VOLUME 27 / NUMBER 4
FEBRUARY 23, 1989
ACC. NOS. N89-12535 TO N89-13393

STAR

AN ABSTRACT JOURNAL

Scientific and Technical Aerospace Reports

PRODUCED BY THE
SCIENTIFIC AND TECHNICAL
INFORMATION
BRANCH

NASA

NATIONAL AERONAUTICS AND SPACE ADMINISTRATION

WHAT YOU CAN DO FOR *STAR*

All users of this abstract service are urged to forward reports to be considered for announcement in *STAR*. This will aid NASA in its efforts to provide the fullest possible coverage of all scientific and technical publications that might support aeronautics and space research and development. If you have prepared relevant reports (other than those that you will transmit to NASA, DoD, or DOE through the usual contract- or grant-reporting channels), please send them for consideration to the NASA Scientific and Technical Information Facility, P.O. Box 8757, BWI Airport, Maryland 21240.

Reprints of journal articles, book chapters, and conference papers are also welcome. These will be considered for announcement in *STAR's* companion journal, *International Aerospace Abstracts*.

You may specify a particular source to be included in a report announcement if you wish; otherwise the report will be placed on public sale at the National Technical Information Service. Copyrighted publications will be announced but not distributed or sold.

PURCHASE OF *STAR*

The semimonthly issues are available to registered users on annual subscription for $99.00 from the NASA Scientific and Technical Information Facility, ATTN: Registration Services, P.O. Box 8757, BWI Airport, MD 21240. *STAR* is publically available on annual subscription for $99.00 from the Superintendent of Documents, U.S. Government Printing Office, Washington, DC 20402.

PUBLISHED BY:

UNITED STATES GOVERNMENT
NATIONAL AERONAUTICS AND SPACE ADMINISTRATION
SCIENTIFIC AND TECHNICAL INFORMATION DIVISION
Scientific and Technical Aerospace Reports, Volume 27, is prepared by the NASA Scientific and Technical Information Facility operated for the National Aeronautics and Space Administration by RMS Associates.

The Administrator of the National Aeronautics and Space Administration has determined that the publication of this periodical is necessary in the transaction of the public business required by law of this Agency. Use of funds for printing this periodical has been approved by the Director of the Office of Management and Budget through March 22, 1989.

US ISSN 0036-8741

INTRODUCTION

Scientific and Technical Aerospace Reports (STAR) is a major component of a comprehensive National Aeronautics and Space Administration information system covering aeronautics, space, and supporting disciplines. *STAR* is issued on the 8th and 23rd of each month and announces current publications of the following types:

- NASA, NASA contractor, and NASA grantee reports
- Reports issued by other U.S. Government Agencies, domestic and foreign institutions, universities, and private firms
- Translations in report form
- NASA-owned patents and patent applications
- Other U.S. Government Agency and foreign patents and patent applications
- Domestic and foreign dissertations and theses

Journal, book, and conference literature, cover-to-cover journal translations, and certain foreign dissertations are announced in a companion journal, *International Aerospace Abstracts (IAA),* available on subscription from the American Institute of Aeronautics and Astronautics, Technical Information Service, 555 West 57th Street, 12th Floor, New York, New York 10019.

SUBJECT SCOPE

Subject scope of *STAR,* and *IAA* includes all aspects of aeronautics and space research and development, supporting basic and applied research, and applications. Aerospace aspects of earth resources, energy development, conservation, oceanography, environmental protection, urban transportation, and other topics of high national priority are also covered.

OTHER NASA PUBLICATIONS

Other NASA publications and information services are described in the publication, *The NASA Scientific and Technical Information System ... and How to Use It,* available without charge from the NASA Scientific and Technical Information Facility, P.O. Box 8757, BWI Airport, Maryland 21240.

HOW TO USE *STAR* SUBJECT CATEGORIES

STAR is categorized by 10 major subject divisions divided into 76 specific subject categories and one general category/division. The major subject divisions are listed in the Table of Contents, together with a note for each that defines its scope and provides any cross-references. For example:

AERONAUTICS

Includes aeronautics (general); aerodynamics; air transportation and safety; aircraft communications and navigation; aircraft design, testing and performance; aircraft instrumentation; aircraft propulsion and power; aircraft stability and control; and research and support facilities (air).

For related information see also *Astronautics.*

Each major division is further divided into as many as nine specific categories, which are identified by category numbers.

Abstracts in *STAR* are grouped by specific category, the categories appearing in sequential order. Category breaks in the abstract section are identified by the category number and title, and a scope note. Cross-references to other categories are provided as appropriate. For example:

02 AERODYNAMICS

Includes aerodynamics of bodies, combinations, wings, rotors, and control surfaces; and internal flow in ducts and turbomachinery.

For related information see also *34 Fluid Mechanics and Heat Transfer.*

CROSS-REFERENCES

Individual *STAR* abstracts are not ordinarily cross-referenced, except for certain conference reports or book translations that have had separate abstracts written for their component papers or chapters. Citations and abstracts of the components follow immediately after those of the parent document. When the subject content of a component differs sufficiently from the general content of the parent, a cross-reference citation also is printed at the end of the category to which it normally would have been assigned if it were independent.

DOCUMENTS ON MICROFICHE

Documents on microfiche[1] are designated by a pound sign (#) following the accession number. The pound sign is used without regard to the source or quality of the microfiche.

AVAILABILITIES

One or more sources from which a document announced in *STAR* is available to the public is given in each citation. The most commonly indicated sources and their acronyms or abbreviations are listed below. If the publication is available from a source other than those listed, the publisher and his address will be displayed on the availability line or in combination with the corporate source line.

Avail: NTIS. Sold by the National Technical Information Service. Prices for hard copy (HC) and microfiche (MF) are indicated by a price code following the letters HC or MF in the *STAR* citation. Current values for the price codes are given in the tables on page vii.

Initially distributed microfiche under the NTIS SRIM (Selected Research in Microfiche) is available at greatly reduced unit prices. For this service and for information concerning subscription to NASA printed reports, consult the NTIS Subscription Section, Springfield, Va. 22161.

NOTE ON ORDERING DOCUMENTS: When ordering NASA publications (those followed by the * symbol), use the N accession number. NASA patent applications (only the specifications are offered) should be ordered by the US-Patent-Appl-SN number. Non-NASA publications (no asterisk) should be ordered by the AD, PB, or other *report number* shown on the last line of the citation, not by the N accession number. It is also advisable to cite the title and other bibliographic identification.

Avail: SOD (or GPO). Sold by the Superintendent of Documents, U.S. Government Printing Office, in hard copy. The current price and order number are given following the availability line. (NTIS will fill microfiche requests, as indicated above, for those documents identified by a # symbol.)

(1) A microfiche is a transparent sheet of film, 105 by 148 mm in size, containing as many as 60 to 98 pages of information reduced to micro images (not to exceed 26:1 reduction).

Avail: BLL (formerly NLL): British Library Lending Division, Boston Spa, Wetherby, Yorkshire, England. Photocopies available from this organization at the price shown. (If none is given, inquiry should be addressed to the BLL.)

Avail: DOE Depository Libraries. Organizations in U.S. cities and abroad that maintain collections of Department of Energy reports, usually in microfiche form, are listed in *Energy Research Abstracts.* Services available from the DOE and its depositories are described in a booklet, *DOE Technical Information Center - Its Functions and Services* (TID-4660), which may be obtained without charge from the DOE Technical Information Center.

Avail: ESDU. Pricing information on specific data, computer programs, and details on ESDU topic categories can be obtained from ESDU International Ltd. Requesters in North America should use the Virginia address while all other requesters should use the London address, both of which are on page vi.

Avail: Fachinformationszentrum, Karlsruhe. Sold by the Fachinformationszentrum Energie, Physik, Mathematik GMBH, Eggenstein Leopoldshafen, Federal Republic of Germany, at the price shown in deutschmarks (DM).

Avail: HMSO. Publications of Her Majesty's Stationery Office are sold in the U.S. by Pendragon House, Inc. (PHI), Redwood City, California. The U.S. price (including a service and mailing charge) is given, or a conversion table may be obtained from PHI.

Avail: NASA Public Document Rooms. Documents so indicated may be examined at or purchased from the National Aeronautics and Space Administration, Public Documents Room (Room 126), 600 Independence Ave., S.W., Washington, D.C. 20546, or public document rooms located at each of the NASA research centers, the NASA Space Technology Laboratories, and the NASA Pasadena Office at the Jet Propulsion Laboratory.

Avail: Univ. Microfilms. Documents so indicated are dissertations selected from *Dissertation Abstracts* and are sold by University Microfilms as xerographic copy (HC) and microfilm. All requests should cite the author and the Order Number as they appear in the citation.

Avail: US Patent and Trademark Office. Sold by Commissioner of Patents and Trademarks, U.S. Patent and Trademark Office, at the standard price of $1.50 each, postage free. (See discussion of NASA patents and patent applications below.)

Avail: (US Sales Only). These foreign documents are available to users within the United States from the National Technical Information Service (NTIS). They are available to users outside the United States through the International Nuclear Information Service (INIS) representative in their country, or by applying directly to the issuing organization.

Avail: USGS. Originals of many reports from the U.S. Geological Survey, which may contain color illustrations, or otherwise may not have the quality of illustrations preserved in the microfiche or facsimile reproduction, may be examined by the public at the libraries of the USGS field offices whose addresses are listed in this Introduction. The libraries may be queried concerning the availability of specific documents and the possible utilization of local copying services, such as color reproduction.

Avail: Issuing Activity, or Corporate Author, or no indication of availability. Inquiries as to the availability of these documents should be addressed to the organization shown in the citation as the corporate author of the document.

NASA PATENTS AND PATENT APPLICATIONS

Patents and patent applications owned by NASA are announced in *STAR* under appropriate subject categories and are referenced in the *STAR* indexes. In the Report/Accession Number Index, patents are indexed by the NASA Case Number (which appears in lieu of the report number in other indexes), the U.S. Patent Number, the U.S. Patent Application Serial Number, and the U.S. Patent Class. Patent applications for which patents have not yet been issued are indexed by the NASA Case Number and the U.S. Patent Application Serial Number.

NASA *patent application specifications* are sold in paper copy by the National Technical Information Service at price code A02. Microfiche are sold at price code A01. The US-Patent-Appl-SN- number should be used in ordering either paper copy or microfiche from NTIS. Printed copies of *patents* (which are not microfiched) are available for purchase at $1.50 per copy from:

Commissioner of Patents and Trademarks
U.S. Patent and Trademark Office
Washington, D.C. 20231

When ordering patents, the U.S. Patent Number should be used, and payment must be remitted in advance, preferably by money order or check payable to the Commissioner of Patents and Trademarks. Prepaid purchase coupons for ordering are also available from the Patent and Trademark Office. The patents and patent applications announced in *STAR* are owned by NASA and are available for royalty-free licensing. Requests for licensing terms and further information should be addressed to:

Associate General Counsel for Intellectual Property/Code GP
National Aeronautics and Space Administration
Washington, D.C. 20546

ELIGIBILITY AND REGISTRATION FOR NASA INFORMATION PRODUCTS AND SERVICES

A variety of services is available to organizations of the following types that have registered with NASA to receive specific services or products:

1. NASA offices, research centers, contractors, subcontractors, grantees, and consultants;
2. Other U.S. Government agencies and their contractors;
3. Libraries in the United States that have arrangements with NASA to maintain collections of NASA documents for public reference;
4. Other organizations in the United States having a need for NASA documents in work related to aeronautics and space research;
5. Organizations abroad that have established reciprocal document exchange arrangements with NASA.

Only the central service points or central points of document acquisition and control within qualified organizations are eligible to register for NASA products and services. Domestic organizations that may be eligible to receive various classes of NASA publications and services should address their requests for registration or for further information to:

NASA Scientific and Technical Information Facility
ATTN: Registration Services
Post Office Box 8757
BWI Airport, Maryland 21240

Organizations abroad should direct requests to Manager, International STI Activities, NTT, NASA Headquarters, Washington, D.C. 20546.

AVAILABILITY OF *STAR* ABSTRACTS ON MICROFICHE

Microfiche of the abstract sections of this issue and other issues of *STAR* are available on annual subscription from NTIS as PB89-911300, Attn: Subscriptions, 5285 Port Royal Road, Springfield, Virginia 22161. Annual subscription rates are $70.00 North America; $140.00 foreign. Abstract sections for previous years retroactive to 1964 are available at the current rates. Microfiche for individual *STAR* issue abstract sections are not available.

PUBLIC COLLECTIONS OF NASA DOCUMENTS

DOMESTIC: NASA and NASA-sponsored documents and a large number of aerospace publications are available to the public for reference purposes at the library maintained by the American Institute of Aeronautics and Astronautics, Technical Information Service, 555 West 57th Street, 12th Floor, New York, New York 10019

EUROPEAN: An extensive collection of NASA and NASA-sponsored publications is maintained by the British Library Lending Division, Boston Spa, Wetherby, Yorkshire, England for public access. The British Library Lending Division also has available many of the non-NASA publications cited in *STAR*. European requesters may purchase facsimile copy or microfiche of NASA and NASA-sponsored documents, those identified by both the symbols # and * from ESA - Information Retrieval Service European Space Agency, 8-10 rue Mario-Nikis, 75738 Paris CEDEX 15, France.

FEDERAL DEPOSITORY LIBRARY PROGRAM

In order to provide the general public with greater access to U.S. Government publications, Congress established the Federal Depository Library Program under the Government Printing Office (GPO), with 50 regional depositories responsible for permanent retention of material, inter-library loan, and reference services. At least one copy of nearly every NASA and NASA-sponsored publication, either in printed or microfiche format, is received and retained by the 50 regional depositories. A list of the regional GPO libraries, arranged alphabetically by state, appears on the inside back cover. These libraries are *not* sales outlets. A local library can contact a Regional Depository to help locate specific reports, or direct contact may be made by an individual.

ADDRESSES OF ORGANIZATIONS

American Institute of Aeronautics and Astronautics
Technical Information Service
555 West 57th Street, 12th Floor
New York, New York 10019

British Library Lending Division,
Boston Spa, Wetherby, Yorkshire,
England

Commissioner of Patents and Trademarks
U.S. Patent and Trademark Office
Washington, D.C. 20231

Department of Energy
Technical Information Center
P.O. Box 62
Oak Ridge, Tennessee 37830

ESA-Information Retrieval Service
ESRIN
Via Galileo Galilei
00044 Frascati (Rome) Italy

ESDU International
P.O. Box 1633
Manassas, Virginia 22110

ESDU International, Ltd.
251-259 Regent Street
London, W1R 7AD, England

Fachinformationszentrum Energie, Physik, Mathematik GMBH
7514 Eggenstein Leopoldshafen
Federal Republic of Germany

Her Majesty's Stationery Office
P.O. Box 569, S.E. 1
London, England

NASA Scientific and Technical Information Facility
P.O. Box 8757
B.W.I. Airport, Maryland 21240

National Aeronautics and Space Administration
Scientific and Technical Information Division (NTT)
Washington, D.C. 20546

National Technical Information Service
5285 Port Royal Road
Springfield, Virginia 22161

Pendragon House, Inc.
899 Broadway Avenue
Redwood City, California 94063

Superintendent of Documents
U.S. Government Printing Office
Washington, D.C. 20402

University Microfilms
A Xerox Company
300 North Zeeb Road
Ann Arbor, Michigan 48106

University Microfilms, Ltd.
Tylers Green
London, England

U.S. Geological Survey Library
National Center - MS 950
12201 Sunrise Valley Drive
Reston, Virginia 22092

U.S. Geological Survey Library
2255 North Gemini Drive
Flagstaff, Arizona 86001

U.S. Geological Survey
345 Middlefield Road
Menlo Park, California 94025

U.S. Geological Survey Library
Box 25046
Denver Federal Center, MS914
Denver, Colorado 80225

NTIS PRICE SCHEDULES

(Effective January 1, 1989)

Schedule A
STANDARD PRICE DOCUMENTS AND MICROFICHE

PRICE CODE	NORTH AMERICAN PRICE	FOREIGN PRICE
A01	$ 6.95	$13.90
A02	10.95	21.90
A03	13.95	27.90
A04-A05	15.95	31.90
A06-A09	21.95	43.90
A10-A13	28.95	57.90
A14-A17	36.95	73.90
A18-A21	42.95	85.90
A22-A25	49.95	99.90
A99	*	*
NO1	55.00	70.00
NO2	55.00	80.00

Schedule E
EXCEPTION PRICE DOCUMENTS AND MICROFICHE

PRICE CODE	NORTH AMERICAN PRICE	FOREIGN PRICE
E01	$ 9.00	18.00
E02	11.50	23.00
E03	13.00	26.00
E04	15.50	31.00
E05	17.50	35.00
E06	20.50	41.00
E07	23.00	46.00
E08	25.50	51.00
E09	28.00	56.00
E10	31.00	62.00
E11	33.50	67.00
E12	36.50	73.00
E13	39.00	78.00
E14	42.50	85.00
E15	46.00	92.00
E16	50.50	101.00
E17	54.50	109.00
E18	59.00	118.00
E19	65.50	131.00
E20	76.00	152.00
E99	*	*

*Contact NTIS for price quote.

IMPORTANT NOTICE

NTIS Shipping and Handling Charges
U.S., Canada, Mexico — ADD $3.00 per TOTAL ORDER
All Other Countries — ADD $4.00 per TOTAL ORDER

Exceptions — Does NOT apply to:
ORDERS REQUESTING NTIS RUSH HANDLING
ORDERS FOR SUBSCRIPTION OR STANDING ORDER PRODUCTS *ONLY*

NOTE: Each additional delivery address on an order requires a separate shipping and handling charge.

VOLUME 27 NUMBER 4 / FEBRUARY 23, 1989

TABLE OF CONTENTS

AERONAUTICS

Includes aeronautics (general); aerodynamics; air transportation and safety; aircraft communications and navigation; aircraft design, testing and performance; aircraft instrumentation; aircraft propulsion and power; aircraft stability and control; and research and support facilities (air).

For related information see also *Astronautics.*

01 AERONAUTICS (GENERAL) 417

02 AERODYNAMICS 418

Includes aerodynamics of bodies, combinations, wings, rotors, and control surfaces; and internal flow in ducts and turbomachinery.

For related information see also *34 Fluid Mechanics and Heat Transfer*

03 AIR TRANSPORTATION AND SAFETY 420

Includes passenger and cargo air transport operations; and aircraft accidents.

For related information see also *16 Space Transportation* and *85 Urban Technology and Transportation.*

04 AIRCRAFT COMMUNICATIONS AND NAVIGATION 421

Includes digital and voice communication with aircraft; air navigation systems (satellite and ground based); and air traffic control.

For related information see also *17 Space Communications, Spacecraft Communications, Command and Tracking* and *32 Communications and Radar.*

05 AIRCRAFT DESIGN, TESTING AND PERFORMANCE 421

Includes aircraft simulation technology.

For related information see also *18 Spacecraft Design, Testing and Performance* and *39 Structural Mechanics.* For land transportation vehicles see *85 Urban Technology and Transportation.*

06 AIRCRAFT INSTRUMENTATION N.A.

Includes cockpit and cabin display devices; and flight instruments.

For related information see also *19 Spacecraft Instrumentation* and *35 Instrumentation and Photography.*

07 AIRCRAFT PROPULSION AND POWER 422

Includes prime propulsion systems and systems components, e.g., gas turbine engines and compressors; and onboard auxiliary power plants for aircraft.

For related information see also *20 Spacecraft Propulsion and Power, 28 Propellants and Fuels,* and *44 Energy Production and Conversion.*

08 AIRCRAFT STABILITY AND CONTROL 424

Includes aircraft handling qualities; piloting; flight controls; and autopilots.

For related information see also *05 Aircraft Design, Testing and Performance.*

09 RESEARCH AND SUPPORT FACILITIES (AIR) 424

Includes airports, hangars and runways; aircraft repair and overhaul facilities; wind tunnels; shock tubes; and aircraft engine test stands.

For related information see also *14 Ground Support Systems and Facilities (Space).*

ASTRONAUTICS

Includes astronautics (general); astrodynamics; ground support systems and facilities (space); launch vehicles and space vehicles; space transportation; space communications, spacecraft communications, command and tracking; spacecraft design, testing and performance; spacecraft instrumentation; and spacecraft propulsion and power.

For related information see also *Aeronautics*

12 ASTRONAUTICS (GENERAL) 425

For extraterrestrial exploration see *91 Lunar and Planetary Exploration.*

13 ASTRODYNAMICS 425

Includes powered and free-flight trajectories; and orbital and launching dynamics.

14 GROUND SUPPORT SYSTEMS AND FACILITIES (SPACE) 425

Includes launch complexes, research and production facilities; ground support equipment, e.g., mobile transporters; and simulators.

For related information see also *09 Research and Support Facilities (Air).*

15 LAUNCH VEHICLES AND SPACE VEHICLES 426

Includes boosters; operating problems of launch/space vehicle systems; and reusable vehicles.

For related information see also *20 Spacecraft Propulsion and Power.*

16 SPACE TRANSPORTATION 427

Includes passenger and cargo space transportation, e.g., shuttle operations; and space rescue techniques.

For related information see also *03 Air Transportation and Safety* and *18 Spacecraft Design, Testing and Performance.* For space suits see *54 Man/System Technology and Life Support.*

17 SPACE COMMUNICATIONS, SPACECRAFT COMMUNICATIONS, COMMAND AND TRACKING N.A.

Includes telemetry; space communications networks; astronavigation and guidance; and radio blackout.

For related information see also *04 Aircraft Communications and Navigation* and *32 Communications and Radar.*

18 SPACECRAFT DESIGN, TESTING AND PERFORMANCE 427

Includes satellites; space platforms; space stations; spacecraft systems and components such as thermal and environmental controls; and attitude controls.

For life support systems see *54 Man/System Technology and Life Support.* For related information see also *05 Aircraft Design, Testing and Performance, 39 Structural Mechanics,* and *16 Space Transportation.*

19 SPACECRAFT INSTRUMENTATION N.A.

For related information see also *06 Aircraft Instrumentation* and *35 Instrumentation and Photography.*

20 SPACECRAFT PROPULSION AND POWER 434

Includes main propulsion systems and components, e.g. rocket engines; and spacecraft auxiliary power sources.

For related information see also *07 Aircraft Propulsion and Power, 28 Propellants and Fuels, 44 Energy Production and Conversion,* and *15 Launch Vehicles and Space Vehicles.*

CHEMISTRY AND MATERIALS

Includes chemistry and materials (general); composite materials; inorganic and physical chemistry; metallic materials; nonmetallic materials; propellants and fuels; and materials processing.

23 CHEMISTRY AND MATERIALS (GENERAL) 441

24 COMPOSITE MATERIALS 442

Includes physical, chemical, and mechanical properties of laminates and other composite materials.

For ceramic materials see *27 Nonmetallic Materials.*

25 INORGANIC AND PHYSICAL CHEMISTRY 444

Includes chemical analysis, e.g., chromatography; combustion theory; electrochemistry; and photochemistry.

For related information see also *77 Thermodynamics and Statistical Physics.*

26 METALLIC MATERIALS 447

Includes physical, chemical, and mechanical properties of metals, e.g., corrosion; and metallurgy.

27 NONMETALLIC MATERIALS 452

Includes physical, chemical, and mechanical properties of plastics, elastomers, lubricants, polymers, textiles, adhesives, and ceramic materials.

For composite materials see *24 Composite Materials.*

28 PROPELLANTS AND FUELS 457

Includes rocket propellants, igniters and oxidizers; their storage and handling procedures; and aircraft fuels.

For related information see also *07 Aircraft Propulsion and Power, 20 Spacecraft Propulsion and Power,* and *44 Energy Production and Conversion.*

29 MATERIALS PROCESSING 458

Includes space-based development of products and processes for commercial application.

For biological materials see *55 Space Biology.*

ENGINEERING

Includes engineering (general); communications and radar; electronics and electrical engineering; fluid mechanics and heat transfer; instrumentation and photography; lasers and masers; mechanical engineering; quality assurance and reliability; and structural mechanics.

For related information see also *Physics.*

31 ENGINEERING (GENERAL) 458

Includes vacuum technology; control engineering; display engineering; cryogenics; and fire prevention.

32 COMMUNICATIONS AND RADAR 464

Includes radar; land and global communications; communications theory; and optical communications.

For related information see also *04 Aircraft Communications and Navigation* and *17 Space Communications, Spacecraft Communications, Command and Tracking.* For search and rescue see *03 Air Transportation and Safety,* and *16 Space Transportation.*

33 ELECTRONICS AND ELECTRICAL ENGINEERING 471

Includes test equipment and maintainability; components, e.g., tunnel diodes and transistors; microminiaturization; and integrated circuitry.

For related information see also *60 Computer Operations and Hardware* and *76 Solid-State Physics.*

34 FLUID MECHANICS AND HEAT TRANSFER 472

Includes boundary layers; hydrodynamics; fluidics; mass transfer and ablation cooling.

For related information see also *02 Aerodynamics* and *77 Thermodynamics and Statistical Physics.*

35 INSTRUMENTATION AND PHOTOGRAPHY 477

Includes remote sensors; measuring instruments and gages; detectors; cameras and photographic supplies; and holography.

For aerial photography see *43 Earth Resources and Remote Sensing.* For related information see also *06 Aircraft Instrumentation* and *19 Spacecraft Instrumentation.*

36 LASERS AND MASERS 479

Includes parametric amplifiers.

For related information see also *76 Solid-State Physics.*

37 MECHANICAL ENGINEERING 481

Includes auxiliary systems (nonpower); machine elements and processes; and mechanical equipment.

38 QUALITY ASSURANCE AND RELIABILITY 484

Includes product sampling procedures and techniques; and quality control.

39 STRUCTURAL MECHANICS 484

Includes structural element design and weight analysis; fatigue; and thermal stress.

For applications see *05 Aircraft Design, Testing and Performance* and *18 Spacecraft Design, Testing and Performance.*

GEOSCIENCES

Includes geosciences (general); earth resources and remote sensing; energy production and conversion; environment pollution; geophysics; meteorology and climatology; and oceanography.

For related information see also *Space Sciences.*

42 GEOSCIENCES (GENERAL) 495

43 EARTH RESOURCES AND REMOTE SENSING 520

Includes remote sensing of earth resources by aircraft and spacecraft; photogrammetry; and aerial photography.

For instrumentation see *35 Instrumentation and Photography.*

44 ENERGY PRODUCTION AND CONVERSION 528

Includes specific energy conversion systems, e.g., fuel cells; global sources of energy; geophysical conversion; and windpower.

For related information see also *07 Aircraft Propulsion and Power, 20 Spacecraft Propulsion and Power,* and *28 Propellants and Fuels.*

45 ENVIRONMENT POLLUTION 530

Includes atmospheric, noise, thermal, and water pollution.

46 GEOPHYSICS 530

Includes aeronomy; upper and lower atmosphere studies; ionospheric and magnetospheric physics; and geomagnetism.

For space radiation see *93 Space Radiation.*

47 METEOROLOGY AND CLIMATOLOGY 532

Includes weather forecasting and modification.

48 OCEANOGRAPHY 535

Includes biological, dynamic, and physical oceanography; and marine resources.

For related information see also *43 Earth Resources and Remote Sensing.*

LIFE SCIENCES

Includes life sciences (general); aerospace medicine; behavioral sciences; man/system technology and life support; and space biology.

51 LIFE SCIENCES (GENERAL) 536

52 AEROSPACE MEDICINE 537

Includes physiological factors; biological effects of radiation; and effects of weightlessness on man and animals.

53 BEHAVIORAL SCIENCES 538

Includes psychological factors; individual and group behavior; crew training and evaluation; and psychiatric research.

54 MAN/SYSTEM TECHNOLOGY AND LIFE SUPPORT 539

Includes human engineering; biotechnology; and space suits and protective clothing.

For related information see also *16 Space Transportation.*

55 SPACE BIOLOGY 539

Includes exobiology; planetary biology; and extraterrestrial life.

MATHEMATICAL AND COMPUTER SCIENCES

Includes mathematical and computer sciences (general); computer operations and hardware; computer programming and software; computer systems; cybernetics; numerical analysis; statistics and probability; systems analysis; and theoretical mathematics.

59 MATHEMATICAL AND COMPUTER SCIENCES (GENERAL) N.A.

60 COMPUTER OPERATIONS AND HARDWARE 540

Includes hardware for computer graphics, firmware, and data processing.

For components see *33 Electronics and Electrical Engineering.*

61 COMPUTER PROGRAMMING AND SOFTWARE 540

Includes computer programs, routines, algorithms, and specific applications, e.g., CAD/CAM.

62 COMPUTER SYSTEMS 541

Includes computer networks and special application computer systems.

63 CYBERNETICS 545

Includes feedback and control theory, artificial intelligence, robotics and expert systems.

For related information see also *54 Man/System Technology and Life Support.*

64 NUMERICAL ANALYSIS 549

Includes iteration, difference equations, and numerical approximation.

65 STATISTICS AND PROBABILITY 551

Includes data sampling and smoothing; Monte Carlo method; and stochastic processes.

66 SYSTEMS ANALYSIS 552

Includes mathematical modeling; network analysis; and operations research.

67 THEORETICAL MATHEMATICS N.A.

Includes topology and number theory.

PHYSICS

Includes physics (general); acoustics; atomic and molecular physics; nuclear and high-energy physics; optics; plasma physics; solid-state physics; and thermodynamics and statistical physics.

For related information see also *Engineering.*

70 PHYSICS (GENERAL) 552

For precision time and time interval (PTTI) see *35 Instrumentation and Photography;* for geophysics, astrophysics or solar physics see *46 Geophysics, 90 Astrophysics,* or *92 Solar Physics.*

71 ACOUSTICS 554
Includes sound generation, transmission, and attenuation.
For noise pollution see *45 Environment Pollution.*

72 ATOMIC AND MOLECULAR PHYSICS 555
Includes atomic structure, electron properties, and molecular spectra.

73 NUCLEAR AND HIGH-ENERGY PHYSICS 556
Includes elementary and nuclear particles; and reactor theory.
For space radiation see *93 Space Radiation.*

74 OPTICS 557
Includes light phenomena and optical devices.
For lasers see *36 Lasers and Masers.*

75 PLASMA PHYSICS 558
Includes magnetohydrodynamics and plasma fusion.
For ionospheric plasmas see *46 Geophysics.* For space plasmas see *90 Astrophysics.*

76 SOLID-STATE PHYSICS 562
Includes superconductivity.
For related information see also *33 Electronics and Electrical Engineering* and *36 Lasers and Masers.*

77 THERMODYNAMICS AND STATISTICAL PHYSICS 564
Includes quantum mechanics; theoretical physics; and Bose and Fermi statistics.
For related information see also *25 Inorganic and Physical Chemistry* and *34 Fluid Mechanics and Heat Transfer.*

SOCIAL SCIENCES

Includes social sciences (general); administration and management; documentation and information science; economics and cost analysis; law, political science, and space policy; and urban technology and transportation.

80 SOCIAL SCIENCES (GENERAL) 565
Includes educational matters.

81 ADMINISTRATION AND MANAGEMENT 565
Includes management planning and research.

82 DOCUMENTATION AND INFORMATION SCIENCE 565
Includes information management; information storage and retrieval technology; technical writing; graphic arts; and micrography.
For computer documentation see *61 Computer Programming and Software.*

83 ECONOMICS AND COST ANALYSIS N.A.
Includes cost effectiveness studies.

84 LAW, POLITICAL SCIENCE AND SPACE POLICY 567
Includes NASA appropriation hearings; aviation law; space law and policy; international law; international cooperation; and patent policy.

85 URBAN TECHNOLOGY AND TRANSPORTATION 567
Includes applications of space technology to urban problems; technology transfer; technology assessment; and surface and mass transportation.
For related information see *03 Air Transportation and Safety, 16 Space Transportation,* and *44 Energy Production and Conversion.*

SPACE SCIENCES

Includes space sciences (general); astronomy; astrophysics; lunar and planetary exploration; solar physics; and space radiation.
For related information see also *Geosciences.*

88 SPACE SCIENCES (GENERAL) 567

89 ASTRONOMY 567
Includes radio, gamma-ray, and infrared astronomy; and astrometry.

90 ASTROPHYSICS 577
Includes cosmology; celestial mechanics; space plasmas; and interstellar and interplanetary gases and dust.
For related information see also *75 Plasma Physics.*

91 LUNAR AND PLANETARY EXPLORATION N.A.
Includes planetology; and manned and unmanned flights.
For spacecraft design or space stations see *18 Spacecraft Design, Testing and Performance.*

92 SOLAR PHYSICS 580
Includes solar activity, solar flares, solar radiation and sunspots.
For related information see *93 Space Radiation.*

93 SPACE RADIATION 580
Includes cosmic radiation; and inner and outer earth's radiation belts.
For biological effects of radiation see *52 Aerospace Medicine.* For theory see *73 Nuclear and High-Energy Physics.*

GENERAL

Includes aeronautical, astronautical, and space science related histories, biographies, and pertinent reports too broad for categorization; histories or broad overviews of NASA programs.

99 GENERAL 580

Note: N.A. means that no abstracts were assigned to this category for this issue.

SUBJECT INDEX I-1
PERSONAL AUTHOR INDEX I-49
CORPORATE SOURCE INDEX I-57
CONTRACT NUMBER INDEX I-69
REPORT/ACCESSION NUMBER INDEX I-71

TYPICAL CITATION AND ABSTRACT

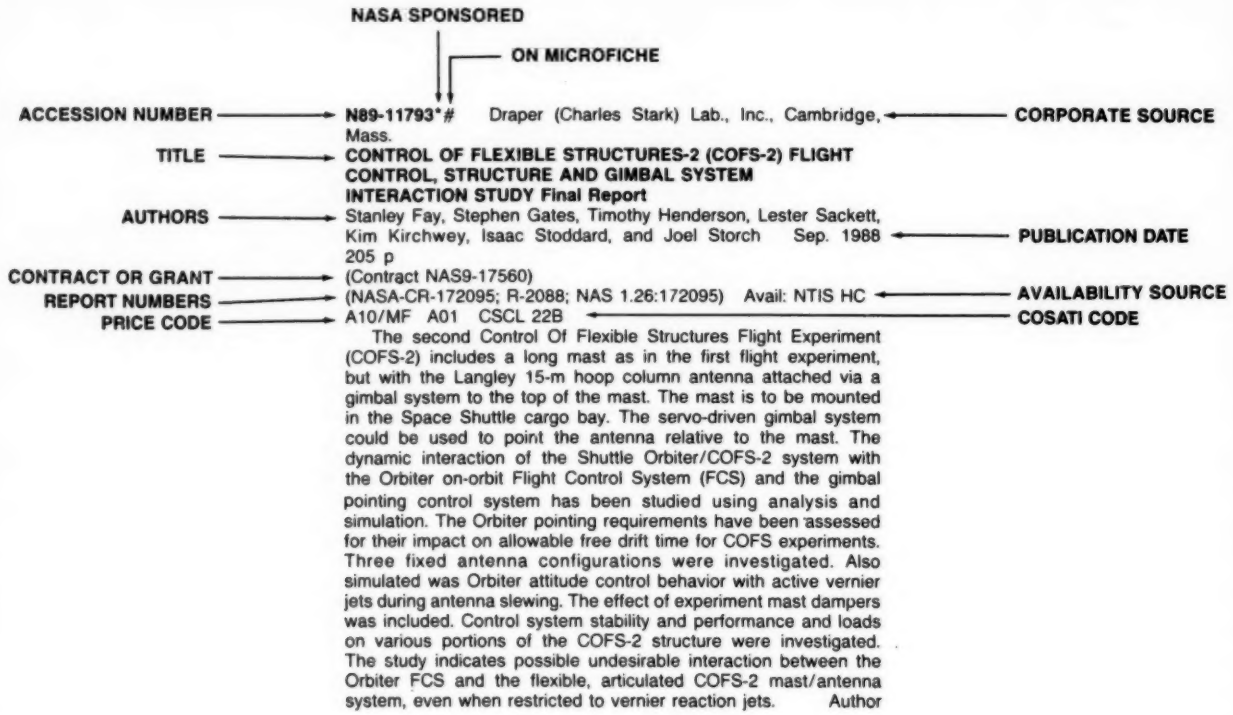
NASA SPONSORED
ON MICROFICHE
ACCESSION NUMBER
N89-11793*#
Draper (Charles Stark) Lab., Inc., Cambridge, Mass.
CORPORATE SOURCE
TITLE
CONTROL OF FLEXIBLE STRUCTURES-2 (COFS-2) FLIGHT CONTROL, STRUCTURE AND GIMBAL SYSTEM INTERACTION STUDY Final Report
AUTHORS
Stanley Fay, Stephen Gates, Timothy Henderson, Lester Sackett, Kim Kirchwey, Isaac Stoddard, and Joel Storch
Sep. 1988
205 p
PUBLICATION DATE
CONTRACT OR GRANT
(Contract NAS9-17560)
REPORT NUMBERS
(NASA-CR-172095; R-2088; NAS 1.26:172095)
Avail: NTIS HC
AVAILABILITY SOURCE
PRICE CODE
A10/MF A01 CSCL 22B
COSATI CODE
The second Control Of Flexible Structures Flight Experiment (COFS-2) includes a long mast as in the first flight experiment, but with the Langley 15-m hoop column antenna attached via a gimbal system to the top of the mast. The mast is to be mounted in the Space Shuttle cargo bay. The servo-driven gimbal system could be used to point the antenna relative to the mast. The dynamic interaction of the Shuttle Orbiter/COFS-2 system with the Orbiter on-orbit Flight Control System (FCS) and the gimbal pointing control system has been studied using analysis and simulation. The Orbiter pointing requirements have been assessed for their impact on allowable free drift time for COFS experiments. Three fixed antenna configurations were investigated. Also simulated was Orbiter attitude control behavior with active vernier jets during antenna slewing. The effect of experiment mast dampers was included. Control system stability and performance and loads on various portions of the COFS-2 structure were investigated. The study indicates possible undesirable interaction between the Orbiter FCS and the flexible, articulated COFS-2 mast/antenna system, even when restricted to vernier reaction jets.
Author

VOLUME 27 NUMBER 4 / FEBRUARY 23, 1989

Scientific and Technical Aerospace Reports

A Semimonthly Publication of the National Aeronautics and Space Administration

01 AERONAUTICS (GENERAL)

N89-12535# Northrop Corp., Hawthorne, Calif.
AUTOMATED AIRFRAME ASSEMBLY PROGRAM (AAAP) SURVEY OF CIM STATUS IN THE AIRCRAFT INDUSTRY Final Report, 30 Nov. 1986 - 30 Oct. 1987
Apr. 1988 42 p
(Contract F33615-87-C-5217)
(AD-A197368; AFWAL-TR-88-4051) Avail: NTIS HC A03/MF A01 CSCL 13H

The purpose of this survey was to evaluate different airframe manufacturing environments. Price Waterhouse and Northrop Aircraft Division (NAD) personnel developed the survey questions jointly to evaluate the Needs and Requirements definition for the Automated Airframe Assembly Program (AAAP). AAAP focused on major and minor subassembly operations and related areas. The survey breaks these down into two timeframes: the next 1 to 5 years (today) and the future (5 to 10 years). The Survey consisted of seven major functional sections including an integration section. The Survey sections were completed by those individuals most familiar with the issues being addressed. The results respondents to this survey are being kept strictly confidential. Price Waterhouse gathered combined and evaluated survey results. NAD personnel do not have access to an individual company's responses. GRA

N89-12536* National Aeronautics and Space Administration, Washington, D.C.
AERONAUTICAL ENGINEERING: A CONTINUING BIBLIOGRAPHY WITH INDEXES (SUPPLEMENT 232)
Nov. 1988 126 p
(NASA-SP-7037(232); NAS 1.21:7037(232)) Avail: NTIS HC A07; NTIS standing order as PB88-914100, $8.50 domestic, $17.00 foreign CSCL 01A

This bibliography lists 422 reports, articles, and other documents introduced into the NASA scientific and technical information system in October, 1988. Author

N89-12537# National Transportation Safety Board, Washington, D. C. Bureau of Safety Programs.
ANNUAL REVIEW OF AIRCRAFT ACCIDENT DATA, US GENERAL AVIATION, CALENDAR YEAR 1985
13 Oct. 1987 238 p
(PB88-115787; NTSB-ARG-87-03) Avail: NTIS HC A11/MF A01 CSCL 01C

A statistical compilation and review of general aviation accidents which occurred in 1985 in the United States, its territories and possessions, and in international waters are presented. The accidents reported are all those involving U.S. registered aircraft not conducting operations under 14 CFR 121, 14 CFR 125, 14 CFR 127, or 14 CFR 135. The report is divided into sections, each of which presents a review of a subset of all general aviation accidents. Each subset represents aircraft of similar types or aircraft being operated for particular purposes. Several tables present accident parameters for 1985 only, and each section includes tabulations which present comparative statistics for 1985 and for the five-year period 1980 through 1984. GRA

N89-12538*# Georgia Inst. of Tech., Atlanta. School of Aerospace Engineering.
TRAJECTORY OPTIMIZATION AND GUIDANCE LAW DEVELOPMENT FOR NATIONAL AEROSPACE PLANE APPLICATIONS Final Report, 1 Jul. 1987 - 30 Nov. 1988
A. J. Calise, G. A. Flandro, and J. E. Corban Dec. 1988 130 p
Prepared for General Dynamics Corp., St. Louis, Mo.
(Grant NAG1-784)
(NASA-CR-182994; NAS 1.26:182994) Avail: NTIS HC A07/MF A01 CSCL 01B

The work completed to date is comprised of the following: a simple vehicle model representative of the aerospace plane concept in the hypersonic flight regime, fuel-optimal climb profiles for the unconstrained and dynamic pressure constrained cases generated using a reduced order dynamic model, an analytic switching condition for transition to rocket powered flight as orbital velocity is approached, simple feedback guidance laws for both the unconstrained and dynamic pressure constrained cases derived via singular perturbation theory and a nonlinear transformation technique, and numerical simulation results for ascent to orbit in the dynamic pressure constrained case. Author

N89-12539*# National Aeronautics and Space Administration. Ames Research Center, Moffett Field, Calif.
AIRCRAFT TECHNOLOGY OPPORTUNITIES FOR THE 21ST CENTURY
James A. Albers and John Zuk Nov. 1988 49 p Presented at the Conference on New Technology and the Aviation System, Los Angeles, Calif., 16-18 Nov. 1988
(NASA-TM-101060; A-89009; NAS 1.15:101060) Avail: NTIS HC A03/MF A01 CSCL 01B

New aircraft technologies are presented that have the potential to expand the air transportation system and reduce congestion through new operating capabilities, and at the same time provide greater levels of safety and environmental compatibility. Both current and planned civil aeronautics technology at the NASA Ames, Lewis, and Langley Research Centers are addressed. The complete spectrum of current aircraft and new vehicle concepts is considered including rotorcraft (helicopters and tiltrotors), vertical and short takeoff and landing (V/STOL) and short takeoff and landing (STOL) aircraft, subsonic transports, high speed transports, and hypersonic/transatmospheric vehicles. New technologies for current aircraft will improve efficiency, affordability, safety, and environmental compatibility. Research and technology promises to enable development of new vehicles that will revolutionize or greatly change the transportation system. These vehicles will provide new capabilities which will lead to enormous market opportunities and economic growth, as well as improve the competitive position of the U.S. aerospace industry. Author

02 AERODYNAMICS

Includes aerodynamics of bodies, combinations, wings, rotors, and control surfaces; and internal flow in ducts and turbomachinery.

For related information see also *34 Fluid Mechanics and Heat Transfer.*

N89-12540 Auburn Univ., Ala.
THE LAMINAR BOUNDARY LAYER ON AN AIRFOIL STARTED IMPULSIVELY FROM REST Ph.D. Thesis
Ruben RojasOviedo 1987 130 p
Avail: Univ. Microfilms Order No. DA8805021

The numerical solution to the unsteady two-dimensional boundary layer equations was obtained for the Joukowski and Karman-Treftz airfoils, impulsively set into uniform motion. The boundary layer development is calculated using an implicit finite difference technique. For a Joukowski airfoil 9.6 percent thick at zero angle of attack, the resulting flow structure shows that as time increases, a bubble of recirculating fluid forms near the trailing edge, increases size, becoming open at the trailing edge, and finally bursting, perturbing further calculations. These results indicate the formation of a system of symmetric vortices near the trailing edge. The computed characteristics of the boundary layer support the concept of a spontaneous singularity at separation. The effects of certain numerical parameters on the numerical calculation and on the computed boundary layer characteristics are also investigated. For the Karman-Treftz airfoil, 12.66 percent thick at zero angle of attack, the results indicate the immediate occurrence of a singularity at the trailing edge of the airfoil. Dissert. Abstr.

N89-12541 Lehigh Univ., Bethlehem, Pa.
UNSTEADY STRUCTURE OF FLOW PAST A PITCHING DELTA WING Ph.D. Thesis
Rasheed A. Atta 1987 226 p
Avail: Univ. Microfilms Order No. DA8729528

The unsteady flow structure generated by flow past a delta wing is addressed. The wing oscillates in the pitching mode about its trailing-edge. Emphasis is on the structure of the instabilities arising from flow separation at the leading- and trailing-edges of the wing. Dissert. Abstr.

N89-12542*# National Aeronautics and Space Administration. Langley Research Center, Hampton, Va.
A TWO-DIMENSIONAL NUMERICAL SIMULATION OF A SUPERSONIC, CHEMICALLY REACTING MIXING LAYER
J. Philip Drummond Washington, D.C. Dec. 1988 106 p
(NASA-TM-4055; L-16415; NAS 1.15:4055) Avail: NTIS HC A06/MF A01 CSCL 01A

Research has been undertaken to achieve an improved understanding of physical phenomena present when a supersonic flow undergoes chemical reaction. A detailed understanding of supersonic reacting flows is necessary to successfully develop advanced propulsion systems now planned for use late in this century and beyond. In order to explore such flows, a study was begun to create appropriate physical models for describing supersonic combustion, and to develop accurate and efficient numerical techniques for solving the governing equations that result from these models. From this work, two computer programs were written to study reacting flows. Both programs were constructed to consider the multicomponent diffusion and convection of important chemical species, the finite rate reaction of these species, and the resulting interaction of the fluid mechanics and the chemistry. The first program employed a finite difference scheme for integrating the governing equations, whereas the second used a hybrid Chebyshev pseudospectral technique for improved accuracy. Author

N89-12543*# National Aeronautics and Space Administration. Langley Research Center, Hampton, Va.
A SPECTRAL COLLOCATION SOLUTION TO THE COMPRESSIBLE STABILITY EIGENVALUE PROBLEM
Michele G. Macaraeg, Craig L. Streett, and M. Yousuff Hussaini Washington, D.C. Dec. 1988 42 p
(NASA-TP-2858; L-16470; NAS 1.60:2858) Avail: NTIS HC A03/MF A01 CSCL 01A

A newly developed spectral compressible linear stability code (SPECLS) (staggered pressure mesh) is presented for analysis of shear flow stability, and applied to high speed boundary layers and free shear flows. The formulation utilizes the first application of a staggered mesh for a compressible flow analysis by a spectral technique. An order of magnitude less number of points is needed for equivalent accuracy of growth rates compared to those calculated by a finite difference formulation. Supersonic disturbances which are found to have oscillatory structures were resolved by a spectral multi-domain discretization, which requires a factor of three fewer points than the single domain spectral stability code. It is indicated, as expected, that stability of mixing layers is enhanced by viscosity and increasing Mach number. The mean flow involves a jet being injected into a quiescent gas. Higher temperatures of the injected gas is also found to enhance stability characteristics of the free shear layer. Author

N89-12544*# Vigyan Research Associates, Inc., Hampton, Va.
SIDEWALL BOUNDARY-LAYER MEASUREMENTS WITH UPSTREAM SUCTION IN THE LANGLEY 0.3-METER TRANSONIC CRYOGENIC TUNNEL
A. V. Murthy Washington NASA Nov. 1988 57 p
(Contract NAS1-17919)
(NASA-CR-4192; NAS 1.26:4192) Avail: NTIS HC A04/MF A01 CSCL 01A

The Langley 0.3 Meter Transonic Cryogenic Tunnel has provision for boundary removal from the sidewalls to reduce sidewall interference effects on the test data. The tests carried out to determine the change in the empty test section sidewall boundary layer thickness at the model station with upstream boundary layer mass removal are described. The boundary layer measurements showed that the upstream removal region is effective in reducing the boundary layer thickness at the model station. The boundary layer displacement thickness reduced from about 1.2 percent to about .4 percent of the test section width. The boundary layer velocity profiles followed a power law variation in the outer region and showed good correlation when plotted in terms of boundary layer momentum thickness. Author

N89-12545 George Washington Univ., Washington, D.C.
THEORETICAL AND EXPERIMENTAL STUDIES OF THE TRANSONIC FLOW FIELD AND ASSOCIATED BOUNDARY CONDITIONS NEAR A LONGITUDINALLY-SLOTTED WIND-TUNNEL WALL Ph.D. Thesis
Joel Lee Everhart 1988 320 p
Avail: Univ. Microfilms Order No. DA8808314

A theoretical examination of the slotted-wall flow field is conducted to determine the appropriate wall pressure-drop (or boundary condition) equation. This analysis improves the understanding of the fluid physics of these types of flow fields and helps to evaluate uncertainties and limitations existing in previous mathematical developments. It is shown that the resulting slotted-wall boundary conditions contains contributions due to the airfoil-induced streamline curvature and the nonlinear quadratic, slot cross-flow in addition to an often-neglected, linear term that results from viscous shearing in the slot. Existing and newly acquired experimental data are examined in light of this formulation and previous theoretical development. A detailed, previously unpublished set of slot-flow measurements obtained in the NASA Langley Research Center's diffuser flow apparatus is analyzed, and the resulting conclusions on the character of slot flows are discussed. A description is also given of a series of wind-tunnel experiments conducted expressly for this investigation in the Research Center's 6 x 19 inch transonic tunnel. Dissert. Abstr.

N89-12546 Leicester Univ. (England).
FLOW FIELD CHARACTERISTICS AROUND BLUFF PARACHUTE CANOPIES Ph.D. Thesis
C. Q. Shen 1987 227 p
Avail: Univ. Microfilms Order No. BRD-81832

The objectives of the present investigation are to determine the nature of the flow field around bluff parachute canopies, considering the effects of canopy shape parameters on this flow and hence on the resulting aerodynamic forces and moments which are developed on the canopy surface. To relate the flow field developed around bluff parachute canopies to their aerodynamic characteristics, a series of experiments in the Leicester University wind tunnel has been conducted on a family of particularly significant canopy shapes. These cross-shaped canopies have excellent drag and stability characteristics if arm ratios of about 4:1 are selected. Flow visualization, using both helium bubbles and wool tufts, was used to determine the flow field around the canopy. The most probable description of the wake flow is chains of irregularly-shaped vortex loops which move at about 0.7 times the undisturbed free stream velocity. Aerodynamic forces and moments measured on the various canopies correspond with the observed flow characteristics. Statistical correlation analyses made with hot wire anemometers in their wake indicate the periodic structure of the wakes formed behind these bluff bodies and reveal their basic similarities. Strouhal numbers of about 0.15 were obtained in the wake formed behind an imporous rigid hemispherical canopy. These are increased as canopy porosity is made larger.
Dissert. Abstr.

N89-12547 Pennsylvania State Univ., University Park.
A ZONAL EQUATION METHOD FOR THREE-DIMENSIONAL LOCALLY ELLIPTIC LAMINAR AND TURBULENT FLOWS Ph.D. Thesis
Matthew James Warfield 1987 194 p
Avail: Univ. Microfilms Order No. DA8807877

The Navier-Stokes equations governing fluid flow are computationally expensive to solve in exact form. Parabolized equations, when suitable, greatly increase the efficiency of the solution. This thesis describes a zonal equation method whereby incompressible elliptic and parabolic fluid flow formulations are utilized in distinct zones to efficiently resolve two- and three-dimensional laminar and turbulent flow-fields. In the present application the elliptic formulation consisted of the full Navier-Stokes equations and was solved by the pseudocompressibility time-marching technique while the parabolic formulation consisted of the parabolized Navier-Stokes equations and was solved by space-marching. The zonal equation method, as applied, is a viscous/viscous interaction technique with overlapping zonal boundaries and both local and global interaction. Local interaction is achieved either through direct variable exchange at the zonal boundaries or by the proposed solution of a simplified set of correction equations which correct the base parabolic solution within the buffer region between zones. The concept of localized ellipticity is examined and ellipticity parameters are proposed for use with the zonal equation method algorithm.
Dissert. Abstr.

N89-12548# Ballistic Research Labs., Aberdeen Proving Ground, Md.
AERODYNAMICS ANALYSIS OF SOLID FUEL RAMJET PROJECTILES
Asher Sigal and James E. Danberg May 1988 61 p
(AD-A196755; BRL-MR-3687; BRL-IMR-0896) Avail: NTIS HC A04/MF A01 CSCL 19A

The aerodynamic characteristics of several Solid Fuel Ramjet (SFRJ) projectiles are estimated by a combination of the NSWC-Aeroprediction code and a post-processing analysis that account for the effects of inlet and the buttress threads. Comparison between predicted and measured normal-force curve slope for two SFRJ-SPINNER configurations show good agreement in one case and 18 to 23 percent analytical under-prediction in the other. The agreement in center-of-pressure location is very good in both cases. The analysis explains the unstable flight of the 60mm SFRJ-FINNER Projectile, having original fins. The analysis predicts, for the projectile with extended fins, a static margin of 0.5 calibers at low supersonic Mach numbers, marginal stability as Mach number approaches 4.3 and instability at Mach numbers larger then 4:3. Wind-tunnel tests of this configuration show that the open inlet contributes more normal-force than accounted for in the analysis and that contribution of the fin set is slightly underpredicted by the NSWC code. The predicted normal-force curve slope is up to 11 percent smaller than experimentally obtained and the center-of-pressure location is in good agreement with test results.
GRA

N89-12549# Air Force Inst. of Tech., Wright-Patterson AFB, Ohio.
A VORTEX PANEL METHOD FOR POTENTIAL FLOWS WITH APPLICATIONS TO DYNAMICS AND CONTROL Ph.D. Thesis
Curtis P. Mracek Aug. 1988 312 p
(AD-A197091; AFIT/CI/NR-88-182) Avail: NTIS HC A14/MF A01 CSCL 20D

A general nonlinear, nonplanar unsteady vortex panel method for potential-flow is developed. The surface is modeled as a collection of triangular elements on which the vorticity vector is piecewise linearly varying. The wake emanates from the sides and trailing edges of the thin lifting surfaces and is modeled as a progressively formed collection of vortex filaments. This model provides a continuous pressure distribution on the surface while allowing the wake to roll up as tightly as needed. The wake position is determined as part of the solution and no prior knowledge of the position or strength is assumed. An adaptive grid technique is used to redistribute the circulation of the vortex filaments of the wake as the wake sheet spreads. The aerodynamic model is coupled with dynamic equations of motion. Forced oscillation tests are conducted on flat rectangular and delta wings. Dynamic tests are performed to predict wing rock of a slender delta wing restricted to one degree of freedom in roll. The aerodynamic/dynamic model is coupled with control laws that govern the motion of flaperons so that a prescribed pitch motion is executed and wing rock is suppressed.
GRA

N89-12550# Stanford Univ., Calif. Dept. of Aeronautics and Astronautics.
FOUNDATIONS OF THE BLADE-VORTEX INTERACTION PROBLEM: STRUCTURE AND BEHAVIOR OF TRAVELLING COMPRESSIBLE VORTICES Final Summary Report, 1 Oct. 1983 - 31 Dec. 1987
Daniel Bershader Apr. 1988 191 p
(Contract DAAG29-83-K-0146)
(AD-A197370; ARO-20670.2-EG) Avail: NTIS HC A09/MF A01 CSCL 01A

The structure of a compressible free vortex has been analyzed while undergoing convection in a quasi-uniform stream flow. Holographic interferograms reveal radial density profiles of the vortex at different stages of its development during convection. A general mathematical expression is found which closely describes the distribution of density inside the vortex. By use of experimental data and the governing equations in an empirical/theoretical analysis, an extended physical description of the vortex is developed. The time behavior of the density, determined from the experiments, allows the solution of the Continuity Equation and a distribution of the radial component of fluid velocity relative to the vortex center is obtained. The density information, supplemented by an independent determination of pressure is then used in the Radial Momentum Equation to obtain a distribution of the circumferential component of fluid velocity relative to the vortex center, thus completing the description of the radial dependence of the velocities inside the vortex. Furthermore, the calculated velocities are used to evaluate the magnitudes of the convective and diffusive terms of the Angular Momentum Equation.
GRA

N89-12551* National Aeronautics and Space Administration. Langley Research Center, Hampton, Va.
METHOD FOR LAMINAR BOUNDARY LAYER TRANSITION VISUALIZATION IN FLIGHT Patent
Bruce J. Holmes, inventor (to NASA) and Peter D. Gall, inventor (to NASA) 4 Oct. 1988 5 p Filed 13 Nov. 1986 Supersedes N87-18535 (25 - 11, p 1435)
(NASA-Case-LAR-13554-1; US-Patent-4,774,835;

US-Patent-Appl-SN-929862; US-Patent-Class-73-147; US-Patent-Class-116-265; US-Patent-Class-116-DIG.43) Avail: US Patent and Trademark Office CSCL 01A

Disclosed is a method of visualizing laminar to turbulent boundary layer transition, shock location, and laminar separation bubbles around a test surface. A liquid crystal coating is formulated using an unencapsulated liquid crystal operable in a temperature bandwidth compatible with the temperature environment around the test surface. The liquid crystal coating is applied to the test surface, which is preferably pretreated by painting with a flat, black paint to achieve a deep matte coating, after which the surface is subjected to a liquid or gas flow. Color change in the liquid crystal coating is produced in response to differences in relative shear stress within the boundary layer around the test surface. The novelty of this invention resides in the use of liquid crystals which are sensitive to shear stress to show aerodynamic phenomena such as a boundary layer transition, shock location, and laminar separation bubbles around a test surface.

Official Gazette of the U.S. Patent and Trademark Office

N89-12552*# National Aeronautics and Space Administration. Lewis Research Center, Cleveland, Ohio.

CONTROL OF LAMINAR SEPARATION OVER AIRFOILS BY ACOUSTIC EXCITATION

K. B. M. Q. Zaman and D. J. McKinzie [1988] 19 p Prepared for presentation at the 27th Aerospace Sciences Meeting, Reno, Nev., 9-12 Jan. 1989; sponsored in part by AIAA (NASA-TM-101379; E-4434; NAS 1.15:101379; AIAA-89-0565) Avail: NTIS HC A03/MF A01 CSCL 01A

The effect of acoustic excitation in reducing laminar separation over two-dimensional airfoils at low angles of attack is investigated experimentally. Airfoils of two different cross sections, each with two different chord lengths, are studied in the chord Reynolds number range of 25,000 is less than R sub c is less than 100,000. While keeping the amplitude of the excitation induced velocity perturbation a constant, it is found that the most effective frequency scales as U (sup 3/2)(sub infinity). The parameter St/R (sup 1/2)(sub c), corresponding to the most effective f sub p for all the cases studied, falls in the range of 0.02 to 0.03, St being the Strouhal number based on the chord. Author

N89-12553*# Cincinnati Univ., Ohio. Dept. of Aerospace Engineering and Engineering Mechanics.

SIMULATION OF 2-DIMENSIONAL VISCOUS FLOW THROUGH CASCADES USING A SEMI-ELLIPTIC ANALYSIS AND HYBRID C-H GRIDS Final Report

R. Ramamurti, U. Ghia, and K. N. Ghia Washington NASA Oct. 1988 194 p (Grant NAG3-194) (NASA-CR-4180; Rept-86-9-71; E-4286; NAS 1.26:4180) Avail: NTIS HC A09/MF A01 CSCL 01A

A semi-elliptic formulation, termed the interacting parabolized Navier-Stokes (IPNS) formulation, is developed for the analysis of a class of subsonic viscous flows for which streamwise diffusion is neglible but which are significantly influenced by upstream interactions. The IPNS equations are obtained from the Navier-Stokes equations by dropping the streamwise viscous-diffusion terms but retaining upstream influence via the streamwise pressure-gradient. A two-step alternating-direction-explicit numerical scheme is developed to solve these equations. The quasi-linearization and discretization of the equations are carefully examined so that no artificial viscosity is added externally to the scheme. Also, solutions to compressible as well as nearly compressible flows are obtained without any modification either in the analysis or in the solution process. The procedure is applied to constricted channels and cascade passages formed by airfoils of various shapes. These geometries are represented using numerically generated curvilinear boundary-oriented coordinates forming an H-grid. A hybrid C-H grid, more appropriate for cascade of airfoils with rounded leading edges, was also developed. Satisfactory results are obtained for flows through cascades of Joukowski airfoils. Author

N89-12554*# National Aeronautics and Space Administration. Ames Research Center, Moffett Field, Calif.

DEVELOPMENT AND VALIDATION OF AN ADVANCED LOW-ORDER PANEL METHOD

Dale L. Ashby, Steven K. Iguchi (Sterling Federal Systems, Inc., Palo Alto, Calif.), and Michael Dudley Oct. 1988 48 p (NASA-TM-101024; A-88275; NAS 1.15:101024) Avail: NTIS HC A03/MF A01 CSCL 01A

A low-order potential-flow panel code, PMARC, for modeling complex three-dimensional geometries, is currently being developed at NASA Ames Research Center. The PMARC code was derived from a code named VSAERO that was developed for Ames Research Center by Analytical Methods, Inc. In addition to modeling potential flow over three-dimensional geometries, the present version of PMARC includes several advanced features such as an internal flow model, a simple jet wake model, and a time-stepping wake model. Data management within the code was optimized by the use of adjustable size arrays for rapidly changing the size capability of the code, reorganization of the output file and adopting a new plot file format. Preliminary versions of a geometry preprocessor and a geometry/aerodynamic data postprocessor are also available for use with PMARC. Several test cases are discussed to highlight the capabilities of the internal flow model, the jet wake model, and the time-stepping wake model. Author

N89-12555*# National Aeronautics and Space Administration. Lewis Research Center, Cleveland, Ohio.

EVALUATION OF THREE TURBULENCE MODELS FOR THE PREDICTION OF STEADY AND UNSTEADY AIRLOADS

Jiunn-Chi Wu, Dennis L. Huff, and L. N. Sankar (Georgia Inst. of Tech., Atlanta.) [1988] 13 p Proposed for presentation at the 27th Aerospace Sciences Meeting, Reno, Nev., 9-12 Jan. 1989; sponsored by AIAA (NASA-TM-101413; E-4507; NAS 1.15:101413; AIAA-89-0609) Avail: NTIS HC A03/MF A01 CSCL 01A

Two dimensional quasi-three dimensional Navier-Stokes solvers were used to predict the static and dynamic airload characteristics of airfoils. The following three turbulence models were used: the Baldwin-Lomax algebraic model, the Johnson-King ODE model for maximum turbulent shear stress, and a two equation k-e model with law-of-the-wall boundary conditions. It was found that in attached flow the three models have good agreement with experimental data. In unsteady separated flows, these models give only a fair correlation with experimental data. Author

03 AIR TRANSPORTATION AND SAFETY

Includes passenger and cargo air transport operations; and aircraft accidents.

For related information see also *16 Space Transportation* and *85 Urban Technology and Transportation.*

N89-12556# Henschel Flugzeug-Werke G.m.b.H., Kassel (West Germany).

LOCATING AND SEARCH PROCEDURES WITH HELICOPTERS FOR SEA AND/OR AIR EMERGENCIES Final Report

Gerald Abich, Hans-Dieter Eisbrecher, Ulrich vonEitzen, and Klaus Koenig Bonn, Fed. Republic of Germany BMFT Mar. 1987 58 p In GERMAN; ENGLISH summary Sponsored by BMFT Prepared in cooperation with Reedereigemeinschaft Forschungsschiffahrt G.m.b.H., Bremen, Fed. Republic of Germany (FPN-0079; ETN-88-93222) Avail: NTIS HC A04/MF A01

Helicopter flight procedures and tables to assist locating and search procedures were developed. The variety of problems encountered in flight tests reveals that most of the equipment available from industry sources for the intended application is either unusable or not compatible. Actual values were determined, followed by deliberations and, where possible, tests and trials to find the reasons for the nonsatisfactory operation. These results and the instruments and equipment available are a basis for further

tests to establish the general engineering specifications for the design of such equipment. Underwater sound ranging tests yield positive results. ESA

04 AIRCRAFT COMMUNICATIONS AND NAVIGATION

Includes digital and voice communication with aircraft; air navigation systems (satellite and ground based); and air traffic control.

For related information see also *17 Space Communications, Spacecraft Communications, Command and Tracking* and *Communications and Radar.*

N89-12557*# Boeing Commercial Airplane Co., Seattle, Wash.
PILOT FACTORS GUIDELINES FOR THE OPERATIONAL INSPECTION OF NAVIGATION SYSTEMS Final Report
J. F. Sadler and G. P. Boucek Sep. 1988 179 p
(Contract NAS1-18027)
(NASA-CR-181644; NAS 1.26:181644) Avail: NTIS HC A09/MF A01 CSCL 17G

A computerized human engineered inspection technique is developed for use by FAA inspectors in evaluating the pilot factors aspects of aircraft navigation systems. The short title for this project is Nav Handbook. A menu-driven checklist, computer program and data base (Human Factors Design Criteria) were developed and merged to form a self-contained, portable, human factors inspection checklist tool for use in a laboratory or field setting. The automated checklist is tailored for general aviation navigation systems and can be expanded for use with other aircraft systems, transports or military aircraft. The Nav Handbook inspection concept was demonstrated using a lap-top computer and an Omega/VLF CDU. The program generates standardized inspection reports. Automated checklists for LORAN/C and R NAV were also developed. A Nav Handbook User's Guide is included. Author

N89-12558# Federal Aviation Administration, Atlantic City, N.J. Technical Center.
LORAN C OFFSHORE FLIGHT FOLLOWING (LOFF) IN THE GULF OF MEXICO
Frank Lorge Feb. 1988 68 p
(AD-A197179; DOT/FAA/CT-TN88/8) Avail: NTIS HC A04/MF A01 CSCL 17G

This report describes results of tests conducted by the FAA Technical Center to evaluate the LOFF system. Simulation and flight test were used to measure system performance under operational conditions. The LOFF system is the first implementation of Automatic Dependent Surveillance (ADS) by the FAA to track aircraft. It uses aircraft derived position as determined by Loran, transmitted by VHF data link for use by air traffic controllers. A converter unit was installed in the Houston Air Route Traffic Control Center (ARTCC) to process incoming LOFF messages and convert them into a radar data format. Results of this conversion are input to the Enhanced Direct Access Radar Channel (EDARC) which presents the aircraft as a conventional radar target. The system provides coverage in areas not currently served by radar, offshore in the Gulf of Mexico. Simulated inputs were used during testing to determine accuracy of the LOFF converter, to measure timing delays, and to relate aircraft position in latitude/longitude to a displayed position as seen by the controller. Flight tests were conducted to determine VHF coverage using the system, to measure Loran accuracy in the area, to compare dynamic performance with nondynamic performance of the EDARC system, and to provide an overall evaluation of the operational system. Overall results of the LOFF test program were favorable. The system performs in a predictable and reasonable manner and is comparable to that of radar. GRA

N89-12559# Air Force Inst. of Tech., Wright-Patterson AFB, Ohio.
VOICE RECOGNITION AND ARTIFICIAL INTELLIGENCE IN AN AIR TRAFFIC CONTROL ENVIRONMENT M.S. Thesis
Robert F. Hall May 1988 117 p
(AD-A197219; AFIT/CI/NR-88-171) Avail: NTIS HC A06/MF A01 CSCL 25D

The rapid growth of air carrier, general aviation, and military traffic has strained this nation's Air Traffic Control (ATC) system. The symptoms of this strain appear as controller fatigue, low controller moral, and the occasional creation of a hazardous situation caused by human error. The current method employed to improve the ATC system has been in the form of increasing its air traffic handling capacity by adding more machinery and manpower. Thus, machines with greater processing power and more humans are coupled into a man machine system which is destined to continually grow. Little has been done to find new forms of technology to increase the joint efficiency of man and machine. Two relatively new technologies which could create a path towards greater system efficiency are the technologies of voice recognition and artificial intelligence. With greater system efficiency, less controller fatigue and better air safety are expected. Where to apply these technologies, in what form, and how deep these technologies can be integrated into the ATC system are questions which deserve inquiry. This research details a method to answer these questions, develops prototype equipment from which to experiment, and establishes a basis from which other research efforts may be launched. A review of literature indicates that current efforts at applying voice recognition in flight operations are centered around pilot task improvement and special projects such as the space shuttle. GRA

N89-12560# Aeronautical Systems Div., Wright-Patterson AFB, Ohio.
AN EVALUATION OF GROUND COLLISION AVOIDANCE SYSTEM ALGORITHM Final Report
Horace A. Orr, Richard Geiselhart, and Mark A. DiPadua Oct. 1987 83 p
(AD-A197831; ASD-TR-87-5040) Avail: NTIS HC A05/MF A01 CSCL 01B

Controlled flight into terrain (CFIT) accidents, which constitute the second largest category of tactical Air Force Class A mishaps, could be greatly reduced by installing forward-looking Terrain-Following Radar (TFR) Systems. In an effort to design a less costly solution to this problem, a software-oriented generic Ground Collision Avoidance System (GCAS) with application to more complex tactical missions was developed. A simulation study of the system evaluated the adequacy of the algorithm in a variety of tactical scenarios. Results indicate GCAS is a variable system for partial solution of CFIT. Although some modifications to the system are necessary prior to implementation, the concept of terrain estimation may give GCAS a capability unmatched by any similar systems. GRA

05 AIRCRAFT DESIGN, TESTING AND PERFORMANCE

Includes aircraft simulation technology.

For related information see also *18 Spacecraft Design, Testing and Performance* and *39 Structural Mechanics.* For land transportation vehicles see *85 Urban Technology and Transportation.*

N89-12561 California Univ., Los Angeles.
NUMERICAL METHODS FOR THE GUIDANCE AND CONTROL OF AIR-TO-AIR MISSILES Ph.D. Thesis
Falin Shieh 1987 159 p
Avail: Univ. Microfilms Order No. DA8803656

An indirect numerical solution method for the guidance and control problem of general air-to-air missiles is presented. The system model is formulated as a nonlinear two-person zero-sum differential game. The system equations of motion consist of eight relative kinematic variables to describe the dynamics of the pursuing missile and its evading target both maneuvering freely in a real three-dimensional space. Control functions are subjected to state dependent constraints. The information structure is nonlinear and

allows different types of noise. The quadratic payoff functional is to be minimized by the missile and maximized by its target. The original problem is decomposed into three smaller solvable problems: the open-loop perfect information differential game problem; the real-time state estimation problem, and the near-closed-loop updating problem. Jacobson and Mayne's second order Differential Dynamic Programming method is extended to the differential games problems with state dependent control constraints. The real-time nonlinear state estimator algorithm is similar to the Extended Kalman Filter. It minimizes the variance of the error propagation matrix and uses the most recent measurement data only to compute the filter updates. Numerical simulations are performed for several types of target interception problems. Many optimal pursuit and evasion tactics are found. The solution method shows very promising future toward the realization of differential game methodology for missile guidance problems. Dissert. Abstr.

N89-12562# Army Aviation Engineering Flight Activity, Edwards AFB, Calif.
AH-1F INSTRUMENT METEOROLOGICAL CONDITIONS (IMC) FLIGHT EVALUATIONS Final Report, 9 Jun. 1984 - 10 Feb. 1987
John S. Lawrence, John R. Martin, Austin R. Omlie, Patrick J. Sullivan, and Terrance L. Reininger Feb. 1988 118 p
(AD-A197128) Avail: NTIS HC A06/MF A01 CSCL 01C

Four deficiencies and seven shortcomings associated with flying the AH-1F in IMC were identified. The deficiencies were: (1) the easily excited lateral gust response; (2) the unsatisfactory location of avionics controls; (3) the poor cyclic flight control system mechanical characteristics; and (4) the large change in airspeed position error in climbs. The AH-1F is unacceptable for flight in IMC. Modifications evaluated in an attempt to correct the aircraft deficiencies included use of the air data system as a pitot-static source, reduction of cyclic control friction, reduction of cyclic centering spring preloads, addition of a Gurney flap to the vertical stabilizer, removal of the 90-degree gearbox fairings, addition of a ventral fin, changes in pitch and roll stability and control augmentation system gains, addition of attitude holds in the pitch and roll axes, and changes in cockpit avionics configurations. The AH-1F is acceptable for flight in IMC when the following modifications are incorporated: attitude hold capability in the pitch and roll axes, cyclic control friction adjusted to 1.0 pounds, and cyclic centering spring preloads adjusted to 3.0 pounds. The suitability of the AH-1F for flight in IMC is enhanced with VOR navigation and VHF communication control panels. GRA

N89-12563# Department of Defense, Washington, D. C.
DOD JOINT UNMANNED AERIAL VEHICLE (UAV) PROGRAM MASTER PLAN, 1988 Final Report
Richard L. Mosier 27 Jun. 1988 52 p
(AD-A197751) Avail: NTIS HC A04/MF A01 CSCL 01C

In FY88, the Congress eliminated separate program elements for remotely piloted vehicle (RPV) programs within each of the military Services, consolidated these efforts in a Joint RPV Program in the office of the Secretary of Defense, and authorized and appropriated reduced levels of RDT and E and procurement funding for such activities in FY88. In addition, the Congress directed that FY88 RDT and E funding is available only for the Joint Remotely Piloted Vehicles (RPV) Program and may not be obligated or expended until the Secretary of Defense submits to the Committees on Appropriation of the Senate and the House of Representatives an updated master plan fully explaining his decisions as to which RPVs will be supported with the available funds and assessing the cooperation by the military Services with efforts to coordinate RPV programs and to eliminate duplication within and among the programs (Title IV, Public Law 100-180). This master plan, developed in response to this direction, describes the changes made by the Department in the management of RPV programs, outlines the requirements for RPV capabilities, defines the Department's strategy for acquisition of a family of RPV systems, and provides the detailed explanation of the programs that are to be supported with available FY88, and requested FY89 funds. GRA

N89-12564# Advisory Group for Aerospace Research and Development, Neuilly-Sur-Seine (France).
GUIDANCE AND CONTROL/FLIGHT MECHANICS PANELS JOINT SYMPOSIUM ON THE MAN-MACHINE INTERFACE IN TACTICAL AIRCRAFT DESIGN AND COMBAT AUTOMATION Technical Evaluation Report
Rudiger Seifert (Messerschmitt-Boelkow-Blohm G.m.b.H., Munich, West Germany) 1988 21 p Symposium held in Stuttgart, Federal Republic of Germany, 28 Sep. - 1 Oct. 1987
(AGARD-AR-249) Copyright Avail: NTIS HC A03/MF A01

A Keynote address and thirty-one papers were presented at the Joint Guidance Control Panel/Flight Mechanics Panel Symposium, held in Stuttgart, Germany from 28 September to 1 October 1987, under the following headings: Combat scenarios and mission segment requirements; Human capabilities and limitations; Technological capabilities and limitations of combat automation; Crew station implementation; System integration. The Keynote Address and twenty-five papers are published in CP-425 (one paper was not available at time of printing) and the four remaining classified papers are included in CP-425(Supplement). Author

06 AIRCRAFT INSTRUMENTATION

Includes cockpit and cabin display devices; and flight instruments.

For related information see also *19 Spacecraft Instrumentation* and *35 Instrumentation and Photography.*

No abstracts in this category.

07 AIRCRAFT PROPULSION AND POWER

Includes prime propulsion systems and systems components, e.g., gas turbine engines and compressors; and onboard auxilliary power plants for aircraft.

For related information see also *20 Spacecraft Propulsion and Power, 28 Propellants and Fuels,* and *44 Energy Production and Conversion.*

N89-12565*# National Aeronautics and Space Administration. Lewis Research Center, Cleveland, Ohio.
ADVANCED TURBOPROP PROJECT
Roy D. Hager and Deborah Vrabel (Sverdrup Technology, Inc., Cleveland, Ohio.) 1988 130 p Original contains color illustrations
(NASA-SP-495; NAS 1.21:495; LC88-1690) Avail: NTIS HC A07/MF A01 CSCL 21E

At the direction of Congress, a task force headed by NASA was organized in 1975 to identify potential fuel saving concepts for aviation. The result was the Aircraft Energy Efficiency (ACEE) Program implemented in 1976. An important part of the program was the development of advanced turboprop technology for Mach 0.65 to 0.85 applications having the potential fuel saving of 30 to 50 percent relative to existing turbofan engines. A historical perspective is presented of the development and the accomplishments that brought the turboprop to successful flight tests in 1986 and 1987. Author

N89-12566*# Sverdrup Technology, Inc., Cleveland, Ohio.
A CONTROL-VOLUME METHOD FOR ANALYSIS OF UNSTEADY THRUST AUGMENTING EJECTOR FLOWS Final Report
Colin K. Drummond Nov. 1988 170 p

(Contract NAS3-25266)
(NASA-CR-182203; E-4461; NAS 1.26:182203) Avail: NTIS HC A08/MF A01 CSCL 21E

A method for predicting transient thrust augmenting ejector characteristics is presented. The analysis blends classic self-similar turbulent jet descriptions with a control volume mixing region discretization to solicit transient effects in a new way. Division of the ejector into an inlet, diffuser, and mixing region corresponds with the assumption of viscous-dominated phenomenon in the latter. Inlet and diffuser analyses are simplified by a quasi-steady analysis, justified by the assumptions that pressure is the forcing function in those regions. Details of the theoretical foundation, the solution algorithm, and sample calculations are given.

Author

N89-12567*# Sverdrup Technology, Inc., Cleveland, Ohio.
A REVIEW OF TURBOMACHINERY BLADE-ROW INTERACTION RESEARCH Final Report
Todd E. Smith Nov. 1988 38 p
(Contract NAS3-25266)
(NASA-CR-182211; E-4422; NAS 1.26:182211) Avail: NTIS HC A03/MF A01 CSCL 21E

Analytical and experimental research in the area of unsteady aerodynamics of turbomachinery has conventionally been applied to blading which oscillates when placed in a uniformly flowing fluid. Comparatively less effort has been offered for the study of blading which is subjected to nonuniformities within the flow field. The fluid dynamic environment of a blade-row embedded within multi-stage turbomachines is dominated by such highly unsteady fluid flow conditions. The production of wakes and circumferential pressure variations from adjacent blade-rows causes large unsteady energy transfers between the fluid and the blades. Determination of the forced response of a blade requires the ability to predict the unsteady loads which are induced by these aerodynamic sources. A review of research publications was done to determine recent investigations of the response of turbomachinery blading subjected to aerodynamic excitations. Such excitations are a direct result of the blade-row aerodynamic interaction which occurs between adjacent cascades of blades. The reports and papers reviewed have been organized into areas emphasizing experimental or analytical efforts.

Author

N89-12568*# National Aeronautics and Space Administration. Lewis Research Center, Cleveland, Ohio.
DEVELOPMENT OF A THERMAL AND STRUCTURAL ANALYSIS PROCEDURE FOR COOLED RADIAL TURBINES
Ganesh N. Kumar and Russell G. DeAnna (Army Aviation Research and Development Command, Cleveland, Ohio.) [1988] 10 p Presented at the 33rd International Gas Turbine and Aeroengine Congress and Exposition, Amsterdam, The Netherlands, 6-9 Jun. 1988; sponsored by the American Society of Mechanical Engineers
(NASA-TM-101416; E-4515; NAS 1.15:101416; AVSCOM-TR-88-C-037) Avail: NTIS HC A02/MF A01 CSCL 21E

A procedure for computing the rotor temperature and stress distributions in a cooled radial turbine are considered. Existing codes for modeling the external mainstream flow and the internal cooling flow are used to compute boundary conditions for the heat transfer and stress analysis. The inviscid, quasi three dimensional code computes the external free stream velocity. The external velocity is then used in a boundary layer analysis to compute the external heat transfer coefficients. Coolant temperatures are computed by a viscous three dimensional internal flow cade for the momentum and energy equation. These boundary conditions are input to a three dimensional heat conduction code for the calculation of rotor temperatures. The rotor stress distribution may be determined for the given thermal, pressure and centrifugal loading. The procedure is applied to a cooled radial turbine which will be tested at the NASA Lewis Research Center. Representative results are given.

Author

N89-12768# Washington State Univ., Pullman. Dept. of Mechanical and Materials Engineering.
GROUND RUN-UP AFTERBURNER DETECTION AND NOISE SUPPRESSION Final Report
Jeffrey J. Girard *In* Universal Energy Systems, Inc., United States Air Force Graduate Student Summer Support Program, Volume 1 Dec. 1987 8 p (For primary document see N89-12754 04-31)
Avail: NTIS HC A99/MF E03 CSCL 21E

N89-12877*# National Aeronautics and Space Administration. Lewis Research Center, Cleveland, Ohio.
TURBINE ENGINE HOT SECTION TECHNOLOGY (HOST) PROJECT
Daniel E. Sokolowski and C. Robert Ensign *In its* Turbine Engine Hot Section Technology 1986 Oct. 1986 p 1-6 Previously announced as N86-11496 (For primary document see N89-12876 04-39)
Avail: NTIS HC A21/MF A01 CSCL 20K

N89-12878*# National Aeronautics and Space Administration. Lewis Research Center, Cleveland, Ohio.
HOST INSTRUMENTATION R AND D PROGRAM OVERVIEW
D. R. Englund *In its* Turbine Engine Hot Section Technology 1986 Oct. 1986 p 7-8 Previously announced as N86-11497 (For primary document see N89-12876 04-39)
Avail: NTIS HC A21/MF A01 CSCL 20K

N89-12879*# National Aeronautics and Space Administration. Lewis Research Center, Cleveland, Ohio.
HOST COMBUSTION R AND T OVERVIEW
Raymond E. Gaugler *In its* Turbine Engine Hot Section Technology 1986 Oct. 1986 p 9-11 (For primary document see N89-12876 04-39)
Avail: NTIS HC A21/MF A01 CSCL 21E

N89-12880*# National Aeronautics and Space Administration. Lewis Research Center, Cleveland, Ohio.
HOST TURBINE HEAT TRANSFER SUBPROJECT OVERVIEW
Herbert J. Gladden *In its* Turbine Engine Hot Section Technology 1986 Oct. 1986 p 13-17 (For primary document see N89-12876 04-39)
Avail: NTIS HC A21/MF A01 CSCL 21E

N89-12893*# Garrett Turbine Engine Co., Phoenix, Ariz.
COMBUSTOR DIFFUSER INTERACTION PROGRAM
Ram Srinivasan and Daniel Thorp *In* NASA, Lewis Research Center, Turbine Engine Hot Section Technology 1986 Oct. 1986 p 133-139 (For primary document see N89-12876 04-39)
(Contract F33615-84-C-2427)
Avail: NTIS HC A21/MF A01 CSCL 21E

N89-12907*# General Electric Co., Fairfield, Conn.
COMPONENT SPECIFIC MODELING
R. J. Maffeo, R. L. McKnight, M. T. Tipton, and G. Weber *In* NASA, Lewis Research Center, Turbine Engine Hot Section Technology 1986 Oct. 1986 p 269-282 (For primary document see N89-12876 04-39)
(Contract NAS3-23687)
Avail: NTIS HC A21/MF A01 CSCL 21E

08 AIRCRAFT STABILITY AND CONTROL

Includes aircraft handling qualities; piloting; flight controls; and autopilots.

For related information see also *05 Aircraft Design, Testing and Performance.*

N89-12569*# National Aeronautics and Space Administration. Langley Research Center, Hampton, Va.
SINGULAR PERTURBATIONS AND TIME SCALES IN THE DESIGN OF DIGITAL FLIGHT CONTROL SYSTEMS
Desineni S. Naidu (Old Dominion Univ., Norfolk, Va.) and Douglas B. Price Washington, D.C. Dec. 1988 30 p
(NASA-TP-2844; L-16440; NAS 1.60:2844) Avail: NTIS HC A03/MF A01 CSCL 01C

The results are presented of application of the methodology of Singular Perturbations and Time Scales (SPATS) to the control of digital flight systems. A block diagonalization method is described to decouple a full order, two time (slow and fast) scale, discrete control system into reduced order slow and fast subsystems. Basic properties and numerical aspects of the method are discussed. A composite, closed-loop, suboptimal control system is constructed as the sum of the slow and fast optimal feedback controls. The application of this technique to an aircraft model shows close agreement between the exact solutions and the decoupled (or composite) solutions. The main advantage of the method is the considerable reduction in the overall computational requirements for the evaluation of optimal guidance and control laws. The significance of the results is that it can be used for real time, onboard simulation. A brief survey is also presented of digital flight systems. Author

N89-12570*# Princeton Univ., N. J. Dept. of Mechanical and Aerospace Engineering.
DESIGN AND NUMERICAL EVALUATION OF FULL-AUTHORITY FLIGHT CONTROL SYSTEMS FOR CONVENTIONAL AND THRUSTER-AUGMENTED HELICOPTERS EMPLOYED IN NOE OPERATIONS Interim Report
Todd A. Perri, R. M. McKillip, Jr., and H. C. Curtiss, Jr. Aug. 1987 199 p
(Grant NAG2-244)
(NASA-CR-183311; NAS 1.26:183311; TR-1789T) Avail: NTIS HC A09/MF A01 CSCL 01C

The development and methodology is presented for development of full-authority implicit model-following and explicit model-following optimal controllers for use on helicopters operating in the Nap-of-the Earth (NOE) environment. Pole placement, input-output frequency response, and step input response were used to evaluate handling qualities performance. The pilot was equipped with velocity-command inputs. A mathematical/computational trajectory optimization method was employed to evaluate the ability of each controller to fly NOE maneuvers. The method determines the optimal swashplate and thruster input histories from the helicopter's dynamics and the prescribed geometry and desired flying qualities of the maneuver. Three maneuvers were investigated for both the implicit and explicit controllers with and without auxiliary propulsion installed: pop-up/dash/descent, bob-up at 40 knots, and glideslope. The explicit controller proved to be superior to the implicit controller in performance and ease of design. Author

N89-12571# Centre Aeroporte de Toulouse (France).
REMOTE GUIDANCE OF PAYLOADS UNDER MANEUVERABLE PARACHUTES [TELEGUIDAGE DES CHARGES SOUS PARACHUTES MANOEUVRABLES]
M. Carol Mar. 1988 173 p In FRENCH
(E-639; Rept-88/03; ETN-88-93109) Avail: NTIS HC A08/MF A01

A remote control system for testing on maneuverable parachutes was designed. The feasibility of trajectory control of heavy load parachutes by a remote system was analyzed. The feasibility of automatic guidance of payloads accompanied by a parachutist was examined. A parachute wing and a parachute model were constructed. Analysis and test results enabled the characteristics of an operational system to be derived. ESA

09 RESEARCH AND SUPPORT FACILITIES (AIR)

Includes airports, hangars and runways; aircraft repair and overhaul facilities; wind tunnels; shock tubes; and aircraft engine test stands.

For related information see also *14 Ground Support Systems and Facilities (Space).*

N89-12572*# Old Dominion Univ., Norfolk, Va. Dept. of Electrical and Computer Engineering.
SUPPORT OF THE EIGHT-FOOT HIGH-TEMPERATURE TUNNEL MODIFICATIONS PROJECT Final Report. 16 May 1985 - 15 May 1986
Donald Y. Hodges and John V. Shebalin Dec. 1987 3 p
(Contract NAS1-17993)
(NASA-CR-183356; NAS 1.26:183356) Avail: NTIS HC A02/MF A01 CSCL 14B

An ultrasonic level sensor was developed to measure the liquid level in a storage vessel under high pressures, namely up to 6000 psi. The sensor is described. A prototype sensor was installed in the cooling-water storage vessel of the Eight-Foot High-Temperature Tunnel. Plans are being made to install the readout instrument in the control room, so that tunnel operators can monitor the water level during the course of a tunnel run. It was discovered that the sensor will operate at cryogenic temperatures. Consequently, a sensor will be installed in the modified Eight-Foot High-Temperature Tunnel to measure the sound speed of liquid oxygen (LOX) as it is transferred from a storage vessel to the tunnel combustor at pressure of about 3000 psi. The sound speed is known to be a reliable indicator of contamination of LOX by pressurized gaseous nitrogen, which will be used to effect the transfer. Subjecting the sensor to a temperature cycle from room temperature to liquid nitrogen temperature and back again several times revealed no deterioration in sensor performance. The method using this sensor is superior to the original method, which was to bleed samples of LOX from the storage vessel to an independent chamber for measurement of the sound speed. Author

N89-12573# BSO/Aerospace B.V., Utrecht (Netherlands).
ADVANCED WORKSTATIONS FOR METEOSAT COMMAND AND CONTROL, VOLUME 1 Final Report
J. Jongert and A. M. Bos Paris, France ESA Mar. 1987 41 p
(Contract ESA-6684/86-D-MD(SC))
(BSO/AETR87030101-Vol-1; ESA-CR(P)-2576-Vol-1; ETN-88-93164) Avail: NTIS HC A03/MF A01

To investigate the applicability of expert systems in the Meteosat environment, a demonstration expert system was built. Based on the evaluation results of the demonstration system and the outcome of a functional analysis of the Meteosat system, the role of expert systems in different control tasks was considered. Combined with the requirements for future operations, these considerations lead to a configuration concept for the command and control center. A literature search into man machine interface design was used in the definition of a global design concept for the user interface of future workstations. Especially in anomaly handling expert system support can lead to improved performance. Tasks such as command generation can be automated without requiring considerable expert system support. Automatic execution of standard procedures prevents erroneous actions. Due to the unpredictable nature of most anomalies, no substantial improvements may be expected from expert system anomaly prediction. Distribution of tasks between operator and computer should be such that the operator retains an active role in the control system. In order to enable multiple satellite operations it

is recommended to create a command and control center consisting of at least three identical workstations, connected to a central configuration manager. Distribution of control tasks among the workstations can best be satellite oriented. This results in independent control per satellite, including its active missions and relevant ground subsystems. ESA

N89-12574# BSO/Aerospace B.V., Utrecht (Netherlands).
ADVANCED WORKSTATIONS FOR METEOSAT COMMAND AND CONTROL. VOLUME 2: APPENDICES Final Report
J. Jongert and A. M. Bos Paris, France ESA Mar. 1987 70 p
(Contract ESA-6684/86-D-MD(SC))
(BSO/AETR87030101-Vol-2; ESA-CR(P)-2576-Vol-2; ETN-88-93165) Avail: NTIS HC A04/MF A01

In order to investigate the applicability of expert systems in the Meteosat environment, a demonstration expert system was built. Evaluation of the system; a literature study into the man machine interface for Meteosat workstations; symbol explanation; process description; physical dataflow diagrams; and logical dataflow diagrams are covered. ESA

12 ASTRONAUTICS (GENERAL)

For extraterrestrial exploration see *91 Lunar and Planetary Exploration.*

N89-12575# Martin Marietta Corp., New Orleans, La.
A TEACHER'S COMPANION TO THE SPACE STATION: A MULTI-DISCIPLINARY RESOURCE
Lynn P. Hagan and Liz Elsen [1988] 67 p Prepared in cooperation with Louisiana Nature and Science Center, New Orleans
Avail: NTIS HC A04/MF A01

The United States Space Station promises to be an adventure in enterprise and ingenuity. This collection of activities, geared for students from kindergarten through high school, promises to help them become aware of the potential of space. Within their lifetime, men and women will be living in space on a routine basis, carrying out activities once only dreamt of in books. Author

N89-12576# Consiglio Nazionale delle Ricerche, Frascati (Italy). Istituto di Fisica dello Spazio Interplanetario.
MODES OF OPERATION OF THE RETE EXPERIMENT
M. Dobrowolny and U. Guidoni May 1988 29 p
(IFSI-88-5; ETN-88-93472) Avail: NTIS HC A03/MF A01

The experiment RETE consist of two parts: an ac electric and magnetic field experiment and a so-called plasma package. The sensors for the two parts are housed in two canisters which are placed at the tip of the satellite deployable booms. The electric field fluctuations are measured in all three axes by means of two dipoles. The instruments include two search coils, three Langmuir probes, and one ion trap. A list of all the modes of operation of the RETE experiment is included. ESA

N89-12980# National Space Development Agency, Tokyo (Japan).
RESULTS OF ADVANCED EARTH OBSERVING SATELLITE (ADEOS) CONCEPTUAL STUDY
N. Hara, M. Homma, T. Igarashi, A. Tsuiki, and K. Ohta *In* ESA, Proceedings of the 1988 International Geoscience and Remote Sensing Symposium (IGARSS 1988) on Remote Sensing: Moving Towards the 21st Century, Volume 1 Aug. 1988 p 179-182 (For primary document see N89-12936 04-42)
Copyright Avail: NTIS HC A99/MF E03; ESA Publications Div., ESTEC, Noordwijk, Netherlands, 120 US dollars or 250 Dutch guilders

N89-12983# Marconi Space and Defence Systems Ltd., Portsmouth (England). Remote Sensing and Science Div.
ON-ORBIT SERVICING AND COST EFFECTIVENESS OF COLUMBUS POLAR PLATFORM CONCEPTS
R. G. W. Hathaway *In* ESA, Proceedings of the 1988 International Geoscience and Remote Sensing Symposium (IGARSS 1988) on Remote Sensing: Moving Towards the 21st Century, Volume 1 Aug. 1988 p 191-194 (For primary document see N89-12936 04-42)
Copyright Avail: NTIS HC A99/MF E03; ESA Publications Div., ESTEC, Noordwijk, Netherlands, 120 US dollars or 250 Dutch guilders

13 ASTRODYNAMICS

Includes powered and free-flight trajectories; and orbital and launching dynamics.

N89-12577 Virginia Polytechnic Inst. and State Univ., Blacksburg.
RESULTS OF TRUE-ANOMALY REGULARIZATION IN ORBITAL MECHANICS Ph.D. Thesis
Paul Wayne Schumacher, Jr. 1987 531 p
Avail: Univ. Microfilms Order No. DA8804426

Presented are some analytical results available from regularization of the differential equations of satellite motion. True-anomaly regularization is developed as a special case of a more general Sundman-type transformation of the independent variable (time) in the equations of motion. Constants of the unperturbed motion are introduced as extra state variables, and regularization with several types of coordinates is considered. Because analytical results are sought, those regularizing transformations which produce rigorously linear governing equations are of main interest. When solutions of the linear regular equations in the true-anomaly domain are examined, it is found that the initial value and boundary value problems of unperturbed motion, typically requiring iterative solutions of the time equation, can be solved with only a single transcendental function evaluation per iteration cycle. Various means are described which can accelerate the evaluation of this function. The time equation developed is an universal relation between time of flight and true anomaly, and applies uniformly to all types of orbits, including rectilinear ones. Once its time equation is solved, the initial and final state vectors on the transfer arc can be related to each other by rational algebraic formulae; no other transcendental function is needed. Additional results are also presented, including exact solutions of the first-order averaged differential equations governing secular variations of the regular orbital elements in the true-anomaly domain. Dissert. Abstr.

14 GROUND SUPPORT SYSTEMS AND FACILITIES (SPACE)

Includes launch complexes, research and production facilities; ground support equipment, e.g., mobile transporters; and simulators.

For related information see also *09 Research and Support Facilities (Air).*

N89-12578# Lawrence Livermore National Lab., Calif.
A DECADE OF RAILGUN DEVELOPMENT FOR HIGH PRESSURE RESEARCH
R. S. Hawke 20 Jul. 1988 5 p Presented at the Shock Wave Symposium, Pullman, Wash., 1 Sep. 1988
(Contract W-7405-eng-48)
(DE88-017024; UCRL-99246; CONF-8809109-5) Avail: NTIS HC A02/MF A01

This paper summarizes a decade of effort towards development of railguns into useful high pressure tools. In 1942 the first successful railgun accelerated a 10-g projectile to about 1 km/s, and in the 1960's velocities approaching 10 km/s were achieved, but without verification of projectile integrity. Later work at the Australian National University showed the potential of railguns to launch intact projectiles. About 10 years ago efforts began to develop railguns for a variety of purposes, including high pressure shock wave equation-of-state (EOS) research. Problems and their

causes in this research are now more clearly understood and efforts are being made to develop the railgun into a hypervelocity EOS tool. DOE

N89-12586*# TRW Defense and Space Systems Group, Redondo Beach, Calif. Operations and Support Group.
CLASS 100 LARGE SPACECRAFT FACILITY Abstract Only
L. E. Ryan *In* NASA, Goddard Space Flight Center, 15th Space Simulation Conference: Support the Highway to Space Through Testing 1988 p 29 (For primary document see N89-12582 04-18)
Avail: NTIS HC A21/MF A01 CSCL 14B

N89-12593*# General Electric Co., Philadelphia, Pa. Astro Space Div.
PYRO SHOCK SIMULATION: EXPERIENCE WITH THE MIPS SIMULATOR
Thomas J. Dwyer and David S. Moul *In* NASA, Goddard Space Flight Center, 15th Space Simulation Conference: Support the Highway to Space Through Testing 1988 p 125-138 (For primary document see N89-12582 04-18)
Avail: NTIS HC A21/MF A01 CSCL 14B

N89-12595*# Control Dynamics Co., Huntsville, Ala.
THE FLIGHT ROBOTICS LABORATORY
Patrick A. Tobbe, Marlin J. Williamson, and John R. Glaese *In* NASA, Goddard Space Flight Center, 15th Space Simulation Conference: Support the Highway to Space Through Testing 1988 p 158-167 (For primary document see N89-12582 04-18)
(Contract NAS8-36570)
Avail: NTIS HC A21/MF A01 CSCL 14B

N89-12599*# Massachusetts Inst. of Tech., Cambridge.
LIGO VACUUM SYSTEM STUDY
Jeffrey C. Livas and Boude C. Moore (California Inst. of Tech., Pasadena.) *In* NASA, Goddard Space Flight Center, 15th Space Simulation Conference: Support the Highway to Space Through Testing 1988 p 206-220 (For primary document see N89-12582 04-18)
(Grant NSF PHY-88-03557)
Avail: NTIS HC A21/MF A01 CSCL 14B

N89-12600*# European Space Agency. European Space Research and Technology Center, ESTEC, Noordwijk (Netherlands).
THE TWO AXIS MOTION SIMULATOR FOR THE LARGE SPACE SIMULATOR AT ESTEC (EUROPEAN SPACE RESEARCH AND TECHNOLOGY CENTER)
Kurt A. Beckel and Joop Hutchison *In* NASA, Goddard Space Flight Center, 15th Space Simulation Conference: Support the Highway to Space Through Testing 1988 p 221-234 (For primary document see N89-12582 04-18)
Avail: NTIS HC A21/MF A01 CSCL 14B

N89-12601*# High Vacuum Equipment Corp., Hingham, Mass.
INDIAN LSSC (LARGE SPACE SIMULATION CHAMBER) FACILITY
A. S. Brar, V. S. PrasadaRao, R. D. Gambhir, and M. Chandramouli (ISRO Satellite Centre, Peenya, Bangalore, India) *In* NASA, Goddard Space Flight Center, 15th Space Simulation Conference: Support the Highway to Space Through Testing 1988 p 235-238 (For primary document see N89-12582 04-18)
Avail: NTIS HC A21/MF A01 CSCL 14B

N89-12603*# Aeritalia S.p.A., Turin (Italy). Space Systems Group.
IRIS THERMAL BALANCE TEST WITHIN ESTEC LSS
Piero Messidoro, Marino Ballesio, and J. P. Vessaz (European Space Agency. European Space Research and Technology Center, ESTEC, Noordwijk, Netherlands) *In* NASA, Goddard Space Flight Center, 15th Space Simulation Conference: Support the Highway to Space Through Testing 1988 p 253-267 (For primary document see N89-12582 04-18)
Avail: NTIS HC A21/MF A01 CSCL 14B

N89-12605*# Industrienlagen-Betriebsgesellschaft m.b.H., Munich (West Germany).
SOLAR SIMULATION WITH A RECTANGULAR BEAM
O. G. Feil and H. U. Frey *In* NASA, Goddard Space Flight Center, 15th Space Simulation Conference: Support the Highway to Space Through Testing 1988 p 278-288 (For primary document see N89-12582 04-18)
Avail: NTIS HC A21/MF A01 CSCL 14B

N89-12609*# Wyle Labs., Inc., Huntsville, Ala.
TEST STAND DESIGN AND ANALYSIS FOR TITAN 34D STATIC FIRING
Shayan Pazargadi *In* NASA, Goddard Space Flight Center, 15th Space Simulation Conference: Support the Highway to Space Through Testing 1988 p 336-352 (For primary document see N89-12582 04-18)
(Contract UTC-CSD-268024)
Avail: NTIS HC A21/MF A01 CSCL 14B

N89-12610*# California Polytechnic State Univ., San Luis Obispo.
TEST STAND FOR TITAN 34D SRM STATIC FIRING
Vladimir Glozman and George Shipway (Wyle Labs., Inc., Huntsville, Ala.) *In* NASA, Goddard Space Flight Center, 15th Space Simulation Conference: Support the Highway to Space Through Testing 1988 p 353-367 (For primary document see N89-12582 04-18)
Avail: NTIS HC A21/MF A01 CSCL 14B

N89-12619*# Martin Marietta Aerospace, Denver, Colo. Space Systems Co.
COST EFFECTIVE ALTERNATIVE TO LOW IRRADIANCE MEASUREMENTS
Scott T. OLeary *In* NASA, Goddard Space Flight Center, 15th Space Simulation Conference: Support the Highway to Space Through Testing 1988 p 466-475 (For primary document see N89-12582 04-18)
Avail: NTIS HC A21/MF A01 CSCL 14B

N89-12620*# Gavazzi (Carlo) Controls S.p.A., Milan (Italy).
TEST DATA ACQUISITION SYSTEM FOR THE ESTEC LARGE SOLAR SIMULATOR AT ESA/ESTEC
G. Buroni and L. Zucconi *In* NASA, Goddard Space Flight Center, 15th Space Simulation Conference: Support the Highway to Space Through Testing 1988 p 476-498 (For primary document see N89-12582 04-18)
Avail: NTIS HC A21/MF A01 CSCL 14B

N89-12780# Louisiana State Univ., Baton Rouge. Dept. of Mechanical Engineering.
A COMPUTER SIMULATION OF A PLASMA ARMATURE RAILGUN Final Report
Christopher B. Leger *In* Universal Energy Systems, Inc., United States Air Force Graduate Student Summer Support Program, Volume 1 Dec. 1987 24 p (For primary document see N89-12754 04-31)
Avail: NTIS HC A99/MF E03 CSCL 14B

15 LAUNCH VEHICLES AND SPACE VEHICLES

Includes boosters; operating problems of launch/space vehicle systems; and reusable vehicles.

For related information see also *20 Spacecraft Propulsion and Power.*

N89-12611*# European Space Agency, Paris (France).
ARIANE 5 VERIFICATION AND ASSOCIATED TEST FACILITIES

M. Vedrenne and A. L. Gonzalez *In* NASA, Goddard Space Flight Center, 15th Space Simulation Conference: Support the Highway to Space Through Testing 1988 p 368-371 (For primary document see N89-12582 04-18)
Avail: NTIS HC A21/MF A01 CSCL 22B

N89-12612*# Contraves Corp., Zurich (Switzerland).
THE SEPARATION TEST IN VACUUM OF THE ARIANE 4 PAYLOAD FAIRING
J. R. Butcher *In* NASA, Goddard Space Flight Center, 15th Space Simulation Conference: Support the Highway to Space Through Testing 1988 p 372-391 (For primary document see N89-12582 04-18)
Avail: NTIS HC A21/MF A01 CSCL 22B

16 SPACE TRANSPORTATION

Includes passenger and cargo space transportation, e.g., shuttle operations; and space rescue techniques.

For related information see also *03 Air Transportation and Safety* and *18 Spacecraft Design, Testing and Performance.* For space suits see *54 Man/System Technology and Life Support.*

N89-12579*# Martin Marietta Aerospace, New Orleans, La. Manned Space Systems.
DEFINITION OF A SPACE TRANSPORTATION SYSTEMS CARGO ELEMENT (SHUTTLE-C). ORIENTATION
Nov. 1987 161 p
(Contract NAS8-37143)
(NASA-CR-179404; NAS 1.26:179404) Avail: NTIS HC A08/MF A01 CSCL 22B

The Martin Marietta Shuttle-C project organization has been tailored to fit the tasks required for the Phase B study. Lead responsibilities have been assigned for Program Control, Safety, Reliability, and Quality Assurance (SR and QA); Systems Engineering and Integration (SE and I); Design and Analysis; Production and Test; and Operations. Details of the Performance Review and Orientation Program of November 1987 are given.
Author

17 SPACE COMM., SPACECRAFT COMM., COMMAND & TRACKING

Includes telemetry; space communications networks; astronavigation and guidance; and radio blackout.

For related information see also *04 Aircraft Communications and Navigation* and *32 Communications and Radar.*

No abstracts in this category.

18 SPACECRAFT DESIGN, TESTING AND PERFORMANCE

Includes satellites; space platforms; space stations; spacecraft systems and components such as thermal and environmental controls; and attitude controls.

For life support systems see *54 Man/System Technology and Life Support.* For related information see also *05 Aircraft Design, Testing and Performance, 39 Structural Mechanics,* and *16 Space Transportation.*

N89-12580*# National Aeronautics and Space Administration. Langley Research Center, Hampton, Va.
LIGHTWEIGHT STRUCTURAL DESIGN OF A BOLTED CASE JOINT FOR THE SPACE SHUTTLE SOLID ROCKET MOTOR
John T. Dorsey, Peter A. Stein (Coast Guard, Yorktown, Va.), and Harold G. Bush Washington, D.C. Nov. 1988 24 p
(NASA-TP-2851; L-16496; NAS 1.60:2851) Avail: NTIS HC A03/MF A01 CSCL 22B

The structural design of a bolted joint with a static face seal which can be used to join Space Shuttle Solid Rocket Motor (SRM) case segments is given. Results from numerous finite element parametric studies indicate that the bolted joint meets the design requirement of preventing joint opening at the O-ring locations during SRM pressurization. A final design recommended for further development has the following parameters: 180 one-in.-diam. studs, stud centerline offset of 0.5 in radially inward from the shell wall center line, flange thickness of 0.75 in, bearing plate thickness of 0.25 in, studs prestressed to 70 percent of ultimate load, and the intermediate alcove. The design has a mass penalty of 1096 lbm, which is 164 lbm greater than the currently proposed capture tang redesign.
Author

N89-12581*# Martin Marietta Aerospace, Denver, Colo. Space Station Program.
SPACE STATION INTEGRATED PROPULSION AND FLUID SYSTEMS STUDY
L. Rose, D. Bergman, B. Bicknell, and S. Wilson 25 Aug. 1987 77 p
(Contract NAS8-36438)
(NASA-CR-179393; NAS 1.26:179393; MCR-87-580) Avail: NTIS HC A05/MF A01 CSCL 22B

This Databook addresses the integration of fluid systems of the Space Station program. It includes a catalog of components required for the Space Station elements fluid systems and information on potential hardware commonality. The components catalog is in four parts. The first part lists the components defined for all the fluid systems identified in EP 2.1, Space Station Program Fluid Systems Configuration Databook. The components are cross-referenced in three sections. Section 2.1 lists the components by the fluid system in which they are used. Section 2.2 lists the components by type. Section 2.3 lists by the type of fluid media handled by the component. The next part of the catalog provides a description of the individual component. This section (2.4) is made up of data retrieved from Martin Marietta Denver Aerospace component data base. The third part is an assessment of propulsion hardware technology requirements. Section 2.5 lists components identified during the study as requiring development prior to flight qualification. Finally, Section 2.6 presents the results of the evaluation of commonality between components. The specific requirements of each component have been reviewed and duplication eliminated.
Author

N89-12582*# National Aeronautics and Space Administration. Goddard Space Flight Center, Greenbelt, Md.
FIFTEENTH SPACE SIMULATION CONFERENCE: SUPPORT THE HIGHWAY TO SPACE THROUGH TESTING
Joseph Stecher, ed. 1988 492 p Conference held in Williamsburg, Va., 31 Oct. - 3 Nov. 1988; sponsored by NASA, Inst. of Environmental Sciences, AIAA, and the American Society for Testing and Materials
(NASA-CP-3015; Rept-88B0253; NAS 1.55:3015) Avail: NTIS HC A21/MF A01 CSCL 22B

The Institute of Environmental Sciences Fifteenth Space Simulation Conference, Support the Highway to Space Through Testing, provided participants a forum to acquire and exchange information on the state-of-the-art in space simulation, test technology, thermal simulation and protection, contamination, and techniques of test measurements. For individual titles, see N89-12583 through N89-12620.

N89-12583*# Jet Propulsion Lab., California Inst. of Tech., Pasadena.
WF/PC INTERNAL MOLECULAR CONTAMINATION DURING SYSTEM THERMAL-VACUUM TEST c19
Daniel M. Taylor, J. Barengoltz, T. Jenkins, K. Leschly, and J. Triolo *In* NASA, Goddard Space Flight Center, 15th Space Simulation Conference: Support the Highway to Space Through

Testing 1988 p 1-10 (For primary document see N89-12582 04-18)
Avail: NTIS HC A21/MF A01 CSCL 14B

During the recent system thermal vacuum test of the Wide-Field/Planetary Camera (WF/PC), instrumentation was added to the WF/PC to characterize the internal molecular contamination and verify the instrument throughput down to 1470 angstroms. Analysis of data elements revealed two contaminants affecting the far-ultraviolet (FUV) performance of the WF/PC. The one contaminant (heavy volatile) is correlated with the electronic and housing temperature, and the contamination is significantly reduced when the electronics are operated below plus 8 degrees to plus 10 degrees C. The other contaminant (light volatile) is controlled by the heat pipe temperature, and the contamination is significantly reduced when the Thermal Electric Cooler (TEC) hot-junction temperature is below minus 40 degrees to minus 50 degrees C. The utility of contamination sensors located behind instruments during system tests was demonstrated. Author

N89-12584*# Jet Propulsion Lab., California Inst. of Tech., Pasadena.
WIDE FIELD/PLANETARY CAMERA (WF/PC) CONTAMINATION CONTROL ASSESSMENT Abstract Only **c35**

C. Maag, J. Millard, and M. Anderson *In* NASA, Goddard Space Flight Center, 15th Space Simulation Conference: Support the Highway to Space Through Testing 1988 p 11 (For primary document see N89-12582 04-18)
Avail: NTIS HC A21/MF A01 CSCL 14B

The major concern of this study was the formation of a haze on the transmissive optics when exposed to a vacuum environment. The phenomena was determined to be a result of molecular transport from a low outgassing structural adhesive. Detailed analysis, both chemical and analytical, were conducted to assess the formation of the haze. Results of the study are given as well as information on clean-up and problem elimination. Author

N89-12585*# Jet Propulsion Lab., California Inst. of Tech., Pasadena. Applied Technologies Sect.
CHARACTERIZATION OF A GRAPHITE EPOXY OPTICAL BENCH DURING THERMAL VACUUM CYCLING **c35**

Patricia A. Hansen, Teresa K. Jenkins, Carl R. Maag, and Daniel M. Taylor *In* NASA, Goddard Space Flight Center, 15th Space Simulation Conference: Support the Highway to Space Through Testing 1988 p 12-25 (For primary document see N89-12582 04-18)
Avail: NTIS HC A21/MF A01 CSCL 14B

In-situ monitoring of the Wide-Field/Planetary Camera, a Hubble Space Telescope science instrument, was performed in a vacuum environment to better understand the formation of ice on cooled optical detectors. Several diagnostic instruments were mounted on an access plate to view the interior of the instrument housing and the graphite epoxy optical bench. The instrumentation chosen and the rationale for choosing the instrumentation are discussed. In addition, the performance of the instrumentation during monitoring operations is discussed. Author

N89-12586*# TRW Defense and Space Systems Group, Redondo Beach, Calif. Operations and Support Group.
CLASS 100 LARGE SPACECRAFT FACILITY Abstract Only **c14**

L. E. Ryan *In* NASA, Goddard Space Flight Center, 15th Space Simulation Conference: Support the Highway to Space Through Testing 1988 p 29 (For primary document see N89-12582 04-18)
Avail: NTIS HC A21/MF A01 CSCL 14B

A new, large spacecraft dedicated clean facility was built and is operating at TRW Space and Defense, Redondo Beach, California. The facility includes typical integration and test and laboratory capabilities. Over 4500 square feet of filtered, air conditioned, hydrocarbon monitored, and personnel controlled working area is currently being used in state-of-the-art aerospace applications. Author

N89-12587*# Hughes Aircraft Co., Long Beach, Calif.
CORRELATION STUDIES ON SURFACE PARTICLE DETECTION METHODS

Ronald V. Peterson and James C. White *In* NASA, Goddard Space Flight Center, 15th Space Simulation Conference: Support the Highway to Space Through Testing 1988 p 30-46 (For primary document see N89-12582 04-18)
(Contract F20602-85-C-0279)
Avail: NTIS HC A21/MF A01 CSCL 22B

The accurate determination of dust levels on optical surfaces is necessary to assess sensor system performance. A comparison study was made on several particle measurement methods including those based on direct imaging and light scattering. The effectiveness of removing the particles from the surface prior to determining particle size distributions was also assessed. These studies revealed that some methods, especially those requiring particle removal before analysis, are subject to large systematic errors affecting particle size distributions. Thus, an understanding of the particle measurement methods employed is necessary before any surface cleanliness or obstruction value assignments are accepted as true representations of an optical surface contamination condition. Author

N89-12588*# TRW Defense and Space Systems Group, Redondo Beach, Calif. Operations and Support Group.
PRECISION CLEANING METHODS FOR SPACECRAFT APPLICATIONS Abstract Only

L. E. Ryan and H. Lindewall *In* NASA, Goddard Space Flight Center, 15th Space Simulation Conference: Support the Highway to Space Through Testing 1988 p 47 (For primary document see N89-12582 04-18)
Avail: NTIS HC A21/MF A01 CSCL 22B

A small CO2 snow cleaning apparatus to clean both molecular films and particles from small and large components and surfaces was constructed. Various types of surfaces were cleaned using the CO2 technique. Vacuum deposited and sputtered metallic coatings such as germanium, aluminum, and silver and silicon wafers, and polished copper conical mirrors were purposely contaminated with everyday aerospace contaminants, including particle fallout and fingerprints. Precleaning characterization by Bidirectional Reflectance Distribution Function (BRDF), ellipsometry, nonvolatile residue, and microscopic particle evaluation served as evaluation of cleaning efficiency. Good results were obtained in trial application. Author

N89-12589*# National Aeronautics and Space Administration. Lewis Research Center, Cleveland, Ohio.
THE NASA ATOMIC OXYGEN EFFECTS TEST PROGRAM **c25**

Bruce A. Banks, Sharon K. Rutledge, and Joyce A. Brady *In* NASA, Goddard Space Flight Center, 15th Space Simulation Conference: Support the Highway to Space Through Testing 1988 p 51-65 (For primary document see N89-12582 04-18)
Avail: NTIS HC A21/MF A01 CSCL 07D

The NASA Atomic Oxygen Effects Test Program was established to compare the low earth orbital simulation characteristics of existing atomic oxygen test facilities and utilize the collective data from a multitude of simulation facilities to promote understanding of mechanisms and erosion yield dependence upon energy, flux, metastables, charge, and environmental species. Four materials chosen for this evaluation include Kapton HN polyimide, FEP Teflon, polyethylene, and graphite single crystals. The conditions and results of atomic oxygen exposure of these materials is reported by the participating organizations and then assembled to identify degrees of dependency of erosion yields that may not be observable from any single atomic oxygen low earth orbital simulation facility. To date, the program includes 30 test facilities. Characteristics of the participating test facilities and results to date are reported. Author

N89-12590*# National Aeronautics and Space Administration. Lyndon B. Johnson Space Center, Houston, Tex.
MATERIALS SELECTION FOR LONG LIFE IN LEO: A CRITICAL EVALUATION OF ATOMIC OXYGEN TESTING WITH THERMAL ATOM SYSTEMS **c25**
S. L. Koontz, J. Kuminecz, L. Leger, and P. Nordine *In* NASA, Goddard Space Flight Center, 15th Space Simulation Conference: Support the Highway to Space Through Testing 1988 p 66-88 (For primary document see N89-12582 04-18)
Avail: NTIS HC A21/MF A01 CSCL 07D

The use of thermal atom test methods as a materials selection and screening technique for low-Earth orbit (LEO) spacecraft is critically evaluated. The chemistry and physics of thermal atom environments are compared with the LEO environment. The relative reactivities of a number of materials determined to be in thermal atom environments are compared to those observed in LEO and in high quality LEO simulations. Reaction efficiencies measured in a new type of thermal atom apparatus are one-hundredth to one-thousandth those observed in LEO, and many materials showing nearly identical reactivities in LEO show relative reactivities differing by as much as a factor of 8 in thermal atom systems. A simple phenomenological kinetic model for the reaction of oxygen atoms with organic materials can be used to explain the differences in reactivity in different environments. Certain specific thermal test environments can be used as reliable materials screening tools. Using thermal atom methods to predict material lifetime in LEO requires direct calibration of the method against LEO data or high quality simulation data for each material. Author

N89-12591*# Toronto Univ., Downsview (Ontario). Inst. for Aerospace Studies.
ATOMIC OXYGEN STUDIES ON POLYMERS **c27**
W. D. Morison, R. C. Tennyson, J. B. French, T. Braithwaite, M. Moisan, and J. Hubert (Montreal Univ., Quebec) *In* NASA, Goddard Space Flight Center, 15th Space Simulation Conference: Support the Highway to Space Through Testing 1988 p 89-109 (For primary document see N89-12582 04-18)
(Contracts N60921-86-C-A226; AUSPI-86-207; TP2-325)
Avail: NTIS HC A21/MF A01 CSCL 11C

The purpose was to study the effects of atomic oxygen on the erosion of polymer based materials. The development of an atomic oxygen neutral beam facility using a SURFATRON surface wave launcher that can produce beam energies between 2 and 3 eV at flux levels as high as approx. 10 to the 17th power atoms/cm (2)-sec is described. Thin film dielectric materials were studied to determine recession rates and and reaction efficiencies as a function of incident beam energy and fluence. Accelerated testing was also accomplished and the values of reaction efficiency compared to available space flight data. Electron microscope photomicrographs of the samples' surface morphology were compared to flight test specimens. Author

N89-12592*# McDonnell-Douglas Astronautics Co., Huntington Beach, Calif.
ATOMIC OXYGEN EFFECTS ON CANDIDATE COATINGS FOR LONG-TERM SPACECRAFT IN LOW EARTH ORBIT
E. H. Lan, Charles A. Smith, and J. B. Cross (Los Alamos National Lab., N. Mex.) *In* NASA, Goddard Space Flight Center, 15th Space Simulation Conference: Support the Highway to Space Through Testing 1988 p 110-121 (For primary document see N89-12582 04-18)
Avail: NTIS HC A21/MF A01 CSCL 22B

Candidate atomic oxygen protective coatings for long-term low Earth orbit (LEO) spacecraft were evaluated using the Los Alamos National Laboratory O-atom exposure facility. The coatings studied include Teflon, Al2O3, SiO2, and SWS-V-10, a silicon material. Preliminary results indicate that sputtered PTFE Teflon (0.1 micrometers) has a fluence lifetime of 10 to the 19th power O-atoms/cm (2), and sputtered silicon dioxide (0.1 micrometers), aluminum oxide (0.1 micrometers), and SWS-V-10, a silicone, (4 micrometers) have fluence lifetimes of 10 to the 20th power to 10 to the 21st power O-atoms/cm (2). There are large variations in fluence lifetime data for these coatings. Author

N89-12593*# General Electric Co., Philadelphia, Pa. Astro Space Div.
PYRO SHOCK SIMULATION: EXPERIENCE WITH THE MIPS SIMULATOR **c14**
Thomas J. Dwyer and David S. Moul *In* NASA, Goddard Space Flight Center, 15th Space Simulation Conference: Support the Highway to Space Through Testing 1988 p 125-138 (For primary document see N89-12582 04-18)
Avail: NTIS HC A21/MF A01 CSCL 14B

The Mechanical Impulse Pyro Shock (MIPS) Simulator at GE Astro Space Division is one version of a design that is in limited use throughout the aerospace industry, and is typically used for component shock testing at levels up to 10,000 response g's. Modifications to the force imput, table and component boundary conditions have allowed a range of test conditions to be achieved. Twelve different designs of components with weights up to 23 Kg are in the process or have completed qualification testing in the Dynamic Simulation Lab at GE in Valley Forge, Pa. A summary of the experience gained through the use of this simulator is presented as well as examples of shock experiments that can be readily simulated at the GE Astro MIPS facility. Autho

N89-12594*# Southwest Research Inst., San Antonio, Tex.
MULTIPLE INPUT/OUTPUT RANDOM VIBRATION CONTROL SYSTEM **c39**
James F. Unruh *In* NASA, Goddard Space Flight Center, 15th Space Simulation Conference: Support the Highway to Space Through Testing 1988 p 139-157 (For primary document see N89-12582 04-18)
Avail: NTIS HC A21/MF A01 CSCL 20K

A multi-input/output random vibration control algorithm was developed based on system identification concepts derived from random vibration spectral analysis theory. The unique features of the algorithm are: (1) the number of input excitors and the number of output control responses need not be identical; (2) the system inverse response matrix is obtained directly from the input/output spectral matrix; and (3) the system inverse response matrix is updated every control loop cycle to accommodate system amplitude nonlinearities. A laboratory demonstration case of two imputs with three outputs is presented to demonstrate the system capabilities. Author

N89-12595*# Control Dynamics Co., Huntsville, Ala.
THE FLIGHT ROBOTICS LABORATORY **c14**
Patrick A. Tobbe, Marlin J. Williamson, and John R. Glaese *In* NASA, Goddard Space Flight Center, 15th Space Simulation Conference: Support the Highway to Space Through Testing 1988 p 158-167 (For primary document see N89-12582 04-18)
(Contract NAS8-36570)
Avail: NTIS HC A21/MF A01 CSCL 14B

The Flight Robotics Laboratory of the Marshall Space Flight Center is described in detail. This facility, containing an eight degree of freedom manipulator, precision air bearing floor, teleoperated motion base, reconfigurable operator's console, and VAX 11/750 computer system, provides simulation capability to study human/system interactions of remote systems. The facility hardware, software and subsequent integration of these components into a real time man-in-the-loop simulation for the evaluation of spacecraft contact proximity and dynamics are described. Author

N89-12596*# Control Dynamics Co., Huntsville, Ala.
SPACE STATION DOCKING MECHANISM DYNAMIC TESTING
Thomas G. Howsman and John R. Glaese *In* NASA, Goddard Space Flight Center, 15th Space Simulation Conference: Support the Highway to Space Through Testing 1988 p 168-175 (For primary document see N89-12582 04-18)
Avail: NTIS HC A21/MF A01 CSCL 22B

A prototype docking mechanism for the Space Station was designed and fabricated for NASA. This docking mechanism is actively controlled and uses a set of electromechanical actuators for alignment and load attenuation. Dynamic tests are planned

using the Marshall Space Flight Center's 6-DOF Motion Simulator. The proposed tests call for basic functionality verification as well as complete hardware-in-the-loop docking dynamics simulations. Author

N89-12597*# Tenney Engineering, Inc.
SPACE SIMULATORS FOR LASER OPTICS **c71**
Frank H. Gardner *In* NASA, Goddard Space Flight Center, 15th Space Simulation Conference: Support the Highway to Space Through Testing 1988 p 179-186 (For primary document see N89-12582 04-18)
Avail: NTIS HC A21/MF A01 CSCL 20F

Different approaches that are being utilized to test laser optical systems are described. One of the most crucial areas in the testing phase is the stability of the laser optics mounted inside the space simulator. The thermal vacuum system, the refrigeration system, and the space simulator are discussed. Author

N89-12598*# Contraves Goerz Corp., Pittsburgh, Pa.
DEVELOPMENT OF A TWO AXIS MOTION SIMULATION SYSTEM FOR THERMAL/VACUUM SATELLITE TESTING
David Henderson, Bert Popovich, Louis DeMore, and Joe Elm *In* NASA, Goddard Space Flight Center, 15th Space Simulation Conference: Support the Highway to Space Through Testing 1988 p 187-205 (For primary document see N89-12582 04-18)
Avail: NTIS HC A21/MF A01 CSCL 22B

A two-axis motion simulation system for thermal vacuum testing of large satellites in a space simulation chamber was developed. Satellites as large as 3000 kilograms with a 4-meter diameter and a 5-meter length can be tested. This motion simulator (MS) incorporates several unique features which result in a less complicated design with improved performance when compared to previous satellite motion simulators. The design of the simulator is discussed in detail. Author

N89-12599*# Massachusetts Inst. of Tech., Cambridge.
LIGO VACUUM SYSTEM STUDY **c14**
Jeffrey C. Livas and Boude C. Moore (California Inst. of Tech., Pasadena.) *In* NASA, Goddard Space Flight Center, 15th Space Simulation Conference: Support the Highway to Space Through Testing 1988 p 206-220 (For primary document see N89-12582 04-18)
(Grant NSF PHY-88-03557)
Avail: NTIS HC A21/MF A01 CSCL 14B

A laser interferometer gravitational wave observatory (LIGO) is being developed with sensitivities which will have a high probability of detecting gravitational waves from astrophysical sources. A major component of LIGO is a total of 16 km of 1.2 m (48 inch) diameter tube at a pressure of less than 10 to the minus 8th power torr. It will be of 304L stainless steel procured directly from the steel mills with the initial hydrogen content specially reduced. Projections of the outgassing rates of hydrogen and of water vapor as a function of time are given and the uncertainties discussed. Based on these, a preliminary analysis of the vacuum system is presented. Author

N89-12600*# European Space Agency. European Space Research and Technology Center, ESTEC, Noordwijk (Netherlands).
THE TWO AXIS MOTION SIMULATOR FOR THE LARGE SPACE SIMULATOR AT ESTEC (EUROPEAN SPACE RESEARCH AND TECHNOLOGY CENTER) **c14**
Kurt A. Beckel and Joop Hutchison *In* NASA, Goddard Space Flight Center, 15th Space Simulation Conference: Support the Highway to Space Through Testing 1988 p 221-234 (For primary document see N89-12582 04-18)
Avail: NTIS HC A21/MF A01 CSCL 14B

The Large Space Simulator at the European Space Research and Technology Center (ESTEC) has been recently equipped with a motion simulator capable of handling test items of 5 tons mass and having a volume of 7m in diameter and a length of 7m. The motion simulator has a modular set-up. It consists of a spinbox as a basic unit on which the test article is mounted and which allows continuous rotation (spin) . This spinbox can be used in two operational configurations; the spin axis is vertical to 30 degrees when mounted on a gimbalstand; and the spin axis is horizontal when mounted on a turntable-yoke combination. The turntable provides rotation within plus or minus 90 degrees. This configuration allows one to bring a test article to all possible relative positions viv-a-vis the sun vector (which is horizontal in this case). The spinbox allows fast rotation between 1 to 6 rpm or slow rotation between 1 to 25 rotations per day as well as positioning within plus or minus 0.4 degrees accuracy. Author

N89-12601*# High Vacuum Equipment Corp., Hingham, Mass.
INDIAN LSSC (LARGE SPACE SIMULATION CHAMBER) FACILITY **c14**
A. S. Brar, V. S. PrasadaRao, R. D. Gambhir, and M. Chandramouli (ISRO Satellite Centre, Peenya, Bangalore, India) *In* NASA, Goddard Space Flight Center, 15th Space Simulation Conference: Support the Highway to Space Through Testing 1988 p 235-238 (For primary document see N89-12582 04-18)
Avail: NTIS HC A21/MF A01 CSCL 14B

The Indian Space Agency has undertaken a major project to acquire in-house capability for thermal and vacuum testing of large satellites. This Large Space Simulation Chamber (LSSC) facility will be located in Bangalore and is to be operational in 1989. The facility is capable of providing 4 meter diameter solar simulation with provision to expand to 4.5 meter diameter at a later date. With such provisions as controlled variations of shroud temperatures and availability of infrared equipment as alternative sources of thermal radiation, this facility will be amongst the finest anywhere. The major design concept and major aspects of the LSSC facility are presented here. Author

N89-12602*# Analytic Sciences Corp., Washington, D. C.
THERMAL/STRUCTURAL DESIGN VERIFICATION STRATEGIES FOR LARGE SPACE STRUCTURES
David Benton *In* NASA, Goddard Space Flight Center, 15th Space Simulation Conference: Support the Highway to Space Through Testing 1988 p 241-252 (For primary document see N89-12582 04-18)
Avail: NTIS HC A21/MF A01 CSCL 22B

Requirements for space structures of increasing size, complexity, and precision have engendered a search for thermal design verification methods that do not impose unreasonable costs, that fit within the capabilities of existing facilities, and that still adequately reduce technical risk. This requires a combination of analytical and testing methods. This requires two approaches. The first is to limit thermal testing to sub-elements of the total system only in a compact configuration (i.e., not fully deployed). The second approach is to use a simplified environment to correlate analytical models with test results. These models can then be used to predict flight performance. In practice, a combination of these approaches is needed to verify the thermal/structural design of future very large space systems. Author

N89-12603*# Aeritalia S.p.A., Turin (Italy). Space Systems Group.
IRIS THERMAL BALANCE TEST WITHIN ESTEC LSS **c14**
Piero Messidoro, Marino Ballesio, and J. P. Vessaz (European Space Agency. European Space Research and Technology Center, ESTEC, Noordwijk, Netherlands) *In* NASA, Goddard Space Flight Center, 15th Space Simulation Conference: Support the Highway to Space Through Testing 1988 p 253-267 (For primary document see N89-12582 04-18)
Avail: NTIS HC A21/MF A01 CSCL 14B

The Italian Research Interim Stage (IRIS) thermal balance test was successfully performed in the ESTEC Large Space Simulator (LSS) to qualify the thermal design and to validate the thermal mathematical model. Characteristics of the test were the complexity of the set-up required to simulate the Shuttle cargo bay and allowing IRIS mechanism actioning and operation for the first time in the new LSS facility. Details of the test are presented, and test results for IRIS and the LSS facility are described. Author

N89-12604*# National Aeronautics and Space Administration. Goddard Space Flight Center, Greenbelt, Md.
THE INSTRUMENT TEST DEWAR (ITD): TESTING SATELLITE INSTRUMENTS AT 1.5 K
Laura J. Milam *In its* 15th Space Simulation Conference: Support t he Highway to Space Through Testing 1988 p 268-277 (For primary document see N89-12582 04-18)
Avail: NTIS HC A21/MF A01 CSCL 22B

The Instrument Test Dewar (ITD) is a cryogenic facility designed and built to test Cosmic Background Explorer (COBE) satellite instruments at 1.5 K. The facility provides a high vacuum and thermal environment with payload thermal, electrical and optical interfaces. There are two concentric vacuum spaces which are not hermitically sealed. The instrument vacuum space is 81.28 cm by 243.84 cm and is cooled by an LHe shroud. The guard vacuum space surrounds an LN2 shroud. There are two separate cryosorption pumping systems and a mechanical LHe pumping system. The data acquisition systems provide payload and housekeeping data. There have been various problems with the facility, and changes and improvements have been made to assure optimum test conditions. COBE instrument testing has been completed on structural, thermal model hardware and the protoflight units. Author

N89-12605*# Industrienlagen-Betriebsgesellschaft m.b.H., Munich (West Germany).
SOLAR SIMULATION WITH A RECTANGULAR BEAM c14
O. G. Feil and H. U. Frey *In* NASA, Goddard Space Flight Center, 15th Space Simulation Conference: Support the Highway to Space Through Testing 1988 p 278-288 (For primary document see N89-12582 04-18)
Avail: NTIS HC A21/MF A01 CSCL 14B

An existing space simulation test facility was modified by enlarging the solar simulator. Because of the restrictions imposed by existing equipment, the shape of the solar beam was altered from a circular to a rectangular cross section in order to adapt the test facility to test objects of increased size. This modification is described together with the results of preliminary measurements. Author

N89-12606*# Messerschmitt-Boelkow-Blohm G.m.b.H., Bremen (West Germany).
CONTROL OF THE INDUCED MICROGRAVITY ENVIRONMENT OF THE MAN TENDED FREE FLYER (MTFF) c29
Juergen Schlund *In* NASA, Goddard Space Flight Center, 15th Space Simulation Conference: Support the Highway to Space Through Testing 1988 p 289-307 (For primary document see N89-12582 04-18)
Avail: NTIS HC A21/MF A01 CSCL 22A

Induced disturbance sources have been identified on board the Man Tended Free Flyer (MTFF). Vibration responses at sensitive payload/spacecraft interfaces have been predicted by the application of an empirically found spacecraft dynamic transfer function. Vibrations from fluid loops (Freon, water) and of reaction wheels are assessed to be the main contributors to the induced microgravity environment. The expected payload acceleration response amplitudes presented here are more than one hundred times higher than the admissible values given by the MTFF system requirement, not considering the structural striction-friction effects which could be avoided by appropriate design. Real responses will be significantly lower because the derivation of excitation and transmission functions are based on worst case assumptions. The results indicate that future activities must be concentrated on equipment design improvement and the implementation of vibration reduction along the disturbance transmission path. The activities must be accompanied by early equipment and assembly development tests and transmissibility measurements with the integrated spacecraft engineering and structural models in order to improve the accuracy of payload response predictions. Author

N89-12607*# Boeing Aerospace Co., Seattle, Wash.
SIMULATION OF THE EFFECTS OF THE ORBITAL DEBRIS ENVIRONMENT ON SPACECRAFT Abstract Only
Michael D. Bjorkman *In* NASA, Goddard Space Flight Center, 15th Space Simulation Conference: Support the Highway to Space Through Testing 1988 p 311 (For primary document see N89-12582 04-18)
Avail: NTIS HC A21/MF A01 CSCL 22B

A remedy for the lack of a technique for testing the effects of orbital debris impacts has been sought along two paths at Boeing and elsewhere, firstly through the development of new launcher techniques capable of impact velocities between 8 and 16 km/s and secondly through the development of similitude techniques for modeling 8 to 16 km/s impacts using the present capabilities of projectile launchers. These two approaches are briefly discussed. Author

N89-12608*# Aerospace Corp., El Segundo, Calif.
A STEAM INERTING SYSTEM FOR HYDROGEN DISPOSAL FOR THE VANDENBERG SHUTTLE c20
Stuart B. Belknap *In* NASA, Goddard Space Flight Center, 15th Space Simulation Conference: Support the Highway to Space Through Testing 1988 p 312-335 (For primary document see N89-12582 04-18)
Avail: NTIS HC A21/MF A01 CSCL 21H

A two-year feasibility and test program to solve the problem of unburned confined hydrogen at the Vandenberg Space Launch Complex Six (SLC-6) during Space Shuttle Main Engine (SSME) firings is discussed. A novel steam inerting design was selected for development. Available sound suppression water is superheated to flash to steam at the duct entrance. Testing, analysis, and design during 1987 showed that the steam inerting system (SIS) solves the problem and meets other flight-critical system requirements. The SIS design is complete and available for installation at SLC-6 to support shuttle or derivative vehicles. Author

N89-12609*# Wyle Labs., Inc., Huntsville, Ala.
TEST STAND DESIGN AND ANALYSIS FOR TITAN 34D STATIC FIRING c14
Shayan Pazargadi *In* NASA, Goddard Space Flight Center, 15th Space Simulation Conference: Support the Highway to Space Through Testing 1988 p 336-352 (For primary document see N89-12582 04-18)
(Contract UTC-CSD-268024)
Avail: NTIS HC A21/MF A01 CSCL 14B

The Test Stand 1C at the Air Force Astronautic Laboratory (AFAL), Edwards AFB, Calif., was originally designed for F-1 liquid propellant engines. The stand was modified to handle a five and one half segment Solid Rocket Motor (SRM) Titan 34D vertical static firing test. The main design drivers and analysis effort utilized in the modification of the test stand are discussed. Author

N89-12610*# California Polytechnic State Univ., San Luis Obispo.
TEST STAND FOR TITAN 34D SRM STATIC FIRING c14
Vladimir Glozman and George Shipway (Wyle Labs., Inc., Huntsville, Ala.) *In* NASA, Goddard Space Flight Center, 15th Space Simulation Conference: Support the Highway to Space Through Testing 1988 p 353-367 (For primary document see N89-12582 04-18)
Avail: NTIS HC A21/MF A01 CSCL 14B

An existing liquid engine test stand at the AF Astronautics Laboratory was refurbished and extensively modified to accommodate the static firing of the Titan 34D solid rocket motor (SRM) in the vertical nozzle down orientation. The main load restraint structure was designed and built to secure the SRM from lifting off during the firing. In addition, the structure provided weather protection, temperature conditioning of the SRM, and positioning of the measurement and recording equipment. The structure was also used for stacking/de-stacking of SRM segments and other technological processes. The existing stand, its foundation and anchorage were thoroughly examined and reanalyzed. Necessary stand modifications were carried out to comply with the requirements of the Titan 34D SRM static firing. Author

N89-12611*# European Space Agency, Paris (France).
ARIANE 5 VERIFICATION AND ASSOCIATED TEST FACILITIES **c15**
M. Vedrenne and A. L. Gonzalez *In* NASA, Goddard Space Flight Center, 15th Space Simulation Conference: Support the Highway to Space Through Testing 1988 p 368-371 (For primary document see N89-12582 04-18)
Avail: NTIS HC A21/MF A01 CSCL 22B

The philosophy of verification tests of the Ariane 5 launcher program is already established. It corresponds to the development and the ground and flight qualification phases for both unmanned and manned launches. The different types of test are outlined for the system, booster, main core and upper structures, allowing the identification of the associated test facilities which are described.
Author

N89-12612*# Contraves Corp., Zurich (Switzerland).
THE SEPARATION TEST IN VACUUM OF THE ARIANE 4 PAYLOAD FAIRING **c15**
J. R. Butcher *In* NASA, Goddard Space Flight Center, 15th Space Simulation Conference: Support the Highway to Space Through Testing 1988 p 372-391 (For primary document see N89-12582 04-18)
Avail: NTIS HC A21/MF A01 CSCL 22B

The separation tests performed during the qualification test program of the Ariane 4 Payload Fairing are described. This is the first fairing structure to be developed using carbon fiber technology. Two separation tests were performed under vacuum conditions. The primary objectives of these tests were to verify compliance with the vehicle imposed requirements and to establish the behavioral characteristics of the fairing structure itself.
Author

N89-12613*# Selenia Spazio S.p.A., Rome (Italy).
THE SOLAR SIMULATION TEST OF THE ITALSAT THERMAL STRUCTURAL MODEL Abstract Only
M. Giommi, S. Liverani, and G. P. Santin *In* NASA, Goddard Space Flight Center, 15th Space Simulation Conference: Support the Highway to Space Through Testing 1988 p 395-396 (For primary document see N89-12582 04-18)
Avail: NTIS HC A21/MF A01 CSCL 22B

The ITALSAT structural/thermal model (STM) was submitted to a solar simulation test in order to verify the spacecraft thermal design and the thermal mathematical model which will be used to predict the on orbit temperatures. The STM was representative of the flight model in terms of configuration, structures, appendages and thermal hardware; dissipating dummy units were used to simulate the electronic units. The test consisted of the main phases: on station (beginning of life), on station (end of life), and transfer orbit. Preliminary results indicate that the test performances were satisfactory. The spacecraft measured temperatures were up to 15 degrees higher than the predicted ones. This imposes a careful correlation analysis in order to have reliable flight temperature predictions.
Author

N89-12614*# Lockheed Missiles and Space Co., Sunnyvale, Calif.
DEVELOPMENT OF OPTIMIZED, GRADED-PERMEABILITY AXIAL GROOVE HEAT PIPES **c34**
Michael R. Kapolnek and H. Rolland Holmes *In* NASA, Goddard Space Flight Center, 15th Space Simulation Conference: Support the Highway to Space Through Testing 1988 p 397-408 (For primary document see N89-12582 04-18)
Avail: NTIS HC A21/MF A01 CSCL 20D

Heat pipe performance can usually be improved by uniformly varying or grading wick permeability from end to end. A unique and cost effective method for grading the permeability of an axial groove heat pipe is described - selective chemical etching of the pipe casing. This method was developed and demonstrated on a proof-of-concept test article. The process improved the test article's performance by 50 percent. Further improvement is possible through the use of optimally etched grooves.
Author

N89-12615*# CCS Associates, Bethel Park, Pa.
HEAT PIPE COOLING SYSTEM WITH SENSIBLE HEAT SINK **c34**
Calvin C. Silverstein *In* NASA, Goddard Space Flight Center, 15th Space Simulation Conference: Support the Highway to Space Through Testing 1988 p 409-415 (For primary document see N89-12582 04-18)
(Contract SNL-33-0878)
Avail: NTIS HC A21/MF A01 CSCL 20D

A heat pipe cooling system which employs a sensible heat sink is discussed. With this type of system, incident aerodynamic heat is transported via a heat pipe from the stagnation region to the heat sink and absorbed by raising the temperature of the heat sink material. The use of a sensible heat sink can be advantageous for situations where the total mission heat load is limited, as it is during re-entry, and a suitable radiation sink is not available.
Author

N89-12616*# National Aeronautics and Space Administration. Goddard Space Flight Center, Greenbelt, Md.
REQUIREMENTS AND TEST RESULTS FOR THE QUALIFICATION OF THERMAL CONTROL COATINGS **c27**
J. E. Brzuskiewicz, G. A. Zerlaut (DSET Labs., Inc., Phoenix, Ariz.), K. Lauder, and G. M. Miller *In its* 15th Space Simulation Conference: Support the Highway to Space Through Testing 1988 p 419-436 (For primary document see N89-12582 04-18)
Avail: NTIS HC A21/MF A01 CSCL 11C

Paint type coatings are often used as engineering materials in critical satellite temperature control applications. The functional features of coatings used for temperature control purposes must remain stable throughout the satellite manufacturing process and the satellite mission. The selection of a particular coating depends on matching coating characteristics to mission requirements. The use of paint coatings on satellites, although having an extensive history, requires that the paint be qualified to each application on an individual basis. Thus, the qualification process through testing serves to ensure that paint coatings as engineering materials will fulfill design requirements.
Author

N89-12617*# McDonnell-Douglas Corp., Huntington Beach, Calif.
COMPARISON OF SULFURIC AND OXALIC ACID ANODIZING FOR PREPARATION OF THERMAL CONTROL COATINGS FOR SPACECRAFT
Huong G. Le, John M. Watcher, and Charles A. Smith *In* NASA, Goddard Space Flight Center, 15th Space Simulation Conference: Support the Highway to Space Through Testing 1988 p 437-451 (For primary document see N89-12582 04-18)
Avail: NTIS HC A21/MF A01 CSCL 22B

The development of thermal control surfaces, which maintain stable solar absorptivity and infrared emissivity over long periods, is challenging due to severe conditions in low-Earth orbit (LEO). Some candidate coatings are second-surface silver-coated Teflon; second-surface, silvered optical solar reflectors made of glass or quartz; and anodized aluminum. Sulfuric acid anodized and oxalic acid anodized aluminum was evaluated under simulated LEO conditions. Oxalic acid anodizing shows promise of greater stability in LEO over long missions, such as the 30 years planned for the Space Station. However, sulfuric acid anodizing shows lower solar absorptivity.
Author

N89-12618*# Jet Propulsion Lab., California Inst. of Tech., Pasadena.
MOISTURE INTERACTION AND STABILITY OF ZOT (ZINC ORTHOTITANATE) THERMAL CONTROL SPACECRAFT COATING
Gordon R. Mon, Charles C. Gonzalez, Ronald G. Ross, Jr., Liang C. Wen, and Timothy ODonnell *In* NASA, Goddard Space Flight Center, 15th Space Simulation Conference: Support the Highway to Space Through Testing 1988 p 452-465 (For primary document see N89-12582 04-18)

(Contract NAS7-918)
Avail: NTIS HC A21/MF A01 CSCL 22B

Two of the many performance requirements of the zinc orthotitanate (ZOT) ceramic thermal control paint covering parts of the Jupiter-bound Galileo spacecraft are that it be sufficiently electrically conductive so as to prevent electrostatic discharge (ESD) damage to onboard electronics and that it adhere to and protect the substrate from corrosion in terrestrial environments. The bulk electrical resistivity of ZOT on an aluminum substrate was measured over the ranges 22 C to 90 C and 0 percent RH to 100 percent RH, and also in soft (10 (minus 2) Torr) and hard (10 (minus 7) Torr) vacuums. No significant temperature dependence was evident, but measured resistivity values ranged over 9 orders of magnitude: 10 to the 5th power ohm-cm at 100 percent RH greater than 10 to the 12th power ohm-cm in a hard vacuum. The latter value violates the ESD criterion for a typical 0.019 cm thick coating. The corrosion study involved exposing typical ZOT substrate combinations to two moisture environments - 30 C/85 percent RH and 85 C/85 percent RH - for 2000 hours, during which time the samples were periodically removed for front-to-back electrical resistance and scratch/peel test measurements. It was determined that the ZOT/Al and ZOT/Mg systems are stable (no ZOT delamination), although some corrosion (oxide formation) and resistivity increases observed among the ZOT/Mg samples warrant that exposure of some parts to humid environments be minimized. Author

N89-12619*# Martin Marietta Aerospace, Denver, Colo. Space Systems Co.
COST EFFECTIVE ALTERNATIVE TO LOW IRRADIANCE MEASUREMENTS **c14**
Scott T. OLeary *In* NASA, Goddard Space Flight Center, 15th Space Simulation Conference: Support the Highway to Space Through Testing 1988 p 466-475 (For primary document see N89-12582 04-18)
Avail: NTIS HC A21/MF A01 CSCL 14B

Martin Marietta's Space Simulation Laboratory (SSL) has a Thermal Environment Simulator (TES) with 56 individually controlled heater zones. The TES has a temperature range of approximately minus 129 C to plus 149 C. Because of the ability of TES to provide complex irradiance distributions, it is necessary to be able to measure a wide range of irradiance levels. SSL currently uses ambient temperature controlled radiometers with the capacity to measure sink irradiance levels of approximately 42.6 mw/sq cm, sink temperature equals 21 C and up. These radiometers could not be used to accurately measure the lower irradiance levels of the TES. Therefore, it was necessary to obtain a radiometer or develop techniques which could be used to measure lower irradiance levels. Author

N89-12620*# Gavazzi (Carlo) Controls S.p.A., Milan (Italy).
TEST DATA ACQUISITION SYSTEM FOR THE ESTEC LARGE SOLAR SIMULATOR AT ESA/ESTEC **c14**
G. Buroni and L. Zucconi *In* NASA, Goddard Space Flight Center, 15th Space Simulation Conference: Support the Highway to Space Through Testing 1988 p 476-498 (For primary document see N89-12582 04-18)
Avail: NTIS HC A21/MF A01 CSCL 14B

A prototype data acquisition system is described. The device characteristics, its performance and the system aspects connected to the integration of the data acquisition system into the space simulator instrumentation and environment are discussed. The data acquisition system has a modular architecture and manifold configuration capability. The input characteristics feature high resolution and accuracy/stability for the measurement of low level (thermocouple originated) analog signals, even in the presence of high common mode and S/N figures. The output is serial digital, compatible with ESA data handling standards. The device is designed to be installed in particularly hostile environments, such as that of a solar simulator. Author

N89-12621* National Aeronautics and Space Administration. Lyndon B. Johnson Space Center, Houston, Tex.
SPACE STATION ERECTABLE MANIPULATOR PLACEMENT SYSTEM Patent
Margaret E. Grimaldi, inventor (to NASA) 20 Sep. 1988 7 p Filed 13 Nov. 1986 Supersedes N87-18596 (25 - 11, p 1446)
(NASA-Case-MSC-21096-1; US-Patent-4,772,175; US-Patent-Appl-SN-929865; US-Patent-Class-414-689; US-Patent-Class-414-718; US-Patent-Class-414-735; US-Patent-Class-212-225; US-Patent-Class-212-257; US-Patent-Class-182-103) Avail: US Patent and Trademark Office CSCL 22A

A habitable space station was proposed for low earth orbit, to be constructed from components which will be separately carried up from the earth and thereafter assembled. A suitable manipulating system having extraordinary manipulative capability is required. The invention is an erectable manipulator placement system for use on a space station and comprises an elongate, lattice-like boom having guide tracks attached thereto, a carriage-like assembly pivotally mounted on and extending from said dolly. The system further includes a turntable base pivotally interconnected with the proximal end of the boom and positioned either on a part of a transferring vehicle, or on another payload component being carried by the said transferring vehicle, or on the space station. Novelty resides in the use of a turntable base having a hinged boom with a dolly translatable therealong to carry the arm-like assembly, thus providing an additional 3 degrees of freedom to the arm.
Official Gazette of the U.S. Patent and Trademark Office

N89-12622*# National Aeronautics and Space Administration. Ames Research Center, Moffett Field, Calif.
RECENT ADVANCES AT NASA IN CALCULATING THE ELECTRONIC SPECTRA OF DIATOMIC MOLECULES
Ellis E. Whiting (Eloret Corp., Sunnyvale, Calif.) and John A. Paterson Oct. 1988 26 p Presented at the Meeting on High Resolution Electronic Spectroscopy of Molecules, Tihany, Hungary, 19-24 Sep. 1988
(NASA-TM-101034; A-88297; NAS 1.15:101034) Avail: NTIS HC A03/MF A01 CSCL 22B

Advanced entry vehicles, such as the proposed Aero-assisted Orbital Transfer Vehicle, provide new and challenging problems for spectroscopy. Large portions of the flow field about such vehicles will be characterized by chemical and thermal nonequilibrium. Only by considering the actual overlap of the atomic and rotational lines emitted by the species present can the impact of radiative transport within the flow field be assessed correctly. To help make such an assessment, a new computer program is described that can generate high-resolution, line-by-line spectra for any spin-allowed transitions in diatomic molecules. The program includes the matrix elements for the rotational energy and distortion to the fourth order; the spin-orbit, spin-spin, and spin-rotation interactions to first order; and the lambda splitting by a perturbation calculation. An overview of the Computational Chemistry Branch at Ames Research Center is also presented. Author

N89-12623*# National Aeronautics and Space Administration. Ames Research Center, Moffett Field, Calif.
A CONCEPTUAL DESIGN STUDY OF THE REUSABLE REENTRY SATELLITE
Byron L. Swenson, Alfred C. Mascy, Bruce Carter, Alan Cartledge, Robert E. Corridan, Larry E. Edsinger, Robert W. Jackson, Robert Keller, Marcus S. Murbach, and Paul F. Wercinski et al. Oct. 1988 91 p
(NASA-TM-101043; A-88310; NAS 1.15:101043) Avail: NTIS HC A05/MF A01 CSCL 22B

Experimentation leading to an understanding of life processes under reduced and extremely low gravitational forces will profoundly contribute to the success of future space missions involving humans. In addition to research on gravitational biology, research on the effects of cosmic radiation and the interruption and change of circadian rhythms on life systems is also of prime importance. Research in space, however, is currently viewed by biological scientists as an arena that is essential, yet largely inaccessible to

them for their experimentation. To fulfill this need, a project and spacecraft system described as the Reusuable Reentry Satellite or Lifesat has been proposed by NASA. Author

N89-12624*# Yale Univ., New Haven, Conn. Center for Systems Science.
VIBRATION SUPPRESSION IN A LARGE SPACE STRUCTURE
Final Report
Kumpati S. Narendra Aug. 1988 12 p
(Contract NAS9-17395)
(NASA-CR-182831; NAS 1.26:182831) Avail: NTIS HC A03/MF A01 CSCL 22B

The Yale University Center for Systems Science and the NASA Johnson Space Center collaborated in a study of vibration suppression in a large space structure during the period January 1985 to August 1987. The research proposal submitted by the Center to NASA concerned disturbance isolation in flexible space structures. The general objective of the proposal was to create within the Center a critical mass of expertise on problems related to the dynamics and control of large flexible space structures. A specific objective was to formulate both passive and active control strategies for the disturbance isolation problem. Both objectives were achieved during the period of the contract. While an extensive literature exists on the control of flexible space structures, it is generally acknowledged that many important questions remain open at even a fundamental level. Hence, instead of studying grossly simplified models of complex structural systems, it was decided as a first step to confine attention to detailed and thorough analyses of simple structures. Author

N89-12761# Cincinnati Univ., Ohio. Dept. of Aerospace Engineering.
PRELIMINARY APPLICATIONS OF DECENTRALIZED ESTIMATION TO LARGE FLEXIBLE SPACE STRUCTURES
Final Report
Susan M. Dumbacher *In* Universal Energy Systems, Inc., United States Air Force Graduate Student Summer Support Program, Volume 1 Dec. 1987 16 p (For primary document see N89-12754 04-31)
Avail: NTIS HC A99/MF E03 CSCL 22B

N89-12978# British Aerospace Public Ltd. Co., Bristol (England). Space and Communications Div.
EUROPEAN REMOTE SENSING SATELLITE PLATFORMS FOR THE 1990'S
P. Truss *In* ESA, Proceedings of the 1988 International Geoscience and Remote Sensing Symposium (IGARSS 1988) on Remote Sensing: Moving Towards the 21st Century, Volume 1 Aug. 1988 p 171-174 (For primary document see N89-12936 04-42)
Copyright Avail: NTIS HC A99/MF E03; ESA Publications Div., ESTEC, Noordwijk, Netherlands, 120 US dollars or 250 Dutch guilders

N89-12979# New South Wales Univ., Kensington (Australia). Dept. of Electrical Engineering.
AUSTRALIAN PREPARATIONS FOR THE POLAR PLATFORM
J. A. Richards, J. Kingwell, and K. N. OSullivan (CRA Exploration Proprietary Ltd., Fyshwick, Australia) *In* ESA, Proceedings of the 1988 International Geoscience and Remote Sensing Symposium (IGARSS 1988) on Remote Sensing: Moving Towards the 21st Century, Volume 1 Aug. 1988 p 177-178 (For primary document see N89-12936 04-42)
Copyright Avail: NTIS HC A99/MF E03; ESA Publications Div., ESTEC, Noordwijk, Netherlands, 120 US dollars or 250 Dutch guilders

N89-12981# National Space Development Agency, Ohashi (Japan).
REQUIREMENTS FOR THE ADVANCED EARTH OBSERVING SATELLITE (ADEOS) ORBIT, ORBIT AND A ATTITUDE CONTROL, AND RATE JITTER
K. Arai *In* ESA, Proceedings of the 1988 International Geoscience and Remote Sensing Symposium (IGARSS 1988) on Remote Sensing: Moving Towards the 21st Century, Volume 1 Aug. 1988 p 183-186 (For primary document see N89-12936 04-42)
Copyright Avail: NTIS HC A99/MF E03; ESA Publications Div., ESTEC, Noordwijk, Netherlands, 120 US dollars or 250 Dutch guilders

19 SPACECRAFT INSTRUMENTATION

For related information see also *06 Aircraft Instrumentation* and *35 Instrumentation and Photography.*

N89-12583*# Jet Propulsion Lab., California Inst. of Tech., Pasadena.
WF/PC INTERNAL MOLECULAR CONTAMINATION DURING SYSTEM THERMAL-VACUUM TEST
Daniel M. Taylor, J. Barengoltz, T. Jenkins, K. Leschly, and J. Triolo *In* NASA, Goddard Space Flight Center, 15th Space Simulation Conference: Support the Highway to Space Through Testing 1988 p 1-10 (For primary document see N89-12582 04-18)
Avail: NTIS HC A21/MF A01 CSCL 14B

20 SPACECRAFT PROPULSION AND POWER

Includes main propulsion systems and components, e.g., rocket engines; and spacecraft auxilliary power sources.

For related information see also *07 Aircraft Propulsion and Power, 28 Propellants and Fuels, 44 Energy Production and Conversion,* and *15 Launch Vehicles and Space Vehicles.*

N89-12625# Sandia National Labs., Albuquerque, N. Mex.
SEMICONDUCTOR BRIDGE (SCB) IGNITER STUDIES. 2: COMPARISON OF SCB AND HOT-WIRE DIRECT PROPULSION THRUSTERS
R. W. Bickes, Jr., S. L. Schlobohm, A. G. Bonas, and P. S. Headley (Crane Unidynamics, Phoenix, Ariz.) 1988 7 p Presented at the 13th International Pyrotechnics Seminar, Grand Junction, Colo., 11 Jul. 1988 Prepared in cooperation with Crane Unidynamics Phoenix, Ariz.
(Contract DE-AC04-76DP-00789)
(DE88-008803; SAND-87-3095-C2; CONF-880750-2) Avail: NTIS HC A02/MF A01

In this paper we present a comparison of the Crane Unidynamics/Phoenix hot-wire thrusters with the same thrusters made with Type 3-2 SCB igniters. (See paper I for details about the SCB igniter.) For both types of thrusters we obtained pressure versus time profiles and determined the function times, the peak pressures and the thruster impulses. The function times for the SCB components were shorter than the hot-wire device times, 350 versus 700 microsec respectively. However, despite the shorter function times, the firing energies for the SCB devices were approximately 4 mJ, as opposed to 36 mJ required for the hot-wire thrusters. In addition, the SCB bridges were completely consumed in less than 10 microsec compared to the hot-wire burst times of 665 microsec; therefore, the repetition interval for the SCB thrusters could be as short as 10 microsec allowing several SCB devices to be fired during the same time interval required for one hot-wire thruster. We believe that the lower energy, faster functioning and faster repetition rate of SCB thrusters offer advantages for future guidance control systems. DOE

N89-12626*# National Aeronautics and Space Administration. Marshall Space Flight Center, Huntsville, Ala.
ADVANCED EARTH-TO-ORBIT PROPULSION TECHNOLOGY 1986, VOLUME 2
R. J. Richmond, ed. and S. T. Wu, ed. (Alabama Univ., Huntsville.) Oct. 1986 775 p Conference held in Huntsville,

Ala., 13-15 May 1986
(NASA-CP-2437-Vol-2; M-541-Vol-2; NAS 1.55:2437-Vol-2) Avail: NTIS HC A99/MF E03 CSCL 21H

Technology issues related to oxygen/hydrogen and oxygen/hydrocarbon propulsion are addressed. Specific topics addressed include: rotor dynamics; fatigue/fracture and life; bearings; combustion and cooling processes; and hydrogen environment embrittlement in advanced propulsion systems. For individual titles, see N89-12627 through N89-12661.

N89-12627*# National Aeronautics and Space Administration. Marshall Space Flight Center, Huntsville, Ala.
DAMPING SEAL TESTER PROGRESS AND INITIAL TEST RESULTS **c37**
K. L. Cappel (Wyle Labs., Inc., Huntsville, Ala.) and George L. vonPragenau *In its* Advanced Earth-To-Orbit Propulsion Technology 1986, Volume 2 Oct. 1986 p 2-8 (For primary document see N89-12626 04-20)
Avail: NTIS HC A99/MF E03 CSCL 21H

The design of the test rig, including modifications made since the original concept, are summarized and initial test results are presented. B.G.

N89-12628*# National Aeronautics and Space Administration. Marshall Space Flight Center, Huntsville, Ala.
LOW-SPEED FLEXIBLE ROTOR BALANCING FOR SMOOTH, HIGH-SPEED OPERATION **c37**
E. Zorzi, John Giordano (Mechanical Technology, Inc., Latham, N. Y.), and George L. vonPragenau *In its* Advanced Earth-To-Orbit Propulsion Technology 1986, Volume 2 Oct. 1986 p 9-32 (For primary document see N89-12626 04-20)
Avail: NTIS HC A99/MF E03 CSCL 21H

A method for balancing flexible rotors at low speeds while ensuring smooth high-speed operation was developed and demonstrated through proof-of-principle tests. A potential application of this method is for the Space Shuttle Main Engine (SSME) turbopump rotors. These rotors operate above one or more critical speeds and must be balanced to ensure smooth operation at those speeds. Conventional low-speed rigid balancing is inadequate. The SSME hardware and geometry restrictions preclude the use of high-speed, flexible rotor, in-housing balancing. The use of a low-speed flexible rotor balancing method could substantially improve the state of balance of these rotors, because this technique eliminates the need for the high-speed runs during the balancing process required by classical flexible rotor balancing methods. The analytic formulation of the low-speed flexible rotor balancing method is described and the results of the proof-of-principle tests are presented. These results indicate that low-speed flexible rotor balancing is not only a viable technology, but that it is a valuable method for ensuring smooth operation above more than one bending critical speed. Also, the High-Pressure Oxygen Turbopump (HPOTP) rotor is shown to be a candidate application for this month. Author

N89-12629*# Mechanical Technology, Inc., Latham, N. Y.
THE EFFECTS OF INTERNAL ROTOR FRICTION ON DYNAMIC CHARACTERISTICS OF TURBOPUMPS **c37**
J. Walton, A. Artiles, J. Lund, and C. Lee *In* NASA, Marshall Space Flight Center, Advanced Earth-To-Orbit Propulsion Technology 1986, Volume 2 Oct. 1986 p 33-61 (For primary document see N89-12626 04-20)
(Contract NAS8-35601)
Avail: NTIS HC A99/MF E03 CSCL 21H

An analytic model developed to determine the stiffness and damping for an axial spline is presented. Following the analytical development, a series of parametric evolutions showing the destabilizing effects of the axial spline on a supercritical rotor system is also presented. B.G.

N89-12630*# National Aeronautics and Space Administration. Marshall Space Flight Center, Huntsville, Ala.
EFFICIENT TRANSIENT ANALYSIS METHODS FOR THE SPACE SHUTTLE MAIN ENGINE (SSME) TURBOPUMPS **c37**
Sherif T. Noah, U. J. Fan, Y.-S. Choi (Texas A&M Univ., College Station.), and T. Fox *In its* Advanced Earth-To-Orbit Propulsion Technology 1986, Volume 2 Oct. 1986 p 62-82 (For primary document see N89-12626 04-20)
(Contract NAS8-36182)
Avail: NTIS HC A99/MF E03 CSCL 21H

Effective procedures are presented for the response analysis of the Space Shuttle Main Engine (SSME) under transient loading conditions. Of particular concern is the determination of the nonlinear response of the systems to rotor imbalance in the presence of bearing clearances. The proposed methods take advantage of the nonlinearities involved being localized at only few rotor/housing coupling points. The methods include those based on alternative integral formulations for the incremental solutions involving the transition matrices of the rotor and housing. Alternatively, a convolutional representation of the housing displacements at the coupling points can be utilized to an advantage. For purposes of assessing the numerical integration results for the nonlinear rotor/housing systems, an FFT-based harmonic balance procedure is being developed to enable determining all possible harmonic, subharmonic, and nonperiodic solutions of the systems. A brief account of the Fourier approach is presented. Author

N89-12631*# Auburn Univ., Ala. Computer Science and Engineering Div.
VIBRATIONS INDUCED BY NONLINEARITIES IN ROTORDYNAMICS **c37**
William B. Day *In* NASA, Marshall Space Flight Center, Advanced Earth-To-Orbit Propulsion Technology 1986, Volume 2 Oct. 1986 p 83-105 (For primary document see N89-12626 04-20)
(Contracts NAS8-35992; NAS8-36475)
Avail: NTIS HC A99/MF E03 CSCL 21H

Special nonlinearities of the Jeffcott equations in rotordynamics are examined. The immediate application of this analysis is directed toward understanding the excessive vibration recorded in the LOX pump of the Space Shuttle Main Engine (SSME) during hot firing ground testing. Deadband, side force, and rubbing are three possible sources of inducing nonlinearity in the Jeffcott equations. The present analysis initially reduces these problems to the same mathematical description. A special frequency, named the nonlinear natural frequency, is defined and used to develop the solution of the nonlinear Jeffcott equations as singular asymptotic expansions. This nonlinear natural frequency, which is the ratio of the cross-stiffness and the damping, plays a major role in determining response frequencies. Numerical solutions are included for comparison with the analysis. Also nonlinear frequency-response tables are made for a typical range of values. Author

N89-12632*# National Aeronautics and Space Administration. Lewis Research Center, Cleveland, Ohio.
SIMPLIFIED CYCLIC STRUCTURAL ANALYSIS OF SSME TURBINE BLADES
Albert Kaufman and J. M. Manderscheid *In* NASA, Marshall Space Flight Center, Advanced Earth-To-Orbit Propulsion Technology 1986, Volume 2 Oct. 1986 p 107-124 Previously announced as N86-16615 (For primary document see N89-12626 04-20)
Avail: NTIS HC A99/MF E03 CSCL 21H

Anisotropic high-temperature alloys are used to meet the safety and durability requirements of turbine blades for high-pressure turbopumps in reusable space propulsion systems. The applicability to anisotropic components of a simplified inelastic structural analysis procedure developed at the NASA Lewis Research Center is assessed. The procedure uses as input the history of the total strain at the critical crack initiation location computed from elastic finite-element analyses. Cyclic heat transfer and structural analyses are performed for the first stage high-pressure fuel turbopump blade of the space shuttle main engine. The blade alloy is directionally solidified MAR-M 246 (nickel base). The analyses are based on a typical test stand engine cycle. Stress-strain histories for the airfoil critical location are computed using both the MARC nonlinear finite-element computer code and the simplified

procedure. Additional cases are analyzed in which the material yield strength is arbitrarily reduced to increase the plastic strains and, therefore, the severity of the problem. Good agreement is shown between the predicted stress-strain solutions from the two methods. The simplified analysis uses about 0.02 percent (5 percent with the required elastic finite-element analyses) of the CPU time used by the nonlinear finite element analysis. Author

N89-12633*# Argonne National Lab., Ill. Materials Science and Technology Div.
EFFECTS OF HIGH MEAN STRESS ON THE HIGH-CYCLE FATIGUE OF PWA 1480 AND DS MAR M 246 + Hf AT 1000 F **c26**
Saurin Majumdar *In* NASA, Marshall Space Flight Center, Advanced Earth-To-Orbit Propulsion Technology 1986, Volume 2 Oct. 1986 p 125-133 Sponsored by NASA. Lewis Research Center, Cleveland, Ohio (For primary document see N89-12626 04-20)
(Contract W-31-109-eng-38)
Avail: NTIS HC A99/MF E03 CSCL 21H

Results showing the effects of high mean stress on the high-cycle fatigue lives of single crystal PWA 1480 and DS MAR M 246 + Hf alloys at 1000 F are summarized. Selected specimens of PWA 1480 were examined by scanning electron microscopy after the fatigue tests were completed. The results indicate that the high-cycle fatigue resistance of PWA 1480 is less than that of DS MAR M 246 + Hf at low mean stress. However, at high mean stress, PWA 1480 is slightly stronger than MAR M 246 + Hf. The relatively low high-cycle fatigue resistance of PWA 1480 at low mean stress was traced to the presence of porosities that nucleate fatigue cracks rather early in life. A simplified linear elastic fracture mechanics analysis, which assumes that the cracks are present at the beginning of life, provides reasonable correlation between the present data and the limited crack growth data available for the same material. Author

N89-12634*# Georgia Inst. of Tech., Atlanta. Fracture and Fatigue Research Lab.
CONSTITUTIVE BEHAVIOR OF SINGLE CRYSTAL PWA 1480 AND DIRECTIONALLY SOLIDIFIED MAR-M 246 UNDER MONOTONIC AND CYCLIC LOADS AT HIGH AND LOW TEMPERATURE **c26**
Walter W. Milligan, Eric S. Huron, and Stephen D. Antolovich *In* NASA, Marshall Space Flight Center, Advanced Earth-To-Orbit Propulsion Technology 1986, Volume 2 Oct. 1986 p 134-171 (For primary document see N89-12626 04-20)
(Grant NAG3-503)
Avail: NTIS HC A99/MF E03 CSCL 21H

Strain rate, temperature, time, and microstructure had strong effects on the mechanical properties of Directionally Solidified MAR-M 246 + Hf and PWA 1480, and physical damage. This is the first step toward characterizing the constitutive behavior of the alloys from the physical point of view. In the remaining portion of the program, these relationships will be further explored, in hopes of developing constitutive models which will be based on actual microstructural deformation mechanisms in the alloys. B.G.

N89-12635*# National Aeronautics and Space Administration. Lewis Research Center, Cleveland, Ohio.
HIGH-TEMPERATURE LCF OF Ni-201 AND 304L STAINLESS STEEL **c26**
Gary R. Halford, L. R. Johnson, and James A. Brown (Aerojet TechSystems Co., Sacramento, Calif.) *In* NASA, Marshall Space Flight Center, Advanced Earth-To-Orbit Propulsion Technology 1986, Volume 2 Oct. 1986 p 172-204 (For primary document see N89-12626 04-20)
Avail: NTIS HC A99/MF E03 CSCL 21H

The high-temperature, low-cycle fatigue characteristics were investigated for two candidate alloys for use in the nozzle of an advanced design Orbital Maneuverable System (OMS) engine. Strain-controlled, low-cycle, creep-fatigue tests were performed in air on a commercially pure nickel (Ni2O1) at 483, 594, and 760 C, and on AISI Type 304L stainless steel at 650, 760, and 870 C. Both continuous strain-cycling tests and compressive-strain, hold-time tests were used in the evaluation. Direct comparisons are made between the two materials, and recommendations are presented as to which material offers the greatest potential for use. Author

N89-12636*# Rockwell International Corp., Canoga Park, Calif. Rocketdyne Div.
FATIGUE CRACK RETARDATION FOLLOWING OVERLOADS IN INCONEL 718, Ti-5Al-2.5Sn, AND HAYNES 188 **c26**
Dan E. Matejczyk, R. P. Jewett, D. W. Schmidt, and G. C. Hresko, III (Professional Services Group, Hellertown, Pa.) *In* NASA, Marshall Space Flight Center, Advanced Earth-To-Orbit Propulsion Technology 1986, Volume 2 Oct. 1986 p 205-219 (For primary document see N89-12626 04-20)
(Contract NAS8-35507)
Avail: NTIS HC A99/MF E03 CSCL 21H

Overload effects on fatigue crack growth were studied in Inconel 718, Ti-5Al-2.5Sn ELI, and Haynes 188 at several temperatures as a function of load ratio and of overload magnitude. Over the range of materials and experimental conditions studied, a range of overload mechanisms may be operative. Results are compared to a crack tip plastic zone model and a plastic wake closure model. Ti-5Al-2.5Sn ELI results are discussed in terms of crack branching and fracture surface microroughness. Author

N89-12637*# SKF Industries, Inc., King of Prussia, Pa.
THERMO-MECHANICAL PERFORMANCE EVALUATION OF CRYOGENIC TURBOPUMP BALL BEARINGS **c26**
Robert A. Pallini *In* NASA, Marshall Space Flight Center, Advanced Earth-To-Orbit Propulsion Technology 1986, Volume 2 Oct. 1986 p 221-240 (For primary document see N89-12626 04-20)
(Contract NAS8-35341)
Avail: NTIS HC A99/MF E03 CSCL 21H

The Space Shuttle Main Engine (SSME) high pressure oxidizer turbopump (HPOTP) presents a severe and demanding operating environment for the rotor-bearing system. The life requirement for the angular contact ball bearings that support the shaft is on the order of 7.5 hours. In actual operation bearing distress was observed after much shorter time. A thermo-mechanical analysis of the HPOTP rotor-bearing system was performed with the SHABERTH (SHaft-BEaring-THermal) computer code. Bearing performance was evaluated as a function of its thermal and mechanical environment. Bearing operating temperatures, heat generation and rolling fatigue life were quantified as functions of operating loads and ball-to-race friction. The latter of these was shown to greatly influence bearing performance. Recommendations for easing the sensitivity of bearing performance to friction levels is addressed. Author

N89-12638*# Spectra Research Systems, Inc., Huntsville, Ala.
THERMAL ANALYSIS OF SSME TURBOPUMP BEARINGS **c26**
Joe C. Cody, David Marty, and Bruce K. Tiller *In* NASA, Marshall Space Flight Center, Advanced Earth-To-Orbit Propulsion Technology 1986, Volume 2 Oct. 1986 p 241-265 (For primary document see N89-12626 04-20)
Avail: NTIS HC A99/MF E03 CSCL 21H

A lumped node thermal network model of the pump end bearing of the Space Shuttle Main Engine (SSME) was developed. The bearing elements, the shaft, isolator, housing, and cryogenic coolant flow characteristics are included. Two phase heat transfer characteristics of the LOX coolant are used in the model. Two computer codes, one thermal, and the other a bearing performance code, were coupled to provide an overall evaluation of the bearing operating characteristics. Software was developed to allow automatic iteration between the models until a compatible solution was found. The model was used to develop sensitivity characteristics for the pump and the bearing. A broad range of parameters such as contact friction, preload, heat transfer coefficient, coolant flow, subcooling, and outer race misalignments

were investigated. In many cases, the solutions of the thermal and performance model would not agree indicating a thermally unstable operating conditions which leads to excessive bearing temperatures and possible failure. The results show that bearing component temperatures are very sensitive to contact friction, preloads and heat transfer coefficients. Although not as sensitive to coolant flow and subcooling, these parameters are very important for marginal conditions. In some cases, thermal instability could be induced by reducing flow or by raising coolant temperature to saturation. Author

N89-12639*# Battelle Columbus Labs., Ohio.
LUBRICATION EVALUATION OF SSME TURBOPUMP BEARINGS **c37**
K. F. Dufrane, J. W. Kannel, and S. A. Barber *In* NASA, Marshall Space Flight Center, Advanced Earth-To-Orbit Propulsion Technology 1986, Volume 2 Oct. 1986 p 266-292 (For primary document see N89-12626 04-20)
Avail: NTIS HC A99/MF E03 CSCL 21H

The power density and longevity of the Space Shuttle Main Engine (SSME) has put enormous demands on the fuel and oxidizer turbopumps. The high pressure oxidizer turbopumps (HPOTP) have required shaft speeds in excess of 30,000 rpm on 57 mm bore bearings in order to deliver the needed oxygen to the engines. Liquid oxygen is pumped through the bearings to serve as a coolant. With no conventional positive lubrication system, the bearings are lubricated by initial solid films and by possible transfer of polytetrafluoroethylene (PTFE) from the bearing cage to the ball-race interface. Despite the hostile environment, the design goal for the bearings is 27,000 seconds with a high degree of reliability. The current bearing performance, while still short of the goals, is adequate for multiple launches. This performance was achieved through an evolutionary process. The process has involved significant effort in evaluating and controlling radial and axial loads, coolant flow, bearing dimensions and tolerances, solid film lubrication, and duty cycles. Some of the rationale for bearing improvements and problems remaining to be solved in order to achieve the optimum life are described. Author

N89-12640*# Rockwell International Corp., Canoga Park, Calif. Rocketdyne Div.
SURFACE CHARACTERISTICS OF LIQUID OXYGEN COOLED BALL BEARINGS **c37**
Myles Butner and Mary Shoemaker *In* NASA, Marshall Space Flight Center, Advanced Earth-To-Orbit Propulsion Technology 1986, Volume 2 Oct. 1986 p 293-310 (For primary document see N89-12626 04-20)
(Contract NAS8-27980)
Avail: NTIS HC A99/MF E03 CSCL 21H

The bearings used in the Space Shuttle Main Engine operate at high loads and speeds while being cooled by liquid oxygen at temperatures of -250 to -280 F. As a consequence of the lack of lubrication supplied by the coolant, bearing service lives are limited by wear of the balls and races rather than by the classic spalling of subsurface origin expected for more typical operating conditions. Transfer films of Teflon from the cage and dry films of MoS2 are the only means of lubrication currently available. In assessing the effectiveness of these measures and in searching for more long-lasting lubrication, the as-run surfaces of balls and races were analyzed for evidence of heating, residual lubricant films, adhesive, and abrasive wear. Techniques used included metallography, optical, and SEM (Scanning Electron Microscopy) imaging, AES (Auger Electron Spectroscopy), ellipsometry, and PEE (Photoelectron Emission). The results of these investigations are summarized. Author

N89-12641*# National Aeronautics and Space Administration. Marshall Space Flight Center, Huntsville, Ala.
POWDER METALLURGY BEARINGS FOR ADVANCED ROCKET ENGINES **c26**
B. N. Bhat, T. S. Humphries, Robert L. Thom, G. I. Friedman, and V. Moxson (TRW Aircraft Components Group, Cleveland, Ohio.) *In its* Advanced Earth-To-Orbit Propulsion Technology 1986, Volume 2 Oct. 1986 p 311-325 (For primary document see N89-12626 04-20)
Avail: NTIS HC A99/MF E03 CSCL 21H

Six different powder metallurgy bearing alloys (X-405, MRC-2001, T-440V, 14-4/6V, WD-65, and D-5) were tested for rolling contact fatigue (RCF) life and stress corrosion cracking and the results were compared with standard 440C. The RCF test results clearly showed that the candidate PM alloys were superior to 440C; B sub 10 lives were better by factors ranging from 1.2 to 5.0. Stress corrosion cracking resistance of these alloys was as good as or better than that of 440C. B.G.

N89-12642*# National Aeronautics and Space Administration. Marshall Space Flight Center, Huntsville, Ala.
ROLLING CONTACT FATIGUE LIFE OF ZIRCONIUM AND MOLYBDENUM NITRIDE SPUTTER PLATED AMS 5749 BEARING STEEL **c37**
Robert L. Thom and Fred J. Dolan *In its* Advanced Earth-To-Orbit Propulsion Technology 1986, Volume 2 Oct. 1986 p 327-340 (For primary document see N89-12626 04-20)
Avail: NTIS HC A99/MF E03 CSCL 21H

Hardened AMS 5749 (Latrobes BG42) bearing steel test specimens were reactively sputter plated with zirconium nitride or molybdenum nitride to thicknesses of 0.5 to 1.0 microns. The test specimens were evaluated for rolling contact fatigue (RCF) resistance at stresses of both 5.42 GPa (786 ksi) and 4.04 GPa (586 ksi) using a ball on rod test setup. Significant improvements in RCF lives of over 100 percent were obtained for coated test specimens over the baseline uncoated AMS 5749. These results indicate improvements that can be made to bearings using reactive sputter plating methods. Author

N89-12643*# Rockwell International Corp., Canoga Park, Calif. Rocketdyne Div.
MEASUREMENT OF ROTORDYNAMIC COEFFICIENTS FOR A HYDROSTATIC RADIAL BEARING **c37**
B. T. Murphy and M. N. Wagner *In* NASA, Marshall Space Flight Center, Advanced Earth-To-Orbit Propulsion Technology 1986, Volume 2 Oct. 1986 p 341-366 (For primary document see N89-12626 04-20)
Avail: NTIS HC A99/MF E03 CSCL 21H

Measurement of rotordynamic coefficients is presented for a hydrostatic radial bearing, including direct and cross-coupled stiffness and damping. Two hydrostatic configurations were tested: an externally fed bearing 74.9 mm in diameter with a nominal direct stiffness of approximately 210 MN/m and an internally fed bearing 54.6 mm in diameter with a nominal direct stiffness of approximately 88 MN/m. Each bearing had six equally spaced hydrostatic pressure pockets, stationary for the externally fed bearing and rotating for the internally fed bearing. Also, both bearings had extended exit regions to provide additional damping. The top rotational speed was 378 Hz and the maximum axial Reynolds number was 50,000 using a Freon derivative (Freon-113) as the working fluid. The test apparatus was a synchronous rig as an intentionally eccentric journal was used as the sole source of excitation. Results showed the externally fed bearing to be 20 percent less stiff than predicted, and to have a significant amount of damping that agrees well with predictions. The internally fed bearing was found to be about 60 percent less stiff than predicted, and to be roughly neutral in terms of damping, as predicted. Author

N89-12644*# Rockwell International Corp., Canoga Park, Calif. Rocketdyne Div.
SURFACE MODIFICATION FOR WEAR RESISTANCE IN A LIQUID OXYGEN TURBOPUMP ENVIRONMENT **c37**
Lillian Ng and Yngve Naerheim (Rockwell International Science Center, Thousand Oaks, Calif.) *In* NASA, Marshall Space Flight Center, Advanced Earth-To-Orbit Propulsion Technology 1986, Volume 2 Oct. 1986 p 366-376 (For primary document see N89-12626 04-20)
Avail: NTIS HC A99/MF E03 CSCL 21H

Bearing elements for the Space Shuttle Main Engine oxidizer

turbopumps operate in the low viscosity environments of liquid oxygen, which results in an operating condition of poor lubrication. High transient axial loads and high coefficient of friction due to lack of lubricant in the high pressure oxidizer turbopump bearings has resulted in surface wear. Hard coatings were utilized to reduce the coefficient of friction and increase the wear resistance of steels. In this study, three bearing alloys (AMS 5618 (VIM-VAR), AMS 5900, and AMS 6491) were coated with TiN or thin-dense-Cr for evaluating the effects of surface modification on wear. Testing was performed in a cone-three-ball tester modified to provide both rolling and sliding friction that simulates operating conditions. Also, a liquid oxygen environment was used to simulate the operating environment. Test results including detailed Scanning Electron Microscopy (SEM), Electron Microscopy for Chemical Analysis (ESCA), and optical analysis will be presented. Author

N89-12645*# Rockwell International Corp., Canoga Park, Calif. Rocketdyne Div.

SSME BEARING HEALTH MONITORING USING A FIBEROPTIC DEFLECTOMETER

Michael E. Hampson, J. J. Collins, M. R. Randall, and Sarkis Barkhoudarian *In* NASA, Marshall Space Flight Center, Advanced Earth-To-Orbit Propulsion Technology 1986, Volume 2 Oct. 1986 p 377-391 (For primary document see N89-12626 04-20)

Avail: NTIS HC A99/MF E03 CSCL 21H

A fiberoptic deflectometer was used to investigate rocket engine turbopump bearing health monitoring. Two Space Shuttle Main Engine (SSME) high pressure oxidizer turbopump turbine-end bearings were tested under simulated high pressure oxidizer turbopump conditions. The deflectometers measured outer raceway deflection, due to ball passage, in the radial direction. The test data were analyzed and plotted several different ways. Accelerometer data from the tests were also analyzed and plotted for comparison. The results determined that bearing health could be successfully monitored using the deflectometer. Several algorithms stood out as the most useful. The 2C and 3C vs time consistently showed increases as bearing condition degraded. Indications became obvious approximately 100 seconds before the accelerometers began to register changes. BPO/Sync, and its time spent above threshold, also clearly indicated degrading conditions. This processing provided a measure of the onset and duration of ball slip in the bearing, a strong driver of wear. Indications became obvious approximately 400 seconds before the accelerometers began to register changes. Author

N89-12646*# Aerojet TechSystems Co., Sacramento, Calif.

AEROJET TECHSYSTEMS COMPANY CONTRIBUTION TO LOX/HC COMBUSTION AND COOLING TECHNOLOGY

Stephen D. Mercer and Don C. Rousar *In* NASA, Marshall Space Flight Center, Advanced Earth-To-Orbit Propulsion Technology 1986, Volume 2 Oct. 1986 p 393-438 (For primary document see N89-12626 04-20)

Avail: NTIS HC A99/MF E03 CSCL 21H

The LOX/HC combustion and cooling data generated by the ATC programs of the past ten years were examined. In addition, ATC is currently conducting LOX/HC combustion technology programs that could have a significant impact on future engine development. The scope and preliminary results from these ongoing programs are presented. Finally, recommendations are made in terms of how future technology programs might be focused in order to have maximum benefit to the engine development program. B.G.

N89-12647*# Pratt and Whitney Aircraft, West Palm Beach, Fla.

SURVEY OF LOX/HYDROCARBON COMBUSTION AND COOLING

A. I. Masters, W. A. Visek, and R. G. Carroll *In* NASA, Marshall Space Flight Center, Advanced Earth-To-Orbit Propulsion Technology 1986, Volume 2 Oct. 1986 p 439-460 (For primary document see N89-12626 04-20)

Avail: NTIS HC A99/MF E03 CSCL 21H

Achieving high chamber pressure in oxygen/hydrocarbon booster engines will require different approaches to regenerative cooling, propellant injection, and combustion stabilization than engines of the past. Comparisons are made with substantiated oxygen/hydrogen combustion technology which has resulted in demonstrated high pressure capability. Means of applying this technology to hydrocarbon booster engines are discussed including: tripropellant cycles with hydrogen cooling, injection techniques for stable efficient combustion and use of acoustic liners as combustion stabilization devices. Author

N89-12648*# Rockwell International Corp., Canoga Park, Calif. Rocketdyne Div.

LOX/HYDROCARBON COMBUSTION AND COOLING SURVEY

R. T. Cook and F. M. Kirby *In* NASA, Marshall Space Flight Center, Advanced Earth-To-Orbit Propulsion Technology 1986, Volume 2 Oct. 1986 p 461-473 (For primary document see N89-12626 04-20)

Avail: NTIS HC A99/MF E03 CSCL 21H

Liquid oxygen (LOX) and hydrocarbon fuels (methane, propane, and RP-1) are very attractive for booster rocket engine applications because of their high bulk density and respectful performance. Vehicle payload capability is dependent on the attainable engine chamber pressure and the combustion efficiency of the selected propellant combination. Combustor design approaches are presented to attain maximum cooling, stability, combustion efficiency, and reusable life. Experimental combustion efficiency and hot-gas heat-transfer rates are discussed as related to combustor contour, thrust level scaling, and injector characteristics including mixture ratio biasing and film cooling. These experimental data are compared to theory, and empirical relationships are derived. Conventional cooling relationships and coking limits are presented for potential hydrocarbon fuels as derived from high heat flux and high pressure electrically heated tube experiments. Experimental results of combustor coolant liner materials compatibility with hydrocarbon fuels are discussed. The application of the results of these studies to future LOX/hydrocrabon engines are delineated. Author

N89-12649*# National Aeronautics and Space Administration. Lewis Research Center, Cleveland, Ohio.

LIQUID OXYGEN COOLING OF HIGH PRESSURE LOX/HYDROCARBON ROCKET THRUST CHAMBERS

Harold G. Price *In* NASA, Marshall Space Flight Center, Advanced Earth-To-Orbit Propulsion Technology 1986, Volume 2 Oct. 1986 p 474-528 (For primary document see N89-12626 04-20)

Avail: NTIS HC A99/MF E03 CSCL 21H

An experimental program using liquid oxygen (LOX) and RP-1 as the propellants and supercritical LOX as the coolant was conducted at 4.14, 8.274, and 13.79 MN/sq m (600, 1200, and 2000 psia) chamber pressure. The objectives of this program were to evaluate the cooling characteristics of LOX with the LOX/RP-1 propellants, the buildup of soot on the hot-gas-side chamber wall and the effect of an internal LOX leak on the structural integrity of the combustor. Five thrust chambers with throat diameters of 6.6 cm (2.6 in) were tested successfully. The first three were tested at 4.14 MN/sq m (600 psia) chamber pressure over a mixture ratio range of 2.25 to 2.92. One of these three was tested over 22 cyclic tests after the first through crack from the coolant channel to the combustion zone was observed with no apparent metal burning or distress. The fourth chamber was tested at 8.274 MN/sq m (1200 psia) chamber pressure over a mixture range of 1.93 to 2.98. The fourth and fifth chambers were tested at 13.79 MN/sq m (2000 psia) chamber pressure over a mixture ratio range of 1.79 to 2.68. Author

N89-12650*# National Aeronautics and Space Administration. Marshall Space Flight Center, Huntsville, Ala.

RP-1 AND METHANE COMBUSTION AND COOLING EXPERIMENTS

C. R. Bailey *In its* Advanced Earth-To-Orbit Propulsion Technology

1986, Volume 2 Oct. 1986 p 529-548 (For primary document see N89-12626 04-20)
Avail: NTIS HC A99/MF E03 CSCL 21H

A program was conducted to investigate ignition, combustion, and heat transfer characteristics of liquid oxygen and either RP-1 or methane fuel applicable to advanced booster engines. Experimental data for both staged combustion and gas generator cycles were obtained for methane. Testing using RP-1 was conducted in support of the gas generator cycle. A pressure-fed combustion system rated at 40,000 pounds thrust was used for all testing. Preburner and gas generator combustion data for both propellant combinations were obtained at pressures ranging from 1500 to 3100 psia and temperatures from 1600 to 2000 degrees Rankine. Main injector evaluations were accomplished primarily with test firings using a water-cooled calorimeter main combustion chamber. With this chamber, heat flux profiles and combustion performance were obtained at pressures to approximately 2200 psia. Several tests were conducted using a methane-cooled combustion chamber. Author

N89-12651*# Rockwell International Corp., Canoga Park, Calif. Rocketdyne Div.
RESULTS OF COAXIAL INJECTOR ELEMENT TESTING
Steven C. Fisher *In* NASA, Marshall Space Flight Center, Advanced Earth-To-Orbit Propulsion Technology 1986, Volume 2 Oct. 1986 p 550-569 (For primary document see N89-12626 04-20)
Avail: NTIS HC A99/MF E03 CSCL 21H

The Turbine Drive Combustor Ignition and Durability Technology Program was created to develop technology that can be utilized to support the design and/or modification of reliable and durable future generation high performance oxygen/hydrogen rocket engine turbine drive combustors. The general objective was broken down into the two specific tasks of developing an analytical code for liquid rocket engine combustion systems and gathering part of the data required to anchor/verify this code and future codes. Hot fire tests were conducted to gain insight into the low mixture ratio ignition and combustion characteristics of coaxial elements as well as to collect data to support the code work. A portion of the recent hot fire testing conducted in this program is discussed. A total of 51 low pressure (100 to 200 psia) hot fire tests were run on a single Space Shuttle Main Engine oxidizer preburner element injector. The results of these tests are the main topic of this paper. Author

N89-12652*# Rockwell International Corp., Canoga Park, Calif. Rocketdyne Div.
COMBUSTION MODELING: PROGRESS AND PROJECTIONS
P. Y. Liang *In* NASA, Marshall Space Flight Center, Advanced Earth-To-Orbit Propulsion Technology 1986, Volume 2 Oct. 1986 p 570-579 (For primary document see N89-12626 04-20)
Avail: NTIS HC A99/MF E03 CSCL 21H

In 1985 Rocketdyne's ARICC combustion code entered operational phase from developmental phase with a successful engineering analysis of the Space Shuttle Main Engine (SSME) preburner injector element flows. The cases studied correspond to two design geometries and two engine operation conditions. Based on this experience, a much better understanding of the unique challenges of combustion modeling for multiphase flows and of the weakest links in the physical model is obtained. This presentation will discuss the nature of combustion model development and highlight the results of the injector study, especially the qualitative features of the problem that pertains to the choice of the numerical methodology. Numerical issues encountered that are peculiar to the simulation of combustion flows wil' be briefly discussed. Finally, the plan for future refinement of ARICC and its subcomponents into a reliable combustion model will be outlined. Author

N89-12653*# Aerojet TechSystems Co., Sacramento, Calif.
EFFECTS OF OXYGEN/HYDROGEN COMBUSTION CHAMBER ENVIRONMENT ON COPPER ALLOYS
Mike Murphy, R. E. Anderson, Don C. Rousar, and J. A. VanKleeck *In* NASA, Marshall Space Flight Center, Advanced Earth-To-Orbit Propulsion Technology 1986, Volume 2 Oct. 1986 p 580-617 (For primary document see N89-12626 04-20)
Avail: NTIS HC A99/MF E03 CSCL 21H

Main chamber liner deterioration in the Space Shuttle Main Engine (SSME) is sufficient to cause local chamber wall failures in the form of cracks through the copper alloy chamber wall. This deterioration is termed blanching and is characterized by an increase in local wall roughness and a bright, shiny, new penny type appearance. One of the objectives is to develop an understanding of the blanching phenomenon. The specific scope of this program includes: thermochemical analysis of the copper-oxygen-hydrogen system; thermogravimetric analysis (TGA) oxidation tests of NARloy-Z copper samples; metallurgical analyses of samples from 40K and full-scale SSME chamber liners, and TGA surface study tests under oxidation-reduction conditions with NARloy-Z, NARloy-A, OFHC, and zirconium copper alloys. B.G.

N89-12654*# Rockwell International Corp., Canoga Park, Calif. Rocketdyne Div.
HYDROGEN-ENVIRONMENT EMBRITTLEMENT AND ITS CONTROL IN HIGH PRESSURE HYDROGEN/OXYGEN ROCKET ENGINES
W. T. Chandler *In* NASA, Marshall Space Flight Center, Advanced Earth-To-Orbit Propulsion Technology 1986, Volume 2 Oct. 1986 p 618-634 (For primary document see N89-12626 04-20)
(Contract NAS8-27980)
Avail: NTIS HC A99/MF E03 CSCL 21H

The workshop on hydrogen environment embrittlement was organized to examine in some detail the effects on metallic materials of the hydrogen environments encountered in high pressure hydrogen/oxygen rocket engines and to discuss methods of preventing hydrogen environment induced failures under such exposure conditions. The Space Shuttle Main Engine (SSME) is the most advanced high pressure hydrogen/oxygen rocket engine currently in service. To serve as a basis for the discussions to follow, the conditions under which materials are exposed to hydrogen environments in the SSME will be outlined and methods used in the design of the SSME to prevent hydrogen environment induced failures will be described. Data generated at Rocketdyne on the effects of high pressure hydrogen on properties of metallic materials will be presented. Author

N89-12655*# IIT Research Inst., Chicago, Ill. Surface Engineering Center.
MULTISPECIMEN TEST FACILITY FOR HIGH-PRESSURE HYDROGEN CREEP STUDIES **c39**
S. K. Verma *In* NASA, Marshall Space Flight Center, Advanced Earth-To-Orbit Propulsion Technology 1986, Volume 2 Oct. 1986 p 635-659 (For primary document see N89-12626 04-20)
Avail: NTIS HC A99/MF E03 CSCL 21H

The IITRI-developed equipment for creep rupture evaluation of materials in hydrogen at up to 20.7 MPa and 925 C is described. This facility can test six specimens simultaneously within a single vessel with continuous measurement of specimen extension within the vessel. A double-wall vessel design concept with balanced pressure across the inner wall was adopted successfully. All temperature and strain measurements are transmitted to a data logger for storage and analysis. Typical rupture life, minimum creep rate, and time to 1 percent strain for selected alloys are presented, as well as analysis using Orowan-Sherby-Dorm temperature-compensated technique to estimate 3500 h rupture life and stress to obtain 1 percent strain in 3500 h. Author

N89-12656*# MTS Systems Corp., Minneapolis, Minn.
A HIGH PRESSURE, HIGH TEMPERATURE HYDROGEN ENVIRONMENT FOR METALS PROPERTIES TESTING SYSTEM **c26**
Michael J. Rother *In* NASA, Marshall Space Flight Center,

Advanced Earth-To-Orbit Propulsion Technology 1986, Volume 2 Oct. 1986 p 661-671 (For primary document see N89-12626 04-20)
Avail: NTIS HC A99/MF E03 CSCL 21H

The use of materials in an adverse environment is always a concern of design engineers. The additional constraints of today's aerodynamic requirements, especially high strength-to-weight ratios for engineering components, have increased the necessity for detailed information of the environmental effects on material properties. The MTS system designed and is in the process of manufacturing a test system for NASA-MSFC to evaluate the effects of high pressure, high temperature hydrogen gas on the material properties of metals. The design process for the system is discussed with a presentation of the system's final configuration.
Author

N89-12657*# National Aeronautics and Space Administration. Marshall Space Flight Center, Huntsville, Ala.
DEVELOPMENT OF A COMPUTER-CONTROLLED TECHNIQUE TO DETERMINE CRACK GROWTH RATE PROPERTIES IN CONTROLLED ENVIRONMENTS USING CRACK OPENING DISPLACEMENT **c39**
Dennis Moore, Dan Drinan, and J. Hodo *In its* Advanced Earth-To-Orbit Propulsion Technology 1986, Volume 2 Oct. 1986 p 672-697 (For primary document see N89-12626 04-20)
Avail: NTIS HC A99/MF E03 CSCL 21H

A computer-controlled testing technique was developed that utilizes crack opening displacement to predict crack lengths for compact tension specimens in crack growth rates (da/dN versus delta K) determinations. The crack growth rate data generated by the developed technique was compared statistically to data results of a highly reliable optical method. No significant difference could be determined between the data generated by either method. The computer-controlled method did prove, however, to be a reliable and cost effective method of determining crack growth rate data and can be incorporated in controlled environment crack growth rate determinations.
Author

N89-12658*# Carnegie-Mellon Univ., Pittsburgh, Pa.
HYDROGEN EFFECTS ON THE FATIGUE AND TENSILE BEHAVIOR OF CMSX-2 NICKEL BASE SUPERALLOY SINGLE CRYSTALS **c26**
I. Mel Bernstein, Scott Walston, M. Dollar, A. Domnanovich, and W. Kromp *In* NASA, Marshall Space Flight Center, Advanced Earth-To-Orbit Propulsion Technology 1986, Volume 2 Oct. 1986 p 698-714 (For primary document see N89-12626 04-20)
Avail: NTIS HC A99/MF E03 CSCL 21H

A number of studies have suggested that specific nickel-based superalloy single crystal materials can be susceptible to varying degrees of hydrogen embrittlement under a variety of testing conditions in gaseous high pressure hydrogen, an important environment, for example, for space shuttle main engine turbopumps. Three areas will be stressed: extension of the low cycle fatigue tests to a lower plastic strain range and to hydrogen conditions produced by high pressure thermal charging; a more detailed fractographic study to ascertain the hydrogen induced fracture plane; and an enhanced solutionizing treatment to break up the dendritic macrostructure and an evaluation of how this thermal processing change affects hydrogen compatibility. B.G.

N89-12659*# National Aeronautics and Space Administration. Marshall Space Flight Center, Huntsville, Ala.
THE DETERMINATION OF MOBILE HYDROGEN IN AEROSPACE ENGINE ALLOYS **c26**
Merlin D. Danford *In its* Advanced Earth-To-Orbit Propulsion Technology 1986, Volume 2 Oct. 1986 p 715-726 (For primary document see N89-12626 04-20)
Avail: NTIS HC A99/MF E03 CSCL 21H

Hydrogen desorption data (coulombs desorbed vs. time) were obtained for Waspaloy and Rene' 41 using electrochemical methods. A more general method of analysis, using diffusion theory, was developed and applied. The method may assume an initial hydrogen distribution which conforms to that predicted by diffusion theory or a uniform initial distribution. The data are interpreted in terms of either of these initial distributions or a combination thereof. It was found that the initial hydrogen distribution for Waspaloy and Rene' 41, after both electrolytic charging and charging at 5000 psi hydrogen pressure, conformed closely to those predicted by diffusion theory. The hydrogen desorption is completely explained by the nature of the initial hydrogen distribution in the metal, which was previously assumed to be uniform, and the fast hydrogen is not due to surface and subsurface hydride formation, as was previously supposed. Finally, the hydrogen solubilities in the metals, for electrolytically charged samples, depend strongly on the charging rate and are about the same for Rene' 41 and Waspaloy.
Author

N89-12660*# Pratt and Whitney Aircraft, West Palm Beach, Fla. Engineering Div.
LCF AND CRACK GROWTH RATE OF TURBINE BLADE ALLOYS IN HYDROGEN AND HYDROGEN/STEAM ENVIRONMENTS **c26**
B. A. Cowles, D. P. Deluca, J. R. Warren, and F. K. Haake *In* NASA, Marshall Space Flight Center, Advanced Earth-To-Orbit Propulsion Technology 1986, Volume 2 Oct. 1986 p 727-748 (For primary document see N89-12626 04-20)
Avail: NTIS HC A99/MF E03 CSCL 21H

The low cycle fatigue (LCF) and fatigue crack growth testing of MAR-M246+Hf and PWA 1480 in high pressure hydrogen and hydrogen enriched steam at elevated temperatures are described. The PWA 1480 single crystal exhibited the best properties overall, compared to both single crystal and directionally solidified MAR-M246+Hf. Addition of water vapor to the hydrogen atmosphere caused more pronounced reduction in the properties of the directionally solidified material than in the single crystal.
Author

N89-12661*# National Aeronautics and Space Administration. Marshall Space Flight Center, Huntsville, Ala.
THE DEVELOPMENT OF A HYDROGEN RESISTANT ALLOY Progress Report **c26**
W. Bryan McPherson *In its* Advanced Earth-To-Orbit Propulsion Technology 1986, Volume 2 Oct. 1986 p 749-757 (For primary document see N89-12526 04-20)
Avail: NTIS HC A99/MF E03 CSCL 21H

In the continuous search for hydrogen tolerant alloys, the latest evaluation of various compositions of the Fe-Ni-Co-Cr system with elemental additions of Cb, Ti, and Al is described. After processing, notched tensile specimens were tested in 34.5 MPa (5000 psi) hydrogen at room temperature as the main screening test. The H2/air ratio was used as the selection/rejection criteria. Several compositions approach the objective strength, 1241 MPa (180 ksi) ultimate and 1103 MPa (160 ksi) yield, with little or no degradation in hydrogen.
Author

N89-12662# Ebasco Services, Inc., New York.
A MULTIMEGAWATT SPACE POWER SOURCE RADIATOR DESIGN
Jacek Jedruch 28 Jan. 1988 19 p Presented at the 5th Symposium on Space Nuclear Power Systems, Albuquerque, N. Mex., 11 Jan. 1988
(Contract DE-AC07-76ID-01570)
(DE88-015185; EGG-M-38487; CONF-880122-17) Avail: NTIS HC A03/MF A01

The multimegawatt space power sources (MMSPS) proposed for deployment in the late 1990s to meet mission burst power requirements, require an increase by four orders of magnitude in the power rating of equipment currently used in space. Prenger and Sullivan (1982) describe various radiator concepts proposed for such applications. They range from the innovative liquid droplet radiator (Mattick and Hertzberg 1981) to the more conventional heat pipe concept (Girrens 1982). The present paper deals with the design of the radiator for one such system, characterized by both high temperature and high pressure. It provides an estimate

of the size, mass, and problems of orbiting such a radiator, based on the assumption that the next generation of heavy launch vehicle with 120-tonne carrying capacity, and 4000-cu m cargo volume, will be available for putting hardware into orbit. DOE

N89-12663# Veritay Technology, Inc., Amherst, N.Y.
21ST CENTURY PROPULSION CONCEPT Final Report, 7 Jul. 1987 - 7 Jan. 1988
Robert L. Talley Apr. 1988 73 p
(Contract F06411-87-C-0058)
(AD-A197537; VERITAY-F04-88-1; AFAL-TR-88-031) Avail: NTIS HC A04/MF A01 CSCL 21C

This Phase 1 effort was intended to explore the Biefield-Brown effect, which allegedly converts electrostatic energy into a propulsive force. Activities under this program emphasized the experimental exploration of this electrostatic thrust-generation concept to verify its existence, to verify its operation in a vacuum, and to establish the magnitude of its thrust. To meet these goals an overall laboratory test configuration was designed and developed for quantifying the electrostatically induced propulsive forces on selected experimental devices. This configuration utilized a vacuum chamber with a torsion fiber type measurement system for direct assessment of propulsive forces. Geometrical symmetries were incorporated in the design to minimize the influence of reaction forces which can arise from nearby bodies, including the walls of the vacuum chamber itself. Tests were conducted at atmospheric pressure and over a range of partial vacuum conditions. Direct experimental results indicate that when an electrostatic potential difference is applied between asymmetrical electrodes of an all metal test device, a residual propulsive force is generated and acts on the device. This residual force acts in the opposite direction to electrical wind forces and to the forces claimed to have been measured in a vacuum by T. T. Brown. GRA

N89-12664# Edgerton, Germeshausen and Grier, Inc., Idaho Falls, Idaho.
FISSION FRAGMENT ROCKETS: A POTENTIAL BREAKTHROUGH
George F. Chapline, Paul W. Dickson, and Brice G. Schnitzler 1988 10 p Presented at the International Reactor Physics Conference, Jackson Hole, Wyo., 18 Sep. 1988
(Contracts DE-AC07-76ID-01570; W-7405-eng-48)
(DE88-016953; EGG-M-88285; CONF-880911-18) Avail: NTIS HC A03/MF A01

A new reactor concept which has the potential of enabling extremely energetic and ambitious space propulsion missions is described. Fission fragments are directly utilized as the propellant by guiding them out of a very low density core using magnetic fields. The very high fission fragment exhaust velocities yield specific impulses of approximately a million seconds while maintaining respectable thrust levels. Specific impulses of this magnitude allow acceleration of significant payload masses to several percent of the velocity of light and enable a variety of interesting missions, e.g., payloads to the nearest star, Alpha Centauri, in about a hundred years for very rapid solar system transport. The parameters reported in this paper are based on a very preliminary analysis. Considerable trade-off studies will be required to find the optimum system. We hope the optimum system proves to be as attractive as our preliminary analysis indicates, although we must admit that our limited effort is insufficient to guarantee any specific level of performance. DOE

N89-12665*# National Aeronautics and Space Administration. Lewis Research Center, Cleveland, Ohio.
SP-100 NUCLEAR SPACE POWER SYSTEMS WITH APPLICATION TO SPACE COMMERCIALIZATION
John M. Smith [1988] 17 p Proposed for presentation at Space Commercialization: Roles of Developing Countries, Nashville, Tenn., 5-10 Mar. 1989; sponsored by AIAA
(NASA-TM-101403; E-4487; NAS 1.15:101403) Avail: NTIS HC A03/MF A01 CSCL 18I

The purpose of this paper is to familiarize the Space Commercialization Community with the status and characteristics of the SP-100 space nuclear power system. The program is a joint undertaking by the Department of Defense, the Department of Energy and NASA. The goal of the program is to develop, validate, and demonstrate the technology for space nuclear power systems in the range of 10 to 1000 kWe electric for use in the future civilian and military space missions. Also discussed are mission applications which are enhanced and/or enabled by SP-100 technology and how this technology compares to that of more familiar solar power systems. The mission applications include earth orbiting platforms and lunar/Mars surface power. Author

N89-12608*# Aerospace Corp., El Segundo, Calif.
A STEAM INERTING SYSTEM FOR HYDROGEN DISPOSAL FOR THE VANDENBERG SHUTTLE
Stuart B. Belknap *In* NASA, Goddard Space Flight Center, 15th Space Simulation Conference: Support the Highway to Space Through Testing 1988 p 312-335 (For primary document see N89-12582 04-18)
Avail: NTIS HC A21/MF A01 CSCL 21H

N89-12758# Texas A&M Univ., College Station. Dept. of Nuclear Engineering.
PRELIMINARY THERMAL ANALYSIS OF A BIMODAL NUCLEAR ROCKET CORE Final Report
David C. Carpenter *In* Universal Energy Systems, Inc., United States Air Force Graduate Student Summer Support Program, Volume 1 Dec. 1987 14 p (For- primary document see N89-12754 04-31)
Avail: NTIS HC A99/MF E03 CSCL 21H

23 CHEMISTRY AND MATERIALS (GENERAL)

N89-12666# North Carolina Univ., Chapel Hill. Dept. of Chemistry.
CHARGE TRANSFER IN MULTIPLE SITE CHEMICAL SYSTEMS Final Report
Thomas J. Meyer 3 Jun. 1988 14 p
(Contract DAAG29-85-K-0121)
(AD-A197143; ARO-22611.20-PH) Avail: NTIS HC A03/MF A01 CSCL 07D

This report covers work done in the areas of mixed valence chemistry, preparation and characterization of multiple redox sites in soluble polymers, the immobilization of catalysts of polymeric films and polymer supports, and controlling redox effects in polymeric films. GRA

N89-12667* National Aeronautics and Space Administration. Langley Research Center, Hampton, Va.
POLYENAMINES FROM AROMATIC DIACETYLENIC DIKETONES AND DIAMINES Patent
Paul M. Hergenrother, inventor (to NASA), Robert G. Bass, inventor (to NASA), Mark S. Sinsky, inventor (to NASA), and John W. Connell, inventor (to NASA) (Virginia Commonwealth Univ., Richmond.) 27 Sep. 1988 7 p Division of US-Patent-4,663,483; US-Patent-Appl-SN-734,366, filed 15 May 1985
(NASA-Case-LAR-13444-2-CU; US-Patent-4,774,359; US-Patent-Appl-SN-000692; US-Patent-Class-564-396; US-Patent-Class-564-315; US-Patent-Class-564-323; US-Patent-Class-564-330; US-Patent-Class-564-342; US-Patent-Class-564-344; US-Patent-Class-564-430) Avail: US Patent and Trademark Office CSCL 07A

The synthesis and characterization of several polyenamine ketones are discussed wherein conjugated diacetylenic diketones and aromatic diamines are used as a route to the formation of high molecular weight polyenamine ketones which exhibit good mechanical properties and can be cast into creasible films. Typical polymerization conditions involved the reaction of stoichiometric amounts of 1,4- or 1,3-PPPO and a diamine at 60 to 130 C in m-cresol at (w/w) solids content of 8 to 26 percent for a specified

period of time under a nitrogen atmosphere. Novel polyenamine ketones were prepared with inherent viscosities as high as 1.99 dl/g and tough, clear amber films with tensile strengths of 12,400 psi and tensile moduli of 397,000 psi were cast from solutions of the polymers in chloroform.
Official Gazette of the U.S. Patent and Trademark Office

24 COMPOSITE MATERIALS

Includes physical, chemical, and mechanical properties of laminates and other composite materials.
For ceramic materials see *27 Nonmetallic Materials*.

N89-12668 California Univ., Irvine.
THE EFFECT OF DELAMINATION ON THE RESPONSE OF ADVANCED COMPOSITE LAMINATES Ph.D. Thesis
John Joseph Tracy 1987 341 p
Avail: Univ. Microfilms Order No. DA8803633

Advanced composites are very susceptible to internal delamination failures. The effects of delaminations on the stiffness dominated response of a simple structural element, the beam-column are studied. Graphite-epoxy beam-column samples with various length delaminations were tested in static bending, free vibration, and buckling response. The finite element method was used to corroborate the experimental results. Beam theory models capable of analyzing delaminated cross-ply laminates composed of symmetric sublaminates were developed to allow efficient analysis of delamination effects. Both three and four point bending tests were used to determine the effect of delaminations on laminate bending stiffness. The effect of delaminations of the free vibration response was determined using experimental modal analysis. Degradation of the buckling loads was determined by three separate techniques. In the first technique, an axial load was applied to the samples and the lateral deflection was measured. The second technique by which the buckling load degradation was determined was through the use of unloaded free vibration test results. The final method made use of free vibration data which was collected with the samples under various levels of axial load. Dissert. Abstr.

N89-12669 Drexel Univ., Philadelphia, Pa.
MIXED-MODE FRACTURE IN FIBER-REINFORCED COMPOSITE MATERIALS Ph.D. Thesis
Wieslaw Kazimierz Binienda 1987 212 p
Avail: Univ. Microfilms Order No. DA8806511

The problems of mixed-mode crack extension in unidirectionally fiber-reinforced composite materials are examined. Previous studies on this subject were aimed at establishing an appropriate criterion for mixed-mode matrix fracture by using specimens in the form of multilayer laminates. One common difficulty encountered was the strong dependence of fracture on specimen geometry due to insufficient analytical rigor in formulating and solving the test problems. This results in different criteria for different specimen geometries. This difficulty is being circumvented by devising a combined analytical, numerical, and experimental effort. Specifically, the analytical problem concerns a line crack which is situated in an infinite orthotropic plate; the crack makes an arbitrary angle with the fibers and the plate is loaded in uniform tension normal to the crack. The numerical effort involves developing a finite element solutions of the same problem. An the accuracy of the finite element solutions depends on the particular scheme used, an optimum scheme can be turned through comparisons with the analytical solutions. The experimental effort involves testing specimens with similar crack configurations and crack extension characteristics. Fracture analysis of the experimental data by the tuned finite element scheme provides the necessary correlation for a criterion. The results suggest that the total energy release G sub Tau is a proper criterion for mixed-mode cracking in laminates made of graphite-epoxy composite. Dissert. Abstr.

N89-12670# National Bureau of Standards, Boulder, Colo. Chemical Engineering Science Div.
ROUND-ROBIN MEASUREMENTS OF THE APPARENT THERMAL CONDUCTIVITY OF TWO REFRACTORY INSULATION MATERIALS, USING HIGH-TEMPERATURE GUARDED-HOT-PLATE APPARATUS
J. G. Hust and D. R. Smith Apr. 1988 31 p Sponsored by ORNL, Tenn.
(PB88-215421; NBSIR-88-3087) Avail: NTIS HC A03/MF A01 CSCL 11D

Test results and analysis are presented of round-robin measurements of apparent thermal conductivity for two kinds of refractory insulation board using high-temperature guarded-hot-plate apparatus. The round robin was carried out under the sponsorship of the American Society for Testing and Materials (ASTM) Subcommittee C-16.30 on Thermal Measurements. To complete the measurement program in a timely manner the participants chose to measure different specimens, selected, however, from the same production lot. The test results for apparent thermal conductivity illustrate the inter-laboratory reproducibility as well as the temperature and density dependence. The data include the temperature range from 297 to 773 K. The standard deviation is 7.4 percent for the 48 test results reported by seven participating laboratories for fibrous alumina-silica. The standard deviation is 8.0 percent for the 58 test results reported for calcium silicate.
GRA

N89-12671 Illinois Univ., Urbana-Champaign.
PREDICTION OF FIBER ORIENTATION DURING PROCESSING OF SHORT FIBER COMPOSITES Ph.D. Thesis
Suresh Gopaldas Advani 1987 231 p
Avail: Univ. Microfilms Order No. DA8802973

The fiber orientation pattern created by the flow of a suspension of short fibers controls the physical and mechanical properties of a short fiber composite material. The orientation of the fibers at any point in the composite plays the role of a structural state variable. Two sets of even-order tensors are used to describe the distribution of orientation of fibers in suspensions and composites containing short rigid fibers. These orientation tensors offer a description which is concise, unambiguous and independent of coordinate system. They provide very efficient calculations for planar orientations and make the prediction of 3-D orientation states feasible. Equations of change for the tensors are derived to predict the orientation of fibers caused by flow during processing. The accuracy of various closure approximations is explored through calculations of mechanical properties of solid composites and the dynamics of orientation in flowing suspensions. A hybrid closure approximation, which combines previous linear and quadratic forms, is introduced. It performs best and permits the use of the second order tensor alone. A Galerkin finite element method is formulated for solution of the equations of change in arbitrary 2-D geometries. A computer simulation is developed, which can perform fiber orientation predictions for the compression mold filling process.
Dissert. Abstr.

N89-12672 Minnesota Univ., Minneapolis.
FINITE ELEMENT ANALYSIS OF COMPOSITE LAMINATES Ph.D. Thesis
Li-ren Tsau 1987 177 p
Avail: Univ. Microfilms Order no. DA8802424

Since composite materials are heterogeneous and anisotropic, the analysis of structural elements made of composites is more difficult than that for those made of homogeneous and isotropic materials. Using the macromechanics approach, a finite element analysis can be used to study the behavior, such as stress distribution and failure analysis, and the effects of the constituent materials are considered only as averaged apparent properties. A three-dimensional finite element computer program was developed for fiber-reinforced laminates. A symmetric eight layer fiber-reinforced composite lamniate of SP-286T300 material with a central hole was adopted for the comparison of analytic with experimental results. Composite material can sustain much higher load after the occurrence of localized damage owing to the features

of heterogeneity and anisotropy. A failure criterion first proposed by Hashin was used because the fiber and matrix mode failure can be predicted separately in the damaged elements. Progressive failure of the elements can be predicted with finite element analysis. Both values of the load for final catastrophic failure and the failure pattern in progressive failure simulation compare well with experimental results. Dissert. Abstr.

N89-12673 Michigan Univ., Ann Arbor.
SHORT FIBER REINFORCED THERMOPLASTICS Ph.D. Thesis
Bora Tekkanat 1987 178 p
Avail: Univ. Microfilms Order No. DA8801430

The PS-PPO blend system was studied systematically as a model matrix system to provide some understanding of special problems associated with short fiber reinforced thermoplastics (SFRTPs). Mechanical properties and failure behavior of short fiber composites are complicated by the nonuniformity of the fiber length, distribution of the fiber orientation, and fiber and configurations. One objective was to explore the simplest predictive theories for composite stiffness and strength in injection molded SFRTP materials which would be easy to use and would be accurate over a wide range of materials. The intention was also to try to understand the predicted dependence of stiffness and strength on fiber length for SFRTPs. The effects of matrix ductility on the mechanical properties and failure mechanisms of SFRTPs were investigated by controlling the matrix ductility via composition in PS-PPO system. In addition to the matrix ductility, consideration was given to the following parameters: fiber length distribution, fiber orientation distribution, fiber volume fraction, aspect ratio, and fiber end configuration to understand the role they play on the mechanical properties, efficiency of reinforcement, and failure mechanisms of SFRTPs. Subsurface analysis by transmission optical microscopy under polarized light was utilized along with fracture surface analysis and found to be a useful technique in determining the detailed microdeformation mechanisms of both matrix and short fiber reinforced systems. Dissert. Abstr.

N89-12674 Virginia Polytechnic Inst. and State Univ., Blacksburg.
AN AXISYMMETRIC LINEAR/HIGH-ORDER FINITE ELEMENT FOR FILAMENT WOUND COMPOSITE STRUCTURES Ph.D. Thesis
Craig A. Rogers 1987 205 p
Avail: Univ. Microfilms Order No. DA8804423

The development of an axisymmetric linear by high-order finite element to model filament-wound structures is presented. The primary objective was to develop a design code to analyze filament wound spherical pressure vessels. In order to develop a design-oriented analysis capability which can produce accurate results rather quickly with reduced input-data requirements, the total number of system equations must be reduced. To accomplish this task, a linear by high-order element was formulated which uses a single high-order displacement field finite element to model the total thickness of an axisymmetric composite structure. The displacement order for the in-plane direction remains linear, while the transverse order is user selectable. Numerical integration for stiffness is evaluated with respect to varying material properties and lamina thicknesses in each individual element. The accuracy of the element was evaluated by comparing the finite element results to elasticity solutions for isotropic, orthotropic, and filament-wound cylindrical pressure vessels. Also presented is an outline of the design code and sample results for spherically wound pressure vessels. Dissert. Abstr.

N89-12675*# Forest Products Lab., Madison, Wis.
IMPROVING THE FATIGUE RESISTANCE OF ADHESIVE JOINTS IN LAMINATED WOOD STRUCTURES
Theodore L. Laufenberg, Bryan H. River, Lidija L. Murmanis, and Alfred W. Christiansen Aug. 1988 96 p
(Contract NASA Order C-80015-F; DE-AI01-76ET-20320)
(NASA-CR-182165; DOE/NASA/0015-1; NAS 1.26:182165)
Avail: NTIS HC A05/MF A01 CSCL 11D

The premature fatigue failure of a laminated wood/epoxy test beam containing a cross section finger joint was the subject of a multi-disciplinary investigation. The primary objectives were to identify the failure mechanisms which occurred during the finger joint test and to provide avenues for general improvements in the design and fabrication of adhesive joints in laminated wood structures. Author

N89-12676# Harvard Univ., Cambridge, Mass. Div. of Applied Sciences.
TOUGHENING BY ALIGNED, FRICTIONALLY CONSTRAINED FIBERS
Bernard Budiansky and John C. Amazigo Mar. 1988 24 p
(Contracts N00014-86-K-0753; N00014-84-K-0510)
(AD-A197194; MECH-119) Avail: NTIS HC A03/MF A01
CSCL 11D

The Mode-I fracture toughness of a brittle material reinforced by aligned brittle fibers is studied theoretically. The fibers are assumed to slip relative to the matrix when a critical interface shear stress is reached, and the toughening action of the fibers is presumed to be due to bridging of crack faces in the vicinity of the crack front. The toughening due to the fiber reinforcement is related to basic parameters associated with the related problem of steady-state matrix cracking in the presence of intact fibers. Bridge lengths at fracture and fracture resistance curves are calculated. GRA

N89-12677# SARMA Equipement Aviation, Saint-Vallier (France).
COMPOSITE RODS IN CARBON-EPOXY FIBREDUX 914 C/TS-6T-6K-34 Final Report [BIELLES COMPOSITES EN CARBONE EPOXY FIBREDUX 914 C/TS-6T-6K-34]
4 Jul. 1988 69 p In FRENCH
(Contract STPA-85-96-011-00-471-75-86)
(SARMA-TR-87-2431A; ETN-88-93314) Avail: NTIS HC A04/MF A01

Mechanical compression tests were performed in order to study the behavior of aircraft command rods as a function of the L/D ratio. The theoretical Euler and Euler-Johnson approaches were considered. The Euler Johnson theoretical curves are found to estimate better the observed phenomena, but anomalies remain for ratios of 50. It is concluded that the performance prediction is accurate enough to use the method as a design tool. ESA

N89-12678# SARMA Equipement Aviation, Saint-Vallier (France).
CARBON-EPOXY COMPOSITE RODS FIBREDUX 914 C/TS-6T-6K-34 Final Report [ETUDE DE COMPOSANTS MECANIQUES EN FIBRES DE CARBONE EPOXY FIBREDUX 914 C/TS-6T-6K-34]
B. Pruvost and J. C. Pourrat 31 Mar. 1988 36 p In FRENCH
(Contract STPA-84-96-013-00-471-75-86)
(SARMA-TR-872429-A; ETN-88-93315) Avail: NTIS HC A03/MF A01

The characterization of composite material rods used in servomechanisms for aircraft construction is investigated. Different rod sizes are studied with different specimen geometries in carbon fiber and glass fiber composites. Compression tests were performed for different rod lengths. The computed values agree with the observed results. The environment and aging actions are found significant, and must be included in the computation procedures. ESA

N89-12679# Los Alamos National Lab., N. Mex.
SYNTHESIS AND CHARACTERIZATION OF VLS-DERIVED SILICON CARBIDE WHISKERS
P. D. Shalek, D. S. Phillips, D. E. Christianson, J. D. Katz, W. J. Parkinson, and J. J. Petrovic 1988 11 p Presented at the International Conference on Whisker- and Fiber-toughened Ceramics, Oak Ridge, Tenn., 7 Jun. 1988
(Contract W-7405-eng-36)
(DE88-016226; LA-UR-88-2536; CONF-8806103-2) Avail: NTIS HC A03/MF A01

Silicon carbide (SiC) whiskers have great potential, some already

realized, in reinforcing ceramic matrix composites to give significant improvements in toughness and strength. Los Alamos has been developing the vapor-liquid-solid (VLS) process to grow single crystal BETA-SiC fibers having relatively few defects and diameters of from 3 to 5 microns and lengths up to 100 mm. These whiskers have superb mechanical properties-strengths up to 16 GPa (2.3 Msi) and elastic modulus of 580 GPa (84 Msi) - and should have excellent stability at high temperatures. Two basic synthesis routes were investigated: (1) in situ SiO generation, and (2) external gaseous Si source. Process 1 had a much more extensive prior developmental history and has been developed at Los Alamos to the point where significant and reproducible yields of prime whiskers can be obtained and scaleup could be considered. What we have learned about this process and its product will be the subject of this paper. DOE

N89-12680# Los Alamos National Lab., N. Mex.
SiC WHISKER-REINFORCED MoSi2 Ph.D. Thesis
David H. Carter Sep. 1988 140 p
(Contract W-7405-eng-36)
(DE88-016674; LA-11411-T) Avail: NTIS HC A07/MF A01

The mechanical characteristics of an intermetallic matrix with two different reinforcements were studied. The matrix materials was MoSi2, with two different reinforcements, Los Alamos VLS SiC whiskers and Huber VS SiC whiskers. The purpose of the reinforcement was to provide toughening at ambient temperature and strengthening at elevated temperatures. The VLS whiskers doubled the strength of the matrix at 1200 C, and greatly improved the ambient temperature toughness of the matrix. The VS whiskers were added because they are much smaller in length and diameter, and therefore decreased the mean free path between whiskers, at the same volume fraction. The VS whiskers improved the toughness of the matrix at ambient temperature, and more than tripled the strength of MoSi2 at elevated temperatures. The high strength of this new composite places this material in the realm of attractive engineering materials for high-temperature applications. A method to quantitatively describe fracture surfaces was used to study these composites. This induced the use of 3-D representations of the fracture surface, from which quantitative information about the roughness was obtained. DOE

N89-12681*# Virginia Polytechnic Inst. and State Univ., Blacksburg. Center for Composite Materials and Structures.
COMBINED MECHANICAL LOADING OF COMPOSITE TUBES
Mark S. Derstine, Marek-Jerzy Pindera, and David E. Bowles Jun. 1988 200 p
(Grant NAG1-343)
(NASA-CR-183012; NAS 1.26:183012; CCMS-88-11; VPI-E-88-18) Avail: NTIS HC A09/MF A01 CSCL 11D

An analytical/experimental investigation was performed to study the effect of material nonlinearities on the response of composite tubes subjected to combined axial and torsional loading. The effect of residual stresses on subsequent mechanical response was included in the investigation. Experiments were performed on P75/934 graphite-epoxy tubes with a stacking sequence of (15/0/ + or - 10/0/ -15), using pure torsion and combined axial/torsional loading. In the presence of residual stresses, the analytical model predicted a reduction in the initial shear modulus. Experimentally, coupling between axial loading and shear strain was observed in laminated tubes under combined loading. The phenomenon was predicted by the nonlinear analytical model. The experimentally observed linear limit of the global shear response was found to correspond to the analytically predicted first ply failure. Further, the failure of the tubes was found to be path dependent above a critical load level. Author

N89-12682# SARMA Equipement Aviation, Saint-Vallier (France). Dept. Equipements Aeronautiques.
DAMAGE OF CARBON FIBER TUBES AND RODS Final Report [ENDOMMAGEMENT DE TUBES ET BIELLES EN FIBRES DE CARBONE]
J. C. Pourrat and B. Pruvost 15 Mar. 1988 32 p In FRENCH
(Contract STPA-86-96-028-00-471-75-86)
(SARMA-TR-882401; ETN-88-93313) Avail: NTIS HC A03/MF A01

The behavior of fiber composite servomechanism elements used in aircraft construction is investigated. Typical defects were induced in order to verify the effects on static and dynamic performance. Tubes of 35 and 50 mm diameter and 300 to 600 mm long were prepared, both with and without defects. The tests performed included Euler Johnson theoretical curves and standard compression tests. The general dispersion of results is larger for the 35 mm tubes for any length. The correlation between defects and effective failure is highly significant. ESA

N89-12683# Aerospatiale, Suresnes (France). Direction de la Qualite.
SHOCK DETECTION IN COMPOSITE STRUCTURES. TEST REPORT 48-915/F [DETECTION DES CHOCS SUR STRUCTURES COMPOSITES. PROCES-VERBAL 48-915/F]
J. Odorico, D. Lecuru, and J. P. Choffy 26 May 1988 65 p In FRENCH
(Contract STPA-86-96-009)
(Rept-48-915/F; ETN-88-93318) Avail: NTIS HC A04/MF A01

Nondestructive methods used to evaluate damage after impact in composite materials are compared. The methods include high frequency ultrasonics, low frequency ultrasonics (400 kHz), and eddy currents. The evaluation of the delaminated surface is made accurately with the high frequency ultrasonics only. In that case the ultrasonics are coupled with a SIAM R-Theta system. No method allows the detection of stiffener break. That is possible using X-ray control. ESA

N89-12684*# National Aeronautics and Space Administration. Lewis Research Center, Cleveland, Ohio.
A PROBABILISTIC APPROACH TO COMPOSITE MICROMECHANICS
T. A. Stock, P. X. Bellini, P. L. N. Murthy (Cleveland State Univ., Ohio.), and C. C. Chamis [1988] 21 p Presented at the 29th Structures, Structural Dynamics and Materials Conference, Williamsburg, Va., 18-20 Apr. 1988; sponsored by AIAA, ASME, ASCE, AHS and ACS Previously announced in IAA as A88-32312
(NASA-TM-101366; E-4405; NAS 1.15:101366) Avail: NTIS HC A03/MF A01 CSCL 11D

Probabilistic composite micromechanics methods are developed that simulate expected uncertainties in unidirectional fiber composite properties. These methods are in the form of computational procedures using Monte Carlo simulation. A graphite/epoxy unidirectional composite (ply) is studied to demonstrate fiber composite material properties at the micro level. Regression results are presented to show the relative correlation between predicted and response variables in the study. Author

N89-12755# Johns Hopkins Univ., Baltimore, Md. Dept. of Materials Science.
CHARACTERIZATION OF GRAPHITE FIBERS BY X-RAY DIFFRACTION Final Report
Peter Arsenovic *In* Universal Energy Systems, Inc., United States Air Force Graduate Student Summer Support Program, Volume 1 Dec. 1987 20 p (For primary document see N89-12754 04-31) Avail: NTIS HC A99/MF E03 CSCL 11D

25 INORGANIC AND PHYSICAL CHEMISTRY

Includes chemical analysis, e.g., chromatography; combustion theory; electrochemistry; and photochemistry.

For related information see also *77 Thermodynamics and Statistical Physics.*.

N89-12685 Drexel Univ., Philadelphia, Pa.
SPARK IGNITION OF MONODISPERSE FUEL SPRAYS Ph.D.

Thesis
Allen Michael Danis 1987 147 p
Avail: Univ. Microfilms Order No. DA8800630

Spark ignition energy requirements were studied with a monodisperse spray system allowing independent control of droplet size, equivalence ratio, and fuel type. Minimum ignition energies were measured for n-heptane and methanol sprays characterized at the spark gap in terms of droplet diameter. The droplet diameter was varied. In addition to sprays, minimum ignition energies were measured for completely prevaporized mixtures of the same fuels over a range of equivalence ratios to provide data at the lower limit of droplet size. Results showed that spray ignition was enhanced with decreasing droplet size and increasing equivalence ratio over the ranges of the parameters studied. By comparing the spray ignition and prevaporized ignition results, the existence of an optimum droplet size for ignition was indicated for both fuels. Fuel volatility was seen to be a critical factor in spray ignition. Spray ignition was observed to be probabilistic in nature, and ignition was qualified in terms of an ignition frequency for a given spark energy. The criterion for the minimum ignition energy was the spark energy which produced an ignition frequency of 50 percent. A model was developed to predict ignition frequencies based on the variation in spark energy and equivalence ration (number density) in the spark gap. Dissert. Abstr.

N89-12686# California Univ., Berkeley. Lawrence Berkeley Lab. Materials and Chemical Sciences Div.
QUANTUM MONTE CARLO CALCULATION OF THE PROPERTIES OF ATOMIC CARBON AND DIAMOND
S. Fahy, X. W. Wang, and S. G. Louie Jun. 1988 6 p Presented at the 19th International Conference on the Physics of Semiconductors, Warsaw, Poland, 1 Aug. 1988
(Contract DE-AC03-76SF-00098)
(DE88-014659; LBL-25544; CONF-880884-2) Avail: NTIS HC A02/MF A01

A new method of calculating total energies of solids using non-local pseudopotentials in conjunction with the variational quantum Monte Carlo approach is presented. By using pseudopotentials, the large fluctuations of the energies in the core region of the atoms which occur in quantum Monte Carlo all-electron schemes are avoided. The method is applied to calculate the cohesive energy and structural properties of diamond and the first ionization energy and electron affinity of the carbon atom. Results are in excellent agreement with experiment. DOE

N89-12687 Council for National Academic Awards (England).
STABILITY LIMITS AND COMBUSTION MEASUREMENTS IN LOW CALORIFIC VALUE GAS FLAMES Ph.D. Thesis
Rooktabir Mandan Sauba 1987 223 p
Avail: Univ. Microfilms Order No. BRD-80893

A Hilton combustor was substantially modified to a suitable symmetrical configuration for research purposes. Provisions for swirl, preheat, and injection of LCV gases were incorporated with appropriate burner management systems for safe operation. Instrumentation for temperature, velocity, and concentration measurements was developed and fully automated by interfacing to a microprocessor for rapid data acquisition. Flame stability limits were determined over a wide range of operating conditions by varying swirl, secondary air temperature, and excess air levels while maintaining the burner momentum constant. With LCV gas flames the excess air factor (EAF) had a major influence on values of temperature, species concentration, and velocity. The combustion data were analyzed to extract the characteristic mixing and chemical reaction times the ratio of which gave the parameter epsilon, originally proposed for uncontrolled flames. Dissert. Abstr.

N89-12688# Massachusetts Inst. of Tech., Cambridge. Dept. of Materials Science and Engineering.
LEC (LIQUID ENCAPSULATED CZOCHRALSKI) GROWTH OF InP WITH MAGNETIC FIELD ASSISTED MELT STABILIZATION AND HEAT TRANSFER CONTROL Final Technical Report, Jan. 1984 - Feb. 1987
August F. Witt Feb. 1988 59 p
(Contract F19628-84-K-0011)
(AD-A196748; RADC-TR-88-27) Avail: NTIS HC A04/MF A01 CSCL 07B

The research focuses on the optimization of InP growth by the Liquid Encapsulated Czochralski (LEC) technique using magnetic fields for melt stabilization and heat pipes for the control of critical thermal fields. GRA

N89-12689# Utah Univ., Salt Lake City.
THE CONVERSION OF SMALLER BORANE FRAGMENTS TO LARGER STRUCTURES. SYSTEMATICS OF BORON HYDRIDE REACTIONS Final Report, 1 Jan. 1985 - 31 Mar. 1988
Robert W. Parry and Goji Kodama 24 Jun. 1988 100 p
(Contract DAAG29-85-K-0034)
(AD-A197068; ARO-22381.15-CH) Avail: NTIS HC A05/MF A01 CSCL 07C

The borane framework expansion reaction by the use of B2H4.2P (CH3)3, was developed to be a more general type of reaction. The B2H4 adducts containing Lewis bases other than P(CH3)3 were tested for the expansion reaction or used to interpret formations of higher borane compounds. The formation of B5H11.PH2(-) from B4H8.PH3 and NaBH4 is cited as a case of new in situ BH3 addition to borane species. A further insight into the formation of the B2H4 adducts from the B3H7 adduct was obtained. The treatment of B3H7.S(CH3)2 with N(CH3)3 in CH2Cl2 at -80 C resulted in the immediate formation of B2H4.2N(CH3)3, suggesting that the same type of reaction might be advantageously used to prepare thermally unstable B2H4 adducts. The number of homolog series of polyboron complex cations has now been increased to five. Similarities and differences in reactivities between these cationic species and the corresponding isoelectronic, neutral borane species have been encountered. Preparation of polyboron complex cations containing SR2 was intended. The B3H6-2S(CH3)(2+) cation was tentatively identified. GRA

N89-12690# Clarkson Univ., Potsdam, N.Y. Dept. of Chemistry.
HOMOGENEOUS CATALYTIC PRODUCTION OF HYDROGEN AND OTHER MOLECULES FROM WATER-DMF (N-DIMETHYLFORMAMIDE) SOLUTIONS Technical Report No. 4
James Y. Yu, Serge Schreiner, and L. Vaska 8 Jul. 1988 12 p
(Contract N00014-84-K-0658)
(AD-A197072) Avail: NTIS HC A03/MF A01 CSCL 07D

The reaction between water and DMF at 100 C under nitrogen (less than 1 atm) mediated by platinum, ruthenium, osmium, rhodium or iridium complexes leads to the evolution of H2, CO2, and CO as a minor product; Me2NH is also obtained, but it reacts in situ with one half of the CO2 produced to yield (Me2NH2)+(Me2NC(O)O)-. The various possible steps in this complex catalytic system are briefly examined. We wish to report a non-photochemical, non-electrochemical catalysis of hydrogen evolution from aqueous solutions at mild conditions. GRA

N89-12691# Texas Univ., Austin.
ELECTROGENERATED CHEMILUMINESCENCE Final Report, 15 Apr. 1985 - 14 Apr. 1988
Allen J. Bard Jun. 1988 10 p
(Contract DAAG29-85-K-0104)
(AD-A197163; ARO-22448.9-CH) Avail: NTIS HC A02/MF A01 CSCL 07B

Electrogenerated chemiluminescence (ECL) has been investigated in a variety of systems under various conditions. Eleven completed publications plus one manuscript in preparation address the following areas: (1) ECL of novel inorganic complexes. (2) ECL from peroxyoxalate/luminescer systems. (3) ECL in micelle systems. (4) ECL at polymer modified electrodes. (5) Electroluminescence at semiconductor electrodes. (6) ECL from systems containing no added luminescer. (7) Inverse photoemission from metal electrodes. GRA

N89-12692# Naval Postgraduate School, Monterey, Calif.
FIRE SPREAD IN A THREE-DIMENSIONAL PRESSURE VESSEL WITH RADIATION EXCHANGE AND WALL HEAT LOSSES
J. Raycraft, M. D. Kelleher, H. Q. Yang, and K. Y. Yang 1 Aug. 1988 60 p Prepared in cooperation with Notre Dame Univ., Ind.
(AD-A197271; AD-E900802; NPS-69-88-008) Avail: NTIS HC A04/MF A01 CSCL 20M

A three dimensional differential field model for the spread of fire and smoke, on general orthogonal coordinate systems is developed. The model, which is designed for closed spaces, also includes the physical effects of turbulence, strong buoyancy, full compressibility, pressure rise due to fire loading, surface-surface and surface-flame radiation exchange, and heat losses through the wall. It is based on a control-volume staggered-cell finite-difference approach with primitive variables. Results of numerical calculations based on the field model are compared with test data for a methanol fire in the NRL FIRE I test facility which is in the form of a closed pressure vessel. Reasonable comparisons of the resulting pressure and temperatures at several locations have been obtained. Also shown are the detailed velocity and temperature fields inside the vessel at different time instants after the commencement of the fire. GRA

N89-12693# M L Energia, Inc., Princeton, N.J.
RADIATIVE AUGMENTED COMBUSTION Final Technical Report, 15 Jul. 1983 - 31 May 1987
Moshe Lavid 1 Mar. 1988 34 p
(Contract F49620-85-C-0145)
(AD-A197300; AFOSR-88-0494TR) Avail: NTIS HC A03/MF A01 CSCL 21B

Many combustion applications are presently limited by constraints such as flammability, flame propagation, ignition and stability imposed by the combustion process itself. Consequently much attention is being given to techniques which can augment combustion by extending these limits. One such promising technique is Radiative Augmented Combustion. It is based on the fact that radiation of selected wavelengths is capable of photodissociating stable molecule, combustion intermediates and other inhibiting species into reactive radicals. Subsequent increases in concentration of these radicals can modify the overall kinetics and produce radiative ignition and combustion enhancements. The potential of this technique was previously demonstrated under static conditions. GRA

N89-12694# Army Armament Research, Development and Engineering Center, Watervliet, N.Y.
DETERMINATION OF SULFURIC ACID, OXALIC ACID, AND THEIR MATRIX EFFECTS IN ALUMINUM ANODIZING SOLUTIONS BY ION CHROMATOGRAPHY Final Report
Samuel Sopok Jun. 1988 14 p
(AD-A197734; ARCCB-TR-88026) Avail: NTIS HC A03/MF A01 CSCL 11C

Anodizing and hardcoating (hard anodizing) of aluminum improve corrosion and wear resistance. Acid concentrations (sulfuric, oxalic), pH, and physical plating variables (current, temperature, time) affect oxide coating thickness, porousness, hardness, solubility, and conductivity. Hardcoating solutions typically contain 120 to 160 g/l sulfuric acid (H2SO4) and 12 to 21 g/l oxalic acid (H2C2O4), while anodizing solutions typically contain 160 to 200 g/l H2SO4. Lower acid concentration hardcoating solutions give oxide coatings that are thicker, harder, less porous, less soluble, and more wear resistant compared to higher acid concentration anodizing solutions. Sodium hydroxide (NaOH) and hydrochloric acid (HC1) are commonly used to adjust the pH of these metal finishing solutions. The acids and sodium salts of sulfate and oxalate have been determined in a variety of matrices, although not for anodizing and hardcoating solutions. A reference standard for instrumental analysis of sulfate or oxalate ions is commonly made from either the acids or the sodium salts. Anodizing and hardcoating sample solution acids and sodium salts are present for these analytes and cause matrix effects when compared to the reference standards. GRA

N89-12695# Massachusetts Inst. of Tech., Cambridge. Dept. of Physics.
SURFACE STRUCTURES AND TRANSITIONS AND THE EVOLUTION FROM FIRM TO BULK BEHAVIOR Final Report, 11 Mar. 1985 - 10 Mar. 1988
Robert J. Birgeneau and A. N. Berker 22 Jul. 1988 9 p
(Contract DAAG28-85-K-0058)
(AD-A197788; ARO-21732.7-PH) Avail: NTIS HC A02/MF A01 CSCL 07D

This research program has concentrated on two main areas of research: the structures and transitions of monolayers and multilayers of rare gases including krypton and xenon on single crystal graphite and the thermal roughening of simple metal surfaces. The simple systems of rare gases on a triangular surface have shown a remarkable variety of solid phases. This is due to the substrate potential which may have a slightly different periodicity from the bulk phase of the adsorbed species. Advances in cell powder design, together with high brightness synchrotron radiation X-ray sources, have made possible studies on one single crystal substrate; this allows one to investigate the structures and orientations of these solid layers in fine detail. Xenon monolayers on a single crystal graphite surface and investigated using beam-line X-20A. A 1 mm x 1 mm focused beam is used with an Di double monochromator and a Ge analyzer. GRA

N89-12696# Missouri Univ., Rolla. Chemical Research, Development and Engineering Center.
OPTICAL CONSTANTS OF MINERALS AND OTHER MATERIALS FROM THE MILLIMETER TO THE ULTRAVIOLET Contractor Report, Jun. 1985 - May 1987
R. J. Bell, R. W. Alexander, Jr., L. A. Newquist, R. VanDiver, M. A. Ordal, L. L. Long, and R. E. Paul Jun. 1988 138 p
(Contract DAAA15-85-K-0004)
(AD-A197803; CRDEC-CR-88074) Avail: NTIS HC A07/MF A01 CSCL 08G

The optical constants of a wide variety of materials were measured for this contract period. This report covers the work done at the Univ. of Missouri-Rolla. The spectral range of the measurements covered from the millimeter to the ultraviolet. The millimeter and submillimeter (far infrared) measurements were made on the Rolla Campus and the infrared, visible and ultraviolet measurements were made on the Kansas City Campus. This wide spectral range means that Kramers-Kronig analyses can be made with better precision than when reflectance data is available only over a limited spectral range. The construction of a homodyning interferometer that is capable of measuring small (diameter approximately 1 cm) samples at millimeter wavelengths and samples that are highly absorbing. To our knowledge no other instruments with this capability exist. The measurement of refractive indices of gypsum, both as a single crystal and as a powder in the far and near infrared for use as a standard. The measurement of several types of graphite. We have found that Dixon 200-10 shows a large positive real part of the dielectric constant at low frequencies. This contradicts the usual free electron picture for graphite at low frequencies. GRA

N89-12697# Lawrence Livermore National Lab., Calif.
AUTOIGNITION CHEMISTRY OF N-BUTANE IN A MOTORED ENGINE: A COMPARISON OF EXPERIMENTAL AND MODELING RESULTS
W. J. Pitz, W. R. Leppard (General Motors Research Labs., Warren, Mich.), and C. K. Westbrook 20 Jun. 1988 27 p Presented at the Society of Automotive Engineers Fuels and Lubricants Meeting, Portland, Oreg., 10 Oct. 1988
(Contract W-7405-eng-48)
(DE88-014153; UCRL-98970; CONF-8810120-1) Avail: NTIS HC A03/MF A01

A detailed chemical kinetic mechanism was used to simulate the oxidation of n-butane/air mixtures in a motored engine. The modeling results were compared to species measurements

obtained from the exhaust of a CFR engine and to measured critical compression ratios. Pressures, temperatures and residence times were considered that are in the range relevant to automotive engine knock. The compression ratio was varied from 6.6 to 15.5 to affect the recycle fraction and the maximum pressure and temperature of the fuel/air mixture. Engine speeds of 600 and 1600 rpm were examined which corresponded to different fuel/air residence times. The relative yields of intermediate species calculated by the model matched the measured yields generally to within a factor of two. The residual fraction derived from the previous engine cycle had a significant impact on the overall reaction rate in the current cycle. The influence of different components in the residual fraction, such as the peroxides, on fuel oxidation chemistry during the engine cycle was investigated. DOE

N89-12698# Pacific Northwest Labs., Richland, Wash.
PREDICTION OF HEAT TRANSFER BETWEEN THE COMBUSTION SPACE AND THE LOAD
Dongmoon Kim and Tae-Ho Song Mar. 1988 22 p Presented at the 25th American Society of Mechanical Engineers/American Inst. of Chemical Engineers/American Nuclear Society National Heat Transfer Conference, Houston, Tex., 24 Jul. 1988
(Contract DE-AC06-76RL-01830)
(DE88-016313; PNL-SA-15359; CONF-880724-24) Avail: NTIS HC A03/MF A01

A computational model has been developed to examine two-dimensional flow and heat transfer in a combustion chamber with emphasis on the interaction between the combustion space and the load. The load is considered semitransparent to thermal radiation. Therefore, conduction and radiation through the load has been considered in the model. The heat flux incident on the load surface is calculated from the temperature field resulting from combustion and heat transfer simulation. Compressible flow and combustion phenomena, along with radiative and convective heat transfer, are simulated in a natural gas-fired combustion chamber. The results provide the temperature distribution and heat flux along the load surface. The study predicts the local peak heat flux to the load from the combustion space. DOE

N89-12699# Pacific Northwest Labs., Richland, Wash.
SUPERCRITICAL FLUID CHROMATOGRAPHY: THE EFFECT OF THE PARTIAL MOLAR VOLUME IN THE STATIONARY PHASE ON RETENTION
C. R. Yonker and R. D. Smith Jul. 1988 20 p Presented at the 12th International Symposium on Column Liquid Chromatography, Washington, D.C., 19 Jun. 1988
(Contract DE-AC06-76RL-01830)
(DE88-016959; PNL-SA-15424; CONF-880621-1) Avail: NTIS HC A03/MF A01

Retention in supercritical fluid chormatography (SFC) is a dynamic mechanism involving intermolecular interactions in the mobile phase and stationary phase. A simple thermodynamic model describing solute retention has been investigated based on the macroscopic thermodynamic variables of the solute partial molar volume in the stationary and mobile phases. Solute-solvent interactions in the mobile phase are dominant at lower pressures. Solute interaction with the five different stationary phases reflects the polarizability difference between these phases as shown by the partial molar volume of the solute in the stationary phase. DOE

N89-12700# State Univ. of New York, Stony Brook. Dept. of Mechanical Engineering.
NEW METHODS FOR LOCATING PHASE BOUNDARIES
George Fescos, John M. Kincaid, and Graham Morrison (National Bureau of Standards, Washington, D.C.) 1988 16 p
(Contract DE-FG02-87ER-13648)
(DE88-017084; DOE/ER-13648/3) Avail: NTIS HC A03/MF A01

A new geometric representation for the dew/bubble conditions of a special class of polydisperse fluids is used to develop series expansion representations for the location of the top of the dew/bubble and shadow curves, and for an expansion around the top of the dew/bubble and shadow curves. An excellent approximation for the 1-component van der Waals coexistence is given as a special illustration of the method. DOE

N89-12589*# National Aeronautics and Space Administration. Lewis Research Center, Cleveland, Ohio.
THE NASA ATOMIC OXYGEN EFFECTS TEST PROGRAM
Bruce A. Banks, Sharon K. Rutledge, and Joyce A. Brady *In* NASA, Goddard Space Flight Center, 15th Space Simulation Conference: Support the Highway to Space Through Testing 1988 p 51-65 (For primary document see N89-12582 04-18)
Avail: NTIS HC A21/MF A01 CSCL 07D

N89-12590*# National Aeronautics and Space Administration. Lyndon B. Johnson Space Center, Houston, Tex.
MATERIALS SELECTION FOR LONG LIFE IN LEO: A CRITICAL EVALUATION OF ATOMIC OXYGEN TESTING WITH THERMAL ATOM SYSTEMS
S. L. Koontz, J. Kuminecz, L. Leger, and P. Nordine *In* NASA, Goddard Space Flight Center, 15th Space Simulation Conference: Support the Highway to Space Through Testing 1988 p 66-88 (For primary document see N89-12582 04-18)
Avail: NTIS HC A21/MF A01 CSCL 07D

N89-12760# Tennessee Univ. Space Inst., Tullahoma. Dept. of Physics.
DIRECTED MOTION DOPPLER SHIFT EFFECTS ON NITRIC OXIDE (0.0) GAMMA BAND RESONANCE ABSORPTION Final Report
James A. Drakes *In* Universal Energy Systems, Inc., United States Air Force Graduate Student Summer Support Program, Volume 1 Dec. 1987 19 p (For primary document see N89-12754 04-31)
Avail: NTIS HC A99/MF E03 CSCL 07D

N89-12782# Georgia Inst. of Tech., Atlanta. School of Mechanical Engineering.
LIQUID SCINTILLATION COUNTING WITH THE PACKARD 1500 ANALYZER Final Report
Randal L. Mandock *In* Universal Energy Systems, Inc., United States Air Force Graduate Student Summer Support Program, Volume 1 Dec. 1987 11 p (For primary document see N89-12754 04-31)
Avail: NTIS HC A99/MF E03 CSCL 07D

26 METALLIC MATERIALS

Includes physical, chemical, and mechanical properties of metals, e.g., corrosion; and metallurgy.

N89-12701# Kawasaki Steel Corp., Kobe (Japan).
HIGHLY MAGNETIC POWDER
Shigeaki Takashiro and Yasunori Yonehana 1988 16 p Transl. into ENGLISH of Japanese Patent no. 61-238901 (24 Oct. 1986) 7 p
(Contract DE-AC05-84OR-21400)
(DE88-010838; ORNL/tr-88/14) Avail: NTIS HC A03/MF A01

The highly magnetic powder (Fe--magnetite) invention is a superior powder that can be used for electric wave absorber and electromagnetic shielding materials. Furthermore, since it possesses a high degree of saturated magnetization and weather resistance, it has sufficient fatigue resistance and can be used for the other purposes such as for carriers in dry copy machines. DOE

N89-12702# Virginia Univ., Charlottesville. Dept. of Materials Science.
IN-SITU OXIDATION OF NI3AI ALLOYS
K. R. Lawless, J. V. Cathcart, and E. A. Kenik (Oak Ridge National Lab., Tenn.) 1988 3 p Presented at the MAS/EMSA Microbeam Analysis Conference, Milwaukee, Wis., 7 Aug. 1988

(Contract DE-AC05-84OR-21400)
(DE88-007177; CONF-880841-3) Avail: NTIS HC A02/MF A01

Ni sub 3 Al is subject to dynamic embrittlement when tested in an oxidizing environment; whereas pre-oxidation under stress does not embrittle the alloy. In-situ high voltage electron microscopy (HVEM) oxidation studies of several ordered intermetallic (Ll sub 2 structure) Ni sub 3 Al alloys with small additions of boron and hafnium are reported. Electron microscopy studies of the oxidized specimens were also made to fully characterize the microstructure. Specimens were annealed and then electropolished to penetration just prior to insertion in the hot stage of the HVEM. Oxidations were carried out at an oxygen pressure of 13 to 60 mPa at 750 degree C. Gas pressure and composition were monitored with a residual gas analyzer. Specimens raised to the operating temperature in the base vacuum showed no indication of oxide in the diffraction pattern and were almost entirely free of dislocations. DOE

N89-12703# Oak Ridge National Lab., Tenn.
COBLE CREEP, CAVITY SINTERING AND CAVITY GROWTH
J. H. Schneibel and L. Martinez (Universidad Nacional Autonoma de Mexico, Cuernavaca.) 1988 13 p Presented at the Symposium on the Sintering of Advanced Ceramics, Cincinnati, Ohio, 1 May 1988
(Contract DE-AC05-84OR-21400)
(DE88-013846; CONF-8805164-1) Avail: NTIS HC A03/MF A01

The close relationships between Coble creep, cavity sintering and cavity growth are discussed. The measurement of size distributions of crack-like cavities is useful for determining grain boundary and surface diffusivities. In nickel aluminide (Ni3Al) intermetallics the grain boundary diffusivity determined in this manner agrees well with that obtained from Coble creep measurements. A critical comparison of the zero-creep technique and the zero-growth technique (critical cavity radius determination) to measure surface free energies is given. DOE

N89-12704# Los Alamos National Lab., N. Mex. Center for Materials Science.
AMORPHOUS POWDERS OF Al-Hf PREPARED BY MECHANICAL ALLOYING
R. B. Schwarz, J. W. Hannigan, H. Sheinberg, and T. Tiainen (Tampere Univ. of Technology, Finland) 1988 13 p Presented at the International Powder Metallurgy Conference and Exhibition, Orlando, Fla., 5 Jun. 1988
(Contract W-7405-eng-36)
(DE88-014459; LA-UR-88-1820; CONF-880667-2) Avail: NTIS HC A03/MF A01

The synthesis of amorphous Al50Hf50 alloy powder by mechanically alloying an equimolar mixture of crystalline powders of Al and Hf using hexane as a dispersant is described. The powder is characterized as a function of mechanical-alloying time by scanning electron microscopy, X-ray diffraction, and differential scanning calorimetry. Amorphous Al50Hf50 powder heated at 10 K/s crystallizes polymorphously at 1003 K into orthorhombic AlHf (CrB-type structure). During mechanical alloying, some hexane decomposes and hydrogen and carbon are incorporated into the amorphous alloy powder. The hydrogen can be removed by annealing the powder by hot pressing at a temperature approximately 30 K below the crystallization temperature. The amorphous compacts have a diamond pyramidal hardness of 1025 DPH. DOE

N89-12705 Council for National Academic Awards (England).
HIGH STRAIN RATE PROPERTIES OF STRUCTURAL ALUMINIUM Ph.D. Thesis
Talal Nayef Minwer AlHaddid 1987 385 p
Avail: Univ. Microfilms Order No. BRD-80668

A number of theories and techniques were used in the past to determine the stress-strain relationships of metals and alloys at high strain rates. Three aluminum alloys, HE15, HE30TF, and DTD5044 were investigated due to their importance in the aircraft, motor, and construction industries. En-8 steel was also investigated for the purpose of comparison. A simple approach using high velocity compression testing in conjunction with a finite-difference numerical technique was adopted, developed, used, and modified to suit different situations. Incremental compression tests were conducted on the materials to obtain the quasi-static stress-strain properties and used in the high strain rate deformation theoretical analysis and calculations. The temperature rise during deformation, specimen size, and deformation history were investigated and found to alter the material constants and therefore affect the flow stress. The approach caters for material inertia, strain hardening, strain rate sensitivity, friction, and temperature rise during deformation. This technique provides a simple, inexpensive method of obtaining the stress-strain characteristics of materials at high strain rates without sacrificing accuracy. Dissert. Abstr.

N89-12706# Portsmouth Gaseous Diffusion Plant, Ohio. Chemistry and Materials Technology Dept.
CORROSION OF NICKEL AND MONEL WELDS OF STEEL IN CHLORINE TRIFLUORIDE
S. L. Fout 25 Jul. 1988 14 p
(Contract DE-AC05-76OR-00001)
(DE88-014122; POEF-T-3487) Avail: NTIS HC A03/MF A01

Failures in the weld areas of nickel-plated steel pipe carrying chlorine trifluoride, ClF3, prompted this investigation to determine the effect of weld composition on corrosion by ClF3. Monel/steel and nickel/steel alloys of composition to simulate weld overlays were tested to determine their corrosion rates in ClF3 at 200 F and 300 F. For both nickel/steel and Monel/steel, the corrosion rate was higher at the higher temperature. For nickel/steel alloys at compositions up to 50 percent iron, which would cover a range considered normal for welding, the corrosion rate would be within acceptable limits. For Monel/steel alloys, compositions up to 35 percent iron have an acceptable corrosion rate. Above this, the corrosion would be greater than a tolerable amount. It should pose no problem to keep the heat input to the weld low enough to produce a Monel weld with an iron content below 35 percent. DOE

N89-12707# Kansas State Univ., Manhattan. Dept. of Chemistry.
THIN FILMS FROM SOLVATED METAL ATOMS AND METAL-METAL BONDED COMPOUNDS Final Report, Aug. 1985 - Aug. 1988
Kenneth J. Klabunde Jul. 1988 21 p
(Contract N00014-85-K-0821)
(AD-A197132) Avail: NTIS HC A03/MF A01 CSCL 07B

Metals such as Pd, Pt, Cu, Ag, Ga, In, Ge, Sn, and Pb are evaporated under vacuum and the vapors (atoms) condensed at 77 K with excess organic solvents. In this way solvated metal atoms are produced. Upon warmup to room temperature metal atom agglomeration occurs in certain solvents to yield stable colloidal particles in solution. In many cases these are the first examples of non-aqueous colloids of these metals, and they are very novel in that they are free of contaminating reducing agents, halide ions, etc., and they are living colloids--by removal of solvent metallic films can be grown on various substrates under very mile conditions. Characterizing these colloidal particles and the films therefrom is an important part of this project. A second area is the proposed synthesis of new metal-metal bonded compounds, eg. R2A1-A1R2, as possible new Chemical Vapor Deposition materials for thin film production. Unusual synthetic approaches, some involving metal vapors, are underway. Compounds containing Al, Ga, In, and level, is that two metal atoms could be deposited at a time on a hot substrate target, thereby generating films of novel structure/stoichiometry (when mixed metals are being codeposited). GRA

N89-12708# Arizona State Univ., Tempe. Dept. of Physics.
FRACTON DYNAMICS ON FRACTAL NETWORKS Annual Summary Report, Nov. 1987 - Jun. 1988
Ralph V. Chamberlin 6 Jul. 1988 3 p
(Contract N00014-88-K-0094)
(AD-A197166) Avail: NTIS HC A02/MF A01 CSCL 07B

An annual progress report of research on the dynamics of fractal systems is discussed. Accomplishments include construction, and initial testing, of a high-frequency susceptometer and SQUID magnetometer, capable of measurements from 0.01 to 100 MHz, and .000001 to 100,000 seconds. Preliminary investigations of 11.9 percent Au:Fe indicate the presence of large, strongly coupled, ferromagnetic domains which obey a stretched-exponential relaxation with a time constant t approx 10 to the 17th s. Future experiments and collaborations are discussed. GRA

N89-12709# Naval Postgraduate School, Monterey, Calif.
AN ELECTRON MICROSCOPY STUDY OF TWEED MICROSTRUCTURES AND PREMARTENSITIC EFFECTS IN HIGH DAMPING 53Cu45Mn2Al ALLOY M.S. Thesis
Larry L. Mayes Mar. 1988 62 p
(AD-A197317) Avail: NTIS HC A04/MF A01 CSCL 11F

The evolution of tweed microstructure upon aging a 53Cu45Mn2Al alloy was studied in the transmission electron microscope (TEM). Characteristic (110) tweed contrast develops after the alloy is aged for 4 hours or longer at 400 C, which apparently is just within the miscibility gap, and is then cooled to room temperature. The microstructure evolved is proposed to consist of a small proportion of Mn-rich regions in a Cu-rich matrix. As the phase separation proceeds, the Neel temperature and the FCC-to-FCT transition temperature both rise within these Mn-rich domains, and as a result they begin to display incipient lattice instabilities when observed at room temperature. This takes the form of a flickering effect in the TEM image. The flickering consists of consistent and repetitive contrast variations at specific locations in the microstructure. The significance of these microstructural features to damping is discussed. GRA

N89-12710# Applied Research Lab., State College, Pa.
INFLUENCE OF PROCESS PARAMETERS ON LASER WELD CHARACTERISTICS IN ALUMINUM ALLOYS Ph.D. Thesis
Nagesh Sonti Aug. 1988 179 p
(Contract N00024-85-C-6041)
(AD-A197398; TR-88-011) Avail: NTIS HC A09/MF A01 CSCL 11F

Multi-kilowatt CO2 lasers are increasingly being used for welding applications due to their capability of producing deep penetration welds at high welding speeds. Although most metals are being successfully welded, laser welding of aluminum alloys is proving to be difficult. Combination of high thermal diffusivity and optical reflectivity to CO2 laser radiation causes difficulty in coupling the laser energy to the material. Much higher laser intensities are required to ensure coupling and to form the keyhole, than to maintain the keyhole and obtain smooth fusion, as absorption of laser energy improves dramatically with the keyhole formation. Laser welds in aluminum alloys contain extensive porosity, and excessive vaporization of alloying elements occurs from the fusion zone. The welds have severe undercuts and large discontinuous cavities on the bead surface. A more precise control of the weld heat input and a better understanding of the influence of process parameters and the alloying content on the weld characteristics is required to improve the laser weldability of aluminum alloys. GRA

N89-12711# Advanced Communications Engineering Co., Altamonte Springs, Fla.
FUNDAMENTAL UNDERSTANDING OF THE INTRINSIC DUCTILITY IN NICKEL-BASE L12 TYPE ALLOYS Final Report, 15 Feb. 1986 - 14 Feb. 1988
C. C. Law, D. W. Shah, and J. Lin 30 Jun. 1988 84 p
(Contract F49620-86-C-0033)
(AD-A197605; PWA-FR-20424; AFOSR-88-0771TR) Avail: NTIS HC A05/MF A01 CSCL 11F

A basic approach for understanding the ductility behavior of intermetallics through studies of mechanical properties and dislocation characteristics of single crystals was applied to a nickel-base Li2 phase compound. Large single crystals of binary and tantalum-modified Ni3Al alloys with various stoichiometry were produced for tensile testing at 293 to 1144 K along four major orientations: (001), (011), (111) and (123). For the binary alloys the tensile ductility generally decreases with temperature for all orientations and reaches a minimum at about 1000 K for the nickel-rich (hypostoichiometric) alloy Al240. For a given temperature the ductility decreases in the order (110), (123), (001) and (111) in Al240. The ductility of the stoichiometric and hypostoichiometric binary alloys is lower and shows a more complex temperature and orientation dependence than Al240. GRA

N89-12712# Naval Ship Research and Development Center, Bethesda, Md. Ship Materials Engineering Dept.
FATIGUE CRACK GROWTH OF 5456-H116 ALUMINUM AND HSLA-80 WELDMENTS Research and Development Report, Sep. 1986 - Mar. 1988
L. R. Link Jul. 1988 31 p
(AD-A197830; DTRC/SME-88-39) Avail: NTIS HC A03/MF A01 CSCL 11F

Fatigue crack growth rate experiments were performed on 4W-type compact tension specimens of baseplate and weldments of 5556-H116 Al and of baseplate and HAZ of HSLA-80 steel. Stress ratios for the tests were 0.1 for both materials with the Al weld also being tested at R=0.5. Crack opening levels were determined for both the weld and baseplate in the aluminum material and for the A710 material in the as-welded and as-stress relieved conditions. The fatigue crack growth rates, when using the total applied load, of the welds and HAZ were significantly less than those of plate for both materials. Using the effective stress intensity at the crack tip, results in a shift of the da/dN versus delta K curves to a faster growth rate. Comparison of the curves show that the fatigue crack growth rates of the aluminum material fall in the same scatter band of data for baseplate, and for the HSLA-80 material the growth rate of the HAZ is shifted to faster growth rates than the baseplate. This shift of data leads to more conservative estimates on fatigue life. GRA

N89-12713# Oak Ridge National Lab., Tenn.
IRRADIATION-ASSISTED STRESS CORROSION CRACKING AND GRAIN BOUNDARY SEGREGATION IN HEAT TREATED TYPE 304SS
A. J. Jacobs, R. E. Clausing, L. Heatherly, and R. M. Kruger (General Electric Co., San Jose, Calif.) 1988 32 p Presented at the 14th International Symposium on Effects of Radiation and Materials, Andover, Mass., 27 Jun. 1988
(Contract DE-AC05-84OR-21400)
(DE88-008382; CONF-880613-3) Avail: NTIS HC A03/MF A01

Evidence was obtained correlating the susceptibility of Type-304 stainless steel (SS) to irradiation-assisted stress corrosion cracking (IASCC) and grain boundary segregation. IASCC susceptibility was measured in constant extension rate tensile (CERT) tests, and grain boundary segregation was demonstrated by Auger Electron Spectroscopy and HNO sub 3/Cr (+6) corrosion tests. DOE

N89-12714# California Univ., Berkeley. Lawrence Berkeley Lab. Center for Advanced Materials.
MECHANICAL HEHAVIOR OF SUPERPLASTICALLY-FORMED Al-Cu-Li-Zr ALLOY 2090
J. Glazer, T. G. Nieh, J. Wadsworth (Lockheed Missiles and Space Co., Palo Alto, Calif.), and J. W. Morris, Jr. May 1988 16 p Presented at the MRS International Meeting on Advanced Materials, Tokyo, Japan, 30 May 1988
(Contract DE-AC03-76SF-00098)
(DE88-016241; LBL-25020; CONF-880529-5) Avail: NTIS HC A03/MF A01

The design, manufacture and post-forming analyses of a complex shape produced by superplastic forming of the aluminum-lithium alloy 2090 are described. With appropriate prior thermomechanical processing to produce fine-grained superplastic sheet, this alloy displays excellent superplastic properties at commercially desirable strain rates and temperatures of formed and unformed sheet after solution heat treatment and aging was investigated. In both cases, tensile properties improve significantly at low temperatures over their room temperature values. However,

these increases are not accompanied by an increase in fracture toughness at low temperature over the moderate value measured at room temperature. DOE

N89-12715# Maryland Univ., College Park. Dept. of Physics and Astronomy.
ADSORPTION ON METAL SURFACES Final Report
Theodore L. Einstein, Rolfe E. Glover, III, and Robert L. Park 1987 13 p
(Contract DE-FG05-84ER-45071)
(DE88-016557; DOE/ER-45071/T1) Avail: NTIS HC A03/MF A01

This report discusses the progress at the University of Maryland Department of Physics on the adsorption of atoms or molecules on the surfaces of metals. Also discussed are phase transformation studies; the use of transfer matrices to study the 2-d, 3-state chiral Potts model; electron-induced ionization of core electrons of atoms; the reflected electron energy loss fine structure above the M sub 2,3 core excitation edge of Cu; and other research in atomic and solid state physics. DOE

N89-12716# Ohio State Univ., Columbus. Dept. of Metallurgical Engineering.
IN-SITU HIGH TEMPERATURE OXIDATION STUDIES Final Technical Report
Robert A. Rapp Aug. 1988 12 p
(Contract DE-FG02-84ER-45136)
(DE88-017092; DOE/ER-45136/2) Avail: NTIS HC A03/MF A01

The growth of oxidation scales on the pure metals iron and copper were examined. Professor Rapp (with B. Pieraggi) developed a new theory to explain the annihilation of vacancies and stress generation in the growth of cation/vacancy diffusing scales on pure metals. Results are briefly discussed. DOE

N89-12717*# National Aeronautics and Space Administration. Lewis Research Center, Cleveland, Ohio.
INFLUENCE OF ALLOYING ELEMENTS ON THE OXIDATION BEHAVIOR OF NbAl3
M. G. Hebsur (Sverdrup Technology, Inc., Cleveland, Ohio.), J. R. Stephens, J. L. Smialek, C. A. Barrett, and D. S. Fox 30 Sep. 1988 14 p Presented at the Workshop on the Oxidation of High-Temperature Intermetallics, 22-23 Sep. 1988; sponsored in part by NASA-Lewis Research Center, ASM International, Case Western Reserve Univ., The Metallurgical Society of AIME and TMS-AIME, Cleveland
(NASA-TM-101398; E-4275; NAS 1.15:101398) Avail: NTIS HC A03/MF A01 CSCL 11F

NbAL3 is one candidate material for advanced aeropropulsion systems because of its high melting point, low density, and good oxidation resistance. Although NbAl3 has the lowest oxidation rate among the binary Nb-Al alloys, it does not form exclusive layers of protective Al2O3 scales. Recently Perkin et al., have shown the feasibility of forming alumina scales on Nb-Al alloys at greatly reduced Al contents. However, the objective was to maintain the high Al content, and hence low density, while achieving the capability of growing protective alumina scales. Alloy development followed approaches similar to those used successfully for superalloys and oxidation resistant MCrAlY coatings. Among the three elements examined (Ti, Si, and Cr) as ternary additions to Nb-Al3, Cr was the most effective in favoring the selective oxidation of Al. Nb-41Al-8Cr formed exclusive layers of alumina and had a k sub p value of 0.22 mg squared/cm (sup 4)/hr at 1200 C. The addition of 1 wt percent Y to this alloy was also beneficial, resulting in nearly an order of magnitude decrease in K sub p at 1200 C. Further improvements were achieved by adding about 1 wt percent Si to the quaternary alloy. The k sub p value of 0.012 mg squared/cm (sup 4)/hr for Nb-40Al-8Cr-1Y-1Si at 1200 C was identical to the best NiAl + Zr alloys. These NbAl3 alloys also exhibited excellent cyclic oxidation resistance for 100 hr at 1200 C, being nearly equivalent to NiAl + Zr. Author

N89-12718# Technische Univ., Munich (West Germany). Fakultaet fuer Physik.
ELECTRONIC TRANSPORT PROPERTIES OF THE METALLIC GLASS Cu SUB 100-x Ti SUB x Ph.D. Thesis [ELEKTRONISCHE TRANSPORTEIGENSCHAFTEN DES METALLISCHEN GLASES CU SUB 100-X TI SUB X]
Werner Dyckhoff 1987 181 p In GERMAN
(ETN-88-93231) Avail: NTIS HC A09/MF A01

Electronic transport properties, atomic structure, and electron densities of amorphous metals of Cu Ti alloys are studied. Electrical resistance versus temperature and pressure and thermoelectric forces in dependance of temperature; and low temperature behavior as a function of concentration and pressure variations are surveyed. Compressibility and thermal elongation effects on sample geometry and electrical resistance are examined. Experimental data are analyzed with theories concerning electronic distribution and their effects on disordered structures. Corrections of the Boltzmann transport theory related to electrical resistance behavior in low temperature are discussed. ESA

N89-12719# Deutsche Forschungs- und Versuchsanstalt fuer Luft- und Raumfahrt, Cologne (West Germany). Inst. fuer Werkstoff-Forschung.
PROPERTIES OF RAPIDLY SOLIDIFIED ALUMINUM ALLOYS. GERMAN-NORWEGIAN PROJECT (1983-1987) Final Report
Horst Buhl, Guenter Marci, Guenter Staniek, and Guenter Wirth Apr. 1988 177 p
(DFVLR-FB-88-24; ISSN-0171-1342; ETN-88-93524) Avail: NTIS HC A09/MF A01; DFVLR VB-PL-DO, 90 60 58, 5000 Cologne, Federal Republic of Germany, 61.50 deutsche marks

Tensile tests were made on high temperature Al alloys heat treated at the anticipated service temperature for an appropriate number of hours together with tensile tests on the material in the as-received state. The fatigue properties correlate to the tensile data. Fracture toughness in planes parallel to the deformation direction seems to be very critical with PM aluminum. Checking fracture toughness is mandatory with this material either via chevron-notched specimens or estimation from da/dN-versus delta K curves. With higher strength materials an improvement of ductility is necessary. Creep rupture tests show that RSR alloys exhibit better creep rupture strengths at 275 C than IM alloys having the same chemical composition. The ranking of the creep rupture strengths at the testing temperature of 150 C of the alloy Al6Fe compacts corresponds to the solidification rates, and hence to fineness of the microstructures. Small grain size becomes detrimental at temperatures where significant grain boundary sliding occurs. Improvement of creep rupture strength of the RSR materials could be achieved by avoiding severe internal defects. It is necessary to improve consolidation techniques in order to use the full potential of rapid solidification. ESA

N89-12720*# National Aeronautics and Space Administration. Lewis Research Center, Cleveland, Ohio.
EFFECT OF GRAIN SIZE ON THE HIGH TEMPERATURE PROPERTIES OF B2 ALUMINIDES
J. Daniel Whittenberger [1987] 26 p Presented at the 1987 Northeast Regional Meeting on High Temperature Structural Composites: Synthesis, Characterization and Properties, Hoboken, N.J., 27-29 May 1987; sponsored by the Metallurgy Society of AIME and the Materials Research Society
(NASA-TM-101382; E-3557; NAS 1.15:101382) Avail: NTIS HC A03/MF A01 CSCL 11F

Measurements of the slow plastic flow behavior of cobalt, iron and nickel B2 crystal structure aluminides were conducted on materials fabricated by metallurical techniques. Due to this processing, the aluminides invariably had small equiaxed grains, ranging in size from about 3 to 60 microns in diameter. Grain size was dependent on the extrusion temperature used for powder consolidation, and it proved to be remarkably stable at elevated temperatures. Mechanical properties of all three aluminides were determined via constant velocity compression testing in air between 1000 and 1400 K at strain rates ranging from approx. 10 to the minus 3 power to 10 to the minus 7 power s (-1). Author

N89-12633*# Argonne National Lab., Ill. Materials Science and Technology Div.
EFFECTS OF HIGH MEAN STRESS ON THE HIGH-CYCLE FATIGUE OF PWA 1480 AND DS MAR M 246 + Hf AT 1000 F
Saurin Majumdar *In* NASA, Marshall Space Flight Center, Advanced Earth-To-Orbit Propulsion Technology 1986, Volume 2 Oct. 1986 p 125-133 Sponsored by NASA. Lewis Research Center, Cleveland, Ohio (For primary document see N89-12626 04-20)
(Contract W-31-109-eng-38)
Avail: NTIS HC A99/MF E03 CSCL 21H

N89-12634*# Georgia Inst. of Tech., Atlanta. Fracture and Fatigue Research Lab.
CONSTITUTIVE BEHAVIOR OF SINGLE CRYSTAL PWA 1480 AND DIRECTIONALLY SOLIDIFIED MAR-M 246 UNDER MONOTONIC AND CYCLIC LOADS AT HIGH AND LOW TEMPERATURE
Walter W. Milligan, Eric S. Huron, and Stephen D. Antolovich *In* NASA, Marshall Space Flight Center, Advanced Earth-To-Orbit Propulsion Technology 1986, Volume 2 Oct. 1986 p 134-171 (For primary document see N89-12626 04-20)
(Grant NAG3-503)
Avail: NTIS HC A99/MF E03 CSCL 21H

N89-12635*# National Aeronautics and Space Administration. Lewis Research Center, Cleveland, Ohio.
HIGH-TEMPERATURE LCF OF Ni-201 AND 304L STAINLESS STEEL
Gary R. Halford, L. R. Johnson, and James A. Brown (Aerojet TechSystems Co., Sacramento, Calif.) *In* NASA, Marshall Space Flight Center, Advanced Earth-To-Orbit Propulsion Technology 1986, Volume 2 Oct. 1986 p 172-204 (For primary document see N89-12626 04-20)
Avail: NTIS HC A99/MF E03 CSCL 21H

N89-12636*# Rockwell International Corp., Canoga Park, Calif. Rocketdyne Div.
FATIGUE CRACK RETARDATION FOLLOWING OVERLOADS IN INCONEL 718, Ti-5Al-2.5Sn, AND HAYNES 188
Dan E. Matejczyk, R. P. Jewett, D. W. Schmidt, and G. C. Hresko, III (Professional Services Group, Hellertown, Pa.) *In* NASA, Marshall Space Flight Center, Advanced Earth-To-Orbit Propulsion Technology 1986, Volume 2 Oct. 1986 p 205-219 (For primary document see N89-12626 04-20)
(Contract NAS8-35507)
Avail: NTIS HC A99/MF E03 CSCL 21H

N89-12637*# SKF Industries, Inc., King of Prussia, Pa.
THERMO-MECHANICAL PERFORMANCE EVALUATION OF CRYOGENIC TURBOPUMP BALL BEARINGS
Robert A. Pallini *In* NASA, Marshall Space Flight Center, Advanced Earth-To-Orbit Propulsion Technology 1986, Volume 2 Oct. 1986 p 221-240 (For primary document see N89-12626 04-20)
(Contract NAS8-35341)
Avail: NTIS HC A99/MF E03 CSCL 21H

N89-12638*# Spectra Research Systems, Inc., Huntsville, Ala.
THERMAL ANALYSIS OF SSME TURBOPUMP BEARINGS
Joe C. Cody, David Marty, and Bruce K. Tiller *In* NASA, Marshall Space Flight Center, Advanced Earth-To-Orbit Propulsion Technology 1986, Volume 2 Oct. 1986 p 241-265 (For primary document see N89-12626 04-20)
Avail: NTIS HC A99/MF E03 CSCL 21H

N89-12641*# National Aeronautics and Space Administration. Marshall Space Flight Center, Huntsville, Ala.
POWDER METALLURGY BEARINGS FOR ADVANCED ROCKET ENGINES
B. N. Bhat, T. S. Humphries, Robert L. Thom, G. I. Friedman, and V. Moxson (TRW Aircraft Components Group, Cleveland, Ohio.) *In its* Advanced Earth-To-Orbit Propulsion Technology 1986, Volume 2 Oct. 1986 p 311-325 (For primary document see N89-12626 04-20)
Avail: NTIS HC A99/MF E03 CSCL 21H

N89-12656*# MTS Systems Corp., Minneapolis, Minn.
A HIGH PRESSURE, HIGH TEMPERATURE HYDROGEN ENVIRONMENT FOR METALS PROPERTIES TESTING SYSTEM
Michael J. Rother *In* NASA, Marshall Space Flight Center, Advanced Earth-To-Orbit Propulsion Technology 1986, Volume 2 Oct. 1986 p 661-671 (For primary document see N89-12626 04-20)
Avail: NTIS HC A99/MF E03 CSCL 21H

N89-12658*# Carnegie-Mellon Univ., Pittsburgh, Pa.
HYDROGEN EFFECTS ON THE FATIGUE AND TENSILE BEHAVIOR OF CMSX-2 NICKEL BASE SUPERALLOY SINGLE CRYSTALS
I. Mel Bernstein, Scott Walston, M. Dollar, A. Domnanovich, and W. Kromp *In* NASA, Marshall Space Flight Center, Advanced Earth-To-Orbit Propulsion Technology 1986, Volume 2 Oct. 1986 p 698-714 (For primary document see N89-12626 04-20)
Avail: NTIS HC A99/MF E03 CSCL 21H

N89-12659*# National Aeronautics and Space Administration. Marshall Space Flight Center, Huntsville, Ala.
THE DETERMINATION OF MOBILE HYDROGEN IN AEROSPACE ENGINE ALLOYS
Merlin D. Danford *In its* Advanced Earth-To-Orbit Propulsion Technology 1986, Volume 2 Oct. 1986 p 715-726 (For primary document see N89-12626 04-20)
Avail: NTIS HC A99/MF E03 CSCL 21H

N89-12660*# Pratt and Whitney Aircraft, West Palm Beach, Fla. Engineering Div.
LCF AND CRACK GROWTH RATE OF TURBINE BLADE ALLOYS IN HYDROGEN AND HYDROGEN/STEAM ENVIRONMENTS
B. A. Cowles, D. P. Deluca, J. R. Warren, and F. K. Haake *In* NASA, Marshall Space Flight Center, Advanced Earth-To-Orbit Propulsion Technology 1986, Volume 2 Oct. 1986 p 727-748 (For primary document see N89-12626 04-20)
Avail: NTIS HC A99/MF E03 CSCL 21H

N89-12661*# National Aeronautics and Space Administration. Marshall Space Flight Center, Huntsville, Ala.
THE DEVELOPMENT OF A HYDROGEN RESISTANT ALLOY Progress Report
W. Bryan McPherson *In its* Advanced Earth-To-Orbit Propulsion Technology 1986, Volume 2 Oct. 1986 p 749-757 (For primary document see N89-12626 04-20)
Avail: NTIS HC A99/MF E03 CSCL 21H

N89-12911*# Cincinnati Univ., Ohio.
CONSTITUTIVE MODELING FOR SINGLE CRYSTAL SUPERALLOYS
D. C. Stouffer, N. Jayaraman, M. Sheh, and D. Alden *In* NASA, Lewis Research Center, Turbine Engine Hot Section Technology 1986 Oct. 1986 p 327-334 (For primary document see N89-12876 04-39)
(Grant NAG3-511)
Avail: NTIS HC A21/MF A01 CSCL 11F

N89-12912*# Connecticut Univ., Storrs.
CONSTITUTIVE MODELLING OF SINGLE CRYSTAL AND DIRECTIONALLY SOLIDIFIED SUPERALLOYS Progress Report
E. H. Jordan and K. P. Walker (Engineering Science Software, Inc., Smithfield, R.I.) *In* NASA, Lewis Research Center, Turbine Engine Hot Section Technology 1986 Oct. 1986 p 335-339 (For primary document see N89-12876 04-39)
(Grant NAG3-512)
Avail: NTIS HC A21/MF A01 CSCL 11F

N89-12918*# Syracuse Univ., N. Y. Dept. of Mechanical and Aerospace Engineering.
GRAIN BOUNDARY OXIDATION AND ITS EFFECTS ON HIGH TEMPERATURE FATIGUE LIFE
H. W. Liu and Yoshiki Oshida *In* NASA, Lewis Research Center, Turbine Engine Hot Section Technology 1986 Oct. 1986 p 407-414 (For primary document see N89-12876 04-39)
(Grant NAG3-348)
Avail: NTIS HC A21/MF A01 CSCL 11F

27 NONMETALLIC MATERIALS

Includes physical, chemical, and mechanical properties of plastics, elastomers, lubricants, polymers, textiles, adhesives, and ceramic materials.

For composite materials see *24 Composite Materials*.

N89-12721# International Centre for Theoretical Physics, Trieste (Italy).
ELECTRONIC STRUCTURE OF LIGHT IMPURITIES IN ALPHA-Fe AND V
Xin-gao Gong, Zhi Zeng, and Wing-qi Zheng (Academia Sinica, Hefei, China) Jul. 1987 13 p
(DE88-702958; IC-87/198) Avail: NTIS (US Sales Only) HC A03/MF A01

The electronic structure of alpha-Fe and V with hydrogen and carbon as impurities is calculated using the embedded cluster models in the framework of self-consistent local density theory. The results obtained reveal that the charge transfer between the H atom and the host atom is small, but the magnetic moments of neighboring Fe atoms are reduced. The total energy implies that hydrogen in alpha-Fe is more easily found to occupy the octahedral interstitial site. On the other hand, there is a charge transfer between the C atom and the host atoms. The distance between the carbon and the nearest neighbor iron atoms is 23 percent elongated. The interaction between the hydrogen and the carbon impurities was studied using a set of clusters of Fe10CH in which the atoms were located in five kinds of configuration. The energy of clusters with hydrogen on octahedral interstitial site is lower than that on the tetrahedral interstitial site. DOE

N89-12722*# HITCO, Santa Ana, Calif. Materials Div.
FINGERPRINT TEST DATA REPORT: FM 5834 TEST LOTS NO. 1, 3, 4, AND 5
[1986] 272 p
(Contract NAS8-36298)
(NASA-CR-179419; NAS 1.26:179419) Avail: NTIS HC A12/MF A01 CSCL 11B

Quality control testing is presented for various lots of resin matrix composites. The tests conducted were filler test, resin test, fabric test, and prepreg test for lots 1, 3, 4, and 5. The results of the tests are presented in chart forms. E.R.

N89-12723*# HITCO, Santa Ana, Calif. Materials Div.
FINGERPRINT TEST DATA REPORT: FM 5064J (KAISER) LOTS NO. 1 (K) - NO. 4 (K)
[1986] 276 p
(Contract NAS8-36298)
(NASA-CR-179409; NAS 1.26:179409) Avail: NTIS HC A13/MF A01 CSCL 11B

Quality control tests are presented for resin matrix and carbon-carbon composites. Tests performed are filler test, resin test, prepregs test, and fabric test. The test results are presented in chart form. E.R.

N89-12724# Edgerton, Germeshausen and Grier, Inc., Idaho Falls, Idaho. National Engineering Lab.
SOL-GEL ROUTES TO SUPERCONDUCTING CERAMICS
Jagadish C. Debsikdar 1988 20 p Presented at the International Conference on the First Two Years of High-T(sub c) Superconductivity, Tuscaloosa, Ala., 11 Apr. 1988
(Contract DE-AC07-76ID-01570)
(DE88-015128; EGG-M-88055; CONF-880431-4) Avail: NTIS HC A03/MF A01

Potential processing advantages of sol-gel techniques for fabricating ceramic end products are discussed with special reference to some typical sol-gel approaches outlined in the literature for producing high temperature ceramic superconducting materials. Moreover, the current state of sol-gel research at the Idaho National Engineering Laboratory has been reported with reference to synthesis of metallo-organic precursor materials, sol-gel processing with those precursor materials, and characterization of high temperature superconducting materials in the BaO-Y2O3-CuO system. DOE

N89-12725# Oak Ridge National Lab., Tenn.
ANALYSIS OF ADHESION TEST METHODS AND THE EVALUATION OF THEIR USE FOR ION-BEAM-MIXED METAL/CERAMIC SYSTEMS
J. E. Pawel Jul. 1988 112 p
(Contract DE-AC05-84OR-21400)
(DE88-015358; ORNL/TM-10468) Avail: NTIS HC A06/MF A01

Several thin film adhesion tests have been examined to determine which provides the most reliable method for the measurement of the adhesion of thin metallic films to ceramic substrate. An attempt was made to use the testing techniques described to measure adhesion changes caused by ion beam mixing for a variety of metal/ceramic systems. The techniques analyzed were the scratch test, the acoustic-emission test, and the pull test. The major variables of the scratch test include film thickness, substrate hardness, and stylus radius, but it is not known precisely what effects changes in these have on the measurement of adhesion. The scratch analyses methods discussed in the literature, each describing a load or stress on the system that is presumed to cause de-adhesion, do not always hold because none of the analyses account for both plastic and elastic deformation or incorporate many of the important parameters. The scratch test was much more likely to reveal a critical value for de-adhesion for relatively brittle films such as chromium than for ductile films such as nickel. DOE

N89-12726# Hughes Aircraft Co., El Segundo, Calif. Electro-Optical and Data Systems Group.
HIGH TEMPERATURE ADHESIVE SYSTEMS Interim Report, 25 Sep. 1985 - 31 Jan. 1988
E. H. Catsiff, T. K. Dougherty, W. E. Elias, D. J. Vachon, R. W. Seibold, W. G. Knauss, S. Shimabukuro, and K. M. Liechti (Texas Univ., Austin.) Feb. 1988 155 p
(Contract N00014-85-C-0881)
(AD-A197077; HAC-REF-F7896) Avail: NTIS HC A08/MF A01 CSCL 11A

Under this program, a comprehensive technical effort was undertaken with the goal of developing high-temperature adhesive systems with inherent processibility and toughness. The approach was to perform a multidisciplinary integrated research effort involving a combination of polymer chemistry and fracture mechanics to tailor, characterize, and qualify tough adhesive systems for bonding to titanium and ferrous alloys. Performance goals for the adhesive systems included the ability to withstand extended duty cycles at high temperature while remaining viable under hot-wet and cold dry conditions. The polymer chemistry effort, which has been completed, entailed employment of novel methods of synthesis to develop appropriate polymer-ceramic systems. The mechanics effort involves the development of test methods and a data base for determining adhesion failure mechanism under severe environments. This interim report summarizes progress from 25 September 1985 through 31 January 1988. GRA

N89-12727# Air Force Wright Aeronautical Labs., Wright-Patterson AFB, Ohio.
BORIC OXIDE AS A SOLID LUBRICANT ADDITIVE IN MOLYBDENUM DISULFIDE Final Report, Jan. - Jun. 1987

Chris J. Klenke 3 Mar. 1988 22 p
(AD-A197109; AFWAL-TR-88-2024) Avail: NTIS HC A03/MF A01 CSCL 11H

A recent investigation suggests that antimony trioxide (Sb2O3) performs well as an additive in molybdenum disulfide because of its ability to soften at asperity contacts so that the solid lubricant can attain and retain a preferred tribological orientation. This research determined the effectiveness of boric oxide (B2O3), when used as an additive in MoS2, for substrate temperatures ranging from 21C to 316C. This range was used to allow the asperity contact temperature to vary below and above the softening point of B2O3. It was found that a moderate friction coefficient and high wear, which is attributed to the additive acting abrasively, occurred when the asperity contact temperature was well below the softening point of the oxide. When the asperity contact temperature neared the softening point of the oxide, the friction coefficient increased dramatically and the wear volume was reduced. GRA

N89-12728# Texas Univ., Arlington. Dept. of Chemistry.
ELECTRONIC AND IONIC TRANSPORT IN POLYMERS Quarterly Technical Report No. 6, 1 Apr. - 30 Jun. 1988
Martin Pomerantz, John R. Reynolds, Krishnan Rajeshwar, Dennis S. Marynick, and Timothy D. Shaffer 12 Jul. 1988 7 p
(Contract N00014-86-K-0769)
(AD-A197142) Avail: NTIS HC A02/MF A01 CSCL 07D

A comparative electrochemical charge transport and morphological study of poly (3-methylthiophene) has shown that the redox switching speed of the polymer is affected by the growth morphology which in turn is affected by the electrolyte. The anodic deactivation of polythiophenes has been examined using voltammetry, coulometry, FT-IR spectroscopy and chemical analysis. Molecular orbital calculations have uncovered steric interactions in polyisothianaphthene and polyisonaphthiophene which causes them to be nonplanar. A series of liquid crystalline polyazomethine ethers with two different highly conjugated mesogenic units and flexible alkyl spacers have been prepared and studied with carbon 13 CP/MAS NMR spectroscopy and by comparison with model compounds. Anomalous amino end groups, which give rise to distorted thermal behavior, could be end capped with benzaldehyde. These compounds were found to exhibit nematic mesomorphism. For the first time a transition metal nickel (II) and Copper (II) has been used to control the mesomorphic character of a liquid crystal. Thus, chelates using N, N'-bis(5-alkoxysalicyl-idene) ethylene diamine (Salen) show smectic mesomorphism whose transition temperatures could be controlled by changing the transition metal or by varying the length of the alkoxy unit. GRA

N89-12729# Kent State Univ., Ohio. Liquid Crystal Inst.
LIGHT EXTINCTION IN A DISPERSION OF SMALL NEMATIC DROPLETS Technical Report No. 9
S. Zumer, A. Golemme, and J. W. Doane 13 Jul. 1988 43 p Submitted for publication Prepared for Connecticut Univ., Storrs
(Contract N00014-86-K-0772)
(AD-A197201) Avail: NTIS HC A03/MF A01 CSCL 07C

The light transmission properties of materials in which submicron size nematic droplets are dispersed in a solid polymeric matrix are studied. Theoretical calculations of the differential and total cross sections have been performed in the Rayleigh-Gans approximation for different nematic director configurations. The effect of interdroplet interference is discussed in relation to the droplet distribution, and different models for the pair correlation function are taken into account. An attenuation coefficient is defined and calculated for different director configurations. Theoretical calculations are in excellent agreement with experimental data obtained from thin films of materials consisting of droplets of cyanobiphenyls is dispersed in an epoxy resin. GRA

N89-12730# Princeton Univ., N. J. Polymer Materials Program.
A METHODOLOGY FOR CHARACTERIZING REACTIVE COATINGS: TIME-TEMPERATURE-TRANSFORMATION (TTT) ANALYSIS OF THE COMPETITION BETWEEN CURE, EVAPORATION AND THERMAL DEGRADATION FOR AN EPOXY-PHENOLIC SYSTEM Technical Report No. 14, 21 Jan. 1987 - 6 Jan. 1988
S. Gan, J. K. Gillham, and R. B. Prime Jun. 1988 32 p
(Contract N00014-84-K-0021)
(AD-A197254) Avail: NTIS HC A03/MF A01 CSCL 11I

A methodology, in terms of a macroscopic isothermal time-temperature-transformation (TTT) diagram, is presented for characterizing the changes which occur isothermally in a reactive thermosetting system in which evaporation, cure, and thermal degradation occur. Iso-weight loss contours show the progress of the loss of volatile material (mostly solvent). The gelation contour corresponds to the macroscopic viscosity rising to a definite level. The vitrification contour corresponds to the glass transition temperature (T sub g) rising to the temperature of cure. Iso-T sub g contours show the progress of cure in terms of the easily measured T sub g (rather than chemical conversion). The iso-T sub g contours also show the influence of thermal degradation competing with cure. Degradation is responsible for difficulties in assigning the glass transition temperature of the fully cured material. GRA

N89-12731# Stanford Univ., Calif. Dept. of Chemical Engineering.
STUDIES OF ULTRATHIN POLYMER FILMS FOR LITHOGRAPHIC APPLICATIONS Technical Report No. 6
S. W. Kuan, C. C. Fu, R. F. Pease, and C. W. Frank 13 Jul. 1988 7 p
(Contract N00014-87-K-0426)
(AD-A197297) Avail: NTIS HC A02/MF A01 CSCL 14E

The advantages of minimizing polymer resist thickness to the macromolecular dimensions are manifold. In optical lithography, ultrathin resists can improve exposure and focus latitude and alleviate the problem of absorption in conventional resists for deep ultraviolet (UV) exposure. In electron beam lithography it is desirable to reduce the resist thickness to minimize forward electron scattering in the resist, and to allow penetration when using the scanning tunneling microscope (STM) as a very low voltage exposure source. Moreover, we can better understand many phenomena such as the nature of the pinholes and etching resistance, which are still puzzles for the thicker films. GRA

N89-12732# Stanford Univ., Calif. Dept. of Chemical Engineering.
ULTRATHIN POLYMER FILMS FOR MICROLITHOGRAPHY Technical Report No. 10
S. W. Kuan, C. W. Frank, C. C. Fu, D. R. Alee, and P. Maccagno 13 Jul. 1988 22 p
(Contract N00014-87-K-0426)
(AD-A197298) Avail: NTIS HC A03/MF A01 CSCL 07F

Ultrathin (14 to 22 nm) poly(methylmethacrylate) (PMMA) films prepared by both spin-casting and Langmuir-Blodgett (LB) techniques and novolac films prepared by spincasting have been explored as high resolution electron-beam resists. One-eighth micron lines-and-spaces patterns (equal to the smallest beam diameter available) have been achieved by using a Perkin Elmer MEBES I pattern generation system as the exposure tool, and the definition of 45 nm features has recently been achieved by using a high resolution electron beam lithography system. The etch resistance of such films is sufficiently good to allow patterning of a chromium film suitable for photomask fabrication. The most surprising result has been that the pinhole densities in 14.3 nm LB PMMA film and 22 nm spin-cast novolac film are only a few per sq. cm., considerably lower than the density in spin-cast PMMA films of comparable thickness. GRA

N89-12733# Naval Air Development Center, Warminster, Pa. Air Vehicle and Crew Systems Technology Dept.
SOILING, CLEANING, AND WEATHERING EFFECTS ON AIRCRAFT POLYURETHANE TOPCOATS Phase Report, Oct. - Dec. 1987
Donald J. Hirst and Charles R. Hegedus Mar. 1988 28 p
(AD-A197302; NADC-88031-60) Avail: NTIS HC A03/MF A01 CSCL 11C

The synergetic effects of weathering, soiling, and cleaning on Navy aircraft polyurethane topcoats has been investigated. Three lusterless, low gloss, coatings matching Federal Standard 595 color 36320, a gray color with a 32 percent reflectance, were studied. Two of the coatings qualify under MIL-C-83286, Coating, Urethane, Aliphatic Isocyanate for Aerospace Application, which is the standard topcoat used on U.S. Navy aircraft. The third coating contains polymer bead pigments and is applied to production F-18 aircraft. Color change of the polyurethane topcoats during weathering and weathering/cleaning conditions was negligible. Color change when specimens were weathered, soiled, and cleaned was significant, especially for low gloss topcoats. However, polymer bead coatings of equivalent gloss (1.1) to conventionally pigmented camouflage coatings performed better, undergoing less color change. None of the three exposure conditions significantly changed the gloss of the coatings analyzed. However, all three exposure conditions caused the coatings surface to become more hydrophilic. Topcoats which were weathered and weathered/cleaned were more cleanable after soiling than their unexposed counterparts because of their hydrophilic surface. Weathering caused slight erosion and chalking of the polyurethane topcoat surfaces. GRA

N89-12734# Naval Postgraduate School, Monterey, Calif.
ON THE RESISTANCE OF CERAMICS TO HIGH VELOCITY PENETRATION
Joseph Sternberg Jul. 1988 47 p
(AD-A197320; NPS73-88-001) Avail: NTIS HC A03/MF A01 CSCL 19D

It is known that high velocity penetration for ductile materials can be represented analytically by a modified hydrodynamic theory. The strength term for the target corresponds to the pressure required to expand a cavity, if the dynamic yield strength is substituted for the static yield strength. Indentation pressures are closely related to the cavity expansion pressures. In this paper it is shown that the key parameters for indentation in brittle materials are similar to but not identical to those for ductile materials. The strength terms for ceramics as measured in ballistic tests are much lower than would be predicted on the basis of the indentation measurements. It is found that the ratio of the target strength term to hardness increases as the fracture toughness of the targets increases. The findings on penetration resistance are used together with cavity expansion theory to estimate the relative size of the craters in ceramic targets. GRA

N89-12735# Gordon Research Conferences, Inc., Kingston, R.I.
GORDON CONFERENCE ON MICROBIAL ADHESION Final Report, Jun. 1987 - Jul. 1988
R. J. Doyle 1 Jul. 1988 9 p Conference held at Newport, R.I., 25-31 Jul. 1987
(Contract N00014-87-G-0268; Proj. RR0-4106)
(AD-A197352) Avail: NTIS HC A02/MF A01 CSCL 06C

A Gordon Conference on the molecular mechanisms of microbial adhesion was held at Salve Regina College, Newport, R.I. on 25 to 31 July, 1987. The Conference was attended by 128 scientists from the U.S.A., Israel, FRG, The Netherlands, Finland, Mexico, Japan, Australia, England and Sweden. The scientific programs dealt with microbial adhesion to animal, plant and artificial surfaces. The program emphasized the molecular aspects of adhesion. GRA

N89-12736# Army Belvoir Research and Development Center, Fort Belvoir, Va.
DIFFERENTIAL SCANNING CALORIMETRY AS A METHOD FOR INDICATING HYDROLYSIS OF URETHANE ELASTOMERS Final Report, Mar. 1987 - Mar. 1988
Dawn M. Crawford, Alan R. Teets, and David Flanagan Jun. 1988 28 p
(AD-A197673; BRDEC-2463) Avail: NTIS HC A03/MF A01 CSCL 11J

Polyether and polyester urethane elastomers were aged in humidity (98 percent), water, and air at 160, 170, and 185 F for 7, 14, 28, 42, 70, and 100 days. After each aging condition, tensile strength of the materials was determined and Differential Scanning Calorimetry (DSC) traces were run to observe changes in thermal transitions of the aged specimens. An effort was made to relate these transitions with actual reduction in tensile strength. Results were evaluated using DSC as a method for indicating hydrolytic degradation of the urethane elastomers studied in this investigation. GRA

N89-12737# Army Military Personnel Center, Alexandria, Va. Program Analysis Office.
POLY(ETHYL ACRYLATE) AND POLY(GAMMA-BENZYL-L-GLUTAMATE): AN INTERPENETRATING POLYMER SYSTEM M.S. Thesis
Peter R. Gibson 13 Jun. 1988 127 p
(AD-A197783) Avail: NTIS HC A07/MF A01 CSCL 07F

The rigid rod polymer poly(gamma-benzyl-L-glutamate) (PBLG) dissolves in ethyl acrylate (EA) at elevated temperatures. Upon cooling to room temperature, a gel is formed. Phase separation occurs on a submicron level. The PBLG forms a continuous submicron network. The sample is homogeneous to the eye. With the addition of an initiator to the EA, the vinyl monomer may be polymerized to form poly(ethyl acrylate) (PEA). When the polymerization initiated by photochemical initiator occurs from the EA-PBLG gel state, no gross change in the PBLG network occurs. A polymer film of linear PEA and PBLG is formed. With the addition of an initiator and crosslinker to the EA, EA may be crosslinked upon polymerization from the EA-PBLG gel state. An interpenetrating polymer network (IPN) of crosslinked PEA and PBLG is formed. Rheologically, the storage and loss moduli variations due to changes in frequency, strain, and PBLG concentration are examined for each type of sample. Additionally, the effects of crosslinker concentration is examined for IPN's. The characteristics of the PEA made in the laboratory are compared to commercial PEA samples by nuclear magnetic resonance (NMR) spectroscopy and gel permeation chromatography (GPC). The swelling and leaching traits of the PEA-PBLG samples are investigated using methanol. GRA

N89-12738# Arizona State Univ., Tempe. Dept. of Chemistry.
SYNTHETIC POLYMERS AS ANALOGS OF POLYSACCHARIDES Final Report, 31 Mar. 1985 - 31 Mar. 1988
Edwin J. Vandenberg and R. S. Juvet, Jr. 15 Jun. 1988 4 p
(Contract MIPR-117-87)
(AD-A197842; ARO-22284.3-CH) Avail: NTIS HC A02/MF A01 CSCL 07C

The major thrust of this program was to make and characterize hydrophilic hydroxy polyethers which are interesting analogues of the important naturally occurring polysaccharides. The work, as described below, centered largely around the synthesis, properties and mechanism aspects of poly(3,3-bis(hydroxymethyl)oxetane), (PBHMO) and poly(3-hydroxyoxetane) (PHO). Two U.S. patents were filed and two publications were prepared. GRA

N89-12739# North Carolina State Univ., Raleigh. Dept. of Materials Science and Engineering.
FUNDAMENTAL STUDIES AND DEVICE DEVELOPMENT IN BETA SILICON CARBIDE Final Report, 1 Feb. 1985 - 31 Jan. 1988
Robert F. Davis 30 Mar. 1988 63 p

(Contract N00014-82-K-0182; Proj. RR0-2102)
(AD-A197843; Rept-243-043-00012) Avail: NTIS HC A04/MF A01 CSCL 20L

High purity monocrystalline Beta-Silicon Carbide films have been chemically vapor deposited on Si(100) and alpha-SiC(001) at 1660K to 1823K and 0.1 MPa using Silane and Ethylene carried in Hydrogen. Films grown on the on-axis Si(100) contained substantial concentrations of dislocations, stacking faults and antiphase boundaries; those deposited on alpha-SiC(0001) contained primarily double positioning boundaries. These boundaries were eliminated by using off-axis orientations of the respective substrates. Films produced on Si(100) have also been doped during growth and via ion implantation with Boron or Aluminum (p-type) or Phosphorus or Nitrogen(n-type) at liquid nitrogen, room and elevated temperatures. Results from the former procedure showed the ionized dopant/total dopant concentration ratios for N, P, B, and Al. The solubility limits of N, P and B at 1660K were determined. High temperature ion implantation coupled with dynamic and post annealing resulted in a markedly reduced defect and precipitate concentration relative to that observed in similar research at the lower temperatures. Dry etching in Carbon Tetrafluoride and Nitrogen trifluoride by reactive ion etching (RIE) and in Sulfur Hexafluoride by plasma etching have also been conducted. Device-compatible surface impurity chemistry and morphology were only obtained using RIE and NF3 combined with a C cathode. Schottky diode, p-n junctions, MESFET and MOSFET devices have been fabricated. GRA

N89-12740# Pittsburgh Univ., Pa. Dept. of Materials Science and Engineering.
INFLUENCE OF SIDE-GROUPS ON THERMOTROPIC BEHAVIOR OF POLYORGANOPHOSPHAZENES Technical Report No. 8
M. Kojima and J. H. Magill 8 Jul. 1988 24 p
(Contract N00014-85-K-0358)
(AD-A197852) Avail: NTIS HC A03/MF A01 CSCL 07F

Structural and morphological investigations of polyphosphazenes with different kinds of side groups were made in an attempt to understand the T(1) thermotropic transitions. Solution grown crystals and cast films of phosphazene homopolymers were prepared and investigated by DSC, electron microscopy and X-ray diffraction. It has been established that the T(1) and the Tg values are roughly linearly related with the size of side groups. The interplanar distances expressed as d(100) delta in thermotropic state also shows a linear relation with the side group dimensions. Polymorphic forms have been found for most polyphosphazenes that exhibit a T(1) temperature, the location of which is influenced by the side groups. GRA

N89-12741* National Aeronautics and Space Administration. Langley Research Center, Hampton, Va.
CRYOGENIC INSULATION SYSTEM Patent
Randall C. Davis, inventor (to NASA), Allan H. Taylor, inventor (to NASA), L. Robert Jackson, inventor (to NASA), and Patrick S. McAuliffe, inventor (to NASA) (Lockheed-California Co., Burbank.) 27 Sep. 1988 8 p Filed 10 Jun. 1987 Supersedes N87-25478 (25 - 19, p 2598)
(NASA-Case-LAR-13506-1; US-Patent-4,774,118;
US-Patent-Appl-SN-060182; US-Patent-Class-428-71;
US-Patent-Class-156-297; US-Patent-Class-156-299;
US-Patent-Class-428-44; US-Patent-Class-428-47;
US-Patent-Class-428-58; US-Patent-Class-428-76) Avail: US Patent and Trademark Office CSCL 11C

This invention relates to reusable, low density, high temperature cryogenic foam insulation systems and the process for their manufacture. A pacing technology for liquid hydrogen fueled, high speed aircraft is the development of a fully reusable, flight weight cryogenic insulation system for propellant tank structures. In the invention cryogenic foam insulation is adhesively bonded to the outer wall of the fuel tank structure. The cryogenic insulation consists of square sheets fabricated from an array of abutting square blocks. Each block consists of a sheet of glass cloth adhesively bonded between two layers of polymethacrylimide foam. Each block is wrapped in a vapor impermeable membrane, such as Kapton(R) aluminum Kapton(R), to provide a vapor barrier. Very beneficial results can be obtained by employing the present invention in conjunction with fibrous insulation and an outer aeroshell, a hot fuselage structure with an internal thermal protection system.

Official Gazette of the U.S. Patent and Trademark Office

N89-12742# Du Pont de Nemours (E. I.) and Co., Aiken, S.C.
CHALLENGING APPLICATIONS FOR HYDRATED AND CHEMICALLY REACTED CERAMICS
C. A. Langton 1 Aug. 1988 13 p Presented at the Australian Ceramic Society Meeting, Sydney, Australia, 12 Jul. 1988
(Contract DE-AC09-76SR-00001)
(DE88-015397; DP-MS-88-163; CONF-8807102-1) Avail: NTIS HC A03/MF A01

Approximately 400 times 10 to the 6th power liters of low-level alkaline salt solution will be treated at the Savannah River Plant (SRP) Defense Waste Processing Facility (DWPF) prior to disposal in concrete vaults at SRP. Treatment involves removal of Cs(+) and Sr (+2) followed by solidification and stabilization of potential contaminants in saltstone, a hydrated ceramic waste form. Chromium, technetium, and nitrate releases from saltstone can be significantly reduced by substituting hydraulic blast furnace slag for portland cement in the formulation designs. Slag-based mixes are also compatible with Class F fly ash used in saltstone as a functional extender to control heat of hydration and reduce permeability. (Class F fly ash is also locally available at SRP.) A monolithic waste form is produced by the hydration of the slag and fly ash. Soluble ion release (NO sub 3 -) is controlled by the saltstone microstructure. Chromium and technetium are less leachable from slag mixes compared to cement-based waste forms because these species are chemically reduced to a lower valence state by ferrous iron in the slag and precipitated as relatively insoluble phases, such as CR(OH) sub 3 and TcO sub 2. DOE

N89-12743# Vanderbilt Univ., Nashville, Tenn.
MODIFIED PULL TEST FOR THE TESTING OF VERY ADHERENT FILMS
J. E. Pawel and C. J. McHargue (Oak Ridge National Lab., Tenn.) 1988 7 p Presented at the NATO Advanced Study Institute on Structure-Property Relationships in Ion-Beam Surface-Modified Ceramics: Theory and Applications, Ciocco, Italy, 28 Aug. 1988
(Contract DE-AC05-84OR-21400)
(DE88-016363; CONF-8808108-1) Avail: NTIS HC A02/MF A01

The effectiveness of a thin film on a substrate depends largely on the degree of adhesion of the film to its substrate. Much effort has been put into developing reproducible, quantitative adhesion tests. The pull test is a direct measure of the tensile force required to remove the test film normal to the substrate surface. A technique was developed to introduce a reproducible flaw at the film/substrate interface in an attempt to lower the apparent adhesion of the film to within the range of the pull tester. This technique also promotes film failure at the artificial flaw and subsequent crack propagation along the film/substrates interface. Zirconium films approximately 500 nm were electron beam evaporated onto the basal plane of single crystal sapphire substrates. The pull test was performed using a Sebastian I adherence tester. The pins were 3 mm in diameter and coated with epoxy. The adhesion of these zirconium films to their sapphire substrates was greater than the strength of the epoxy used to bond the test pin to the specimen. A thin layer of gold was sputter deposited onto a small portion of the sapphire substrate after the substrate had been cleaned. The test film was then deposited through a mask such that a portion of this new film overlapped the gold layer. Since the gold layer was non-adherent (experimentally) to the sapphire substrates used in this experiment, this served as a release layer for the test films. The mild shadowing effect of the mask used during gold deposition caused the edge of the gold layer under the test film to be tapered and thus this was treated as a reproducible crack and the analysis made using the concept of fracture toughness as indicated by the stress intensity factor, K. Results are discussed. DOE

N89-12744# Oak Ridge National Lab., Tenn. Metals and Ceramics Div.
ION BEAM MIXING OF METALS AND CERAMICS: MATERIAL CONSIDERATIONS
Carl J. McHargue 1988 8 p Presented at the NATO Advanced Study Institute on Structure-Property Relationships in Ion-Beam Surface-Modified Ceramics: Theory and Applications, Ciocco, Italy, 28 Aug. 1988
(Contract DE-AC05-84OR-21400)
(DE88-016797; CONF-8808108-4) Avail: NTIS HC A03/MF A01

Most studies on ion beam mixing have been concerned with metal-metal or metal-silicon systems. The great activity in this field is attested by the fact that a 1983 review tabulated data for 38 bilayer and 25 multilayer systems. The initial models for mixing focused on the dynamics of ion-solid interactions and produced models based on direct recoils, cascades, and enhanced diffusion due to radiation-produced defects. An earlier chapter contains a description of ion beam mixing processes and the mechanisms that have been proposed to describe material transport across the layer/substrate interface. In this chapter, the issues raised by the application of ion beam mixing to a system where at least one component is an insulating compound, e.g., a ceramic, are discussed. In order to narrow the subject, this chapter will deal with some of the questions arising from ion bombardment of thin metal films and insulator substrate systems. Much of the interest in ion beam mixing as applied to metal-insulator couples arises from the observation that bombardment with an ion beam often increases the adhesion of the film to the substrate. However, this chapter will not address that issue but will discuss the role of the materials properties that influence the microstructures so produced. DOE

N89-12745*# Dayton Univ., Ohio. Research Inst.
DEVELOPMENT OF POLYISOCYANURATE POUR FOAM FORMULATION FOR SPACE SHUTTLE EXTERNAL TANK THERMAL PROTECTION SYSTEM Final Technical Report, Mar. 1986 - Oct. 1987
James A. Harvey, John M. Butler, and Richard P. Chartoff Aug. 1988 49 p
(Contract NAS8-36280)
(NASA-CR-183511; NAS 1.26:183511; UDR-TR-88-96) Avail: NTIS HC A03/MF A01 CSCL 11C

Four commercially available polyisocyanurate polyurethane spray-foam insulation formulations are used to coat the external tank of the space shuttle. There are several problems associated with these formulations. For example, some do not perform well as pourable closeout/repair systems. Some do not perform well at cryogenic temperatures (poor adhesion to aluminum at liquid nitrogen temperatures). Their thermal stability at elevated temperatures is not adequate. A major defect in all the systems is the lack of detailed chemical information. The formulations are simply supplied to NASA and Martin Marietta, the primary contractor, as components; Part A (isocyanate) and Part B (poly(s) and additives). Because of the lack of chemical information the performance behavior data for the current system, NASA sought the development of a non-proprietary room temperature curable foam insulation. Requirements for the developed system were that it should exhibit equal or better thermal stability both at elevated and cryogenic temperatures with better adhesion to aluminum as compared to the current system. Several formulations were developed that met these requirements, i.e., thermal stability, good pourability, and good bonding to aluminum. Author

N89-12746*# National Aeronautics and Space Administration. Lewis Research Center, Cleveland, Ohio.
SLURRY-PRESSING CONSOLIDATION OF SILICON NITRIDE
William A. Sanders, James D. Kiser, and Marc R. Freedman Nov. 1988 19 p
(NASA-TM-101365; E-4352; NAS 1.15:101365) Avail: NTIS HC A03/MF A01 CSCL 11C

A baseline slurry-pressing method for a silicon nitride material is developed. The Si3N4 composition contained 5.8 wt percent SiO2 and 6.4 wt percent Y2O3. Slurry-pressing variables included volume percent solids, application of ultrasonic energy, and pH. Twenty vol percent slurry-pressed material was approximately 11 percent stronger than both 30 vol percent slurry-pressed and dry-pressed materials. The Student's t-test showed the difference to be significant at the 99 percent confidence level. Twenty volume percent (300 h) slurry-pressed test bars exhibited strengths as high as 980 MPa. Large, columnar beta-Si3N4 grains caused failure in the highest strength specimens. The improved strength correlated with better structural uniformity as determined by radiography, optical microscopy, and image analysis. Author

N89-12747*# National Aeronautics and Space Administration. Langley Research Center, Hampton, Va.
THERMOPLASTIC ADHESIVES BASED ON 4,4'-ISOPHTHALOYLDIPHTHALIC ANHYDRIDE (IDPA)
Donald J. Progar, Terry L. StClair, and J. Richard Pratt (PRC Systems Services Co., Hampton, Va.) Nov. 1988 32 p
(NASA-TM-101508; NAS 1.15:101508) Avail: NTIS HC A03/MF A01 CSCL 11C

Thermoplastic polyimides were prepared and evaluated as adhesives. These materials are based on 4,4'-isophthaloyl-diphathalic anhydride (IDAP) and either metalphenylene diamine (MPD) or 3,3'-diaminobenzophenone (DBAP). Both polymers exhibit excellent adhesive properties; however, the IDPA-MPD is the more attractive system because of a combination of high mechanical and physical properties as well as being made from commercially attractive monomers. The IDPA-MPD is an isomeric form of the commercially available adhesive and matrix resin, LARC-TPI and both systems have the same glass transition temperature and exhibit similar adhesive properties. Author

N89-12591*# Toronto Univ., Downsview (Ontario). Inst. for Aerospace Studies.
ATOMIC OXYGEN STUDIES ON POLYMERS
W. D. Morison, R. C. Tennyson, J. B. French, T. Braithwaite, M. Moisan, and J. Hubert (Montreal Univ., Quebec) *In* NASA, Goddard Space Flight Center, 15th Space Simulation Conference: Support the Highway to Space Through Testing 1988 p 89-109 (For primary document see N89-12582 04-18)
(Contracts N60921-86-C-A226; AUSPI-86-207; TP2-325)
Avail: NTIS HC A21/MF A01 CSCL 11C

N89-12616*# National Aeronautics and Space Administration. Goddard Space Flight Center, Greenbelt, Md.
REQUIREMENTS AND TEST RESULTS FOR THE QUALIFICATION OF THERMAL CONTROL COATINGS
J. E. Brzuskiewicz, G. A. Zerlaut (DSET Labs., Inc., Phoenix, Ariz.), K. Lauder, and G. M. Miller *In its* 15th Space Simulation Conference: Support the Highway to Space Through Testing 1988 p 419-436 (For primary document see N89-12582 04-18)
Avail: NTIS HC A21/MF A01 CSCL 11C

N89-12883*# National Aeronautics and Space Administration. Lewis Research Center, Cleveland, Ohio.
HOST SURFACE PROTECTION R AND T OVERVIEW
Robert A. Miller *In its* Turbine Engine Hot Section Technology 1986 Oct. 1986 p 45-50 (For primary document see N89-12876 04-39)
Avail: NTIS HC A21/MF A01 CSCL 11C

N89-12919*# National Aeronautics and Space Administration. Lewis Research Center, Cleveland, Ohio.
A STUDY ON THERMAL BARRIER COATINGS INCLUDING THERMAL EXPANSION MISMATCH AND BOND COAT OXIDATION
George C. Chang, Woraphat Phucharoen (Cleveland State Univ., Ohio.), and Robert A. Miller *In its* Turbine Engine Hot Section Technology 1986 Oct. 1986 p 415-434 (For primary document see N89-12876 04-39)

(Contract NCC3-27)
Avail: NTIS HC A21/MF A01 CSCL 11C

N89-12920*# Garrett Turbine Engine Co., Phoenix, Ariz.
THERMAL BARRIER COATING LIFE PREDICTION MODEL DEVELOPMENT
T. E. Strangman, J. F. Neumann, and A. Liu *In* NASA, Lewis Research Center, Turbine Engine Hot Section Technology 1986 Oct. 1986 p 435-445 (For primary document see N89-12876 04-39)
(Contract NAS3-23945)
Avail: NTIS HC A21/MF A01 CSCL 11C

N89-12921*# General Electric Co., Fairfield, Conn. Aircraft Engine Business Group.
THERMAL BARRIER COATING LIFE PREDICTION MODEL
B. H. Pilsner, R. V. Hillery, R. L. McKnight, T. S. Cook, K. S. Kim, and E. C. Duderstadt *In* NASA, Lewis Research Center, Turbine Engine Hot Section Technology 1986 Oct. 1986 p 447-467 (For primary document see N89-12876 04-39)
(Contract NAS3-23943)
Avail: NTIS HC A21/MF A01 CSCL 11C

N89-12922*# Pratt and Whitney Aircraft, East Hartford, Conn.
THERMAL BARRIER COATING LIFE PREDICTION MODEL DEVELOPMENT
J. T. DeMasi and K. D. Sheffler *In* NASA, Lewis Research Center, Turbine Engine Hot Section Technology 1986 Oct. 1986 p 469-483 (For primary document see N89-12876 04-39)
(Contract NAS3-23944)
Avail: NTIS HC A21/MF A01 CSCL 11C

N89-13228# Idaho State Univ., Pocatello.
EVALUATION OF BORON CARBIDE COATINGS
David Levinskas *In* New Mexico Univ., Nuclear Technology for the Year 2000 1987 p 68-71 (For primary document see N89-13223 04-70)
Avail: NTIS HC A06/MF A01

28 PROPELLANTS AND FUELS

Includes rocket propellants, igniters, and oxidizers; their storage and handling procedures; and aircraft fuels.

For related information see also *07 Aircraft Propulsion and Power, 20 Spacecraft Propulsion and Power,* and *44 Energy Production and Conversion.*

N89-12748# Svensk Drivmedeksteknik A.B., Stockholm.
FUEL ALCOHOL FORMULATIONS
Sep. 1988 48 p
(Contract DE-GI01-87CE-50181)
(DE88-016753; DOE/CE-50181/H1) Avail: NTIS HC A03/MF A01

This work was conducted through the collaborative efforts of the International Energy Agency (IEA) Working Group on Alcohols and Alcohol Blends as Motor Fuel, consisting of representatives from Canada, Italy, Japan, Sweden and the United States. Under Annex 2 of the IEA Agreement on this subject, Technology Information Exchange on Motor Alcohols, the Swedish Motor Fuel Technology Company (SMAB) seeks, collects, collates, and sometimes assesses data and information on new work in the field. This information supplements the three-volume report of early 1987 on the state-of-the-art of production and utilization technology titled, Alcohols and Alcohol Blends as Motor Fuel. Since there is considerable interest in and a future need for fuel alcohol specifications, one of the efforts under Annex 2 was to review the fuel formulations used in field activities and the results of previous workshops on the subject. This document presents the results of that plus discussion on key points that would be considered in determining specifications. The contribution of Dr. Claes Pilo of SMAB was key to achieving this. The Executive Committee of this IEA working group recognizes that development and adoption of fuel specifications are functions of individual countries wherein there are existing organizations and procedures to do this. This document may be helpful to those organizations, and is intended as a service to aiding the technical community as it moves in that direction. DOE

N89-12749# Ballistic Research Labs., Aberdeen Proving Ground, Md.
COMBINED PRESSURE-SHEAR IGNITION SENSITIVITY TEST
Vincent M. Boyle, Deborah L. Pilarski, and Oliver H. Blake Jul. 1988 52 p
(AD-A197076; BRL-TR-2927) Avail: NTIS HC A04/MF A01 CSCL 19A

A procedure is described for using a high pressure activator to test explosives and propellants for sensitivity to ignition under conditions of combined pressure and shear. Data are presented for TNT and Comp B explosive and Composite Modified Double Base (CMDB) propellant showing that sensitivity increases from TNT to Comp B to CMDB. The maximum pressure and shear velocity were around 1.0 GPa and 60 m/sec, respectively. An analysis of the data in terms of viscous heating of the shear zone is presented. In this analysis, the energy deposition rate per unit volume (due to viscous heating) was equated to the energy loss rate per unit volume (due to thermal conduction) to obtain a relationship between pressure and shear velocity required for ignition. This relationship defines a boundary curve in the pressure-shear velocity plane between ignition and non-ignition. GRA

N89-12750# Air Force Wright Aeronautical Labs., Wright-Patterson AFB, Ohio.
PROPERTIES OF JP-8 JET FUEL Summary Report, Aug. 1984 - Apr. 1988
Charles R. Martel May 1988 19 p
(AD-A197270; AD-E900802; AFWAL-TR-88-2040) Avail: NTIS HC A03/MF A01 CSCL 21D

This report provides a summary of 80 JP-8 jet fuels produced over the time period of August 1984 to April 1988. The data were obtained from the test reports provided by the fuel supplier or receiving terminal. Averages, standards deviations, minimum and maximum values of the various data have been determined and are reported. GRA

N89-12751# Ballistic Research Labs., Aberdeen Proving Ground, Md.
REPORT ON JANNAF WORKSHOP INFLUENCE OF GAS-PHASE CHEMICAL KINETICS ON LOW-PRESSURE IGNITION AND FLAMESPREADING IN SOLID PROPELLANT Technical Report, period ending Oct. 1986
George K. Keller Jul. 1988 22 p Workshop held in Hampton, Va., 23-24 Oct. 1986
(AD-A197854; BRL-TR-2918) Avail: NTIS HC A03/MF A01 CSCL 19A

A workshop on the subject influence of Gas-Phase Chemical Kinetics on the Low-Pressure Ignition and Flamespreading in Solid Propellants was held at Hampton, Va., on 23 and 24 October 1986 in conjunction with the 23rd JANNAF Combustion Meeting. The objectives of the workshop were to: (1) force a synergisitc interaction between those whose measurements have provided evidence for the participation of chemical kinetics in low-pressure solid propellant burning and those who are striving to simulate these events with interior ballistic models, and (2) address problems of anomalous ignition behavior in gun propelling charges. The workshop participants: (1) reviewed the evidence for the participation of chemical kinetics in the low-pressure burning of solid propellants, (2) reviewed model simulations which include finite-rate kinetics, and (3) determined which model simulations and further experimental characterizations would be most fruitful. This report documents the workshop. GRA

29 MATERIALS PROCESSING

Includes space-based development of products and processes for commercial applications.
For biological materials see *55 Space Biology*.

N89-12752*# National Aeronautics and Space Administration, Washington, D.C.
MICROGRAVITY SCIENCE AND APPLICATIONS PROGRAM TASKS, 1987 REVISION
Aug. 1988 239 p
(NASA-TM-4068; NAS 1.15:4068) Avail: NTIS HC A11/MF A01 CSCL 12A

A compilation is presented of the active research tasks as of the end of the FY87 of the Microgravity Science and Applications Program, NASA-Office of Space Science and Applications, involving several NASA centers and other organizations. An overview is provided of the program scope for managers and scientists in industry, university, and government communities. An introductory description is provided of the program along with the strategy and overall goal, identification of the organizational structures and people involved, and a description of each task. A list of recent publications is also provided. The tasks are grouped into six major categories: Electronic Materials; Solidification of Metals, Alloys, and Composites; Fluid Dynamics and Transport Phenomena; Biotechnology; Glasses and Ceramics; and Combustion. Other categories include Experimental Technology, General Studies and Surveys; Foreign Government Affiliations; Industrial Affiliations; and Physics and Chemistry Experiments (PACE). The tasks are divided into ground based and flight experiments. Author

N89-12753*# National Aeronautics and Space Administration. Lewis Research Center, Cleveland, Ohio.
CONVECTIVE FLOWS IN ENCLOSURES WITH VERTICAL TEMPERATURE OR CONCENTRATION GRADIENTS
L. W. Wang, A. T. Chai, and D. J. Sun (National Cheng Kung Univ., Tainan, Taiwan) [1988] 18 p Presented at the 27th Aerospace Sciences Meeting, Reno, Nev., 9-12 Jan. 1989; sponsored by the American Institute of Aeronautics and Astronautics
(NASA-TM-101373; E-4421; NAS 1.15:101373; AIAA-89-0069)
Avail: NTIS HC A03/MF A01 CSCL 22A

The transport process in the fluid phase during the growth of a crystal has a profound influence on the structure and quality of the solid phase. In vertical growth techniques the fluid phase is often subjected to vertical temperature and concentration gradients. The main objective is to obtain more experimental data on convective flows in enclosures with vertical temperature or concentration gradients. Among actual crystal systems the parameters vary widely. The parametric ranges studied for mass transfer are mainly dictated by the electrochemical system employed to impose concentration gradients. Temperature or concentration difference are maintained between two horizontal end walls. The other walls are kept insulated. Experimental measurements and observations were made of the heat transfer or mass transfer, flow patterns, and the mean and fluctuating temperature distribution. The method used to visualize the flow pattern in the thermal cases is an electrochemical pH-indicator method. Laser shadowgraphs are employed to visualize flow patterns in the solutal cases. Author

N89-12606*# Messerschmitt-Boelkow-Blohm G.m.b.H., Bremen (West Germany).
CONTROL OF THE INDUCED MICROGRAVITY ENVIRONMENT OF THE MAN TENDED FREE FLYER (MTFF)
Juergen Schlund *In* NASA, Goddard Space Flight Center, 15th Space Simulation Conference: Support the Highway to Space Through Testing 1988 p 289-307 (For primary document see N89-12582 04-18)
Avail: NTIS HC A21/MF A01 CSCL 22A

31 ENGINEERING (GENERAL)

Includes vacuum technology; control engineering; display engineering; cryogenics; and fire prevention.

N89-12754# Universal Energy Systems, Inc., Dayton, Ohio.
UNITED STATES AIR FORCE GRADUATE STUDENT SUMMER SUPPORT PROGRAM, VOLUME 1 Program Technical Report, 1987
Rodney C. Darrah and Susan K. Espy Dec. 1987 695 p Program held in 1987; sponsored by AFOSR, AFSC, and USAF
(Contract F49620-85-C-0013; AF Proj. 3396)
(AD-A191121; AFOSR-88-0209TR-Vol-1) Avail: NTIS HC A99/MF E03 CSCL 13B

The U.S. AF 1987 Graduate Student Summer Support Program (USAF-GSSSP) was conducted under the United States Air Force Summer Faculty Research Program. The program provides funds for graduate students to work at an Air Force Facility with a supervising professor or with a supervising Air Force Engineer. The students are selected on a nationally advertised competitive basis for a ten-week assignment during the summer intersession period to perform research at Air Force laboratories/centers. Each assignment is in a subject area and at the Air Force facility mutually agreed upon by the students and the Air Force. The USAF-GSSSP is sponsored by the Air Force Office of Scientific Research, Air Force Systems Command, United States Air Force, and is conducted by Universal Energy Systems, Inc. For individual titles, see N89-12755 through N89-12784.

N89-12755# Johns Hopkins Univ., Baltimore, Md. Dept. of Materials Science.
CHARACTERIZATION OF GRAPHITE FIBERS BY X-RAY DIFFRACTION Final Report **c24**
Peter Arsenovic *In* Universal Energy Systems, Inc., United States Air Force Graduate Student Summer Support Program, Volume 1 Dec. 1987 20 p (For primary document see N89-12754 04-31)
Avail: NTIS HC A99/MF E03 CSCL 11D

Samples of different types of graphite fibers were prepared for measurement in a Picker diffractometer. Young's modulus and crystallite orientation measurements were made, as well as equatorial and meridional scans on the fibers. The results show that the higher modulus fibers have improved crystallite orientation, and that applying tensile stress will increase the orientation by a small amount. The diffraction peaks become less sharp for fibers with a lower modulus. This work was an important step toward the formulating of a model that will explain the mechanical behavior of graphite fibers in terms of their internal structure. Author

N89-12756# Kent State Univ., Ohio. Dept. of Physics.
COMPUTER EVALUATION OF ION-IMPLANTED DOPANT PROFILE EVOLUTION DURING ANNEALING Final Report **c76**
Steven W. Rucev *In* Universal Energy Systems, Inc., United States Air Force Graduate Student Summer Support Program, Volume 1 Dec. 1987 14 p (For primary document see N89-12754 04-31)
Avail: NTIS HC A99/MF E03 CSCL 20L

The project is to study the partial annealing of dopant implanted GaAs or silicon. Dr. David Moroi has developed an analytical solution for the concentration profile during ion-implantation which had not been evaluated. A computer analysis was made to compare with a numerical solution. For the case of the linear dependence of the diffusion parameter excellent agreement was found between the solutions for a constant diffusion, but for a concentration dependence an overall relative error of about 5 percent is shown over the range of significant concentration. Author

N89-12757# Missouri Univ., Rolla. Dept. of Electrical Engineering.
ISOLATION OF OSTEOGENIC CELLS FROM THE TRAUMA-ACTIVATED PERIOSTEUM Final Report **c44**
Chang-Hsiao Wu and John Bullock *In* Universal Energy Systems, Inc., United States Air Force Graduate Student Summer Support

Program, Volume 1 Dec. 1987 11 p (For primary document see N89-12754 04-31)
Avail: NTIS HC A99/MF E03 CSCL 10A

Closed, greenstick type fractures were created in adult male white New Zealand rabbits. After a waiting period of 5 days the developing callous and bone approximately 1 cm to each side of the callous was harvested and cell cultures established. Biochemical assays for total protein, alkaline phosphatase activity and glycosamino-glycan content were performed on spent media collected at each change and upon the cells after their termination, in an attempt to more fully characterize the osteoblast population. Since little is known about bone forming cells isolated from this source it is important to establish baseline data so as to be able to relate reactions of these cells to altered environmental conditions. Author

N89-12758# Texas A&M Univ., College Station. Dept. of Nuclear Engineering.
PRELIMINARY THERMAL ANALYSIS OF A BIMODAL NUCLEAR ROCKET CORE Final Report **c20**
David C. Carpenter *In* Universal Energy Systems, Inc., United States Air Force Graduate Student Summer Support Program, Volume 1 Dec. 1987 14 p (For primary document see N89-12754 04-31)
Avail: NTIS HC A99/MF E03 CSCL 21H

The framework for a general purpose finite element analysis code was developed to study the 2-D temperature distribution in a hot-channel hexagonal fuel element in the core of a bimodal nuclear rocket. Preliminary thermal-hydraulic analysis of the core pressure drops under helium coolant conditions were also performed. Hydrogen coolant analysis was not performed due to insufficient property data in a usable form. Although the thermal gradients observed in the fuel element did not seem to present a problem, a more detailed thermal stress analysis was initiated. The stress analysis is not fully implemented in the code at this time. Code development also progressed into 3-D temperature distributions in anticipation of projected research. Author

N89-12759# New Mexico Univ., Albuquerque. Dept. of Physics and Astronomy.
CONSTRUCTION OF A PHASE CONJUGATE LASER RESONATOR USING BRILLOUIN ENHANCED FOUR WAVE MIXING Final Report **c36**
Kyunam Choi *In* Universal Energy Systems, Inc., United States Air Force Graduate Student Summer Support Program, Volume 1 Dec. 1987 17 p (For primary document see N89-12754 04-31)
Avail: NTIS HC A99/MF E03 CSCL 20E

A study on the realization of a phase conjugate laser resonator employing the Brillouin enhanced four wave mixing as its main phase conjugation mechanism is discussed. The resonator output beam can maintain monochromatic laser wavelengths with excellent temporal and spatial beam profile while enjoying high phase-conjugate fidelity. Details on experimental procedures together with experimental results are reported. Author

N89-12760# Tennessee Univ. Space Inst., Tullahoma. Dept. of Physics.
DIRECTED MOTION DOPPLER SHIFT EFFECTS ON NITRIC OXIDE (0.0) GAMMA BAND RESONANCE ABSORPTION Final Report **c25**
James A. Drakes *In* Universal Energy Systems, Inc., United States Air Force Graduate Student Summer Support Program, Volume 1 Dec. 1987 19 p (For primary document see N89-12754 04-31)
Avail: NTIS HC A99/MF E03 CSCL 07D

An investigation into the effects of flowfield-induced Doppler shifts was performed. The directed motion Doppler shift arises in expanding flowfields where the gas molecules are traveling with non-parallel trajectories. It was found that the shifting of the line center frequency of the absorption lines in the medium, caused by the gas expansion, lead to a marked increase in the transmittance of the medium. Our study examined an absorbing conical flow, using both a homogeneous model, the transmittance at the second band head, located at approximately 2262 Angstroms, was increased in the range of 5- to 17- percent upon the inclusion of flowfield Doppler shifts, depending on the exit velocity of the flow. The transmittance at the second band head of the annular flowfield showed an increase with the inclusion of the directed motion Doppler shift of from 8- to 22- percent, varying with the exit velocity. Author

N89-12761# Cincinnati Univ., Ohio. Dept. of Aerospace Engineering.
PRELIMINARY APPLICATIONS OF DECENTRALIZED ESTIMATION TO LARGE FLEXIBLE SPACE STRUCTURES Final Report **c18**
Susan M. Dumbacher *In* Universal Energy Systems, Inc., United States Air Force Graduate Student Summer Support Program, Volume 1 Dec. 1987 16 p (For primary document see N89-12754 04-31)
Avail: NTIS HC A99/MF E03 CSCL 22B

The advent of space travel requires the examination of Large Flexible Space Structures (LFSS) as a means to achieve it. Much experimentation is being done in the field of control and estimation of parameters on these structures, since adequate testing cannot be done on earth to determine exactly the damping, frequencies and mode shapes of these structures. To vibrationally suppress a LFSS, or maintain it at a state of equilibrium, actuators and sensors are placed at various locations along the structure which are then used to damp out selected modes. To determine modal positions and velocities of a LFSS, decentralized estimation/control is examined here as an alternative to a fully centralized system. Author

N89-12762# Alabama Univ., Tuscaloosa. Dept. of Health Education.
VALIDITY OF HEAT INDEX AS INDICATOR OF LEVEL OF HEAT STORAGE FOR PERSONNEL WEARING PROTECTIVE CLOTHING IN HOT ENVIRONMENTS Final Report **c54**
K. Suzanne Enlow *In* Universal Energy Systems, Inc., United States Air Force Graduate Student Summer Support Program, Volume 1 Dec. 1987 18 p (For primary document see N89-12754 04-31)
Avail: NTIS HC A99/MF E03 CSCL 05H

The use of protective clothing such as the Chemical Defense Ensemble (CDE) in moderate to hot environments substantially reduces work capacity due to heat stress. The purpose of this research was to determine the validity of a heat stress index in predicting the level of heat storage when used during work/rest cycles with intermittent microenvironmental cooling. Author

N89-12763# Notre Dame Univ., Ind. Dept. of Civil Engineering.
INVESTIGATION INTO THE APPLICABILITY OF FRACTURE MECHANICS TECHNIQUES TO AIRCRAFT WHEEL LIFE STUDIES Final Report **c39**
Thomas J. Enneking *In* Universal Energy Systems, Inc., United States Air Force Graduate Student Summer Support Program, Volume 1 Dec. 1987 20 p (For primary document see N89-12754 04-31)
Avail: NTIS HC A99/MF E03 CSCL 20K

In response to a specified logistic need, an in-house program was started in late 1986 to investigate test and analytical methods for wheel life estimation and verification. In conjunction with this program, an additional ten week study was initiated June 1, 1987 to explore analytical techniques for fatigue analysis and experimental methods to verify these analytical techniques. In particular, the applicability and feasibility of applying fracture mechanics concepts to aircraft wheel assemblies was assessed. A literature review was performed to identify current research activity involving aircraft wheels and fatigue studies. This was expanded to include finite element techniques and stochastic methods as applied to wheel life and reliability estimates. Based on the results of this study, and previous studies, a combined analytical and experimental methodology was proposed for the estimation and verification of aircraft wheel service life. This proposed multi-task approach contains several alternatives within

the individual tasks. The optimum alternatives, i.e., those with the highest probability of success and an acceptable cost (effort), will be the object of further studies. Author

N89-12764# Ohio Univ., Lancaster. Dept. of Psychology.
THE EFFECTS OF HIGH NOISE LEVELS ON THE ACOUSTIC-PHONETIC STRUCTURE OF SPEECH: A PRELIMINARY INVESTIGATION **c71**
Beverley A. Gable *In* Universal Energy Systems, Inc., United States Air Force Graduate Student Summer Support Program, Volume 1 Dec. 1987 20 p (For primary document see N89-12754 04-31)
Avail: NTIS HC A99/MF E03 CSCL 20A

The purpose of this study was to provide some preliminary data concerning the acoustic-phonetic structure of speech produced under high noise levels. Acoustical measurements were made of a set of sentences spoken by four subjects in two conditions: the 95dB noise condition and the no-noise condition. Sentences produced under 95dB noise were different from sentences produced under ambient noise in both durational and spectral characteristics. Author

N89-12765# State Univ. of New York, Buffalo. Dept. of Psychology.
THE EFFECT OF ATTENTIONAL FOCUS LEVEL ON TASK PERFORMANCE UTILIZING INFORMATION FROM DIFFERENT STIMULUS STRUCTURE LEVELS Final Report **c53**
Deborah A. Gagnon *In* Universal Energy Systems, Inc., United States Air Force Graduate Student Summer Support Program, Volume 1 Dec. 1987 21 p (For primary document see N89-12754 04-31)
Avail: NTIS HC A99/MF E03 CSCL 05I

An experiment is described that will allow for the analysis of performance on an object and scene two-alternative forced choice task under different stimulus structure attention focuses. Seventeen subjects participated in a pilot study at the State University of New York at Buffalo. Suggestions for a data analysis are made. Author

N89-12766# Oregon State Univ., Corvallis. Dept. of Computer Science.
PROVIDING ON-LINE GUIDANCE TO COMPUTER USERS Final Report **c61**
Edward M. Gellenbeck *In* Universal Energy Systems, Inc., United States Air Force Graduate Student Summer Support Program, Volume 1 Dec. 1987 20 p (For primary document see N89-12754 04-31)
Avail: NTIS HC A99/MF E03 CSCL 09B

The conceptual design for an on-line guidance interface is presented. The design is based on research in user-oriented interface design and artificial intelligence. The on-line guidance interface offers help to users in goal-oriented, context-sensitive terms. It is accessed through a window on a multi-tasking computer system. The guidance interface is examined as an interface to information retrieval services. The paper concludes with a list of references in the area of user-oriented interface design. Author

N89-12767# New Mexico State Univ., University Park. Dept. of Electrical and Computer Engineering.
MODE EXTRACTION FROM AN ELECTROMAGNETIC SLOW WAVE SYSTEM Final Report **c32**
James A. Gerald *In* Universal Energy Systems, Inc., United States Air Force Graduate Student Summer Support Program, Volume 1 Dec. 1987 20 p (For primary document see N89-12754 04-31)
Avail: NTIS HC A99/MF E03 CSCL 20N

Expressions for the electromagnetic fields in a coaxial waveguide with a corrugated outer conductor were obtained. In this analysis, the depth, width, and period of the corrugations remained variable along with the radius of the inner conductor and the overall radius of the structure. Also, for the purpose of analysis, the structure has been divided into two regions, 1 and 2. Region 1 is the portion of the waveguide contained within the corrugations or slots. To meet the boundary conditions, several functions have been used to approximate the z-directed component of the electric field at the radius b. A comparison of how well the fields match at the radius b for each approximation has been made. The phase velocity in the slow wave structure was of particular interest, and methods for obtaining it have been presented. Author

N89-12768# Washington State Univ., Pullman. Dept. of Mechanical and Materials Engineering.
GROUND RUN-UP AFTERBURNER DETECTION AND NOISE SUPPRESSION Final Report **c07**
Jeffrey J. Girard *In* Universal Energy Systems, Inc., United States Air Force Graduate Student Summer Support Program, Volume 1 Dec. 1987 8 p (For primary document see N89-12754 04-31)
Avail: NTIS HC A99/MF E03 CSCL 21E

Two projects were completed, both related to aircraft station engine run-up noise. A purchase description was written for an acoustic detection system to determine whether an aircraft in a shelter has engaged afterburners. A test plan was written for a test to supply information required for evaluation of noise suppression techniques employed in hush houses for ground round-up. Author

N89-12769# Ohio State Univ., Columbus. Dept. of Exercise Physiology and Physiological Chemistry.
ALTERATIONS OF SEGMENTAL VOLUME DURING ORTHOSTATIC STRESS IN NONHUMAN PRIMATES Final Report **c51**
Beverly Elaine Girten *In* Universal Energy Systems, Inc., United States Air Force Graduate Student Summer Support Program, Volume 1 Dec. 1987 20 p (For primary document see N89-12754 04-31)
Avail: NTIS HC A99/MF E03 CSCL 06P

The effect of exposure to short-term simulated weightlessness on the volume changes that occur in young adult nonhuman primates is investigated. A series of experiments involving head-up and head-down tilt protocols were conducted to test feasibility of using impedance plethysmographic equipment and procedures to define segmental volume changes in Rhesus monkeys. The specific objectives involved monitoring the calf, thigh, pelvic, abdominal and thoracic volumes prior to, during, and following exposure to short-term orthostatic and antiorthostatic stress. Initial work on this project involved preliminary testing of the data recording system. Four adult male Rhesus monkeys were tested during this phase, and impedance plethysmography was utilized to determine segmental volume changes. Ten animals were tested during the primary experiment. The data obtained indicated that fluid exchange between the peripheral and the more head-up or head-down, and the redistribution seems to be graded and a function of the angle of tilt. These results suggest that the peripheral arterial/venous system is able to compensate for mild stresses produced by low angles of head-up and head-down tilt; however, it is not able to maintain this compensation during or following the higher angles of tilt. Author

N89-12770# San Diego State Univ., Calif. Dept. of Psychology.
DESIGNING SIMULATOR TASKS TO STUDY THE HIGH SPEED, LOW ALTITUDE ENVIRONMENT Final Report **c53**
Laura Giusti *In* Universal Energy Systems, Inc., United States Air Force Graduate Student Summer Support Program, Volume 1 Dec. 1987 12 p (For primary document see N89-12754 04-31)
Avail: NTIS HC A99/MF E03 CSCL 05I

An experiment was designed as an instrument to measure the effectiveness of proposed experimental training regimes and display designs. A computer simulation of a terrain-following, terrain-avoidance task was used to determine the subjects' capabilities in the high-speed, low altitude flying environment. Subjects controlled only the pitch and altitude of their aircraft and were instructed to successfully maneuver over and between twenty equidistant buildings. Preliminary results suggest that the task will

be an effective measure for evaluating training regimes and display designs. Author

N89-12771# Louisiana State Univ., Baton Rouge. Dept. of Mechanical Engineering.
SIX DEGREE OF FREEDOM SIMULATION COMPUTER PROGRAM FOR AEROELASTIC FREE-FLIGHT PROJECTILES Final Report **c61**
Thomas Harkins *In* Universal Energy Systems, Inc., United States Air Force Graduate Student Summer Support Program, Volume 1 Dec. 1987 18 p (For primary document see N89-12754 04-31)
Avail: NTIS HC A99/MF E03 CSCL 09B

The objective of this research effort was to determine how much influence aeroelastic effects had on determining the aerodynamic coefficients of a free-flight projectile. These coefficients were determined from parameter estimation techniques based on rigid body motion. A general six degree of freedom simulation program was developed in FORTRAN code. The program was then modified by adding elastic inertia terms. The flight simulator was run with the rigid body aerodynamic coefficients, but the model itself was allowed to flex during its flight. Preliminary results showed that the body's flexing had no effect on the trajectory. Author

N89-12772# Meharry Medical Coll., Nashville, Tenn. Dept. of Biomedical Sciences.
THE EFFECTS OF HYPERBARIC OXYGEN AND ANTIOXIDANT DEFICIENCIES ON RAT RETINAL ULTRASTRUCTURE Final Report **c51**
Adrienne L. Hollis *In* Universal Energy Systems, Inc., United States Air Force Graduate Student Summer Support Program, Volume 1 Dec. 1987 19 p (For primary document see N89-12754 04-31)
Avail: NTIS HC A99/MF E03 CSCL 06C

It was shown previously that the electro-physiological response of the rat retina is rapidly diminished in animals fed diets deficient in both vitamin E and selenium for 6 weeks and treated with hyperbaric oxygen (HBO). Animals deficient in vitamin E alone also show diminished electroretinograms but only after prolonged hyperbaric oxygen treatment. Through quantitative histopathological studies, damage to the retinal pigment epithelial layer as well as the outer nuclear layer has been observed in animals fed a diet for 15 weeks that was deficient in vitamin E only. The alterations in retinal tissues observed by electrophysiology and quantitative histopathology should correlate with ultrastructural studies. In this study, we have prepared retinal tissue samples for electronmicroscopy studies and have obtained electron micrographs for future cytopathological analyses. The parameters to be studied include outer segment disk membrane deterioration, lipofuscin content of the RPE, phagosome number in the RPE, separations between tips of photoreceptors and apical surface of RPE, and migration of photoreceptor cells into the inner retina. Author

N89-12773# Colorado Univ., Boulder. Dept. of Aerospace Engineering Sciences.
A COMPARATIVE STUDY OF DIFFERING VORTEX STRUCTURES ARISING IN UNSTEADY SEPARATED FLOWS Final Report **c34**
Stephen A. Huyer *In* Universal Energy Systems, Inc., United States Air Force Graduate Student Summer Support Program, Volume 1 Dec. 1987 19 p (For primary document see N89-12754 04-31)
Avail: NTIS HC A99/MF E03 CSCL 20D

The vortex structures arising in two separate unsteady separated flow cases were examined in detail. The flowfields resulting from the deployment of a periodically deforming leading edge (PDLE) and an oscillating flat plate were studied and compared. The PDLE produced two separate vortex structures during each cycle. It was found through flow visualization and hot-wire anemometry that these two structures exhibited different behavior. The primary vortex was characterized by low, constant velocities within the vortex, increasing threefold to 120 percent freestream values in a space of 3 mm. The second vortex exhibited a more even vortex rotation rate. The vortex structures produced by an oscillating flat plate were also examined. It was found that a reduced frequency of 3 yielded a more cohesive vortex compared to that produced by a reduced frequency of 1. The structures produced by PDLE deployment were also considerably weaker than those produced by an oscillating flat plate. Author

N89-12774# University of Eastern Illinois, Charleston. Dept. of Mathematics.
PERTURBED FUNCTIONAL ITERATION APPLIED TO THE NAVIER-STOKES EQUATIONS Final Report **c34**
David L. James *In* Universal Energy Systems, Inc., United States Air Force Graduate Student Summer Support Program, Volume 1 Dec. 1987 9 p (For primary document see N89-12754 04-31)
Avail: NTIS HC A99/MF E03 CSCL 20D

The Navier-Stokes partial differential equations were written as a set of averaged finite difference equations. Of the methods available, Perturbed Functional Iteration was chosen to solve the Navier-Stokes equations. The Perturbed Functional Iteration Scheme (PFIS) was applied to both a two dimensional problem, both implicitly and explicitly, and a three dimensional problem, explicity. PFIS quickly gave accurate results in the test cases. Author

N89-12775# Texas A&M Univ., College Station. Dept. of Aerospace Engineering.
AN OPTICAL SENSOR SYSTEM FOR MONITORING STRUCTURAL DYNAMICS WITH APPLICATIONS TO SYSTEM IDENTIFICATION Final Report **c74**
George Henry James, III *In* Universal Energy Systems, Inc., United States Air Force Graduate Student Summer Support Program, Volume 1 Dec. 1987 20 p (For primary document see N89-12754 04-31)
Avail: NTIS HC A99/MF E03 CSCL 20F

A unique optical sensor system using video cameras, digital processing, and photogrammetric triangulation has been shown to be feasible for use in monitoring structural dynamics. The system can determine natural frequencies, mode shapes, and displacement time histories. The major advantages of the system are the possibility of non-contact measurement, ease of marker application, simple operation and upkeep, the ability to cover a large area, and excellent large amplitude and low frequency response. The major disadvantages of the system are low spatial resolution and long processing times. Using the ERA algorithm, the first five natural frequencies of the 5 X 5 ft, aluminum grid test structure were calculated in a high coverage mode, in a high resolution mode, and in a 2D mode. The first three mode shapes were calculated using ERA with the high coverage data. Recommendations for improvements in the system, future research, and possible uses are provided. Author

N89-12776# Cornell Univ., Ithaca, N.Y. School of Electrical Engineering.
A SYSTEM TO INVESTIGATE SYNTHESIZED VOICE FEEDBACK IN MAN-MACHINE INTERFACES Final Report **c54**
Michele E. Johnson *In* Universal Energy Systems, Inc., United States Air Force Graduate Student Summer Support Program, Volume 1 Dec. 1987 17 p (For primary document see N89-12754 04-31)
Avail: NTIS HC A99/MF E03 CSCL 05H

The Rome Air Development Center (RADC), Intelligence Analysis Branch, is sponsoring an in-house research effort to study and develop advanced man-machine interfaces. At present, most interfaces consist of a keyboard and a display terminal, and feedback to a user is visual. Verbal dialog is an alternative interface that has the potential to reduce the human operator's visual load, and to take advantage of the verbal communication skills that almost every human being possesses. This paper described the elements of a system that RADC will use to investigate verbal

feedback to a human operator, more specifically to examine the interactions between synthesized message characteristics and the performance of tasks requiring comprehension of audio information. Author

N89-12777# Auburn Univ., Ala. Dept. of Civil Engineering.
WAVE PROPAGATION IN LAYERED STRUCTURES Final Report **c32**
David W. Landis *In* Universal Energy Systems, Inc., United States Air Force Graduate Student Summer Support Program, Volume 1 Dec. 1987 20 p (For primary document see N89-12754 04-31)
Avail: NTIS HC A99/MF E03 CSCL 20N

Protective military shelters are typically constructed of massive, monolithic, reinforced concrete slabs. This is considered necessary in order to protect personnel and vital equipment inside the shelter from the spall caused by the high-intensity blast waves caused by convectional weaponry. Recent studies show that layered structures may be an alternative to the massive monolithic construction. The objective of this study is to show that the implementation of layered structures can significantly reduce or eliminate the incidence of interior spalling of the concrete walls. The layered structures considered in this study are concrete-sand-concrete and concrete-polystyrene-concrete models. This study presents the results of a numerical analysis to evaluate the effectiveness of layered structures in reducing the transmission of high-intensity blast waves. The results show that layered structures can be very effective in the reduction in stress wave transmission. Author

N89-12778# Auburn Univ., Ala. Dept. of Computer Science and Engineering.
INSTALLATION OF THE ADINA FEM COMPUTER PROGRAMS Final Report **c61**
Sharon K. Landis *In* Universal Energy Systems, Inc., United States Air Force Graduate Student Summer Support Program, Volume 1 Dec. 1987 13 p (For primary document see N89-12754 04-31)
Avail: NTIS HC A99/MF E03 CSCL 09B

The ADINA computer program package consists of four separate computer programs to be used in conjunction with one another: ADINA-IN, ADINA, ADINAT, and ADINA-PLOT. The ADINA programs are for the static and dynamic, linear and nonlinear finite element analysis of solids, structures, and fluid-structure systems. Due to the large size of the ADINA programs, ADINA-IN, ADINA, ADINAT and ADINA-PLOT must be broken into smaller modules to minimize the amount of central memory occupied by the ADINA programs. If the ADINA programs occupy less central memory, then a larger finite element problem can be solved. Also, a user-friendly interface was developed to aid the users at HQ AFESC/RDC in executing any of the ADINA programs. Author

N89-12779# Ohio State Univ., Columbus. Dept. of Mechanical Engineering.
EXPERIMENTAL STUDY OF ISOTHERMAL FLOWS IN A DUMP COMBUSTOR Final Report **c34**
Craig A. Langenfeld *In* Universal Energy Systems, Inc., United States Air Force Graduate Student Summer Support Program, Volume 1 Dec. 1987 16 p (For primary document see N89-12754 04-31)
Avail: NTIS HC A99/MF E03 CSCL 20D

Isothermal flows in a dump combustor were studied for configuration of no swirl and of weak swirl, S = 0.3. Detailed mean flow and turbulence measurements in the axial and radial directions were obtained using a two-component coincident LDV system. Mean axial and radial velocity, axial and radial turbulence intensities and Reynolds stress profiles are plotted. The relativity of the data to previous work in the same model but for the axial and tangential directions is discussed. For the no swirl case, the flow does not become fully developed flow even at 24 step heights downstream. Turbulence intensities and Reynolds stresses peak at a shear layer generated by recirculating flow for locations before reattachment and decay out further downstream. For both no swirl and weak swirl, the Reynolds stress in the axial-radial plane was greater than for axial-tangential plane for the shear layer region between the main flow and the recirculating flow. Author

N89-12780# Louisiana State Univ., Baton Rouge. Dept. of Mechanical Engineering.
A COMPUTER SIMULATION OF A PLASMA ARMATURE RAILGUN Final Report **c14**
Christopher B. Leger *In* Universal Energy Systems, Inc., United States Air Force Graduate Student Summer Support Program, Volume 1 Dec. 1987 24 p (For primary document see N89-12754 04-31)
Avail: NTIS HC A99/MF E03 CSCL 14B

A computer simulation for a plasma armature railgun was developed for use on a Zenith 248 microcomputer. The purpose of the simulation is to predict gun performance both for design purposes and to estimate the results of specific shot conditions. The simulation models projectile velocity, power supply currents, armature mass, and armature length. These parameters are modeled using equations expressing their time rates of change and then using numerical integration. The acceleration includes terms for ablation and viscous drag effects, and the ablation is made velocity dependent. This gives good agreement with experimental results. Author

N89-12781# New Mexico Univ., Albuquerque. Dept. of Physics and Astronomy.
INVESTIGATION OF LASER DIODE COUPLING USING NONLINEAR OPTICS Final Report **c36**
Bruce W. Liby *In* Universal Energy Systems, Inc., United States Air Force Graduate Student Summer Support Program, Volume 1 Dec. 1987 8 p (For primary document see N89-12754 04-31)
Avail: NTIS HC A99/MF E03 CSCL 20E

A discussion of the original goals is contained, as well as how they were changed and why. The pertinent operating characteristics of the laser diodes to be used are described, and recommendations for follow on experiments are presented. Author

N89-12782# Georgia Inst. of Tech., Atlanta. School of Mechanical Engineering.
LIQUID SCINTILLATION COUNTING WITH THE PACKARD 1500 ANALYZER Final Report **c25**
Randal L. Mandock *In* Universal Energy Systems, Inc., United States Air Force Graduate Student Summer Support Program, Volume 1 Dec. 1987 11 p (For primary document see N89-12754 04-31)
Avail: NTIS HC A99/MF E03 CSCL 07D

Alpha and beta particles were detected with the Packard 1500 Liquid Scintillation Analyzer. Six tests of the EPA Radon-222 in water by liquid scintillation produced results which agreed with the known activities within the uncertainty when three regions were analyzed. The alpha activity measured for Pu-242 was consistently high, although the majority of the measurements taken in Region B agreed with the known activity within the uncertainty. The alpha activity measured for Am-241 agreed well with the known activity for every measurement in Region B. Measured tritium activities decreased due to color quenching as urine color progressed from light to dark. Background determination was found to be a key element when measuring low levels of activity. Author

N89-12783# Oregon Graduate Center for Study and Research, Beaverton. Dept. of Applied Physics and Electrical Engineering.
DE-EMBEDDING S-PARAMETER MEASUREMENTS USING TSD TECHNIQUE **c32**
James W. Mattern *In* Universal Energy Systems, Inc., United States Air Force Graduate Student Summer Support Program, Volume 1 Dec. 1987 14 p (For primary document see N89-12754 04-31)
Avail: NTIS HC A99/MF E03 CSCL 20N

Scattering-parameter measurement of devices embedded in microstrip lines are de-embedded using the Thru-Short-Delay method. A computer algorithm was developed to calculate the error adjustment terms needed to adjust the error matrix supplied

by the network analyzer. The results are new error terms that shift the measurement plane to device level. The algorithm was tested successfully by using a pair of 10 cm airlines with APC7 connectors to simulate a pair of arbitrary launchers. Author

N89-12784# Vanderbilt Univ., Nashville, Tenn. Dept. of Electrical Engineering.

AN EXPERT SYSTEM FOR DIAGNOSIS AND REPAIR OF ANALOG CIRCUITS Final Report c33

Matthew B. McBeth *In* Universal Energy Systems, Inc., United States Air Force Graduate Student Summer Support Program, Volume 1 Dec. 1987 18 p (For primary document see N89-12754 04-31)

Avail: NTIS HC A99/MF E03 CSCL 09C

The purpose for this research project is to study the use of artificial intelligence in the domains of electronic diagnosis and repair. This paper describes a framework for building expert systems in such a domain, concentrating on an amplifier circuit board frequently used in data acquisition systems at Sverdrup Technology. The system under development is designed to aid the technicians in diagnosing and repairing the amplifier board down to the component level. This system will detect a potential fault and have the technician either adjust, check, or replace a component. It will then verify whether that was the problem and make a record of all repairs. This paper will also discuss the knowledge acquisition techniques used for the system, and the knowledge that was gained from each. Author

N89-12785* National Aeronautics and Space Administration. Pasadena Office, Calif.

SELF-ACTUATING HEAT SWITCHES FOR REDUNDANT REFRIGERATION SYSTEMS Patent

Chung K. Chan, inventor (to NASA) (Jet Propulsion Lab., California Inst. of Tech., Pasadena.) 20 Sep. 1988 8 p

(NASA-Case-NPO-17085-1-CU; US-Patent-4,771,823; US-Patent-Appl-SN-087282; US-Patent-Class-165-61; US-Patent-Class-62-467; US-Patent-Class-62-514-R; US-Patent-Class-165-96) Avail: US Patent and Trademark Office CSCL 13B

A dual refrigeration system for cooling a sink device is described, which automatically thermally couples the cold refrigerator to the sink device while thermally isolating the warm refrigerator from the sink device. The system includes two gas gap heat switches that each thermally couples one of the refrigerators to the sink device, and a pair of sorption pumps that are coupled through tubes to the heat switches. When the first refrigerator is operated and therefore cold, the first pump which is thermally coupled to it is also cooled and adsorbs gas to withdraw it from the second heat switch, to thereby thermally isolate the sink device from the warm second refrigerator. With the second refrigerator being warm, the second pump is also warm and desorbs gas, so the gas lies in the first switch, to close that switch and therefore thermally couple the cold first refrigerator to the sink device. Thus. the heat switches are automatically switched according to the temperature of the corresponding refrigerator.

Official Gazette of the U.S. Patent and Trademark Office

N89-12786* National Aeronautics and Space Administration. Langley Research Center, Hampton, Va.

TRUSS-CORE CORRUGATION FOR COMPRESSIVE LOADS Patent

Randall C. Davis, inventor (to NASA) and Robert Jackson, inventor (to NASA) 13 Sep. 1988 9 p Filed 5 Mar. 1987 Supersedes N87-25496 (25 - 19, p 2601)

(NASA-Case-LAR-13438-1; US-Patent-4,769,968; US-Patent-Appl-SN-022298; US-Patent-Class-52-814; US-Patent-Class-52-821; US-Patent-Class-428-182) Avail: US Patent and Trademark Office CSCL 13B

A corrugated panel structure for supporting compressive loads is described which includes curved cap strips separated by truss-core web segments. The truss-core web segments are formed from first and second flat panels with a corrugated filler in between them. The corrugated filler extends in the direction of the compressive load. As a result, all components of the panel structure have a compressive load carrying capability resulting in a high strength-to-weight ratio when the compressive load is limiting. Application to rocket and aircraft structures is suggested.

Official Gazette of the U.S. Patent and Trademark Office

N89-12787# Sandia National Labs., Albuquerque, N. Mex. Fluid and Thermal Sciences Dept.

INVESTIGATIONS INTO THE PLASMA SPRAY PROCESS

R. C. Dykhuizen and M. F. Smith 1988 11 p Presented at the National Thermal Spray Conference, Cincinnati, Ohio, 24 Oct. 1988

(Contract DE-AC04-76DP-00789)

(DE88-014524; SAND-88-1132C; CONF-881026-1) Avail: NTIS HC A03/MF A01

A simple analytical model that was developed to examine momentum and thermal transfer from the plasma jet to the spray particles in low-pressure plasma spray deposition is described. This model correctly predicts a previously unreported maximum in spray particle acceleration at intermediate chamber pressure and, for conditions appropriate to the simplifying assumptions, the calculated results were in good agreement with experimentally measured spray particle size and mass density on particle velocity. The model has also been used to explore the thermal effects of variations in selected process parameters. The analytical and experimental results for particle velocity are again in good agreement, with substantially lower acceleration rates and lower peak velocities for larger, more massive particles. The results of the thermal calculations indicate that particle melting is influenced by many mechanisms. The net effect is that better particle melting is obtained at higher chamber pressure levels. Detailed thermal data are not yet available to enable verification of the thermal model; however, the predictions of the thermal model appear to be in qualitative agreement with empirically developed spray conditions for good particle melting. The model indicates that difficulties in melting refractory materials at very low chamber pressures are related to decreased plasma temperatures and plasma densities at low chamber pressures. DOE

N89-12788# Los Alamos National Lab., N. Mex.

FIRE AEROSOL EXPERIMENT AND COMPARISONS WITH COMPUTER CODE PREDICTIONS

W. S. Gregory, B. D. Nichols, B. W. White, P. R. Smith, I. H. Leslie, and J. R. Corkran (New Mexico State Univ., Las Cruces.) 1988 14 p Presented at the 20th DOE/NRC Nuclear Air Cleaning Conference, Boston, Mass., 22 Aug. 1988

(Contract W-7405-eng-36)

(DE88-016328; LA-UR-88-2666; CONF-880815-7) Avail: NTIS HC A03/MF A01

Los Alamos National Laboratory, in cooperation with New Mexico State University, has carried on a series of tests to provide experimental data on fire-generated aerosol transport. These data will be used to verify the aerosol transport capabilities of the FIRAC computer code. FIRAC was developed by Los Alamos for the U.S. Nuclear Regulatory Commission. It is intended to be used by safety analysts to evaluate the effects of hypothetical fires on nuclear plants. One of the most significant aspects of this analysis deals with smoke and radioactive material movement throughout the plant. The tests have been carried out using an industrial furnace that can generate gas temperatures to 300 C. To date, we have used quartz aerosol with a median diameter of about 10 microns as the fire aerosol simulant. We also plan to use fire-generated aerosols of polystyrene and polymethyl methacrylate (PMMA). The test variables include two nominal gas flow rates (150 and 300 cu ft/min) and three nominal gas ter peratures (ambient, 150 C, and 300 C). The test results are pr sented in the form of plots of aerosol deposition vs length of duct. in addition, the mass of aerosol caught in a high-efficiency particulate air (HEPA) filter during the tests is reported. The tests are simulated with the FIRAC code, and the results are compared with the experimental data. DOE

N89-12789# California Univ., Berkeley. Sensor and Actuator Center.
AS-DEPOSITED LOW-STRAIN LPCVD (LOW-PRESSURE, CHEMICAL-VAPOR-DEPOSITION) POLYSILICON
L. S. Fan and R. S. Muller Aug. 1988 7 p Prepared for Lawrence Livermore National Lab., Calif.
(Contract W-7405-eng-48)
(DE88-016980; UCRL-21092) Avail: NTIS HC A02/MF A01

As-deposited polysilicon films with very low residual strain (lower than 5 x .00001) are obtained by a low pressure, chemical vapor deposition (LPCVD) process. Straight polysilicon bridges 300 microns long, 1.2 microns thick, and 2 to 20 microns wide, made using this process. No buckling has been observed in any of the nearly one thousand bridges of this type made in two separate process runs. In addition, no problems of sticking between the bridges and the substrate were encountered with these structures. The polysilicon films from which the beams were fabricated were deposited by pyrolyzing silane at 605 C on a phosphosilicate-glass (PSG) layer (8 wt percent P). The PSG layer serves as a sacrificial layer to be subsequently etched away to free the bridge. Our research is aimed at obtaining an understanding of these relationships through consideration of the role of interfacial stresses and the kinetics of initial crystalline nucleation. The technique for producing these low-strain films is significant, however, because no high-temperature annealing steps are required to produce them. DOE

32 COMMUNICATIONS AND RADAR

Includes radar; land and global communications; communications theory; and optical communications.

For related information see also *04 Aircraft Communications and Navigation* and *17 Space Communications, Spacecraft Communications, Command and Tracking.* For search and rescue see *03 Air Transportation and Safety,* and *16 Space Transportation.*

N89-12790# Applied Research Corp., Huntsville, Ala.
ANTENNA PATTERN STUDY Final Report
Warren Harper 15 Jul. 1988 62 p Prepared in cooperation with Uwohali, Inc., Huntsville, Ala.
(ARI/R-88-510Z) Avail: NTIS HC A04/MF A01

Prediction of antenna radiation patterns has long been an important function in the design of command, communication, and tracking systems for rocket vehicles and spacecraft. An acceptable degree of assurance that a radio link will provide the required quality of data or certainty of correct command execution must be acquired by some means if the system is to be certified as reliable. Two methods have been used to perform this function: (1) Theoretical analysis, based on the known properties of basic antenna element types and their behavior in the presence of conductive structures of simple shape, and (2) Measurement of the patterns on scale models of the spacecraft or rocket vehicle on which the antenna is located. Both of these methods are ordinarily employed in the antenna design process. Author

N89-12791# Oak Ridge National Lab., Tenn.
BIOELECTROMAGNETIC EFFECTS OF EMP: PRELIMINARY FINDINGS
T. E. Aldrich, C. E. Easterly, P. C. Gailey, and C. B. Hamilton (Tennessee Univ., Knoxville.) Jun. 1988 120 p Prepared in cooperation with Tennessee Univ., Knoxville; EC Corp., Knoxville, Tenn.
(Contract DE-AC05-84OR-21400)
(DE88-012118; ORNL/TM-10784) Avail: NTIS HC A06/MF A01

Facilities to simulate electromagnetic pulses (EMPs) are used to test military equipment and electrical communications devices for resistance to the effects of an EMP caused by an upper-atmospheric nuclear detonation. The rapid rise time and high field strengths (0.1 to 50 kV/m) of an EMP distinguish it from other electromagnetic phenomena. Certain types of EMP simulators also expose facility operators and members of the public to electromagnetic fields of varying intensity as do other natural sources such as the fields produced near a lightning bolt. Limited biological effects data have been collected to assess the potential EMP health hazards to humans. Evidence from the available database does not establish that EMPs represent either an occupational or a public health hazard. A critique is presented of the EMP research published to date in order to explore its limitations and similarities with related outcome experience from other electromagnetic field research. Laboratory research and multiple years of observations on workers in existing EMP manufacturing and simulation facilities suggest that there are no acute or short-term health effects. The occupational exposure guideline for EMP is 100 kV/m, which is far in excess of usual exposures with EMP simulators. DOE

N89-12792 Syracuse Univ., N. Y.
ON ADAPTIVE CELL-AVERAGING CFAR RADAR SIGNAL DETECTION Ph.D. Thesis
Mourad Barkat 1987 172 p
Avail: Univ. Microfilms Order No. DA8805159

In radar signal detection, the problem is to automatically detect a target in a nonstationary noise and clutter background while maintaining a constant probability of false-alarm. Classical detection using a matched filter receiver and a fixed threshold is not applicable due to the nonstationary nature of the background noise. Therefore, adaptive threshold techniques are needed to maintain a constant false-alarm rate (CFAR). One approach to adaptive detection in nonstationary noise and clutter background is to compare the processed target signal to an adaptive threshold. In the cell-averaging CFAR processing, an estimate of the background noise from the leading and the lagging reference windows is used to set the adaptive threshold. A threshold multiplier (or scaling factor) is used to scale the threshold to achieve the desired probability of false-alarm. Two modified cell-averaging detectors for multiple target situations are proposed. The theory of distributed CFAR detection with data fusion is developed. Two topologies, namely, a parallel and a tandem topology are investigated. The overall systems are optimized so that the probability of detection is maximum while CFAR is achieved. Dissert. Abstr.

N89-12793# Sandia National Labs., Albuquerque, N. Mex.
MICROWAVE RF COUPLING RESPONSE THROUGH ADJACENT CAVITIES
R. P. Toth 1988 5 p Presented at the 4th National High Power Microwave Conference, Monterey, Calif., 9 May 1988
(Contract DE-AC04-76DP-00789)
(DE88-012430; SAND-87-2872C; CONF-8805132-8) Avail: NTIS HC A02/MF A01

The segmentation of the interior volume of a modern weapon system into functionally associated compartments is viewed as a series of multiple connected microwave resonators. It is known that the magnitude of the microwave coupling phenomena is affected by the presence of apertures, conductors, and dielectrics and that each of these factors may interact to exhibit a complex frequency dependence. A large resonator test object was subdivided with adjustable bulkheads which included openings and monopoles connecting adjoining volumes. Microwave signal injection was by either an external monopole receiving antenna or by seam leakage into the test object interior. DOE

N89-12794*# Massachusetts Inst. of Tech., Cambridge. Dept. of Electrical Engineering and Computer Science.
THE OPTIMAL POLARIZATIONS FOR ACHIEVING MAXIMUM CONTRAST IN RADAR IMAGES
A. A. Swartz, H. A. Yueh, J. A. Kong, L. M. Novak, and R. T. Shin (Massachusetts Inst. of Tech., Lexington.) [1988] 33 p
(Grant NAG5-270)
(NASA-CR-183349; NAS 1.26:183349) Avail: NTIS HC A03/MF A01 CSCL 17I

There is considerable interest in determining the optimal polarizations that maximize contrast between two scattering classes in polarimetric radar images. A systematic approach is presented

for obtaining the optimal polarimetric matched filter, i.e., that filter which produces maximum contrast between two scattering classes. The maximization procedure involves solving an eigenvalue problem where the eigenvector corresponding to the maximum contrast ratio is an optimal polarimetric matched filter. To exhibit the physical significance of this filter, it is transformed into its associated transmitting and receiving polarization states, written in terms of horizontal and vertical vector components. For the special case where the transmitting polarization is fixed, the receiving polarization which maximizes the contrast ratio is also obtained. Polarimetric filtering is then applies to synthetic aperture radar images obtained from the Jet Propulsion Laboratory. It is shown, both numerically and through the use of radar imagery, that maximum image contrast can be realized when data is processed with the optimal polarimeter matched filter. Author

N89-12795# Air Force Inst. of Tech., Wright-Patterson AFB, Ohio.
ROBUST RECOGNITION OF LOUD AND LOMBARD SPEECH IN THE FIGHTER COCKPIT ENVIRONMENT Ph.D. Thesis
Bill J. Stanton, Jr. Aug. 1988 433 p
(AD-A197093; AFIT/CI/NR-88-178) Avail: NTIS HC A19/MF A01 CSCL 25D

There are a number of challenges associated with incorporating speech recognition technology into the fighter cockpit. One of the major problems is the wide range of variability in the pilot's voice. That can result from changing levels of stress and workload. Increasing the training set to include abnormal speech is not an attractive option because of the innumerable conditions that would have to be represented and the inordinate amount of time to collect such a training set. A more promising approach is to study subsets of abnormal speech that have been produced under controlled cockpit conditions with the purpose of characterizing reliable shifts that occur relative to normal speech. Such was the initiative of this research. Analyses were conducted for 18 features on 17671 phoneme tokens across eight speakers for normal, loud, and Lombard speech. It was discovered that there was a consistent migration of energy in the sonorants. This discovery of reliable energy shifts led to the development of a method to reduce or eliminate these shifts in the Euclidean distances between LPC log magnitude spectra. This combination significantly improved recognition performance of loud and Lombard speech. Discrepancies in recognition error rates between normal and abnormal speech were reduced by approximately 50 percent for all eight speakers combined. GRA

N89-12796# Air Force Inst. of Tech., Wright-Patterson AFB, Ohio.
TEMPORAL CLUSTERING IN THE MULTI-TARGET TRACKING ENVIRONMENT Ph.D. Thesis
Thomas S. Kelso Aug. 1988 142 p
(AD-A197153; AFIT/CI/NR-88-179) Avail: NTIS HC A07/MF A01 CSCL 15C

In multi-target tracking problems such as those found in high-energy particle physics, fluid mechanics, and ballistic missile defense, the common objective is to separate the data into observations associated with individual targets and to use this data to estimate the targets' trajectories. In defense related applications, it is necessary to have algorithms which are computationally efficient, robust, and minimize data storage requirements. Recently developed approaches in the field of multi-target tracking, however, have been shown to have significant computational disadvantages. In this study, non-hierarchical clustering methods are combined with computationally efficient algorithms such as those used to solve assignment and quadratic programming problems to provide an integrated procedure which is computationally efficient, minimizes data storage requirements, and gives a reasonable estimate of the number of targets. Combined with a sequential estimation filter such as the extended Kalman filter, the procedure can provide estimates of a target's state and state covariance after three observations and continuously maintain updated target state estimates in real time. Empirical results based on 100 targets in ballistic trajectories have demonstrated this method's effectiveness by properly clustering data with four measurement attributes (range, range rate, azimuth, and elevation) in over 98 percent of the cases. GRA

N89-12797# Communications Research Centre, Ottawa (Ontario). Radar and Communications Technology Branch.
PHASE COHERENCE AND SIGNAL-TO-NOISE RATIO CONSIDERATIONS FOR SAMPLED APERTURE RADAR SYSTEMS
J. Litva and H. C. Chan Dec. 1987 47 p
(AD-A197180; CRC-1412) Avail: NTIS HC A03/MF A01 CSCL 17I

This report describes the application of Sampled Aperture Radar (SAMPAR) technology to the tracking of low-angle targets of low-angle targets at sea. In particular, expressions are developed and presented describing aperture signals for a conventional (SAMPAR) configuration which uses coherent local oscillators. The radar signals are shown to contain an interference term in which is contained all of the information used during Correlation Height Analysis (CHA) processing. A continuous wave (CW) experiment designed to evaluate the CHA algorithm is described. This system employs a beacon source and self-cohering receivers. It is shown that the same interference term is also contained in the self-cohered received signal. Some pre-processing of the interference term is required prior to CHA processing to optimize the results. A discussion is given of the implementation of Doppler processing for various target velocities. Finally a discussion is given of signal-to-noise ratios for typical target geometries and sea-state conditions, in which forward-scatter clutter, back-scatter clutter and system noise are taken into account. GRA

N89-12798# Naval Weapons Center, China Lake, Calif.
REVIEW OF ELECTROMAGNETIC SURFACE WAVES, 1960 THROUGH 1987 Final Report, Aug. 1987 - Oct. 1987
P. L. Overfelt Jan. 1988 38 p
(AD-A197278; AD-E900801; NWC-TP-6880) Avail: NTIS HC A03/MF A01 CSCL 20N

This report contains a literature survey on electromagnetic surface waves for the years 1960 through 1987. GRA

N89-12799# Applied Research Lab., State College, Pa.
USE OF PROXIMITY EFFECT IN HEARING AID MICROPHONES TO INCREASE TELEPHONE INTELLIGIBILITY IN NOISE M.S. Thesis
Kathryn R. Wilson Jul. 1988 84 p
(AD-A197311; ARL/PSU/TR-88-007) Avail: NTIS HC A05/MF A01 CSCL 25C

This thesis describes an experiment to test the use of the proximity effect to increase the intelligibility of telephone speech for hearing-aid wearers. NU-6 word lists were played through the equivalent of long-distance telephone lines with a standard Bell 500 handset, while Multi-Talker noise was played in the background at three different levels. The signals were picked up with one of three microphones placed by the ear of a dummy head: a first-order pressure-gradient microphone (bi-directional), a zero-order microphone (omni-directional), or one with order between zero and one (cardioid). The signal picked up by these microphones was recorded and played back to normal-hearing subjects through a modified hearing aid, while the Multi-Talker noise was played in the background. The pressure gradient microphones allowed significant better understanding of the telephone signal than did the pressure microphone and this difference was more pronounced at higher noise levels. The bidirectional and cardioid microphones did not provide significantly different scores at any noise level. It is argued that this similarity may be due to head effects reducing the pressure-gradient sensitivity of the microphones. The use of the proximity effect to enable hearing aids to pick up a telephone conversation while discriminating against background noise appears to be successful. GRA

N89-12800# Air Force Inst. of Tech., Wright-Patterson AFB, Ohio.
NATURAL LANGUAGE GENERATION

Mark T. Maybury 1988 28 p
(AD-A197321; AFIT/CI/NR-88-142) Avail: NTIS HC A03/MF A01 CSCL 05G

The goal of natural language generation is to replicate human writers or speakers: to generate fluent, grammatical, and coherent text or speech. Produced language, using both explicit and implicit means, must clearly and effectively express some intended message. This demands the use of a lexicon and a grammar together with mechanisms which exploit semantic, discourse and pragmatic knowledge to constrain production. Furthermore, special processors may be required to guide focus, extract presuppositions, and maintain coherency. As with interpretation, generation may require knowledge of the world, including information about the discourse participants as well as knowledge of the specific domain of discourse. All of these processes and knowledge sources must cooperate to produce well-written, unambiguous language. Natural language generation has received less attention than language interpretation due to the nature of language: it is important to interpret all the ways of expressing a message but we need to generate only one. Furthermore, the generative task can often be accomplished by canned text (e.g., error messages or user instructions). The advent of more sophisticated computer systems, however, has intensified the need to express multisentential English. GRA

N89-12801# Air Force Inst. of Tech., Wright-Patterson AFB, Ohio.
AUDITORY MODELS FOR SPEECH ANALYSIS
Mark T. Maybury 1988 35 p
(AD-A197322; AFIT/CI/NR-88-143) Avail: NTIS HC A03/MF A01 CSCL 12I

This paper reviews the psychophysical basis for auditory models and discusses their application to automatic speech recognition. First an overview of the human auditory system is presented, followed by a review of current knowledge gleaned from neurological and psychoacoustic experimentation. Next, a general framework describes established peripheral auditory models which are based on well-understood properties of the peripheral auditory system. This is followed by a discussion of current enhancements to that models to include nonlinearities and synchrony information as well as other higher auditory functions. Finally, the initial performance of auditory models in the task of speech recognition is examined and additional applications are mentioned. GRA

N89-12802# Naval Ocean Systems Center, San Diego, Calif.
THE DESIGN OF ANTENNA MATCHING NETWORKS USING A MICROCOMPUTER Professional Paper, Mar. - May 1988
S. T. Li and D. W. Tam May 1988 2 p
(AD-A197364) Avail: NTIS HC A02/MF A01 CSCL 12G

In a communication system one of the primary concerns is maximum efficiency in signal transmission and reception. For maximum power transfer there must be an impedance match between the antenna and transmitter (or receiver). A basic problem is to design a coupling network between a given source and a given load so that the transfer of power from the source to the load is maximized over a given frequency band of interest. The device used to perform this impedance matching is called an antenna matching network. The number of pieces of equipment requiring an antenna connection in some applications may exceed the number of acceptable locations available for antennas. One solution is the use of broadband antennas that have a low VSWR (voltage standing-wave ratio) over the operating band. Broadband antennas are used in conjunction with multicouplers (filters with multiple inputs) to provide a sufficient number of antenna connections. Despite the aid of Smith Charts, the traditional design of an antenna matching network by engineering experience and manual calculation means is an extremely time-consuming task. This paper is intended to relieve the engineer of the tedious numerical calculation involved in the network design. GRA

N89-12803# Naval Ocean Systems Center, San Diego, Calif.
EXPLORING THE BACK-PROPAGATION NETWORK FOR SPEECH APPLICATIONS Presentation Report, Apr. 1988
Stephen Luse, Doug Martin, Stephen Nunn, and Jeff Waters Jun. 1988 6 p
(AD-A197385) Avail: NTIS HC A02/MF A01 CSCL 25D

Neural networks have sophisticated abilities for processing and filtering signals. In particular, Elman and Zipser demonstrated that the back-propagation network develops significant feature representations which may be useful for both segmenting and recognizing speech. Such networks might find applications in speech compression and/or normalization. The network's apparent potential for speech applications justifies further exploration, and this paper describes our work in progress. GRA

N89-12804# Army Communications-Electronics Command, Fort Monmouth, N.J.
A COMPARISON OF PROPAGATION MODEL PREDICTIONS WITH EPLRS (ENHANCED POSITION LOCATION AND REPORTING SYSTEM) UHF NETWORK MEASUREMENTS
William M. Brennan and Paul F. Sass Aug. 1988 18 p
(AD-A197473; CECOM-TR-88-2) Avail: NTIS HC A03/MF A01 CSCL 25B

This report presents the results of a comparison between measurements at White Sands Missile Range (WSMR), New Mexico, and several propagation prediction models. One of these models is called Ground Network Communications Model (GNCM), which uses the point-to-point path loss prediction capability of the Irregular terrain Model (ITM, or Longley-Rice model). The analysis was completed using measurement data taken at WSMR with a 41-node EPLRS (Enhanced Position Location and Reporting System) network. Several models are compared with the measurements, demonstrating the reliability of propagation models. GRA

N89-12805# Defence Research Establishment, Ottawa. (Ontario). Electronic Warfare Div.
APPLICATION OF AUTOREGRESSIVE METHODS TO ADAPTIVE EXCISION OF INTERFERING TONES FROM DIRECT SEQUENCE SPREAD SPECTRUM COMMUNICATIONS SYSTEMS
Brian W. Kozminchuk Mar. 1988 47 p
(AD-A197801; DREO-TN-88-4) Avail: NTIS HC A03/MF A01 CSCL 12I

A Computer Simulation of a BPSK Direct Sequence Spread Spectrum System has been developed to investigate the effects of adaptively filtering stable tone interferers covering twenty percent of the communication band. Preliminary results for the swept tone interfering signal are also presented and shows that the block filter is effective when the tones are stable, but degrades in performance as the tone sweeps quickly across the band. To combat the non-stationary signal environment, either shorter block lengths may be required or the use of recursive algorithms that are based on gradient or least square concepts may have to be examined. GRA

N89-12806*# National Aeronautics and Space Administration. Goddard Space Flight Center, Greenbelt, Md.
ANALYSIS OF GEOSAT RADAR ALTIMETER ERRORS BASED ON PRE-LAUNCH TEST DATA Final Report, Aug. 1986 - Jul. 1987
L. Miller, A. Uliana, J. Shuhy, L. Choy (Naval Research Lab., Washington, D.C.), G. Hayne, and D. Hancock 28 Jun. 1988 60 p
(NASA-TM-101230; NAS 1.15:101230; AD-A197818; NRL-MR-6244) Avail: NTIS HC A04/MF A01 CSCL 17I

Prelaunch test results conducted on the GEOSAT radar altimeter are discussed. This report is for documentation of results. The results are applicable to new sensor engineering design and testing, and post launch monitoring of performance degradation. These tests were to exercise the radar altimeter under: (1) conditions of transient and rapidly varying signal conditions, (2) nominal operating conditions, and (3) slowly varying conditions. The results have shown that the GEOSAT altimeter meets specifications, however, several subtle effects which will be important for designing future high precision altimeters are

discussed. These effects relate to the temporal stability of the height, AGC, and waveform data; to interactions between AGC transients and height perturbations; and to height data statistics. GRA

N89-12807# Booz-Allen and Hamilton, Inc., Bethesda, Md.
EMP (ELECTROMAGNETIC PULSE) MITIGATION PROGRAM APPROACH Final Report
10 Sep. 1987 82 p
(Contract DCA100-82-C-0034)
(AD-A197849; NCS-TIB-87-17) Avail: NTIS HC A05/MF A01 CSCL 20O

The function of the EMP Mitigation Program is to assess, and where possible, lessen the potential adverse effects of electromagnetic pulse (EMP) on the nation's telecommunications infrastructure. The Office of the Manager, National Communications System (OMNCS) focuses its efforts on the Public Switched Network (PSN) because the majority of critical government users rely on the PSN to conduct their National Security Emergency Preparedness (NSEP) communication requirements. This document presents an overall plan for the EMP Mitigation Program. To date, the OMNCS has a series of tools for quantifying EMP effects on the PSN. These tools include models for predicting the effect of EMP on network equipment and estimating the EMP stress levels that equipment are exposed to. Also available is a data base for describing the topology of a major portion of the post-divestiture PSN. Results of these activities are then synthesized into a network level model, whose function is to evaluate the performance capabilities of the MEP exposed network. In addition the network level model has the ability to perform sensitivity studies. Sensitivity studies can assess the importance of different equipment types, and they are therefore useful for identifying which equipment types are require EMP testing. Present plans call for testing of the Northern Telecom DMS-100 and AT and T 4ESS switches. GRA

N89-12808# Ohio State Univ., Columbus. Electroscience Lab.
MODELING AND PERFORMANCE OF HF/OTH (HIGH-FREQUENCY/OVER-THE-HORIZON) RADAR TARGET IDENTIFICATION SYSTEMS
Donald J. Strausberger and Fred D. Garber Dec. 1987 152 p
(Contract N00014-86-K-0202)
(AD-A197850; ESL-718048-8) Avail: NTIS HC A08/MF A01 CSCL 17I

The effects of various channels on the performance of a Radar Target Identification system are investigated. Coherent, incoherent, and multiplicative component channel models are developed to synthesize estimation of features. In addition, a frequency-selective fading channel model is developed to observe the effects of multipath propagation on the identification system. A Monte-Carlo computer simulation provides performance estimates of various channels. It is shown that decreasing the frequency band degrades classification performance. It is also shown that given a highly correlated fading channel, classification performance using relative radar cross section (RCS) estimates may approach that of using coherent absolute RCS estimates. GRA

N89-12809# European Satellite Consulting Organization, Montrouge (France).
STUDY OF THE INTEGRATION OF ADVANCED COMMUNICATIONS SATELLITE SYSTEMS AND TERRESTRIAL NETWORKS, EXECUTIVE SUMMARY Final Report
Paris, France ESA Apr. 1988 52 p
(Contract ESTEC-6781/86-NL-DG)
(ESA-CR(P)-2655; ETN-88-93252) Avail: NTIS HC A04/MF A01

Two levels of integration of satellite and terrestrial communication networks were examined: level 1 where 1 earth station is installed at each of the existing or planned 48 international switching centers in Europe; and level 2 where earth stations are installed at the first significant hierarchical level (850 nodes) of the future network of the European countries. Both levels are technically feasible. The main source of economies lies in the ability of the satellite system to derive Erlang advantages by the aggregation of relatively low density international traffic streams, which would otherwise flow via numerous terrestrial routes, through a single transmission facility. An implementation plan based on EUTELSAT 2 and 3 is suggested. ESA

N89-12810*# North Carolina State Univ., Raleigh. Dept. of Electrical and Computer Engineering.
FOCAL REGION FIELDS OF DISTORTED REFLECTORS Final Report
N. E. Buris and J. F. Kauffman Jul. 1988 72 p
(Grant NAG1-738)
(NASA-CR-183001; NAS 1.26:183001) Avail: NTIS HC A04/MF A01 CSCL 20N

The problem of the focal region fields scattered by an arbitrary surface reflector under uniform plane wave illumination is solved. The physical optics (PO) approximation is used to calculate the current induced on the reflector. The surface of the reflector is described by a number of triangular domain-wise 5th degree bivariate polynomials. A 2-dimensional Gaussian quadrature is employed to numerically evaluate the integral expressions of the scattered fields. No Freshnel or Fraunhofer zone approximations are made. The relation of the focal fields problem to surface compensation techniques and other applications are mentioned. Several examples of distorted parabolic reflectors are presented. The computer code developed is included, together with instructions on its usage. Author

N89-12811# Office of Naval Research, London (England).
THE RACE PROGRAM OF THE EUROPEAN COMMUNITIES
J. F. Blackburn 17 Aug. 1988 11 p
(ONRL-8-014-R) Avail: NTIS HC A03/MF A01

The background of R and D in Advanced Communications technology for Europe (RACE), the program for research and development in advanced communications technology for Europe is discussed. Progress in switching, transmission, customer access, terminal and display, and coding are discussed. Author

N89-12767# New Mexico State Univ., University Park. Dept. of Electrical and Computer Engineering.
MODE EXTRACTION FROM AN ELECTROMAGNETIC SLOW WAVE SYSTEM Final Report
James A. Gerald *In* Universal Energy Systems, Inc., United States Air Force Graduate Student Summer Support Program, Volume 1 Dec. 1987 20 p (For primary document see N89-12754 04-31)
Avail: NTIS HC A99/MF E03 CSCL 20N

N89-12777# Auburn Univ., Ala. Dept. of Civil Engineering.
WAVE PROPAGATION IN LAYERED STRUCTURES Final Report
David W. Landis *In* Universal Energy Systems, Inc., United States Air Force Graduate Student Summer Support Program, Volume 1 Dec. 1987 20 p (For primary document see N89-12754 04-31)
Avail: NTIS HC A99/MF E03 CSCL 20N

N89-12783# Oregon Graduate Center for Study and Research, Beaverton. Dept. of Applied Physics and Electrical Engineering.
DE-EMBEDDING S-PARAMETER MEASUREMENTS USING TSD TECHNIQUE
James W. Mattern *In* Universal Energy Systems, Inc., United States Air Force Graduate Student Summer Support Program, Volume 1 Dec. 1987 14 p (For primary document see N89-12754 04-31)
Avail: NTIS HC A99/MF E03 CSCL 20N

N89-12943# Deutsche Forschungs- und Versuchsanstalt fuer Luft- und Raumfahrt, Wesseling (West Germany). Inst. for Radio Frequency Technology.
REAL-TIME ADAPTIVE RADIOMETRIC CORRECTION FOR IMAGING RADAR SYSTEMS
J. A. Moreira and W. Poetzsch *In* ESA, Proceedings of the 1988 International Geoscience and Remote Sensing Symposium

(IGARSS 1988) on Remote Sensing: Moving Towards the 21st Century, Volume 1 Aug. 1988 p 23-24 (For primary document see N89-12936 04-42)
Copyright Avail: NTIS HC A99/MF E03; ESA Publications Div., ESTEC, Noordwijk, Netherlands, 120 US dollars or 250 Dutch guilders

N89-12944# Joint Research Centre of the European Communities, Ispra (Italy).
EURACS: A EUROPEAN RADAR CROSS SECTION DATABASE
P. N. Churchill and A. J. Sieber *In* ESA, Proceedings of the 1988 International Geoscience and Remote Sensing Symposium (IGARSS 1988) on Remote Sensing: Moving Towards the 21st Century, Volume 1 Aug. 1988 p 29-31 (For primary document see N89-12936 04-42)
Copyright Avail: NTIS HC A99/MF E03; ESA Publications Div., ESTEC, Noordwijk, Netherlands, 120 US dollars or 250 Dutch guilders

N89-12945# GEC-Marconi Electronics Ltd., Chelmsford (England).
CONSTRAINTS ON TWO-SCALE DESCRIPTIONS OF RADAR BACKSCATTERING FROM THE SEA SURFACE USING SCATTEROMETER MODEL FUNCTIONS
J. A. Conway, R. A. Cordey, and J. T. Macklin *In* ESA, Proceedings of the 1988 International Geoscience and Remote Sensing Symposium (IGARSS 1988) on Remote Sensing: Moving Towards the 21st Century, Volume 1 Aug. 1988 p 33-34 (For primary document see N89-12936 04-42)
Copyright Avail: NTIS HC A99/MF E03; ESA Publications Div., ESTEC, Noordwijk, Netherlands, 120 US dollars or 250 Dutch guilders

N89-12948# Texas Univ., Arlington. Wave Scattering Research Center.
SCATTERING FROM A SKEWED RANDOM SURFACE
A. K. Fung *In* ESA, Proceedings of the 1988 International Geoscience and Remote Sensing Symposium (IGARSS 1988) on Remote Sensing: Moving Towards the 21st Century, Volume 1 Aug. 1988 p 41-43 (For primary document see N89-12936 04-42)
(Contract N60530-85-C-0365)
Copyright Avail: NTIS HC A99/MF E03; ESA Publications Div., ESTEC, Noordwijk, Netherlands, 120 US dollars or 250 Dutch guilders

N89-12949*# Texas Univ., Arlington. Wave Scattering Research Center.
POLARIMETRIC MICROWAVE SCATTERING FROM KNOWN RANDOMLY ROUGH SURFACES
C. E. Nance, A. J. Blanchard, and M. F. Chen *In* ESA, Proceedings of the 1988 International Geoscience and Remote Sensing Symposium (IGARSS 1988) on Remote Sensing: Moving Towards the 21st Century, Volume 1 Aug. 1988 p 47-50 (For primary document see N89-12936 04-42)
(Grant NAG5-486)
Copyright Avail: NTIS HC A99/MF E03; ESA Publications Div., ESTEC, Noordwijk, Netherlands, 120 US dollars or 250 Dutch guilders CSCL 20N

N89-12952# Illinois Univ., Chicago. Communications Lab.
STATISTICAL ANALYSIS AND SOME POLARIMETRIC SIGNATURES OF A POLARIMETRIC SYNTHETIC APERTURE RADAR IMAGE
M. Walther, A. B. Kostinski, H. J. Eom, and W.-M. Boerner *In* ESA, Proceedings of the 1988 International Geoscience and Remote Sensing Symposium (IGARSS 1988) on Remote Sensing: Moving Towards the 21st Century, Volume 1 Aug. 1988 p 59-64 (For primary document see N89-12936 04-42)
Copyright Avail: NTIS HC A99/MF E03; ESA Publications Div., ESTEC, Noordwijk, Netherlands, 120 US dollars or 250 Dutch guilders

N89-12953# Illinois Univ., Chicago. Dept. of Electrical Engineering and Computer Science.
STATISTICAL PROPERTIES OF PHASE DIFFERENCE BETWEEN TWO ORTHOGONALLY-POLARISED SAR SIGNALS
H. J. Eom and W.-M. Boerner *In* ESA, Proceedings of the 1988 International Geoscience and Remote Sensing Symposium (IGARSS 1988) on Remote Sensing: Moving Towards the 21st Century, Volume 1 Aug. 1988 p 65-66 (For primary document see N89-12936 04-42)
Copyright Avail: NTIS HC A99/MF E03; ESA Publications Div., ESTEC, Noordwijk, Netherlands, 120 US dollars or 250 Dutch guilders

N89-12954# Illinois Univ., Chicago. Communications Lab.
ON THE CONCEPT OF THE POLARIMETRIC MATCHED FILTER IN HIGH RESOLUTION RADAR IMAGING: AN ALTERNATIVE FOR SPECKLE RADIATION
W.-M. Boerner, A. B. Kostinski, and B. D. James *In* ESA, Proceedings of the 1988 International Geoscience and Remote Sensing Symposium (IGARSS 1988) on Remote Sensing: Moving Towards the 21st Century, Volume 1 Aug. 1988 p 69-72 (For primary document see N89-12936 04-42)
Copyright Avail: NTIS HC A99/MF E03; ESA Publications Div., ESTEC, Noordwijk, Netherlands, 120 US dollars or 250 Dutch guilders

N89-12955# Karlsruhe Univ. (West Germany). Inst. fuer Hochfrequenztechnik und Elektronik.
POLARIZATION-DEPENDENT ATTENUATION OF DIELECTRIC CYLINDER ARRAYS
W. Wiesbeck, D. Kaehny, and S. Riegger *In* ESA, Proceedings of the 1988 International Geoscience and Remote Sensing Symposium (IGARSS 1988) on Remote Sensing: Moving Towards the 21st Century, Volume 1 Aug. 1988 p 73-74 (For primary document see N89-12936 04-42)
Copyright Avail: NTIS HC A99/MF E03; ESA Publications Div., ESTEC, Noordwijk, Netherlands, 120 US dollars or 250 Dutch guilders

N89-12956*# Jet Propulsion Lab., California Inst. of Tech., Pasadena.
THE EFFECTS OF UNDERSAMPLING ON MULTIPOLARIZATION SAR IMAGES
A. Freeman, P. C. Dubois, and J. D. Klein *In* ESA, Proceedings of the 1988 International Geoscience and Remote Sensing Symposium (IGARSS 1988) on Remote Sensing: Moving Towards the 21st Century, Volume 1 Aug. 1988 p 75-78 (For primary document see N89-12936 04-42)
Copyright Avail: NTIS HC A99/MF E03; ESA Publications Div., ESTEC, Noordwijk, Netherlands, 120 US dollars or 250 Dutch guilders CSCL 17I

N89-12957# Karlsruhe Univ. (West Germany). Inst. fuer Hochfrequenztechnik und Elektronik.
INTERPRETATION OF COHERENT POLARIMETRIC SIGNATURES BY DIELECTRIC CYLINDER MODELS
D. Kaehny, S. Riegger, W. Wiesbeck, and A. J. Sieber (Joint Research Centre of the European Communities, Ispra, Italy) *In* ESA, Proceedings of the 1988 International Geoscience and Remote Sensing Symposium (IGARSS 1988) on Remote Sensing: Moving Towards the 21st Century, Volume 1 Aug. 1988 p 79-82 Sponsored in part by the Joint Research Center of the European Communities, Ispra, Italy (For primary document see N89-12936 04-42)
Copyright Avail: NTIS HC A99/MF E03; ESA Publications Div., ESTEC, Noordwijk, Netherlands, 120 US dollars or 250 Dutch guilders

N89-12975# Ministry of Posts and Telecommunications, Tokyo (Japan). Communications Research Lab.
INFERENCE OF RADIO SCATTERING PARAMETERS OF ANTARCTIC ICE SHEET USING 179 MHz AIRBORNE RADIO ECHO SOUNDING DATA

S. Uratsuka, F. Nishio, H. Ohmae, and S. Mae (Hokkaido Univ., Sapporo, Japan) *In* ESA, Proceedings of the 1988 International Geoscience and Remote Sensing Symposium (IGARSS 1988) on Remote Sensing: Moving Towards the 21st Century, Volume 1 Aug. 1988 p 157-160 (For primary document see N89-12936 04-42)
Copyright Avail: NTIS HC A99/MF E03; ESA Publications Div., ESTEC, Noordwijk, Netherlands, 120 US dollars or 250 Dutch guilders

N89-12977# Scott Polar Research Inst., Cambridge (England).
SYNTHETIC APERTURE RADAR OVER TERRESTRIAL ICE
W. G. Rees *In* ESA, Proceedings of the 1988 International Geoscience and Remote Sensing Symposium (IGARSS 1988) on Remote Sensing: Moving Towards the 21st Century, Volume 1 Aug. 1988 p 165-168 (For primary document see N89-12936 04-42)
Copyright Avail: NTIS HC A99/MF E03; ESA Publications Div., ESTEC, Noordwijk, Netherlands, 120 US dollars or 250 Dutch guilders

N89-13008# Illinois Univ., Chicago. Communications Lab.
OPTIMAL RECEPTION IN DEPOLARISING CLUTTER
W.-M. Boerner *In* ESA, Proceedings of the 1988 International Geoscience and Remote Sensing Symposium (IGARSS 1988) on Remote Sensing: Moving Towards the 21st Century, Volume 1 Aug. 1988 p 289-290 (For primary document see N89-12936 04-42)
Copyright Avail: NTIS HC A99/MF E03; ESA Publications Div., ESTEC, Noordwijk, Netherlands, 120 US dollars or 250 Dutch guilders

N89-13009# Dornier-Werke G.m.b.H., Friedrichshafen (West Germany).
PERFORMANCE MODELING AND RESULTS FOR X-SAR
D. Miller *In* ESA, Proceedings of the 1988 International Geoscience and Remote Sensing Symposium (IGARSS 1988) on Remote Sensing: Moving Towards the 21st Century, Volume 1 Aug. 1988 p 293-296 (For primary document see N89-12936 04-42)
Copyright Avail: NTIS HC A99/MF E03; ESA Publications Div., ESTEC, Noordwijk, Netherlands, 120 US dollars or 250 Dutch guilders

N89-13010# Aerospatiale, Les Mureaux (France). Dept. Measures.
IMAGE SIMULATION OF COMPLEX GEOMETRIC TARGETS FOR SPACEBORNE SYNTHETIC APERTURE RADAR
J. M. Nasr and D. Vidal-Madjar (Centre de Recherches en Physique de l'Environnement, Issy-les-Moulineaux, France) *In* ESA, Proceedings of the 1988 International Geoscience and Remote Sensing Symposium (IGARSS 1988) on Remote Sensing: Moving Towards the 21st Century, Volume 1 Aug. 1988 p 297-301 (For primary document see N89-12936 04-42)
Copyright Avail: NTIS HC A99/MF E03; ESA Publications Div., ESTEC, Noordwijk, Netherlands, 120 US dollars or 250 Dutch guilders

N89-13011# Duisburg Univ. (West Germany). Dept. of Electrical Engineering.
SCATTERING BEHAVIOR OF A THREE-AXIAL ELLIPSOID
A. Beyer and B. Roth *In* ESA, Proceedings of the 1988 International Geoscience and Remote Sensing Symposium (IGARSS 1988) on Remote Sensing: Moving Towards the 21st Century, Volume 1 Aug. 1988 p 303-306 (For primary document see N89-12936 04-42)
Copyright Avail: NTIS HC A99/MF E03; ESA Publications Div., ESTEC, Noordwijk, Netherlands, 120 US dollars or 250 Dutch guilders

N89-13012# Texas Univ., Arlington. Wave Scattering Research Center.
ATTENUATION AND SCATTERING MEASUREMENTS FROM DENSE MEDIA
I. Syed, A. J. Blanchard, and A. K. Fung *In* ESA, Proceedings of the 1988 International Geoscience and Remote Sensing Symposium (IGARSS 1988) on Remote Sensing: Moving Towards the 21st Century, Volume 1 Aug. 1988 p 307-310 (For primary document see N89-12936 04-42)
Copyright Avail: NTIS HC A99/MF E03; ESA Publications Div., ESTEC, Noordwijk, Netherlands, 120 US dollars or 250 Dutch guilders

N89-13013# Texas Univ., Arlington. Wave Scattering Research Center.
BISTATIC FREQUENCY DIVERSE IMAGING OF COMPLEX SCATTERING TARGETS
A. J. Blanchard and M. Dolaty *In* ESA, Proceedings of the 1988 International Geoscience and Remote Sensing Symposium (IGARSS 1988) on Remote Sensing: Moving Towards the 21st Century, Volume 1 Aug. 1988 p 311-314 (For primary document see N89-12936 04-42)
(Grant NAG5-486)
Copyright Avail: NTIS HC A99/MF E03; ESA Publications Div., ESTEC, Noordwijk, Netherlands, 120 US dollars or 250 Dutch guilders

N89-13014*# Jet Propulsion Lab., California Inst. of Tech., Pasadena.
DESIGN CONSIDERATIONS FOR ADVANCED MULTI-POLARISATION SAR
J. D. Klein and A. Freeman *In* ESA, Proceedings of the 1988 International Geoscience and Remote Sensing Symposium (IGARSS 1988) on Remote Sensing: Moving Towards the 21st Century, Volume 1 Aug. 1988 p 317-321 (For primary document see N89-12936 04-42)
Copyright Avail: NTIS HC A99/MF E03; ESA Publications Div., ESTEC, Noordwijk, Netherlands, 120 US dollars or 250 Dutch guilders CSCL 17I

N89-13015# Environmental Research Inst. of Michigan, Ann Arbor. Radar Science Lab.
PHASE CALIBRATION OF POLARIMETRIC SAR
D. R. Sheen, E. S. Kasischke, and R. A. Shuchman *In* ESA, Proceedings of the 1988 International Geoscience and Remote Sensing Symposium (IGARSS 1988) on Remote Sensing: Moving Towards the 21st Century, Volume 1 Aug. 1988 p 323-326 (For primary document see N89-12936 04-42)
Copyright Avail: NTIS HC A99/MF E03; ESA Publications Div., ESTEC, Noordwijk, Netherlands, 120 US dollars or 250 Dutch guilders

N89-13016*# Kansas Univ., Kansas City. Radar Systems and Remote Sensing Lab.
A FINE RESOLUTION MULTIFREQUENCY POLARIMETRIC FM RADAR
J. Bredow, S. Gogineni, T. Leung, and R. K. Moore *In* ESA, Proceedings of the 1988 International Geoscience and Remote Sensing Symposium (IGARSS 1988) on Remote Sensing: Moving Towards the 21st Century, Volume 1 Aug. 1988 p 327-329
Sponsored by NASA, ONR, and Kansas Univ. General Research Fund No. 3790 (For primary document see N89-12936 04-42)
Copyright Avail: NTIS HC A99/MF E03; ESA Publications Div., ESTEC, Noordwijk, Netherlands, 120 US dollars or 250 Dutch guilders CSCL 17I

N89-13017# Academia Sinica, Beijing (China). Inst. of Electronics.
A SYNTHETIC APERTURES RADAR WITH MULTICHANNEL AND MULTIPOLARISATION
Cheng Bo Zhang *In* ESA, Proceedings of the 1988 International Geoscience and Remote Sensing Symposium (IGARSS 1988) on Remote Sensing: Moving Towards the 21st Century, Volume 1 Aug. 1988 p 331-333 (For primary document see N89-12936 04-42)
Copyright Avail: NTIS HC A99/MF E03; ESA Publications Div.,

ESTEC, Noordwijk, Netherlands, 120 US dollars or 250 Dutch guilders

N89-13018*# Jet Propulsion Lab., California Inst. of Tech., Pasadena.
CALIBRATION OF MULTIPOLARISATION IMAGING RADAR
A. Freeman, C. Werner, and Yuhshen Shen *In* ESA, Proceedings of the 1988 International Geoscience and Remote Sensing Symposium (IGARSS 1988) on Remote Sensing: Moving Towards the 21st Century, Volume 1 Aug. 1988 p 335-339 (For primary document see N89-12936 04-42)
Copyright Avail: NTIS HC A99/MF E03; ESA Publications Div., ESTEC, Noordwijk, Netherlands, 120 US dollars or 250 Dutch guilders CSCL 17I

N89-13019# Texas Instruments, Inc., McKinney. Radar Systems Technology.
EXAMINING THE POLARISATION PHASE RETRIEVAL OF A DUAL CHANNEL MULTIPOLARISATION RADAR
B. Derryberry, A. J. Blanchard, and V. Kaupp (Arkansas Univ., Fayetteville.) *In* ESA, Proceedings of the 1988 International Geoscience and Remote Sensing Symposium (IGARSS 1988) on Remote Sensing: Moving Towards the 21st Century, Volume 1 Aug. 1988 p 341-344 (For primary document see N89-12936 04-42)
Copyright Avail: NTIS HC A99/MF E03; ESA Publications Div., ESTEC, Noordwijk, Netherlands, 120 US dollars or 250 Dutch guilders

N89-13020*# Jet Propulsion Lab., California Inst. of Tech., Pasadena.
THE NASA/JPL MULTIFREQUENCY, MULTIPOLARISATION AIRBORNE SAR SYSTEM
D. N. Held, W. E. Brown, A. Freeman, J. D. Klein, H. A. Zebker, T. Sato, T. Miller, Q. Nguyen, and Y. Lou *In* ESA, Proceedings of the 1988 International Geoscience and Remote Sensing Symposium (IGARSS 1988) on Remote Sensing: Moving Towards the 21st Century, Volume 1 Aug. 1988 p 345-349 (For primary document see N89-12936 04-42)
Copyright Avail: NTIS HC A99/MF E03; ESA Publications Div., ESTEC, Noordwijk, Netherlands, 120 US dollars or 250 Dutch guilders CSCL 17I

N89-13021# Illinois Univ., Chicago. Communications Lab.
FORMULATION OF THE PROPER EQUATIONS FOR DEVELOPING STANDARDS IN COHERENT DUAL POLARISATION SAR IMAGING
W.-M. Boerner and A. B. Kostinski *In* ESA, Proceedings of the 1988 International Geoscience and Remote Sensing Symposium (IGARSS 1988) on Remote Sensing: Moving Towards the 21st Century, Volume 1 Aug. 1988 p 351-353 (For primary document see N89-12936 04-42)
Copyright Avail: NTIS HC A99/MF E03; ESA Publications Div., ESTEC, Noordwijk, Netherlands, 120 US dollars or 250 Dutch guilders

N89-13029# GEC-Marconi Electronics Ltd., Chelmsford (England).
COMPLEX SAR IMAGERY AND SPECKLE FILTERING FOR ERS-1 WAVE MODE
R. A. Cordey and J. T. Macklin *In* ESA, Proceedings of the 1988 International Geoscience and Remote Sensing Symposium (IGARSS 1988) on Remote Sensing: Moving Towards the 21st Century, Volume 1 Aug. 1988 p 387-390 (For primary document see N89-12936 04-42)
Copyright Avail: NTIS HC A99/MF E03; ESA Publications Div., ESTEC, Noordwijk, Netherlands, 120 US dollars or 250 Dutch guilders

N89-13030# Naval Ocean Research and Development Activity, Bay St. Louis, Miss.
SOME CHARACTERISTICS OF SHORT OCEAN WAVES AS MICROWAVE SCATTERERS
P. Smith and D. Johnson *In* ESA, Proceedings of the 1988 International Geoscience and Remote Sensing Symposium (IGARSS 1988) on Remote Sensing: Moving Towards the 21st Century, Volume 1 Aug. 1988 p 395-396 (For primary document see N89-12936 04-42)
Copyright Avail: NTIS HC A99/MF E03; ESA Publications Div., ESTEC, Noordwijk, Netherlands, 120 US dollars or 250 Dutch guilders

N89-13031# Kansas Univ., Lawrence. Radar Systems and Remote Sensing Lab.
MODULATION OF THE RADAR BACKSCATTER FROM THE OCEAN SURFACE BY A LONG GRAVITY WAVE
J. C. Holtzman, J. C. West, S. P. Gogineni, and R. K. Moore *In* ESA, Proceedings of the 1988 International Geoscience and Remote Sensing Symposium (IGARSS 1988) on Remote Sensing: Moving Towards the 21st Century, Volume 1 Aug. 1988 p 397-398 (For primary document see N89-12936 04-42)
Copyright Avail: NTIS HC A99/MF E03; ESA Publications Div., ESTEC, Noordwijk, Netherlands, 120 US dollars or 250 Dutch guilders

N89-13032*# Johns Hopkins Univ., Laurel, Md. Applied Physics Lab.
ESTIMATING AIRCRAFT SAR RESPONSE CHARACTERISTICS AND APPROXIMATING OCEAN WAVE SPECTRA IN THE LABRADOR SEA
D. G. Tilley *In* ESA, Proceedings of the 1988 International Geoscience and Remote Sensing Symposium (IGARSS 1988) on Remote Sensing: Moving Towards the 21st Century, Volume 1 Aug. 1988 p 399-402 Sponsored by NASA and the ONR (For primary document see N89-12936 04-42)
Copyright Avail: NTIS HC A99/MF E03; ESA Publications Div., ESTEC, Noordwijk, Netherlands, 120 US dollars or 250 Dutch guilders CSCL 17I

N89-13033# Canada Centre for Remote Sensing, Ottawa (Ontario). RADARSAT Project Office.
PHASE VERSUS ORBITAL VELOCITY IN SAR WAVE IMAGING: PARADOX LOST
R. K. Raney and P. W. Vachon *In* ESA, Proceedings of the 1988 International Geoscience and Remote Sensing Symposium (IGARSS 1988) on Remote Sensing: Moving Towards the 21st Century, Volume 1 Aug. 1988 p 405-406 (For primary document see N89-12936 04-42)
Copyright Avail: NTIS HC A99/MF E03; ESA Publications Div., ESTEC, Noordwijk, Netherlands, 120 US dollars or 250 Dutch guilders

N89-13034# Environmental Research Inst. of Michigan, Ann Arbor.
SAR IMAGE STATISTICS RELATED TO ATMOSPHERIC DRAG OVER SEA ICE
B. A. Burns and A. Wegener (Institute for Polar and Marine Research, Bremerhaven, West Germany) *In* ESA, Proceedings of the 1988 International Geoscience and Remote Sensing Symposium (IGARSS 1988) on Remote Sensing: Moving Towards the 21st Century, Volume 1 Aug. 1988 p 409-412 (For primary document see N89-12936 04-42)
(Contract N00014-81-C-0295)
Copyright Avail: NTIS HC A99/MF E03; ESA Publications Div., ESTEC, Noordwijk, Netherlands, 120 US dollars or 250 Dutch guilders

N89-13038# Helsinki Univ. of Technology, Espoo (Finland). Dept. of Space Technology.
A 35 GHz HELICOPTER-BORNE POLARIMETER RADAR
M. T. Hallikainen and J. T. Pulliainen *In* ESA, Proceedings of the 1988 International Geoscience and Remote Sensing Symposium (IGARSS 1988) on Remote Sensing: Moving Towards the 21st Century, Volume 1 Aug. 1988 p 423-424 (For primary document see N89-12936 04-42)
Copyright Avail: NTIS HC A99/MF E03; ESA Publications Div.,

ESTEC, Noordwijk, Netherlands, 120 US dollars or 250 Dutch guilders

N89-13074*# National Aeronautics and Space Administration. Wallops Flight Facility, Wallops Island, Va.
EFFECTS OF RAINFALL ON SCATTEROMETER DERIVED WIND SPEEDS
L. F. Bliven and G. Norcross (Computer Sciences Corp., Wallops Island, Va.) *In* ESA, Proceedings of the 1988 International Geoscience and Remote Sensing Symposium (IGARSS 1988) on Remote Sensing: Moving Towards the 21st Century, Volume 1 Aug. 1988 p 565-566 (For primary document see N89-12936 04-42)
(Contract ONR-146-70-03)
Copyright Avail: NTIS HC A99/MF E03; ESA Publications Div., ESTEC, Noordwijk, Netherlands, 120 US dollars or 250 Dutch guilders

N89-13075# Marconi Space and Defence Systems Ltd., Portsmouth (England).
RADAR CONTROL, DETECTION AND PROCESSING ELECTRONICS DESIGN AS USED FOR THE ERS-1 WIND SCATTEROMETER SPACE SEGMENT
N. P. Fillery *In* ESA, Proceedings of the 1988 International Geoscience and Remote Sensing Symposium (IGARSS 1988) on Remote Sensing: Moving Towards the 21st Century, Volume 1 Aug. 1988 p 567-568 (For primary document see N89-12936 04-42)
Copyright Avail: NTIS HC A99/MF E03; ESA Publications Div., ESTEC, Noordwijk, Netherlands, 120 US dollars or 250 Dutch guilders

N89-13086# Academia Sinica, Beijing (China). Inst. of Electronics.
A LUMINANCE EDGE EXTRACTION METHOD USING GRADIENT OF GRAY LEVEL FOR SYNTHETIC APERTURE RADAR IMAGERIES
Wei Xu and Zongzhi Chen *In* ESA, Proceedings of the 1988 International Geoscience and Remote Sensing Symposium (IGARSS 1988) on Remote Sensing: Moving Towards the 21st Century, Volume 1 Aug. 1988 p 625-628 (For primary document see N89-12936 04-42)
Copyright Avail: NTIS HC A99/MF E03; ESA Publications Div., ESTEC, Noordwijk, Netherlands, 120 US dollars or 250 Dutch guilders

33 ELECTRONICS AND ELECTRICAL ENGINEERING

Includes test equipment and maintainability; components, e.g., tunnel diodes and transistors; microminiaturization; and integrated circuitry.

For related information see also *60 Computer Operations and Hardware* and *76 Solid-State Physics*.

N89-12812# Stanford Linear Accelerator Center, Calif.
ALGORITHMS FOR THE SELF-CONSISTENT SIMULATION OF HIGH POWER KLYSTRONS
K. Eppley May 1988 6 p Presented at the Workshop on Accelerator and Beam Optics Codes, San Diego, Calif., 19 Jan. 1988
(Contract DE-AC03-76SF-00515)
(DE88-010684; SU-SLAC-PUB-4622; CONF-880178-5) Avail: NTIS HC A02/MF A01

We discuss an improvement to the algorithm developed by Yu for modelling RF cavities in klystrons using the port approximation. In this method, the cavity is simulated by imposing an RF voltage as a boundary condition across the outer wall. The voltage and phase are chosen to be consistent with the cavity impedence and with the RF current induced by the electron beam. In the original method, each cavity was calculated successively using either linear theory or an iterative method to achieve a self-consistent voltage. The new method relaxes the voltage and phase of several cavities simultaneously during the simulation. The time dependence of the voltages are calculated from a relaxation equation. The new algorithm reduces the total computation time by about a factor of five for a complete klystron. DOE

N89-12813*# Jet Propulsion Lab., California Inst. of Tech., Pasadena.
FUNCTIONAL DESCRIPTION OF SIGNAL PROCESSING IN THE ROGUE GPS RECEIVER
J. B. Thomas 1 Jun. 1988 53 p
(Contract NAS7-918)
(NASA-CR-183314; NAS 1.26:183314; JPL-Publ-88-15) Avail: NTIS HC A04/MF A01 CSCL 09C

Over the past year, two Rogue GPS prototype receivers have been assembled and successfully subjected to a variety of laboratory and field tests. A functional description is presented of signal processing in the Rogue receiver, tracing the signal from RF input to the output values of group delay, phase, and data bits. The receiver can track up to eight satellites, without time multiplexing among satellites or channels, simultaneously measuring both group delay and phase for each of three channels (L1-C/A, L1-P, L2-P). The Rogue signal processing described requires generation of the code for all three channels. Receiver functional design, which emphasized accuracy, reliability, flexibility, and dynamic capability, is summarized. A detailed functional description of signal processing is presented, including C/A-channel and P-channel processing, carrier-aided averaging of group delays, checks for cycle slips, acquistion, and distinctive features. Author

N89-12814# Instituto de Pesquisas Espaciais, Sao Jose dos Campos (Brazil).
CIRCUIT FOR ACTUATION OF A STEPPING MOTOR [MOTOR DE PASSO CIRCUITO DE CONTROLE]
Luis Carlos Russo Aug. 1988 47 p In PORTUGESE
(INPE-4633-NTE/281) Avail: NTIS HC A03/MF A01

A system of actuation and control of a stepping motor was developed for use in laboratory crystal growth and optical characterization of radiation sensors. A stepping motor (Digimotor Model DM27) was utilized. Its torque characteristics, velocity, and positional precision were adequate for the required applications. Also presented is a summary of the operational principles of these motors. Author

N89-12815# Columbia Univ., New York, N.Y. Radiation Lab.
JOINT SERVICES ELECTRONICS PROGRAM Final Report, 1 Apr. 1985 - 31 Mar. 1988
George W. Flynn and Richard M. Osgood, Jr. May 1988 15 p
(Contract DAAG29-85-K-0049)
(AD-A197140; ARO-22371.13-EL) Avail: NTIS HC A03/MF A01 CSCL 20L

Several milestones have been reached in GaAs research. The first active GaAs device, a 1 micrometer channel width MESFET, has been made at Columbia. This device is a basic building block in the GaAs CCD program. GaAs surface studies have also born fruit. UV light has been found to oxidize rapidly the surface of GaAs in an UHV environment containing traces of water vapor and O2. The mechanism appears to be related to the generation of hot photocarriers. GRA

N89-12816# Utah Univ., Salt Lake City. Dept. of Chemistry.
THE BEHAVIOR OF DISK ELECTRODES: OPTICAL IMAGING OF THE CONCENTRATION DISTRIBUTION OVER A DISK ELECTRODE UNDER GALVANOSTATIC CONDITIONS Technical Report No. 9, Sep. 1987 - Jul. 1988
J. Daschbach, S. F. Simpson, J. M. Harris, M. Fleischmann, and S. Pons 15 Jul. 1988 21 p
(Contract N00014-85-K-0712)
(AD-A197355) Avail: NTIS HC A03/MF A01 CSCL 07D

This paper describes the theoretical and experimental determination of the integrated time dependent concentration distribution of an electrogenerated species over a disk electrode

embedded in an insulated plane. We have derived this result for case of constant applied flux (chronopotentiometry). The experimental technique used for observing the integrated concentration distribution over the electrode was imaging by a low noise charge coupled device camera with time and spatial resolution of approximately 20 ms and 20 micrometers respectively. The experiment demonstrates the contribution of the tertiary current distribution across the surface of the electrode. GRA

N89-12817# Colorado Univ., Boulder.
SUPERIONIC CONDUCTORS AS FAST, REPETITIVE OPENING SWITCHES Annual Report, Jun. 1987 - Jun. 1988
James Scott 6 Jun. 1988 10 p
(Contract N00014-86-K-0516)
(AD-A197365; Rept-153-4705) Avail: NTIS HC A02/MF A01 CSCL 07E

The use of superionic conductors, in particular Ag13I9W2O8, as fast, repetitive, optically triggered opening switches for power conditioning applications in spacecraft has been investigated. It was found, unexpectedly, that serious shelf-life degradation in this material exists, caused by conversion of Ag(+) ions to neutral silver. This degradation can be minimized by storage at 150 C or above, but irreversible conversion from Ag13I9W2O8 to Ag4I2WO4 and Ag5IW2O8 is greatly accelerated by the presence of laser light. GRA

N89-12818# Giner, Inc., Waltham, Mass.
ADVANCED DOUBLE LAYER CAPACITOR Quarterly Report No. 1, 1 May - 31 Jul. 1988
Anthony B. LaConti and Philip Lessner Aug. 1988 7 p
(Contract N00014-88-C-0391; ARPA Order 9526)
(AD-A197739; C87A-25) Avail: NTIS HC A02/MF A01 CSCL 09A

The overall goal of this project is to develop electrochemical capacitors utilizing an electrode-solid ionomer electrolyte composite. An advantage of these devices over conventional double layer capacitors would be the absence of free liquid electrolyte and thus greater safety and reliability. In the first quarter, we have concentrated our efforts on Task IA of the Work Plan. Specifically, we have fabricated noble metal oxides of the RuO(x) type into electrodes, and a laboratory test cell is constructed to determine which electrode structures are the most promising. In addition, several methods of forming catalyst-ionomer composites are investigated. GRA

N89-12819*# National Aeronautics and Space Administration. Lewis Research Center, Cleveland, Ohio.
RADIATION RESISTANCE AND COMPARATIVE PERFORMANCE OF ITO/InP AND n/p InP HOMOJUNCTION SOLAR CELLS
I. Weinberg, C. K. Swartz, R. E. Hart, Jr., and T. J. Coutts (Midwest Research Inst., Golden, Colo.) 30 Sep. 1988 11 p Presented at the 20th Photovoltaic Specialists Conference, Las Vegas, Nev., 26-30 Sep. 1988; sponsored in part by IEEE
(NASA-TM-101387; E-4447; NAS 1.15:101387) Avail: NTIS HC A03/MF A01 CSCL 09A*

The radiation resistance of ITO/InP cells processed by DC magnetron sputtering is compared to that of standard n/p InP and GaAs homojunction cells. After 20 MeV proton irradiations, it is found that the radiation resistance of the present ITO/InP cell is comparable to that of the n/p homojunction InP cell and that both InP cell types have radiation resistance significantly greater than GaAs. The relatively lower radiation resistance, observed at higher fluence, for the InP cell with the deepest junction depth, is attributed to losses in the cells emitter region. Diode parameters obtained from I sub sc - V sub oc plots, data from surface Raman spectroscopy, and determinations of surface conductivity types are used to investigate the configuration of the ITO/InP cells. It is concluded that thesee latter cells are n/p homojunctions, the n-region consisting of a disordered layer at the oxide semiconductor. Author

N89-12820*# Case Western Reserve Univ., Cleveland, Ohio. Dept. of Electrical Engineering and Applied Physics.
MICROWAVE CHARACTERISTICS OF INTERDIGITATED PHOTOCONDUCTORS ON A HEMT STRUCTURE M.S. Thesis. Final Contractor Report
Scott M. Hill and Paul C. Claspy Nov. 1988 90 p
(Contract NCC3-99)
(NASA-CR-182197; NAS 1.26:182197) Avail: NTIS HC A05/MF A01 CSCL 09A

Interdigitated photoconductive detectors of various geometries were fabricated on AlGaAs/GaAs heterostructure material. The processes used in the fabrication of these devices are described, and the results of a study of their optical and electrical characteristics are presented. Author

N89-12784# Vanderbilt Univ., Nashville, Tenn. Dept. of Electrical Engineering.
AN EXPERT SYSTEM FOR DIAGNOSIS AND REPAIR OF ANALOG CIRCUITS Final Report
Matthew B. McBeth *In* Universal Energy Systems, Inc., United States Air Force Graduate Student Summer Support Program, Volume 1 Dec. 1987 18 p (For primary document see N89-12754 04-31)
Avail: NTIS HC A99/MF E03 CSCL 09C

34 FLUID MECHANICS AND HEAT TRANSFER

Includes boundary layers; hydrodynamics; fluidics; mass transfer; and ablation cooling.

For related information see also *02 Aerodynamics* and *77 Thermodynamics and Statistical Physics.*

N89-12821 California Inst. of Tech., Pasadena.
STRUCTURE MEASUREMENTS IN A SYNTHETIC TURBULENT BOUNDARY LAYER Ph.D. Thesis
Jaywant H. Arakeri 1987 312 p
Avail: Univ. Microfilms Order No. DA8803384

Extensive hot-wire measurements were made to determine the structure of the large eddy in a synthetic turbulent boundary layer on a flat-plate model. The experiments were carried out in a wind tunnel at a nominal free-stream velocity of 12 m/s. The synthetic turbulent boundary layer had a hexagonal pattern of eddies and a ratio of streamwise scale to spanwise scale of 3.2:1. The measured celerity of the large eddy was 84.2 percent of the free-stream velocity. There was some loss of coherence, but very little distortion, as the eddies moved downstream. Several mean properties of the synthetic boundary layer were found to agree quite well with the mean properties of a natural turbulent boundary layer at the same Reynolds number. The large eddy is composed of a pair of primary counter-rotating vortices about five delta long in the steamwise direction and about one delta apart in the spanwise direction, where delta is the mean boundary-layer thickness. Definite signatures are obtained in terms of the mean skin-friction coefficient and the mean wake parameter averaged at constant phase. Velocities induced by the vortices are partly responsible for entrainment of irrotational fluid, for transport of momentum, for generation of Reynolds stresses, and for maintenance of streamwise and normal velocity in the outer flow. Dissert. Abstr.

N89-12822*# National Aeronautics and Space Administration. Langley Research Center, Hampton, Va.
AERODYNAMIC PRESSURES AND HEATING RATES ON SURFACES BETWEEN SPLIT ELEVONS AT MACH 6.6
L. Roane Hunt Washington, D.C. Dec. 1988 85 p
(NASA-TP-2855; L-16460; NAS 1.60:2855) Avail: NTIS HC A05/MF A01 CSCL 20D

An aerothermal study was performed in the Langley 8-Foot High Temperature Tunnel at Mach number 6.6 to define the pressures and heating rates on the surfaces between split elevons

similar to those used on the Space Shuttle. Tests were performed with both laminar and turbulent boundary layers on the wing surface upstream of the elevons. The flow in the chordwise gap between the elevons was characterized by flow separation at the gap entrance and flow reattachment at a depth into the gap inversely proportional to the gap width. The gap pressure and heating rate increased significantly with decrease of elevon gap width, and the maximum gap heating rate was proportional to the maximum gap pressure. Correlation of the present results indicate that the gap heating was directly proportional to the elevon windward surface pressure and was not dependent upon whether the boundary layer on the windward elevon surface was laminar or turbulent. Author

N89-12823 Sussex Univ., Brighton (England).
HEAT TRANSFER TO ROUGH TURBINE BLADING Ph.D. Thesis
Fathi Hasan Ali Tarada 1987 460 p
Avail: Univ. Microfilms Order No. BRDX81097

The project arose from an industrial interest in the quantification of the effects of external surface roughness on the temperatures, both local and means, of internally cooled gas turbine blades, with a view to estimating the possible changes in operating life. Such roughness may occur due to the process involved in the production of the blades or during operation in hostile environments. A dual theoretical and experimental approach was employed to better understand and predict the complex mechanisms influencing the boundary-layer heat transfer on turbine blade surfaces. In order to quantify typical blade roughness levels, a blade roughness survey was undertaken as a pre-cursor to the experimental investigations. The experimental component consisted of heat transfer measurements to one rotor blade and two nozzle guide vanes, with different levels and types of external surface roughness, and with and without significant free-stream turbulence intensity, using two heat transfer measurement techniques. The (dominant) theoretical component comprised the derivation of a low Reynolds number k-epsilon turbulence model, supplemented by an algebraic stress model, for rough curved boundary layer flow, and the development of topographical models of stochastic surface roughness. Computer programs were written to implement the theoretical models developed, and extensive validation tests were conducted with reference to published data sets. Dissert. Abstr.

N89-12824 Rutgers - The State Univ., New Brunswick, N. J.
THERMAL TRANSPORT BETWEEN A CONTINUOUSLY MOVING HEATED PLATE AND A QUIESCENT AMBIENT MEDIUM Ph.D. Thesis
Mukund Vishnu Karwe 1987 229 p
Avail: Univ. Microfilms Order No. DA8803486

A numerical and experimental investigation of the heat transfer and the fluid flow associated with a continuously moving flat surface was carried out. This circumstance is encountered in manufacturing processes such as hot rolling, extrusion, and continuous casting. The resulting temperature distribution within the solid, the appropriate conditions that arise at the location where the plate emerges from the furnace of the die, and the nature of the induced flow field and the heat transfer rate, are of interest. These considerations are important in the simulation, design, control, and optimization of the practical systems. In the numerical part of the study, the thermal transport from a flat, infinitely wide, continuously moving plate, was studied assuming a two-dimensional steady circumstance. The boundary layer equations as well as full governing equations, including buoyancy effects, were solved employing finite difference techniques. Conjugate transport, involving conduction within the plate, radiative loss from the plates surface and convection to the fluid, was considered. The temperature measurements were carried out for a heated aluminum plate moving vertically downward in water and moving upward or downward in the air. The temperature distributions, within the moving plate and the induced flow, were measured, using a microcomputer-controlled data acquisition system. The flow was visualized by means of a shadowgraph. Dissert. Abstr.

N89-12825 Exeter Univ. (England).
THE STABILITY OF TIME-DEPENDENT FLUID FLOWS Ph.D. Thesis
David Stuart Lawrenc Lettis 1987 189 p
Avail: Univ. Microfilms Order No. BRDX81113

The stability of time-dependent fluid flows are examined. In the first problem of Bernard convention in a finite two-dimensional box, the time-dependence is introduced via a small modulation imposed on the temperature of the lower surface. Weakly nonlinear theory is used to obtain an amplitude equations governing the resulting motion, and this equation is solved both asymptotically and numerically for various sizes of imperfections at the sidewalls of the box. The second problem remains with Benard convection, but now, an infinite layer of fluid rotating about a vertical axis is considered. The final problem considers high Reynolds number flow over a semi-infinite flat plate where the free stream has a small, high frequency modulation imposed on top of the usually steady streaming. Here, a linear triple-deck theory is adopted to consider the stability of the resulting flow. The stability parameters are found to be given by the solution of a partial differential equation which is solved asymptotically for a particle parameter regime. This analyis is then checked and extended by a numerical solution of the equation. Dissert. Abstr.

N89-12826# Energy International, Inc., Bellevue, Wash. Industrial Processes Program.
ASSESSMENT OF JAPANESE VARIABLE SPEED HEAT PUMP TECHNOLOGY
Kenji Ushimaru 1988 9 p Presented at the 2nd DOE/ORNL Heat Pump Conference: Research and Development on the Heat Pump for Space Conditioning Applications, Washington, D.C., 17 Apr. 1988
(Contract DE-AC05-84OR-21400)
(DE88-013246; CONF-8804100-2) Avail: NTIS HC A02

An analysis of critical component technologies and design methodologies for Japanese variable speed heat pumps are presented. The market for variable speed heat pumps in Japan is predominantly residential split-type, between the fractional to 2.5 ton capacity range. Approximately 1.1 million residential inverter-driven heat pumps were sold in 1987. Based on the market trends, component technology and several advanced features are described. Similarities and differences between Japanese and U.S. system design methodologies are discussed. Finally, the outlook for future technology trends is briefly described. DOE

N89-12827 City Univ., London (England).
HEAT TRANSFER FROM ROUGHENED SURFACES USING INTERFEROMETRY Ph.D. Thesis
John Francis Lockett 1987 233 p
Avail: Univ. Microfilms Order No. BRDX80265

Holographic interferometry is used to study the thermal fields over numerous two-dimensional ribbed geometry and to ascertain the Nusselt number distribution around them. Full field information is provided as the fringe pattern generated is essentially an isotherm contour map of the flow situation. Hence, this makes it ideally suited to verify the theoretical solutions obtained from Large Eddy Simulations (LES) and Finite Element predictions. Initially, a smooth surface geometry was investigated to verify the accuracy of the experimental technique. Ribbed geometries with a pitch to height ratio of 7.2:1 were then studied. Double exposure and real-time techniques enabled both detailed thermal measurements to be made and any time-dependency of the field to be identified. Flow rates up to nuclear reactor conditions were studied and typical interferograms are illustrated. Numerical simulations of the flow were taken using the K-epsilon and q-f models employed in the finite element code FEAT. Incorrect modelling of the length scles in the near wall region using a low Reynolds number model led to errors in the thermal field predictions. Hence, only a qualitative comparison with the experimental results is undertaken.
Dissert. Abstr.

N89-12828# California Univ., Berkeley. Dept. of Materials Science and Mineral Engineering.
PHYSICAL MODELING OF BUBBLE PHENOMENA, ELECTROLYTE FLOW AND MASS TRANSFER IN SIMULATED ADVANCED HALL CELLS Progress Report, 15 Apr. - 31 Jul. 1988
J. W. Evans Aug. 1988 26 p
(Contract DE-AM03-76SF-00115)
(DE88-015585; DOE/SF-00115/T13) Avail: NTIS HC A03/MF A01

The objectives of this project are to define mathematically dimensionless numbers, using physical models and specialized apparatus and selected working fluids, to develop quantitative correlations of dimensionless groups, to recommend designs, and to predict advanced (low-energy) Hall-Heroult cell performance. Most of the important aspects of this project like the design of the near-vertical and the near-horizontal electrode configurations, and preliminary selection of the working fluid have been accomplished. Unfortunately, because of the problems associated with the tank which will house the electrode assembly, measurements in the physical model will be delayed by at least 2 to 3 weeks. DOE

N89-12829# Air Force Inst. of Tech., Wright-Patterson AFB, Ohio.
THE EFFECTS OF EXPANSION DEVICES ON THE TRANSIENT RESPONSE CHARACTERISTICS OF THE AIR-SOURCE HEAT PUMP DURING THE REVERSE CYCLE DEFROST M.S. Thesis
Kurt T. Peterson Aug. 1988 129 p
(AD-A197150; AFIT/CI/NR-88-170) Avail: NTIS HC A07/MF A01 CSCL 13A

The effects of the defrost expansion device on the transient performance of the air source heat pump during the reverse cycle defrost was investigated. A base case test was established using an average response thermal expansion valve in the experimental setup. The base case test was compared to tests using fast and slow response TXVs and different diameter orifices. The overall performance of each test was analyzed as well as a detailed investigation of the refrigerant dynamics. The results of the investigation for TXVs indicated bulb/suction line contact was more critical to the response of the TXV than the internal bulb charge. The orifice investigation showed a general trend of faster defrost times with larger orifices, although the largest orifices allowed liquid refrigerant to enter the compressor intake. The investigation also described the different refrigerant flow control of the TXV and the orifice. GRA

N89-12830*# National Aeronautics and Space Administration. Goddard Space Flight Center, Greenbelt, Md.
THEORETICAL STUDY OF TURBULENT CHANNEL FLOW: BULK PROPERTIES, PRESSURE FLUCTUATIONS, AND PROPAGATION OF ELECTROMAGNETIC WAVES
V. M. Canuto, G. J. Hartke, A. Battaglia, J. Chasnov, and G. F. Albrecht (Lawrence Livermore National Lab., Calif.) 1988 84 p
(Contract W-7405-eng-48)
(NASA-TM-101248; NAS 1.15:101248; DE88-016174; UCRL-21085) Avail: NTIS HC A05/MF A01

In this paper, we apply two theoretical turbulence models, DIA and the recent GISS model, to study properties of a turbulent channel flow. Both models provide a turbulent kinetic energy spectral function E(k) as the solution of a non-linear equation; the two models employ the same source function but different closures. The source function is characterized by a rate n sub s (k) which is derived from the complex eigenvalues of the Orr--Sommerfeld (OS) equation in which the basic flow is taken to be of a Poiseuille type. The O--S equation is solved for a variety of Reynolds numbers corresponding to available experimental data. A physical argument is presented whereby the central line velocity characterizing the basic flow, U0 sup L, is not to be identified with the U0 appearing in the experimental Reynolds number. The theoretical results are compared with two types of experimental data: (1) turbulence bulk properties, and (2) properties that depend stongly on the structure of the turbulence spectrun at low wave numbers. The only existing analytical expression for Pi (k) cannot be used in the present case because it applies to the case of a flat plate, not a finite channel. DOE

N89-12831# Sandia National Labs., Albuquerque, N. Mex. Aerothermodynamics Div.
TEMPERATURE PROFILE IN SEMI-INFINITE PLANAR SLAB WITH EXPONENTIAL SOURCE AND CONVECTIVE BOUNDARY CONDITION: APPLICATION TO LASER HEATING
B. F. Blackwell Aug. 1988 23 p
(Contract DE-AC04-76DP-00789)
(DE88-016746; SAND-87-1940) Avail: NTIS HC A03/MF A01

An analytical solution for the temperature profile in a semi-infinite planar slab with an exponentially decaying (with position) source and convective boundary condition is obtained using Laplace transforms. The appropriate dimensionless parameters are identified and the temperature as a function of these parameters is presented in graphical form. With cooling at the front surface, the maximum temperature occurs in the interior of the slab instead of at the exposed surface. The location of the temperature maximum as a function of the various system parameters is presented in graphical form. Approximate relationships are presented for small values of dimensionless time. Example calculations are presented for laser drilling with external cooling. DOE

N89-12832# Argonne National Lab., Ill. Fusion Power Program.
LIQUID METAL FLOW IN A LARGE-RADIUS ELBOW WITH A UNIFORM MAGNETIC FLUID
T. J. Moon and J. S. Walker Jul. 1988 32 p
(Contract W-31-109-eng-38)
(DE88-016957; ANL/FPP/TM-227) Avail: NTIS HC A03/MF A01

This paper treats the liquid-metal flow in an elbow between two straight, rectangular ducts. There is a uniform magnetic field in the plane of the elbow. The duct has thin, electrically conducting walls. The Hartmann number and the interaction parameter are assumed to be large, while the magnetic Reynolds number is assumed to be small. Solutions for the velocity at each cross section of the elbow and for the pressure drop due to three-dimensional effects are presented. DOE

N89-12833# Catholic Univ. of America, Washington, D.C. Dept. of Civil Engineering.
ADVANCED INSTRUMENTATION FOR LOCAL MEASUREMENT OF GAS-SOLID SUSPENSION FLOWS Quarterly Technical Progress Report No. 7, 1 May - 31 Jul. 1988
S. C. Ling and H. P. Pao 1988 8 p
(Contract DE-FG22-86PC-90956)
(DE88-017087; DOE/PC-90956/T6) Avail: NTIS HC A02/MF A01

The study of gas-solid suspension flow is being conducted in two parts: the lifting of heavy particles from the flow boundary by micro-hairpin vortices and the design of an optical instrument to investigate the characteristics of turbulent flows has particle-size concentrations. The study of micro-hairpin vortices is based on the observation of these vortices in a cavitation water-tunnel. The micro-vortices exist within the laminar and intermediate sublayer of the turbulent flow field where the velocity gradient is most intense. These vortices are believed to be the major production source of turbulence which are also responsible for the picking up of heavy solid particles from the flow boundary at the bottom of the pipe. However, this important transport mechanism near the bottom boundary was not taken into account in all previous theories of solid transport. It is hoped that this work will provide a more basic understanding on the mechanics of solid transport. Our major research effort in this quarter has been concentrated on the construction of the experimental test-setup and the development of an optical particle-size and concentration detector. The optical detector also provides the information on flow characteristics. DOE

N89-12834*# National Aeronautics and Space Administration. Langley Research Center, Hampton, Va.

DIRECT SIMULATION OF THREE-DIMENSIONAL FLOW ABOUT THE AFE VEHICLE AT HIGH ALTITUDES

M. Cevdet Celenligil, James N. Moss, and Graeme A. Bird (Sydney Univ., Australia) Sep. 1988 32 p Presented at the 16th International Symposium on Rarefied Gas Dynamics, Pasadena, Calif., 10-16 Jul. 1988

(NASA-TM-101492; NAS 1.15:101492) Avail: NTIS HC A03/MF A01 CSCL 20D

Three-dimensional hypersonic rarefied flow about the Aeroassist Flight Experiment (AFE) vehicle was studied using the direct simulation Monte Carlo (DSMC) technique. Results are presented for the transitional flow regime encountered between 120 and 200 km altitudes with a reentry velocity of 9.92 km/s. In the simulations, a five-species reacting real-gas model that accounts for internal energies (rotational and vibrational) is used. The results indicate that the transitional effects are significant even at an altitude of 200 km and influence the overall vehicle aerodynamics. For the cases considered, the aerodynamic coefficients, surface pressures, convective heating, and flow field structure variations with rarefaction effects are presented. Author

N89-12835*# Naval Postgraduate School, Monterey, Calif. Dept. of Aeronautics.

A NUMERICAL METHOD FOR COMPUTING UNSTEADY 2-D BOUNDARY LAYER FLOWS Interim Contractor Report

Andreas Krainer Washington NASA Dec. 1988 62 p

(NASA Order C-80017-F)

(NASA-CR-4198; E-4394; NAS 1.26:4198) Avail: NTIS HC A04/MF A01 CSCL 20D

A numerical method for computing unsteady two-dimensional boundary layers in incompressible laminar and turbulent flows is described and applied to a single airfoil changing its incidence angle in time. The solution procedure adopts a first order panel method with a simple wake model to solve for the inviscid part of the flow, and an implicit finite difference method for the viscous part of the flow. Both procedures integrate in time in a step-by-step fashion, in the course of which each step involves the solution of the elliptic Laplace equation and the solution of the parabolic boundary layer equations. The Reynolds shear stress term of the boundary layer equations is modeled by an algebraic eddy viscosity closure. The location of transition is predicted by an empirical data correlation originating from Michel. Since transition and turbulence modeling are key factors in the prediction of viscous flows, their accuracy will be of dominant influence to the overall results. Author

N89-12836*# Science Applications International Corp., Sunnyvale, Calif.

MASS FLOW METER USING THE TRIBOELECTRIC EFFECT FOR MEASUREMENT IN CRYOGENICS Final Report

Henry Bernatowicz, Jock Cunningham, and Steve Wolff Apr. 1987 76 p

(Contract NAS3-24648)

(NASA-CR-179572; NAS 1.26:179572; SAIC-87/1612) Avail: NTIS HC A05/MF A01 CSCL 20D

The use of triboelectric charge to measure the mass flow rate of cryogens for the Space Shuttle Main Engine was investigated. Cross correlation of the triboelectric charge signals was used to determine the transit time of the cryogen between two sensor locations in a .75-in tube. The ring electrode sensors were mounted in a removable spool piece. Three spool pieces were constructed for delivery, each with a different design. One set of electronics for implementation of the cross correlation and flow calculation was constructed for delivery. Tests were made using a laboratory flow loop using liquid freon and transformer oil. The measured flow precision was 1 percent and the response was linear. The natural frequency distribution of the triboelectric signal was approximately 1/f. The sensor electrodes should have an axial length less than approximately one/tenth pipe diameter. The electrode spacing should be less than approximately one pipe diameter. Tests using liquid nitrogen demonstrated poor tribo-signal to noise ratio. Most of the noise was microphonic and common to both electrode systems. The common noise rejection facility of the correlator was successful in compensating for this noise but the signal was too small to enable reliable demonstration of the technique in liquid nitrogen. Author

N89-12837*# Auburn International, Inc., Danvers, Mass.

MASS FLOW MEASUREMENT OF LIQUID CRYOGENS USING THE TRIBOELECTRIC EFFECT Final Report

Ronald L. Dechene 12 Aug. 1986 65 p

(Contract NAS3-24873)

(NASA-CR-179519; NAS 1.26:179519) Avail: NTIS HC A04/MF A01 CSCL 20D

A cross correlator technique using triboelectric technology has been shown to be a feasible method to measure liquid flow rate for liquid nitrogen and JP4 jet fuel. This technology, invented and pioneered by Auburn International, Inc., is also expected to be suitable for use with all other insulating liquids and cryogens. The technology described is particularly well suited for cryogenic use, since the sensor is non-contacting and non-intrusive, and therefore, causes no additional pressure drop within the flow stream. Further development of the in-line sensor is required to produce a prototypical version for the test purposes under SSME fuel flow conditions. However, with the knowledge gained from this feasibility study, it is very likely that an acceptable sensor design for a full test bed evaluation could be produced. Author

N89-12838*# Tennessee Univ. Space Inst., Tullahoma.

INFLUENCE OF BULK TURBULENCE AND ENTRANCE BOUNDARY LAYER THICKNESS ON THE CURVED DUCT FLOW FIELD Final Contractor Report

R. A. Crawford Nov. 1988 88 p

(Grant NAG3-617)

(NASA-CR-4188; E-4458; NAS 1.26:4188; UTSI/88-07) Avail: NTIS HC A05/MF A01 CSCL 20D

The influence of bulk turbulence and boundary layer thickness on the secondary flow development in a square, 90 degree turning duct was investigated. A three-dimensional laser velocimetry system was utilized to measure the mean and fluctuating components of velocity at six cross-planes in the duct. The results from this investigation, with entrance boundary layer thickness of 20 percent, were compared with the thin boundary layer results documented in NASA CR-174811. The axial velocity profiles, cross-flow velocities, and turbulence intensities were compared and evaluated with regard to the influence of bulk turbulence intensity and boundary layer thickness, and the influence was significant. The results of this investigation expand the 90 degree curved duct experimental data base to higher turbulence levels and thicker entrance boundary layers. The experimental results provide a challenging benchmark data base for computational fluid dynamics code development and validation. The variation of inlet bulk turbulence intensity provides additional information to aid in turbulence model evaluation. Author

N89-12839# Deutsche Forschungs- und Versuchsanstalt fuer Luft- und Raumfahrt, Goettingen (West Germany). Abteilung Instationaere Aerodynamik.

NUMERICAL INTEGRATION OF INFLUENCE COEFFICIENTS FOR PANEL METHODS ABOUT AXISYMMETRIC BODIES BY MEANS OF THE ROMBERG ALGORITHM

Edgar Katzer Jun. 1988 49 p In GERMAN; ENGLISH summary

(DFVLR-Mitt-88-18; ISSN-0176-7739; ETN-88-93521) Avail: NTIS HC A03/MF A01; DFVLR, VB-PL-DO, 90 60 58, 5000 Cologne, Federal Republic of Germany, 19.50 deutsche marks

The influence coefficients of axisymmetric panel elements with continuous vorticity distribution are calculated. The circumferential integrals are reduced to elliptic integrals; the integration along the panel is performed numerically. The ROMBERG integration procedure is applied and the number of integration nodes are chosen according to the smoothness of the integrands and the accuracy. The induced field variables may be calculated even close to the panel surface and they approach continuously the values

on the surface. A quadrature formula is applied for the integration of the Cauchy and a logarithmic singularity. The ROMBERG algorithm is vectorized and sufficiently large vector lengths are achieved. ESA

N89-12614*# Lockheed Missiles and Space Co., Sunnyvale, Calif.
DEVELOPMENT OF OPTIMIZED, GRADED-PERMEABILITY AXIAL GROOVE HEAT PIPES
Michael R. Kapolnek and H. Rolland Holmes *In* NASA, Goddard Space Flight Center, 15th Space Simulation Conference: Support the Highway to Space Through Testing 1988 p 397-408 (For primary document see N89-12582 04-18)
Avail: NTIS HC A21/MF A01 CSCL 20D

N89-12615*# CCS Associates, Bethel Park, Pa.
HEAT PIPE COOLING SYSTEM WITH SENSIBLE HEAT SINK
Calvin C. Silverstein *In* NASA, Goddard Space Flight Center, 15th Space Simulation Conference: Support the Highway to Space Through Testing 1988 p 409-415 (For primary document see N89-12582 04-18)
(Contract SNL-33-0878)
Avail: NTIS HC A21/MF A01 CSCL 20D

N89-12773# Colorado Univ., Boulder. Dept. of Aerospace Engineering Sciences.
A COMPARATIVE STUDY OF DIFFERING VORTEX STRUCTURES ARISING IN UNSTEADY SEPARATED FLOWS Final Report
Stephen A. Huyer *In* Universal Energy Systems, Inc., United States Air Force Graduate Student Summer Support Program, Volume 1 Dec. 1987 19 p (For primary document see N89-12754 04-31)
Avail: NTIS HC A99/MF E03 CSCL 20D

N89-12774# University of Eastern Illinois, Charleston. Dept. of Mathematics.
PERTURBED FUNCTIONAL ITERATION APPLIED TO THE NAVIER-STOKES EQUATIONS Final Report
David L. James *In* Universal Energy Systems, Inc., United States Air Force Graduate Student Summer Support Program, Volume 1 Dec. 1987 9 p (For primary document see N89-12754 04-31)
Avail: NTIS HC A99/MF E03 CSCL 20D

N89-12779# Ohio State Univ., Columbus. Dept. of Mechanical Engineering.
EXPERIMENTAL STUDY OF ISOTHERMAL FLOWS IN A DUMP COMBUSTOR Final Report
Craig A. Langenfeld *In* Universal Energy Systems, Inc., United States Air Force Graduate Student Summer Support Program, Volume 1 Dec. 1987 16 p (For primary document see N89-12754 04-31)
Avail: NTIS HC A99/MF E03 CSCL 20D

N89-12890*# General Motors Corp., Detroit, Mich. Gas Turbine Engine Div.
AEROTHERMAL MODELING PROGRAM, PHASE 2
K. C. Karki, H. C. Mongia, Suhas V. Patankar, and A. K. Runchal *In* NASA, Lewis Research Center, Turbine Engine Hot Section Technology 1986 Oct. 1986 p 105-113 (For primary document see N89-12876 04-39)
(Contract NAS3-24350)
Avail: NTIS HC A21/MF A01 CSCL 20D

N89-12891*# General Motors Corp., Detroit, Mich. Gas Turbine Engine Div.
AEROTHERMAL MODELING PROGRAM, PHASE 2. ELEMENT B: FLOW INTERACTION EXPERIMENT
M. Nikjooy, H. C. Mongia, S. N. B. Murthy, and J. P. Sullivan *In* NASA, Lewis Research Center, Turbine Engine Hot Section Technology 1986 Oct. 1986 p 115-124 (For primary document see N89-12876 04-39)
(Contract NAS3-24350)
Avail: NTIS HC A21/MF A01 CSCL 20D

N89-12892*# General Motors Corp., Detroit, Mich. Gas Turbine Engine Div.
AEROTHERMAL MODELING PROGRAM, PHASE 2. ELEMENT C: FUEL INJECTOR-AIR SWIRL CHARACTERIZATION
A. A. Mostafa, H. C. Mongia, V. G. McDonnell, and G. S. Samuelsen *In* NASA, Lewis Research Center, Turbine Engine Hot Section Technology 1986 Oct. 1986 p 125-131 (For primary document see N89-12876 04-39)
(Contract NAS3-24350)
Avail: NTIS HC A21/MF A01 CSCL 20D

N89-12894*# Minnesota Univ., Minneapolis. Dept. of Mechanical Engineering.
EFFICIENT NUMERICAL TECHNIQUES FOR COMPLEX FLUID FLOWS
Suhas V. Patankar *In* NASA, Lewis Research Center, Turbine Engine Hot Section Technology 1986 Oct. 1986 p 141-143 (For primary document see N89-12876 04-39)
(Grant NAG3-596)
Avail: NTIS HC A21/MF A01 CSCL 20D

N89-12895*# Avco-Everett Research Lab., Mass.
IMPROVED NUMERICAL METHODS FOR TURBULENT VISCOUS RECIRCULATING FLOWS
J. P. VanDoormaal, A. Turan, and G. D. Raithby *In* NASA, Lewis Research Center, Turbine Engine Hot Section Technology 1986 Oct. 1986 p 145-150 (For primary document see N89-12876 04-39)
(Contract NAS3-24351)
Avail: NTIS HC A21/MF A01 CSCL 20D

N89-12896*# Tennessee Univ. Space Inst., Tullahoma.
INFLUENCE OF BULK TURBULENCE AND ENTRANCE BOUNDARY LAYER THICKNESS ON THE CURVED DUCT FLOW FIELD
Roger A. Crawford and Carroll E. Peters *In* NASA, Lewis Research Center, Turbine Engine Hot Section Technology 1986 Oct. 1986 p 151-157 (For primary document see N89-12876 04-39)
(Grant NAG3-617)
Avail: NTIS HC A21/MF A01 CSCL 20D

N89-12897*# United Technologies Research Center, East Hartford, Conn.
MEASUREMENT OF AIRFOIL HEAT TRANSFER COEFFICIENTS ON A TURBINE STAGE
Robert P. Dring, Michael F. Blair, and H. David Joslyn *In* NASA, Lewis Research Center, Trubine Engine Hot Section Technology 1986 Oct. 1986 p 159-176 (For primary document see N89-12876 04-39)
(Contract NAS3-2317)
Avail: NTIS HC A21/MF A01 CSCL 20D

N89-12898*# Arizona State Univ., Tempe. Dept. of Mechanical and Aerospace Engineering.
HEAT TRANSFER IN THE TIP REGION OF A ROTOR BLADE SIMULATOR
M. K. Chyu, H. K. Moon, and D. E. Metzger *In* NASA, Lewis Research Center, Turbine Engine Hot Section Technology 1986 Oct. 1986 p 177-192 (For primary document see N89-12876 04-39)
(Grant NAG3-623)
Avail: NTIS HC A21/MF A01 CSCL 20D

N89-12899*# Pratt and Whitney Aircraft, East Hartford, Conn.
COOLANT PASSAGE HEAT TRANSFER WITH ROTATION
T. J. Hajek, J. Wagner, and B. V. Johnson *In* NASA, Lewis Research Center, Turbine Engine Hot Section Technology 1986 Oct. 1986 p 193-206 (For primary document see N89-12876 04-39)
(Contract NAS3-23691)
Avail: NTIS HC A21/MF A01 CSCL 20D

N89-12900*# Stanford Univ., Calif. Dept. of Mechanical Engineering.
HEAT TRANSFER WITH VERY HIGH FREE-STREAM TURBULENCE AND STREAMWISE VORTICES
Robert J. Moffat, Paul Maciejewski, John K. Eaton, and Wayne Pauley *In* NASA, Lewis Research Center, Trubine Engine Hot Section Technology 1986 Oct. 1986 p 207-217 (For primary document see N89-12876 04-39)
(Grant NAG3-522)
Avail: NTIS HC A21/MF A01 CSCL 20D

N89-12901*# Minnesota Univ., Minneapolis. Dept. of Mechanical Engineering.
DEVELOPMENT OF LOW REYNOLDS NUMBER TWO EQUATION TURBULENCE MODELS FOR PREDICTING EXTERNAL HEAT TRANSFER ON TURBINE BLADES
Suhas V. Patankar and Rodney C. Schmidt *In* NASA, Lewis Research Center, Turbine Engine Hot Section Technology 1986 Oct. 1986 p 219-232 (For primary document see N89-12876 04-39)
(Grant NAG3-579)
Avail: NTIS HC A21/MF A01 CSCL 20D

N89-12902*# National Aeronautics and Space Administration. Lewis Research Center, Cleveland, Ohio.
TURBINE STATOR FLOW FIELD SIMULATIONS
R. C. Buggeln, W. R. Briley, S. J. Shamroth, and H. McDonald *In* NASA, Lewis Research Center, Trubine Engine Hot Section Technology 1986 Oct. 1986 p 233-235 (For primary document see N89-12876 04-39)
(Contract NAS3-24358)
Avail: NTIS HC A21/MF A01 CSCL 20D

N89-12903*# General Motors Corp., Detroit, Mich. Gas Turbine Div.
TURBINE AIRFOIL FILM COOLING
Larry D. Hylton *In* NASA, Lewis Research Center, Turbine Engine Hot Section Technology 1986 Oct. 1986 p 237-241 (For primary document see N89-12876 04-39)
(Contract NAS3-24619)
Avail: NTIS HC A21/MF A01 CSCL 20D

35 INSTRUMENTATION AND PHOTOGRAPHY

Includes remote sensors; measuring instruments and gages; detectors; cameras and photographic supplies; and holography.

For aerial photography see *43 Earth Resources and Remote Sensing.* For related information see also *06 Aircraft Instrumentation,* and *19 Spacecraft Instrumentation.*

N89-12840# Sandia National Labs., Albuquerque, N. Mex.
THE STANDARDIZED BAUER PIEZOELECTRIC POLYMER SHOCK GAUGE
R. A. Graham, F. Bauer, L. M. Lee (Ktech Corp., Albuquerque, N. Mex.), and R. P. Reed 1988 4 p Presented at the Shock Wave Symposium, Pullman, Wash., 1 Sep. 1988
(Contract DE-AC04-76DP-00789)
(DE88-014963; SAND-88-2152C; CONF-8809109-3) Avail: NTIS HC A02/MF A01

Earlier reports have described work to establish feasibility for a shock-compression, stress-rate or stress gauge based on a high quality polymer film, polyvinylidene difluoride (PVDF). We have now established standardized procedures to provide large quantities of PVDF guage elements with highly reproducible electrical characteristics based on the process developed by Bauer. (The standard remanent polarization of a group of 100 gauges centered around a mean of 9.1 microcoulombs per square centimeter showed a standard deviation of 0.83 percent.) We have also carried out piezoelectric response measurements of standardized guage elements from 300 MPa to 46 GPa. Based on these measurements, it is now clear that the gauge provides the capability to carry out time-resolved stress pulse measurements over a broad stress range. Unlike gauges utilizing piezoelectric crystals, the 25 micron thickness of the Bauer piezoelectric polymer gauge provides for unobtrusive and highly versatile gauge locations. The ability to provide a direct measure of stress-rate provides an unusually sensitive record of stress pulses. DOE

N89-12841* National Aeronautics and Space Administration. Langley Research Center, Hampton, Va.
POROUS PLUG FOR REDUCING ORIFICE INDUCED PRESSURE ERROR IN AIRFOILS Patent
Elizabeth B. Plentovich, inventor (to NASA), Blair B. Gloss, inventor (to NASA), John W. Eves, inventor (to NASA), and John P. Stack, inventor (to NASA) 13 Sep. 1988 8 p Filed 5 Feb. 1987 Supersedes N87-25559 (25 - 19, p 2612)
(NASA-Case-LAR-13569-1; US-Patent-4,770,032; US-Patent-Appl-SN-010943; US-Patent-Class-73-147; US-Patent-Class-73-180) Avail: US Patent and Trademark Office CSCL 14B

A porous plug is provided for the reduction or elimination of positive error caused by the orifice during static pressure measurements of airfoils. The porous plug is press fitted into the orifice, thereby preventing the error caused either by fluid flow turning into the exposed orifice or by the fluid flow stagnating at the downstream edge of the orifice. In addition, the porous plug is made flush with the outer surface of the airfoil, by filing and polishing, to provide a smooth surface which alleviates the error caused by imperfections in the orifice. The porous plug is preferably made of sintered metal, which allows air to pass through the pores, so that the static pressure measurements can be made by remote transducers.
Official Gazette of the U.S. Patent and Trademark Office

N89-12842*# National Aeronautics and Space Administration. Lyndon B. Johnson Space Center, Houston, Tex.
IMPROVED DOCKING ALIGNMENT SYSTEM Patent Application
Leo G. Monford, inventor (to NASA) 15 Sep. 1988 19 p
(NASA-Case-MSC-21372-1; NAS 1.71:MSC-21372-1; US-Patent-Appl-SN-246595) Avail: NTIS HC A03/MF A01 CSCL 14B

Improved techniques are provided for the alignment of two objects. The present invention is particularly suited for 3-D translation and 3-D rotational alignment of objects in outer space. A camera is affixed to one object, such as a remote manipulator arm of the spacecraft, while the planar reflective surface is affixed to the other object, such as a grapple fixture. A monitor displays in real-time images from the camera such that the monitor displays both the reflected image of the camera and visible marking on the planar reflective surface when the objects are in proper alignment. The monitor may thus be viewed by the operator and the arm manipulated so that the reflective surface is perpendicular to the optical axis of the camera, the roll of the reflective surface is at a selected angle with respect to the camera, and the camera is spaced a pre-selected distance from the reflective surface.
NASA

N89-12843*# National Aeronautics and Space Administration. Lyndon B. Johnson Space Center, Houston, Tex.
TANK GAUGING APPARATUS AND METHOD Patent Application
Brian G. Morris, inventor (to NASA) 11 Jul. 1988 22 p
(NASA-Case-MSC-21059-1; NAS 1.71:MSC-21059-1; US-Patent-Appl-SN-217725) Avail: NTIS HC A03/MF A01 CSCL 14B

An apparatus for gauging the amount of liquid in a container of liquid and gas under low or zero gravity net conditions includes an accumulator and appropriate connector apparatus for communicating gas between the accumulator and the container. In one form of the invention, gas is removed from the container and compressed into the accumulator. The pressure and temperature of the fluid in the container is measured before and

after removal of the gas; the pressure and temperature of the gas in the accumulator is measured before and after compression of the gas into the accumulator from the container. These pressure and temperature measurements are used to determine the volume of gas in the container, whereby the volume of the liquid in the container can be determined from the difference between the known volume of the container and the volume of gas in the container. Gas from the accumulator may be communicated into the container in a similar process as a verification of the gauging of the liquid volume, or as an independent process for determining the volume of liquid in the container. NASA

N89-12844# California Univ., Berkeley. Sensor and Actuator Center.
APPLICATIONS OF POLYSILICON FILMS IN MICROSENSORS AND MICROACTUATORS
Roger T. Howe Aug. 1988 15 p Presented at the Fall Meeting of the Materials Research Society, Boston, Mass., 30 Nov. 1987 Prepared for Lawrence Livermore National Lab., Calif.
(Contract W-7405-eng-48)
(DE88-016979; UCRL-21091; CONF-871124-104) Avail: NTIS HC A03/MF A01

This paper reviews the applications of polysilicon in microsensor technology and in the emerging field of microfabricated actuators. Polysilicon is an attractive material for thin-film strain gauges, and is also used to fabricate micromechanical structures. The need for better understanding of the non-electrical properties of polysilicon, such as Young's modulus, residual strain, ultimate strength, friction, and wear, is emphasized. DOE

N89-12845*# National Aeronautics and Space Administration. Lewis Research Center, Cleveland, Ohio.
PERFORMANCE OF THE FORWARD SCATTERING SPECTROMETER PROBE IN NASA's ICING RESEARCH TUNNEL
Edward A. Hovenac and Robert F. Ide (Army Aviation Research and Development Command, Cleveland, Ohio.) [1988] 11 p Proposed for presentation at the 27th Aerospace Sciences Meeting, Reno, Nev., 9-12 Jan. 1989; sponsored by AIAA
(NASA-TM-101381; E-4435; NAS 1.15:101381; AVSCOM-TR-88-C-036; AIAA-89-0769) Avail: NTIS HC A03/MF A01 CSCL 14B

Two Forward Scattering Spectrometer Probes were used to measure droplet distributions in the NASA Lewis Icing Research Tunnel. The instruments showed good agreement when the median volume diameter (MVD) was approximately 16 micrometers. Coincidence events affect much of the data and caused the measured MVD to be about 2 to 3 micrometers larger than expected. Coincidence events were reduced by shutting down half of the spray bars in the tunnel during certain tests. Author

N89-12846# Consiglio Nazionale delle Ricerche, Frascati (Italy). Istituto di Fisica dello Spazio Interplanetario.
THE FRASCATI (ITALY) GRAVITATIONAL ANTENNA, 1987 [L'ANTENNA GRAVITAZIONALE DI FRASCATI 1987]
M. Bassan, P. Bonifazi, F. Bordoni, G. Chionchio, M. G. Castellano, D. DeBugaro, V. Iafolla, M. Iannilli, M. Maiani, and I. Modena (Rome Univ., Italy) et al. May 1988 27 p In ITALIAN
(IFSI-88-4; ETN-88-93471) Avail: NTIS HC A03/MF A01

A gravitational wave experiment is described. The antenna, consisting of a cylindrical aluminum mass of 390 kg was cooled in a liquid helium cryostat. The cooling device consists of a series of concentric chambers cooled with different cryogenic media. The suspension system reduces by 70 dB the external noise at the antenna frequency. A special capacitance resonant transducer was developed and tested. The device, equipped with a dc amplifier, operated at a noise temperature of 110 mK. ESA

N89-12847# Environmental Protection Agency, Research Triangle Park, N.C. Atmospheric Sciences Research Lab.
WIND TUNNEL INVESTIGATION OF THE RESPONSE OF A SONIC ANEMOMETER
Robert E. Eskridge and C. Bruce Baker Aug. 1988 22 p
(PB88-249826; EPA-600/D-88-192) Avail: NTIS HC A03/MF A01 CSCL 14B

An Applied Technology, Inc. (ATI) sonic of the type used by J. C. Kaimal at the Boulder Tower was tested in the large wind tunnel at the U.S. EPA Fluid Modeling Facility. The wind tunnel is approximately 6 ft high, 10 ft wide with a test section bed 60 ft long. The air speed in the tunnel can be varied from about 0.20 to 7.0 m/s. The sonic probe was mounted near the center of the tunnel to study the effect of shadowing of the probe and mount as a function of azimuth angle at speeds of 1.0, 3.0, and 7.0 m/s. Experiments were performed to determine if there is a Reynolds number dependency of the instrument when the tunnel speed was varied from 0.20 to 7.0 m/s. Velocity correction curves are somewhat different from those published by J. C. Kaimal. No Reynolds number dependency of the flow on the velocity components under maximum shadowing was found. GRA

N89-12584*# Jet Propulsion Lab., California Inst. of Tech., Pasadena.
WIDE FIELD/PLANETARY CAMERA (WF/PC) CONTAMINATION CONTROL ASSESSMENT Abstract Only
C. Maag, J. Millard, and M. Anderson *In* NASA, Goddard Space Flight Center, 15th Space Simulation Conference: Support the Highway to Space Through Testing 1988 p 11 (For primary document see N89-12582 04-18)
Avail: NTIS HC A21/MF A01 CSCL 14B

N89-12585*# Jet Propulsion Lab., California Inst. of Tech., Pasadena. Applied Technologies Sect.
CHARACTERIZATION OF A GRAPHITE EPOXY OPTICAL BENCH DURING THERMAL VACUUM CYCLING
Patricia A. Hansen, Teresa K. Jenkins, Carl R. Maag, and Daniel M. Taylor *In* NASA, Goddard Space Flight Center, 15th Space Simulation Conference: Support the Highway to Space Through Testing 1988 p 12-25 (For primary document see N89-12582 04-18)
Avail: NTIS HC A21/MF A01 CSCL 14B

N89-12884*# Pratt and Whitney Aircraft, East Hartford, Conn. Engineering Div.
FURTHER DEVELOPMENT OF THE DYNAMIC GAS TEMPERATURE MEASUREMENT SYSTEM
D. L. Elmore, W. W. Robinson, and W. B. Watkins *In* NASA, Lewis Research Center, Turbine Engine Hot Section Technology 1986 Oct. 1986 p 51-60 (For primary document see N89-12876 04-39)
(Contract NAS3-24228)
Avail: NTIS HC A21/MF A01 CSCL 14B

N89-12886*# Northwestern Univ., Evanston, Ill.
ELEVATED TEMPERATURE STRAIN GAGES
J. O. Brittain, D. Geslin, and J. F. Lei *In* NASA, Lewis Research Center, Turbine Engine Hot Section Technology 1986 Oct. 1986 p 69-84 (For primary document see N89-12876 04-39)
(Grant NAG3-501)
Avail: NTIS HC A21/MF A01 CSCL 14B

N89-12887*# National Aeronautics and Space Administration. Lewis Research Center, Cleveland, Ohio.
DEVELOPMENT OF A HIGH TEMPERATURE STATIC STRAIN SENSOR
Charles O. Hulse, Richard S. Bailey, and Howard P. Grant *In* NASA, Lewis Research Center, Turbine Engine Hot Section Technology 1986 Oct. 1986 p 85-90 (For primary document see N89-12876 04-39)
(Contract NAS3-23722)
Avail: NTIS HC A21/MF A01 CSCL 14B

N89-12888*# National Aeronautics and Space Administration. Lewis Research Center, Cleveland, Ohio.
THE NASA LEWIS STRAIN GAUGE LABORATORY: AN UPDATE
H. F. Hobart *In its* Turbine Engine Hot Section Technology

1986 Oct. 1986 p 91-96 (For primary document see N89-12876 04-39)
Avail: NTIS HC A21/MF A01 CSCL 14B

N89-12938# Hughes Aircraft Co., Tucson, Ariz.
AUTOMATIC CONTROL OF A MULTI-CHANNEL MILLIMETER WAVE RADIOMETER
D. A. Zielinskie, C. A. Wassenberg, and J. A. Reagan *In* ESA, Proceedings of the 1988 International Geoscience and Remote Sensing Symposium (IGARSS 1988) on Remote Sensing: Moving Towards the 21st Century, Volume 1 Aug. 1988 p 13-14 (For primary document see N89-12936 04-42)
Copyright Avail: NTIS HC A99/MF E03; ESA Publications Div., ESTEC, Noordwijk, Netherlands, 120 US dollars or 250 Dutch guilders

N89-12939# Deutsche Forschungs- und Versuchsanstalt fuer Luft- und Raumfahrt, Oberpfaffenhofen (West Germany).
THE AIRBORNE RADIOMETRY EXPERIMENT (ABREX) INSTRUMENT, AN EXPERIMENTAL TEST BED FOR THE SPECIFICATION OF SATELLITE-BORNE MICROWAVE RADIOMETER AT 90 GHz
W. Keydel and H. Goessl *In* ESA, Proceedings of the 1988 International Geoscience and Remote Sensing Symposium (IGARSS 1988) on Remote Sensing: Moving Towards the 21st Century, Volume 1 Aug. 1988 p 15-16 (For primary document see N89-12936 04-42)
Copyright Avail: NTIS HC A99/MF E03; ESA Publications Div., ESTEC, Noordwijk, Netherlands, 120 US dollars or 250 Dutch guilders

N89-12942# Marconi Space Systems Ltd., Portsmouth (England).
PROPOSED DESIGN OF THE TEMPERATURE CONTROL SYSTEM FOR THE VARIABLE TEMPERATURE CALIBRATION TARGET FOR THE ADVANCED MICROWAVE SOUNDING UNIT B
L. J. Banfield *In* ESA, Proceedings of the 1988 International Geoscience and Remote Sensing Symposium (IGARSS 1988) on Remote Sensing: Moving Towards the 21st Century, Volume 1 Aug. 1988 p 21-22 Sponsored by the Ministry of Defence Procurement Executive, London, United Kingdom (For primary document see N89-12936 04-42)
Copyright Avail: NTIS HC A99/MF E03; ESA Publications Div., ESTEC, Noordwijk, Netherlands, 120 US dollars or 250 Dutch guilders

36 LASERS AND MASERS

Includes parametric amplifiers.
For related information see also *76 Solid-State Physics*.

N89-12848# Mound Lab., Miamisburg, Ohio.
LASER ILLUMINATED HIGH SPEED PHOTOGRAPHY OF ENERGETIC MATERIALS
Larry R. Dosser, John W. Reed, and Margaret A. Stark 1988 5 p Presented at the Medical and Material Processing Applications of Various Types of Lasers, Cincinnati, Ohio, 21 Apr. 1988
(Contract DE-AC04-76DP-00053)
(DE88-012870; MLM-3498(OP); CONF-8804159-2) Avail: NTIS HC A02/MF A01

The evaluation of the properties of energetic materials, such as burn rate and ignition, is of primary importance in understanding their reactions and how devices containing them perform their function. We have recently applied high speed photography at rates of up to 20,000 images per second to this problem. When a copper vapor laser is synchronized to the high speed camera, laser illuminated images can be recorded that detail the performance of a component in a manner never before possible. The copper vapor laser used for these experiments had an average power of 30 watts, and produced pulses at a rate of up to 10 kHz. The 30 nanosecond pulsewidth of the laser essentially freezes all motion in the functioning component, thus providing stop-action pictures at a rate of up to 10,000 per second. Each laser pulse has a peak power of approximately 170,000 watts which provides ample illumination for the high speed photography. Several energetic materials and components studied include the pyrotechnic Ti/2B, a pyrotechnic torch, laser ignition of high explosives, and a functioning igniter. DOE

N89-12849# Advisory Group for Aerospace Research and Development, Neuilly-Sur-Seine (France).
LASER APPLICATIONS IN FLOW DIAGNOSTICS
J. D. Trolinger and J. J. Ginoux, ed. (Von Karman Inst. for Fluid Dynamics, Rhode-Saint-Genese, Belgium) Oct. 1988 189 p
(AGARD-AG-296; ISBN-92-835-0480-1) Copyright Avail: NTIS HC A09/MF A01

This is an explanation and update of AGARDograph No. 186, Laser Instrumentation for Flow Field Diagnostics, which was published in 1974. A brief introduction to coherent optics and lasers is given to provide a review and common language to the reader. The material is presented at a level to be understood by engineers who are working in the aerospace field and who are interested in the experimental application of lasers in research and development. An emphasis is placed on applications in aerodynamics, and examples were selected from a number of laboratories in the NATO countries visited while the material was being prepared. The applications include holography, laser velocimetry, spectroscopy, and the use of lasers simply as efficient light sources in conventional measurement methods. Author

N89-12850# Rochester Univ., N. Y. Inst. of Optics.
LASER SPECKLE FROM THIN AND CASCADED DIFFUSERS Ph.D. Thesis
Lyle Gordon Shirley May 1988 206 p Sponsored by Army Research Office, Washington, D.C.
(AD-A197066; ARO-24626-PH-UIR; ARO-24749-PH) Avail: NTIS HC A10/MF A01 CSCL 09F

The scattering of laser light from a single diffuser and from a cascade of two diffusers is analyzed with particular emphasis on remote sensing. It is shown that diffuser surface properties and the spacing between diffuser planes can be determined remotely by measuring the angular distribution of the radiation pattern or the decorrelation of the far-zone speckle pattern with respect to changes in the wavelength or the angle of incidence of an input plane wave. A general expression is derived for the two-state correlation function of far-zone complex amplitude from a cascade of two diffusers, where the two states are the initial and final values of the wavelength, angle of incidence, angle of observation, and spacing. This function is then related to the two-state correlation function of intensity, which is a measure of the correlation between the initial and final speckle patterns. The two-state correlation function of intensity is evaluated for various double diffuser combinations. The effect of surface height profiles on the radiation pattern is studied. Of particular interest are strong diffusers that have a normally distributed height profile and whose surface height autocorrelation functions are paraboloidal or conical for small spatial offsets. GRA

N89-12851# Michigan Univ., Ann Arbor. Dept. of Chemistry.
ION MOBILITY SPECTROMETRY WITH LASER-PRODUCED IONS Final Report, 1 May 1985 - 31 Mar. 1988
David M. Lubman 10 May 1988 14 p
(Contract DAAG29-85-K-0105)
(AD-A197117; ARO-22444.16-CH) Avail: NTIS HC A03/MF A01 CSCL 09A

The purpose of this work has been to investigate laser multiphoton ionization (MPI) as an atmospheric pressure ionization source for ion mobility spectrometry (IMS). This has included a study of the potential of MPI for improving selectivity and specificity in IMS and also an investigation of the fundamentals of laser MPI under atmospheric conditions. A second focus of this work has been to extend IMS to nonvolatile molecules using a pulsed laser desorption method for volatilization. The final report contains the research findings. GRA

N89-12852# Physical Sciences, Inc., Alexandria, Va.
SURVEY OF LASER-PRODUCED PRESSURE AND IMPULSE DATA Final Report, Aug. 1986 - Sep. 1987
J. A. McKay and P. M. Laufer Jan. 1988 243 p
(Contract N00014-86-C-2241)
(AD-A197313; PSI-1012/TR-757) Avail: NTIS HC A11/MF A01 CSCL 09C

The objective of the present work is the collection of all laser generation pressure and impulse data of good quality, and the display of those data in a single format. It should now be possible not only to discover what data regimes have been investigated and which neglected, but to compare experimental results for consistency and the detection of overall patterns. The data are organized first by pressure and impulse, then by the ambient conditions, i.e., in air, in reduced-pressure air, and in vacuum. Within each category the reports are organized by wavelength, beginning with the middle infrared and proceeding to the ultraviolet. Within each wavelength category the data are presented in chronological order of publication. The graphic display of each set is selected to emphasize the most important single variable. GRA

N89-12853# Texas Univ., Dallas. Center for Quantum Electronics.
PROOF OF THE FEASIBILITY OF COHERENT AND INCOHERENT SCHEMES FOR PUMPING A GAMMA-RAY LASER Quarterly Report, 1 Jan. - 31 Mar. 1988
Carl B. Collins Apr. 1988 91 p
(Contract N00014-86-C-2488)
(AD-A197333; GRL/8704) Avail: NTIS HC A05/MF A01 CSCL 09C

Recent approaches to the problem of the gamma-ray laser have focused upon upconversion techniques in which metastable nuclei are pumped with long wavelength radiation. At the nuclear level, the storage of energy on approach teraJoules (10 to the 12th power J) per liter for thousands of years. This report focuses upon the nuclear analog of the optical double resonance method which produced much of the database at the molecular level that was of such essential use in the development of conventional lasers. Applied most recently to the study of levels which might be used in dumping isomeric populations into freely radiating states, it produced an unexpected result of major importance. In several test isotopes, a class of extremely useful states was discovered that could radiatively couple to both normal and isomeric states of a nucleus spanning large changes of angular momentum. Demonstrated was the excitation of populations of the second of the 29 actual candidates for a gamma-ray laser. Another of the less attractive of the 29 isomers because of a large change in angular momentum of 5 h, 123Te superscript m was one of the few which had both a radioactive signature sufficiently distinctive for detection and a stable ground state from which to fabricate a target. GRA

N89-12854# Air Force Systems Command, Wright-Patterson AFB, Ohio. Foreign Technology Div.
POPULATION INVERSION NON-EQUILIBRIUM FLOW SIMULATION CALCULATIONS OF THE CAPABILITIES OF CONVECTION FLOW LASERS
Wu Zhongxiang 24 Jun. 1988 20 p Transl. into ENGLISH from Lixue Jinzhan (Peoples Republic of China), v. 16, no. 2, 25 May 1986 p 221-227
(AD-A197741; FTD-ID(RS)T-0263-88) Avail: NTIS HC A03/MF A01 CSCL 09C

Fluid mechanics and non-equilibrium state thermal dynamics are brought together to form hot gas dynamics. The test production of high power lasers has quickly developed. The flow movements of working media have important effects on high power laser devices: (1) the convectionary heat diffusion heat dissipation; (2) flow movements make the working medium constantly replace itself, making it possible to maintain the stability of the working medium as well as to continuously replenish the energy source; (3) and it is possible to make use of rapid expansion to directly form population inversion. Because of this, the high power lasers which currently exist - gas flow lasers, flow movement and electrical discharge lasers, quasimolecular lasers, chemical lasers, and similar devices - make use of reactive flow gases to act as working media. GRA

N89-12855# National Bureau of Standards, Boulder, Colo. Quantum Physics Div.
DETECTION OF EXCITED STATES BY LASER-INDUCED FLUORESCENCE AND ANALYSIS OF ENERGY TRANSFER Final Report, Oct. 1986 - Sep. 1987
A. B. Wedding and A. V. Phelps Jul. 1988 63 p
(AF Proj. 2301)
(AD-A197770; MIPR-FY1455-86-N0652; AFWAL-TR-88-2033)
Avail: NTIS HC A04/MF A01 CSCL 07B

The objective of this research is to develop diagnostics and models required for measurement and prediction of the properties of electrical discharges in molecular gases. Discharges in molecular gases are important in Air Force technology because of their use in devices such as plasma processors, high power switches, and negative ion sources and because of their role in phenomena such as corona and lightning. The research program includes: (1) the development and application of laser fluorescence and absorption techniques to the measurement of excited state densities in electric discharges; (2) the measurement of the properties of the excited states of importance in molecular discharges of current interest; (3) the application of various diagnostic techniques to the determination of the characteristics of moderate current density, transient electrical discharges; and (4) the quantitative comparison of these results with appropriate discharge models. GRA

N89-12856*# National Aeronautics and Space Administration. Pasadena Office, Calif.
Tm,Ho:YLF LASER END-PUMPED BY A SEMICONDUCTOR DIODE LASER ARRAY Patent Application
Hamid Hemmati, inventor (to NASA) (Jet Propulsion Lab., California Inst. of Tech., Pasadena.) 23 Aug. 1988 16 p
(Contract NAS7-918)
(NASA-Case-NPO-17282-1-CU; NAS 1.71:NPO-17282-1-CU; US-Patent-Appl-SN-235150) Avail: NTIS HC A03/MF A01 CSCL 20E

An Ho:YLF crystal including Tm as sensitizers for the activator Ho, is optically pumped with a semiconductor diode laser array to generate 2.1 micron radiation with a pump power to output power of efficiency as high as 68 percent. The prior-art dual sensitizer system of Er and Tm requires cooling, such as by LN2, but by using Tm alone and decreasing the concentrations of Tm and Ho, and decreasing the length of the laser rod to about 1 cm, it has been demonstrated that laser operation can be obtained from a temperature of 77 K with an efficiency as high as 68 percent up to ambient room temperature with an efficiency at that temperature as high as 9 percent. NASA

N89-12857# Sandia National Labs., Albuquerque, N. Mex.
RESONATOR DESIGN WITH AN INTRACAVITY TIME-VARYING INDEX GRADIENT
D. R. Neal, W. C. Sweatt, and J. R. Torczynski 1988 12 p Presented at the 32nd International Technical Symposium on Optical and Opto-Electronic Applied Sciences and Engineering, San Diego, Calif., 14 Aug. 1988
(Contract DE-AC04-76DP-00789)
(DE88-015259; SAND-88-0494C; CONF-880887-6) Avail: NTIS HC A03/MF A01

Side-pumped lasers such as flashlamp- or reactor-pumped lasers often have a nonuniform energy deposition in the gain medium, which can establish a significant transverse index gradient. This gradient significantly complicates energy extraction. A normalized resonator analysis method is developed that predicts resonator stability transitions and mode sizes for parabolic index fields. Parameter studies for some practical classes of resonators are presented, along with some design guidelines. Experimental comparison for a long-pulse gas laser shows good agreement

with stability transition times. Two resonator-design approaches are presented for increasing the extraction efficiency in the presence of intracavity index gradients. DOE

N89-12858# Los Alamos National Lab., N. Mex. Laser Science and Applications Group.
OVERVIEW OF RECENT ADVANCES IN EXCIMER LASER TECHNOLOGY AT LOS ALAMOS
Irving J. Bigio, Robert C. Sze, Antoinette J. Taylor, and Robert B. Gibson 1988 6 p Presented at the Excimer Laser Session, Hamburg, Fed. Republic of Germany, 22 Sep. 1988
(Contract W-7405-eng-36)
(DE88-016236; LA-UR-88-2745; CONF-8809124-1) Avail: NTIS HC A02/MF A01

From among the areas of excimer laser development at Los Alamos two are selected for further discussion: ultra-high brightness excimer laser systems and discharge-pumped XeF(C yields A) lasers operating in the blue-green portion of the spectrum. Two different high brightness systems are described. One is based on small-aperture KrF amplifiers, while the other is based on a large-aperture XeCl amplifier. The XeF(C yields A) laser is tunable from 435 to 525 nm, and may one day become a viable alternative to pulsed dye lasers for many applications. DOE

N89-12859# Sandia National Labs., Albuquerque, N. Mex.
RADIATION EFFECTS IN SEMICONDUCTOR LASER DIODE ARRAYS
Richard F. Carson 1988 19 p Presented at the Optoelectronic Materials and Devices 2, Boston, Mass., 6 Sep. 1988
(Contract DE-AC04-76DP-00789)
(DE88-016318; SAND-88-1049C; CONF-8809111-2) Avail: NTIS HC A03/MF A01

The effects of radiation events are important for many of the present and future applications that involve optoelectronic components. Laser diodes show a strong resistance to degradation by gamma rays, prompt X-rays and (to a lesser extent), neutrons. This is due to the short carrier lifetime that is associated with stimulated emission and the high current injection conditions that are present in these devices. Radiation-resistant properties should carry over to many of the more recently developed devices such as multi-stripe array and broad area laser diodes. There are, however, additional considerations for radiation tolerance that are introduced by these devices. Arrays and other high power laser diodes have larger active region volumes than lower power single stripe devices. In addition, evanescent field coupling between stripes, the material quality available from newer MOCVD epitaxial growth techniques, and stripe definition methods may all influence the radiation tolerance of the high power laser diode devices. Radiation tests have been conducted on various GaAs-GaAlAs laser diode array and broad area devices. Tests involving total gamma dose have indicated that high power laser diodes and arrays have small degradations in light power output with current input after 4 MRad(Si) of radiation from a Co^{60} source. DOE

N89-12860# Lawrence Livermore National Lab., Calif.
HIGH POWER Nd:GLASS LASERS AS DRIVERS FOR INERTIAL CONFINEMENT FUSION
Howard T. Powell, John H. Campbell, John T. Hunt, W. Howard Lowdermilk, John R. Murray, and D. Ralph Speck Sep. 1988 21 p Presented at the Course and Workshop on Inertial Confinement Fusion, Varenna, Italy, 6 Sep. 1988
(Contract W-7405-eng-48)
(DE88-017016; UCRL-99517; CONF-880928-3) Avail: NTIS HC A03/MF A01

We review the design and performance of the 100-kJ Nova laser used for inertial confinement fusion research. In particular, we describe a major upgrade to the Nova system which is in progress. We also discuss briefly the design of a potential 10-MJ, 1000 TW laser, which we have named Athena. DOE

N89-12759# New Mexico Univ., Albuquerque. Dept. of Physics and Astronomy.
CONSTRUCTION OF A PHASE CONJUGATE LASER RESONATOR USING BRILLOUIN ENHANCED FOUR WAVE MIXING Final Report
Kyunam Choi *In* Universal Energy Systems, Inc., United States Air Force Graduate Student Summer Support Program, Volume 1 Dec. 1987 17 p (For primary document see N89-12754 04-31)
Avail: NTIS HC A99/MF E03 CSCL 20E

N89-12781# New Mexico Univ., Albuquerque. Dept. of Physics and Astronomy.
INVESTIGATION OF LASER DIODE COUPLING USING NONLINEAR OPTICS Final Report
Bruce W. Liby *In* Universal Energy Systems, Inc., United States Air Force Graduate Student Summer Support Program, Volume 1 Dec. 1987 8 p (For primary document see N89-12754 04-31)
Avail: NTIS HC A99/MF E03 CSCL 20E

N89-12885*# National Aeronautics and Space Administration. Lewis Research Center, Cleveland, Ohio.
LASER ANEMOMETRY: A STATUS REPORT
Mark P. Wernet, Richard G. Seasholtz, Donald H. Weikle, and Lawrence G. Oberle *In its* Turbine Engine Hot Section Technology 1986 Oct. 1986 p 61-68 (For primary document see N89-12876 04-39)
Avail: NTIS HC A21/MF A01 CSCL 20E

N89-12889*# National Aeronautics and Space Administration. Lewis Research Center, Cleveland, Ohio.
SUMMARY OF LASER SPECKLE PHOTOGRAMMETRY FOR HOST
Frank G. Pollack *In its* Turbine Engine Hot Section Technology 1986 Oct. 1986 p 97-103 (For primary document see N89-12876 04-39)
Avail: NTIS HC A21/MF A01 CSCL 20E

N89-12982*# National Aeronautics and Space Administration. Goddard Space Flight Center, Greenbelt, Md.
GEODYNAMICS LASER RANGING SYSTEM: PERFORMANCE SIMULATIONS AND DEVELOPMENT OF THE EOS FACILITY
S. C. Cohen *In* ESA, Proceedings of the 1988 International Geoscience and Remote Sensing Symposium (IGARSS 1988) on Remote Sensing: Moving Towards the 21st Century, Volume 1 Aug. 1988 p 187-189 (For primary document see N89-12936 04-42)
Copyright Avail: NTIS HC A99/MF E03; ESA Publications Div., ESTEC, Noordwijk, Netherlands, 120 US dollars or 250 Dutch guilders CSCL 20E

37 MECHANICAL ENGINEERING

Includes auxiliary systems (nonpower); machine elements and processes; and mechanical equipment.

N89-12861# Gaydon Technology Ltd., Warwick (England).
GAS FLOW AND GLOBAL CODE PROGRAMME Summary Report, 1 Apr. 1985 - 31 Mar. 1986
S. F. Benjamin Feb. 1987 18 p Sponsored in part by the Commission of the European Communities, Luxembourg
(Contract EN3E.0005.UK(H))
(DE88-012635; EUR-11186) Avail: NTIS (US Sales Only) HC A03/MF A01

This contract (Contract 2) forms a bridging program between contract EE.CI.210 (UK(H) (1.3.83-31.12.84) (Contract 1) entitled, The development and evaluation of three dimensional models of cold flow in an internal combustion engine, and proposal EN3 E/CI/041 GB (Contract 3) entitled, Basic Gas Flow Code for Reciprocating Engines, (planned start dte 1.4.86). The objectives of these programs are to develop a series of computer codes capable of simulating the in-cylinder flow and turbulence fields in reciprocating engines. This program involves both computational work for the construction of the computer codes along with an

experimental program aimed at providing flow measurements for code evaluation. During the contract period problems were encountered with the MICE code. An earlier development code EPISO, on which MICE was based was therefore used as the basis for continued refinement, and to support the first steps in the development of the SPEED code. A combustion module was incorporated into EPISO. Development of the SPEED code has met the interim objectives, so that this work is on schedule for release of the first version (Code 1) at the end of 1986. The experimental program has largely concentrated on the development of hardware necessary for the high speed laser Doppler anemometry measurements that are to be obtained as part of the ongoing program. Testing of the mechanical and electronic hardware for the high speed model engine system is complete. Measurements were obtained from an idealized port under steady state conditions prior to incorporation on the model engine.
DOE

N89-12862*# Eagle Engineering, Inc., Houston, Tex.
LUNAR SURFACE TRANSPORTATION SYSTEMS CONCEPTUAL DESIGN LUNAR BASE SYSTEMS STUDY TASK 5.2
7 Jul. 1988 188 p
(Contracts NAS9-17878; EEI-TO-87-57)
(NASA-CR-172077; NAS 1.26:172077; EEI-88-188) Avail: NTIS HC A09/MF A01 CSCL 13F

Conceptual designs for three categories of lunar surface transportation were described. The level of understanding for the capabilities and design approach varies between the vehicles representing these categories. A summary of the vehicle categories and current state of conceptual design is provided. Finally, a brief evaluation and discussion is provided for a systematic comparison of transportation categories and effectiveness in supporting transportation objectives.
Author

N89-12863# Centre Aeroporte de Toulouse (France).
AUTOMATIC RELEASE MECHANISM FOR THE EL 32 BAG [LIBERATEUR AUTOMATIQUE DE SAC GAINE EL 32]
T. E. F. Seigneurie Jan. 1988 82 p In FRENCH
(E-768; Rept-88/05; ETN-88-93110) Avail: NTIS HC A05/MF A01

An automatic release mechanism for the weapon holder of a parachutist, based on a chrono-accelerometer principal, is discussed. Tests of the device show that it does not work in every case, because of the effects of rubbing against objects, e.g., the parachute cords can prevent the pins attaching the bag from being withdrawn. The system also has difficulty in distinguishing between shocks caused by normal opening of the parachute and random shocks.
ESA

N89-12864# Dayton Univ., Ohio. Research Inst.
RESEARCH ON MECHANICAL PROPERTIES FOR ENGINE LIFE PREDICTION Final Report, Aug. 1984 - Sep. 1987
M. Khobaib, Noel E. Ashbaugh, George A. Hartman, Tusit Weerasooriya, and David C. Maxwell May 1988 120 p
(Contract F33615-84-C-5051)
(AD-A197816; UDR-TR-88-08; AFWAL-TR-88-4062) Avail: NTIS HC A06/MF A01 CSCL 11F

Analytical and experimental investigations have been performed to determine crack growth behavior of turbine engine disk and blade alloys under various loading conditions typical of service environments. Tests were performed at elevated temperature in vacuum also to evaluate the baseline crack growth behavior. Substructural analysis of creep rupture specimens were conducted to understand the basic mechanism of time-dependent elevated temperature deformation. The work performed can be divided into three categories -- development of experimental techniques, material characterization techniques, and data maintenance and test support activities. The capability of the IDG laser system to monitor extended gage length was analyzed and found feasible. New grips and specimens have been designed and fabricated for high temperature composite testing. Enhancements to existing systems for crack length and displacement measurements were made.
GRA

N89-12865*# National Aeronautics and Space Administration. Lyndon B. Johnson Space Center, Houston, Tex.
GRIPPING DEVICE Patent Application
George F. Parma, inventor (to NASA) 19 Jul. 1988 21 p
(NASA-Case-MSC-21365-1; NAS 1.71:MSC-21365-1;
US-Patent-Appl-SN-221388) Avail: NTIS HC A03/MF A01
CSCL 13I

This invention relates to a gripping device, and more particularly to one with a large moment carrying capability for handling long workpieces of various diameters and which can be particularly used as an end effector on a robotic arm.
NASA

N89-12866*# National Aeronautics and Space Administration. Lyndon B. Johnson Space Center, Houston, Tex.
MAGNETIC ATTACHMENT MECHANISM Patent Application
Mitchell B. Wu, inventor (to NASA) and William D. Harwell, inventor (to NASA) 23 Sep. 1988 20 p
(NASA-Case-MSC-21095-1; NAS 1.71:MSC-21095-1;
US-Patent-Appl-SN-248010) Avail: NTIS HC A03/MF A01
CSCL 13I

A magnetic attachment mechanism adapted for interfacing with the manipulator arm of a remote manipulator system and comprising a pair of permanent magnets of rare earth material are arranged in a stator-rotor relationship. The rotor magnet is journalled for rotation about its longitudinal axis between pole plates of the stator magnet, each of which includes an adhering surface. In a first rotary position corresponding to the ON condition, each of the poles of the rotor magnet is closely adjacent to a stator magnet pole plate of like polarity whereby the respective magnet fields are additive for producing a strong magnetic field emanating from the adhering surfaces for attracting a ferrous magnetic plate, or the like, affixed to the payload. When the rotor magnet is rotated to a second position corresponding to the OFF condition, each of the poles of the rotor magnet is disposed closely adjacent to a pole plate of unlike polarity whereby the magnetic fields of the magnets are in cancelling relationship at the adhering surfaces, which permits the release of a payload. An actuator for selectively rotating the rotor magnet between the ON and OFF positions is provided for interfacing and connecting the magnetic attachment mechanism with a manipulator arm. For affecting an optimal rigidized attachment the payload is provided with guide means cooperable with guide means on the housing of the mechanism for directing adhering surfaces of the polar plates to the ferrous plate.
NASA

N89-12867*# National Aeronautics and Space Administration. Langley Research Center, Hampton, Va.
PULTRUSION DIE ASSEMBLY Patent Application
Maywood L. Wilson, inventor (to NASA), Gary S. Johnson, inventor (to NASA), Mark W. Frye, inventor (to NASA), and Clarence E. Stanfield, inventor (to NASA) 1 Sep. 1988 20 p
(NASA-Case-LAR-13719-1; NAS 1.71:LAR-13719-1;
US-Patent-Appl-SN-239260) Avail: NTIS HC A03/MF A01
CSCL 13I

This invention relates generally to pultrusion die assemblies, and more particularly, to a pultrusion die assembly which incorporates a plurality of functions in order to produce a continuous, thin composite fiber reinforced thermoplastic material. The invention is useful for making high performance thermoplastic composite materials in sheets which can be coiled on a spool and stored for further processing.
NASA

N89-12868*# National Aeronautics and Space Administration. Marshall Space Flight Center, Huntsville, Ala.
OPTICALLY CONTROLLED WELDING SYSTEM Patent Application
Stephen S. Gordon, inventor (to NASA) (Rockwell International Corp., Huntsville, Ala.) 28 Sep. 1988 16 p
(NASA-Case-MFS-29291-1; NAS 1.71:MFS-29291-1;

US-Patent-Appl-SN-250196) Avail: NTIS HC A03/MF A01 CSCL 13H

An optically controlled welding system wherein a welding torch having through-the-torch viewing capabilities is provided with an optical beam splitter to create a transmitted view and a reflective view of a welding operation. These views are converted to digital signals which are then processed and utilized by a computerized robotic welder to make the welding torch responsive thereto. Other features include an actively cooled electrode holder which minimizes a blocked portion of the view by virtue of being constructed of a single spoke or arm, and a weld pool contour detector comprising a laser beam directed onto the weld pool with the position of specular radiation reflected therefrom, being characteristic of a penetrated or unpenetrated condition of the weld pool. NASA

N89-12869# Oak Ridge National Lab., Tenn.
BES WELDING SCIENCE CONTRACTORS Summary Report, 1987-1988
S. A. David, comp., J. M. Vitek, T. Zacharia, A. J. McEvily, T. DebRoy, J. Szekely, D. K. Matlock, and D. L. Olson (Colorado School of Mines, Golden.) 1988 37 p
(Contract DE-AC05-84OR-21400)
(DE88-016589; ORNL/M-612) Avail: NTIS HC A03/MF A01

The principal aim of the Fundamental Welding Science Program is to investigate the physical metallurgy of weldments and to develop the capability to predict weld metal microstructure and properties. The program consists of four major parts relating to the study of: (1) solidification behavior of weld metal, (2) correlation of thermal history and phase stability of weldment microstructure, (3) mathematical modeling, and its verification, of welding processes, and (4) activities related to coordination of BES welding programs and ORNL-industry cooperative programs. DOE

N89-12870*# Carnegie-Mellon Univ., Pittsburgh, Pa. Dept. of Mechanical Engineering.
DYNAMICS OF FACE AND ANNULAR SEALS WITH TWO-PHASE FLOW Final Report, 15 Mar. 1981 - 18 Nov. 1988
William F. Hughes, Prithwish Basu, Paul A. Beatty, Richard M. Beeler, and Stephen Lau Nov. 1988 270 p
(Grant NAG3-166)
(NASA-CR-183352; NAS 1.26:183352) Avail: NTIS HC A12/MF A01 CSCL 11A

A detailed study was made of face and annular seals under conditions where boiling, i.e., phase change of the leaking fluid, occurs within the seal. Many seals operate in this mode because of flashing due to pressure drop and/or heat input from frictional heating. Some of the distinctive behavior characteristics of two phase seals are discussed, particularly their axial stability. The main conclusions are that seals with two phase flow may be unstable if improperly balanced. Detailed theoretical analyses of low (laminar) and high (turbulent) leakage seals are presented along with computer codes, parametric studies, and in particular a simplified PC based code that allows for rapid performance prediction: calculations of stiffness coefficients, temperature and pressure distributions, and leakage rates for parallel and coned face seals. A simplified combined computer code for the performance prediction over the laminar and turbulent ranges of a two phase flow is described and documented. The analyses, results, and computer codes are summarized. Author

N89-12627*# National Aeronautics and Space Administration. Marshall Space Flight Center, Huntsville, Ala.
DAMPING SEAL TESTER PROGRESS AND INITIAL TEST RESULTS
K. L. Cappel (Wyle Labs., Inc., Huntsville, Ala.) and George L. vonPragenau *In its* Advanced Earth-To-Orbit Propulsion Technology 1986, Volume 2 Oct. 1986 p 2-8 (For primary document see N89-12626 04-20)
Avail: NTIS HC A99/MF E03 CSCL 21H

N89-12628*# National Aeronautics and Space Administration. Marshall Space Flight Center, Huntsville, Ala.
LOW-SPEED FLEXIBLE ROTOR BALANCING FOR SMOOTH, HIGH-SPEED OPERATION
E. Zorzi, John Giordano (Mechanical Technology, Inc., Latham, N. Y.), and George L. vonPragenau *In its* Advanced Earth-To-Orbit Propulsion Technology 1986, Volume 2 Oct. 1986 p 9-32 (For primary document see N89-12626 04-20)
Avail: NTIS HC A99/MF E03 CSCL 21H

N89-12629*# Mechanical Technology, Inc., Latham, N. Y.
THE EFFECTS OF INTERNAL ROTOR FRICTION ON DYNAMIC CHARACTERISTICS OF TURBOPUMPS
J. Walton, A. Artiles, J. Lund, and C. Lee *In* NASA, Marshall Space Flight Center, Advanced Earth-To-Orbit Propulsion Technology 1986, Volume 2 Oct. 1986 p 33-61 (For primary document see N89-12626 04-20)
(Contract NAS8-35601)
Avail: NTIS HC A99/MF E03 CSCL 21H

N89-12630*# National Aeronautics and Space Administration. Marshall Space Flight Center, Huntsville, Ala.
EFFICIENT TRANSIENT ANALYSIS METHODS FOR THE SPACE SHUTTLE MAIN ENGINE (SSME) TURBOPUMPS
Sherif T. Noah, U. J. Fan, Y.-S. Choi (Texas A&M Univ., College Station.), and T. Fox *In its* Advanced Earth-To-Orbit Propulsion Technology 1986, Volume 2 Oct. 1986 p 62-82 (For primary document see N89-12626 04-20)
(Contract NAS8-36182)
Avail: NTIS HC A99/MF E03 CSCL 21H

N89-12631*# Auburn Univ., Ala. Computer Science and Engineering Div.
VIBRATIONS INDUCED BY NONLINEARITIES IN ROTORDYNAMICS
William B. Day *In* NASA, Marshall Space Flight Center, Advanced Earth-To-Orbit Propulsion Technology 1986, Volume 2 Oct. 1986 p 83-105 (For primary document see N89-12626 04-20)
(Contracts NAS8-35992; NAS8-36475)
Avail: NTIS HC A99/MF E03 CSCL 21H

N89-12639*# Battelle Columbus Labs., Ohio.
LUBRICATION EVALUATION OF SSME TURBOPUMP BEARINGS
K. F. Dufrane, J. W. Kannel, and S. A. Barber *In* NASA, Marshall Space Flight Center, Advanced Earth-To-Orbit Propulsion Technology 1986, Volume 2 Oct. 1986 p 266-292. (For primary document see N89-12626 04-20)
Avail: NTIS HC A99/MF E03 CSCL 21H

N89-12640*# Rockwell International Corp., Canoga Park, Calif. Rocketdyne Div.
SURFACE CHARACTERISTICS OF LIQUID OXYGEN COOLED BALL BEARINGS
Myles Butner and Mary Shoemaker *In* NASA, Marshall Space Flight Center, Advanced Earth-To-Orbit Propulsion Technology 1986, Volume 2 Oct. 1986 p 293-310 (For primary document see N89-12626 04-20)
(Contract NAS8-27980)
Avail: NTIS HC A99/MF E03 CSCL 21H

N89-12642*# National Aeronautics and Space Administration. Marshall Space Flight Center, Huntsville, Ala.
ROLLING CONTACT FATIGUE LIFE OF ZIRCONIUM AND MOLYBDENUM NITRIDE SPUTTER PLATED AMS 5749 BEARING STEEL
Robert L. Thom and Fred J. Dolan *In its* Advanced Earth-To-Orbit Propulsion Technology 1986, Volume 2 Oct. 1986 p 327-340 (For primary document see N89-12626 04-20)
Avail: NTIS HC A99/MF E03 CSCL 21H

N89-12643*# Rockwell International Corp., Canoga Park, Calif. Rocketdyne Div.
MEASUREMENT OF ROTORDYNAMIC COEFFICIENTS FOR A HYDROSTATIC RADIAL BEARING
B. T. Murphy and M. N. Wagner *In* NASA, Marshall Space Flight Center, Advanced Earth-To-Orbit Propulsion Technology 1986, Volume 2 Oct. 1986 p 341-366 (For primary document see N89-12626 04-20)
Avail: NTIS HC A99/MF E03 CSCL 21H

N89-12644*# Rockwell International Corp., Canoga Park, Calif. Rocketdyne Div.
SURFACE MODIFICATION FOR WEAR RESISTANCE IN A LIQUID OXYGEN TURBOPUMP ENVIRONMENT
Lillian Ng and Yngve Naerheim (Rockwell International Science Center, Thousand Oaks, Calif.) *In* NASA, Marshall Space Flight Center, Advanced Earth-To-Orbit Propulsion Technology 1986, Volume 2 Oct. 1986 p 366-376 (For primary document see N89-12626 04-20)
Avail: NTIS HC A99/MF E03 CSCL 21H

38 QUALITY ASSURANCE AND RELIABILITY

Includes product sampling procedures and techniques; and quality control.

N89-12871 Iowa State Univ. of Science and Technology, Ames.
LASER DYNAMIC PHOTOELASTICITY AND DIGITAL IMAGE ANALYSIS FOR NONDESTRUCTIVE EVALUATION OF SURFACE AND NEAR SURFACE FLAWS THROUGH ULTRASONIC SPECTROSCOPY Ph.D. Thesis
Babak Raj 1987 236 p
Avail: Univ. Microfilms Order No. DA8805129

The interaction of Rayleigh surface waves with artificial surface-breaking and near surface flaws in a half-space was investigated. The validity of ultrasonic spectroscopy was substantiated as an effective tool in nondestructive evaluation of the depth of such flaws. Dynamic photoelasticity was used to obtain full-field visualization of ultrasonic waves propagating in birefringent materials and their interaction with flaws of interest. PSM-1, which is a tough polymer of very low stress fringe value, was chosen as the birefringent material for this research. Sufficient short exposure times were achieved with a high-power pulsed YAG laser which has a pulse duration of about 15 nsec. The output was coupled into an optical fiber which then illuminated the dynamic model. The results are photoelastic pictures with excellent fringe resolution and negligible smearing effect. The Fast Fourier Transform of the constructed spatial waveforms was performed to yield the frequency spectrums of the wave-trains. The optimal ranges for the detection of the depth of surface slits and the ligament sizes for near surface slit were determined with respect to the Rayleigh wavelength in different materials. In both cases, an estimation was made as to the maximum depth of a surface slit or a ligament size which could be detected and characterized using ultrasonic spectroscopy. Dissert. Abstr.

N89-12872# California Univ., Berkeley. Lawrence Berkeley Lab. Center for X-ray Optics.
A REFINED MODEL FOR CHARACTERIZING X-RAY MULTILAYERS Ph.D. Thesis
Abraham L. Oren and Burke L. Henke Dec. 1987 61 p
(Contract DE-AC03-76SF-00098)
(DE88-013592; LBL-25401) Avail: NTIS HC A04/MF A01

The ability to quickly and accurately characterize arbitrary multilayers is very valuable for not only can we use the characterizations to predict the reflectivity of a multilayer for any soft X-ray wavelength, we also can generalize the results to apply to other multilayers of the same type. In addition, we can use the characterizations as a means of evaluating various sputtering environments and refining sputtering techniques to obtain better multilayers. In this report we have obtained improved characterizations for sample molybdenum-silicon and vanadium-silicon multilayers. However, we only examined five crystals overall, so the conclusions that we could draw about the structure of general multilayers is limited. Research involving many multilayers manufactured under the same sputtering conditions is clearly in order. In order to best understand multilayer structures it may be necessary to further refine our model, e.g., adopting a Gaussian form for the interface regions. With such improvements we can expect even better agreement with experimental values and continued concurrence with other characterization techniques. DOE

N89-12873# McDonnell Aircraft Co., St. Louis, Mo.
COMPOSITE CURING PROCESS NONDESTRUCTIVE EVALUATION Final Report, Sep. 1985 - Dec. 1987
Paul W. Harruff, Ram L. Levy, Ronald T. Harrold, Zal N. Sanjana, and Scott Schwab Jun. 1988 139 p
(Contract F33615-85-C-5024)
(AD-A197834; AFWAL-TR-88-4085) Avail: NTIS HC A07/MF A01 CSCL 11D

The objective of this program was to develop nondestructive evaluation techniques that can be used for in-process monitoring of the 350 F carbon/epoxy cure cycle. The techniques developed should have the capability of measuring composite material properties that can be used as a real time measure of the state of composite cure. Fluorescence Optrode and Acoustic Waveguide sensors were selected for development as cure-monitoring techniques. Miniature pressure sensors were also evaluated for tracking laminate resin hydrostatic pressures. Development efforts undertaken to establish optimum sensor responses, evaluate sensor-laminate interface methods, establish factory-capable data acquisition and presentation systems, determine sensor response-material property relationships, and demonstrate sensor capability for monitoring typical autoclave composite cure cycles are described. GRA

N89-12914*# Pratt and Whitney Aircraft, East Hartford, Conn.
CREEP FATIGUE LIFE PREDICTION FOR ENGINE HOT SECTION MATERIALS (ISOTROPIC): FOURTH YEAR PROGRESS REVIEW
Richard S. Nelson and John F. Schoendorf *In* NASA, Lewis Research Center, Turbine Engine Hot Section Technology 1986 Oct. 1986 p 359-370 (For primary document see N89-12876 04-39)
(Contract NAS3-23288)
Avail: NTIS HC A21/MF A01 CSCL 14D

N89-12916*# Pratt and Whitney Aircraft, East Hartford, Conn.
LIFE PREDICTION AND CONSTITUTIVE MODELS FOR ENGINE HOT SECTION
G. A. Swanson, T. G. Meyer, and D. M. Nissley *In* NASA, Lewis Research Center, Turbine Engine Hot Section Technology 1986 Oct. 1986 p 385-397 (For primary document see N89-12876 04-39)
(Contract NAS3-23939)
Avail: NTIS HC A21/MF A01 CSCL 14D

39 STRUCTURAL MECHANICS

Includes structural element design and weight analysis; fatigue; and thermal stress.

For applications see *05 Aircraft Design, Testing and Performance* and *18 Spacecraft Design, Testing and Performance*.

N89-12874 Ohio State Univ., Columbus.
DYNAMIC SYNTHESIS OF JOINED/HERMETIC SHELL STRUCTURES USING STATE SPACE METHOD Ph.D. Thesis
Massoud Seyed Tavakoli 1987 187 p
Avail: Univ. Microfilms Order No. DA8804114

Structures composed of shell elements find a wide range of applications in such areas as refrigeration systems, pressure

vessels, nuclear reactors, and aircraft. The dynamic behavior and design techniques for reduced noise and vibration of such structures are poorly understood because structural synthesis methods capable of handling the associated complexities are not well investigated. Accordingly, a synthesis method based on state space mathematics is proposed for the dynamic analysis of joined/hermetic shell structures. Chief strengths of this method include distributed patameter modeling, systematic substructuring, and exact matching of all of the boundary variables. The solution procedure is unified for both space-variant and space-invariant substructures using a spatial discretization scheme. Presently, the method is restricted to the determination of undamped eigensolutions of thin elactic structures. The proposed mehtod is first validated extensively by applying it to various well-known clasical beam, plate, and shell geometries, and comparing its results with those given by theory and finite element modeling. Further, the analytical design capability of the method is illustrated by examining the dynamics of a hermetic refrigeration compressor shell through five approximate models. The results of the proposed method compare excellently with finite element model predictions. Based on these studies, design recommendations for increased stiffness of the compressor shell are made. Dissert. Abstr.

N89-12875 Southern Methodist Univ., Dallas, Tex.
ON THE EFFECT OF R-RATIO AND Kfmax ON FRACTURE TOUGHNESS MEASUREMENT, FATIGUE CRACK PROPAGATION, AND FATIGUE CRACK CLOSURE Ph.D. Thesis
Angela Ann Steffen 1987 249 p
Avail: Univ. Microfilms Order No. DA8804369

A fundamental assumption of fracture toughness testing is that the resistance of the material to the presence of cracks is a material constant. This constant could be either sigma, K sub Q, CTOD, or J sub c, which is generally assumed to be experimentally measured for the material. The standards should be a measure of the true value of this material constant and if not should estimate the lower bound of the material property. An experimental investigation was undertaken to determine the effects of R-ratio and K sub fmax on fracture toughness measurements in 4130 steel. Both K sub 1c and CTOD test methods were considered. The K sub fmax values above 0.6K sub Q (the present limit in fracture toughness testing) were found to overestimate both K sub 1c and CTOD fracture toughness measurements. Stress ratios greater than 0.1 led to lower bound estimates of K sub 1c fracture toughness. Based on the lower bound stress estimate for fracture toughness, the use of R-ratios greater than 0.1 was encouraged. Stress ratios greater than 0.1 led to increases in CTOD. Based on a lower bound displacement estimate for fracture toughness estimate, the use of R-ratio greater than 0.1 in CTOD is discouraged. A model was developed to account for the variation in K sub Q as a function of K sub kmax and R. Dissert. Abstr.

N89-12876*# National Aeronautics and Space Administration. Lewis Research Center, Cleveland, Ohio.
TURBINE ENGINE HOT SECTION TECHNOLOGY 1986
Oct. 1986 488 p Workshop held in Cleveland, Ohio, 21-22 Oct. 1986
(NASA-CP-2444; E-3205; NAS 1.55:2444) Avail: NTIS HC A21/MF A01 CSCL 20K

The Turbine Engine Hot Section Technology (HOST) Project of the NASA Lewis Research Center sponsored a workshop to discuss current research pertinent to turbine engine durability problems. Presentations were made concerning the hot-section environment and the behavior of combustion liners, turbine blades, and turbine vanes. The presentations were divided into six sessions: Instrumentation, Combustion, Turbine Heat Transfer, Structural Analysis, Fatigue and Fracture, and Surface Protection. Topics discussed included modeling of thermal and fluid-flow phenomena, structural analysis, fatigue and fracture, surface protective coatings, constitutive behavior of materials, stress-strain response, and life-prediction methods. Researchers from industry, academia, and government presented results of their work sponsored by the HOST project. For individual titles, see N89-12877 through N89-12922.

N89-12877*# National Aeronautics and Space Administration. Lewis Research Center, Cleveland, Ohio.
TURBINE ENGINE HOT SECTION TECHNOLOGY (HOST) PROJECT **c07**
Daniel E. Sokolowski and C. Robert Ensign *In its* Turbine Engine Hot Section Technology 1986 Oct. 1986 p 1-6 Previously announced as N86-11496 (For primary document see N89-12876 04-39)
Avail: NTIS HC A21/MF A01 CSCL 20K

The Hot Section Technology (HOST) Project is a NASA-sponsored endeavor to improve the durability of advanced gas turbine engines for commercial and military aircraft. Through improvements in the analytical models and life prediction systems, designs for future hot section components, the combustor and turbine, will be more accurately analyzed and will incorporate features required for longer life in the more hostile operating environment of high performance engines. E.R.

N89-12878*# National Aeronautics and Space Administration. Lewis Research Center, Cleveland, Ohio.
HOST INSTRUMENTATION R AND D PROGRAM OVERVIEW **c07**
D. R. Englund *In its* Turbine Engine Hot Section Technology 1986 Oct. 1986 p 7-8 Previously announced as N86-11497 (For primary document see N89-12876 04-39)
Avail: NTIS HC A21/MF A01 CSCL 20K

The HOST Instrumentation R and D program is focused on two categories of instrumentation. One category is that required to characterize the environment imposed on the hot section components of turbine engines. This category includes instruments for measuring gas flow, gas temperature, and heat flux. The second category is that for measuring the effect of the environment on the hot section components. This category includes strain measuring instruments and an optical system for viewing the interior of an operating combustor to detect cracks, buckling, carbon buildup, etc. E.R.

N89-12879*# National Aeronautics and Space Administration. Lewis Research Center, Cleveland, Ohio.
HOST COMBUSTION R AND T OVERVIEW **c07**
Raymond E. Gaugler *In its* Turbine Engine Hot Section Technology 1986 Oct. 1986 p 9-11 (For primary document see N89-12876 04-39)
Avail: NTIS HC A21/MF A01 CSCL 21E

The overall objective of the Turbine Engine Hot Section Technology Combustion Project was to develop and verify improved and more accurate numerical analysis methods for increasing the ability to design with confidence combustion systems for advanced aircraft gas turbine engines. The objective was approached from two directions: computational and experimental. On the computational side, the approach was to first assess and evaluate existing combustor aerothermal analysis models. On the experimental side, three types of experiments are identified; first, fundamental experiments directed toward improved understanding of the flow physics and chemistry; second, experiments run to provide data for the empirical modeling of complex phenomena; and third, benchmark experiments for computer code validation. E.R.

N89-12880*# National Aeronautics and Space Administration. Lewis Research Center, Cleveland, Ohio.
HOST TURBINE HEAT TRANSFER SUBPROJECT OVERVIEW **c07**
Herbert J. Gladden *In its* Turbine Engine Hot Section Technology 1986 Oct. 1986 p 13-17 (For primary document see N89-12876 04-39)
Avail: NTIS HC A21/MF A01 CSCL 21E

The experimental part of the turbine heat transfer subproject consists of six large experiments, which are highlighted in this overview, and three of somewhat more modest scope. One of

the initial efforts was the stator airfoil heat transfer program. The non-film cooled and the showerhead film cooled data have already been reported. The gill region film cooling effort is currently underway. The investigation of secondary flows in a 90 deg curved duct, was completed. The first phase examined flows with a relatively thin inlet boundary layer and low free stream turbulence. The second phase studied a thicker inlet boundary layer and higher free stream turbulence. A comparison of analytical and experimental cross flow velocity vectors is shown for the 60 deg plane. Two experiments were also conducted in the high pressure facility. One examined full coverage film cooled vanes, and the other, advanced instrumentation. The other three large experimental efforts were conducted in a rotation reference frame. An experiment to obtain gas path airfoil heat transfer coefficients in the large, low speed turbine was completed. Single-stage data with both high and low-inlet turbulence were taken. The second phase examined a one and one-half stage turbine and focused on the second vane row. Under phase 3 aerodynamic quantities such as interrow time-averaged and rms values of velocity, flow angle, inlet turbulence, and surface pressure distribution were measured. E.R.

N89-12881*# National Aeronautics and Space Administration. Lewis Research Center, Cleveland, Ohio.

HOST STRUCTURAL ANALYSIS PROGRAM OVERVIEW

Robert L. Thompson *In its* Turbine Engine Hot Section Technology 1986 Oct. 1986 p 19-31 (For primary document see N89-12876 04-39)

Avail: NTIS HC A21/MF A01 CSCL 20K

Hot-section components of aircraft gas turbine engines are subjected to severe thermal structural loading conditions, especially during the startup and takeoff portions of the engine cycle. The most severe and damaging stresses and strains are those induced by the steep thermal gradients induced during the startup transient. These transient stresses and strains are also the most difficult to predict, in part because the temperature gradients and distributions are not well known or readily predictable and, in part, because the cyclic elastic-viscoplastic behavior of the materials at these extremes of temperature and strain are not well known or readily predictable. A broad spectrum of structures related technology programs is underway to address these deficiencies at the basic as well as the applied level. The three key program elements in the HOST structural analysis program are computations, constitutive modeling, and experiments for each research activity. Also shown are tables summarizing each of the activities. E.R.

N89-12882*# National Aeronautics and Space Administration. Lewis Research Center, Cleveland, Ohio.

FATIGUE AND FRACTURE OVERVIEW

Gary R. Halford *In its* Turbine Engine Hot Section Technology 1986 Oct. 1986 p 33-43 (For primary document see N89-12876 04-39)

Avail: NTIS HC A21/MF A01 CSCL 20K

The accomplishments achieved under the isotropic creep-fatigue crack initiation life prediction program are summarized. A sizeable creep-fatigue crack initiation data base was generated on the nickel-base superalloy, B-1900. Companion constitutive modeling programs have also generated extensive data bases on the same heat of material. The crack initiation results have formed the basis of a new approach to creep-fatigue life prediction. The term Cyclic Damage Accumulation (CDA) was coined for the method, which was evaluated under isothermal, uniaxial conditions. Stringent laboratory verification experiments were used to test the accuracy of the method. Considering the quite limited material property data needed to evaluate the constants in the approach, the prediction accuracy is acceptable. At the expense of the larger data base required, Lewis developed total strain- strainrange partitioning method (TS-SRP) is capable of a higher degree of accuracy. E.R.

N89-12883*# National Aeronautics and Space Administration. Lewis Research Center, Cleveland, Ohio.

HOST SURFACE PROTECTION R AND T OVERVIEW **c27**

Robert A. Miller *In its* Turbine Engine Hot Section Technology 1986 Oct. 1986 p 45-50 (For primary document see N89-12876 04-39)

Avail: NTIS HC A21/MF A01 CSCL 11C

Most of the efforts in the HOST Surface Protection Subproject were focused on thermal barrier coating (TBC) life prediction. Also, a small effort, consisting primarily of wrapping up and reporting the work of previous years, remained on the airfoil deposition modeling. The work performed under the airfoil deposition modeling program element was concerned with modeling the deposition of corrodants onto turbine airfoils. Accomplishments included verification of the chemically frozen boundary (CFBL) theory. Encouraging results were also achieved with the recently developed local thermochemical equilibrium (LTCE) theory. The surface protection subprogram was devoted to thermal-barrier-coating life modeling. This modeling is an essential step in the development of TBC's. E.R.

N89-12884*# Pratt and Whitney Aircraft, East Hartford, Conn. Engineering Div.

FURTHER DEVELOPMENT OF THE DYNAMIC GAS TEMPERATURE MEASUREMENT SYSTEM **c35**

D. L. Elmore, W. W. Robinson, and W. B. Watkins *In* NASA, Lewis Research Center, Turbine Engine Hot Section Technology 1986 Oct. 1986 p 51-60 (For primary document see N89-12876 04-39)

(Contract NAS3-24228)

Avail: NTIS HC A21/MF A01 CSCL 14B

The objective of this effort was to experimentally verify a dynamic gas temperature measurement system in laboratory experiments. The dynamic gas temperature measurement system verification program is described. A brief description of the sensor geometry and construction is followed by a discussion of the probe heat transfer analysis and subsequent compensation method. The laboratory experiments are described and experimental results are discussed. Finally, directions for further investigation are given. E.R.

N89-12885*# National Aeronautics and Space Administration. Lewis Research Center, Cleveland, Ohio.

LASER ANEMOMETRY: A STATUS REPORT **c36**

Mark P. Wernet, Richard G. Seasholtz, Donald H. Weikle, and Lawrence G. Oberle *In its* Turbine Engine Hot Section Technology 1986 Oct. 1986 p 61-68 (For primary document see N89-12876 04-39)

Avail: NTIS HC A21/MF A01 CSCL 20E

A laser anemometer system is being developed for the warm turbine facility as part of the HOST program. The system will be built using results obtained from the analytical and experimental research program. The status report of the laser anemometry applications research effort is presented. The designs for the turbine casing, the windows, and the positioning system were completed. A block diagram of the laser anemometer system, signal processing scheme, and computer system is given. Author

N89-12886*# Northwestern Univ., Evanston, Ill.

ELEVATED TEMPERATURE STRAIN GAGES **c35**

J. O. Brittain, D. Geslin, and J. F. Lei *In* NASA, Lewis Research Center, Turbine Engine Hot Section Technology 1986 Oct. 1986 p 69-84 (For primary document see N89-12876 04-39)

(Grant NAG3-501)

Avail: NTIS HC A21/MF A01 CSCL 14B

One of the goals of the HOST Program is the development of electrical resistance strain gages for static strain measurements at temperatures equal to or greater than 1273 K. Strain gage materials must have a reproducible or predictable response to temperature, time and strain. It is the objective of this research to investigate criteria for the selection of materials for such applications through electrical properties studies. The results of the investigation of two groups of materials, refractory compounds and binary alloy solid solutions are presented. Author

N89-12887*# National Aeronautics and Space Administration. Lewis Research Center, Cleveland, Ohio.
DEVELOPMENT OF A HIGH TEMPERATURE STATIC STRAIN SENSOR **c35**
Charles O. Hulse, Richard S. Bailey, and Howard P. Grant *In* NASA, Lewis Research Center, Turbine Engine Hot Section Technology 1986 Oct. 1986 p 85-90 (For primary document see N89-12876 04-39)
(Contract NAS3-23722)
Avail: NTIS HC A21/MF A01 CSCL 14B

The goal of this program is to develop an electrical resistance strain gage system which will accurately measure the static strains of superalloy blades and vanes in gas turbine engines running on a test stand. Accurate knowledge of these strains is essential to reaching the goals of the HOST program in the selection and experimental verification of the various theoretical models developed to understand and improve the performance of these engines. The specific objective is to develop a complete system capable of making strain measurements of up to + or - 10 percent of full scale during a 50 hour period at temperatures as high as 1250 K. In addition to survival and stability, attaining a low temperature coefficient of resistance, of the order of 20 ppm/K or less, was a major goal. This requirement arises from the presently unavoidable uncertainties in measurement of the exact temperatures inside gas turbines for use in making corrections for apparent strain due to temperature. Author

N89-12888*# National Aeronautics and Space Administration. Lewis Research Center, Cleveland, Ohio.
THE NASA LEWIS STRAIN GAUGE LABORATORY: AN UPDATE **c35**
H. F. Hobart *In its* Turbine Engine Hot Section Technology 1986 Oct. 1986 p 91-96 (For primary document see N89-12876 04-39)
Avail: NTIS HC A21/MF A01 CSCL 14B

Efforts continue in the development and evaluation of electrical resistance strain gauges of the thin film and small diameter wire type. Results obtained early in 1986 on some Chinese gauges and Kanthal A-1 gauges mounted on a Hastelloy-X substrate are presented. More recent efforts include: (1) the determination of the uncertainty in the ability to establish gauge factor, (2) the evaluation of sputtered gauges that were fabricated at Lewis, (3) an investigation of the efficacy of dual element temperature compensated gauges when using strain gauge alloys having large thermal coefficients of resistance, and (4) an evaluation of the practical methods of stabilizing gauges whose apparent strain is dependent on cooling rate (e.g., FeCrAl gauges). Author

N89-12889*# National Aeronautics and Space Administration. Lewis Research Center, Cleveland, Ohio.
SUMMARY OF LASER SPECKLE PHOTOGRAMMETRY FOR HOST **c36**
Frank G. Pollack *In its* Turbine Engine Hot Section Technology 1986 Oct. 1986 p 97-103 (For primary document see N89-12876 04-39)
Avail: NTIS HC A21/MF A01 CSCL 20E

High temperature static strain measurement capability is important for the success of the HOST program. As part of the NASA Lewis effort to develop the technology for improved hot-section durability, the HOST instrumentation program has, as a major goal, the development of methods for measuring strain at high temperature. Development work includes both improvements in resistance strain-gauge technology and, as an alternative approach, the development of optical techniques for high temperature strain measurement. Author

N89-12890*# General Motors Corp., Detroit, Mich. Gas Turbine Engine Div.
AEROTHERMAL MODELING PROGRAM, PHASE 2 **c34**
K. C. Karki, H. C. Mongia, Suhas V. Patankar, and A. K. Runchal *In* NASA, Lewis Research Center, Turbine Engine Hot Section Technology 1986 Oct. 1986 p 105-113 (For primary document see N89-12876 04-39)
(Contract NAS3-24350)
Avail: NTIS HC A21/MF A01 CSCL 20D

The main objective of the NASA sponsored Aerothermal Modeling Program, Phase 2--Element A, is to develop an improved numerical scheme for predicting combustor flow fields. This effort consists of the following three technical tasks. Task 1 involves the selection and evaluation of various candidate numerical techniques. Task 2 involves an in-depth evaluation of the selected numerical schemes. Task 3 involves the convection-diffusion scheme and the direct solver that will be incorporated in the NASA 3-D elliptic code (COM3S). E.R.

N89-12891*# General Motors Corp., Detroit, Mich. Gas Turbine Engine Div.
AEROTHERMAL MODELING PROGRAM, PHASE 2. ELEMENT B: FLOW INTERACTION EXPERIMENT **c34**
M. Nikjooy, H. C. Mongia, S. N. B. Murthy, and J. P. Sullivan *In* NASA, Lewis Research Center, Turbine Engine Hot Section Technology 1986 Oct. 1986 p 115-124 (For primary document see N89-12876 04-39)
(Contract NAS3-24350)
Avail: NTIS HC A21/MF A01 CSCL 20D

The design process was improved and the efficiency, life, and maintenance costs of the turbine engine hot section was enhanced. Recently, there has been much emphasis on the need for improved numerical codes for the design of efficient combustors. For the development of improved computational codes, there is a need for an experimentally obtained data base to be used at test cases for the accuracy of the computations. The purpose of Element-B is to establish a benchmark quality velocity and scalar measurements of the flow interaction of circular jets with swirling flow typical of that in the dome region of annular combustor. In addition to the detailed experimental effort, extensive computations of the swirling flows are to be compared with the measurements for the purpose of assessing the accuracy of current and advanced turbulence and scalar transport models. Author

N89-12892*# General Motors Corp., Detroit, Mich. Gas Turbine Engine Div.
AEROTHERMAL MODELING PROGRAM, PHASE 2. ELEMENT C: FUEL INJECTOR-AIR SWIRL CHARACTERIZATION **c34**
A. A. Mostafa, H. C. Mongia, V. G. McDonnell, and G. S. Samuelsen *In* NASA, Lewis Research Center, Turbine Engine Hot Section Technology 1986 Oct. 1986 p 125-131 (For primary document see N89-12876 04-39)
(Contract NAS3-24350)
Avail: NTIS HC A21/MF A01 CSCL 20D

The main objectives of the NASA-sponsored Aerothermal Modeling Program, Phase 2--Element C, are experimental evaluation of the air swirler interaction with a fuel injector in a simulated combustor chamber, assessment of the current two-phase models, and verification of the improved spray evaporation/dispersion models. This experimental and numerical program consists of five major tasks. Brief descriptions of the five tasks are given. Author

N89-12893*# Garrett Turbine Engine Co., Phoenix, Ariz.
COMBUSTOR DIFFUSER INTERACTION PROGRAM **c07**
Ram Srinivasan and Daniel Thorp *In* NASA, Lewis Research Center, Turbine Engine Hot Section Technology 1986 Oct. 1986 p 133-139 (For primary document see N89-12876 04-39)
(Contract F33615-84-C-2427)
Avail: NTIS HC A21/MF A01 CSCL 21E

Advances in gas turbine engine performance are achieved by using compressor systems with high stage loading and low part count, which result in high exit Mach numbers. The diffuser and combustor systems in such engines should be optimized to reduce system pressure loss and to maximize the engine thrust-to-weight ratio and minimize length. The state-of-the-art combustor-diffuser systems do not meet these requirements. Detailed understanding of the combustor-diffuser flow field interaction is required for designing advanced gas turbine engines. An experimental study

of the combustor-diffuser interaction (CDI) is being conducted to obtain data for the evaluation and improvement of analytical models applicable to a wide variety of diffuser designs. The CDI program consists of four technical phases: Literature Search; Baseline Configuration; Parametric Configurations; and Performance Configurations. Phase 2 of the program is in progress. Author

N89-12894*# Minnesota Univ., Minneapolis. Dept. of Mechanical Engineering.

EFFICIENT NUMERICAL TECHNIQUES FOR COMPLEX FLUID FLOWS **c34**

Suhas V. Patankar *In* NASA, Lewis Research Center, Turbine Engine Hot Section Technology 1986 Oct. 1986 p 141-143 (For primary document see N89-12876 04-39)

(Grant NAG3-596)

Avail: NTIS HC A21/MF A01 CSCL 20D

The central feature in any flow prediction method is the treatment of the coupling between the momentum and continuity equations. In natural-convection flows, the energy equation also becomes strongly coupled with the momentum equations. Because of the nonlinear nature of the coupling, these equations are solved iteratively. Iterative methods are often prone to slow convergence, divergence, and extreme sensitivity to underrelaxation factors. The aim of the present research is to develop more efficient and reliable solution schemes for the coupled flow equations. Such schemes will significantly reduce the expense of computing complex flows encountered in combustion chambers, gas turbines, heat exchangers, and other practical equipment. In the work completed so far, a technique employing norm reduction in conjunctine with the successive-substitution and Newton-Raphson techniques was developed. Also, a block-correction procedure for the flow equations is currently being formulated and tested. Author

N89-12895*# Avco-Everett Research Lab., Mass.

IMPROVED NUMERICAL METHODS FOR TURBULENT VISCOUS RECIRCULATING FLOWS **c34**

J. P. VanDoormaal, A. Turan, and G. D. Raithby *In* NASA, Lewis Research Center, Turbine Engine Hot Section Technology 1986 Oct. 1986 p 145-150 (For primary document see N89-12876 04-39)

(Contract NAS3-24351)

Avail: NTIS HC A21/MF A01 CSCL 20D

The objective of the present study is to improve both the accuracy and computational efficiency of existing numerical techniques used to predict viscous recirculating flows in combustors. A review of the status of the study is presented along with some illustrative results. The effort to improve the numerical techniques consists of the following technical tasks: (1) selection of numerical techniques to be evaluated; (2) two dimensional evaluation of selected techniques; and (3) three dimensional evaluation of technique(s) recommended in Task 2. Author

N89-12896*# Tennessee Univ. Space Inst., Tullahoma.

INFLUENCE OF BULK TURBULENCE AND ENTRANCE BOUNDARY LAYER THICKNESS ON THE CURVED DUCT FLOW FIELD **c34**

Roger A. Crawford and Carroll E. Peters *In* NASA, Lewis Research Center, Turbine Engine Hot Section Technology 1986 Oct. 1986 p 151-157 (For primary document see N89-12876 04-39)

(Grant NAG3-617)

Avail: NTIS HC A21/MF A01 CSCL 20D

The objective of this investigation was the experimental evaluation of bulk turbulence and boundary thickness influence on the secondary flow development in a square, 90 deg turning duct. A three dimensional laser velocimetry system was utilized to measure the mean and fluctuating components of velocity in the large curved duct facility. The three dimensional development of the viscous shear layers in the curved duct has a strong influence on the complete flow field. Since ducted three dimensional flows are found in many engineering applications, including gas turbine engines, and contain high turbulence levels and high wall heat transfer rates, they present a difficult challenge to computational fluid mechanics codes. Turbulence modeling remains one of constraints to CFD advance due to inadequate physical understanding and experimental definition of turbulent shear flows. The results of this investigation expand the curved duct data base to higher turbulence levels and thicker entrance boundary layers. The experimental results provide a challenging benchmark data base for computational fluid dynamics code development and validation. The variation of inlet bulk turbulence intensity provides additional information to aid in turbulence model evaluation. Author

N89-12897*# United Technologies Research Center, East Hartford, Conn.

MEASUREMENT OF AIRFOIL HEAT TRANSFER COEFFICIENTS ON A TURBINE STAGE **c34**

Robert P. Dring, Michael F. Blair, and H. David Joslyn *In* NASA, Lewis Research Center, Trubine Engine Hot Section Technology 1986 Oct. 1986 p 159-176 (For primary document see N89-12876 04-39)

(Contract NAS3-2317)

Avail: NTIS HC A21/MF A01 CSCL 20D

The Primary basis for heat transfer analysis of turbine airfoils is experimental data obtained in linear cascades. These data were very valuable in identifying the major heat transfer and fluid flow features of a turbine airfoil. The first program objective is to obtain a detailed set of heat transfer coefficients along the midspan of a stator and a rotor in a rotating turbine stage. The data are to be compared to some standard analysis of blade boundary layer heat transfer which is in use today. A second program objective is to obtain a detailed set of heat transfer coefficients along the midspan of a stator located in the wake of an upstream turbine stage. E.R.

N89-12898*# Arizona State Univ., Tempe. Dept. of Mechanical and Aerospace Engineering.

HEAT TRANSFER IN THE TIP REGION OF A ROTOR BLADE SIMULATOR **c34**

M. K. Chyu, H. K. Moon, and D. E. Metzger *In* NASA, Lewis Research Center, Turbine Engine Hot Section Technology 1986 Oct. 1986 p 177-192 (For primary document see N89-12876 04-39)

(Grant NAG3-623)

Avail: NTIS HC A21/MF A01 CSCL 20D

In gas turbines, the blades of axial turbine stages rotate in close proximity to a stationary peripheral wall. Differential expansion of the turbine wheel, blades, and the shroud causes variations in the size of the clearance gap between blade tip and stationary shroud. The necessity to tolerate this differential thermal expansion dictates that the clearance gap cannot be eliminated altogether, despite accurate engine machining. Pressure differences between the pressure and suction sides of a blade drives a flow through the clearance gap. This flow, the tip leakage flow, is detrimental to engine performance. The primary detrimental effect of tip leakage flow is the reduction of turbine stage efficiency, and a second is the convective heat transfer associated with the flow. The surface area at the blade tip in contact with the hot working gas represents an additional thermal loading on the blade which, together with heat transfer to the suction and pressure side surface area, must be removed by the blade internal cooling flows. Experimental results concerned with the local heat transfer characteristics on all surfaces of shrouded, rectangular cavities are reported. A brief discussion of the mass transfer system used is given. Author

N89-12899*# Pratt and Whitney Aircraft, East Hartford, Conn.

COOLANT PASSAGE HEAT TRANSFER WITH ROTATION **c34**

T. J. Hajek, J. Wagner, and B. V. Johnson *In* NASA, Lewis Research Center, Turbine Engine Hot Section Technology 1986 Oct. 1986 p 193-206 (For primary document see N89-12876 04-39)

(Contract NAS3-23691)

Avail: NTIS HC A21/MF A01 CSCL 20D

In current and advanced gas turbine engines, increased speeds,

pressures and temperatures are used to reduce specific fuel consumption and increase thrust/weight ratios. Hence, the turbine airfoils are subjected to increased heat loads escalating the cooling requirements to satisfy life goals. The efficient use of cooling air requires that the details of local geometry and flow conditions be adequately modeled to predict local heat loads and the corresponding heat transfer coefficients. The objective of this program is to develop a heat transfer and pressure drop data base, computational fluid dynamic techniques and correlations for multi-pass rotating coolant passages with and without flow turbulators. The experimental effort is focused on the simulation of configurations and conditions expected in the blades of advanced aircraft high pressure turbines. With the use of this data base, the effects of Coriolis and buoyancy forces on the coolant side flow can be included in the design of turbine blades. Author

N89-12900*# Stanford Univ., Calif. Dept. of Mechanical Engineering.

HEAT TRANSFER WITH VERY HIGH FREE-STREAM TURBULENCE AND STREAMWISE VORTICES **c34**

Robert J. Moffat, Paul Maciejewski, John K. Eaton, and Wayne Pauley *In* NASA, Lewis Research Center, Trubine Engine Hot Section Technology 1986 Oct. 1986 p 207-217 (For primary document see N89-12876 04-39)

(Grant NAG3-522)

Avail: NTIS HC A21/MF A01 CSCL 20D

Results are presented for two experimental programs related to augmentation of heat transfer by complex flow characteristics. In one program, high free stream turbulence (up to 63 percent) was shown to increase the Stanton number by more than a factor of 5, compared with the normally expected value based on x-Reynolds number. These experiments are being conducted in a free-jet facility, near the margins of the jet. To a limited extent, the mean velocity, turbulence intensity, and integral length scale can be separately varied. The results show that scale is a very important factor in determining the augmentation. Detailed studies of the turbulence structure are being carried out using an orthogonal triple hot-wire anemometer equipped with a fourth wire for measuring temperature. The v' component of turbulence appears to be distributed differently from u' or w'. In the second program, the velocity distributions and boundary layer thicknesses associated with a pair of counter-rotating, streamwise vortices were measured. There is a region of considerably thinned boundary layer between the two vortices when they are of approximately the same strength. If one vortex is much stronger than the other, the weaker vortex may be lifted off the surface and absorbed into the stronger. Author

N89-12901*# Minnesota Univ., Minneapolis. Dept. of Mechanical Engineering.

DEVELOPMENT OF LOW REYNOLDS NUMBER TWO EQUATION TURBULENCE MODELS FOR PREDICTING EXTERNAL HEAT TRANSFER ON TURBINE BLADES **c34**

Suhas V. Patankar and Rodney C. Schmidt *In* NASA, Lewis Research Center, Turbine Engine Hot Section Technology 1986 Oct. 1986 p 219-232 (For primary document see N89-12876 04-39)

(Grant NAG3-579)

Avail: NTIS HC A21/MF A01 CSCL 20D

A research effort was underway to study the use of two equation low Reynolds number turbulence models in predicting gas side heat transfer on turbine blades. The major objectives of this work are basicly threefold: study the predictive capabilities of two equation low Reynolds number turbulence models under the conditions characteristic of modern gas turbine blades; explore potential improvements to the models themselves as well as to the specification of initial conditions; and provide a comparison of the predictions of these models with the experimental data from a broad range of recently available turbine cascade experiments. The problems associated with predicting the boundary layer transition from laminar to turbulent flow are emphasized, as this may be the most serious deficiency of current modeling techniques. The results and conclusions of the first two phases are briefly described. Author

N89-12902*# National Aeronautics and Space Administration. Lewis Research Center, Cleveland, Ohio.

TURBINE STATOR FLOW FIELD SIMULATIONS **c34**

R. C. Buggeln, W. R. Briley, S. J. Shamroth, and H. McDonald *In* NASA, Lewis Research Center, Trubine Engine Hot Section Technology 1986 Oct. 1986 p 233-235 (For primary document see N89-12876 04-39)

(Contract NAS3-24358)

Avail: NTIS HC A21/MF A01 CSCL 20D

The increased capability and accessibility of modern computers, coupled with increasingly sophisticated and accurate numerical and physical modeling, has led to a marked impact of numerical simulations upon current turbine design and research problems. The turbine section represents a considerable challenge as it contains significant regions of complex three-dimensional flow, including both aerodynamic and heat transfer phenomena. The focus of the present effort is the development of an efficient and accurate three-dimensional Navier-Stokes calculation procedure for application to the turbine stator and rotor problems. In particular, an effective procedure is sought which: (1) adequately represents the flow physics, (2) allows for sufficient resolution in regions of small length scale, and (3) has sufficiently good convergence properties so as to allow use on a regular basis. Author

N89-12903*# General Motors Corp., Detroit, Mich. Gas Turbine Div.

TURBINE AIRFOIL FILM COOLING **c34**

Larry D. Hylton *In* NASA, Lewis Research Center, Turbine Engine Hot Section Technology 1986 Oct. 1986 p 237-241 (For primary document see N89-12876 04-39)

(Contract NAS3-24619)

Avail: NTIS HC A21/MF A01 CSCL 20D

Emphasis is placed on developing more accurate analytical models for predicting turbine airfoil external heat transfer rates. Performance goals of new engines require highly refined, accurate design tools to meet durability requirements. In order to obtain improvements in analytical capabilities, programs are required which focus on enhancing analytical techniques through verification of new models by comparison with relevant experimental data. The objectives of the current program are to develop an analytical approach, based on boundary layer theory, for predicting the effects of airfoil film cooling on downstream heat transfer rates and to verify the resulting analytical method by comparison of predictions with hot cascade data obtained under this program. Author

N89-12904*# Southwest Research Inst., San Antonio, Tex.

CONSTITUTIVE MODELING FOR ISOTROPIC MATERIALS

Ulric S. Lindholm and Kwai S. Chan *In* NASA, Lewis Research Center, Turbine Engine Hot Section Technology 1986 Oct. 1986 p 243-253 (For primary document see N89-12876 04-39)

(Contract NAS3-23925)

Avail: NTIS HC A21/MF A01 CSCL 20K

The objective of the program is to evaluate and develop existing constitutive models for use in finite-element structural analysis of turbine engine hot section components. The class of constitutive equation studied is considered unified in that all inelastic deformation including plasticity, creep, and stress relaxation are treated in a single term rather than a classical separation of plasticity (time independent) and creep (time dependent) behavior. The unified theories employed also do not utilize the classical yield surface or plastic potential concept. The models are constructed from an appropriate flow law, a scalar kinetic relation between strain rate, temperature and stress, and evolutionary equations for internal variables describing strain or work hardening, both isotropic and directional (kinematic). This and other studies have shown that the unified approach is particularly suited for determining the cyclic behavior of superalloy type blade and vane materials and is entirely compatible with three-dimensional inelastic finite-element formulations. The behavior was examined of a second nickel-base alloy, MAR-M247, and compared it with the

Bodner-Partom model, further examined procedures for determining the material-specific constants in the models, and exercised the MARC code for a turbine blade under simulated flight spectrum loading. Results are summarized. Author

N89-12905*# Pratt and Whitney Aircraft, East Hartford, Conn.
ON 3-D INELASTIC ANALYSIS METHODS FOR HOT SECTION COMPONENTS
E. S. Todd *In* NASA, Lewis Research Center, Turbine Engine Hot Section Technology 1986 Oct. 1986 p 255-256 (For primary document see N89-12876 04-39)
Avail: NTIS HC A21/MF A01 CSCL 20K

The objective of this program is to produce a series of new computer codes that permit more accurate and efficient three-dimensional inelastic structural analysis of combustor liners, turbine blades, and turbine vanes. Each code embodies a progression of mathematical models for increasingly comprehensive representation of the geometrical features, loading conditions, and forms of nonlinear material response that distinguish these three groups of hot section components. Author

N89-12906*# General Electric Co., Fairfield, Conn.
ON 3D INELASTIC ANALYSIS METHODS FOR HOT SECTION COMPONENTS
R. L. McKnight, P. C. Chen, L. T. Dame, R. V. Holt, H. Huang, M. Hartle, S. Gellin, D. H. Allen, and W. E. Haisler *In* NASA, Lewis Research Center, Turbine Engine Hot Section Technology 1986 Oct. 1986 p 257-268 (For primary document see N89-12876 04-39)
(Contract NAS3-23698)
Avail: NTIS HC A21/MF A01 CSCL 20K

Accomplishments are described for the 2-year program, to develop advanced 3-D inelastic structural stress analysis methods and solution strategies for more accurate and cost effective analysis of combustors, turbine blades and vanes. The approach was to develop a matrix of formulation elements and constitutive models. Three constitutive models were developed in conjunction with optimized iterating techniques, accelerators, and convergence criteria within a framework of dynamic time incrementing. Three formulations models were developed; an eight-noded mid-surface shell element, a nine-noded mid-surface shell element and a twenty-noded isoparametric solid element. A separate computer program was developed for each combination of constitutive model-formulation model. Each program provides a functional stand alone capability for performing cyclic nonlinear structural analysis. In addition, the analysis capabilities incorporated into each program can be abstracted in subroutine form for incorporation into other codes or to form new combinations. Author

N89-12907*# General Electric Co., Fairfield, Conn.
COMPONENT SPECIFIC MODELING **c07**
R. J. Maffeo, R. L. McKnight, M. T. Tipton, and G. Weber *In* NASA, Lewis Research Center, Turbine Engine Hot Section Technology 1986 Oct. 1986 p 269-282 (For primary document see N89-12876 04-39)
(Contract NAS3-23687)
Avail: NTIS HC A21/MF A01 CSCL 21E

The overall objective of this program is to develop and verify a series of interdisciplinary modeling and analysis techniques that were specialized to address three specific hot section components. These techniques incorporate data as well as theoretical methods from many diverse areas including cycle and performance analysis, heat transfer analysis, linear and nonlinear stress analysis, and mission analysis. Building on the proven techniques already available in these fields, the new methods developed are integrated to provide an accurate, efficient, and unified approach to analyzing combustor burner liners, hollow air-cooled turbine blades, and air-cooled turbine vanes. For these components, the methods developed predict temperature, deformation, stress, and strain histories throughout a complete flight mission. Author

N89-12908*# Akron Univ., Ohio.
A MULTIAXIAL THEORY OF VISCOPLASTICITY FOR ISOTROPIC MATERIALS
D. N. Robinson and J. R. Ellis *In* NASA, Lewis Research Center, Turbine Engine Hot Section Technology 1986 Oct. 1986 p 283-291 (For primary document see N89-12876 04-39)
(Grant NAG3-379)
Avail: NTIS HC A21/MF A01 CSCL 20K

Many viscoplastic constitutive models for high temperature structural alloys are based exclusively on uniaxial test data. Generalization to multiaxial states of stress is made by assuming the stress dependence to be on the second principal invariant (J sub 2) of the deviatoric stress, frequently called the effective stress. If such a J sub 2 theory, based on uniaxial testing, is called upon to predict behavior under conditions other than uniaxial, e.g., pure shear, and it does so poorly, nothing is left to adjust in the theory. For a fully isotropic material whose inelastic deformation behavior is relatively independent of hydrostatic stress, the most general stress dependence is on the two (non-zero) principal invariants of the deviatoric stress, J sub 2 and J sub 3. These invariants constitute what is known as an integrity basis for the material. A time dependent constitutive theory with stress dependence on J sub 2 and J sub 3 is presented, that reduces to a known J sub 2 theory as a special case. Author

N89-12909*# National Aeronautics and Space Administration. Lewis Research Center, Cleveland, Ohio.
THERMOMECHANICAL CHARACTERIZATION OF HASTELLOY-X UNDER UNIAXIAL CYCLIC LOADING
J. R. Ellis, P. A. Bartolotta, G. P. Allen, and D. N. Robinson (Akron Univ., Ohio.) *In its* Turbine Engine Hot Section Technology 1986 Oct. 1986 p 293-305 (For primary document see N89-12876 04-39)
Avail: NTIS HC A21/MF A01 CSCL 20K

In most high-temperature engineering applications, components are subjected to complex combinations of thermal and mechanical loading during service. A number of viscoplastic constitutive models were proposed which potentially can provide mathematical descriptions of material response under such conditions. Implementation of these models into large finite element codes such as MARC has already resulted in much improved inelastic analysis capability for hot-section aircraft engine components. However, a number of questions remain regarding the validity of methods adopted in characterizing these constitutive models for particular high-temperature materials. One area of concern is that the majority of experimental data available for this purpose are determined under isothermal conditions. This is in contrast to service conditions which, as noted above, almost always involve some form of thermal cycling. The obvious question arises as to whether a constitutive model characterized using an isothermal data base can adequately predict material response under thermomechanical conditions. An experimental program was initiated within the HOST program to address this particular concern. The results of the most recent isothermal and thermomechanical experiments are described. Author

N89-12910*# Oak Ridge National Lab., Tenn.
DETERMINATION OF SURFACES OF CONSTANT INELASTIC STRAIN RATE AT ELEVATED TEMPERATURE
R. L. Battiste and S. J. Ball *In* NASA, Lewis Research Center, Turbine Engine Hot Section Technology 1986 Oct. 1986 p 307-325 (For primary document see N89-12876 04-39)
(Contract DE-AC05-84OR-21400)
Avail: NTIS HC A21/MF A01 CSCL 20K

An experimental effort to perform special exploratory multiaxial deformation tests on tubular specimens of type 316 stainless steel at 650 C (1200 F) is described. One test specimen was subjected to a time-independent torsional shear strain test history, and surfaces of constant inelastic strain rate (SCISRs) in an axial/torsional stress space were measured at various predetermined points during the test. A second specimen was subjected to a 14-week time-dependent (creep-recovery-creep periods) torsional shear stress histogram SCISRs determinations

made at 17 points during the test. The tests were conducted in a high temperature, computer controlled axial/torsional test facility using high-temperature multiaxial extensometer. The effort was successful, and for the first time the existence of surfaces of constant inelastic strain rate was experimentally demonstrated.
Author

N89-12911*# Cincinnati Univ., Ohio.
CONSTITUTIVE MODELING FOR SINGLE CRYSTAL SUPERALLOYS **c26**
D. C. Stouffer, N. Jayaraman, M. Sheh, and D. Alden *In* NASA, Lewis Research Center, Turbine Engine Hot Section Technology 1986 Oct. 1986 p 327-334 (For primary document see N89-12876 04-39)
(Grant NAG3-511)
Avail: NTIS HC A21/MF A01 CSCL 11F

The inelastic response of single crystal gamma/gamma prime superalloys is quite different from the behavior of polycrystalline nickel base superalloys. Upto a critical temperature the yield stress of single crystal alloys is a function of the material orientation relative to the direction of the applied stress and the material exhibits significant tension/compression asymmetry. This behavior is primarily due to slip on the octahedral slip system. Above the critical temperature there is a sharp drop in the yield stress, cube slip becomes more predominant and the tension/compression asymmetry is reduced. Similar orientation and tension/compression asymmetry is observed in creep and secondary creep above the critical temperature is inferred to occur by octahedral slip. There are two exceptions to this behavior. First, loading near the (111) orientation exhibits cube slip at all temperatures, and; second, loading near the (001) orientation produces only octahedral slip at all temperatures. The constitutive model is based on separating the total global strain into elastic and inelastic components. This model is developed and briefly discussed. Author

N89-12912*# Connecticut Univ., Storrs.
CONSTITUTIVE MODELLING OF SINGLE CRYSTAL AND DIRECTIONALLY SOLIDIFIED SUPERALLOYS Progress Report **c26**
E. H. Jordan and K. P. Walker (Engineering Science Software, Inc., Smithfield, R.I.) *In* NASA, Lewis Research Center, Turbine Engine Hot Section Technology 1986 Oct. 1986 p 335-339 (For primary document see N89-12876 04-39)
(Grant NAG3-512)
Avail: NTIS HC A21/MF A01 CSCL 11F

The trend towards improved engine efficiency and durability places increasing demands on materials that operate in the hot section of the gas turbine engine. These demands are being met by new coatings and materials such as single crystal and directionally solidified nickel-base superalloys which have greater creep/fatigue resistance at elevated temperatures and reduced susceptibility to grain boundary creep, corrosion and oxidation than conventionally cast alloys. Work carried out as part of a research program aimed at the development of constitutive equations to describe the elevated temperature stress-strain-time behavior of single crystal and directionally solidified turbine blade superalloys is discussed. The program involves both development of suitable constitutive models and their verification through elevated temperature tension-torsion testing of single crystals of PWA 1480. Author

N89-12913*# National Aeronautics and Space Administration. Lewis Research Center, Cleveland, Ohio.
HIGH TEMPERATURE STRESS-STRAIN ANALYSIS
Robert L. Thompson and Paul E. Moorhead *In its* Turbine Engine Hot Section Technology 1986 Oct. 1986 p 341-357 (For primary document see N89-12876 04-39)
Avail: NTIS HC A21/MF A01 CSCL 20K

The objectives of the high-temperature structures program are threefold: to assist in the development of analytical tools needed to improve design analyses and procedures for the efficient and accurate prediction of the nonlinear structural response of hot-section components; to aid in the calibration, validation, and evaluation of the analytical tools by comparing predictions with experimental data; and to evaluate existing as well as advanced temperature and strain measurement instrumentation. As the analytical tools, test methods, tests, instrumentations, as well as data acquisition, management, and analysis methods are developed and evaluated, a proven, integrated analysis and experiment method will result in a more accurate prediction of the cyclic life of hot section components. Author

N89-12914*# Pratt and Whitney Aircraft, East Hartford, Conn.
CREEP FATIGUE LIFE PREDICTION FOR ENGINE HOT SECTION MATERIALS (ISOTROPIC): FOURTH YEAR PROGRESS REVIEW **c38**
Richard S. Nelson and John F. Schoendorf *In* NASA, Lewis Research Center, Turbine Engine Hot Section Technology 1986 Oct. 1986 p 359-370 (For primary document see N89-12876 04-39)
(Contract NAS3-23288)
Avail: NTIS HC A21/MF A01 CSCL 14D

As gas turbine technology continues to advance, the need for advanced life prediction methods for hot section components is becoming more and more evident. The complex local strain and temperature histories at critical locations must be accurately interpreted to account for the effects of various damage mechanisms (such as fatigue, creep, and oxidation) and their possible interactions. As part of the overall NASA HOST effort, this program is designed to investigate these fundamental damage processes, identify modeling strategies, and develop practical models which can be used to guide the early design and development of new engines and to increase the durability of existing engines. Author

N89-12915*# General Electric Co., Fairfield, Conn.
ELEVATED TEMPERATURE CRACK GROWTH
S. N. Malik, R. H. VanStone, K. S. Kim, and J. H. Laflen *In* NASA, Lewis Research Center, Turbine Engine Hot Section Technology 1986 Oct. 1986 p 371-383 (For primary document see N89-12876 04-39)
(Contract NAS3-23940)
Avail: NTIS HC A21/MF A01 CSCL 20K

It is necessary to relate the processes that control crack growth in the immediate vicinity of the crack tip to parameters that can be calculated from remote quantities, such as forces, stresses, or displacements. The most likely parameters appear to be certain path-independent (PI) integrals, several of which have already been proposed for application to high temperature inelastic problems. The ability of currently available PI-integrals to correlate fatigue crack propagation under conditions that simulate the engine combustor liner environment was determined. The utility of advanced fracture mechanics measurements will also be evaluated and determined during the course of the program. E.R.

N89-12916*# Pratt and Whitney Aircraft, East Hartford, Conn.
LIFE PREDICTION AND CONSTITUTIVE MODELS FOR ENGINE HOT SECTION **c38**
G. A. Swanson, T. G. Meyer, and D. M. Nissley *In* NASA, Lewis Research Center, Turbine Engine Hot Section Technology 1986 Oct. 1986 p 385-397 (For primary document see N89-12876 04-39)
(Contract NAS3-23939)
Avail: NTIS HC A21/MF A01 CSCL 14D

The purpose of this program is to develop life prediction models for coated anisotropic materials used in gas turbine airfoils. In the program, two single crystal alloys and two coatings are being tested. These include PWA 1480, Alloy 185, overlay coating (PWA 286), and aluminide coating (PWA 273). Constitutive models are also being developed for these materials to predict the time independent (plastic) and time dependent (creep) strain histories of the materials in the lab tests and for actual design conditions. This nonlinear material behavior is particularly important for high temperature gas turbine applications and is basic to any life prediction system. Some of the accomplishments of the program are highlighted. Author

N89-12917*# National Aeronautics and Space Administration. Lewis Research Center, Cleveland, Ohio.
AUTOMATION SOFTWARE FOR A MATERIALS TESTING LABORATORY **c61**
Michael A. McGaw and Peter J. Bonacuse *In its* Turbine Engine Hot Section Technology 1986 Oct. 1986 p 399-406 (For primary document see N89-12876 04-39)
Avail: NTIS HC A21/MF A01 CSCL 09B

A comprehensive software system for automating much of the experimental process has recently been completed at the Lewis Research Center's high-temperature fatigue and structures laboratory. The system was designed to support experiment definition and conduct, results analysis and archiving, and report generation activities. This was accomplished through the design and construction of several software systems, as well as through the use of several commercially available software products, all operating on a local, distributed minicomputer system. Experimental capabilities currently supported in an automated fashion include both isothermal and thermomechanical fatigue and deformation testing capabilities. The future growth and expansion of this system will be directed toward providing multiaxial test control, enhanced thermomechanical test control, and higher test frequency (hundreds of hertz). Author

N89-12918*# Syracuse Univ., N. Y. Dept. of Mechanical and Aerospace Engineering.
GRAIN BOUNDARY OXIDATION AND ITS EFFECTS ON HIGH TEMPERATURE FATIGUE LIFE **c26**
H. W. Liu and Yoshiki Oshida *In* NASA, Lewis Research Center, Turbine Engine Hot Section Technology 1986 Oct. 1986 p 407-414 (For primary document see N89-12876 04-39)
(Grant NAG3-348)
Avail: NTIS HC A21/MF A01 CSCL 11F

Fatigue lives at elevated temperatures are often shortened by creep and/or oxidation. Creep causes grain boundary void nucleation and grain boundary cavitation. Grain boundary voids and cavities will accelerate fatigue crack nucleation and propagation, and thereby shorten fatigue life. The functional relationships between the damage rate of fatigue crack nucleation and propagation and the kinetic process of oxygen diffusion depend on the detailed physical processes. The kinetics of grain boundary oxidation penetration was investigated. The statistical distribution of grain boundary penetration depth was analyzed. Its effect on high temperature fatigue life are discussed. A model of intermittent micro-ruptures of grain boundary oxide was proposed for high temperature fatigue crack growth. The details of these studies are reported. Author

N89-12919*# National Aeronautics and Space Administration. Lewis Research Center, Cleveland, Ohio.
A STUDY ON THERMAL BARRIER COATINGS INCLUDING THERMAL EXPANSION MISMATCH AND BOND COAT OXIDATION **c27**
George C. Chang, Woraphat Phucharoen (Cleveland State Univ., Ohio.), and Robert A. Miller *In its* Turbine Engine Hot Section Technology 1986 Oct. 1986 p 415-434 (For primary document see N89-12876 04-39)
(Contract NCC3-27)
Avail: NTIS HC A21/MF A01 CSCL 11C

The present investigation deals with a plasma-sprayed thermal barrier coating (TBC) intended for high temperature applications to advanced gas turbine blades. Typically, this type of coating system consists of a zirconia-yttria ceramic layer with a nickel-chromium-aluminum bond coat on a superalloy substrate. The problem on hand is a complex one due to the fact that bond coat oxidation and thermal mismatch occur in the TBC. Cracking in the TBC has also been experimentally illustrated. A clearer understanding of the mechanical behavior of the TBC is investigated. The stress states in a model thermal barrier coating as it cools down in air is studied. The powerful finite element method was utilized to model a coating cylindrical specimen. Four successively refined finite element models were developed. Some results obtained using the first two models have been reported previously. The major accomplishment is the successful development of an elastic TBC finite element model known as TBCG with interface geometry between the ceramic layer and the bond coat. An equally important milestone is the near-completion of the new elastic-plastic TBC finite element model called TBCGEP which yielded initial results. Representative results are presented. Author

N89-12920*# Garrett Turbine Engine Co., Phoenix, Ariz.
THERMAL BARRIER COATING LIFE PREDICTION MODEL DEVELOPMENT **c27**
T. E. Strangman, J. F. Neumann, and A. Liu *In* NASA, Lewis Research Center, Turbine Engine Hot Section Technology 1986 Oct. 1986 p 435-445 (For primary document see N89-12876 04-39)
(Contract NAS3-23945)
Avail: NTIS HC A21/MF A01 CSCL 11C

Thermal barrier coatings (TBCs) for turbine airfoils in high-performance engines represent an advanced materials technology with both performance and durability benefits. The foremost TBC benefit is the reduction of heat transferred into air-cooled components, which yields performance and durability benefits. This program focuses on predicting the lives of two types of strain-tolerant and oxidation-resistant TBC systems that are produced by commercial coating suppliers to the gas turbine industry. The plasma-sprayed TBC system, composed of a low-pressure plasma-spray (LPPS) or an argon shrouded plasma-spray (ASPS) applied oxidation resistant NiCrAlY (or CoNiCrAlY) bond coating and an air-plasma-sprayed yttria (8 percent) partially stabilized zirconia insulative layer, is applied by Chromalloy, Klock, and Union Carbide. The second type of TBC is applied by the electron beam-physical vapor deposition (EB-PVD) process by Temescal. Author

N89-12921*# General Electric Co., Fairfield, Conn. Aircraft Engine Business Group.
THERMAL BARRIER COATING LIFE PREDICTION MODEL **c27**
B. H. Pilsner, R. V. Hillery, R. L. McKnight, T. S. Cook, K. S. Kim, and E. C. Duderstadt *In* NASA, Lewis Research Center, Turbine Engine Hot Section Technology 1986 Oct. 1986 p 447-467 (For primary document see N89-12876 04-39)
(Contract NAS3-23943)
Avail: NTIS HC A21/MF A01 CSCL 11C

The objectives of this program are to determine the predominant modes of degradation of a plasma sprayed thermal barrier coating system, and then to develop and verify life prediction models accounting for these degradation modes. The program is divided into two phases, each consisting of several tasks. The work in Phase 1 is aimed at identifying the relative importance of the various failure modes, and developing and verifying life prediction model(s) for the predominant model for a thermal barrier coating system. Two possible predominant failure mechanisms being evaluated are bond coat oxidation and bond coat creep. The work in Phase 2 will develop design-capable, causal, life prediction models for thermomechanical and thermochemical failure modes, and for the exceptional conditions of foreign object damage and erosion. Author

N89-12922*# Pratt and Whitney Aircraft, East Hartford, Conn.
THERMAL BARRIER COATING LIFE PREDICTION MODEL DEVELOPMENT **c27**
J. T. DeMasi and K. D. Sheffler *In* NASA, Lewis Research Center, Turbine Engine Hot Section Technology 1986 Oct. 1986 p 469-483 (For primary document see N89-12876 04-39)
(Contract NAS3-23944)
Avail: NTIS HC A21/MF A01 CSCL 11C

The objective of this program is to establish a methodology to predict Thermal Barrier Coating (TBC) life on gas turbine engine components. The approach involves experimental life measurement coupled with analytical modeling of relevant degradation modes. The coating being studied is a flight qualified two layer system, designated PWA 264, consisting of a nominal ten mil layer of

seven percent yttria partially stabilized zirconia plasma deposited over a nominal five mil layer of low pressure plasma deposited NiCoCrAlY. Thermal barrier coating degradation modes being investigated include: thermomechanical fatigue, oxidation, erosion, hot corrosion, and foreign object damage. Author

N89-12923*# Old Dominion Univ., Norfolk, Va. Dept. of Mechanical Engineering and Mechanics.
PREDICTION OF STRESSES IN AIRCRAFT PANELS SUBJECTED TO ACOUSTIC FORCES Final Report, 1 Oct. 1985 - 15 Dec. 1987
Chuh Mei Mar. 1988 13 p
(Contract NAS1-17993)
(NASA-CR-182513; NAS 1.26:182513) Avail: NTIS HC A03/MF A01 CSCL 20K

Summarized are the progress and accomplishments performed under NASA/Langley Research Center Master Agreement NAS1-17993, Task Assignment No. 22, entitled Prediction of Stresses in Aircraft Panels Subjected to Acoustic Forces, for the period October 1, 1985 to December 15, 1987. The primary effort of this task is the development of analytical methods for prediction of stresses in aircraft panels subjected to acoustic forces. The progress and accomplishments of various activities are discussed first. Then, publications, presentations and thesis are presented. Author

N89-12924 Arizona Univ., Tucson.
THE DEVELOPMENT OF A NEAR-INFRARED POLARIMETER AND ITS APPLICATION TO THE CONTINUUM POLARIZATION OF MAGNETIC WHITE DWARFS Ph.D. Thesis
Steven Charles West 1987 162 p
Avail: Univ. Microfilms Order No. DA8804193

An astronomical polarimeter is presented that incorporates a fused silica stress-birefringent modulator which simultaneously allows the selection of chopping frequency and spectral tuning with very high modulation efficiency. Two integrating detector packages are discussed. The instrumental polarizations of the MMT are calculated using Mueller calculus and experimentally verified. The continuum polarizations of five isolated highly magnetic white dwarfs are investigated both observationally and theoretically. Hydrogen Balmer photoionization occurring from the magnetically perturbed bound states into the Coulomb-Lorentz mixed quasi-Landau continuum is investigated with the aid of recent high field calculations. Finally, the continuum polarization of Grw + 70 deg 8247 is compared to models for cyclotron and inverse magnetobremsstrahlung absorptions in a dipolar field. The conclusion is that the continuum polarizations of these objects still eludes an exact description. Observations of BG C Mi reveal the first definitive discovery of polarized cyclotron emission in any intermediate polar and confirms that the long-held basic model of a magnetically accreting white dwarf is correct. Dissert. Abstr.

N89-12925# Ottawa Univ. (Ontario). Dept. of Mechanical Engineering.
CHARACTERIZATION OF ADHESIVELY BONDED JOINTS USING ACOUSTO-ULTRASONICS M.S. Thesis
Samsir Tanary Apr. 1988 229 p
Avail: NTIS HC A11/MF A01

The mechanical performance of adhesively bonded joints is characterized using nondestructive acousto-ultrasonic and destructive shear testing techniques. The research program is intended to assess the feasibility of utilizing acousto-ultrasonics in characterization and strength prediction of adhesively bonded joints. The basic principles of the acousto-ultrasonic technique are described. The instruments, operating procedures and factors affecting acousto-ultrasonic measurements are explained. Factors affecting the joint strength such as the material and geometry of the joint are also discussed. Experimental results obtained in a series of characterization tests on adhesively bonded specimens are presented. Author

N89-12926# California Univ., Berkeley. Computer Science Div.
PERFORMANCE STUDIES OF DYNAMIC LOAD BALANCING IN DISTRIBUTED SYSTEMS Progress Report, 7 Aug. 1984 - 6 Aug. 1987
Songnian Zhou Oct. 1987 120 p
(Contract N00039-84-C-0089; ARPA Order 4871)
(AD-A197130; UCB/CSD-87/376; PR-87-6) Avail: NTIS HC A06/MF A01 CSCL 12G

Distributed systems are often characterized by uneven loads on hosts and other resources. In this thesis, the problems concerning dynamic load balancing in loosely-coupled distributed systems are studied using trace-driven simulation, implementation, and measurement. Information about job CPU and input/output demands is collected from three production systems and used as input to a simulator that includes a representative central processing units scheduling policy and considers the message exchange and job transfer costs explicitly. A prototype load balancer is implemented in the Berkeley UNIX and Sun/UNIX environments, and the results of a large number of measurement experiments performed on six workstations are presented. The quality of two families of load indices, one based on resource queue length, the other on resource utilization, is evaluated in the context of dynamic load balancing. The performances of seven algorithms using different load information exchange and job placement strategies are compared. The factors that affect load balancing performance, and the impacts of load balancing on individuals hosts and on each type of job are also quantitatively investigated. GRA

N89-12927# Army Armament Research and Development Command, Watervliet, N. Y. Weapons Lab.
FRACTURE AND FATIGUE Final Report
R. O. Ritchie, W. W. Gerberich, and J. H. Underwood Apr. 1988 77 p
(AD-A197310; ARCCB-TR-88016) Avail: NTIS HC A05/MF A01 CSCL 20K

In the last twenty years, much progress has been made with the continuum mechanics characterization of crack growth rates through the application of linear elastic and elastic-plastic fracture mechanics, and such analyses are now in widespread use for defect-tolerant design codes. Similarly, an understanding of the role of microstructure in improving the resistance to fracture and fatigue has emerged to the point where alloy design guidelines exist for the production of alloys with optimum resistance to fatigue failure. However, much work remains in the definition of mechanisms associated with environmentally-influenced crack growth, with the effect of variable amplitude loading, with the problem of the short flaw, and in the fracture of microscopic structures (e.g., packaging problems in the electronics industry). GRA

N89-12928# Virginia Polytechnic Inst. and State Univ., Blacksburg. Center for Adhesive and Sealant Science.
THE DURABILITY OF ADHESIVE JOINTS: AN ENGINEERING STUDY Final Report, 1 Jun. 1985 - 30 Jun. 1988
Didier R. Lefebvre, D. A. Dillard, and H. F. Brinson Jun. 1988 174 p
(Contracts N00014-82-K-0185; N00014-85-K-0145)
(AD-A197754; VPI-88-19; CASS/ESM-88-7) Avail: NTIS HC A08/MF A01 CSCL 11A

Water diffusion through the adhesive is the rate controlling factor for the durability of many metal-to-polymer bonds exposed to moist environments. A methodology is proposed, to relate the diffusion coefficient of water in polymers to temperature, strain and penetrant concentration. The approach used is based on well known free volume theories. In the rubbery state, it is assumed that the transport kinetics is governed by the constant redistribution of the free volume, caused by the segmental motions of the polymeric chains. An expression for the diffusion coefficient is inferred from the temperature, strain and penetrant concentration of the free volume. It is shown that the free volume treatment can be extended to the glassy range by introducing a few additional

features in the model. The stress dependence of solubility as well as the non-fickian driving forces contributing to mass transport are predicted from the Flory-Huggins theory. GRA

N89-12929# Lawrence Livermore National Lab., Calif. Applied Mechanics Group.

STRUCTURAL RESPONSE CALCULATIONS FOR A METAL BOOSTER TANK MODEL

Tod A. Laursen and Gregory J. Kay 25 Jul. 1988 18 p
(Contract W-7405-eng-48)
(DE88-017095; UCID-21475) Avail: NTIS HC A03/MF A01

An analysis has been carried out to computationally predict the response of a pressurized thin metal tank to short pulse laser loading. The analysis used a 3-D Lagrangian explicit finite element code to predict structural response and included consideration tank wall reductions due to rear surface spall and front surface melt. The wall reductions, the result of the initial laser energy deposition, were predicted with a one-dimensional material response code. Possible buckling behavior and initial stresses resulting from tank pressurization were included in the calculations. This report details the methodology and results of the analysis. We conclude that high confidence computational prediction of failure of metal booster tanks subjected to short-pulse laser loading is not possible, due to the lack of verified failure models and of a suitable experimental data base. DOE

N89-12930*# National Aeronautics and Space Administration. Lewis Research Center, Cleveland, Ohio.

CALCULATION OF WEIBULL STRENGTH PARAMETERS AND BATDORF FLOW-DENSITY CONSTANTS FOR VOLUME- AND SURFACE-FLAW-INDUCED FRACTURE IN CERAMICS

Shantaram S. Pai and John P. Gyekenyesi Oct. 1988 32 p
Presented at the 3rd International Symposium on Ceramic Materials and Components for Engines, Las Vegas, Nev., 27-30 Nov. 1988; sponsored in part by the American Ceramic Society
(NASA-TM-100890; E-4128; NAS 1.15:100890) Avail: NTIS HC A03/MF A01 CSCL 20K

The calculation of shape and scale parameters of the two-parameter Weibull distribution is described using the least-squares analysis and maximum likelihood methods for volume- and surface-flaw-induced fracture in ceramics with complete and censored samples. Detailed procedures are given for evaluating 90 percent confidence intervals for maximum likelihood estimates of shape and scale parameters, the unbiased estimates of the shape parameters, and the Weibull mean values and corresponding standard deviations. Furthermore, the necessary steps are described for detecting outliers and for calculating the Kolmogorov-Smirnov and the Anderson-Darling goodness-of-fit statistics and 90 percent confidence bands about the Weibull distribution. It also shows how to calculate the Batdorf flaw-density constants by uing the Weibull distribution statistical parameters. The techniques described were verified with several example problems, from the open literature, and were coded. The techniques described were verified with several example problems from the open literature, and were coded in the Structural Ceramics Analysis and Reliability Evaluation (SCARE) design program. Author

N89-12931*# Georgia Inst. of Tech., Atlanta. Dept. of Aerospace Engineering.

NON-ISOTHERMAL BUCKLING BEHAVIOR OF VISCOPLASTIC SHELL STRUCTURES

Richard Riff and G. J. Simitses [1988] 6 p
(Grant NAG3-534)
(NASA-CR-183013; NAS 1.26:183013) Avail: NTIS HC A02/MF A01 CSCL 20K

Described are the mathematical model and solution methodologies for analyzing the structural response of thin, metallic elasto-viscoplastic shell structures under large thermomechanical loads and their non-isothermal buckling behavior. Among the system responses associated with these loads and conditions are snap-through, buckling, thermal buckling, and creep buckling. This geometric and material nonlinearities (of high order) can be anticipated and are considered in the model and the numerical treatment. Author

N89-12932*# Georgia Inst. of Tech., Atlanta. School of Aerospace Engineering.

CONSIDERATIONS IN DEVELOPMENT AND IMPLEMENTATION OF ELASTO-VISCOPLASTIC CONSTITUTIVE MODEL FOR HIGH TEMPERATURE APPLICATIONS

Richard Riff [1988] 2 p
(Grant NAG3-534)
(NASA-CR-183403; NAS 1.26:183403) Avail: NTIS HC A02/MF A01 CSCL 20K

The prediction of inelastic behavior of metallic materials at elevated temperatures has increased in importance in recent years. The operating conditions within the hot section of a rocket motor or a modern gas turbine engine present an extremely harsh thermomechanical environment. Large thermal transients are induced each time the engine is started or shut down. Additional thermal transients from an elevated ambient occur whenever the engine power level is adjusted to meet flight requirements. The structural elements employed in such hot sections, as well as any engine components located therein, must be capable of withstanding such extreme conditions. Failure of a component would, due to the critical nature of the hot section, lead to an immediate and catastrophic loss in power. Consequently, assuring satisfactory long term performance for such components is a major concern. Nonisothermal loading of structures often causes excursion of stress well into the inelastic range. Moreover, the influence of geometry changes on the response is also significant in most cases. Therefore, both material and geometric nonlinear effects are considered. Author

N89-12933# Deutsche Forschungs- und Versuchsanstalt fuer Luft- und Raumfahrt, Brunswick (West Germany). Inst. fuer Strukturmechanik.

TWO DIFFERENT METHODS FOR SHELL BUCKLING CALCULATION IN THE ELASTIC-PLASTIC REGION

Maria Esslinger and Gert Poblotzki Jun. 1988 53 p In GERMAN; ENGLISH summary
(DFVLR-FB-88-26; ISSN-0171-1342; ETN-88-93526) Avail: NTIS HC A04/MF A01; DFVLR VB-PL-DO, 90 60 58, 5000 Cologne, Federal Republic of Germany, 20.50 deutsche marks

A shell buckling calculation procedure that transfers the criterion for loading or unloading from the buckling, rather than from the prebuckling mode of the ideal shell, is presented. Application is demonstrated by numerical examples. ESA

N89-12934# Southampton Univ. (England). Inst. of Sound and Vibration Research.

APPROXIMATE MOBILITIES OF BUILT UP STRUCTURES

R. J. Pinnington 1988 92 p Sponsored by the Ministry of Defence Procurement Executive, London, England
(ISVR-TR-162; ETN-88-93550) Avail: NTIS HC A05/MF A01

Point mobility formulas of typical structures for use in estimating vibration transmission from machinery are presented. Input mobilities of homogeneous beams, rings and plates; input mobilities of orthotropic plates in flexure; two regime systems: cylinders and spherical shells; two wave type systems: thick plates with firm or compliant cores; beam stiffened plates and cylinders; stiffness controlled systems; and isolator transfer impedances are covered. ESA

N89-12935*# National Aeronautics and Space Administration. Langley Research Center, Hampton, Va.

ANALYSIS OF THE SPACE SHUTTLE ORBITER SKIN PANELS UNDER SIMULATED HYDRODYNAMIC LOADS

Huey D. Carden, Edwin L. Fasanella, and Lisa E. Jones (PRC Systems Services Co., Hampton, Va.) Dec. 1988 15 p
(NASA-TM-4082; L-16511; NAS 1.15:4082) Avail: NTIS HC A03/MF A01 CSCL 20K

The Space Shuttle orbiter skin panels were analyzed under pressure loads simulating hydrodynamic loads to determine their

capability to sustain a potential ditching and to determine pressures that typically would produce failures. Two Dynamic Crash Analysis of Structures (DYCAST) finite element models were used. One model was used to represent skin panels (bays) in the center body, while a second model was used to analyze a fuselage bay in the wing region of the orbiter. From an assessment of the DYCAST nonlinear computer results, it is concluded that the probability is extremely high that most, if not all, of the lower skin panels would rupture under ditching conditions. Extremely high pressure loads which are produced under hydrodynamic planning conditions far exceed the very low predicted failure pressures for the skin panels. Consequently, a ditching of the orbiter is not considered to have a high probability of success and should not be considered a means of emergency landing unless no other option exists. Author

N89-12594*# Southwest Research Inst., San Antonio, Tex.
MULTIPLE INPUT/OUTPUT RANDOM VIBRATION CONTROL SYSTEM
James F. Unruh *In* NASA, Goddard Space Flight Center, 15th Space Simulation Conference: Support the Highway to Space Through Testing 1988 p 139-157 (For primary document see N89-12582 04-18)
Avail: NTIS HC A21/MF A01 CSCL 20K

N89-12655*# IIT Research Inst., Chicago, Ill. Surface Engineering Center.
MULTISPECIMEN TEST FACILITY FOR HIGH-PRESSURE HYDROGEN CREEP STUDIES
S. K. Verma *In* NASA, Marshall Space Flight Center, Advanced Earth-To-Orbit Propulsion Technology 1986, Volume 2 Oct. 1986 p 635-659 (For primary document see N89-12626 04-20)
Avail: NTIS HC A99/MF E03 CSCL 21H

N89-12657*# National Aeronautics and Space Administration. Marshall Space Flight Center, Huntsville, Ala.
DEVELOPMENT OF A COMPUTER-CONTROLLED TECHNIQUE TO DETERMINE CRACK GROWTH RATE PROPERTIES IN CONTROLLED ENVIRONMENTS USING CRACK OPENING DISPLACEMENT
Dennis Moore, Dan Drinan, and J. Hodo *In its* Advanced Earth-To-Orbit Propulsion Technology 1986, Volume 2 Oct. 1986 p 672-697 (For primary document see N89-12626 04-20)
Avail: NTIS HC A99/MF E03 CSCL 21H

N89-12763# Notre Dame Univ., Ind. Dept. of Civil Engineering.
INVESTIGATION INTO THE APPLICABILITY OF FRACTURE MECHANICS TECHNIQUES TO AIRCRAFT WHEEL LIFE STUDIES Final Report
Thomas J. Enneking *In* Universal Energy Systems, Inc., United States Air Force Graduate Student Summer Support Program, Volume 1 Dec. 1987 20 p (For primary document see N89-12754 04-31)
Avail: NTIS HC A99/MF E03 CSCL 20K

42 GEOSCIENCES (GENERAL)

N89-12936# European Space Agency, Paris (France).
PROCEEDINGS OF THE 1988 INTERNATIONAL GEOSCIENCE AND REMOTE SENSING SYMPOSIUM (IGARSS 1988) ON REMOTE SENSING: MOVING TOWARDS THE 21ST CENTURY, VOLUME 1
T. D. Guyenne, ed. and J. J. Hunt, ed. Aug. 1988 673 p Partly in ENGLISH and FRENCH Symposium held in Edinburgh, United Kingdom, 12-16 Sep. 1988; sponsored by the Remote Sensing Society, the Geoscience and Remote Sensing Society, IEEE, and IURS
(ESA-SP-284-Vol-1; IEEE-88CH2497-6-Vol-1; ISSN-0379-6566; LC-87-83254; ETN-88-93242) Copyright Avail: NTIS HC A99/MF E03; ESA Publications Div., ESTEC, Noordwijk, Netherlands, 120 US dollars or 250 Dutch guilders

Radiometry; radar cross section data bases and modeling services; multipolarization SAR; geographic information systems; ocean waves; land ice; future space remote sensing systems; pattern recognition and feature extraction; rain; calibration and verification of ground-based measurements; backscatter modeling of volume scattering; multipolarization SAR systems; geology; sea ice (SAR); snow; SPOT; and wind measurement were discussed. For individual titles, see N89-12937 through N89-13087.

N89-12937# Cologne Univ. (West Germany). Inst. fuer Geophysik und Meteorologie.
THE AIRBORNE VERSION CONICAL SCAN RADIOMETER (AVCSR): AN AIRBORNE RADIOMETER AS A TOOL FOR SATELLITE DATA VALIDATION **c43**
J. Wirth and M. Peeters *In* ESA, Proceedings of the 1988 International Geoscience and Remote Sensing Symposium (IGARSS 1988) on Remote Sensing: Moving Towards the 21st Century, Volume 1 Aug. 1988 p 11-12 (For primary document see N89-12936 04-42)
Copyright Avail: NTIS HC A99/MF E03; ESA Publications Div., ESTEC, Noordwijk, Netherlands, 120 US dollars or 250 Dutch guilders

The airborne radiation budget radiometer AVCSR for satellite radiometer data validation by development of a special validation strategy to define a best estimate standard satellite instrument, to establish the AVCSR as a stable transfer standard for satellite data validation is described. The calibration strategy of the AVCSR is presented. Expected accuracies are 2 to 5 percent in the solar spectral range; 3 to 10 percent in the terrestrial. Campaigns are planned to validate the data of the Scanner for Radiation Budget (ScaRaB) on the USSR satellites METEOR and of the ATSR on ERS-1. ESA

N89-12938# Hughes Aircraft Co., Tucson, Ariz.
AUTOMATIC CONTROL OF A MULTI-CHANNEL MILLIMETER WAVE RADIOMETER **c35**
D. A. Zielinskie, C. A. Wassenberg, and J. A. Reagan *In* ESA, Proceedings of the 1988 International Geoscience and Remote Sensing Symposium (IGARSS 1988) on Remote Sensing: Moving Towards the 21st Century, Volume 1 Aug. 1988 p 13-14 (For primary document see N89-12936 04-42)
Copyright Avail: NTIS HC A99/MF E03; ESA Publications Div., ESTEC, Noordwijk, Netherlands, 120 US dollars or 250 Dutch guilders

A real time distributed architecture for a multichannel radiometer is presented. Digital signal processing and automated control of the system are summarized. The system consists of four microwave radiometer subsystems which provide a total of nine frequency channels, a steerable reflector to permit slantpath measurements, and a host computer for recording and evaluating the data. The nine channels span the water vapor and oxygen absorption lines in the 20 to 60 GHz range with the lowest frequencies (20.6, 22.235, and 31.65 GHz) to be used for water vapor and liquid water retrievals and the six highest frequencies (50.3, 52.85, 53.85, 55.45, 58.8, and 61.15 GHz) to be used for temperature profile retrievals. The zenith angle scanning capability is for calibration and the study of temporal/spatial variations in atmospheric water vapor and temperature. ESA

N89-12939# Deutsche Forschungs- und Versuchsanstalt fuer Luft- und Raumfahrt, Oberpfaffenhofen (West Germany).
THE AIRBORNE RADIOMETRY EXPERIMENT (ABREX) INSTRUMENT, AN EXPERIMENTAL TEST BED FOR THE SPECIFICATION OF SATELLITE-BORNE MICROWAVE RADIOMETER AT 90 GHz **c35**
W. Keydel and H. Goessl *In* ESA, Proceedings of the 1988 International Geoscience and Remote Sensing Symposium (IGARSS 1988) on Remote Sensing: Moving Towards the 21st Century, Volume 1 Aug. 1988 p 15-16 (For primary document see N89-12936 04-42)

Copyright Avail: NTIS HC A99/MF E03; ESA Publications Div., ESTEC, Noordwijk, Netherlands, 120 US dollars or 250 Dutch guilders

The AirBorne Radiometry Experiment (ABREX), a 90 GHz Hach-radiometer breadboard realization of a planned satellite radiometer is described. It was built following the Phase A study results of a satellite-borne radiometer experiment as a testbed for future satellite radiometers with respect to components, calibration, measurement possibilities, etc., and as an instrument for pre-experiments and accompanying measurements of similar 90 GHz satellite-borne radiometers as well. The goals of the experiment, the specifications, and the realized hardware are presented, as well as measurement results. ESA

N89-12940# Technical Univ. of Denmark, Lyngby. Electromagnetics Inst.

ON THE SAMPLING IN IMAGING MICROWAVE RADIOMETERS **c43**

N. Skou *In* ESA, Proceedings of the 1988 International Geoscience and Remote Sensing Symposium (IGARSS 1988) on Remote Sensing: Moving Towards the 21st Century, Volume 1 Aug. 1988 p 17-18 (For primary document see N89-12936 04-42)

Copyright Avail: NTIS HC A99/MF E03; ESA Publications Div., ESTEC, Noordwijk, Netherlands, 120 US dollars or 250 Dutch guilders

Imaging radiometer system sampling time dependence on the dwell time per footprint is discussed. Two different approaches are seen: either a sampling time equal to the dwell time per footprint, or sampling twice per dwell time. The correct sampling is between these 2 extremes: a sampling time of 70 percent of the dwell time per footprint is required for realistic antenna patterns. ESA

N89-12941# National Oceanic and Atmospheric Administration, Boulder, Colo. Wave Propagation Lab.

VERIFICATION OF THE ACCURACY OF A NETWORK OF WATER-VAPOR RADIOMETERS **c43**

J. B. Snider *In* ESA, Proceedings of the 1988 International Geoscience and Remote Sensing Symposium (IGARSS 1988) on Remote Sensing: Moving Towards the 21st Century, Volume 1 Aug. 1988 p 19-20 (For primary document see N89-12936 04-42)

Copyright Avail: NTIS HC A99/MF E03; ESA Publications Div., ESTEC, Noordwijk, Netherlands, 120 US dollars or 250 Dutch guilders

Calibration of a network of water vapor radiometers by means of a mobile radiometer used as a standard is described. Precipitable water vapor (PWV) calculated from radiosonde data is consistently lower than that measured by the radiometers by approximately 0.8 mm. The low bias of the radiometer measurement may be caused by inaccuracies in the radiosonde hygristor, deficiencies in microwave absorption theory, or undetected errors in the tipping curve calibration. Differences in PWV measured at 2 min intervals by the radiometric systems are less than 0.58 mm considering the network as a whole. The mobile radiometer indicates slightly lower PWV values than the network systems. A well calibrated radiometer can continuously monitor short and long-term variations in water vapor with accuracy comparable to or better than that of the radiosonde. Although questions remain in regard to absorption theory and the radiosonde moisture sensor, these uncertainties have a relatively small effect upon the radiometric vapor measurement. Therefore, deployment of vapor-liquid radiometers to complement the wind profiler network is feasible. ESA

N89-12942# Marconi Space Systems Ltd., Portsmouth (England).

PROPOSED DESIGN OF THE TEMPERATURE CONTROL SYSTEM FOR THE VARIABLE TEMPERATURE CALIBRATION TARGET FOR THE ADVANCED MICROWAVE SOUNDING UNIT B **c35**

L. J. Banfield *In* ESA, Proceedings of the 1988 International Geoscience and Remote Sensing Symposium (IGARSS 1988) on Remote Sensing: Moving Towards the 21st Century, Volume 1 Aug. 1988 p 21-22 Sponsored by the Ministry of Defence Procurement Executive, London, United Kingdom (For primary document see N89-12936 04-42)

Copyright Avail: NTIS HC A99/MF E03; ESA Publications Div., ESTEC, Noordwijk, Netherlands, 120 US dollars or 250 Dutch guilders

The Advanced Microwave Sounding Unit B for the Tiros N/NOAA series of weather satellites performance calibration using a highly absorptive target precisely temperature controlled is described. The standard thermal control solution is a closed loop pumped fluid system which may not be the optimum approach in this application. A stepped conductance design is an alternative. This system uses sequential flooding of annular chambers with cryogenic fluid, to achieve progressively lower operating temperatures, with cooling offset by electrical heating. A mathematical model of the system was analyzed and its thermal performance predicted. ESA

N89-12943# Deutsche Forschungs- und Versuchsanstalt fuer Luft- und Raumfahrt, Wesseling (West Germany). Inst. for Radio Frequency Technology.

REAL-TIME ADAPTIVE RADIOMETRIC CORRECTION FOR IMAGING RADAR SYSTEMS **c32**

J. A. Moreira and W. Poetzsch *In* ESA, Proceedings of the 1988 International Geoscience and Remote Sensing Symposium (IGARSS 1988) on Remote Sensing: Moving Towards the 21st Century, Volume 1 Aug. 1988 p 23-24 (For primary document see N89-12936 04-42)

Copyright Avail: NTIS HC A99/MF E03; ESA Publications Div., ESTEC, Noordwijk, Netherlands, 120 US dollars or 250 Dutch guilders

A solution of a real time radiometric image correction that also minimizes the quantization and saturation noise introduced by the process of analog to digital (A/D) conversion of raw data of coherent and noncoherent imaging radar systems is proposed. The range dependent decrease of the backscattered signal power is compensated by varying the gain of the IF-section of the radar. The range dependent IF-gain is calculated in real time using an adaptive control system that analyzes the digitized backscattered signal. The technique of the nonlinear adaptive control and its implementation is explained. A simulation of this procedure with the parameters of an experimental L/C-Band SAR-system shows that a residual signal level error before the A/D-conversion of less than 1 dB is achievable. ESA

N89-12944# Joint Research Centre of the European Communities, Ispra (Italy).

EURACS: A EUROPEAN RADAR CROSS SECTION DATABASE **c32**

P. N. Churchill and A. J. Sieber *In* ESA, Proceedings of the 1988 International Geoscience and Remote Sensing Symposium (IGARSS 1988) on Remote Sensing: Moving Towards the 21st Century, Volume 1 Aug. 1988 p 29-31 (For primary document see N89-12936 04-42)

Copyright Avail: NTIS HC A99/MF E03; ESA Publications Div., ESTEC, Noordwijk, Netherlands, 120 US dollars or 250 Dutch guilders

A European radar cross section database, EURACS, is being developed. The philosophy behind the development and implementation of EURACS, and preliminary work undertaken during the European Agrisar 1986 and Agriscatt 1987 airborne microwave campaigns are described. Potential applications of EURACS are suggested. ESA

N89-12945# GEC-Marconi Electronics Ltd., Chelmsford (England).

CONSTRAINTS ON TWO-SCALE DESCRIPTIONS OF RADAR BACKSCATTERING FROM THE SEA SURFACE USING SCATTEROMETER MODEL FUNCTIONS **c32**

J. A. Conway, R. A. Cordey, and J. T. Macklin *In* ESA, Proceedings of the 1988 International Geoscience and Remote Sensing Symposium (IGARSS 1988) on Remote Sensing: Moving Towards

the 21st Century, Volume 1 Aug. 1988 p 33-34 (For primary document see N89-12936 04-42)
Copyright Avail: NTIS HC A99/MF E03; ESA Publications Div., ESTEC, Noordwijk, Netherlands, 120 US dollars or 250 Dutch guilders

Scatterometer model functions for Seasat and ERS-1 are used to obtain constraints on the cut-off wavenumber kd required in the composite-surface description of radar backscattering from the sea surface. These data are inverted, neglecting specular backscatter, to obtain the short-wave spectral energy density E(kB) at a particular Bragg wavenumber kB, for a wide range of values of kd. Due to the overlap of the Seasat and ERS-1 data, a constraint on kd can be obtained by requiring E(kB) to be a power-law smoothly connecting the data sets. The value of kd obtained is 0.3kr (kr being the radar wavenumber) with a weak dependence on wind speed, thus agreeing with results of other investigators. ESA

N89-12946# Naval Research Lab., Washington, D.C.
SHADOWS AND WEDGES IN SCATTERING FROM THE SEA **c74**
L. B. Wetzel *In* ESA, Proceedings of the 1988 International Geoscience and Remote Sensing Symposium (IGARSS 1988) on Remote Sensing: Moving Towards the 21st Century, Volume 1 Aug. 1988 p 35-38 (For primary document see N89-12936 04-42)
Copyright Avail: NTIS HC A99/MF E03; ESA Publications Div., ESTEC, Noordwijk, Netherlands, 120 US dollars or 250 Dutch guilders

By using simple physical optics diffraction theory to calculate the distribution of diffracted illumination over the trough of a trochoidal wave model, it was found that geometrical optics can provide a reasonable shadowing approximation only for the higher wind speeds and radar frequencies, e.g., the greater than 15kts at 10GHz. Under these conditions, the modified illumination profile implied by a threshold shadowing theory leads to a shadowing function with a sharp cut-off below 2 deg. The standard asymptotic approximations used in wedge scattering are found to be unsuitable for describing scattering from the randomly oriented features on a real sea surface. Generalizations turn out to be noncausal, and alternative theories give wrong results at intermediate angles. The failure of both wedge and Bragg scattering theories to provide a self-consistent model of sea scatter is discussed in relation to the actual scattering structures appearing on the surface of an active sea. ESA

N89-12947# Virginia Polytechnic Inst. and State Univ., Blacksburg. Dept. of Electrical Engineering.
THE E-PARALLEL POLARIZATION RESPONSE OF A TWO-DIMENSIONAL HETEROGENEOUS LAYER MODELLED BY TWO THIN SHEETS **c43**
R. C. Robertson *In* ESA, Proceedings of the 1988 International Geoscience and Remote Sensing Symposium (IGARSS 1988) on Remote Sensing: Moving Towards the 21st Century, Volume 1 Aug. 1988 p 39-40 (For primary document see N89-12936 04-42)
Copyright Avail: NTIS HC A99/MF E03; ESA Publications Div., ESTEC, Noordwijk, Netherlands, 120 US dollars or 250 Dutch guilders

The flexibility of the thin sheet technique to model two-dimensional structures is extended by analyzing the response to E-parallel to the strike of the anomaly polarization when a heterogeneous Earth is modeled by two thin sheets over a horizontally stratified half-space. The electromagnetic fields induced by the heterogeneous layer when a uniform plane wave is normally incident on the Earth are expressed as integral equations which are evaluated using the method of moments. The resulting matrix equations are solved by the Gauss-Seidel method, and the magnetotelluric (MT) impedance is calculated. Numerical results are obtained for a representative model using both one and two thin sheets, and the results are compared. At frequencies where the anomalous layer is not electrically thin, the phase error in the MT impedance that results from the single thin sheet model is much more severe than the error in magnitude. This behavior is similar to that obtained for the E-Perpendicular to the strike of the anomaly polarization response. ESA

N89-12948# Texas Univ., Arlington. Wave Scattering Research Center.
SCATTERING FROM A SKEWED RANDOM SURFACE **c32**
A. K. Fung *In* ESA, Proceedings of the 1988 International Geoscience and Remote Sensing Symposium (IGARSS 1988) on Remote Sensing: Moving Towards the 21st Century, Volume 1 Aug. 1988 p 41-43 (For primary document see N89-12936 04-42)
(Contract N60530-85-C-0365)
Copyright Avail: NTIS HC A99/MF E03; ESA Publications Div., ESTEC, Noordwijk, Netherlands, 120 US dollars or 250 Dutch guilders

By incorporating skewness in surface elevation into a standard Kirchhoff surface scattering model, it is shown that additional terms are generated which can account for the difference in the backscattering coefficient due to a change in the sense of the direction of observation. For the sea surface this offers an explanation for the difference between the upwind and downwind observations. Major changes in the backscattering coefficient due to change in direction appear through the directional surface spectrum while a change in the sense of the direction is reflected through the skewness function of the surface. ESA

N89-12949*# Texas Univ., Arlington. Wave Scattering Research Center.
POLARIMETRIC MICROWAVE SCATTERING FROM KNOWN RANDOMLY ROUGH SURFACES **c32**
C. E. Nance, A. J. Blanchard, and M. F. Chen *In* ESA, Proceedings of the 1988 International Geoscience and Remote Sensing Symposium (IGARSS 1988) on Remote Sensing: Moving Towards the 21st Century, Volume 1 Aug. 1988 p 47-50 (For primary document see N89-12936 04-42)
(Grant NAG5-486)
Copyright Avail: NTIS HC A99/MF E03; ESA Publications Div., ESTEC, Noordwijk, Netherlands, 120 US dollars or 250 Dutch guilders CSCL 20N

Scattering from rough surfaces is reviewed, and artificial randomly rough surfaces are described. Measurements were made from 4 to 18 GHz for the 4 linear polarization states. The target consists of a metalized randomly rough surface constructed from known surface statistical information. The surface was generated using surface generation routines on the computer, and then the data was converted for the machining of the surface on a computer controlled mill. Bistatic and monostatic measurements were acquired at incident angles from 25 to 60 deg. At the 13.5 to 18 GHz frequencies, the effects of backscatter enhancement and depolarization effects can be studied in a regime which does not satisfy Kirchoff or small perturbation assumptions. This allows scattering mechanisms to be introduced into models, which may show missing elements in the more standard formulations. At lower frequency bands such as 4 to 8.5 GHz the scattering behavior was also examined to see the behavior as assumptions of other formulations are satisfied. ESA

N89-12950*# Jet Propulsion Lab., California Inst. of Tech., Pasadena.
INFERENCE OF GEOLOGIC SURFACE PARAMETERS FROM POLARIMETRIC RADAR OBSERVATIONS AND MODEL INVERSION **c43**
Jakob J. VanZyl, P. C. Dubois, H. A. Zebker, and T. G. Farr *In* ESA, Proceedings of the 1988 International Geoscience and Remote Sensing Symposium (IGARSS 1988) on Remote Sensing: Moving Towards the 21st Century, Volume 1 Aug. 1988 p 51-52 (For primary document see N89-12936 04-42)
Copyright Avail: NTIS HC A99/MF E03; ESA Publications Div., ESTEC, Noordwijk, Netherlands, 120 US dollars or 250 Dutch guilders CSCL 08G

The results of inferring geologic parameters such as rms surface height, correlation length, and dielectric constant of rough surfaces

by fitting observed polarization signatures with those predicted by the second order Rice model are discussed. The inferred results are compared to measured values of rms height and correlation length. The rms height values inferred are in good agreement with in situ measurements. The inferred correlation lengths generally do not agree with measured values. The results allow the separation of the effects of surface roughness and dielectric constant on the overall backscatter from rough surfaces. ESA

N89-12951*# National Aeronautics and Space Administration. Goddard Space Flight Center, Greenbelt, Md.
MODELLING OF SAR POLARISATION PHASE DIFFERENCE FROM TREES **c43**
Tsan Mo (Computer Sciences Corp., Beltsville, Md.) and J. R. Wang *In* ESA, Proceedings of the 1988 International Geoscience and Remote Sensing Symposium (IGARSS 1988) on Remote Sensing: Moving Towards the 21st Century, Volume 1 Aug. 1988 p 55-58 (For primary document see N89-12936 04-42)
Copyright Avail: NTIS HC A99/MF E03; ESA Publications Div., ESTEC, Noordwijk, Netherlands, 120 US dollars or 250 Dutch guilders CSCL 02F

The data for polarization phase difference Delta Phi between the HH- and VV-polarized backscattered waves from tree-covered fields were obtained with an airborne synthetic aperture radar at 1.225 GHz. The mean values over tree-covered fields were derived from the images of the phase difference and were examined as a function of incident beam angle from 15 to 55 deg. A theoretical model for simulating these data, based on the electromagnetic wave scatterings from the tree trunk and its branches, both of which are assumed as very long dielectric cylinders was developed. The radius and direction of a tree branch are taken as random variables and are chosen by a Monte Carlo method to encounter the incident waves in producing the scattering events. The Monte Carlo simulated results are in good agreement with the observations within experimental uncertainty. ESA

N89-12952# Illinois Univ., Chicago. Communications Lab.
STATISTICAL ANALYSIS AND SOME POLARIMETRIC SIGNATURES OF A POLARIMETRIC SYNTHETIC APERTURE RADAR IMAGE **c32**
M. Walther, A. B. Kostinski, H. J. Eom, and W.-M. Boerner *In* ESA, Proceedings of the 1988 International Geoscience and Remote Sensing Symposium (IGARSS 1988) on Remote Sensing: Moving Towards the 21st Century, Volume 1 Aug. 1988 p 59-64 (For primary document see N89-12936 04-42)
Copyright Avail: NTIS HC A99/MF E03; ESA Publications Div., ESTEC, Noordwijk, Netherlands, 120 US dollars or 250 Dutch guilders

Complete polarimetric SAR image data obtained with an L-band system on the San Francisco Bay area were analyzed. Results concerning deviations of amplitude (one-look) images from Rayleigh statistics depending on the terrain type (roughness) and the nature of the polarimetric scattering are shown. The behavior of important polarimetric functions of the scattering matrix versus the terrain texture, e.g., double bounce/corner reflector behavior of the urban area section of the image, is discussed. Physical models describing the observed effects are provided. ESA

N89-12953# Illinois Univ., Chicago. Dept. of Electrical Engineering and Computer Science.
STATISTICAL PROPERTIES OF PHASE DIFFERENCE BETWEEN TWO ORTHOGONALLY-POLARISED SAR SIGNALS **c32**
H. J. Eom and W.-M. Boerner *In* ESA, Proceedings of the 1988 International Geoscience and Remote Sensing Symposium (IGARSS 1988) on Remote Sensing: Moving Towards the 21st Century, Volume 1 Aug. 1988 p 65-66 (For primary document see N89-12936 04-42)
Copyright Avail: NTIS HC A99/MF E03; ESA Publications Div., ESTEC, Noordwijk, Netherlands, 120 US dollars or 250 Dutch guilders

The theoretical behavior of two linearly polarized (VV and HH polarization states) radar backscattered fields is examined statistically. The coherency between two polarized signals is studied in terms of their statistical behavior on phase difference between two signals. The probability density function corresponding to the phase difference between two signals is derived and studied in terms of the degree of polarization, and the variance of each polarized signal. The phase difference is considered with respect to the polarimetric SAR data collected over rugged terrain and ocean. It is found that the phase coherency between two copolarized channels (VV and HH polarizations) strongly depends upon the degree of terrain roughness structure. The degree of polarization is also found to be closely related to terrain/oceanic surface roughness and anisotropy. ESA

N89-12954# Illinois Univ., Chicago. Communications Lab.
ON THE CONCEPT OF THE POLARIMETRIC MATCHED FILTER IN HIGH RESOLUTION RADAR IMAGING: AN ALTERNATIVE FOR SPECKLE RADIATION **c32**
W.-M. Boerner, A. B. Kostinski, and B. D. James *In* ESA, Proceedings of the 1988 International Geoscience and Remote Sensing Symposium (IGARSS 1988) on Remote Sensing: Moving Towards the 21st Century, Volume 1 Aug. 1988 p 69-72 (For primary document see N89-12936 04-42)
Copyright Avail: NTIS HC A99/MF E03; ESA Publications Div., ESTEC, Noordwijk, Netherlands, 120 US dollars or 250 Dutch guilders

The potential of an exclusively polarimetric image filtering approach, i.e., filtering which takes full advantage of the POL-SAR matrix data provided on a pixel-by-pixel basis and which complements the existing scalar speckle reduction techniques, was assessed. The three stage polarimetric optimization procedure search for optimal polarizations on a pixel-by-pixel basis is combined with a subsequent statistical analysis of polarization eigenvectors (versus surface category), and the digital adjustment of polarimetric variables. Results are encouraging. In order to improve the efficiency of the polarimetric filtering method, it must be combined with other image processing and statistical communication theory techniques. Filter efficiency depends critically on peak sharpness of the histograms, and multilook incoherent averaging, block discretization, and nonuniform quantization can be used to improve peakedness. ESA

N89-12955# Karlsruhe Univ. (West Germany). Inst. fuer Hochfrequenztechnik und Elektronik.
POLARIZATION-DEPENDENT ATTENUATION OF DIELECTRIC CYLINDER ARRAYS **c32**
W. Wiesbeck, D. Kaehny, and S. Riegger *In* ESA, Proceedings of the 1988 International Geoscience and Remote Sensing Symposium (IGARSS 1988) on Remote Sensing: Moving Towards the 21st Century, Volume 1 Aug. 1988 p 73-74 (For primary document see N89-12936 04-42)
Copyright Avail: NTIS HC A99/MF E03; ESA Publications Div., ESTEC, Noordwijk, Netherlands, 120 US dollars or 250 Dutch guilders

Land use inventory by remote sensing is reviewed, and the characteristics of the transmitted signal, concerning the polarization dependency as a function of the dielectric properties and the size and orientation of cylinders, are studied. Measurements from 5 to 20 GHz on lossy dielectric cylinders show that transmitted power decreases continuously with frequency. This is due to the increasing reflected power and increasing losses. Transmission attenuation is considerably higher for vertical polarization than for horizontal polarization. Slant linear polarized signals are attenuated accordingly. The resonances, which occur at circumferences of multiples of half a wavelength for dielectric cylinders, are not significant. ESA

N89-12956*# Jet Propulsion Lab., California Inst. of Tech., Pasadena.
THE EFFECTS OF UNDERSAMPLING ON MULTIPOLARIZATION SAR IMAGES **c32**
A. Freeman, P. C. Dubois, and J. D. Klein *In* ESA, Proceedings of the 1988 International Geoscience and Remote Sensing Symposium (IGARSS 1988) on Remote Sensing: Moving Towards

the 21st Century, Volume 1 Aug. 1988 p 75-78 (For primary document see N89-12936 04-42)
Copyright Avail: NTIS HC A99/MF E03; ESA Publications Div., ESTEC, Noordwijk, Netherlands, 120 US dollars or 250 Dutch guilders CSCL 17I

The scattering matrix and Stokes matrix formats for multipolarization synthetic aperture radar (SAR) images are introduced. The effects of converting to the Stokes matrix format, without first doubling the sampling rate to allow for the conversion from a complex to an intensity format is quantified and discussed. It is shown that for most applications the Stokes matrix format is acceptable, since errors introduced by undersampling tend to average out when large numbers of pixels are averaged. For those applications requiring analysis of single image pixels, the scattering matrix format is recommended. ESA

N89-12957# Karlsruhe Univ. (West Germany). Inst. fuer Hochfrequenztechnik und Elektronik.
INTERPRETATION OF COHERENT POLARIMETRIC SIGNATURES BY DIELECTRIC CYLINDER MODELS **c32**
D. Kaehny, S. Riegger, W. Wiesbeck, and A. J. Sieber (Joint Research Centre of the European Communities, Ispra, Italy) *In* ESA, Proceedings of the 1988 International Geoscience and Remote Sensing Symposium (IGARSS 1988) on Remote Sensing: Moving Towards the 21st Century, Volume 1 Aug. 1988 p 79-82 Sponsored in part by the Joint Research Center of the European Communities, Ispra, Italy (For primary document see N89-12936 04-42)
Copyright Avail: NTIS HC A99/MF E03; ESA Publications Div., ESTEC, Noordwijk, Netherlands, 120 US dollars or 250 Dutch guilders

Polarimetric radar cross section theory and measurement for simple coniferous tree models, represented by lossy dielectric cylinders, are compared. The theory uses the principle of linear superposition, neglecting the interactions between different scattering components. The selected polarimetric signatures, the depolarization, and the traces show good agreement between theory and measurement. This verifies that for configurations used, more complex theories for signature interpretation need not be applied. However, single frequency measurement in many cases is not sufficient for signature interpretation. ESA

N89-12958*# National Aeronautics and Space Administration. Goddard Space Flight Center, Greenbelt, Md.
REQUIREMENTS FOR ONGOING DEVELOPMENT OF THE PILOT LAND DATA SYSTEM (PLDS) **c43**
S. W. Wharton and J. A. Newcomer (ST Systems Corp., Lanham, Md.) *In* ESA, Proceedings of the 1988 International Geoscience and Remote Sensing Symposium (IGARSS 1988) on Remote Sensing: Moving Towards the 21st Century, Volume 1 Aug. 1988 p 85-88 Sponsored by NASA, Washington D.C. (For primary document see N89-12936 04-42)
Copyright Avail: NTIS HC A99/MF E03; ESA Publications Div., ESTEC, Noordwijk, Netherlands, 120 US dollars or 250 Dutch guilders CSCL 05B

The Pilot Land Data System being developed to address the information processing needs of the NASA land sciences research community is presented. The objective of the pilot program is to establish a limited-scale, distributed information system for the archival, location, transfer, integration, and manipulation of data across multiple sites connected by a high-speed communications network. Functional capabilities required for users to create, access, and maintain local and distributed data bases containing various types of data in support of land sciences research are summarized. ESA

N89-12959# Reading Univ. (England). NERC Unit for Thematic Information Systems.
THE USE OF REMOTE SENSING IN CONJUNCTION WITH GEOGRAPHIC INFORMATION SYSTEMS FOR LOCAL PLANNING **c43**
N. A. Quarmby, J. L. Cushnie, and J. Smith (National Remote Sensing Centre, Farnborough, England) *In* ESA, Proceedings of the 1988 International Geoscience and Remote Sensing Symposium (IGARSS 1988) on Remote Sensing: Moving Towards the 21st Century, Volume 1 Aug. 1988 p 89-92 (For primary document see N89-12936 04-42)
(Contract NERC-F60/G6/12)
Copyright Avail: NTIS HC A99/MF E03; ESA Publications Div., ESTEC, Noordwijk, Netherlands, 120 US dollars or 250 Dutch guilders

The use of remote sensing and other types of geographic information for local planning purposes is discussed. Perspective views, combining remotely sensed data and digital elevation data, are a useful tool in the decision-making process for housing land supply. Weighting, overlay, and dilation operations were performed on digitized information showing environmental constraints and communication networks to illustrate the ability of a geographic information system to provide alternative solutions to the problem of assessing the potential impact of new housing developments. ESA

N89-12960# Katholieke Universiteit te Leuven (Belgium). Lab. for Land Management.
AN INTEGRATED REMOTE SENSING APPROACH FOR REGIONAL AGROSTATISTICS AND LAND MONITORING **c43**
M. Rockaerts, W. Devos, H. Peeters, H. Eerens, and P. Gombeer *In* ESA, Proceedings of the 1988 International Geoscience and Remote Sensing Symposium (IGARSS 1988) on Remote Sensing: Moving Towards the 21st Century, Volume 1 Aug. 1988 p 93-96 (For primary document see N89-12936 04-42)
Copyright Avail: NTIS HC A99/MF E03; ESA Publications Div., ESTEC, Noordwijk, Netherlands, 120 US dollars or 250 Dutch guilders

Nine satellite images of six different recording dates were merged after radiometric recalibration and geometrical correction to the Belgian Lambert cartographic projection. This multitemporal dataset was classified with a decision tree incorporating single channel level-slicing, different vegetation-indices, and a minimum distance classification algorithm, all based on the recalibrated digital values. Fourteen terrain-classes are distinguished including 10 crops, deciduous and coniferous forest, waterbodies, and urbanization. The classification proves to be in accordance with the data gathered by the National Institute of Statistics. ESA

N89-12961# Eidgenoessische Technische Hochschule, Zurich (Switzerland). Inst. for Communication Technology.
DEVELOPMENT OF A GEOGRAPHIC INFORMATION SYSTEM WITH THE AID OF DIGITAL IMAGE PROCESSING TECHNIQUES **c43**
K. Seidel and M. Keller (Zurich Univ., Switzerland) *In* ESA, Proceedings of the 1988 International Geoscience and Remote Sensing Symposium (IGARSS 1988) on Remote Sensing: Moving Towards the 21st Century, Volume 1 Aug. 1988 p 97-100 Sponsored by the Swiss National Research Council, Berne (For primary document see N89-12936 04-42)
Copyright Avail: NTIS HC A99/MF E03; ESA Publications Div., ESTEC, Noordwijk, Netherlands, 120 US dollars or 250 Dutch guilders

The mutual effects of economic activities, tourism, and land use on the state of the natural system were studied in a test site around Davos, Switzerland. Field work was carried out to yield a reliable data base. The venture covered geomorphology, soil science, climatology, geobotany, forestry, game biology, and landscape history. All spatial information was collected in a geographical information system. Image processing techniques were used to digitize the incoming survey maps and to control the consistency of the data. On the basis of a mathematical model, natural elements such as soil type, vegetation type, agricultural yield, game dispersal, avalanche hazard, etc., were simulated. Several scenarios were investigated showing contrasting concepts for landuse. This results in a series of thematic maps (e.g., productivity, avalanche hazard maps) which can be displayed for interactive examination using digital image processing facilities. ESA

N89-12962# Leeds Univ. (England). School of Geography.
MODELLING LAND RESOURCES WITHIN A PILOT GEOGRAPHICAL INFORMATION SYSTEM **c43**
J. Hogg *In* ESA, Proceedings of the 1988 International Geoscience and Remote Sensing Symposium (IGARSS 1988) on Remote Sensing: Moving Towards the 21st Century, Volume 1 Aug. 1988 p 101-105 (For primary document see N89-12936 04-42)
Copyright Avail: NTIS HC A99/MF E03; ESA Publications Div., ESTEC, Noordwijk, Netherlands, 120 US dollars or 250 Dutch guilders

A pilot geographical information system (GIS) for regional evaluation of land resources is outlined and its scope for modeling is considered in the context of remote sensing of upland vegetation in northern England. The pilot GIS uses a proprietary relational database management system to handle objects abstracted from a spatial database or supplied by users. The spatial database is made up of binary square images encoded and held as linear quadtrees. To illustrate how the pilot GIS is used, spatial and aspatial data are analyzed to identify homogeneous land units for resource management and planning. Different strategies for modeling land resources within such units are outlined using geographic data from digital maps, LANDSAT TM, and climatic records. ESA

N89-12963# Aberdeen Univ. (Scotland). Dept. of Geography.
COMMUNICATION: THE KEY TO INTEGRATING REMOTE SENSING AND GEOGRAPHIC INFORMATION SYSTEMS **c43**
D. R. Green, J. J. vanderSanden, and J. A. T. Young (Edinburgh Univ., Scotland) *In* ESA, Proceedings of the 1988 International Geoscience and Remote Sensing Symposium (IGARSS 1988) on Remote Sensing: Moving Towards the 21st Century, Volume 1 Aug. 1988 p 107-109 (For primary document see N89-12936 04-42)
Copyright Avail: NTIS HC A99/MF E03; ESA Publications Div., ESTEC, Noordwijk, Netherlands, 120 US dollars or 250 Dutch guilders

The need for designers and users of remote sensing and geographic information systems to communicate better to realize the full potential of joint work is discussed. A communication framework is proposed. ESA

N89-12964# Edinburgh Univ. (Scotland). Dept. of Geography.
INTEGRATING REMOTE SENSING DATA INTO A GEOGRAPHICAL INFORMATION SYSTEM: A FOUNDATION FOR RURAL LAND USE STRATEGIES: NATURE CONSERVANCY COUNCIL PROJECT **c43**
R. Healey, P. Dowie, A. Mowle, and J. Holbrook (Natural Environmental Research Council, Edinburgh, Scotland) *In* ESA, Proceedings of the 1988 International Geoscience and Remote Sensing Symposium (IGARSS 1988) on Remote Sensing: Moving Towards the 21st Century, Volume 1 Aug. 1988 p 111-112 (For primary document see N89-12936 04-42)
Copyright Avail: NTIS HC A99/MF E03; ESA Publications Div., ESTEC, Noordwijk, Netherlands, 120 US dollars or 250 Dutch guilders

The development of a geographic information system, and approaches to the integration of digital cartographic and remote sensing data to support this process, are described. Data from available map sources, as well as detailed field survey, combined with LANDSAT TM imagery allow different land use classifications to be assessed at different scales. The possible effects of alternative policies for resolving conflicts of interest in rural development can be examined, including specific problems such as the impact of designating areas as sites of special scientific interest. ESA

N89-12965# Strasbourg Univ. (France).
DATA BASES AND REMOTE SENSING [BASES DE DONNEES ET TELEDETECTION] **c43**
J. F. Dufourd and C. Silber *In* ESA, Proceedings of the 1988 International Geoscience and Remote Sensing Symposium (IGARSS 1988) on Remote Sensing: Moving Towards the 21st Century, Volume 1 Aug. 1988 p 113-114 In FRENCH (For primary document see N89-12936 04-42)
Copyright Avail: NTIS HC A99/MF E03; ESA Publications Div., ESTEC, Noordwijk, Netherlands, 120 US dollars or 250 Dutch guilders

The design of a data base for remote sensing is discussed. Definition of the role and limits of the base; types of data; and functional design are considered. ESA

N89-12966# Reading Univ. (England).
AN INTERNATIONAL APPROACH TO GIS BASED ON REMOTE SENSING AND TERRAIN CLASSIFICATION **c43**
C. W. Mitchell *In* ESA, Proceedings of the 1988 International Geoscience and Remote Sensing Symposium (IGARSS 1988) on Remote Sensing: Moving Towards the 21st Century, Volume 1 Aug. 1988 p 117-118 (For primary document see N89-12936 04-42)
Copyright Avail: NTIS HC A99/MF E03; ESA Publications Div., ESTEC, Noordwijk, Netherlands, 120 US dollars or 250 Dutch guilders

Geographic information systems (GIS) which emphasize environmental data based on remote sensing are discussed. The use of terrain units, recognizable on remotely sensed imagery, as a framework offers a number of advantages, including ready comprehensibility, economy, applicability to different disciplines, mapping scales and technological levels, a capability for self-refinement, and a recognition of analogs between different areas. The UK, the Middle East, and North Africa provide examples of the method. An outline design for linked national and international GIS is proposed. ESA

N89-12967# Leeds Univ. (England). School of Geography.
ANALYSIS OF POTATO CROP DISTRIBUTION USING REMOTELY SENSED AND ENVIRONMENTAL DATA IN A PILOT GEOGRAPHICAL INFORMATION SYSTEM **c43**
N. Stuart, J. Hogg, G. G. Wright, and J. G. Morrice (MacAulay Land Use Research Inst., Aberdeen, Scotland) *In* ESA, Proceedings of the 1988 International Geoscience and Remote Sensing Symposium (IGARSS 1988) on Remote Sensing: Moving Towards the 21st Century, Volume 1 Aug. 1988 p 119-124 (For primary document see N89-12936 04-42)
Copyright Avail: NTIS HC A99/MF E03; ESA Publications Div., ESTEC, Noordwijk, Netherlands, 120 US dollars or 250 Dutch guilders

Use of geographic information systems (GIS) to predict production of potato crops in Scotland is described. To quantify the extent to which the crop may be subject to drought stress, soil types and soil water deficits in the potato growing areas were studied. In the light of results obtained using raster images, the potential of a pilot GIS is assessed for the inventory and analysis of the potato crop distribution. Spatial and statistical analyses are used to describe and measure associations between the presence of crop and a range of environmental conditions. These relationships can be explored interactively, used to describe and explain crop distribution, and as the basis of predictive models of crop suitability or drought risk. ESA

N89-12968# Ecole Nationale Superieure des Telecommunications, Brest (France). Groupe Traitement d'Images.
SPECTRAL ANALYSIS OF OCEAN WAVE IMAGERY USING 2-D LINEAR PREDICTION **c48**
C. Cariou, J.-M. Boucher, C. Roux, and P. Larouche (Institut Maurice Lamontagne, Mont-Joli, Quebec) *In* ESA, Proceedings of the 1988 International Geoscience and Remote Sensing Symposium (IGARSS 1988) on Remote Sensing: Moving Towards the 21st Century, Volume 1 Aug. 1988 p 127-130 (For primary document see N89-12936 04-42)
Copyright Avail: NTIS HC A99/MF E03; ESA Publications Div., ESTEC, Noordwijk, Netherlands, 120 US dollars or 250 Dutch guilders

A method for spectral estimation based on 2-D linear prediction for the determination of wavelength and propagation direction of

swell fields given by Seasat synthetic aperture radar (SAR) and SPOT imaging is presented. The method is shown to provide interesting results when compared to classical Fourier analysis. It allows the estimation of wavelength and propagation direction over small analysis windows (up to 400 sqm) and makes possible the analysis of nonstationary phenomena such as waves refracted by bathymetry or internal waves. ESA

N89-12969# Johns Hopkins Univ., Laurel, Md. Applied Physics Lab.
ON THE USE OF SPECKLE STATISTICS FOR THE EXTRACTION OF OCEAN WAVE SPECTRA FROM SAR IMAGERY **c48**
F. M. Monaldo *In* ESA, Proceedings of the 1988 International Geoscience and Remote Sensing Symposium (IGARSS 1988) on Remote Sensing: Moving Towards the 21st Century, Volume 1 Aug. 1988 p 133-136 (For primary document see N89-12936 04-42)
Copyright Avail: NTIS HC A99/MF E03; ESA Publications Div., ESTEC, Noordwijk, Netherlands, 120 US dollars or 250 Dutch guilders

The effects of speckle noise on a synthetic aperture radar (SAR) image spectrum and the necessity for accounting for speckle noise in calibrating ocean wave height-variance spectra derived from SAR imagery are discussed. Speckle noise complicates the procedure of estimating wave slope and height variance spectra from SAR imagery. The incorrect compensation for the speckle noise floor in SAR image spectra causes errors in the total level of ocean wave height or slope-variance estimates from SAR imagery. To alleviate this problem, it is proposed that high resolution SAR ocean wave imagery be averaged to reduced speckle noise. A moderate amount of averaging leaves sufficient resolution to image typical ocean surface waves, but still very significantly reduces speckle noise and its attendant problems. ESA

N89-12970# Forut, Tromsoe (Norway).
OCEAN WAVE NUMBER SPECTRA AND SPATIAL AUTOCORRELATION FUNCTIONS FROM SAR IMAGES **c48**
H. Johnsen, T. Eltoft, and S. Jacobsen (Tromsoe Univ., Norway) *In* ESA, Proceedings of the 1988 International Geoscience and Remote Sensing Symposium (IGARSS 1988) on Remote Sensing: Moving Towards the 21st Century, Volume 1 Aug. 1988 p 137-140 (For primary document see N89-12936 04-42)
Copyright Avail: NTIS HC A99/MF E03; ESA Publications Div., ESTEC, Noordwijk, Netherlands, 120 US dollars or 250 Dutch guilders

Optimal estimates of the directional long gravity ocean wavenumber spectra were computed from digitally processed X and L-band synthetic aperture radar (SAR) images. An unspeckled estimate of the ocean wave spectrum was obtained from the speckled image spectrum. By performing an inverse Fourier transformation on the wave spectrum, an estimate of the long gravity ocean wave autocorrelation is obtained. For near range traveling waves, the main peak of the wave spectrum is in good agreement with in-situ measured swell wavelength. The direction of propagation (azimuth angle) however, is 15 percent larger than the in-situ measured swell direction. This may be caused by the loss of azimuth resolution caused by the motion of the scatterer. In the case of azimuth traveling waves, no imaging of waves is observed in the X or in the L-band under the present sea conditions. A combination of nonlinear imaging and loss of azimuth resolution may explain the observations. ESA

N89-12971# Canada Centre for Remote Sensing, Ottawa (Ontario). RADARSAT Project Office.
SAR-SEEN MULTIMODE WAVES IN ICE: EVIDENCE OF IMAGING NONLINEARITIES **c48**
R. K. Raney and P. W. Vachon *In* ESA, Proceedings of the 1988 International Geoscience and Remote Sensing Symposium (IGARSS 1988) on Remote Sensing: Moving Towards the 21st Century, Volume 1 Aug. 1988 p 141-144 (For primary document see N89-12936 04-42)
Copyright Avail: NTIS HC A99/MF E03; ESA Publications Div., ESTEC, Noordwijk, Netherlands, 120 US dollars or 250 Dutch guilders

A two dimensional wave field analytic model based on the synthetic aperture radar (SAR) velocity bunching mechanism that is extended to the multi-modal case and includes the effects of wave component translation between looks is discussed. Using this model, directional spectra results are presented for a bimodal sea. As significant wave height is increased, the image spectra evolve from the correct bimodal form through suppression of the correct modes to creation of a new and dominant spectral artifact propagating at approximately 90 deg to the true wave direction. The simulated wave images compare favorably to actual imagery of waves in ice from the LIMEX/LEWEX 87 EXPERIMENT using similar radar, viewing geometry, and wave parameters. It is concluded that coherence time limitation is beneficial, as it expands the effective linear domain of the SAR imaging process. ESA

N89-12972# Oceanor, Trondheim (Norway).
AN INTERCOMPARISON OF SAR AND BUOY DIRECTIONAL WAVE SPECTRA FROM THE LABRADOR SEA EXTREME WAVES EXPERIMENT (LEWEX) **c48**
H. E. Krogstad and R. B. Olsen *In* ESA, Proceedings of the 1988 International Geoscience and Remote Sensing Symposium (IGARSS 1988) on Remote Sensing: Moving Towards the 21st Century, Volume 1 Aug. 1988 p 147-148 (For primary document see N89-12936 04-42)
Copyright Avail: NTIS HC A99/MF E03; ESA Publications Div., ESTEC, Noordwijk, Netherlands, 120 US dollars or 250 Dutch guilders

The Labrador Sea Extreme Waves Experiment (LEWEX) provided an opportunity to compare several airborne remote sensing and in situ wave measuring instruments. Comparisons of C-band synthetic aperture radar (SAR) data with measurements from a heave/pitch/roll buoy are discussed. A method for modifying the buoy data to provide spectra which are equivalent to those expected from an ideal airborne scanning instrument is suggested. Scanning distortion is demonstrated to have a significant effect on the appearance of the spectra. Directional distributions for different wavelengths indicate a fair agreement between the two instruments. However, components in the SAR spectra are not identified in the buoy spectra. ESA

N89-12973# Johns Hopkins Univ., Laurel, Md. Applied Physics Lab.
DIRECTIONAL OCEAN WAVE SPECTRA: PROSPECTS FOR ACQUIRING A GLOBAL DATA BASE FROM SIR-C **c48**
R. C. Beal, J. L. MacArthur, F. M. Monaldo, and S. F. Oden *In* ESA, Proceedings of the 1988 International Geoscience and Remote Sensing Symposium (IGARSS 1988) on Remote Sensing: Moving Towards the 21st Century, Volume 1 Aug. 1988 p 149-150 (For primary document see N89-12936 04-42)
Copyright Avail: NTIS HC A99/MF E03; ESA Publications Div., ESTEC, Noordwijk, Netherlands, 120 US dollars or 250 Dutch guilders

Use of SIR-C to collect directional ocean wave spectra over global scales is discussed. The very low shuttle range-to-velocity ratio will allow the synthetic aperture radar (SAR) to image ocean waves that are reasonably undistorted by Doppler motion blur in the azimuth direction. To take advantage of this opportunity, an experimental on-board processor which, if continually activated below 30S, will provide more than 100,000 directional spectral estimates over a 5 day interval will be implemented. This data base may be sufficiently dense in space and time (one 7 km x 7 km sample per second) to allow a fairly accurate reconstruction of a time-space history of the directional wave spectrum over the entire southern ocean. ESA

N89-12974# Johns Hopkins Univ., Laurel, Md. Applied Physics Lab.
THE LABRADOR SEA EXTREME WAVES EXPERIMENT: OBJECTIVES, STATUS AND PLANS **c48**
R. C. Beal and T. W. Gerling *In* ESA, Proceedings of the 1988

International Geoscience and Remote Sensing Symposium (IGARSS 1988) on Remote Sensing: Moving Towards the 21st Century, Volume 1 Aug. 1988 p 151-154 (For primary document see N89-12936 04-42)
Copyright Avail: NTIS HC A99/MF E03; ESA Publications Div., ESTEC, Noordwijk, Netherlands, 120 US dollars or 250 Dutch guilders

The Labrador Sea Extreme Waves Experiment (LEWEX) is an international effort to assess method of measuring and modeling the directional aspects of wind-generated ocean waves, especially their evolution in the presence of rapidly turning winds. The main data-gathering period of LEWEX occurred from 13 through 19 March 1987, and was supported by a large number of ship and aircraft-based estimates of the directional wave spectrum. Directional spectra were forecast by first, second, and third generation wave models (using their own separately determined wind fields) and will be hindcast by these same models (using a common wind field). A final consensus wind field history may be synthesized by iteration, using a consensus wave field history.
ESA

N89-12975# Ministry of Posts and Telecommunications, Tokyo (Japan). Communications Research Lab.
INFERENCE OF RADIO SCATTERING PARAMETERS OF ANTARCTIC ICE SHEET USING 179 MHz AIRBORNE RADIO ECHO SOUNDING DATA **c32**
S. Uratsuka, F. Nishio, H. Ohmae, and S. Mae (Hokkaido Univ., Sapporo, Japan) *In* ESA, Proceedings of the 1988 International Geoscience and Remote Sensing Symposium (IGARSS 1988) on Remote Sensing: Moving Towards the 21st Century, Volume 1 Aug. 1988 p 157-160 (For primary document see N89-12936 04-42)
Copyright Avail: NTIS HC A99/MF E03; ESA Publications Div., ESTEC, Noordwijk, Netherlands, 120 US dollars or 250 Dutch guilders

Characteristics of radio wave scattering of Antarctic ice sheet are inferred from the 179 MHz airborne radio echo sounding data. The A-scope data from the sounder with wide beam antennas include information on the scattering characteristics at the air/ice interface, at the inner region of the ice sheet, and at the ice/bedrock interface. These characteristics are derived from the A-scope form by using expanded radar equations. These parameters are available to survey the roughness of the air/ice interface of the ice sheet and ice/bedrock the interface, and the temperature of inner regions of the ice sheet.
ESA

N89-12976# Scott Polar Research Inst., Cambridge (England).
TOPOGRAPHIC EFFECTS ON LIGHT SCATTERING FROM SNOW **c43**
W. G. Rees and J. A. Dowdeswell (University Coll. of Wales, Aberystwyth.) *In* ESA, Proceedings of the 1988 International Geoscience and Remote Sensing Symposium (IGARSS 1988) on Remote Sensing: Moving Towards the 21st Century, Volume 1 Aug. 1988 p 161-164 (For primary document see N89-12936 04-42)
Copyright Avail: NTIS HC A99/MF E03; ESA Publications Div., ESTEC, Noordwijk, Netherlands, 120 US dollars or 250 Dutch guilders

The influence of surface topography on the appearance of a LANDSAT image of a snow-covered ice surface is quantitatively assessed. The correlation of pixel brightness against surface slope (parallel to the solar azimuth) is shown to be 0.8 to 0.9. The accuracy with which this correlation allows surface slope to be deduced from the LANDSAT image is 0.5 deg. The possibility of using this correlation to deduce surface topography from a satellite image is investigated. A theoretical model was developed, and its application to the LANDSAT data gives typical errors of 100m, although when nearest-neighbor smoothing is applied this is reduced to 40m. The most likely applications of the methods, and the surface truth requirements of each of them are discussed.
ESA

N89-12977# Scott Polar Research Inst., Cambridge (England).
SYNTHETIC APERTURE RADAR OVER TERRESTRIAL ICE **c32**
W. G. Rees *In* ESA, Proceedings of the 1988 International Geoscience and Remote Sensing Symposium (IGARSS 1988) on Remote Sensing: Moving Towards the 21st Century, Volume 1 Aug. 1988 p 165-168 (For primary document see N89-12936 04-42)
Copyright Avail: NTIS HC A99/MF E03; ESA Publications Div., ESTEC, Noordwijk, Netherlands, 120 US dollars or 250 Dutch guilders

The physical properties of snow and ice near the surface of a terrestrial ice mass are reviewed, and surface and volume scattering models are discussed. Synthetic aperture radar (SAR) images are presented to support the conclusion that it is difficult to do more than distinguish ice-covered and ice-free areas from a SAR image. Nevertheless, even this may be useful. It may in future be possible to use SAR data to distinguish, without ambiguity, bare ice, dry and wet snow cover, but before this end can be attained much experimental work must be performed. The possible adverse effects of ionospheric irregularities on the formation of SAR images are noted.
ESA

N89-12978# British Aerospace Public Ltd. Co., Bristol (England). Space and Communications Div.
EUROPEAN REMOTE SENSING SATELLITE PLATFORMS FOR THE 1990'S **c18**
P. Truss *In* ESA, Proceedings of the 1988 International Geoscience and Remote Sensing Symposium (IGARSS 1988) on Remote Sensing: Moving Towards the 21st Century, Volume 1 Aug. 1988 p 171-174 (For primary document see N89-12936 04-42)
Copyright Avail: NTIS HC A99/MF E03; ESA Publications Div., ESTEC, Noordwijk, Netherlands, 120 US dollars or 250 Dutch guilders

Requirements and constraints on a polar orbiting remote sensing system are reviewed. It is concluded that a series of 2 ton payload multi-mission platforms achieve the defined objectives.
ESA

N89-12979# New South Wales Univ., Kensington (Australia). Dept. of Electrical Engineering.
AUSTRALIAN PREPARATIONS FOR THE POLAR PLATFORM **c18**
J. A. Richards, J. Kingwell, and K. N. OSullivan (CRA Exploration Proprietary Ltd., Fyshwick, Australia) *In* ESA, Proceedings of the 1988 International Geoscience and Remote Sensing Symposium (IGARSS 1988) on Remote Sensing: Moving Towards the 21st Century, Volume 1 Aug. 1988 p 177-178 (For primary document see N89-12936 04-42)
Copyright Avail: NTIS HC A99/MF E03; ESA Publications Div., ESTEC, Noordwijk, Netherlands, 120 US dollars or 250 Dutch guilders

Australian preparations for the Polar Platform era are described in relation to plans being formulated to ensure effective data acquisition and dissemination, advice given to the user community, and proposals submitted in response to Announcements of Opportunity. The deliberations and recommendations of a study group, established to act as a focus for Australian and New Zealand involvement are reviewed.
ESA

N89-12980# National Space Development Agency, Tokyo (Japan).
RESULTS OF ADVANCED EARTH OBSERVING SATELLITE (ADEOS) CONCEPTUAL STUDY **c12**
N. Hara, M. Homma, T. Igarashi, A. Tsuiki, and K. Ohta *In* ESA, Proceedings of the 1988 International Geoscience and Remote Sensing Symposium (IGARSS 1988) on Remote Sensing: Moving Towards the 21st Century, Volume 1 Aug. 1988 p 179-182 (For primary document see N89-12936 04-42)
Copyright Avail: NTIS HC A99/MF E03; ESA Publications Div., ESTEC, Noordwijk, Netherlands, 120 US dollars or 250 Dutch guilders

The results of the conceptual study on the Advanced Earth

Observing Satellite (ADEOS), particularly the mission operation concept, are reviewed. The ADEOS is viewed as an intermediate step between ERS-1 (Japan) and the technically more sophisticated Japanese Polar Platform. The Earth observation system centering around ADEOS involves a data relay and tracking satellite to provide a time rate of link visibility of 72 percent instead of 3.1 percent in the case of support by one ground station in Japan. This corresponds to the number of global coverages every year, 9 times for land cover with high spatial resolution, and 122 times for the ocean elated sensor with 1500km in swath width. ESA

N89-12981# National Space Development Agency, Ohashi (Japan).
REQUIREMENTS FOR THE ADVANCED EARTH OBSERVING SATELLITE (ADEOS) ORBIT, ORBIT AND A ATTITUDE CONTROL, AND RATE JITTER **c18**
K. Arai *In* ESA, Proceedings of the 1988 International Geoscience and Remote Sensing Symposium (IGARSS 1988) on Remote Sensing: Moving Towards the 21st Century, Volume 1 Aug. 1988 p 183-186 (For primary document see N89-12936 04-42)
Copyright Avail: NTIS HC A99/MF E03; ESA Publications Div., ESTEC, Noordwijk, Netherlands, 120 US dollars or 250 Dutch guilders

The Advanced Earth Observing Satellite: (ADEOS) orbit was determined from the subcycle period for Ocean Color and Temperature Scanner: (OCTS) onboard ADEOS with swath width of 1400 km and side-lapping condition for the Advanced Visible and Near Infrared Radiometer with swath width of 80 km. The requirements for the orbit and attitude control were also determined from how to keep the recurrency of the satellite orbit and its accuracy. Pointing accuracy, geometric distortion and degradation of modulation transfer function were determined through a rate jitter analysis. ESA

N89-12982*# National Aeronautics and Space Administration. Goddard Space Flight Center, Greenbelt, Md.
GEODYNAMICS LASER RANGING SYSTEM: PERFORMANCE SIMULATIONS AND DEVELOPMENT OF THE EOS FACILITY **c36**
S. C. Cohen *In* ESA, Proceedings of the 1988 International Geoscience and Remote Sensing Symposium (IGARSS 1988) on Remote Sensing: Moving Towards the 21st Century, Volume 1 Aug. 1988 p 187-189 (For primary document see N89-12936 04-42)
Copyright Avail: NTIS HC A99/MF E03; ESA Publications Div., ESTEC, Noordwijk, Netherlands, 120 US dollars or 250 Dutch guilders CSCL 20E

The NASA Geodynamics Laser Ranging System is a spaceborne multicolor laser ranger to be used for studying regional and local scale crustal movements and will provide a capability for height profiling of ice-sheets, land terrains, cloud-tops, and other surfaces. Ranging measurements to retroreflector targets will produce intersite distances and relative heights with subcentimeter accuracy over baselines up to several hundred kilometers long. Arrays containing up to a few hundred targets can be surveyed nearly simultaneously. Altimetric profiling can be performed with spatial resolution of 80m and vertical accuracy of 10cm with the latter depending on the roughness and slope of the terrain. ESA

N89-12983# Marconi Space and Defence Systems Ltd., Portsmouth (England). Remote Sensing and Science Div.
ON-ORBIT SERVICING AND COST EFFECTIVENESS OF COLUMBUS POLAR PLATFORM CONCEPTS **c12**
R. G. W. Hathaway *In* ESA, Proceedings of the 1988 International Geoscience and Remote Sensing Symposium (IGARSS 1988) on Remote Sensing: Moving Towards the 21st Century, Volume 1 Aug. 1988 p 191-194 (For primary document see N89-12936 04-42)
Copyright Avail: NTIS HC A99/MF E03; ESA Publications Div., ESTEC, Noordwijk, Netherlands, 120 US dollars or 250 Dutch guilders

Payload servicing of a 17-instrument Polar Platform complement is determined from the available design data, reliability of the platform subsystems, and the servicing interval of each component. On-orbit and ground servicing analytical background and cost modeling are summarized. The most suitable grouping of the scientific and commercially biased instruments and their servicing needs is discussed. It is suggested that dedicated platforms are more cost effective in terms of servicing lifetime. The Orbital Replacement Unit philosophy is considered and its effect on basic design concepts are reflected in the robotic and extra vehicular activity approach. ESA

N89-12984*# National Aeronautics and Space Administration. Goddard Space Flight Center, Greenbelt, Md.
PIPS: A PROCEDURE FOR INTERACTIVE PYRAMID SEGMENTATION **c43**
S. W. Wharton *In* ESA, Proceedings of the 1988 International Geoscience and Remote Sensing Symposium (IGARSS 1988) on Remote Sensing: Moving Towards the 21st Century, Volume 1 Aug. 1988 p 197-200 Sponsored by the Director's Discretionary Fund, Greenbelt, Md. (For primary document see N89-12936 04-42)
Copyright Avail: NTIS HC A99/MF E03; ESA Publications Div., ESTEC, Noordwijk, Netherlands, 120 US dollars or 250 Dutch guilders CSCL 08B

The Procedure for Interactive Pyramid Segementation was designed to identify regions of spatially connected and spectrally homogeneous pixels in multispectral image data, and to allow these regions to be interactively manipulated without the use of processing parameters. The objective is to provide the user with the capability to easily extract and identify regions corresponding to target objects of interest. The approach is to segment a multispectral image into a set of regions and to allow the analyst to interactively refine the segmentation by direct manipulation. The user can elect to: interactively display maps of the spatial distribution of regions for any designated image subset; display the statistics of a given region; and label, merge, or split regions. ESA

N89-12985# North Carolina Univ., Raleigh.
MULTITEMPORAL RESOURCE COMPLEX ANALYSIS OF CATINIA PROVINCE, ITALY FROM LANDSAT-TM DATA **c43**
S. Khorram, J. Brockhaus, and A. Gerachi (Catania Univ., Italy) *In* ESA, Proceedings of the 1988 International Geoscience and Remote Sensing Symposium (IGARSS 1988) on Remote Sensing: Moving Towards the 21st Century, Volume 1 Aug. 1988 p 201-204 (For primary document see N89-12936 04-42)
Copyright Avail: NTIS HC A99/MF E03; ESA Publications Div., ESTEC, Noordwijk, Netherlands, 120 US dollars or 250 Dutch guilders

Thematic Mapper (TM) digital data were used to analyze a multiresource complex. Nineteen Anderson (USGS) Level 1, 2, and 3 land use/land cover types were studied and mapped. Spectral signatures characterizing the land use/land cover types were generated through interactive guided clustering of training sites representative of these types. Editing of the signatures resulted in 55 clusters being required to represent the 19 cover types of interest. Raw TM digital data were assigned to the land use/land cover types with a minimum distance to means classifier. The patterns seen in the classified image seem to correspond to those observed in the field. ESA

N89-12986# Karlsruhe Univ. (West Germany). Inst. fuer Photogrammetrie und Fernerkundung.
LARGE AREA TM LAND COVER CLASSIFICATION OF MITTLERER OBERRHEIN COUNTY, SOUTHWEST GERMANY, AND ITS USE FOR REGIONAL PLANNING AND CROP SURVEYS **c43**
C. Schmullius *In* ESA, Proceedings of the 1988 International Geoscience and Remote Sensing Symposium (IGARSS 1988) on Remote Sensing: Moving Towards the 21st Century, Volume 1 Aug. 1988 p 207-210 (For primary document see N89-12936 04-42)

Copyright Avail: NTIS HC A99/MF E03; ESA Publications Div., ESTEC, Noordwijk, Netherlands, 120 US dollars or 250 Dutch guilders

The spectral problems of classifying a whole, geographically very heterogenic county were investigated. A map is presented and its use for regional planning and crop surveys discussed. The influence of three distinctive natural regions on the phenological situation of six different crop types is demonstrated. Diagrams show how the dynamics of crop development differ due to varying locations. Differences in reflections of one crop type in several training sites are illustrated in histograms. Classification results are compared to official land inventory statistics. It is concluded that the classification is of little use for such a large area, but the mapping possibilities are interesting. ESA

N89-12987# Liege Univ. (Belgium). Dept. of Geography.
TOWARDS AN URBAN LAND-USE CLASSIFICATION USING TEXTURAL AND MORPHOLOGICAL CRITERIA **c43**
Y. Baudot, I. Nadasdi, and J.-P. Donnay *In* ESA, Proceedings of the 1988 International Geoscience and Remote Sensing Symposium (IGARSS 1988) on Remote Sensing: Moving Towards the 21st Century, Volume 1 Aug. 1988 p 211-212 (For primary document see N89-12936 04-42)
Copyright Avail: NTIS HC A99/MF E03; ESA Publications Div., ESTEC, Noordwijk, Netherlands, 120 US dollars or 250 Dutch guilders

The use of satellite data to provide land use maps suitable for urban planners is discussed. Spatial resolutions of civilian satellites are not adapted to the complexity of urban milieu. A land use does not correspond to a specific spectral signature; thus a classification of land uses cannot be reached only by means of radiometric information, but requires morphological and topological elements, in a way inspired by the proceses involved in visual interpretation of aerial photographs. ESA

N89-12988# Kingston Polytechnic, Kingston-Upon-Thames (England). School of Geography.
THE DETECTION OF UNIMPROVED GRASSLAND IN BERKSHIRE USING A BINARY DECISION TREE APPROACH **c43**
N. M. Trodd and A. J. Morton (Imperial Coll. of Science and Technology, London, England) *In* ESA, Proceedings of the 1988 International Geoscience and Remote Sensing Symposium (IGARSS 1988) on Remote Sensing: Moving Towards the 21st Century, Volume 1 Aug. 1988 p 213-214 (For primary document see N89-12936 04-42)
Copyright Avail: NTIS HC A99/MF E03; ESA Publications Div., ESTEC, Noordwijk, Netherlands, 120 US dollars or 250 Dutch guilders

In order to detect unimproved grassland, a binary discard decision tree method of classification was used to target this land cover. The flexibility of the algorithm allowed multidate LANDSAT-TM data to be incorporated into the best practical method. Per-field criteria show more promise than per-pixel to discriminate unimproved from improved grassland. The results are compatible with, but do not mimic, existing ecological survey procedures and should enhance a regional detection strategy. ESA

N89-12989# National Inst. for Environmental Studies, Tsukuba (Japan).
DETECTION OF SEASONAL AND LONG-TERM CHANGES IN LAND COVER FROM MULTITEMPORAL LANDSAT MSS DATA **c43**
T. Yokota and Y. Matsumoto *In* ESA, Proceedings of the 1988 International Geoscience and Remote Sensing Symposium (IGARSS 1988) on Remote Sensing: Moving Towards the 21st Century, Volume 1 Aug. 1988 p 215-216 (For primary document see N89-12936 04-42)
Copyright Avail: NTIS HC A99/MF E03; ESA Publications Div., ESTEC, Noordwijk, Netherlands, 120 US dollars or 250 Dutch guilders

Procedures for detecting changes in land cover by using multitemporal LANDSAT MSS data were developed and tested, to detect seasonal changes and long-term changes in land cover. Four observation dates by LANDSAT were selected in spring and winter at an interval of 7 or 8 yr. Four bands of MSS were used for each date. The CCT values were transformed to the values comparable to spectral reflectances by using references. The change detection procedures proposed use no training data, and are preclassification methods. In one procedure spectral differences are calculated at each pixel between every two dates out of four by using a Euclidean distance norm of the four band data. From these norms the spectral changes among the four dates are checked in every pixel, and seasonal and long-term changes are detected. The principal component procedure is also tested. Results are variable. ESA

N89-12990# Kingston Polytechnic, Kingston-Upon-Thames (England). School of Geography.
CROP CLASSIFICATION WITH MULTI-TEMPORAL X-BAND SAR DATA **c43**
G. M. Foody, P. J. Curran, G. B. Groom, and D. C. Munro (Hawaii Univ., Manoa.) *In* ESA, Proceedings of the 1988 International Geoscience and Remote Sensing Symposium (IGARSS 1988) on Remote Sensing: Moving Towards the 21st Century, Volume 1 Aug. 1988 p 217-220 (For primary document see N89-12936 04-42)
Copyright Avail: NTIS HC A99/MF E03; ESA Publications Div., ESTEC, Noordwijk, Netherlands, 120 US dollars or 250 Dutch guilders

Multitemporal X-band HH polarized synthetic aperture radar data were used to classify crop type. Prior to the classification, the influence of non-crop variables on crop separability were evaluated. While the influence of the soil moisture content was unimportant, the data sets had to be radiometrically corrected and intercalibrated. A per-field classification of these data enables the 3 main crop types of the test site to be classified with accuracies approaching 90 percent when the complete multitemporal data set acquired four data is used. Comparable levels of accuracy can, however, be obtained from the use of data recorded on only two of the four dates. ESA

N89-12991# Rothamsted Experimental Station, Harpenden (England).
SPATIAL RESOLUTION FOR REMOTE SENSING OF FOREST PLANTATIONS **c43**
P. M. Atkinson and F. M. Danson (Sheffield Univ., England) *In* ESA, Proceedings of the 1988 International Geoscience and Remote Sensing Symposium (IGARSS 1988) on Remote Sensing: Moving Towards the 21st Century, Volume 1 Aug. 1988 p 221-223 Sponsored by the Natural Environment Research Council, London, United Kingdom (For primary document see N89-12936 04-42)
Copyright Avail: NTIS HC A99/MF E03; ESA Publications Div., ESTEC, Noordwijk, Netherlands, 120 US dollars or 250 Dutch guilders

The optimum spatial resolution for the collection of remotely sensed data of forest plantations was determined by modeling the spatial dependence in high resolution airborne multispectral scanner (MSS) data. It is shown that spatial dependence is present in coniferous and oak plantations and that the range is related to the stand age and species. Three methodologies for determining the optimum spatial resolution using the semivariance at lag one (gamma (h=1) max) are discussed. The method provides an approximation of this statistic but where it is possible to estimate (h=1)max by degrading the image a sound and tractable estimate of the optimum resolution is be obtained. Further work is required to investigate the precision of estimates obtained by regularization of the semi-variogram. ESA

N89-12992*# National Aeronautics and Space Administration. Goddard Space Flight Center, Greenbelt, Md.
AN ALGORITHM TO DERIVE PRECIPITATION PROFILES FROM A DOWNWARD VIEWING RADAR AND A MULTIFREQUENCY PASSIVE RADIOMETER **c47**

J. A. Weinman, C. D. Kummerow, and C. S. Atwater (Applied Research Corp., Landover, Md.) *In* ESA, Proceedings of the 1988 International Geoscience and Remote Sensing Symposium (IGARSS 1988) on Remote Sensing: Moving Towards the 21st Century, Volume 1 Aug. 1988 p 229-234 (For primary document see N89-12936 04-42)
Copyright Avail: NTIS HC A99/MF E03; ESA Publications Div., ESTEC, Noordwijk, Netherlands, 120 US dollars or 250 Dutch guilders CSCL 04B

An algorithm that yields a robust solution of the radar equation subjected to constraints imposed by measurements of dual polarized, multifrequency microwave radiances is developed. Using simulated data, it is shown that this algorithm generates retrieved hydrometeor profiles that overcome limitations of the radar retrievals introduced by noise and ambiguities in the phase of the hydrometeors. ESA

N89-12993# Rutherford High Energy Lab., Chilton (England).
CROSS-POLAR RADAR MEASUREMENTS IN ICE AND RAIN **c47**
J. F. W. Goddard, S. M. Cherry, and K. Holloway *In* ESA, Proceedings of the 1988 International Geoscience and Remote Sensing Symposium (IGARSS 1988) on Remote Sensing: Moving Towards the 21st Century, Volume 1 Aug. 1988 p 235-236 (For primary document see N89-12936 04-42)
Copyright Avail: NTIS HC A99/MF E03; ESA Publications Div., ESTEC, Noordwijk, Netherlands, 120 US dollars or 250 Dutch guilders

Linear cross-polar measurements to characterize hydrometeor types and size distributions were made using a 3 GHz radar. Different hydrometeor phases are clearly distinguished, and tight limits can be put on the degree of canting present in different conditions, by comparisons with theoretical modeling of cross-polar and copolar characteristics. ESA

N89-12994# Essex Univ., Colchester (England). Dept. of Mathematics.
SOME ADVANTAGES OF USING POLARISATION DIVERSITY ILLUSTRATED THROUGH THE ANALYSIS OF RADAR DATA FROM A STORM IN CENTRAL ALBERTA (CANADA) **c47**
A. R. Holt, R. G. Humphries (MacDonald, Dettwiler and Associates Ltd., Richmond, British Columbia), and B. McGuinness *In* ESA, Proceedings of the 1988 International Geoscience and Remote Sensing Symposium (IGARSS 1988) on Remote Sensing: Moving Towards the 21st Century, Volume 1 Aug. 1988 p 237-240 (For primary document see N89-12936 04-42)
(Grant SERC-GR/E/27164)
Copyright Avail: NTIS HC A99/MF E03; ESA Publications Div., ESTEC, Noordwijk, Netherlands, 120 US dollars or 250 Dutch guilders

The advantages of using polarization-diversity in ground-based radar remote sensing of storms is illustrated using data from an S band circular depolariztion ratio radar. It is shown that the polarization can identify precipitation regions containing ice. It also identifies clear-air effects. These effects include a line-echo which appears to be coincident with the passage of a cold front. Possible mechanisms for the observed scatter are discussed. ESA

N89-12995# Manchester Coll. of Science and Technology (England). Dept. of Pure and Applied Physics.
DUAL LINEAR POLARISATION TIME SERIES AS AN AID TO HYDROMETEOR IDENTIFICATION **c47**
I. J. Caylor and A. J. Illingworth *In* ESA, Proceedings of the 1988 International Geoscience and Remote Sensing Symposium (IGARSS 1988) on Remote Sensing: Moving Towards the 21st Century, Volume 1 Aug. 1988 p 241-242 (For primary document see N89-12936 04-42)
(Grants NERC-GR3/5896; AF-AFOSR-0121-88)
Copyright Avail: NTIS HC A99/MF E03; ESA Publications Div., ESTEC, Noordwijk, Netherlands, 120 US dollars or 250 Dutch guilders

Radar observations of precipitation particles using a polarization parameter, p(H,V), which is the correlation of the time series of ZH and ZV (the radar reflectivity factors measured with horizontal and vertical polarization) are presented. Parameter p(H,V) is very close to unity in most precipitation. In stratiform precipitation, low values of p(H,V) are found only in the melting layer, and so may be used as a simple means of identifying the bright band. It is suggested that in convective clouds, p(H,V) is low only where hailstones are large enough to enter the Mie scattering region. Observations are made at S band, but, because p(H,V) should be little affected by propagation problems, the technique could be implemented at shorter wavelengths. ESA

N89-12996# National Severe Storms Lab., Norman, Okla.
PROCESSING AND INTERPRETATION OF ALTERNATELY POLARISED WEATHER RADAR ECHOES **c47**
D. S. Zrnic, N. Balakrishnan, and M. Sachidananda *In* ESA, Proceedings of the 1988 International Geoscience and Remote Sensing Symposium (IGARSS 1988) on Remote Sensing: Moving Towards the 21st Century, Volume 1 Aug. 1988 p 243-246 (For primary document see N89-12936 04-42)
Copyright Avail: NTIS HC A99/MF E03; ESA Publications Div., ESTEC, Noordwijk, Netherlands, 120 US dollars or 250 Dutch guilders

Processing methods to derive polarimetric measurables differential phase constant K sub DP, and the correlation coefficient between horizontally and vertically polarized echoes, rho HV(o) simultaneously with Doppler velocity from an alternating sequence of horizontally and vertically polarized echoes are described. It is shown that K sub DP yields a good estimate of liquid water in a rain-hail mixture and that it can be used together with the differential reflectivity and reflectivity factor to infer the hail rate. This is because K sub DP is sensitive to anisotropic scatterers (rain); pure hail which is nearly isotropic and has a small refractive index is almost transparent to K sub DP. A method to categorize hail size based on rho HV(o) is proposed. Physical reasons for a decrease in rho HV(o) stem from a broader distribution of sizes and shapes in a rain-hail mixture; observations that larger hail has a larger protuberance to diameter ratio; and the fact that larger hail falls with minor axis gyrating about the horizontal. The first mechanism is consistent with data from two hailstorms in that it correctly qualifies hail size. ESA

N89-12997# Centre de Recherches en Physique de l'Environnement, Issy-les-Moulineaux (France).
DESIGN OF A SPACEBORNE RADAR FOR TROPICAL RAIN MAPPING AT THE CLIMATOLOGICAL SCALE **c47**
M. Marzoug, P. Amayenc, and N. Karouche (Centre National d'Etudes Spatiales, Toulouse, France) *In* ESA, Proceedings of the 1988 International Geoscience and Remote Sensing Symposium (IGARSS 1988) on Remote Sensing: Moving Towards the 21st Century, Volume 1 Aug. 1988 p 247-248 (For primary document see N89-12936 04-42)
Copyright Avail: NTIS HC A99/MF E03; ESA Publications Div., ESTEC, Noordwijk, Netherlands, 120 US dollars or 250 Dutch guilders

A high resolution spaceborne radar designed to perform rainfall rate profiling in tropical rain, from the low-inclination platform of the BEST mission project on tropical system energy budget is presented. The main characteristics and the expected performances of the nominal system (one operating frequency in Ku-band, cross-track scanning antenna beam with 1.6 km footprint size) are listed. System characteristics improvement in more sophisticated options are also mentioned. ESA

N89-12998*# National Aeronautics and Space Administration. Goddard Space Flight Center, Greenbelt, Md.
RAINFALL INDEX OVER OCEANS DERIVED FROM SSM/I DATA **c47**
A. T. C. Chang and T. T. Wilheit *In* ESA, Proceedings of the 1988 International Geoscience and Remote Sensing Symposium (IGARSS 1988) on Remote Sensing: Moving Towards the 21st Century, Volume 1 Aug. 1988 p 251-252 (For primary document see N89-12936 04-42)

Copyright Avail: NTIS HC A99/MF E03; ESA Publications Div., ESTEC, Noordwijk, Netherlands, 120 US dollars or 250 Dutch guilders CSCL 04B

Ths Special Sensor Microwave/Imager radiometer on board the DMSP satellite measured microwave radiation at 19.35, 22.235, 37.0, and 85.5 GHz with a swath width of 1400 km, providing an opportunity to study global precipitation distributions. A monthly averaged rainfall index was derived using only the 19.35 GHz data. It covers the + or - 50 deg portion of the world with a 5 deg x 5 deg grid. The brightness temperature histogram is analyzed to derive the rainfall distribution. Estimates of the freezing level heights and the water vapor contents are utilized to understand the rainfall distribution better. Log normal and gamma distribution functions are fitted to the data and the derived monthly rainfall index compares favorably with historical precipitation patterns. ESA

N89-12999# Recherche en Prevision Numerique, Dorval (Quebec).

PRODUCTION OF PROBABILITY OF PRECIPITATION MAPS OVER OCEANIC AREAS FROM AUTOMATED CLOUD CLASSIFICATION **c47**

L. Garand *In* ESA, Proceedings of the 1988 International Geoscience and Remote Sensing Symposium (IGARSS 1988) on Remote Sensing: Moving Towards the 21st Century, Volume 1 Aug. 1988 p 255-256 (For primary document see N89-12936 04-42)

Copyright Avail: NTIS HC A99/MF E03; ESA Publications Div., ESTEC, Noordwijk, Netherlands, 120 US dollars or 250 Dutch guilders

Cloud fields are classified in 17 classes at the scale of 130 km using the scheme of Garand (1988). From collocation with ship observations, the probability of precipitation is established for each class. From independent data taken in 1984 (1067 cases) and 1986 (673 cases) the absolute accuracy of the method is found to be 1.1 percent at monthly scale. However the rms differences between various months can be as large as 5.8 percent, showing the validity of the method as a climate indicator. ESA

N89-13000# Direction de la Meteorologie Nationale, Paris (France). Div. Prevision.

TOWARDS DIRECT VARIATIONAL ASSIMILATION OF SCATTEROMETER BACKSCATTER MEASUREMENTS INTO NUMERICAL WEATHER PREDICTION MODELS **c47**

H. Roquet and A. Ratier (Centre National d'Etudes Spatiales, Toulouse, France) *In* ESA, Proceedings of the 1988 International Geoscience and Remote Sensing Symposium (IGARSS 1988) on Remote Sensing: Moving Towards the 21st Century, Volume 1 Aug. 1988 p 257-260 (For primary document see N89-12936 04-42)

Copyright Avail: NTIS HC A99/MF E03; ESA Publications Div., ESTEC, Noordwijk, Netherlands, 120 US dollars or 250 Dutch guilders

As a step towards variational assimilation of scatterometer backscatter measurements into numerical weather forecasting models, a variational surface wind analysis scheme was developed, whereby a field of unique surface wind vectors is directly retrieved from sigma naught triplets, through the minimization of a cost function involving observation error penalty and smoothness constraint terms. Realistic ERS1 simulations lead to promising wind retrieval performances as regards accuracy, implicit ambiguity removal, preservation of actual wind structures of dynamical significance, and cost efficiency. No sensitivity is found to the initial wind field, and smoothness constraints are shown to reduce the rms error induced by instrumental noise on wind divergence and key ocean forcing parameters. ESA

N89-13001# National Oceanic and Atmospheric Administration, Boulder, Colo. Wave Propagation Lab.

RADIOMETRIC OBSERVATIONS OF CLOUD LIQUID WATER DURING FIRE **c47**

J. B. Snider *In* ESA, Proceedings of the 1988 International Geoscience and Remote Sensing Symposium (IGARSS 1988) on Remote Sensing: Moving Towards the 21st Century, Volume 1 Aug. 1988 p 261-262 (For primary document see N89-12936 04-42)

Copyright Avail: NTIS HC A99/MF E03; ESA Publications Div., ESTEC, Noordwijk, Netherlands, 120 US dollars or 250 Dutch guilders

An experimental study of the characteristics of marine stratocumulus clouds was conducted off the coast of southern California. An extensive array of remote and in situ sensors located on the ground, aircraft, tethered balloons and satellites were utilized. Ground-based observations of liquid water made by a microwave radiometer are shown. ESA

N89-13002# Sheffield Univ. (England). Dept. of Geography.

RELATIONSHIPS BETWEEN THE NITROGEN CONTENT OF GRASS AND REFLECTANCE **c43**

S. E. Plummer *In* ESA, Proceedings of the 1988 International Geoscience and Remote Sensing Symposium (IGARSS 1988) on Remote Sensing: Moving Towards the 21st Century, Volume 1 Aug. 1988 p 265-267 (For primary document see N89-12936 04-42)

Copyright Avail: NTIS HC A99/MF E03; ESA Publications Div., ESTEC, Noordwijk, Netherlands, 120 US dollars or 250 Dutch guilders

The results of an experiment to test the hypothesized negative relationship between green reflectance and leaf nitrogen content and the positive relationship between near infrared reflectance and leaf nitrogen content under field conditions are reported. It is concluded that neither relationship holds unless the effect of canopy geometry is suppressed in visible wavelengths and the effect of biomass is suppressed in near infrared wavelengths. ESA

N89-13003# Joint Research Centre of the European Communities, Ispra (Italy).

SMALL FORMAT AIR PHOTO FROM ULTRAHIGH AIRCRAFT AS AN AID FOR DATA COLLECTION OF AGRICULTURAL STATISTICS IN SAHELIAN COUNTRIES **c43**

E. Bartholome, J.-M. Gregoire, and R. Zeyen *In* ESA, Proceedings of the 1988 International Geoscience and Remote Sensing Symposium (IGARSS 1988) on Remote Sensing: Moving Towards the 21st Century, Volume 1 Aug. 1988 p 269-270 (For primary document see N89-12936 04-42)

Copyright Avail: NTIS HC A99/MF E03; ESA Publications Div., ESTEC, Noordwijk, Netherlands, 120 US dollars or 250 Dutch guilders

An experiment was carried out in Mali to assess the feasibility in Sahelian conditions of 70 mm air photography for field mapping of ground segments to be used for the crop statistics and crop surface assessment. It is found that the ultralight aircraft is an efficient tool for air photograhy at the local or subregional level. Accurate field mapping can be achieved if the photos are made during the growing season. Black and white film and scales smaller than 1/15000 are sufficient. Such a procedure could be applied on an operational basis without major difficulty. For crop classification, 1/5000 infrared photos are required. They allow only the recognition of major crop types, which is sufficient for production forecasting, not for agricultural statistics. The operational use of this technique is difficult because of the special film processing involved, and the manpower required for the data analysis. ESA

N89-13004# National Space Development Agency, Ohashi (Japan). Earth Observation Center.

VERIFICATION RESULTS OF MOS-1 MULTISPECTRAL SELF SCANNING RADIOMETER (MESSR) DATA **c43**

K. Maeda, H. Wakabayashi, K. Tasaki, M. Shimada, and H. Sato *In* ESA, Proceedings of the 1988 International Geoscience and Remote Sensing Symposium (IGARSS 1988) on Remote Sensing: Moving Towards the 21st Century, Volume 1 Aug. 1988 p 271-274 (For primary document see N89-12936 04-42)

Copyright Avail: NTIS HC A99/MF E03; ESA Publications Div., ESTEC, Noordwijk, Netherlands, 120 US dollars or 250 Dutch guilders

The first MESSR imagery was obtained 4 days after the launch of MOS-1, and MESSR is found to be as expected during mission check period (3 months after the launch). Initial verification results of MESSR radiometric and geometric performance are presented. ESA

N89-13005# Iwate Univ., Morioka (Japan). Dept. of Computer Science.
ESTIMATION OF SEA SURFACE TEMPERATURE VIA NOAA-AVHRR SENSOR: COMPARISON WITH SEA TRUTH DATA BY FIXED BUOYS **c48**
R. Yokoyama and Sumio Tanba *In* ESA, Proceedings of the 1988 International Geoscience and Remote Sensing Symposium (IGARSS 1988) on Remote Sensing: Moving Towards the 21st Century, Volume 1 Aug. 1988 p 275-280 (For primary document see N89-12936 04-42)
Copyright Avail: NTIS HC A99/MF E03; ESA Publications Div., ESTEC, Noordwijk, Netherlands, 120 US dollars or 250 Dutch guilders

Brightness temperatures observed by channels 4 and 5 HRPT data of the Advanced Very High Resolution Radiometer (AVHRR) aboard NOAA-9 were compared with in situ sea surface temperature provided by fixed buoys in Mutsu bay in northern Japan. The total of 154 match-ups of the coincidence within 30 min and 3 pixels were screened out. Linear regression analysis was applied to the three grouped data sets, i.e., the total data, the daytime data and the nighttime data. The standard errors in both single and double variate regression functions are comparable (0.5C), but the maximum residues are improved in the double variate regression. ESA

N89-13006# Department of Agriculture, Beltsville, Md. Hydrology Lab.
LABORATORY EVALUATION OF A FIELD PORTABLE DIELECTRIC/SOIL MOISTURE PROBE **c43**
T. J. Jackson *In* ESA, Proceedings of the 1988 International Geoscience and Remote Sensing Symposium (IGARSS 1988) on Remote Sensing: Moving Towards the 21st Century, Volume 1 Aug. 1988 p 281-282 (For primary document see N89-12936 04-42)
Copyright Avail: NTIS HC A99/MF E03; ESA Publications Div., ESTEC, Noordwijk, Netherlands, 120 US dollars or 250 Dutch guilders

A 125 GHz soil moisture probe was evaluated. Results suggest that the observations do not exhibit as wide a range of response as would be expected and that a single functional relationship between e' and volumetric soil moisture might work well. The differences between the observed and predicted relationships is attributed to the compaction that occurs when the probe tip is in contact with the ground. These results indicate that the instrument makes an excellent soil moisture measurement device if the effects of texture and density are ignored and a single relationship between e' and soil moisture is used. If the device is used to estimate in situ dielectric properties, care must be taken to minimize compaction or else correct for it. ESA

N89-13007# National Space Development Agency, Ohashi (Japan). Earth Observation Center.
DATA COLLECTION SYSTEM OPERATING ON JAPAN'S FIRST MARINE OBSERVATION SATELLITE: INFLIGHT EVALUATION OF THE SYSTEM PERFORMANCE **c43**
M. Shimada, T. Yamazaki, M. Tsuji, and K. Ayabe *In* ESA, Proceedings of the 1988 International Geoscience and Remote Sensing Symposium (IGARSS 1988) on Remote Sensing: Moving Towards the 21st Century, Volume 1 Aug. 1988 p 283-286 (For primary document see N89-12936 04-42)
Copyright Avail: NTIS HC A99/MF E03; ESA Publications Div., ESTEC, Noordwijk, Netherlands, 120 US dollars or 250 Dutch guilders

Location accuracy of the marine observation satellite (MOS) data collection system was assessed. The location determination algorithm and correction parameters are described. Analysis shows that location of data collection platforms (DCP) is accurate to within 500 m for DCP located between 100 and 2000 km from the MOS-1 subsatellite track. ESA

N89-13008# Illinois Univ., Chicago. Communications Lab.
OPTIMAL RECEPTION IN DEPOLARISING CLUTTER **c32**
W.-M. Boerner *In* ESA, Proceedings of the 1988 International Geoscience and Remote Sensing Symposium (IGARSS 1988) on Remote Sensing: Moving Towards the 21st Century, Volume 1 Aug. 1988 p 289-290 (For primary document see N89-12936 04-42)
Copyright Avail: NTIS HC A99/MF E03; ESA Publications Div., ESTEC, Noordwijk, Netherlands, 120 US dollars or 250 Dutch guilders

The physics of partially polarized waves are discussed with applications to optical (lidar) reception problems. Optimal intensity reception of partially polarized waves scattered off a fluctuating object (ensemble of scatterers) of known polarization properties (measured Mueller matrix) is considered. Expressions for total available intensity and adjustable (polarization-dependent) intensity are derived via the coherency matrix approach. A general numerical technique is developed and illustrated for the optimization of adjustable intensity as a function of transmitted polarization. Closed form expressions are derived for two important subcases, and numerical illustrations for the general case are discussed, including the use of relevant experimental data. ESA

N89-13009# Dornier-Werke G.m.b.H., Friedrichshafen (West Germany).
PERFORMANCE MODELING AND RESULTS FOR X-SAR **c32**
D. Miller *In* ESA, Proceedings of the 1988 International Geoscience and Remote Sensing Symposium (IGARSS 1988) on Remote Sensing: Moving Towards the 21st Century, Volume 1 Aug. 1988 p 293-296 (For primary document see N89-12936 04-42)
Copyright Avail: NTIS HC A99/MF E03; ESA Publications Div., ESTEC, Noordwijk, Netherlands, 120 US dollars or 250 Dutch guilders

Image performance of X-synthetic aperture radar (X-SAR) objectives are reviewed; modeling algorithms are summarized, and predicted performance results examples are given. The problems of beam pointing errors and consequent processing errors are highlighted. ESA

N89-13010# Aerospatiale, Les Mureaux (France). Dept. Measures.
IMAGE SIMULATION OF COMPLEX GEOMETRIC TARGETS FOR SPACEBORNE SYNTHETIC APERTURE RADAR **c32**
J. M. Nasr and D. Vidal-Madjar (Centre de Recherches en Physique de l'Environnement, Issy-les-Moulineaux, France) *In* ESA, Proceedings of the 1988 International Geoscience and Remote Sensing Symposium (IGARSS 1988) on Remote Sensing: Moving Towards the 21st Century, Volume 1 Aug. 1988 p 297-301 (For primary document see N89-12936 04-42)
Copyright Avail: NTIS HC A99/MF E03; ESA Publications Div., ESTEC, Noordwijk, Netherlands, 120 US dollars or 250 Dutch guilders

A spaceborne synthetic aperture radar (SAR) image simulator is presented. The images are composed of an actual SAR background taken from existing satellite images over which are incrusted simulated complex targets. The raw signal backscattered by these targets is computed using known radar cross section prediction techniques. Then the target image is evaluated from raw simulated signal using Doppler processing by fast Fourier transform techniques. The incrustation then operates on the two previous raw images (each pixel is represented by a complex). The results permit quantifying the contribution of a human or natural target in a SAR background. ESA

N89-13011# Duisburg Univ. (West Germany). Dept. of Electrical Engineering.
SCATTERING BEHAVIOR OF A THREE-AXIAL ELLIPSOID **c32**

A. Beyer and B. Roth *In* ESA, Proceedings of the 1988 International Geoscience and Remote Sensing Symposium (IGARSS 1988) on Remote Sensing: Moving Towards the 21st Century, Volume 1 Aug. 1988 p 303-306 (For primary document see N89-12936 04-42)
Copyright Avail: NTIS HC A99/MF E03; ESA Publications Div., ESTEC, Noordwijk, Netherlands, 120 US dollars or 250 Dutch guilders

A method for the solution of the electromagnetic wave problem of a three-axial ellipsoid is presented. It is explained how to determine the field components in the inner and outer space of the ellipsoid. Knowing the general solution, boundary conditions and the eigenvalue equation are discussed. The eigensolutions are found in the form of Lame's wave-functions. The applicability of the method is proved by numerical results. ESA

N89-13012# Texas Univ., Arlington. Wave Scattering Research Center.
ATTENUATION AND SCATTERING MEASUREMENTS FROM DENSE MEDIA c32
I. Syed, A. J. Blanchard, and A. K. Fung *In* ESA, Proceedings of the 1988 International Geoscience and Remote Sensing Symposium (IGARSS 1988) on Remote Sensing: Moving Towards the 21st Century, Volume 1 Aug. 1988 p 307-310 (For primary document see N89-12936 04-42)
Copyright Avail: NTIS HC A99/MF E03; ESA Publications Div., ESTEC, Noordwijk, Netherlands, 120 US dollars or 250 Dutch guilders

Bistatic radar measurements were conducted while varying the incidence angles on a vertically oriented single dielectric volumetric target to examine the effect of target density. Measurements are made on an experimental model to obtain bistatic data from high density volumetric targets for evaluating the applicability of theoretical scattering models. The volumetric density of wooden cylinders comprising the target was varied from 1 percent to 10 percent. The measurements were made in the frequency range from 4 to 8.5 GHz using an HP 8510 network analyzer configured into a FM radar system. The target was observed at phi 180 deg (forward scatter) at two incidence angles for a variety of scattered angles. ESA

N89-13013# Texas Univ., Arlington. Wave Scattering Research Center.
BISTATIC FREQUENCY DIVERSE IMAGING OF COMPLEX SCATTERING TARGETS c32
A. J. Blanchard and M. Dolaty *In* ESA, Proceedings of the 1988 International Geoscience and Remote Sensing Symposium (IGARSS 1988) on Remote Sensing: Moving Towards the 21st Century, Volume 1 Aug. 1988 p 311-314 (For primary document see N89-12936 04-42)
(Grant NAG5-486)
Copyright Avail: NTIS HC A99/MF E03; ESA Publications Div., ESTEC, Noordwijk, Netherlands, 120 US dollars or 250 Dutch guilders

Tomographic imaging of a complex shape and a prefectly conducting object is discussed. Far field data was collected at a selected bistatic transmit/receive antenna configuration. The data was transformed to create tomographic image of the object. The frequency swept technique in the range 4 to 12 GHz was used to achieve centimeter resolution in the reconstructed image. The cross section of the scattering object for a number of transmit/receive polarization is presented as well as the combination of like and cross polarized images. ESA

N89-13014*# Jet Propulsion Lab., California Inst. of Tech., Pasadena.
DESIGN CONSIDERATIONS FOR ADVANCED MULTI-POLARISATION SAR c32
J. D. Klein and A. Freeman *In* ESA, Proceedings of the 1988 International Geoscience and Remote Sensing Symposium (IGARSS 1988) on Remote Sensing: Moving Towards the 21st Century, Volume 1 Aug. 1988 p 317-321 (For primary document see N89-12936 04-42)
Copyright Avail: NTIS HC A99/MF E03; ESA Publications Div., ESTEC, Noordwijk, Netherlands, 120 US dollars or 250 Dutch guilders CSCL 17I

System design and verification of an airborne imaging radar (AIR) system are discussed. Issues of importance to multipolarization systems (e.g., mutual coherence and amplitude balance between channels) are emphasized. Methods of detecting and correcting channel imbalances are discussed, and AIR test results are presented. ESA

N89-13015# Environmental Research Inst. of Michigan, Ann Arbor. Radar Science Lab.
PHASE CALIBRATION OF POLARIMETRIC SAR c32
D. R. Sheen, E. S. Kasischke, and R. A. Shuchman *In* ESA, Proceedings of the 1988 International Geoscience and Remote Sensing Symposium (IGARSS 1988) on Remote Sensing: Moving Towards the 21st Century, Volume 1 Aug. 1988 p 323-326 (For primary document see N89-12936 04-42)
Copyright Avail: NTIS HC A99/MF E03; ESA Publications Div., ESTEC, Noordwijk, Netherlands, 120 US dollars or 250 Dutch guilders

Techniques to measure the phase characteristics of a polarimetric imaging SAR were developed. Techniques to calibrate the phase portion of the radar signature from an airborne, polarimetric SAR system, targets (dihedral and trihedral corner reflectors) with known characteristics were deployed, and several passes of polarimetric data collected. The techniques used to reduce and analyze these data are presented. The radar-measured scattering matrix is compared to the theoretical scattering matrix. The results of this calibration are discussed in the context of the rms phase errors achieved for the SAR system utilized in the experiment. ESA

N89-13016*# Kansas Univ., Kansas City. Radar Systems and Remote Sensing Lab.
A FINE RESOLUTION MULTIFREQUENCY POLARIMETRIC FM RADAR c32
J. Bredow, S. Gogineni, T. Leung, and R. K. Moore *In* ESA, Proceedings of the 1988 International Geoscience and Remote Sensing Symposium (IGARSS 1988) on Remote Sensing: Moving Towards the 21st Century, Volume 1 Aug. 1988 p 327-329 Sponsored by NASA, ONR, and Kansas Univ. General Research Fund No. 3790 (For primary document see N89-12936 04-42)
Copyright Avail: NTIS HC A99/MF E03; ESA Publications Div., ESTEC, Noordwijk, Netherlands, 120 US dollars or 250 Dutch guilders CSCL 17I

A fine resolution polarimetric FM SAR was developed for optimization of polarimetric SARs and interpretation of SAR data via controlled experiments with surface-base sensors. The system is designed for collecting polarimetric data at 5.3 and 10 GHz over incidence angles from 0 to 60 deg. Features of the system include broad bandwidth to obtain fine range resolution, phase stabilization and linearization loop circuitry, and digital signal processing capability. The system is used in a research program to collect polarimetric backscatter data from artificial sea ice research and design trade-offs, laboratory and field evaluation, as well as results from experiments on artificial sea ice are presented. ESA

N89-13017# Academia Sinica, Beijing (China). Inst. of Electronics.
A SYNTHETIC APERTURES RADAR WITH MULTICHANNEL AND MULTIPOLARISATION c32
Cheng Bo Zhang *In* ESA, Proceedings of the 1988 International Geoscience and Remote Sensing Symposium (IGARSS 1988) on Remote Sensing: Moving Towards the 21st Century, Volume 1 Aug. 1988 p 331-333 (For primary document see N89-12936 04-42)
Copyright Avail: NTIS HC A99/MF E03; ESA Publications Div., ESTEC, Noordwijk, Netherlands, 120 US dollars or 250 Dutch guilders

A SAR system, which has quadri-mapping channel and quadri-polarization was developed. The system, designed to provide

capabilities for land use, includes an airborne radar installed in a small aircraft, a real-time down link subsystem, a ground based image processor, and a data film analyzer. The design concept, main features of the system, and its applications are described. The SAR imagery is presented. ESA

N89-13018*# Jet Propulsion Lab., California Inst. of Tech., Pasadena.
CALIBRATION OF MULTIPOLARISATION IMAGING RADAR **c32**
A. Freeman, C. Werner, and Yuhshen Shen *In* ESA, Proceedings of the 1988 International Geoscience and Remote Sensing Symposium (IGARSS 1988) on Remote Sensing: Moving Towards the 21st Century, Volume 1 Aug. 1988 p 335-339 (For primary document see N89-12936 04-42)
Copyright Avail: NTIS HC A99/MF E03; ESA Publications Div., ESTEC, Noordwijk, Netherlands, 120 US dollars or 250 Dutch guilders CSCL 17I

An experiment was designed to calibrate airborne imaging radar (AIR) images, in terms of relative and absolute backscatter, and relative phase between polarization channels. The calibration uses measurements made within the radar system itself (internal calibration) and using ground-based corner reflectors and transponders (external calibration). The techniques developed for the AIR calibration campaign will form the basis of the calibration approach for SIR-C. ESA

N89-13019# Texas Instruments, Inc., McKinney. Radar Systems Technology.
EXAMINING THE POLARISATION PHASE RETRIEVAL OF A DUAL CHANNEL MULTIPOLARISATION RADAR **c32**
B. Derryberry, A. J. Blanchard, and V. Kaupp (Arkansas Univ., Fayetteville.) *In* ESA, Proceedings of the 1988 International Geoscience and Remote Sensing Symposium (IGARSS 1988) on Remote Sensing: Moving Towards the 21st Century, Volume 1 Aug. 1988 p 341-344 (For primary document see N89-12936 04-42)
Copyright Avail: NTIS HC A99/MF E03; ESA Publications Div., ESTEC, Noordwijk, Netherlands, 120 US dollars or 250 Dutch guilders

Three multipolarization radar system models are evaluated with emphasis on usage in calibration and polarization phase retrieval. The first one models the radar as a dual channel system with a diode switch and circulators for switching and isolating between the two polarization channels during transmission and reception. Nonreciprocal impedances and cross-over leakage between channels is included in the model with realization of principal and cross-polarization antenna patterns. The second model simplifies the first by assuming no cross-over leakage and ideal microwave components. The third model is based upon Sinclair's signal model with no cross-polarization antenna patterns and uniformly illuminating principal patterns. The results of sensitivity analysis reveal that the dual channel model should be used whenever the microwave components have on/off ratios in the range -20 to -40 dB. ESA

N89-13020*# Jet Propulsion Lab., California Inst. of Tech., Pasadena.
THE NASA/JPL MULTIFREQUENCY, MULTIPOLARISATION AIRBORNE SAR SYSTEM **c32**
D. N. Held, W. E. Brown, A. Freeman, J. D. Klein, H. A. Zebker, T. Sato, T. Miller, Q. Nguyen, and Y. Lou *In* ESA, Proceedings of the 1988 International Geoscience and Remote Sensing Symposium (IGARSS 1988) on Remote Sensing: Moving Towards the 21st Century, Volume 1 Aug. 1988 p 345-349 (For primary document see N89-12936 04-42)
Copyright Avail: NTIS HC A99/MF E03; ESA Publications Div., ESTEC, Noordwijk, Netherlands, 120 US dollars or 250 Dutch guilders CSCL 17I

Polarimetric synthetic aperture radars, operating at L-, C- and P-band, were designed to replace and upgrade a system destroyed in an aircraft accident. Ground and flight tests were conducted, and the radar was flown over a calibration site in a sequence of experiments designed to calibrate the system. The radar also took part in science campaigns. ESA

N89-13021# Illinois Univ., Chicago. Communications Lab.
FORMULATION OF THE PROPER EQUATIONS FOR DEVELOPING STANDARDS IN COHERENT DUAL POLARISATION SAR IMAGING **c32**
W.-M. Boerner and A. B. Kostinski *In* ESA, Proceedings of the 1988 International Geoscience and Remote Sensing Symposium (IGARSS 1988) on Remote Sensing: Moving Towards the 21st Century, Volume 1 Aug. 1988 p 351-353 (For primary document see N89-12936 04-42)
Copyright Avail: NTIS HC A99/MF E03; ESA Publications Div., ESTEC, Noordwijk, Netherlands, 120 US dollars or 250 Dutch guilders

Crucial inconsistencies in the basic equations of radar polarimetry which are common in the literature were detected. The formulations of the polarization state definitions given in the IEEE/ANSI Standards 149-1979 are in error. These and other inconsistencies and conceptual errors are discussed. The correct formulae for the proposed revision of the polarimetric standards together with a well-defined and consistent procedure for measuring target scattering matrices in monostatic and bistatic arrangements are given. The proposed procedure can be applied to an arbitrary measurement process in any general elliptical polarization basis. ESA

N89-13022# Griffiths Remote Sensing, London (England).
THE RELATIVITY UTILITY OF LANDSAT MSS AND SIR-A IMAGERY IN RECONNAISSANCE GEOLOGICAL MAPPING IN NORTHERN SUDAN **c43**
P. S. Griffiths *In* ESA, Proceedings of the 1988 International Geoscience and Remote Sensing Symposium (IGARSS 1988) on Remote Sensing: Moving Towards the 21st Century, Volume 1 Aug. 1988 p 359-362 (For primary document see N89-12936 04-42)
Copyright Avail: NTIS HC A99/MF E03; ESA Publications Div., ESTEC, Noordwijk, Netherlands, 120 US dollars or 250 Dutch guilders

Reconnaissance geological mapping for mineral exploration of crystalline basement in the Sudanese Nubian Desert was carried out by interpretation of LANDSAT MSS, LANDSAT RBV, and SIR-A imagery, helped by a field-check. Radar and simply-enhanced MSS imagery are compared. Although the SIR-A data provide the greater density of structural information, both image types give a similar overall impression of rock-unit variation, structure and geological history. Since reconnaissance work normally demands acquisition by the simplest means of a broad range of goelogical information, it is concluded that the required result could be obtained using MSS imagery alone, although the interpretation of other image types raises confidence in the result. ESA

N89-13023# Open Univ., Milton (England). Dept. of Earth Sciences.
A REGIONAL TECTONIC STUDY OF NE AND E AFRICA AND ITS IMPLICATION FOR MINERAL EXPLORATION: A SYNOPTIC VIEW FROM SATELLITE IMAGERY **c43**
S. M. Behre *In* ESA, Proceedings of the 1988 International Geoscience and Remote Sensing Symposium (IGARSS 1988) on Remote Sensing: Moving Towards the 21st Century, Volume 1 Aug. 1988 p 363-366 (For primary document see N89-12936 04-42)
Copyright Avail: NTIS HC A99/MF E03; ESA Publications Div., ESTEC, Noordwijk, Netherlands, 120 US dollars or 250 Dutch guilders

The regional tectonic framework of NE and E Africa was established, based on a study of published maps and reports, fieldwork, and remote sensing data. The major lineaments identified in the Horn of Africa are 010 + or - 10 deg., 055 to 065 deg. and 145 to 165 deg. The earliest conjugate fractures are N-S and NW-SE trending. A later deformation episode produced NE-SW lineaments but also reactiviated NW-SE trending lineaments. These

lineaments extended histories from the late Proterozoic to the Tertiary and were reactivated repeatedly during the breakup of Gondwanaland. They controlled ore deposits, basin sedimentation and subsequently controlled the evolution of the East African Rift system. Tectonic and metallogenic evolution of the NE Sudan-Eritrea region is cited as a case study. ESA

N89-13024# Reading Univ. (England). NERC Unit for Thematic Informations Systems.
MAPPING THE DISTRIBUTION AND ABUNDANCE OF LITHOLOGICAL UNITS AND SURFACE MINERALOGIES AT JABAL SA'ID, SAUDI ARABIA: AN APPLICATION OF SPECTRAL MIXTURE MODELLING **c43**
N. Drake, S. Mackin, T. J. Munday, J. Settle, and A. Al-Sari (Durham Univ., England) *In* ESA, Proceedings of the 1988 International Geoscience and Remote Sensing Symposium (IGARSS 1988) on Remote Sensing: Moving Towards the 21st Century, Volume 1 Aug. 1988 p 367-368 (For primary document see N89-12936 04-42)
Copyright Avail: NTIS HC A99/MF E03; ESA Publications Div., ESTEC, Noordwijk, Netherlands, 120 US dollars or 250 Dutch guilders

The spatial distribution of various lithologies, and in particular the abundance of particular surface mineralogies relating to the alteration found around Jabal Sa'id (Saudi Arabia), were examined and compared using data acquired by LANDSAT TM and an airborne multispectral scanner. These systems provide information on the spatial distributions of certain mineralogies based upon the strength and position of spectral absorption features located in the wavelength region 0.4 to 2.4 micrometer. In the study area, observed absorptions are due primarily to the presence of iron (hematite and limonite) and various phyllosilicates (chlorite, sericite). Airborne and LANDSAT data agree. ESA

N89-13025# Open Univ., Milton (England). Dept. of Earth Sciences.
THE NEED FOR VOLCANO MONITORING AND THE ABILITY TO DETECT ACTIVITY USING EMITTED SHORT WAVELENGTH INFRARED **c43**
D. A. Rothery *In* ESA, Proceedings of the 1988 International Geoscience and Remote Sensing Symposium (IGARSS 1988) on Remote Sensing: Moving Towards the 21st Century, Volume 1 Aug. 1988 p 369-372 (For primary document see N89-12936 04-42)
Copyright Avail: NTIS HC A99/MF E03; ESA Publications Div., ESTEC, Noordwijk, Netherlands, 120 US dollars or 250 Dutch guilders

It is argued that remote sensing in the short wavelength infrared (SWIR) has the potential for providing a great deal of information about activity at volcanoes, by virtue of the radiation emitted by hot surfaces. This can be used to give warning of imminent eruptions, monitor their progress, and model volcanic processes. The LANDSAT TM is the only operational instrument which returns suitable data. This is particularly valuable because it incorporates two SWIR bands enabling constraints to be put on the sub-pixel structure of the image. Current orbital thermal infrared imagery (e.g., AVHRR, TM band 6) cannot resolve most volcanic thermal anomalies because the pixel size is too coarse. Moreover, the gains of operational thermal infrared sensors make them unsuitable for measuring volcanic temperatures. ESA

N89-13026# Sheffield Univ. (England). Dept. of Geography.
IMPROVING THE ACCESSIBILITY OF SPATIALLY REFERENCED GEOLOGICAL INFORMATION **c43**
S. M. Black *In* ESA, Proceedings of the 1988 International Geoscience and Remote Sensing Symposium (IGARSS 1988) on Remote Sensing: Moving Towards the 21st Century, Volume 1 Aug. 1988 p 373-374 (For primary document see N89-12936 04-42)
Copyright Avail: NTIS HC A99/MF E03; ESA Publications Div., ESTEC, Noordwijk, Netherlands, 120 US dollars or 250 Dutch guilders

The structure and operation of an idealized data integration and analysis system is outlined. It is based on an advanced micro or minicomputer and embodies aspects of graphics/image processing and geographic information systems (GIS) technology within a desktop environment. The aim of the system is to improve the accessibility of spatially referenced information for geological research and application on a local and regional level. However, the system's operational capabilities and structures are equally applicable in other areas of Earth science and nonrelated fields. ESA

N89-13027# Dundee Univ. (Scotland). Dept. of Applied Physics and Electronic and Mfg. Engineering.
THE INTERPRETATION OF ICELANDIC TUNDRA FEATURES FROM LANDSAT-MSS DATA **c43**
R. A. Vaughan and P. O. Vaughan (Imperial Coll. of Science and Technology, London, England) *In* ESA, Proceedings of the 1988 International Geoscience and Remote Sensing Symposium (IGARSS 1988) on Remote Sensing: Moving Towards the 21st Century, Volume 1 Aug. 1988 p 375-376 (For primary document see N89-12936 04-42)
Copyright Avail: NTIS HC A99/MF E03; ESA Publications Div., ESTEC, Noordwijk, Netherlands, 120 US dollars or 250 Dutch guilders

A multidisciplinary expedition to Iceland collected summer ground truth data from the area east of the Vatnajokull ice-cap. Geological and geomorphological features within this area were identified on the ground and using air photographs, and correlated with LANDSAT MSS imagery. Because of the very low percentage of vegetation cover, exposed rock surfaces, gravel plains, and large (over 200 m high) scree slopes can be identified on such imagery. These features are particularly well-defined on principal component color composites, although attempts at meaningful classification are not successful due to poor discrimination in feature space and high correlation between bands. ESA

N89-13028# Reading Univ. (England). Dept. of Geography.
MONITORING PLAYAS USING THEMATIC MAPPER DATA **c43**
A. C. Millington, N. A. Quarmby, N. Drake, A. J. Reading, and J. R. G. Townshend *In* ESA, Proceedings of the 1988 International Geoscience and Remote Sensing Symposium (IGARSS 1988) on Remote Sensing: Moving Towards the 21st Century, Volume 1 Aug. 1988 p 377-380 (For primary document see N89-12936 04-42)
(Contracts NERC-F60/G6/12; NERC-GT4/85/GS/85)
Copyright Avail: NTIS HC A99/MF E03; ESA Publications Div., ESTEC, Noordwijk, Netherlands, 120 US dollars or 250 Dutch guilders

Image analysis techniques were applied to multitemporal Thematic Mapper data to monitor sediment transfer processes in semi-arid Tunisia. This enabled process-domains on salt playas to be identified, and the detection of seasonal, inter-seasonal, and spatial changes in salt playas which were related to variations in sediment, salt, and moisture fluxes. Surface water and groundwater activity, and eolian processes are all identified as important sediment transfer processes. ESA

N89-13029# GEC-Marconi Electronics Ltd., Chelmsford (England).
COMPLEX SAR IMAGERY AND SPECKLE FILTERING FOR ERS-1 WAVE MODE **c32**
R. A. Cordey and J. T. Macklin *In* ESA, Proceedings of the 1988 International Geoscience and Remote Sensing Symposium (IGARSS 1988) on Remote Sensing: Moving Towards the 21st Century, Volume 1 Aug. 1988 p 387-390 (For primary document see N89-12936 04-42)
Copyright Avail: NTIS HC A99/MF E03; ESA Publications Div., ESTEC, Noordwijk, Netherlands, 120 US dollars or 250 Dutch guilders

A method to predict the wavenumber dependence of the speckle component in spectra of SAR intensity images is described. Filtering of this component is an important step in recovering wave height spectra from SAR images of the ocean, and an effective

means of doing so is required for the wave mode of ERS-1. The method uses the correlation function of the corresponding complex images and was tested using airborne and spaceborne imagery obtained over land and sea. Examples of successful and unsuccessful applications of the method are shown. The successes show a great improvement in speckle filtering over previous techniques, while the failures can be explained in terms of artefacts of an individual SAR processor or too coarse a digitization of complex pixel amplitudes. ESA

N89-13030# Naval Ocean Research and Development Activity, Bay St. Louis, Miss.

SOME CHARACTERISTICS OF SHORT OCEAN WAVES AS MICROWAVE SCATTERERS **c32**

P. Smith and D. Johnson *In* ESA, Proceedings of the 1988 International Geoscience and Remote Sensing Symposium (IGARSS 1988) on Remote Sensing: Moving Towards the 21st Century, Volume 1 Aug. 1988 p 395-396 (For primary document see N89-12936 04-42)

Copyright Avail: NTIS HC A99/MF E03; ESA Publications Div., ESTEC, Noordwijk, Netherlands, 120 US dollars or 250 Dutch guilders

In order to assess the applicability of scattering models, and to estimate the range of values for their parameters, a spar buoy equipped with 6 capacitance wave gages spaced at distances appropriate to the 100 to 10 cm scale of ocean waves was developed. Directional wave spectra derived from this data set show that 10 to 100 cm waves in the vicinity of roughness transitions propagate in the downwind direction. The directional resolution is + or - 15 deg. However the confidence limits on the spectral amplitude are not sufficiently small to determine the amplitude of the Bragg scatterers with enough precision to evaluate the relative importance of the Rice perturbation theory. An increase in the number of wires to 14 will alleviate this problem. The directional spectra derived in this manner can give useful information about the wave components present, however. ESA

N89-13031# Kansas Univ., Lawrence. Radar Systems and Remote Sensing Lab.

MODULATION OF THE RADAR BACKSCATTER FROM THE OCEAN SURFACE BY A LONG GRAVITY WAVE **c32**

J. C. Holtzman, J. C. West, S. P. Gogineni, and R. K. Moore *In* ESA, Proceedings of the 1988 International Geoscience and Remote Sensing Symposium (IGARSS 1988) on Remote Sensing: Moving Towards the 21st Century, Volume 1 Aug. 1988 p 397-398 (For primary document see N89-12936 04-42)

Copyright Avail: NTIS HC A99/MF E03; ESA Publications Div., ESTEC, Noordwijk, Netherlands, 120 US dollars or 250 Dutch guilders

The modulation of the scattering cross-section as a function of position on a long gravity wave is calculated from experimental data. The phase position of the signal on the long wave is determined from spectral analysis of the wave-height time series. Samples of return power from the same phase position are averaged together to reduce the effects of phase-interference (Rayleigh) fading. The resulting modulation curves suggest that hydrodynamic and aerodynamic effects are responsible for the radar cross-section modulation. Sea spikes are most common on the front face of the wave, suggesting they are associated with wave breaking. ESA

N89-13032*# Johns Hopkins Univ., Laurel, Md. Applied Physics Lab.

ESTIMATING AIRCRAFT SAR RESPONSE CHARACTERISTICS AND APPROXIMATING OCEAN WAVE SPECTRA IN THE LABRADOR SEA **c32**

D. G. Tilley *In* ESA, Proceedings of the 1988 International Geoscience and Remote Sensing Symposium (IGARSS 1988) on Remote Sensing: Moving Towards the 21st Century, Volume 1 Aug. 1988 p 399-402 Sponsored by NASA and the ONR (For primary document see N89-12936 04-42)

Copyright Avail: NTIS HC A99/MF E03; ESA Publications Div., ESTEC, Noordwijk, Netherlands, 120 US dollars or 250 Dutch guilders CSCL 17I

The data processing methods employed to compute estimates of two-dimensional wave height-variance spectra from the ocean imagery obtained in the Labrador Sea by a C-band airborne SAR system are described. The SAR spectra are compared for high and low altitude geometries with large and small elevation angles. A surface contour radar and a radar ocean wave spectrometer aboard an aircraft are used to verify the surface wave spectrum. ESA

N89-13033# Canada Centre for Remote Sensing, Ottawa (Ontario). RADARSAT Project Office.

PHASE VERSUS ORBITAL VELOCITY IN SAR WAVE IMAGING: PARADOX LOST **c32**

R. K. Raney and P. W. Vachon *In* ESA, Proceedings of the 1988 International Geoscience and Remote Sensing Symposium (IGARSS 1988) on Remote Sensing: Moving Towards the 21st Century, Volume 1 Aug. 1988 p 405-406 (For primary document see N89-12936 04-42)

Copyright Avail: NTIS HC A99/MF E03; ESA Publications Div., ESTEC, Noordwijk, Netherlands, 120 US dollars or 250 Dutch guilders

The focus paradox in ocean wave SAR imaging from the air is reconciled. Improved wave imagery from an airborne SAR is possible by compensating individual looks (in a multilook data set) for wave movement prior to look summation. By observing the direction of wave motion between looks, the omnipresent 180 deg ambiguity (in wave direction estimation through spectral analysis) may be resolved using only the SAR data from one pass of the sensor. (There are known methods for resolution of the directional ambiguity for a single mode sea using two opposed passes). Approximation of the required image shift by focus adjustment is not recommended because the azimuth impulse response is degraded in the process, the method by definition is tuned to only one wave component, and the resulting image shift is in the azimuthal direction only and thus not necessarily in the direction of wave propagation. For directional spectral calculations, Fourier transformation of individual looks by magnitude summation leads to better results than the normal method of Fourier transformation of the look summed wave image. These results do not depend on invocation of any particular wave imaging mechanism. ESA

N89-13034# Environmental Research Inst. of Michigan, Ann Arbor.

SAR IMAGE STATISTICS RELATED TO ATMOSPHERIC DRAG OVER SEA ICE **c32**

B. A. Burns and A. Wegener (Institute for Polar and Marine Research, Bremerhaven, West Germany) *In* ESA, Proceedings of the 1988 International Geoscience and Remote Sensing Symposium (IGARSS 1988) on Remote Sensing: Moving Towards the 21st Century, Volume 1 Aug. 1988 p 409-412 (For primary document see N89-12936 04-42)

(Contract N00014-81-C-0295)

Copyright Avail: NTIS HC A99/MF E03; ESA Publications Div., ESTEC, Noordwijk, Netherlands, 120 US dollars or 250 Dutch guilders

The possibility of using SAR data to distinguish sea ice regions with different atmospheric drag is explored. The amplitude of the radar backscatter cross section and the areal statistics derived from SAR imagery are examined. Using surface roughness data from pack ice areas it is shown that the scattering coefficients for radar wavelengths presently used are insensitive to the roughness elements responsible for drag coefficient variations. For seasonal ice zones, where ice concentration and floe deformation contribute to atmopheric drag, statistical filters applied to 23.5 cm SAR digital image data are found to produce maps related to these quantities. ESA

N89-13035# GEC-Marconi Electronics Ltd., Chelmsford (England).
ANALYSIS OF SEASAT SAR SEA-ICE DATA FROM THE BEAUFORT SEA **c48**
K. C. Partington *In* ESA, Proceedings of the 1988 International Geoscience and Remote Sensing Symposium (IGARSS 1988) on Remote Sensing: Moving Towards the 21st Century, Volume 1 Aug. 1988 p 413-416 (For primary document see N89-12936 04-42)
Copyright Avail: NTIS HC A99/MF E03; ESA Publications Div., ESTEC, Noordwijk, Netherlands, 120 US dollars or 250 Dutch guilders

Seasat synthetic aperture radar imagery of the Beaufort sea is analyzed. Despite the presence of a large proportion of new ice and a limited dynamic range in the data, computationally-efficient correlation algorithms are highly successful at measuring the motion. The good performance is explained by analysis of the speckle properties of segmented regions of the image. A maximum of 7 percent of the area of the analyzed image is characterized by fully-developed speckle. ESA

N89-13036# Helsinki Univ. of Technology, Espoo (Finland). Dept. of Space Technology.
MICROWAVE DIELECTRIC PROPERTIES OF LOW-SALINITY SEA ICE **c48**
M. T. Hallikainen, M. V. O. Toikka, and J. M. Hyyppa *In* ESA, Proceedings of the 1988 International Geoscience and Remote Sensing Symposium (IGARSS 1988) on Remote Sensing: Moving Towards the 21st Century, Volume 1 Aug. 1988 p 419-420 (For primary document see N89-12936 04-42)
Copyright Avail: NTIS HC A99/MF E03; ESA Publications Div., ESTEC, Noordwijk, Netherlands, 120 US dollars or 250 Dutch guilders

A waveguide transmission system was used to measure the dielectric properties of sea ice during the Bothnian Experiment in Preparation for ERS-1 Campaign in the Gulf of Bothnia, March 31 - April 3, 1987. The temperature range of the ice samples was minus 6.0 to minus 0.3 C and the salinity range 0.0 to 1.0 per mille. The dielectric properties of the sea ice are dominated by those of the brine liquid. ESA

N89-13037# Canada Centre for Remote Sensing, Ottawa (Ontario).
THE LIMEX 1987 PILOT PROJECT, LIMEX 1989 AND LONG-TERM OBJECTIVE FOR DATA COLLECTION ON THE CANADIAN EAST COAST **c48**
L. McNutt and R. K. Raney *In* ESA, Proceedings of the 1988 International Geoscience and Remote Sensing Symposium (IGARSS 1988) on Remote Sensing: Moving Towards the 21st Century, Volume 1 Aug. 1988 p 421-422 (For primary document see N89-12936 04-42)
Copyright Avail: NTIS HC A99/MF E03; ESA Publications Div., ESTEC, Noordwijk, Netherlands, 120 US dollars or 250 Dutch guilders

The Labrador Ice Margin (LIMEX) Series to develop techniques to combine remotely sensed data with meteorological and oceanographic information into air/sea ice interaction models to predict ice and ocean conditions, both short-term and seasonally is introduced. The results obtained from LIMEX '87; the experiment planned for LIMEX '89; and the approach to be used in LIMEX '91 are described. Another followon study will be prepared for the RADARSAT Program, based on experience gained in the previous experiments. ESA

N89-13038# Helsinki Univ. of Technology, Espoo (Finland). Dept. of Space Technology.
A 35 GHz HELICOPTER-BORNE POLARIMETER RADAR **c32**
M. T. Hallikainen and J. T. Pulliainen *In* ESA, Proceedings of the 1988 International Geoscience and Remote Sensing Symposium (IGARSS 1988) on Remote Sensing: Moving Towards the 21st Century, Volume 1 Aug. 1988 p 423-424 (For primary document see N89-12936 04-42)
Copyright Avail: NTIS HC A99/MF E03; ESA Publications Div., ESTEC, Noordwijk, Netherlands, 120 US dollars or 250 Dutch guilders

A helicopter-borne 35-GHz polarimeter radar is described. An HP 8753A network analyzer is employed in the system as a signal generator and processing unit. The 1 to 3 GHz signal from the network analyzer is up-converted to the 35 to 37 GHz band for transmission. The backscattered signal is down-converted and then processed by the network analyzer. The HP 8753A complex math operation capability includes subtraction of background or leakage noise (from within the system) from the return signal, and averaging of several measurements. These features along with the 90 dB dynamic range and the range-gating capability make the polarimeter radar suitable for several applications. ESA

N89-13039# Environmental Research Inst. of Michigan, Ann Arbor. Radar Science Lab.
SEA ICE TYPE CLASSIFICATION OF SAR IMAGERY **c48**
C. C. Wackerman, R. R. Jentz, and R. A. Shuchman *In* ESA, Proceesings of the 1988 International Geoscience and Remote Sensing Symposium (IGARSS 1988) on Remote Sensing: Moving Towrds the 21st Century, Volume 1 Aug. 1988 p 425-428 (For primary document see N89-12936 04-42)
(Contracts N00014-87-C-0418; N00014-81-C-0195)
Copyright Avail: NTIS HC A99/MF E03; ESA Publications Div., ESTEC, Noordwijk, Netherlands, 120 US dollars or 250 Dutch guilders

Fully automatic algorithms were developed to produce sea ice type classification maps and sea ice concentration estimates of SAR imagery. The sea ice type classification algorithm uses local statistics to determine ice type boundaries, and the ice concentration algorithm iteratively decomposes the histogram into ice and water histograms. The algorithms were used on simulated imagery and actual SAR imagery gathered during the 1984 and 1987 Marginal Ice Zone Experiments (MIZEX). The results are compared with ground truth data gathered during MIZEX '87. ESA

N89-13040# Zurich Univ. (Switzerland). Remote Sensing Labs.
IMPROVEMENT IN NOAA-AVHRR SNOWCOVER DETERMINATION FOR RUNOFF PREDICTION **c43**
C. Frank, K. I. Itten, and K. Staenz *In* ESA, Proceedings of the 1988 International Geoscience and Remote Sensing Symposium (IGARSS 1988) on Remote Sensing: Moving Towards the 21st Century, Volume 1 Aug. 1988 p 433-435 (For primary document see N89-12936 04-42)
Copyright Avail: NTIS HC A99/MF E03; ESA Publications Div., ESTEC, Noordwijk, Netherlands, 120 US dollars or 250 Dutch guilders

Computer based theme masking and specific image enhancement techniques are demonstrated for an accurate and fast determination of the snow covered area. Cloud masks and height classes from a digital elevation model combined with region masks form the basis for a principal component analysis of NOAA-AVHRR multispectral imagery for an efficient snow cover classification for runoff prediction. ESA

N89-13041# Helsinki Univ. of Technology, Espoo (Finland). Dept. of Space Technology.
MICROWAVE EMISSION BEHAVIOR OF SNOW **c43**
M. T. Hallikainen and V. I. Jaaskelainen *In* ESA, Proceedings of the 1988 International Geoscience and Remote Sensing Symposium (IGARSS 1988) on Remote Sensing: Moving Towards the 21st Century, Volume 1 Aug. 1988 p 437-438 (For primary document see N89-12936 04-42)
Copyright Avail: NTIS HC A99/MF E03; ESA Publications Div., ESTEC, Noordwijk, Netherlands, 120 US dollars or 250 Dutch guilders

The brightness temperature of snow-covered terrain was monitored throughout the winter. Radiometers operating at 1, 16.5, and 37 GHz (vertical and horizontal polarization) were used. The snow conditions varied from fine-grained to refrozen snow and

from dry snow to wetnesses of different levels. The effects of snow water equivalent, liquid water content, structure, and grain size were ascertained. ESA

N89-13042# Kanazawa Univ. (Japan). Lab. of Information Science.
SNOWMELT RUNOFF ESTIMATION USING SNOW COVER EXTENT DATA AND ITS APPLICATION TO OPTIMUM CONTROL OF DAM WATER LEVEL **c43**
Y. Kawata, T. Kusaka, and S. Ueno (Kyoto Inst. of Tech., Japan) *In* ESA, Proceedings of the 1988 International Geoscience and Remote Sensing Symposium (IGARSS 1988) on Remote Sensing: Moving Towards the 21st Century, Volume 1 Aug. 1988 p 439-440 (For primary document see N89-12936 04-42)
Copyright Avail: NTIS HC A99/MF E03; ESA Publications Div., ESTEC, Noordwijk, Netherlands, 120 US dollars or 250 Dutch guilders

Using LANDSAT MSS data and meteorological information, the daily runoff volume in the Sai river basin (Japan) for 3 years was estimated. Simulation of streamflow based on the Martinec Snowmelt Runoff Model (SRM) has an accuracy of 90 percent in the Sai river basin. The snow-cover depletion curve may be estimated from the value of maximum snow depth in the basin. Computer simulation shows that the optimum water level of the Sai River dam can be maintained with the aid of predicted inflow by the SRM. ESA

N89-13043# Puget Sound Univ., Tacoma, Wash.
POLARISATION OF PASSIVE MICROWAVE SIGNALS AS INDICATOR OF SNOW WATER EQUIVALENT **c43**
Z. F. Danes and P. L. R. Danes *In* ESA, Proceedings of the 1988 International Geoscience and Remote Sensing Symposium (IGARSS 1988) on Remote Sensing: Moving Towards the 21st Century, Volume 1 Aug. 1988 p 441-442 (For primary document see N89-12936 04-42)
(Contract GS-14-08-0001-A-0353)
Copyright Avail: NTIS HC A99/MF E03; ESA Publications Div., ESTEC, Noordwijk, Netherlands, 120 US dollars or 250 Dutch guilders

Difference in polarization between the 37 GHz and the 18 GHz passive microwave signals from the upper Colorado River watershed shows strong correlation with the amount of snow on the ground in areas of sparse vegetation. Under such conditions, this difference may become a measure of the snow-water equivalent. However, in wooded areas the correlation is weak if any, probably due to the large amount of energy radiated by the trees. ESA

N89-13044# Zurich Univ. (Switzerland). Remote Sensing Labs.
MONITORING OF SEASONAL SNOW COVER ON GLACIERS **c43**
H. Haefner and P. Laager *In* ESA, Proceedings of the 1988 International Geoscience and Remote Sensing Symposium (IGARSS 1988) on Remote Sensing: Moving Towards the 21st Century, Volume 1 Aug. 1988 p 443-445 (For primary document see N89-12936 04-42)
Copyright Avail: NTIS HC A99/MF E03; ESA Publications Div., ESTEC, Noordwijk, Netherlands, 120 US dollars or 250 Dutch guilders

The delineation of the transient snow line on a glacier was studied for the melting period by comparing the data from an automatic camera, aerial photographs, and LANDSAT-TM images. The accuracy achieved from TM band 2 regarding the course of the snow line lies, except at a few areas of very low contrast, within 1 pixel. The highest snow line in fall and the separation of the firn line allow direct conclusions on the position of the equilibrium line. The dynamics of the melting pattern and the melting curve were established. This allows the influence of weather conditions on the seasonal snow cover and consequently on the runoff pattern to be assessed. ESA

N89-13045*# National Aeronautics and Space Administration. Goddard Space Flight Center, Greenbelt, Md.
AVERAGE AREAL WATER EQUIVALENT OF SNOW IN A MOUNTAIN BASIN USING MICROWAVE AND VISIBLE SATELLITE DATA
A. Rango, J. Martinec, A. T. C. Chang, J. L. Foster, and V. vanKatwijk (Vrije Univ., Amsterdam, Netherlands) *In* ESA, Proceedings of the 1988 International Geoscience and Remote Sensing Symposium (IGARSS 1988) on Remote Sensing: Moving Towards the 21st Century, Volume 1 Aug. 1988 p 447-448 (For primary document see N89-12936 04-42)
Copyright Avail: NTIS HC A99/MF E03; ESA Publications Div., ESTEC, Noordwijk, Netherlands, 120 US dollars or 250 Dutch guilders

Satellite microwave data were used to evaluate the average areal water equivalent of snow cover in the mountainous Rio Grande basin of Colorado. Areal water equivalent data for the basin were obtained from contoured values of point measurements and from zonal water volume values generated by a snowmelt runoff model. Comparison of these snow water equivalent values shows the model values to consistently exceed the contoured values, probably because of the narrow elevation range in the lower part of the basin where the point measurements are concentrated. A significant relationship between the difference in microwave brightness temperatures at two different wavelengths and a basin-wide average snow water equivalent value is obtained. The average water equivalent of the snow cover in the basin was derived from differences of the microwave brightness temperatures. ESA

N89-13046# Massachusetts Univ., Amherst. Microwave Remote Sensing Lab.
MILLIMETER-WAVE BACKSCATTER MEASUREMENTS OF VARIOUS SNOW FORMS **c43**
R. M. Narayanan, P. M. Langlois, P. W. Gaiser, and R. E. McIntosh *In* ESA, Proceedings of the 1988 International Geoscience and Remote Sensing Symposium (IGARSS 1988) on Remote Sensing: Moving Towards the 21st Century, Volume 1 Aug. 1988 p 451-452 (For primary document see N89-12936 04-42)
Copyright Avail: NTIS HC A99/MF E03; ESA Publications Div., ESTEC, Noordwijk, Netherlands, 120 US dollars or 250 Dutch guilders

Normalized radar cross section measurements of various snow profiles for VV, VH, HM, and HV polarizations at 215 GHz are presented. Combined backscatter model calculations based on surface and volume scattering theory, together with shadowing corrections, agree with the measured data reasonably well. ESA

N89-13047# Georgia Inst. of Tech., Atlanta.
STATISTICS AND HIGH RESOLUTION IMAGING OF SNOWPACK AT 35 GHz USING A MICROCOMPUTER **c43**
J. M. Trostel *In* ESA, Proceedings of the 1988 International Geoscience and Remote Sensing Symposium (IGARSS 1988) on Remote Sensing: Moving Towards the 21st Century, Volume 1 Aug. 1988 p 453-454 (For primary document see N89-12936 04-42)
Copyright Avail: NTIS HC A99/MF E03; ESA Publications Div., ESTEC, Noordwijk, Netherlands, 120 US dollars or 250 Dutch guilders

Millimeter wave (MMW) reflectivity data from snow-covered ground was collected during the winter by two polarization-agile, frequency-stepped radars. One radar gathered data over a bandwidth of 640 MHz centered about 35 GHz and the other gathered data over a 256 MHz bandwidth centered about 95 GHz. A microcomputer-based system, consisting of a microcomputer with two 9-track tape drives and a color printer, is being developed for use in data calibration, statistical analysis of data, and production of high resolution range and inverse synthetic aperture images from frequency-agile MMW data bases. This analysis system was used to look at snow measurement data. ESA

N89-13048# Trier Univ., Trier-Tarforst (West Germany). Dept. of Geography and Remote Sensing.
SNOW COVER TO ALTER TERRAIN SIGNATURES ON RADAR IMAGES **c43**
W. Geile *In* ESA, Proceedings of the 1988 International Geoscience and Remote Sensing Symposium (IGARSS 1988) on Remote Sensing: Moving Towards the 21st Century, Volume 1 Aug. 1988 p 455-457 (For primary document see N89-12936 04-42)
Copyright Avail: NTIS HC A99/MF E03; ESA Publications Div., ESTEC, Noordwijk, Netherlands, 120 US dollars or 250 Dutch guilders

Differences of an HH-polarized X-band airborne SAR image recorded with the terrain covered by to 10 to 15 cm of dry snow compared to imagery of the same test site also recorded in winter but without snow are detailed. A drastically increased contrast between overall low returning open agricultural areas (largely irrespective of the soil surface roughness within the field pattern) and high returning textures such as forests and settlements is seen. An increased brightness and signal compression of individual target returns, strongly enhancing small targets and relief features of the smallest order such as dams or ditches on the background of a more favorable target-to-noise or target-to-clutter ratio is shown. ESA

N89-13049# Department of Agriculture, Beltsville, Md. Hydrology Lab.
MICROCOMPUTERS (PCS) FOR SNOW COVER ANALYSES USING MULTISENSOR SATELLITE DATA **c43**
M. F. Baumgartner and A. Rango *In* ESA, Proceedings of the 1988 International Geoscience and Remote Sensing Symposium (IGARSS 1988) on Remote Sensing: Moving Towards the 21st Century, Volume 1 Aug. 1988 p 459-460 (For primary document see N89-12936 04-42)
Copyright Avail: NTIS HC A99/MF E03; ESA Publications Div., ESTEC, Noordwijk, Netherlands, 120 US dollars or 250 Dutch guilders

The design of a general snow cover mapping scheme which can be used in basins with different geographical characteristics is considered. Selecting the appropriate procedures, the scheme allows precise snow cover mapping taking into account topographical effect, solar illumination, and vegetation and cloud coverage. Based on tests of PC image processing systems, limitations for operational snow cover mapping on microcomputers are presented. ESA

N89-13050# Research Inst. for Soil Science and Agricultural Chemistry, Budapest (Turkey).
AGROELECOLOGICAL INFORMATION CONTENT OF SPOT DATA **c43**
F. Csillag, G. Buttner (FOMI Remote Sensing Center, Budapest, Hungary), and I. Juhasz *In* ESA, Proceedings of the 1988 International Geoscience and Remote Sensing Symposium (IGARSS 1988) on Remote Sensing: Moving Towards the 21st Century, Volume 1 Aug. 1988 p 465-470 Sponsored by the Ministry of Agriculture, Budapest, Hungary and Spot Image, Toulouse, France (For primary document see N89-12936 04-42)
Copyright Avail: NTIS HC A99/MF E03; ESA Publications Div., ESTEC, Noordwijk, Netherlands, 120 US dollars or 250 Dutch guilders

Four SPOT scenes acquired over Hungary are evaluated in terms of their potential use for agroecological mapping. Extremely variable soil conditions characteristic of the study area are found to be limiting factors of crop growth. In-field heterogeneities were mapped based on bi-temporal (spring and summer) data using soil brightness and normalized vegetation index. They were field checked and identified as well as on color infrared aerial photography. ESA

N89-13051# Edinburgh Univ. (Scotland). Dept. of Geography.
EVALUATION OF LANDSAT TM AND SPOT IMAGERY FOR AGRICULTURAL LAND USE PLANNING IN LESS DEVELOPED COUNTRIES **c43**
J. R. Wheeler, C. Jarvis, A. J. B. Mitchell, R. B. King, and R. J. White *In* ESA, Proceedings of the 1988 International Geoscience and Remote Sensing Symposium (IGARSS 1988) on Remote Sensing: Moving Towards the 21st Century, Volume 1 Aug. 1988 p 471-472 (For primary document see N89-12936 04-42)
Copyright Avail: NTIS HC A99/MF E03; ESA Publications Div., ESTEC, Noordwijk, Netherlands, 120 US dollars or 250 Dutch guilders

Imagery from SPOT and LANDSAT-TM were acquired for a part of Tabora Region (Tanzania) to investigate the value of both types of imagery for interpreting areas of agricultural potential, current land use, vegetation, cultural features, and clarity and ease of interpretation. Satellite imagery with ground resolution of 20 to 30 m at a scale of 1:50,000 is shown to be extremely useful for land use planners in less developed countries. It provides a means of rapidly appraising areas of cultivation, eroded areas and likely sources of erosion, natural vegetation, and areas with potential for increased population. The main advantages of satellite imagery compared with aerial photography are synopsis and provision of up to date information. ESA

N89-13052# Universite Catholique de Louvain (Belgium). Lab. for Cartography.
COMBINING SPECTRAL AND STRUCTURAL ANALYSES TO SELECT USEFUL CARTOGRAPHIC INFORMATION FROM SPOT IMAGERY **c43**
H. Willemsen *In* ESA, Proceedings of the 1988 International Geoscience and Remote Sensing Symposium (IGARSS 1988) on Remote Sensing: Moving Towards the 21st Century, Volume 1 Aug. 1988 p 473-475 (For primary document see N89-12936 04-42)
Copyright Avail: NTIS HC A99/MF E03; ESA Publications Div., ESTEC, Noordwijk, Netherlands, 120 US dollars or 250 Dutch guilders

The possibilities of cartographic applications of SPOT-imagery are investigated, emphasizing spectral analysis and structural analysis. A maximum of information is achieved through combination of both approaches. Examples of applied techniques and their results are given. ESA

N89-13053# MacDonald, Dettwiler and Associates Ltd., Richmond (British Columbia).
EXTRACTION OF DENSE DIGITAL ELEVATION MODELS FROM SPOT STEREO IMAGERY **c43**
D. S. Kauffman and S. R. Haja (Digim, 1983, Inc. Montreal, Quebec) *In* ESA, Proceedings of the 1988 International Geoscience and Remote Sensing Symposium (IGARSS 1988) on Remote Sensing: Moving Towards the 21st Century, Volume 1 Aug. 1988 p 477-478 (For primary document see N89-12936 04-42)
Copyright Avail: NTIS HC A99/MF E03; ESA Publications Div., ESTEC, Noordwijk, Netherlands, 120 US dollars or 250 Dutch guilders

Automatic techniques for accurately extracting dense digital elevation models from SPOT PLA data are reviewed. Digital techniques of extracting terrain height from stereo satellite images that match or better the accuracy and throughput of traditional photogrammetric techniques exist. While digital methods develop, there are issues to resolve. They involve making sure that the cartographic specifications of the Earth's geoid are accurate, and beginning to address standard methods of storing and accessing the huge quantities of data available. ESA

N89-13054# University Coll., London (England). Dept. of Geography.
THE DIFFERENTIAL RECTIFICATION OF SPOT HRV PANCHROMATIC AND MULTISPECTRAL IMAGERY USING A DIGITAL ELEVATION MODEL **c43**
S. Kay *In* ESA, Proceedings of the 1988 International Geoscience and Remote Sensing Symposium (IGARSS 1988) on Remote Sensing: Moving Towards the 21st Century, Volume 1 Aug. 1988 p 479-481 Sponsored by the Natural Environment

Research Council, London, United Kingdom (For primary document see N89-12936 04-42)
Copyright Avail: NTIS HC A99/MF E03; ESA Publications Div., ESTEC, Noordwijk, Netherlands, 120 US dollars or 250 Dutch guilders

For SPOT image differential rectification, a semi-automated method, utilizing a parametric solution and a digital terrain model, is described. Elevation point interpolation and radiometric resampling are achieved by bilinear interpolation. Two panchromatic subscenes were processed. Geometric rectification is achieved reliably and quickly. Similar results are expected for multispectral data. ESA

N89-13055# Stockholm Univ. (Sweden). Dept. of Physical Geography.
LANDSAT THEMATIC MAPPING (TM) AND SPOT HRV FOR SURVEY MAPPING OF BEDROCK OUTCROPS **c43**
B. Lunden and K. Wester *In* ESA, Proceedings of the 1988 International Geoscience and Remote Sensing Symposium (IGARSS 1988) on Remote Sensing: Moving Towards the 21st Century, Volume 1 Aug. 1988 p 483-484 (For primary document see N89-12936 04-42)
Copyright Avail: NTIS HC A99/MF E03; ESA Publications Div., ESTEC, Noordwijk, Netherlands, 120 US dollars or 250 Dutch guilders

It is shown that LANDSAT TM and SPOT HRV provide good possibilities for mapping of bedrock outcrop areas to be presented on the Swedish topographical map on the scale of 1:50,000. The classification errors can be reduced by the use of a slicing procedure on the training data, and by combining the automatic classification with a subsequent manual improvement. ESA

N89-13056# Reading Univ. (England). Dept. of Geography.
THE PRODUCTION OF ANAGLYPHS FROM SPOT-HRV PANCHROMATIC DATA FOR GEOMORPHOLOGICAL MAPPING **c43**
P. J. Styles *In* ESA, Proceedings of the 1988 International Geoscience and Remote Sensing Symposium (IGARSS 1988) on Remote Sensing: Moving Towards the 21st Century, Volume 1 Aug. 1988 p 485-487 (For primary document see N89-12936 04-42)
(Grant NERC-CASE-GT4/86/GS/90)
Copyright Avail: NTIS HC A99/MF E03; ESA Publications Div., ESTEC, Noordwijk, Netherlands, 120 US dollars or 250 Dutch guilders

The production of geomorphological maps from nadir SPOT-HRV data is discussed. Problems arise due to the masking of topographic features by vegetation cover. Given the availability of off nadir HRV imagery, the quality of maps may be improved by the use of imagery stereo-pairs. Methods of combining of nadir imagery into stereo pairs are described, and the processing steps necessary to produce a stereo view are outlined. The improvements in interpretability that result from the use of data in this form are considered together with problems encountered in map production. ESA

N89-13057# Aston Univ., Birmingham (England). Remote Sensing Unit.
AN EVALUATION OF SATELLITE IMAGERY, LANDSAT THEMATIC MAPPER AND SPOT-1 HRV, FOR GRASSLAND INVENTORY IN THE UK **c43**
J. McGuire and W. G. Collins *In* ESA, Proceedings of the 1988 International Geoscience and Remote Sensing Symposium (IGARSS 1988) on Remote Sensing: Moving Towards the 21st Century, Volume 1 Aug. 1988 p 489-491 (For primary document see N89-12936 04-42)
Copyright Avail: NTIS HC A99/MF E03; ESA Publications Div., ESTEC, Noordwijk, Netherlands, 120 US dollars or 250 Dutch guilders

Grassland classification and mapping using the spectral discrimination properties of LANDSAT Thematic Mapper (TM) and SPOT-1 HRV data, as a basis for the production of grassland cover maps is discussed. From such derived maps, the extent, distribution, and general quality of lowland grassland types can be surveyed, providing an information system capable of creating landcover/grassland maps, quickly and inexpensively, as an aid to environmental, agroeconomical, and ecological planning and for monitoring change. Classifications are evaluated with the assistance of detailed field survey vegetation maps. The use of temporal and spatial features for classification are investigated and the spectral characteristics of different grassland types analyzed. ESA

N89-13058# National Remote Sensing Centre, Farnborough (England).
MONITORING URBAN CHANGE FROM LANDSAT TM AND SPOT SATELLITE IMAGERY BY IMAGE DIFFERENCING **c43**
G. H. Griffiths *In* ESA, Proceedings of the 1988 International Geoscience and Remote Sensing Symposium (IGARSS 1988) on Remote Sensing: Moving Towards the 21st Century, Volume 1 Aug. 1988 p 493-497 (For primary document see N89-12936 04-42)
Copyright Avail: NTIS HC A99/MF E03; ESA Publications Div., ESTEC, Noordwijk, Netherlands, 120 US dollars or 250 Dutch guilders

It is shown that visual interpretation of satellite imagery is the most accurate technique for detecting urban change. This would particularly be the case if enhanced SPOT imagery combining the spectral information of the multispectral channels (XS) and the spatial information of the panchromatic channels was available for both image dates. However, at county, regional, and national scales a more automated technique is required to provide a unified record of the distribution of urban change at specified time intervals. This can be achieved by using a modified form of image differencing in which unwanted agricultural change is differentiated from the urban change of interest by using the variance of the SPOT panchromatic channel as a textural discrimator. In this way it is possible to discriminate between areas of reflectance change on the difference image that display a high variance and correspond to urban land, and areas of reflectance change with low variance which are generally nonurban. ESA

N89-13059# Oslo Univ. (Norway). Dept. of Geography.
EFFECTS OF CHANGING SATELLITE SENSOR ATTRIBUTES **c43**
A. K. Gjertsen *In* ESA, Proceedings of the 1988 International Geoscience and Remote Sensing Symposium (IGARSS 1988) on Remote Sensing: Moving Towards the 21st Century, Volume 1 Aug. 1988 p 501-504 (For primary document see N89-12936 04-42)
Copyright Avail: NTIS HC A99/MF E03; ESA Publications Div., ESTEC, Noordwijk, Netherlands, 120 US dollars or 250 Dutch guilders

A satellite scene is classified into a land cover/land use map, and the effects of changing sensor attributes like, e.g., the resolution cells are evaluated. To quantitatively evaluate the effects of the different attributes of the TM sensor a statistical method for analysis of variance was employed. A three factor, two level fixed effect model was adopted. Finer resolution cells (30 m) result in a reduction in total classification accuracy, but 30 m cells show better results than with 80 m cells to classify the forest into quality classes. ESA

N89-13060# National Inst. for Environment, Ibaraki (Japan).
EFFICIENT CLASSIFICATION OF MULTISPECTRAL IMAGES BY A BEST LINEAR DISCRIMINANT FUNCTION **c43**
Y. Iikura, T. Mizoguchi, and Y. Yasuoka *In* ESA, Proceedings of the 1988 International Geoscience and Remote Sensing Symposium (IGARSS 1988) on Remote Sensing: Moving Towards the 21st Century, Volume 1 Aug. 1988 p 505-508 (For primary document see N89-12936 04-42)
Copyright Avail: NTIS HC A99/MF E03; ESA Publications Div., ESTEC, Noordwijk, Netherlands, 120 US dollars or 250 Dutch guilders

An algorithm for satellite imagery classification which uses best linear discrimination (BLD) as a decision rule of binary decision

tree is proposed. Performance of the proposed method is shown by applying it to multispectral data of LANDSAT 5. Conventional methods (maximum likelihood, Fisher's linear discrimination, and binary decision tree) were also applied to the same data and were compared with the proposed method. The BLD method is a better classifier, although maximum likelihood can be more time efficient. ESA

N89-13061# Tokai Univ., Kanagawa (Japan). Research and Information Center.
A NEW SPATIAL CLASSIFICATION ALGORITHM FOR HIGH GROUND RESOLUTION IMAGES **c43**
Zi-jue Zhang, H. Shimoda, K. Fukue, and T. Sakata *In* ESA, Proceedings of the 1988 International Geoscience and Remote Sensing Symposium (IGARSS 1988) on Remote Sensing: Moving Towards the 21st Century, Volume 1 Aug. 1988 p 509-512 (For primary document see N89-12936 04-42)
Copyright Avail: NTIS HC A99/MF E03; ESA Publications Div., ESTEC, Noordwijk, Netherlands, 120 US dollars or 250 Dutch guilders

A landcover/use classification algorithm to increase classification accuracies for high resolution images is presented. The algorithm is based on a two stage recognition model of landcover/use. Each concept of landcover categories is defined by the component ratio of landcover elements surrounding the corresponding pixel. The classification procedure can be divided into three steps: the first step is the land cover element recognition of each pixel using a pixelwise classifier; the second step is the calculation of the component ratio of each element within local image region; the third step is the final decision for landcover categories using a minimum distance classifier. The results of experiments using TM data show that this algorithm achieves 7 percent improvements of classification accuracies. ESA

N89-13062# Kingston Polytechnic, Kingston-Upon-Thames (England). School of Geography.
CLASSIFICATION DECISION RULE MODIFICATION ON THE BASIS OF INFORMATION EXTRACTED FROM TRAINING DATA **c43**
G. M. Foody, T. F. Wood, and N. M. Trodd *In* ESA, Proceedings of the 1988 International Geoscience and Remote Sensing Symposium (IGARSS 1988) on Remote Sensing: Moving Towards the 21st Century, Volume 1 Aug. 1988 p 513-516 (For primary document see N89-12936 04-42)
Copyright Avail: NTIS HC A99/MF E03; ESA Publications Div., ESTEC, Noordwijk, Netherlands, 120 US dollars or 250 Dutch guilders

Classification of training data to increase thematic classification accuracy is discussed. Not only does it indicate the distribution of misclassification but it can provide data which can enable the modification of classifier decision rules. This can lead to significant increases in classification accuracy. Rule modification also permits the definition of uncertainty classes which may be used to delimit transitional zones between cover-types. Rule modification and uncertainty class definition are discussed in relation to the classification of seminatural vegetation in England from LANDSAT-TM data. ESA

N89-13063# University Coll., London (England). Dept. of Computer Science.
LAPWING: A TRAINABLE SPATIAL FEATURE RECOGNITION SYSTEM **c43**
I. Poole, G. G. Wilkinson, and G. P. Otto *In* ESA, Proceedings of the 1988 International Geoscience and Remote Sensing Symposium (IGARSS 1988) on Remote Sensing: Moving Towards the 21st Century, Volume 1 Aug. 1988 p 517-518 Sponsored by the Natural Environment Research Council, London, United Kingdom (For primary document see N89-12936 04-42)
Copyright Avail: NTIS HC A99/MF E03; ESA Publications Div., ESTEC, Noordwijk, Netherlands, 120 US dollars or 250 Dutch guilders

A method for supervised image-pixel labeling is described. A decision tree is constructed from training data, near optimal splitting rules being found at each node by an optimization strategy (a genetic algorithm). A significantly sized neighborhood of pixels is considered, thus permitting spatial characteristics such as texture, edges, and lines to be exploited. The technique can be iterated to construct a trained relaxation process to exploit contextual dependencies between labels. The method is illustrated with an application to urban area-detection from airborne thematic mapper data. ESA

N89-13064# Missouri Univ., Rolla.
CO-OCCURRENCE MATRIX MODIFICATION FOR SMALL REGION TEXTURE MEASUREMENT AND COMPARISON **c43**
G. E. Carlson and W. J. Ebel *In* ESA, Proceedings of the 1988 International Geoscience and Remote Sensing Symposium (IGARSS 1988) on Remote Sensing: Moving Towards the 21st Century, Volume 1 Aug. 1988 p 519-520 (For primary document see N89-12936 04-42)
Copyright Avail: NTIS HC A99/MF E03; ESA Publications Div., ESTEC, Noordwijk, Netherlands, 120 US dollars or 250 Dutch guilders

Modification of a typical co-occurrence matrix used to measure image region texture is discussed. For small regions, it produces a co-occurrence array whose size varies with the number of pixel adjacencies available to produce more effective and consistent texture comparisons. A segmentation example is presented. ESA

N89-13065# Reading Univ. (England). Dept. of Geography.
THE INTERRELATIONSHIP BETWEEN RESAMPLING METHOD AND INFORMATION EXTRACTION TECHNIQUE **c43**
P. Atkinson *In* ESA, Proceedings of the 1988 International Geoscience and Remote Sensing Symposium (IGARSS 1988) on Remote Sensing: Moving Towards the 21st Century, Volume 1 Aug. 1988 p 521-527 (For primary document see N89-12936 04-42)
(Grant NERC-GT4/83/TLS/43)
Copyright Avail: NTIS HC A99/MF E03; ESA Publications Div., ESTEC, Noordwijk, Netherlands, 120 US dollars or 250 Dutch guilders

The interrelationship between the type of resampling algorithm and the quality of information extracted, and additional features which influence resampling effects are reviewed. The spatial and radiometric resolution of a sensor, together with the location of its bands within the electromagnetic spectrum are fundamental influences on the potential information content of a given scene. The location of a band within the electromagnetic spectrum, and the spatial and radiometric resolution of a sensor also influences the standard deviation of a class. Changes in the standard deviation of a class are also affected by the size of the mean and the number and type of classes (textures). The unpopularity of bilinear interpolation can be attributed to the blurred image it produces. However, this blurring is confined to edges. It produces a gray level distribution closest to the unresampled image, so it is the most appropriate algorithm for single band studies. Its classification accuracy is less satisfactory than either nearest neighbor or cubic convolution, so it is not recommended that this algorithm be used when classification is the primary information extraction technique. ESA

N89-13066# Tokai Univ., Kanagawa (Japan). Reserch and Information Center.
ACCURACY OF LAND COVER CLASSIFICATION OF THEMATIC MAPPER (TM) AND SPOT DATA **c43**
H. Shimoda, K. Fukue, R. Yamaguchi, Zi-jue Zhang, and T. Sakata *In* ESA, Proceedings of the 1988 International Geoscience and Remote Sensing Symposium (IGARSS 1988) on Remote Sensing: Moving Towards the 21st Century, Volume 1 Aug. 1988 p 529-535 (For primary document see N89-12936 04-42)
Copyright Avail: NTIS HC A99/MF E03; ESA Publications Div., ESTEC, Noordwijk, Netherlands, 120 US dollars or 250 Dutch guilders

Land cover/use classification capabilities of a conventional

classifier for SPOT HRV and LANDSAT TM data were evaluated as to ground resolution, spectral resolution, and utilization of spatial feature characteristics. Accuracies of classified results were evaluated with the aid of digital land cover/use test site data. The increase of spatial resolution does not necessarily provide higher classification accuracies. This indicates that spatial information should be utilized to obtain higher accuracies. However, a simple addition of texture features to spectral features can not increase the classification accuracy. The addition of spectral bands, i.e., band 1, 5, and 7 in TM increases land cover classification accuracy. These bands greatly increase the number of discriminable categories. ESA

N89-13067# Hydrological Research Inst., Pretoria (South Africa). Dept. of Water Affairs.

THE EXTRAPOLATION OF SPECTRAL SIGNATURES ILLUSTRATES LANDSATS' POTENTIAL TO DETECT WETLANDS

A. Howman *In* ESA, Proceedings of the 1988 International Geoscience and Remote Sensing Symposium (IGARSS 1988) on Remote Sensing: Moving Towards the 21st Century, Volume 1 Aug. 1988 p 537-539 (For primary document see N89-12936 04-42)

Copyright Avail: NTIS HC A99/MF E03; ESA Publications Div., ESTEC, Noordwijk, Netherlands, 120 US dollars or 250 Dutch guilders

Spectral signatures of a wetland area were determined using LANDSAT MSS data, hydromorphic soil information, and a pixel extraction technique. Investigations indicate that wetlands could be identified and that the same wetland signatures could be extrapolated to another part of the same image to classify similar wetland systems. ESA

N89-13068# New South Wales Univ., Kensington (Australia). Center for Remote Sensing.

CHANGE DIRECTION ANALYSIS USING LANDSAT IMAGERY: A REVIEW OF METHODOLOGY **c43**

A. K. Milne *In* ESA, Proceedings of the 1988 International Geoscience and Remote Sensing Symposium (IGARSS 1988) on Remote Sensing: Moving Towards the 21st Century, Volume 1 Aug. 1988 p 541-544 (For primary document see N89-12936 04-42)

Copyright Avail: NTIS HC A99/MF E03; ESA Publications Div., ESTEC, Noordwijk, Netherlands, 120 US dollars or 250 Dutch guilders

Techniques that can be applied to LANDSAT data in order to detect changes in land surface conditions once potential sources of error introduced through variations in illumination conditions, atmospheric differences, sensor observations, and plant phenology are removed are reviewed. The development of change detection procedures suitable for use in monitoring land cover changes over an extended period of time is related to providing a routine that can be regularly and systematically applied to data collected from satellite sensors and that can be easily integrated with other information sources in order to facilitate decision making in relation to environmental management. The suitability of such a procedure needs to be assessed according to its complexity, ease of implementation, costs in terms of man hours involved, computer time, and the amount of fieldwork and ground truth information required. ESA

N89-13069# British Antarctic Survey, Cambridge (England).

CLOUD TRACK WINDS FROM POLAR ORBITING SATELLITES **c47**

D. Warren and J. Turner *In* ESA, Proceedings of the 1988 International Geoscience and Remote Sensing Symposium (IGARSS 1988) on Remote Sensing: Moving Towards the 21st Century, Volume 1 Aug. 1988 p 549-550 (For primary document see N89-12936 04-42)

Copyright Avail: NTIS HC A99/MF E03; ESA Publications Div., ESTEC, Noordwijk, Netherlands, 120 US dollars or 250 Dutch guilders

A means of estimating wind speed and direction at high latitudes from polar orbiting satellite data is described. The method is similar to that used to obtain cloud track winds from geostationary satellite imagery and takes advantage of the large overlap between successive AVHRR images at latitudes poleward of 70 deg. Sources of error inherent in the techniques are described along with the quality control criteria applied to eliminate inaccurate estimates. ESA

N89-13070# University of Southern California, Los Angeles.

MODEL-BASED ESTIMATION OF WIND FIELDS OVER THE OCEAN FROM WIND SCATTEROMETER MEASUREMENTS **c47**

D. G. Long and J. M. Mendel *In* ESA, Proceedings of the 1988 International Geoscience and Remote Sensing Symposium (IGARSS 1988) on Remote Sensing: Moving Towards the 21st Century, Volume 1 Aug. 1988 p 553-556 (For primary document see N89-12936 04-42)

Copyright Avail: NTIS HC A99/MF E03; ESA Publications Div., ESTEC, Noordwijk, Netherlands, 120 US dollars or 250 Dutch guilders

A model-based approach to estimating the entire wind field over the swath simultaneously is described. The approach incorporates dynamical constraints provided by a mathematical model of the wind field and eliminates the dealiasing required in a traditional wind retrievel process. The approach results in more accurate wind estimates and the ability to quantify the accuracy of the resulting wind field estimates. The development of the wind field model, and a comparison of the model-based and traditional wind estimation schemes are reviewed. ESA

N89-13071# GEC-Marconi Electronics Ltd., Chelmsford (England).

AN ANALYSIS OF DIRECTIONAL AMBIGUITIES IN WIND SCATTEROMETER MEASUREMENTS **c47**

J. Laycock *In* ESA, Proceedings of the 1988 International Geoscience and Remote Sensing Symposium (IGARSS 1988) on Remote Sensing: Moving Towards the 21st Century, Volume 1 Aug. 1988 p 557-560 (For primary document see N89-12936 04-42)

Copyright Avail: NTIS HC A99/MF E03; ESA Publications Div., ESTEC, Noordwijk, Netherlands, 120 US dollars or 250 Dutch guilders

The dependence of the accuracy with which wind scatterometers are able to measure wind fields on solving the problem of directional ambiguities, is discussed. The results of a simulation to analyze the performance of systems of a similar configuration to the ERS-1 wind scatterometer are assessed. The results show that an initial skill of between 70 percent to 80 percent is expected. Most errors are caused by ambiguities, and although any ambiguous solution which is chosen as rank 1 is bound to be highly inaccurate, this does mean that substantially correct wind measurements are achievable, provided that the problem of ambiguities can be overcome. Ambiguity removal techniques are reviewed. Promising results are obtained using smoothing algorithms. Ways in which algorithm performance might be further improved are identified. ESA

N89-13072# Marconi Space Systems Ltd., Portsmouth (England).

MULTISTATIC SCATTEROMETRY **c45**

C. D. Hall and R. A. Cordey (GEC-Marconi Electronics Ltd., Chelmsford, England) *In* ESA, Proceedings of the 1988 International Geoscience and Remote Sensing Symposium (IGARSS 1988) on Remote Sensing: Moving Towards the 21st Century, Volume 1 Aug. 1988 p 561-562 (For primary document see N89-12936 04-42)

Copyright Avail: NTIS HC A99/MF E03; ESA Publications Div., ESTEC, Noordwijk, Netherlands, 120 US dollars or 250 Dutch guilders

The concept of a scatterometer based on multistatic principles is described. The performance of a system using GPSS transmitters and a radiometer style receiver is shown to be inadequate. It is

shown that transmitters of much higher power and a longer code modulation than GPSS are required to realise a system with useful performance. ESA

N89-13073*# Jet Propulsion Lab., California Inst. of Tech., Pasadena.

PERFORMANCE OF A SCANNING PENCIL-BEAM SPACEBORNE SCATTEROMETER FOR OCEAN WIND MEASUREMENTS

R. K. Moore (Kansas Univ. Center for Research, Inc., Lawrence.), R. G. Kennett, and K. Fuk *In* ESA, Proceedings of the 1988 International Geoscience and Remote Sensing Symposium (IGARSS 1988) on Remote Sensing: Moving Towards the 21st Century, Volume 1 Aug. 1988 p 563-564 (For primary document see N89-12936 04-42)

Copyright Avail: NTIS HC A99/MF E03; ESA Publications Div., ESTEC, Noordwijk, Netherlands, 120 US dollars or 250 Dutch guilders

Simulation results show that a scatterometer design using two pencil beams scanning at different incidence angles measures the near-surface oceanic winds from a satellite better under most conditions than previous designs. The return signals from the ocean surface are much stronger than those from the fan beams used previously. Performance on a polar-orbiting satellite is compared with that of a fan beam spaceborne scatterometer. A wider and continuous swath is covered. The improvement in performance is higher at low wind speeds, so it is particularly suitable for measuring the low-mean-speed tropical wind fields. Performance on a low altitude tropic-orbiting platform such as the Space Station is also shown. ESA

N89-13074*# National Aeronautics and Space Administration. Wallops Flight Facility, Wallops Island, Va.

EFFECTS OF RAINFALL ON SCATTEROMETER DERIVED WIND SPEEDS **c32**

L. F. Bliven and G. Norcross (Computer Sciences Corp., Wallops Island, Va.) *In* ESA, Proceedings of the 1988 International Geoscience and Remote Sensing Symposium (IGARSS 1988) on Remote Sensing: Moving Towards the 21st Century, Volume 1 Aug. 1988 p 565-566 (For primary document see N89-12936 04-42)

(Contract ONR-146-70-03)

Copyright Avail: NTIS HC A99/MF E03; ESA Publications Div., ESTEC, Noordwijk, Netherlands, 120 US dollars or 250 Dutch guilders

Rainfall modification of scatterometer response from the sea surface was simulated in wind-wave tank experiments. Data show that for a given wind speed, radar cross section increases as rainfall rate increases, but this effect decreases as wind speed increases. An empirical model accounts for these observations. ESA

N89-13075# Marconi Space and Defence Systems Ltd., Portsmouth (England).

RADAR CONTROL, DETECTION AND PROCESSING ELECTRONICS DESIGN AS USED FOR THE ERS-1 WIND SCATTEROMETER SPACE SEGMENT **c32**

N. P. Fillery *In* ESA, Proceedings of the 1988 International Geoscience and Remote Sensing Symposium (IGARSS 1988) on Remote Sensing: Moving Towards the 21st Century, Volume 1 Aug. 1988 p 567-568 (For primary document see N89-12936 04-42)

Copyright Avail: NTIS HC A99/MF E03; ESA Publications Div., ESTEC, Noordwijk, Netherlands, 120 US dollars or 250 Dutch guilders

A design philosophy and structure as used successfully by the ERS-1 scatterometer electronics is presented. Key aspects affecting performance and producibility, including hardware/software partitioning, are discussed. The detailed design techniques used for radar control, signal detection, and processing are described. A fully representative engineering model is used as the basis for presenting performance. ESA

N89-13076# Canada Centre for Remote Sensing, Ottawa (Ontario).

THE CANADA CENTRE FOR REMOTE SENSING (CCRS) GROUND-BASED MICROWAVE FACILITY **c43**

B. Brisco, R. J. Brown, and G. J. Sofko (Saskatchewan Univ., Saskatoon.) *In* ESA, Proceedings of the 1988 International Geoscience and Remote Sensing Symposium (IGARSS 1988) on Remote Sensing: Moving Towards the 21st Century, Volume 1 Aug. 1988 p 575-576 (For primary document see N89-12936 04-42)

Copyright Avail: NTIS HC A99/MF E03; ESA Publications Div., ESTEC, Noordwijk, Netherlands, 120 US dollars or 250 Dutch guilders

The Canada Center for Remote Sensing (CCRS) truck-mounted scatterometer is described. This microwave facility is being used to provide data regarding the fundamental interactions of microwaves with agricultural targets (i.e., crops and soils). The 1987 measurement campaign is described and an example of the data generated by the scatterometer system is presented. Analyses topics to be addressed with these data are outlined and the goals and objectives of the CCRS ground-based microwave project are described. ESA

N89-13077# Scott, Wilson, Kirkpatrick and Partners, Basingstoke (England).

COTTON AREA MAPPING USING MULTITEMPORAL SATELLITE DATA INTEGRATED WITHIN A GEOGRAPHICAL INFORMATION SYSTEM APPLIED TO A COTTON BOLL WEEVIL CONTROL PROGRAMME IN PARAGUAY **c43**

B. J. Denore, T. E. Beaumont, J. Pender, D. G. Campion, B. R. Critchley, and L. R. M. Marengo (Ministry of Agriculture and Livestock, Ascuncion, Paraguay) *In* ESA, Proceedings of the 1988 International Geoscience and Remote Sensing Symposium (IGARSS 1988) on Remote Sensing: Moving Towards the 21st Century, Volume 1 Aug. 1988 p 581-582 (For primary document see N89-12936 04-42)

Copyright Avail: NTIS HC A99/MF E03; ESA Publications Div., ESTEC, Noordwijk, Netherlands, 120 US dollars or 250 Dutch guilders

An attempt to map the distribution of cotton using satellite imagery in a pest control program is described. Image classification is performed using GIST, a system incorporating image processing, digital mapping, and a relational database. If resulting cotton maps are accurate a program of pest control can be undertaken, which will involve creating a cotton free buffer zone. The location and implementation of a buffer zone depends on many factors including socioeconomic conditions. The biogeography of the boll weevil, the feasibility of monitoring the spread of the pest, and the cotton distribution can be incorporated into GIST to assist in formulating an integrated control program. ESA

N89-13078# European Space Agency. ESRIN, Frascati (Italy).

ERS DATA POLICY **c81**

L. Marelli *In its* Proceedings of the 1988 International Geoscience and Remote Sensing Symposium (IGARSS 1988) on Remote Sensing: Moving Towards the 21st Century, Volume 1 Aug. 1988 p 585-586 (For primary document see N89-12936 04-42)

Copyright Avail: NTIS HC A99/MF E03; ESA Publications Div., ESTEC, Noordwijk, Netherlands, 120 US dollars or 250 Dutch guilders

Factors which affect ERS-1 data policy are summarized. The pricing policy is aimed at three major targets: (1) to identify a partnership with meteorological/sea state forecasting organizations which is consistent with their modus operandi which at the same time will preserve the motivation of member states to guarantee ERS continuity, (2) to price SAR product and services coherent with prevailing conditions of equivalent systems operating in parallel, and (3) to make sure through appropriate mechanisms (Announcement of Opportunity, pilot/demonstration projects), that ERS data will be fully exploited by the scientific/research community and will contribute to the major effort anticipated for

the 90s in order to improve the understanding of world climate and environment changes. ESA

N89-13079# Goettingen Univ. (West Germany). Inst. fuer Forsteinrichtung.
BUILDING A MONITORING SYSTEM BASED ON SATELLITE DATA TO DETECT VEGETATION AND LAND USE CHANGES IN A SUBTROPICAL REGION OF MEXICO **c43**
J. Schnurr *In* ESA, Proceedings of the 1988 International Geoscience and Remote Sensing Symposium (IGARSS 1988) on Remote Sensing: Moving Towards the 21st Century, Volume 1 Aug. 1988 p 587-588 Sponsored by the Deutsche Forschungsgemeinschaft, Bonn, Fed. Republic of Germany (For primary document see N89-12936 04-42)
Copyright Avail: NTIS HC A99/MF E03; ESA Publications Div., ESTEC, Noordwijk, Netherlands, 120 US dollars or 250 Dutch guilders

A project was carried out in an area in Mexico typical of subtropical regions to compare different satellite systems as to classification accuracy for subtropical vegetation types; for a multitemporal analysis (1973 - 1986) to build up a monitoring system for such an area based on satellite data only; and to develop software. The resulting maps and tables demonstrate the potential of satellite data for change detection in extensively used subtropical areas. The images were analyzed by applying a classification method based on discriminant analysis in combination with a global F-test, which provides a measure to describe the separability of training areas. ESA

N89-13080# Instituto de Pesquisas Espaciais, Sao Jose dos Campos (Brazil).
MICROWAVE REMOTE SENSING AT THE INSTITUTE FOR SPACE RESEARCH (INPE) BRAZIL: CONCEPTS AND FUTURE PROSPECTS OF SOIL MOISTURE STUDIES **c43**
H. J. H. Kux and J. V. Soares *In* ESA, Proceedings of the 1988 International Geoscience and Remote Sensing Symposium (IGARSS 1988) on Remote Sensing: Moving Towards the 21st Century, Volume 1 Aug. 1988 p 591-593 (For primary document see N89-12936 04-42)
Copyright Avail: NTIS HC A99/MF E03; ESA Publications Div., ESTEC, Noordwijk, Netherlands, 120 US dollars or 250 Dutch guilders

Experience in microwave remote sensing, applied specifically to soil moisture studies, including the main concepts and prospects for future research is summarized. In the approach proposed, information derived from ground truth, airborne and orbital data, as well as meteorological data, are important inputs. ESA

N89-13081# Deutsche Forschungs- und Versuchsanstalt fuer Luft- und Raumfahrt, Oberpfaffenhofen (West Germany). Inst. for Optoelectronics.
THE MEOSS EXPERIMENT: A TEST CASE FOR FUTURE CARTOGRAPHIC MISSIONS **c43**
F. Lanzl, A. Drescher, K. Hiller, M. Hauck, and D. Beran *In* ESA, Proceedings of the 1988 International Geoscience and Remote Sensing Symposium (IGARSS 1988) on Remote Sensing: Moving Towards the 21st Century, Volume 1 Aug. 1988 p 599-604 (For primary document see N89-12936 04-42)
Copyright Avail: NTIS HC A99/MF E03; ESA Publications Div., ESTEC, Noordwijk, Netherlands, 120 US dollars or 250 Dutch guilders

The Indian/West German monocular electro optical stereo CCD line scanner planned to be launched in 1988 as a joint satellite experiment is presented. The camera system, the mission aspects, and the planned evaluation methods are summarized. ESA

N89-13082# Indian Inst. of Tech., Bombay. Center of Studies in Resources Engineering.
IMPORTANT ASPECTS OF TECHNOLOGY TRANSFER: TRAINING OF INSERVICE ENGINEERS AND SCIENTISTS; SATELLITE REMOTE SENSING **c85**
T. V. Pavate *In* ESA, Proceedings of the 1988 International Geoscience and Remote Sensing Symposium (IGARSS 1988) on Remote Sensing: Moving Towards the 21st Century, Volume 1 Aug. 1988 p 607-608 (For primary document see N89-12936 04-42)
Copyright Avail: NTIS HC A99/MF E03; ESA Publications Div., ESTEC, Noordwijk, Netherlands, 120 US dollars or 250 Dutch guilders

Technology transfer, especially with respect to emerging areas such as satellite remote sensing, and operationalization in multidisciplinary user agencies is discussed. There is a certain amount of urgency being felt in this regard as the conventional method of university education has limited scope in training of large numbers of inservice engineers and scientists who are already working in different capacities. A new approach is mandatory in training of very large number of engineers and scientists towards operationalization of uses of satellite remote sensing to identify, quantify, and manage natural resources on the global scale. ESA

N89-13083*# National Aeronautics and Space Administration. Goddard Space Flight Center, Greenbelt, Md.
THE DERIVATION OF SUB-CANOPY SURFACE TERRAIN MODELS OF COASTAL FORESTS USING SYNTHETIC APERTURE RADAR
M. L. Imhoff and D. B. Gesch (Science Applications Research, Lanham, Md.) *In* ESA, Proceedings of the 1988 International Geoscience and Remote Sensing Symposium (IGARSS 1988) on Remote Sensing: Moving Towards the 21st Century, Volume 1 Aug. 1988 p 613-617 Sponsored by the Overseas Development Administration, Surrey, United Kingdom (For primary document see N89-12936 04-42)
Copyright Avail: NTIS HC A99/MF E03; ESA Publications Div., ESTEC, Noordwijk, Netherlands, 120 US dollars or 250 Dutch guilders

Radar data acquired by the Shuttle Imaging Radar-B mission covering a portion of the Mouths of the Ganges forests were used to create a terrain model for use in determining tidal flow and eventual nutrient transport from the forest to the marine habitat. Results show that good digital topographic terrain models of wet coastal forests can be generated using multiple sets of L-band SAR and ancillary tide elevation data. The dominance of the interaction phenomenon in the radar backscatter of flooded forests can be used to create sub-canopy inundation maps which when merged with tide surface data can be used to generate reasonable topographic models. Ideally models could be improved by using multiple sets of data at a constant incidence angle over the total tide range. The optimal angle for the SAR depends upon the characteristics of the forest. The range of 46 to 57 deg seems applicable to the 12.5 m tall closed canopy in this example. Such models can be an extremely valuable tool for studying and mapping the mangal ecosystem. ESA

N89-13084# Joint Research Centre of the European Communities, Ispra (Italy).
THE CLASSIFICATION OF SEMI-NATURAL VEGETATION FROM LANDSAT THEMATIC MAPPER IMAGERY: A USER'S PERSPECTIVE **c43**
A. S. Belward, J. C. Taylor, M. J. Stuttard, E. Bignal, J. Mathews (Nature Conservatory Council, London, England), and D. Curtis *In* ESA, Proceedings of the 1988 International Geoscience and Remote Sensing Symposium (IGARSS 1988) on Remote Sensing: Moving Towards the 21st Century, Volume 1 Aug. 1988 p 621-622 (For primary document see N89-12936 04-42)
Copyright Avail: NTIS HC A99/MF E03; ESA Publications Div., ESTEC, Noordwijk, Netherlands, 120 US dollars or 250 Dutch guilders

An unsupervised maximum likelihood classification of LANDSAT Thematic Mapper imagery is found to provide the basis for a thematic map of broad habitat types over an area of complex seminatural vegetation. The cover categories to be mapped must be selected such that they have spectral homogeneity in addition to ecological significance. The use of photographic prints of satellite imagery in the field is found to be invaluable in this respect. Where

cover categories are selected on the basis of ecological divisions alone, results are shown to be poor. ESA

N89-13085# Deutsche Forschungs- und Versuchsanstalt fuer Luft- und Raumfahrt, Oberpfaffenhofen (West Germany).
SPECTRAL CHARACTERIZATION OF FOREST DAMAGE IN BEECH, OAK AND PINE STANDS **c43**
W. Kirchhof, S. Guttmann, M. Schramm, I. Zwenger, and M. Lamberty (Forstamt, Frankfurt, West Germany) *In* ESA, Proceedings of the 1988 International Geoscience and Remote Sensing Symposium (IGARSS 1988) on Remote Sensing: Moving Towards the 21st Century, Volume 1 Aug. 1988 p 623-624 (For primary document see N89-12936 04-42)
Copyright Avail: NTIS HC A99/MF E03; ESA Publications Div., ESTEC, Noordwijk, Netherlands, 120 US dollars or 250 Dutch guilders

Multispectral scanner data were gathered at 2000 and 4000 m flight altitudes over a test site to serve as data basis for the development of operational methods for the detection, classification, and mapping of forest disease in larger areas of Germany. In the visible, near IR and short wave IR region, radiance values of beech and oak decrease with increasing damage level. The spectral behavior of pine is nonuniform and influenced by understory vegetation, expect one dense homogenous stand. It shows yellowing of foliage in the visible, which could not be measured for deciduous leaves; decreasing reflectance in the near IR; and slight rise in the short wave IR for the damaged class. Experience suggests important influence of secondary effects mainly caused by loss of biomass, increase of shadow areas, background, and understory vegetation. ESA

N89-13086# Academia Sinica, Beijing (China). Inst. of Electronics.
A LUMINANCE EDGE EXTRACTION METHOD USING GRADIENT OF GRAY LEVEL FOR SYNTHETIC APERTURE RADAR IMAGERIES **c32**
Wei Xu and Zongzhi Chen *In* ESA, Proceedings of the 1988 International Geoscience and Remote Sensing Symposium (IGARSS 1988) on Remote Sensing: Moving Towards the 21st Century, Volume 1 Aug. 1988 p 625-628 (For primary document see N89-12936 04-42)
Copyright Avail: NTIS HC A99/MF E03; ESA Publications Div., ESTEC, Noordwijk, Netherlands, 120 US dollars or 250 Dutch guilders

A method for the extraction of luminance edge of SAR images is proposed. The method uses the relative average gradient and combines detection with tracking. ESA

N89-13087# Geological Survey of Britain, Nottingham.
APPLICATIONS OF REMOTE SENSING FOR GEOLOGICAL MAPPING IN EASTERN EGYPT **c43**
E. A. OConnor and A. J. W. McDonald *In* ESA, Proceedings of the 1988 International Geoscience and Remote Sensing Symposium (IGARSS 1988) on Remote Sensing: Moving Towards the 21st Century, Volume 1 Aug. 1988 p 631-632 (For primary document see N89-12936 04-42)
Copyright Avail: NTIS HC A99/MF E03; ESA Publications Div., ESTEC, Noordwijk, Netherlands, 120 US dollars or 250 Dutch guilders

Results from a mapping project illustrate the relative contributions from multivariate remote sensing data sets to structural and lithological discrimination in a tectonically-mixed terrain of a hyper-arid climatic zone. Structural and morphological detail are well served by air and space photography depending on map-scale requirements. Shuttle-borne radar fulfils a similar role but can yield additional information in areas veneered by thin sand sheets, e.g., dykes in degraded granite plutons. The LANDSAT MSS data is widely available at modest cost and provides an efficient means of producing scalimetrically-accurate image interpreted geological and topographical maps. When more highly detailed lithological extraction is required for mineral exploration and groundwater assessment, the wider infrared wavebands and improved pixel resolution of the LANDSAT TM is an indispensable and cost-effective data base. ESA

43 EARTH RESOURCES AND REMOTE SENSING

Includes remote sensing of earth resources by aircraft and spacecraft; photogrammetry; and aerial photography.

For instrumentation see *35 Instrumentation and Photography.*

N89-13088*# Wyoming Univ., Laramie. Dept. of Botany.
BIOGEOCHEMICAL PROCESSES IN SAGEBRUSH STEPPE: INTERACTIONS OF TERRAIN, VEGETATION AND CHEMICAL CYCLES Final Technical Report, 1 Jun. 1985 - 29 Feb. 1988
William A. Reiners 1988 8 p
(Grant NAG2-355)
(NASA-CR-181486; NAS 1.26:181486) Avail: NTIS HC A02/MF A01 CSCL 02C

Publications, manuscripts in various stages of progress, presentations made at scientific meetings, and undergraduate honor thesis and one Ph.D. dissertation are contained. B.G.

N89-13089 California Univ., San Diego.
MASS AND HEAT BALANCES IN THE UPPER OCEAN Ph.D. Thesis
Daniel Lars Rudnick 1987 114 p
Avail: Univ. Microfilms Order No. DA8804753

The mass and heat balances in the upper ocean are examined from both theoretical and observational points of view. The theoretical model investigates the conditions necessary for frontogenesis in mixed layers. The objective is to understand the roles of advection and turbulent mixing. A unified theory of frontogenesis in mixed layers is proposed. Analytical solutions of the nonlinear mass and density balances in a mixed layer are found in the Lagrangian frame for a wide class of entrainment parameterizations. These solutions show mixed-layer depth and density to be functions of particle position and separation, where mixing is represented by an integral over time following a particle. Thus, given a knowledge of only the cross-front velocity field, the likelihood of frontal formation can be predicted. Both surface convergence and divergence in conjunction with vertical mixing can be frontogenetic. The mass and heat budgets on the northern California continental shelf between Point Arena and Point Reyes are examined using moored measurements of horizontal water velocity and temperature made during the second Coastal Ocean Dynamics Experiment (CODE-2). Dissert. Abstr.

N89-13090# Instituto de Pesquisas Espaciais, Cachoeira Paulista (Brazil).
PHOTOGRAMMETRIC MODEL FOR CORRECTION OF MSS-LANDSAT IMAGERY
Antonio Jose F. MachadoeSilva Aug. 1988 15 p In PORTUGUESE; ENGLISH summary Presented at the 3rd Brazilian Symposium on Remote Sensing, Rio de Janeiro, Brazil, 28-30 Nov. 1984
(INPE-4652-PRE/1359) Avail: NTIS HC A03/MF A01

This photogrammetric model for the correction of MSS-LANDSAT imagery is based on collinearity equations. Using geodetic coordinates (latitude and longitude) it associates each point of the image to a point on the Earth's surface. Internal and external image system distortion are eliminated by the model. The resulting improved geometric image accuracy is reached (about 1 pixel) independently of the Ground Control Point (GCP). Many possibilities exist for refinement of the image using GCP, and cartographic projection images can be generated to satisfy user requirements. Author

N89-13091*# Massachusetts Inst. of Tech., Cambridge. Lab. for Water Resources and Hydrodynamics.
THE STRUCTURE OF RED-INFRARED SCATTERGRAMS OF SEMIVEGETATED LANDSCAPES

Michael F. Jasinski and Peter S. Eagleson 25 Nov. 1988 46 p Submitted for publication
(Grant NAG5-510)
(NASA-CR-183385; NAS 1.26:183385) Avail: NTIS HC A03/MF A01 CSCL 02F

A physically based linear stochastic geometric canopy soil reflectance model is presented for characterizing spatial variability of semivegetated landscapes at subpixel and regional scales. Landscapes are conceptualized as stochastic geometric surfaces, incorporating not only the variability in geometric elements, but also the variability in vegetation and soil background reflectance which can be important in some scenes. The model is used to investigate several possible mechanisms which contribute to the often observed characteristic triangular shape of red-infrared scattergrams of semivegetated landscapes. Scattergrams of simulated and semivegetated scenes are analyzed with respect to the scales of the satellite pixel and subpixel components. Analysis of actual aerial radiometric data of a pecan orchard is presented in comparison with ground observations as preliminary confirmation of the theoretical results. Author

N89-13092# Naval Postgraduate School, Monterey, Calif.
MULTISPECTRAL SATELLITE ANALYSIS OF MARINE STRATOCUMULUS CLOUD MICROPHYSICS M.S. Thesis
Gary M. Mineart Mar. 1988 149 p
(AD-A197316) Avail: NTIS HC A07/MF A01 CSCL 04A

Variations in marine stratocumulus cloud microphysics during FIRE IFO 1987 are observed and analyzed through the use of NOAA-9/10 AVHRR satellite data and aircraft in-cloud measurements. The relationships between channel 3 reflectance and cloud microphysical properties are examined through model reflectances based on Mie theory and the delta-Eddington approximation, and reveal a channel 3 reflectance dependence on cloud droplet size distribution. Satellite observations show significant regions of continental influence over the ocean through higher channel 3 reflectances resulting from the injection of continental aerosols and the associated modification of cloud droplet characteristics. Channel 3 reflectance gradients across individual cloud elements correspond to radially varying cloud droplet size distributions within the elements. Various mesoscale and microscale features such as ship stack effluent tracks and pollution sources are observed in the data. Correlations between reflectance values and aircraft measurements illustrate the potential of estimating cloud droplet size distribution and marine atmospheric boundary layer aerosol composition and concentration through use of satellite data. Such an estimation technique may prove useful in determining climatic implications of cloud reflectance changes due to the influence of natural and man-made aerosol sources, and provide a means to assess the performance of boundary layer electro-optic systems. GRA

N89-13093# Alaska Univ., Fairbanks. Petroleum Development Lab.
DEVELOPMENT OF ALASKAN GAS HYDRATE RESOURCES Annual Report, Oct. 1986 - Sep. 1987
G. D. Sharma, V. A. Kamath, S. P. Godbole, S. L. Patil, Suresh G. Paranjpe, Pralhad Mutalik, and Mehrdad Nadem Oct. 1987 223 p
(Contract DE-FG21-86FE-61114)
(DE88-010270; DOE/FE-61114/2608) Avail: NTIS HC A10/MF A01

Solid ice-like mixtures of natural gas and water in the form of natural gas hydrated have been found immobilized in the rocks beneath the permafrost in Arctic basins and in muds under the deep water along the American continental margins, in the North Sea and several other locations around the world. It is estimated that the arctic areas of the United States may contain as much as 500 trillion SCF of natural gas in the form of gas hydrates (Lewin and Associates, 1983). While the U.S. Arctic gas hydrate resources may have enormous potential and represent long term future source of natural gas, the recovery of this resource from reservoir frozen with gas hydrates has not been commercialized yet. Continuing study and research is essential to develop technologies which will enable a detailed characterization and assessment of this alternative natural gas resource, so that development of cost effective extraction technology. This study presents a state-of-the-art review of the various aspects related to gas hydrates. Reviews on gas hydrated have been published earlier by Byk and Fomina (1968) and Makogen (1981). Since then, many articles have been published on different aspects of gas hydrates. An attempt has been made in this review to provide a more complete and up-to-date information of gas hydrate literature. DOE

N89-13094# National Oceanic and Atmospheric Administration, Washington, D. C. National Environmental Satellite, Data and Information Service.
PRECIPITATION DETECTION WITH SATELLITE MICROWAVE DATA
Y. Chenggang and A. Timchalk Jun. 1988 37 p Prepared in cooperation with Chinese Academy of Meteorological Sciences, Beijing
(PB88-240239; NOAA-TR-NESDIS-32) Avail: NTIS HC A03/MF A01 CSCL 04B

When all four channels of the NOAA polar-orbiting satellite Microwave Sounding Unite (MSU) instrument were screened against a measure of rainrate, MSU Ch 2 (53.74 GHz) was found to be the most useful channel for detecting precipitation over land. The MFA2 values were found to be correlated with an Effective Rain Rate (ERR). In the winter cases, convection was relatively weak and rain rates were small. Results indicate that the MFA2 is marginally useful in detecting rain rates. Its operational use in the TIROS Operational Vertical Sounding (TOVS) algorithm, however, does serve well to prevent cold biased temperature retrievals from being calculated in areas where precipitation contamination is strong. GRA

N89-12937# Cologne Univ. (West Germany). Inst. fuer Geophysik und Meteorologie.
THE AIRBORNE VERSION CONICAL SCAN RADIOMETER (AVCSR): AN AIRBORNE RADIOMETER AS A TOOL FOR SATELLITE DATA VALIDATION
J. Wirth and M. Peeters *In* ESA, Proceedings of the 1988 International Geoscience and Remote Sensing Symposium (IGARSS 1988) on Remote Sensing: Moving Towards the 21st Century, Volume 1 Aug. 1988 p 11-12 (For primary document see N89-12936 04-42)
Copyright Avail: NTIS HC A99/MF E03; ESA Publications Div., ESTEC, Noordwijk, Netherlands, 120 US dollars or 250 Dutch guilders

N89-12940# Technical Univ. of Denmark, Lyngby. Electromagnetics Inst.
ON THE SAMPLING IN IMAGING MICROWAVE RADIOMETERS
N. Skou *In* ESA, Proceedings of the 1988 International Geoscience and Remote Sensing Symposium (IGARSS 1988) on Remote Sensing: Moving Towards the 21st Century, Volume 1 Aug. 1988 p 17-18 (For primary document see N89-12936 04-42)
Copyright Avail: NTIS HC A99/MF E03; ESA Publications Div., ESTEC, Noordwijk, Netherlands, 120 US dollars or 250 Dutch guilders

N89-12941# National Oceanic and Atmospheric Administration, Boulder, Colo. Wave Propagation Lab.
VERIFICATION OF THE ACCURACY OF A NETWORK OF WATER-VAPOR RADIOMETERS
J. B. Snider *In* ESA, Proceedings of the 1988 International Geoscience and Remote Sensing Symposium (IGARSS 1988) on Remote Sensing: Moving Towards the 21st Century, Volume 1 Aug. 1988 p 19-20 (For primary document see N89-12936 04-42)
Copyright Avail: NTIS HC A99/MF E03; ESA Publications Div., ESTEC, Noordwijk, Netherlands, 120 US dollars or 250 Dutch guilders

N89-12947# Virginia Polytechnic Inst. and State Univ., Blacksburg. Dept. of Electrical Engineering.
THE E-PARALLEL POLARIZATION RESPONSE OF A TWO-DIMENSIONAL HETEROGENEOUS LAYER MODELLED BY TWO THIN SHEETS
R. C. Robertson *In* ESA, Proceedings of the 1988 International Geoscience and Remote Sensing Symposium (IGARSS 1988) on Remote Sensing: Moving Towards the 21st Century, Volume 1 Aug. 1988 p 39-40 (For primary document see N89-12936 04-42)
Copyright Avail: NTIS HC A99/MF E03; ESA Publications Div., ESTEC, Noordwijk, Netherlands, 120 US dollars or 250 Dutch guilders

N89-12950*# Jet Propulsion Lab., California Inst. of Tech., Pasadena.
INFERENCE OF GEOLOGIC SURFACE PARAMETERS FROM POLARIMETRIC RADAR OBSERVATIONS AND MODEL INVERSION
Jakob J. VanZyl, P. C. Dubois, H. A. Zebker, and T. G. Farr *In* ESA, Proceedings of the 1988 International Geoscience and Remote Sensing Symposium (IGARSS 1988) on Remote Sensing: Moving Towards the 21st Century, Volume 1 Aug. 1988 p 51-52 (For primary document see N89-12936 04-42)
Copyright Avail: NTIS HC A99/MF E03; ESA Publications Div., ESTEC, Noordwijk, Netherlands, 120 US dollars or 250 Dutch guilders CSCL 08G

N89-12951*# National Aeronautics and Space Administration. Goddard Space Flight Center, Greenbelt, Md.
MODELLING OF SAR POLARISATION PHASE DIFFERENCE FROM TREES
Tsan Mo (Computer Sciences Corp., Beltsville, Md.) and J. R. Wang *In* ESA, Proceedings of the 1988 International Geoscience and Remote Sensing Symposium (IGARSS 1988) on Remote Sensing: Moving Towards the 21st Century, Volume 1 Aug. 1988 p 55-58 (For primary document see N89-12936 04-42)
Copyright Avail: NTIS HC A99/MF E03; ESA Publications Div., ESTEC, Noordwijk, Netherlands, 120 US dollars or 250 Dutch guilders CSCL 02F

N89-12958*# National Aeronautics and Space Administration. Goddard Space Flight Center, Greenbelt, Md.
REQUIREMENTS FOR ONGOING DEVELOPMENT OF THE PILOT LAND DATA SYSTEM (PLDS)
S. W. Wharton and J. A. Newcomer (ST Systems Corp., Lanham, Md.) *In* ESA, Proceedings of the 1988 International Geoscience and Remote Sensing Symposium (IGARSS 1988) on Remote Sensing: Moving Towards the 21st Century, Volume 1 Aug. 1988 p 85-88 Sponsored by NASA, Washington D.C. (For primary document see N89-12936 04-42)
Copyright Avail: NTIS HC A99/MF E03; ESA Publications Div., ESTEC, Noordwijk, Netherlands, 120 US dollars or 250 Dutch guilders CSCL 05B

N89-12959# Reading Univ. (England). NERC Unit for Thematic Information Systems.
THE USE OF REMOTE SENSING IN CONJUNCTION WITH GEOGRAPHIC INFORMATION SYSTEMS FOR LOCAL PLANNING
N. A. Quarmby, J. L. Cushnie, and J. Smith (National Remote Sensing Centre, Farnborough, England) *In* ESA, Proceedings of the 1988 International Geoscience and Remote Sensing Symposium (IGARSS 1988) on Remote Sensing: Moving Towards the 21st Century, Volume 1 Aug. 1988 p 89-92 (For primary document see N89-12936 04-42)
(Contract NERC-F60/G6/12)
Copyright Avail: NTIS HC A99/MF E03; ESA Publications Div., ESTEC, Noordwijk, Netherlands, 120 US dollars or 250 Dutch guilders

N89-12960# Katholieke Universiteit te Leuven (Belgium). Lab. for Land Management.
AN INTEGRATED REMOTE SENSING APPROACH FOR REGIONAL AGROSTATISTICS AND LAND MONITORING
M. Rockaerts, W. Devos, H. Peeters, H. Eerens, and P. Gombeer *In* ESA, Proceedings of the 1988 International Geoscience and Remote Sensing Symposium (IGARSS 1988) on Remote Sensing: Moving Towards the 21st Century, Volume 1 Aug. 1988 p 93-96 (For primary document see N89-12936 04-42)
Copyright Avail: NTIS HC A99/MF E03; ESA Publications Div., ESTEC, Noordwijk, Netherlands, 120 US dollars or 250 Dutch guilders

N89-12961# Eidgenoessische Technische Hochschule, Zurich (Switzerland). Inst. for Communication Technology.
DEVELOPMENT OF A GEOGRAPHIC INFORMATION SYSTEM WITH THE AID OF DIGITAL IMAGE PROCESSING TECHNIQUES
K. Seidel and M. Keller (Zurich Univ., Switzerland) *In* ESA, Proceedings of the 1988 International Geoscience and Remote Sensing Symposium (IGARSS 1988) on Remote Sensing: Moving Towards the 21st Century, Volume 1 Aug. 1988 p 97-100 Sponsored by the Swiss National Research Council, Berne (For primary document see N89-12936 04-42)
Copyright Avail: NTIS HC A99/MF E03; ESA Publications Div., ESTEC, Noordwijk, Netherlands, 120 US dollars or 250 Dutch guilders

N89-12962# Leeds Univ. (England). School of Geography.
MODELLING LAND RESOURCES WITHIN A PILOT GEOGRAPHICAL INFORMATION SYSTEM
J. Hogg *In* ESA, Proceedings of the 1988 International Geoscience and Remote Sensing Symposium (IGARSS 1988) on Remote Sensing: Moving Towards the 21st Century, Volume 1 Aug. 1988 p 101-105 (For primary document see N89-12936 04-42)
Copyright Avail: NTIS HC A99/MF E03; ESA Publications Div., ESTEC, Noordwijk, Netherlands, 120 US dollars or 250 Dutch guilders

N89-12963# Aberdeen Univ. (Scotland). Dept. of Geography.
COMMUNICATION: THE KEY TO INTEGRATING REMOTE SENSING AND GEOGRAPHIC INFORMATION SYSTEMS
D. R. Green, J. J. vanderSanden, and J. A. T. Young (Edinburgh Univ., Scotland) *In* ESA, Proceedings of the 1988 International Geoscience and Remote Sensing Symposium (IGARSS 1988) on Remote Sensing: Moving Towards the 21st Century, Volume 1 Aug. 1988 p 107-109 (For primary document see N89-12936 04-42)
Copyright Avail: NTIS HC A99/MF E03; ESA Publications Div., ESTEC, Noordwijk, Netherlands, 120 US dollars or 250 Dutch guilders

N89-12964# Edinburgh Univ. (Scotland). Dept. of Geography.
INTEGRATING REMOTE SENSING DATA INTO A GEOGRAPHICAL INFORMATION SYSTEM: A FOUNDATION FOR RURAL LAND USE STRATEGIES: NATURE CONSERVANCY COUNCIL PROJECT
R. Healey, P. Dowie, A. Mowle, and J. Holbrook (Natural Environmental Research Council, Edinburgh, Scotland) *In* ESA, Proceedings of the 1988 International Geoscience and Remote Sensing Symposium (IGARSS 1988) on Remote Sensing: Moving Towards the 21st Century, Volume 1 Aug. 1988 p 111-112 (For primary document see N89-12936 04-42)
Copyright Avail: NTIS HC A99/MF E03; ESA Publications Div., ESTEC, Noordwijk, Netherlands, 120 US dollars or 250 Dutch guilders

N89-12965# Strasbourg Univ. (France).
DATA BASES AND REMOTE SENSING [BASES DE DONNEES ET TELEDETECTION]
J. F. Dufourd and C. Silber *In* ESA, Proceedings of the 1988 International Geoscience and Remote Sensing Symposium

(IGARSS 1988) on Remote Sensing: Moving Towards the 21st Century, Volume 1 Aug. 1988 p 113-114 In FRENCH (For primary document see N89-12936 04-42)
Copyright Avail: NTIS HC A99/MF E03; ESA Publications Div., ESTEC, Noordwijk, Netherlands, 120 US dollars or 250 Dutch guilders

N89-12966# Reading Univ. (England).
AN INTERNATIONAL APPROACH TO GIS BASED ON REMOTE SENSING AND TERRAIN CLASSIFICATION
C. W. Mitchell *In* ESA, Proceedings of the 1988 International Geoscience and Remote Sensing Symposium (IGARSS 1988) on Remote Sensing: Moving Towards the 21st Century, Volume 1 Aug. 1988 p 117-118 (For primary document see N89-12936 04-42)
Copyright Avail: NTIS HC A99/MF E03; ESA Publications Div., ESTEC, Noordwijk, Netherlands, 120 US dollars or 250 Dutch guilders

N89-12967# Leeds Univ. (England). School of Geography.
ANALYSIS OF POTATO CROP DISTRIBUTION USING REMOTELY SENSED AND ENVIRONMENTAL DATA IN A PILOT GEOGRAPHICAL INFORMATION SYSTEM
N. Stuart, J. Hogg, G. G. Wright, and J. G. Morrice (MacAulay Land Use Research Inst., Aberdeen, Scotland) *In* ESA, Proceedings of the 1988 International Geoscience and Remote Sensing Symposium (IGARSS 1988) on Remote Sensing: Moving Towards the 21st Century, Volume 1 Aug. 1988 p 119-124 (For primary document see N89-12936 04-42)
Copyright Avail: NTIS HC A99/MF E03; ESA Publications Div., ESTEC, Noordwijk, Netherlands, 120 US dollars or 250 Dutch guilders

N89-12976# Scott Polar Research Inst., Cambridge (England).
TOPOGRAPHIC EFFECTS ON LIGHT SCATTERING FROM SNOW
W. G. Rees and J. A. Dowdeswell (University Coll. of Wales, Aberystwyth.) *In* ESA, Proceedings of the 1988 International Geoscience and Remote Sensing Symposium (IGARSS 1988) on Remote Sensing: Moving Towards the 21st Century, Volume 1 Aug. 1988 p 161-164 (For primary document see N89-12936 04-42)
Copyright Avail: NTIS HC A99/MF E03; ESA Publications Div., ESTEC, Noordwijk, Netherlands, 120 US dollars or 250 Dutch guilders

N89-12984*# National Aeronautics and Space Administration. Goddard Space Flight Center, Greenbelt, Md.
PIPS: A PROCEDURE FOR INTERACTIVE PYRAMID SEGMENTATION
S. W. Wharton *In* ESA, Proceedings of the 1988 International Geoscience and Remote Sensing Symposium (IGARSS 1988) on Remote Sensing: Moving Towards the 21st Century, Volume 1 Aug. 1988 p 197-200 Sponsored by the Director's Discretionary Fund, Greenbelt, Md. (For primary document see N89-12936 04-42)
Copyright Avail: NTIS HC A99/MF E03; ESA Publications Div., ESTEC, Noordwijk, Netherlands, 120 US dollars or 250 Dutch guilders CSCL 08B

N89-12985# North Carolina Univ., Raleigh.
MULTITEMPORAL RESOURCE COMPLEX ANALYSIS OF CATINIA PROVINCE, ITALY FROM LANDSAT-TM DATA
S. Khorram, J. Brockhaus, and A. Gerachi (Catania Univ., Italy) *In* ESA, Proceedings of the 1988 International Geoscience and Remote Sensing Symposium (IGARSS 1988) on Remote Sensing: Moving Towards the 21st Century, Volume 1 Aug. 1988 p 201-204 (For primary document see N89-12936 04-42)
Copyright Avail: NTIS HC A99/MF E03; ESA Publications Div., ESTEC, Noordwijk, Netherlands, 120 US dollars or 250 Dutch guilders

N89-12986# Karlsruhe Univ. (West Germany). Inst. fuer Photogrammetrie und Fernerkundung.
LARGE AREA TM LAND COVER CLASSIFICATION OF MITTLERER OBERRHEIN COUNTY, SOUTHWEST GERMANY, AND ITS USE FOR REGIONAL PLANNING AND CROP SURVEYS
C. Schmullius *In* ESA, Proceedings of the 1988 International Geoscience and Remote Sensing Symposium (IGARSS 1988) on Remote Sensing: Moving Towards the 21st Century, Volume 1 Aug. 1988 p 207-210 (For primary document see N89-12936 04-42)
Copyright Avail: NTIS HC A99/MF E03; ESA Publications Div., ESTEC, Noordwijk, Netherlands, 120 US dollars or 250 Dutch guilders

N89-12987# Liege Univ. (Belgium). Dept. of Geography.
TOWARDS AN URBAN LAND-USE CLASSIFICATION USING TEXTURAL AND MORPHOLOGICAL CRITERIA
Y. Baudot, I. Nadasdi, and J.-P. Donnay *In* ESA, Proceedings of the 1988 International Geoscience and Remote Sensing Symposium (IGARSS 1988) on Remote Sensing: Moving Towards the 21st Century, Volume 1 Aug. 1988 p 211-212 (For primary document see N89-12936 04-42)
Copyright Avail: NTIS HC A99/MF E03; ESA Publications Div., ESTEC, Noordwijk, Netherlands, 120 US dollars or 250 Dutch guilders

N89-12988# Kingston Polytechnic, Kingston-Upon-Thames (England). School of Geography.
THE DETECTION OF UNIMPROVED GRASSLAND IN BERKSHIRE USING A BINARY DECISION TREE APPROACH
N. M. Trodd and A. J. Morton (Imperial Coll. of Science and Technology, London, England) *In* ESA, Proceedings of the 1988 International Geoscience and Remote Sensing Symposium (IGARSS 1988) on Remote Sensing: Moving Towards the 21st Century, Volume 1 Aug. 1988 p 213-214 (For primary document see N89-12936 04-42)
Copyright Avail: NTIS HC A99/MF E03; ESA Publications Div., ESTEC, Noordwijk, Netherlands, 120 US dollars or 250 Dutch guilders

N89-12989# National Inst. for Environmental Studies, Tsukuba (Japan).
DETECTION OF SEASONAL AND LONG-TERM CHANGES IN LAND COVER FROM MULTITEMPORAL LANDSAT MSS DATA
T. Yokota and Y. Matsumoto *In* ESA, Proceedings of the 1988 International Geoscience and Remote Sensing Symposium (IGARSS 1988) on Remote Sensing: Moving Towards the 21st Century, Volume 1 Aug. 1988 p 215-216 (For primary document see N89-12936 04-42)
Copyright Avail: NTIS HC A99/MF E03; ESA Publications Div., ESTEC, Noordwijk, Netherlands, 120 US dollars or 250 Dutch guilders

N89-12990# Kingston Polytechnic, Kingston-Upon-Thames (England). School of Geography.
CROP CLASSIFICATION WITH MULTI-TEMPORAL X-BAND SAR DATA
G. M. Foody, P. J. Curran, G. B. Groom, and D. C. Munro (Hawaii Univ., Manoa.) *In* ESA, Proceedings of the 1988 International Geoscience and Remote Sensing Symposium (IGARSS 1988) on Remote Sensing: Moving Towards the 21st Century, Volume 1 Aug. 1988 p 217-220 (For primary document see N89-12936 04-42)
Copyright Avail: NTIS HC A99/MF E03; ESA Publications Div., ESTEC, Noordwijk, Netherlands, 120 US dollars or 250 Dutch guilders

N89-12991# Rothamsted Experimental Station, Harpenden (England).
SPATIAL RESOLUTION FOR REMOTE SENSING OF FOREST PLANTATIONS
P. M. Atkinson and F. M. Danson (Sheffield Univ., England) *In*

ESA, Proceedings of the 1988 International Geoscience and Remote Sensing Symposium (IGARSS 1988) on Remote Sensing: Moving Towards the 21st Century, Volume 1 Aug. 1988 p 221-223 Sponsored by the Natural Environment Research Council, London, United Kingdom (For primary document see N89-12936 04-42)
Copyright Avail: NTIS HC A99/MF E03; ESA Publications Div., ESTEC, Noordwijk, Netherlands, 120 US dollars or 250 Dutch guilders

N89-13002# Sheffield Univ. (England). Dept. of Geography.
RELATIONSHIPS BETWEEN THE NITROGEN CONTENT OF GRASS AND REFLECTANCE
S. E. Plummer *In* ESA, Proceedings of the 1988 International Geoscience and Remote Sensing Symposium (IGARSS 1988) on Remote Sensing: Moving Towards the 21st Century, Volume 1 Aug. 1988 p 265-267 (For primary document see N89-12936 04-42)
Copyright Avail: NTIS HC A99/MF E03; ESA Publications Div., ESTEC, Noordwijk, Netherlands, 120 US dollars or 250 Dutch guilders

N89-13003# Joint Research Centre of the European Communities, Ispra (Italy).
SMALL FORMAT AIR PHOTO FROM ULTRAHIGH AIRCRAFT AS AN AID FOR DATA COLLECTION OF AGRICULTURAL STATISTICS IN SAHELIAN COUNTRIES
E. Bartholome, J.-M. Gregoire, and R. Zeyen *In* ESA, Proceedings of the 1988 International Geoscience and Remote Sensing Symposium (IGARSS 1988) on Remote Sensing: Moving Towards the 21st Century, Volume 1 Aug. 1988 p 269-270 (For primary document see N89-12936 04-42)
Copyright Avail: NTIS HC A99/MF E03; ESA Publications Div., ESTEC, Noordwijk, Netherlands, 120 US dollars or 250 Dutch guilders

N89-13004# National Space Development Agency, Ohashi (Japan). Earth Observation Center.
VERIFICATION RESULTS OF MOS-1 MULTISPECTRAL SELF SCANNING RADIOMETER (MESSR) DATA
K. Maeda, H. Wakabayashi, K. Tasaki, M. Shimada, and H. Sato *In* ESA, Proceedings of the 1988 International Geoscience and Remote Sensing Symposium (IGARSS 1988) on Remote Sensing: Moving Towards the 21st Century, Volume 1 Aug. 1988 p 271-274 (For primary document see N89-12936 04-42)
Copyright Avail: NTIS HC A99/MF E03; ESA Publications Div., ESTEC, Noordwijk, Netherlands, 120 US dollars or 250 Dutch guilders

N89-13006# Department of Agriculture, Beltsville, Md. Hydrology Lab.
LABORATORY EVALUATION OF A FIELD PORTABLE DIELECTRIC/SOIL MOISTURE PROBE
T. J. Jackson *In* ESA, Proceedings of the 1988 International Geoscience and Remote Sensing Symposium (IGARSS 1988) on Remote Sensing: Moving Towards the 21st Century, Volume 1 Aug. 1988 p 281-282 (For primary document see N89-12936 04-42)
Copyright Avail: NTIS HC A99/MF E03; ESA Publications Div., ESTEC, Noordwijk, Netherlands, 120 US dollars or 250 Dutch guilders

N89-13007# National Space Development Agency, Ohashi (Japan). Earth Observation Center.
DATA COLLECTION SYSTEM OPERATING ON JAPAN'S FIRST MARINE OBSERVATION SATELLITE: INFLIGHT EVALUATION OF THE SYSTEM PERFORMANCE
M. Shimada, T. Yamazaki, M. Tsuji, and K. Ayabe *In* ESA, Proceedings of the 1988 International Geoscience and Remote Sensing Symposium (IGARSS 1988) on Remote Sensing: Moving Towards the 21st Century, Volume 1 Aug. 1988 p 283-286 (For primary document see N89-12936 04-42)
Copyright Avail: NTIS HC A99/MF E03; ESA Publications Div., ESTEC, Noordwijk, Netherlands, 120 US dollars or 250 Dutch guilders

N89-13022# Griffiths Remote Sensing, London (England).
THE RELATIVITY UTILITY OF LANDSAT MSS AND SIR-A IMAGERY IN RECONNAISSANCE GEOLOGICAL MAPPING IN NORTHERN SUDAN
P. S. Griffiths *In* ESA, Proceedings of the 1988 International Geoscience and Remote Sensing Symposium (IGARSS 1988) on Remote Sensing: Moving Towards the 21st Century, Volume 1 Aug. 1988 p 359-362 (For primary document see N89-12936 04-42)
Copyright Avail: NTIS HC A99/MF E03; ESA Publications Div., ESTEC, Noordwijk, Netherlands, 120 US dollars or 250 Dutch guilders

N89-13023# Open Univ., Milton (England). Dept. of Earth Sciences.
A REGIONAL TECTONIC STUDY OF NE AND E AFRICA AND ITS IMPLICATION FOR MINERAL EXPLORATION: A SYNOPTIC VIEW FROM SATELLITE IMAGERY
S. M. Behre *In* ESA, Proceedings of the 1988 International Geoscience and Remote Sensing Symposium (IGARSS 1988) on Remote Sensing: Moving Towards the 21st Century, Volume 1 Aug. 1988 p 363-366 (For primary document see N89-12936 04-42)
Copyright Avail: NTIS HC A99/MF E03; ESA Publications Div., ESTEC, Noordwijk, Netherlands, 120 US dollars or 250 Dutch guilders

N89-13024# Reading Univ. (England). NERC Unit for Thematic Informations Systems.
MAPPING THE DISTRIBUTION AND ABUNDANCE OF LITHOLOGICAL UNITS AND SURFACE MINERALOGIES AT JABAL SA'ID, SAUDI ARABIA: AN APPLICATION OF SPECTRAL MIXTURE MODELLING
N. Drake, S. Mackin, T. J. Munday, J. Settle, and A. Al-Sari (Durham Univ., England) *In* ESA, Proceedings of the 1988 International Geoscience and Remote Sensing Symposium (IGARSS 1988) on Remote Sensing: Moving Towards the 21st Century, Volume 1 Aug. 1988 p 367-368 (For primary document see N89-12936 04-42)
Copyright Avail: NTIS HC A99/MF E03; ESA Publications Div., ESTEC, Noordwijk, Netherlands, 120 US dollars or 250 Dutch guilders

N89-13025# Open Univ., Milton (England). Dept. of Earth Sciences.
THE NEED FOR VOLCANO MONITORING AND THE ABILITY TO DETECT ACTIVITY USING EMITTED SHORT WAVELENGTH INFRARED
D. A. Rothery *In* ESA, Proceedings of the 1988 International Geoscience and Remote Sensing Symposium (IGARSS 1988) on Remote Sensing: Moving Towards the 21st Century, Volume 1 Aug. 1988 p 369-372 (For primary document see N89-12936 04-42)
Copyright Avail: NTIS HC A99/MF E03; ESA Publications Div., ESTEC, Noordwijk, Netherlands, 120 US dollars or 250 Dutch guilders

N89-13026# Sheffield Univ. (England). Dept. of Geography.
IMPROVING THE ACCESSIBILITY OF SPATIALLY REFERENCED GEOLOGICAL INFORMATION
S. M. Black *In* ESA, Proceedings of the 1988 International Geoscience and Remote Sensing Symposium (IGARSS 1988) on Remote Sensing: Moving Towards the 21st Century, Volume 1 Aug. 1988 p 373-374 (For primary document see N89-12936 04-42)
Copyright Avail: NTIS HC A99/MF E03; ESA Publications Div., ESTEC, Noordwijk, Netherlands, 120 US dollars or 250 Dutch guilders

N89-13027# Dundee Univ. (Scotland). Dept. of Applied Physics and Electronic and Mfg. Engineering.
THE INTERPRETATION OF ICELANDIC TUNDRA FEATURES FROM LANDSAT-MSS DATA
R. A. Vaughan and P. O. Vaughan (Imperial Coll. of Science and Technology, London, England) *In* ESA, Proceedings of the 1988 International Geoscience and Remote Sensing Symposium (IGARSS 1988) on Remote Sensing: Moving Towards the 21st Century, Volume 1 Aug. 1988 p 375-376 (For primary document see N89-12936 04-42)
Copyright Avail: NTIS HC A99/MF E03; ESA Publications Div., ESTEC, Noordwijk, Netherlands, 120 US dollars or 250 Dutch guilders

N89-13028# Reading Univ. (England). Dept. of Geography.
MONITORING PLAYAS USING THEMATIC MAPPER DATA
A. C. Millington, N. A. Quarmby, N. Drake, A. J. Reading, and J. R. G. Townshend *In* ESA, Proceedings of the 1988 International Geoscience and Remote Sensing Symposium (IGARSS 1988) on Remote Sensing: Moving Towards the 21st Century, Volume 1 Aug. 1988 p 377-380 (For primary document see N89-12936 04-42)
(Contracts NERC-F60/G6/12; NERC-GT4/85/GS/85)
Copyright Avail: NTIS HC A99/MF E03; ESA Publications Div., ESTEC, Noordwijk, Netherlands, 120 US dollars or 250 Dutch guilders

N89-13040# Zurich Univ. (Switzerland). Remote Sensing Labs.
IMPROVEMENT IN NOAA-AVHRR SNOWCOVER DETERMINATION FOR RUNOFF PREDICTION
C. Frank, K. I. Itten, and K. Staenz *In* ESA, Proceedings of the 1988 International Geoscience and Remote Sensing Symposium (IGARSS 1988) on Remote Sensing: Moving Towards the 21st Century, Volume 1 Aug. 1988 p 433-435 (For primary document see N89-12936 04-42)
Copyright Avail: NTIS HC A99/MF E03; ESA Publications Div., ESTEC, Noordwijk, Netherlands, 120 US dollars or 250 Dutch guilders

N89-13041# Helsinki Univ. of Technology, Espoo (Finland). Dept. of Space Technology.
MICROWAVE EMISSION BEHAVIOR OF SNOW
M. T. Hallikainen and V. I. Jaaskelainen *In* ESA, Proceedings of the 1988 International Geoscience and Remote Sensing Symposium (IGARSS 1988) on Remote Sensing: Moving Towards the 21st Century, Volume 1 Aug. 1988 p 437-438 (For primary document see N89-12936 04-42)
Copyright Avail: NTIS HC A99/MF E03; ESA Publications Div., ESTEC, Noordwijk, Netherlands, 120 US dollars or 250 Dutch guilders

N89-13042# Kanazawa Univ. (Japan). Lab. of Information Science.
SNOWMELT RUNOFF ESTIMATION USING SNOW COVER EXTENT DATA AND ITS APPLICATION TO OPTIMUM CONTROL OF DAM WATER LEVEL
Y. Kawata, T. Kusaka, and S. Ueno (Kyoto Inst. of Tech., Japan) *In* ESA, Proceedings of the 1988 International Geoscience and Remote Sensing Symposium (IGARSS 1988) on Remote Sensing: Moving Towards the 21st Century, Volume 1 Aug. 1988 p 439-440 (For primary document see N89-12936 04-42)
Copyright Avail: NTIS HC A99/MF E03; ESA Publications Div., ESTEC, Noordwijk, Netherlands, 120 US dollars or 250 Dutch guilders

N89-13043# Puget Sound Univ., Tacoma, Wash.
POLARISATION OF PASSIVE MICROWAVE SIGNALS AS INDICATOR OF SNOW WATER EQUIVALENT
Z. F. Danes and P. L. R. Danes *In* ESA, Proceedings of the 1988 International Geoscience and Remote Sensing Symposium (IGARSS 1988) on Remote Sensing: Moving Towards the 21st Century, Volume 1 Aug. 1988 p 441-442 (For primary document see N89-12936 04-42)
(Contract GS-14-08-0001-A-0353)
Copyright Avail: NTIS HC A99/MF E03; ESA Publications Div., ESTEC, Noordwijk, Netherlands, 120 US dollars or 250 Dutch guilders

N89-13044# Zurich Univ. (Switzerland). Remote Sensing Labs.
MONITORING OF SEASONAL SNOW COVER ON GLACIERS
H. Haefner and P. Laager *In* ESA, Proceedings of the 1988 International Geoscience and Remote Sensing Symposium (IGARSS 1988) on Remote Sensing: Moving Towards the 21st Century, Volume 1 Aug. 1988 p 443-445 (For primary document see N89-12936 04-42)
Copyright Avail: NTIS HC A99/MF E03; ESA Publications Div., ESTEC, Noordwijk, Netherlands, 120 US dollars or 250 Dutch guilders

N89-13046# Massachusetts Univ., Amherst. Microwave Remote Sensing Lab.
MILLIMETER-WAVE BACKSCATTER MEASUREMENTS OF VARIOUS SNOW FORMS
R. M. Narayanan, P. M. Langlois, P. W. Gaiser, and R. E. McIntosh *In* ESA, Proceedings of the 1988 International Geoscience and Remote Sensing Symposium (IGARSS 1988) on Remote Sensing: Moving Towards the 21st Century, Volume 1 Aug. 1988 p 451-452 (For primary document see N89-12936 04-42)
Copyright Avail: NTIS HC A99/MF E03; ESA Publications Div., ESTEC, Noordwijk, Netherlands, 120 US dollars or 250 Dutch guilders

N89-13047# Georgia Inst. of Tech., Atlanta.
STATISTICS AND HIGH RESOLUTION IMAGING OF SNOWPACK AT 35 GHz USING A MICROCOMPUTER
J. M. Trostel *In* ESA, Proceedings of the 1988 International Geoscience and Remote Sensing Symposium (IGARSS 1988) on Remote Sensing: Moving Towards the 21st Century, Volume 1 Aug. 1988 p 453-454 (For primary document see N89-12936 04-42)
Copyright Avail: NTIS HC A99/MF E03; ESA Publications Div., ESTEC, Noordwijk, Netherlands, 120 US dollars or 250 Dutch guilders

N89-13048# Trier Univ., Trier-Tarforst (West Germany). Dept. of Geography and Remote Sensing.
SNOW COVER TO ALTER TERRAIN SIGNATURES ON RADAR IMAGES
W. Geile *In* ESA, Proceedings of the 1988 International Geoscience and Remote Sensing Symposium (IGARSS 1988) on Remote Sensing: Moving Towards the 21st Century, Volume 1 Aug. 1988 p 455-457 (For primary document see N89-12936 04-42)
Copyright Avail: NTIS HC A99/MF E03; ESA Publications Div., ESTEC, Noordwijk, Netherlands, 120 US dollars or 250 Dutch guilders

N89-13049# Department of Agriculture, Beltsville, Md. Hydrology Lab.
MICROCOMPUTERS (PCS) FOR SNOW COVER ANALYSES USING MULTISENSOR SATELLITE DATA
M. F. Baumgartner and A. Rango *In* ESA, Proceedings of the 1988 International Geoscience and Remote Sensing Symposium (IGARSS 1988) on Remote Sensing: Moving Towards the 21st Century, Volume 1 Aug. 1988 p 459-460 (For primary document see N89-12936 04-42)
Copyright Avail: NTIS HC A99/MF E03; ESA Publications Div., ESTEC, Noordwijk, Netherlands, 120 US dollars or 250 Dutch guilders

N89-13050# Research Inst. for Soil Science and Agricultural Chemistry, Budapest (Turkey).
AGROELECOLOGICAL INFORMATION CONTENT OF SPOT DATA
F. Csillag, G. Buttner (FOMI Remote Sensing Center, Budapest, Hungary), and I. Juhasz *In* ESA, Proceedings of the 1988

International Geoscience and Remote Sensing Symposium (IGARSS 1988) on Remote Sensing: Moving Towards the 21st Century, Volume 1 Aug. 1988 p 465-470 Sponsored by the Ministry of Agriculture, Budapest, Hungary and Spot Image, Toulouse, France (For primary document see N89-12936 04-42)
Copyright Avail: NTIS HC A99/MF E03; ESA Publications Div., ESTEC, Noordwijk, Netherlands, 120 US dollars or 250 Dutch guilders

N89-13051# Edinburgh Univ. (Scotland). Dept. of Geography.
EVALUATION OF LANDSAT TM AND SPOT IMAGERY FOR AGRICULTURAL LAND USE PLANNING IN LESS DEVELOPED COUNTRIES
J. R. Wheeler, C. Jarvis, A. J. B. Mitchell, R. B. King, and R. J. White *In* ESA, Proceedings of the 1988 International Geoscience and Remote Sensing Symposium (IGARSS 1988) on Remote Sensing: Moving Towards the 21st Century, Volume 1 Aug. 1988 p 471-472 (For primary document see N89-12936 04-42)
Copyright Avail: NTIS HC A99/MF E03; ESA Publications Div., ESTEC, Noordwijk, Netherlands, 120 US dollars or 250 Dutch guilders

N89-13052# Universite Catholique de Louvain (Belgium). Lab. for Cartography.
COMBINING SPECTRAL AND STRUCTURAL ANALYSES TO SELECT USEFUL CARTOGRAPHIC INFORMATION FROM SPOT IMAGERY
H. Willemsen *In* ESA, Proceedings of the 1988 International Geoscience and Remote Sensing Symposium (IGARSS 1988) on Remote Sensing: Moving Towards the 21st Century, Volume 1 Aug. 1988 p 473-475 (For primary document see N89-12936 04-42)
Copyright Avail: NTIS HC A99/MF E03; ESA Publications Div., ESTEC, Noordwijk, Netherlands, 120 US dollars or 250 Dutch guilders

N89-13053# MacDonald, Dettwiler and Associates Ltd., Richmond (British Columbia).
EXTRACTION OF DENSE DIGITAL ELEVATION MODELS FROM SPOT STEREO IMAGERY
D. S. Kauffman and S. R. Haja (Digim, 1983, Inc. Montreal, Quebec) *In* ESA, Proceedings of the 1988 International Geoscience and Remote Sensing Symposium (IGARSS 1988) on Remote Sensing: Moving Towards the 21st Century, Volume 1 Aug. 1988 p 477-478 (For primary document see N89-12936 04-42)
Copyright Avail: NTIS HC A99/MF E03; ESA Publications Div., ESTEC, Noordwijk, Netherlands, 120 US dollars or 250 Dutch guilders

N89-13054# University Coll., London (England). Dept. of Geography.
THE DIFFERENTIAL RECTIFICATION OF SPOT HRV PANCHROMATIC AND MULTISPECTRAL IMAGERY USING A DIGITAL ELEVATION MODEL
S. Kay *In* ESA, Proceedings of the 1988 International Geoscience and Remote Sensing Symposium (IGARSS 1988) on Remote Sensing: Moving Towards the 21st Century, Volume 1 Aug. 1988 p 479-481 Sponsored by the Natural Environment Research Council, London, United Kingdom (For primary document see N89-12936 04-42)
Copyright Avail: NTIS HC A99/MF E03; ESA Publications Div., ESTEC, Noordwijk, Netherlands, 120 US dollars or 250 Dutch guilders

N89-13055# Stockholm Univ. (Sweden). Dept. of Physical Geography.
LANDSAT THEMATIC MAPPING (TM) AND SPOT HRV FOR SURVEY MAPPING OF BEDROCK OUTCROPS
B. Lunden and K. Wester *In* ESA, Proceedings of the 1988 International Geoscience and Remote Sensing Symposium (IGARSS 1988) on Remote Sensing: Moving Towards the 21st Century, Volume 1 Aug. 1988 p 483-484 (For primary document see N89-12936 04-42)
Copyright Avail: NTIS HC A99/MF E03; ESA Publications Div., ESTEC, Noordwijk, Netherlands, 120 US dollars or 250 Dutch guilders

N89-13056# Reading Univ. (England). Dept. of Geography.
THE PRODUCTION OF ANAGLYPHS FROM SPOT-HRV PANCHROMATIC DATA FOR GEOMORPHOLOGICAL MAPPING
P. J. Styles *In* ESA, Proceedings of the 1988 International Geoscience and Remote Sensing Symposium (IGARSS 1988) on Remote Sensing: Moving Towards the 21st Century, Volume 1 Aug. 1988 p 485-487 (For primary document see N89-12936 04-42)
(Grant NERC-CASE-GT4/86/GS/90)
Copyright Avail: NTIS HC A99/MF E03; ESA Publications Div., ESTEC, Noordwijk, Netherlands, 120 US dollars or 250 Dutch guilders

N89-13057# Aston Univ., Birmingham (England). Remote Sensing Unit.
AN EVALUATION OF SATELLITE IMAGERY, LANDSAT THEMATIC MAPPER AND SPOT-1 HRV, FOR GRASSLAND INVENTORY IN THE UK
J. McGuire and W. G. Collins *In* ESA, Proceedings of the 1988 International Geoscience and Remote Sensing Symposium (IGARSS 1988) on Remote Sensing: Moving Towards the 21st Century, Volume 1 Aug. 1988 p 489-491 (For primary document see N89-12936 04-42)
Copyright Avail: NTIS HC A99/MF E03; ESA Publications Div., ESTEC, Noordwijk, Netherlands, 120 US dollars or 250 Dutch guilders

N89-13058# National Remote Sensing Centre, Farnborough (England).
MONITORING URBAN CHANGE FROM LANDSAT TM AND SPOT SATELLITE IMAGERY BY IMAGE DIFFERENCING
G. H. Griffiths *In* ESA, Proceedings of the 1988 International Geoscience and Remote Sensing Symposium (IGARSS 1988) on Remote Sensing: Moving Towards the 21st Century, Volume 1 Aug. 1988 p 493-497 (For primary document see N89-12936 04-42)
Copyright Avail: NTIS HC A99/MF E03; ESA Publications Div., ESTEC, Noordwijk, Netherlands, 120 US dollars or 250 Dutch guilders

N89-13059# Oslo Univ. (Norway). Dept. of Geography.
EFFECTS OF CHANGING SATELLITE SENSOR ATTRIBUTES
A. K. Gjertsen *In* ESA, Proceedings of the 1988 International Geoscience and Remote Sensing Symposium (IGARSS 1988) on Remote Sensing: Moving Towards the 21st Century, Volume 1 Aug. 1988 p 501-504 (For primary document see N89-12936 04-42)
Copyright Avail: NTIS HC A99/MF E03; ESA Publications Div., ESTEC, Noordwijk, Netherlands, 120 US dollars or 250 Dutch guilders

N89-13060# National Inst. for Environment, Ibaraki (Japan).
EFFICIENT CLASSIFICATION OF MULTISPECTRAL IMAGES BY A BEST LINEAR DISCRIMINANT FUNCTION
Y. Iikura, T. Mizoguchi, and Y. Yasuoka *In* ESA, Proceedings of the 1988 International Geoscience and Remote Sensing Symposium (IGARSS 1988) on Remote Sensing: Moving Towards the 21st Century, Volume 1 Aug. 1988 p 505-508 (For primary document see N89-12936 04-42)
Copyright Avail: NTIS HC A99/MF E03; ESA Publications Div., ESTEC, Noordwijk, Netherlands, 120 US dollars or 250 Dutch guilders

N89-13061# Tokai Univ., Kanagawa (Japan). Research and Information Center.
A NEW SPATIAL CLASSIFICATION ALGORITHM FOR HIGH GROUND RESOLUTION IMAGES

Zi-jue Zhang, H. Shimoda, K. Fukue, and T. Sakata *In* ESA, Proceedings of the 1988 International Geoscience and Remote Sensing Symposium (IGARSS 1988) on Remote Sensing: Moving Towards the 21st Century, Volume 1 Aug. 1988 p 509-512 (For primary document see N89-12936 04-42)
Copyright Avail: NTIS HC A99/MF E03; ESA Publications Div., ESTEC, Noordwijk, Netherlands, 120 US dollars or 250 Dutch guilders

N89-13062# Kingston Polytechnic, Kingston-Upon-Thames (England). School of Geography.
CLASSIFICATION DECISION RULE MODIFICATION ON THE BASIS OF INFORMATION EXTRACTED FROM TRAINING DATA
G. M. Foody, T. F. Wood, and N. M. Trodd *In* ESA, Proceedings of the 1988 International Geoscience and Remote Sensing Symposium (IGARSS 1988) on Remote Sensing: Moving Towards the 21st Century, Volume 1 Aug. 1988 p 513-516 (For primary document see N89-12936 04-42)
Copyright Avail: NTIS HC A99/MF E03; ESA Publications Div., ESTEC, Noordwijk, Netherlands, 120 US dollars or 250 Dutch guilders

N89-13063# University Coll., London (England). Dept. of Computer Science.
LAPWING: A TRAINABLE SPATIAL FEATURE RECOGNITION SYSTEM
I. Poole, G. G. Wilkinson, and G. P. Otto *In* ESA, Proceedings of the 1988 International Geoscience and Remote Sensing Symposium (IGARSS 1988) on Remote Sensing: Moving Towards the 21st Century, Volume 1 Aug. 1988 p 517-518 Sponsored by the Natural Environment Research Council, London, United Kingdom (For primary document see N89-12936 04-42)
Copyright Avail: NTIS HC A99/MF E03; ESA Publications Div., ESTEC, Noordwijk, Netherlands, 120 US dollars or 250 Dutch guilders

N89-13064# Missouri Univ., Rolla.
CO-OCCURRENCE MATRIX MODIFICATION FOR SMALL REGION TEXTURE MEASUREMENT AND COMPARISON
G. E. Carlson and W. J. Ebel *In* ESA, Proceedings of the 1988 International Geoscience and Remote Sensing Symposium (IGARSS 1988) on Remote Sensing: Moving Towards the 21st Century, Volume 1 Aug. 1988 p 519-520 (For primary document see N89-12936 04-42)
Copyright Avail: NTIS HC A99/MF E03; ESA Publications Div., ESTEC, Noordwijk, Netherlands, 120 US dollars or 250 Dutch guilders

N89-13065# Reading Univ. (England). Dept. of Geography.
THE INTERRELATIONSHIP BETWEEN RESAMPLING METHOD AND INFORMATION EXTRACTION TECHNIQUE
P. Atkinson *In* ESA, Proceedings of the 1988 International Geoscience and Remote Sensing Symposium (IGARSS 1988) on Remote Sensing: Moving Towards the 21st Century, Volume 1 Aug. 1988 p 521-527 (For primary document see N89-12936 04-42)
(Grant NERC-GT4/83/TLS/43)
Copyright Avail: NTIS HC A99/MF E03; ESA Publications Div., ESTEC, Noordwijk, Netherlands, 120 US dollars or 250 Dutch guilders

N89-13066# Tokai Univ., Kanagawa (Japan). Reserch and Information Center.
ACCURACY OF LAND COVER CLASSIFICATION OF THEMATIC MAPPER (TM) AND SPOT DATA
H. Shimoda, K. Fukue, R. Yamaguchi, Zi-jue Zhang, and T. Sakata *In* ESA, Proceedings of the 1988 International Geoscience and Remote Sensing Symposium (IGARSS 1988) on Remote Sensing: Moving Towards the 21st Century, Volume 1 Aug. 1988 p 529-535 (For primary document see N89-12936 04-42)
Copyright Avail: NTIS HC A99/MF E03; ESA Publications Div., ESTEC, Noordwijk, Netherlands, 120 US dollars or 250 Dutch guilders

N89-13068# New South Wales Univ., Kensington (Australia). Center for Remote Sensing.
CHANGE DIRECTION ANALYSIS USING LANDSAT IMAGERY: A REVIEW OF METHODOLOGY
A. K. Milne *In* ESA, Proceedings of the 1988 International Geoscience and Remote Sensing Symposium (IGARSS 1988) on Remote Sensing: Moving Towards the 21st Century, Volume 1 Aug. 1988 p 541-544 (For primary document see N89-12936 04-42)
Copyright Avail: NTIS HC A99/MF E03; ESA Publications Div., ESTEC, Noordwijk, Netherlands, 120 US dollars or 250 Dutch guilders

N89-13076# Canada Centre for Remote Sensing, Ottawa (Ontario).
THE CANADA CENTRE FOR REMOTE SENSING (CCRS) GROUND-BASED MICROWAVE FACILITY
B. Brisco, R. J. Brown, and G. J. Sofko (Saskatchewan Univ., Saskatoon.) *In* ESA, Proceedings of the 1988 International Geoscience and Remote Sensing Symposium (IGARSS 1988) on Remote Sensing: Moving Towards the 21st Century, Volume 1 Aug. 1988 p 575-576 (For primary document see N89-12936 04-42)
Copyright Avail: NTIS HC A99/MF E03; ESA Publications Div., ESTEC, Noordwijk, Netherlands, 120 US dollars or 250 Dutch guilders

N89-13077# Scott, Wilson, Kirkpatrick and Partners, Basingstoke (England).
COTTON AREA MAPPING USING MULTITEMPORAL SATELLITE DATA INTEGRATED WITHIN A GEOGRAPHICAL INFORMATION SYSTEM APPLIED TO A COTTON BOLL WEEVIL CONTROL PROGRAMME IN PARAGUAY
B. J. Denore, T. E. Beaumont, J. Pender, D. G. Campion, B. R. Critchley, and L. R. M. Marengo (Ministry of Agriculture and Livestock, Ascuncion, Paraguay) *In* ESA, Proceedings of the 1988 International Geoscience and Remote Sensing Symposium (IGARSS 1988) on Remote Sensing: Moving Towards the 21st Century, Volume 1 Aug. 1988 p 581-582 (For primary document see N89-12936 04-42)
Copyright Avail: NTIS HC A99/MF E03; ESA Publications Div., ESTEC, Noordwijk, Netherlands, 120 US dollars or 250 Dutch guilders

N89-13079# Goettingen Univ. (West Germany). Inst. fuer Forsteinrichtung.
BUILDING A MONITORING SYSTEM BASED ON SATELLITE DATA TO DETECT VEGETATION AND LAND USE CHANGES IN A SUBTROPICAL REGION OF MEXICO
J. Schnurr *In* ESA, Proceedings of the 1988 International Geoscience and Remote Sensing Symposium (IGARSS 1988) on Remote Sensing: Moving Towards the 21st Century, Volume 1 Aug. 1988 p 587-588 Sponsored by the Deutsche Forschungsgemeinschaft, Bonn, Fed. Republic of Germany (For primary document see N89-12936 04-42)
Copyright Avail: NTIS HC A99/MF E03; ESA Publications Div., ESTEC, Noordwijk, Netherlands, 120 US dollars or 250 Dutch guilders

N89-13080# Instituto de Pesquisas Espaciais, Sao Jose dos Campos (Brazil).
MICROWAVE REMOTE SENSING AT THE INSTITUTE FOR SPACE RESEARCH (INPE) BRAZIL: CONCEPTS AND FUTURE PROSPECTS OF SOIL MOISTURE STUDIES
H. J. H. Kux and J. V. Soares *In* ESA, Proceedings of the 1988 International Geoscience and Remote Sensing Symposium (IGARSS 1988) on Remote Sensing: Moving Towards the 21st Century, Volume 1 Aug. 1988 p 591-593 (For primary document see N89-12936 04-42)

Copyright Avail: NTIS HC A99/MF E03; ESA Publications Div., ESTEC, Noordwijk, Netherlands, 120 US dollars or 250 Dutch guilders

N89-13081# Deutsche Forschungs- und Versuchsanstalt fuer Luft- und Raumfahrt, Oberpfaffenhofen (West Germany). Inst. for Optoelectronics.
THE MEOSS EXPERIMENT: A TEST CASE FOR FUTURE CARTOGRAPHIC MISSIONS
F. Lanzl, A. Drescher, K. Hiller, M. Hauck, and D. Beran *In* ESA, Proceedings of the 1988 International Geoscience and Remote Sensing Symposium (IGARSS 1988) on Remote Sensing: Moving Towards the 21st Century, Volume 1 Aug. 1988 p 599-604 (For primary document see N89-12936 04-42)
Copyright Avail: NTIS HC A99/MF E03; ESA Publications Div., ESTEC, Noordwijk, Netherlands, 120 US dollars or 250 Dutch guilders

N89-13084# Joint Research Centre of the European Communities, Ispra (Italy).
THE CLASSIFICATION OF SEMI-NATURAL VEGETATION FROM LANDSAT THEMATIC MAPPER IMAGERY: A USER'S PERSPECTIVE
A. S. Belward, J. C. Taylor, M. J. Stuttard, E. Bignal, J. Mathews (Nature Conservatory Council, London, England), and D. Curtis *In* ESA, Proceedings of the 1988 International Geoscience and Remote Sensing Symposium (IGARSS 1988) on Remote Sensing: Moving Towards the 21st Century, Volume 1 Aug. 1988 p 621-622 (For primary document see N89-12936 04-42)
Copyright Avail: NTIS HC A99/MF E03; ESA Publications Div., ESTEC, Noordwijk, Netherlands, 120 US dollars or 250 Dutch guilders

N89-13085# Deutsche Forschungs- und Versuchsanstalt fuer Luft- und Raumfahrt, Oberpfaffenhofen (West Germany).
SPECTRAL CHARACTERIZATION OF FOREST DAMAGE IN BEECH, OAK AND PINE STANDS
W. Kirchhof, S. Guttmann, M. Schramm, I. Zwenger, and M. Lamberty (Forstamt, Frankfurt, West Germany) *In* ESA, Proceedings of the 1988 International Geoscience and Remote Sensing Symposium (IGARSS 1988) on Remote Sensing: Moving Towards the 21st Century, Volume 1 Aug. 1988 p 623-624 (For primary document see N89-12936 04-42)
Copyright Avail: NTIS HC A99/MF E03; ESA Publications Div., ESTEC, Noordwijk, Netherlands, 120 US dollars or 250 Dutch guilders

N89-13087# Geological Survey of Britain, Nottingham.
APPLICATIONS OF REMOTE SENSING FOR GEOLOGICAL MAPPING IN EASTERN EGYPT
E. A. OConnor and A. J. W. McDonald *In* ESA, Proceedings of the 1988 International Geoscience and Remote Sensing Symposium (IGARSS 1988) on Remote Sensing: Moving Towards the 21st Century, Volume 1 Aug. 1988 p 631-632 (For primary document see N89-12936 04-42)
Copyright Avail: NTIS HC A99/MF E03; ESA Publications Div., ESTEC, Noordwijk, Netherlands, 120 US dollars or 250 Dutch guilders

44 ENERGY PRODUCTION AND CONVERSION

Includes specific energy conversion systems, e.g., fuel cells; global sources of energy; geophysical conversion; and windpower.

For related information see also *07 Aircraft Propulsion and Power, 20 Spacecraft Propulsion and Power,* and *28 Propellants and Fuels.*

N89-13095# Sandia National Labs., Albuquerque, N. Mex. Solar Energy Dept.
PHASE 2 TESTING OF A MOLTEN SALT CENTRAL RECEIVER
James W. Grossman, James M. Chavez, Eugene S. Riley, and Robert F. Boehm (Utah Univ., Salt Lake City.) 1988 10 p Presented at the 4th International Symposium on Research, Development and Applications of Solar Thermal Technology, Santa Fe, N. Mex., 13 Jun. 1988
(Contract DE-AC04-76DP-00789)
(DE88-012701; SAND-87-2921C; CONF-880655-7) Avail: NTIS HC A02/MF A01

A 5-MWt molten salt cavity receiver was designed, constructed, and tested in a program funded by the U.S. Department of Energy. The receiver testing was conducted at the Solar Central Receiver Test Facility (CRTF) in Albuquerque, New Mexico. The initial testing, Phase 1, was performed to characterize the operational capabilities of the receiver. The follow-up testing, Phase 2, was initiated to measure thermal losses and to refine the receiver control algorithm to supplement the data from the Phase 1 testing. The receiver's thermal losses were measured with improved salt mass flow measurements and more accurate temperature measurements to improve the accuracy of the thermal loss data. Additional testing of the receiver control algorithm was undertaken to improve the receiver's control response for recovery from the effects of a cloud transient. In this paper we present the results of the Phase 2 receiver testing and compare them to the Phase 1 test data on receiver thermal loss and cloud transients. DOE

N89-13096# International Centre for Theoretical Physics, Trieste (Italy).
METALLIZATION AND CHARACTERIZATION OF A SILICON p-n JUNCTION DIODE FABRICATED FROM A SOLAR-CELL-TYPE SILICON SUBSTRATE
A. U. Ebong (Port Harcourt Univ., Nigeria) and S. K. Adjepong Dec. 1987 7 p
(DE88-703007; IC-87/405) Avail: NTIS (US Sales Only) HC A02/MF A01

The paper describes the metallization and characterization of a silicon p-n junction diode fabricated, in the laboratory, from a solar-cell-type silicon substrate, using simple equipment and locally-available materials. Metallization of the fabricated device was achieved by electroless nickel plating without the use of a chemical activator such as palladous chloride (PdCl4) which is very expensive. On the basis of the abrupt-junction approximation, values for the substrate concentration and the built-in potential of the fabricated device are calculated from the latter C-V profile and found to be approximately 8.5 x 10 to the 15th/cu cm and 0.53V respectively. The value of the substrate concentration agrees fairly well with that estimated from the resistivity of the substrate. DOE

N89-13097# Department of Energy, Morgantown, W. Va. Energy Technology Center.
FUEL CELLS: A BIBLIOGRAPHY
May 1988 340 p Prepared in cooperation with DOE, Oak Ridge, Tenn.
(DE88-001081; DOE/METC-88-6091; DOE/OSTI-3359-Suppl-3)
Avail: NTIS HC A15/MF A01

This bibliography includes 1392 citations of domestic and foreign reports, journal articles, patents, conference papers and proceedings and books. The citations were taken from the DOE Energy Data Base covering the period March 1985 through February 1988. These citations are arranged in the following six subject categories: general; design and development; performance testing; materials, components, and auxiliaries; applications; and electrochemistry, mass transfer, and thermodynamics. Within each category, the report citations are arranged alphanumerically by report numbers, and nonreport literature citations are arranged in reverse chronological order. Indexes are provided for corporate author, personal author, subject, contract number, and report number. DOE

N89-13098# Glasstech Solar, Inc., Wheatridge, Colo.
PREPARATION AND PROPERTIES OF HIGH-DEPOSITION-RATE a-Si:H FILMS AND SOLAR CELLS USING DISILANE Annual Subcontract Report, 1 May 1987 - 30 Apr. 1988
P. K. Bhat, H. Chatham, and A. Madan Jun. 1988 38 p Prepared for Midwest Research Inst., Golden, Colo.
(Contract DE-AC02-83CH-10093)
(DE88-001191; SERI/STR-211-3364) Avail: NTIS HC A03/MF A01

This report contains results of the first year of research on producing p-i-n amorphous silicon solar cells with the intrinsic layer deposited from higher order silanes at deposition rates of 1 nm/s or more. The research was divided into three major areas: diagnostic studies of monosilane and disilane RF discharges using optical emission spectroscopy and mass spectrometry to assist in optimizing discharge conditions and gas-phase processes; parametric studies of material properties of 1-layers prepared form disilane as a function of deposition rate and other process parameters; and parametric studies of p-i-n devices with the i-layer prepared from disilane at various deposition rates. The focus during the first year was to fabricate a p-i-n solar cell with 9 percent AM1.5 efficiency over an area greater than 0.08 sq cm with the i-layer deposited at 1 nm/s or more. Material properties such as the dark and AM1.5 light conductivities, optical band gap, and conductivity activation energy showed a weak dependence on deposition rate. The performance characteristics of unoptimized p-i-n solar cells with i-layers prepared from disilane were independent of the deposition rate of the i-layer. A p-i-n device was prepared at a rate close to 1 nm/s with an AM1.5 efficiency of 9 percent. DOE

N89-13099# Edgerton, Germeshausen and Grier, Inc., Idaho Falls, Idaho.
IMPROVING THE EFFICIENCY OF BINARY CYCLES
G. L. Mines and C. J. Bliem 1988 6 p Presented at the 6th DOE Geothermal Program Review, San Francisco, Calif., 19 Apr. 1988
(Contract DE-AC07-76ID-01570)
(DE88-015108; EGG-M-88131; CONF-880477-11) Avail: NTIS HC A02/MF A01

The performance of binary geothermal power plants can be improved through the proper choice of a working fluid, and optimization of component designs and operating conditions. This paper summarizes the investigations at the Idaho National Engineering Laboratory (INEL) which are examining binary cycle performance improvements for moderate temperature (350 to 400 F) resources. These investigations examine performance improvements resulting from the supercritical vaporization and countercurrent integral condensation of mixed hydrocarbon working fluids, as well as the modification of the turbine inlet state points to achieve supersaturated turbine vapor expansions. For resources, with the brine outlet temperature restricted, the use of turbine exhaust recuperators is examined. The reference plant used to determine improvements in plant performance in these studies operates at conditions similar to the 45 MW Heber binary plant. The brine effectiveness (watt-hours per pound of brine) is used as an indicator for improvements in performance. The performance of the binary cycle can be improved by 25 to 30 percent relative to the reference plant through the selection of the optimum working fluids and operating conditions, achieving countercurrent integral condensation, and allowing supersaturated vapor expansions in the turbine. DOE

N89-13100# Lawrence Livermore National Lab., Calif.
MICRO HEAT PIPES
Dolores U. Oiness Aug. 1988 10 p
(Contract W-7405-eng-48)
(DE88-016113; UCID-21471) Avail: NTIS HC A02/MF A01

Under the direction of Dr. Tomas Hirschfeld, a preliminary set of experiments was carried out in the spring of 1982 to examine the heat transmitting properties of micro heat pipes. The miniaturized heat pipes were observed to conduct heat better than copper wires of comparable size; calculations indicate a potential conductivity four orders of magnitude greater than that of aluminum. The experiments are described and the calculations are presented. DOE

N89-13101# Midwest Research Inst., Golden, Colo. Wind Research Branch.
PRELIMINARY RESULTS FROM THE DYNAMIC RESPONSE TESTING OF THE NORTHERN POWER SYSTEMS 100-kW WIND TURBINE
R. M. Osgood and S. M. Hock Jun. 1988 5 p Presented at IECEC '88, Denver, Colo., 1 Aug. 1988
(Contract DE-AC02-83CH-10093)
(DE88-001166; SERI/TP-217-3342; CONF-880885-1) Avail: NTIS HC A02/MF A01

The Solar Energy Research Institute (SERI), in cooperation with Northern Power Systems (NPS), conducted a series of dynamic response tests on the NPS 100 kW Wind Turbine as part of the Department of Energy's (DOE) Cooperative Field Test Program. This paper presents a preliminary review of the test data, including average and cyclic machine response characteristics. The mean turbine operating conditions are analyzed as a function of mean wind speed and rotor azimuth position using the method of bins. Rotor bending loads are also presented in the frequency domain to investigate the relative effects of low- and high-frequency wind turbulence. DOE

N89-13102# Midwest Research Inst., Golden, Colo. Solar Energy Research Inst.
SOLAR PHOTOVOLTAIC TECHNOLOGY: THE THIN FILM OPTION
H. S. Ullal, K. Zweibel, E. S. Sabisky, and T. Surek 1988 10 p Presented at the American Institute of Chemical Engineers Summer National Meeting, Denver, Colo., 21 Aug. 1988
(Contract DE-AC02-83CH-10093)
(DE88-001195; SERI/TP-211-3390; CONF-880850-13) Avail: NTIS HC A02/MF A01

Photovoltaics (PV), the direct conversion of sunlight to electricity, was first discovered by scientists at the Bell Labs in 1954. In the late 1960's and 1970's most of the solar cell technology has been used for space applications to power satellites. The main work horse for the PV technology has been crystalline silicon (Si) solar cells. Over the past 15 years this has led to cost reduction from $35/kWh to about $0.30/kWh at the present time. Demonstrated reliability of 20 years or more has resulted in acceptance by several utilities. However, cost reductions in crystalline Si solar cells have been limited by the cost of wafering of ingots and the attendant loss of material. A number of Si sheet solar cells are also being investigated. In the past decade the emphasis of the research and development effort has been focused on thin film solar cells, which have the potential for generating power at much lower cost of $1 to 2/Wp. Thin film solar cells that are presently being investigated and are generating global attention are: amorphous silicon (a-Si:H), cadmium telluride (CdTe), and copper indium diselenide (CuInSe sub 2, or CIS). In the past few years, considerable progress has been made by all three of these thin film solar cells. This paper reviews the current status and future potential of these exiting thin film solar cell technologies. DOE

N89-13103*# Cleveland State Univ., Ohio. Dept. of Chemical Engineering.
ASSESSMENT AND COMPARISON OF 100-MW COAL GASIFICATION PHOSPHORIC ACID FUEL CELL POWER PLANTS
Cheng-Yi Lu Aug. 1988 9 p Presented at the 1988 Fuel Cell Seminar, Long Beach, Calif., 23-26 Oct. 1988; sponsored by the National Fuel Cell Coordinating Group
(Contracts NCC3-17; DE-AI21-80ET-17088)
(NASA-CR-182189; E-4320; DOE/NASA/0017-7; NAS 1.26:182189) Avail: NTIS HC A02/MF A01 CSCL 10A

One of the advantages of fuel cell (FC) power plants is fuel versatility. With changes only in the fuel processor, the power

plant will be able to accept a variety of fuels. This study was performed to design process diagrams, evaluate performance, and to estimate cost of 100 MW coal gasifier (CG)/phosphoric acid fuel cell (PAFC) power plant systems utilizing coal, which is the largest single potential source of alternate hydrocarbon liquids and gases in the United States, as the fuel. Results of this study will identify the most promising integrated CG/PAFC design and its near-optimal operating conditions. The comparison is based on the performance and cost of electricity which is calculated under consistent financial assumptions. Author

N89-12757# Missouri Univ., Rolla. Dept. of Electrical Engineering.
ISOLATION OF OSTEOGENIC CELLS FROM THE TRAUMA-ACTIVATED PERIOSTEUM Final Report
Chang-Hsiao Wu and John Bullock *In* Universal Energy Systems, Inc., United States Air Force Graduate Student Summer Support Program, Volume 1 Dec. 1987 11 p (For primary document see N89-12754 04-31)
Avail: NTIS HC A99/MF E03 CSCL 10A

45 ENVIRONMENT POLLUTION

Includes atmospheric, noise, thermal, and water pollution.

N89-13104 United Nations Environment Programme, Paris (France).
ENVIRONMENTAL MANAGEMENT PRACTICES IN OIL REFINERIES AND TERMINALS: AN OVERVIEW
1987 106 p
(ISBN-92-807-1108-3) Copyright Avail: Issuing Activity

Within the concept of the UNEP (UN Environmental Programme) ongoing review of the environmental effects of specific industries, a seminar was held in Paris in March 1977 on the petroleum industry. An overview document, Environmental Aspects of the Petroleum Industry, was published in 1978 as a synthesis of their evaluation. It discusses policy aspects of the environmental issues to enable appropriate action to take place. To provide a forum for consultation and communication to exchange experiences among governments, industry and relevant international institutions, UNEP established an Environmental Consultative Committee on the Petroleum Industry which held its first meeting in Paris in September 1978 and second in the same city in June 1981. A broad range of views and information were exchanged, such as the environmental impact of oil exploration and production, marine transportation, aspects of pipeline construction and operation, refining, oil spill control, long term effects on hydrocarbons on the marine environment, sulphur in petroleum and its role in acid rain, disposal of oily wastes, environmental management in refineries, terminals, coastal installations, etc. Author

N89-13105# Department of Energy, New York. Environmental Measurements Lab.
WORLDWIDE DEPOSITION OF Sr-90 THROUGH 1985
Z. Russell Juzdan Jun. 1988 34 p
(DE88-015577; EML-515) Avail: NTIS HC A03/MF A01

The total deposition of Sr-90 on the surface of the earth during 1985 was 0.2 PBq, with approximately equal amounts deposited in the Northern and Southern Hemispheres. This is the lowest total deposit since the initiation of the global fallout program of the Environmental Measurements Laboratory in the mid-1950's. The cumulative deposit of Sr-90 decreased to 264 PBq in the Northern Hemisphere and 85 PBq in the Southern Hemisphere, making a worldwide cumulative deposit of 349 PBq (9.4 MCi). DOE

N89-13106# Lawrence Livermore National Lab., Calif.
ASPECTS OF CFC RELATIVE OZONE DESTRUCTION EFFICIENCIES DETERMINED IN THE LLNL 2-D MODEL
P. Connell, K. Grant, and D. Wuebbles Aug. 1988 5 p Presented at the International Quadrennial Ozone Symposium, Gottingen, Fed. Republic of Germany, 8 Aug. 1988
(Contract W-7405-eng-48)
(DE88-015431; UCRL-97987; CONF-8808102-4) Avail: NTIS HC A02/MF A01

We have investigated the efficiency of surface emission of several individual chlorofluorocarbons (CFCs) and hydrogen-containing chlorofluorocarbons (HCFCs) for reducing the calculated steady state total ozone column in both one- and two-dimensional models, relative to the effects of CFC-11 (CFCl sub 3) emission. We find that CFC and HCFC relative efficiencies can vary over two orders of magnitude, mostly as a result of atmospheric lifetimes. For CFCs and HCFCs with long stratospheric lifetimes the calculated efficiency is also reduced by the effects of lower and mid stratospheric photochemistry. Ozone in this region changes according to the net effect of changing rates of oxygen photolysis, direct chlorine-catalyzed ozone loss and interference by active chlorine species in the nitrogen oxide-catalyzed ozone loss process. In these cases, the relative efficiencies show a marked latitudinal dependence, being larger at high latitudes and smaller at lower latitudes. Additionally in these cases, the one-dimensional model appears to overestimate the globally and annually averaged result that is obtained from the two-dimensional model. These considerations should be taken into account when quantities similar to the relative efficiency defined here are applied to CFC production and emission decisions. DOE

N89-13072# Marconi Space Systems Ltd., Portsmouth (England).
MULTISTATIC SCATTEROMETRY
C. D. Hall and R. A. Cordey (GEC-Marconi Electronics Ltd., Chelmsford, England) *In* ESA, Proceedings of the 1988 International Geoscience and Remote Sensing Symposium (IGARSS 1988) on Remote Sensing: Moving Towards the 21st Century, Volume 1 Aug. 1988 p 561-562 (For primary document see N89-12936 04-42)
Copyright Avail: NTIS HC A99/MF E03; ESA Publications Div., ESTEC, Noordwijk, Netherlands, 120 US dollars or 250 Dutch guilders

46 GEOPHYSICS

Includes aeronomy; upper and lower atmosphere studies; ionospheric and magnetospheric physics; and geomagnetism.

For space radiation see *93 Space Radiation.*

N89-13107*# Illinois Univ., Urbana-Champaign. Electro-Optic Systems Lab.
RAYLEIGH LIDAR OBSERVATIONS OF GRAVITY WAVE ACTIVITY IN THE UPPER STRATOSPHERE AT URBANA, ILL. Semiannual Report
C. S. Gardner, M. S. Miller, and C. H. Liu Sep. 1988 67 p
(Grant NsG-5049)
(NASA-CR-182738; NAS 1.26:182738) Avail: NTIS HC A04/MF A01 CSCL 04A

During 13 nights of Rayleigh lidar measurements at Urbana, Ill. in 1984 to 1986, thirty-six quasi-monochromatic gravity waves were observed in the 35 to 50 km altitude region of the stratosphere. The characteristics of the waves are compared with other lidar and radar measurements of gravity waves and the theoretical models of wave saturation and dissipation phenomena. The measured vertical wavelengths ranged from 2 to 11.5 km and the measured vertical phase velocities ranged from 10 to 85 cm/s. The vertical wavelengths and vertical phase velocities were used to infer observed wave periods which ranged from 100 to 1000 min and horizontal wavelengths which ranged from 70 to 2000 km. Dominant wave activity was found at vertical wavelengths between 2 to 4 km and 7 to 10 km. No significant seasonal variations were evident in the observed parameters. Vertical and horizontal wavelengths showed a clear tendency to increase with wave periods, which is consistent with recent sodium lidar studies of quasi-monochromatic waves near the mesopause. An average

amplitude growth length of 20.9 km for the rms wind perturbations was estimated from the data. Kinetic energy density associated with the waves decreased with height, suggesting that waves in this altitude region were subject to dissipation or saturation effects. Author

N89-13108 Iowa Univ., Iowa City.
SPACE-TIME SPECTRAL STUDIES OF GLOBAL STRATOSPHERIC TEMPERATURE FIELDS Ph.D. Thesis
Leslie Robert Lait 1987 124 p
Avail: Univ. Microfilms Order No. DA8805099

A method proposed by Salby for computing the zonal space-time Fourier transform of asynoptically acquired soundings from polar-orbiting satellites was implemented, tested, and applied in two investigations of atmospheric motions. It is demonstrated that the technique is robust under real data conditions, providing meaningful results in the presence of randomly varying signals, sampling errors, and missing data. The spectra computed display several advantageous characteristics: a frequency range which includes very short periods, a lack of distortion due to the asynoptic nature of the data, and a closely-spaced spectra. The method is well suited for detecting features with small amplitudes and/or short periods. The method is applied to measurements of brightness temperature from the Southern Hemisphere polar winter. Finally, the method is applied to a search for two fast-moving waves predicted in a numerical model. The ability of the method to detect very small signals is used to demonstrate the nonexistence of the modes during the time period analyzed. Dissert. Abstr.

N89-13109 Purdue Univ., West Lafayette, Ind.
ON THE INTERACTIONS OF LONGWAVE RADIATION, MICROPHYSICS AND TURBULENCE IN BOUNDARY LAYER CLOUDS Ph.D. Thesis
Adil Rainier Alves 1987 201 p
Avail: Univ. Microfilms Order No. DA8729715

A detailed model for longwave radiative transfer in general cloudy atmospheres was developed and applied to microphysical and macrophysical studies of the radiation regime within typical boundary layer clouds. The model uses high vertical and spectral resolution to provide broadband flux divergence and cloud cooling rates, using LOWTRAN 6 and Chou and Arking's radiative transmission functions and Wiscombe's Mie code to provide the cloud droplet optical characteristics. The model is applicable to clouds with either homogeneous or inhomogeneous liquid water distributions. The spectral resolution of the model is important in determining cooling rates at the cloud top, especially for arbitrary temperature inversions. The substantial cloud-top cooling rates destabilize the cloud convectively, and an analysis of the relative time constants for radiative and convective processes confirms that convection occurs on a much shorter time scale. A mixed layer model version is used to show, at first order, that an accurate representation of the vertical distribution of radiation is important in calculating turbulent fluxes and entrainment rates. The longwave radiative budget of individual droplets is also determined, and shows a dependence on droplet radius. Dissert. Abstr.

N89-13110# Cambridge Univ. (England). Dept. of Applied Mathematics and Theoretical Physics.
FUNDAMENTALS OF MIDDLE-ATMOSPHERIC DYNAMICS Annual Report, 1 Apr. 1987 - 31 Mar. 1988
M. E. McIntyre 31 Mar. 1988 4 p
(Contract N00014-87-G-0170)
(AD-A197358) Avail: NTIS HC A02/MF A01 CSCL 04B

The aim over three years is to advance fundamental understanding of middle atmospheric dynamics, particularly with regard to the vertical and horizontal dynamical coupling associated with planetary scale motions and their interactions with other scales. The immediate aims of the first year are to continue with high-resolution barotropic planetary wave-breaking simulations, to extend these to fully three-dimensional baroclinic simulations using the Cray X-MP/48. The approach is to build and use a sophisticated numerical modelling capability, exploiting the Global Atmospheric Modelling Project, to develop abstract theoretical concepts that are likely to lead to dynamical insight and test them in numerical experiments, and to develop new and efficient ways for scientists to interact with numerical models, exploiting modern workstation facilities. One milestone was the successful initiation of three-dimensional, high-resolution numerical simulations of breaking planetary waves, building upon the barotropic modelling work initiated earlier and still continuing. GRA

N89-13111*# Utah Univ., Salt Lake City. Dept. of Meteorology.
BACKSCATTER LASER DEPOLARIZATION STUDIES OF SIMULATED STRATOSPHERIC AEROSOLS: CRYSTALLIZED SULFURIC ACID DROPLETS Final Report, 2 Jun. 1986 - 1 Jun. 1988
Kenneth Sassen, Hongjie Zhao, and Bing-Kun Yu 15 Nov. 1988 20 p
(Grant NAG1-686)
(NASA-CR-183387; NAS 1.26:183387) Avail: NTIS HC A03/MF A01 CSCL 04A

The optical depolarizing properties of simulated stratospheric aerosols were studied in laboratory laser (0.633 micrometer) backscattering experiments for application to polarization lidar observations. Clouds composed of sulfuric acid solution droplets, some treated with ammonia gas, were observed during evaporation. The results indicate that the formation of minute ammonium sulfate particles from the evaporation of acid droplets produces linear depolarization ratios of beta equivalent to 0.02, but beta equivalent to 0.10 to 0.15 are generated from aged acid cloud aerosols and acid droplet crystallization effects following the introduction of ammonia gas into the chamber. It is concluded that partially crystallized sulfuric acid droplets are a likely candidate for explaining the lidar beta equivalent to 0.10 values that have been observed in the lower stratosphere in the absence of the relatively strong backscattering from homogeneous sulfuric acid droplet (beta equivalent to 0) or ice crystal (beta equivalent to 0.5) clouds. Author

N89-13112# Consiglio Nazionale delle Ricerche, Frascati (Italy). Istituto di Fisica dello Spazio Interplanetario.
INTERACTION OF A HOLLOW-CATHODE SOURCE WITH AN IONOSPHERIC PLASMA
G. Vannaroni, C. B. Cosmovici, U. Guidoni, L. Iess, and L. Scandurra Jul. 1988 35 p
(IFSI-88-10; ETN-88-93477) Avail: NTIS HC A03/MF A01

Hollow cathodes to be used as plasma contactors on rocket or shuttle based experiments are under development. A large plasma chamber was used to permit the simulation of an ionospheric plasma with magnetic field compensation and variation. The interaction between a hollow cathode (HC) plasma plume with an ionospheric plasma beam was investigated by means of Langmuir probes at different distances from the HC source. Preliminary spectroscopic work was also carried out on the HC source. The results are discussed in connection with space plasma physics applications, and are also compared with a theoretical model describing the physical phenomena involved in two plasmas coupling. ESA

N89-13113# Consiglio Nazionale delle Ricerche, Frascati (Italy). Istituto di Fisica dello Spazio Interplanetario.
INJECTION OF IONOSPHERIC IONS INTO THE PLASMA SHEET IN THE EARTH'S MAGNETOTAIL
S. Orsini, M. Candidi, M. Stokholm, and H. Balsiger (Bern Univ., Switzerland) Sep. 1987 32 p Original contains color illustrations
(IFSI-88-13; ETN-88-93480) Avail: NTIS HC A03/MF A01

The ISEE-1 and ISEE-2 observations of the lobe/mantle region and the plasma sheet boundary layer region at distances between 10 and 20 Re downstream during 1978 and 1979, were examined. Cold, tailward flowing ionospheric C(+) streams observed during geomagnetically disturbed periods were statistically analyzed. At the crossing between the lobe/mantle region and the plasma sheet boundary layer region the characteristics of the streams change significantly. These changes suggest the action of energization and isotropization processes which accelerate and make the

ionospheric ions a part of the plasma sheet plasma. It is shown that the stream flow pattern in the lobe/mantle region is in good agreement with the tail lobe ion spectrometer model in the thermal speed distribution as well, as shown previously for the flow velocity and density distributions. Such agreement is extended to the plasma sheet boundary layer qualitatively in the appropriate field configuration. ESA

N89-13114# Observatorio del Ebro, Roquetas (Spain).
IONOSPHERE 1970, VOLUME 58 [IONOSFERA 1970, VOL. 58]
J. O. Cardus and E. Galdon 1987 159 p In SPANISH
(ISSN-0211-5166; ETN-88-93527) Avail: NTIS HC A08/MF A01

The ionospheric sounding measurements made by the Ebro Observatory (Spain) in 1970 are presented. The instruments used include an automatic ionospheric sounding radar working at 0.25 to 20 MHz emitting 50 pulses/sec of up to microsec length. The accuracy of the E1 and ES critical frequency data is less than 0.05 MHz, and for F1 and F2 less than 0.1 MHz. ESA

N89-13115# Instituto Geografico Nacional, Madrid (Spain). Centro Geofisico de Canarias.
[ACTIVITIES REPORT OF THE CANARY GEOPHYSICAL CENTER] Annual Report, 1987 [ANUARIO DEL CENTRO GEOFISICO DE CANARIAS, ANO 1984]
1987 61 p In SPANISH
(ISBN-8-45-055434-9; ETN-88-93528) Avail: NTIS HC A04/MF A01

Data includes absolute horizontal and vertical components of the Earth magnetic field, time and space variation, and secular trends. ESA

47 METEOROLOGY AND CLIMATOLOGY

Includes weather forecasting and modification.

N89-13116 Arizona Univ., Tucson.
THE INCORPORATION OF SULFUR DIOXIDE INTO SNOW AND DEPOSITING ICE Ph.D. Thesis
Marc Philip Valdez 1987 189 p
Avail: Univ. Microfilms Order No. DA8803267

Depth profiles of S(IV) and S(VI) in snow exposed to 20-140 ppbv SO2 for 6 to 12 hours were determined in 48 laboratory experiments. Surface deposition velocity (v sub d) was averaged 0.06 cm/s. Well metamorphosed snow, longer run times, higher SO2 concentrations and colder snow were associated with lower values of v sub d, and vice versa. Melting followed by draining increased v sub d greatly. Four NO2 deposition experiments and one combined SO2-NO2 deposition experiment were conducted. The deposition of SO2 into a snowpack is modelled as an aqeous system, where the liquid water is considered to be present on snow grain surfaces. Gas transport into the snow, air-water partitioning, and aqeous-phase reactions are explicitly considered. Three oxidants (Fe- or Mn-catalyzed O2, O3, and H2O2) act to convert S(IV) to S (VI), acidify the film, and inhibit further S(IV) uptake. Experiments were also conducted on the incorporation of SO2 into ice depositing from the vapor at -7 to -15 C. An aqeous-film model accounting for the capture of SO2 by depositing ice was developed. Dissert. Abstr.

N89-13117 North Carolina State Univ., Raleigh.
AN ANALYSIS OF THE ERROR CHARACTERISTICS OF ATLANTIC TROPICAL CYCLONE TRACK PREDICTION MODELS Ph.D. Thesis
James T. Kroll 1987 120 p
Avail: Univ. Microfilms Order No. DA8804841

Using 140 track forecasts between 1976-1985, the error characteristics of the National Hurricane Center's tropical cyclone track prediction models are assessed with special emphasis on the Moveable Fine Mesh (MFM) model. The results indicate that beyond the 12 hour forecast, the MFM has the lowest mean forecast error of the NHC models. The forecast error component, relative to storm motion, are also analyzed. A consensus style track forecast known as the Combined Confidence Weighted Forecast (CCWF) scheme is tested using the track prediction output from NHC models. The CCWF provides improved track forecasts at 12 and 24 hours relative to the individual track prediction models. An attempt is made to develop linear regression models, using independent variables which describe storm characteristics and the large-scale wind field, to predict the magnitude of the NHC track prediction model forecast errors. Finally, a spectral barotropic model is used to identify the effects that sparse data and initial position errors have upon track forecast errors. Dissert. Abstr.

N89-13118# ST Systems Corp., Lexington, Mass.
C CLOUD S (CLIMATOLOGY OF CLOUD STATISTICS) DATABASE (USERS MANUAL) Scientific Technical Report No. 1, 15 Feb. 1987 - 14 Feb. 1988
James H. Willand 15 Mar. 1988 53 p
(Contract F19628-87-C-0046; AF Proj. 2310)
(AD-A196497; AFGL-TR-88-0060) Avail: NTIS HC A04/MF A01 CSCL 04B

This report provides detailed instructions to access and utilize a prototype computer-based global climatology of total sky cover cloud statistics known as C Cloud S. GRA

N89-13119# Air Force Inst. of Tech., Wright-Patterson AFB, Ohio.
AN ANALYSIS OF THE ERROR CHARACTERISTICS OF ATLANTIC TROPICAL CYCLONE TRACK PREDICTION MODELS Ph.D. Thesis
James T. Kroll 1988 121 p
(AD-A197146; AFIT/CI/NR-88-132) Avail: NTIS HC A06/MF A01 CSCL 04B

Using 140 track forecasts between 1976 to 1985, the error characteristics of the National Hurricane Center's tropical cyclone track prediction models are assessed with special emphasis on the Moveable Fine Mesh (MFM) model. The results indicate that beyond the 12-hour forecast, the MFM has the lowest mean forecast error of the NHC models. The forecast error component, relative to storm motion, are also analyzed. The MFM displayed the smallest mean across-track error, which is a measure of the accuracy of the path of movement. A consensus style track forecast known as the Combined Confidence Weighted Forecast (CCWF) scheme is tested using the track prediction output from NHC models. The CCWF provides improved track forecasts at 12 and 24 hours relative to the individual track prediction models. The CCWF scheme, on average, is also more accurate than the official forecast disseminated by NHC. An attempt is made to develop linear regression models, using independent variables which describe storm characteristics and the large-scale wind field, to predict the magnitude of the NHC track prediction model forecast errors. Finally, a spectral barotropic model is used to identify the effects that sparse data and initial position errors have upon track forecast errors. Various scales of motion are removed from the initial wind field to test the effect of sparse data. GRA

N89-13120# Air Force Inst. of Tech., Wright-Patterson AFB, Ohio.
THE EFFECT OF VERTICAL WIND SHEAR ON TROPICAL CYCLONE MOVEMENT M.S. Thesis
Kim M. Talbert 1988 116 p
(AD-A197218; AFIT/CI/NR-88-133) Avail: NTIS HC A06/MF A01 CSCL 04A

A 3-dimensional primitive equation model based upon Ooyama's 3-layer incompressible fluid model is used to investigate tropical cyclone motion. The governing equations are solved on a doubly periodic midlatitude beta-plane using a spectral method with Fourier basis functions. Numerical f-plane simulations are run which successively include a nearly linear horizontal barotropic basic current, surface drag, and cumulus convection. Simulations are then run, under identical conditions, with increasingly greater magnitudes of westerly vertical wind shear. All simulations are repeated using a variable Coriolis parameter to incorporate the beta-effect. Relative vorticity advection had the most dominant

effect on tropical cyclone motion followed by the beta-effect. Inclusion of surface drag and cumulus convection also had significant effects. Surface drag retarded vortex speed and resulted in a rightward deviation of the vortex relative to the direction of the basic current. Cumulus convection also resulted in vortex deviations to the right of the tract towards the regions of diabatic heating associated with areas of maximum boundary layer convergence. The primary effect of unidirectional vertical wind shear on cyclone movement, evident in all shear simulations, results in an initial deviation of the simulated cyclone towards the right of the direction of the wind shear vector. GRA

N89-13121# Air Force Inst. of Tech., Wright-Patterson AFB, Ohio.
A GLOBAL ANALYSIS AND CORRELATION OF NIMBUS 7 CLOUD AND LONGWAVE RADIATION DATA M.S. Thesis
Deanna R. Ramirez 24 May 1988 78 p
(AD-A197223; AFIT/CI/NR-88-181) Avail: NTIS HC A05/MF A01 CSCL 04B

Cloud data obtained from the Temperature Humidity Infrared Radiometer and Total Ozone Mapping Spectrometer and longwave radiation obtained from the Earth Radiation Budget instrument, all aboard the NIMBUS 7 satellite, have been used to present global analyses of the total cloud, high cloud and radiation fields and a correlation between the fields. The horizontal projections of the seasonal variation of the ITCZ by a maximum of cloud cover. The SH middle latitudes depict a zonal pattern of cloud amount for winter and summer, while the NH reveals an increase of cloud from summer to winter over the storm tracks. The dry subtropics are defined by a minimum of cloud cover. Areas of small or large amount of total cloud are defined by a small standard deviation, while the transition zones between maximum and minimum centers of total cloud are characterized by a large standard deviation. The standard deviation of the high cloud reveals that in areas of large high cloud amount, the variation of cloud is largely due to the advective or convective processes with which the cloud is associated. For small amount of high cloud, the variation of the cloud is small. Analyses of the global distribution of the seasonal mean field for infrared radiation (IR) indicate that areas that are defined by high cloud amount are also characterized by low IR due to the low radiative temperatures of the high cloud. GRA

N89-13122# Science Applications International Corp., Monterey, Calif.
FORECASTING AIDS FOR SETTING TROPICAL CYCLONE CONDITIONS: SASEBO AND IWAKUNI, JAPAN Final Report, 31 Dec. 1985 - 31 Dec. 1987
Jerry D. Jarrell Mar. 1988 46 p
(Contract N00228-86-C-3040)
(AD-A197802; SAIC-PN-1-425-07-809; NEPRF-CR-88-02) Avail: NTIS HC A03/MF A01 CSCL 04B

Forecast aids for predicting winds associated with tropical cyclones at Sasebo and Iwakuni, Japan, are developed. His report is divided into two parts: the first contains charts that relate winds observed at Sasebo and Iwakuni to tropical cyclone center winds as a function of storm location; and the second provides diagrams that estimate the worst case arrival time of winds of at least 50 kt. GRA

N89-13123# Pacific Northwest Labs., Richland, Wash.
HANFORD METEOROLOGICAL STATION COMPUTER CODES. VOLUME 8: THE REVIEW COMPUTER CODE
G. L. Andrews and K. W. Burk Aug. 1988 132 p
(Contract DE-AC06-76RL-01830)
(DE88-015958; PNL-6279-Vol-8) Avail: NTIS HC A07/MF A01

The Hanford Meteorological Station (HMS) routinely collects meteorological data from sources on and off the Hanford Site. The data are averaged over both 15 minutes and 1 hour and are maintained in separate databases on the Digital Equipment Corporation (DEC) VAX 11/750 at the HMS. The databases are transferred to the Emergency Management System (EMS) DEC VAX 11/750 computer. The EMS is part of the Unified Dose Assessment Center, which is located on the ground-level floor of the Federal building in Richland and operated by Pacific Northwest Laboratory. The computer program REVIEW is used to display meteorological data in graphical and alphanumeric form from either the 15-minute or hourly database. The code is available on the HMS and EMS computer. The REVIEW program helps maintain a high level of quality assurance on the instruments that collect the data and provides a convenient mechanism for analyzing meteorological data on a routine basis and during emergency response situations. DOE

N89-13124# Deutsche Forschungs- und Versuchsanstalt fuer Luft- und Raumfahrt, Oberpfaffenhofen (West Germany). Abteilung Lasertechnik.
CIRRUS-EXPERIMENT ICE-1987: MICROLIDAR MEASUREMENTS
Christian Werner, Hartmut Herrmann, and Juergen Streicher Apr. 1988 42 p In GERMAN; ENGLISH summary Original contains color illustrations
(DFVLR-Mitt-88-17; ISSN-0176-7739; ETN-88-93520) Avail: NTIS HC A03/MF A01; DFVLR, VB-PL-DO, 90 60 58, 5000 Cologne, Federal Republic of Germany, 31 deutsche marks

A microlidar developed as a small aerosol lidar was installed during the cirrus experiment in a Falcon-20 aircraft. Results were obtained at a few flight passages through the cirrus clouds and above it. Range-resolved measurements show the scattering profiles of the clouds; depolarization is of the order 0.4 to 0.5. ESA

N89-13125# National Weather Service, Garden City, N.Y.
TURB: TURBULENCE FORECASTING FOR SMALL/MEDIUM AND LARGE AIRCRAFT
Steven J. Naglic Jul. 1988 52 p
(PB88-246368; NOAA-NWS-ERCP-44) Avail: NTIS HC A04/MF A01 CSCL 04B

The program was developed to provide Center Weather Service Unit (CWSU) meteorologists and FAA flight service station personnel with a local product they can use to describe areas of significant turbulence. The program takes upper air data from any raob site, processes it, and generates a turbulence forcast for the areas within a 100 nm radius from the raob site. This information is quite valuable to the CWSU meteorologists as their forecasts, meteorological impact statements, and center weather advisories are used by the FAA for planning purposes and for the routing or rerouting of air traffic. The forecast product gives the layers analyzed in thousands of feet, the wind shear per thousand feet, and the turbulence forecast for small/medium aircraft and large aircraft. GRA

N89-12992*# National Aeronautics and Space Administration. Goddard Space Flight Center, Greenbelt, Md.
AN ALGORITHM TO DERIVE PRECIPITATION PROFILES FROM A DOWNWARD VIEWING RADAR AND A MULTIFREQUENCY PASSIVE RADIOMETER
J. A. Weinman, C. D. Kummerow, and C. S. Atwater (Applied Research Corp., Landover, Md.) *In* ESA, Proceedings of the 1988 International Geoscience and Remote Sensing Symposium (IGARSS 1988) on Remote Sensing: Moving Towards the 21st Century, Volume 1 Aug. 1988 p 229-234 (For primary document see N89-12936 04-42)
Copyright Avail: NTIS HC A99/MF E03; ESA Publications Div., ESTEC, Noordwijk, Netherlands, 120 US dollars or 250 Dutch guilders CSCL 04B

N89-12993# Rutherford High Energy Lab., Chilton (England).
CROSS-POLAR RADAR MEASUREMENTS IN ICE AND RAIN
J. F. W. Goddard, S. M. Cherry, and K. Holloway *In* ESA, Proceedings of the 1988 International Geoscience and Remote Sensing Symposium (IGARSS 1988) on Remote Sensing: Moving Towards the 21st Century, Volume 1 Aug. 1988 p 235-236 (For primary document see N89-12936 04-42)
Copyright Avail: NTIS HC A99/MF E03; ESA Publications Div., ESTEC, Noordwijk, Netherlands, 120 US dollars or 250 Dutch guilders

N89-12994# Essex Univ., Colchester (England). Dept. of Mathematics.
SOME ADVANTAGES OF USING POLARISATION DIVERSITY ILLUSTRATED THROUGH THE ANALYSIS OF RADAR DATA FROM A STORM IN CENTRAL ALBERTA (CANADA)
A. R. Holt, R. G. Humphries (MacDonald, Dettwiler and Associates Ltd., Richmond, British Columbia), and B. McGuinness *In* ESA, Proceedings of the 1988 International Geoscience and Remote Sensing Symposium (IGARSS 1988) on Remote Sensing: Moving Towards the 21st Century, Volume 1 Aug. 1988 p 237-240 (For primary document see N89-12936 04-42)
(Grant SERC-GR/E/27164)
Copyright Avail: NTIS HC A99/MF E03; ESA Publications Div., ESTEC, Noordwijk, Netherlands, 120 US dollars or 250 Dutch guilders

N89-12995# Manchester Coll. of Science and Technology (England). Dept. of Pure and Applied Physics.
DUAL LINEAR POLARISATION TIME SERIES AS AN AID TO HYDROMETEOR IDENTIFICATION
I. J. Caylor and A. J. Illingworth *In* ESA, Proceedings of the 1988 International Geoscience and Remote Sensing Symposium (IGARSS 1988) on Remote Sensing: Moving Towards the 21st Century, Volume 1 Aug. 1988 p 241-242 (For primary document see N89-12936 04-42)
(Grants NERC-GR3/5896; AF-AFOSR-0121-88)
Copyright Avail: NTIS HC A99/MF E03; ESA Publications Div., ESTEC, Noordwijk, Netherlands, 120 US dollars or 250 Dutch guilders

N89-12996# National Severe Storms Lab., Norman, Okla.
PROCESSING AND INTERPRETATION OF ALTERNATELY POLARISED WEATHER RADAR ECHOES
D. S. Zrnic, N. Balakrishnan, and M. Sachidananda *In* ESA, Proceedings of the 1988 International Geoscience and Remote Sensing Symposium (IGARSS 1988) on Remote Sensing: Moving Towards the 21st Century, Volume 1 Aug. 1988 p 243-246 (For primary document see N89-12936 04-42)
Copyright Avail: NTIS HC A99/MF E03; ESA Publications Div., ESTEC, Noordwijk, Netherlands, 120 US dollars or 250 Dutch guilders

N89-12997# Centre de Recherches en Physique de l'Environnement, Issy-les-Moulineaux (France).
DESIGN OF A SPACEBORNE RADAR FOR TROPICAL RAIN MAPPING AT THE CLIMATOLOGICAL SCALE
M. Marzoug, P. Amayenc, and N. Karouche (Centre National d'Etudes Spatiales, Toulouse, France) *In* ESA, Proceedings of the 1988 International Geoscience and Remote Sensing Symposium (IGARSS 1988) on Remote Sensing: Moving Towards the 21st Century, Volume 1 Aug. 1988 p 247-248 (For primary document see N89-12936 04-42)
Copyright Avail: NTIS HC A99/MF E03; ESA Publications Div., ESTEC, Noordwijk, Netherlands, 120 US dollars or 250 Dutch guilders

N89-12998*# National Aeronautics and Space Administration. Goddard Space Flight Center, Greenbelt, Md.
RAINFALL INDEX OVER OCEANS DERIVED FROM SSM/I DATA
A. T. C. Chang and T. T. Wilheit *In* ESA, Proceedings of the 1988 International Geoscience and Remote Sensing Symposium (IGARSS 1988) on Remote Sensing: Moving Towards the 21st Century, Volume 1 Aug. 1988 p 251-252 (For primary document see N89-12936 04-42)
Copyright Avail: NTIS HC A99/MF E03; ESA Publications Div., ESTEC, Noordwijk, Netherlands, 120 US dollars or 250 Dutch guilders CSCL 04B

N89-12999# Recherche en Prevision Numerique, Dorval (Quebec).
PRODUCTION OF PROBABILITY OF PRECIPITATION MAPS OVER OCEANIC AREAS FROM AUTOMATED CLOUD CLASSIFICATION
L. Garand *In* ESA, Proceedings of the 1988 International Geoscience and Remote Sensing Symposium (IGARSS 1988) on Remote Sensing: Moving Towards the 21st Century, Volume 1 Aug. 1988 p 255-256 (For primary document see N89-12936 04-42)
Copyright Avail: NTIS HC A99/MF E03; ESA Publications Div., ESTEC, Noordwijk, Netherlands, 120 US dollars or 250 Dutch guilders

N89-13000# Direction de la Meteorologie Nationale, Paris (France). Div. Prevision.
TOWARDS DIRECT VARIATIONAL ASSIMILATION OF SCATTEROMETER BACKSCATTER MEASUREMENTS INTO NUMERICAL WEATHER PREDICTION MODELS
H. Roquet and A. Ratier (Centre National d'Etudes Spatiales, Toulouse, France) *In* ESA, Proceedings of the 1988 International Geoscience and Remote Sensing Symposium (IGARSS 1988) on Remote Sensing: Moving Towards the 21st Century, Volume 1 Aug. 1988 p 257-260 (For primary document see N89-12936 04-42)
Copyright Avail: NTIS HC A99/MF E03; ESA Publications Div., ESTEC, Noordwijk, Netherlands, 120 US dollars or 250 Dutch guilders

N89-13001# National Oceanic and Atmospheric Administration, Boulder, Colo. Wave Propagation Lab.
RADIOMETRIC OBSERVATIONS OF CLOUD LIQUID WATER DURING FIRE
J. B. Snider *In* ESA, Proceedings of the 1988 International Geoscience and Remote Sensing Symposium (IGARSS 1988) on Remote Sensing: Moving Towards the 21st Century, Volume 1 Aug. 1988 p 261-262 (For primary document see N89-12936 04-42)
Copyright Avail: NTIS HC A99/MF E03; ESA Publications Div., ESTEC, Noordwijk, Netherlands, 120 US dollars or 250 Dutch guilders

N89-13069# British Antarctic Survey, Cambridge (England).
CLOUD TRACK WINDS FROM POLAR ORBITING SATELLITES
D. Warren and J. Turner *In* ESA, Proceedings of the 1988 International Geoscience and Remote Sensing Symposium (IGARSS 1988) on Remote Sensing: Moving Towards the 21st Century, Volume 1 Aug. 1988 p 549-550 (For primary document see N89-12936 04-42)
Copyright Avail: NTIS HC A99/MF E03; ESA Publications Div., ESTEC, Noordwijk, Netherlands, 120 US dollars or 250 Dutch guilders

N89-13070# University of Southern California, Los Angeles.
MODEL-BASED ESTIMATION OF WIND FIELDS OVER THE OCEAN FROM WIND SCATTEROMETER MEASUREMENTS
D. G. Long and J. M. Mendel *In* ESA, Proceedings of the 1988 International Geoscience and Remote Sensing Symposium (IGARSS 1988) on Remote Sensing: Moving Towards the 21st Century, Volume 1 Aug. 1988 p 553-556 (For primary document see N89-12936 04-42)
Copyright Avail: NTIS HC A99/MF E03; ESA Publications Div., ESTEC, Noordwijk, Netherlands, 120 US dollars or 250 Dutch guilders

N89-13071# GEC-Marconi Electronics Ltd., Chelmsford (England).
AN ANALYSIS OF DIRECTIONAL AMBIGUITIES IN WIND SCATTEROMETER MEASUREMENTS
J. Laycock *In* ESA, Proceedings of the 1988 International Geoscience and Remote Sensing Symposium (IGARSS 1988) on Remote Sensing: Moving Towards the 21st Century, Volume 1 Aug. 1988 p 557-560 (For primary document see N89-12936

04-42)
Copyright Avail: NTIS HC A99/MF E03; ESA Publications Div., ESTEC, Noordwijk, Netherlands, 120 US dollars or 250 Dutch guilders

48 OCEANOGRAPHY

Includes biological, dynamic, and physical oceanography; and marine resources.

For related information see also *43 Earth Resources and Remote Sensing.*

N89-13126# Naval Training Systems Center, Orlando, Fla.
ARCTIC OCEANOGRAPHY AND METEOROLOGY REVIEW Final Report, Jul. - Nov. 1987
Paul C. Etter 31 Dec. 1987 58 p Prepared in cooperation with SYNTEK Engineering and Computer Systems, Inc., Rockville, Md.
(AD-A196533; NTSC-TR-87-032) Avail: NTIS HC A04/MF A01 CSCL 20A

This report presents an overview of Arctic oceanography and meteorology in addition to acoustic properties of the Arctic Ocean relevant to sonar system performance. Acoustic modeling techniques appropriate to ice-covered ocean areas are also discussed. Environmental-acoustic data are identified which can support sonar performance modeling efforts. GRA

N89-13127# Naval Ship Research and Development Center, Bethesda, Md. Ship Hydromechanics Dept.
BERING SEA WAVE AND ICE MEASUREMENTS IN SUPPORT OF ARCTIC WEST WINTER 1986 Final Report
William L. Thomas, III Apr. 1988 52 p
(AD-A197196; DTRC/SHD-1212-03) Avail: NTIS HC A04/MF A01 CSCL 08C

Arctic West Winter 1986 (AWW-86) was conducted aboard USCGC POLAR SEA (WAGB-11) from 1 April to 30 April 1986 in the Northeast Pacific Ocean and Southern Bering Sea. During the first leg of the trial, three open ocean wave measurements were made using Delft University wave buoys. Five wave measurements were made during the remainder of the trial in the Bering Sea. Wave measurements were compared with Global Spectral Ocean Wave Model (GSOWM) forecasts which were provided by the Fleet Numerical Oceanography Center in Monterey, California. Ice edge observations were compared with ice edge forecasts provided by the Naval Polar Oceanography Center in Suitland, Maryland. Observations related to ice accretion were compared to Wise and Comisky nomogram predictions. Interviews were conducted with officers and crewmembers aboard USCGC POLAR SEA in an effort to document experience in cold weather operations which may be beneficial to the U.S. Navy. GRA

N89-13128# Washington Univ., Seattle. Inst. for Study of Atmosphere and Ocean.
A NUMERICAL MODEL FOR THE COMPUTATION OF RADIANCE DISTRIBUTIONS IN NATURAL WATERS WITH WIND-ROUGHENED SURFACES
Curtis D. Mobley and Rudolph W. Preisendorfer Jan. 1988 201 p
(Contract N00014-87-K-0525)
(AD-A197207; CONTRIB-40; NOAA/PMEL-TM-75; NOAA/PMEL-CONTRIB-813) Avail: NTIS HC A10/MF A01 CSCL 08H

The details are compiled of the derivation of a numerical procedure to determine the unpolarized radiance distribution as a function of depth, direction, and wavelength, in a natural hydrosol such as a lake or sea. The input to the model consists of the incidence radiance distribution at the air water surface, the state of randomness of the air water surface as a function of wind speed, the volume scattering and volume attenuation functions of the medium as a function of depth and wavelength, and the type of bottom boundary. The fundamental mathematical operation is the discretization over direction space of the continuous radiative transfer equation. The directionally discretized radiances, called quadaveraged radiances, are the averages over a finite set of solid angles of the directionally continuous radiance. The quadaveraged equations are azimuthally decomposed using standard Fourier analysis to obtain equations for the quadaveraged radiances are assembled from the solution reflectances and transmittances of the water body, in combination with the boundary conditions. The model has an expandable library of derived quantities that are of use in various applications of optics to natural waters, such as marine biological studies, underwater visual search tasks, remote sensing, and climatology. GRA

N89-13129# North Carolina Univ., Greensboro. Dept. of Biology.
OPTICAL MODELING OF CLEAR OCEAN LIGHT FIELDS: RAMAN SCATTERING EFFECTS Semiannual Report
Robert Hans Stavn and Alan Dean Weidemann (Naval Ocean Research and Development Activity, Bay St. Louis, Miss.) 1988 47 p
(Contract N00014-86-K-0606)
(AD-A197249) Avail: NTIS HC A03/MF A01 CSCL 08C

A Monte Carlo simulation (the NORDA optical model) and the Three-Parameter Model of the submarine light field are used to analyze the effect of water Raman emission at 520nm in clear ocean waters. Reported optical anomalies for clear ocean waters at longer wavelengths (520nm +) are explained by the effects of water Raman emission and the simulation results are confirmed by Biowatt-NORDA observations made in the Sargasso Sea. A new optical parameterization for clear ocean water is proposed. GRA

N89-12968# Ecole Nationale Superieure des Telecommunications, Brest (France). Groupe Traitement d'Images.
SPECTRAL ANALYSIS OF OCEAN WAVE IMAGERY USING 2-D LINEAR PREDICTION
C. Cariou, J.-M. Boucher, C. Roux, and P. Larouche (Institut Maurice Lamontagne, Mont-Joli, Quebec) *In* ESA, Proceedings of the 1988 International Geoscience and Remote Sensing Symposium (IGARSS 1988) on Remote Sensing: Moving Towards the 21st Century, Volume 1 Aug. 1988 p 127-130 (For primary document see N89-12936 04-42)
Copyright Avail: NTIS HC A99/MF E03; ESA Publications Div., ESTEC, Noordwijk, Netherlands, 120 US dollars or 250 Dutch guilders

N89-12969# Johns Hopkins Univ., Laurel, Md. Applied Physics Lab.
ON THE USE OF SPECKLE STATISTICS FOR THE EXTRACTION OF OCEAN WAVE SPECTRA FROM SAR IMAGERY
F. M. Monaldo *In* ESA, Proceedings of the 1988 International Geoscience and Remote Sensing Symposium (IGARSS 1988) on Remote Sensing: Moving Towards the 21st Century, Volume 1 Aug. 1988 p 133-136 (For primary document see N89-12936 04-42)
Copyright Avail: NTIS HC A99/MF E03; ESA Publications Div., ESTEC, Noordwijk, Netherlands, 120 US dollars or 250 Dutch guilders

N89-12970# Forut, Tromsoe (Norway).
OCEAN WAVE NUMBER SPECTRA AND SPATIAL AUTOCORRELATION FUNCTIONS FROM SAR IMAGES
H. Johnsen, T. Eltoft, and S. Jacobsen (Tromsoe Univ., Norway) *In* ESA, Proceedings of the 1988 International Geoscience and Remote Sensing Symposium (IGARSS 1988) on Remote Sensing: Moving Towards the 21st Century, Volume 1 Aug. 1988 p 137-140 (For primary document see N89-12936 04-42)
Copyright Avail: NTIS HC A99/MF E03; ESA Publications Div., ESTEC, Noordwijk, Netherlands, 120 US dollars or 250 Dutch guilders

N89-12971# Canada Centre for Remote Sensing, Ottawa (Ontario). RADARSAT Project Office.
SAR-SEEN MULTIMODE WAVES IN ICE: EVIDENCE OF IMAGING NONLINEARITIES
R. K. Raney and P. W. Vachon *In* ESA, Proceedings of the 1988 International Geoscience and Remote Sensing Symposium (IGARSS 1988) on Remote Sensing: Moving Towards the 21st Century, Volume 1 Aug. 1988 p 141-144 (For primary document see N89-12936 04-42)
Copyright Avail: NTIS HC A99/MF E03; ESA Publications Div., ESTEC, Noordwijk, Netherlands, 120 US dollars or 250 Dutch guilders

N89-12972# Oceanor, Trondheim (Norway).
AN INTERCOMPARISON OF SAR AND BUOY DIRECTIONAL WAVE SPECTRA FROM THE LABRADOR SEA EXTREME WAVES EXPERIMENT (LEWEX)
H. E. Krogstad and R. B. Olsen *In* ESA, Proceedings of the 1988 International Geoscience and Remote Sensing Symposium (IGARSS 1988) on Remote Sensing: Moving Towards the 21st Century, Volume 1 Aug. 1988 p 147-148 (For primary document see N89-12936 04-42)
Copyright Avail: NTIS HC A99/MF E03; ESA Publications Div., ESTEC, Noordwijk, Netherlands, 120 US dollars or 250 Dutch guilders

N89-12973# Johns Hopkins Univ., Laurel, Md. Applied Physics Lab.
DIRECTIONAL OCEAN WAVE SPECTRA: PROSPECTS FOR ACQUIRING A GLOBAL DATA BASE FROM SIR-C
R. C. Beal, J. L. MacArthur, F. M. Monaldo, and S. F. Oden *In* ESA, Proceedings of the 1988 International Geoscience and Remote Sensing Symposium (IGARSS 1988) on Remote Sensing: Moving Towards the 21st Century, Volume 1 Aug. 1988 p 149-150 (For primary document see N89-12936 04-42)
Copyright Avail: NTIS HC A99/MF E03; ESA Publications Div., ESTEC, Noordwijk, Netherlands, 120 US dollars or 250 Dutch guilders

N89-12974# Johns Hopkins Univ., Laurel, Md. Applied Physics Lab.
THE LABRADOR SEA EXTREME WAVES EXPERIMENT: OBJECTIVES, STATUS AND PLANS
R. C. Beal and T. W. Gerling *In* ESA, Proceedings of the 1988 International Geoscience and Remote Sensing Symposium (IGARSS 1988) on Remote Sensing: Moving Towards the 21st Century, Volume 1 Aug. 1988 p 151-154 (For primary document see N89-12936 04-42)
Copyright Avail: NTIS HC A99/MF E03; ESA Publications Div., ESTEC, Noordwijk, Netherlands, 120 US dollars or 250 Dutch guilders

N89-13005# Iwate Univ., Morioka (Japan). Dept. of Computer Science.
ESTIMATION OF SEA SURFACE TEMPERATURE VIA NOAA-AVHRR SENSOR: COMPARISON WITH SEA TRUTH DATA BY FIXED BUOYS
R. Yokoyama and Sumio Tanba *In* ESA, Proceedings of the 1988 International Geoscience and Remote Sensing Symposium (IGARSS 1988) on Remote Sensing: Moving Towards the 21st Century, Volume 1 Aug. 1988 p 275-280 (For primary document see N89-12936 04-42)
Copyright Avail: NTIS HC A99/MF E03; ESA Publications Div., ESTEC, Noordwijk, Netherlands, 120 US dollars or 250 Dutch guilders

N89-13035# GEC-Marconi Electronics Ltd., Chelmsford (England).
ANALYSIS OF SEASAT SAR SEA-ICE DATA FROM THE BEAUFORT SEA
K. C. Partington *In* ESA, Proceedings of the 1988 International Geoscience and Remote Sensing Symposium (IGARSS 1988) on Remote Sensing: Moving Towards the 21st Century, Volume 1 Aug. 1988 p 413-416 (For primary document see N89-12936 04-42)
Copyright Avail: NTIS HC A99/MF E03; ESA Publications Div., ESTEC, Noordwijk, Netherlands, 120 US dollars or 250 Dutch guilders

N89-13036# Helsinki Univ. of Technology, Espoo (Finland). Dept. of Space Technology.
MICROWAVE DIELECTRIC PROPERTIES OF LOW-SALINITY SEA ICE
M. T. Hallikainen, M. V. O. Toikka, and J. M. Hyyppa *In* ESA, Proceedings of the 1988 International Geoscience and Remote Sensing Symposium (IGARSS 1988) on Remote Sensing: Moving Towards the 21st Century, Volume 1 Aug. 1988 p 419-420 (For primary document see N89-12936 04-42)
Copyright Avail: NTIS HC A99/MF E03; ESA Publications Div., ESTEC, Noordwijk, Netherlands, 120 US dollars or 250 Dutch guilders

N89-13037# Canada Centre for Remote Sensing, Ottawa (Ontario).
THE LIMEX 1987 PILOT PROJECT, LIMEX 1989 AND LONG-TERM OBJECTIVE FOR DATA COLLECTION ON THE CANADIAN EAST COAST
L. McNutt and R. K. Raney *In* ESA, Proceedings of the 1988 International Geoscience and Remote Sensing Symposium (IGARSS 1988) on Remote Sensing: Moving Towards the 21st Century, Volume 1 Aug. 1988 p 421-422 (For primary document see N89-12936 04-42)
Copyright Avail: NTIS HC A99/MF E03; ESA Publications Div., ESTEC, Noordwijk, Netherlands, 120 US dollars or 250 Dutch guilders

N89-13039# Environmental Research Inst. of Michigan, Ann Arbor. Radar Science Lab.
SEA ICE TYPE CLASSIFICATION OF SAR IMAGERY
C. C. Wackerman, R. R. Jentz, and R. A. Shuchman *In* ESA, Proceesings of the 1988 International Geoscience and Remote Sensing Symposium (IGARSS 1988) on Remote Sensing: Moving Towrds the 21st Century, Volume 1 Aug. 1988 p 425-428 (For primary document see N89-12936 04-42)
(Contracts N00014-87-C-0418; N00014-81-C-0195)
Copyright Avail: NTIS HC A99/MF E03; ESA Publications Div., ESTEC, Noordwijk, Netherlands, 120 US dollars or 250 Dutch guilders

51 LIFE SCIENCES (GENERAL)

N89-13130# Massachusetts Inst. of Tech., Cambridge. Harvard-MIT Div. of Health Sciences and Technology.
ELECTROPORATION: THEORY OF BASIC MECHANISMS Annual Progress Report, 1 Jun. 1987 - 31 May 1988
James C. Weaver 30 Jun. 1988 3 p
(Contract N00014-87-K-0479; Proj. RR0-4108)
(AD-A197391) Avail: NTIS HC A02/MF A01 CSCL 06D

The objective of our investigation is to develop a theory of the mechanism of electroporation, by providing a quantitative description of key features of this dramatic phenomenon. Electroporation is now believed to be a universal cell membrane phenomenon, involving both the lipid bilayer and membrane macromolecules. It provides a general method for introducing molecules into cells, or releasing molecules from cells, with potentially major applications in science and technology, and yet is presently poorly understood. Our specific goals are extension of our first, successful theory of reversible electrical breakdown (REB) to one with more solid foundations, i.e., elimination of the approximate switch on criteria of pores; and development of a theory which describes quantitatively the transmembrane potential, U(t), during irreversible rupture, such that a unified theory of both REB and rupture is provided by one model; extension of our first,

successful theory of the reversible electrical breakdown of electroporation to include metastable pores associated with a pore-membrane macromolecule interaction; and development of a more complex theory which also predicts the amount of transmembrane transport of molecules. GRA

N89-13131*# National Aeronautics and Space Administration. Lyndon B. Johnson Space Center, Houston, Tex.
HORIZONTALLY ROTATED CELL CULTURE SYSTEM Patent Application
David A. Wolf, inventor (to NASA), Ray Schwarz, inventor (to NASA), and Tinh Trinh, inventor (to NASA) (Krug International, Houston, Tex.) 30 Jun. 1988 17 p
(NASA-Case-MSC-21294-1; NAS 1.71:MSC-21294-1; US-Patent-Appl-SN-213558) Avail: NTIS HC A03/MF A01 CSCL 06C

The present invention relates to a horizontally rotating bioreactor useful for carrying out cell and tissue culture. For processing of mammalian cells, the system is sterilized and fresh fluid medium, microcarrier beads, and cells are admitted to completely fill the cell culture vessel. An oxygen containing gas is admitted to the interior of the permeable membrane which prevents air bubbles from being introduced into the medium. The cylinder is rotated at a low speed within an incubator so that the circular motion of the fluid medium uniformly suspends the microbeads throughout the cylinder during the cell growth period. The unique design of this cell and tissue culture device was initially driven by two requirements imposed by its intended use for feasibility studies for three dimensional culture of living cells and tissues in space by JSC. They were compatibility with microgravity and simulation of microgravity in one G. The vessels are designed to approximate the extremely quiescent low shear environment obtainable in space. NASA

N89-12769# Ohio State Univ., Columbus. Dept. of Exercise Physiology and Physiological Chemistry.
ALTERATIONS OF SEGMENTAL VOLUME DURING ORTHOSTATIC STRESS IN NONHUMAN PRIMATES Final Report
Beverly Elaine Girten *In* Universal Energy Systems, Inc., United States Air Force Graduate Student Summer Support Program, Volume 1 Dec. 1987 20 p (For primary document see N89-12754 04-31)
Avail: NTIS HC A99/MF E03 CSCL 06P

N89-12772# Meharry Medical Coll., Nashville, Tenn. Dept. of Biomedical Sciences.
THE EFFECTS OF HYPERBARIC OXYGEN AND ANTIOXIDANT DEFICIENCIES ON RAT RETINAL ULTRASTRUCTURE Final Report
Adrienne L. Hollis *In* Universal Energy Systems, Inc., United States Air Force Graduate Student Summer Support Program, Volume 1 Dec. 1987 19 p (For primary document see N89-12754 04-31)
Avail: NTIS HC A99/MF E03 CSCL 06C

52 AEROSPACE MEDICINE

Includes physiological factors; biological effects of radiation; and effects of weightlessness on man and animals.

N89-13132# Army Research Inst. of Environmental Medicine, Natick, Mass.
DERIVATION OF ANTHROPOMETRY BASED BODY FAT EQUATIONS FOR THE ARMY'S WEIGHT CONTROL PROGRAM Technical Report, Jun. - Nov. 1984
J. A. Vogel, J. W. Kirkpatrick, P. I. Fitzgerald, J. A. Hodgdon, and E. A. Harman May 1988 55 p
(AD-A197371; USARIEM-17-88) Avail: NTIS HC A04/MF A01 CSCL 05I

Large inter-observer variability is a major disadvantage to the use of skinfold measurements for the prediction of percent body fat. This is particularly relevant in the Army's weight control program where standardized training is difficult for the large number of required observers located worldwide and who frequently turn over due to reassignment. This necessitated the development of an alternative method that required no formal training, could be administered by non-technical personnel and had low inter-observer variability. This report describes circumference-based equations that were developed to replace the skinfold equations. The equations apply to all ages and racial groups. Conversion tables were developed for easy calculation of percent body fat from the raw measurements of circumferences, height and weight. In those individuals exceeding the weight-height table, the equation was more accurate in males in correctly classifying individuals than the weight-height table but only marginally better in women. In addition to the ease of measurement by non-technical observers, the equations better predict percent body fat measured by hydrostatic weighing than do the previously used Durnin-Womersley skinfold equations when considering all ages, racial groups and degrees of adiposity. GRA

N89-13133# Technology, Inc., San Antonio, Tex. Life Sciences Div.
RESEARCH AND DEVELOPMENT OF ANTI-g LIFE SUPPORT SYSTEMS. PART 2: DECOMPRESSION SICKNESS RESEARCH Final Report, 1 Apr. 1981 - 31 Jul. 1985
Robert W. Krutz, Robert M. Olson, Bijan Eshaghian, Emily M. Gause, and William T. Harvey May 1988 28 p
(Contract F33615-81-C-0600)
(AD-A197675; USAFSAM-TR-86-36-Pt-2) Avail: NTIS HC A03/MF A01 CSCL 06J

Instrumentation and techniques for differentiating bends-prone and bends-resistant individuals were developed. Studies were conducted to determine bends- and bubble-formation altitudes using a variety of simulated pressure-suit pressures and breathing gas mixtures. A pressure of 9.5 psia eliminated the occurrence of bends under the conditions of these studies. In vitro studies of intravenous bubble formation were undertaken. United States Air Force (U.S.A.F.) aircrews must be prepared to encounter loss of cabin pressure caused by either mechanical failure or deliberate maneuvering of aircraft. Aircrews generally tolerate short-duration depressurization well, but decompression sickness (DCS) occurs much more often than is reported. Symptoms of DCS range in severity from minor to life threatening; however, all incidences of DCS require medical attention to preclude subsequent problems. The physiological mechanisms involved in DCS are not completely understood, but DCS is considered to result from supersaturation of body tissues with nitrogen (N2). Supersaturation sets in as the ambient pressure (hence the absolute pressure of N2) decreases. Nitrogen is less soluble in blood than in tissues so that the rate of decrease of partial pressure of N2 in tissues lags behind the rate of decrease in atmospheric N2 pressure, resulting in formation of N2 bubbles in blood and tissues. The tendency for bubbles to form is greater as the difference between the two pressure increases. GRA

N89-13134# Naval Submarine Medical Center, Groton, Conn.
DISCRIMINATION AND IDENTIFICATION OF MODULATION-FREQUENCY USING NOISE, TONE AND TONAL-COMPLEX CARRIERS
Thomas E. Hanna 23 May 1988 26 p
(AD-A197780; NSMRL-1117) Avail: NTIS HC A03/MF A01 CSCL 06D

A two-interval, two-alternative, forced-choice discrimination task (2I-2AFC) and an identification task were used to measure listeners' abilities to resolve modulation frequency, using three different types of carrier--noise, a 1-kHz tone, or a tonal complex. Identification performance was not simply related to 2I-2AFC discrimination performance. Identification of stimuli near the edges of the range was relatively good compared with listeners' abilities to discriminate these stimuli, a result which has been found for other stimuli (e.g., Berliner, Durlach, and Braida, 1977). In addition, certain midrange stimuli were identified relatively well, indicating the effects of central factors that enhance the encoding of these stimuli.

Results for the 1-kHz and the tonal-complex carrier showed enhanced identification of modulation frequencies in the range 50 to 80 Hz. The results for the noise carrier, however, indicated enhanced resolution only for modulation frequencies less than 54 Hz. Possible explanations for these effects are discussed, and it is suggested that a more detailed examination of the role of the stimulus context would provide some answers. GRA

N89-13135# Oak Ridge National Lab., Tenn. Office of Risk Analysis.
HUMAN EXPOSURE TO DIOXIN FROM COMBUSTION SOURCES
Holly A. Hattemer-Frey and Curtis C. Travis 1988 20 p Presented at the Symposium on Emissions From Combustion Processes, Toronto, Ontario, 5 Jun. 1988
(Contract DE-AC05-84OR-21400)
(DE88-013825; CONF-8806227-1) Avail: NTIS HC A03/MF A01

Because of their extreme toxicity, much concern and debate has arisen about the nature and extent of human exposure to dioxin. Since municipal solid waste (MSW) incinerators are known to emit polychorinated dibenzo-p-dioxins (PCDDs) and polycholorinated dibenzofurnas (PCDFs), many people who live near MSW incinerators fear that they will be exposed to high levels of dioxin and subsequently develop cancer. What is often overlooked in this debate, however, is the fact that the general population is continuously being exposed to trace amounts of dioxin as exemplified by the fact that virtually all human adipose tissue samples contain dioxin at levels of 3 parts per trillion (ppt) or greater. This paper provides a perspective on MSW incineration as a source of human exposure to dioxin by comparing this exposure source with exposure to background environmental contamination and evaluates some of the potential key sources of PCDD/PCDF input into the enviroment. DOE

N89-13136# Deutsche Forschungs- und Versuchsanstalt fuer Luft- und Raumfahrt, Cologne (West Germany). Inst. fuer Flugmedizin.
GLUCOSE TOLERANCE AND INSULIN SECRETION DURING 0-g SIMULATION Ph.D. Thesis - Technische Hochschule, Aachen
Sabine Trumbach Aug. 1987 86 p In GERMAN; ENGLISH summary
(DFVLR-FB-88-25; ISSN-0171-1342; ETN-88-93525) Avail: NTIS HC A05/MF A01; DFVLR VB-PL-DO, 90 60 58, 5000 Cologne, Federal Republic of Germany, 29.50 deutsche marks

To improve the health conditions of astronauts during space missions, 12 male volunteers were examined with regard to glucose and insulin metabolism during 7 days of 0 g simulation (6 deg head down tilt). Before, during, and after simulation oral glucose-tolerance tests were done; glucose, insulin and c-peptide concentration in serum was measured, along with creatinine, osmolality, hematocrit and electrolytes. During the simulation, glucose-tolerance decreases. Parallel to this insulin concentration increases, due to increased secretion, whereas a decreased decomposition of insulin is improbable. Comparing six trained with six less trained volunteers (discovered by spiroergometry) shows no significant differences. ESA

53 BEHAVIORAL SCIENCES

Includes psychological factors; individual and group behavior; crew training and evaluation; and psychiatric research.

N89-13137# Washington Univ., St. Louis, Mo. Dept. of Neurology.
IS WORD RECOGNITION AUTOMATIC: A COGNITIVE-ANATOMICAL APPROACH
Michael I. Posner, Jennifer Sandson, Meena Dhawan, and Gordon L. Shulman 30 May 1988 35 p
(Contract N00014-86-K-0289; Proj. RR0-4206)
(AD-A197089; TR-88-4-ONR) Avail: NTIS HC A03/MF A01 CSCL 06D

It is generally accepted that two tasks will interfere to the extent that they require attention or involve shared non-attentional processing systems. The authors used anatomical data from studies of blood flow during lexical processing to generate hypotheses about the conditions under which an auditory shadowing task would interfere with three common visual priming tasks. Data from blood flow studies suggest that visual priming involves automatic activation of a set of posterior visual areas that are not activated by auditory language processing. In accord with this account, we found no reduction in visual priming during simultaneous shadowing. Cueing covert visual attention involves posterior parietal areas that are not involved in auditory shadowing. However, these posterior areas are part of a unified attention system. In accord with this idea, cueing covert attention is greatly affected by simultaneous auditory shadowing. Blood flow data indicate that semantic involves both an anterior attention system and an area of lateral frontal cortex. Both these areas can also be activated by auditory information. GRA

N89-13138# Georgia Inst. of Tech., Atlanta.
CONSEQUENCES OF INDIVIDUAL DIFFERENCES IN BRAIN ORGANIZATION FOR HUMAN PERFORMANCE Interim Report, Jul. 1986 - Jul. 1987
Joanne Green, Philip D. West, David C. Hartup, and Dennis F. Folds Jul. 1988 127 p
(Contract MDA903-86-K-0320; DA Proj. 2Q1-61102-B-74-F)
(AD-A197667; ARI-RN-88-47) Avail: NTIS HC A07/MF A01 CSCL 06D

This research note summarizes the work done during the first year of a four-year research program to identify how measurement of brain functioning, especially individual differences in brain functioning, can be used to understand and predict human performance in complex human machine systems. A major objective of the completed work was to define measures which identify characteristics of individual brain functioning. The results suggest that electrophysiological measures have the greatest potential to measure performance related aspects of brain functioning. Given the sensitivity of the electrophysiological measures to variation in brain functioning, and their potential as measures of workload, it is planned to include further evaluation of these measures in future work, as indices of performance related aspects of brain functioning. GRA

N89-13139# Johns Hopkins Univ., Baltimore, Md. Dept. of Physiology.
PREATTENTIVE AND ATTENTIVE VISUAL INFORMATION PROCESSING Interim Report, 1 Apr. 1987 - 31 Mar. 1988
Howard E. Egeth 15 Jun. 1988 62 p
(Grant AF-AFOSR-0180-87; AF Proj. 2313)
(AD-A197670; AFOSR-88-0726TR) Avail: NTIS HC A04/MF A01 CSCL 05H

Twelve (12) experiments are described in this report. The first nine (9) are concerned with the hypothesis that the identification of the values of stimulus features in multielement visual displays requires serial processing. Contrary to this hypothesis, the weight of the evidence suggests that feature identification can be carried out by spatially parallel processes. The remaining three (3) experiments are concerned with the ability to extract semantic information from several stimuli in parallel. Both alphanumeric character classification and lexical (i.e., word vs. nonword) decisions can be accomplished by parallel processes, but semantic categorization of words cannot. The implications of these findings for theories of attention are discussed. GRA

N89-13140# Deutsche Forschungs- und Versuchsanstalt fuer Luft- und Raumfahrt, Hamburg (West Germany). Abteilung Luft- und Raumfahrtpsychologie.
DIFFERENTIAL-PSYCHOLOGICAL ANALYSIS OF A COMPUTER-BASED AUDIO-VISUAL TEST OF VIGILANCE
Peter Maschke and Georg Finell May 1988 48 p In GERMAN;

ENGLISH summary Report will also be announced as translation (ESA-TT-1136)
(DFVLR-FB-88-23; ISSN-0171-1342; ETN-88-93523) Avail: NTIS HC A03/MF A01; DFVLR VB-PL-DO, 90 60 58, 5000 Cologne, Federal Republic of Germany, 18 deutsche marks

An audio-visual test of vigilance, in which visual (indicator deflections) and auditory (letter) signals are presented simultaneously, is evaluated with regard to its differential and diagnostical value. The sample consisted of 261 airline pilot and 241 air traffic controller applicants. Correlation and factor analyses with reference tests suggest the existence of two independent constructs of vigilance: signal detection and false alarms. In both modalities and in both samples these scores prove to be sufficiently reliable. ESA

N89-12765# State Univ. of New York, Buffalo. Dept. of Psychology.
THE EFFECT OF ATTENTIONAL FOCUS LEVEL ON TASK PERFORMANCE UTILIZING INFORMATION FROM DIFFERENT STIMULUS STRUCTURE LEVELS Final Report
Deborah A. Gagnon *In* Universal Energy Systems, Inc., United States Air Force Graduate Student Summer Support Program, Volume 1 Dec. 1987 21 p (For primary document see N89-12754 04-31)
Avail: NTIS HC A99/MF E03 CSCL 05I

N89-12770# San Diego State Univ., Calif. Dept. of Psychology.
DESIGNING SIMULATOR TASKS TO STUDY THE HIGH SPEED, LOW ALTITUDE ENVIRONMENT Final Report
Laura Giusti *In* Universal Energy Systems, Inc., United States Air Force Graduate Student Summer Support Program, Volume 1 Dec. 1987 12 p (For primary document see N89-12754 04-31)
Avail: NTIS HC A99/MF E03 CSCL 05I

54 MAN/SYSTEM TECHNOLOGY AND LIFE SUPPORT

Includes human engineering; biotechnology; and space suits and protective clothing.

For related information see also *16 Space Transportation.*

N89-13141*# Eagle Engineering, Inc., Houston, Tex.
LUNAR STORM SHELTER CONCEPTUAL DESIGN
1 May 1988 92 p
(Contract NAS9-17878)
(NASA-CR-172078; NAS 1.26:172078; EEI-88-189) Avail: NTIS HC A05/MF A01 CSCL 06K

The requirements for a radiation protection program for the exploration and permanent occupancy of the lunar surface are described. B.G.

N89-13142# Naval Postgraduate School, Monterey, Calif.
THREE-DIMENSIONAL VISUAL DISPLAY FOR A PROTOTYPE COMMAND AND CONTROL WORKSTATION M.S. Thesis
Milton D. Abner Jun. 1988 68 p
(AD-A197319) Avail: NTIS HC A04/MF A01 CSCL 25E

The development of a real-time three-dimensional visual display for the Command and Control Workstation of the Future (CCWF) is a means of rapidly interpreting large amounts of important information. In this study, we examine the realistic versus real-time trade-offs required to achieve such a display and the components effecting these trade-offs, i.e., hidden surface technique, lighting and shading models, etc. We also present a unified data structure that is used in storing various properties that create the display. GRA

N89-13143# Princeton Univ., N. J. Dept. of Mechanical and Aerospace Engineering.
AUTOCREW IMPLEMENTATION: INBOUND SURFACE-TO-AIR MISSILE SIMULATION Interim Technical Report
Brenda L. Belkin May 1988 45 p
(Contract DAAG29-84-K-0048)
(AD-A197674; ARO-20155.16-MA) Avail: NTIS HC A03/MF A01 CSCL 12I

Nine multiple cooperating rule-based systems for the combat aircraft environment were developed and implemented in the AUTOCREW expert system. Each component rule-based system is modelled on a typical World War II bomber crew member having specific task responsibilities. The bases for modelling integrated rule-based systems as crew members are twofold. First, tasks performed by crew members are easily identified, well-defined, and familiar to operations personnel and aircraft system designers. The issue of task familiarity is essential from a human engineering standpoint. The pilot of a single-seat combat aircraft categorizes the tasks he performs into logical groups such as navigation, flight control, systems monitoring, failure diagnosis, and fire control operations. Implementing an AI-based pilot aid as a logical extension of human operations is highly desirable. The pilot must identify with the task performed by the on-board aid, so a crew-model design of component knowledge bases is commensurate with the pilot's experience and training. The modelled crew members are COPILOT (flight control), ENGINEER (system diagnosis, reconfiguration), NAVIGATOR (navigation), COMMUNICATOR (radio/data operations), OBSERVER (lookout and alarm) ATTACKER (offensive weapon control), DEFENDER (defensive weapon control), and SPOOFER (countermeasures). The ninth rule-based system (EXECUTIVE) coordinates mission-specific tasks and has knowledge of the mission plan. GRA

N89-12762# Alabama Univ., Tuscaloosa. Dept. of Health Education.
VALIDITY OF HEAT INDEX AS INDICATOR OF LEVEL OF HEAT STORAGE FOR PERSONNEL WEARING PROTECTIVE CLOTHING IN HOT ENVIRONMENTS Final Report
K. Suzanne Enlow *In* Universal Energy Systems, Inc., United States Air Force Graduate Student Summer Support Program, Volume 1 Dec. 1987 18 p (For primary document see N89-12754 04-31)
Avail: NTIS HC A99/MF E03 CSCL 05H

N89-12776# Cornell Univ., Ithaca, N.Y. School of Electrical Engineering.
A SYSTEM TO INVESTIGATE SYNTHESIZED VOICE FEEDBACK IN MAN-MACHINE INTERFACES Final Report
Michele E. Johnson *In* Universal Energy Systems, Inc., United States Air Force Graduate Student Summer Support Program, Volume 1 Dec. 1987 17 p (For primary document see N89-12754 04-31)
Avail: NTIS HC A99/MF E03 CSCL 05H

55 SPACE BIOLOGY

Includes exobiology; planetary biology; and extraterrestrial life.

N89-13144*# National Aeronautics and Space Administration. Ames Research Center, Moffett Field, Calif.
NASA NEWSLETTERS FOR THE WEBER STUDENT SHUTTLE INVOLVEMENT PROJECT
E. R. Morey-Holton, P. D. Sebesta, A. M. Ladwig, J. T. Jackson, and W. M. Knott, III (National Aeronautics and Space Administration. John F. Kennedy Space Center, Cocoa Beach, Fla.) Nov. 1988 317 p
(NASA-TM-101001; A-88182; NAS 1.15:101001) Avail: NTIS HC A14/MF A01 CSCL 06C

Biweekly reports generated for the Weber Student Shuttle Involvement Project (SSIP) are discussed. The reports document the evolution of science, hardware, and logistics for this Shuttle project aboard the eleventh flight of the Space Transportation System (STS-41B), launched from Kennedy Space Center on February 3, 1984, and returned to KSC 8 days later. The reports were intended to keep all members of the team aware of progress

in the project and to avoid redundancy and misunderstanding. Since the Weber SSIP was NASA's first orbital rat project, documentation of all actions was essential to assure the success of this complex project. Eleven reports were generated: October 3, 17 and 31; November 14 and 28; and December 12 and 17, 1983; and January 3, 16, and 23; and May 1, 1984. A subject index of the reports is included. The final report of the project is included as an appendix. Author

59 MATHEMATICAL AND COMPUTER SCIENCES (GENERAL)

No abstracts in this category.

60 COMPUTER OPERATIONS AND HARDWARE

Includes hardware for computer graphics, firmware, and data processing.

For components see *33 Electronics and Electrical Engineering.*

N89-13145*# Illinois Univ., Urbana. Coordinated Science Lab.
PERFORMANCE ANALYSIS OF THE ALLIANT FX/8 MULTIPROCESSOR USING STATISTICAL CLUSTERING
Robert Tod Dimpsey Nov. 1988 39 p
(Grant NAG1-613)
(NASA-CR-183221; NAS 1.26:183221; UILU-ENG-88-2255; CSG-91) Avail: NTIS HC A03/MF A01 CSCL 09B

Results for two distinct, real, scientific workloads executed on an Alliant FX/8 are discussed. A combination of user concurrency and system overhead measurements was taken for both workloads. Preliminary analysis shows that the first sampled workload is comprised of consistently high user concurrency, low system overhead, and little paging. The second sample has much less user concurrency, but significant paging and system overhead. Statistical cluster analysis is used to extract a state transition model to jointly characterize user concurrency and system overhead. A skewness factor is introduced and used to bring out the effects of unbalanced clustering when determining states with important transitions. The results from the models show that during the collection of the first sample, the system was operating in states of high user concurrency approximately 75 percent of the time. The second workload sample shows the system in high user concurrency states only 26 percent of the time. In addition, it is ascertained that high system overhead is usually accompanied by low user concurrency. The analysis also shows a high predictability of system behavior for both workloads. Author

N89-13146# California Univ., Berkeley. Computer Science Div.
SPEED AND DATA STRUCTURES IN COMPUTER ALGEBRA SYSTEMS Technical Report, 7 Aug. 1984 - 6 Aug. 1987
Richard J. Fateman and Carl G. Ponder 31 Aug. 1987 10 p
(Contract N00039-84-C-0089; ARPA Order 4871)
(AD-A197131) Avail: NTIS HC A02/MF A01 CSCL 12F

Comparing the speed of computation in algebra systems is a perennial occupation of system designers, algorithm implementors, and, more recently, marketing personnel. At least some people have observed that for many problems, the choice of a system makes much less difference than the approach used to represent the problem. The mapping from mathematics to a data representation and the choice of algorithms can make significant, and separate, contributions to efficiency. Systems which have the flexibility to provide several data structures and algorithms can provide an advantage in this respect. Macsyma is probably the system with the largest selection, currently. On the other hand, Macsyma has not taken advantage of recent advances such as the extensive use of hash-coding incorporated in the University of Waterloo's Maple system. For the one somewhat artificial benchmark discussed in this paper, it appears that the Maple system does considerably better than any representation in Macsyma by precisely this mechanism. GRA

N89-13147# Du Pont de Nemours (E. I.) and Co., Aiken, S.C. Technical Div.
DATA ACQUISITION OF THE THERMOGRAVIMETRIC ANALYSIS TESTING SUMMARY
Michael S. Elks 17 Dec. 1987 7 p
(Contract DE-AC09-76SR-00001)
(DE88-016062; DPST-87-878) Avail: NTIS HC A02/MF A01

Environmental and Chemical Sciences of New Ellenton, South Carolina, performs thermogravimetric analysis (TGA) tests for the Savannah River Laboratory. In the past, the TGA's data acquisition system consisted of a Micromac 4000 computer connected to a Commodore CBM computer with two floppy drives and a printer. Because the data required several transfers, a new, simpler acquisition system was developed. The new system includes the Micromac 4000 coupled to an IBM PC/XT, IOMEGA 10+10 Bernoulli Box, and graphics printer. The new system is faster and more accurate and requires less technical time for data analysis. A BASIC program was written for the IBM to acquire the data. DOE

N89-13148 Plessey Research Roke Manor Ltd., Romsey (England).
ARCHITECTURES FOR OPTOELECTRONIC COMPUTING
A. M. King Jun. 1988 39 p
(Rept-72/88/R260/U; ETN-88-93565) Copyright Avail: Plessey Research Roke Manor Ltd., Roke Manor, Romsey, Hants, SO51 0ZN, United Kingdom

The limitations of electrical communication are reviewed to assess the potential benefits of applying waveguide and holographic connection systems to clock distribution and data interchange between different components of a computer. Optical interconnect is also attractive for implementing artificial neural systems. As well as providing the high degree of interconnect, optics can perform mathematical operations that underlie many neural models. Optical phenomena for implementing residue arithmetic are reviewed. Optical substitution architectures are described, as well as data encoding schemes, and basic components of a computer are formulated in terms of symbolic substitution rules. The principles of shadow casting logic are presented together with implementations for different data coding systems. The relationship between cellular logic and symbolic substitution is explored as a foundation for image processing architectures to perform parallel shifting, boundary detection, and pattern matching operations. Virtual cellular processors are introduced to solve image partitioning problems, and to distribute the image processing tasks evenly over a network of processors. Optical reconfigurability to dynamically match the interconnect topology to the image processing task is investigated, and the possibility of finding a good static interconnect pattern is explored. ESA

61 COMPUTER PROGRAMMING AND SOFTWARE

Includes computer programs, routines, alogorithms, and specific applications, e.g., CAD/CAM.

N89-13149# National Aeronautical Lab., Bangalore (India). Aerodynamics Div.
MATHEMATICAL MODELLING AND COMPUTER SIMULATION USING CARTESIAN GRID
S. S. Desai and R. Rangarajan Jul. 1988 24 p
(TM-AE-8804) Avail: NTIS HC A03/MF A01

Math models and computer simulation continue to grow as competitive alternatives to experiment in the analysis of flow over

aircraft and space vehicles, as also in the design of efficient shapes that produce air flow with desirable features. Whereas the math model aims to capture the essence of the physical phenomena in the form of governing equations and their boundary conditions, computer simulation aims to display the essence of the equations and their boundary conditions in the form of intelligible numbers and illuminating graphs and pictures. Though math models are as old as science itself, it is the growth of computers in their ability to handle numbers at ever-increasing speed and in their ability to exhibit graphs of these numbers that is fast making this activity an alternative to experimentation. Most of the physical features of fluid flow are embodied mathematically in the Navier-Stokes equations which are a system of nonlinear partial differential equations. The presentation is covered in two broad categories: 2-D and 3-D flow simulation. The mathematical details are ignored and only an attempt is made to bring out the spirit of approximations involved in modeling techniques and the resulting software for flow simulation for industry standard aerodynamic applications. Research and development in the Aerodynamics Division of the National Aeronautics Laboratory on math modelling and computer simulation using cartesian grids is summarized. Author

N89-13150*# College of William and Mary, Williamsburg, Va. Dept. of Computer Science.
DESIGN DOCUMENT FOR GCS VERSION
Jeffrey M. Voas 15 Sep. 1988 32 p
(Grant NAG1-824)
(NASA-CR-183278; NAS 1.26:183278) Avail: NTIS HC A03/MF A01 CSCL 09B

This design document shows the module and design calling hierarchy for the William and Mary GCS version. Also, all code written to date is shown. This is a complete compiling version, however, no testing other than syntax compilation was performed. Author

N89-13151# Lawrence Livermore National Lab., Calif.
BOEING MILITARY AIRPLANE COMPANY TECHNICAL ORDER TRANSFER TESTS
1 Feb. 1988 29 p Prepared in cooperation with SYSCON Corp., San Diego, Calif.
(Contract W-7405-eng-48)
(DE88-012233; UCRL-21058; AITI-87-005) Avail: NTIS HC A03

This report covers testing being conducted by the Air Force Logistics Command on the Military Standard for the Automated Interchange of Technical Information (AITI). The objective is to demonstrate the validity of the transfer protocol defined in the standard and the viability of standardized formats for the transfer of technical information defined in other specifications used by the standard. DOE

N89-13152*# College of William and Mary, Williamsburg, Va.
FAULT DIAGNOSIS BASED ON CONTINUOUS SIMULATION MODELS Final Report, 1 Oct. 1986 - 31 Dec. 1987
Stefan Feyock 1987 91 p
(Grant NAG1-618)
(NASA-CR-182737; NAS 1.26:182737) Avail: NTIS HC A05/MF A01 CSCL 09B

The results are described of an investigation of techniques for using continuous simulation models as basis for reasoning about physical systems, with emphasis on the diagnosis of system faults. It is assumed that a continuous simulation model of the properly operating system is available. Malfunctions are diagnosed by posing the question: how can we make the model behave like that. The adjustments that must be made to the model to produce the observed behavior usually provide definitive clues to the nature of the malfunction. A novel application of Dijkstra's weakest precondition predicate transformer is used to derive the preconditions for producing the required model behavior. To minimize the size of the search space, an envisionment generator based on interval mathematics was developed. In addition to its intended application, the ability to generate qualitative state spaces automatically from quantitative simulations proved to be a fruitful avenue of investigation in its own right. Implementations of the Dijkstra transform and the envisionment generator are reproduced in the Appendix. Author

N89-13153*# George Washington Univ., Washington, D.C. School of Engineering and Applied Science.
MAKING STATISTICAL INFERENCES ABOUT SOFTWARE RELIABILITY Progress Report
Douglas R. Miller Dec. 1988 25 p
(Grant NAG1-771)
(NASA-CR-4197; NAS 1.26:4197) Avail: NTIS HC A03/MF A01 CSCL 09B

Failure times of software undergoing random debugging can be modelled as order statistics of independent but nonidentically distributed exponential random variables. Using this model inferences can be made about current reliability and, if debugging continues, future reliability. This model also shows the difficulty inherent in statistical verification of very highly reliable software such as that used by digital avionics in commercial aircraft. Author

N89-13154# Carnegie-Mellon Univ., Pittsburgh, Pa. Software Engineering Inst.
SOFTWARE PROCESS MODELING Final Report
Marc I. Kellner and Gregory A. Hansen May 1988 53 p
(Contract F19628-85-C-0003)
(AD-A197137; CMU/SEI-88-TR-9; ESD-TR-88-010) Avail: NTIS HC A04/MF A01 CSCL 12E

This paper discusses the topic of software process modeling, a means of reasoning about the processes used to develop and maintain software. Although this term is beginning to come into common use, its meaning varies widely. For the purposes of this paper, software process modeling is defined as a methodology that encompasses a representation approach, comprehensive analysis capabilities, and the capability to make predictions regarding the effects of changes to a process. This paper reports the approach we have taken to software process modeling and summarizes our experiences on the Post Deployment Software Support (PDSS) Project. The paper is structured as follows: Chapter 1 - Introduction; Chapter 2 - Overview of the objectives and capabilities of software processing modeling; Chapter 3 - Overview of the PDSS Information Management Project, describing the context for our modeling experience; Chapter 4 - Details and examples of the modeling approach used on the PDSS Project; Chapter 5 - Outcomes and results of those modeling efforts; Chapter 6 - Lessons learned from this effort, and a list of the capabilities required for successful software process modeling; and Chapter 7 - Conclusions and directions for future work. GRA

N89-13155# American Coll. Testing Program, Iowa city, Iowa.
MULTIDIMENSIONAL ITEM RESPONSE THEORY ESTIMATION: A COMPUTER PROGRAM
James E. Carlson Apr. 1988 27 p
(Contract N00014-85-C-0241)
(AD-A197160; ONR-87-2; ACT-RR-87-19) Avail: NTIS HC A03/MF A01 CSCL 12E

The MIRTE computer program, which provides estimates of item parameters and individuals' proficiencies (abilities) based on the multidimensional two-parameter logistic (M2PL) item response theory model, is described. The program uses a modified Newton-Raphson algorithm to iteratively estimate the parameters and proficiencies. The algorithm, use of the program, and some results based on simulated datasets are described. GRA

N89-13156# Washington Univ., Seattle. Dept. of Computer Science.
PARALLEL DEBUGGING USING GRAPHICAL VIEWS
Mary L. Bailey, David Socha, and David Notkin Mar. 1988 13 p
(Contract N00014-86-K-0264; AF-AFOSR-0023-88)
(AD-A197197; TR-88-03-05) Avail: NTIS HC A03/MF A01 CSCL 12E

Graphical views are essential for debugging parallel programs

because of the large quantity of state information contained in parallel programs. Voyeur, a prototype system for creating graphical views of parallel programs, provides a cost-effective way to construct such views for any parallel programming system. We illustrate Voyeur by discussing four views created for debugging Poker programs. One is a general trace facility for any Poker program. The other three are tailored to display a specific type of algorithmic information. Each of these views has been instrumental in detecting bugs that would have been difficult to detect otherwise, yet were obvious with the views. GRA

N89-13157# Mitre Corp., Bedford, Mass.
EUCLIDEAN DECODERS FOR BCH CODES Final Technical Report, Oct. 1985 - Oct. 1986
Willard L. Eastman Apr. 1988 192 p
(Contract F19628-86-C-0001)
(AD-A197242; MTR-101197; RADC-TR-88-44) Avail: NTIS HC A09/MF A01 CSCL 12I

This report investigates conventional decoding algorithms for BCH codes. The algorithm of Sugiyama, Kasahara, Hirasawa and Namekawa, Mills' continued fraction algorithm, and the Berlekamp-Massey algorithm are all viewed as slightly differing variants of Euclid's algorithm. An improved version of Euclid's algorithm for polynomials is developed. The Berlekamp-Massey algorithm is extended within the Euclidean framework to avoid computation of vector inner products. Inversionless forms of the algorithms are considered and the results are extended to provide for decoding of erasures as well as errors. GRA

N89-13158# Washington Univ., Seattle. Dept. of Computer Science.
PRACTICAL ALGORITHMS FOR IMAGE COMPONENT LABELING ON SIMD MESH CONNECTED COMPUTERS
R. E. Cypher, Larry Snyder, and J. L. Sanz Dec. 1987 11 p
(Contract N00014-86-K-0164)
(AD-A197341; TR-87-12-05) Avail: NTIS HC A03/MF A01 CSCL 12F

Two new parallel algorithms are presented for the problem of labeling the connected components of a binary image, which is also known as the connected ones problem. The machine model is an SIMD two-dimensional mesh connected computer consisting of an N x N array of processing elements, each containing a single pixel of an N x N image. Both new algorithms use a shrinking operation defined by Levialdi and have time complexities of O(N log N) bit operations, which makes them the fastest local algorithms for the problem. Compared with other approaches having similar or better time complexities, this local approach dramatically simplifies the algorithms and reduces the constants of proportionality by nearly two orders of magnitude, thus making them the first practical algorithms for the problem. The two algorithms differ in the amount of memory required per processing element; the first uses O(N) bits while the second employs a novel compression scheme to reduce the requirement to O(log N) bits. GRA

N89-13159# Massachusetts Inst. of Tech., Cambridge. Lab. for Computer Science.
GRAPHICAL PROGRAMMING AND MONITORING Final Report, Sep. 1982 - Sep. 1986
J. C. Licklider Jan. 1988 65 p
(Contract F30602-82-K-0170; ARPA Order 4469)
(AD-A197342; LCS-1986/AF 1; RADC-TR-TR-88-7) Avail: NTIS HC A04/MF A01 CSCL 12E

The goal of this research was to explore graphical programming and graphical monitoring of the interpretation of computer programs and develop a concept demonstration system for creating programs graphically. The system, GRAPPLE, is essentially a graphical interface to a LISP-like language called MDL. Using GRAPPLE, the programmer develops a diagrammatic representation of a program by making selections from menus with a mouse and typing some short labels on a keyboard. GRAPPLE then creates a symbolic MDL program as a subprogram in further programming or run it with whatever data it requires. The report describes the programming process in detail and includes a discussion of issues, conclusions and recommendations. GRA

N89-13160# California Univ., Berkeley. Dept. of Electrical Engineering and Computer Science.
PAN 1: AN INTRODUCTION FOR USERS, REVISION
S. L. Graham Sep. 1987 65 p
(Contract N00039-84-C-0089; ARPA Order 4871)
(AD-A197344; PIPER-WP-87-5) Avail: NTIS HC A04/MF A01 CSCL 12E

Pan is a prototype and testbed for language-based editors and viewers. Its design addresses the needs of experienced users who manage complex objects such as large software systems. All of Pan's components are multi-lingual, incremental, description-driven, customizable, and extensible. Viewing is facilitated by semantics-based browsing and an object model which integrates text and structure. Pan is intended to share information with other tools, allowing integration into a larger language, program, and document development environment. This document, a users manual, describes the basic operational facilities of Pan 1, the current implementation. It explains the concepts behind Pan's editing environment, introduces editing commands, and discusses techniques for customization. Appendices list commanded bindings (to both keystrokes and menus), buffer options, buffer flags, and a compatibility guide for GNU Emacs users. GRA

N89-13161# Scripps Institution of Oceanography, La Jolla, Calif. Marine Physical Lab.
PARABOLIC EQUATION MODEL Summary Report
Jean-Marie Tran Apr. 1988 61 p
(Contract N00014-87-C-0127)
(AD-A197480; MPL-TM-401; MPL-U-9/88) Avail: NTIS HC A04/MF A01 CSCL 20A

This report deals with a parabolic propagation model now implemented at the Marine Physical Laboratory. This parabolic equation (PE) program is a FORTRAN 77 version of the SACLANTPAREQ program. The parabolic methods were a major development in the field of acoustic modeling. The advantage of the method is the simple way range dependence is handled. Diffraction effects are included, but neither reverberation nor backscattering are accounted for in an earlier document. The parabolic equation requires small angles of propagation from the horizontal and cannot handle steep sound velocity gradients or high frequency propagation because of computer speed considerations. The parabolic equations are derived, the associated numerical algorithms are presented, the environment and the program inputs are described. Finally examples are given. The goal of this report is to provide the potential user the necessary information to understand and use the PE program. GRA

N89-13162# Naval Ocean Research and Development Activity, Bay St. Louis, Miss.
IMPLEMENTATION ISSUES FOR LEVEL O IMAGE PROCESSOR SOFTWARE WITHIN AN APPLICATION PACKAGE Final Report
James E. Lennox Feb. 1988 30 p
(AD-A197768; NORDA-203) Avail: NTIS HC A03/MF A01 CSCL 12E

Image processing is rapidly emerging as a field with many interesting areas for the computer scientist. Packages are available that allow images to be manipulated in an interactive environment by applying functions to the image. Functions are defined as transformations from the image memory domain to the display domain, which may permanently alter image memory values. This paper describes minimum hardware constraints and the scope of modifications necessary to implement different image processors with in the Earth Resources Laboratory Applications Software (ELAS) environment. It also contrasts the impact on software engineering principles related to the implementation of low-level software to support the imaging functions. GRA

N89-13163# Illinois Univ., Urbana. Coordinated Science Lab.
DISCOVERING SUBSTRUCTURE IN EXAMPLES M.S. Thesis
Lawrence B. Holder, Jr. May 1988 117 p
(Contracts N00014-82-K-0186; N00014-87-K-0874)
(AD-A197778; UILI-ENG-88-2223) Avail: NTIS HC A06/MF A01 CSCL 12E

This thesis describes a method for discovering substructure concepts and gives examples. The method involves a computationally constrained best-first search guided by four heuristics: cognitive savings, compactness, connectivity and coverage. Each heuristic is described in detail along with its role in evaluating an individual substructure concept. The SUBDUE computer program that implements the method contains a substructure discovery module, a substructure specialization module and an incremental substructure background knowledge module for applying previously discovered substructures in a hierarchy that is used to determine which substructures are present in the input examples. The system has performed well on a number of examples from different domains and has discovered many interesting substructure concepts such as an aromatic ring and a macro-operator for stacking blocks. The method and implementation of the SUBDUE system are described, and an analysis of experimental results is presented. GRA

N89-13164# Mission Research Corp., Albuquerque, N. Mex.
MICROWAVE AND ELECTRON BEAM COMPUTER PROGRAMS Final Report, Aug. 1986 - Jan. 1988
Brendan B. Godfrey Jun. 1988 31 p
(Contract F29601-86-C-0216)
(AD-A197798; AMRC-R-886; AFWL-TR-87-69) Avail: NTIS HC A03/MF A01 CSCL 20N

This report discusses some computer programs available for addressing the physics of highpower microwave and charged particle beam generation and propagation. Codes range from simple lumped parameter models to detailed multidimensional simulations. Described here are the capabilities and underlying models of the microwave source, particle beam accelerator, and particle beam propagation codes. Although the more powerful of these programs can also be used for microwave propagation and antenna design, other programs specifically designed for these applications are typically employed instead. GRA

N89-13165*# Jet Propulsion Lab., California Inst. of Tech., Pasadena.
APPLICATIONS OF PARALLELISM TO CURRENT ALGORITHMS FOR INTELLIGENCE ANALYSIS Final Report
Martha A. Griesel, J. Steven Hughes, and Beth R. Moore 10 Jul. 1987 23 p Prepared for Army Intelligence Center and School, Fort Huachuca, Ariz.
(Contract NAS7-918)
(NASA-CR-183351; JPL-D-4719; NAS 1.26:183351; AD-A197838; ALGO-Publ-0125) Avail: NTIS HC A03/MF A01 CSCL 09B

The purpose of this document is to detail a study of concurrent processing by the Concurrent Processing Subgroup of the U.S. Army Intelligence Center and School (USAMS) task in association with the Advanced Computing Research Facility (ACRF) at Argonne National Laboratory (ANL). The study centered on the effect of different concurrent architectures (hypercube and shared memory) on Intelligence and Electronic Warfare (IEW) algorithm performance. This study examined implementation of a spatial aggregation algorithm on a hypercube and a shared memory machine with special attention given to data partitioning. The difference in implementation of the algorithm is due to data partitioning, data dependence, and communication between processors. Two parallel machines were used: the Cal Tech-JPL Mark 2 Hypercube, and the Sequent Balance at the Advanced Computing Research Facility at the Argonne National Laboratory. The hypercube is a 32 node concurrent processor consisting of 32 identical processors linked by a communications network. The Sequent Balance is a high-performance, general-purpose computer system that uses 2 to 12 National Semiconductor Series 32000 CPUs in a tightly-coupled multiprocessing architecture. This study indicates that task oriented algorithms with a low degree of data interdependence are better suited to a shared memory implementation and data-driven algorithms to a hypercube implementation. GRA

N89-13166# Johns Hopkins Univ., Laurel, Md. Applied Physics Lab.
A GLR (GENERALIZED LIKELIHOOD RATIO) ALGORITHM FOR POLYLINE APPROXIMATION OF WAVEFORMS
Richard A. Steinberg Jun. 1988 78 p
(Contract N00039-87-C-5301)
(AD-A197846; JHU/APL/TG-1370) Avail: NTIS HC A05/MF A01 CSCL 12A

New algorithms are derived for the polyline approximation of digital waveforms, using recursive least squares and generalized likelihood ratio techniques. Numerical experiments indicate that the new algorithms may in some applications offer significant speed and accuracy advantages compared to prior polyline algorithms. GRA

N89-13167# Sandia National Labs., Albuquerque, N. Mex.
SIMULATING VEHICLE DYNAMICS: THE IMPORTANCE OF A VALID FORCING FUNCTION
G. L. Ferguson 1988 14 p Presented at the 59th Shock and Vibration Symposium, Albuquerque, N. Mex., 18 Oct. 1988
(Contract DE-AC04-76DP-00789)
(DE88-010527; SAND-88-1350C; CONF-881076-1) Avail: NTIS HC A03/MF A01

The recent evolution of vehicle systems has required they be structurally sound with minimum weight. Historically, a trial and error approach to marketing a vehicle was used. The 1970s saw mainframe computers speed the vehicle design process. In the early 1980s simulating vehicle dynamics became the accepted design procedure. The forcing function used in this technique is also its major drawback. This paper summarizes the results of one sled vehicle used in a detailed study done at the U. S. Air Force's High Speed Test Track. The study concluded that results from simulation studies are valid only if an accurate forcing function is used. DOE

N89-13168# Argonne National Lab., Ill. Mathematics and Computer Science Div.
ALGORITHMS FOR BOUND CONSTRAINED QUADRATIC PROGRAMMING PROBLEMS
Jorge J. More and Gerardo Toraldo May 1988 25 p
(Contract W-31-109-eng-38)
(DE88-016470; ANL/MCS-TM-117) Avail: NTIS HC A03/MF A01

We present an algorithm which combines standard active set strategies with the gradient projection method for the solution of quadratic programming problems subject to bounds. We show, in particular, that if the quadratic is bounded below on the feasible set then termination occurs at a stationary point in a finite number of iterations. Moreover, if all stationary points are nondegenerate, termination occurs at a local minimizer. A numerical comparison of the algorithm based on the gradient projection algorithm with a standard active set strategy shows that on mildly degenerate problems the gradient projection algorithm requires considerable less iterations typically decreases by at least a factor of 10. For strongly degenerate problems, the performance of the gradient projection algorithms deteriorates, but it still performs better than the active set method. DOE

N89-13169# Department of Energy, Washington, D. C. Energy Information Administration.
HLP30: A SET OF LINEAR PROGRAMMING PROCEDURES SYSTEM MANUAL
William Orchard-Hays Jun. 1988 163 p
(DE88-016571; DOE/EIA-M031) Avail: NTIS HC A08/MF A01

HLP30 is a set of programs for solving large LP problems on a large IBM 370 computer with virtual storage. The programs were developed on the IBM 370/3033 (now a 3084) at the Energy Information Administration (EIA) computer facility. They are largely written in Assembly Language but have FORTRAN caps so they

may be adapted to larger modelling environments. There is no concession either to limited resources or to portability to other types of equipment. A large model requires a large region of virtual storage. The programs utilize very few files, most work files for the algorithmic routines has been completely dispensed with. Files are used for initial data input in standard MPS CONVERT and REVISE formats, for result output in standard Filed SOLUTION format, and for a compact form of model file. Beyond this, only eight other files are used throughout the set of programs. DOE

N89-13170# Lawrence Livermore National Lab., Calif.
THE STATE OF PC-BASED CADD (COMPUTER-AIDED DESIGN AND DRAFTING) SYSTEMS
G. L. Brandt, J. M. Bowers, T. S. Gorman, and L. E. Taylor 11 Jul. 1988 75 p
(Contract W-7405-eng-48)
(DE88-017326; UCRL-53877) Avail: NTIS HC A04

This report provides an overview of the state of the art of personal computer (PC)-based computer-aided design and drafting (CADD) systems for mechanical engineering applications. It presents the results of an evaluation performed on seven systems during October 1987 to March 1988 and summarizes the strengths and weaknesses of the systems. DOE

N89-13171*# National Aeronautics and Space Administration. Ames Research Center, Moffett Field, Calif.
EFFICIENT USE OF BIT PLANES IN THE GENERATION OF MOTION STIMULI
Jeffrey B. Mulligan and Leland S. Stone Oct. 1988 26 p
(NASA-TM-101022; A-88269; NAS 1.15:101022) Avail: NTIS HC A03/MF A01 CSCL 09B

The production of animated motion sequences on computer-controlled display systems presents a technical problem because large images cannot be transferred from disk storage to image memory at conventional frame rates. A technique is described in which a single base image can be used to generate a broad class of motion stimuli without the need for such memory transfers. This technique was applied to the generation of drifting sine-wave gratings (and by extension, sine wave plaids). For each drifting grating, sine and cosine spatial phase components are first reduced to 1 bit/pixel using a digital halftoning technique. The resulting pairs of 1-bit images are then loaded into pairs of bit planes of the display memory. To animate the patterns, the display hardware's color lookup table is modified on a frame-by-frame basis; for each frame the lookup table is set to display a weighted sum of the spatial sine and cosine phase components. Because the contrasts and temporal frequencies of the various components are mutually independent in each frame, the sine and cosine components can be counterphase modulated in temporal quadrature, yielding a single drifting grating. Using additional bit planes, multiple drifting gratings can be combined to form sine-wave plaid patterns. A large number of resultant plaid motions can be produced from a single image file because the temporal frequencies of all the components can be varied independently. For a graphics device having 8 bits/pixel, up to four drifting gratings may be combined, each having independently variable contrast and speed. Author

N89-13172# Helsinki Univ. of Technology, Espoo (Finland). Dept. of Information Technology.
AN APPROACH TO AUTOMATE DIGITAL SIGNAL PROCESSOR CODE GENERATION Ph.D. Thesis
Olli Hyvarinen 1988 17 p
(ETN-88-93530) Avail: NTIS HC A03/MF A01

Methods for digital processing (DSP) firmware implementation generation are discussed. Hardware modeling and code generation are considered. Two high level DSP-oriented languages were developed. A hardware extension for an ordinary signal processor which implements developed control structures was built. The advantages of graph format realization descriptions are reviewed. ESA

N89-13173# Office of Naval Research, London (England).
EUROPEAN SEMINAR ON NEURAL COMPUTING
Claire Zomzely-Neurath 31 Aug. 1988 38 p Seminar held in London, United Kingdom, Feb. 1988
(ONRL-8-010-C) Avail: NTIS HC A03/MF A01

Topics range from neural systems and models through languages and architectures to the respective European and American perspectives on neurocomputing. Author

N89-12766# Oregon State Univ., Corvallis. Dept. of Computer Science.
PROVIDING ON-LINE GUIDANCE TO COMPUTER USERS Final Report
Edward M. Gellenbeck *In* Universal Energy Systems, Inc., United States Air Force Graduate Student Summer Support Program, Volume 1 Dec. 1987 20 p (For primary document see N89-12754 04-31)
Avail: NTIS HC A99/MF E03 CSCL 09B

N89-12771# Louisiana State Univ., Baton Rouge. Dept. of Mechanical Engineering.
SIX DEGREE OF FREEDOM SIMULATION COMPUTER PROGRAM FOR AEROELASTIC FREE-FLIGHT PROJECTILES Final Report
Thomas Harkins *In* Universal Energy Systems, Inc., United States Air Force Graduate Student Summer Support Program, Volume 1 Dec. 1987 18 p (For primary document see N89-12754 04-31)
Avail: NTIS HC A99/MF E03 CSCL 09B

N89-12778# Auburn Univ., Ala. Dept. of Computer Science and Engineering.
INSTALLATION OF THE ADINA FEM COMPUTER PROGRAMS Final Report
Sharon K. Landis *In* Universal Energy Systems, Inc., United States Air Force Graduate Student Summer Support Program, Volume 1 Dec. 1987 13 p (For primary document see N89-12754 04-31)
Avail: NTIS HC A99/MF E03 CSCL 09B

N89-12917*# National Aeronautics and Space Administration. Lewis Research Center, Cleveland, Ohio.
AUTOMATION SOFTWARE FOR A MATERIALS TESTING LABORATORY
Michael A. McGaw and Peter J. Bonacuse *In its* Turbine Engine Hot Section Technology 1986 Oct. 1986 p 399-406 (For primary document see N89-12876 04-39)
Avail: NTIS HC A21/MF A01 CSCL 09B

62 COMPUTER SYSTEMS

Includes computer networks and special application computer systems.

N89-13174# Swedish Inst. of Computer Science, Uppsala.
PRACTICAL ISSUES RELATING TO THE INTERNAL DATABASE PREDICATES IN AN OR-PARALLEL PROLOG: EXTENSIONS AND USEFUL HACKS
M. Carlsson, K. Danhof, and R. Overbeek (Argonne National Lab., Ill.) 1988 14 p Presented at the 5th International Logic Programming Conference, Seattle, Wash., 15 Aug. 1988 Prepared in cooperation with Southern Illinois Univ., Carbondale; Argonne National Lab., Ill.
(Contract W-31-109-eng-38)
(DE88-010019; CONF-880859-1) Avail: NTIS HC A03/MF A01

This technical report is being written to document and explain some of the insights the authors have gained during the implementation of two OR-parallel Prolog systems for shared-memory multiprocessors. We have been quite amazed by how much power and functionality can be achieved through the implementation of just a few primitive predicates. We introduce a few relatively trival predicates which allow one to implement versions of findall/3, bagof/3, and setof/3 for the multiprocessors

environment. Then we show how these predicates can be used to implement AND-parallelism. Finally, we illustrate their use for implementing a limited notion of streams, and how such streams can be used to create a compiler that achieves excellent speedups for multiprocessors with a limited number of processors. DOE

N89-13175# Mentor Technologies, Inc., Bayside, N.Y.
MICRO-COMPUTER NETWORK ARCHITECTURE FOR RANGE INSTRUMENTATION APPLICATIONS Final Report, 16 Sep. 1987 - 13 Mar. 1988
M. R. Belzer and Y. M. Cho 13 Mar. 1988 58 p
(Contract DAAD07-87-C-0103)
(AD-A196971) Avail: NTIS HC A04/MF A01 CSCL 12F

VLSI technology has been developed to the point where special purpose processors may be concatenated to form supercomputers with far greater throughput rates than uniprocessor machines. MTI has developed a parallel form of the conventional Kalman filter that is well suited to being implemented in a multiprocessing environment. Moreover, our Decentralized Square Root Information Filter (DSRIF) has several very unique features which could be incorporated into the design of an integrated test range tracking system with much improved performance over existing methods. Phase 1 research demonstrated feasibility of the DSRIF as a means for solving the linear least squares estimation problem in decentralized form. Also, an extended form of the DSRIF was derived and successfully used to track real Multiple Rocket Launch System Data provided by the White Sands Missile Range. GRA

N89-13176# Washington Univ., Seattle. Dept. of Computer Science.
ACHIEVING SPEEDUPS FOR A SHARED MEMORY MODEL LANGUAGE ON AN SIMD PARALLEL COMPUTER
Ray Greenlaw and Larry Snyder Sep. 1987 22 p
(Contract N00014-86-K-0264; NSF DCR-84-16878)
(AD-A197102; TR-87-09-03) Avail: NTIS HC A03/MF A01 CSCL 12E

The potential for speeding up a shared memory model sequential programming language, APL, by using an idealized non-shared memory parallel computer is investigated. The authors simulated the running of APL's dyadic, reduction, and subscript operators on a 4-connected mesh SIMD parallel computer. The simulation results indicate that these operations can be accelerated significantly using parallelism. These findings support the thesis that parallelism can speed up a majority of 'typical' APL (A Programming Language) programs and not just those programs that are especially suited to parallelization. The sequential APL language requires no sophisticated compilation techniques like Paraphase and PFC, because the operators in APL are inherently parallel. It is felt that exploiting this property of APL is interesting. GRA

N89-13177# Washington Univ., Seattle. Dept. of Computer Science.
VOYEUR: GRAPHICAL VIEWS OF PARALLEL PROGRAMS
David Socha, Mary L. Bailey, and David Notkin Apr. 1988 12 p
(Contract N00014-86-K-0264; NSF CCR-84-16878)
(AD-A197103; TR-88-04-03) Avail: NTIS HC A03/MF A01 CSCL 12E

Voyeur is a prototype system that facilitates the construction of application-specific, visual views of parallel programs. These views range from textual views showing the contents of variables to graphical maps of the state of the computational domain of the program. These views have been instrumental in quickly detecting bugs that would have been difficult to detect otherwise. GRA

N89-13178# Carnegie-Mellon Univ., Pittsburgh, Pa. Dept. of Mathematics.
PARALLEL ALGORITHMS IN THE FINITE ELEMENT APPROXIMATION OF FLOW PROBLEMS Final Report, May 1987 - May 1988
Max D. Gunburger 29 May 1988 20 p
(Grant AF-AFOSR-0101-83; AF Proj. 2301)
(AD-A197454; AFOSR-88-0764TR) Avail: NTIS HC A03/MF A01 CSCL 20D

We discuss a portion of the research of the which has been carried out during the past years under AFOSR sponsorship. This includes work on finite element methods for a Ladyshenskaya model of viscous incompressible flow, hyperbolic partial differential equations, exterior problems, algebraic turbulence models, streamfunction vorticity formulations of viscous flows and first order elliptic systems of partial differential equations, and on substructing methods for the approximate solution of partial differential equations. GRA

N89-13179# Massachusetts Inst. of Tech., Lexington. Lincoln Lab.
NEURAL NETWORK PERFORMANCE ON THE STOCHASTIC EXCLUSIVE-OR PROBLEM Technical Report No. 808
R. Y. Levine 8 Jul. 1988 50 p
(Contract F19628-85-C-0002)
(AD-A197789; ESD-TR-88-125) Avail: NTIS HC A03/MF A01 CSCL 17I

The application of neural networks to the detection of variance transitions in Gaussian noise is considered. The problem, which consists of transition detection between a pair of input sample variances, is a benchmark example of hypothesis testing on a nonstationary stochastic process. In the case of neural net algorithms the testing of hypotheses results from the decision space output of the last layer of neurons. Variance transition detection in a Gaussian random process is probably the most tractable example upon which to study machine analysis of a nonstationary stochastic process. It is an obvious test bed for the analysis of neural network decisioning of stochastic data. In this report the modeling of the process as Gaussian is dictated by the desire for a comparison of neural network and classical detection techniques. For specific applications, other data-derived parameters, such as correlation length, may be more appropriate for the analysis of transitions. It is expected, however, that neural network structures required for hypothesis testing are independent of the nature of the sufficient statistics; dependent instead upon the pattern of mean values. The purpose of this research is to provide a theoretical foundation for work currently being done on satellite maneuver detection. The detection of maneuvers is performed by neural networks which have been trained upon signal variances, spectral widths, and autoregressive model coefficients from radar cross section data. This research is also relevant to the data fusion effort, in which these parameters are obtained from different sensors. GRA

63 CYBERNETICS

Includes feedback and control theory, artificial intelligence, robotics and expert systems.

For related information see also *54 Man/System Technology and Life Support.*

N89-13180# Syracuse Univ., N. Y.
NORTHEAST ARTIFICIAL INTELLIGENCE CONSORTIUM (NAIC). REVIEW OF TECHNICAL TASKS, VOLUME 2, PART 1 Interim Report, Dec. 1984 - Dec. 1985
J. F. Allen, P. B. Berra, J. A. Biles, K. A. Bowen, S. E. Conry, W. B. Croft, V. R. Lesser, R. A. Meyer, J. W. Modestino, and G. Nagy et al. Jul. 1987 479 p Consortium held in Syracuse, N.Y.; sponsored by RADC Sponsored in part by the Laboratory Director's Fund
(Contract F30602-85-C-0008; AF Proj. 2304)
(AD-A189773; RADC-TR-86-218-Vol-2-Pt-1) Avail: NTIS HC A21/MF A01 CSCL 09B

The Northeast Artificial Intelligence Consortium (NAIC) was created by the Air Force Systems Command, Rome Air Development Center, and the Office of Scientific Research. Its purpose is to conduct pertinent research in artificial intelligence and to perform activities ancillary to this research. Progress that

was made in the first year of the existence of the NAIC on the technical research tasks undertaken at the member universities is described. The topics covered are: versatile expert system for equipment maintenance, distributed AI for communications system control, automatic photointerpretation, time-oriented problem solving, speech understanding systems, knowledge base maintenance, hardware architectures for very large systems, knowledge-based reasoning and planning, and a knowledge acquisition, assistance, and explanation system. For individual titles, see N89-13181 through N89-13191.

N89-13181# State Univ. of New York, Buffalo. Dept. of Computer Science.
A FAULT DIAGNOSIS SYSTEM BASED ON AN INTEGRATED KNOWLEDGE BASE
Stuart C. Shapiro, Sargur N. Srihari, James Geller, and Ming-Ruey Taie *In* Syracuse Univ., N. Y. Northeast Artificial Intelligence Consortium (NAIC). Review of Technical Tasks, Volume 2, Part 1 Jul. 1987 p 27-29 (For primary document see N89-13180 04-63)
Avail: NTIS HC A21/MF A01 CSCL 09B

A versatile maintenance expert system (VMES) was developed for trouble-shooting electrical circuits. The VMES is able to diagnose a variety of common faults of electrical equipment. It can easily be adapted to new devices, and can communicate with the user through natural language, graphics, and menus. The system was successfully adapted to a simplified real device, a six channel PCM board used for telephone communications. Future plans include the investigation of domain knowledge, and further development of the knowledge representation scheme for reasoning and display. Author

N89-13182# Instituto Superior Tecnico, Lisbon (Portugal). Dept. de Engenharia Mecanica.
A LOGIC FOR BELIEF REVISION
Joao P. Martins and Stuart C. Shapiro (State Univ. of New York, Buffalo.) *In* Syracuse Univ., N. Y. Northeast Artificial Intelligence Consortium (NAIC). Review of Technical Tasks, Volume 2, Part 1 Jul. 1987 p 31-89 (For primary document see N89-13180 04-63)
Avail: NTIS HC A21/MF A01 CSCL 09B

Artificial Intelligence (AI) is the branch of computer science which studies how to enable computers to exhibit intelligent behavior. One of the central problems in AI research, automated reasoning, is that of how computers can automatically draw conclusions from bodies of information. One branch of automated reasoning is concerned with what to do when a contradiction is found during the reasoning process. Systems that are able to detect contradictions and/or identify their causes were implemented by several researchers. A logic suitable to support belief revision systems is presented and the properties of a belief revision system based on that logic is discussed. One of the fundamental problems that any logic underlying a belief revision system has to address is how to keep track of and propagate propositional dependencies. The SWM system is based on relevance logic and makes use of the bookkeeping mechanisms of relevance logic. In addition, SWM has some other mechanisms to remember the contradictions that were derived, to prevent their re-derivation. Author

N89-13183# Instituto Superior Tecnico, Lisbon (Portugal). Dept. de Engenharia Mecanica.
A MODEL FOR BELIEF REVISION
Joao P. Martins and Stuart C. Shapiro (State Univ. of New York, Buffalo.) *In* Syracuse Univ., N. Y. Northeast Artificial Intelligence Consortium (NAIC). Review of Technical Tasks, Volume 2, Part 1 Jul. 1987 p 91-180 (For primary document see N89-13180 04-63)
Avail: NTIS HC A21/MF A01 CSCL 09B

It is generally recognized that the possibility of detecting contradictions and identifying their sources is an important feature of an intelligent system. Systems that are able to detect contradictions and/or identify their causes, called Belief Revision Systems, Truth Maintenance Systems, or Reason Maintenance Systems, were implemented. A logic suitable to support belief revision systems is presented, the properties that a belief revision system based on this logic will exhibit is discussed, and a particular implementation of the model of a belief revision system is presented. The system presented, SNeBR, differs from most of the systems developed so far in two respects. First, it is based on a logic which was developed to support belief revision systems. Second, its implementation relies on the manipulation of sets of assumptions, not justifications. The first feature allows the study of the formal properties of the system independently of its implementation, and the second one enables the system to work effectively and efficiently with inconsistent information, to switch reasoning contexts without processing overhead, and to avoid most backtracking. Author

N89-13184# State Univ. of New York, Buffalo. Dept. of Computer Science.
SNePS CONSIDERED AS A FULLY INTENSIONAL PROPOSITIONAL SEMANTIC NETWORK
Stuart C. Shapiro and William J. Rapaport *In* Syracuse Univ., N. Y. Northeast Artificial Intelligence Consortium (NAIC). Review of Technical Tasks, Volume 2, Part 1 Jul. 1987 p 181-226 (For primary document see N89-13180 04-63)
(Contract F30602-85-C-0008; SUNY-BRDF-150-9216)
Avail: NTIS HC A21/MF A01 CSCL 09B

A semantic network is a data structure typically consisting of labeled nodes and labeled, directed arcs. The Semantic Network Processing System (SNePS) can be viewed as a semantic network language with facilities for building semantic networks to represent virtually any kind of information or knowledge; retrieving information from them; and performing inference with them. The interpretation of a particular use of SNePS in terms of a philosophical theory of mental entities inspired by Alexius Meinong's Theory of Objects is offered. Presentation of the nodes and arcs used in the interaction, together with some other important ones is given. The criteria for a semantic network are discussed. Author

N89-13185# Instituto Superior Tecnico, Lisbon (Portugal). Dept. de Engenharia Mecanica.
BELIEF REVISION IN SNePS
Joao P. Martins and Stuart C. Shapiro *In* Syracuse Univ., N. Y. Northeast Artificial Intelligence Consortium (NAIC). Review of Technical Tasks, Volume 2, Part 1 Jul. 1987 p 227-243 (For primary document see N89-13180 04-63)
(Contract F30602-85-C-0008; NSF MCS-80-06314)
Avail: NTIS HC A21/MF A01 CSCL 09B

The Semantic Network Processing System (SNePS) is a powerful knowledge representation system which allows multiple beliefs (beliefs from multiple agents, contradictory beliefs, hypothetical beliefs) to be simultaneously represented, and performs both forward and backward reasoning within sets of these beliefs. The SNePS Belief Revision (SNeBR) relies on a logic developed to support belief revision systems, the SWM system, and its implementation relies on the manipulation of assumptions, rather than justifications, as is common in other belief revision systems. The first aspect guarantees, among other things, that every proposition in SNeBR is associated with those (and only those) hypotheses from which it was derived. The second aspect enables it to effectively switch reasoning contexts and to avoid having to mark every proposition which should not be considered by the knowledge base retrieval operation. Author

N89-13186# Clarkson Coll. of Technology, Potsdam, N.Y. Electrical and Computer Engineering.
DISTRIBUTED PROBLEM SOLVING
Susan E. Conry, Robert A. Meyer, and Janice E. Searleman *In* Syracuse Univ., N. Y. Northeast Artificial Intelligence Consortium (NAIC). Review of Technical Tasks, Volume 2, Part 1 Jul. 1987 p 245-265 (For primary document see N89-13180 04-63)
Avail: NTIS HC A21/MF A01 CSCL 09B

The research efforts during the past year are described. The work is in the area of distributed artificial intelligence. Distributed AI is the study of systems involving the cooperation and

coordination of a group of loosely coupled knowledge based component systems working together to solve common problems. Interest is in the systems which are naturally distributed as the result of a distributed problem domain. Specifically, the system currently under study is both functionally distributed and geographically distributed. The long term goals are to answer fundamental questions about distributed problem solving activities in such systems. In order to investigate the questions an application domain was selected in which to study the ideas about distributed problem solving. The specific domain used in this research is described. Research objectives are reviewed and progress in meeting these objectives, and the directions for future research are outlined. Author

N89-13187# Clarkson Coll. of Technology, Potsdam, N.Y.
A SHARED KNOWLEDGE BASE FOR INDEPENDENT PROBLEM SOLVING AGENTS
S. E. Conry, R. A. Meyer, and J. E. Searleman *In* Syracuse Univ., N. Y. Northeast Artificial Intelligence Consortium (NAIC). Review of Technical Tasks, Volume 2, Part 1 Jul. 1987 p 267-275 (For primary document see N89-13180 04-63)
(Contract F30602-85-C-0008)
Avail: NTIS HC A21/MF A01 CSCL 09B

A knowledge representation scheme that is intended to be compatible with two modes of problem solving activity in a distributed problem solving environment is described. The application domain of the interest involves the situation assessment, diagnosis, and planning necessary for monitoring and control of image communication systems. Author

N89-13188# Colgate Univ., Hamilton, N.Y.
PLANNER SYSTEM FOR THE APPLICATION OF INDICATIONS AND WARNING
Sergei Nirenburg *In* Syracuse Univ., N. Y. Northeast Artificial Intelligence Consortium (NAIC). Review of Technical Tasks, Volume 2, Part 1 Jul. 1987 p 277-326 (For primary document see N89-13180 04-63)
Avail: NTIS HC A21/MF A01 CSCL 09B

A planner system for the application of indications and warning (A and I) is designed. The task of the project is two-pronged: obtain as input messages concerning events in a model of a real-life subworld; understand these events by detecting what plans they are part of and, whenever applicable, what goals are pursued; and produce (suggestion for possible) plans of action necessary in connection with the suituation in the world. Author

N89-13189# Colgate Univ., Hamilton, N.Y.
PROVIDING INTELLIGENT ASSISTANCE IN DISTRIBUTED OFFICE ENVIRONMENTS
Sergei Nirenburg and Victor Lesser (Massachusetts Univ., Amherst.) *In* Syracuse Univ., N. Y. Northeast Artificial Intelligence Consortium (NAIC). Review of Technical Tasks, Volume 2, Part 1 Jul. 1987 p 327-344 (For primary document see N89-13180 04-63)
(Contract F30602-85-C-0008)
Avail: NTIS HC A21/MF A01 CSCL 09B

It is argued that a task-centered, an agent-centered, and a cognition-oriented perspective are all needed for providing intelligent assistance in distributed office environments. The architecture is presented for a system called OFFICE that combines these three perspectives. The architecture is illustrated through an example. Author

N89-13190# Colgate Univ., Hamilton, N.Y.
POPLAR: A TESTBED FOR COGNITIVE MODELING
Irene Nirenburg, Sergei Nirenburg, and James H. Reynolds *In* Syracuse Univ., N. Y. Northeast Artificial Intelligence Consortium (NAIC). Review of Technical Tasks, Volume 2, Part 1 Jul. 1987 p 345-374 (For primary document see N89-13180 04-63)
Avail: NTIS HC A21/MF A01 CSCL 09B

An overview of a cognitive modeling system centered around a personally-oriented planner is presented and then the types of knowlede it uses to make control decisions is described in detail. POPLAR is a model of an intelligent actor capable of planning sequences of control and domain actions in a simulated world that exists independently of the planner. The world is a simplification of the Dungeon computer game environment. The actor makes control decisions on the basis of situational knowledge as well as its personality characteristics and its beliefs about personality of other cognitive entities in the world. POPLAR is a step toward an AI system whose behavior is psychologically justified and can provide the basis for an experimental testbed in cognitive modeling. Author

N89-13191# Massachusetts Univ., Amherst. Dept. of Computer and Information Science.
PLAN RECOGNITION, KNOWLEDGE ACQUISITION AND EXPLANATION IN AN INTELLIGENT INTERFACE Year End Report, 1984 - 1985
Victor Lesser, W. Bruce Croft, and Beverly Woolf *In* Syracuse Univ., N. Y. Northeast Artificial Intelligence Consortium (NAIC). Review of Technical Tasks, Volume 2, Part 1 Jul. 1987 p 375-466 (For primary document see N89-13180 04-63)
Avail: NTIS HC A21/MF A01 CSCL 09B

The primary focus was to support users in their interactions with an intelligent database and with each other, in a case of a distributed interface. The research effort has two complementary aims: development of a planner, plan recognizer, and associated database that knows about the user tasks and can begin to automate execution of the tasks; and development of intelligent interface tools, such as natural language parsers and generators, and graphics facilities, to increase a user's ability to interact with the system. Both efforts are directed at enabling a machine to provide assistance to a user while describing its own actions and decisions. The achievements for fiscal year 1984 to 1985 are outlined. Author

N89-13192# Massachusetts Inst. of Tech., Cambridge. Lab. for Information and Decision Systems.
EVALUATION OF EXPERT SYSTEMS IN DECISIONMAKING ORGANIZATIONS
Didier M. Perdu and Alexander H. Levis Jul. 1988 15 p
(Contract N00014-85-K-0782)
(AD-A196448; LIDS-P-1788) Avail: NTIS HC A03/MF A01 CSCL 23B

A class of decision aids that is receiving attention in the development community is based on artificial intelligence and especially expert systems. This paper presents a procedure for assessing to what extent the measures of performance of an organization are modified when an expert system is introduced. First, a model of symbolic computation with fuzzy logic, using Predicate Transition Nets, is presented to model the most common kind of expert systems - the consultant expert systems. This model allows evaluation of its response time for a given input. An Air Defense problem in which command and control involves a hierarchical two decisionmaker organization, where the expert system is used as an aid in the fusion of inconsistent information, is then presented. A strategy involving the use of the expert system is compared to two other strategies expected to be used by a decisionmaker facing this problem. Measures of performance (workload, timeliness and accuracy) are evaluated for each of these strategies. The results show that the strategy involving the use of the expert system improves significantly the accuracy of the organization, but requires more time and increases the workload of the decisionmaker using it. GRA

N89-13193# Defense Systems, Inc., McLean, Va.
USER-COMPUTER INTERFACE TECHNOLOGY: AN ASSESSMENT OF THE CURRENT STATE OF THE ART Interim Report, Jul. 1986 - Mar. 1987
Sam Landee-Thompson Jun. 1988 86 p Prepared in cooperation with International Information Systems, Inc., McLean, Va.
(Contract MDA903-86-C-0204; DA Proj. 2Q1-62717-A-790)
(AD-A196839; ARI-RN-88-50) Avail: NTIS HC A05/MF A01 CSCL 12E

There is an obvious challenge for those doing research and development work in user-computer interaction to identify and track research developments from a wide range of related fields. This assessment of relevant literature is intended to extend the user-computer R and D community's appreciation for some of the current trends, directions, accomplishments and challenges in developing intelligent interactive system interfaces. The basic document consists of an assessment of the state-of-the-art based upon the analysis of 39 representative recent publications. These are analyzed in terms of defining the problem, recent developments toward intelligent interfacing and difficulties in developing intelligent interfaces. Conclusions and suggestions are offered concerning promising areas for research and development. The document also contains an annotated bibliography in which the contents of 57 recent publications relevant to user-computer interface technology are summarized. This document will prove useful to anyone seeking a definition and synopsis of the state-of-the-art in intelligent user-computer interface technology. GRA

N89-13194# University of Southern California, Marina del Rey. Information Sciences Inst.
APPLICATIONS OF THE ISI (INFORMATION SCIENCES INSTITUTE) GRAPHER
Gabriel Robins Jun. 1988 31 p
(Contract MDA903-81-C-0335)
(AD-A197230; ISI/RS-88-210) Avail: NTIS HC A03/MF A01 CSCL 12E

Described are various end-user applications that were built using the ISI Grapher, a portable software tool for displaying graphs pictorially. Numerous current research projects that already utilize the ISI Grapher are listed, and several general domains are identified where a grapher would be of considerable benefit. Throughout this paper, the term user denotes someone using the ISI Grapher for applications such as the NIKL/LOOM Browser. On the other hand, the term application-builder will be used to denote a person who is actually building an application using the ISI Grapher as a foundation. GRA

N89-13195# Princeton Univ., N. J. Dept. of Mechanical and Aerospace Engineering.
ARTIFICIAL INTELLIGENCE THEORY AND RECONFIGURABLE CONTROL SYSTEMS Final Report, 12 Mar. 1984 - 11 Mar. 1984
Robert F. Stengel Jun. 1988 28 p
(Contract DAAG29-84-K-0048)
(AD-A197255; MAE-1826; ARO-20155.15-MA) Avail: NTIS HC A03/MF A01 CSCL 12E

The principal topic of research in this effort was the development of analysis and design methods for fault-tolerant control systems, using artificial intelligence concepts to screen failure hypotheses, and more conventional control theory for reconfiguration and actual control. Methods developed include new graphical presentations of logic trees and signal dependency graphs, procedures for translating expert systems from LISP to Pascal, the definition of performance metrics for real-time expert systems, a Control Equation Parser computer program for computer-aided control system design, and a control-reconfiguration strategy based on proportional-integral implicit model-following. A Rule-Based Flight Control System for a tandem-rotor helicopter, implemented with parallel microprocessors and operating in real time, was developed in the course of this research. This task made use of the Princeton Rule-Based Controller, a unique software architecture for combining procedural and symbolic processing. The knowledge base is developed in the LISP computer language and is translated with the inference engine into the Pascal language. The ease with which Pascal code can be embedded in the knowledge-base structure makes this a highly suitable tool for task and algorithm scheduling. GRA

N89-13196# JAYCOR, Vienna, Va.
BAYESIAN REASONING TOOL
26 May 1988 87 p
(Contract N00014-86-C-2352)
(AD-A197351) Avail: NTIS HC A05/MF A01 CSCL 12E

Many real problems are associated with uncertainty; the evidence people observe which helps them to reason about some goal event is almost always uncertain and incomplete. Still, people make judgements based on this uncertain and incomplete evidence. These uncertain evidences can be combined in various ways to find the validity or strength of a hypothesis, Bayesian probability theory is a normative theory that allows one to reason about and combine uncertain evidences in a way the conforms to the tenets of probability theory, but avoids the disadvantages usually associated with probabilistic computations of belief. BaRT is a Bayesian Reasoning Tool which implements Pearl's ideas. It has been implemented as an AI programming environment which can perform classification problem solving, and it has been used to classify ships. Section 2 provides an overview of the theoretical background for this work. Section 3 explains how to use BaRT and provides an example. Sections 4 and 5 provide details concerning the implementation of this system. This manual describes a preliminary version of a system which is under development. Later versions of BaRT will have greater capabilities, so any of the functions and capabilities described here are subject to change. GRA

N89-13197# George Mason Univ., Fairfax, Va. School of Information Technology and Engineering.
COMPUTER BASED INTELLIGENCE SUPPORT: AN INTEGRATED EXPERT SYSTEM AND DECISION SUPPORT SYSTEMS APPROACH Interim Report, Oct. 1984 - Oct. 1985
Andrew P. Sage and Adolfo Lagomasino Jun. 1988 31 p
(Contract MDA903-82-C-0124; DA Proj. 2Q1-61102-B-74-F)
(AD-A197386; ARI-RN-88-41) Avail: NTIS HC A03/MF A01 CSCL 12I

This research note summarizes research and design needs in the area of computer based intelligence support, particularly the command and control area. It is argued that an integrating approach is needed. A discussion of knowledge representation emphasizes this, and an approach that accommodates both probabilistic and logical support, and which is able to cope with several types of imperfect information is described. GRA

N89-13198*# National Aeronautics and Space Administration. Langley Research Center, Hampton, Va.
ADVANCING AUTOMATION AND ROBOTICS TECHNOLOGY FOR THE SPACE STATION AND FOR THE US ECONOMY Progress Report No. 6, Oct. 1987 - Mar. 1988
Robert Nunamaker 15 Jun. 1988 54 p Prepared in cooperation with NASA, Lyndon B. Johnson Space Center, Houston, Tex.
(NASA-TM-100989; NAS 1.15:100989) Avail: NTIS HC A04/MF A01 CSCL 09B

In April 1985, as required by Public Law 98-371, the NASA Advanced Technology Advisory Committee (ATAC) reported to Congress the results of its studies on advanced automation and robotics technology for use on the Space Station. This material was documented in the initial report (NASA Technical Memo 87566). A further requirement of the law was that ATAC follow NASA's progress in this area and report to Congress semiannually. This report is the sixth in a series of progress updates and covers the period between October 1, 1987 and March 1, 1988. NASA has accepted the basic recommendations of ATAC for its Space Station efforts. ATAC and NASA agree that the thrust of Congress is to build an advanced automation and robotics technology base that will support an evolutionary Space Station program and serve as a highly visible stimulator affecting the U.S. long-term economy. The progress report identifies the work of NASA and the Space Station study contractors, research in progress, and issues connected with the advancement of automation and robotics technology on the Space Station. Author

N89-13199# Pennsylvania Univ., Philadelphia. School of Electrical Engineering.
OPTICAL COMPUTING BASED ON NEURONAL MODELS Final Report, 15 Sep. 1985 - 15 Feb. 1988
Nabil H. Farhat May 1988 75 p
(Contract N00014-85-K-2036)
(AD-A197749; EO/MO-14) Avail: NTIS HC A04/MF A01 CSCL 12I

The ultimate goal of the research work carried out under this grant is understanding the computational algorithms used by the nervous system and development of systems that emulate, match, or surpass in their performance the computational power of biological brain. Tasks such as seeing, hearing, touch, walking, and cognition are far too complex for existing sequential digital computers. Therefore new architectures, hardware, and algorithms modeled after neural circuits must be considered in order to deal with real-world problems. Neural net models and their analogs represent a new approach to collective signal processing that is robust, fault tolerant and can be extremely fast. These properties stem directly from the massive interconnectivity of neurons (the logic elements) in the brain and their ability to perform many-to-one mappings with varied degree of nonlinearity and to store information as weights of the links between them, i.e., their synaptic interconnections, in a distributed non-localized manner. As a result signal processing tasks such as nearest neighbor searches in associative memory can be performed in time durations equal to a few time constants of the decision making elements, the neurons, of the net. GRA

64 NUMERICAL ANALYSIS

Includes iteration, difference equations, and numerical approximation.

N89-13200*# National Aeronautics and Space Administration. Ames Research Center, Moffett Field, Calif.
ON THE CONSTRAINED CHEBYSHEV APPROXIMATION PROBLEM ON ELLIPSES
Roland Freund and Bernd Fischer Aug. 1988 20 p Submitted for publication
(Contract NCC2-387)
(NASA-CR-183209; NAS 1.26:183209; RIACS-TR-88.20) Avail: NTIS HC A03/MF A01 CSCL 12A

Constrained Chebyshev approximation problems of the type with minimum (p is an element of Pi(sub n):p(c)=1) and maximum (z is an element of E) with /p(z)/ are considered. Here Pi(sub n) denotes the set of all complex polynomials of degree at most n, E is any ellipse in the complex plane, and c is an element of C/E. Such approximation problems arise in the context of optimizing semi-iterative methods for the solution of large, sparse systems of linear equations Ax=b with complex non-Hermitian coefficient matrices A. The problem of obtaining optimal polynomial preconditioners for conjugate gradient type methods for Ax=b also leads to problems of this type. A new family of polynomials -- q(sub n)(z;c), n is an element of N, and c is an element of C/E -- are introduced as the polynomials which are optimal for a modified version of the Chebyshev approximation problem with Pi(sub n) replaced by a certain subfamily. Some simple properties of q(sub n) are also listed. A necessary and sufficient condition for q(sub n) to be the extremal polynomial for the approximation problem is then derived. Finally, it is shown that q(sub n) is indeed optimal for the problem for all fixed n whenever the distance between c and E is sufficiently large. Results of some numerical tests are presented. M.G.

N89-13201# International Centre for Theoretical Physics, Trieste (Italy).
NONLINEAR PERTURBATIONS OF DIFFERENTIAL OPERATORS WITH NONTRIVIAL KERNEL AND APPLICATIONS TO THIRD ORDER PERIODIC BOUNDARY VALUE PROBLEMS
Anthony Uyl Afuwape, Pierpaolo Omari, and Fabio Zanolin (Udine Univ., Italy) Nov. 1987 29 p
(DE88-702991; IC-87/371) Avail: NTIS (US Sales Only) HC A03/MF A01

This paper deals with the solvability of the nonlinear operator equations in normed spaces Lx = EGx + f, where L is a linear map with possible nontrivial kernel. Applications are given to the existence of periodic solutions for the third order scalar differential equation x''' + ax'' + bx' + g(t,x) = p(t), under various conditions on the interaction of g(t,x)/x with spectral configurations of a, b, and c. DOE

N89-13202*# Awesome Computing, Inc.
THE SOLUTION OF LINEAR SYSTEMS OF EQUATIONS WITH A STRUCTURAL ANALYSIS CODE ON THE NAS CRAY-2
Eugene L. Poole and Andrea L. Overman Washington NASA Dec. 1988 33 p Prepared for Analytical Services and Materials, Inc., Hampton, Va.
(Contract NAS1-18599)
(NASA-CR-4159; NAS 1.26:4159) Avail: NTIS HC A03/MF A01 CSCL 12A

Two methods for solving linear systems of equations on the NAS Cray-2 are described. One is a direct method; the other is an iterative method. Both methods exploit the architecture of the Cray-2, particularly the vectorization, and are aimed at structural analysis applications. To demonstrate and evaluate the methods, they were installed in a finite element structural analysis code denoted the Computational Structural Mechanics (CSM) Testbed. A description of the techniques used to integrate the two solvers into the Testbed is given. Storage schemes, memory requirements, operation counts, and reformatting procedures are discussed. Finally, results from the new methods are compared with results from the initial Testbed sparse Choleski equation solver for three structural analysis problems. The new direct solvers described achieve the highest computational rates of the methods compared. The new iterative methods are not able to achieve as high computation rates as the vectorized direct solvers but are best for well conditioned problems which require fewer iterations to converge to the solution. Author

N89-13203*# National Aeronautics and Space Administration. Langley Research Center, Hampton, Va.
ENGINEERING APPLICATIONS OF HEURISTIC MULTILEVEL OPTIMIZATION METHODS
Jean-Francois M. Barthelemy Oct. 1988 10 p Presented at the 2nd NASA/Air Force Symposium on Recent Advances in Multidisciplinary Analysis and Optimization, Hampton, Va., 28-30 Sep. 1988 and GAMM Seminar, Siegen, Fed. Republic of Germany, 5-7 Oct. 1988
(NASA-TM-101504; NAS 1.15:101504) Avail: NTIS HC A02/MF A01 CSCL 12A

Some engineering applications of heuristic multilevel optimization methods are presented and the discussion focuses on the dependency matrix that indicates the relationship between problem functions and variables. Coordination of the subproblem optimizations is shown to be typically achieved through the use of exact or approximate sensitivity analysis. Areas for further development are identified. GRA

N89-13204# Carnegie-Mellon Univ., Pittsburgh, Pa. Management Sciences Research Group.
SENSITIVITY ANALYSIS FOR SHORTEST HAMILTONIAN PATH AND TRAVELING SALESMAN PROBLEMS
Marek Libura Apr. 1988 27 p
(AD-A197167; MSRR-540; WP-87-88-39) Avail: NTIS HC A03/MF A01 CSCL 12D

The problem considered in this paper belongs to so called sensitivity analysis in combinatorial optimization. This term is used for a phase of solution procedure when an optimal solution of problem has been already found and additional calculations are performed in order to investigate, how this optimal solution depends on changes of problems parameters. In this paper two well known combinatorial optimization problems are considered: the shortest Hamiltonian path problem in undirected weighted graph and the

symmetric traveling salesman problem. It is assumed that an optimal solution of given problem is known. The goal of sensitivity analysis consists in finding by how much we can perturb each edge weight individually without changing the optimality of the solution. The maximum increment and decrement of the edge weight that preserve the optimality of solution are called the edge tolerances with respect to this solution. In this paper, a method of computing lower bounds of the edge tolerances with respect to the optimal solution of the shortest Hamiltonian path problem and traveling salesman problem is described. The method is based on solving the sensitivity analysis problem for appropriate relaxation of the original optimization problem. This paper gives a description of the approach and its microcomputer implementation and we report preliminary results of computational experiments. GRA

N89-13205# Florida State Univ., Tallahassee. Dept. of Statistics.

IDENTIFYING NONLINEAR COVARIATE EFFECTS IN SEMIMARTINGALE REGRESSION MODELS

Ian W. McKeague and Klaus J. Utikal Jun. 1988 23 p
(Contract DAAL03-86-K-0094; AF-AFOSR-0040-88)
(AD-A197323; FSU-TR-M783; TR-D103-ARO; ARO-23699.19-MA; AFOSR-88-129TR) Avail: NTIS HC A03/MF A01 CSCL 12C

Let X sub t be a semimartingale which is either continuous or of counting process type and which satisfies the stochastic differential equation dX sub t = Y sub t alpha (t, Z sub t) dt + dM sub t, where Y and Z are predictable covariate processes, M is a martingale and alpha is an unknown, nonrandom function. The authors study inference for alpha by introducing an estimator and deriving a functional central limit theorem for it. The asymptotic distribution turns out to be given by a Gaussian random field that admits a representation as a stochastic integral with respect to a multiparameter Wiener process. This result is used to develop a test for independence of X from the covariate Z, a test for time-homogeneity of alpha, and a goodness-of-fit test for the proportional hazards model alpha (t,z) = alpha sub 1 (t) alpha sub 2 (z) used in survival analysis. GRA

N89-13206# Georgia Inst. of Tech., Atlanta. Production and Distribution Research Center.

GLOBAL OPTIMIZATION OF CONCAVE FUNCTIONS SUBJECT TO SEPARABLE QUADRATIC CONSTRAINTS AND OF ALL-QUADRATIC SEPARABLE PROBLEMS

Faiz A. Al-Khayyal, Reiner Horst, and Panos M. Pardalos Apr. 1988 20 p
(Contract N00014-86-K-0173)
(AD-A197747; PDRC-88-04) Avail: NTIS HC A03/MF A01 CSCL 12D

Different methods are proposed for finding the global minimum of concave function subject to quadratic separable constraints. The first method is of the branch and bound type, and is based on rectangular partitions to obtain upper and lower bounds. Convergence of the proposed algorithm is also proved. For computational purposes, different procedures that accelerate the convergence of the proposed algorithm are analyzed. The second method is based on piecewise linear approximations of the constraint functions. When the constraints are convex the problem is reduced to global concave minimization subject to linear constraints. In the case of non-convex constraints we use zero-one integer variables to linearize the constraints. The number of integer variables depends only on the concave parts of the constraint functions. GRA

N89-13207# Texas A&M Univ., College Station. Dept. of Statistics.

OPTIMAL RATES OF CONVERGENCE FOR DECONVOLVING A DENSITY Technical Report No. 3, Aug. 1987 - Aug. 1988

Raymond J. Carroll and Peter Hall Aug. 1988 8 p
(Contract F49620-85-C-0144)
(AD-A197748; AFOSR-88-0775TR) Avail: NTIS HC A02/MF A01 CSCL 07D

Suppose we observe the sum of two independent random variables X and Z, where Z denotes measurement error and has a known distribution, and where the unknown density f of X is to be estimated. It is shown that if Z is normally distributed and if f has k bounded derivatives, then the fastest attainable convergence rate of any nonparametric estimator of f is only (log n)-k/1. Therefore deconvolution with normal errors may not be a practical proposition. Other error distributions are also treated. Stefanski-Carroll (1978b) estimators achieve the optimal rates. Our results have versions for multiplicative errors, where they imply that even optimal rates are exceptionally slow. GRA

N89-13208# Army Armament Research and Development Command, Watervliet, N. Y.

AN ADAPTIVE METHOD WITH MESH MOVING AND LOCAL MESH REFINEMENT FOR TIME-DEPENDENT PARTIAL DIFFERENTIAL EQUATIONS Final Report

David C. Arney and Joseph E. Flaherty Apr. 1988 56 p
(AD-A197772; ARCCB-TR-88017) Avail: NTIS HC A04/MF A01 CSCL 12A

The authors discuss mesh moving, static mesh regeneration, and local mesh refinement algorithms that can be used with a finite difference or finite element scheme to solve initial-boundary value problems for vector systems of time-dependent partial differential equations in two-space dimensions and time. A coarse base mesh of quadrilateral cells is moved by an algebraic mesh movement function so that it may follow and isolate spatially distinct phenomena. The local mesh refinement method recursively divides the time step and spatial cells of the moving base mesh in regions were error indicators are high until a prescribed tolerance is satisfied. The static mesh regeneration procedure is used to create a new base mesh when the existing ones become too distorted. In order to test our adaptive algorithms, the authors implemented them in a system code with an initial mesh generator, a MacCormack finite difference scheme for hyperbolic systems, and an error indicator based upon estimates of the local discretization error obtained by Richardson extrapolation. Results are presented for several computational examples. GRA

N89-13209# Texas A&M Univ., College Station. Dept. of Mathematics.

MULTIVARIATE REGRESSION WITH EMPHASIS ON MULTIVARIATE SPLINE METHODS Final Report

Charles K. Chui 12 Jul. 1988 14 p
(Contract DAAG29-84-K-0154)
(AD-A197793; ARO-21091.17-MA) Avail: NTIS HC A03/MF A01 CSCL 12C

The notion of vertex splines in introduced to generalize the univariate spline theory with arbitrary knot sequence to higher dimensions. These are in fact Hermite elements and to facilitate the construction process, the notion of super splines is also introduced. The advantages include efficiency in computing a locally supported basis, guaranteeing the full order of approximation, and various applications to finite element methods, computer-aided geometric design, data analysis, etc. In general, computaticnal schemes are studied and constructed, and interpolation as well as quasi-interpolation problems are solved. Shape-preserved approximation and interpolation by bivariate splines is also studied. Development of general multivariate spline theory including the dimension and basis problems is also a portion of this subject. On the other hand, applications to engineering problems are included in our study. GRA

N89-13210# Naval Research Lab., Washington, D.C. Engineering Services Div.

A NOTE ON INCOMPLETE INTEGRALS OF CYLINDRICAL FUNCTIONS Final Report

Allen R. Miller 21 Jun. 1988 10 p
(AD-A197822; NRL-9127) Avail: NTIS HC A02/MF A01 CSCL 12B

Representations for incomplete Lipschitz-Hankel integrals of cylindrical functions are given in closed form by using Kampe de Feriet double hypergeometric functions. In addition, reduction formulas for the Kampe de Feriet functions associated with these integrals are provided for some cases. GRA

N89-13211*# Jet Propulsion Lab., California Inst. of Tech., Pasadena.
OPTIMAL FIX ESTIMATORS AND A VARIATION ON THE CRAMER RAO LOWER BOUND Final Report
3 Sep. 1987 25 p Prepared for Army Intelligence Center and School, Fort Huachuca, Ariz.
(Contract NAS7-918)
(NASA-CR-183011; JPL-D-4718; NAS 1.26:183011; AD-A197836; ALGO-Publ-0124) Avail: NTIS HC A03/MF A01 CSCL 12A

The fix estimators MARC (Mathematical Analysis Research Corporation) has examined in fielded systems have a property which implies that these fix estimators approach optimality. Explaining the meaning of this statement and the qualifications that go with it is the purpose of the main body of this report. Contents include: (1) Optimal Estimators in Statistics; (2) Fix Modeling Assumptions; (3) Problems with Fix Modeling Assumptions; Optimality to within Terms of Order. GRA

N89-13212# Los Alamos National Lab., N. Mex.
SOME STRATEGIES FOR ENHANCING THE PERFORMANCE OF THE BLOCK LANCZOS METHOD
J. D. Kress, S. B. Woodruff, G. A. Parker, and R. T. Pack 1988 8 p Presented at the Workshop on Practical Iterative Methods for Large Scale Computations, Minneapolis, Minn., 23 Oct. 1988
(Contract W-7405-eng-36)
(DE88-014401; LA-UR-88-2482; CONF-8810119-2) Avail: NTIS HC A02/MF A01

The block Lanczos method is used to calculate the eigenfunctions for a generalized eigenvalue problem constructed for a finite element solution to a 2-D Schroedinger equation on the surface of a hypersphere. This equation results from a treatment of the 3-D reactive scattering problem using Adiabatically adjusting, Principal axes Hyperspherical (APH) coordinates. Three strategies are considered with respect to increasing the CPU performance of the block Lanczos (with selective orthogonalization) method: (1) the effect of varying the Lanczos block size; (2) the effect of solving the block tridiagonal ordinary eigenvalue problem upon every other Lanczos iteration; and (3) the effect of dividing a single problem of finding p eigenvalues into a set of p sub i problems, where each subproblem consists of finding p/p sub i eigenvalues. DOE

N89-13213# Stanford Linear Accelerator Center, Calif. Dept. of Statistics.
FITTING FUNCTIONS TO NOISY DATA IN HIGH DIMENSIONS
Jerome H. Friedman Jul. 1988 41 p Presented at the 20th Symposium on the Interface: Computing Science and Statistics, Washington, D.C., 20 Apr. 1988
(Contract DE-AC03-76SF-00515)
(DE88-015922; SU-SLAC-PUB-4676; CONF-8804183-1) Avail: NTIS HC A03/MF A01

Consider an arbitrary domain of interest in n-dimensional Euclidean space and an unknown function of n arguments defined on that domain. Suppose we are given the value of the function (perhaps perturbed with additive noise) at some set of points. The problem is to find a function that provides a reasonable approximation to the unknown one over the domain of interest. This paper presents a brief review of current methodology aimed at dealing with this problem, and presents a new technique - multivariate adaptive regression splines - that has the potential to overcome some of the limitations of previous approaches. DOE

N89-13214*# National Aeronautics and Space Administration. Ames Research Center, Moffett Field, Calif.
TWO ALTERNATE PROOFS OF WANG'S LUNE FORMULA FOR SPARSE DISTRIBUTED MEMORY AND AN INTEGRAL APPROXIMATION
Louis A. Jaeckel 3 Feb. 1988 35 p
(Contract NCC2-408)
(NASA-CR-184555; RIACS-TR-88.5; NAS 1.26:184555) Avail: NTIS HC A03/MF A01 CSCL 12A

In Kanerva's Sparse Distributed Memory, writing to and reading from the memory are done in relation to spheres in an n-dimensional binary vector space. Thus it is important to know how many points are in the intersection of two spheres in this space. Two proofs are given of Wang's formula for spheres of unequal radii, and an integral approximation for the intersection in this case. Author

N89-13215*# California Univ., Los Angeles. Dept. of Mathematics.
AN ARTIFICIAL COMPRESSION METHOD FOR ENO SCHEMES: THE SLOPE MODIFICATION METHOD
Huanan Yang 8 Sep. 1988 61 p
(Contracts NAG1-270; N00014-86-K-0691; F49620-86-C-0115; NSF DMS-85-03294)
(NASA-CR-184613; NAS 1.26:184613) Avail: NTIS HC A04/MF A01 CSCL 12A

A simple and effective method of artificial compression is introduced. This method is based on a modification of the slopes of the ENO (essentially nonoscillatory) reconstruction and, with the help of suitable chosen parameters, greatly improves the resolution of the contact discontinuities. Numerical examples are provided to test the performance of the method and to give some suggestions as to the choice of the parameters. Author

65 STATISTICS AND PROBABILITY

Includes data sampling and smoothing; Monte Carlo method; and stochastic processes.

N89-13216# Washington Univ., Seattle. Dept. of Chemistry.
WAVELENGTH OR SENSOR SELECTION BY MINIMIZATION OF PREDICTION ERROR Interim Technical Report No. 42
Kenneth R. Beebe and Bruce R. Kowalski 1 Jul. 1988 28 p
(Contract N00014-75-C-0536)
(AD-A197231) Avail: NTIS HC A03/MF A01 CSCL 12E

A method of variable selection based on prediction error is presented. An algorithm based on this approach is developed and used to select variables using a simulated data set. The results of this procedure are compared to those expected using signal averaging with a smaller set of variables. GRA

N89-13217# Florida State Univ., Tallahassee. Dept. of Statistics.
STOCHASTIC CALCULUS AND SURVIVAL ANALYSIS
Ian W. McKeague and Klaus J. Utikal Jun. 1988 23 p
(Contract DAAL03-86-K-0094)
(AD-A197324; FSU-TR-M790; TR-D102-ARO; ARO-23699.18-MA) Avail: NTIS HC A03/MF A01 CSCL 12C

This paper gives a brief survey of the uses of stochastic calculus in survival analysis. The role played by martingale central limit theory in deriving asymptotic distributions of estimators and test statistics is described. The Nelson-Aalen estimator, Kaplan-Meier estimator, Cox's proportional hazards model, Aalen's additive risk model and a goodness-of-fit test for Cox's model are discussed. Sketches of the proofs of the main results are included. GRA

N89-13218# Pennsylvania State Univ., University Park. Dept. of Statistics.
TWO-SAMPLE INFERENCE FOR MEDIAN SURVIVAL TIMES BASED ON ONE-SAMPLE PROCEDURES FOR CENSORED SURVIVAL DATA Technical Report No. 74
Jane-Ling Wang and Thomas P. Hettmansperger Aug. 1988 29 p
(Contract N00014-80-C-0741; AF-AFOSR-0268-85)
(AD-A197776) Avail: NTIS HC A03/MF A01 CSCL 12C

Nonparametric two-sample tests based on ranks, e.g., median and Wilcoxon tests, have been extended by Gehan, Efron, and Brookmeyer and Crowley among others to accommodate censored survival data. While there is a vast literature on general linear rank test procedures with censored observations, two-sample confidence intervals have received much less attention. Nonparametric confidence intervals for the ratio of two scale parameters were derived for randomly right censored data by Wei and Gail based on the idea of Hodges and Lehmann. Their method

can also be applied to obtain confidence intervals for the difference of two location parameters. The confidence intervals for the difference of two location parameters. The confidence sets were computed by a numerical method based on a grid search and may not yield an interval. This paper focuses on the problem of testing and confidence intervals of the difference of two population medians with randomly right censored data. The authors show how to construct a two-sample test and confidence interval based on one-sample confidence intervals for the median of each population. GRA

N89-13219*# Jet Propulsion Lab., California Inst. of Tech., Pasadena.
BEARING ERROR AND THE CENTRAL LIMIT THEOREM Final Technical Memoorandum No. 32
24 Aug. 1987 13 p Prepared in cooperation with Mathematical Analysis Research Corp., Claremont, Calif. Prepared for Army Intelligence Center and School, Fort Huachuca. Ariz.
(Contract NAS7-918)
(NASA-CR-183009; JPL-D-4711; NAS 1.26:183009; AD-A197837; ALGO-Publ-0121) Avail: NTIS HC A03/MF A01 CSCL 12A

The approach of bearing error to a Normal distribution is examined by obtaining the distribution curve for different averages of bearing error (N=1, N=2, N=3). These curves are then compared against the corresponding normal. The bearing errors are taken from a Uniform distribution, a quadratic nonsymmetric, and a quadratic symmetric distribution - both concave up and concave down. Author

N89-13220*# Jet Propulsion Lab., California Inst. of Tech., Pasadena.
USE OF DISTANCE VERSUS STATISTICAL DISTANCE IN ACCEPTANCE TESTS Final Technical Memorandum No. 35
29 Sep. 1987 8 p Prepared in cooperation with Mathematical Analysis Research Corp., Claremont, Calif. Prepared for Army Intelligence Center and School, Fort Huachuca, Ariz.
(Contract NAS7-918)
(NASA-CR-183353; JPL-D-4817; NAS 1.26:183353; AD-A197839; ALGO-Publ-0144) Avail: NTIS HC A02/MF A01 CSCL 12A

The problem treated in this report is that of deciding, with a given (50 percent) confidence level and based on distance alone, whether two estimated fixes belong to the same emitter. In place of geometric distance - (x-y)T(x-y) - the authors propose use of statistical distance - (x-y)TB-1(x-y) - where B is a covariance matrix computed from those matrices of the fixes. The two methods are compared for various ratios of the axes of the 50 percent probability ellipse. GRA

N89-13221# Oak Ridge National Lab., Tenn.
PEOPLE VERSUS PROBABILITY
Bruce Tonn and Richard Goeltz Aug. 1988 32 p
(Contract DE-AC05-84OR-21400)
(DE88-017380; ORNL/TM-10898) Avail: NTIS HC A03/MF A01

This research explores how subjects combine estimates of uncertainty in probabilistic and evidential contexts. Two major computer programs written in Common Lisp asked subjects questions about the likelihoods and conjunctions of independent events. The results suggest that in the probabilistic context the best model to describe individual decision making is not the product rule but a minimum rule, and models varied as the magnitude of the likelihoods varied. In the evidential context, subjects appeared to use a maximum rule, although some evidence supports the use of the certainty factor rule. Subjects had difficulty in combining contradictory evidence. DOE

66 SYSTEMS ANALYSIS

Includes mathematical modeling; network analysis; and operations research.

N89-13222# Science Applications International Corp., Billerica, Mass.
ADAPTIVE MACHINE VISION Annual Report
William W. Stoner, Michael H. Brill, and Doreen W. Bergeron 8 Mar. 1988 91 p
(Contract N00014-86-C-0601)
(AD-A197039) Avail: NTIS HC A05/MF A01 CSCL 14D

The mission of the Strategic Defense Initiative is to develop defenses against threatening ballistic missiles. There are four distinct phases to the SDI defense; boost, post boost, midcourse and terminal. In each of these phases, one or more machine vision functions are required, such as pattern recognition, stereo image fusion, clutter rejection and discrimination. In this document the SDI missions of coarse track, stereo track and discrimination are examined from the point of view of a machine vision system. GRA

67 THEORETICAL MATHEMATICS

Includes topology and number theory.

No abstracts in this category.

70 PHYSICS (GENERAL)

For precision time and time interval (PTTI) see *35 Instrumentation and Photography;* for geophysics, astrophysics or solar physics see *46 Geophysics, 90 Astrophysics,* or *92 Solar Physics.*

N89-13223# New Mexico Univ., Albuquerque. Student Branch of the American Nuclear Society.
NUCLEAR TECHNOLOGY FOR THE YEAR 2000
1987 112 p Proceedings of the 1987 Western Region American Nuclear Society Student Conference, Albuquerque, N. Mex., 19-21 Mar. 1987
(Contract DE-FG02-85ER-75172)
(DE88-005041; DOE/ER-75172/5; CONF-8703231-Summs)
Avail: NTIS HC A06/MF A01

Topics addressed include: space nuclear power; dosimetry and health physics; nuclear design and thermal hydraulics; nuclear diagnostics; fusion technology and plasma physics; and an overview of chernobyl. For individual titles, see N89-13224 through N89-13231.

N89-13224# New Mexico Univ., Albuquerque.
RADIOISOTOPE SPACE POWER GENERATORS: DESIGN CONCEPTS **c73**
Tina Forsman and George Simion *In its* Nuclear Technology for the Year 2000 1987 p 7-1 (For primary document see N89-13223 04-70)
Avail: NTIS HC A06/MF A01

The use of radioisotope power systems for space applications was a key part of some of the most ambitious astronautical undertakings of the United States. Nuclear power sources have provided the electrical energy for the NASA Pioneer, Viking, and Voyager missions as well as earlier earth orbital and Apollo missions. Recently developed, radioisotope thermoelectric generators (RTGs) will be used in future space missions, such as the Galileo Project (Jupiter study) and the International Solar Polar Mission. Present design concepts of RTGs and related dynamic isotope power systems (DIPS) are surveyed. Author

N89-13225# New Mexico Univ., Albuquerque.
DOWN SCALE OF THE SP-100 CONCEPT FOR 5 kWe **c73**
Brad Evans and William Schueler *In its* Nuclear Technology for the Year 2000 1987 p 13-17 (For primary document see N89-13223 04-70)
Avail: NTIS HC A06/MF A01

The feasibility of using a SP-100 thermoelectric space reactor design as a 5 kWe power source, called the SP-5, was examined. The SP-100 is scaled down in size to give a high specific power by using the neutronics program FEMP2D. Possible future space missions may require a power source able to provide 5 kWe of power. There is an interest in using nuclear reactors in place of Radioactive Thermoelectric Generators (RTGs) for this low power demand because of the possibility of spreading toxic plutonium by the heat source if there was a launch accident. The SP-5 design will be compared to the RTGs on the basis of specific power, safety, and reliability. The reactor studied is the lithium cooled SP-100. The core was reduced in size by using the neutronics program FEMP2D. A reactor was designed that is 35 cm high and 15.2 cm in radius. The shield mass is as high as 270 kg and to cool the reactor a radiator with a surface area of 5 square meters (50 kg) is required. This gives a total specific power of 8 We/kg. Author

N89-13226# New Mexico Univ., Albuquerque.
THE 5 kWe SCALE-DOWN OF THE SPAR/SP-100 HEAT PIPE REACTOR **c73**
John M. Adrian and Steven M. Benke *In its* Nuclear Technology for the Year 2000 1987 p 18-23 (For primary document see N89-13223 04-70)
Avail: NTIS HC A06/MF A01

The SPAR/SP-100 heat pipe reactor was designed to operate at 100 kWe. Work done on a 5 kWe scaled-down version of the SPAR/SP-100 is presented. This scale-down was done in order to compare the performance of a small heat pipe reactor to Radioisotope Thermoelectric Generators (RTGs). The work on this design is broken into the following categories: reactor core modeling, control drum modeling, heat rejection modeling, and shadow shield modeling. The reactor core modeling will be completed using the already available computer programs FEMP2D and ORIGEN. The REMP2D will be used to complete the neutronics survey through the core and control drums and it will also be used to ensure the core will be subcritical in case of a water abort. Another safety aspect that will be investigated using FEMP2D is ensuring that a fuel element remains subcritical in the event of reactor break-up during reentry. The ORIGEN wil be used to check the burn-up characteristics of the core design. The reactor control drums will be modeled using a FORTRAN program in order to provide atom density information for use in FEMP2D. The heat rejection system will be modeled in order to determine weight requirements of the radiator. The shadow shield model will also provide information on the weight requirements of the shield with respect to the reactor size. The data obtained from the different categories wil be used to compare the performance of a small heat pipe reactor to the RTG. Comparisons will be made in the following areas: specific power, operating characteristics, and safety. Author

N89-13227*# Oregon State Univ., Corvallis.
SPACE REACTOR ASSESSMENT AND VALIDATION STUDY
Abstract Only **c73**
Stephen Gedeon and Dennis Morey *In* New Mexico Univ., Nuclear Technology for the Year 2000 1987 p 24 (For primary document see N89-13223 04-70)
(Grant NAG3-752)
Avail: NTIS HC A06/MF A01

The present difficulties experienced by the United States in launching payloads into space has suggested a number of problems which are associated with the handling of hazardous materials in spacecraft. The question has arisen as to the safety of launching highly radioactive material such as plutonium-238, related to the possibility of its dispersion into the atmosphere during a launch vehicle explosion. An alternative is the use of a small nuclear reactor which is not started until it is in space and contains little or no radioactivity at launch. A first order assessment of six small reactor concepts with power levels up to 100 MWe was performed. Both the nuclear feasibility of these concepts to operate at their rated power levels between 7 and 10 years and the capability of these concepts to remain subcritical both before and during launch and also in the case of water immersion during a potential launch failure or abort were investigated. Author

N89-13228# Idaho State Univ., Pocatello.
EVALUATION OF BORON CARBIDE COATINGS **c27**
David Levinskas *In* New Mexico Univ., Nuclear Technology for the Year 2000 1987 p 68-71 (For primary document see N89-13223 04-70)
Avail: NTIS HC A06/MF A01

A method of depositing pure boron carbide directly onto various metal surfaces was recently developed. The coating may provide design engineers with a material form for criticality control in spent fuel shipping casks and storage pools. The AGN-201 reactor at the Idaho State University was used to determine the neutron attenuation characteristics of boron carbide applied as a thin coating over a metal surface. Initial results indicate that boron carbide coatings as thin as 0.040 inches will attenuate 90 percent of an incident thermal neutron beam. The neutron attenuation experiment and resulting data are described. The coating density, calculated from the data obtained in the attenuation experiment, is compared to the density given for boron carbide in standard references. The advantages of directly coating structural materials as a means of achieving criticality control, instead of the current practice of using boron loaded aluminum plates, are examined. The possibility of using boron carbide coatings in a number of nuclear applications are suggested. Author

N89-13229# Arizona State Univ., Tempe. Dept. of Electrical Engineering.
LASER DRIVEN INERTIAL CONFINEMENT FUSION **c75**
William Derks *In* New Mexico Univ., Nuclear Technology for the Year 2000 1987 p 97-99 (For primary document see N89-13223 04-70)
Avail: NTIS HC A06/MF A01

Mechanics, design requirements, and recent developments of the three major components used in laser driven inertial confinement fusion reactors are examined. These components are the laser, the fuel pellet, and the blast chamber. The objective is to provide a general feasibility study on this specific approach to fusion power production. A general overview is given of the basic operations, nuclear physics, fuel pellet fabrication, pellet injection, fuel pellet density, laser power requirements and pulse length, different reactor cavity designs, and blast chamber protection with a lithium blanket. Author

N89-13230# Washington Univ., Seattle.
FIREBIRD: A CONCEPTUAL DESIGN OF A FIELD REVERSED CONFIGURATION COMPACT TORUS FUSION REACTOR (CTFR) **c75**
Roger Raman and Robert M. Zubrin *In* New Mexico Univ., Nuclear Technology for the Year 2000 1987 p 100-104 (For primary document see N89-13223 04-70)
Avail: NTIS HC A06/MF A01

Work carried out by the Nuclear Engineering 512 design team at the University of Washington on a conceptual design study of a Compact-Torus (field-reverse) Fusion Reactor Configuration (CTFR) is summarized. The primary objective was to develop a reactor design for high engineering power density, modest recirculating power, and competitive cost of electrical power. A conceptual design was developed for a translating field-reversed configuration reactor; based on the physics developed by Tuszewski and Lindford at LANL and by Hoffman and Milroy at MSNW. Furthermore, it also appears possible to operate a simplified form of this reactor using a pure D-D fuel cycle after an initial D-T ignition ramp to reach the advanced fuel operating regime. One optimistic reactor so designed has a length of about 35 meters, producing a net electrical power of about 375 MWe. Author

N89-13231# New Mexico Univ., Albuquerque.
TESLA'S COHERENT PLASMA DISCHARGE AND A PLAN FOR MEGAVOLTS AT MEGAHERTZ
James D. Nichson *In its* Nuclear Technology for the Year 2000 1987 p 105-107 (For primary document see N89-13223 04-70)
Avail: NTIS HC A06/MF A01

In the lecture on Experiments With Alternative Currents of High Potential and High Frequency before the Institute of Electircal Engineers in London (1892), Tesla reports a discharge through a partially evacuated air tube of 1 meter length and 1 inch diameter. It is characterized by the following properties. The filamentary discharge may be locally displaced by a nearby dielectric body or a magnet. When the filament is released, it demonstrates behavior similar to that of a string which suspends a weight, including the formation of standing waves with distinct nodes. Its decay time is on the order of 8 minutes. The vibrating filament may be split with a magnet to produce two vibrating filaments. This effect could only be formed with a dynamo-driven coil at low air pressures in the tube. The disruptive discharge coil failed to produce the effect with its superior voltage and frequency range. It is proposed that this phenomenon is related to positive leader formation. A model for this, consistent for ac and dc discharges, is advanced. Also, a method for regulation of a nitrogen-filled spark gap will be proposed. It is hoped that this device will produce smooth, uniform discharges from the Tesla coil. This, if the theory is correct on many points, will reproduce Tesla's coherent plasma at higher pressures in free-standing form, and will allow other effects. Author

71 ACOUSTICS

Includes sound generation, transmission and attenuation. For noise pollution see *45 Environmental Pollution.*

N89-13232 Virginia Polytechnic Inst. and State Univ., Blacksburg.
A STUDY OF ACTIVE CONTROL TECHNIQUES FOR NOISE REDUCTION IN AN AIRCRAFT FUSELAGE MODEL Ph.D. Thesis
James D. Jones 1987 302 p
Avail: Univ. Microfilms Order No. DA8804408

A simplified cylindrical model is used to investigate the elementary mechanisms of control of sound transmission into aircraft cabins by two active control techniques: propeller synchrophasing and active vibration control. Propeller synchrophasing involves controlling the relative rotational phase of the engines to achieve maximum cabin noise reduction. Active vibration control involves structurally controlling the vibrational response of the cabin wall to reduce the important modes which transmit their energy into the cabin. Noise reductions for harmonic excitation at acoustic cavity resonance are shown to be in excess of 20 dB throughout most of the cavity whether synchrophasing or active vibration control is used. Off-resonance reductions are substantially less due to increase modal density requiring a larger number of actuators for effective control of the complex sound fields. Additional studies were performed using synchrophasing in conjunction with active vibration control to study their joint capabilities in controlling complex sound fields. The dual control system displayed improved control performance with noise reductions on the order of 25 to 35 dB and a more uniform sound field. An independent study was performed to identify the effects of a complex geometry on sound transmission into an aircraft fuselage model interior. This investigation identified the fundamental mechanisms of control of sound transmission into simplified models of aircraft fuselages by active control techniques. Dissert. Abstr.

N89-13233# Brown Univ., Providence, R. I. Dept. of Physics.
SURFACES AND THIN FILMS STUDIED BY PICOSECOND ULTRASONICS Annual Progress Report, 1 Dec. 1987 - 30 Nov. 1988
H. J. Maris and J. Tauc 1988 5 p
(Contract DE-FG02-86ER-45267)
(DE88-015268; DOE/ER-45267/2) Avail: NTIS HC A02/MF A01

The research is in two related areas. The first is the development of the techniques of picosecond ultrasonics and the practical application of these techniques to the non-destructive study of thin film structures. The second area is the study using this technique of fundamental problems in ultrasonics and lattice dynamics. We have completed our study of the vibrational normal modes Ge:Si multilayer structures, including a theoretical investigation of the conditions under which surface modes occur in such structures. We have continued our experimental study of the Kapitza resistance and its temperature dependence, and have compared experimental results with a theoretical calculation. We have used the picosecond ultrasonic technique to measure the sound velocity and refractive index of AlAs, and we have studied the sound velocity in a series of silicon oxynitride films of varying composition. DOE

N89-13234# Naval Underwater Systems Center, New London, Conn. Environmental and Tactical Support Systems Dept.
NEARFIELD ACOUSTIC RADIATION FROM A POINT-EXCITED CYLINDRICAL SHELL Ph.D. Thesis
Richard D. Vogelsong 26 May 1988 223 p
(AD-A197282; NUSC-TD-8043) Avail: NTIS HC A10/MF A01 CSCL 20A

The surface force exerted by a dense medium such as water upon an elastic structure undergoing dynamic motion is often comparable to the inertial and damping forces found within the structure. Fluid loading may alter the structural response by strongly coupling the elastic and acoustic media. Any attempt to locally deform the structure may lead to a slowly decaying pressure field that excites the elastic structure further away. In this study, the acoustic nearfield and radial surface deformation of a cylindrical shell of infinite axial extent is examined. The shell is subject to external fluid loading and is excited by a radically acting, time harmonic point force. The shell is modeled using Flugge's thin shell theory. Eigenfunction and integral transform methods are used to formulate the shell's radial deformation and the radiated acoustic pressure in terms of an infinite Fourier series of inverse transform integrals. The inverse transform integrals are solved by Cauchy's theorem. In the acoustic nearfield and at frequencies below the classical plate coincidence frequency, the solutions are shown to be dependent only upon the residue contribution of a single real singularity at each of a small number of modes. Strong acoustical coupling exists between the driving-point excitation and the acoustic nearfield. GRA

N89-13235# Naval Research Lab., Washington, D.C.
ON THE SIMULATION OF HARMONICALLY RELATED SIGNALS Interim Report
Albert A. Gerlach, Edward L. Kunz, Wendell L. Anderson, and Kenneth D. Flowers 27 Jun. 1988 14 p
(AD-A197821; NRL-9125) Avail: NTIS HC A03/MF A01 CSCL 12E

Narrowband harmonically related signals, embedded in broadband noise and other unrelated signals, occur in specific applications. To study these signals and to evaluate techniques for their discernment, it is convenient to model or simulate harmonically related signals in the laboratory. A means of accomplishing this task on a conventional digital computer is developed in discrete algorithm format. The resulting simulator uses parameters that allow one to select the mean frequency and harmonic ratio of the signals and to control both the extent and autocorrelation (or power spectral density) of the random signal-frequency fluctuations. Broadband noise and other nonharmonically related signals may also be accommodated in the simulator concept. Examples, using the algorithm, demonstrate its performance and its conformance with theoretical predictions. Conclusions: A relatively simple algorithm is formulated to simulate harmonically related narrowband signals with random frequency fluctuations in discrete format on a digital computer. Signal parameters are incorporated into the algorithm to select the signal

mean frequencies and to control both the spectral bounds and the autocorrelation (or power spectral density) of the signal fluctuations. Examples, using the algorithm, demonstrate the performance of the signal simulator and its conformance with theoretical predictions. GRA

N89-13236* National Aeronautics and Space Administration. Pasadena Office, Calif.
STABILIZATION AND OSCILLATION OF AN ACOUSTICALLY LEVITATED OBJECT Patent
Martin B. Barmatz, inventor (to NASA) and Steven L. Garrett, inventor (to NASA) (Jet Propulsion Lab., California Inst. of Tech., Pasadena.) 27 Sep. 1988 12 p
(NASA-Case-NPO-16896-1-CU; US-Patent-4,773,266; US-Patent-Appl-SN-087283; US-Patent-Class-73-505) Avail: US Patent and Trademark Office CSCL 20A

Methods are described for rapidly damping oscillation of an acoustically levitated object or for causing and maintaining such oscillations, and a method is provided for determining the restoring force constant K on the levitated object by measuring its frequency of oscillation. Oscillations of a levitated object are damped by applying levitating acoustic energy at a frequency slightly less than the center resonant frequency. Oscillations are maintained by applying acoustic energy slightly greater than the center resonant frequency. The restoring force constant of the levitation force is proportional to the square of the frequency of oscillation of the object. Official Gazette of the U.S. Patent and Trademark Office

N89-12597*# Tenney Engineering, Inc.
SPACE SIMULATORS FOR LASER OPTICS
Frank H. Gardner *In* NASA, Goddard Space Flight Center, 15th Space Simulation Conference: Support the Highway to Space Through Testing 1988 p 179-186 (For primary document see N89-12582 04-18)
Avail: NTIS HC A21/MF A01 CSCL 20F

N89-12764# Ohio Univ., Lancaster. Dept. of Psychology.
THE EFFECTS OF HIGH NOISE LEVELS ON THE ACOUSTIC-PHONETIC STRUCTURE OF SPEECH: A PRELIMINARY INVESTIGATION
Beverley A. Gable *In* Universal Energy Systems, Inc., United States Air Force Graduate Student Summer Support Program, Volume 1 Dec. 1987 20 p (For primary document see N89-12754 04-31)
Avail: NTIS HC A99/MF E03 CSCL 20A

72 ATOMIC AND MOLECULAR PHYSICS

Includes atomic structure, electron properties, and molecular spectra.

N89-13237# Tokyo Univ. (Japan). Inst. of Space and Astronautical Science.
DIFFERENTIAL CROSS SECTIONS FOR ELECTRON-IMPACT EXCITATION OF ATOMIC IONS
Yukikazu Itikawa and Kazuhiro Sakimoto Jul. 1987 28 p Presented at the UK-Japan Seminar on the Theory of Atomic Collisions, Royal Holloway and Bedford New College, 3-6 Aug. 1987
(ISAS-RN-365) Avail: NTIS HC A03/MF A01

In the study of electron collision with neutral atoms and molecules, it is customary to calculate differential cross sections (DCS) when a comparison is made between theory and experiment or between different theories. In the case of electron-ion collisions, on the other hand, a very limited number of papers have reported DCS. It is difficult to obtain DCS experimentally for electron-ion collisions, though a few attempts have been made. The DCS, however, is valuable in getting insight into the physical mechanism of the collision process. Furthermore, differences in theoretical approximation can be seen easily in DCS. Consequently, a systematic study of DCS for the electron-impact excitation of atomic ions has begun. The excitation cross section is calculated by the distorted-wave method (called DWXA). For a comparison, the Coulomb-Born-type calculation is also done in some cases. These methods are rather easily adapted to a systematic study. In the future more elaborate calculations (e.g., the close-coupling one) would be carried out to compare with the present approximate methods. As the first example of the study, He-like ions are chosen as a target and preliminary results of their DCS are given.
Author

N89-13238# Auburn Univ., Ala. Dept. of Physics.
ELECTRON-IMPACT IONIZATION OF HEAVY ATOMIC IONS
M. S. Pindzola, D. C. Griffin, and C. Bottcher (Oak Ridge National Lab., Tenn.) 1987 8 p Presented at the 15th International Conference on the Physics of Electronic and Atomic Collisions, Brighton, England, 22 Jul. 1987 Prepared in cooperation with Rollins Coll., Winter Park, Fl.; Oak Ridge National Lab., Tenn.
(Contract DE-AC05-84OR-21400)
(DE88-008371; CONF-870715-9) Avail: NTIS HC A02/MF A01

General theoretical methods for the calculation of direct and indirect processes in the electron-impact ionization of heavy atomic ions are reviewed. Cross section results for Xe (8+) and U (89+) are presented. DOE

N89-13239# Iowa Univ., Iowa City.
DETERMINATION OF STEPSIZE PARAMETERS FOR INTERMOLECULAR VIBRATIONAL ENERGY TRANSFER Progress Report, 1 May 1987 - 30 Apr. 1988
D. C. Tardy May 1988 18 p
(Contract DE-FG02-87ER-13700)
(DE88-010904; DOE/ER-13700/1) Avail: NTIS HC A03/MF A01

Intermolecular vibrational energy transfer for highly excited polyatomic molecules is involved in any mechanism in which excitation energy is required (pyrolysis) or in which energy must be removed from a hot source (cooling). The average energy removed per collision, (DELTA E), is a useful quantity to compare efficiency for energy transfer. The objectives of this work are: to determine the dependence of (DELTA E) on excitation energy and on the molecular complexity (number of vibrational modes) of substrate and deactivator; to assess the importance of intermolecular attractions (complex formation) on vibrational energy transfer; to obtain detailed information on the energy distribution after collision and to evaluate the importance of (DELTA E) on high-temperature unimolecular reactions. This information will be obtained by monitoring the time dependence of the infrared emission, ultraviolet absorption, refractive index and pressure. The results from these complementary techniques will be benchmarked with (DELTA E) values from previous studies on the relaxation of chemically activated alkyl and fluoroalkyl radicals. Trajectory calculations simulating energy transfer are being performed for generic substrate/deactivator pairs to provide additional details and insight on the important parameters. Model calculations are also being performed to determine the feasibility of obtaining (DELTA E) information from experimental data for high-temperature uhimolecular reactions. DOE

N89-13240*# Arizona Univ., Tucson. Dept. of Physics.
HOLOGRAPHIC PARTICLE DETECTION Semiannual Progress Report, 1 Feb. - 31 Jul. 1988
Theodore Bowen 31 Jul. 1988 15 p
(Grant NAG5-831)
(NASA-CR-183315; NAS 1.26:183315) Avail: NTIS HC A03/MF A01 CSCL 20H

The feasibility was studied of developing a novel particle track detector based on the detection of 1p-1s emission radiation from electron bubbles in liquid helium. The principles, design, construction, and initial testing of the detection system have been described in previous reports. The main obstacle encountered was the construction of the liquid-helium tight infrared windows. Despite numerous efforts in testing and redesigning the windows, the problem of window leakage at low temperature persisted. Due to limited time and resources, attention was switched to investigating the possibility of using room-temperature liquid as the detection

medium. A possible mechanism was the detection of de-excitation radiation emitted from localized electrons in common liquids where electrons exhibit low mobilities, as suggested in the previous report. The purity of the liquid is critical in this method as the dissolved impurities (such as oxygen), even in trace amounts, will act as scavengers of electrons. Another mechanism is discussed whereby the formation of the superoxide ions by electron scavenging behavior of dissolved oxygen is exploited to detect the track of ionizing particles. An experiment to measure the ionization current produced in a liquid by a pulsed X-ray beam in order to study propertiies of the ions is also reported. Author

N89-13241# State Univ. of New York, Buffalo. Dept. of Chemistry.
LARGE SILICON CLUSTERS: CONFIRMATION OF PHILLIPS' CONJECTURE
Daniel A. Jelski, Z. C. Wu, and Thomas F. George Jul. 1988 30 p
(Contract N00014-86-K-0043)
(AD-A197487; UBUFFALO/DC/88/TR-78) Avail: NTIS HC A03/MF A01 CSCL 20H

This paper attempts to verify the hypothesis put forward by Phillips that large silicon clusters are arranged in a cylindrical shape, as stacked quasigraphitic rings. It is shown that the periodic variations in reactivity can probably be explained by this hypothesis. A tight-binding calculation is employed, and the geometry and charge distribution of clusters ranging in size from 30 to 45 atoms is explored. GRA

N89-13242# Texas Univ., Arlington. Center for Accelerator Science and Technology.
INVESTIGATION OF ACCELERATION AND DENSIFICATION OF ELECTRONS UTILIZING TRAVELLING MAGNETIC WAVES Final Report, 30 Sep. 1983 - 31 Oct. 1987
K. W. Chen and S. H. Kim 19 Apr. 1988 20 p
(Grant AF-AFOSR-0368-83; AF Proj. 2301)
(AD-A197700; AFOSR-88-0706TR) Avail: NTIS HC A03/MF A01 CSCL 20G

Experimental investigation of electron beam physics: naturally occurring and externally driven low frequency (6 to 500 KHz) diocotron oscillations are observed and the m = 1 rotating structure of these oscillations are measured by using electrostatic probes. Systematic analysis of the circuit system for the generation of a fast-rising pinching magnetic field: a circuit consisted of distributed circuit (transmission line) part and lumped circuit parts included a coil are systematically analyzed from the first principles of circuit. Computer code to calculate expediently the temporal profile of the pinching magnetic is developed. Theoretical study of acceleration of high-energy electron beams by a laser-light through net inverse bremsstrahlung in plasma fields: the absorption of the incident laser photons by net inverse bremsstrahlung can give rise to the dc ponderomotive force whose strength is far greater than the amplitude of the Lorentz force of the laser wave. Study of a soft X-ray free electron laser (FEL) scheme using a two-beam elliptical pill-box wake-field cavity: it is found that the scheme provides sufficient gain as a coherent radiation source down to the X-ray regime. Wake field acceleration research: the theoretical result from the modal analysis developed here agrees with the recent experiment in both profile (shape) and magnitude of the wake potential. GRA

N89-13243# Consiglio Nazionale delle Ricerche, Frascati (Italy). Istituto di Fisica dello Spazio Interplanetario.
NEUTRON FLUX MEASUREMENTS IN THE GRAN SASSO UNDERGROUND LABORATORY (ITALY) (PART 2)
G. Villoresi, N. Iucci, R. Bernabei, S. DAngelo, L. Paoluzi, R. Santonico, F. Re, M. P. DePascale, and N. Taborgna (Istituto Nazionale di Fisica Nucleare, Rome, Italy) Jun. 1988 14 p
(IFSI-88-7; ETN-88-93474) Avail: NTIS HC A03/MF A01

Measurements of the neutron flux were done, where the thermal neutron flux and the upper limit of the neutron energy are estimated. The 5 large cylindrical BE3 proportional counters were arranged not only in a vertical plane, but also in a horizontal plane in order to reveal a possible anisotropy in the high-energy neutron flux. ESA

N89-13244# Technical Research Centre of Finland, Espoo. Instrument Lab.
COLLOID VIBRATION POTENTIALS
Auvo Penttinen, Matti Ryynaenen, Vaeinoe Kelhae, Allan Johansson, and Vesa Arpiainen May 1988 46 p In FINNISH; ENGLISH summary
(VTT-RR-535; ISBN-9-51-383158-2; ISSN-0358-5077; ETN-88-93532) Copyright Avail: NTIS HC A03/MF A01; Technical Research Centre of Finland, Vuorimiehentie 5, SF-02150, Finland, 85 Finnish marks

The so called Zeta potential is used to describe the electrical potential at the particle surface. The origin of the electrical double layer and Zeta potential is described. The charge distributions associated with this double layer were distorted using ultrasonic waves, which resulted in measurable vibration potentials. A theory of vibration potentials is derived and its dependence on the number of colloidal particles and the electrolyte concentration is given. Results on colloidal systems in various electrolytes are also given. ESA

73 NUCLEAR AND HIGH-ENERGY PHYSICS

Includes elementary and nuclear particles; and reactor theory.

For space radiation see *93 Space Radiation.*

N89-13245# Continuous Electron Beam Accelerator Facility, Newport New, Va.
COMMENTS ON THE HIGH FREQUENCY BEHAVIOR OF THE COUPLING OF AN ACCELERATOR BEAM TO ITS ENVIRONMENT
Joseph J. Bisognano [1988] 17 p
(Contract DE-AC05-84ER-40150)
(CEBAF-PR-88-006) Avail: NTIS HC A03/MF A01

The short bunch lengths and the associated high frequencies found in the latest designs of linear colliders, superconducting linacs, FEL drivers, damping rings, and synchrotron light sources increase the importance of understanding the high-frequency behavior of the interaction of an accelerator beam with its environment. This parametric domain is at the limits of both the numerical and analytical tools which have been developed to date, and consequently there is some question as to the correct asymptotic frequency dependence. The resulting uncertainty in the coupling of a particle beam to vacuum chamber discontinuities hinders evaluation of bunch lengthening in storage rings and transverse beam blowup in linacs, and limits confidence in assessments of beam quality in proposed designs. Another high-frequency phenomenon, of particular concern in damping and storage rings, is the synchrotron radiation process in the presence of conductive boundaries. Estimates indicate that this effect can provide the dominant limit on peak beam current in small, smooth-walled machines, but earlier work does not take into account fully the complex, finite-Q resonance structure which is present. The charge to the August 1987 Impedance Beyond cutoff Workshop at Lawrence Berkeley Laboratory was to investigate these issues in depth and to provide clarification of the main features of the beam coupling impedance at frequencies well above the lowest propagation frequency of the beam pipe. Workshop results are given. Author

N89-13246# Sandia National Labs., Albuquerque, N. Mex.
A RADIO-FREQUENCY QUADRUPOLE ACCELERATOR LONGITUDINAL FIELD STABILIZER
E. R. Gray, G. Spalek, and A. Shapiro 1988 25 p Presented at the Linear Accelerator Conference, Williamsburg, Va., 3 Oct. 1988

(Contract W-7405-eng-48)
(DE88-014399; LA-UR-88-2465; CONF-881049-1) Avail: NTIS HC A03/MF A01

The fields in a 600-MHz model of a radio-frequency quadrupole (RFQ) accelerator have been longitudinally stabilized over 86 percent of its length. The stabilizing elements consist of four external transverse electromagnetic (TEM) lines. Each line is coupled to the RFQ by two magnetic loops attached to voltage maxima of the TEM line. These resonant lines stabilize the RFQ fields by providing an alternate longitudinal power flow path in the RFQ. Stabilization depends on the TEM line Q and the TEM line RFQ coupling. Each stabilizer coupling-loop location in the RFQ needs to be fully azimuthally stabilized. Substantial coupling between stabilizer elements destroys stabilization. DOE

N89-13247# Brookhaven National Lab., Upton, N. Y. National Synchrotron Light Source.
DESIGN OF VACUUM CHAMBERS DOWNSTREAM OF NSLS X-RAY RING INSERTION DEVICES
J. C. Schuchman and S. Sharma 1988 7 p Presented at the Topical Conference on Vacuum Design of Advanced and Compact Synchrotron Light Sources, Upton, N.Y., 16 May 1988
(Contract DE-AC02-76CH-00016)
(DE88-015715; BNL-41555; CONF-880552-6) Avail: NTIS HC A02/MF A01

In an electron storage ring the maximum power deposited in the vacuum chamber walls is that produced by the electron beam as it is accelerated through the bending magnets. In the NSLS X-ray ring this power is 58 watts per linear cm of arc chamber length, or 2 kw/sq cm taking into account the beam size. Standard water cooling techniques are adequate to protect the chambers from overheating under this range of power density. However, with the installation of wigglers and undulators, cooling of the chambers is no longer a trivial matter. Without proper interlocks and cooling, beams from these insertion devices can easily do permanent thermal damage to the chamber walls. As part of the NSLS Phase 2 project three insertion devices are planned for the beamlines X-1, X-17 and X-25, namely, a soft X-ray undulator, a superconducting wiggler and a hybrid wiggler. The effect of these insertion devices on the design of vacuum chambers downstream of these devices is the subject of this paper. DOE

N89-13224# New Mexico Univ., Albuquerque.
RADIOISOTOPE SPACE POWER GENERATORS: DESIGN CONCEPTS
Tina Forsman and George Simion *In its* Nuclear Technology for the Year 2000 1987 p 7-1 (For primary document see N89-13223 04-70)
Avail: NTIS HC A06/MF A01

N89-13225# New Mexico Univ., Albuquerque.
DOWN SCALE OF THE SP-100 CONCEPT FOR 5 kWe
Brad Evans and William Schueler *In its* Nuclear Technology for the Year 2000 1987 p 13-17 (For primary document see N89-13223 04-70)
Avail: NTIS HC A06/MF A01

N89-13226# New Mexico Univ., Albuquerque.
THE 5 kWe SCALE-DOWN OF THE SPAR/SP-100 HEAT PIPE REACTOR
John M. Adrian and Steven M. Benke *In its* Nuclear Technology for the Year 2000 1987 p 18-23 (For primary document see N89-13223 04-70)
Avail: NTIS HC A06/MF A01

N89-13227*# Oregon State Univ., Corvallis.
SPACE REACTOR ASSESSMENT AND VALIDATION STUDY Abstract Only
Stephen Gedeon and Dennis Morey *In* New Mexico Univ., Nuclear Technology for the Year 2000 1987 p 24 (For primary document see N89-13223 04-70)
(Grant NAG3-752)
Avail: NTIS HC A06/MF A01

74 OPTICS

Includes light phenomena; and optical devices.
For lasers see *36 Lasers and Masers.*

N89-13248 Arizona Univ., Tucson.
PHASE MEASUREMENT ACCURACY LIMITATION IN PHASE SHIFTING INTERFEROMETRY Ph.D. Thesis
Chiayu Ai 1987 146 p
Avail: Univ. Microfilms Order No. DA8804161

In phase shift interferometry (PSI), several factors affect measurement accuracy, such as piezoelectric transducer (PZT) calibration and PZT nonlinearity, vibration, spurious reflection, source bandwidth, detector nonlinearity, and detector noise. The effects of these error sources on several algorithms to solve the phase of the wavefront are studied. Dissert. Abstr.

N89-13249*# California Univ., Berkeley. Space Sciences Lab.
DEVELOPMENT OF HIGH EFFICIENCY OPAQUE PHOTOCATHODES FOR THE REGION 900 ANGSTROM TO 1200 ANGSTROM Final Status Report
M. Lampton and O. Siegmund 1988 9 p
(Grant NAG5-1007)
(NASA-CR-180597; NAS 1.26:180597) Avail: NTIS HC A02/MF A01 CSCL 20F

Progress in the following three areas is reported: investigation of the basic properties of candidate photocathode materials; measurement of the quantum detection efficiency (QDE) of KCl, RbBr, and CsBr as a function of wavelength and incident angle; and assessment of the stability of these photocathodes. Author

N89-13250# Air Force Systems Command, Wright-Patterson AFB, Ohio. Foreign Technology Div.
THE 6TH ALL-UNION CONFERENCE ON NONLINEAR OPTICS (TABLE OF CONTENTS)
15 Jun. 1988 5 p Transl. into ENGLISH from Zhurnal Prikladnoy Spektroskopii (USSR), v. 17, no. 5, Nov. 1972 p 269-261 Conference held in Minsk (USSR), 27 Jun. - 1 Jul. 1972
(AD-A197347; FTD-ID(RS)T-0463-88) Avail: NTIS HC A02/MF A01 CSCL 20F

The self reaction of light waves; nonlinear processes in crystals; nonlinear spectroscopy; general questions of the interactions of radiation with matter; lasers on organic compounds; resonance nonlinear effects; the optics of ultra short pulses; instruments based on nonlinear effects; the generation of optical harmonics; forced scattering; nonlinear effects of atoms and molecules; and the nonlinear optics of semiconductors are discussed. GRA

N89-13251# Johns Hopkins Univ., Laurel, Md. Applied Physics Lab.
SURVEY OF IMAGE RESTORATION TECHNIQUES Technical Memo, Apr. - Aug. 1986
P. K. Murphy Jul. 1988 32 p
(Contract N00039-87-C-5301)
(AD-A197470; JHU/APL/TG-1368) Avail: NTIS HC A03/MF A01 CSCL 17E

This survey of image restoration techniques presents a concise overview of the most useful restoration methods. Linear spatially invariant and linear spatially variant image restoration techniques are described and the strengths and weaknesses of each approach are identified. Examples of restored images for the various techniques are given. To provide guidelines for choosing a restoration technique for a particular application, a comparison of the techniques is made. The restoration methods are compared and evaluated based on the following circuit: restored image visual quality, performance in the presence of additive image-independent noise, degree of a priori knowledge required, and computational complexity. GRA

N89-13252# Honeywell, Inc., Bloomington, Minn. Sensors and Signal Processing Lab.
OPTICAL SYMBOLIC PROCESSOR FOR EXPERT SYSTEM EXECUTION Annual Technical Report, 1 Jun. 1987 - 31 May 1988

Aloke Guha, Julian Bristow, and Subra Natarajan 31 May 1988 102 p
(Contract F49620-86-C-0082; ARPA Order 5794)
(AD-A197668; AFOSR-88-0735TR) Avail: NTIS HC A06/MF A01 CSCL 12F

A detailed performance evaluation was begun for our optical architecture, SPARO, for combinator graph reduction. Since the interconnection network was the bottleneck in the performance of the architecture, the focus was on the message throughput of the simple register-based network. An accurate performance model was derived for the equivalent bidirectional ring network and found, both by analysis and simulation, that the net parallelism in the architecture was restricted by the low message traffic in the network. When messages exhibited no locality, the throughput for a 1024 processor network was limited to 8. With local messages, the maximum throughput for the same network was 27. GRA

N89-13253*# National Aeronautics and Space Administration. Marshall Space Flight Center, Huntsville, Ala.
A REFERENCE STANDARD FOR BIDIRECTIONAL REFLECTION DISTRIBUTION FUNCTION AND BIDIRECTIONAL TRANSMISSION DISTRIBUTION FUNCTION MEASUREMENT Patent Application
William K. Witherow, inventor (to NASA) 15 Sep. 1988 15 p
(NASA-Case-MFS-28183-1; NAS 1.71:MFS-28183-1; US-Patent-Appl-SN-244367) Avail: NTIS HC A03/MF A01 CSCL 20F

A Lambertian reference standard for uniformly scattering a beam of light is constructed of a plate having a planar surface with a layer of glue disposed on the surface. An evenly packed layer of monodisperse spheres is set in the layer, and when the standard is used for bi-directional (BRDF) measurements, the spheres are coated with a layer of highly relective substance, such as gold or silver. When the standard is used for bi-directional transmittance distribution function (BTDF) measurements, the spheres are of a transparent material and are provided with a roughened surface, as by acid etching. In this case, the layer of glue is an optical cement, and the plate is of glass, with the spheres, the layer, and the plate all possessing a similar refractive index. NASA

N89-13254# Lawrence Livermore National Lab., Calif.
TIME-RESOLVED SOLID-STATE ARRAY IMAGING SYSTEMS: DEVELOPMENTS AND APPLICATIONS
H. A. Koehler 1 Aug. 1988 17 p Presented at the 18th International Congress on High-Speed Photography and Photonics, Xian, China, 28 Aug. 1988
(Contract W-7405-eng-48)
(DE88-016274; UCRL-98606; CONF-8808103-2) Avail: NTIS HC A03/MF A01

Several optical, single transient data imaging systems have been developed at the Lawrence Livermore National Laboratory for providing time-, space-, and intensity information of pulsed radiation sources. The basic components of these systems are fast-gated cameras, large-bandwidth transmission lines, large memories, and image processors. Several methods are currently investigated to: (1) produce faster optical gates without significant irising or reduction in resolution, and (2) to improve spatial resolution. Both photodiode arrays and charge-coupled devices (CCD) are used for the imagers in the solid-state cameras. These cameras are designed to achieve a large dynamic range (500:1), low saturation fluence (less than or equal to 1.5 erg/ sq cm at 420 nm), and small frame time (less than or equal to 2.5 msec). Current investigations are concentrating on large segmented (512 x 512) photodiode arrays with CCD readout. All cameras are designed for fiber-optic or lens coupling. Maximum dynamic range and maximum signal-to-noise is achieved by using 8-, 10-, or 12-bit A/D converters. A technique known as data compression is applied to take advantage of a 10-bit system using an 8-bit data acquisition arrangement. The advent of large array cameras requires modifications in calibration procedure, data acquisition, and image processing. DOE

N89-13255# Sandia National Labs., Albuquerque, N. Mex. Photovoltaic Technology Div.
RE-EVALUATION OF AN IMPROVED EFFICIENCY POLYMERIC WEB POINT-FOCUS FRESNEL LENS
Charles B. Stillwell Aug. 1988 18 p
(Contract DE-AC04-76DP-00789)
(DE88-016892; SAND-88-0903) Avail: NTIS HC A03/MF A01

The optical efficiency of the lens developed by 3M and reported in Development and Evaluation of an Improved Efficiency Polymeric Web Point-Focus Fresnel Lens was measured by Sandia and reported to be 82 percent. Subsequent to publication of that report, additional lens tests at Sandia showed a lens efficiency of only 79 percent. This report presents the results of a study to determine why the lens efficiency is now lower than originally observed. DOE

N89-13256*# General Electric Co., Cincinnati, Ohio. Aircraft Engine Business Group.
FIBER OPTIC CONTROL SYSTEM INTEGRATION Final Report
G. L. Poppel, W. M. Glasheen, and J. C. Russell Feb. 1987 72 p
(Contract NAS3-24624)
(NASA-CR-179568; NAS 1.26:179568; R87AEB111) Avail: NTIS HC A04/MF A01 CSCL 20F

A total fiber optic, integrated propulsion/flight control system concept for advanced fighter aircraft is presented. Fiber optic technology pertaining to this system is identified and evaluated for application readiness. A fiber optic sensor vendor survey was completed, and the results are reported. The advantages of centralized/direct architecture are reviewed, and the concept of the protocol branch is explained. Preliminary protocol branch selections are made based on the F-18/F404 application. Concepts for new optical tools are described. Development plans for the optical technology and the described system are included. Author

N89-12775# Texas A&M Univ., College Station. Dept. of Aerospace Engineering.
AN OPTICAL SENSOR SYSTEM FOR MONITORING STRUCTURAL DYNAMICS WITH APPLICATIONS TO SYSTEM IDENTIFICATION Final Report
George Henry James, III *In* Universal Energy Systems, Inc., United States Air Force Graduate Student Summer Support Program, Volume 1 Dec. 1987 20 p (For primary document see N89-12754 04-31)
Avail: NTIS HC A99/MF E03 CSCL 20F

N89-12946# Naval Research Lab., Washington, D.C.
SHADOWS AND WEDGES IN SCATTERING FROM THE SEA
L. B. Wetzel *In* ESA, Proceedings of the 1988 International Geoscience and Remote Sensing Symposium (IGARSS 1988) on Remote Sensing: Moving Towards the 21st Century, Volume 1 Aug. 1988 p 35-38 (For primary document see N89-12936 04-42)
Copyright Avail: NTIS HC A99/MF E03; ESA Publications Div., ESTEC, Noordwijk, Netherlands, 120 US dollars or 250 Dutch guilders

75 PLASMA PHYSICS

Includes magnetohydrodynamics and plasma fusion.

For ionospheric plasmas see *46 Geophysics*. For space plasmas see *90 Astrophysics*.

N89-13257# Air Force Inst. of Tech., Wright-Patterson AFB, Ohio.
SAMPLE INTRODUCTION USING THE HILDEBRAND GRID NEBULIZER FOR PLASMA SPECTROMETRY Ph.D. Thesis
Timothy J. Brotherton 1988 240 p
(AD-A197145; AFIT/CI/NR-88-112) Avail: NTIS HC A11/MF A01 CSCL 07D

The Hildebrand grid nebulizer is evaluated for use with

Inductively Coupled Plasma-Optical Emission Spectrometry (ICP-OES) and Mass Spectrometry (ICP/MS) detection. Limiting aspiration rates for various organic solvents were determined for the grid nebulizer with a mini-pyrex spray chamber, a cooled spray chamber and a conical spray chamber. Detection limits and linear dynamic ranges were determined for various species. Indirect solvent transport efficiencies were determined as a function of spray chamber, flow rate, temperature and solvent. A comparison was made between the grid, cross-flow, concentric and glass frit. Three interfaces for volatile organic solvents used to couple Flow Injection Analysis (FIA) with ICP-OES detection were evaluated. Detection limits, linear dynamic ranges, precision, and peak width were determined for elements in methanol and acetonitrile solutions. GRA

N89-13258# Los Alamos National Lab., N. Mex.
THE NEXT LOGICAL STEP IN LASER-FUSION DEVELOPMENT
C. A. Fenstermacher, D. B. Harris, D. J. Dudziak, T. E. McDonald, and D. C. Cartwright 1988 5 p Presented at the 8th Topical Meeting on Technology of Fusion Energy, Salt Lake City, Utah, 9 Oct. 1988
(Contract W-7405-eng-36)
(DE88-007825; LA-UR-88-981; CONF-881031-1) Avail: NTIS HC A02/MF A01

Present and future facilities for laser produced fusion energy are discussed. Cost and efficiency are the major underlying topics developed. DOE

N89-13259# Los Alamos National Lab., N. Mex.
CONFINEMENT DYNAMICS IN THE REVERSED FIELD PINCH
K. F. Schoenberg 1988 2 p Presented at the 12th International Conference on Plasma Physics and Controlled Nuclear Fusion Research, Nice, France, 12 Oct. 1988
(Contract W-7405-eng-36)
(DE88-009148; LA-UR-88-1103; CONF-881015-2) Avail: NTIS HC A02/MF A01

The study of basic transport and confinement dynamics is central to the development of the reversed field pinch (RFP) as a confinement concept. Thus, the goal of RFP research is to understand the connection between processes that sustain the RFP configuration and related transport/confinement properties. Recently, new insights into confinement have emerged from a detailed investigation of RFP electron and ion physics. These insights derive from the recognition that both magnetohydrodynamic (MHD) and electron kinetic effects play an important and strongly coupled role in RFP sustainment and confinement dynamics. In this paper, we summarize the results of these studies on the ZT-40M experiment. DOE

N89-13260# Los Alamos National Lab., N. Mex.
MODIFIED MAGNETIC CONFINEMENT CONFIGURATIONS BASED ON UNDERSTANDING HELICITY DISSIPATION AND PRESSURE DRIVEN MODES IN THE SPHEROMAK
T. R. Jarboe, C. W. Barnes, J. C. Fernandez, I. Henins, G. J. Marklin, and F. J. Wysocki 1988 2 p Presented at the 12th International Conference on Plasma Physics and Controlled Nuclear Fusion Research, Nice, France, 12 Oct. 1988
(Contract W-7405-eng-36)
(DE88-009149; LA-UR-88-1104; CONF-881015-1) Avail: NTIS HC A02/MF A01

Recent results from the spheromak work at Los Alamos include: In decaying spheromaks in the mesh flux conserver, the rate of current decay dI/dt depends only on the density n sub e (not on I or T sub e as might be expected classically). The particular dependence of dI/dt on n sub e suggests that most of the helicity is dissipated in the field error regions at the edge where electron-neutral hydrogen collisions dominate the electrical resistance. A new solid-wall, titanium-gettered flux conserver has been commissioned, resulting in less field errors than with previous mesh flux conserver. A factor of four decrease in dI/dt has been observed. In this new flux conserver, clear evidence of a pressure-driven instability has been obtained. To our knowledge, this is the first time a pressure driven interchange mode has been directly observed in a toroidal geometry. Peak beta values observed before the onset of the mode are of the same order as those predicted at the corresponding Mercier limits (beta sub c approx 1 percent). As a result, flux conserver shapes with higher beta sub c are now being considered. The beta sub c calculations have been made using Taylor-like (minimum energy) magnetic profiles. By changing the flux conserver shape, the q profile of the minimum-energy state can be varied continuously from RFP-like to tokamak-like. The highest beta sub c (approx 10 percent) are found at these two extremes of the range of magnetic configurations. DOE

N89-13261# Los Alamos National Lab., N. Mex. Materials Science and Technology Div.
A MASS SPECTROMETRIC ANALYSIS OF CF4/O2 PLASMAS: EFFECT OF OXYGEN CONCENTRATION AND PLASMA POWER
Joseph C. Martz, Dennis W. Hess (California Univ., Berkeley.), and Wallace E. Anderson 1988 25 p Presented at the NATO ASI on Plasma Surface Interaction and Processing of Materials, Alicante, Spain, 4 Sep. 1988
(Contract W-7405-eng-36)
(DE88-016237; LA-UR-88-2751; CONF-8809125-1) Avail: NTIS HC A03/MF A01

A quadrupole mass analyzer was used to detect the neutral products extracted downstream from a CF4/O2 RF discharge at 80 mtorr. Stable discharge products are reported as a function of plasma power, residence time, oxygen concentration, and plasma voltage standing-wave ratio. In general, as plasma power increased from 10 to 200 W, production of CO increased while the measured mole fractions of CO2 and COF2 stabilized. The ratio of CO to CO2 decreased at low plasma powers as the oxygen concentration increased. An increase in the relative conversion of CF4 to oxygenated products occurred at both low plasma powers and low oxygen concentrations. Several mechanisms are suggested to account for these results. DOE

N89-13262# Stanford Univ., Calif. High-Temperature Gasdynamics Lab.
NONEQUILIBRIUM EFFECTS IN THERMAL PLASMAS: RADIATION TRANSPORT AND CHEMICAL REACTIVITY
Charles H. Kruger 1988 8 p Presented at the 6th Symposium on Energy Engineering Sciences, Argonne, Ill., 4 May 1988
(Contract DE-FG03-85ER-13393)
(DE88-016841; DOE/ER-13393/T3; CONF-8805106-2) Avail: NTIS HC A02/MF A01

This paper describes one aspect of research on optical diagnostics in the High-Temperature Gasdynamics Laboratory at Stanford. The focus, intended to be in keeping with the theme of this Symposium, is on the possible importance of nonequilibrium effects in so-called thermal plasmas at pressures of approximately one atmosphere. Numerical calculations are described which investigate conditions such that electron-temperature non-equilibrium in thermal plasmas and charged-particle reaction channels might influence the chemical reactivity of such plasmas in plasma synthesis and plasma processing applications. Results for dissociation rates in the presence of elevated electron temperatures show that nonequilibrium in a plasma torch itself or in an auxiliary discharge can have significant effects on the state of the plasma and its reactivity. To address such effects experimentally and to develop plasma diagnostics suitable for nonequilibrium situations, experiments are under way in a plasma facility incorporating a 50 kW RF induction torch. Results from spectroscopic measurements show differences between Boltzmann excitation temperatures and those inferred assuming local thermodynamic equilibrium. DOE

N89-13263# Stanford Univ., Calif. High Temperature Gasdynamics Lab.
NONEQUILIBRIUM EFFECTS IN THERMAL PLASMA CHEMISTRY
Charles H. Kruger 1987 7 p Presented at the 8th International Symposium on Plasma Chemistry, Tokyo, Japan, 31 Aug. 1987

(Contract DE-FG03-85ER-13393)
(DE88-016842; DOE/ER-13393/T4; CONF-870810-1) Avail: NTIS HC A02/MF A01

Numerical calculations have been performed to assess the potential significance of nonequilibrium effects on chemical reactivity in thermal plasmas. The calculations consider situations where the electron temperature and/or the electron density are elevated above their equilibrium values corresponding to the local gas temperature. Such nonequilibrium may occur in the plasma torch itself, or could be purposefully imposed by a controlled hybrid discharge in a downstream reactor region so as to augment reactivity over a longer residence time. The calculations account for finite ionization/recombination rates of atomic and molecular species, electron-impact dissociation, dissociative recombination, dissociative attachment, and predissociation effects, as well as thermal reactions between neutral chemical species. As an example of the possible nonequilibrium enhancement of molecular decomposition, initial consideration has focused on the dissociation rates of diatomic species where heavy particle reaction rates and cross-sections can be reasonably estimated. The results show that for O sub 2 or H sub 2 in argon at moderate temperatures, electron temperature elevation can give rise to a notable enhancement of the dissociation rate, in comparison with the equilibrium case. DOE

N89-13264# Texas Univ., Austin. Inst. for Fusion Studies.
TOROIDAL STUDIES OF SAWTOOTH OSCILLATIONS IN TOKAMAKS
A. Y. Aydemir, J. C. Wiley, and D. W. Ross Aug. 1988 53 p
(Contract DE-FG05-80ET-53088)
(DE88-017115; DOE/ET-53088/303; IFSR-303) Avail: NTIS HC A04/MF A01

Tokamak sawtooth oscillations are studied with a nonreduced, fully toroidal, resistive MHD (magnetohydrodynamic) model that includes ohmic heating, and parallel and perpendicular thermal conduction. Effects of perpendicular transport in producing different types of sawteeth, varying form simple, periodic oscillations to giant sawteeth with temperature modulations of order unity, and compound sawteeth with multiple relaxations, are demonstrated. Some of the recent experimental observations from large tokamaks, such as the fast crash times and a presumed topological anomaly in the X-ray tomography pictures, thought to be inconsistent with the Kadomtsev reconnection model, are examined and possible explanations are offered. DOE

N89-13265# Argonne National Lab., Ill. Fusion Power Program.
INTERACTION OF IMPURITY IONS WITH A WEAKLY NON-MAXWELLIAN SIMPLE HYDROGENIC PLASMA
William K. Terry Aug. 1988 48 p
(Contract W-31-109-eng-38)
(DE88-017137; ANL/FPP/TM-215-Rev-1) Avail: NTIS HC A03/MF A01

The average acceleration of an ensemble of test particles in a plasma is called the dynamical friction; the average rate at which their velocity vectors spread out in velocity space is expressed in a velocity-space diffusion-rate tensor. These quantities are derived for impurity ions interacting with a weakly non-Maxwellian simple hydrogenic plasma. The distribution functions for the plasma ions and electrons are written explicitly. DOE

N89-13266# FOM-Inst. voor Plasmafysica, Rijnhuizen, Jutphaas (Netherlands).
FOM CONTRIBUTIONS TO THE 15TH EUROPEAN CONFERENCE ON CONTROLLED FUSION AND PLASMA HEATING
Jun. 1988 43 p Conference held in Dubrovnic, Yugoslavia, 16-20 May 1988 Sponsored by the Netherlands Organization for the Advancement of Pure Research and Euratom
(Rept-88-178; ETN-88-93376) Avail: NTIS HC A03/MF A01

The subjects studied include internal kink modes, toroidal plasmas, tokamak devices, plasma stability, screw pinch plasmas, ion-kinetics regimes, temperature measurement, RF stabilization, computerized simulations, and optimization of drive currents. For individual titles, see N89-13267 through N89-13276.

N89-13267# FOM-Inst. voor Plasmafysica, Rijnhuizen, Jutphaas (Netherlands).
THE m=1 INTERNAL KINK MODE IN A TOROIDAL PLASMA WITH A FLAT q-PROFILE NEAR q=1
H. J. deBLank and T. J. Schep *In its* FOM Contributions to the 15th European Conference on Controlled Fusion and Plasma Heating Jun. 1988 p 1-4 (For primary document see N89-13266 04-75)
Avail: NTIS HC A03/MF A01

Ideal magnetohydrodynamic stability is studied using the energy principle. The equilibrium configuration is allowed to have a broad region with q close to unity. The minimization of the energy functional yields an implicit equation for the growth rate that can be solved by simple numerical means. The growth rate depends very sensitively on q. The conditions of highest growth rate are given. ESA

N89-13268# FOM-Inst. voor Plasmafysica, Rijnhuizen, Jutphaas (Netherlands).
KINETIC EFFECTS ON ELECTRON CYCLOTRON EMISSION DURING ELECTRON CYCLOTRON HEATING IN TOKAMAKS
G. Giruzzi *In its* FOM Contributions to the 15th European Conference on Controlled Fusion and Plasma Heating Jun. 1988 p 5-8 (For primary document see N89-13266 04-75)
Avail: NTIS HC A03/MF A01

The properties of the radiation emitted by non-Mawellian distributions generated by high-power electron cyclotron plasma heating are studied. The electron distribution is determined by solving the time dependent bounce averaged quasilinear Fokker-Plank equation by means of a three dimensional Fokker-Plank code. The computed steady state distribution function is then used to calculate the emission and transmission spectra for different locations of the receiving antennas, polarizations, and harmonics. The results yield insights on the impact of quasi-linear flattening and electron trapping. ESA

N89-13269# FOM-Inst. voor Plasmafysica, Rijnhuizen, Jutphaas (Netherlands).
FUNDAMENTAL HARMONIC ELECTRON CYCLOTRON EMISSION FOR HOT, LOSS-CONE TYPE DISTRIBUTIONS
M. Bornatici, U. Ruffina (Pavia Univ., Italy), and E. Westerhof *In its* FOM Contributions to the 15th European Conference on Controlled Fusion and Plasma Heating Jun. 1988 p 9-12 (For primary document see N89-13266 04-75)
Avail: NTIS HC A03/MF A01

The consequences of the dispersion properties for the emissivity of the fundamental harmonic X mode are analyzed for perpendicular propagation. The emissivity is calculated for two types of distribution functions having a loss-cone anisotropy in the parameter regime for which the dispersion properties are discussed. The calculations of the polarization vector and of the normalized power flux ocurring in the equations require the knowledge of the dielectric tensor and the wave refractive index and, hence, the solution of the dispersion equation. The sharp peaks existing in the presented results are a sensitive function of the temperature and are close to maximum for the parameters chosen. ESA

N89-13270# FOM-Inst. voor Plasmafysica, Rijnhuizen, Jutphaas (Netherlands).
TRANSPORT CODE STUDIES OF m=2 MODE CONTROL BY LOCAL ELECTRON CYCLOTRON HEATING IN TFR
E. Westerhof and W. J. Goedheer *In its* FOM Contributions to the 15th European Conference on Controlled Fusion and Plasma Heating Jun. 1988 p 13-16 (For primary document see N89-13266 04-75)
Avail: NTIS HC A03/MF A01

Transport code simulations of TFR experiments were carried out to determine whether positive results obtained by local electron cyclotron heating are indeed a consequence of profile tailoring. The evolution of the m=2, n=1 tearing mode was evaluated for

cylindrical geometry using quasi-linear theory. The conclusion is that the suppression of the magnetohydrodynamic activity with electron cyclotron heating on TFR cannot be due to current profile tailoring alone. The most probable cause is the effect of electron cyclotron heating on the plasma position. ESA

N89-13271# FOM-Inst. voor Plasmafysica, Rijnhuizen, Jutphaas (Netherlands).
RECENT RESULTS OF THE TOROIDAL SCREW PINCH SPICA 2
H. S. Lassing, J. Lok, A. F. G. vanderMeer, G. A. Navratil (Columbia Univ., New York, N.Y.), D. Oepts, A. A. M. Oomens, and M. Verreck *In its* FOM Contributions to the 15th European Conference on Controlled Fusion and Plasma Heating Jun. 1988 p 17-20 (For primary document see N89-13266 04-75)
Avail: NTIS HC A03/MF A01

With discharges in the slow screw pinch mode (without shock wave heating), high beta plasmas were studied. In this mode the power crowbar banks are switched on when the predischarge current and the bias field reach their maximum value. At these low plasma currents (less than 70 kA) the stabilization by the conducting wall could not prevent disastrous plasma-wall contact. It is concluded that for this mode of operation a pulsed vertical field is essential. ESA

N89-13272# FOM-Inst. voor Plasmafysica, Rijnhuizen, Jutphaas (Netherlands).
TOKAMAK EQUILIBRIUM DETERMINATION THROUGH FUNCTION PARAMETERIZATION
B. Ph. vanMilligen and N. J. LopesCardozo *In its* FOM Contributions to the 15th European Conference on Controlled Fusion and Plasma Heating Jun. 1988 p 21-24 (For primary document see N89-13266 04-75)
Avail: NTIS HC A03/MF A01

A Grad-Shafranov equilibrium solver is being developed to determine the magnetic flux surfaces in a tokamak plasma. The flux surfaces are identified from magnetic measurements made with 12 radial and 12 poloidal field coils and 12 flux loops. Additional measurements may be used to improve the accuracy including sawtooth inversion radius (by means of soft X ray observations of the poloidal field profile and of the local current density). The code is designed to be fast enough, so that a fingerprint is available soon after termination of a discharge. This computational speed is allowed by using the function parameterization statistical method. ESA

N89-13273# FOM-Inst. voor Plasmafysica, Rijnhuizen, Jutphaas (Netherlands).
THE APPLICABILITY OF RUTHERFORD SCATTERING FOR Ti MEASUREMENTS AT MEDIUM AND LARGE-SIZED EXPERIMENTS
E. P. Barbian, A. A. E. vanBlokland, and H. W. vanderVen *In its* FOM Contributions to the 15th European Conference on Controlled Fusion and Plasma Heating Jun. 1988 p 25-28 (For primary document see N89-13266 04-75)
Avail: NTIS HC A03/MF A01

The general applicability of the beam scattering diagnotic for experiments beyond the parameter sets are discussed. The estimates are supported by a comparison with an example of JT-60 data and are also extended to even higher probing beam energies of 300 to 500 keV which are suitable velues for large fusion devices. The choice of higher beam energies improves strongly the main distribution. No limitations from the impurity component appear to limit the potential of the beam diagnostic for application at large fusion devices. ESA

N89-13274# FOM-Inst. voor Plasmafysica, Rijnhuizen, Jutphaas (Netherlands).
INTERNAL KINK MODES IN THE ION-KINETIC REGIME
T. J. Schep, F. Pegoraro, and F. Porcelli (Joint European Torus Project, Abingdon, England) *In its* FOM Contributions to the 15th European Conference on Controlled Fusion and Plasma Heating Jun. 1988 p 29-32 (For primary document see N89-13266 04-75)
Avail: NTIS HC A03/MF A01

The m=1 kink mode is investigated in the high temperature regime where the width of the singular layer is determined by the mean ion gyroradius. A dispersion relation that contains the full ion dynamics is presented. The growth rates are larger than the corresponding ones obtained from fluid theory. Diamagnetic stabilization is weaker than in the fluid case. Unstable modes are found for certain limiting conditions. ESA

N89-13275# FOM-Inst. voor Plasmafysica, Rijnhuizen, Jutphaas (Netherlands).
RF STABILIZATION OF EXTERNAL KINK MODES
J. P. Goedbloed and D. A. Dippolito (Lodestar Research Corp., Boulder, Colo.) *In its* FOM Contributions to the 15th European Conference on Controlled Fusion and Plasma Heating Jun. 1988 p 33-36 (For primary document see N89-13266 04-75)
Avail: NTIS HC A03/MF A01

The effect of a term due to ponderomotive force in an external RF field in low beta plasmas is computed for two idealized cases: a single coil toroidal antenna situated at theta=0 and producing a field A(theta) at the plasma boundary which couples the poloidal harmonics, and a poloidal antenna system at phi=0 producing a field A(phi) which couples the toroidal harmonics. The results for a highly localized RF field show that the stabilization becomes genuine when an RF field of finite extent is considered. Analogous results for a poloidal antenna system are also found. The m=2 external kink modes are easily stabilized by a poloidal RF field. ESA

N89-13276# FOM-Inst. voor Plasmafysica, Rijnhuizen, Jutphaas (Netherlands).
OPTIMIZING CURRENT DRIVE BY ELECTRON CYCLOTRON WAVES IN THE PRESENCE OF TRAPPED PARTICLES
G. Giruzzi *In its* FOM Contributions to the 15th European Conference on Controlled Fusion and Plasma Heating Jun. 1988 p 37-40 (For primary document see N89-13266 04-75)
Avail: NTIS HC A03/MF A01

Moving the absorption region to the inboard side of the magnetic surfaces and combining electron cyclotron waves and lower hybrid waves are investigated in order to solve problems caused by electron trapping in tokamak devices. The time dependent bounce averaged quasilinear Fokker Planck equation is solved in order to evaluate the current drive efficiency for realistic wave power levels. It is shown that moving the absorption region is ineffective in enhancing the current drive efficiency, because of the interplay of quasilinear and toroidal effects for high wave power. On the other hand, combination with lower hybrid waves can be quite efficient in minimizing the negative impact of electron trapping. ESA

N89-13229# Arizona State Univ., Tempe. Dept. of Electrical Engineering.
LASER DRIVEN INERTIAL CONFINEMENT FUSION
William Derks *In* New Mexico Univ., Nuclear Technology for the Year 2000 1987 p 97-99 (For primary document see N89-13223 04-70)
Avail: NTIS HC A06/MF A01

N89-13230# Washington Univ., Seattle.
FIREBIRD: A CONCEPTUAL DESIGN OF A FIELD REVERSED CONFIGURATION COMPACT TORUS FUSION REACTOR (CTFR)
Roger Raman and Robert M. Zubrin *In* New Mexico Univ., Nuclear Technology for the Year 2000 1987 p 100-104 (For primary document see N89-13223 04-70)
Avail: NTIS HC A06/MF A01

76 SOLID-STATE PHYSICS

Includes superconductivity.

For related information, see also *33 Electronics and Electrical Engineering* and *36 Lasers and Masers.*

N89-13277# Delaware Univ., Newark. Dept. of Physics.
NEUTRON STUDIES OF LIQUID AND SOLID HELIUM Progress Report, 1 May 1987 - 30 Apr. 1988
H. R. Glyde 1988 20 p
(Contract DE-FG02-84ER-45082)
(DE88-009096; DOE/ER-45082/4) Avail: NTIS HC A03

Liquid and solid helium are prototype simple liquids and solids displaying a wide spectrum of quantum properties. Understanding gained in these simple systems can be readily applied to more complicated materials. Neutron scattering studies carried out at DOE supported national facilities and the associated development of theory and models continue to reveal new physics in these fascinating materials. During the past year we have measured the dynamic form factor, S(Q,omega), in superfluid and normal liquid He-4 accurately as a function of temperature. This shows that the sharp one-phonon excitation, which exists in the superfluid phase below T sub lambda, either disappears at or changes entirely in character at the transition to the normal phase. Thus the sharp one-phonon excitation can be associated with superfluidity (or a condensate). However, we find the weight of scattering in the one-phonon peak, Z(Q,T), is not porportional to the superfluid density, rho sub S (T). We have also measured S(Q,omega) in the range 3 less than or equal to Q less than or equal to 15 angstrom sup minus 1 in order to obtain the width W(Q) and peak position, E(Q), of S(Q,omega) as a function of Q. We have made microscopic calculations of S(Q,omega) in the range 3 less than or equal to Q less than or equal to 15 angstrom sup minus 1 in both liquid He-3 and He-4. The aim is a first principles evaluation of W(Q) and E(Q) as a function of Q for comparsion with experiments. DOE

N89-13278# California Univ., Berkeley. Lawrence Berkeley Lab. Engineering Div.
GENERATION OF THE J(SUB c), H(SUB c), T(SUB c) SURFACE FOR COMMERCIAL SUPERCONDUCTOR USING REDUCED-STATE PARAMETERS
Michael A. Green Apr. 1988 67 p
(Contract DE-AC03-76SF-00098)
(DE88-014038; LBL-24875) Avail: NTIS HC A04/MF A01

This report presents a method for calculating the J sub C, H sub C, T sub C surface for Type II Superconductors. The method requires that one knows T sub C at zero current and field, H sub c2 at zero current and temperature, and J sub c at at least one temperature and field. The theory presented in this report agrees with the measured data quite well over virtually the entire J sub c, H sub c, T sub c surface given the value of J sub c versus H at one or two temperatures. This report presents calculated and measured values of J sub c versus T and B for niobium titanium, niobium zirconium, niobium tin, niobium titanium tin, niobium tantalum tin, vanadium zirconium hafnium, and vanadium gallium. Good agreement of theory with measured data was obtained for commercial niobium titanium and niobium tin. DOE

N89-13279# California Univ., Berkeley. Lawrence Berkeley Lab.
HIGH T(SUB c) SUPERCONDUCTORS: WILL THEY REPLACE HELIUM TEMPERATURE SUPERCONDUCTORS FOR MAGNETS
Michael A. Green Jul. 1988 6 p Presented at the 12th International Cryogenic Engineering Conference and Exhibition, Southhampton, United Kingdom, 12 Jul. 1988
(Contract DE-AC03-76SF-00098)
(DE88-016632; LBL-25733; CONF-880736-3) Avail: NTIS HC A02/MF A01

This compares the properties of a Y-Ba-Cu-O high T(sub c) conductor (T(sub c) = 93 K) with niobium titanium (T(sub c) = 9.4 K). If one assumes that the critical current density for the high T(sub c) superconductor is the same as niobium titanium and they are both in a conducting matrix, one can make a direct comparison of the two types of superconductor. The comparisons in the paper include: adiabatic and dynamic stability diameter, normal region propagation rates, the burnout integral of J^2 dt, quench initiation energy, and matrix current density for cryogenic stability. From such a comparison, it is clear that high T(sub c) superconductor may not be the superconductor of choice for many applications. An example of such an application is the use of high T(sub c) conductors for accelerator magnets. DOE

N89-13280# Massachusetts Inst. of Tech., Lexington. Lincoln Lab.
TRANSITION-METAL OXIDE SUPERCONDUCTIVITY
Gerald F. Dionne 20 Apr. 1988 99 p
(Contract F19628-85-C-0002)
(AD-A197069; TR-802; ESD-TR-87-277) Avail: NTIS HC A05/MF A01 CSCL 20L

Superconductivity in transition-metal oxides is discussed from the standpoints of electron transfer mechanisms and the transition from superconduction to normal conduction. As explanations for the reported superconducting effects, it is suggested that polarons associated with ion pairs of the d9 yields d8 ion combination in 180-degree bond geometries (e.g., Cu(2+) yields Cu(3+) + e(-) ion perovskites) and d1 yields d0 combination in 90-degree geometries (e.g., Ti(3+) yields Ti(4+) + e(-) in spinels) become itinerant within cell boundaries through energy-free electron transfers made possible by strong orbital exchange coupling. The proposed superconduction model is based on continuous linkages between cells that result in moving chains of uniformly spaced charge carriers. A phenomenological theory of normal resistivity and superconduction transition temperature as functions of composition for the La(2-x)Sr(x)CuO4 and YBa2Cu3O(y) perovskite families provides excellent agreement with experiment. Reported superconduction and structural data for the related Bi2(Sr,Ca)3Cu2O(8+y) system are also included. Optimized lattice ordering of the sources that produce the mixed-valence Cu(2+)(3+) ions could result in critical temperatures above 300 K. GRA

N89-13281# Air Force Inst. of Tech., Wright-Patterson AFB, Ohio.
NONLINEAR EFFECTS IN PHOTOREFRACTIVE CRYSTALS Ph.D. Thesis
Donald R. Erbschloe 1988 200 p Original contains color illustrations
(AD-A197152; AFIT/CI/NR-88-174) Avail: NTIS HC A09/MF A01 CSCL 07B

Photorefractive crystals are materials whose index of refraction is altered under illumination by light. These crystals are both photoconductive and electrooptic. When a nonuniform light intensity pattern is present in the material, photocarriers are generated and redistributed, creating space charge electric fields which change the refractive index locally. These crystals are ideal media for real time holography, and applications include wave amplification, image processing, phase conjugation, and laser beam steering for optical interconnects. This thesis investigates many novel aspects of the photorefractive effect. A study of nonreciprocal behavior identifies a new important consideration in the theory of two-wave mixing between counterpropagating beams-namely the presence of a photocurrent, or frequency detuning between the beams results in a spatially varying beam coupling. A numerical treatment of these important cases provides the first systematic theoretical assessment the control of nonreciprocal transmission and phase shift in lithium niobate, a representative photorefractive crystal. A comparison between crystal types suggests candidates for nonreciprocal applications such as an optical diode. GRA

N89-13282# Rensselaer Polytechnic Inst., Troy, N.Y.
RESEARCH ON MERCURY CADMIUM TELLURIDE Annual Technical Report, 15 Feb. 1987 - 14 Feb. 1988
S. K. Ghandhi 21 Jun. 1988 127 p
(Contract N00014-85-K-0151)
(AD-A197238) Avail: NTIS HC A07/MF A01 CSCL 07B

This report summarizes work done during the third year of a program entitled, Research on Mercury Cadmium Telluride. CdTe studies were extended to the DLTS of both n- and p- material. The wide gap materials effort was expanded with the growth of Zinc Selenides, which is lattice matched to Gallium Arsenides. Significant (100 to 200 times) improvement in the photoluminescence of GaAs was demonstrated by the use of a pseudomorphic ZnSe layer. The new reactor is fully operational, and is capable of growing HgCdTe with a Cd composition control of + or - 0.002 across a 1 cm x 1 cm slice. In addition, significant improvement in MCT quality was obtained by the use of CdTeSe substrates. Work with CdTeZn substrates was also carried out during this year. GRA

N89-13283# California Univ., Los Angeles. Dept. of Materials Science and Engineering.
PREPARATION AND STRUCTURE OF Li-STABILIZED Na(+) BETA' ALUMINA SINGLE CRYSTALS Technical Report No. 16, Aug. 1987 - Aug. 1988
B. Dunn, B. B. Schwarz, J. O. Thomas, and P. E. D. Morgan (Rockwell International Corp., Thousand Oaks, Calif.) 1 Jul. 1988 16 p Submitted for publication
(Contract N00014-83-K-0498)
(AD-A197245) Avail: NTIS HC A03/MF A01 CSCL 11F

Single crystals of Lithium-stabilized Sodium-Beta alumina were grown from homogeneous melts of NaAlO2 and LiVO3 on slow cooling from 1600 to 1300 C. Single crystal X-ray diffraction indicates that Li substitutes for Al(2) and Al(4) in an ordered fashion. The sodium ion distribution exhibits no short-range order effects. GRA

N89-13284# Pennsylvania State Univ., University Park. Dept. of Chemistry.
CHEMICAL PRECURSORS TO ZINC SULFIDE: ZnS WHISKER SYNTHESIS Technical Report No. 3
T. A. Guiton, C. L. Czekaj, M. S. Rau, G. L. Geoffroy, and C. G. Pantano 11 Jul. 1988 8 p
(Contract N00014-86-K-0191)
(AD-A197262; AD-E900802) Avail: NTIS HC A02/MF A01 CSCL 07A

Currently, Chemical Vapor Deposition (CVD) derived zinc sulfide is one of the most widely used infrared optical window materials. Unfortunately, for numerous applications it does not possess optimum mechanical properties. To fabricate infrared transmitting ZnS/ZnS composites requires the development of high aspect ratio, micron sized ZnS whiskers. Although larger ZnS single crystals and whiskers have been made by a variety of high temperature routes, alternative routes have been sought for greater ZnS whisker morphology control. Low temperature organometallic routes are attractive for this purpose. The precursor compound used in this study is the known pentameric species (EtZn(SBut))5. One of the most successful routes involves the reaction of (EtZn(SBU sup t))5 with hydrogen sulfide at ambient or sub-ambient temperature to yield a precipitate which is subsequently heated under flowing H2S at 500 C to yield a mixture of sub-micron particles and single-crystal ZnS whiskers. Transmission electron micrographs of the (EtZn(SBU sup t))5 products indicate that the ZnS morphology is critically dependent on the rate of H2S reaction. Corresponding X-ray/electron diffraction, electron microscopy, elemental analysis, NMR and infrared spectroscopies have been conducted. A summary of the chemical methods, product characterization results, and proposed synthesis mechanisms are presented. GRA

N89-13285# State Univ. of New York, Buffalo. Dept. of Chemistry.
OVERVIEW OF HIGH-TEMPERATURE SUPERCONDUCTIVITY: THEORY, SURFACES, INTERFACES AND BULK SYSTEMS
D. Sahu, A. Langner, Thomas F. George, J. H. Weaver, and H. M. Meyer, III Jun. 1988 23 p
(Contract N00014-86-K-0043)
(AD-A197383; UBUFFALO/DC/88/TR-75) Avail: NTIS HC A03/MF A01 CSCL 20C

An overview of the theoretical and experimental aspects of the recently discovered superconducting compounds is presented. This overview is divided into three sections. In the first section a review of some of the theoretical and computational works is presented under the subsections entitled pairing mechanisms, electronic structure calculations and thermophysical properties. In the second section surface and interface chemistry issues related to the fabrication and use of high-temperature superconductors for high-performance applications are presented. Specific issues that are discussed include metallization and the formation of stable ohmic contacts, and chemically-stable overlayers that are suitable for passivation, protection and encapsulation of superconducting material structures that can then be used under a wide range of environmental conditions. Lastly, issues are discussed that are related to each of the bulk high-temperature superconducting ceramic oxides which have received so much attention the past two years. These include Tl2Ba2Ca2Cu3O10 with a critical temperature of 125 K, which is the current record. GRA

N89-13286# Illinois Univ., Chicago.
MBE GROWTH, CHARACTERIZATION AND ELECTRONIC DEVICE PROCESSING OF HgCdTe, HgZnTe RELATED HETEROJUNCTIONS AND HgCdTe-CdTe SUPERLATTICES Annual Report
Jean-Pierre Faurie 31 Dec. 1987 42 p
(Contract F49620-87-C-0021)
(AD-A197752; AFOSR-88-0723TR) Avail: NTIS HC A03/MF A01 CSCL 20L

A report is made on growth and characterization of high quality HgCdTe epilayers, MBE growth and characterization of two-inch diameter p- and n-type Hg(1-x)Cd(X)Te films on GaAs(100) substrate. The n-type intrinsic and extrinsic doping is discussed. The incorporation of As has been photo assisted using a Nd-YAG pulsed laser. X-ray photoemission of Hg clusters on Hg(1-x)Cd(x)Te surfaces has been studied. Direct measurement by XPS and electrical determination of HgTe-CdTe valence band discontinuity give values of 300 to 400 meV at 300K. Silicon has been used as a n-type dopant to grow a homojunction which electrical characteristics are presented here. GRA

N89-13287# Naval Ocean Systems Center, San Diego, Calif.
ELECTRONIC PROPERTIES AND CURRENT CARRYING CAPACITY OF HIGH-TEMPERATURE CERAMIC SUPERCONDUCTORS Final Report
T. E. Jones, W. C. McGinnis, R. D. Boss, E. W. Jacobs, J. W. Schindler, and C. D. Rees Jul. 1988 11 p
(AD-A197819; NOSC/TD-1306) Avail: NTIS HC A03/MF A01 CSCL 20C

Samples of both the YBa2Cu3O7 family of high-temperature ceramic superconductor and the layered set of bismuth based superconductors, described by the set of crystal structures Bi2Sr2Ca(n-1)CunO(2n+4+delta), were synthesized and characterized by X-ray diffraction, and temperature dependent resistivity and thermoelectric-power measurements. Superconductivity in the yttrium-based materials is relatively insensitive to rare earth substitutions for the yttrium. Critical current measurements on these materials reveal two characteristic critical current values. The intrinsic critical current, determined by the suppression of the transition midpoint, is estimated to be greater than 10,000 A/sq cm at 77 K. The critical current defined by the R=0 point is much less in bulk ceramics and limited by intercrystalline weak links. For the bismuth based materials, two high-temperature superconducting phases have been observed with transition temperatures near 80 K and 110 K. Evidence from thermoelectric power measurements is presented which shows both electronlike and holelike carriers contribute to the electrical transport in this family of ceramic superconductors. However, all of superconducting transitions observed involve with transition temperatures near 80 K and 110 K. GRA

N89-13288# Los Alamos National Lab., N. Mex. Theoretical Div.
A NOVEL EXCITONIC MECHANISM FOR HIGH TEMPERATURE SUPERCONDUCTIVITY
Z. Tesanovic, A. R. Bishop, and R. L. Martin 1988 9 p Presented at the International Conference on Science and Technology of Synthetic Metals, Santa Fe, N. Mex., 26 Jun. 1988
(Contract W-7405-eng-36)
(DE88-016227; LA-UR-88-2535; CONF-880669-16) Avail: NTIS HC A02/MF A01

We propose a novel mechanism for superconductivity, based on intra and interband Cu (equilibrium) O charge transfer excitations in oxide superconductors. The dynamic polarizability of the environment surrounding CuO2 planes plays an important role in enhancing T sub c. The sandwich structure in which CuO2 planes are separated by a highly polarizable medium is ideally suited for this mechanism. Our proposal is consistent with a variety of available data, and suggests several new experimental directions. DOE

N89-13289# California Univ., Berkeley. Dept. of Physics.
SUPERCONDUCTIVITY: PHENOMENOLOGY
L. M. Falicov Aug. 1988 16 p Presented at the Topsoe Summer School on Superconductivity, Risoe, Denmark, 20 Jun. 1988 Prepared in cooperation with California Univ., Berkeley, Lawrence Berkeley Lab.
(Contract DE-AC03-76SF-00098)
(DE88-016659; LBL-25678; CONF-8806233-1) Avail: NTIS HC A03/MF A01

This document discusses first the following topics: (1) The superconducting transition temperature; (2) Zero resistivity; (3) The Meissner effect; (4) The isotope effect; (5) Microwave and optical properties; and (7) The superconducting energy gap. Part 2 of this document investigates the Ginzburg-Landau equations by discussing: (1) The coherence length; (2) The penetration depth; (3) Flux quantization; (4) Magnetic-field dependence of the energy gap; (5) Quantum interference phenomena; and (6) The Josephson effect. DOE

N89-13290# Keuring van Electrotechnische Materialen N.V., Arnhem (Netherlands). Chemical Research Dept.
MICROSTRUCTURE AND NONLINEARITY OF ZnO VARISTORS, VOLUME 5, NUMBER 8
H. P. A. M. vanderStaak, C. D. Andriesse, and A. J. VanLoon, ed. 1987 12 p
(B8735659; ISBN-9-03-530055-6; ISSN-0167-8590; ETN-88-93440) Avail: NTIS HC A03/MF A01

Good and poor ZnO varistor materials were prepared by variation of the amount of barrier-forming and grain-controlling additives. Good varistors show a clear correlation between grain size and nonlinearity. A theory to explain this correlation was developed. The good varistors are characterized by narrow intergranular layers. There is insufficient understanding of the correlation for poor varistors. They have wide intergranular layers which are rich in spinel and pyrochlore. An explanation might be that the energy gradients could be small in these thick barriers. ESA

N89-13291# Office of Naval Research, London (England).
HIGH TEMPERATURE SUPERCONDUCTIVITY RESEARCH IN SELECTED LABORATORIES IN WEST GERMANY
Donald H. Liebenberg and Alan Clark 8 Jul. 1988 10 p
(ONRL-8-011-R) Avail: NTIS HC A02/MF A01

The superconductivity work at eight West German laboratories is reviewed. The laboratories are (or located at): the University of Giessen; the Technical University at Darmstadt; Hoechst AG; Siemens AG; KFA Julich; KFK, Karlsruhe; the Walter Meissner Institute, Garching; and the Max Planck Institute, Stuttgart. Author

N89-13292# Los Alamos National Lab., N. Mex.
LOW CONTACT-RESISTIVITY JUNCTION TO CERAMIC SUPERCONDUCTORS
M. P. Maley, J. O. Willis, J. D. Katz, R. G. Castro, and R. M. Aikin 1988 10 p Presented at the Applied Superconductivity Conference, San Francisco, Calif., 21 Aug. 1988
(Contract W-7405-eng-36)
(DE88-016155; LA-UR-88-2815; CONF-880812-2) Avail: NTIS HC A02/MF A01

We report on the development of a plasma-arc spray process for the application of low resistivity silver contact junctions onto YBa2Cu3O7 sintered ceramic materials. The contact resistances decrease monotonically with decreasing temperature and are typically approximately 10 to the -8 omega/sq cm at 75 K. I-V characteristics are linear up to a critical current density that agrees with that of the underlying superconducting material. Advantages over other contact methods include: ease of application, absence of any post-processing treatment, and applicability to large areas and arbitrary shapes. DOE

N89-12756# Kent State Univ., Ohio. Dept. of Physics.
COMPUTER EVALUATION OF ION-IMPLANTED DOPANT PROFILE EVOLUTION DURING ANNEALING Final Report
Steven W. Rucev *In* Universal Energy Systems, Inc., United States Air Force Graduate Student Summer Support Program, Volume 1 Dec. 1987 14 p (For primary document see N89-12754 04-31)
Avail: NTIS HC A99/MF E03 CSCL 20L

77 THERMODYNAMICS AND STATISTICAL PHYSICS

Includes quantum mechanics; theoretical physics; and Bose and Fermi statistics.

For related information see also *25 Inorganic and Physical Chemistry* and *34 Fluid Mechanics and Heat Transfer.*

N89-13293# International Centre for Theoretical Physics, Trieste (Italy).
HOW TO TEST THE SPECIAL THEORY OF RELATIVITY ON ROTATING EARTH
H. Abolghasem, M. R. Khadjehpoor (Sharif Univ. of Technology, Tehran, Iran), and R. Mansouri Feb. 1988 6 p
(DE88-703048; IC-88/44) Avail: NTIS (US Sales Only) HC A02/MF A01

In the framework of a one parameter test theory of special relativity, the difference between Transport- and Einstein synchronization on the rotating earth is calculated. For the special theory of relativity this difference vanishes. Therefore, experiments in which these synchronization procedures are compared, test the special theory of relativity. DOE

N89-13294# Los Alamos National Lab., N. Mex. Theoretical Div.
NEW GRAVITATIONAL FORCES FROM QUANTUM THEORY
Michael Martin Nieto (Niels Bohr Inst., Copenhagen, Denmark), T. Goldman, and R. J. Hughes 1988 7 p Presented at the 5th Marcel Grossmann Conference, Perth, Australia, 8 Aug. 1988
(Contract W-7405-eng-36)
(DE88-016231; LA-UR-88-2563; CONF-8808112-1) Avail: NTIS HC A02/MF A01

When a classical theory is quantized, new physical effects result. The prototypical example is the Lamb Shift of quantum electrodynamics. Even though this phenomenon could be parametrized by the Uehling Potential, it was always realized that it was a quantum aspect of electromagnetism, not a new force of nature. So, too, with theories of quantum gravity. Generically they predict that there will be spin-1 (graviphoton) and spin-0 (graviscalar) partners of the spin-2 graviton. At some level, these partners will generate new effects. Among them are (1) non-Newtonian gravitational forces, and (2) substance dependance (violation of the Principle of Equivalence). We discuss these ideas in the context of recent experiments. (Experiments usually test only one of the above effects, which could be distinct.) We contrast

these ideas with the alternative point of view, that there actually may be a fifth force of nature. DOE

80 SOCIAL SCIENCES (GENERAL)

Includes educational matters.

N89-13295# Maryland Univ., College Park. Dept. of Aerospace Engineering.
ESTABLISHMENT OF CENTER FOR ROTORCRAFT EDUCATION AND RESEARCH Final Report, 22 Nov. 1982 - 31 Dec. 1987
Alfred Gessow 2 May 1988 25 p
(Contract DAAG29-83-K-0002)
(AD-A197141; ARO-19392.19-EG-RW) Avail: NTIS HC A03/MF A01 CSCL 01C

Under a five-year contract with the U.S. Army Research Office, a rotorcraft Center of Excellence was established in the Fall of 1982 at the University of Maryland. As one of the universities chosen for the program, Maryland had the responsibility to attract and involve a significant number of experienced faculty into the program; to develop and add to its graduate curriculum a number of specialized rotorcraft courses which cover the disciplines applicable to rotorcraft design; to attract the best and brightest students into the program and motivate them into rotorcraft as a career; to upgrade and develop experimental facilities which meet the specialized needs of rotorcraft research; to blend faculty, students and facilities into a research combination which concentrated on leading edge research areas; and finally, to disseminate widely the results of the research. The degree to which these responsibilities were met at the end of the contract period is summarized herein. GRA

81 ADMINISTRATION AND MANAGEMENT

Includes management planning and research.

N89-13296# Automation Research Systems Ltd., Alexandria, Va.
MANPRINT (MANPOWER AND PERSONNEL INTEGRATION PROGRAM) PRIMER Final Report, 1 May - 24 Jun. 1988
William O. Blackwood and Jack W. Dice 24 Jun. 1988 139 p
(Contract MDA903-86-C-0092)
(AD-A197681) Avail: NTIS HC A07/MF A01 CSCL 12E

The Manpower and Personnel Integration program (MANPRINT) is a comprehensive management and technical program to enhance human performance and reliability in the operation, maintenance and use of weapon systems and equipment (hereafter referred to as system). MANPRINT achieves this objective by focusing attention on human resource goals and constraints during system design, development, production and upgrade. This MANPRINT primer is designed for both Army and industry MANPRINT practitioners. It provides a basis for their activities and specific how to guidance to deal with MANPRINT activities that must occur throughout the materiel acquisition life cycle. Chapter 1 is an introduction to MANPRINT. It provides the Army's conceptual basis and thrust in MANPRINT. Primary roles and responsibilities for Army and industry are shown in Chapter 2 and Appendix F. Chapter 3 focuses on various aspects of program management--organization planning, scheduling, and resourcing of a comprehensive MANPRINT program throughout the design and development cycle. Technical MANPRINT management is addressed in Chapter 4 in discussions of force level analyses; issues in each of the MANPRINT domains; and planning for and selecting analytical techniques and methodologies for use in satisfying information needed. GRA

N89-13078# European Space Agency. ESRIN, Frascati (Italy).
ERS DATA POLICY
L. Marelli *In its* Proceedings of the 1988 International Geoscience and Remote Sensing Symposium (IGARSS 1988) on Remote Sensing: Moving Towards the 21st Century, Volume 1 Aug. 1988 p 585-586 (For primary document see N89-12936 04-42)
Copyright Avail: NTIS HC A99/MF E03; ESA Publications Div., ESTEC, Noordwijk, Netherlands, 120 US dollars or 250 Dutch guilders

82 DOCUMENTATION AND INFORMATION SCIENCE

Includes information management; information storage and retrieval technology; technical writing; graphic arts; and micrography.

For computer documentation see *61 Computer Programming and Software.*

N89-13297 California Univ., Los Angeles.
THE PROCESSING OF QUALITATIVE INFORMATION IN A NATURAL LANGUAGE CONTEXT Ph.D. Thesis
Bryan C. Hsiao 1987 202 p
Avail: Univ. Microfilms Order No. DA8803649

Although nonstructured decision problems are difficult to handle, human decision makers are effective in this domain in terms of providing answers to fulfill the decision needs promptly. To embed such a capability in computing systems, various approaches, including Bayesian inference, fuzzy logic, and monotonic reasoning were proposed to work on the notion of inexactness. All seem persuasive in certain aspects, yet none functions as robust as human decision makers. By taking information in the form of natural language, different perceptions of inexactness are compared and it is suggested that qualitativeness in natural language is an advantage, not a drawback; it should be identified, not modeled, and processed, not resolved. It is proposed that qualitative lexical items from scales, and these scales can be bundled into a boolean lattice (Q-context). This lattice then is interpreted in Keenan and Faltz's boolean semantic theory to establish a theoretic linguistic connection. Further, to examine the properties of the Q-context, results in other lattice related studies are adopted to check several computational issues. Research in switching theory helps to explore the limitations on its representation, Hall's node placement algorithm provides some insights for allocating lexical items within it, and fractal theory allows the study of its recursiveness for the learning potential.
Dissert. Abstr.

N89-13298*# National Aeronautics and Space Administration, Washington, D.C.
NASA THESAURUS. VOLUME 2: ACCESS VOCABULARY
Jul. 1988 410 p
(NASA-SP-7064-Vol-2; NAS 1.21:7064-Vol-2) Avail: NTIS HC A18 CSCL 05B

The access vocabulary, which is essentially a permuted index, provides access to any word or number in authorized postable and nonpostable terms. Additional entries include postable and nonpostable terms, other word entries and pseudo-multiword terms that are permutations of words that contain words within words. The access vocabulary contains almost 42,000 entries that give increased access to the hierarchies in Volume 1 - Hierarchical Listing. Author

N89-13299# National Oceanic and Atmospheric Administration, Boulder, Colo. Space Environment Lab.
SPACE ENVIRONMENT LABORATORY DATA ACQUISITION AND DISPLAY SYSTEM 2
J. R. Abeyta, C. C. Balch, W. P. Barrett, F. C. Cowley, and C. M. Cruickshank Mar. 1988 96 p
(PB88-205471; NOAA-TM-ERL-SEL-76) Avail: NTIS HC A05/MF A01 CSCL 05B

The purpose of the publication is to document the effort undertaken by the staff of the Space Environment Laboratory to design and implement the Space Environment Laboratory Data

Acquisition and Display System 2 (SELDADS 2). The information presented here is intended for a broad spectrum of readers, both management and technical, who may be involved with computer system design and implementation. SELDADS 2 is the second generation of dedicated computer support for the Space Environment Services Center operation. The first part of the report, describing the purpose and the history of the operation, is intended to provide the reader with a framework for understanding why and how SELDADS 2 came into existence. GRA

N89-13300# Commerce Dept., Washington, D.C. Office of Economic Affairs.
SURVEY OF SUPPLY/DEMAND RELATIONSHIPS FOR JAPANESE TECHNICAL INFORMATION IN THE UNITED STATES: THE FIELD OF ADVANCED CERAMICS RESEARCH AND DEVELOPMENT
7 Mar. 1988 132 p Prepared in cooperation with Technology International Corp., Potomac, Md.
(PB88-210943) Avail: NTIS HC A07/MF A01 CSCL 05B

In conformance with the Japanese Technical Literature Act of 1986, a significant level of effort was made by government agencies and commercial and not-for-profit information providers to acquire and disseminate Japanese technical information. The survey described in the report was undertaken to determine why the demand from users has lagged behind supply. Because the survey is limited to the field of advanced ceramics, its results can not be freely extrapolated to other fields. However, the responses do provide a snapshot view of current U.S. efforts to use Japanese information and encapsulate some of the challenges faced by providers as well as users. GRA

N89-13301*# National Aeronautics and Space Administration, Washington, D.C.
NASA THESAURUS. VOLUME 3: DEFINITIONS
Jul. 1988 148 p
(NASA-SP-7064-Vol-3; NAS 1.21:7064-Vol-3) Avail: NTIS HC A07 CSCL 05B

Publication of NASA Thesaurus definitions began with Supplement 1 to the 1985 NASA Thesaurus. The definitions given here represent the complete file of over 3,200 definitions, complimented by nearly 1,000 use references. Definitions of more common or general scientific terms are given a NASA slant if one exists. Certain terms are not defined as a matter of policy: common names, chemical elements, specific models of computers, and nontechnical terms. The NASA Thesaurus predates by a number of years the systematic effort to define terms, therefore not all Thesaurus terms have been defined. Nevertheless, definitions of older terms are continually being added. The following data are provided for each entry: term in uppercase/lowercase form, definition, source, and year the term (not the definition) was added to the NASA Thesaurus. The NASA History Office is the authority for capitalization in satellite and spacecraft names. Definitions with no source given were constructed by lexicographers at the NASA Scientific and Technical Information (STI) Facility who rely on the following sources for their information: experts in the field, literature searches from the NASA STI database, and specialized references. Author

N89-13302*# National Aeronautics and Space Administration, Washington, D.C.
NASA THESAURUS. VOLUME 1: HIERARCHICAL LISTING
Jul. 1988 875 p
(NASA-SP-7064-Vol-1; NAS 1.21:7064-Vol-1) Avail: NTIS HC A99 CSCL 05B

There are over 17,000 postable terms and nearly 4,000 nonpostable terms approved for use in the NASA scientific and technical information system in the Hierarchical Listing of the NASA Thesaurus. The generic structure is presented for many terms. The broader term and narrower term relationships are shown in an indented fashion that illustrates the generic structure better than the more widely used BT and NT listings. Related terms are generously applied, thus enhancing the usefulness of the Hierarchical Listing. Greater access to the Hierarchical Listing may be achieved with the collateral use of Volume 2 - Access Vocabulary and Volume 3 - Definitions. Author

N89-13303# Rutgers - The State Univ., New Brunswick, N. J. Center for Expert Systems Research.
EMPIRICAL ANALYSIS AND REFINEMENT OF EXPERT SYSTEM KNOWLEDGE BASES Quarterly Report
Sholom M. Weiss and Casimir A. Kulikowski 31 May 1988 6 p
(Contract N00014-87-K-0398)
(AD-A197241) Avail: NTIS HC A02/MF A01 CSCL 12G

Knowledge base refinement is the modification of an existing expert system knowledge base with the goals of localizing specific weaknesses in a knowledge base and improving an expert system's performance. Systems that automate some aspects of knowledge base refinement can have a significant impact on the related problems of knowledge base acquisition, maintenance, verification, and learning from experience. The SEEK system was the first expert system framework to integrate large-scale performance information into all phases of knowledge base development and to provide automatic information about the refinement. A recently developed successor system, SEEK2, significantly expands the scope of the original system in terms of generality and automated capabilities. Based on promising results using the SEEK approach, we believe that significant progress will be made in expert system techniques for knowledge acquisition, knowledge base refinement, maintenance, and verification. We are proposing to demonstrate a rule refinement system in an application of the diagnosis of complex equipment failure. The expected candidate application is computer network troubleshooting. The expert system should demonstrate the following advanced capabilities: (1) automatic localization of knowledge base weaknesses; (2) automatic repair (refinement) of poorly performing rules; (3) automatic verification of new knowledge base rules; and (4) some automatic learning capabilities. GRA

N89-13304# Massachusetts Inst. of Tech., Cambridge. Artificial Intelligence Lab.
A LEXICAL CONCEPTUAL APPROACH TO GENERATION FOR MACHINE TRANSLATION Memorandum Report, Sep. 1987 - Jan. 1988
Bonnie J. Dorr Jan. 1988 26 p
(Contract N00014-85-K-0124)
(AD-A197356; AI-M-1015) Avail: NTIS HC A03/MF A01 CSCL 12I

Current approaches to generation for machine translation make use of direct-replacement templates, large grammars, and knowledge-based inferencing techniques. Not only are rules language-specific, but they are too simplistic to handle sentences that exhibit more complex phenomena. Furthermore, these systems are not easily extendable to other languages because the rules that map the internal representation to the surface form are entirely dependent on both the domain of the system and the language being generated. Finally an adequate interlingual representation has not yet been discovered; thus, knowledge-based inferencing is necessary and syntactic cross-linguistic generalization cannot be exploited. This report introduces a plan for the development of a theoretically based computational scheme of natural language generation for a translation system. The emphasis of the project is the mapping from the lexical conceptual structure of sentences to an underlying or base syntactic structure called deep structure. This approach tackles the problems of thematic and structural divergence, i.e., it allows generation of target language sentences that are not thematically or structurally equivalent to their conceptually equivalent source language counterparts. GRA

N89-13305# California Univ., Berkeley. Dept. of Computer Sciences.
MULTIPLE REPRESENTATION DOCUMENT DEVELOPMENT Technical Report, 7 Aug. 1984 - 6 Aug. 1987
Pehong Chen and Michael A. Harrison 6 Aug. 1987 38 p
(Contract N00039-84-C-0089; ARPA Order 4871)

(AD-A197369; UCB/CSD-87/367) Avail: NTIS HC A03/MF A01 CSCL 12E

The world of electronic publishing software seems to divide into two camps: the conventional batch-oriented programming language approach versus the more elaborate direct manipulation paradigm. This paper indicates which aspects of document preparation are more conveniently handled under which model and points out several instances of a hybrid approach which takes advantage of multiple representations. The authors introduce a framework for analyzing the structure of multiple representation systems in general. Based upon this simple but robust framework, a top-down design methodology is derived. The design of a fairly sophisticated document development environment is discussed as a case study of the methodology. GRA

83 ECONOMICS AND COST ANALYSIS

Includes cost effectiveness studies.

No abstracts in this category.

84 LAW, POLITICAL SCIENCE AND SPACE POLICY

Includes NASA appropriation hearings; aviation law; space law and policy; international law; international cooperation; and patent policy.

N89-13306# Los Alamos National Lab., N. Mex.
UNITED STATES SPACE POLICY: REVIEW AND ASSESSMENT
Patrick J. Garrity Jun. 1988 40 p
(Contract W-7405-eng-36)
(DE88-015538; LA-11181; CNSS-3) Avail: NTIS HC A03/MF A01

This report summarizes two key documents that reflect official U.S. space policy: (1) the January 1988 Presidential directive on overall U.S. national space policy; and (2) the February 1987 Department of Defense space policy. The report examines various U.S. military, civilian, commercial, and arms control activities as they relate to space. DOE

85 URBAN TECHNOLOGY AND TRANSPORTATION

Includes applications of space technology to urban problems; technology transfer; technology assessment; and surface and mass transportation.

For related information see also *03 Air Transportation and Safety, 16 Space Transportation,* and *44 Energy Production and Conversion.*

N89-13307# Federal Lab. Consortium, Washington, D. C.
FEDERAL LABORATORY CONSORTIUM FOR TECHNOLOGY TRANSFER: PUTTING TECHNOLOGY TO WORK. EXAMPLES OF INDUSTRY-LABORATORY COOPERATION CONTRIBUTING TO OUR NATION'S ECONOMIC STRENGTH
Mar. 1988 141 p
(PB88-243357) Avail: NTIS HC A07/MF A01 CSCL 05A

The Nations's Federal laboratories are proving increasingly effective in contributing to the economy through technology transfer. Laboratory technologies, expertise, and mission program interests have formed the basis for many commercial innovations. From the spinoff of small high technology companies into local incubator facilities, to long-term joint research and development with large companies, many Federal laboratories and agencies are demonstrating their commitment, the workability of their cooperative mechanisms, and the wealth of commercially attractive opportunities. The document is a collection of examples from 31 laboratories representing 7 government agencies; it should be viewed as indicative of the full potential for industry-laboratory cooperation to contribute to the nation's economic strength. GRA

N89-13082# Indian Inst. of Tech., Bombay. Center of Studies in Resources Engineering.
IMPORTANT ASPECTS OF TECHNOLOGY TRANSFER: TRAINING OF INSERVICE ENGINEERS AND SCIENTISTS; SATELLITE REMOTE SENSING
T. V. Pavate *In* ESA, Proceedings of the 1988 International Geoscience and Remote Sensing Symposium (IGARSS 1988) on Remote Sensing: Moving Towards the 21st Century, Volume 1 Aug. 1988 p 607-608 (For primary document see N89-12936 04-42)
Copyright Avail: NTIS HC A99/MF E03; ESA Publications Div., ESTEC, Noordwijk, Netherlands, 120 US dollars or 250 Dutch guilders

88 SPACE SCIENCES (GENERAL)

N89-13308# Max-Planck-Inst. fuer Physik und Astrophysik, Garching (West Germany). Inst. fuer Extraterrestrische Physik.
[ACTIVITIES REPORT OF THE INSTITUTE OF EXTRATERRESTRIAL ACTIVITIES] Status Report, 1985-1988
May 1988 107 p
(MPE-208; ISSN-0178-7101; ETN-88-93519) Copyright Avail: NTIS HC A06/MF A01

Research concerning solar and space plasma physics; the solar system; life cycle of stars; the interstellar medium; activity in galactic nuclei; and laboratory astrophysics is summarized. ESA

N89-13309# Observatorio del Ebro, Tortosa (Spain).
GEOMAGNETISM, A DYNAMIC SCIENCE [EL GEOMAGNETISMO CIENCIA EN PROGRESO]
J. O. Cardus 1988 55 p In SPANISH
(Rept-37; ETN-88-93545) Avail: NTIS HC A04/MF A01

The development of knowledge on geomagnetism is described to present important events throughout the last few centuries. Solar wind, magnetic storms, Earth magnetic field variability, ionospheric phenomena, and long range variations are discussed. ESA

89 ASTRONOMY

Includes radio, gamma-ray, and infrared astronomy, and astrometry.

N89-13310*# National Aeronautics and Space Administration. Ames Research Center, Moffett Field, Calif.
SECOND WORKSHOP ON IMPROVEMENTS TO PHOTOMETRY
William J. Borucki, ed. Sep. 1988 314 p Workshop held in Gaithersburg, Md., 5-6 Oct. 1987; sponsored by NASA, Ames Research Center, Moffett Field, Calif. and NBS, Gaithersburg, Md.
(NASA-CP-10015; A-88125; NAS 1.55:10015) Avail: NTIS HC A14/MF A01 CSCL 03A

The papers in these proceedings show that a major effort is under way to improve all aspects of photometry. Astronomical multichannel photometry, photodiodes, analog-to-digital converters, data reduction techniques, interference filters and optical fibers are discussed. For individual titles, see N89-13311 through N89-13327.

N89-13311*# National Science Foundation, Washington, D.C. Div. of Astronomical Sciences.
THE HUBBLE SPACE TELESCOPE HIGH SPEED PHOTOMETER
G. W. VanCitters, Jr., R. C. Bless, J. F. Dolan, J. L. Elliot, E. L. Robinson, and R. L. White *In* NASA, Ames Research Center,

Second Workshop on Improvements to Photometry Sep. 1988 p 1-15 (For primary document see N89-13310 04-89)
Avail: NTIS HC A14/MF A01 CSCL 03A

The Hubble Space Telescope will provide the opportunity to perform precise astronomical photometry above the disturbing effects of the atmosphere. The High Speed Photometer is designed to provide the observatory with a stable, precise photometer with wide dynamic range, broad wavelenth coverage, time resolution in the microsecond region, and polarimetric capability. Here, the scientific requirements for the instrument are examined, the unique design features of the photometer are explored, and the improvements to be expected over the performance of ground-based instruments are projected. Author

N89-13312*# Rome Univ. (Italy). Instituto Astronomico.
PRECISION LIMITS OF THE TWIN-BEAM MULTIBAND URSULA
G. A. DeBiase, L. Paterno, B. Fedel, G. Santagati, and R. Ventura (Catania Astrophysical Observatory, Italy) *In* NASA, Ames Research Center, Second Workshop on Improvements to Photometry Sep. 1988 p 17-33 (For primary document see N89-13310 04-89)
Avail: NTIS HC A14/MF A01 CSCL 03A

URSULA is a multiband astronomical photoelectric photometer which minimizes errors introduced by the presence of the atmosphere. It operates with two identical channels, one for the star to be measured and the other for a reference star. After a technical description of the present version of the apparatus, some measurements of stellar sources of different brightness, and in different atmospheric conditions are presented. These measurements, based on observations made with the 91 cm Cassegrain telescope of the Catania Astrophysical Observatory, are used to check the photometer accuracy and compare its performance with that of standard photometers. Author

N89-13313*# Technische Univ., Munich (West Germany).
A MULTICHANNEL FIBER OPTIC PHOTOMETER PRESENT PERFORMANCE AND FUTURE DEVELOPMENTS
H. Barwig, R. Schoembs, and G. Huber *In* NASA, Ames Research Center, Second Workshop on Improvements to Photometry Sep. 1988 p 35-46 (For primary document see N89-13310 04-89) (Grant Ba-867/2-1)
Avail: NTIS HC A14/MF A01 CSCL 03A

A three channel photometer for simultaneous multicolor observations was designed with the aim of making possible highly efficient photometry of fast variable objects like cataclysmic variables. Experiences with this instrument over a period of three years are presented. Aspects of the special techniques applied are discussed with respect to high precision photometry. In particular, the use of fiber optics is critically analyzed. Finally, the development of a new photometer concept is discussed. Author

N89-13314*# National Aeronautics and Space Administration. Ames Research Center, Moffett Field, Calif.
TESTS OF A MULTICHANNEL PHOTOMETER BASED ON SILICON DIODE DETECTORS
William J. Borucki, L. E. Allen, S. W. Taylor, E. B. Torbet, A. R. Schaefer, and J. Fowler (National Bureau of Standards, Gaithersburg, Md.) *In its* Second Workshop on Improvements to Photometry Sep. 1988 p 47-55 (For primary document see N89-13310 04-89)
Avail: NTIS HC A14/MF A01 CSCL 03A

A breadboard photometer was constructed that demonstrates a precision of 2 times 10 to the 4th power in the laboratory and scintillation-limited performance when used with an 0.5 m aperture telescope. Because the detectors and preamps are not cooled, only stars with m sub v approx. less than 4 are bright enough to allow the photometer to attain a precision of 1 times 10 to the 3rd power for three minute observations with an 0.5 m aperture telescope. Cooling the telescope should allow much fainter stars to be observed. Increasing the aperture of the telescope will allow higher precision and the observation of fainter stars. Author

N89-13315*# Royal Greenwich Observatory, Herstmonceux (England). Deudneys Cottage.
A FIBRE OPTIC, FOUR CHANNEL COMPARATIVE PHOTOMETER
E. N. Walker *In* NASA, Ames Research Center, Second Workshop on Improvements to Photometry Sep. 1988 p 57-81 (For primary document see N89-13310 04-89)
Avail: NTIS HC A14/MF A01 CSCL 03A

Development of a four channel comparative photometer is described. Tests have shown that it is stable from night to night and is capable of working in very poor sky conditions. Even when the sky conditions are so poor that stars are barely visible, light curves can still be obtained with an r.m.s. value of 0.0016 mag., provided that integration times that are long compared with the transparancy changes are possible. Author

N89-13316*# International Research and Development Co. Ltd., Newcastle (England).
OPTICAL AND ELECTRICAL MEASUREMENTS ON UV SENSITIVE PHOTODIODES
H. Lyall and A. D. Wilson (Barr and Stroud Ltd., Glasgow, Scotland) *In* NASA, Ames Research Center, Second Workshop on Improvements to Photometry Sep. 1988 p 85-109 (For primary document see N89-13310 04-89)
Avail: NTIS HC A14/MF A01 CSCL 03A

The optical and electrical characteristics of the various types of photodiodes potentially useful for UV radiometers were studied. It was concluded that both GaAsP and GaP photodiodes have advantages over silicon photodiodes in terms of spectral response and UV stability. Both GaAsP and GaP have excellent electrical characteristics for low frequency radiometers, although their high capacitance could be inconvenient for high frequency applications. GaAsP is particularly good with respect to dynamic range.
Author

N89-13317*# National Bureau of Standards, Gaithersburg, Md.
APPLICATION OF PN AND AVALANCHE SILICON PHOTODIODES TO LOW-LEVEL OPTICAL
G. Eppeldauer (Hungarian Academy of Sciences, Budapest.) and A. R. Schaefer *In* NASA, Ames Research Center, Second Workshop on Improvements to Photometry Sep. 1988 p 111-151 (For primary document see N89-13310 04-89)
Avail: NTIS HC A14/MF A01 CSCL 03A

New approaches to the discovery of other planetary systems require very sensitive and stable detection techniques in order to succeed. Two methods in particular, the astrometric and the photometric methods, require this. To begin understanding the problems and limitations of solid state detectors regarding this application, preliminary experiments were performed at the National Bureau of Standards and a low light level detector characterization facility was built. This facility is briefly described, and the results of tests conducted in it are outlined. A breadboard photometer that was used to obtain stellar brightness ratio precision data is described. The design principles of PN and avalanche silicon photodiodes based on low light level measuring circuits are discussed. Author

N89-13318*# Cambridge Research and Instrumentation, Inc., Mass.
ABSOLUTE PHOTOMETRIC CALIBRATION OF DETECTORS TO 0.3 mmag USING AMPLITUDE-STABILIZED LASERS AND A HELIUM-COOLED ABSOLUTE RADIOMETER
Peter J. Miller *In* NASA, Ames Research Center, Second Workshop on Improvements to Photometry Sep. 1988 p 153-178 (For primary document see N89-13310 04-89)
Avail: NTIS HC A14/MF A01 CSCL 03A

Laser sources whose intensity is determined with a cryogenic electrical substitution radiometer are described. Detectors are then calibrated against this known flux, with an overall error of 0.028 percent (0.3 mmag). Ongoing research has produced laser intensity stabilizers with flicker and drift of less than 0.01 percent. Recently, the useful wavelength limit of these stabilizers have been extended to 1.65 microns by using a new modular technology and InGaAs

detector systems. Data from Si photodiode calibration using the method of Zalewski and Geist are compared against an absolute cavity radiometer calibration as an internal check on the calibration system. Author

N89-13319*# McDonald Observatory, Austin, Tex.
ANALOG-TO-DIGITAL CONVERSION TECHNIQUES FOR PRECISION PHOTOMETRY
Chet B. Opal *In* NASA, Ames Research Center, Second Workshop on Improvements to Photometry Sep. 1988 p 179-192 (For primary document see N89-13310 04-89)
Avail: NTIS HC A14/MF A01 CSCL 03A

Three types of analog-to-digital converters are described: parallel, successive-approximation, and integrating. The functioning of comparators and sample-and-hold amplifiers is explained. Differential and integral linearity are defined, and good and bad examples are illustrated. The applicability and relative advantages of the three types of converters for precison astronomical photometric measurements are discussed. For most measurements, integral linearity is more important than differential linearity. Successive-approximation converters should be used with multielement solid state detectors because of their high speed, but dual slope integrating converters may be superior for use with single element solid state detectors where speed of digitization is not a factor. In all cases, the input signal should be tailored so that they occupy the upper part of the converter's dynamic range; this can be achieved by providing adjustable gain, or better by varying the integration time of the observation if possible. Author

N89-13320*# National Bureau of Standards, Gaithersburg, Md.
AN INTRODUCTION TO BLOCKED IMPURITY BAND DETECTORS Abstract Only
Jon Geist *In* NASA, Ames Research Center, Second Workshop on Improvements to Photometry Sep. 1988 p 193 (For primary document see N89-13310 04-89)
Avail: NTIS HC A14/MF A01 CSCL 03A

Blocked impurity band detectors fabricated using standard silicon technologies offer the possibility of combining high sensitivity and high accuracy in a single detector operating in a low background environment. The solid state photomultiplier described by Petroff et al., which is a new type of blocked impurity band detector, offers even higher sensitivity as well as operation in the visible spectral region. The principle of operation and possible application of blocked impurity band detectors for stellar seismology and the search for extra-solar planets are described. Author

N89-13321*# Lowell Observatory, Flagstaff, Ariz.
MONITORING SOLAR-TYPE STARS FOR LUMINOSITY VARIATIONS
G. W. Lockwood and B. A. Skiff *In* NASA, Ames Research Center, Second Workshop on Improvements to Photometry Sep. 1988 p 197-214 (For primary document see N89-13310 04-89)
Avail: NTIS HC A14/MF A01 CSCL 03A

Since 1984, researchers have made more than 1500 differential photometric b (471 nm) and y (551 nm) measurements of three dozen solar-like lower main sequence stars whose chromospheric activity was previosly studied by O. C. Wilson. Here, researchers describe their methodology and the statistical tests used to distinguish intrinsic stellar variability from observational and instrument errors. The incidence of detected variability among the program and comparison stars is summarized. Among the 100 plus pairs of stars measured differentially, only a dozen were found that were unusually constant, with peak-to-peak amplitudes of seasonal mean brightness smaller than 0.3 percent (0.003 mag) over a two-to-three-year interval. Author

N89-13322*# San Diego State Univ., Calif. Dept. of Astronomy.
IMPROVEMENTS TO PHOTOMETRY. PART 1: BETTER ESTIMATION OF DERIVATIVES IN EXTINCTION AND TRANSFORMATION EQUATIONS
Andrew T. Young *In* NASA, Ames Research Center, Second Workshop on Improvements to Photometry Sep. 1988 p 215-245 (For primary document see N89-13310 04-89)
Avail: NTIS HC A14/MF A01 CSCL 03A

Atmospheric extinction in wideband photometry is examined both analytically and through numerical simulations. If the derivatives that appear in the Stromgren-King theory are estimated carefully, it appears that wideband measurements can be transformed to outside the atmosphere with errors no greater than a millimagnitude. A numerical analysis approach is used to estimate derivatives of both the stellar and atmospheric extinction spectra, avoiding previous assumptions that the extinction follows a power law. However, it is essential to satify the requirements of the sampling theorem to keep aliasing errors small. Typically, this means that band separations cannot exceed half of the full width at half-peak response. Further work is needed to examine higher order effects, which may well be significant. Author

N89-13323*# National Bureau of Standards, Gaithersburg, Md.
AN OPTICAL HETERODYNE DENSITOMETER
A. L. Migdall, Ying Cong Zheng, J. Hardis, and J. J. Snyder *In* NASA, Ames Research Center, Second Workshop on Improvements to Photometry Sep. 1988 p 249-253 (For primary document see N89-13310 04-89)
Avail: NTIS HC A14/MF A01 CSCL 03A

Researchers are developing an optical heterodyne densitometer with the potential to measure optical density over an unprecedented dynamic range with high accuracy and sensitivity. This device uses a Mach-Zender interferometer configuration with heterodyne detection to make direct comparisons between optical and RF attenuators. Researchers expect to attain measurements of filter transmittance down to 10 to the minus 12th power with better than 1 percent uncertainty. In addition, they intend to extend the technique to the problem of measuring low levels of light scattering from reflective and transmissive optics. Author

N89-13324*# PTR Optics Corp., Waltham, Mass.
FIBER OPTIC WAVELENGTH DIVISION MULTIPLEXING: PRINCIPLES AND APPLICATIONS IN TELECOMMUNICATIONS AND SPECTROSCOPY
R. K. Erdmann and B. D. Walton *In* NASA, Ames Research Center, Second Workshop on Improvements to Photometry Sep. 1988 p 255-276 (For primary document see N89-13310 04-89)
Avail: NTIS HC A14/MF A01 CSCL 03A

Design and fabrication tradeoffs of wavelength division multiplexers are discussed and performance parameters are given. The same multiplexer construction based on prism gratings has been used in spectroscopic applications, in the wavelength region from 450 to 1600 nm. For shorter wavelengths down to 200 nm, a similar instrument based on longer fibers (500 to 1000 micrometer) has been constructed and tested with both a fiber array and a photodiode detector array at the output. Author

N89-13325*# Pennsylvania State Univ., University Park.
USE OF OPTICAL FIBERS IN SPECTROPHOTOMETRY
Lawrence W. Ramsey *In* NASA, Ames Research Center, Second Workshop on Improvements to Photometry Sep. 1988 p 277-288 (For primary document see N89-13310 04-89)
Avail: NTIS HC A14/MF A01 CSCL 03A

The use of single or small numbers of fiber optic fibers in astronomical spectroscopy with the goal of greater spectrophotometric and radial velocity accuracy is discussed. The properties of multimode step index fibers which are most important for this application are outlined, as are laboratory tests of currently available fibers. Author

N89-13326*# Hawaii Univ., Hilo. Dept. of Physics and Astronomy.
A CONSIDERATION OF THE USE OF OPTICAL FIBERS TO REMOTELY COUPLE PHOTOMETERS TO TELESCOPES
William D. Heacox *In* NASA, Ames Research Center, Second

Workshop on Improvements to Photometry Sep. 1988 p 289-301 (For primary document see N89-13310 04-89)
Avail: NTIS HC A14/MF A01 CSCL 03A

The possible use of optical fiers to remotely couple photometers to telescopes is considered. Such an application offers the apparent prospect of enhancing photometric stability as a consequence of the benefits of remote operation and decreased sensitivity to image details. A properly designed fiber optic coupler will probably show no significant changes in optical transmisssion due to normal variations in the fiber configuration. It may be more difficult to eliminate configuration-dependent effects on the pupil of the transmitted beam, and thus achieve photometric stability to guiding and seeing errors. In addition, there is some evidence for significant changes in the optical throughputs of fibers over the temperature range normally encountered in astronomical observatories. Author

N89-13327*# Arizona Univ., Tucson. Optical Sciences Center.
MOISTURE ADSORPTION IN OPTICAL COATINGS
H. Angus Macleod *In* NASA, Ames Research Center, Second Workshop on . Improvements to Photometry Sep. 1988 p 303-320 (For primary document see N89-13310 04-89)
Avail: NTIS HC A14/MF A01 CSCL 03A

The thin film filter is a very large aperture component which is exceedingly useful because of its small size, flexibility and ease of mounting. Thin film components, however, do have defects of performance and especially of stability which can cause problems in systems, particularly where long-term measurements are being made. Of all of the problems, those associated with moisture absorption are the most serious. Moisture absorption occurs in the pore-shaped voids inherent in the columnar structure of the layers. Ion-assisted deposition is a promising technique for substantially reducing moisture adsorption effects in thin film structures. Author

N89-13328 Michigan Univ., Ann Arbor.
OBSERVATIONS OF A COMPLETE SAMPLE OF EMISSION-LINE GALAXIES Ph.D. Thesis
John Joseph Salzer 1987 265 p
Avail: Univ. Microfilms Order No. DA8801411

Optical spectroscopic and broad band imaging observations have been obtained for all 172 emission-line galaxy (ELG) candidates in Lists IV and V of the University of Michigan Curtis Schmidt Objective Prism (UM) Survey. These data allow for the accurate determination of the completeness limits and selection characteristics of the survey and provide valuable information about the physical nature of the survey constituents. The UM survey is found to be comprehensive in the sense that it includes a wide range of types of active galaxies. Analysis of the data shows that the completeness characteristics of this survey are most accurately parameterized using emission-line flux and equivalent width. This result leads to the definition of a complete sample of UM galaxies which is used to determine the relative populations of the various types of ELGs found in the survey. Dissert. Abstr.

N89-13329 California Inst. of Tech., Pasadena.
A FAR-INFRARED HETERODYNE SPECTROMETER FOR AIRBORNE ASTRONOMY Ph.D. Thesis
Erich Nathan Grossman 1988 221 p
Avail: Univ. Microfilms Order No. DA8803395

The design and construction of a heterodyne spectrometer for airborne astronomy in the 50 to 200 micrometer wavelength range is described, along with laboratory measurements of its performance. The astronomical and technical context of the project, the constraints which the astronomical goals set on the instrument, and the advantages and drawbacks of each of the various broad instrumental strategies that are available for spectrometer design are described. An extensive series of measurements of bandwidth, photoconductive gain, and direct detection responsibility for a series of highly compensated, NTD detectors grown specifically for this purpose are presented. The operating principles and construction of the FIR laser are described. The construction and performance of the corner-cubes is outlined, including the first direct measurement of the main beam efficiency of a corner-cube antenna in the FIR, and a comparison with theory. A detailed, quantitative model was developed for the conversion efficiency obtainable from Schottky diodes in this application. Dissert. Abstr.

N89-13330*# National Aeronautics and Space Administration, Washington, D.C.
INFRARED OBSERVATIONS OF COMETS HALLEY AND WILSON AND PROPERTIES OF THE GRAINS
Martha S. Hanner, ed. (Jet Propulsion Lab., California Inst. of Tech., Pasadena.) Sep. 1988 200 p Workshop held at Ithaca, N.Y., 10-12 Aug. 1987
(NASA-CP-3004; NAS 1.55:3004) Avail: NTIS HC A09/MF A01 CSCL 03A

The presented papers and discussions at a workshop held at Cornell Univ. are summarized. The infrared observations of Comet Halley and Comet Wilson are reviewed and they are related to optical properties and composition of cometary grains. Relevant laboratory studies are also discussed. Recommendations are made for future infrared comet observations and supporting laboratory investigations. For individual titles, see N89-13331 through N89-13368.

N89-13331*# Planetary Science Inst., Tucson, Ariz.
INFRARED OBSERVATIONS OF THE DUST COMA
Humberto C. Campins and Alan T. Tokunaga (Hawaii Univ., Honolulu.) *In* NASA, Washington, Infrared Observations of Comets Halley and Wilson and Properties of the Grains Sep. 1988 p 1-21 (For primary document see N89-13330 04-89)
Avail: NTIS HC A09/MF A01 CSCL 03A

The main infrared observational results were briefly reviewed at the start of this session. The new results are summarized. All of these results have yet to be synthesized into a self-consistent picture of the dust grain composition, dust production history, outburst mechanisms, and composition of the nucleus. The workshop discussion was helpful in pointing out problems faced by theorists, such as data quality, the lack of the proper theory for computing the scattering and emission of irregular particles, and in some cases the lack of optical constants of realistic materials. It is expected that the gross spectral and dynamical properties of Halley's Comet can be understood in time, even if the details of the observations and the theoretical calculations continue to vex us in the future. Author

N89-13332*# Jet Propulsion Lab., California Inst. of Tech., Pasadena.
GRAIN OPTICAL PROPERTIES
Martha Hanner *In* NASA, Washington, Infrared Observations of Comets Halley and Wilson and Properties of the Grains Sep. 1988 p 22-49 (For primary document see N89-13330 04-89)
Avail: NTIS HC A09/MF A01 CSCL 03A

The optical properties of small grains provide the link between the infrared observations presented in Chapter 1 and the dust composition described in Chapter 3. In this session, the optical properties were discussed from the viewpoint of modeling the emission from the dust coma and the scattering in order to draw inference about the dust size distribution and composition. The optical properties are applied to the analysis of the infrared data in several ways, and these different uses should be kept in mind when judging the validity of the methods for applying optical constants to real grains. Author

N89-13333*# Minnesota Univ., Minneapolis.
COMETARY DUST COMPOSITION
R. D. Gehrz and M. S. Hanner (Jet Propulsion Lab., California Inst. of Tech., Pasadena.) *In* NASA, Washington, Infrared Observations of Comets Halley and Wilson and Properties of the Grains Sep. 1988 p 50-63 (For primary document see N89-13330 04-89)
Avail: NTIS HC A09/MF A01 CSCL 03A

The earth based measurements and in situ sampling of Comet Halley have provided new data about the chemical composition of cometary grains. Recent progress in laboratory studies of

interplanetary dust particles (IDPs) complement the comet data, allowing inferences about the mineralogy and physical structure of the comet dust to be drawn from the observed elemental composition and infrared spectra. The in situ dust composition measurements at Halley, the composition of IDPs and their relation to comet dust, and the origin of the 3.4 micron hydrocarbon feature is discussed. Related discussion is also presented on aromatic components in comets and the 3.4 micron feature. These topics are briefly summarized. Author

N89-13334*# Martin Marietta Aerospace, Denver, Colo. Planetary Sciences Lab.
PIA UPDATE: CORRELATION ANALYSES OF MASS SPECTRA
L. W. Mason and B. C. Clark *In* NASA, Washington, Infrared Observations of Comets Halley and Wilson and Properties of the Grains Sep. 1988 p 64-65 (For primary document see N89-13330 04-89)
Avail: NTIS HC A09/MF A01 CSCL 03A

The PIA instrument aboard the Giotto spacecraft (a time of flight spectrometer) has been presented elsewhere. The mass spectra used in this analysis were decoded and mass numbers assigned according to the presence of carbon and silver, using the global values for these elements in their spectral absence. The results presented here were obtained using a frequency of occurrence based on analysis which correlated how often mass numbers appear in the mass spectra and which mass numbers tend to occur together in the same spectra; no amplitude information is utilized. The data are presented as plots of mass vs coincident mass for different subsets of the PIA data set, with both axes having units of atomic mass. Frequency contours are plotted at approximately five percent contour intervals, relative to the maximum AMU occurrence in that plot. The plots presented are symmetrical about the matrix diagonal, i.e., every mass is coincident with itself in a given spectra. Author

N89-13335*# Washington Univ., Seattle. Dept. of Astronomy.
A COMPARISON OF HALLEY DUST WITH METEORITES, INTERPLANETARY DUST AND INTERSTELLAR GRAINS
D. E. Brownlee *In* NASA, Washington, Infrared Observations of Comets Halley and Wilson and Properties of the Grains Sep. 1988 p 66-67 (For primary document see N89-13330 04-89)
Avail: NTIS HC A09/MF A01 CSCL 03A

The variability of the mineral forming elements in the submicron Halley grains provides a powerful basis for comparison of Halley with the different classes of meteoritic materials that have been studied in the lab. The degree of variability in the Halley samples is larger than that seen in chondrites implying that Halley is more heterogeneous at the submicron scale. A critical distinction is that Halley contains abundant pure Mg silicates at the size scale while the carbon rich meteorites do not. The submicron dispersion composition seen in Halley is dramatically different from the narrowly constrained compositions seen in CI and CM (type 1 and 2) carbonaceous chondrites. These meteorites are carbon rich but are dominated by a hydrated silicate with a very narrow range of Mg/Si ratio. The Halley results are also unlike the composition variations seen in most of interplanetary dust types that are dominated by hydrated materials. The only known class of meteoritic material that appear to closely resemble the Halley data is a class of cosmic dust composed entirely of anhydrous minerals. The composition implies that Halley is dominated by olivine, pyroxene, iron sulfide, glass and amorphous carbonaceous matter. Author

N89-13336*# National Aeronautics and Space Administration. Ames Research Center, Moffett Field, Calif.
THE SPECTRAL PROPERTIES OF INTERPLANETARY DUST PARTICLES
Scott A. Sandford *In* NASA, Washington, Infrared Observations of Comets Halley and Wilson and Properties of the Grains Sep. 1988 p 68-72 (For primary document see N89-13330 04-89)
Avail: NTIS HC A09/MF A01 CSCL 03A

The observed spectral and mineralogical properties of interplanetary dust particles (IDP) allows the conclusion that: (1) the majority of IDP infrared spectra are dominated by olivine, pyroxene, or layer lattice silicate minerals, (2) to the first order the emission spectra of comets Halley and Kohoutek can be matched by mixtures of these IDP infrared types, implying that comets contain mixtures of these different crystalline silicates and may vary from comet to comet and perhaps even within a single comet, (3) do not expect to observe a single 20 micron feature in cometary spectra, (4) carbonaceous materials dominate the visible spectra properties of the IDPs even though the mass in these particles consists primarily of silicates, and (5) the particle characteristics summarized need to be properly accounted for in future cometary emission models. Author

N89-13337*# National Aeronautics and Space Administration. Ames Research Center, Moffett Field, Calif.
AROMATIC COMPONENTS IN COMETARY MATERIALS
Abstract Only
Louis J. Allamandola, Scott A. Sandford, and B. Wopenka (Washington Univ., St. Louis, Mo.) *In* NASA, Washington, Infrared Observations of Comets Halley and Wilson and Properties of the Grains Sep. 1988 p 73-74 (For primary document see N89-13330 04-89)
Avail: NTIS HC A09/MF A01 CSCL 03A

The Raman spectra of interplanetary dust particles (IDPs) collected in the stratosphere show that two bands at about 1350 and 1600 delta/cm and a broader feature between 2200 and 3300 delta/cm that are characteristic of aromatic molecular units with ordered domains smaller than 25 A in diameter. This suggests that the carbonaceous material in IDPs may be similar to the polymeric component seen in meteorites, where this material is thought to consist of aromatic molecular units that are randomly interlinked by short aliphatic bridges. The features in the Raman spectra of IDPs are similar in position, and relative strength to interstellar infrared emission features that have been attributed to vibrational transitions in free molecular polycyclic aromatic hydrocarbons. Taken together, these observations suggest that some fraction of the carbonaceous materials in IDPs may have been produced in circumstellar dust shells and only slightly modified in interstellar space. Author

N89-13338*# State Univ. of New York, Stony Brook. Astronomy Program.
THE 3.4 MICROMETER EMISSION FEATURE IN COMET HALLEY
Timothy Y. Brooke and R. F. Knacke *In* NASA, Washington, Infrared Observations of Comets Halley and Wilson and Properties of the Grains Sep. 1988 p 75-78 (For primary document see N89-13330 04-89)
Avail: NTIS HC A09/MF A01 CSCL 03A

Several teams of ground based observers reported observations of the emission feature centered at 3.36 micrometers in comet Halley following its discovery by the Vega 1 spacecraft. The position and shape of the band indicate a superposition of emissions by C-H groups. But the mechanism for the excitation of these C-H3 groups is still not agreed upon. Three possibilities are summarized. Elucidation of the emission mechanism is needed to determine whether the source is predominately solid or gas. In addition, is it shown that the derived carbon abundance in Halley depends strongly on the assumed mechanism. Author

N89-13339*# Hawaii Univ., Honolulu.
COMPARISON OF THE 3.36 MICROMETER FEATURE TO THE ISM
Alan T. Tokunaga and Timothy Y. Brooke (State Univ. of New York, Stony Brook.) *In* NASA, Washington, Infrared Observations of Comets Halley and Wilson and Properties of the Grains Sep. 1988 p 79-82 (For primary document see N89-13330 04-89)
Avail: NTIS HC A09/MF A01 CSCL 03A

It has been noted that the 3.36 micrometer emission feature is not the same as that of any ISM band at 3.4 micrometer. This is documented herein. There is no convincing analog to the cometary 3.36 micrometer emission feature seen in the Interstellar Matter band. This fact suggests that if the carbonaceous material in comets

came from the ISM, it was either further processed in the solar nebula or has a different appearance because of the different excitation environment of the sun and ISM. Author

N89-13340*# Cornell Univ., Ithaca, N.Y. Lab. for Planetary Studies
A TWO COMPONENT MODEL FOR THERMAL EMISSION FROM ORGANIC GRAINS IN COMET HALLEY
Christopher Chyba and Carl Sagan *In* NASA, Washington, Infrared Observations of Comets Halley and Wilson and Properties of the Grains Sep. 1988 p 83-84 (For primary document see N89-13330 04-89)
Avail: NTIS HC A09/MF A01 CSCL 03A

Observations of Comet Halley in the near infrared reveal a triple-peaked emission feature near 3.4 micrometer, characteristic of C-H stretching in hydrocarbons. A variety of plausible cometary materials exhibit these features, including the organic residue of irradiated candidate cometary ices (such as the residue of irradiated methane ice clathrate, and polycyclic aromatic hydrocarbons. Indeed, any molecule containing -CH3 and -CH2 alkanes will emit at 3.4 micrometer under suitable conditions. Therefore tentative identifications must rest on additional evidence, including a plausible account of the origins of the organic material, a plausible model for the infrared emission of this material, and a demonstration that this conjunction of material and model not only matches the 3 to 4 micrometer spectrum, but also does not yield additional emission features where none is observed. In the case of the residue of irradiated low occupancy methane ice clathrate, it is argued that the lab synthesis of the organic residue well simulates the radiation processing experienced by Comet Halley. Author

N89-13341*# Observatoire de Paris-Meudon (France).
ON THE CARBON ABUNDANCE IN COMET HALLEY DERIVED FROM THE 3 MICRON FEATURE: COMPARISON WITH INTERSTELLAR DUST Abstract Only
Therese Encrenaz, J. L. Puget, and Louis dHendecourt *In* NASA, Washington, Infrared Observations of Comets Halley and Wilson and Properties of the Grains Sep. 1988 p 85 (For primary document see N89-13330 04-89)
Avail: NTIS HC A09/MF A01 CSCL 03A

In spite of some similarities with the infrared features observed in the interstellar medium, the 3 micron signature observed in comet Halley's spectrum shows two distinct differences: (1) the 3.28 micron and 3.37 micron cometary features are both in emission, while the 3.37 micron interstellar feature is most often observed in absorption; and (2) there is no associated emission feature beyond 6 micron in the cometary spectrum. These two facts can be simply explained if it is assumed that the excitation mechanism is resonance fluorescence by the solar IR radiation field. With this assumption, it is found that hydrocarbons are present in roughly equal quantities in both the saturated forms, with a total carbon abundance of about 30 percent of H2O. This carbon abundance can be compared with the abundances derived for the interstellar dust when all condensed (or condensable) components are considered. Author

N89-13342*# Applied Research Corp., Landover, Md.
POSSIBLE IDENTIFICATIONS OF THE 3.4 MICROMETER FEATURE
Anthony C. Danks and D. L. Lambert (Texas Univ., Austin.) *In* NASA, Washington, Infrared Observations of Comets Halley and Wilson and Properties of the Grains Sep. 1988 p 86-90 (For primary document see N89-13330 04-89)
Avail: NTIS HC A09/MF A01 CSCL 03A

A feature at 3.4 micrometer was first detected in Comet Halley by the IKS spectrometer on board the Vega 1 probe; and subsequently from the ground. The feature has since been reported in Comet Wilson. The presence of the feature is of considerable interest for a number of reasons. First, it may represent the detection of a new parent molecule, and when combined with data from Giotto and Vega yield new information on cometary chemistry and the early solar system composition. Secondly, it may represent a link to the interstellar medium, the feature corresponds in wavelength and shape with an interstellar feature seen in absorption in a luminous star, towards the Galactic center known as GC-IRS7. The feature in turn is thought to be related with a growing family of unidentified infrared emission features seen in stellar objects, planetary nebulae, reflection nebulae, HII regions and extra galactic sources. These features occur at wavelengths 3.3, 3.4, 3.5, 6.2, 7.7, 8.6, and 11.25 micrometers. Further identification theory is given. Author

N89-13343*# Aerospace Corp., Los Angeles, Calif. Space Sciences Lab.
LABORATORY INVESTIGATIONS
Ray W. Russell *In* NASA, Washington, Infrared Observations of Comets Halley and Wilson and Properties of the Grains Sep. 1988 p 91-104 (For primary document see N89-13330 04-89)
Avail: NTIS HC A09/MF A01 CSCL 03A

Laboratory studies related to cometary grains and the nuclei of comets can be broken down into three areas which relate to understanding the spectral properties, the formation mechanisms, and the evolution of grains and nuclei: (1) Spectral studies to be used in the interpretation of cometary spectra; (2) Sample preparation experiments which may shed light on the physical nature and history of cometary grains and nuclei by exploring the effects on grain emissivities resulting from the ways in which the samples are created; and (3) Grain processing experiments which should provide insight on the interaction of cometary grains with the environment in the immediate vicinity of the cometary nucleus as the comet travels from the Oort cloud through perihelion, and perhaps even suggestions regarding the relationship between interstellar grains and cometary matter. A summary is presented with a different view of lab experiments than is found in the literature, concentrating on measurement techniques and sample preparations especially relevant to cometary dust. Author

N89-13344*# Jet Propulsion Lab., California Inst. of Tech., Pasadena.
FOCUS ON THE FUTURE
Martha S. Hanner *In* NASA, Washington, Infrared Observations of Comets Halley and Wilson and Properties of the Grains Sep. 1988 p 105-116 (For primary document see N89-13330 04-89)
Avail: NTIS HC A09/MF A01 CSCL 03A

An assessment is made of what was learned from Halley and recommendations are made for future directions for infrared studies of comets and supporting lab investigations. The following issues are addressed: (1) What steps can be taken to achieve consistent interpretation of Halley infrared data; (2) How successful has the Halley Watch been for infrared studies; (3) What supporting lab research is needed; (4) What are the key infrared observations needed for future comets; and (5) How do current and future NASA programs relate to comet studies. Author

N89-13345*# State Univ. of New York, Stony Brook. Dept. of Earth and Space Sciences.
CURRENT STATUS OF THE INTERNATIONAL HALLEY WATCH INFRARED NET ARCHIVE
Brian B. McGuinness *In* NASA, Washington, Infrared Observations of Comets Halley and Wilson and Properties of the Grains Sep. 1988 p 117-122 (For primary document see N89-13330 04-89)
Avail: NTIS HC A09/MF A01 CSCL 03A

The primary purposes of the Halley Watch have been to promote Halley observations, coordinate and standardize the observing where useful, and to archive the results in a database readily accessible to cometary scientists. The intention of IHW is to store the observations themselves, along with any information necessary to allow users to understand and use the data, but to exclude interpretations of these data. Each of the archives produced by the IHW will appear in two versions: a printed archive and a digital archive on CD-ROMs. The archive is expected to have a very long lifetime. The IHW has already produced an archive for P/Crommelin. This consists of one printed volume and two 1600

bpi tapes. The Halley archive will contain at least twenty gigabytes of information. Author

N89-13346*# National Aeronautics and Space Administration. Ames Research Center, Moffett Field, Calif.

INTERSTELLAR GRAIN CHEMISTRY AND THE COMPOSITION OF COMETS Abstract Only

Louis J. Allamandola, Scott A. Sandford, and F. P. J. Valero *In* NASA, Washington, Infrared Observations of Comets Halley and Wilson and Properties of the Grains Sep. 1988 p 127-128 (For primary document see N89-13330 04-89)

Avail: NTIS HC A09/MF A01 CSCL 03A

During the past 15 years considerable progress in observational techniques has been achieved in the middle infrared, the spectral region most diagnostic of molecular vibrations. Spectra of many different astronomical infrared sources are now available. By comparing these astronomical spectra with the spectra of lab ices, one can determine the composition and abundance of the icy materials frozen on the cold dust grains present in the interior of molecular clouds. In the experiments described, the assumption is made that cometary ices are similar to interstellar ices. As an illustration of the processes which can take place as an ice is irradiated and subsequently warmed, the infrared spectra is presented of the mixture H2O:CH3OH:CO:NH3:C6H14 (100:50:-10:10:10). Apart from the last species, the ratio of these compounds is representative of the simplest ices found in interstellar clouds. Author

N89-13347*# National Aeronautics and Space Administration. Ames Research Center, Moffett Field, Calif.

THE SPECTRAL APPEARANCE OF COMETS FROM 5 TO 20 MICROMETERS: A SURVEY OF THE DATA Abstract Only

Jesse D. Bregman *In* NASA, Washington, Infrared Observations of Comets Halley and Wilson and Properties of the Grains Sep. 1988 p 129-133 (For primary document see N89-13330 04-89)

Avail: NTIS HC A09/MF A01 CSCL 03A

Based on the concept of comets as being conglomerates of rocks and ices, it is expected that they reflect these components in their emission spectra. Silicate materials (rocks) are common in many astronomical environments and show prominent features at about 10 and 18 micrometers. Carbon should be abundant, but is much more difficult to detect spectroscopically since it has no strong features (except for the hydrogenated form). Ices are present in comets, but they are difficult to detect since they are volatile enough to dissipate when the comet is bright enough to be easily observed in the IR, with present equipment. There are other materials present in comets, but the ones listed above should be the most common and thus dominate the thermal IR spectrum. Most of the IR observations made on comets between 5 and 20 micrometers are summarized. They fall into three broad categories: (1) filter photometry; (2) circular variable filter wheel spectroscopy; and (3) spectra obtained with multidetector grating spectrometers. Author

N89-13348*# State Univ. of New York, Stony Brook. Astronomy Program.

THE NEAR-INFRARED POLARIZATION AND COLOR OF COMET HALLEY: WHAT CAN WE LEARN ABOUT THE GRAINS Abstract Only

Timothy Y. Brooke and R. F. Knacke *In* NASA, Washington, Infrared Observations of Comets Halley and Wilson and Properties of the Grains Sep. 1988 p 134-135 (For primary document see N89-13330 04-89)

Avail: NTIS HC A09/MF A01 CSCL 03A

The near infrared polarization and JHK colors of light scattered by dust grains in comet Halley were measured over a wide range in phase angle and heliocentric distance. Colors were redder than solar with no statistically significant variation with phase angle, heliocentric distance, or pre- and post-perihelion. This suggests that the grain population did not change drastically over time and that the data may be combined and modeled. However, short term variations in visible polarization and dust albedo were seen in Halley. Also, near infrared colors became systematically bluer after the observations were completed. The near infrared colors of Halley fall in the range of those of other comets. The near infrared polarization is similar to the visible polarization of Halley and other comets in showing a negative branch at small phase angles and an approximately linear rise toward positive values at larger phase angles. Mie theory calculations and a size distribution based on spacecraft data were used to model the near infrared polarization and color of comet Halley. Numerous lines of evidence point to the presence of dark, absorbing, probably carbonaceous materials in comets. Author

N89-13349*# Atmospheric and Environmental Research, Inc., Cambridge, Mass.

IR-DUST OBSERVATIONS OF COMET TEMPEL 2 WITH CRAF VIMS Abstract Only

Michael R. Combi, T. B. McCord, J. F. Bell, R. H. Brown, R. N. Clark, D. P. Cruikshank, T. V. Johnson, L. A. Lebofsky, and D. L. Matson (Jet Propulsion Lab., California Inst. of Tech., Pasadena.) *In* NASA, Washington, Infrared Observations of Comets Halley and Wilson and Properties of the Grains Sep. 1988 p 136 (For primary document see N89-13330 04-89)

Avail: NTIS HC A09/MF A01 CSCL 03A

Measurement strategies are now being planned for using the Visual and Infrared Mapping Spectrometer (VIMS) to observe the asteroid Hestia, and the nucleus, and the gas and dust in the coma of comet P/Tempel 2 as part of the Comet Rendezvous Asteroid Flyby (CRAF) mission. The spectral range of VIMS will cover wavelengths from 0.35 to 5.2 micrometers, with a spectral resolution of 11 nm from 0.35 to 2.4 micrometers and of 22 nm from 2.4 to 5.2 micrometers. The instantaneous field of view (IFOV) provided by the foreoptics is 0.5 milliradians, and the current design of the instrument provides for a scanning secondary mirror which will scan a swath of length 72 IFOVs. The CRAF high resolution scan platform motion will permit slewing VIMS in a direction perpendicular to the swath. This enables the building of a two dimensional image in any or all wavelength channels. Important measurements of the dust coma will include the onset of early coma activity, the mapping of gas and dust jets and correlations with active nucleus areas, observations of the dust coma from various scattering phase angles, coverage of the low wavelength portion of the thermal radiation, and the 3.4 micrometer hydrocarbon emission. A description of the VIMS instrument is presented. Author

N89-13350*# Jet Propulsion Lab., California Inst. of Tech., Pasadena.

COMETARY DUST SIZE DISTRIBUTIONS FROM FLYBY SPACECRAFT Abstract Only

Neil Divine *In* NASA, Washington, Infrared Observations of Comets Halley and Wilson and Properties of the Grains Sep. 1988 p 137-138 (For primary document see N89-13330 04-89)

Avail: NTIS HC A09/MF A01 CSCL 03A

Pior to the Halley flybys in 1986, the distribution of cometary dust grains with particle size were approximated using models which provided reasonable fits to the dynamics of dust tails, anti-tails, and infrared spectra. These distributions have since been improved using fluence data (i.e., particle fluxes integrated over time along the flyby trajectory) from three spacecraft. The fluence derived distributions are appropriate for comparison with simultaneous infrared photometry (from Earth) because they sample the particles in the same way as the IR data do (along the line of sight) and because they are directly proportional to the concentration distribution in that region of the coma which dominates the IR emission. Author

N89-13351*# Durham Univ. (England). Dept. of Physics.

POLARIZATION IMAGES OF COMET HALLEY Abstract Only

N. Eaton, S. M. Scarrott, and R. F. Warren-Smith *In* NASA, Washington, Infrared Observations of Comets Halley and Wilson and Properties of the Grains Sep. 1988 p 139-141 (For

primary document see N89-13330 04-89)
Avail: NTIS HC A09/MF A01 CSCL 03A

Observations from two dates 5 Jan. and 7 Jan. 1986 are presented. The images were obtained with the Durham imaging polarimeter on the 1-m telescope of the Wise Observatory, Israel. The observations were made through a broadband filter centered at 0.67 microns with a 0.17 micron effective bandwidth. This wavelength region should be dominated by continuum radiation. The intensity images cover 46 x 78 arcsecs. The intensity images are shown in logorithmic form and they are analyzed. Author

N89-13352*# Observatoire de Paris-Meudon (France).
DETECTION OF PARENT MOLECULES IN THE IR SPECTRUM OF P/HALLEY WITH THE IKS-VEGA SPECTROMETER
Abstract Only
Therese Encrenaz, J. Crovisier, M. Combes, V. I. Moroz, and A. Grigoriev (Academy of Sciences, USSR, Moscow) *In* NASA, Washington, Infrared Observations of Comets Halley and Wilson and Properties of the Grains Sep. 1988 p 142-144 (For primary document see N89-13330 04-89)
Avail: NTIS HC A09/MF A01 CSCL 03A

The two spectroscopic channels of the IKS experiment on board the Vega probes were designed for the detection of emission bands of parent molecules and/or cometary dust, in the 2.5 to 5 micrometer range and the 6 to 12 micron range respectively. On Vega 1, the experiment worked successfully, and cometary spectra were recorded at distances from the comet nucleus ranging from about 250,000 to 40,000 km. The field of view was 1 deg and the spectral resolving power was about 50. On Vega 2, no result could be obtained due to a failure of the cryogenic system. The emission spectra obtained are briefly analyzed. Author

N89-13353*# Minnesota Univ., Minneapolis. Dept. of Astronomy.
INFRARED OBSERVATIONS OF P/HALLEY AND P/ENCKE
Abstract Only
Robert D. Gehrz and E. P. Ney *In* NASA, Washington, Infrared Observations of Comets Halley and Wilson and Properties of the Grains Sep. 1988 p 145-146 Sponsored in part by NSF, Washington, D.C. (For primary document see N89-13330 04-89)
Avail: NTIS HC A09/MF A01 CSCL 03A

Broadband optical/infrared photometers responding from 0.5 to 23 microns mounted on the Univ. of Minnesota (UM) O'Brien 76-cm telescope, Wyoming Infrared Observatory 234-cm telescope, and UM's Mount Lemmon Infrared Observatory 152-cm telescope were used to measure comet Halley more than 30 times between 12 Dec. 1985 to 6 May 1986. The Wyoming system was used to measure P/Encke on 24 Jul. 1987. The equipment and observations of Halley were fully described by Gehrz and Ney. Conclusions based on a preliminary analysis of the Halley and P/Encke data are reported. Author

N89-13354*# National Aeronautics and Space Administration. Goddard Space Flight Center, Greenbelt, Md.
AIRBORNE 20-65 MICRON SPECTROPHOTOMETRY OF COMET HALLEY Abstract Only
William Glaccum, S. H. Moseley, Humberto C. Campins, and R. F. Loewenstein (Yerkes Observatory, Williams Bay, Wis.) *In* NASA, Washington, Infrared Observations of Comets Halley and Wilson and Properties of the Grains Sep. 1988 p 147-149 (For primary document see N89-13330 04-89)
Avail: NTIS HC A09/MF A01 CSCL 03A

Observations of Comet Halley with a grating spectrometer on board the Kuiper Airborne Observatory on four nights in Dec. 1985 to Apr. 1986 are reported. Low resolution 20 to 65 micrometer spectra of the nucleus with a 40 arcsec FWHM beam was obtained on 17 Dec. 1985, and on 15 and 17 Apr. 1986. On 20 Dec. 1985, only a 20 to 35 micrometer spectrum was obtained. Most of the data have been discussed in a paper where the continuum was dealt with. In that paper, models were fit to the continuum that showed that more micron sized particles of grain similar to amorphous carbon were needed to fit the spectrum than were allowed by the Vega SP-2 mass distribution, or that a fraction of the grains had to be made out of a material whose absorption efficiency fell steeper than lambda sup -1 for lambda greater than 20 micrometers. Spectra was also presented taken at several points on the coma on 15 Apr. which showed that the overall shape to the spectrum is the same in the coma. Tabulated values of the data and calibration curves are available. The spectral features are discussed. Author

N89-13355*# Wyoming Univ., Laramie. Infrared Observatory.
AN ALBEDO MAP OF P/HALLEY ON 13 MARCH 1986
Abstract Only
Thomas L. Hayward, Gary L. Grasdalen, and S. F. Green (Kent Univ., Canterbury, England) *In* NASA, Washington, Infrared Observations of Comets Halley and Wilson and Properties of the Grains Sep. 1988 p 151-153 (For primary document see N89-13330 04-89)
Avail: NTIS HC A09/MF A01 CSCL 03A

An albedo map is presented of comet Halley from a 10 micrometer image taken from the Wyoming Infrared Observatory on 13 Mar. 1986, and a 7311 A CCD image taken from the Anglo-Australian Telescope about an hour later. To construct this map, the CCD image was first converted from 0.49 arcsec/pixel to 1 arcsec/pixel to match the scale of the 10 micron image, then both were calibrated in lambda F sub lambda units. According to the albedo map, most of the inner coma of Halley lies between gamma = 0.04 and 0.08. The overall smoothness of the map is remarkable considering the large dynamic range of the optical and IR maps, and the differences in spatial resolution and image processing. Author

N89-13356*# Arizona Univ., Tucson. Dept. of Physics.
THE PROBLEM OF CLUSTERING IN LABORATORY STUDIES OF COMETARY DUST Abstract Only
Donald R. Huffman *In* NASA, Washington, Infrared Observations of Comets Halley and Wilson and Properties of the Grains Sep. 1988 p 154-155 (For primary document see N89-13330 04-89)
Avail: NTIS HC A09/MF A01 CSCL 03A

In trying to understand the nature of interstellar or interplanetary dust grains it is tempting to simply rely on direct lab measurements of grain properties such as extinction. However, until agreement is achieved between directly measured extinction and the same property calculated from measured optical constants of the solid, application to astronomical observations is questionable. There are two major problems which are discussed: the problem of what optical constants to use in the calculation, and the almost unavoidable problem of particle clustering in lab studies. Regarding small particle measurements, a problem afflicting almost all lab measurements is the clustering of particles. Having failed in efforts to isolate particles, the solution to the problem was attempted with a simple theory which seems to adequately describe the extinction by small, clustered particles in many cases. The theory is briefly explained. Author

N89-13357*# Laboratoire d'Astronomie Spatiale, Marseille (France).
LIGHT SCATTERING OF LARGE ROUGH PARTICLES APPLICATION TO COMETARY GRAINS Abstract Only
Philippe L. Lamy and J. M. Perrin *In* NASA, Washington, Infrared Observations of Comets Halley and Wilson and Properties of the Grains Sep. 1988 p 156-157 (For primary document see N89-13330 04-89)
Avail: NTIS HC A09/MF A01 CSCL 03A

While the electromagnetic field scattered by a spherical particle is classically obtained by the Helmholtz equation, the general case of an arbitrary particle may be investigated in the general framework of the interaction of a wave with a scattering potential. A wave function then satisfies the Schroedinger equation. The general solution of the Schroedinger equation is given. The main disadvantage of this approach are its restriction to large particles and its scalar nature preventing the calculation of the polarization. However, Perrin and Lamy have shown how to avoid the second limitation and retrieve a vectorial description. They proved that in

the case of large spheres when the ad hoc assumptions are satisfied, the expression of the scattering amplitude may be approximated by an expansion series in partial waves, i.e., on a discrete basis. The analogy may be generalized, and the ratio of the two components for a rough particle obtained by taking the ratio of the reflectivities for the two directions of polarization. These reflectivities involve the simple and double reflections calculated following the method developed by Wolff for rough surfaces. The theory is further detailed. Author

N89-13358*# Kansas State Univ., Manhattan. Dept. of Physics.
THERMAL PROPERTIES OF HETEROGENEOUS GRAINS Abstract Only
David J. Lien *In* NASA, Washington, Infrared Observations of Comets Halley and Wilson and Properties of the Grains Sep. 1988 p 158-160 (For primary document see N89-13330 04-89)
Avail: NTIS HC A09/MF A01 CSCL 03A

Cometary dust is not spherical nor homogeneous, yet these are the assumptions used to model its thermal, optical, and dynamical properties. To better understand the effects of heterogeneity on the thermal and optical properties of dust grains, the effective dielectric constant for an admixture of magnetite and a silicate were calculated using two different effective medium theories: the Maxwell-Garnett theory and the Bruggeman theory. In concept, the MG theory describes the effective dielectric constant of a matrix material into which is embedded a large number of very small inclusions of a second material. The Bruggeman theory describes the dielectric constant of a well mixed aggregate of two or more types of materials. Both theories assume that the individual particles are much smaller than the wavelength of the incident radiation. The refractivity for a heterogeneous grain using the MG theory is very similar to the refractivity of the matrix material, even for large volume fractions of the inclusion. The equilibrium grain temperature for spherical particles sized from .001 to 100 microns in radius at 1 astronomical unit from the sun was calculated. Further explanation is given. Author

N89-13359*# Aerospace Corp., Los Angeles, Calif. Space Sciences Lab.
COMET HALLEY'S COLORFUL OUTBURSTS Abstract Only
David K. Lynch and Ray W. Russell *In* NASA, Washington, Infrared Observations of Comets Halley and Wilson and Properties of the Grains Sep. 1988 p 161-164 (For primary document see N89-13330 04-89)
(Contract NAS2-12370)
Avail: NTIS HC A09/MF A01 CSCL 03A

Two preperihelion outbursts by Comet Halley were observed, each showing different brightness changes at 2.3, 3.6, 4.6 and 10.3 micrometers. Neither event was observed from beginning to end. The first observation on 8 Nov. 1985 lasted on the order of a day and was accompanied by a tail-like appendage recorded photographically. During the outburst the IR colors changed dramatically, showing no significant change at 10.3 micrometers but showing progressively more change at shorter wavelengths over a time scale of a few hours. The second outburst measurement extended over several days (10 to 13 Jan. 1986) during which time the intensities at the four wavelengths increased by roughly the same amount. Although the outbursts were of different duration, the IR measurements suggest that the first event involved volatile ice particles that evaporated, while the second was associated with long lived nonvolatile dust grains. Author

N89-13360*# National Aeronautics and Space Administration. Ames Research Center, Moffett Field, Calif.
SOME 5-13 MICROMETER AIRBORNE OBSERVATIONS OF COMET WILSON 1986l: PRELIMINARY RESULTS Abstract Only
David K. Lynch, Ray W. Russell, F. C. Witteborn, Jesse D. Bregman, D. M. Rank, M. C Cohen, and Humberto C. Campins (Planetary Science Inst., Tucson, Ariz.) *In* NASA, Washington, Infrared Observations of Comets Halley and Wilson and Properties of the Grains Sep. 1988 p 165 (For primary document see N89-13330 04-89)
(Contract NAS2-12370)
Avail: NTIS HC A09/MF A01 CSCL 03A

Comet Wilson was observed from the Kuiper Airborne Observatory approximately 23.6 and 25.7 Apr. 1987, UT (approx. 3 to 5 days after perihelion) using the NASA-Ames Faint Object Grating Spectrometer. Spectrophotometric data were observed with a 21 inch aperture between 5 and 13 micrometer and with a spectral resolution of 50 to 100. Spectra of the inner coma and nucleus reveal a fairly smooth continuum with little evidence of silicate emission. The 5 to 8 micrometer color temperature of the comet was 300 + or - 15 K, approx. 15 percent higher than the equilibrium blackbody temperature. All three spectra of the nucleus show a new emission feature at approx. 12.25 micrometer approx. two channels (.22 micrometer) wide. Visual and photographic observations made during the time of these observations showed a broad faint, possible two component tail. No outburst activity was observed. Author

N89-13361*# National Aeronautics and Space Administration. Goddard Space Flight Center, Greenbelt, Md.
AERODYNAMIC PROPERTIES OF FRACTAL GRAINS: IMPLICATIONS FOR THE PRIMORDIAL SOLAR NEBULA
P. Meakin (Du Pont de Nemours, E. I. and Co., Wilmington, Del) and Bertram Donn *In* NASA, Washington, Infrared Observations of Comets Halley and Wilson and Properties of the Grains Sep. 1988 p 166-171 Submitted for publication (For primary document see N89-13330 04-89)
Avail: NTIS HC A09/MF A01 CSCL 03A

Under conditions in the primordial solar nebula and dense interstellar clouds, small grains have low relative velocities. This is the condition for efficient sticking and formation of fractal aggregates. A calculation of the ratio of cross section, sigma, to number of primary particles, N, for fractal clusters yielded 1n sigma/N = 0.2635 + 0.5189N sup (-0.1748). This ratio decreases slowly with N and approaches a constant for large N. Under the usual assumption of collisions producing spherical compact, uniform density aggregates, sigma/N varies as N sup -1/3 and decreases rapidly. Fractal grains are therefore much more closely coupled to the gas than are compact aggregates. This has a significant effect on the aerodynamic behavior of aggregates and consequently on their evolution and that of the nebula. Author

N89-13362*# Hawaii Univ., Honolulu. Inst. for Astronomy.
COLOR GRADIENTS IN THE COMA OF P/HALLEY Abstract Only
Karen Meech *In* NASA, Washington, Infrared Observations of Comets Halley and Wilson and Properties of the Grains Sep. 1988 p 172-173 (For primary document see N89-13330 04-89)
Avail: NTIS HC A09/MF A01 CSCL 03A

Some important information relevant to the understanding of the gas/dust dynamics near the surface of a comet nucleus concerns knowledge of the grain composition and scattering properties as well as the particle size distribution of dust in the coma. Ground based measurements of light scattered from the dust comae can provide some information about the physical grain properties, in particular about the mean optically dominant grain size. Optical spectra of continua of nine comets presented by Jewitt and Meech, 1986, show that all of the scattered light is reddened with respect to the Sun. There is significant scatter in the amount of reddening seen for different comets. In the near IF regions, the reddening decreases until near 2 to 3 micrometers where the reflectivity is nearly neutral. It is of particular interest to see if there are any observable changes in the grain size distribution during outburst. Although no coma colar changes were observed during the Nov. 1985 outbursts, a color gradient within the coma has been observed in Halley. Radial color gradients in J, H, and K images of Halley as reported by Campins have not been observed by the author. Author

N89-13363*# Kanazawa Inst. of Tech. (Japan).
OPTICAL PROPERTIES OF COMETARY GRAINS Abstract Only
Tadashi Mukai *In* NASA, Washington, Infrared Observations of Comets Halley and Wilson and Properties of the Grains Sep. 1988 p 175-177 (For primary document see N89-13330 04-89)
Avail: NTIS HC A09/MF A01 CSCL 03A

An analysis of visible/near IF polarimetry of Comet Halley leads to a variation of the complex refractive index m = n - i x k of grain material with wavelength, i.e., a slight decrease of n from 1.39 at lambda = 0.37 micrometer to 1.37 at lambda = 2.2 micrometers, in constrast to an increase of k from 0.024 at lambda = 0.37 micrometer to 0.042 at lambda 2.2 micrometers. The mass distribution of grains reported by Mazets et al. from in situ measurements of Vega 2 was applied in the analysis. Combining these optical constants with those of astronomical silicate proposed by Draine, cometary silicate is presented as a candidate for cometary grains. The complex refractive index of the proposed cometary silicate is shown. Based on Mie theory, an emission coefficiency of each of the grains in computed as well as its temperature, as functions of grain radius and sun comet (grain) distance. It is found that the tentative thermal spectrum from these cometary silicates, where the mass distribution of grains reported by Mazets from Vega 2 was applied, fits very well to the IR spectrum of Comet Halley. This means that cometary silicate can explain not only the phase angle and wavelength dependences of visible/near IF polarization, but also the thermal emission. Author

N89-13364*# Kent Univ., Canterbury (England). Unit for Space Sciences.
A POSSIBLE EXPLANATION FOR THE INCONSISTENCY BETWEEN THE GIOTTO GRAIN MASS DISTRIBUTION AND GROUND-BASED OBSERVATIONS Abstract Only
C. H. Perry, S. F. Green, and J. A. M. McDonnell *In* NASA, Washington, Infrared Observations of Comets Halley and Wilson and Properties of the Grains Sep. 1988 p 178-180 (For primary document see N89-13330 04-89)
Avail: NTIS HC A09/MF A01 CSCL 03A

Giotto measured the in situ Halley dust grain mass distribution with 2 instruments, Particle Impact Analyzer and Dust Impact Detection System (DIDSY), as well as the total intercepted mass from the deceleration of the spacecraft (Giotto Radio-Science Experiment, GRE). Ground based observations made shortly before encounter have fluxes much higher than would be predicted from Giotto data. It is concluded that Giotto DIDSY and GRE data represent observations of dust originating from a narrow track along the nucleus. They are consistent with ground based data, if assumptions are made about the level of activity along this track. The actual size distribution that should be used for modeling of the whole coma should not include the large mass excess actually observed by Giotto. Extrapolation of the small grain data should be used, since for these grains the velocity dispersion is low and temporal changes at the nucleus would not affect the shape of the mass distribution. Author

N89-13365*# Hawaii Univ., Honolulu. Inst. for Astronomy.
PROPERTIES OF INTERSTELLAR DUST IN REFLECTION NEBULAE Abstract Only
Kristin Seligren *In* NASA, Washington, Infrared Observations of Comets Halley and Wilson and Properties of the Grains Sep. 1988 p 181 (For primary document see N89-13330 04-89)
Avail: NTIS HC A09/MF A01 CSCL 03A

Observations of interstellar dust in reflection nebulae are the closest analog in the interstellar medium to studies of cometary dust in our solar system. The presence of a bright star near the reflection nebula dust provides the opportunity to study both the reflection and emission characteristics of interstellar dust. At 0.1 to 1 micrometer, the reflection nebula emission is due to starlight scattered by dust. The albedo and scattering phase function of the dust is determined from observations of the scattered light. At 50 to 200 micrometers, thermal emission from the dust in equilibrium with the stellar radiation field is observed. The derived dust temperature determines the relative values of the absorption coefficient of the dust at wavelengths where the stellar energy is absorbed and at far infrared wavelengths where the absorbed energy is reradiated. These emission mechanisms directly relate to those seen in the near and mid infrared spectra of comets. In a reflection nebula the dust is observed at much larger distances from the star than in our solar system, so that the equilibrium dust temperature is 50 K rather than 300 K. Thus, in reflection nebulae, thermal emission from dust is emitted at 50 to 200 micrometer. Author

N89-13366*# Los Alamos National Lab., N. Mex.
LABORATORY SIMULATIONS OF COMET SURFACES Abstract Only
John R. Stephens and Bo A. S. Gustafson (Florida Univ., Gainesville.) *In* NASA, Washington, Infrared Observations of Comets Halley and Wilson and Properties of the Grains Sep. 1988 p 182-183 (For primary document see N89-13330 04-89)
Avail: NTIS HC A09/MF A01 CSCL 03A

The geometric albedos of frozen mixtures consisting of colloidal silica and carbon black mixed with water have been measured over the wavelength range of 400 to 800 nm to compare with recent observations of Comet Halley. Data were obtained as a function of sample temperature, scattering angle, and wavelength as the frozen samples warmed to 0 C in vacuum. Scattering from water ice, flat black paint, and Kodak white reflectance paint were also measured. Lab simulations show that the change in albedo of the samples show that sublimation of the water from the sample surface can have a major effect on the albedo of a particle/ice sample in the visible. Such processing may have a marked effect on the visible albedo of comet surfaces as well. Author

N89-13367*# National Aeronautics and Space Administration. Ames Research Center, Moffett Field, Calif.
A MULTICOMPONENT MODEL OF THE INFRARED EMISSION FROM COMET HALLEY Abstract Only
K. S. Krishna Swamy, Scott A. Sandford, Louis J. Allamandola, F. C. Witteborn, and Jesse D. Bregman *In* NASA, Washington, Infrared Observations of Comets Halley and Wilson and Properties of the Grains Sep. 1988 p 184-185 (For primary document see N89-13330 04-89)
Avail: NTIS HC A09/MF A01 CSCL 03A

A model based on a mixture of coated silicates and amorphous carbon grains produces a good spectral match to the available Halley data and is consistent with the compositional and morphological information derived from interplanetary dust particle studies and Halley flyby data. The dark appearance of comets may be due to carbonaceous coatings on the dominant (by mass) silicates. The lack of a 10 micrometer feature may be due to the presence of large silicate grains. The optical properties of pure materials apparently are not representative of cometary materials. The determination of the optical properties of additional silicates and carbonaceous materials would clearly be of use. Author

N89-13368*# Hawaii Univ., Honolulu. Inst. for Astronomy.
THE NASA INFRARED TELESCOPE FACILITY COMET HALLEY MONITORING PROGRAM 2: POST-PERIHELION RESULTS Abstract Only
Alan T. Tokunaga, W. F. Golisch, D. M. Griep, C. D. Kaminski, and Martha S. Hanner (Jet Propulsion Lab., California Inst. of Tech., Pasadena.) *In* NASA, Washington, Infrared Observations of Comets Halley and Wilson and Properties of the Grains Sep. 1988 p 186 (For primary document see N89-13330 04-89)
Avail: NTIS HC A09/MF A01 CSCL 03A

The post perihelion results of a 1 to 20 micrometer infrared monitoring program of Comet Halley are presented. These results complement previous observations of the pre-perihelion passages of Halley. The observations cover the time period of Mar. 1986 to the present time. During the time the comet was observable, two or more observations were obtained per month. The most interesting results were: (1) a detectable change in the J-H and

H-K colors of Halley, and (2) a search for a nucleus rotation at J during 20 Feb. to 10 Mar. was unsuccessful. The perihelion J-H and K-K colors were constant at 0.48 + or - 0.01 and 0.17, respectively. A preliminary reduction of the data is given. It is concluded that the colors were at first similar to pre-perihelion and then changed from July onward to be bluer and more similar to the solar colors. This suggests that a change may have occurred in the composition of the dust coma of Halley in July 1986.
Author

N89-13369 Hawaii Univ., Honolulu.
PROPERTIES OF STELLAR ACTIVITY IN F STARS Ph.D. Thesis
John Roger Varsik 1987 193 p
Avail: Univ. Microfilms Order No. DA8810702

The evolution of chromospheric activity in stars from F2 to G2 as measured by CaII flux as a function of stellar age for a large sample of nearby field and cluster stars is investigated. Ages and masses for the field stars are estimated from theoretical isochrones using Stromgren colors to obtain effective temperatures, absolute magnitudes, and metallicities. The main-sequence F stars of solar composition with M sub * less than 1.325 solar mass follow an exponential chromospheric activity law, with an e-folding time of 2.04 Gyr. For M sub * greater that or equal to 1.324 solar mass the change in activity with age is small but is consistent with an exponential dependence with an e-folding time of 3.12 Gyr. The exponential decay and the small dependence of the e-folding time with mass are consistent with an overall quadrupole magnetiic field as proposed by Gill and Roxburgh (1984), rather than the generally assumed radial field geometry. The V sin i-age dependence for stars of solar composition appears best modeled by an exponential decay, also in agreement with the quadrupole magnetic field model. It has been suggested that the lack of low activity early F stars indicates that there is another component of chromospheric activity for stars with M sub * greater than or = 132 solar mass independent of the magnetic field. However, standard acoustic heating theory (Stein 1981) suggests that if activity in early F stars is generated mainly by acoustic heating, then activity in late F stars and in the Sun would be much greater than that which is observed. Dissert. Abstr.

N89-13370# Ceskoslovenska Akademie Ved, Ondrejov.
TENTH EUROPEAN REGIONAL ASTRONOMY MEETING OF THE IAU: ABSTRACTS
Oct. 1987 120 p Meeting held in Prague, Czechoslovakia, 24 Aug. 1987
(DE88-703273; INIS-mf-11267; CONF-8708269) Avail: NTIS (US Sales Only) HC A06/MF A01

The conference met in 13 sessions. Session 1: Development of active solar regions included papers on sunspots, the photometry thereof, the diagnostics of radio waves of active solar regions, etc. Session 2: The complex of interplanetary bodies included papers on interplanetary dust, meteors, asteroids and comets. Session 3 dealt with resonance in the solar system. Papers presented in the session Structure of galaxies and star formation dealt with the problems of the development of stars and galaxies and their properties immediately after formation. The session: Rapid variability of single, binary and multiple stars contained papers on star observation and star activity. In other sessions participants heard papers on ultraviolet star spectra, cosmology and the formation of galaxies, high-energy astrophysics, active extragalactic objects and binary stars. DOE

N89-13371# Academy of Sciences of the Ukrainian SSR, Kiev. Inst. Teoreticheskoj Fiziki
SPECTRAL VARIABILITY OF WOLF-RAYET STARS
S. V. Marchenko 1987 25 p In RUSSIAN; ENGLISH summary
(DE88-703325; ITF-87-55) Avail: NTIS (US Sales Only) HC A03/MF A01

The equivalent widths (W(sub lambda)) of six Wolf-Rayet stars are given. In the stars HD 193077, HD 192641 W(sub lambda) variability is rare. The HD 192103 spectra show small-scale night-to-night W(sub lambda) variations. The HD 191765 is the most active one among the six WR stars. From the 1984 year data, the periodical changes of W(sub lambda) in three lines are detected: P1/sup d/.74 + or - 0(sup d).38. An interpretation of the eclipsing binary HD 193576 observations are proposed using the hypothesis about a common low-density gas envelope around the system. DOE

N89-13372# Instituto y Observatorio Astronomico de Marina, San Fernando (Spain).
CARLSBERG MERIDIAN CATALOG LA PALMA NO. 3: OBSERVATIONS OF POSITIONS OF STARS AND PLANETS MADE IN THE YEAR 1986
1987 350 p Prepared in cooperation with Copenhagen Univ., Denmark; Royal Greenwich Observatory, Hailsham, United Kingdom; and the Real Inst. y Observatorio de la Armada, San Fernando, Spain
(ISBN-0-98-87006-3; ETN-88-93529) Avail: NTIS HC A15/MF A01

Positions in a smoothed version of the FK5 system for the equinox J2000.0, proper motions, and magnitudes of 19,156 stars north of - 45 deg declination are given. The limiting magnitude is 13.3. The stars include: 10,003 IRS, 2086 Hipparcos stars with poor astrometric history, 1950 reference stars around 204 benchmark radio sources, 2816 F-stars within 100 pc, 1107 G- and K-type stars, and 74 radio stars. The zenith mean errors are epsilon alpha cos delta = 0.arcsec 192, epsilon delta = 0.arcsec 183, and epsilon m = 0 m. 063. The proper motion mean errors are typically 0.arcsec 003 per year. The catalog also contains 2997 observations of 4 major planets, Callisto, and 61 minor planets. Cross-references are given to DM, AGK3, SAO, HD and the double star catalogs ADS and IDS. Tables of systematic corrections are included to transform the positions in Carlsberg Meridian Catalogs 1 and 2 to the same system as this catalog.
ESA

90 ASTROPHYSICS

Includes cosmology; celestial mechanics; space plasmas; and interstellar and interplanetary gases and dust.
For related information see also *75 Plasma Physics.*

N89-13373# Hiroshima Univ., Takehara (Japan). Research Inst. for Theoretical Physics.
STOCHASTIC STAGE OF AN INFLATIONARY UNIVERSE MODEL
Yasusada Nambu and Misao Sasaki Dec. 1987 13 p
(DE88-753149; RRK-87-31) Avail: NTIS (US Sales Only) HC A03/MF A01

Using the stochastic description of a scalar field on its phase space, we analyze the early stage of an inflationary universe model with Higgs-type potential. At this stage, quantum fluctuations play an important role for the dynamics of the scalar field as well as the classical potential force. We find that the velocity dispersion of the field (phi) becomes negligible within the Hubble timescale and the slow roll-over phase is realized, provided that (first derivative of phi sq) equal to or less than (V(phi)) initially. This supports the picture that inflation can set in for a wide class of pre-inflationary states, including thermal states, and the behavior of the scalar field is independent of such states. It also verifies the use of the slow roll-over approximation for most stages of the inflation. DOE

N89-13374 City Univ. of New York, N.Y.
GROWTH AND SEDIMENTATION OF DUST GRAINS IN THE PRIMITIVE SOLAR NEBULA Thesis
Alessandro Battaglia 1987 248 p
Avail: Univ. Microfilms Order No. DA8801681

The formation of the planets in the solar system is envisioned to occur via a gravitational instability in a thin layer of dust located at the midplane of the primitive solar nebula. The break-up of the dust layer gives rise to seed planets that, through successive

collisions, eventually form the present-day planets. The problem of the formation of the dust layer, beginning with a configuration in which the dust particles are uniformly mixed with the nebula's turbulent gas is addressed. In the process, four basic ingredients are needed: a model to describe the properties of turbulence in the nebula's gas; a model for the structure of the primitive solar nebula; a formalism to calculate the velocity of dust particles embedded in a turbulent fluid; and a formalism to calculate the space-time evolution of the initial population of dust grains. To describe the properties of turbulence in the primitive solar nebula, the model by Canuto et al., (1987b) which was favorably tested against a host of laboratory and astrophysical data, is used. The model of the primitive solar nebula by Cabot et al., (1987a,b), is also used, since it constitutes the most recent and physically plausible investigation of the problem. The results concerning the calculation of the velocity of particles embedded in a turbulent fluid were found to be unsatisfactory; therefore a new formalism was developed to express the latter quantity in terms of the properties of the turbulence in the fluid. A byproduct of this calculation is an expression for the coefficient of turbulent diffusion. Following the space-time evolution of the grains, a formalism was developed that stimulates the simultaneous processes of collisions and sedimentation of the dust grains in the primitive solar nebula. Dissert. Abstr.

N89-13375*# Smithsonian Astrophysical Observatory, Cambridge, Mass.
THEORETICAL STUDIES OF MASS LOSS AND SHOCK PHENOMENA IN COOL STAR ENVELOPES Semiannual Progress Reports No. 9 and 10, 1 Oct. 1987 - 30 Sep. 1988
Lee Hartmann Sep. 1988 17 p
(Grant NAGw-511)
(NASA-CR-182708; NAS 1.26:182708) Avail: NTIS HC A03/MF A01 CSCL 03B

Wind-disk interactions; disks in T Tauri stars; and T Tauri stars in the HR diagram are examined. B.G.

N89-13376 Arizona State Univ., Tempe.
ATOMIC AND MOLECULAR ABUNDANCES IN COMETS Ph.D. Thesis
Ichishiro Konno 1987 181 p
Avail: Univ. Microfilms Order No. DA8802787

Spectrophotometric observations of comet Giacobini-Zinner were obtained in March, June, September, and October 1985. The September observations were obtained at perihelion, exactly at the time of the International Cometary Explorer (ICE) encounter with the comet. Spatial profiles extracted from the long-slit spectra were analyzed by using the Monte Carlo method to determine scale lengths and lifetimes for the observed radicals, C2 and NH2, and their respective parent molecules. A spatial profile for H2O(+) along the projected tail axis of the comet was derived from the September data, and analyzed with a fountain model. Dissert. Abstr.

N89-13377# Ceskoslovenska Akademie Ved, Ostrava.
GRAVITATION, BLACK HOLES AND SPACE-TIME PHYSICS
Vojtech Ullmann 1986 273 p In CZECH
(DE88-703054; INIS-mf-11229) Avail: NTIS (US Sales Only) HC A12/MF A01

A wide range of questions relating to the general theory of relativity, the physics of gravitation, and space-time are discussed, including the relationships between gravitation and the other fields of physics, mainly electromagnetism and the special theory of relativity, Einstein general relativity theory (the consequences of the principle of equivalence), the physics of curved space-time, equations of the gravitation fields, properties of gravitational energy and gravitational waves. The properties are analyzed for certain significant solutions of the Einstein field equations, causality and the global structure of space-time, horizons, and the problem of space-time singularities. The physics of black holes is discussed in detail as the extreme manifestation of gravitation, also the problem of the structure and development of the universe with regard to present relativistic cosmology. Finally discussed are the Mach principle, the quantizing of the field of gravitation, and the problems of the unified theories of the field. DOE

N89-13378 Cornell Univ., Ithaca, N.Y.
THE TRANSFER OF CYCLOTRON PHOTONS THROUGH NEUTRON STAR ATAMOSPHERES Ph.D. Thesis
John Chi Lin Wang 1988 333 p
Avail: Univ. Microfilms Order No. DA8804499

An extensive Monte Carlo study of the transfer of cyclotron photons through the polar cap plasmas of accreting magnetized neutron stars was performed. The aim is to understand the physics of line transfer and to model cyclotron line emission features. The polar cap environment was modeled as an isothermal, plane parallel, purely scattering atmosphere threaded by a superstrong magnetic field that points in the direction parallel to the atmospheric normal. Electronic motion is classical along the field and quantized orthogonal to it. All atmospheric electrons reside in the ground state. Excitation to the first excited state occurs only in a resonant scatter. The transfer of unpolarized photons with resonant scattering was studied as the sole transfer mechanism. Recoil, natural line width, Doppler broadening, and noncoherent frequency redistribution effects are all included. Analytic scaling laws for quantities such as the number of scatters per photon experienced prior to escape are derived and confirmed numerically, and fits are obtained for such quantities. This study was extended to include polarization. The cold plasma and magnetic vacuum modes are used. The presence of two modes and mode switching breaks the scaling laws of unpolarized transfer. Cyclotron line emission features were modeled. This study is extended to include polarization using the cold plasma molds. Dissert. Abstr.

N89-13379 Texas Univ., Austin.
CARBON, NITROGEN AND OXYGEN ABUNDANCES IN THE CHEMICALLY PECULIAR STARS OF THE UPPER MAIN SEQUENCE Ph.D. Thesis
Scott Wilson Roby 1987 260 p
Avail: Univ. Microfilms Order No. DA8806407

Abundance of the three light elements, carbon, nitrogen, and oxygen (CNO), are obtained from low-noise, high-resolution reticon spectra of a variety of chemically peculiar (CP) stars with surface temperatures in the range 7000 to 18000 K. The survey includes 13 Am and related stars, 9 HgMn stars, 15 magnetic Ap stars (8 SrCrEu-typer and 7 Si type), 1 He-weak star, and 5 suitable standard composition stars. A quantitative abundance analysis was carried out using neutral lines of CNO and once-ionized lines of C at mostly red and near-infrared wavelengths and line-blanketed model atmospheres. Local thermodynamic equilibrium was assumed. This analysis provides the first comprehensive and uniform set of CNO abundances in the traditional classes of CP stars. The C and O abundances show a roughly monotonic increase with surface temperature in both the nonmagnetic and magnetic stars. The N abundance in the nonmagnetic stars is most deficient in the stars above 10,000 K, which is in conflict with the predictions for an overabundance at these temperatures based on models where diffusion is operating alone. In the magnetic stars, only stars with temperatures between 8000 and 10,000 K show large N deficiencies. It is proposed that a modest stellar wind coupled with upward diffusion can explain the observed large N deficiencies in the HgMn stars, and, perhaps, in the SrCrEu stars. It was also found that the largest N depletions are associated with weak or absent magnetic fields, which provide an argument against an alternative explanation of CP star abundance anomalies, the magnetic accretion theory. Dissert. Abstr.

N89-13380 Ohio State Univ., Columbus.
S-WAVES IN THE SPECTRUM OF CATACLYSMIC BINARIES Ph.D. Thesis
Panayiotis Hantzios 1988 124 p
Avail: Univ. Microfilms Order No. DA8812258

Time-resolved spectroscopy is presented for three cataclysmic binaries: WZ Sagittae, U Geminorum, and LX Serpentis. This study is focused on the S-wave component of the emission lines of

these systems. A procedure has been developed that enables the separation of the S-wave component from the disk component of the emission line profiles. The resulting S-wave profiles have been studied in terms of line flux and radial velocity variations through the orbital cycles. A set of theoretical models has been constructed for the geometrical structure of the gas stream and the hot spot region of the accretion disk around the white dwarf. The observed S-wave profiles have been matched with the theoretical profiles by changing the model parameters. The resulting comparison yields information about the geometry and emissivity distribution of the S-wave emitting region. For the three systems of this study it was found that the observed characteristics of the S-waves are consistent with the model that places the S-wave emitting region on the part of the gas stream that flows above the accretion disk. Dissert. Abstr.

N89-13381 Oxford Univ. (England).
THE LARGE-SCALE STRUCTURE OF THE UNIVERSE: SOME THEORETICAL CONSIDERATIONS Ph.D. Thesis
Colin Andrew McGill 1987 159 p
Avail: Univ. Microfilms Order No. BRD-81581

Several theoretical concepts relating to the large-scale structure of the universe are presented. In particular, various aspects of the hierarchical scenario are investigated. The initial perturbation field and its early evolution are discussed. Two-point correlation functions for galaxies, clusters, and superclusters are examined. Some effects of using velocity as distance measure are described. In particular, it will be argued that caustics in redshift space are an almost inevitable feature of the hierarchical scenario. The possibility that quasar Ly-alpha absorption lines are redshift caustics is suggested. Dissert. Abstr.

N89-13382 Washington Univ., Seattle.
MIXING AND STRUCTURAL CHANGES DURING MASS TRANSFER IN BINARY SYSTEMS Ph.D. Thesis
Charles Raymond Proffitt 1988 112 p
Avail: Univ. Microfilms Order No. DA8810582

Some aspects of the effects of the transfer of nuclear processed material in an interacting binary system are considered. When a main sequence star accretes material that has a higher mean atomic weight than was initially present on the surface of the main sequence star, a composition inversion is created. The stability of such a composition inversion is studied and the rate at which such an inversion will be destroyed by thermal instabilities is estimated. These estimates are applied to models of a one solar mass star just leaving the main sequence. Such a process may cause mixing throughout a substantial fraction of a star's envelope, and a main sequence star with a thin convective envelope may therefore dilute accreted material to an extent comparable to the dilution that would occur in a gaint star with a deep convective envelope. Dissert. Abstr.

N89-13383 University of Wales, Swansea.
THEORETICAL ASPECTS OF GRAVITATIONAL WAVE DETECTION Ph.D. Thesis
Massino Tinto 1987 201 p
Avail: Univ. Microfilms Order No. BRDX81899

Some theoretical problems regarding the detection of gravitational waves are analyzed by using networks of Laser Interferometric Detectors working in coincidence. The first investigation of this work is a study of the effect that a detector's location has on its sensitivity and the effect that the latitudes, relative longitudes and orientations of two detectors have on the probability of coincident detections of linearly polarized bursts. This is done in Appendix D in the form of a paper, written in collaboration with Professor Bernard F. Schutz. In Chapter 1 the main result of Appendix D was extended, namely the formula for the coincidence probability averaged over all thresholds of two antennas working in coincidence to the case of elliptically polarized waves. By plotting this function in terms of the detectors' orientations, for several pairs of likely locations, we can deduce those values optimizing coincidence rates. After pointing out that this function does not contain quantitatively exact information about the probability itself (which depends on the setectors' thresholds), in in Chapter 2 we deduce real coincidence rates for networks of two, three and four detectors observing bursts from coalescing binaries. In Chapter 3 we calculate coincidence rates as functions of the distance to the source by assuming the thresholds to be in a specific proportion. Since binary systems are homogeneously and isotropically distributed in the Universe, we can calculate the fraction of the total number of events out to a certain distance that a network of interferometers will be able to register over a given observing time. Dissert. Abstr.

N89-13384# Lawrence Livermore National Lab., Calif.
SYNTHESIS OF ACCRETION DISK AND NONTHERMAL SOURCE MODELS FOR AGN
David L. Band and Matthew A. Malkan (California Univ., Los Angeles.) 25 May 1988 4 p Presented at the Georgia State University Conference on Active Galactic Nuclei, Atlanta, Ga., 28 Oct. 1987 Submitted for publication
(Contract DE-AC04-76DP-00789)
(DE88-013098; UCRL-97451; CONF-8710344-1) Avail: NTIS HC A02/MF A01

A scenario for the central engine of AGN has been developed consisting of a massive black hole (MBH) onto which gas accretes through an accretion disk. The accretion disk radiates the observed optical and ultraviolet continua. Surrounding the MBH is a nonthermal source which produces the infrared and soft X-ray continua by synchrotron emission, and the X-ray spectrum by inverse Compton scattering of the optical-ultraviolet photons from the accretion disk. Previously we modeled the accretion disk (M.A.M.) and nonthermal source (D.L.B.) separately, and here we combine the two models to form a unified description of the AGN engine. This combined model can be inverted to determine source parameters from observed spectra. A group of AGN for which multiband observations exist can then be modeled to: demonstrate the validity of the combined model for a large number of objects; establish the range of parameter values that describe the source; and search for any correlations between source description and type. DOE

N89-13385# Academy of Sciences of the Ukrainian SSR, Kiev. Inst. Teoretichskoj Fiziki.
ON THE MICROSTRUCTURE THEORY OF A CONDENSATE LAYER IN A WHITE DWARF ATMOSPHERE
V. G. Zubko 1987 17 p In RUSSIAN; ENGLISH summary
(DE88-703324; ITF-87-52) Avail: NTIS (US Sales Only) HC A03/MF A01

The microstructure of a condensed carbon layer in the white dwarf is considered including the nucleation, growth and sedimentation of condensate particles. The stationary solutions of the kinetic equation are obtained for condensate particles. Model estimations show that particles may grow to 1 to 10 mcm and the condensate layer may be optically thick. DOE

N89-13386# Consiglio Nazionale delle Ricerche, Frascati (Italy). Istituto di Fisica dello Spazio Interplanetario.
THE EVOLUTIONARY STATUS OF YOUNG STELLAR MASS LOSS DRIVING SOURCES AS DERIVED FROM IRAS OBSERVATIONS
F. Berrilli, C. Ceccarelli, R. Liseau, D. Lorenzetti, P. Saraceno, and L. Spinoglio Sep. 1988 51 p Submitted for publication
(IFSI-88-12; ETN-88-93479) Avail: NTIS HC A04/MF A01

A statistical analysis of the IRAS data for young stellar objects associated with mass outflows (Herbig-Haro objects and molecular outflows) is presented. Systematic differences are found between the observed far IR behavior and that predicted by the model by Adams and Shu (1986) describing the main accretion phase during the formation of low mass stars. It is suggested that the low mass outflow sources are at a later evolutionary stage and not truly protostellar. The IRAS data permit an accurate derivation of the bolometric luminosities, which span over six orders of magnitude for the driving sources of the molecular outflows. From the observed luminosity function the mass function is mass function for the

stars in the solar neighborhood, suggesting that heavy mass loss was an important phase during the formation of stars at all times in the history of the galaxy. ESA

91 LUNAR AND PLANETARY EXPLORATION

Includes planetology; and manned and unmanned flights.

For spacecraft design or space stations see *18 Spacecraft Design, Testing and Performance.*

No abstracts in this category.

92 SOLAR PHYSICS

Includes solar activity, solar flares, solar radiation and sunspots.

For related information see *93 Space Radiation.*

N89-13387*# Joint Inst. for Lab. Astrophysics, Boulder, Colo.
C IV FLUXES FROM THE SUN AS A STAR, AND THE CORRELATION WITH MAGNETIC FLUX Final Report
C. J. Schrijver, J. L. Linsky, J. Bennett, A. Brown, and S. H. Saar 30 Aug. 1988 13 p
(Grant NAG5-932)
(NASA-CR-182719; NAS 1.26:182719) Avail: NTIS HC A03/MF A01 CSCL 03B

A total of 144 C IV wavelength 1548 Solar Maximum Mission (SMM)-UVSP spectroheliograms of solar plages were analyzed, some of which are series of exposures of the same region on the same day. Also analyzed were the C IV wavelength 1551 rasters of plages and C IV wavelength 1548 rasters of the quiet sun. The sample contained data on 17 different plages, observed on 50 different days. The center-to-limb variations of the active regions show that the optical thickness effects in the C IV wavelength 1548 line can be neglected in the conversion from intensity to flux density. As expected for the nearly optically thin situation, the C IV wavelength 1548 line is twice as bright as the C IV 1551 line. The average C IV wavelength 1548 flux density for a quiet region is 2700 ergs/cm/s and, with surprisingly little scatter, 18,000 erg/cm/s for plages. The intensity histograms of rasters obtained at disk center can be separated into characteristic plage and quiet sun contributions with variable relative filling factors. The relationship between the C IV and magnetic flux densities for spatially resolved data is inferred to be almost the same, with only an additional factor of order unity in the constant of proportionality. Author

N89-13388# Stanford Linear Accelerator Center, Calif.
SOLAR MONOPOLES AND TERRESTRIAL NEUTRINOS
J. Frieman Apr. 1988 4 p Presented at the Extra Solar Neutrino Astronomy Workshop, Los Angeles, Calif., 30 Sep. 1987
(Contract DE-AC03-76SF-00515)
(DE88-010677; SU-SLAC-PUB-4606; CONF-8709275-2) Avail: NTIS HC A02/MF A01

Magnetic monopoles captured in the core of the sun may give rise to a substantial flux of energetic neutrinos by catalyzing the decay of solar hydrogen. We discuss the expected neutrino flux in underground detectors under different assumptions about solar interior conditions. Although a monopole flux as low as F sub M approximately 10 to the -24/cm/sec/sr/sup could give rise to a neutrino flux above atmospheric background, due to M/bar M/ annihilation, this does not translate into a reliable monopole flux bound stronger than the Parker limit. DOE

N89-13389# Arizona Univ., Tucson. Dept. of Physics.
EVIDENCE FOR TEMPORAL VARIATION IN THE ACOUSTIC AND f-MODE EIGENFREQUENCY SPECTRUM OF THE SUN
Paul H. Oglesby, Henry A. Hill, and Gregory F. Rabaey 1988 10 p Presented at the 27th Plenary Meeting of COSPAR, Espoo, Finland, 18 Jul. 1988
(Contract DE-FG02-87ER-13670)
(DE88-015650; DOE/ER-13670/T1; CONF-880780-4) Avail: NTIS HC A03/MF A01

The power spectrum obtained from 1985 solar radiation intensity measurements was tested for evidence of frequency shifts of the low-order, low-degree acoustic modes and intermediate degree f-modes classified at SCLERA (Santa Catalina Laboratory for Experimental Relativity by Astrometry). These classifications were based on 1979 differential radius observations. Maxima in the coincidence rates between the peaks in the 1985 power spectrum and the classified frequency spectrum were found for frequency shifts (of the order of 0.05 microHz) that are dependent on degree. These shifts indicate a change in eigenfrequency spectrum over a 6 year period. The coincidence rates between the peaks in the 1985 power spectrum and the classified frequency spectrum for multiplets taken in subgroups of approx. 5 (same n and contiguous in lambda) were typically 3 to 5 sigma above the accidental coincidence rate. Since these modes primarily reside in the convection zone, details of temporal changes of these eigenfrequencies should yield interesting information about the level of variations in the properties of the convection zone over, for example, the solar cycle. DOE

93 SPACE RADIATION

Includes cosmic radiation; and inner and outer earth's radiation belts.

For biological effects of radiation see *52 Aerospace Medicine.* For theory see *73 Nuclear and High-Energy Physics.*

N89-13390# Science Applications International Corp., McLean, Va.
SOVIET EXOATMOSPHERIC NEUTRAL PARTICLE BEAM RESEARCH
J. E. Leiss, R. H. Abrams, K. W. Ehlers, J. A. Farrell, G. H. Gillespie, R. A. Jameson, D. Keefe, and R. K. Parker (Naval Research Lab., Washington, D.C.) Feb. 1988 240 p Prepared in cooperation with Science Applications International Corp., San Diego, Calif.
(FASAC-TAR-3110) Avail: NTIS HC A11/MF A01

This technical assessment was performed by a panel of eight U.S. scientists and engineers who are familiar with Soviet research through their own research experience, their knowledge of the published scientific literature and conference proceedings, and personal contacts with Soviet scientists and other foreign colleagues. Most of the technical components of a neutral particle beam generating system including the ion source, the accelerator, the accelerator radio frequency power supply, the beam conditioning and aiming system, and the beam neutralizer system are addressed. It does not address a number of other areas important to an exoatmospheric neutral beam system. Author

99 GENERAL

N89-13391# Danish Space Research Inst., Lyngby.
DANISH SPACE RESEARCH INSTITUTE Annual Report, 1987
[1987] 49 p
Avail: NTIS HC A03/MF A01

The year 1987 was one of the few in which the Danish Space Research Institute was not gathering data from a satellite in orbit. Viking operations ceased in January and attempts to reactivate in May failed. However, the year long Viking data accumulation will take a while to interpret. Two successful rocket launches, both carrying magnetometers, complemented the data acquisition activities. The Institute participated in ESA's Cluster project, joining two consortia which provided wave and magnetometer instruments,

respectively. The Institute also agreed to provide technical and engineering support for the Institute of Astronomy at Arhus University in their effort to join the Stellar Seismology proposal for the SOHO mission. The majority of the Institute's production effort was, however, devoted to the Watch project of the Academy of Sciences, U.S.S.R., which was to provide four Watch all-sky monitor units for launch on the Granat satellite in November, 1988. A further opportunity came to participate in the Soviet space program, i.e., the Spectrum X-Gamma missions, the first of a new series to make astronomical measurements over a variety of wavelength bands from radio through gamma ray. The Institute's commitments to the ESA programs Hipparcos, Watch (on Eureca) and ISO received appropriate attention. The first two are delayed by launch schedule difficulties at ESA and NASA and schedules have been adjusted accordingly. F.M.R.

N89-13392# Advisory Group for Aerospace Research and Development, Neuilly-Sur-Seine (France).
AGARD HANDBOOK
Jun. 1988 53 p
Copyright Avail: NTIS HC A04/MF A01

This handbook is intended as an introduction to AGARD and its activities. The handbook includes the official texts of the AGARD charter and by-laws. Author

N89-13393*# National Aeronautics and Space Administration. Ames Research Center, Moffett Field, Calif.
RESEARCH AND TECHNOLOGY Annual Report, 1987
Mar. 1988 209 p Original contains color illustrations
(NASA-TM-100051; A-88044; NAS 1.15:100051) Avail: NTIS HC A10/MF A01 CSCL 05D

This report describes various research and technology activities at Ames Moffett and Ames Dryden Research Centers. Highlights of these accomplishments indicate the Centers' varied and highly productive research efforts for 1987. Author

Typical Subject Index Listing

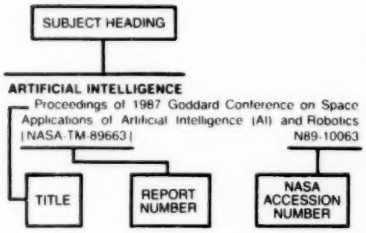

The subject heading is the key to the subject content of the document. Titles, report numbers, and accession numbers of pertinent documents are provided under each subject heading. When the title is insufficiently descriptive of the document content, a title extension has been added, separated from the title by three hyphens. The report number helps to indicate the type of document cited (e.g., NASA report, NASA translation, NASA contractor report). The NASA accession number is the number by which the document abstracts are arranged in this journal and by which the document is sold or requested. The titles, with title extensions if present, are arranged under each subject heading in ascending accession number order. The subject headings have been selected from the latest revision of the *NASA Thesaurus* (NASA SP-7064).

A

ABNORMALITIES
Robust recognition of loud and Lombard speech in the fighter cockpit environment
[AD-A197093] N89-12795

ABSORPTION
Directed motion Doppler shift effects on nitric oxide (0,0) gamma band resonance absorption N89-12760

ABSORPTION SPECTRA
Improvements to photometry. Part 1: Better estimation of derivatives in extinction and transformation equations N89-13322

ABSTRACTS
Biogeochemical processes in sagebrush steppe: Interactions of terrain, vegetation and chemical cycles
[NASA-CR-181486] N89-13088

ABUNDANCE
Atomic and molecular abundances in comets N89-13376
Carbon, nitrogen and oxygen abundances in the chemically peculiar stars of the upper main sequence N89-13379

ACCELERATION (PHYSICS)
Investigation of acceleration and densification of electrons utilizing travelling magnetic waves
[AD-A197700] N89-13242

ACCRETION DISKS
Synthesis of accretion disk and nonthermal source models for AGN
[DE88-013098] N89-13384

ACOUSTIC EXCITATION
Control of laminar separation over airfoils by acoustic excitation
[NASA-TM-101379] N89-12552

ACOUSTIC FATIGUE
Prediction of stresses in aircraft panels subjected to acoustic forces
[NASA-CR-182513] N89-12923

ACOUSTIC LEVITATION
Stabilization and oscillation of an acoustically levitated object
[NASA-CASE-NPO-16896-1-CU] N89-13236

ACOUSTIC MEASUREMENT
Analysis of adhesion test methods and the evaluation of their use for ion-beam-mixed metal/ceramic systems
[DE88-015358] N89-12725

ACOUSTIC PROPERTIES
Arctic oceanography and meteorology review
[AD-A196533] N89-13126

ACOUSTIC VELOCITY
Support of the eight-foot high-temperature tunnel modifications project
[NASA-CR-183356] N89-12572
Surfaces and thin films studied by picosecond ultrasonics
[DE88-015268] N89-13233

ACOUSTICS
The effects of high noise levels on the acoustic-phonetic structure of speech: A preliminary investigation N89-12764
Composite curing process nondestructive evaluation
[AD-A197834] N89-12873
Characterization of adhesively bonded joints using acousto-ultrasonics N89-12925
Arctic oceanography and meteorology review
[AD-A196533] N89-13126
Nearfield acoustic radiation from a point-excited cylindrical shell
[AD-A197282] N89-13234

ACQUISITION
DOD joint Unmanned Aerial Vehicle (UAV) program master plan, 1988
[AD-A197751] N89-12563

ACRYLATES
Poly(ethyl acrylate) and poly(gamma-benzyl-L-glutamate): An interpenetrating polymer system
[AD-A197783] N89-12737

ACTIVE CONTROL
Space station docking mechanism dynamic testing N89-12596
A study of active control techniques for noise reduction in an aircraft fuselage model N89-13232

ACTUATORS
Space station docking mechanism dynamic testing N89-12596
Circuit for actuation of a stepping motor
[INPE-4633-NTE/281] N89-12814
Applications of polysilicon films in microsensors and microactuators
[DE88-016979] N89-12844

ADDITIVES
Computer evaluation of ion-implanted dopant profile evolution during annealing N89-12756

ADHESION
Gordon Conference on Microbial Adhesion
[AD-A197352] N89-12735

ADHESION TESTS
Analysis of adhesion test methods and the evaluation of their use for ion-beam-mixed metal/ceramic systems
[DE88-015358] N89-12725
Modified pull test for the testing of very adherent films
[DE88-016363] N89-12743

ADHESIVE BONDING
Improving the fatigue resistance of adhesive joints in laminated wood structures
[NASA-CR-182165] N89-12675
High temperature adhesive systems
[AD-A197077] N89-12726
Thermoplastic adhesives based on 4,4'-isophthaloyldiphthalic anhydride (IDPA)
[NASA-TM-101508] N89-12747
Characterization of adhesively bonded joints using acousto-ultrasonics N89-12925
The durability of adhesive joints: An engineering study
[AD-A197754] N89-12928

ADHESIVES
Wide Field/Planetary Camera (WF/PC) contamination control assessment N89-12584
Improving the fatigue resistance of adhesive joints in laminated wood structures
[NASA-CR-182165] N89-12675
High temperature adhesive systems
[AD-A197077] N89-12726
The durability of adhesive joints: An engineering study
[AD-A197754] N89-12928

ADIPOSE TISSUES
Derivation of anthropometry based body fat equations for the Army's weight control program
[AD-A197371] N89-13132

ADSORPTION
Adsorption on metal surfaces
[DE88-016557] N89-12715
Moisture adsorption in optical coatings N89-13327

ADVECTION
Mass and heat balances in the upper ocean N89-13089

AERIAL PHOTOGRAPHY
Small format air photo from ultrahigh aircraft as an aid for data collection of agricultural statistics in Sahelian countries N89-13003
Mapping the distribution and abundance of lithological units and surface mineralogies at Jabal Sa'id, Saudi Arabia: An application of spectral mixture modelling N89-13024

AEROASSIST
Direct simulation of three-dimensional flow about the AFE vehicle at high altitudes
[NASA-TM-101492] N89-12834

AERODYNAMIC COEFFICIENTS
Flow field characteristics around bluff parachute canopies N89-12546

AERODYNAMIC DRAG
SAR image statistics related to atmospheric drag over sea ice N89-13034

AERODYNAMIC HEATING
Heat pipe cooling system with sensible heat sink N89-12615
Aerodynamic pressures and heating rates on surfaces between split elevons at Mach 6.6
[NASA-TP-2855] N89-12822

AERODYNAMIC INTERFERENCE
Sidewall boundary-layer measurements with upstream suction in the Langley 0.3-meter transonic cryogenic tunnel
[NASA-CR-4192] N89-12544
A review of turbomachinery blade-row interaction research
[NASA-CR-182211] N89-12567

AERODYNAMIC LOADS
Evaluation of three turbulence models for the prediction of steady and unsteady airloads
[NASA-TM-101413] N89-12555

AERODYNAMICS
Aeronautical engineering: A continuing bibliography with indexes (supplement 232)
[NASA-SP-7037(232)] N89-12536
A vortex panel method for potential flows with applications to dynamics and control
[AD-A197091] N89-12549

AEROELASTICITY
Six degree of freedom simulation computer program for aeroelastic free-flight projectiles N89-12771

AERONAUTICAL ENGINEERING
Aeronautical engineering: A continuing bibliography with indexes (supplement 232)
[NASA-SP-7037(232)] N89-12536

AEROSOLS
Fire aerosol experiment and comparisons with computer code predictions
[DE88-016328] N89-12788
Backscatter laser depolarization studies of simulated stratospheric aerosols: Crystallized sulfuric acid droplets
[NASA-CR-183387] N89-13111

AEROSPACE ENGINEERING
Class 100 large spacecraft facility N89-12586
AGARD handbook N89-13392

AEROSPACE ENVIRONMENTS
Microgravity science and applications program tasks, 1987 revision
[NASA-TM-4068] N89-12752

Tank gauging apparatus and method
[NASA-CASE-MSC-21059-1] N89-12843
Space environment laboratory data acquisition and display system 2
[PB88-205471] N89-13299

AEROSPACE INDUSTRY
Aircraft technology opportunities for the 21st Century
[NASA-TM-101060] N89-12539

AEROSPACE SCIENCES
Danish Space Research Institute N89-13391

AEROSPACE TECHNOLOGY TRANSFER
Important aspects of technology transfer: Training of inservice engineers and scientists; satellite remote sensing N89-13082

AEROTHERMODYNAMICS
Aerothermal modeling program, phase 2 N89-12890
Aerothermal modeling program, phase 2. Element B: Flow interaction experiment N89-12891
Aerothermal modeling program, phase 2. Element C: Fuel injector-air swirl characterization N89-12892

AFRICA
Small format air photo from ultrahigh aircraft as an aid for data collection of agricultural statistics in Sahelian countries N89-13003

AFRICAN RIFT SYSTEM
A regional tectonic study of NE and E Africa and its implication for mineral exploration: A synoptic view from satellite imagery N89-13023

AFTERBURNING
Ground run-up afterburner detection and noise suppression N89-12768

AGING (MATERIALS)
Differential scanning calorimetry as a method for indicating hydrolysis of urethane elastomers
[AD-A197673] N89-12736

AGRICULTURAL AIRCRAFT
Small format air photo from ultrahigh aircraft as an aid for data collection of agricultural statistics in Sahelian countries N89-13003

AGRICULTURE
An integrated remote sensing approach for regional agrostatistics and land monitoring N89-12960
Agroecological information content of SPOT data N89-13050
Evaluation of LANDSAT TM and SPOT imagery for agricultural land use planning in less developed countries N89-13051
The Canada Centre for Remote Sensing (CCRS) ground-based microwave facility --- scatterometer N89-13076

AIR DEFENSE
Evaluation of expert systems in decisionmaking organizations
[AD-A196448] N89-13192

AIR PURIFICATION
Fire aerosol experiment and comparisons with computer code predictions
[DE88-016328] N89-12788

AIR SEA ICE INTERACTIONS
The LIMEX 1987 pilot project, LIMEX 1989 and long-term objective for data collection on the Canadian East coast N89-13037

AIR TO AIR MISSILES
Numerical methods for the guidance and control of air-to-air missiles N89-12561

AIR TRAFFIC CONTROL
LORAN C Offshore Flight Following (LOFF) in the Gulf of Mexico
[AD-A197179] N89-12558
Voice recognition and artificial intelligence in an air traffic control environment
[AD-A197219] N89-12559
TURB: Turbulence forecasting for small/medium and large aircraft
[PB88-246368] N89-13125

AIR WATER INTERACTIONS
A numerical model for the computation of radiance distributions in natural waters with wind-roughened surfaces
[AD-A197207] N89-13128

AIRBORNE EQUIPMENT
The airborne radiometry experiment (ABREX) instrument, an experimental test bed for the specification of satellite-borne microwave radiometer at 90 GHz N89-12939
A synthetic apertures radar with multichannel and multipolarisation N89-13017
The NASA/JPL multifrequency, multipolarisation airborne SAR system N89-13020
Estimating aircraft SAR response characteristics and approximating ocean wave spectra in the Labrador Sea N89-13032
Cirrus-experiment ICE-1987: Microlidar measurements
[DFVLR-MITT-88-17] N89-13124

AIRCRAFT ACCIDENT INVESTIGATION
Annual review of aircraft accident data, US general aviation, calendar year 1985
[PB88-115787] N89-12537

AIRCRAFT ACCIDENTS
An evaluation of ground collision avoidance system algorithm
[AD-A197831] N89-12560

AIRCRAFT COMPARTMENTS
Research and development of anti-g life support systems. Part 2: Decompression sickness research
[AD-A197675] N89-13133

AIRCRAFT CONSTRUCTION MATERIALS
Composite rods in carbon-epoxy Fibredux 914 C/TS-6T-6K-34
[SARMA-TR-87-2431A] N89-12677
Carbon-epoxy composite rods Fibredux 914 C/TS-6T-6K-34
[SARMA-TR-872429-A] N89-12678
Damage of carbon fiber tubes and rods --- aircraft construction materials
[SARMA-TR-882401] N89-12682

AIRCRAFT CONTROL
AH-1F Instrument Meteorological Conditions (IMC) flight evaluations
[AD-A197128] N89-12562
Guidance and Control/Flight Mechanics Panels Joint Symposium on The Man-Machine Interface in Tactical Aircraft Design and Combat Automation
[AGARD-AR-249] N89-12564

AIRCRAFT DESIGN
Guidance and Control/Flight Mechanics Panels Joint Symposium on The Man-Machine Interface in Tactical Aircraft Design and Combat Automation
[AGARD-AR-249] N89-12564
A study of active control techniques for noise reduction in an aircraft fuselage model N89-13232

AIRCRAFT ENGINES
HOST combustion R and T overview N89-12879
HOST structural analysis program overview N89-12881

AIRCRAFT GUIDANCE
Guidance and Control/Flight Mechanics Panels Joint Symposium on The Man-Machine Interface in Tactical Aircraft Design and Combat Automation
[AGARD-AR-249] N89-12564

AIRCRAFT INDUSTRY
Automated Airframe Assembly Program (AAAP) survey of CIM status in the aircraft industry
[AD-A197368] N89-12535

AIRCRAFT MANEUVERS
Design and numerical evaluation of full-authority flight control systems for conventional and thruster-augmented helicopters employed in NOE operations
[NASA-CR-183311] N89-12570
Research and development of anti-g life support systems. Part 2: Decompression sickness research
[AD-A197675] N89-13133

AIRCRAFT NOISE
A study of active control techniques for noise reduction in an aircraft fuselage model N89-13232

AIRCRAFT STRUCTURES
Prediction of stresses in aircraft panels subjected to acoustic forces
[NASA-CR-182513] N89-12923

AIRCRAFT TIRES
Investigation into the applicability of fracture mechanics techniques to aircraft wheel life studies N89-12763

AIRFOIL PROFILES
The laminar boundary layer on an airfoil started impulsively from rest N89-12540

AIRFOILS
Control of laminar separation over airfoils by acoustic excitation
[NASA-TM-101379] N89-12552
Simulation of 2-dimensional viscous flow through cascades using a semi-elliptic analysis and hybrid C-H grids
[NASA-CR-4180] N89-12553
Porous plug for reducing orifice induced pressure error in airfoils
[NASA-CASE-LAR-13569-1] N89-12841
HOST turbine heat transfer subproject overview N89-12880
Measurement of airfoil heat transfer coefficients on a turbine stage N89-12897
Turbine airfoil film cooling N89-12903
Life prediction and constitutive models for engine hot section N89-12916
Thermal barrier coating life prediction model development N89-12920

AIRFRAMES
Automated Airframe Assembly Program (AAAP) survey of CIM status in the aircraft industry
[AD-A197368] N89-12535

ALASKA
Development of Alaskan gas hydrate resources
[DE88-010270] N89-13093

ALBEDO
An albedo map of P/Halley on 13 March 1986 N89-13355
Laboratory simulations of comet surfaces N89-13366

ALCOHOLS
Poly(ethyl acrylate) and poly(gamma-benzyl-L-glutamate): An interpenetrating polymer system
[AD-A197783] N89-12737

ALERTNESS
Differential-psychological analysis of a computer-based audio-visual test of vigilance
[DFVLR-FB-88-23] N89-13140

ALGEBRA
Speed and data structures in computer algebra systems
[AD-A197131] N89-13146
An adaptive method with mesh moving and local mesh refinement for time-dependent partial differential equations
[AD-A197772] N89-13208

ALGORITHMS
Multiple input/output random vibration control system N89-12594
Vibrations induced by nonlinearities in rotordynamics N89-12631
De-embedding S-parameter measurements using TSD technique N89-12783
Temporal clustering in the multi-target tracking environment
[AD-A197153] N89-12796
Algorithms for the self-consistent simulation of high power klystrons
[DE88-010684] N89-12812
An algorithm to derive precipitation profiles from a downward viewing radar and a multifrequency passive radiometer N89-12992
Sea ice type classification of SAR imagery N89-13039
Precipitation detection with satellite microwave data
[PB88-240239] N89-13094
Multidimensional item response theory estimation: A computer program
[AD-A197160] N89-13155
Euclidean decoders for BCH codes
[AD-A197242] N89-13157
A GLR (Generalized Likelihood Ratio) algorithm for polyline approximation of waveforms
[AD-A197846] N89-13166
Algorithms for bound constrained quadratic programming problems
[DE88-016470] N89-13168
Artificial intelligence theory and reconfigurable control systems
[AD-A197255] N89-13195
Optical computing based on neuronal models
[AD-A197749] N89-13199
An adaptive method with mesh moving and local mesh refinement for time-dependent partial differential equations
[AD-A197772] N89-13208
Phase measurement accuracy limitation in phase shifting interferometry N89-13248

ALIGNMENT
Improved docking alignment system
[NASA-CASE-MSC-21372-1] N89-12842

ALKYL COMPOUNDS
Determination of stepsize parameters for intermolecular vibrational energy transfer
[DE88-010904] N89-13239

ALLOYING
Amorphous powders of Al-Hf prepared by mechanical alloying
[DE88-014459] N89-12704

ALLOYS
Fracture and fatigue
[AD-A197310] N89-12927

ALUMINIDES
Effect of grain size on the high temperature properties of B2 aluminides
[NASA-TM-101382] N89-12720

ALUMINUM
Determination of sulfuric acid, oxalic acid, and their matrix effects in aluminum anodizing solutions by ion chromatography
[AD-A197734] N89-12694
Fatigue crack growth of 5456-H116 aluminum and HSLA-80 weldments
[AD-A197830] N89-12712

ALUMINUM ALLOYS
In-situ oxidation of Ni3Al alloys
[DE88-007177] N89-12702

High strain rate properties of structural aluminium N89-12705
Influence of process parameters on laser weld characteristics in aluminum alloys [AD-A197398] N89-12710
Mechanical behavior of superplastically-formed Al-Cu-Li-Zr alloy 2090 [DE88-016241] N89-12714
Influence of alloying elements on the oxidation behavior of NbAl3 [NASA-TM-101398] N89-12717
Properties of rapidly solidified aluminum alloys. German-Norwegian Project (1983-1987) [DFVLR-FB-88-24] N89-12719

ALUMINUM GALLIUM ARSENIDES
Microwave characteristics of interdigitated photoconductors on a HEMT structure [NASA-CR-182197] N89-12820

ALUMINUM OXIDES
Preparation and structure of Li-stabilized Na(+) beta' alumina single crystals [AD-A197245] N89-13283

AMBIGUITY
An analysis of directional ambiguities in wind scatterometer measurements N89-13071

AMORPHOUS MATERIALS
Amorphous powders of Al-Hf prepared by mechanical alloying [DE88-014459] N89-12704
Electronic transport properties of the metallic glass Cu sub 100-x Ti sub x [ETN-88-93231] N89-12718
Fundamental studies and device development in beta silicon carbide [AD-A197843] N89-12739

AMPLIFIERS
Analog-to-digital conversion techniques for precision photometry N89-13319

AMPLITUDE MODULATION
Discrimination and identification of modulation-frequency using noise, tone and tonal-complex carriers [AD-A197780] N89-13134

ANALOG CIRCUITS
An expert system for diagnosis and repair of analog circuits N89-12784

ANALOG TO DIGITAL CONVERTERS
Analog-to-digital conversion techniques for precision photometry N89-13319

ANALOGS
Synthetic polymers as analogs of polysaccharides [AD-A197842] N89-12738

ANATOMY
Is word recognition automatic: A cognitive-anatomical approach [AD-A197089] N89-13137

ANIMALS
Gordon Conference on Microbial Adhesion [AD-A197352] N89-12735

ANIMATION
Efficient use of bit planes in the generation of motion stimuli [NASA-TM-101022] N89-13171

ANISOTROPIC MEDIA
Life prediction and constitutive models for engine hot section N89-12916

ANNEALING
Computer evaluation of ion-implanted dopant profile evolution during annealing N89-12756

ANNUAL VARIATIONS
Detection of seasonal and long-term changes in land cover from multitemporal LANDSAT MSS data N89-12989
A global analysis and correlation of Nimbus 7 cloud and longwave radiation data [AD-A197223] N89-13121

ANODIC COATINGS
Determination of sulfuric acid, oxalic acid, and their matrix effects in aluminum anodizing solutions by ion chromatography [AD-A197734] N89-12694

ANODIZING
Comparison of sulfuric and oxalic acid anodizing for preparation of thermal control coatings for spacecraft N89-12617
Determination of sulfuric acid, oxalic acid, and their matrix effects in aluminum anodizing solutions by ion chromatography [AD-A197734] N89-12694

ANOMALIES
Results of true-anomaly regularization in orbital mechanics N89-12577

ANTARCTIC REGIONS
Inference of radio scattering parameters of Antarctic ice sheet using 179 MHz airborne radio echo sounding data N89-12975

ANTENNA RADIATION PATTERNS
Antenna pattern study [ARI/R-88-510Z] N89-12790
Examining the polarisation phase retrieval of a dual channel multipolarisation radar N89-13019

ANTENNAS
The design of antenna matching networks using a microcomputer [AD-A197364] N89-12802
Microwave and electron beam computer programs [AD-A197798] N89-13164

ANTHROPOMETRY
Derivation of anthropometry based body fat equations for the Army's weight control program [AD-A197371] N89-13132

ANTIBODIES
Gordon Conference on Microbial Adhesion [AD-A197352] N89-12735

ANTIMISSILE MISSILES
Adaptive machine vision [AD-A197039] N89-13222

ANTIMONY COMPOUNDS
Boric oxide as a solid lubricant additive in molybdenum disulfide [AD-A197109] N89-12727

ANTIOXIDANTS
The effects of hyperbaric oxygen and antioxidant deficiencies on rat retinal ultrastructure N89-12772

APERTURES
Phase coherence and Signal-To-Noise ratio considerations for sampled aperture radar systems [AD-A197180] N89-12797

APPROXIMATION
A GLR (Generalized Likelihood Ratio) algorithm for polyline approximation of waveforms [AD-A197846] N89-13166
Parallel algorithms in the finite element approximation of flow problems [AD-A197454] N89-13178
Two alternate proofs of Wang's lune formula for sparse distributed memory and an integral approximation [NASA-CR-184555] N89-13214

ARCHITECTURE
Micro-computer network architecture for range instrumentation applications [AD-A196971] N89-13175

ARCHITECTURE (COMPUTERS)
Architectures for optoelectronic computing [REPT-72/88/R260/U] N89-13148
Applications of parallelism to current algorithms for intelligence analysis [NASA-CR-183351] N89-13165
The state of PC-based CADD (Computer-Aided Design and Drafting) systems [DE88-017326] N89-13170
European Seminar on Neural Computing [ONRL-8-010-C] N89-13173
Optical computing based on neuronal models [AD-A197749] N89-13199
Optical symbolic processor for expert system execution [AD-A197668] N89-13252

ARCTIC OCEAN
Arctic oceanography and meteorology review [AD-A196533] N89-13126

ARCTIC REGIONS
Arctic oceanography and meteorology review [AD-A196533] N89-13126
Bering Sea wave and ice measurements in support of Arctic west winter 1986 [AD-A197196] N89-13127

ARIANE LAUNCH VEHICLE
Ariane 5 verification and associated test facilities N89-12611

ARMATURES
A computer simulation of a plasma armature railgun N89-12780

ARMED FORCES (UNITED STATES)
United States Air Force Graduate Student Summer Support Program, volume 1 [AD-A191121] N89-12754

ARMOR
On the resistance of ceramics to high velocity penetration [AD-A197320] N89-12734

ARRAYS
Tm,Ho:YLF laser end-pumped by a semiconductor diode laser array [NASA-CASE-NPO-17282-1-CU] N89-12856
Time-resolved solid-state array imaging systems: Developments and applications [DE88-016274] N89-13254

ARTIFICIAL INTELLIGENCE
Voice recognition and artificial intelligence in an air traffic control environment [AD-A197219] N89-12559
AUTOCREW implementation: Inbound surface-to-air missile simulation [AD-A197674] N89-13143
Northeast Artificial Intelligence Consortium (NAIC). Review of technical tasks, volume 2, part 1 [AD-A189773] N89-13180
A logic for belief revision N89-13182
A model for belief revision N89-13183
SNePS considered as a fully intensional propositional semantic network N89-13184
Belief revision in SNePS N89-13185
Distributed problem solving N89-13186
Planner system for the application of indications and warning N89-13188
Providing intelligent assistance in distributed office environments N89-13189
POPLAR: A testbed for cognitive modeling N89-13190
User-computer interface technology: An assessment of the current state of the art [AD-A196839] N89-13193
Artificial intelligence theory and reconfigurable control systems [AD-A197255] N89-13195
Bayesian reasoning tool [AD-A197351] N89-13196

ARTIFICIAL SATELLITES
Development of a two axis motion simulation system for thermal/vacuum satellite testing N89-12598
Indian LSSC (Large Space Simulation Chamber) facility N89-12601
Requirements and test results for the qualification of thermal control coatings N89-12616

ASSEMBLING
Magnetic attachment mechanism [NASA-CASE-MSC-21095-1] N89-12866

ASSESSMENTS
Precision limits of the twin-beam multiband URSULA N89-13312

ASTRONOMICAL CATALOGS
Carlsberg meridian catalog La Palma no. 3: Observations of positions of stars and planets made in the year 1986 [ISBN-0-98-87006-3] N89-13372

ASTRONOMICAL MODELS
A multicomponent model of the infrared emission from Comet Halley N89-13367
Growth and sedimentation of dust grains in the primitive solar nebula N89-13374
Theoretical studies of mass loss and shock phenomena in cool star envelopes [NASA-CR-182708] N89-13375

ASTRONOMICAL PHOTOMETRY
Second Workshop on Improvements to Photometry [NASA-CP-10015] N89-13310
Infrared observations of P/Halley and P/Encke N89-13353

ASTRONOMICAL SPECTROSCOPY
Use of optical fibers in spectrophotometry N89-13325

ASTRONOMY
Application of PN and avalanche silicon photodiodes to low-level optical N89-13317
Analog-to-digital conversion techniques for precision photometry N89-13319
Monitoring solar-type stars for luminosity variations N89-13321
A consideration of the use of optical fibers to remotely couple photometers to telescopes N89-13326
Tenth European Regional Astronomy Meeting of the IAU: Abstracts [DE88-703273] N89-13370

ASTROPHYSICS
LIGO vacuum system study N89-12599
Tenth European Regional Astronomy Meeting of the IAU: Abstracts [DE88-703273] N89-13370

ASYMMETRY
Spectral variability of Wolf-Rayet stars [DE88-703325] N89-13371

ASYMPTOTIC METHODS
Stochastic calculus and survival analysis [AD-A197324] N89-13217

ATMOSPHERIC CHEMISTRY
Possible identifications of the 3.4 micrometer feature N89-13342
Laboratory investigations N89-13343

ATMOSPHERIC CIRCULATION
Fundamentals of middle-atmospheric dynamics [AD-A197358] N89-13110

ATMOSPHERIC MODELS
Towards direct variational assimilation of scatterometer backscatter measurements into numerical weather prediction models N89-13000
Model-based estimation of wind fields over the ocean from wind scatterometer measurements N89-13070

Multispectral satellite analysis of marine stratocumulus cloud microphysics
[AD-A197316] N89-13092
Fundamentals of middle-atmospheric dynamics
[AD-A197358] N89-13110
The incorporation of sulfur dioxide into snow and depositing ice N89-13116
An analysis of the error characteristics of Atlantic tropical cyclone track prediction models N89-13117
An analysis of the error characteristics of Atlantic tropical cyclone track prediction models
[AD-A197146] N89-13119
The effect of vertical wind shear on tropical cyclone movement
[AD-A197218] N89-13120

ATMOSPHERIC PRESSURE
Ion mobility spectrometry with laser-produced ions
[AD-A197117] N89-12851

ATMOSPHERIC SOUNDING
Proposed design of the temperature control system for the variable temperature calibration target for the Advanced Microwave Sounding Unit B N89-12942
Cirrus-experiment ICE-1987: Microlidar measurements
[DFVLR-MITT-88-17] N89-13124

ATMOSPHERIC TURBULENCE
TURB: Turbulence forecasting for small/medium and large aircraft
[PB88-246368] N89-13125

ATOMIC EXCITATIONS
Differential cross sections for electron-impact excitation of atomic ions
[ISAS-RN-365] N89-13237

ATOMIC STRUCTURE
Electronic transport properties of the metallic glass Cu sub 100-x Ti sub x
[ETN-88-93231] N89-12718
Electronic structure of light impurities in alpha-Fe and V
[DE88-702958] N89-12721
A novel excitonic mechanism for high temperature superconductivity
[DE88-016227] N89-13288

ATOMIZING
Sample introduction using the Hildebrand grid nebulizer for plasma spectrometry
[AD-A197145] N89-13257

ATOMS
Materials selection for long life in LEO: A critical evaluation of atomic oxygen testing with thermal atom systems N89-12590
Atomic oxygen studies on polymers N89-12591
Atomic oxygen effects on candidate coatings for long-term spacecraft in low earth orbit N89-12592

ATTENTION
The effect of attentional focus level on task performance utilizing information from different stimulus structure levels N89-12765
Is word recognition automatic: A cognitive-anatomical approach
[AD-A197089] N89-13137
Preattentive and attentive visual information processing
[AD-A197670] N89-13139

ATTENUATORS
An optical heterodyne densitometer N89-13323

AUDITORY DEFECTS
Use of proximity effect in hearing aid microphones to increase telephone intelligibility in noise
[AD-A197311] N89-12799

AUDITORY PERCEPTION
A system to investigate synthesized voice feedback in man-machine interfaces N89-12776
Discrimination and identification of modulation-frequency using noise, tone and tonal-complex carriers
[AD-A197780] N89-13134

AUDITORY SIGNALS
Is word recognition automatic: A cognitive-anatomical approach
[AD-A197089] N89-13137

AUDITORY STIMULI
Differential-psychological analysis of a computer-based audio-visual test of vigilance
[DFVLR-FB-88-23] N89-13140

AUGMENTATION
Re-evaluation of an improved efficiency polymeric web point-focus Fresnel lens
[DE88-016892] N89-13255

AUSTENITIC STAINLESS STEELS
High-temperature LCF of Ni-201 and 304L stainless steel N89-12635

AUSTRALIA
Australian preparations for the Polar Platform N89-12979

AUTOCORRELATION
Ocean wave number spectra and spatial autocorrelation functions from SAR images N89-12970

AUTOMATIC CONTROL
Guidance and Control/Flight Mechanics Panels Joint Symposium on The Man-Machine Interface in Tactical Aircraft Design and Combat Automation
[AGARD-AR-249] N89-12564
Space simulators for laser optics N89-12597
Automatic release mechanism for the EL 32 bag --- parachutes
[E-768] N89-12863
Automation software for a materials testing laboratory N89-12917
Automatic control of a multi-channel millimeter wave radiometer N89-12938
Advancing automation and robotics technology for the space station and for the US economy
[NASA-TM-100989] N89-13198

AUTOMATIC FLIGHT CONTROL
Design and numerical evaluation of full-authority flight control systems for conventional and thruster-augmented helicopters employed in NOE operations
[NASA-CR-183311] N89-12570

AUTOMATIC GAIN CONTROL
Analysis of GEOSAT radar altimeter errors based on pre-launch test data
[NASA-TM-101230] N89-12808

AUTOMATIC PILOTS
DOD joint Unmanned Aerial Vehicle (UAV) program master plan, 1988
[AD-A197751] N89-12563

AUTOMATION
An approach to automate digital signal processor code generation
[ETN-88-93530] N89-13172

AUTOMOBILE FUELS
Autoignition chemistry of n-butane in a motored engine: A comparison of experimental and modeling results
[DE88-014153] N89-12697

AUTOREGRESSIVE PROCESSES
Application of autoregressive methods to adaptive excision of interfering tones from direct sequence spread spectrum communications systems
[AD-A197801] N89-12805

AVIONICS
AH-1F Instrument Meteorological Conditions (IMC) flight evaluations
[AD-A197128] N89-12562

AXIAL LOADS
Lubrication evaluation of SSME turbopump bearings N89-12639
Thermomechanical characterization of Hastelloy-X under uniaxial cyclic loading N89-12909

AXIAL STRAIN
Determination of surfaces of constant inelastic strain rate at elevated temperature N89-12910

AXIAL STRESS
Creep fatigue life prediction for engine hot section materials (isotropic): Fourth year progress review N89-12914

AXISYMMETRIC BODIES
Numerical integration of influence coefficients for panel methods about axisymmetric bodies by means of the ROMBERG algorithm
[DFVLR-MITT-88-18] N89-12839

B

BACKSCATTERING
Constraints on two-scale descriptions of radar backscattering from the sea surface using scatterometer model functions N89-12945
Statistical properties of phase difference between two orthogonally-polarised SAR signals N89-12953
Towards direct variational assimilation of scatterometer backscatter measurements into numerical weather prediction models N89-13000
Modulation of the radar backscatter from the ocean surface by a long gravity wave N89-13031
A 35 GHz helicopter-borne polarimeter radar N89-13038
Snow cover to alter terrain signatures on radar images N89-13048
Backscatter laser depolarization studies of simulated stratospheric aerosols: Crystallized sulfuric acid droplets
[NASA-CR-183387] N89-13111

BACTERIA
Gordon Conference on Microbial Adhesion
[AD-A197352] N89-12735

BAGS
Automatic release mechanism for the EL 32 bag --- parachutes
[E-768] N89-12863

BALANCING
Efficient transient analysis methods for the Space Shuttle Main Engine (SSME) turbopumps N89-12630

BALL BEARINGS
Thermo-mechanical performance evaluation of cryogenic turbopump ball bearings N89-12637
Lubrication evaluation of SSME turbopump bearings N89-12639
Surface characteristics of liquid oxygen cooled ball bearings N89-12640
Measurement of rotordynamic coefficients for a hydrostatic radial bearing N89-12643

BALLISTIC TRAJECTORIES
Temporal clustering in the multi-target tracking environment
[AD-A197153] N89-12796

BARIUM OXIDES
High T(sub c) superconductors: Will they replace helium temperature superconductors for magnets
[DE88-016632] N89-13279

BAYES THEOREM
Bayesian reasoning tool
[AD-A197351] N89-13196

BEAM NEUTRALIZATION
Soviet exoatmospheric neutral particle beam research
[FASAC-TAR-3110] N89-13390

BEAMS (RADIATION)
Comments on the high frequency behavior of the coupling of an accelerator beam to its environment
[CEBAF-PR-88-006] N89-13245
Nonlinear effects in photorefractive crystals
[AD-A197152] N89-13281

BEARING (DIRECTION)
Bearing error and the central limit theorem
[NASA-CR-183009] N89-13219

BEARINGS
Advanced Earth-to-Orbit Propulsion Technology 1986, volume 2
[NASA-CP-2437-VOL-2] N89-12626
Low-speed flexible rotor balancing for smooth, high-speed operation N89-12628
Thermal analysis of SSME turbopump bearings N89-12638
Powder metallurgy bearings for advanced rocket engines N89-12641
Rolling contact fatigue life of zirconium and molybdenum nitride sputter plated AMS 5749 bearing steel N89-12642
Surface modification for wear resistance in a liquid oxygen turbopump environment N89-12644
SSME bearing health monitoring using a fiberoptic deflectometer N89-12645

BENARD CELLS
The stability of time-dependent fluid flows N89-12825

BIBLIOGRAPHIES
Aeronautical engineering: A continuing bibliography with indexes (supplement 232)
[NASA-SP-7037(232)] N89-12536
Fuel cells: A bibliography
[DE88-001081] N89-13097

BIDIRECTIONAL REFLECTANCE
A reference standard for bidirectional reflection distribution function and bidirectional transmission distribution function measurement
[NASA-CASE-MFS-28183-1] N89-13253

BINARY ALLOYS
Fundamental understanding of the intrinsic ductility in nickel-base L12 type alloys
[AD-A197605] N89-12711
Elevated temperature strain gages N89-12886

BINARY STARS
Spectral variability of Wolf-Rayet stars
[DE88-703325] N89-13371
S-waves in the spectrum of cataclysmic binaries N89-13380
Mixing and structural changes during mass transfer in binary systems N89-13382

BINARY SYSTEMS (MATERIALS)
Analysis of adhesion test methods and the evaluation of their use for ion-beam-mixed metal/ceramic systems
[DE88-015358] N89-12725

BIOCHEMISTRY
Isolation of osteogenic cells from the trauma-activated periosteum N89-12757
Electroporation: Theory of basic mechanisms
[AD-A197391] N89-13130

BIOELECTRICITY
Electroporation: Theory of basic mechanisms
[AD-A197391] N89-13130

BIOLOGICAL EFFECTS
Liquid scintillation counting with the Packard 1500 analyzer N89-12782
Bioelectromagnetic effects of EMP: Preliminary findings
[DE88-012118] N89-12791

BIOREACTORS
Horizontally rotated cell culture system
[NASA-CASE-MSC-21294-1] N89-13131
BIOSATELLITES
A conceptual design study of the reusable reentry satellite
[NASA-TM-101043] N89-12623
BITS
Efficient use of bit planes in the generation of motion stimuli
[NASA-TM-101022] N89-13171
BIVARIATE ANALYSIS
Multivariate regression with emphasis on multivariate spline methods
[AD-A197793] N89-13209
BLACK BODY RADIATION
Cost effective alternative to low irradiance measurements N89-12619
BLACK HOLES (ASTRONOMY)
Gravitation, black holes and space-time physics
[DE88-703054] N89-13377
BLADE TIPS
Heat transfer in the tip region of a rotor blade simulator N89-12898
BLADE-VORTEX INTERACTION
Foundations of the blade-vortex interaction problem: Structure and behavior of travelling compressible vortices
[AD-A197370] N89-12550
BLOOD VOLUME
Alterations of segmental volume during orthostatic stress in nonhuman primates N89-12769
BLUFF BODIES
Flow field characteristics around bluff parachute canopies N89-12546
BOILING
Dynamics of face and annular seals with two-phase flow
[NASA-CR-183352] N89-12870
BOLL WEEVILS
Cotton area mapping using multitemporal satellite data integrated within a geographical information system applied to a cotton boll weevil control programme in Paraguay N89-13077
BOLTED JOINTS
Lightweight structural design of a bolted case joint for the space shuttle solid rocket motor
[NASA-TP-2851] N89-12580
BOLTZMANN TRANSPORT EQUATION
Electronic transport properties of the metallic glass Cu sub 100-x Ti sub x
[ETN-88-93231] N89-12718
BONES
Isolation of osteogenic cells from the trauma-activated periosteum N89-12757
BOOMS (EQUIPMENT)
Space station erectable manipulator placement system
[NASA-CASE-MSC-21096-1] N89-12621
BOOSTER ROCKET ENGINES
Ariane 5 verification and associated test facilities N89-12611
Advanced Earth-to-Orbit Propulsion Technology 1986, volume 2
[NASA-CP-2437-VOL-2] N89-12626
Aerojet TechSystems Company contribution to LOX/HC combustion and cooling technology N89-12646
Survey of LOX/hydrocarbon combustion and cooling N89-12647
LOX/hydrocarbon combustion and cooling survey N89-12648
RP-1 and methane combustion and cooling experiments N89-12650
BORANES
The conversion of smaller borane fragments to larger structures. Systematics of boron hydride reactions
[AD-A197068] N89-12689
BORON CARBIDES
Evaluation of boron carbide coatings N89-13228
BORON HYDRIDES
The conversion of smaller borane fragments to larger structures. Systematics of boron hydride reactions
[AD-A197068] N89-12689
BORON OXIDES
Boric oxide as a solid lubricant additive in molybdenum disulfide
[AD-A197109] N89-12727
BOUNDARIES
New methods for locating phase boundaries
[DE88-017084] N89-12700
Combined pressure-shear ignition sensitivity test
[AD-A197076] N89-12749
Temperature profile in semi-infinite planar slab with exponential source and convective boundary condition: Application to laser heating
[DE88-016746] N89-12831
BOUNDARY LAYER EQUATIONS
The laminar boundary layer on an airfoil started impulsively from rest N89-12540
The effect of vertical wind shear on tropical cyclone movement
[AD-A197218] N89-13120
BOUNDARY LAYER FLOW
A spectral collocation solution to the compressible stability eigenvalue problem
[NASA-TP-2858] N89-12543
Sidewall boundary-layer measurements with upstream suction in the Langley 0.3-meter transonic cryogenic tunnel
[NASA-CR-4192] N89-12544
Influence of bulk turbulence and entrance boundary layer thickness on the curved duct flow field N89-12896
Turbine airfoil film cooling N89-12903
BOUNDARY LAYER TRANSITION
Method for laminar boundary layer transition visualization in flight
[NASA-CASE-LAR-13554-1] N89-12551
Development of low Reynolds number two equation turbulence models for predicting external heat transfer on turbine blades N89-12901
BOUNDARY LAYERS
A two-dimensional numerical simulation of a supersonic, chemically reacting mixing layer
[NASA-TM-4055] N89-12542
Development of a thermal and structural analysis procedure for cooled radial turbines
[NASA-TM-101416] N89-12568
BOUNDARY VALUE PROBLEMS
Theoretical and experimental studies of the transonic flow field and associated boundary conditions near a longitudinally-slotted wind-tunnel wall N89-12545
Results of true-anomaly regularization in orbital mechanics N89-12577
Nonlinear perturbations of differential operators with nontrivial kernel and applications to third order periodic boundary value problems
[DE88-702991] N89-13201
An adaptive method with mesh moving and local mesh refinement for time-dependent partial differential equations
[AD-A197772] N89-13208
BRAGG ANGLE
Shadows and wedges in scattering from the sea N89-12946
BRAIN
Consequences of individual differences in brain organization for human performance
[AD-A197667] N89-13138
BREAKING
Isolation of osteogenic cells from the trauma-activated periosteum N89-12757
BREMSSTRAHLUNG
Investigation of acceleration and densification of electrons utilizing travelling magnetic waves
[AD-A197700] N89-13242
BRIGHTNESS
Comet Halley's colorful outbursts N89-13359
Spectral variability of Wolf-Rayet stars
[DE88-703325] N89-13371
BRIGHTNESS TEMPERATURE
Microwave emission behavior of snow N89-13041
BRITTLE MATERIALS
Toughening by aligned, frictionally constrained fibers
[AD-A197194] N89-12676
On the resistance of ceramics to high velocity penetration
[AD-A197320] N89-12734
BROADBAND
The design of antenna matching networks using a microcomputer
[AD-A197364] N89-12802
Improvements to photometry. Part 1: Better estimation of derivatives in extinction and transformation equations N89-13322
BUBBLES
Physical modeling of bubble phenomena, electrolyte flow and mass transfer in simulated advanced Hall cells
[DE88-015585] N89-12828
BUOYS
An intercomparison of SAR and buoy directional wave spectra from the Labrador Sea Extreme Waves Experiment (LEWEX) N89-12972
Estimation of sea surface temperature via NOAA-AVHRR sensor: Comparison with sea truth data by fixed buoys N89-13005
BURNERS
Stability limits and combustion measurements in low calorific value gas flames N89-12687
BURNING RATE
Laser illuminated high speed photography of energetic materials
[DE88-012870] N89-12848
BUTANES
Autoignition chemistry of n-butane in a motored engine: A comparison of experimental and modeling results
[DE88-014153] N89-12697

C

CALCULUS
Stochastic calculus and survival analysis
[AD-A197324] N89-13217
CALCULUS OF VARIATIONS
Quantum Monte Carlo calculation of the properties of atomic carbon and diamond
[DE88-014659] N89-12686
CALIBRATING
Cost effective alternative to low irradiance measurements N89-12619
The Airborne Version Conical Scan Radiometer (AVCSR): An airborne radiometer as a tool for satellite data validation N89-12937
Verification of the accuracy of a network of water-vapor radiometers N89-12941
Proposed design of the temperature control system for the variable temperature calibration target for the Advanced Microwave Sounding Unit B N89-12942
Phase calibration of polarimetric SAR N89-13015
Calibration of multipolarisation imaging radar N89-13018
Phase measurement accuracy limitation in phase shifting interferometry N89-13248
Absolute photometric calibration of detectors to 0.3 mmag using amplitude-stabilized lasers and a helium-cooled absolute radiometer N89-13318
CALIFORNIA
Mass and heat balances in the upper ocean N89-13089
CALORIMETERS
Differential scanning calorimetry as a method for indicating hydrolysis of urethane elastomers
[AD-A197673] N89-12736
CAMERAS
WF/PC internal molecular contamination during system thermal-vacuum test N89-12583
Wide Field/Planetary Camera (WF/PC) contamination control assessment N89-12584
Characterization of a graphite epoxy optical bench during thermal vacuum cycling N89-12585
CANADA
The LIMEX 1987 pilot project, LIMEX 1989 and long-term objective for data collection on the Canadian East coast N89-13037
CANOPIES
Flow field characteristics around bluff parachute canopies N89-12546
CANOPIES (VEGETATION)
The structure of red-infrared scattergrams of semivegetated landscapes
[NASA-CR-183385] N89-13091
CAPACITORS
Advanced double layer capacitor
[AD-A197739] N89-12818
CARBOHYDRATE METABOLISM
Glucose tolerance and insulin secretion during 0-g simulation
[DFVLR-FB-88-25] N89-13136
CARBON
Quantum Monte Carlo calculation of the properties of atomic carbon and diamond
[DE88-014659] N89-12686
On the carbon abundance in Comet Halley derived from the 3 micron feature: Comparison with interstellar dust N89-13341
Laboratory simulations of comet surfaces N89-13366
CARBON DIOXIDE
Precision cleaning methods for spacecraft applications N89-12588
A mass spectrometric analysis of CF4/O2 plasmas: Effect of oxygen concentration and plasma power
[DE88-016237] N89-13261
CARBON DIOXIDE LASERS
Influence of process parameters on laser weld characteristics in aluminum alloys
[AD-A197398] N89-12710
CARBON FIBER REINFORCED PLASTICS
Composite rods in carbon-epoxy Fibredux 914 C/TS-6T-6K-34
[SARMA-TR-87-2431A] N89-12677
Carbon-epoxy composite rods Fibredux 914 C/TS-6T-6K-34
[SARMA-TR-872429-A] N89-12678
Damage of carbon fiber tubes and rods --- aircraft construction materials
[SARMA-TR-882401] N89-12682

CARBON MONOXIDE
A mass spectrometric analysis of CF4/O2 plasmas: Effect of oxygen concentration and plasma power
[DE88-016237] N89-13261
CARBON-CARBON COMPOSITES
Fingerprint test data report: FM 5834 test lots No. 1, 3, 4, and 5 --- resin matrix composites
[NASA-CR-179419] N89-12722
Fingerprint test data report: FM 5064J (Kaiser) lots No. 1 (K) - No. 4 (K) --- resin matrix composites
[NASA-CR-179409] N89-12723
CARBONACEOUS MATERIALS
Comparison of the 3.36 micrometer feature to the ISM
N89-13339
CARTESIAN COORDINATES
Mathematical modelling and computer simulation using Cartesian grid
[TM-AE-8804] N89-13149
CASCADE FLOW
Simulation of 2-dimensional viscous flow through cascades using a semi-elliptic analysis and hybrid C-H grids
[NASA-CR-4180] N89-12553
CATACLYSMIC VARIABLES
S-waves in the spectrum of cataclysmic binaries
N89-13380
CATALOGS
Space station integrated propulsion and fluid systems study
[NASA-CR-179393] N89-12581
CATALYSIS
Homogeneous catalytic production of hydrogen and other molecules from water-DMF (N-dimethylformamide) solutions
[AD-A197072] N89-12690
CAVITIES
Coble creep, cavity sintering and cavity growth
[DE88-013846] N89-12703
CAVITY RESONATORS
Microwave RF coupling response through adjacent cavities
[DE88-012430] N89-12793
CELLS (BIOLOGY)
Isolation of osteogenic cells from the trauma-activated periosteum N89-12757
Horizontally rotated cell culture system
[NASA-CASE-MSC-21294-1] N89-13131
CENSORED DATA (MATHEMATICS)
Two-sample inference for median survival times based on one-sample procedures for censored survival data
[AD-A197776] N89-13218
CERAMIC BONDING
A study on thermal barrier coatings including thermal expansion mismatch and bond coat oxidation
N89-12919
CERAMIC MATRIX COMPOSITES
Synthesis and characterization of VLS-derived silicon carbide whiskers
[DE88-016226] N89-12679
CERAMICS
Sol-gel routes to superconducting ceramics
[DE88-015128] N89-12724
Analysis of adhesion test methods and the evaluation of their use for ion-beam-mixed metal/ceramic systems
[DE88-015358] N89-12725
On the resistance of ceramics to high velocity penetration
[AD-A197320] N89-12734
Challenging applications for hydrated and chemically reacted ceramics
[DE88-015397] N89-12742
Ion beam mixing of metals and ceramics: Material considerations
[DE88-016797] N89-12744
Slurry-pressing consolidation of silicon nitride
[NASA-TM-101365] N89-12746
Calculation of Weibull strength parameters and Batdorf flow-density constants for volume- and surface-flaw-induced fracture in ceramics
[NASA-TM-100890] N89-12930
Low contact-resistivity junction to ceramic superconductors
[DE88-016155] N89-13292
Survey of supply/demand relationships for Japanese Technical Information in the United States: The field of advanced ceramics research and development
[PB88-210943] N89-13300
CHANGE DETECTION
Detection of seasonal and long-term changes in land cover from multitemporal LANDSAT MSS data
N89-12989
Monitoring playas using Thematic Mapper data
N89-13028
Monitoring of seasonal snow cover on glaciers
N89-13044
Monitoring urban change from LANDSAT TM and SPOT satellite imagery by image differencing N89-13058
Change direction analysis using LANDSAT imagery: A review of methodology N89-13068
Building a monitoring system based on satellite data to detect vegetation and land use changes in a subtropical region of Mexico N89-13079
CHANNEL FLOW
Theoretical study of turbulent channel flow: Bulk properties, pressure fluctuations, and propagation of electromagnetic waves
[NASA-TM-101248] N89-12830
CHARACTERIZATION
Characterization of a graphite epoxy optical bench during thermal vacuum cycling N89-12585
Synthesis and characterization of VLS-derived silicon carbide whiskers
[DE88-016226] N89-12679
Characterization of graphite fibers by X-ray diffraction
N89-12755
CHARGE CARRIERS
Transition-metal oxide superconductivity
[AD-A197069] N89-13280
CHARGE COUPLED DEVICES
WF/PC internal molecular contamination during system thermal-vacuum test N89-12583
Joint services electronics program
[AD-A197140] N89-12815
The behavior of disk electrodes: Optical imaging of the concentration distribution over a disk electrode under galvanostatic conditions
[AD-A197355] N89-12816
The MEOSS experiment: A test case for future cartographic missions N89-13081
CHARGE DISTRIBUTION
Electronic structure of light impurities in alpha-Fe and V
[DE88-702958] N89-12721
CHARGE TRANSFER
Charge transfer in multiple site chemical systems
[AD-A197143] N89-12666
Electronic structure of light impurities in alpha-Fe and V
[DE88-702958] N89-12721
Electronic and ionic transport in polymers
[AD-A197142] N89-12728
A novel excitonic mechanism for high temperature superconductivity
[DE88-016227] N89-13288
CHEBYSHEV APPROXIMATION
On the constrained Chebyshev approximation problem on ellipses
[NASA-CR-183209] N89-13200
CHECKOUT
Parallel debugging using graphical views
[AD-A197197] N89-13156
CHEMICAL ANALYSIS
Laboratory investigations N89-13343
CHEMICAL ATTACK
Corrosion of nickel and Monel welds of steel in chlorine trifluoride
[DE88-014122] N89-12706
CHEMICAL BONDS
Large silicon clusters: Confirmation of Phillips' conjecture
[AD-A197487] N89-13241
CHEMICAL COMPOSITION
Charge transfer in multiple site chemical systems
[AD-A197143] N89-12666
Determination of sulfuric acid, oxalic acid, and their matrix effects in aluminum anodizing solutions by ion chromatography
[AD-A197734] N89-12694
Corrosion of nickel and Monel welds of steel in chlorine trifluoride
[DE88-014122] N89-12706
The incorporation of sulfur dioxide into snow and depositing ice N89-13116
Grain optical properties N89-13332
Cometary dust composition N89-13333
The spectral properties of interplanetary dust particles
N89-13336
Interstellar grain chemistry and the composition of comets N89-13346
CHEMICAL LASERS
Population inversion non-equilibrium flow simulation calculations of the capabilities of convection flow lasers
[AD-A197741] N89-12854
CHEMICAL PROPERTIES
Chemical precursors to zinc sulfide: ZnS whisker synthesis
[AD-A197262] N89-13284
CHEMICAL REACTIONS
A two-dimensional numerical simulation of a supersonic, chemically reacting mixing layer
[NASA-TM-4055] N89-12542
The conversion of smaller borane fragments to larger structures. Systematics of boron hydride reactions
[AD-A197068] N89-12689
Homogeneous catalytic production of hydrogen and other molecules from water-DMF (N-dimethylformamide) solutions
[AD-A197072] N89-12690
A mass spectrometric analysis of CF4/O2 plasmas: Effect of oxygen concentration and plasma power
[DE88-016237] N89-13261
Nonequilibrium effects in thermal plasma chemistry
[DE88-016842] N89-13263
Chemical precursors to zinc sulfide: ZnS whisker synthesis
[AD-A197262] N89-13284
CHEMILUMINESCENCE
Electrogenerated chemiluminescence
[AD-A197163] N89-12691
CHLORINE FLUORIDES
Corrosion of nickel and Monel welds of steel in chlorine trifluoride
[DE88-014122] N89-12706
CHROMATOGRAPHY
Determination of sulfuric acid, oxalic acid, and their matrix effects in aluminum anodizing solutions by ion chromatography
[AD-A197734] N89-12694
CHROMOSPHERE
C IV fluxes from the Sun as a star, and the correlation with magnetic flux
[NASA-CR-182719] N89-13387
CIRCADIAN RHYTHMS
A conceptual design study of the reusable reentry satellite
[NASA-TM-101043] N89-12623
CIRCUITS
A fault diagnosis system based on an integrated knowledge base N89-13181
CIRCULAR POLARIZATION
The development of a near-infrared polarimeter and its application to the continuum polarization of magnetic white dwarfs N89-12924
Some advantages of using polarisation diversity illustrated through the analysis of radar data from a storm in central Alberta (Canada) N89-12994
CIRRUS CLOUDS
Cirrus-experiment ICE-1987: Microlidar measurements
[DFVLR-MITT-88-17] N89-13124
CIVIL AVIATION
Annual review of aircraft accident data, US general aviation, calendar year 1985
[PB88-115787] N89-12537
CLASSICAL MECHANICS
Stochastic stage of an inflationary universe model
[DE88-753149] N89-13373
CLASSIFICATIONS
An international approach to GIS based on remote sensing and terrain classification --- geographic information system (GIS) N89-12966
Large area TM land cover classification of Mittlerer Oberrhein County, southwest Germany, and its use for regional planning and crop surveys N89-12986
Towards an urban land-use classification using textural and morphological criteria N89-12987
Crop classification with multi-temporal X-band SAR data N89-12990
Production of probability of precipitation maps over oceanic areas from automated cloud classification
N89-12999
Sea ice type classification of SAR imagery
N89-13039
Efficient classification of multispectral images by a best linear discriminant function N89-13060
A new spatial classification algorithm for high ground resolution images N89-13061
Classification decision rule modification on the basis of information extracted from training data --- satellite imagery N89-13062
Lapwing: A trainable spatial feature recognition system
N89-13063
The interrelationship between resampling method and information extraction technique N89-13065
Accuracy of land cover classification of Thematic Mapper (TM) and SPOT data N89-13066
The classification of semi-natural vegetation from LANDSAT Thematic Mapper imagery: A user's perspective N89-13084
Preattentive and attentive visual information processing
[AD-A197670] N89-13139
Bayesian reasoning tool
[AD-A197351] N89-13196
CLEAN ROOMS
Class 100 large spacecraft facility N89-12586

CLEANING
Precision cleaning methods for spacecraft applications N89-12588
CLEANLINESS
Correlation studies on surface particle detection methods N89-12587
CLIMATE
A global analysis and correlation of Nimbus 7 cloud and longwave radiation data
[AD-A197223] N89-13121
CLIMATOLOGY
C Cloud S (Climatology of Cloud Statistics) database (users manual)
[AD-A196497] N89-13118
CLOTHING
Soiling, cleaning, and weathering effects on aircraft polyurethane topcoats
[AD-A197302] N89-12733
CLOUD COVER
C Cloud S (Climatology of Cloud Statistics) database (users manual)
[AD-A196497] N89-13118
A global analysis and correlation of Nimbus 7 cloud and longwave radiation data
[AD-A197223] N89-13121
CLOUD PHOTOGRAPHY
Cloud track winds from polar orbiting satellites N89-13069
CLOUD PHYSICS
Radiometric observations of cloud liquid water during FIRE --- First ISCCP Regional Experiment (FIRE) N89-13001
Multispectral satellite analysis of marine stratocumulus cloud microphysics
[AD-A197316] N89-13092
CLOUDS
On the interactions of longwave radiation, microphysics and turbulence in boundary layer clouds N89-13109
CLOUDS (METEOROLOGY)
Production of probability of precipitation maps over oceanic areas from automated cloud classification N89-12999
CLUSTER ANALYSIS
Performance analysis of the Alliant FX/8 multiprocessor using statistical clustering
[NASA-CR-183221] N89-13145
The problem of clustering in laboratory studies of cometary dust N89-13356
Aerodynamic properties of fractal grains: Implications for the primordial solar nebula N89-13361
CLUTTER
Optimal reception in depolarising clutter N89-13008
CMOS
The RACE Program of the European Communities
[ONRL-8-014-R] N89-12811
COAL GASIFICATION
Assessment and comparison of 100-MW coal gasification phosphoric acid fuel cell power plants
[NASA-CR-182189] N89-13103
COASTAL ECOLOGY
The derivation of sub-canopy surface terrain models of coastal forests using synthetic aperture radar N89-13083
COATINGS
Method for laminar boundary layer transition visualization in flight
[NASA-CASE-LAR-13554-1] N89-12551
Determination of sulfuric acid, oxalic acid, and their matrix effects in aluminum anodizing solutions by ion chromatography
[AD-A197734] N89-12694
Moisture adsorption in optical coatings N89-13327
COBALT ALLOYS
Fatigue crack retardation following overloads in Inconel 718, Ti-5Al-2.5Sn, and Haynes 188 N89-12636
Multispecimen test facility for high-pressure hydrogen creep studies N89-12655
COCKPITS
Robust recognition of loud and Lombard speech in the fighter cockpit environment
[AD-A197093] N89-12795
CODERS
An approach to automate digital signal processor code generation
[ETN-88-93530] N89-13172
CODING
The RACE Program of the European Communities
[ONRL-8-014-R] N89-12811
Euclidean decoders for BCH codes
[AD-A197242] N89-13157
An adaptive method with mesh moving and local mesh refinement for time-dependent partial differential equations
[AD-A197772] N89-13208
COGNITION
Is word recognition automatic: A cognitive-anatomical approach
[AD-A197089] N89-13137
Consequences of individual differences in brain organization for human performance
[AD-A197667] N89-13138
Discovering substructure in examples
[AD-A197778] N89-13163
Providing intelligent assistance in distributed office environments N89-13189
POPLAR: A testbed for cognitive modeling N89-13190
COHERENT RADIATION
Investigation of acceleration and densification of electrons utilizing travelling magnetic waves
[AD-A197700] N89-13242
COILS
Tesla's coherent plasma discharge and a plan for megavolts at megahertz N89-13231
COLLISION AVOIDANCE
An evaluation of ground collision avoidance system algorithm
[AD-A197831] N89-12560
COLLOIDS
Colloid vibration potentials
[VTT-RR-535] N89-13244
COLOR
Method for laminar boundary layer transition visualization in flight
[NASA-CASE-LAR-13554-1] N89-12551
Soiling, cleaning, and weathering effects on aircraft polyurethane topcoats
[AD-A197302] N89-12733
Comet Halley's colorful outbursts N89-13359
Color gradients in the coma of P/Halley N89-13362
The NASA Infrared Telescope Facility Comet Halley monitoring program 2: Post-perihelion results N89-13368
COMBAT
Guidance and Control/Flight Mechanics Panels Joint Symposium on The Man-Machine Interface in Tactical Aircraft Design and Combat Automation
[AGARD-AR-249] N89-12564
The effect of attentional focus level on task performance utilizing information from different stimulus structure levels N89-12765
AUTOCREW implementation: Inbound surface-to-air missile simulation
[AD-A197674] N89-13143
COMBINATORIAL ANALYSIS
Sensitivity analysis for shortest Hamiltonian path and traveling salesman problems
[AD-A197167] N89-13204
COMBUSTION
Radiative augmented combustion
[AD-A197300] N89-12693
Prediction of heat transfer between the combustion space and the load
[DE88-016313] N89-12698
Human exposure to dioxin from combustion sources
[DE88-013825] N89-13135
COMBUSTION CHAMBERS
LOX/hydrocarbon combustion and cooling survey N89-12648
Effects of oxygen/hydrogen combustion chamber environment on copper alloys N89-12653
Stability limits and combustion measurements in low calorific value gas flames N89-12687
Turbine Engine Hot Section Technology (HOST) Project N89-12877
HOST structural analysis program overview N89-12881
Further development of the dynamic gas temperature measurement system N89-12884
Aerothermal modeling program, phase 2 N89-12890
Aerothermal modeling program, phase 2. Element B: Flow interaction experiment N89-12891
Aerothermal modeling program, phase 2. Element C: Fuel injector-air swirl characterization N89-12892
Combustor diffuser interaction program N89-12893
Efficient numerical techniques for complex fluid flows N89-12894
On 3-D inelastic analysis methods for hot section components N89-12905
On 3D inelastic analysis methods for hot section components N89-12906
Component specific modeling N89-12907
Elevated temperature crack growth N89-12915
COMBUSTION EFFICIENCY
Aerothermal modeling program, phase 2. Element B: Flow interaction experiment N89-12891
COMET NUCLEI
Laboratory investigations N89-13343
Polarization images of Comet Halley N89-13351
Airborne 20-65 micron spectrophotometry of Comet Halley N89-13354
Some 5-13 micrometer airborne observations of Comet Wilson 1986l: Preliminary results N89-13360
Color gradients in the coma of P/Halley N89-13362
COMET RENDEZVOUS ASTEROID FLYBY MISSION
IR-dust observations of Comet Tempel 2 with CRAF VIMS N89-13349
COMET TAILS
Comet Halley's colorful outbursts N89-13359
Some 5-13 micrometer airborne observations of Comet Wilson 1986l: Preliminary results N89-13360
COMETARY ATMOSPHERES
Infrared Observations of Comets Halley and Wilson and Properties of the Grains
[NASA-CP-3004] N89-13330
Infrared observations of the dust coma N89-13331
Cometary dust composition N89-13333
PIA update: Correlation analyses of mass spectra N89-13334
A comparison of Halley dust with meteorites, interplanetary dust and interstellar grains N89-13335
The spectral properties of interplanetary dust particles N89-13336
Aromatic components in cometary materials N89-13337
The 3.4 micrometer emission feature in Comet Halley N89-13338
Comparison of the 3.36 micrometer feature to the ISM N89-13339
A two component model for thermal emission from organic grains in Comet Halley N89-13340
Possible identifications of the 3.4 micrometer feature N89-13342
Laboratory investigations N89-13343
Focus on the future N89-13344
Current status of the international Halley Watch infrared net archive N89-13345
Interstellar grain chemistry and the composition of comets N89-13346
The spectral appearance of comets from 5 to 20 micrometers: A survey of the data N89-13347
IR-dust observations of Comet Tempel 2 with CRAF VIMS N89-13349
Cometary dust size distributions from flyby spacecraft N89-13350
Polarization images of Comet Halley N89-13351
An albedo map of P/Halley on 13 March 1986 N89-13355
The problem of clustering in laboratory studies of cometary dust N89-13356
Light scattering of large rough particles application to cometary grains N89-13357
Thermal properties of heterogeneous grains N89-13358
Some 5-13 micrometer airborne observations of Comet Wilson 1986l: Preliminary results N89-13360
Aerodynamic properties of fractal grains: Implications for the primordial solar nebula N89-13361
Laboratory simulations of comet surfaces N89-13366
COMETS
Atomic and molecular abundances in comets N89-13376
COMMAND AND CONTROL
Advanced workstations for Meteosat command and control, volume 1
[BSO/AETR87030101-VOL-1] N89-12573
Advanced workstations for Meteosat command and control. Volume 2: Appendices
[BSO/AETR87030101-VOL-2] N89-12574
Three-dimensional visual display for a prototype command and control workstation
[AD-A197319] N89-13142
Evaluation of expert systems in decisionmaking organizations
[AD-A196448] N89-13192
Computer based intelligence support: An integrated expert system and decision support systems approach
[AD-A197386] N89-13197
COMMERCE
Federal Laboratory Consortium for Technology Transfer: Putting technology to work. Examples of industry-laboratory cooperation contributing to our nation's economic strength
[PB88-243357] N89-13307
COMMUNICATING
Communication: The key to integrating remote sensing and geographic information systems N89-12963
COMMUNICATION EQUIPMENT
Northeast Artificial Intelligence Consortium (NAIC). Review of technical tasks, volume 2, part 1
[AD-A189773] N89-13180
COMMUNICATION NETWORKS
The design of antenna matching networks using a microcomputer
[AD-A197364] N89-12802

A comparison of propagation model predictions with EPLRS (Enhanced Position Location and Reporting System) UHF network measurements
[AD-A197473] N89-12804
Study of the integration of advanced communications satellite systems and terrestrial networks, executive summary
[ESA-CR(P)-2655] N89-12809
The RACE Program of the European Communities
[ONRL-8-014-R] N89-12811
Applications of parallelism to current algorithms for intelligence analysis
[NASA-CR-183351] N89-13165
Distributed problem solving N89-13186
A shared knowledge base for independent problem solving agents N89-13187
Providing intelligent assistance in distributed office environments N89-13189

COMMUNICATION SATELLITES
Fifteenth Space Simulation Conference: Support the Highway to Space Through Testing
[NASA-CP-3015] N89-12582
The solar simulation test of the ITALSAT thermal structural model N89-12613

COMPARISON
A comparative study of differing vortex structures arising in unsteady separated flows N89-12773
Detection of excited states by laser-induced fluorescence and analysis of energy transfer
[AD-A197770] N89-12855

COMPLEX COMPOUNDS
Electrogenerated chemiluminescence
[AD-A197163] N89-12691

COMPONENTS
Space station integrated propulsion and fluid systems study
[NASA-CR-179393] N89-12581

COMPOSITE MATERIALS
Combined mechanical loading of composite tubes
[NASA-CR-183012] N89-12681
Composite curing process nondestructive evaluation
[AD-A197834] N89-12873

COMPOSITE STRUCTURES
Finite element analysis of composite laminates N89-12672
An axisymmetric linear/high-order finite element for filament wound composite structures N89-12674

COMPRESSIBLE FLOW
A spectral collocation solution to the compressible stability eigenvalue problem
[NASA-TP-2858] N89-12543
Foundations of the blade-vortex interaction problem: Structure and behavior of travelling compressible vortices
[AD-A197370] N89-12550

COMPRESSION LOADS
An artificial compression method for ENO schemes: The slope modification method
[NASA-CR-184613] N89-13215

COMPRESSION TESTS
Composite rods in carbon-epoxy Fibredux 914 C/TS-6T-6K-34
[SARMA-TR-87-2431A] N89-12677
Damage of carbon fiber tubes and rods — aircraft construction materials
[SARMA-TR-882401] N89-12682

COMPRESSIVE STRENGTH
Truss-core corrugation for compressive loads
[NASA-CASE-LAR-13436-1] N89-12786

COMPRESSORS
Assessment of Japanese variable speed heat pump technology
[DE88-013246] N89-12826
Combustor diffuser interaction program N89-12893

COMPUTATION
Computer evaluation of ion-implanted dopant profile evolution during annealing N89-12756
A numerical model for the computation of radiance distributions in natural waters with wind-roughened surfaces
[AD-A197207] N89-13128
Speed and data structures in computer algebra systems
[AD-A197131] N89-13146
Voyeur: Graphical views of parallel programs
[AD-A197103] N89-13177
A lexical conceptual approach to generation for machine translation
[AD-A197356] N89-13304

COMPUTATIONAL FLUID DYNAMICS
The laminar boundary layer on an airfoil started impulsively from rest N89-12540
Simulation of 2-dimensional viscous flow through cascades using a semi-elliptic analysis and hybrid C-H grids
[NASA-CR-4180] N89-12553
A control-volume method for analysis of unsteady thrust augmenting ejector flows
[NASA-CR-182203] N89-12566
A numerical method for computing unsteady 2-D boundary layer flows
[NASA-CR-4198] N89-12835
Influence of bulk turbulence and entrance boundary layer thickness on the curved duct flow field
[NASA-CR-4188] N89-12838
Improved numerical methods for turbulent viscous recirculating flows N89-12895

COMPUTATIONAL GRIDS
A spectral collocation solution to the compressible stability eigenvalue problem
[NASA-TP-2858] N89-12543
Simulation of 2-dimensional viscous flow through cascades using a semi-elliptic analysis and hybrid C-H grids
[NASA-CR-4180] N89-12553
An adaptive method with mesh moving and local mesh refinement for time-dependent partial differential equations
[AD-A197772] N89-13208

COMPUTER AIDED DESIGN
The state of PC-based CADD (Computer-Aided Design and Drafting) systems
[DE88-017326] N89-13170
Artificial intelligence theory and reconfigurable control systems
[AD-A197255] N89-13195
Multivariate regression with emphasis on multivariate spline methods
[AD-A197793] N89-13209

COMPUTER AIDED MAPPING
Combining spectral and structural analyses to select useful cartographic information from SPOT imagery N89-13052
Extraction of dense digital elevation models from SPOT stereo imagery N89-13053

COMPUTER GRAPHICS
Improvement in NOAA-AVHRR snowcover determination for runoff prediction N89-13040
Statistics and high resolution imaging of snowpack at 35 GHz using a microcomputer N89-13047
Microcomputers (PCs) for snow cover analyses using multisensor satellite data N89-13049
Graphical programming and monitoring
[AD-A197342] N89-13159
Voyeur: Graphical views of parallel programs
[AD-A197103] N89-13177
Applications of the ISI (Information Sciences Institute) grapher
[AD-A197230] N89-13194

COMPUTER NETWORKS
Implementation issues for level O image processor software within an application package
[AD-A197768] N89-13162
Empirical analysis and refinement of expert system knowledge bases
[AD-A197241] N89-13303

COMPUTER PROGRAMMING
Software process modeling
[AD-A197137] N89-13154
Graphical programming and monitoring
[AD-A197342] N89-13159
Pan 1: An introduction for users, revision
[AD-A197344] N89-13160
Bayesian reasoning tool
[AD-A197351] N89-13196
Engineering applications of heuristic multilevel optimization methods
[NASA-TM-101504] N89-13203
Global optimization of concave functions subject to separable quadratic constraints and of all-quadratic separable problems
[AD-A197747] N89-13206
Tokamak equilibrium determination through function parameterization N89-13272
Multiple representation document development
[AD-A197369] N89-13305

COMPUTER PROGRAMS
Automated Airframe Assembly Program (AAAP) survey of CIM status in the aircraft industry
[AD-A197368] N89-12535
Development and validation of an advanced low-order panel method
[NASA-TM-101024] N89-12554
Evaluation of three turbulence models for the prediction of steady and unsteady airloads
[NASA-TM-101413] N89-12555
Finite element analysis of composite laminates N89-12672
Six degree of freedom simulation computer program for aeroelastic free-flight projectiles N89-12771
Installation of the ADINA FEM computer programs N89-12778
Fire aerosol experiment and comparisons with computer code predictions
[DE88-016328] N89-12788
Exploring the back-propagation network for speech applications
[AD-A197385] N89-12803
Focal region fields of distorted reflectors
[NASA-CR-183001] N89-12810
Gas flow and global code programme
[DE88-012635] N89-12861
Influence of bulk turbulence and entrance boundary layer thickness on the curved duct flow field N89-12896
On 3-D inelastic analysis methods for hot section components N89-12905
Automation software for a materials testing laboratory N89-12917
Hanford Meteorological Station computer codes. Volume 8: The REVIEW computer code
[DE88-015958] N89-13123
Multidimensional item response theory estimation: A computer program
[AD-A197160] N89-13155
Graphical programming and monitoring
[AD-A197342] N89-13159
Implementation issues for level O image processor software within an application package
[AD-A197768] N89-13162
Microwave and electron beam computer programs
[AD-A197798] N89-13164
Applications of the ISI (Information Sciences Institute) grapher
[AD-A197230] N89-13194
The solution of linear systems of equations with a structural analysis code on the NAS CRAY-2
[NASA-CR-4159] N89-13202
Investigation of acceleration and densification of electrons utilizing travelling magnetic waves
[AD-A197700] N89-13242
MANPRINT (Manpower and Personnel Integration Program) primer
[AD-A197681] N89-13296

COMPUTER STORAGE DEVICES
Applications of parallelism to current algorithms for intelligence analysis
[NASA-CR-183351] N89-13165

COMPUTER SYSTEMS DESIGN
Data bases and remote sensing N89-12965
Improving the accessibility of spatially referenced geological information N89-13026
Statistics and high resolution imaging of snowpack at 35 GHz using a microcomputer N89-13047
Architectures for optoelectronic computing
[REPT-72/88/R260/U] N89-13148
An approach to automate digital signal processor code generation
[ETN-88-93530] N89-13172

COMPUTER SYSTEMS PERFORMANCE
Performance analysis of the Alliant FX/8 multiprocessor using statistical clustering
[NASA-CR-183221] N89-13145
Data acquisition of the thermogravimetric analysis testing summary
[DE88-016062] N89-13147
The solution of linear systems of equations with a structural analysis code on the NAS CRAY-2
[NASA-CR-4159] N89-13202

COMPUTER SYSTEMS PROGRAMS
Natural language generation
[AD-A197321] N89-12800
Design document for GCS version
[NASA-CR-183278] N89-13150
Software process modeling
[AD-A197137] N89-13154

COMPUTER VISION
Optically controlled welding system
[NASA-CASE-MFS-29291-1] N89-12868
Optical computing based on neuronal models
[AD-A197749] N89-13199
Adaptive machine vision
[AD-A197039] N89-13222

COMPUTERIZED SIMULATION
Numerical methods for the guidance and control of air-to-air missiles N89-12561
A control-volume method for analysis of unsteady thrust augmenting ejector flows
[NASA-CR-182203] N89-12566
Multiple input/output random vibration control system N89-12594
Thermo-mechanical performance evaluation of cryogenic turbopump ball bearings N89-12637
Thermal analysis of SSME turbopump bearings N89-12638
Results of coaxial injector element testing N89-12651
Combustion modeling: Progress and projections N89-12652

A probabilistic approach to composite micromechanics
[NASA-TM-101366] N89-12684
Prediction of heat transfer between the combustion space and the load
[DE88-016313] N89-12698
A computer simulation of a plasma armature railgun N89-12780
Application of autoregressive methods to adaptive excision of interfering tones from direct sequence spread spectrum communications systems
[AD-A197801] N89-12805
Algorithms for the self-consistent simulation of high power klystrons
[DE88-010684] N89-12812
Direct simulation of three-dimensional flow about the AFE vehicle at high altitudes
[NASA-TM-101492] N89-12834
HOST combustion R and T overview N89-12879
Turbine stator flow field simulations N89-12902
Structural response calculations for a metal booster tank model
[DE88-017095] N89-12929
Fundamentals of middle-atmospheric dynamics
[AD-A197358] N89-13110
C Cloud S (Climatology of Cloud Statistics) database (users manual)
[AD-A196497] N89-13118
The effect of vertical wind shear on tropical cyclone movement
[AD-A197218] N89-13120
AUTOCREW implementation: Inbound surface-to-air missile simulation
[AD-A197674] N89-13143
Mathematical modelling and computer simulation using Cartesian grid
[TM-AE-8804] N89-13149
Fault diagnosis based on continuous simulation models
[NASA-CR-182737] N89-13152
Microwave and electron beam computer programs
[AD-A197798] N89-13164
Simulating vehicle dynamics: The importance of a valid forcing function
[DE88-010527] N89-13167
Kinetic effects on electron cyclotron emission during electron cyclotron heating in tokamaks N89-13268
Fundamental harmonic electron cyclotron emission for hot, loss-cone type distributions N89-13269
Transport code studies of m=2 mode control by local electron cyclotron heating in TFR N89-13270
Optimizing current drive by electron cyclotron waves in the presence of trapped particles N89-13276
Synthesis of accretion disk and nonthermal source models for AGN
[DE88-013098] N89-13384

COMPUTERS
Speed and data structures in computer algebra systems
[AD-A197131] N89-13146

CONCAVITY
Global optimization of concave functions subject to separable quadratic constraints and of all-quadratic separable problems
[AD-A197747] N89-13206

CONCRETES
Challenging applications for hydrated and chemically reacted ceramics
[DE88-015397] N89-12742

CONCURRENT PROCESSING
Performance analysis of the Alliant FX/8 multiprocessor using statistical clustering
[NASA-CR-183221] N89-13145
Applications of parallelism to current algorithms for intelligence analysis
[NASA-CR-183351] N89-13165

CONDENSATES
On the microstructure theory of a condensate layer in a white dwarf atmosphere
[DE88-703324] N89-13385

CONDUCTORS
Superionic conductors as fast, repetitive opening switches
[AD-A197365] N89-12817

CONFERENCES
Definition of a space transportation systems cargo element (Shuttle-C). Orientation
[NASA-CR-179404] N89-12579
Fifteenth Space Simulation Conference: Support the Highway to Space Through Testing
[NASA-CP-3015] N89-12582
Advanced Earth-to-Orbit Propulsion Technology 1986, volume 2
[NASA-CP-2437-VOL-2] N89-12626
Gordon Conference on Microbial Adhesion
[AD-A197352] N89-12735
Report on JANNAF Workshop Influence of Gas-Phase Chemical Kinetics on Low-Pressure Ignition and Flamespreading in Solid Propellant
[AD-A197854] N89-12751
Turbine Engine Hot Section Technology 1986
[NASA-CP-2444] N89-12876
Proceedings of the 1988 International Geoscience and Remote Sensing Symposium (IGARSS 1988) on Remote Sensing: Moving Towards the 21st Century, volume 1
[ESA-SP-284-VOL-1] N89-12936
European Seminar on Neural Computing
[ONRL-8-010-C] N89-13173
Nuclear technology for the year 2000
[DE88-005041] N89-13223
The 6th All-Union Conference on Nonlinear Optics (table of contents)
[AD-A197347] N89-13250
FOM Contributions to the 15th European Conference on Controlled Fusion and Plasma Heating
[REPT-88-178] N89-13266
Second Workshop on Improvements to Photometry
[NASA-CP-10015] N89-13310

CONFIDENCE LIMITS
Two-sample inference for median survival times based on one-sample procedures for censored survival data
[AD-A197776] N89-13218
Use of distance versus statistical distance in acceptance tests
[NASA-CR-183353] N89-13220

CONGRESSIONAL REPORTS
Advancing automation and robotics technology for the space station and for the US economy
[NASA-TM-100989] N89-13198

CONICAL BODIES
Laser speckle from thin and cascaded diffusers
[AD-A197066] N89-12850

CONSOLIDATION
Slurry-pressing consolidation of silicon nitride
[NASA-TM-101365] N89-12746

CONSTITUTIVE EQUATIONS
Constitutive modeling for isotropic materials N89-12904
A multiaxial theory of viscoplasticity for isotropic materials N89-12908
Constitutive modeling for single crystal superalloys N89-12911
Constitutive modelling of single crystal and directionally solidified superalloys N89-12912
Life prediction and constitutive models for engine hot section N89-12916

CONTAINERS
Challenging applications for hydrated and chemically reacted ceramics
[DE88-015397] N89-12742

CONTAMINANTS
WF/PC internal molecular contamination during system thermal-vacuum test N89-12583
Wide Field/Planetary Camera (WF/PC) contamination control assessment N89-12584
Class 100 large spacecraft facility N89-12586

CONTAMINATION
WF/PC internal molecular contamination during system thermal-vacuum test N89-12583
Wide Field/Planetary Camera (WF/PC) contamination control assessment N89-12584
Correlation studies on surface particle detection methods N89-12587

CONTEXT
People versus probability
[DE88-017380] N89-13221

CONTINENTAL SHELVES
Mass and heat balances in the upper ocean N89-13089

CONTINUUM MECHANICS
Fracture and fatigue
[AD-A197310] N89-12927

CONTRACTORS
BES welding science contractors
[DE88-016589] N89-12869

CONTROL
Circuit for actuation of a stepping motor
[INPE-4633-NTE/281] N89-12814

CONTROL SYSTEMS DESIGN
Remote guidance of payloads under maneuverable parachutes
[E-639] N89-12571
Advancing automation and robotics technology for the space station and for the US economy
[NASA-TM-100989] N89-13198

CONTROL THEORY
A vortex panel method for potential flows with applications to dynamics and control
[AD-A197091] N89-12549
Multiple input/output random vibration control system N89-12594
AUTOCREW implementation: Inbound surface-to-air missile simulation
[AD-A197674] N89-13143
Artificial intelligence theory and reconfigurable control systems
[AD-A197255] N89-13195

CONTROLLED FUSION
FOM Contributions to the 15th European Conference on Controlled Fusion and Plasma Heating
[REPT-88-178] N89-13266
The m=1 internal kink mode in a toroidal plasma with a flat q-profile near q=1 N89-13267
The applicability of Rutherford scattering for Ti measurements at medium and large-sized experiments N89-13273

CONTROLLERS
Fiber optic control system integration
[NASA-CR-179568] N89-13256

CONVECTION
The stability of time-dependent fluid flows N89-12825
Temperature profile in semi-infinite planar slab with exponential source and convective boundary condition: Application to laser heating
[DE88-016746] N89-12831
Population inversion non-equilibrium flow simulation calculations of the capabilities of convection flow lasers
[AD-A197741] N89-12854

CONVECTIVE FLOW
Convective flows in enclosures with vertical temperature or concentration gradients
[NASA-TM-101373] N89-12753

CONVECTIVE HEAT TRANSFER
Heat transfer in the tip region of a rotor blade simulator N89-12898

CONVERGENCE
Optimal rates of convergence for deconvolving a density
[AD-A197748] N89-13207
Bearing error and the central limit theorem
[NASA-CR-183009] N89-13219

COOLANTS
Development of a thermal and structural analysis procedure for cooled radial turbines
[NASA-TM-101416] N89-12568

COOLING
LOX/hydrocarbon combustion and cooling survey N89-12648
Liquid oxygen cooling of high pressure LOX/hydrocarbon rocket thrust chambers N89-12649
Tests of a multichannel photometer based on silicon diode detectors N89-13314
Absolute photometric calibration of detectors to 0.3 mmag using amplitude-stabilized lasers and a helium-cooled absolute radiometer N89-13318

COOLING SYSTEMS
Aerojet TechSystems Company contribution to LOX/HC combustion and cooling technology N89-12646
Survey of LOX/hydrocarbon combustion and cooling N89-12647

COPPER ALLOYS
Effects of oxygen/hydrogen combustion chamber environment on copper alloys N89-12653
An electron microscopy study of tweed microstructures and premartensitic effects in high damping 53Cu45Mn2Al alloy
[AD-A197317] N89-12709
Mechanical behavior of superplastically-formed Al-Cu-Li-Zr alloy 2090
[DE88-016241] N89-12714

CORNER FLOW
Liquid metal flow in a large-radius elbow with a uniform magnetic fluid
[DE88-016957] N89-12832

CORRELATION
A global analysis and correlation of Nimbus 7 cloud and longwave radiation data
[AD-A197223] N89-13121

CORROSION
Moisture interaction and stability of ZOT (Zinc Orthotitanate) thermal control spacecraft coating N89-12618
Determination of sulfuric acid, oxalic acid, and their matrix effects in aluminum anodizing solutions by ion chromatography
[AD-A197734] N89-12694
Corrosion of nickel and Monel welds of steel in chlorine trifluoride
[DE88-014122] N89-12706

CORROSION PREVENTION
Moisture interaction and stability of ZOT (Zinc Orthotitanate) thermal control spacecraft coating N89-12618

CORROSION RESISTANCE
The development of a hydrogen resistant alloy N89-12661

CORRUGATED PLATES
Truss-core corrugation for compressive loads
[NASA-CASE-LAR-13438-1] N89-12786
COSMIC BACKGROUND EXPLORER SATELLITE
The Instrument Test Dewar (ITD): Testing satellite instruments at 1.5 K N89-12604
COSMIC DUST
Infrared Observations of Comets Halley and Wilson and Properties of the Grains
[NASA-CP-3004] N89-13330
Infrared observations of the dust coma N89-13331
Grain optical properties N89-13332
Cometary dust composition N89-13333
A two component model for thermal emission from organic grains in Comet Halley N89-13340
On the carbon abundance in Comet Halley derived from the 3 micron feature: Comparison with interstellar dust N89-13341
Laboratory investigations N89-13343
Focus on the future N89-13344
Interstellar grain chemistry and the composition of comets N89-13346
The near-infrared polarization and color of Comet Halley: What can we learn about the grains N89-13348
IR-dust observations of Comet Tempel 2 with CRAF VIMS N89-13349
Cometary dust size distributions from flyby spacecraft N89-13350
Polarization images of Comet Halley N89-13351
Detection of parent molecules in the IR spectrum of P/Halley with the IKS-Vega spectrometer N89-13352
Infrared observations of P/Halley and P/Encke N89-13353
Airborne 20-65 micron spectrophotometry of Comet Halley N89-13354
The problem of clustering in laboratory studies of cometary dust N89-13356
Light scattering of large rough particles application to cometary grains N89-13357
Thermal properties of heterogeneous grains N89-13358
Aerodynamic properties of fractal grains: Implications for the primordial solar nebula N89-13361
Color gradients in the coma of P/Halley N89-13362
Optical properties of cometary grains N89-13363
A possible explanation for the inconsistency between the Giotto grain mass distribution and ground-based observations N89-13364
Properties of interstellar dust in reflection nebulae N89-13365
Laboratory simulations of comet surfaces N89-13366
A multicomponent model of the infrared emission from Comet Halley N89-13367
COSMIC RAYS
A conceptual design study of the reusable reentry satellite
[NASA-TM-101043] N89-12623
COSMOLOGY
Tenth European Regional Astronomy Meeting of the IAU: Abstracts
[DE88-703273] N89-13370
Stochastic stage of an inflationary universe model
[DE88-753149] N89-13373
Gravitation, black holes and space-time physics
[DE88-703054] N89-13377
The large-scale structure of the universe: Some theoretical considerations N89-13381
COST EFFECTIVENESS
Cost effective alternative to low irradiance measurements N89-12619
On-orbit servicing and cost effectiveness of Columbus Polar Platform concepts N89-12983
COTTON
Cotton area mapping using multitemporal satellite data integrated within a geographical information system applied to a cotton boll weevil control programme in Paraguay N89-13077
COUPLING
Fracton dynamics on fractal networks
[AD-A197166] N89-12708
Investigation of laser diode coupling using nonlinear optics N89-12781
The design of antenna matching networks using a microcomputer
[AD-A197364] N89-12802
Comments on the high frequency behavior of the coupling of an accelerator beam to its environment
[CEBAF-PR-88-006] N89-13245
A consideration of the use of optical fibers to remotely couple photometers to telescopes N89-13326
COVALENT BONDS
Transition-metal oxide superconductivity
[AD-A197069] N89-13280
COVARIANCE
Identifying nonlinear covariate effects in semimartingale regression models
[AD-A197323] N89-13205
Use of distance versus statistical distance in acceptance tests
[NASA-CR-183353] N89-13220
CRACK CLOSURE
Fatigue crack retardation following overloads in Inconel 718, Ti-5Al-2.5Sn, and Haynes 188 N89-12636
On the effect of R-ratio and Kfmax on fracture toughness measurement, fatigue crack propagation, and fatigue crack closure N89-12875
CRACK INITIATION
Simplified cyclic structural analysis of SSME turbine blades N89-12632
Effects of oxygen/hydrogen combustion chamber environment on copper alloys N89-12653
Fatigue and fracture overview N89-12882
CRACK OPENING DISPLACEMENT
Development of a computer-controlled technique to determine crack growth rate properties in controlled environments using crack opening displacement N89-12657
CRACK PROPAGATION
Effects of high mean stress on the high-cycle fatigue of PWA 1480 and DS MAR M 246 + Hf at 1000 F N89-12633
Fatigue crack retardation following overloads in Inconel 718, Ti-5Al-2.5Sn, and Haynes 188 N89-12636
Development of a computer-controlled technique to determine crack growth rate properties in controlled environments using crack opening displacement N89-12657
LCF and crack growth rate of turbine blade alloys in hydrogen and hydrogen/steam environments N89-12660
Mixed-mode fracture in fiber-reinforced composite materials N89-12669
Toughening by aligned, frictionally constrained fibers
[AD-A197194] N89-12676
Fatigue crack growth of 5456-H116 aluminum and HSLA-80 weldments
[AD-A197830] N89-12712
Research on mechanical properties for engine life prediction
[AD-A197816] N89-12864
On the effect of R-ratio and Kfmax on fracture toughness measurement, fatigue crack propagation, and fatigue crack closure N89-12875
Elevated temperature crack growth N89-12915
Grain boundary oxidation and its effects on high temperature fatigue life N89-12918
Fracture and fatigue
[AD-A197310] N89-12927
CRACKING (CHEMICAL ENGINEERING)
Homogeneous catalytic production of hydrogen and other molecules from water-DMF (N-dimethylformamide) solutions
[AD-A197072] N89-12690
CRATERS
On the resistance of ceramics to high velocity penetration
[AD-A197320] N89-12734
CREEP BUCKLING
Non-isothermal buckling behavior of viscoplastic shell structures
[NASA-CR-183013] N89-12931
CREEP PROPERTIES
High-temperature LCF of Ni-201 and 304L stainless steel N89-12635
Coble creep, cavity sintering and cavity growth
[DE88-013846] N89-12703
Fatigue and fracture overview N89-12882
Creep fatigue life prediction for engine hot section materials (isotropic): Fourth year progress review N89-12914
Grain boundary oxidation and its effects on high temperature fatigue life N89-12918
CREEP RUPTURE STRENGTH
Multispecimen test facility for high-pressure hydrogen creep studies N89-12655
LCF and crack growth rate of turbine blade alloys in hydrogen and hydrogen/steam environments N89-12660
Properties of rapidly solidified aluminum alloys. German-Norwegian Project (1983-1987)
[DFVLR-FB-88-24] N89-12719
CRITICAL TEMPERATURE
Generation of the J(sub c), H(sub c), T(sub c) surface for commercial superconductor using reduced-state parameters
[DE88-014038] N89-13278
CROP IDENTIFICATION
Crop classification with multi-temporal X-band SAR data N89-12990
CROP INVENTORIES
Analysis of potato crop distribution using remotely sensed and environmental data in a pilot geographical information system N89-12967
Large area TM land cover classification of Mittlerer Oberrhein County, southwest Germany, and its use for regional planning and crop surveys N89-12986
Crop classification with multi-temporal X-band SAR data N89-12990
Small format air photo from ultrahigh aircraft as an aid for data collection of agricultural statistics in Sahelian countries N89-13003
An evaluation of satellite imagery, LANDSAT Thematic Mapper and SPOT-1 HRV, for grassland inventory in the UK N89-13057
CROP VIGOR
Analysis of potato crop distribution using remotely sensed and environmental data in a pilot geographical information system N89-12967
CROSS POLARIZATION
Examining the polarisation phase retrieval of a dual channel multipolarisation radar N89-13019
CROSS SECTIONS
Differential cross sections for electron-impact excitation of atomic ions
[ISAS-RN-365] N89-13237
CRYOGENIC EQUIPMENT
Space simulators for laser optics N89-12597
The Instrument Test Dewar (ITD): Testing satellite instruments at 1.5 K N89-12604
The Frascati (Italy) gravitational antenna, 1987
[IFSI-88-4] N89-12846
CRYOGENIC FLUID STORAGE
Cryogenic insulation system
[NASA-CASE-LAR-13506-1] N89-12741
CRYOGENIC FLUIDS
Mass flow meter using the triboelectric effect for measurement in cryogenics
[NASA-CR-179572] N89-12836
Mass flow measurement of liquid cryogens using the triboelectric effect
[NASA-CR-179519] N89-12837
CRYOGENIC WIND TUNNELS
Sidewall boundary-layer measurements with upstream suction in the Langley 0.3-meter transonic cryogenic tunnel
[NASA-CR-4192] N89-12544
CRYOGENICS
Surface modification for wear resistance in a liquid oxygen turbopump environment N89-12644
CRYSTAL DEFECTS
Fundamental studies and device development in beta silicon carbide
[AD-A197843] N89-12739
CRYSTAL GROWTH
Convective flows in enclosures with vertical temperature or concentration gradients
[NASA-TM-101373] N89-12753
Preparation and structure of Li-stabilized Na(+) beta' alumina single crystals
[AD-A197245] N89-13283
Chemical precursors to zinc sulfide: ZnS whisker synthesis
[AD-A197262] N89-13284
CRYSTAL OPTICS
The 6th All-Union Conference on Nonlinear Optics (table of contents)
[AD-A197347] N89-13250
CRYSTAL STRUCTURE
Preparation and structure of Li-stabilized Na(+) beta' alumina single crystals
[AD-A197245] N89-13283
CRYSTALLIZATION
Backscatter laser depolarization studies of simulated stratospheric aerosols: Crystallized sulfuric acid droplets
[NASA-CR-183387] N89-13111
CULTURE TECHNIQUES
Horizontally rotated cell culture system
[NASA-CASE-MSC-21294-1] N89-13131
CURING
Composite curing process nondestructive evaluation
[AD-A197834] N89-12873
CURRENT DENSITY
High T(sub c) superconductors: Will they replace helium temperature superconductors for magnets
[DE88-016632] N89-13279
CYBERNETICS
AUTOCREW implementation: Inbound surface-to-air missile simulation
[AD-A197674] N89-13143
Optical computing based on neuronal models
[AD-A197749] N89-13199
CYCLIC LOADS
Constitutive behavior of single crystal PWA 1480 and directionally solidified MAR-M 246 under monotonic and cyclic loads at high and low temperature N89-12634

Thermomechanical characterization of Hastelloy-X under uniaxial cyclic loading N89-12909

CYCLONES

An analysis of the error characteristics of Atlantic tropical cyclone track prediction models N89-13117

An analysis of the error characteristics of Atlantic tropical cyclone track prediction models [AD-A197146] N89-13119

The effect of vertical wind shear on tropical cyclone movement [AD-A197218] N89-13120

Forecasting aids for setting tropical cyclone conditions: Sasebo and Iwakuni, Japan [AD-A197802] N89-13122

CYCLOTRON RADIATION

Kinetic effects on electron cyclotron emission during electron cyclotron heating in tokamaks N89-13268

Fundamental harmonic electron cyclotron emission for hot, loss-cone type distributions N89-13269

CYCLOTRON RESONANCE

Kinetic effects on electron cyclotron emission during electron cyclotron heating in tokamaks N89-13268

CYLINDRICAL ANTENNAS

Polarization-dependent attenuation of dielectric cylinder arrays N89-12955

CYLINDRICAL BODIES

Interpretation of coherent polarimetric signatures by dielectric cylinder models N89-12957

A note on incomplete integrals of cylindrical functions [AD-A197822] N89-13210

Large silicon clusters: Confirmation of Phillips' conjecture [AD-A197487] N89-13241

CYLINDRICAL SHELLS

Nearfield acoustic radiation from a point-excited cylindrical shell [AD-A197282] N89-13234

CZOCHRALSKI METHOD

LEC (Liquid Encapsulated Czochralski) growth of InP with magnetic field assisted melt stabilization and heat transfer control [AD-A196748] N89-12688

D

DAMAGE

The NASA atomic oxygen effects test program N89-12589

DAMAGE ASSESSMENT

Fatigue and fracture overview N89-12882

Thermal barrier coating life prediction model development N89-12922

Spectral characterization of forest damage in beech, oak and pine stands N89-13085

DAMPING

Damping seal tester progress and initial test results N89-12627

DAMS

Snowmelt runoff estimation using snow cover extent data and its application to optimum control of dam water level N89-13042

DATA ACQUISITION

Test data acquisition system for the ESTEC large solar simulator at ESA/ESTEC N89-12620

Small format air photo from ultrahigh aircraft as an aid for data collection of agricultural statistics in Sahelian countries N89-13003

Data acquisition of the thermogravimetric analysis testing summary [DE88-016062] N89-13147

Plan recognition, knowledge acquisition and explanation in an intelligent interface N89-13191

Space environment laboratory data acquisition and display system 2 [PB88-205471] N89-13299

DATA BASE MANAGEMENT SYSTEMS

Space station integrated propulsion and fluid systems study [NASA-CR-179393] N89-12581

Practical issues relating to the internal database predicates in an OR-parallel prolog: Extensions and useful hacks [DE88-010019] N89-13174

Multiple representation document development [AD-A197369] N89-13305

DATA BASES

High temperature adhesive systems [AD-A197077] N89-12726

EURACS: A European radar cross section database N89-12944

Data bases and remote sensing N89-12965

Speed and data structures in computer algebra systems [AD-A197131] N89-13146

Current status of the international Halley Watch infrared net archive N89-13345

DATA COLLECTION PLATFORMS

Data collection system operating on Japan's first marine observation satellite: Inflight evaluation of the system performance N89-13007

DATA LINKS

LORAN C Offshore Flight Following (LOFF) in the Gulf of Mexico [AD-A197179] N89-12558

DATA MANAGEMENT

LORAN C Offshore Flight Following (LOFF) in the Gulf of Mexico [AD-A197179] N89-12558

Software process modeling [AD-A197137] N89-13154

Plan recognition, knowledge acquisition and explanation in an intelligent interface N89-13191

DATA PROCESSING

Automation software for a materials testing laboratory N89-12917

Neural network performance on the stochastic exclusive-or problem [AD-A197789] N89-13179

The processing of qualitative information in a natural language context N89-13297

Multiple representation document development [AD-A197369] N89-13305

DATA PROCESSING EQUIPMENT

Micro-computer network architecture for range instrumentation applications [AD-A196971] N89-13175

DATA PROCESSING TERMINALS

Three-dimensional visual display for a prototype command and control workstation [AD-A197319] N89-13142

DATA SAMPLING

On the sampling in imaging microwave radiometers N89-12940

The effects of undersampling on multipolarization SAR images N89-12956

The interrelationship between resampling method and information extraction technique N89-13065

DATA SMOOTHING

An analysis of directional ambiguities in wind scatterometer measurements N89-13071

DATA STORAGE

Temporal clustering in the multi-target tracking environment [AD-A197153] N89-12796

DATA STRUCTURES

Speed and data structures in computer algebra systems [AD-A197131] N89-13146

SNePS considered as a fully intensional propositional semantic network N89-13184

DATA SYSTEMS

Requirements for ongoing development of the Pilot Land Data System (PLDS) N89-12958

DATA TRANSMISSION

The RACE Program of the European Communities [ONRL-8-014-R] N89-12811

Boeing Military Airplane Company technical order transfer tests [DE88-012233] N89-13151

DECISION MAKING

An evaluation of ground collision avoidance system algorithm [AD-A197831] N89-12560

Classification decision rule modification on the basis of information extracted from training data --- satellite imagery N89-13062

A logic for belief revision N89-13182

POPLAR: A testbed for cognitive modeling N89-13190

Plan recognition, knowledge acquisition and explanation in an intelligent interface N89-13191

Evaluation of expert systems in decisionmaking organizations [AD-A196448] N89-13192

Computer based intelligence support: An integrated expert system and decision support systems approach [AD-A197386] N89-13197

People versus probability [DE88-017380] N89-13221

The processing of qualitative information in a natural language context N89-13297

DECODING

Euclidean decoders for BCH codes [AD-A197242] N89-13157

DECOMPRESSION SICKNESS

Research and development of anti-g life support systems. Part 2: Decompression sickness research [AD-A197675] N89-13133

DEFECTS

Calculation of Weibull strength parameters and Batdorf flow-density constants for volume- and surface-flaw-induced fracture in ceramics [NASA-TM-100890] N89-12930

DEFENSE PROGRAM

EMP (electromagnetic pulse) mitigation program approach [AD-A197849] N89-12807

DEFLECTION

SSME bearing health monitoring using a fiberoptic deflectometer N89-12645

DEGRADATION

Materials selection for long life in LEO: A critical evaluation of atomic oxygen testing with thermal atom systems N89-12590

Atomic oxygen effects on candidate coatings for long-term spacecraft in low earth orbit N89-12592

Superionic conductors as fast, repetitive opening switches [AD-A197365] N89-12817

DEGREES OF FREEDOM

Six degree of freedom simulation computer program for aeroelastic free-flight projectiles N89-12771

DELAMINATING

The effect of delamination on the response of advanced composite laminates N89-12668

DELTA WINGS

Unsteady structure of flow past a pitching delta wing N89-12541

DENMARK

Danish Space Research Institute N89-13391

DENSITOMETERS

An optical heterodyne densitometer N89-13323

DENSITY

Investigations into the plasma spray process [DE88-014524] N89-12787

DENSITY DISTRIBUTION

Optimal rates of convergence for deconvolving a density [AD-A197748] N89-13207

DEPOLARIZATION

Optimal reception in depolarising clutter N89-13008

DEPOSITION

Investigations into the plasma spray process [DE88-014524] N89-12787

Preparation and properties of high-deposition-rate a-Si:H films and solar cells using disilane [DE88-001191] N89-13098

Worldwide deposition of Sr-90 through 1985 [DE88-015577] N89-13105

DESIGN ANALYSIS

Space simulators for laser optics N89-12597

The two axis motion simulator for the large space simulator at ESTEC (European Space Research and Technology Center) N89-12600

Thermal/structural design verification strategies for large space structures N89-12602

IRIS thermal balance test within ESTEC LSS N89-12603

Solar simulation with a rectangular beam N89-12605

Test stand design and analysis for Titan 34D static firing N89-12609

Test stand for Titan 34D SRM static firing N89-12610

A multimegawatt space power source radiator design [DE88-015185] N89-12662

Stability limits and combustion measurements in low calorific value gas flames N89-12687

Designing simulator tasks to study the high speed, low altitude environment N89-12770

Dynamic synthesis of joined/hermetic shell structures using state space method N89-12874

Laser driven inertial confinement fusion N89-13229

Design of vacuum chambers downstream of NSLS X-ray ring insertion devices [DE88-015715] N89-13247

A multichannel fiber optic photometer present performance and future developments N89-13313

DESORPTION

The determination of mobile hydrogen in aerospace engine alloys N89-12659

Ion mobility spectrometry with laser-produced ions [AD-A197117] N89-12851

DESTRUCTION

Aspects of CFC relative ozone destruction efficiencies determined in the LLNL 2-D model [DE88-015431] N89-13106

DETECTION

Correlation studies on surface particle detection methods N89-12587

Detection of excited states by laser-induced fluorescence and analysis of energy transfer [AD-A197770] N89-12855

Theoretical aspects of gravitational wave detection N89-13383

Solar monopoles and terrestrial neutrinos
[DE88-010677] N89-13388

DETECTORS
Microwave characteristics of interdigitated photoconductors on a HEMT structure
[NASA-CR-182197] N89-12820
Tests of a multichannel photometer based on silicon diode detectors N89-13314
Application of PN and avalanche silicon photodiodes to low-level optical N89-13317
Absolute photometric calibration of detectors to 0.3 mmag using amplitude-stabilized lasers and a helium-cooled absolute radiometer N89-13318
An introduction to blocked impurity band detectors N89-13320

DEVELOPING NATIONS
Evaluation of LANDSAT TM and SPOT imagery for agricultural land use planning in less developed countries N89-13051

DIAMINES
Polyenamines from aromatic diacetylenic diketones and diamines
[NASA-CASE-LAR-13444-2-CU] N89-12667

DIAMONDS
Quantum Monte Carlo calculation of the properties of atomic carbon and diamond
[DE88-014659] N89-12686

DIATOMIC GASES
The NASA atomic oxygen effects test program N89-12589

DIATOMIC MOLECULES
Recent advances at NASA in calculating the electronic spectra of diatomic molecules
[NASA-TM-101034] N89-12622

DICTIONARIES
NASA thesaurus. Volume 3: Definitions
[NASA-SP-7064-VOL-3] N89-13301
A lexical conceptual approach to generation for machine translation
[AD-A197356] N89-13304

DIELECTRIC PROPERTIES
Optical constants of minerals and other materials from the millimeter to the ultraviolet
[AD-A197803] N89-12696
Microwave dielectric properties of low-salinity sea ice N89-13036

DIELECTRICS
Review of electromagnetic surface waves, 1960 through 1987
[AD-A197278] N89-12798
Polarization-dependent attenuation of dielectric cylinder arrays N89-12955
Interpretation of coherent polarimetric signatures by dielectric cylinder models N89-12957

DIES
Pultrusion die assembly
[NASA-CASE-LAR-13719-1] N89-12867

DIFFERENTIAL EQUATIONS
Nonlinear perturbations of differential operators with nontrivial kernel and applications to third order periodic boundary value problems
[DE88-702991] N89-13201
Identifying nonlinear covariate effects in semimartingale regression models
[AD-A197323] N89-13205

DIFFRACTION
Parabolic equation model
[AD-A197480] N89-13161

DIFFRACTOMETERS
Characterization of graphite fibers by X-ray diffraction N89-12755

DIGITAL COMPUTERS
Computer based intelligence support: An integrated expert system and decision support systems approach
[AD-A197386] N89-13197

DIGITAL SYSTEMS
Singular perturbations and time scales in the design of digital flight control systems
[NASA-TP-2844] N89-12569
An approach to automate digital signal processor code generation
[ETN-88-93530] N89-13172

DIGITAL TECHNIQUES
Development of a geographic information system with the aid of digital image processing techniques N89-12961

DIMENSIONAL STABILITY
Dynamics of face and annular seals with two-phase flow
[NASA-CR-183352] N89-12870

DIMENSIONLESS NUMBERS
Physical modeling of bubble phenomena, electrolyte flow and mass transfer in simulated advanced Hall cells
[DE88-015585] N89-12828

DIMENSIONS
Fitting functions to noisy data in high dimensions
[DE88-015922] N89-13213

DIODES
Investigation of laser diode coupling using nonlinear optics N89-12781
Tests of a multichannel photometer based on silicon diode detectors N89-13314

DIRECTION FINDING
Bearing error and the central limit theorem
[NASA-CR-183009] N89-13219

DIRECTIONAL SOLIDIFICATION (CRYSTALS)
Constitutive modelling of single crystal and directionally solidified superalloys N89-12912

DISPLAY DEVICES
Efficient use of bit planes in the generation of motion stimuli
[NASA-TM-101022] N89-13171
Space environment laboratory data acquisition and display system 2
[PB88-205471] N89-13299

DISSIPATION
Modified magnetic confinement configurations based on understanding helicity dissipation and pressure driven modes in the spheromak
[DE88-009149] N89-13260

DISSOCIATION
Nonequilibrium effects in thermal plasmas: Radiation transport and chemical reactivity
[DE88-016841] N89-13262

DISTRIBUTED PROCESSING
Performance studies of dynamic load balancing in distributed systems
[AD-A197130] N89-12926
European Seminar on Neural Computing
[ONRL-8-010-C] N89-13173
Distributed problem solving N89-13186
Two alternate proofs of Wang's lune formula for sparse distributed memory and an integral approximation
[NASA-CR-184555] N89-13214

DISTRIBUTION (PROPERTY)
Fundamental harmonic electron cyclotron emission for hot, loss-cone type distributions N89-13269

DISTRIBUTION FUNCTIONS
Interaction of impurity ions with a weakly non-Maxwellian simple hydrogenic plasma
[DE88-017137] N89-13265
C IV fluxes from the Sun as a star, and the correlation with magnetic flux
[NASA-CR-182719] N89-13387

DITCHING
Analysis of the Space Shuttle Orbiter skin panels under simulated hydrodynamic loads
[NASA-TM-4082] N89-12935

DOCUMENTS
Biogeochemical processes in sagebrush steppe: Interactions of terrain, vegetation and chemical cycles
[NASA-CR-181486] N89-13088

DOPPLER EFFECT
Directed motion Doppler shift effects on nitric oxide (0,0) gamma band resonance absorption N89-12760

DOPPLER RADAR
Modeling and performance of HF/OTH (High-Frequency/Over-The-Horizon) radar target identification systems
[AD-A197850] N89-12808

DOUBLE BASE PROPELLANTS
Combined pressure-shear ignition sensitivity test
[AD-A197076] N89-12749

DRAFTING MACHINES
The state of PC-based CADD (Computer-Aided Design and Drafting) systems
[DE88-017326] N89-13170

DROP SIZE
Light extinction in a dispersion of small nematic droplets
[AD-A197201] N89-12729

DROPS (LIQUIDS)
Spark ignition of monodisperse fuel sprays N89-12685
On the interactions of longwave radiation, microphysics and turbulence in boundary layer clouds N89-13109
Backscatter laser depolarization studies of simulated stratospheric aerosols: Crystallized sulfuric acid droplets
[NASA-CR-183387] N89-13111

DUCTILITY
Multispecimen test facility for high-pressure hydrogen creep studies N89-12655
Fundamental understanding of the intrinsic ductility in nickel-base L12 type alloys
[AD-A197605] N89-12711
On the resistance of ceramics to high velocity penetration
[AD-A197320] N89-12734

DUCTS
Influence of bulk turbulence and entrance boundary layer thickness on the curved duct flow field
[NASA-CR-4188] N89-12838

DUMP COMBUSTORS
Experimental study of isothermal flows in a dump combustor N89-12779

DURABILITY
The NASA atomic oxygen effects test program N89-12589
Materials selection for long life in LEO: A critical evaluation of atomic oxygen testing with thermal atom systems N89-12590
Atomic oxygen effects on candidate coatings for long-term spacecraft in low earth orbit N89-12592

DUST
Correlation studies on surface particle detection methods N89-12587
Precision cleaning methods for spacecraft applications N89-12588
Growth and sedimentation of dust grains in the primitive solar nebula N89-13374

DYE LASERS
Overview of recent advances in excimer laser technology at Los Alamos
[DE88-016236] N89-12858

DYNAMIC CHARACTERISTICS
LORAN C Offshore Flight Following (LOFF) in the Gulf of Mexico
[AD-A197179] N89-12558
Fracton dynamics on fractal networks
[AD-A197166] N89-12708
Simulating vehicle dynamics: The importance of a valid forcing function
[DE88-010527] N89-13167
Nearfield acoustic radiation from a point-excited cylindrical shell
[AD-A197282] N89-13234

DYNAMIC CONTROL
A vortex panel method for potential flows with applications to dynamics and control
[AD-A197091] N89-12549
The effects of expansion devices on the transient response characteristics of the air-source heat pump during the reverse cycle defrost
[AD-A197150] N89-12829

DYNAMIC LOADS
Measurement of rotordynamic coefficients for a hydrostatic radial bearing N89-12643

DYNAMIC MODELS
Trajectory optimization and guidance law development for national aerospace plane applications
[NASA-CR-182994] N89-12538
A vortex panel method for potential flows with applications to dynamics and control
[AD-A197091] N89-12549

DYNAMIC PRESSURE
Aerodynamic pressures and heating rates on surfaces between split elevons at Mach 6.6
[NASA-TP-2855] N89-12822

DYNAMIC PROGRAMMING
Numerical methods for the guidance and control of air-to-air missiles N89-12561

DYNAMIC RESPONSE
Nearfield acoustic radiation from a point-excited cylindrical shell
[AD-A197282] N89-13234

DYNAMIC STRUCTURAL ANALYSIS
An optical sensor system for monitoring structural dynamics with applications to system identification N89-12775
Non-isothermal buckling behavior of viscoplastic shell structures
[NASA-CR-183013] N89-12931
Approximate mobilities of built up structures
[ISVR-TR-162] N89-12934
Simulating vehicle dynamics: The importance of a valid forcing function
[DE88-010527] N89-13167

DYNAMIC TESTS
Space station docking mechanism dynamic testing N89-12596
The separation test in vacuum of the Ariane 4 payload fairing N89-12612
Preliminary results from the dynamic response testing of the Northern Power Systems 100-kW wind turbine
[DE88-001166] N89-13101

DYNAMICAL SYSTEMS
Confinement dynamics in the reversed field pinch
[DE88-009148] N89-13259

E

EAR
Use of proximity effect in hearing aid microphones to increase telephone intelligibility in noise
[AD-A197311] N89-12799

EARTH ATMOSPHERE
Improvements to photometry. Part 1: Better estimation of derivatives in extinction and transformation equations
N89-13322

EARTH IONOSPHERE
Ionosphere 1970, Volume 58
[ISSN-0211-5166] N89-13114

EARTH OBSERVATIONS (FROM SPACE)
Proceedings of the 1988 international Geoscience and Remote Sensing Symposium (IGARSS 1988) on Remote Sensing: Moving Towards the 21st Century, volume 1
[ESA-SP-284-VOL-1] N89-12936
European remote sensing satellite platforms for the 1990's N89-12978
Results of Advanced Earth Observing Satellite (ADEOS) conceptual study N89-12980
Geodynamics laser ranging system: Performance simulations and development of the EOS facility --- Earth Observing System (EOS) N89-12982
Data collection system operating on Japan's first marine observation satellite: Inflight evaluation of the system performance N89-13007

EARTH ORBITS
Materials selection for long life in LEO: A critical evaluation of atomic oxygen testing with thermal atom systems N89-12590
Atomic oxygen effects on candidate coatings for long-term spacecraft in low earth orbit N89-12592

EARTH RESOURCES
Multitemporal resource complex analysis of Catinia province, Italy from LANDSAT-TM data N89-12985

EARTH ROTATION
How to test the special theory of relativity on rotating earth
[DE88-703048] N89-13293

ECHO SOUNDING
Inference of radio scattering parameters of Antarctic ice sheet using 179 MHz airborne radio echo sounding data
N89-12975

ECOLOGY
Agroelecological information content of SPOT data
N89-13050

ECONOMIC ANALYSIS
Development of Alaskan gas hydrate resources
[DE88-010270] N89-13093

EDDY CURRENTS
Shock detection in composite structures. Test report 48-915/F --- Impact damage
[REPT-48-915/F] N89-12683

EDGES
A luminance edge extraction method using gradient of gray level for synthetic aperture radar imageries
N89-13086

EDITING ROUTINES (COMPUTERS)
Part 1: An introduction for users, revision
[AD-A197344] N89-13160

EDUCATION
A teacher's companion to the space station: A multi-disciplinary resource N89-12575

EFFICIENCY
Aspects of CFC relative ozone destruction efficiencies determined in the LLNL 2-D model
[DE88-015431] N89-13106
Re-evaluation of an improved efficiency polymeric web point-focus Fresnel lens
[DE88-016892] N89-13255

EJECTORS
A control-volume method for analysis of unsteady thrust augmenting ejector flows
[NASA-CR-182203] N89-12566
The separation test in vacuum of the Ariane 4 payload fairing N89-12612

ELASTIC BUCKLING
Two different methods for shell buckling calculation in the elastic-plastic region
[DFVLR-FB-88-26] N89-12933

ELASTIC DEFORMATION
Nearfield acoustic radiation from a point-excited cylindrical shell
[AD-A197282] N89-13234

ELASTIC PROPERTIES
Simplified cyclic structural analysis of SSME turbine blades N89-12632

ELASTOMERS
Differential scanning calorimetry as a method for indicating hydrolysis of urethane elastomers
[AD-A197673] N89-12736

ELASTOPLASTICITY
A study on thermal barrier coatings including thermal expansion mismatch and bond coat oxidation
N89-12919

ELECTRIC BRIDGES
Semiconductor bridge (SCB) igniter studies. 2: Comparison of SCB and hot-wire direct propulsion thrusters
[DE88-008803] N89-12625

ELECTRIC CHARGE
Mass flow meter using the triboelectric effect for measurement in cryogenics
[NASA-CR-179572] N89-12836

ELECTRIC CONTACTS
Overview of high-temperature superconductivity: Theory, surfaces, interfaces and bulk systems
[AD-A197383] N89-13285
Low contact-resistivity junction to ceramic superconductors
[DE88-016155] N89-13292

ELECTRIC DISCHARGES
Detection of excited states by laser-induced fluorescence and analysis of energy transfer
[AD-A197770] N89-12855
Tesla's coherent plasma discharge and a plan for megavolts at megahertz N89-13231

ELECTRIC FIELDS
Modes of operation of the RETE experiment
[IFSI-88-5] N89-12576

ELECTRIC POTENTIAL
Colloid vibration potentials
[VTT-RR-535] N89-13244

ELECTRIC PROPULSION
21st century propulsion concept
[AD-A197537] N89-12663

ELECTRICAL ENGINEERING
Engineering applications of heuristic multilevel optimization methods
[NASA-TM-101504] N89-13203

ELECTRICAL MEASUREMENT
Optical and electrical measurements on UV sensitive photodiodes N89-13316

ELECTRICAL PROPERTIES
Microwave characteristics of interdigitated photoconductors on a HEMT structure
[NASA-CR-182197] N89-12820
Electronic properties and current carrying capacity of high-temperature ceramic superconductors
[AD-A197819] N89-13287
Optical and electrical measurements on UV sensitive photodiodes N89-13316

ELECTRICAL RESISTANCE
Electronic transport properties of the metallic glass Cu sub 100-x Ti sub x
[ETN-88-93231] N89-12718
The NASA Lewis Strain Gauge Laboratory: An update
N89-12888

ELECTRICAL RESISTIVITY
Moisture interaction and stability of ZOT (Zinc Orthotitanate) thermal control spacecraft coating
N89-12618
Low contact-resistivity junction to ceramic superconductors
[DE88-016155] N89-13292

ELECTRO-OPTICAL PHOTOGRAPHY
The behavior of disk electrodes: Optical imaging of the concentration distribution over a disk electrode under galvanostatic conditions
[AD-A197355] N89-12816
The MEOSS experiment: A test case for future cartographic missions N89-13081

ELECTRO-OPTICS
Multispectral satellite analysis of marine stratocumulus cloud microphysics
[AD-A197316] N89-13092
Architectures for optoelectronic computing
[REPT-72/88/R260/U] N89-13148

ELECTROACOUSTICS
Use of proximity effect in hearing aid microphones to increase telephone intelligibility in noise
[AD-A197311] N89-12799

ELECTROCHEMISTRY
The determination of mobile hydrogen in aerospace engine alloys N89-12659
Electronic and ionic transport in polymers
[AD-A197142] N89-12728
Convective flows in enclosures with vertical temperature or concentration gradients
[NASA-TM-101373] N89-12753
Advanced double layer capacitor
[AD-A197739] N89-12818
Fuel cells: A bibliography
[DE88-001081] N89-13097
Electroporation: Theory of basic mechanisms
[AD-A197391] N89-13130

ELECTRODES
The behavior of disk electrodes: Optical imaging of the concentration distribution over a disk electrode under galvanostatic conditions
[AD-A197355] N89-12816
Advanced double layer capacitor
[AD-A197739] N89-12818

ELECTROLUMINESCENCE
Electrogenerated chemiluminescence
[AD-A197163] N89-12691

ELECTROLYTES
Electronic and ionic transport in polymers
[AD-A197142] N89-12728
Advanced double layer capacitor
[AD-A197739] N89-12818
Physical modeling of bubble phenomena, electrolyte flow and mass transfer in simulated advanced Hall cells
[DE88-015585] N89-12828

ELECTROLYTIC CELLS
Physical modeling of bubble phenomena, electrolyte flow and mass transfer in simulated advanced Hall cells
[DE88-015585] N89-12828

ELECTROMAGNETIC FIELDS
Mode extraction from an electromagnetic slow wave system N89-12767
Bioelectromagnetic effects of EMP: Preliminary findings
[DE88-012118] N89-12791

ELECTROMAGNETIC PULSES
EMP (electromagnetic pulse) mitigation program approach
[AD-A197849] N89-12807
Radiation effects in semiconductor laser diode arrays
[DE88-016318] N89-12859

ELECTROMAGNETIC SURFACE WAVES
Review of electromagnetic surface waves, 1960 through 1987
[AD-A197278] N89-12798

ELECTROMAGNETISM
Gravitation, black holes and space-time physics
[DE88-703054] N89-13377

ELECTRON AFFINITY
Quantum Monte Carlo calculation of the properties of atomic carbon and diamond
[DE88-014659] N89-12686

ELECTRON BEAMS
Algorithms for the self-consistent simulation of high power klystrons
[DE88-010684] N89-12812
Microwave and electron beam computer programs
[AD-A197798] N89-13164
Investigation of acceleration and densification of electrons utilizing travelling magnetic waves
[AD-A197700] N89-13242

ELECTRON CYCLOTRON HEATING
FOM Contributions to the 15th European Conference on Controlled Fusion and Plasma Heating
[REPT-88-178] N89-13266
Transport code studies of m=2 mode control by local electron cyclotron heating in TFR N89-13270
Optimizing current drive by electron cyclotron waves in the presence of trapped particles N89-13276

ELECTRON DENSITY (CONCENTRATION)
Nonequilibrium effects in thermal plasma chemistry
[DE88-016842] N89-13263

ELECTRON ENERGY
The applicability of Rutherford scattering for Ti measurements at medium and large-sized experiments
N89-13273

ELECTRON IMPACT
Differential cross sections for electron-impact excitation of atomic ions
[ISAS-RN-365] N89-13237
Electron-impact ionization of heavy atomic ions
[DE88-008371] N89-13238

ELECTRON MICROSCOPES
An electron microscopy study of tweed microstructures and premartensitic effects in high damping 53Cu45Mn2Al alloy
[AD-A197317] N89-12709

ELECTRON MICROSCOPY
An electron microscopy study of tweed microstructures and premartensitic effects in high damping 53Cu45Mn2Al alloy
[AD-A197317] N89-12709

ELECTRON PUMPING
Proof of the feasibility of coherent and incoherent schemes for pumping a gamma-ray laser
[AD-A197333] N89-12853

ELECTRON TRANSFER
Charge transfer in multiple site chemical systems
[AD-A197143] N89-12666
Transition-metal oxide superconductivity
[AD-A197069] N89-13280

ELECTRONIC EQUIPMENT
Studies of ultrathin polymer films for lithographic applications
[AD-A197297] N89-12731
Microgravity science and applications program tasks, 1987 revision
[NASA-TM-4068] N89-12752
MBE growth, characterization and electronic device processing of HgCdTe, HgZnTe related heterojunctions and HgCdTe-CdTe superlattices
[AD-A197752] N89-13286
ELECTRONIC SPECTRA
Recent advances at NASA in calculating the electronic spectra of diatomic molecules
[NASA-TM-101034] N89-12622
ELECTROPHORESIS
Electroporation: Theory of basic mechanisms
[AD-A197391] N89-13130
ELECTROPHOTOMETERS
Precision limits of the twin-beam multiband URSULA N89-13312
ELECTROPLATING
Metallization and characterization of a silicon p-n junction diode fabricated from a solar-cell-type silicon substrate
[DE88-703007] N89-13096
ELECTROSTATIC PROBES
Modes of operation of the RETE experiment
[IFSI-88-5] N89-12576
ELECTROSTATIC PROPULSION
21st century propulsion concept
[AD-A197537] N89-12663
ELEVONS
Aerodynamic pressures and heating rates on surfaces between split elevons at Mach 6.6
[NASA-TP-2855] N89-12822
ELLIPSOIDS
Scattering behavior of a three-axial ellipsoid N89-13011
ELLIPTIC FUNCTIONS
A zonal equation method for three-dimensional locally elliptic laminar and turbulent flows N89-12547
EMBEDDED COMPUTER SYSTEMS
De-embedding S-parameter measurements using TSD technique N89-12783
EMISSION SPECTRA
Observations of a complete sample of emission-line galaxies N89-13328
Grain optical properties N89-13332
The 3.4 micrometer emission feature in Comet Halley N89-13338
Comparison of the 3.36 micrometer feature to the ISM N89-13339
On the carbon abundance in Comet Halley derived from the 3 micron feature: Comparison with interstellar dust N89-13341
Possible identifications of the 3.4 micrometer feature N89-13342
The spectral appearance of comets from 5 to 20 micrometers: A survey of the data N89-13347
IR-dust observations of Comet Tempel 2 with CRAF VIMS N89-13349
Detection of parent molecules in the IR spectrum of P/Halley with the IKS-Vega spectrometer N89-13352
Some 5-13 micrometer airborne observations of Comet Wilson 1986l: Preliminary results N89-13360
Optical properties of cometary grains N89-13363
Properties of interstellar dust in reflection nebulae N89-13365
A multicomponent model of the infrared emission from Comet Halley N89-13367
ENCAPSULATING
LEC (Liquid Encapsulated Czochralski) growth of InP with magnetic field assisted melt stabilization and heat transfer control
[AD-A196748] N89-12688
ENCKE COMET
Infrared observations of P/Halley and P/Encke N89-13353
ENERGY CONSERVATION
Advanced turboprop project
[NASA-SP-495] N89-12565
ENERGY CONVERSION EFFICIENCY
Phase 2 testing of a molten salt central receiver
[DE88-012701] N89-13095
Improving the efficiency of binary cycles
[DE88-015108] N89-13099
ENERGY DISSIPATION
Combined pressure-shear ignition sensitivity test
[AD-A197076] N89-12749
ENERGY LEVELS
Electronic structure of light impurities in alpha-Fe and V
[DE88-702958] N89-12721
Determination of stepsize parameters for intermolecular vibrational energy transfer
[DE88-010904] N89-13239
A novel excitonic mechanism for high temperature superconductivity
[DE88-016227] N89-13288
ENERGY REQUIREMENTS
Spark ignition of monodisperse fuel sprays N89-12685
ENERGY TRANSFER
Detection of excited states by laser-induced fluorescence and analysis of energy transfer
[AD-A197770] N89-12855
Determination of stepsize parameters for intermolecular vibrational energy transfer
[DE88-010904] N89-13239
ENGINE COOLANTS
Coolant passage heat transfer with rotation N89-12899
ENGINE DESIGN
HOST combustion R and T overview N89-12879
ENGINE INLETS
HOST turbine heat transfer subproject overview N89-12880
Influence of bulk turbulence and entrance boundary layer thickness on the curved duct flow field N89-12896
ENGINE MONITORING INSTRUMENTS
SSME bearing health monitoring using a fiberoptic deflectometer N89-12645
ENGINE PARTS
Damping seal tester progress and initial test results N89-12627
Thermo-mechanical performance evaluation of cryogenic turbopump ball bearings N89-12637
Powder metallurgy bearings for advanced rocket engines N89-12641
Research on mechanical properties for engine life prediction
[AD-A197818] N89-12864
Turbine Engine Hot Section Technology (HOST) Project N89-12877
ENGINE TESTS
Test stand design and analysis for Titan 34D static firing N89-12609
Ariane 5 verification and associated test facilities N89-12611
ENTRAINMENT
Structure measurements in a synthetic turbulent boundary layer N89-12821
ENVIRONMENT EFFECTS
Environmental management practices in oil refineries and terminals: An overview
[ISBN-92-807-1108-3] N89-13104
ENVIRONMENTAL MONITORING
Liquid scintillation counting with the Packard 1500 analyzer N89-12782
Monitoring playas using Thematic Mapper data N89-13028
Change direction analysis using LANDSAT imagery: A review of methodology N89-13068
Building a monitoring system based on satellite data to detect vegetation and land use changes in a subtropical region of Mexico N89-13079
Environmental management practices in oil refineries and terminals: An overview
[ISBN-92-807-1108-3] N89-13104
ENVIRONMENTAL TESTS
A high pressure, high temperature hydrogen environment for metals properties testing system N89-12656
LCF and crack growth rate of turbine blade alloys in hydrogen and hydrogen/steam environments N89-12660
ENVIRONMENTS
Designing simulator tasks to study the high speed, low altitude environment N89-12770
Comments on the high frequency behavior of the coupling of an accelerator beam to its environment
[CEBAF-PR-88-006] N89-13245
ENZYME ACTIVITY
Glucose tolerance and insulin secretion during 0-g simulation
[DFVLR-FB-88-25] N89-13136
EPITAXY
Research on mercury cadmium telluride
[AD-A197238] N89-13282
EPOXY RESINS
Characterization of a graphite epoxy optical bench during thermal vacuum cycling N89-12585
EQUATIONS OF MOTION
A vortex panel method for potential flows with applications to dynamics and control
[AD-A197091] N89-12549
The effects of internal rotor friction on dynamic characteristics of turbopumps N89-12629
EQUATIONS OF STATE
A decade of railgun development for high pressure research
[DE88-017024] N89-12578
EQUILIBRIUM
Preliminary applications of decentralized estimation to large flexible space structures N89-12761
EQUILIBRIUM FLOW
New methods for locating phase boundaries
[DE88-017084] N89-12700
EQUIPMENT SPECIFICATIONS
A far-infrared heterodyne spectrometer for airborne astronomy N89-13329
EROSION
The NASA atomic oxygen effects test program N89-12589
ERROR ANALYSIS
Analysis of GEOSAT radar altimeter errors based on pre-launch test data
[NASA-TM-101230] N89-12806
An analysis of the error characteristics of Atlantic tropical cyclone track prediction models N89-13117
An analysis of the error characteristics of Atlantic tropical cyclone track prediction models
[AD-A197146] N89-13119
A fault diagnosis system based on an integrated knowledge base N89-13181
A model for belief revision N89-13183
ERRORS
Natural language generation
[AD-A197321] N89-12800
Porous plug for reducing orifice induced pressure error in airfoils
[NASA-CASE-LAR-13569-1] N89-12841
Formulation of the proper equations for developing standards in coherent dual polarisation SAR imaging N89-13021
Bearing error and the central limit theorem
[NASA-CR-183009] N89-13219
Use of distance versus statistical distance in acceptance tests
[NASA-CR-183353] N89-13220
Phase measurement accuracy limitation in phase shifting interferometry N89-13248
ERS-1 (ESA SATELLITE)
Complex SAR imagery and speckle filtering for ERS-1 wave mode N89-13029
Radar control, detection and processing electronics design as used for the ERS-1 wind scatterometer space segment N89-13075
ERS data policy N89-13078
ESTIMATES
Improvements to photometry. Part 1: Better estimation of derivatives in extinction and transformation equations N89-13322
ESTIMATING
Optimal fix estimators and a variation on the Cramer Rao lower bound
[NASA-CR-183011] N89-13211
ETCHING
Development of optimized, graded-permeability axial groove heat pipes N89-12614
Studies of ultrathin polymer films for lithographic applications
[AD-A197297] N89-12731
ETHERS
Electronic and ionic transport in polymers
[AD-A197142] N89-12728
ETHYL COMPOUNDS
Poly(ethyl acrylate) and poly(gamma-benzyl-L-glutamate): An interpenetrating polymer system
[AD-A197783] N89-12737
EUCLIDEAN GEOMETRY
Euclidean decoders for BCH codes
[AD-A197242] N89-13157
EULER BUCKLING
Composite rods in carbon-epoxy Fibredux 914 C/TS-6T-6K-34
[SARMA-TR-87-2431A] N89-12677
EUROPEAN SPACE PROGRAMS
Modes of operation of the RETE experiment
[IFSI-88-5] N89-12576
EURACS: A European radar cross section database N89-12944
European remote sensing satellite platforms for the 1990's N89-12978
EUTECTIC ALLOYS
Mechanical behavior of superplastically-formed Al-Cu-Li-Zr alloy 2090
[DE88-016241] N89-12714
EVALUATION
Computer evaluation of ion-implanted dopant profile evolution during annealing N89-12756
Re-evaluation of an improved efficiency polymeric web point-focus Fresnel lens
[DE88-016892] N89-13255

EVAPORATION
A methodology for characterizing reactive coatings: Time-Temperature-Transformation (TTT) analysis of the competition between cure, evaporation and thermal degradation for an epoxy-phenolic system
[AD-A197254] N89-12730
EVOLUTION (DEVELOPMENT)
The large-scale structure of the universe: Some theoretical considerations N89-13381
EXCIMER LASERS
Overview of recent advances in excimer laser technology at Los Alamos
[DE88-016236] N89-12858
EXCITATION
Detection of excited states by laser-induced fluorescence and analysis of energy transfer
[AD-A197770] N89-12855
Determination of stepsize parameters for intermolecular vibrational energy transfer
[DE88-010904] N89-13239
EXCITONS
A novel excitonic mechanism for high temperature superconductivity
[DE88-016227] N89-13288
EXHAUST GASES
Fuel alcohol formulations
[DE88-016753] N89-12748
EXPERIMENT DESIGN
Automation software for a materials testing laboratory N89-12917
The Labrador Sea Extreme Waves Experiment: Objectives, status and plans N89-12974
The LIMEX 1987 pilot project, LIMEX 1989 and long-term objective for data collection on the Canadian East coast N89-13037
EXPERT SYSTEMS
An expert system for diagnosis and repair of analog circuits N89-12784
Northeast Artificial Intelligence Consortium (NAIC). Review of technical tasks, volume 2, part 1
[AD-A189773] N89-13180
A fault diagnosis system based on an integrated knowledge base N89-13181
SNePS considered as a fully intensional propositional semantic network N89-13184
A shared knowledge base for independent problem solving agents N89-13187
Planner system for the application of indications and warning N89-13188
Providing intelligent assistance in distributed office environments N89-13189
Evaluation of expert systems in decisionmaking organizations
[AD-A196448] N89-13192
Computer based intelligence support: An integrated expert system and decision support systems approach
[AD-A197386] N89-13197
Optical symbolic processor for expert system execution
[AD-A197668] N89-13252
Empirical analysis and refinement of expert system knowledge bases
[AD-A197241] N89-13303
EXPLOSIONS
Space reactor assessment and validation study N89-13227
EXTERNAL TANKS
Development of polyisocyanurate pour foam formulation for space shuttle external tank thermal protection system
[NASA-CR-183511] N89-12745
EXTINCTION
Light extinction in a dispersion of small nematic droplets
[AD-A197201] N89-12729
EXTRACTION
Mode extraction from an electromagnetic slow wave system N89-12767
EXTREMELY HIGH FREQUENCIES
The airborne radiometry experiment (ABREX) instrument, an experimental test bed for the specification of satellite-borne microwave radiometer at 90 GHz N89-12939
A 35 GHz helicopter-borne polarimeter radar N89-13038

F

F STARS
Properties of stellar activity in F stars N89-13369
FABRICATION
Sol-gel routes to superconducting ceramics
[DE88-015128] N89-12724
Construction of a phase conjugate laser resonator using Brillouin enhanced four wave mixing N89-12759
Dynamic synthesis of joined/hermetic shell structures using state space method N89-12874
Metallization and characterization of a silicon p-n junction diode fabricated from a solar-cell-type silicon substrate
[DE88-703007] N89-13096
Fuel cells: A bibliography
[DE88-001081] N89-13097
Solar photovoltaic technology: The thin film option
[DE88-001195] N89-13102
Development of high efficiency opaque photocathodes for the Region 900 angstrom to 1200 angstrom
[NASA-CR-180597] N89-13249
FAILURE ANALYSIS
Effects of oxygen/hydrogen combustion chamber environment on copper alloys N89-12653
Hydrogen-environment embrittlement and its control in high pressure hydrogen/oxygen rocket engines N89-12654
Short fiber reinforced thermoplastics N89-12673
Modified pull test for the testing of very adherent films
[DE88-016363] N89-12743
Thermal barrier coating life prediction model N89-12921
Thermal barrier coating life prediction model development N89-12922
Analysis of the Space Shuttle Orbiter skin panels under simulated hydrodynamic loads
[NASA-TM-4082] N89-12935
Fault diagnosis based on continuous simulation models
[NASA-CR-182737] N89-13152
FAILURE MODES
Improving the fatigue resistance of adhesive joints in laminated wood structures
[NASA-CR-182165] N89-12675
FAIRINGS
The separation test in vacuum of the Ariane 4 payload fairing N89-12612
FALLOUT
Worldwide deposition of Sr-90 through 1985
[DE88-015577] N89-13105
FALSE ALARMS
On adaptive cell-averaging CFAR radar signal detection N89-12792
FATIGUE (MATERIALS)
Constitutive behavior of single crystal PWA 1480 and directionally solidified MAR-M 246 under monotonic and cyclic loads at high and low temperature N89-12634
Improving the fatigue resistance of adhesive joints in laminated wood structures
[NASA-CR-182165] N89-12675
Research on mechanical properties for engine life prediction
[AD-A197816] N89-12864
On the effect of R-ratio and Kfmax on fracture toughness measurement, fatigue crack propagation, and fatigue crack closure N89-12875
Turbine Engine Hot Section Technology 1986
[NASA-CP-2444] N89-12876
Elevated temperature crack growth N89-12915
Automation software for a materials testing laboratory N89-12917
Fracture and fatigue
[AD-A197310] N89-12927
FATIGUE LIFE
Thermo-mechanical performance evaluation of cryogenic turbopump ball bearings N89-12637
Rolling contact fatigue life of zirconium and molybdenum nitride sputter plated AMS 5749 bearing steel N89-12642
Fatigue crack growth of 5456-H116 aluminum and HSLA-80 weldments
[AD-A197830] N89-12712
Fatigue and fracture overview N89-12882
Creep fatigue life prediction for engine hot section materials (isotropic): Fourth year progress review N89-12914
Grain boundary oxidation and its effects on high temperature fatigue life N89-12918
FATIGUE TESTS
Development of a computer-controlled technique to determine crack growth rate properties in controlled environments using crack opening displacement N89-12657
The development of a hydrogen resistant alloy N89-12661
FAULT TOLERANCE
Fault diagnosis based on continuous simulation models
[NASA-CR-182737] N89-13152
Making statistical inferences about software reliability
[NASA-CR-4197] N89-13153
Artificial intelligence theory and reconfigurable control systems
[AD-A197255] N89-13195
FEEDBACK
A system to investigate synthesized voice feedback in man-machine interfaces N89-12776
FEEDBACK CONTROL
Trajectory optimization and guidance law development for national aerospace plane applications
[NASA-CR-182994] N89-12538
FERROMAGNETIC MATERIALS
Fracton dynamics on fractal networks
[AD-A197166] N89-12708
FIBER COMPOSITES
Mixed-mode fracture in fiber-reinforced composite materials N89-12669
Prediction of fiber orientation during processing of short fiber composites N89-12671
Finite element analysis of composite laminates N89-12672
Toughening by aligned, frictionally constrained fibers
[AD-A197194] N89-12676
SiC whisker-reinforced MoSi2
[DE88-016674] N89-12680
Pultrusion die assembly
[NASA-CASE-LAR-13719-1] N89-12867
FIBER OPTICS
SSME bearing health monitoring using a fiberoptic deflectometer N89-12645
Fiber optic control system integration
[NASA-CR-179568] N89-13256
Second Workshop on Improvements to Photometry
[NASA-CP-10015] N89-13310
A multichannel fiber optic photometer present performance and future developments N89-13313
A fibre optic, four channel comparative photometer N89-13315
Fiber optic wavelength division multiplexing: Principles and applications in telecommunications and spectroscopy N89-13324
Use of optical fibers in spectrophotometry N89-13325
A consideration of the use of optical fibers to remotely couple photometers to telescopes N89-13326
FIBER ORIENTATION
Prediction of fiber orientation during processing of short fiber composites N89-12671
FIBERS
Characterization of graphite fibers by X-ray diffraction N89-12755
FIELD EFFECT TRANSISTORS
Joint services electronics program
[AD-A197140] N89-12815
FIELD THEORY (PHYSICS)
New gravitational forces from quantum theory
[DE88-016231] N89-13294
FIGHTER AIRCRAFT
Guidance and Control/Flight Mechanics Panels Joint Symposium on The Man-Machine Interface in Tactical Aircraft Design and Combat Automation
[AGARD-AR-249] N89-12564
FILAMENT WINDING
An axisymmetric linear/high-order finite element for filament wound composite structures N89-12674
FILM COOLING
Turbine airfoil film cooling N89-12903
FINITE DIFFERENCE THEORY
High strain rate properties of structural aluminium N89-12705
A numerical method for computing unsteady 2-D boundary layer flows
[NASA-CR-4198] N89-12835
An adaptive method with mesh moving and local mesh refinement for time-dependent partial differential equations
[AD-A197772] N89-13208
FINITE ELEMENT METHOD
The effect of delamination on the response of advanced composite laminates N89-12668
Prediction of fiber orientation during processing of short fiber composites N89-12671
Finite element analysis of composite laminates N89-12672
An axisymmetric linear/high-order finite element for filament wound composite structures N89-12674
Installation of the ADINA FEM computer programs N89-12778
Heat transfer from roughened surfaces using interferometry N89-12827
Dynamic synthesis of joined/hermetic shell structures using state space method N89-12874
HOST surface protection R and T overview N89-12883
Constitutive modeling for isotropic materials N89-12904
Structural response calculations for a metal booster tank model
[DE88-017095] N89-12929

Parallel algorithms in the finite element approximation of flow problems
[AD-A197454] N89-13178
An adaptive method with mesh moving and local mesh refinement for time-dependent partial differential equations
[AD-A197772] N89-13208

FINITE VOLUME METHOD
A control-volume method for analysis of unsteady thrust augmenting ejector flows
[NASA-CR-182203] N89-12566

FINS
Aerodynamics analysis of solid fuel Ramjet projectiles
[AD-A196755] N89-12548

FIRES
Fire spread in a three-dimensional pressure vessel with radiation exchange and wall heat losses
[AD-A197271] N89-12692
Fire aerosol experiment and comparisons with computer code predictions
[DE88-016328] N89-12788

FISSILE FUELS
Fission fragment rockets: A potential breakthrough
[DE88-016953] N89-12664

FISSION ELECTRIC CELLS
Fission fragment rockets: A potential breakthrough
[DE88-016953] N89-12664

FISSIONABLE MATERIALS
Fission fragment rockets: A potential breakthrough
[DE88-016953] N89-12664

FITTING
Fitting functions to noisy data in high dimensions
[DE88-015922] N89-13213

FLAME PROPAGATION
Report on JANNAF Workshop Influence of Gas-Phase Chemical Kinetics on Low-Pressure Ignition and Flamespreading in Solid Propellant
[AD-A197854] N89-12751

FLAME STABILITY
Stability limits and combustion measurements in low calorific value gas flames N89-12687
Radiative augmented combustion
[AD-A197300] N89-12693

FLAT PLATES
Structure measurements in a synthetic turbulent boundary layer N89-12821

FLEXIBLE SPACECRAFT
Vibration suppression in a large space structure
[NASA-CR-182831] N89-12624

FLIGHT CHARACTERISTICS
AH-1F Instrument Meteorological Conditions (IMC) flight evaluations
[AD-A197128] N89-12562

FLIGHT CONTROL
An evaluation of ground collision avoidance system algorithm
[AD-A197831] N89-12580
Singular perturbations and time scales in the design of digital flight control systems
[NASA-TP-2844] N89-12569
Fiber optic control system integration
[NASA-CR-179568] N89-13256

FLIGHT CREWS
Research and development of anti-g life support systems. Part 2: Decompression sickness research
[AD-A197675] N89-13133

FLIGHT SIMULATORS
Designing simulator tasks to study the high speed, low altitude environment N89-12770
Six degree of freedom simulation computer program for aeroelastic free-flight projectiles N89-12771

FLIGHT TESTS
AH-1F Instrument Meteorological Conditions (IMC) flight evaluations
[AD-A197128] N89-12562
Designing simulator tasks to study the high speed, low altitude environment N89-12770

FLOW DISTRIBUTION
A spectral collocation solution to the compressible stability eigenvalue problem
[NASA-TP-2858] N89-12543
Theoretical and experimental studies of the transonic flow field and associated boundary conditions near a longitudinally-slotted wind-tunnel wall N89-12545
Flow field characteristics around bluff parachute canopies N89-12546
Development and validation of an advanced low-order panel method
[NASA-TM-101024] N89-12554
Evaluation of three turbulence models for the prediction of steady and unsteady airloads
[NASA-TM-101413] N89-12555
A comparative study of differing vortex structures arising in unsteady separated flows N89-12773
Advanced instrumentation for local measurement of gas-solid suspension flows
[DE88-017087] N89-12833
Influence of bulk turbulence and entrance boundary layer thickness on the curved duct flow field
[NASA-CR-4188] N89-12838
Laser applications in flow diagnostics
[AGARD-AG-296] N89-12849
Aerothermal modeling program, phase 2 N89-12890
Aerothermal modeling program, phase 2. Element B: Flow interaction experiment N89-12891
Influence of bulk turbulence and entrance boundary layer thickness on the curved duct flow field N89-12896
Measurement of airfoil heat transfer coefficients on a turbine stage N89-12897
Turbine stator flow field simulations N89-12902

FLOW EQUATIONS
Efficient numerical techniques for complex fluid flows N89-12894

FLOW MEASUREMENT
Effect of grain size on the high temperature properties of B2 aluminides
[NASA-TM-101382] N89-12720
Advanced instrumentation for local measurement of gas-solid suspension flows
[DE88-017087] N89-12833
Mass flow meter using the triboelectric effect for measurement in cryogenics
[NASA-CR-179572] N89-12836
Mass flow measurement of liquid cryogens using the triboelectric effect
[NASA-CR-179519] N89-12837

FLOW STABILITY
Unsteady structure of flow past a pitching delta wing N89-12541
A spectral collocation solution to the compressible stability eigenvalue problem
[NASA-TP-2858] N89-12543
The stability of time-dependent fluid flows N89-12825

FLOW VELOCITY
Development of a thermal and structural analysis procedure for cooled radial turbines
[NASA-TM-101416] N89-12568
Theoretical study of turbulent channel flow: Bulk properties, pressure fluctuations, and propagation of electromagnetic waves
[NASA-TM-101248] N89-12830
Influence of bulk turbulence and entrance boundary layer thickness on the curved duct flow field
[NASA-CR-4188] N89-12838
Laser anemometry: A status report N89-12885
Heat transfer with very high free-stream turbulence and streamwise vortices N89-12900
Sample introduction using the Hildebrand grid nebulizer for plasma spectrometry
[AD-A197145] N89-13257

FLOW VISUALIZATION
Method for laminar boundary layer transition visualization in flight
[NASA-CASE-LAR-13554-1] N89-12551

FLUID DYNAMICS
Evaluation of three turbulence models for the prediction of steady and unsteady airloads
[NASA-TM-101413] N89-12555

FLUID FLOW
Thermal transport between a continuously moving heated plate and a quiescent ambient medium N89-12824
The stability of time-dependent fluid flows N89-12825
Liquid metal flow in a large-radius elbow with a uniform magnetic field
[DE88-016957] N89-12832
Measurement of airfoil heat transfer coefficients on a turbine stage N89-12897
Improving the efficiency of binary cycles
[DE88-015108] N89-13099

FLUID MANAGEMENT
Space station integrated propulsion and fluid systems study
[NASA-CR-179393] N89-12581

FLUID MECHANICS
A two-dimensional numerical simulation of a supersonic, chemically reacting mixing layer
[NASA-TM-4055] N89-12542
Temporal clustering in the multi-target tracking environment
[AD-A197153] N89-12796
Population inversion non-equilibrium flow simulation calculations of the capabilities of convection flow lasers
[AD-A197741] N89-12854

FLUORIDES
Tm,Ho:YLF laser end-pumped by a semiconductor diode laser array
[NASA-CASE-NPO-17282-1-CU] N89-12856

FLUORINE
A mass spectrometric analysis of CF4/O2 plasmas: Effect of oxygen concentration and plasma power
[DE88-016237] N89-13261

FLUOROHYDROCARBONS
Aspects of CFC relative ozone destruction efficiencies determined in the LLNL 2-D model
[DE88-015431] N89-13106

FOAMS
Development of polyisocyanurate pour foam formulation for space shuttle external tank thermal protection system
[NASA-CR-183511] N89-12745

FOCAL PLANE DEVICES
Re-evaluation of an improved efficiency polymeric web point-focus Fresnel lens
[DE88-016892] N89-13255

FOCUSING
Phase versus orbital velocity in SAR wave imaging: Paradox lost N89-13033

FOKKER-PLANCK EQUATION
Kinetic effects on electron cyclotron emission during electron cyclotron heating in tokamaks N89-13268

FOOD CHAIN
Human exposure to dioxin from combustion sources
[DE88-013825] N89-13135

FORECASTING
Physical modeling of bubble phenomena, electrolyte flow and mass transfer in simulated advanced Hall cells
[DE88-015585] N89-12828
Aspects of CFC relative ozone destruction efficiencies determined in the LLNL 2-D model
[DE88-015431] N89-13106
Hanford Meteorological Station computer codes. Volume 8: The REVIEW computer code
[DE88-015958] N89-13123
Bering Sea wave and ice measurements in support of Arctic west winter 1986
[AD-A197196] N89-13127

FORESTS
Spatial resolution for remote sensing of forest plantations N89-12991
The derivation of sub-canopy surface terrain models of coastal forests using synthetic aperture radar N89-13083
Spectral characterization of forest damage in beech, oak and pine stands N89-13085

FORM FACTORS
Neutron studies of liquid and solid helium
[DE88-009096] N89-13277

FORMAT
On the simulation of harmonically related signals
[AD-A197821] N89-13235

FORMULATIONS
Fuel alcohol formulations
[DE88-016753] N89-12748

FORWARD SCATTERING
Phase coherence and Signal-To-Noise ratio considerations for sampled aperture radar systems
[AD-A197180] N89-12797
Performance of the forward scattering spectrometer probe in NASA's icing research tunnel
[NASA-TM-101381] N89-12845

FOUNDATIONS
Space station erectable manipulator placement system
[NASA-CASE-MSC-21096-1] N89-12621

FOURIER ANALYSIS
The effect of vertical wind shear on tropical cyclone movement
[AD-A197218] N89-13120

FRACTURE MECHANICS
Advanced Earth-to-Orbit Propulsion Technology 1986, volume 2
[NASA-CP-2437-VOL-2] N89-12626
Effects of high mean stress on the high-cycle fatigue of PWA 1480 and DS MAR M 246 + Hf at 1000 F N89-12633
Fatigue crack retardation following overloads in Inconel 718, Ti-5Al-2.5Sn, and Haynes 188 N89-12636
Mixed-mode fracture in fiber-reinforced composite materials N89-12669
Short fiber reinforced thermoplastics N89-12673
Toughening by aligned, frictionally constrained fibers
[AD-A197194] N89-12676
High temperature adhesive systems
[AD-A197077] N89-12726
Modified pull test for the testing of very adherent films
[DE88-016363] N89-12743
Investigation into the applicability of fracture mechanics techniques to aircraft wheel life studies N89-12763
Turbine Engine Hot Section Technology 1986
[NASA-CP-2444] N89-12876
Fatigue and fracture overview N89-12882
Fracture and fatigue
[AD-A197310] N89-12927

Calculation of Weibull strength parameters and Batdorf flow-density constants for volume- and surface-flaw-induced fracture in ceramics [NASA-TM-100890] N89-12930

FRACTURE STRENGTH
Modified pull test for the testing of very adherent films [DE88-016363] N89-12743
On the effect of R-ratio and Kfmax on fracture toughness measurement, fatigue crack propagation, and fatigue crack closure N89-12875

FRACTURES (MATERIALS)
On the resistance of ceramics to high velocity penetration [AD-A197320] N89-12734

FRAGMENTS
The conversion of smaller borane fragments to larger structures. Systematics of boron hydride reactions [AD-A197068] N89-12689

FREE ELECTRON LASERS
Investigation of acceleration and densification of electrons utilizing travelling magnetic waves [AD-A197700] N89-13242

FREE FLIGHT
Six degree of freedom simulation computer program for aeroelastic free-flight projectiles N89-12771

FREE FLOW
Heat transfer with very high free-stream turbulence and streamwise vortices N89-12900

FREQUENCIES
The Frascati (Italy) gravitational antenna, 1987 [IFSI-88-4] N89-12846

FREQUENCY DISTRIBUTION
C Cloud S (Climatology of Cloud Statistics) database (users manual) [AD-A196497] N89-13118

FREQUENCY MODULATION
A fine resolution multifrequency polarimetric FM radar N89-13016
Discrimination and identification of modulation-frequency using noise, tone and tonal-complex carriers [AD-A197780] N89-13134

FRESNEL LENSES
Re-evaluation of an improved efficiency polymeric web point-focus Fresnel lens [DE88-016892] N89-13255

FRICTION
The effects of internal rotor friction on dynamic characteristics of turbopumps N89-12629

FUEL CELL POWER PLANTS
Assessment and comparison of 100-MW coal gasification phosphoric acid fuel cell power plants [NASA-CR-182189] N89-13103

FUEL CELLS
Fuel cells: A bibliography [DE88-001081] N89-13097

FUEL COMBUSTION
Advanced Earth-to-Orbit Propulsion Technology 1986, volume 2 [NASA-CP-2437-VOL-2] N89-12626
Autoignition chemistry of n-butane in a motored engine: A comparison of experimental and modeling results [DE88-014153] N89-12697

FUEL CONSUMPTION
Trajectory optimization and guidance law development for national aerospace plane applications [NASA-CR-182994] N89-12538
Advanced turboprop project [NASA-SP-495] N89-12565

FUEL INJECTION
Survey of LOX/hydrocarbon combustion and cooling N89-12647
Aerothermal modeling program, phase 2. Element C: Fuel injector-air swirl characterization N89-12892

FUEL SPRAYS
Spark ignition of monodisperse fuel sprays N89-12685

FUEL TANKS
Cryogenic insulation system [NASA-CASE-LAR-13506-1] N89-12741
Tank gauging apparatus and method [NASA-CASE-MSC-21059-1] N89-12843

FUNCTIONAL ANALYSIS
Perturbed functional iteration applied to the Navier-Stokes equations N89-12774

FUNCTIONAL DESIGN SPECIFICATIONS
The airborne radiometry experiment (ABREX) instrument, an experimental test bed for the specification of satellite-borne microwave radiometer at 90 GHz N89-12939
Multistatic scatterometry N89-13072

FUNCTIONS (MATHEMATICS)
Implementation issues for level O image processor software within an application package [AD-A197768] N89-13162
Global optimization of concave functions subject to separable quadratic constraints and of all-quadratic separable problems [AD-A197747] N89-13206

FURANS
Human exposure to dioxin from combustion sources [DE88-013825] N89-13135

FUSELAGES
A study of active control techniques for noise reduction in an aircraft fuselage model N89-13232

FUSION REACTORS
FIREBIRD: A conceptual design of a field reversed configuration Compact Torus Fusion Reactor (CTFR) N89-13230

FUSION WELDING
Influence of process parameters on laser weld characteristics in aluminum alloys [AD-A197398] N89-12710

G

GALACTIC CLUSTERS
The large-scale structure of the universe: Some theoretical considerations N89-13381

GALACTIC NUCLEI
Activities report of the Institute of Extraterrestrial Activities [MPE-208] N89-13308
Synthesis of accretion disk and nonthermal source models for AGN [DE88-[illegible],3098] N89-13384

GALAXIES
Observations of a complete sample of emission-line galaxies N89-13328

GALILEO PROJECT
Moisture interaction and stability of ZOT (Zinc Orthotitanate) thermal control spacecraft coating N89-12618

GALLIUM ARSENIDES
Joint services electronics program [AD-A197140] N89-12815
MBE growth, characterization and electronic device processing of HgCdTe, HgZnTe related heterojunctions and HgCdTe-CdTe superlattices [AD-A197752] N89-13286

GAMMA RAY LASERS
Proof of the feasibility of coherent and incoherent schemes for pumping a gamma-ray laser [AD-A197333] N89-12853

GAMMA RAYS
Directed motion Doppler shift effects on nitric oxide (0,0) gamma band resonance absorption N89-12760
Proof of the feasibility of coherent and incoherent schemes for pumping a gamma-ray laser [AD-A197333] N89-12853

GAS DYNAMICS
Population inversion non-equilibrium flow simulation calculations of the capabilities of convection flow lasers [AD-A197741] N89-12854
Aerothermal modeling program, phase 2. Element C: Fuel injector-air swirl characterization N89-12892

GAS FLOW
Population inversion non-equilibrium flow simulation calculations of the capabilities of convection flow lasers [AD-A197741] N89-12854
Gas flow and global code programme [DE88-012635] N89-12861
Spectral variability of Wolf-Rayet stars [DE88-703325] N89-13371

GAS LASERS
Population inversion non-equilibrium flow simulation calculations of the capabilities of convection flow lasers [AD-A197741] N89-12854
Resonator design with an intracavity time-varying index gradient [DE88-015259] N89-12857

GAS TEMPERATURE
Further development of the dynamic gas temperature measurement system N89-12884

GAS TURBINE ENGINES
Development of a thermal and structural analysis procedure for cooled radial turbines [NASA-TM-101416] N89-12568
Turbine Engine Hot Section Technology 1986 [NASA-CP-2444] N89-12876
Turbine Engine Hot Section Technology (HOST) Project N89-12877
HOST instrumentation R and D program overview N89-12878
HOST combustion R and T overview N89-12879
HOST turbine heat transfer subproject overview N89-12880
HOST structural analysis program overview N89-12881
Fatigue and fracture overview N89-12882

HOST surface protection R and T overview N89-12883
Further development of the dynamic gas temperature measurement system N89-12884
Laser anemometry: A status report N89-12885
Aerothermal modeling program, phase 2. Element B: Flow interaction experiment N89-12891
Combustor diffuser interaction program N89-12893
Efficient numerical techniques for complex fluid flows N89-12894
Heat transfer in the tip region of a rotor blade simulator N89-12898
Coolant passage heat transfer with rotation N89-12899
Turbine stator flow field simulations N89-12902
Constitutive modeling for isotropic materials N89-12904
Creep fatigue life prediction for engine hot section materials (isotropic): Fourth year progress review N89-12914

GAS TURBINES
Constitutive behavior of single crystal PWA 1480 and directionally solidified MAR-M 246 under monotonic and cyclic loads at high and low temperature N89-12634
Heat transfer to rough turbine blading N89-12823
HOST structural analysis program overview N89-12881
Considerations in development and implementation of elasto-viscoplastic constitutive model for high temperature applications [NASA-CR-183403] N89-12932

GAS-GAS INTERACTIONS
Combustor diffuser interaction program N89-12893

GAS-METAL INTERACTIONS
Effects of oxygen/hydrogen combustion chamber environment on copper alloys N89-12653
Multispecimen test facility for high-pressure hydrogen creep studies N89-12655
A high pressure, high temperature hydrogen environment for metals properties testing system N89-12656
Hydrogen effects on the fatigue and tensile behavior of CMSX-2 nickel base superalloy single crystals N89-12658
LCF and crack growth rate of turbine blade alloys in hydrogen and hydrogen/steam environments N89-12660

GASES
Stability limits and combustion measurements in low calorific value gas flames N89-12687
Advanced instrumentation for local measurement of gas-solid suspension flows [DE88-017087] N89-12833
Tank gauging apparatus and method [NASA-CASE-MSC-21059-1] N89-12843

GASOHOL (FUEL)
Fuel alcohol formulations [DE88-016753] N89-12748

GENES
Gordon Conference on Microbial Adhesion [AD-A197352] N89-12735

GEODETIC ACCURACY
The differential rectification of SPOT HRV panchromatic and multispectral imagery using a digital elevation model N89-13054

GEODYNAMICS
Geodynamics laser ranging system: Performance simulations and development of the EOS facility — Earth Observing System (EOS) N89-12982

GEOGRAPHIC INFORMATION SYSTEMS
Requirements for ongoing development of the Pilot Land Data System (PLDS) N89-12958
The use of remote sensing in conjunction with geographic information systems for local planning N89-12959
An integrated remote sensing approach for regional agrostatistics and land monitoring N89-12960
Development of a geographic information system with the aid of digital image processing techniques N89-12961
Modelling land resources within a pilot geographical information system N89-12962
Communication: The key to integrating remote sensing and geographic information systems N89-12963
Integrating remote sensing data into a geographical information system: A foundation for rural land use strategies: Nature Conservancy Council project N89-12964
An international approach to GIS based on remote sensing and terrain classification — geographic information system (GIS) N89-12966
Analysis of potato crop distribution using remotely sensed and environmental data in a pilot geographical information system N89-12967
Improving the accessibility of spatially referenced geological information N89-13026

Cotton area mapping using multitemporal satellite data integrated within a geographical information system applied to a cotton boll weevil control programme in Paraguay N89-13077

GEOLOGICAL SURVEYS

Inference of geologic surface parameters from polarimetric radar observations and model inversion N89-12950

The relativity utility of LANDSAT MSS and SIR-A imagery in reconnaissance geological mapping in Northern Sudan N89-13022

Mapping the distribution and abundance of lithological units and surface mineralogies at Jabal Sa'id, Saudi Arabia: An application of spectral mixture modelling N89-13024

LANDSAT Thematic Mapping (TM) and SPOT HRV for survey mapping of bedrock outcrops N89-13055

Applications of remote sensing for geological mapping in eastern Egypt N89-13087

GEOLOGY

Development of Alaskan gas hydrate resources [DE88-010270] N89-13093

GEOMAGNETIC PULSATIONS

Activities report of the Canary Geophysical Center [ISBN-8-45-055434-9] N89-13115

GEOMAGNETIC TAIL

Interaction of a hollow-cathode source with an ionospheric plasma [IFSI-88-10] N89-13112

Injection of ionospheric ions into the plasma sheet in the Earth's magnetotail [IFSI-88-13] N89-13113

GEOMAGNETISM

The E-parallel polarization response of a two-dimensional heterogeneous layer modelled by two thin sheets --- electromagnetic geophysical sounding N89-12947

Activities report of the Canary Geophysical Center [ISBN-8-45-055434-9] N89-13115

Geomagnetism, a dynamic science [REPT-37] N89-13309

GEOMETRIC RECTIFICATION (IMAGERY)

The differential rectification of SPOT HRV panchromatic and multispectral imagery using a digital elevation model N89-13054

GEOMETRICAL OPTICS

Shadows and wedges in scattering from the sea N89-12946

GEOMETRY

Use of distance versus statistical distance in acceptance tests [NASA-CR-183353] N89-13220

GEOMORPHOLOGY

The production of anaglyphs from SPOT-HRV panchromatic data for geomorphological mapping N89-13056

GEOPHYSICAL FLUIDS

Improving the efficiency of binary cycles [DE88-015108] N89-13099

GEOPHYSICS

Activities report of the Canary Geophysical Center [ISBN-8-45-055434-9] N89-13115

GEOSAT SATELLITES

Analysis of GEOSAT radar altimeter errors based on pre-launch test data [NASA-TM-101230] N89-12806

GEOTHERMAL TECHNOLOGY

Improving the efficiency of binary cycles [DE88-015108] N89-13099

GET AWAY SPECIALS (STS)

NASA newsletters for the Weber Student Shuttle Involvement Project [NASA-TM-101001] N89-13144

GLACIERS

Monitoring of seasonal snow cover on glaciers N89-13044

GLASS FIBERS

Preliminary results from the dynamic response testing of the Northern Power Systems 100-kW wind turbine [DE88-001166] N89-13101

GLASS LASERS

High power Nd:glass lasers as drivers for inertial confinement fusion [DE88-017016] N89-12860

GLOBAL POSITIONING SYSTEM

Functional description of signal processing in the Rogue GPS receiver [NASA-CR-183314] N89-12813

GLUCOSE

Glucose tolerance and insulin secretion during 0-g simulation [DFVLR-FB-88-25] N89-13136

GLUTAMIC ACID

Poly(ethyl acrylate) and poly(gamma-benzyl-L-glutamate): An interpenetrating polymer system [AD-A197783] N89-12737

GRADIENTS

Resonator design with an intracavity time-varying index gradient [DE88-015259] N89-12857

GRAIN BOUNDARIES

In-situ oxidation of Ni3Al alloys [DE88-007177] N89-12702

Irradiation-assisted stress corrosion cracking and grain boundary segregation in heat treated Type 304SS [DE88-008382] N89-12713

Grain boundary oxidation and its effects on high temperature fatigue life N89-12918

GRAIN SIZE

Effect of grain size on the high temperature properties of B2 aluminides [NASA-TM-101382] N89-12720

Light scattering of large rough particles application to cometary grains N89-13357

Color gradients in the coma of P/Halley N89-13362

A possible explanation for the inconsistency between the Giotto grain mass distribution and ground-based observations N89-13364

GRAMMARS

A lexical conceptual approach to generation for machine translation [AD-A197356] N89-13304

GRAPHITE

Characterization of a graphite epoxy optical bench during thermal vacuum cycling N89-12585

Surface structures and transitions and the evolution from firm to bulk behavior [AD-A197788] N89-12695

Characterization of graphite fibers by X-ray diffraction N89-12755

GRAPHITE-EPOXY COMPOSITES

The effect of delamination on the response of advanced composite laminates N89-12668

A probabilistic approach to composite micromechanics [NASA-TM-101366] N89-12684

GRASSES

Relationships between the nitrogen content of grass and reflectance N89-13002

GRASSLANDS

The detection of unimproved grassland in Berkshire using a binary decision tree approach N89-12988

An evaluation of satellite imagery, LANDSAT Thematic Mapper and SPOT-1 HRV, for grassland inventory in the UK N89-13057

GRATINGS (SPECTRA)

Fiber optic wavelength division multiplexing: Principles and applications in telecommunications and spectroscopy N89-13324

GRAVITATION

Gravitation, black holes and space-time physics [DE88-703054] N89-13377

GRAVITATIONAL EFFECTS

A conceptual design study of the reusable reentry satellite [NASA-TM-101043] N89-12623

GRAVITATIONAL FIELDS

New gravitational forces from quantum theory [DE88-016231] N89-13294

GRAVITATIONAL PHYSIOLOGY

Glucose tolerance and insulin secretion during 0-g simulation [DFVLR-FB-88-25] N89-13136

GRAVITATIONAL WAVE ANTENNAS

The Frascati (Italy) gravitational antenna, 1987 [IFSI-88-4] N89-12846

GRAVITATIONAL WAVES

LIGO vacuum system study N89-12599

Theoretical aspects of gravitational wave detection N89-13383

GRAVITY WAVES

Modulation of the radar backscatter from the ocean surface by a long gravity wave N89-13031

Phase versus orbital velocity in SAR wave imaging: Paradox lost N89-13033

Rayleigh lidar observations of gravity wave activity in the upper stratosphere at Urbana, Ill. [NASA-CR-182738] N89-13107

GRAY SCALE

A luminance edge extraction method using gradient of gray level for synthetic aperture radar imageries N89-13086

GRID GENERATION (MATHEMATICS)

Mathematical modelling and computer simulation using Cartesian grid [TM-AE-8804] N89-13149

An adaptive method with mesh moving and local mesh refinement for time-dependent partial differential equations [AD-A197772] N89-13208

GROOVES

Development of optimized, graded-permeability axial groove heat pipes N89-12614

GROUND TESTS

Microgravity science and applications program tasks, 1987 revision [NASA-TM-4068] N89-12752

GROUND TRUTH

Verification of the accuracy of a network of water-vapor radiometers N89-12941

GROWTH

Research on mercury cadmium telluride [AD-A197238] N89-13282

H

HAFNIUM ALLOYS

Amorphous powders of Al-Hf prepared by mechanical alloying [DE88-014459] N89-12704

HAIL

Processing and interpretation of alternately polarised weather radar echoes N89-12996

HAILSTORMS

Some advantages of using polarisation diversity illustrated through the analysis of radar data from a storm in central Alberta (Canada) N89-12994

HALLEY'S COMET

Infrared Observations of Comets Halley and Wilson and Properties of the Grains [NASA-CP-3004] N89-13330

Infrared observations of the dust coma N89-13331

Grain optical properties N89-13332

Cometary dust composition N89-13333

PIA update: Correlation analyses of mass spectra N89-13334

A comparison of Halley dust with meteorites, interplanetary dust and interstellar grains N89-13335

The spectral properties of interplanetary dust particles N89-13336

Aromatic components in cometary materials N89-13337

The 3.4 micrometer emission feature in Comet Halley N89-13338

Comparison of the 3.36 micrometer feature to the ISM N89-13339

A two component model for thermal emission from organic grains in Comet Halley N89-13340

On the carbon abundance in Comet Halley derived from the 3 micron feature: Comparison with interstellar dust N89-13341

Possible identifications of the 3.4 micrometer feature N89-13342

Focus on the future N89-13344

Current status of the international Halley Watch infrared net archive N89-13345

The near-infrared polarization and color of Comet Halley: What can we learn about the grains N89-13348

Polarization images of Comet Halley N89-13351

Detection of parent molecules in the IR spectrum of P/Halley with the IKS-Vega spectrometer N89-13352

Infrared observations of P/Halley and P/Encke N89-13353

Airborne 20-65 micron spectrophotometry of Comet Halley N89-13354

An albedo map of P/Halley on 13 March 1986 N89-13355

Comet Halley's colorful outbursts N89-13359

Color gradients in the coma of P/Halley N89-13362

Optical properties of cometary grains N89-13363

A possible explanation for the inconsistency between the Giotto grain mass distribution and ground-based observations N89-13364

Laboratory simulations of comet surfaces N89-13366

A multicomponent model of the infrared emission from Comet Halley N89-13367

The NASA Infrared Telescope Facility Comet Halley monitoring program 2: Post-perihelion results N89-13368

HAMILTONIAN FUNCTIONS

Sensitivity analysis for shortest Hamiltonian path and traveling salesman problems [AD-A197167] N89-13204

HARDNESS TESTS

On the resistance of ceramics to high velocity penetration [AD-A197320] N89-12734

HARMONIC MOTION

Nearfield acoustic radiation from a point-excited cylindrical shell [AD-A197282] N89-13234

HARMONIC RADIATION

Fundamental harmonic electron cyclotron emission for hot, loss-cone type distributions N89-13269

HARMONICS

On the simulation of harmonically related signals [AD-A197821] N89-13235

HASTELLOY (TRADEMARK)
Thermomechanical characterization of Hastelloy-X under uniaxial cyclic loading N89-12909
HAZARDS
Bioelectromagnetic effects of EMP: Preliminary findings
[DE88-012118] N89-12791
HAZE
Wide Field/Planetary Camera (WF/PC) contamination control assessment N89-12584
HEALING
Isolation of osteogenic cells from the trauma-activated periosteum N89-12757
HEARING
Use of proximity effect in hearing aid microphones to increase telephone intelligibility in noise
[AD-A197311] N89-12799
HEAT BALANCE
Mass and heat balances in the upper ocean N89-13089
HEAT FLUX
HOST instrumentation R and D program overview N89-12878
HEAT PIPES
Development of optimized, graded-permeability axial groove heat pipes N89-12614
Heat pipe cooling system with sensible heat sink N89-12615
LEC (Liquid Encapsulated Czochralski) growth of InP with magnetic field assisted melt stabilization and heat transfer control
[AD-A196748] N89-12688
Micro heat pipes
[DE88-016113] N89-13100
The 5 kWe scale-down of the SPAR/SP-100 heat pipe reactor N89-13226
HEAT PUMPS
Assessment of Japanese variable speed heat pump technology
[DE88-013246] N89-12826
The effects of expansion devices on the transient response characteristics of the air-source heat pump during the reverse cycle defrost
[AD-A197150] N89-12829
HEAT RADIATORS
The solar simulation test of the ITALSAT thermal structural model N89-12613
HEAT RESISTANT ALLOYS
Simplified cyclic structural analysis of SSME turbine blades N89-12632
Effects of high mean stress on the high-cycle fatigue of PWA 1480 and DS MAR M 246 + Hf at 1000 F N89-12633
Constitutive behavior of single crystal PWA 1480 and directionally solidified MAR-M 246 under monotonic and cyclic loads at high and low temperature N89-12634
Fatigue crack retardation following overloads in Inconel 718, Ti-5Al-2.5Sn, and Haynes 188 N89-12636
Hydrogen effects on the fatigue and tensile behavior of CMSX-2 nickel base superalloy single crystals N89-12658
LCF and crack growth rate of turbine blade alloys in hydrogen and hydrogen/steam environments N89-12660
A multiaxial theory of viscoplasticity for isotropic materials N89-12908
Constitutive modeling for single crystal superalloys N89-12911
Constitutive modelling of single crystal and directionally solidified superalloys N89-12912
HEAT SINKS
Heat pipe cooling system with sensible heat sink N89-12615
Self-actuating heat switches for redundant refrigeration systems
[NASA-CASE-NPO-17085-1-CU] N89-12785
HEAT TRANSFER
Development of a thermal and structural analysis procedure for cooled radial turbines
[NASA-TM-101416] N89-12568
Fifteenth Space Simulation Conference: Support the Highway to Space Through Testing
[NASA-CP-3015] N89-12582
RP-1 and methane combustion and cooling experiments N89-12650
LEC (Liquid Encapsulated Czochralski) growth of InP with magnetic field assisted melt stabilization and heat transfer control
[AD-A196748] N89-12688
Prediction of heat transfer between the combustion space and the load
[DE88-016313] N89-12698
Heat transfer to rough turbine blading N89-12823
Thermal transport between a continuously moving heated plate and a quiescent ambient medium N89-12824
Heat transfer from roughened surfaces using interferometry N89-12827
Turbine Engine Hot Section Technology 1986
[NASA-CP-2444] N89-12876
HOST turbine heat transfer subproject overview N89-12880
Aerothermal modeling program, phase 2 N89-12890
Heat transfer with very high free-stream turbulence and streamwise vortices N89-12900
Development of low Reynolds number two equation turbulence models for predicting external heat transfer on turbine blades N89-12901
Micro heat pipes
[DE88-016113] N89-13100
The effect of vertical wind shear on tropical cyclone movement
[AD-A197218] N89-13120
HEAT TRANSFER COEFFICIENTS
Measurement of airfoil heat transfer coefficients on a turbine stage N89-12897
Coolant passage heat transfer with rotation N89-12899
Turbine airfoil film cooling N89-12903
HEATING
Combined pressure-shear ignition sensitivity test
[AD-A197076] N89-12749
HEAVY IONS
Electron-impact ionization of heavy atomic ions
[DE88-008371] N89-13238
HELICAL FLOW
Modified magnetic confinement configurations based on understanding helicity dissipation and pressure driven modes in the spheromak
[DE88-009149] N89-13260
HELICOPTER CONTROL
Design and numerical evaluation of full-authority flight control systems for conventional and thruster-augmented helicopters employed in NOE operations
[NASA-CR-183311] N89-12570
HELICOPTERS
Locating and search procedures with helicopters for sea and/or air emergencies
[FPN-0079] N89-12556
Establishment of center for rotorcraft education and research
[AD-A197141] N89-13295
HELIUM
High T(sub c) superconductors: Will they replace helium temperature superconductors for magnets
[DE88-016632] N89-13279
Absolute photometric calibration of detectors to 0.3 mmag using amplitude-stabilized lasers and a helium-cooled absolute radiometer N89-13318
HERTZSPRUNG-RUSSELL DIAGRAM
Theoretical studies of mass loss and shock phenomena in cool star envelopes
[NASA-CR-182708] N89-13375
HETEROCYCLIC COMPOUNDS
Electronic and ionic transport in polymers
[AD-A197142] N89-12728
HETERODYNING
An optical heterodyne densitometer N89-13323
A far-infrared heterodyne spectrometer for airborne astronomy N89-13329
HETEROGENEITY
Thermal properties of heterogeneous grains N89-13358
HETEROJUNCTIONS
MBE growth, characterization and electronic device processing of HgCdTe, HgZnTe related heterojunctions and HgCdTe-CdTe superlattices
[AD-A197752] N89-13286
HEURISTIC METHODS
Discovering substructure in examples
[AD-A197778] N89-13163
Engineering applications of heuristic multilevel optimization methods
[NASA-TM-101504] N89-13203
HIERARCHIES
Design document for GCS version
[NASA-CR-183278] N89-13150
The large-scale structure of the universe: Some theoretical considerations N89-13381
HIGH FREQUENCIES
Modeling and performance of HF/OTH (High-Frequency/Over-The-Horizon) radar target identification systems
[AD-A197850] N89-12808
Comments on the high frequency behavior of the coupling of an accelerator beam to its environment
[CEBAF-PR-88-006] N89-13245
HIGH POWER LASERS
Population inversion non-equilibrium flow simulation calculations of the capabilities of convection flow lasers
[AD-A197741] N89-12854
HIGH RESOLUTION
Statistics and high resolution imaging of snowpack at 35 GHz using a microcomputer N89-13047
HIGH SPEED
Designing simulator tasks to study the high speed, low altitude environment N89-12770
HIGH SPEED PHOTOGRAPHY
Laser illuminated high speed photography of energetic materials
[DE88-012870] N89-12848
HIGH TEMPERATURE
Round-robin measurements of the apparent thermal conductivity of two refractory insulation materials, using high-temperature guarded-hot-plate apparatus
[PB88-215421] N89-12670
Effect of grain size on the high temperature properties of B2 aluminides
[NASA-TM-101382] N89-12720
Turbine Engine Hot Section Technology (HOST) Project N89-12877
Elevated temperature strain gages N89-12886
Development of a high temperature static strain sensor N89-12887
The NASA Lewis Strain Gauge Laboratory: An update N89-12888
Determination of surfaces of constant inelastic strain rate at elevated temperature N89-12910
High temperature stress-strain analysis N89-12913
Overview of high-temperature superconductivity: Theory, surfaces, interfaces and bulk systems
[AD-A197383] N89-13285
Electronic properties and current carrying capacity of high-temperature ceramic superconductors
[AD-A197819] N89-13287
HIGH TEMPERATURE ENVIRONMENTS
Materials selection for long life in LEO: A critical evaluation of atomic oxygen testing with thermal atom systems N89-12590
Cost effective alternative to low irradiance measurements N89-12619
Considerations in development and implementation of elasto-viscoplastic constitutive model for high temperature applications
[NASA-CR-183403] N89-12932
HIGH TEMPERATURE GASES
A high pressure, high temperature hydrogen environment for metals properties testing system N89-12656
Population inversion non-equilibrium flow simulation calculations of the capabilities of convection flow lasers
[AD-A197741] N89-12854
HIGH TEMPERATURE PLASMAS
Fundamental studies and device development in beta silicon carbide
[AD-A197843] N89-12739
HIGH TEMPERATURE RESEARCH
In-situ high temperature oxidation studies
[DE88-017092] N89-12716
HIGH TEMPERATURE SUPERCONDUCTORS
Generation of the J(sub c), H(sub c), T(sub c) surface for commercial superconductor using reduced-state parameters
[DE88-014038] N89-13278
A novel excitonic mechanism for high temperature superconductivity
[DE88-016227] N89-13288
HIGH TEMPERATURE TESTS
High temperature adhesive systems
[AD-A197077] N89-12726
Elevated temperature crack growth N89-12915
HINGES
Space station erectable manipulator placement system
[NASA-CASE-MSC-21096-1] N89-12621
HISTORIES
Geomagnetism, a dynamic science
[REPT-37] N89-13309
HOLDERS
Gripping device
[NASA-CASE-MSC-21365-1] N89-12865
HOLMIUM
Tm,Ho:YLF laser end-pumped by a semiconductor diode laser array
[NASA-CASE-NPO-17282-1-CU] N89-12856
HOLOGRAPHY
Foundations of the blade-vortex interaction problem: Structure and behavior of travelling compressible vortices
[AD-A197370] N89-12550
Laser applications in flow diagnostics
[AGARD-AG-296] N89-12849
Holographic particle detection
[NASA-CR-183315] N89-13240

HOMOGENEITY
Poly(ethyl acrylate) and poly(gamma-benzyl-L-glutamate): An interpenetrating polymer system
[AD-A197783] N89-12737
HUBBLE SPACE TELESCOPE
WF/PC internal molecular contamination during system thermal-vacuum test N89-12583
Wide Field/Planetary Camera (WF/PC) contamination control assessment N89-12584
Characterization of a graphite epoxy optical bench during thermal vacuum cycling N89-12585
The Hubble Space Telescope high speed photometer N89-13311
HUMAN FACTORS ENGINEERING
Pilot factors guidelines for the operational inspection of navigation systems
[NASA-CR-181644] N89-12557
Voice recognition and artificial intelligence in an air traffic control environment
[AD-A197219] N89-12559
AUTOCREW implementation: Inbound surface-to-air missile simulation
[AD-A197674] N89-13143
HUMAN PERFORMANCE
Consequences of individual differences in brain organization for human performance
[AD-A197667] N89-13138
MANPRINT (Manpower and Personnel Integration Program) primer
[AD-A197681] N89-13296
HUMAN RESOURCES
MANPRINT (Manpower and Personnel Integration Program) primer
[AD-A197681] N89-13296
HYDRATES
Development of Alaskan gas hydrate resources
[DE88-010270] N89-13093
HYDRATION
Challenging applications for hydrated and chemically reacted ceramics
[DE88-015397] N89-12742
HYDROCARBON FUELS
Survey of LOX/hydrocarbon combustion and cooling N89-12647
LOX/hydrocarbon combustion and cooling survey N89-12648
HYDROCARBONS
Aromatic components in cometary materials N89-13337
The 3.4 micrometer emission feature in Comet Halley N89-13338
HYDROCHLORIC ACID
Determination of sulfuric acid, oxalic acid, and their matrix effects in aluminum anodizing solutions by ion chromatography
[AD-A197734] N89-12694
HYDRODYNAMICS
Analysis of the Space Shuttle Orbiter skin panels under simulated hydrodynamic loads
[NASA-TM-4082] N89-12935
HYDROGEN
A steam inerting system for hydrogen disposal for the Vandenberg Shuttle N89-12608
A high pressure, high temperature hydrogen environment for metals properties testing system N89-12656
LCF and crack growth rate of turbine blade alloys in hydrogen and hydrogen/steam environments N89-12660
HYDROGEN EMBRITTLEMENT
Advanced Earth-to-Orbit Propulsion Technology 1986, volume 2
[NASA-CP-2437-VOL-2] N89-12626
Hydrogen-environment embrittlement and its control in high pressure hydrogen/oxygen rocket engines N89-12654
Multispecimen test facility for high-pressure hydrogen creep studies N89-12655
Hydrogen effects on the fatigue and tensile behavior of CMSX-2 nickel base superalloy single crystals N89-12658
The determination of mobile hydrogen in aerospace engine alloys N89-12659
The development of a hydrogen resistant alloy N89-12661
HYDROGEN OXYGEN ENGINES
Advanced Earth-to-Orbit Propulsion Technology 1986, volume 2
[NASA-CP-2437-VOL-2] N89-12626
Results of coaxial injector element testing N89-12651
Hydrogen-environment embrittlement and its control in high pressure hydrogen/oxygen rocket engines N89-12654
HYDROGEN PLASMA
Interaction of impurity ions with a weakly non-Maxwellian simple hydrogenic plasma
[DE88-017137] N89-13265
HYDROGEN PRODUCTION
Homogeneous catalytic production of hydrogen and other molecules from water-DMF (N-dimethylformamide) solutions
[AD-A197072] N89-12690
HYDROLYSIS
Differential scanning calorimetry as a method for indicating hydrolysis of urethane elastomers
[AD-A197673] N89-12736
HYDROMETEOROLOGY
Cross-polar radar measurements in ice and rain N89-12993
Dual linear polarisation time series as an aid to hydrometeor identification N89-12995
HYPERBARIC CHAMBERS
The effects of hyperbaric oxygen and antioxidant deficiencies on rat retinal ultrastructure N89-12772
HYPERCUBE MULTIPROCESSORS
Applications of parallelism to current algorithms for intelligence analysis
[NASA-CR-183351] N89-13165
HYPERGEOMETRIC FUNCTIONS
A note on incomplete integrals of cylindrical functions
[AD-A197822] N89-13210
HYPERSONIC AIRCRAFT
Trajectory optimization and guidance law development for national aerospace plane applications
[NASA-CR-182994] N89-12538
HYPERSONIC FLIGHT
Aerodynamic pressures and heating rates on surfaces between split elevons at Mach 6.6
[NASA-TP-2855] N89-12822
HYPERSONIC FLOW
Direct simulation of three-dimensional flow about the AFE vehicle at high altitudes
[NASA-TM-101492] N89-12834
HYPERVELOCITY IMPACT
On the resistance of ceramics to high velocity penetration
[AD-A197320] N89-12734
HYPERVELOCITY PROJECTILES
A decade of railgun development for high pressure research
[DE88-017024] N89-12578
HYPOTHESES
Is word recognition automatic: A cognitive-anatomical approach
[AD-A197089] N89-13137
Neural network performance on the stochastic exclusive-or problem
[AD-A197789] N89-13179

I

ICE
Cross-polar radar measurements in ice and rain N89-12993
The incorporation of sulfur dioxide into snow and depositing ice N89-13116
ICE ENVIRONMENTS
Arctic oceanography and meteorology review
[AD-A196533] N89-13126
ICE FORMATION
Characterization of a graphite epoxy optical bench during thermal vacuum cycling N89-12585
Performance of the forward scattering spectrometer probe in NASA's icing research tunnel
[NASA-TM-101381] N89-12845
Arctic oceanography and meteorology review
[AD-A196533] N89-13126
Bering Sea wave and ice measurements in support of Arctic west winter 1986
[AD-A197196] N89-13127
ICE REPORTING
The LIMEX 1987 pilot project, LIMEX 1989 and long-term objective for data collection on the Canadian East coast N89-13037
ICELAND
The interpretation of Icelandic tundra features from LANDSAT-MSS data N89-13027
IGNITION
Semiconductor bridge (SCB) igniter studies. 2: Comparison of SCB and hot-wire direct propulsion thrusters
[DE88-008803] N89-12625
RP-1 and methane combustion and cooling experiments N89-12650
Results of coaxial injector element testing N89-12651
Autoignition chemistry of n-butane in a motored engine: A comparison of experimental and modeling results
[DE88-014153] N89-12697
Combined pressure-shear ignition sensitivity test
[AD-A197076] N89-12749
ILLUMINATING
Laser illuminated high speed photography of energetic materials
[DE88-012870] N89-12648
IMAGE ANALYSIS
Laser dynamic photoelasticity and digital image analysis for nondestructive evaluation of surface and near surface flaws through ultrasonic spectroscopy N89-12871
Statistical analysis and some polarimetric signatures of a polarimetric synthetic aperture radar image N89-12952
The effects of undersampling on multipolarization SAR images N89-12956
Spectral analysis of ocean wave imagery using 2-D linear prediction N89-12968
On the use of speckle statistics for the extraction of ocean wave spectra from SAR imagery N89-12969
Multitemporal resource complex analysis of Catinia province, Italy from LANDSAT-TM data N89-12985
The detection of unimproved grassland in Berkshire using a binary decision tree approach N89-12988
Detection of seasonal and long-term changes in land cover from multitemporal LANDSAT MSS data N89-12989
The interpretation of Icelandic tundra features from LANDSAT-MSS data N89-13027
Microcomputers (PCs) for snow cover analyses using multisensor satellite data N89-13049
Lapwing: A trainable spatial feature recognition system N89-13063
Co-occurrence matrix modification for small region texture measurement and comparison N89-13064
The interrelationship between resampling method and information extraction technique N89-13065
IMAGE CONTRAST
The optimal polarizations for achieving maximum contrast in radar images
[NASA-CR-183349] N89-12794
IMAGE ENHANCEMENT
Photogrammetric model for correction of MSS-LANDSAT imagery
[INPE-4652-PRE/1359] N89-13090
IMAGE FILTERS
On the concept of the polarimetric matched filter in high resolution radar imaging: An alternative for speckle radiation N89-12954
Complex SAR imagery and speckle filtering for ERS-1 wave mode N89-13029
IMAGE PROCESSING
On the sampling in imaging microwave radiometers N89-12940
Development of a geographic information system with the aid of digital image processing techniques N89-12961
PIPS: A Procedure for Interactive Pyramid Segmentation N89-12984
Performance modeling and results for X-SAR N89-13009
Complex SAR imagery and speckle filtering for ERS-1 wave mode N89-13029
Extraction of dense digital elevation models from SPOT stereo imagery N89-13053
Implementation issues for level O image processor software within an application package
[AD-A197763] N89-13162
Time-resolved solid-state array imaging systems: Developments and applications
[DE88-016274] N89-13254
IMAGE RECONSTRUCTION
Survey of image restoration techniques
[AD-A197470] N89-13251
IMAGE RESOLUTION
Effects of changing satellite sensor attributes N89-13059
IMAGERY
Practical algorithms for image component labeling on SIMD mesh connected computers
[AD-A197341] N89-13158
Survey of image restoration techniques
[AD-A197470] N89-13251
IMAGES
Survey of image restoration techniques
[AD-A197470] N89-13251
IMAGING TECHNIQUES
Correlation studies on surface particle detection methods N89-12587
The optimal polarizations for achieving maximum contrast in radar images
[NASA-CR-183349] N89-12794

The use of remote sensing in conjunction with geographic information systems for local planning N89-12959
Efficient use of bit planes in the generation of motion stimuli [NASA-TM-101022] N89-13171
Time-resolved solid-state array imaging systems: Developments and applications [DE88-016274] N89-13254

IMPACT DAMAGE
Simulation of the effects of the orbital debris environment on spacecraft N89-12607
Shock detection in composite structures. Test report 48-915/F --- Impact damage [REPT-48-915/F] N89-12683

IMPEDANCE MATCHING
The design of antenna matching networks using a microcomputer [AD-A197364] N89-12802

IMPURITIES
Electronic structure of light impurities in alpha-Fe and V [DE88-702958] N89-12721
Interaction of impurity ions with a weakly non-Maxwellian simple hydrogenic plasma [DE88-017137] N89-13265
An introduction to blocked impurity band detectors N89-13320

INCINERATORS
Human exposure to dioxin from combustion sources [DE88-013825] N89-13135

INCOMPRESSIBLE FLOW
Parallel algorithms in the finite element approximation of flow problems [AD-A197454] N89-13178

INCONEL (TRADEMARK)
Fatigue crack retardation following overloads in Inconel 718, Ti-5Al-2.5Sn, and Haynes 188 N89-12636

INDEXES (DOCUMENTATION)
NASA thesaurus. Volume 2: Access vocabulary [NASA-SP-7064-VOL-2] N89-13298
NASA thesaurus. Volume 1: Hierarchical Listing [NASA-SP-7064-VOL-1] N89-13302

INDIUM PHOSPHIDES
Radiation resistance and comparative performance of ITO/InP and n/p InP homojunction solar cells [NASA-TM-101387] N89-12819

INDUSTRIES
Environmental management practices in oil refineries and terminals: An overview [ISBN-92-807-1108-3] N89-13104
Federal Laboratory Consortium for Technology Transfer: Putting technology to work. Examples of industry-laboratory cooperation contributing to our nation's economic strength [PB88-243357] N89-13307

INELASTIC STRESS
On 3D inelastic analysis methods for hot section components N89-12906
Determination of surfaces of constant inelastic strain rate at elevated temperature N89-12910
Considerations in development and implementation of elasto-viscoplastic constitutive model for high temperature applications [NASA-CR-183403] N89-12932

INERTIAL CONFINEMENT FUSION
High power Nd:glass lasers as drivers for inertial confinement fusion [DE88-017016] N89-12860
Nuclear technology for the year 2000 [DE88-005041] N89-13223
Laser driven inertial confinement fusion N89-13229
Confinement dynamics in the reversed field pinch [DE88-009148] N89-13259
Modified magnetic confinement configurations based on understanding helicity dissipation and pressure driven modes in the spheromak [DE88-009149] N89-13260

INFERENCE
Two-sample inference for median survival times based on one-sample procedures for censored survival data [AD-A197776] N89-13218

INFLUENCE COEFFICIENT
Numerical integration of influence coefficients for panel methods about axisymmetric bodies by means of the ROMBERG algorithm [DFVLR-MITT-88-18] N89-12839

INFORMATION DISSEMINATION
Survey of supply/demand relationships for Japanese Technical Information in the United States: The field of advanced ceramics research and development [PB88-210943] N89-13300

INFORMATION RETRIEVAL
Improving the accessibility of spatially referenced geological information N89-13026
NASA thesaurus. Volume 2: Access vocabulary [NASA-SP-7064-VOL-2] N89-13298
NASA thesaurus. Volume 3: Definitions [NASA-SP-7064-VOL-3] N89-13301
NASA thesaurus. Volume 1: Hierarchical Listing [NASA-SP-7064-VOL-1] N89-13302

INFORMATION SYSTEMS
Boeing Military Airplane Company technical order transfer tests [DE88-012233] N89-13151

INFRARED ASTRONOMY
A far-infrared heterodyne spectrometer for airborne astronomy N89-13329
Infrared observations of the dust coma N89-13331
Current status of the international Halley Watch infrared net archive N89-13345
IR-dust observations of Comet Tempel 2 with CRAF VIMS N89-13349
The evolutionary status of young stellar mass loss driving sources as derived from IRAS observations [IFSI-88-12] N89-13386

INFRARED IMAGERY
The need for volcano monitoring and the ability to detect activity using emitted short wavelength infrared N89-13025
An albedo map of P/Halley on 13 March 1986 N89-13355

INFRARED RADIATION
Survey of laser-produced pressure and impulse data [AD-A197313] N89-12852
A global analysis and correlation of Nimbus 7 cloud and longwave radiation data [AD-A197223] N89-13121
Chemical precursors to zinc sulfide: ZnS whisker synthesis [AD-A197262] N89-13284
Comet Halley's colorful outbursts N89-13359

INFRARED SPECTRA
Infrared Observations of Comets Halley and Wilson and Properties of the Grains [NASA-CP-3004] N89-13330
Focus on the future N89-13344
Interstellar grain chemistry and the composition of comets N89-13346
The spectral appearance of comets from 5 to 20 micrometers: A survey of the data N89-13347
Cometary dust size distributions from flyby spacecraft N89-13350
Detection of parent molecules in the IR spectrum of P/Halley with the IKS-Vega spectrometer N89-13352
Infrared observations of P/Halley and P/Encke N89-13353
Comet Halley's colorful outbursts N89-13359
A multicomponent model of the infrared emission from Comet Halley N89-13367
The NASA Infrared Telescope Facility Comet Halley monitoring program 2: Post-perihelion results N89-13368

INFRARED WINDOWS
Chemical precursors to zinc sulfide: ZnS whisker synthesis [AD-A197262] N89-13284

INJECTORS
Results of coaxial injector element testing N89-12651
Combustion modeling: Progress and projections N89-12652

INLET FLOW
Influence of bulk turbulence and entrance boundary layer thickness on the curved duct flow field N89-12896

INPUT
Multiple input/output random vibration control system N89-12594

INPUT/OUTPUT ROUTINES
Performance studies of dynamic load balancing in distributed systems [AD-A197130] N89-12926

INSERTION
Design of vacuum chambers downstream of NSLS X-ray ring insertion devices [DE88-015715] N89-13247

INSPECTION
Pilot factors guidelines for the operational inspection of navigation systems [NASA-CR-181644] N89-12557

INSTRUCTORS
A teacher's companion to the space station: A multi-disciplinary resource N89-12575

INSTRUMENT PACKAGES
HOST instrumentation R and D program overview N89-12878

INSULATION
Round-robin measurements of the apparent thermal conductivity of two refractory insulation materials, using high-temperature guarded-hot-plate apparatus [PB88-215421] N89-12670
Cryogenic insulation system [NASA-CASE-LAR-13506-1] N89-12741
Development of polyisocyanurate pour foam formulation for space shuttle external tank thermal protection system [NASA-CR-183511] N89-12745
The behavior of disk electrodes: Optical imaging of the concentration distribution over a disk electrode under galvanostatic conditions [AD-A197355] N89-12816

INSULIN
Glucose tolerance and insulin secretion during 0-g simulation [DFVLR-FB-88-25] N89-13136

INTEGRAL EQUATIONS
Two alternate proofs of Wang's lune formula for sparse distributed memory and an integral approximation [NASA-CR-184555] N89-13214

INTEGRALS
A note on incomplete integrals of cylindrical functions [AD-A197822] N89-13210

INTELLIGIBILITY
Use of proximity effect in hearing aid microphones to increase telephone intelligibility in noise [AD-A197311] N89-12799

INTERFACES
Guidance and Control/Flight Mechanics Panels Joint Symposium on The Man-Machine Interface in Tactical Aircraft Design and Combat Automation [AGARD-AR-249] N89-12564
Ion beam mixing of metals and ceramics: Material considerations [DE88-016797] N89-12744
Providing on-line guidance to computer users N89-12766
A system to investigate synthesized voice feedback in man-machine interfaces N89-12776
The durability of adhesive joints: An engineering study [AD-A197754] N89-12928
Applications of the ISI (Information Sciences Institute) grapher [AD-A197230] N89-13194
Fitting functions to noisy data in high dimensions [DE88-015922] N89-13213

INTERFACIAL TENSION
As-deposited low-strain LPCVD (Low-Pressure, Chemical-Vapor-Deposition) polysilicon [DE88-016980] N89-12789

INTERFEROMETERS
LIGO vacuum system study N89-12599
The Instrument Test Dewar (ITD): Testing satellite instruments at 1.5 K N89-12604
Phase measurement accuracy limitation in phase shifting interferometry N89-13248

INTERFEROMETRY
Foundations of the blade-vortex interaction problem: Structure and behavior of travelling compressible vortices [AD-A197370] N89-12550

INTERIOR BALLISTICS
Report on JANNAF Workshop Influence of Gas-Phase Chemical Kinetics on Low-Pressure Ignition and Flamespreading in Solid Propellant [AD-A197854] N89-12751

INTERMETALLICS
Coble creep, cavity sintering and cavity growth [DE88-013846] N89-12703

INTERMOLECULAR FORCES
Supercritical fluid chromatography: The effect of the partial molar volume in the stationary phase on retention [DE88-016959] N89-12699

INTERNAL COMBUSTION ENGINES
Autoignition chemistry of n-butane in a motored engine: A comparison of experimental and modeling results [DE88-014153] N89-12697
Fuel alcohol formulations [DE88-016753] N89-12748
Gas flow and global code programme [DE88-012635] N89-12861

INTERNATIONAL COOPERATION
An international approach to GIS based on remote sensing and terrain classification --- geographic information system (GIS) N89-12966
Danish Space Research Institute N89-13391

INTERPLANETARY DUST
A comparison of Halley dust with meteorites, interplanetary dust and interstellar grains N89-13335
The spectral properties of interplanetary dust particles N89-13336
Aromatic components in cometary materials N89-13337

INTERPLANETARY MAGNETIC FIELDS
Tenth European Regional Astronomy Meeting of the IAU: Abstracts [DE88-703273] N89-13370

INTERPOLATION
Multivariate regression with emphasis on multivariate spline methods
[AD-A197793] N89-13209
INTERSTELLAR CHEMISTRY
Interstellar grain chemistry and the composition of comets N89-13346
INTERSTELLAR MATTER
A comparison of Halley dust with meteorites, interplanetary dust and interstellar grains N89-13335
Comparison of the 3.36 micrometer feature to the ISM N89-13339
On the carbon abundance in Comet Halley derived from the 3 micron feature: Comparison with interstellar dust N89-13341
Properties of interstellar dust in reflection nebulae N89-13365
INTERSTELLAR SPACE
Activities report of the Institute of Extraterrestrial Activities
[MPE-208] N89-13308
INVISCID FLOW
A numerical method for computing unsteady 2-D boundary layer flows
[NASA-CR-4196] N89-12835
ION BEAMS
Analysis of adhesion test methods and the evaluation of their use for ion-beam-mixed metal/ceramic systems
[DE88-015358] N89-12725
Ion beam mixing of metals and ceramics: Material considerations
[DE88-016797] N89-12744
Internal kink modes in the ion-kinetic regime N89-13274
ION IMPLANTATION
Fundamental studies and device development in beta silicon carbide
[AD-A197843] N89-12739
Ion beam mixing of metals and ceramics: Material considerations
[DE88-016797] N89-12744
Computer evaluation of ion-implanted dopant profile evolution during annealing N89-12756
ION SOURCES
Soviet exoatmospheric neutral particle beam research
[FASAC-TAR-3110] N89-13390
ION TEMPERATURE
Internal kink modes in the ion-kinetic regime N89-13274
ION TRAPS (INSTRUMENTATION)
Modes of operation of the RETE experiment
[IFSI-88-5] N89-12576
IONIZATION
Adsorption on metal surfaces
[DE88-016557] N89-12715
Electron-impact ionization of heavy atomic ions
[DE88-008371] N89-13238
IONIZATION CROSS SECTIONS
Electron-impact ionization of heavy atomic ions
[DE88-008371] N89-13238
IONIZING RADIATION
Holographic particle detection
[NASA-CR-183315] N89-13240
IONOSPHERIC COMPOSITION
Interaction of a hollow-cathode source with an ionospheric plasma
[IFSI-88-10] N89-13112
Injection of ionospheric ions into the plasma sheet in the Earth's magnetotail
[IFSI-88-13] N89-13113
IONOSPHERIC CURRENTS
Interaction of a hollow-cathode source with an ionospheric plasma
[IFSI-88-10] N89-13112
Injection of ionospheric ions into the plasma sheet in the Earth's magnetotail
[IFSI-88-13] N89-13113
IONOSPHERIC SOUNDING
Ionosphere 1970, Volume 58
[ISSN-0211-5166] N89-13114
IONS
Interaction of impurity ions with a weakly non-Maxwellian simple hydrogenic plasma
[DE88-017137] N89-13265
Transition-metal oxide superconductivity
[AD-A197069] N89-13280
IRON ALLOYS
Multispecimen test facility for high-pressure hydrogen creep studies N89-12655
The development of a hydrogen resistant alloy N89-12661
IRRADIANCE
Cost effective alternative to low irradiance measurements N89-12619
Improvements to photometry. Part 1: Better estimation of derivatives in extinction and transformation equations N89-13322
IRRADIATION
Irradiation-assisted stress corrosion cracking and grain boundary segregation in heat treated Type 304SS
[DE88-008382] N89-12713
IRREVERSIBLE PROCESSES
Superionic conductors as fast, repetitive opening switches
[AD-A197365] N89-12817
ISOTHERMAL FLOW
Experimental study of isothermal flows in a dump combustor N89-12779
ISOTHERMAL PROCESSES
Thermomechanical characterization of Hastelloy-X under uniaxial cyclic loading N89-12909
Non-isothermal buckling behavior of viscoplastic shell structures
[NASA-CR-183013] N89-12931
ISOTROPIC MEDIA
Constitutive modeling for isotropic materials N89-12904
A multiaxial theory of viscoplasticity for isotropic materials N89-12908
ITALIAN SPACE PROGRAM
The solar simulation test of the ITALSAT thermal structural model N89-12613
ITERATION
Algorithms for bound constrained quadratic programming problems
[DE88-016470] N89-13168
ITERATIVE SOLUTION
Perturbed functional iteration applied to the Navier-Stokes equations N89-12774
On the constrained Chebyshev approximation problem on ellipses
[NASA-CR-183209] N89-13200
The solution of linear systems of equations with a structural analysis code on the NAS CRAY-2
[NASA-CR-4159] N89-13202
Some strategies for enhancing the performance of the block Lanczos method
[DE88-014401] N89-13212

J

JAPAN
Forecasting aids for setting tropical cyclone conditions: Sasebo and Iwakuni, Japan
[AD-A197802] N89-13122
Survey of supply/demand relationships for Japanese Technical Information in the United States: The field of advanced ceramics research and development
[PB88-210943] N89-13300
JAPANESE SPACECRAFT
Results of Advanced Earth Observing Satellite (ADEOS) conceptual study N89-12980
Requirements for the Advanced Earth Observing Satellite (ADEOS) orbit, orbit and a attitude control, and rate jitter N89-12981
Verification results of MOS-1 multispectral self scanning radiometer (MESSR) data N89-13004
Data collection system operating on Japan's first marine observation satellite: Inflight evaluation of the system performance N89-13007
JET AIRCRAFT
Ground run-up afterburner detection and noise suppression N89-12768
Fiber optic control system integration
[NASA-CR-179568] N89-13256
JET ENGINE FUELS
Aerodynamics analysis of solid fuel Ramjet projectiles
[AD-A196755] N89-12548
Properties of JP-8 jet fuel
[AD-A197270] N89-12750
JET MIXING FLOW
Aerothermal modeling program, phase 2. Element C: Fuel injector-air swirl characterization N89-12892
JOINTS (JUNCTIONS)
Improving the fatigue resistance of adhesive joints in laminated wood structures
[NASA-CR-182165] N89-12675
JP-8 JET FUEL
Properties of JP-8 jet fuel
[AD-A197270] N89-12750
JUDGMENTS
Bayesian reasoning tool
[AD-A197351] N89-13196
JUNCTION DIODES
Metallization and characterization of a silicon p-n junction diode fabricated from a solar-cell-type silicon substrate
[DE88-703007] N89-13096

K

K-EPSILON TURBULENCE MODEL
Heat transfer to rough turbine blading N89-12823
Heat transfer from roughened surfaces using interferometry N89-12827
KALMAN FILTERS
A GLR (Generalized Likelihood Ratio) algorithm for polyline approximation of waveforms
[AD-A197846] N89-13166
KERNEL FUNCTIONS
Nonlinear perturbations of differential operators with nontrivial kernel and applications to third order periodic boundary value problems
[DE88-702991] N89-13201
KETONES
Polyenamines from aromatic diacetylenic diketones and diamines
[NASA-CASE-LAR-13444-2-CU] N89-12667
KINETIC ENERGY
Internal kink modes in the ion-kinetic regime N89-13274
KINETICS
Materials selection for long life in LEO: A critical evaluation of atomic oxygen testing with thermal atom systems N89-12590
The durability of adhesive joints: An engineering study
[AD-A197754] N89-12928
KLYSTRONS
Algorithms for the self-consistent simulation of high power klystrons
[DE88-010684] N89-12812
KNOWLEDGE BASES (ARTIFICIAL INTELLIGENCE)
Northeast Artificial Intelligence Consortium (NAIC). Review of technical tasks, volume 2, part 1
[AD-A189773] N89-13180
A logic for belief revision N89-13182
A model for belief revision N89-13183
A shared knowledge base for independent problem solving agents N89-13187
Planner system for the application of indications and warning N89-13188
POPLAR: A testbed for cognitive modeling N89-13190
Plan recognition, knowledge acquisition and explanation in an intelligent interface N89-13191
Empirical analysis and refinement of expert system knowledge bases
[AD-A197241] N89-13303
KNOWLEDGE REPRESENTATION
European Seminar on Neural Computing
[ONRL-8-010-C] N89-13173
Northeast Artificial Intelligence Consortium (NAIC). Review of technical tasks, volume 2, part 1
[AD-A189773] N89-13180
A fault diagnosis system based on an integrated knowledge base N89-13181
SNePS considered as a fully intensional propositional semantic network N89-13184
Belief revision in SNePS N89-13185
Distributed problem solving N89-13186
A shared knowledge base for independent problem solving agents N89-13187
Plan recognition, knowledge acquisition and explanation in an intelligent interface N89-13191
KRYPTON
Surface structures and transitions and the evolution from firm to bulk behavior
[AD-A197788] N89-12695

L

LABORATORIES
Class 100 large spacecraft facility N89-12586
The flight robotics laboratory N89-12595
Neutron flux measurements in the Gran Sasso Underground Laboratory (Italy) (part 2)
[IFSI-88-7] N89-13243
Space environment laboratory data acquisition and display system 2
[PB88-205471] N89-13299
Federal Laboratory Consortium for Technology Transfer: Putting technology to work. Examples of industry-laboratory cooperation contributing to our nation's economic strength
[PB88-243357] N89-13307
LAMBERT SURFACE
A reference standard for bidirectional reflection distribution function and bidirectional transmission distribution function measurement
[NASA-CASE-MFS-28183-1] N89-13253
LAME WAVE EQUATIONS
Scattering behavior of a three-axial ellipsoid N89-13011

LAMINAR BOUNDARY LAYER
The laminar boundary layer on an airfoil started impulsively from rest N89-12540
Method for laminar boundary layer transition visualization in flight
[NASA-CASE-LAR-13554-1] N89-12551
LAMINAR FLOW
A zonal equation method for three-dimensional locally elliptic laminar and turbulent flows N89-12547
Control of laminar separation over airfoils by acoustic excitation
[NASA-TM-101379] N89-12552
LAMINATES
Improving the fatigue resistance of adhesive joints in laminated wood structures
[NASA-CR-182165] N89-12675
Shock detection in composite structures. Test report 48-915/F --- impact damage
[REPT-48-915/F] N89-12683
Surface structures and transitions and the evolution from firm to bulk behavior
[AD-A197788] N89-12695
Wave propagation in layered structures N89-12777
LAND ICE
Inference of radio scattering parameters of Antarctic ice sheet using 179 MHz airborne radio echo sounding data N89-12975
Topographic effects on light scattering from snow N89-12976
Synthetic aperture radar over terrestrial ice N89-12977
LAND MANAGEMENT
Modelling land resources within a pilot geographical information system N89-12962
The detection of unimproved grassland in Berkshire using a binary decision tree approach N89-12988
An evaluation of satellite imagery, LANDSAT Thematic Mapper and SPOT-1 HRV, for grassland inventory in the UK N89-13057
LAND USE
Polarization-dependent attenuation of dielectric cylinder arrays N89-12955
The use of remote sensing in conjunction with geographic information systems for local planning N89-12959
An integrated remote sensing approach for regional agrostatistics and land monitoring N89-12960
Development of a geographic information system with the aid of digital image processing techniques N89-12961
Multitemporal resource complex analysis of Catinia province, Italy from LANDSAT-TM data N89-12985
Large area TM land cover classification of Mittlerer Oberrhein County, southwest Germany, and its use for regional planning and crop surveys N89-12986
Towards an urban land-use classification using textural and morphological criteria N89-12987
Detection of seasonal and long-term changes in land cover from multitemporal LANDSAT MSS data N89-12989
A new spatial classification algorithm for high ground resolution images N89-13061
Accuracy of land cover classification of Thematic Mapper (TM) and SPOT data N89-13066
Building a monitoring system based on satellite data to detect vegetation and land use changes in a subtropical region of Mexico N89-13079
LANDING GEAR
Investigation into the applicability of fracture mechanics techniques to aircraft wheel life studies N89-12763
LANDSAT SATELLITES
The relativity utility of LANDSAT MSS and SIR-A imagery in reconnaissance geological mapping in Northern Sudan N89-13022
The interpretation of Icelandic tundra features from LANDSAT-MSS data N89-13027
Change direction analysis using LANDSAT imagery: A review of methodology N89-13068
Photogrammetric model for correction of MSS-LANDSAT imagery
[INPE-4652-PRE/1359] N89-13090
LAP JOINTS
Characterization of adhesively bonded joints using acousto-ultrasonics N89-12925
LARGE SPACE STRUCTURES
Thermal/structural design verification strategies for large space structures N89-12602
Vibration suppression in a large space structure
[NASA-CR-182831] N89-12624
Preliminary applications of decentralized estimation to large flexible space structures N89-12761
LASER ALTIMETERS
Geodynamics laser ranging system: Performance simulations and development of the EOS facility --- Earth Observing System (EOS) N89-12982
LASER ANEMOMETERS
Laser anemometry: A status report N89-12885
LASER APPLICATIONS
Construction of a phase conjugate laser resonator using Brillouin enhanced four wave mixing N89-12759
Laser applications in flow diagnostics
[AGARD-AG-296] N89-12849
Overview of recent advances in excimer laser technology at Los Alamos
[DE88-016236] N89-12858
Optically controlled welding system
[NASA-CASE-MFS-29291-1] N89-12868
Laser dynamic photoelasticity and digital image analysis for nondestructive evaluation of surface and near surface flaws through ultrasonic spectroscopy N89-12871
Backscatter laser depolarization studies of simulated stratospheric aerosols: Crystallized sulfuric acid droplets
[NASA-CR-183387] N89-13111
Laser driven inertial confinement fusion N89-13229
LASER DAMAGE
Survey of laser-produced pressure and impulse data
[AD-A197313] N89-12852
LASER DOPPLER VELOCIMETERS
Laser applications in flow diagnostics
[AGARD-AG-296] N89-12849
LASER FUSION
The next logical step in laser-fusion development
[DE88-007825] N89-13258
LASER HEATING
Temperature profile in semi-infinite planar slab with exponential source and convective boundary condition: Application to laser heating
[DE88-016746] N89-12831
LASER INDUCED FLUORESCENCE
Detection of excited states by laser-induced fluorescence and analysis of energy transfer
[AD-A197770] N89-12855
LASER INTERFEROMETRY
Theoretical aspects of gravitational wave detection N89-13383
LASER OUTPUTS
Laser illuminated high speed photography of energetic materials
[DE88-012870] N89-12848
Laser speckle from thin and cascaded diffusers
[AD-A197066] N89-12850
Summary of laser speckle photogrammetry for HOST N89-12889
Nonlinear effects in photorefractive crystals
[AD-A197152] N89-13281
LASER PUMPING
Proof of the feasibility of coherent and incoherent schemes for pumping a gamma-ray laser
[AD-A197333] N89-12853
Tm,Ho:YLF laser end-pumped by a semiconductor diode laser array
[NASA-CASE-NPO-17282-1-CU] N89-12856
LASER RANGE FINDERS
Geodynamics laser ranging system: Performance simulations and development of the EOS facility --- Earth Observing System (EOS) N89-12982
LASER SPECTROSCOPY
The 6th All-Union Conference on Nonlinear Optics (table of contents)
[AD-A197347] N89-13250
LASER STABILITY
Proof of the feasibility of coherent and incoherent schemes for pumping a gamma-ray laser
[AD-A197333] N89-12853
LASER TARGET INTERACTIONS
The 6th All-Union Conference on Nonlinear Optics (table of contents)
[AD-A197347] N89-13250
LASER WELDING
BES welding science contractors
[DE88-016589] N89-12869
LASERS
LIGO vacuum system study N89-12599
Investigation of laser diode coupling using nonlinear optics N89-12781
Survey of laser-produced pressure and impulse data
[AD-A197313] N89-12852
Absolute photometric calibration of detectors to 0.3 mmag using amplitude-stabilized lasers and a helium-cooled absolute radiometer N89-13318
LEAKAGE
Dynamics of face and annular seals with two-phase flow
[NASA-CR-183352] N89-12870
LEARNING
A teacher's companion to the space station: A multi-disciplinary resource N89-12575
Empirical analysis and refinement of expert system knowledge bases
[AD-A197241] N89-13303
LEARNING MACHINES
Discovering substructure in examples
[AD-A197778] N89-13163
LEAST SQUARES METHOD
A GLR (Generalized Likelihood Ratio) algorithm for polyline approximation of waveforms
[AD-A197846] N89-13166
LEAVES
Relationships between the nitrogen content of grass and reflectance N89-13002
LIFE (DURABILITY)
Low-speed flexible rotor balancing for smooth, high-speed operation N89-12628
The durability of adhesive joints: An engineering study
[AD-A197754] N89-12928
Atomic and molecular abundances in comets N89-13376
LIFE SUPPORT SYSTEMS
Research and development of anti-g life support systems. Part 2: Decompression sickness research
[AD-A197675] N89-13133
LIGHT (VISIBLE RADIATION)
The 6th All-Union Conference on Nonlinear Optics (table of contents)
[AD-A197347] N89-13250
Application of PN and avalanche silicon photodiodes to low-level optical N89-13317
LIGHT EMISSION
Optical modeling of clear ocean light fields: Raman scattering effects
[AD-A197249] N89-13129
LIGHT SCATTERING
Correlation studies on surface particle detection methods N89-12587
Topographic effects on light scattering from snow N89-12976
A reference standard for bidirectional reflection distribution function and bidirectional transmission distribution function measurement
[NASA-CASE-MFS-28183-1] N89-13253
An optical heterodyne densitometer N89-13323
Grain optical properties N89-13332
Light scattering of large rough particles application to cometary grains N89-13357
LIGHT SOURCES
Laser applications in flow diagnostics
[AGARD-AG-296] N89-12849
LIGHT TRANSMISSION
Light extinction in a dispersion of small nematic droplets
[AD-A197201] N89-12729
LIMITERS (FUSION REACTORS)
Liquid metal flow in a large-radius elbow with a uniform magnetic fluid
[DE88-016957] N89-12832
LINE SPECTRA
Recent advances at NASA in calculating the electronic spectra of diatomic molecules
[NASA-TM-101034] N89-12622
Overview of recent advances in excimer laser technology at Los Alamos
[DE88-016236] N89-12858
Observations of a complete sample of emission-line galaxies N89-13328
S-waves in the spectrum of cataclysmic binaries N89-13380
LINEAR ACCELERATORS
A radio-frequency quadrupole accelerator longitudinal field stabilizer
[DE88-014399] N89-13246
LINEAR EQUATIONS
On the constrained Chebyshev approximation problem on ellipses
[NASA-CR-183209] N89-13200
The solution of linear systems of equations with a structural analysis code on the NAS CRAY-2
[NASA-CR-4159] N89-13202
LINEAR POLARIZATION
Statistical properties of phase difference between two orthogonally-polarised SAR signals N89-12953
Polarization-dependent attenuation of dielectric cylinder arrays N89-12955
Dual linear polarisation time series as an aid to hydrometeor identification N89-12995
Processing and interpretation of alternately polarised weather radar echoes N89-12996
Examining the polarisation phase retrieval of a dual channel multipolarisation radar N89-13019
LINEAR PROGRAMMING
HLP30: A set of linear programming procedures system manual
[DE88-016571] N89-13169
Global optimization of concave functions subject to separable quadratic constraints and of all-quadratic separable problems
[AD-A197747] N89-13206

LINEARITY
Fracton dynamics on fractal networks
[AD-A197166] N89-12708
LININGS
On 3-D inelastic analysis methods for hot section components N89-12905
Component specific modeling N89-12907
LIQUID CHROMATOGRAPHY
Supercritical fluid chromatography: The effect of the partial molar volume in the stationary phase on retention
[DE88-016959] N89-12699
LIQUID CRYSTALS
Method for laminar boundary layer transition visualization in flight
[NASA-CASE-LAR-13554-1] N89-12551
LIQUID HELIUM
Neutron studies of liquid and solid helium
[DE88-009096] N89-13277
LIQUID METAL COOLED REACTORS
A multimegawatt space power source radiator design
[DE88-015185] N89-12662
LIQUID METALS
Liquid metal flow in a large-radius elbow with a uniform magnetic fluid
[DE88-016957] N89-12832
LIQUID OXYGEN
Support of the eight-foot high-temperature tunnel modifications project
[NASA-CR-183356] N89-12572
Survey of LOX/hydrocarbon combustion and cooling N89-12647
LOX/hydrocarbon combustion and cooling survey N89-12648
Liquid oxygen cooling of high pressure LOX/hydrocarbon rocket thrust chambers N89-12649
LIQUID PHASES
Convective flows in enclosures with vertical temperature or concentration gradients
[NASA-TM-101373] N89-12753
LIQUID PROPELLANT ROCKET ENGINES
Survey of LOX/hydrocarbon combustion and cooling N89-12647
Liquid oxygen cooling of high pressure LOX/hydrocarbon rocket thrust chambers N89-12649
RP-1 and methane combustion and cooling experiments N89-12650
LIQUID ROCKET PROPELLANTS
A steam inerting system for hydrogen disposal for the Vandenberg Shuttle N89-12608
LIQUID SURFACES
Synthesis and characterization of VLS-derived silicon carbide whiskers
[DE88-016226] N89-12679
LIQUIDS
Mass flow measurement of liquid cryogens using the triboelectric effect
[NASA-CR-179519] N89-12837
Tank gauging apparatus and method
[NASA-CASE-MSC-21059-1] N89-12843
LITERATURE
A review of turbomachinery blade-row interaction research
[NASA-CR-182211] N89-12567
LITHIUM
Tm,Ho:YLF laser end-pumped by a semiconductor diode laser array
[NASA-CASE-NPO-17282-1-CU] N89-12856
Preparation and structure of Li-stabilized Na(+) beta' alumina single crystals
[AD-A197245] N89-13283
LITHIUM ALLOYS
Mechanical behavior of superplastically-formed Al-Cu-Li-Zr alloy 2090
[DE88-016241] N89-12714
LITHOGRAPHY
Studies of ultrathin polymer films for lithographic applications
[AD-A197297] N89-12731
LITHOLOGY
Mapping the distribution and abundance of lithological units and surface mineralogies at Jabal Sa'id, Saudi Arabia: An application of spectral mixture modelling N89-13024
LOAD TESTING MACHINES
A high pressure, high temperature hydrogen environment for metals properties testing system N89-12656
LOAD TESTS
Measurement of rotordynamic coefficients for a hydrostatic radial bearing N89-12643
LOADS (FORCES)
Fatigue crack retardation following overloads in Inconel 718, Ti-5Al-2.5Sn, and Haynes 188 N89-12636
Prediction of heat transfer between the combustion space and the load
[DE88-016313] N89-12698
Analysis of the Space Shuttle Orbiter skin panels under simulated hydrodynamic loads
[NASA-TM-4082] N89-12935
LOGIC DESIGN
A logic for belief revision N89-13182
A model for belief revision N89-13183
Belief revision in SNePS N89-13185
LONG WAVE RADIATION
On the interactions of longwave radiation, microphysics and turbulence in boundary layer clouds N89-13109
LONGITUDINAL STABILITY
A radio-frequency quadrupole accelerator longitudinal field stabilizer
[DE88-014399] N89-13246
LORAN C
LORAN C Offshore Flight Following (LOFF) in the Gulf of Mexico
[AD-A197179] N89-12558
LORENTZ FORCE
Investigation of acceleration and densification of electrons utilizing travelling magnetic waves
[AD-A197700] N89-13242
LOSSES
Fire spread in a three-dimensional pressure vessel with radiation exchange and wall heat losses
[AD-A197271] N89-12692
Theoretical studies of mass loss and shock phenomena in cool star envelopes
[NASA-CR-182708] N89-13375
LOW ALTITUDE
Designing simulator tasks to study the high speed, low altitude environment N89-12770
LOW REYNOLDS NUMBER
Development of low Reynolds number two equation turbulence models for predicting external heat transfer on turbine blades N89-12901
LOW SPEED
Low-speed flexible rotor balancing for smooth, high-speed operation N89-12628
LOW TEMPERATURE ENVIRONMENTS
Cost effective alternative to low irradiance measurements N89-12619
LOW TEMPERATURE TESTS
The Instrument Test Dewar (ITD): Testing satellite instruments at 1.5 K N89-12604
LUBRICATION SYSTEMS
Lubrication evaluation of SSME turbopump bearings N89-12639
LUMINANCE
A luminance edge extraction method using gradient of gray level for synthetic aperture radar imageries N89-13086
LUMINOSITY
Monitoring solar-type stars for luminosity variations N89-13321
LUMINOUS INTENSITY
Nonlinear effects in photorefractive crystals
[AD-A197152] N89-13281
LUNAR BASES
Lunar storm shelter conceptual design
[NASA-CR-172078] N89-13141
LUNAR SHELTERS
Lunar storm shelter conceptual design
[NASA-CR-172078] N89-13141
LUNAR SURFACE VEHICLES
Lunar surface transportation systems conceptual design lunar base systems study Task 5.2
[NASA-CR-172077] N89-12862

M

MACH-ZEHNDER INTERFEROMETERS
An optical heterodyne densitometer N89-13323
MACHINE TRANSLATION
A lexical conceptual approach to generation for machine translation
[AD-A197356] N89-13304
MAGNETIC DISTURBANCES
Geomagnetism, a dynamic science
[REPT-37] N89-13309
MAGNETIC FIELDS
LEC (Liquid Encapsulated Czochralski) growth of InP with magnetic field assisted melt stabilization and heat transfer control
[AD-A196748] N89-12688
Liquid metal flow in a large-radius elbow with a uniform magnetic fluid
[DE88-016957] N89-12832
Magnetic attachment mechanism
[NASA-CASE-MSC-21095-1] N89-12866
The development of a near-infrared polarimeter and its application to the continuum polarization of magnetic white dwarfs N89-12924
Generation of the J(sub c), H(sub c), T(sub c) surface for commercial superconductor using reduced-state parameters
[DE88-014038] N89-13278
Properties of stellar activity in F stars N89-13369
MAGNETIC FLUX
C IV fluxes from the Sun as a star, and the correlation with magnetic flux
[NASA-CR-182719] N89-13387
MAGNETIC MEASUREMENT
Tokamak equilibrium determination through function parameterization N89-13272
MAGNETIC MONOPOLES
Solar monopoles and terrestrial neutrinos
[DE88-010677] N89-13388
MAGNETIC SURVEYS
The E-parallel polarization response of a two-dimensional heterogeneous layer modelled by two thin sheets --- electromagnetic geophysical sounding N89-12947
MAGNETITE
Highly magnetic powder
[DE88-010838] N89-12701
MAGNETIZATION
Highly magnetic powder
[DE88-010838] N89-12701
Fracton dynamics on fractal networks
[AD-A197166] N89-12708
The E-parallel polarization response of a two-dimensional heterogeneous layer modelled by two thin sheets --- electromagnetic geophysical sounding N89-12947
MAGNETOHYDRODYNAMIC STABILITY
FOM Contributions to the 15th European Conference on Controlled Fusion and Plasma Heating
[REPT-88-178] N89-13266
The m=1 internal kink mode in a toroidal plasma with a flat q-profile near q=1 N89-13267
Transport code studies of m=2 mode control by local electron cyclotron heating in TFR N89-13270
RF stabilization of external kink modes --- tokamak plasmas N89-13275
MAGNETOHYDRODYNAMICS
Microwave and electron beam computer programs
[AD-A197798] N89-13164
MAIN SEQUENCE STARS
Monitoring solar-type stars for luminosity variations N89-13321
Carbon, nitrogen and oxygen abundances in the chemically peculiar stars of the upper main sequence N89-13379
MAINTENANCE
An expert system for diagnosis and repair of analog circuits N89-12784
A fault diagnosis system based on an integrated knowledge base N89-13181
SNePS considered as a fully intensional propositional semantic network N89-13184
MAN MACHINE SYSTEMS
Voice recognition and artificial intelligence in an air traffic control environment
[AD-A197219] N89-12559
Guidance and Control/Flight Mechanics Panels Joint Symposium on The Man-Machine Interface in Tactical Aircraft Design and Combat Automation
[AGARD-AR-249] N89-12564
The flight robotics laboratory N89-12595
A system to investigate synthesized voice feedback in man-machine interfaces N89-12776
Consequences of individual differences in brain organization for human performance
[AD-A197667] N89-13138
Belief revision in SNePS N89-13185
MAN-COMPUTER INTERFACE
User-computer interface technology: An assessment of the current state of the art
[AD-A196839] N89-13193
MANGANESE ALLOYS
An electron microscopy study of tweed microstructures and premartensitic effects in high damping 53Cu45Mn2Al alloy
[AD-A197317] N89-12709
MANIPULATORS
The flight robotics laboratory N89-12595
Space station erectable manipulator placement system
[NASA-CASE-MSC-21096-1] N89-12621
Improved docking alignment system
[NASA-CASE-MSC-21372-1] N89-12642
Gripping device
[NASA-CASE-MSC-21365-1] N89-12865
Magnetic attachment mechanism
[NASA-CASE-MSC-21095-1] N89-12866

MANPOWER
MANPRINT (Manpower and Personnel Integration Program) primer
[AD-A197681] N89-13296
MANUFACTURING
Automated Airframe Assembly Program (AAAP) survey of CIM status in the aircraft industry
[AD-A197368] N89-12535
Assessment of Japanese variable speed heat pump technology
[DE88-013246] N89-12826
MAPPING
The MEOSS experiment: A test case for future cartographic missions N89-13081
A global analysis and correlation of Nimbus 7 cloud and longwave radiation data
[AD-A197223] N89-13121
Voyeur: Graphical views of parallel programs
[AD-A197103] N89-13177
MARINE ENVIRONMENTS
Multispectral satellite analysis of marine stratocumulus cloud microphysics
[AD-A197316] N89-13092
Arctic oceanography and meteorology review
[AD-A196533] N89-13126
MARINE METEOROLOGY
Radiometric observations of cloud liquid water during FIRE --- First ISCCP Regional Experiment (FIRE) N89-13001
Multispectral satellite analysis of marine stratocumulus cloud microphysics
[AD-A197316] N89-13092
MARKETING
Assessment of Japanese variable speed heat pump technology
[DE88-013246] N89-12826
MARTINGALES
Identifying nonlinear covariate effects in semimartingale regression models
[AD-A197323] N89-13205
MASS
Theoretical studies of mass loss and shock phenomena in cool star envelopes
[NASA-CR-182708] N89-13375
MASS DISTRIBUTION
Mass and heat balances in the upper ocean N89-13089
A possible explanation for the inconsistency between the Giotto grain mass distribution and ground-based observations N89-13364
MASS FLOW
Mass flow meter using the triboelectric effect for measurement in cryogenics
[NASA-CR-179572] N89-12836
Mass flow measurement of liquid cryogens using the triboelectric effect
[NASA-CR-179519] N89-12837
MASS SPECTRA
PIA update: Correlation analyses of mass spectra N89-13334
MASS SPECTROSCOPY
Sample introduction using the Hildebrand grid nebulizer for plasma spectrometry
[AD-A197145] N89-13257
MASS TRANSFER
Physical modeling of bubble phenomena, electrolyte flow and mass transfer in simulated advanced Hall cells
[DE88-015585] N89-12828
Fuel cells: A bibliography
[DE88-001081] N89-13097
Mixing and structural changes during mass transfer in binary systems N89-13382
MASSIVELY PARALLEL PROCESSORS
Some strategies for enhancing the performance of the block Lanczos method
[DE88-014401] N89-13212
MATHEMATICAL MODELS
A vortex panel method for potential flows with applications to dynamics and control
[AD-A197091] N89-12549
Numerical methods for the guidance and control of air-to-air missiles N89-12561
A control-volume method for analysis of unsteady thrust augmenting ejector flows
[NASA-CR-182203] N89-12566
Development of a thermal and structural analysis procedure for cooled radial turbines
[NASA-TM-101416] N89-12568
The solar simulation test of the ITALSAT thermal structural model N89-12613
Efficient transient analysis methods for the Space Shuttle Main Engine (SSME) turbopumps N89-12630
Vibrations induced by nonlinearities in rotordynamics N89-12631
Combustion modeling: Progress and projections N89-12652
The effect of delamination on the response of advanced composite laminates N89-12668
Mixed-mode fracture in fiber-reinforced composite materials N89-12669
Prediction of heat transfer between the combustion space and the load
[DE88-016313] N89-12698
New methods for locating phase boundaries
[DE88-017084] N89-12700
Coble creep, cavity sintering and cavity growth
[DE88-013846] N89-12703
A comparison of propagation model predictions with EPLRS (Enhanced Position Location and Reporting System) UHF network measurements
[AD-A197473] N89-12804
On the effect of R-ratio and Kfmax on fracture toughness measurement, fatigue crack propagation, and fatigue crack closure N89-12875
Aerothermal modeling program, phase 2 N89-12890
Constitutive modeling for isotropic materials N89-12904
On 3-D inelastic analysis methods for hot section components N89-12905
Component specific modeling N89-12907
Thermomechanical characterization of Hastelloy-X under uniaxial cyclic loading N89-12909
Constitutive modeling for single crystal superalloys N89-12911
Constitutive modelling of single crystal and directionally solidified superalloys N89-12912
Life prediction and constitutive models for engine hot section N89-12916
Thermal barrier coating life prediction model development N89-12920
Thermal barrier coating life prediction model N89-12921
Thermal barrier coating life prediction model development N89-12922
Structural response calculations for a metal booster tank model
[DE88-017095] N89-12929
Analysis of the Space Shuttle Orbiter skin panels under simulated hydrodynamic loads
[NASA-TM-4082] N89-12935
Constraints on two-scale descriptions of radar backscattering from the sea surface using scatterometer model functions N89-12945
The E-parallel polarization response of a two-dimensional heterogeneous layer modelled by two thin sheets --- electromagnetic geophysical sounding N89-12947
Modelling of SAR polarisation phase difference from trees N89-12951
The derivation of sub-canopy surface terrain models of coastal forests using synthetic aperture radar N89-13083
The structure of red-infrared scattergrams of semivegetated landscapes
[NASA-CR-183385] N89-13091
Aspects of CFC relative ozone destruction efficiencies determined in the LLNL 2-D model
[DE88-015431] N89-13106
Space-time spectral studies of global stratospheric temperature fields N89-13108
On the interactions of longwave radiation, microphysics and turbulence in boundary layer clouds N89-13109
An analysis of the error characteristics of Atlantic tropical cyclone track prediction models
[AD-A197146] N89-13119
The effect of vertical wind shear on tropical cyclone movement
[AD-A197218] N89-13120
A numerical model for the computation of radiance distributions in natural waters with wind-roughened surfaces
[AD-A197207] N89-13128
Optical modeling of clear ocean light fields: Raman scattering effects
[AD-A197249] N89-13129
Mathematical modelling and computer simulation using Cartesian grid
[TM-AE-8804] N89-13149
Fault diagnosis based on continuous simulation models
[NASA-CR-182737] N89-13152
Parabolic equation model
[AD-A197480] N89-13161
Identifying nonlinear covariate effects in semimartingale regression models
[AD-A197323] N89-13205
Stochastic stage of an inflationary universe model
[DE88-753149] N89-13373
MATRICES (MATHEMATICS)
Co-occurrence matrix modification for small region texture measurement and comparison N89-13064
Use of distance versus statistical distance in acceptance tests
[NASA-CR-183353] N89-13220
MATRIX MATERIALS
Toughening by aligned, frictionally constrained fibers
[AD-A197194] N89-12676
MEASURING INSTRUMENTS
SSME bearing health monitoring using a fiberoptic deflectometer N89-12645
Advanced instrumentation for local measurement of gas-solid suspension flows
[DE88-017087] N89-12833
The standardized Bauer piezoelectric polymer shock gauge
[DE88-014963] N89-12840
Tank gauging apparatus and method
[NASA-CASE-MSC-21059-1] N89-12843
Turbine Engine Hot Section Technology 1986
[NASA-CP-2444] N89-12876
MECHANICAL ENGINEERING
Approximate mobilities of built up structures
[ISVR-TR-162] N89-12934
Engineering applications of heuristic multilevel optimization methods
[NASA-TM-101504] N89-13203
MECHANICAL PROPERTIES
Constitutive behavior of single crystal PWA 1480 and directionally solidified MAR-M 246 under monotonic and cyclic loads at high and low temperature N89-12634
Hydrogen-environment embrittlement and its control in high pressure hydrogen/oxygen rocket engines N89-12654
A high pressure, high temperature hydrogen environment for metals properties testing system N89-12656
Short fiber reinforced thermoplastics N89-12673
SiC whisker-reinforced MoSi2
[DE88-016674] N89-12680
Combined mechanical loading of composite tubes
[NASA-CR-183012] N89-12681
Damage of carbon fiber tubes and rods --- aircraft construction materials
[SARMA-TR-882401] N89-12682
Synthetic polymers as analogs of polysaccharides
[AD-A197842] N89-12738
Research on mechanical properties for engine life prediction
[AD-A197816] N89-12864
Chemical precursors to zinc sulfide: ZnS whisker synthesis
[AD-A197262] N89-13284
MECHANICAL SHOCK
Pyro shock simulation: Experience with the MIPS simulator N89-12593
MELTING
Snowmelt runoff estimation using snow cover extent data and its application to optimum control of dam water level N89-13042
MELTS (CRYSTAL GROWTH)
LEC (Liquid Encapsulated Czochralski) growth of InP with magnetic field assisted melt stabilization and heat transfer control
[AD-A196748] N89-12688
MEMBRANES
Electroporation: Theory of basic mechanisms
[AD-A197391] N89-13130
MEMORY (COMPUTERS)
Achieving speedups for a shared memory model language on an SIMD parallel computer
[AD-A197102] N89-13176
Two alternate proofs of Wang's lune formula for sparse distributed memory and an integral approximation
[NASA-CR-184555] N89-13214
MENTAL PERFORMANCE
Bayesian reasoning tool
[AD-A197351] N89-13196
MERCURY CADMIUM TELLURIDES
Research on mercury cadmium telluride
[AD-A197238] N89-13282
MBE growth, characterization and electronic device processing of HgCdTe, HgZnTe related heterojunctions and HgCdTe-CdTe superlattices
[AD-A197752] N89-13286
MESH
Practical algorithms for image component labeling on SIMD mesh connected computers
[AD-A197341] N89-13158
MESSAGE PROCESSING
Natural language generation
[AD-A197321] N89-12800
Performance studies of dynamic load balancing in distributed systems
[AD-A197130] N89-12926
Optical symbolic processor for expert system execution
[AD-A197668] N89-13252

METAL COATINGS
Comparison of sulfuric and oxalic acid anodizing for preparation of thermal control coatings for spacecraft
N89-12617

METAL FATIGUE
Advanced Earth-to-Orbit Propulsion Technology 1986, volume 2
[NASA-CP-2437-VOL-2] N89-12626
Effects of high mean stress on the high-cycle fatigue of PWA 1480 and DS MAR M 246 + Hf at 1000 F
N89-12633
High-temperature LCF of Ni-201 and 304L stainless steel N89-12635
Rolling contact fatigue life of zirconium and molybdenum nitride sputter plated AMS 5749 bearing steel
N89-12642
Hydrogen effects on the fatigue and tensile behavior of CMSX-2 nickel base superalloy single crystals
N89-12658
LCF and crack growth rate of turbine blade alloys in hydrogen and hydrogen/steam environments
N89-12660
Properties of rapidly solidified aluminum alloys. German-Norwegian Project (1983-1987)
[DFVLR-FB-88-24] N89-12719

METAL FILMS
Thin films from solvated metal atoms and metal-metal bonded compounds
[AD-A197132] N89-12707

METAL FINISHING
Determination of sulfuric acid, oxalic acid, and their matrix effects in aluminum anodizing solutions by ion chromatography
[AD-A197734] N89-12694

METAL IONS
Thin films from solvated metal atoms and metal-metal bonded compounds
[AD-A197132] N89-12707

METAL OXIDES
Determination of sulfuric acid, oxalic acid, and their matrix effects in aluminum anodizing solutions by ion chromatography
[AD-A197734] N89-12694
Transition-metal oxide superconductivity
[AD-A197069] N89-13280

METAL POWDER
Surface structures and transitions and the evolution from firm to bulk behavior
[AD-A197788] N89-12695
Optical constants of minerals and other materials from the millimeter to the ultraviolet
[AD-A197803] N89-12696
Effect of grain size on the high temperature properties of B2 aluminides
[NASA-TM-101382] N89-12720

METAL SHELLS
Structural response calculations for a metal booster tank model
[DE88-017095] N89-12929

METAL SURFACES
Precision cleaning methods for spacecraft applications
N89-12588
Adsorption on metal surfaces
[DE88-016557] N89-12715
Polarimetric microwave scattering from known randomly rough surfaces N89-12949

METAL-GAS SYSTEMS
The determination of mobile hydrogen in aerospace engine alloys N89-12659

METAL-METAL BONDING
Thin films from solvated metal atoms and metal-metal bonded compounds
[AD-A197132] N89-12707

METALLIC GLASSES
Electronic transport properties of the metallic glass Cu sub 100-x Ti sub x
[ETN-88-93231] N89-12718

METALLIZING
Metallization and characterization of a silicon p-n junction diode fabricated from a solar-cell-type silicon substrate
[DE88-703007] N89-13096

METALS
A high pressure, high temperature hydrogen environment for metals properties testing system
N89-12656
Adsorption on metal surfaces
[DE88-016557] N89-12715
Ion beam mixing of metals and ceramics: Material considerations
[DE88-016797] N89-12744

METEORITES
A comparison of Halley dust with meteorites, interplanetary dust and interstellar grains N89-13335

METEOROLOGICAL RADAR
Some advantages of using polarisation diversity illustrated through the analysis of radar data from a storm in central Alberta (Canada) N89-12994
Processing and interpretation of alternately polarised weather radar echoes N89-12996
Design of a spaceborne radar for tropical rain mapping at the climatological scale N89-12997
Cirrus-experiment ICE-1987: Microlidar measurements
[DFVLR-MITT-88-17] N89-13124

METEOROLOGY
Hanford Meteorological Station computer codes. Volume 8: The REVIEW computer code
[DE88-015958] N89-13123

METEOSAT SATELLITE
Advanced workstations for Meteosat command and control, volume 1
[BSO/AETR87030101-VOL-1] N89-12573
Advanced workstations for Meteosat command and control. Volume 2: Appendices
[BSO/AETR87030101-VOL-2] N89-12574

METHANE
RP-1 and methane combustion and cooling experiments N89-12650

MICROCOMPUTERS
The design of antenna matching networks using a microcomputer
[AD-A197364] N89-12802

MICROELECTRONICS
The RACE Program of the European Communities
[ONRL-8-014-R] N89-12811

MICROINSTRUMENTATION
Applications of polysilicon films in microsensors and microactuators
[DE88-016979] N89-12844

MICROMECHANICS
A probabilistic approach to composite micromechanics
[NASA-TM-101366] N89-12684

MICROORGANISMS
Gordon Conference on Microbial Adhesion
[AD-A197352] N89-12735

MICROSTRIP DEVICES
De-embedding S-parameter measurements using TSD technique N89-12783

MICROSTRUCTURE
In-situ oxidation of Ni3Al alloys
[DE88-007177] N89-12702
An electron microscopy study of twseed microstructures and premartensitic effects in high damping 53Cu45Mn2Al alloy
[AD-A197317] N89-12709
As-deposited low-strain LPCVD (Low-Pressure, Chemical-Vapor-Deposition) polysilicon
[DE88-016980] N89-12789
Microstructure and nonlinearity of ZnO varistors, Volume 5, Number 8
[B8735659] N89-13290
On the microstructure theory of a condensate layer in a white dwarf atmosphere
[DE88-703324] N89-13385

MICROWAVE COUPLING
Microwave RF coupling response through adjacent cavities
[DE88-012430] N89-12793

MICROWAVE EMISSION
Microwave emission behavior of snow N89-13041
Polarisation of passive microwave signals as indicator of snow water equivalent N89-13043

MICROWAVE RADIOMETERS
Automatic control of a multi-channel millimeter wave radiometer N89-12938
The airborne radiometry experiment (ABREX) instrument, an experimental test bed for the specification of satellite-borne microwave radiometer at 90 GHz
N89-12939
On the sampling in imaging microwave radiometers
N89-12940
Verification of the accuracy of a network of water-vapor radiometers N89-12941
An algorithm to derive precipitation profiles from a downward viewing radar and a multifrequency passive radiometer N89-12992
Rainfall index over oceans derived from SSM/I data --- Special Sensor Microwave/Imager (SSM/I) N89-12998
Radiometric observations of cloud liquid water during FIRE --- First ISCCP Regional Experiment (FIRE)
N89-13001
Estimation of sea surface temperature via NOAA-AVHRR sensor: Comparison with sea truth data by fixed buoys N89-13005
Improvement in NOAA-AVHRR snowcover determination for runoff prediction N89-13040
Average areal water equivalent of snow in a mountain basin using microwave and visible satellite data
N89-13045

MICROWAVE SCATTERING
Shadows and wedges in scattering from the sea
N89-12946
Polarimetric microwave scattering from known randomly rough surfaces N89-12949
Scattering behavior of a three-axial ellipsoid
N89-13011
Some characteristics of short ocean waves as microwave scatterers N89-13030
Millimeter-wave backscatter measurements of various snow forms N89-13046

MICROWAVE SOUNDING
Proposed design of the temperature control system for the variable temperature calibration target for the Advanced Microwave Sounding Unit B N89-12942
Precipitation detection with satellite microwave data
[PB88-240239] N89-13094

MIE SCATTERING
Multispectral satellite analysis of marine stratocumulus cloud microphysics
[AD-A197316] N89-13092

MILITARY HELICOPTERS
AH-1F Instrument Meteorological Conditions (IMC) flight evaluations
[AD-A197128] N89-12562

MILITARY OPERATIONS
SP-100 nuclear space power systems with application to space commercialization
[NASA-TM-101403] N89-12665
Wave propagation in layered structures N89-12777
Applications of parallelism to current algorithms for intelligence analysis
[NASA-CR-183351] N89-13165

MILLING
Highly magnetic powder
[DE88-010838] N89-12701

MINERAL EXPLORATION
A regional tectonic study of NE and E Africa and its implication for mineral exploration: A synoptic view from satellite imagery N89-13023

MINERALS
Optical constants of minerals and other materials from the millimeter to the ultraviolet
[AD-A197803] N89-12696

MINIATURIZATION
Micro heat pipes
[DE88-016113] N89-13100

MIRRORS
Correlation studies on surface particle detection methods N89-12587

MISSILE CONTROL
Numerical methods for the guidance and control of air-to-air missiles N89-12561

MISSILE DETECTION
Adaptive machine vision
[AD-A197039] N89-13222

MISSILE TRACKING
Temporal clustering in the multi-target tracking environment
[AD-A197153] N89-12796

MISSION PLANNING
SP-100 nuclear space power systems with application to space commercialization
[NASA-TM-101403] N89-12665
Radioisotope space power generators: Design concepts N89-13224
Down scale of the SP-100 concept for 5 kWe
N89-13225

MIXED CRYSTALS
Nonlinear effects in photorefractive crystals
[AD-A197152] N89-13281

MIXING
A two-dimensional numerical simulation of a supersonic, chemically reacting mixing layer
[NASA-TM-4055] N89-12542
Ion beam mixing of metals and ceramics: Material considerations
[DE88-016797] N89-12744

MIXTURES
Thermal properties of heterogeneous grains
N89-13358

MODELS
Report on JANNAF Workshop Influence of Gas-Phase Chemical Kinetics on Low-Pressure Ignition and Flamespreading in Solid Propellant
[AD-A197854] N89-12751
Auditory models for speech analysis
[AD-A197322] N89-12801
EMP (electromagnetic pulse) mitigation program approach
[AD-A197849] N89-12807
Software process modeling
[AD-A197137] N89-13154
Microwave and electron beam computer programs
[AD-A197798] N89-13164

Optimal fix estimators and a variation on the Cramer Rao lower bound
[NASA-CR-183011] N89-13211
Transition-metal oxide superconductivity
[AD-A197069] N89-13280

MODES
Mode extraction from an electromagnetic slow wave system N89-12767

MODULES
Design document for GCS version
[NASA-CR-183278] N89-13150

MOISTURE
Moisture interaction and stability of ZOT (Zinc Orthotitanate) thermal control spacecraft coating N89-12618
Moisture adsorption in optical coatings N89-13327

MOISTURE CONTENT
Radiometric observations of cloud liquid water during FIRE — First ISCCP Regional Experiment (FIRE) N89-13001
Polarisation of passive microwave signals as indicator of snow water equivalent N89-13043
Average areal water equivalent of snow in a mountain basin using microwave and visible satellite data N89-13045

MOISTURE METERS
Laboratory evaluation of a field portable dielectric/soil moisture probe N89-13006

MOLECULAR BEAM EPITAXY
MBE growth, characterization and electronic device processing of HgCdTe, HgZnTe related heterojunctions and HgCdTe-CdTe superlattices
[AD-A197752] N89-13286

MOLECULAR BIOLOGY
Gordon Conference on Microbial Adhesion
[AD-A197352] N89-12735

MOLECULAR INTERACTIONS
Gordon Conference on Microbial Adhesion
[AD-A197352] N89-12735

MOLECULAR OSCILLATIONS
Determination of stepsize parameters for intermolecular vibrational energy transfer
[DE88-010904] N89-13239

MOLECULAR SPECTRA
Recent advances at NASA in calculating the electronic spectra of diatomic molecules
[NASA-TM-101034] N89-12622

MOLECULAR STRUCTURE
Gordon Conference on Microbial Adhesion
[AD-A197352] N89-12735
Influence of side-groups on thermotropic behavior of polyorganophosphazenes
[AD-A197852] N89-12740
Aromatic components in cometary materials N89-13337
Possible identifications of the 3.4 micrometer feature N89-13342
Detection of parent molecules in the IR spectrum of P/Halley with the IKS-Vega spectrometer N89-13352

MOLECULES
WF/PC internal molecular contamination during system thermal-vacuum test N89-12583
Wide Field/Planetary Camera (WF/PC) contamination control assessment N89-12584

MOLTEN SALTS
Phase 2 testing of a molten salt central receiver
[DE88-012701] N89-13095

MOLYBDENUM
Heat pipe cooling system with sensible heat sink N89-12615
SiC whisker-reinforced MoSi2
[DE88-016674] N89-12680

MOLYBDENUM DISULFIDES
Boric oxide as a solid lubricant additive in molybdenum disulfide
[AD-A197109] N89-12727

MONTE CARLO METHOD
Quantum Monte Carlo calculation of the properties of atomic carbon and diamond
[DE88-014659] N89-12686
Direct simulation of three-dimensional flow about the AFE vehicle at high altitudes
[NASA-TM-101492] N89-12834
Atomic and molecular abundances in comets N89-13376
The transfer of cyclotron photons through neutron star atamospheres N89-13378

MORPHOLOGY
In-situ high temperature oxidation studies
[DE88-017092] N89-12716
Influence of side-groups on thermotropic behavior of polyorganophosphazenes
[AD-A197852] N89-12740
Physical modeling of bubble phenomena, electrolyte flow and mass transfer in simulated advanced Hall cells
[DE88-015585] N89-12828
Towards an urban land-use classification using textural and morphological criteria N89-12987

MOTION SIMULATORS
Space station docking mechanism dynamic testing N89-12596
Development of a two axis motion simulation system for thermal/vacuum satellite testing N89-12598
The two axis motion simulator for the large space simulator at ESTEC (European Space Research and Technology Center) N89-12600
Solar simulation with a rectangular beam N89-12605

MOVING TARGET INDICATORS
Micro-computer network architecture for range instrumentation applications
[AD-A196971] N89-13175

MULTIPLEXING
The RACE Program of the European Communities
[ONRL-8-014-R] N89-12811

MULTIPROCESSING (COMPUTERS)
Performance analysis of the Alliant FX/8 multiprocessor using statistical clustering
[NASA-CR-183221] N89-13145
Practical issues relating to the internal database predicates in an OR-parallel prolog: Extensions and useful hacks
[DE88-010019] N89-13174

MULTISPECTRAL BAND SCANNERS
The relativity utility of LANDSAT MSS and SIR-A imagery in reconnaissance geological mapping in Northern Sudan N89-13022
The interpretation of Icelandic tundra features from LANDSAT-MSS data N89-13027
Photogrammetric model for correction of MSS-LANDSAT imagery
[INPE-4652-PRE/1359] N89-13090

MULTISPECTRAL PHOTOGRAPHY
PIPS: A Procedure for Interactive Pyramid Segmentation N89-12984
Efficient classification of multispectral images by a best linear discriminant function N89-13060

MULTISTATIC RADAR
Attenuation and scattering measurements from dense media — radar N89-13012
Bistatic frequency diverse imaging of complex scattering targets N89-13013
Multistatic scatterometry N89-13072

MULTIVARIATE STATISTICAL ANALYSIS
Multivariate regression with emphasis on multivariate spline methods
[AD-A197793] N89-13209
Wavelength or sensor selection by minimization of prediction error
[AD-A197231] N89-13216

N

NAP-OF-THE-EARTH NAVIGATION
Design and numerical evaluation of full-authority flight control systems for conventional and thruster-augmented helicopters employed in NOE operations
[NASA-CR-183311] N89-12570

NASA PROGRAMS
Research and technology
[NASA-TM-100051] N89-13393

NASA SPACE PROGRAMS
Geodynamics laser ranging system: Performance simulations and development of the EOS facility — Earth Observing System (EOS) N89-12982

NATURAL GAS
Development of Alaskan gas hydrate resources
[DE88-010270] N89-13093

NATURAL LANGUAGE (COMPUTERS)
Natural language generation
[AD-A197321] N89-12800
The processing of qualitative information in a natural language context N89-13297

NAVIER-STOKES EQUATION
Simulation of 2-dimensional viscous flow through cascades using a semi-elliptic analysis and hybrid C-H grids
[NASA-CR-4180] N89-12553
Evaluation of three turbulence models for the prediction of steady and unsteady airloads
[NASA-TM-101413] N89-12555
Perturbed functional iteration applied to the Navier-Stokes equations N89-12774
Turbine stator flow field simulations N89-12902

NAVIGATION
Pilot factors guidelines for the operational inspection of navigation systems
[NASA-CR-181644] N89-12557

NEAR INFRARED RADIATION
The development of a near-infrared polarimeter and its application to the continuum polarization of magnetic white dwarfs N89-12924
The near-infrared polarization and color of Comet Halley: What can we learn about the grains N89-13348

NEODYMIUM LASERS
High power Nd:glass lasers as drivers for inertial confinement fusion
[DE88-017016] N89-12860

NEURAL NETS
Exploring the back-propagation network for speech applications
[AD-A197385] N89-12803
European Seminar on Neural Computing
[ONRL-8-010-C] N89-13173
Neural network performance on the stochastic exclusive-or problem
[AD-A197789] N89-13179
Optical computing based on neuronal models
[AD-A197749] N89-13199

NEUTRAL PARTICLES
Soviet exoatmospheric neutral particle beam research
[FASAC-TAR-3110] N89-13390

NEUTRON ABSORBERS
Neutron flux measurements in the Gran Sasso Underground Laboratory (Italy) (part 2)
[IFSI-88-7] N89-13243

NEUTRON COUNTERS
Neutron flux measurements in the Gran Sasso Underground Laboratory (Italy) (part 2)
[IFSI-88-7] N89-13243

NEUTRON FLUX DENSITY
Solar monopoles and terrestrial neutrinos
[DE88-010677] N89-13388

NEUTRON SCATTERING
Neutron studies of liquid and solid helium
[DE88-009096] N89-13277

NEUTRON STARS
The transfer of cyclotron photons through neutron star atamospheres N89-13378

NEW ZEALAND
Australian preparations for the Polar Platform N89-12979

NEWTON-RAPHSON METHOD
Multidimensional item response theory estimation: A computer program
[AD-A197160] N89-13155

NICKEL
High-temperature LCF of Ni-201 and 304L stainless steel N89-12635
Metallization and characterization of a silicon p-n junction diode fabricated from a solar-cell-type silicon substrate
[DE88-703007] N89-13096

NICKEL ALLOYS
Simplified cyclic structural analysis of SSME turbine blades N89-12632
Effects of high mean stress on the high-cycle fatigue of PWA 1480 and DS MAR M 246 + Hf at 1000 F N89-12633
Constitutive behavior of single crystal PWA 1480 and directionally solidified MAR-M 246 under monotonic and cyclic loads at high and low temperature N89-12634
Fatigue crack retardation following overloads in Inconel 718, Ti-5Al-2.5Sn, and Haynes 188 N89-12636
Hydrogen effects on the fatigue and tensile behavior of CMSX-2 nickel base superalloy single crystals N89-12658
LCF and crack growth rate of turbine blade alloys in hydrogen and hydrogen/steam environments N89-12660
The development of a hydrogen resistant alloy N89-12661
In-situ oxidation of Ni3Al alloys
[DE88-007177] N89-12702
Fundamental understanding of the intrinsic ductility in nickel-base L12 type alloys
[AD-A197605] N89-12711
Constitutive modeling for isotropic materials N89-12904

NIMBUS 7 SATELLITE
A global analysis and correlation of Nimbus 7 cloud and longwave radiation data
[AD-A197223] N89-13121

NIOBIUM
High T(sub c) superconductors: Will they replace helium temperature superconductors for magnets
[DE88-016632] N89-13279

NIOBIUM ALLOYS
Influence of alloying elements on the oxidation behavior of NbAl3
[NASA-TM-101398] N89-12717

NIOBIUM COMPOUNDS
Generation of the J(sub c), H(sub c), T(sub c) surface for commercial superconductor using reduced-state parameters
[DE88-014038] N89-13278

NITRIC OXIDE
Directed motion Doppler shift effects on nitric oxide (0,0) gamma band resonance absorption N89-12760

NITROGEN
Relationships between the nitrogen content of grass and reflectance N89-13002
NOAA SATELLITES
Estimation of sea surface temperature via NOAA-AVHRR sensor: Comparison with sea truth data by fixed buoys N89-13005
Improvement in NOAA-AVHRR snowcover determination for runoff prediction N89-13040
NOISE
Fitting functions to noisy data in high dimensions [DE88-015922] N89-13213
NOISE INTENSITY
Use of proximity effect in hearing aid microphones to increase telephone intelligibility in noise [AD-A197311] N89-12799
NOISE PREDICTION
On the simulation of harmonically related signals [AD-A197821] N89-13235
NOISE REDUCTION
Ground run-up afterburner detection and noise suppression N89-12768
A study of active control techniques for noise reduction in an aircraft fuselage model N89-13232
NOISE SPECTRA
The effects of high noise levels on the acoustic-phonetic structure of speech: A preliminary investigation N89-12764
NONDESTRUCTIVE TESTS
Shock detection in composite structures. Test report 48-915/F — Impact damage [REPT-48-915/F] N89-12683
Laser dynamic photoelasticity and digital image analysis for nondestructive evaluation of surface and near surface flaws through ultrasonic spectroscopy N89-12871
Composite curing process nondestructive evaluation [AD-A197834] N89-12873
Characterization of adhesively bonded joints using acousto-ultrasonics N89-12925
Surfaces and thin films studied by picosecond ultrasonics [DE88-015268] N89-13233
NONEQUILIBRIUM PLASMAS
Nonequilibrium effects in thermal plasmas: Radiation transport and chemical reactivity [DE88-016841] N89-13262
Nonequilibrium effects in thermal plasma chemistry [DE88-016842] N89-13263
Interaction of impurity ions with a weakly non-Maxwellian simple hydrogenic plasma [DE88-017137] N89-13265
NONEQUILIBRIUM THERMODYNAMICS
Population inversion non-equilibrium flow simulation calculations of the capabilities of convection flow lasers [AD-A197741] N89-12854
NONLINEAR EQUATIONS
Nonlinear perturbations of differential operators with nontrivial kernel and applications to third order periodic boundary value problems [DE88-702991] N89-13201
NONLINEAR OPTICS
Investigation of laser diode coupling using nonlinear optics N89-12781
The 6th All-Union Conference on Nonlinear Optics (table of contents) [AD-A197347] N89-13250
NONLINEAR PROGRAMMING
Algorithms for bound constrained quadratic programming problems [DE88-016470] N89-13168
NONLINEAR SYSTEMS
Fracton dynamics on fractal networks [AD-A197166] N89-12708
Identifying nonlinear covariate effects in semimartingale regression models [AD-A197323] N89-13205
Nonlinear effects in photorefractive crystals [AD-A197152] N89-13281
NONLINEARITY
Vibrations induced by nonlinearities in rotordynamics N89-12631
Simplified cyclic structural analysis of SSME turbine blades N89-12632
SAR-seen multimode waves in ice: Evidence of imaging nonlinearities N89-12971
Microstructure and nonlinearity of ZnO varistors, Volume 5, Number 8 [B8735659] N89-13290
NONOSCILLATORY ACTION
An artificial compression method for ENO schemes: The slope modification method [NASA-CR-184613] N89-13215
NONPARAMETRIC STATISTICS
Two-sample inference for median survival times based on one-sample procedures for censored survival data [AD-A197776] N89-13218
NORMAL DENSITY FUNCTIONS
Optimal fix estimators and a variation on the Cramer Rao lower bound [NASA-CR-183011] N89-13211
Stochastic calculus and survival analysis [AD-A197324] N89-13217
NORMALITY
Bearing error and the central limit theorem [NASA-CR-183009] N89-13219
NORTH ATLANTIC TREATY ORGANIZATION (NATO)
AGARD handbook N89-13392
NOVA LASER SYSTEM
High power Nd:glass lasers as drivers for inertial confinement fusion [DE88-017016] N89-12860
NOZZLE GEOMETRY
High-temperature LCF of Ni-201 and 304L stainless steel N89-12635
NUCLEAR EXPLOSIONS
Worldwide deposition of Sr-90 through 1985 [DE88-015577] N89-13105
NUCLEAR FUEL ELEMENTS
Preliminary thermal analysis of a bimodal nuclear rocket core N89-12758
NUCLEAR FUSION
Nuclear technology for the year 2000 [DE88-005041] N89-13223
NUCLEAR POWER PLANTS
Fire aerosol experiment and comparisons with computer code predictions [DE88-016328] N89-12768
NUCLEAR REACTORS
Liquid metal flow in a large-radius elbow with a uniform magnetic fluid [DE88-016957] N89-12832
Down scale of the SP-100 concept for 5 kWe N89-13225
Evaluation of boron carbide coatings N89-13228
NUCLEAR ROCKET ENGINES
Preliminary thermal analysis of a bimodal nuclear rocket core N89-12758
NUMERICAL ANALYSIS
The laminar boundary layer on an airfoil started impulsively from rest N89-12540
A two-dimensional numerical simulation of a supersonic, chemically reacting mixing layer [NASA-TM-4055] N89-12542
Focal region fields of distorted reflectors [NASA-CR-183001] N89-12810
HOST combustion R and T overview N89-12879
Fundamentals of middle-atmospheric dynamics [AD-A197358] N89-13110
A numerical model for the computation of radiance distributions in natural waters with wind-roughened surfaces [AD-A197207] N89-13128
A GLR (Generalized Likelihood Ratio) algorithm for polyline approximation of waveforms [AD-A197846] N89-13166
NUMERICAL CONTROL
Phase 2 testing of a molten salt central receiver [DE88-012701] N89-13095
Efficient use of bit planes in the generation of motion stimuli [NASA-TM-101022] N89-13171
NUMERICAL INTEGRATION
Numerical integration of influence coefficients for panel methods about axisymmetric bodies by means of the ROMBERG algorithm [DFVLR-MITT-88-18] N89-12839
NUMERICAL WEATHER FORECASTING
Towards direct variational assimilation of scatterometer backscatter measurements into numerical weather prediction models N89-13000
NUTRIENTS
The effects of hyperbaric oxygen and antioxidant deficiencies on rat retinal ultrastructure N89-12772

O

OBSERVATORIES
LIGO vacuum system study N89-12599
OCEAN DATA ACQUISITIONS SYSTEMS
An intercomparison of SAR and buoy directional wave spectra from the Labrador Sea Extreme Waves Experiment (LEWEX) N89-12972
Directional ocean wave spectra: Prospects for acquiring a global data base from SIR-C N89-12973
The Labrador Sea Extreme Waves Experiment: Objectives, status and plans N89-12974
OCEAN MODELS
Mass and heat balances in the upper ocean N89-13089
OCEAN SURFACE
Constraints on two-scale descriptions of radar backscattering from the sea surface using scatterometer model functions N89-12945
Shadows and wedges in scattering from the sea N89-12946
Scattering from a skewed random surface — radar scattering N89-12948
Spectral analysis of ocean wave imagery using 2-D linear prediction N89-12958
On the use of speckle statistics for the extraction of ocean wave spectra from SAR imagery N89-12969
Ocean wave number spectra and spatial autocorrelation functions from SAR images N89-12970
Some characteristics of short ocean waves as microwave scatterers N89-13030
Modulation of the radar backscatter from the ocean surface by a long gravity wave N89-13031
Estimating aircraft SAR response characteristics and approximating ocean wave spectra in the Labrador Sea N89-13032
OCEANOGRAPHIC PARAMETERS
The Labrador Sea Extreme Waves Experiment: Objectives, status and plans N89-12974
Model-based estimation of wind fields over the ocean from wind scatterometer measurements N89-13070
Performance of a scanning pencil-beam spaceborne scatterometer for ocean wind measurements N89-13073
OCEANOGRAPHY
Arctic oceanography and meteorology review [AD-A196533] N89-13126
OCEANS
Rainfall index over oceans derived from SSM/I data — Special Sensor Microwave/Imager (SSM/I) N89-12998
Production of probability of precipitation maps over oceanic areas from automated cloud classification N89-12999
OIL EXPLORATION
Environmental management practices in oil refineries and terminals: An overview [ISBN-92-807-1108-3] N89-13104
ON-LINE SYSTEMS
Providing on-line guidance to computer users N89-12766
OPERATING TEMPERATURE
Turbine Engine Hot Section Technology (HOST) Project N89-12877
OPTICAL COMPUTERS
Optical computing based on neuronal models [AD-A197749] N89-13199
Optical symbolic processor for expert system execution [AD-A197668] N89-13252
OPTICAL COUPLING
Nonlinear effects in photorefractive crystals [AD-A197152] N89-13281
OPTICAL DATA PROCESSING
Optical symbolic processor for expert system execution [AD-A197668] N89-13252
OPTICAL EQUIPMENT
Correlation studies on surface particle detection methods N89-12587
Moisture adsorption in optical coatings N89-13327
OPTICAL MATERIALS
Optical constants of minerals and other materials from the millimeter to the ultraviolet [AD-A197803] N89-12696
OPTICAL MEASUREMENT
Development of a computer-controlled technique to determine crack growth rate properties in controlled environments using crack opening displacement N89-12657
Application of PN and avalanche silicon photodiodes to low-level optical N89-13317
OPTICAL MEASURING INSTRUMENTS
An optical sensor system for monitoring structural dynamics with applications to system identification N89-12775
An optical heterodyne densitometer N89-13323
OPTICAL POLARIZATION
The near-infrared polarization and color of Comet Halley: What can we learn about the grains N89-13348
Polarization images of Comet Halley N89-13351
OPTICAL PROPERTIES
Microwave characteristics of interdigitated photoconductors on a HEMT structure [NASA-CR-182197] N89-12820
Optical modeling of clear ocean light fields: Raman scattering effects [AD-A197249] N89-13129
The 6th All-Union Conference on Nonlinear Optics (table of contents) [AD-A197347] N89-13250

Re-evaluation of an improved efficiency polymeric web point-focus Fresnel lens
[DE88-016892] N89-13255
Optical and electrical measurements on UV sensitive photodiodes N89-13316
Grain optical properties N89-13332

OPTICAL RADAR
Rayleigh lidar observations of gravity wave activity in the upper stratosphere at Urbana, Ill.
[NASA-CR-182738] N89-13107
Backscatter laser depolarization studies of simulated stratospheric aerosols: Crystallized sulfuric acid droplets
[NASA-CR-183387] N89-13111
Cirrus-experiment ICE-1987: Microlidar measurements
[DFVLR-MITT-88-17] N89-13124

OPTICAL SWITCHING
The RACE Program of the European Communities
[ONRL-8-014-R] N89-12811

OPTIMAL CONTROL
Trajectory optimization and guidance law development for national aerospace plane applications
[NASA-CR-182994] N89-12538
Singular perturbations and time scales in the design of digital flight control systems
[NASA-TP-2844] N89-12569

OPTIMIZATION
The optimal polarizations for achieving maximum contrast in radar images
[NASA-CR-183349] N89-12794
Algorithms for bound constrained quadratic programming problems
[DE88-016470] N89-13168
Engineering applications of heuristic multilevel optimization methods
[NASA-TM-101504] N89-13203
Global optimization of concave functions subject to separable quadratic constraints and of all-quadratic separable problems
[AD-A197747] N89-13206
Optimal fix estimators and a variation on the Cramer Rao lower bound
[NASA-CR-183011] N89-13211
Optimizing current drive by electron cyclotron waves in the presence of trapped particles N89-13276

ORBIT MANEUVERING ENGINE (SPACE SHUTTLE)
High-temperature LCF of Ni-201 and 304L stainless steel N89-12635

ORBITAL MECHANICS
Results of true-anomaly regularization in orbital mechanics N89-12577

ORBITAL SERVICING
On-orbit servicing and cost effectiveness of Columbus Polar Platform concepts N89-12983

ORGANIC MATERIALS
Thin films from solvated metal atoms and metal-metal bonded compounds
[AD-A197132] N89-12707
A two component model for thermal emission from organic grains in Comet Halley N89-13340

ORGANIC SEMICONDUCTORS
The 6th All-Union Conference on Nonlinear Optics (table of contents)
[AD-A197347] N89-13250

ORTHOGONALITY
Fire spread in a three-dimensional pressure vessel with radiation exchange and wall heat losses
[AD-A197271] N89-12692
Statistical properties of phase difference between two orthogonally-polarised SAR signals N89-12953

ORTHOSTATIC TOLERANCE
Alterations of segmental volume during orthostatic stress in nonhuman primates N89-12769

ORTHOTROPIC PLATES
Mixed-mode fracture in fiber-reinforced composite materials N89-12669

OSCILLATIONS
A review of turbomachinery blade-row interaction research
[NASA-CR-182211] N89-12567
Stabilization and oscillation of an acoustically levitated object
[NASA-CASE-NPO-16896-1-CU] N89-13236
Toroidal studies of sawtooth oscillations in tokamaks
[DE88-017115] N89-13264

OSMOSIS
Electroporation: Theory of basic mechanisms
[AD-A197391] N89-13130

OUTCROPS
LANDSAT Thematic Mapping (TM) and SPOT HRV for survey mapping of bedrock outcrops N89-13055

OUTGASSING
Wide Field/Planetary Camera (WF/PC) contamination control assessment N89-12584

OUTPUT
Multiple input/output random vibration control system N89-12594

OVER-THE-HORIZON RADAR
Modeling and performance of HF/OTH (High-Frequency/Over-The-Horizon) radar target identification systems
[AD-A197850] N89-12808

OXALIC ACID
Comparison of sulfuric and oxalic acid anodizing for preparation of thermal control coatings for spacecraft N89-12617
Determination of sulfuric acid, oxalic acid, and their matrix effects in aluminum anodizing solutions by ion chromatography
[AD-A197734] N89-12694

OXIDATION
In-situ oxidation of Ni3Al alloys
[DE88-007177] N89-12702
In-situ high temperature oxidation studies
[DE88-017092] N89-12716
Grain boundary oxidation and its effects on high temperature fatigue life N89-12918
A study on thermal barrier coatings including thermal expansion mismatch and bond coat oxidation N89-12919

OXIDATION RESISTANCE
Influence of alloying elements on the oxidation behavior of NbAl3
[NASA-TM-101398] N89-12717

OXIDATION-REDUCTION REACTIONS
Charge transfer in multiple site chemical systems
[AD-A197143] N89-12666
Electronic and ionic transport in polymers
[AD-A197142] N89-12728

OXYGEN
The NASA atomic oxygen effects test program N89-12589
Materials selection for long life in LEO: A critical evaluation of atomic oxygen testing with thermal atom systems N89-12590
Atomic oxygen studies on polymers N89-12591
Atomic oxygen effects on candidate coatings for long-term spacecraft in low earth orbit N89-12592
The effects of hyperbaric oxygen and antioxidant deficiencies on rat retinal ultrastructure N89-12772

OZONE
Aspects of CFC relative ozone destruction efficiencies determined in the LLNL 2-D model
[DE88-015431] N89-13106

OZONE DEPLETION
Aspects of CFC relative ozone destruction efficiencies determined in the LLNL 2-D model
[DE88-015431] N89-13106

P

P-I-N JUNCTIONS
Preparation and properties of high-deposition-rate a-Si:H films and solar cells using disilane
[DE88-001191] N89-13098

P-N JUNCTIONS
Metallization and characterization of a silicon p-n junction diode fabricated from a solar-cell-type silicon substrate
[DE88-703007] N89-13096

PADE APPROXIMATION
Dynamic synthesis of joined/hermetic shell structures using state space method N89-12874

PAINTS
Requirements and test results for the qualification of thermal control coatings N89-12616
Moisture interaction and stability of ZOT (Zinc Orthotitanate) thermal control spacecraft coating N89-12618

PANEL METHOD (FLUID DYNAMICS)
A vortex panel method for potential flows with applications to dynamics and control
[AD-A197091] N89-12549
Development and validation of an advanced low-order panel method
[NASA-TM-101024] N89-12554
A numerical method for computing unsteady 2-D boundary layer flows
[NASA-CR-4198] N89-12835
Numerical integration of influence coefficients for panel methods about axisymmetric bodies by means of the ROMBERG algorithm
[DFVLR-MITT-88-18] N89-12839

PANELS
Truss-core corrugation for compressive loads
[NASA-CASE-LAR-13438-1] N89-12786
Prediction of stresses in aircraft panels subjected to acoustic forces
[NASA-CR-182513] N89-12923

PARABOLIC ANTENNAS
Laser speckle from thin and cascaded diffusers
[AD-A197066] N89-12850

PARABOLIC DIFFERENTIAL EQUATIONS
Parabolic equation model
[AD-A197480] N89-13161

PARABOLIC REFLECTORS
Focal region fields of distorted reflectors
[NASA-CR-183001] N89-12810

PARACHUTE DESCENT
Automatic release mechanism for the EL 32 bag --- parachutes
[E-768] N89-12863

PARACHUTES
Flow field characteristics around bluff parachute canopies N89-12546
Remote guidance of payloads under maneuverable parachutes
[E-639] N89-12571

PARALLEL COMPUTERS
Achieving speedups for a shared memory model language on an SIMD parallel computer
[AD-A197102] N89-13176
Voyeur: Graphical views of parallel programs
[AD-A197103] N89-13177

PARALLEL FLOW
Parallel algorithms in the finite element approximation of flow problems
[AD-A197454] N89-13178

PARALLEL PROCESSING (COMPUTERS)
Practical algorithms for image component labeling on SIMD mesh connected computers
[AD-A197341] N89-13158
Applications of parallelism to current algorithms for intelligence analysis
[NASA-CR-183351] N89-13165
European Seminar on Neural Computing
[ONRL-8-010-C] N89-13173
Practical issues relating to the internal database predicates in an OR-parallel prolog: Extensions and useful hacks
[DE88-010019] N89-13174
Parallel algorithms in the finite element approximation of flow problems
[AD-A197454] N89-13178

PARALLEL PROGRAMMING
Parallel debugging using graphical views
[AD-A197197] N89-13156

PARAMETER IDENTIFICATION
Tokamak equilibrium determination through function parameterization N89-13272

PARAMETERIZATION
Multidimensional item response theory estimation: A computer program
[AD-A197160] N89-13155

PARTIAL DIFFERENTIAL EQUATIONS
Parallel algorithms in the finite element approximation of flow problems
[AD-A197454] N89-13178
An adaptive method with mesh moving and local mesh refinement for time-dependent partial differential equations
[AD-A197772] N89-13208

PARTICLE ACCELERATORS
Comments on the high frequency behavior of the coupling of an accelerator beam to its environment
[CEBAF-PR-88-006] N89-13245

PARTICLE BEAMS
Microwave and electron beam computer programs
[AD-A197798] N89-13164
Soviet exoatmospheric neutral particle beam research
[FASAC-TAR-3110] N89-13390

PARTICLE COLLISIONS
Determination of stepsize parameters for intermolecular vibrational energy transfer
[DE88-010904] N89-13239

PARTICLE MASS
PIA update: Correlation analyses of mass spectra N89-13334

PARTICLE PRODUCTION
Thin films from solvated metal atoms and metal-metal bonded compounds
[AD-A197132] N89-12707

PARTICLE SIZE DISTRIBUTION
Correlation studies on surface particle detection methods N89-12587
Highly magnetic powder
[DE88-010838] N89-12701
Investigations into the plasma spray process
[DE88-014524] N89-12787
Advanced instrumentation for local measurement of gas-solid suspension flows
[DE88-017087] N89-12833
Performance of the forward scattering spectrometer probe in NASA's icing research tunnel
[NASA-TM-101381] N89-12845
Cometary dust size distributions from flyby spacecraft N89-13350

On the microstructure theory of a condensate layer in a white dwarf atmosphere
[DE88-703324] N89-13385
PARTICLE TRACKS
Holographic particle detection
[NASA-CR-183315] N89-13240
PARTICULATES
Fire aerosol experiment and comparisons with computer code predictions
[DE88-016328] N89-12788
PATHOGENS
Gordon Conference on Microbial Adhesion
[AD-A197352] N89-12735
PATTERN RECOGNITION
Efficient classification of multispectral images by a best linear discriminant function N89-13060
Lapwing: A trainable spatial feature recognition system N89-13063
A luminance edge extraction method using gradient of gray level for synthetic aperture radar imageries N89-13086
Adaptive machine vision
[AD-A197039] N89-13222
PAYLOADS
Remote guidance of payloads under maneuverable parachutes
[E-639] N89-12571
The separation test in vacuum of the Ariane 4 payload fairing N89-12612
PECULIAR STARS
Carbon, nitrogen and oxygen abundances in the chemically peculiar stars of the upper main sequence N89-13379
PENCIL BEAMS
Performance of a scanning pencil-beam spaceborne scatterometer for ocean wind measurements N89-13073
PENETRATION
On the resistance of ceramics to high velocity penetration
[AD-A197320] N89-12734
PERCEPTION
Preattentive and attentive visual information processing
[AD-A197670] N89-13139
Efficient use of bit planes in the generation of motion stimuli
[NASA-TM-101022] N89-13171
PERFORMANCE PREDICTION
Damping seal tester progress and initial test results N89-12627
Efficient transient analysis methods for the Space Shuttle Main Engine (SSME) turbopumps N89-12630
Stability limits and combustion measurements in low calorific value gas flames N89-12687
A computer simulation of a plasma armature railgun N89-12780
Modeling and performance of HF/OTH (High-Frequency/Over-The-Horizon) radar target identification systems
[AD-A197850] N89-12808
Research on mechanical properties for engine life prediction
[AD-A197816] N89-12864
HOST surface protection R and T overview N89-12883
PERFORMANCE TESTS
A vortex panel method for potential flows with applications to dynamics and control
[AD-A197091] N89-12549
Test data acquisition system for the ESTEC large solar simulator at ESA/ESTEC N89-12620
Measurement of rotordynamic coefficients for a hydrostatic radial bearing N89-12643
Combined pressure-shear ignition sensitivity test
[AD-A197076] N89-12749
Properties of JP-8 jet fuel
[AD-A197270] N89-12750
EMP (electromagnetic pulse) mitigation program approach
[AD-A197849] N89-12807
Radiation resistance and comparative performance of ITO/InP and n/p InP homojunction solar cells
[NASA-TM-101387] N89-12819
The effects of expansion devices on the transient response characteristics of the air-source heat pump during the reverse cycle defrost
[AD-A197150] N89-12829
Performance of the forward scattering spectrometer probe in NASA's icing research tunnel
[NASA-TM-101381] N89-12845
Gas flow and global code programme
[DE88-012635] N89-12861
Research on mechanical properties for engine life prediction
[AD-A197816] N89-12864
Laboratory evaluation of a field portable dielectric/soil moisture probe N89-13006
Preparation and properties of high-deposition-rate a-Si:H films and solar cells using disilane
[DE88-001191] N89-13098
Tests of a multichannel photometer based on silicon diode detectors N89-13314
PERMEABILITY
Development of optimized, graded-permeability axial groove heat pipes N89-12614
PERSONAL COMPUTERS
The state of PC-based CADD (Computer-Aided Design and Drafting) systems
[DE88-017326] N89-13170
PERSONNEL DEVELOPMENT
Important aspects of technology transfer: Training of inservice engineers and scientists; satellite remote sensing N89-13082
PERSONNEL MANAGEMENT
MANPRINT (Manpower and Personnel Integration Program) primer
[AD-A197681] N89-13296
PERTURBATION
Perturbed functional iteration applied to the Navier-Stokes equations N89-12774
Nonlinear perturbations of differential operators with nontrivial kernel and applications to third order periodic boundary value problems
[DE88-702991] N89-13201
PERTURBATION THEORY
Singular perturbations and time scales in the design of digital flight control systems
[NASA-TP-2844] N89-12569
PESTICIDES
Cotton area mapping using multitemporal satellite data integrated within a geographical information system applied to a cotton boll weevil control programme in Paraguay N89-13077
PHASE COHERENCE
Phase coherence and Signal-To-Noise ratio considerations for sampled aperture radar systems
[AD-A197180] N89-12797
PHASE CONJUGATION
Construction of a phase conjugate laser resonator using Brillouin enhanced four wave mixing N89-12759
PHASE SHIFT
Phase measurement accuracy limitation in phase shifting interferometry N89-13248
Nonlinear effects in photorefractive crystals
[AD-A197152] N89-13281
PHASE TRANSFORMATIONS
Synthesis and characterization of VLS-derived silicon carbide whiskers
[DE88-016226] N89-12679
New methods for locating phase boundaries
[DE88-017084] N89-12700
Adsorption on metal surfaces
[DE88-016557] N89-12715
Neutron studies of liquid and solid helium
[DE88-009096] N89-13277
PHENOLIC EPOXY RESINS
A methodology for characterizing reactive coatings: Time-Temperature-Transformation (TTT) analysis of the competition between cure, evaporation and thermal degradation for an epoxy-phenolic system
[AD-A197254] N89-12730
PHENOMENOLOGY
Superconductivity: Phenomenology
[DE88-016659] N89-13289
PHONETICS
The effects of high noise levels on the acoustic-phonetic structure of speech: A preliminary investigation N89-12764
PHONONS
Ion mobility spectrometry with laser-produced ions
[AD-A197117] N89-12851
PHOSPHAZENE
Influence of side-groups on thermotropic behavior of polyorganophosphazenes
[AD-A197852] N89-12740
PHOSPHORIC ACID
Assessment and comparison of 100-MW coal gasification phosphoric acid fuel cell power plants
[NASA-CR-182169] N89-13103
PHOTOCATHODES
Development of high efficiency opaque photocathodes for the Region 900 angstrom to 1200 angstrom
[NASA-CR-180597] N89-13249
PHOTOCHEMICAL REACTIONS
Radiative augmented combustion
[AD-A197300] N89-12693
PHOTOCONDUCTORS
Microwave characteristics of interdigitated photoconductors on a HEMT structure
[NASA-CR-182197] N89-12820
PHOTODECOMPOSITION
Joint services electronics program
[AD-A197140] N89-12815
PHOTODIODES
Optical and electrical measurements on UV sensitive photodiodes N89-13316
Application of PN and avalanche silicon photodiodes to low-level optical N89-13317
PHOTODISSOCIATION
The NASA atomic oxygen effects test program N89-12589
PHOTOELASTICITY
Laser dynamic photoelasticity and digital image analysis for nondestructive evaluation of surface and near surface flaws through ultrasonic spectroscopy N89-12871
PHOTOELECTRIC EMISSION
Electrogenerated chemiluminescence
[AD-A197163] N89-12691
PHOTOGRAMMETRY
Summary of laser speckle photogrammetry for HOST N89-12889
Photogrammetric model for correction of MSS-LANDSAT imagery
[INPE-4652-PRE/1359] N89-13090
PHOTOIONIZATION
Ion mobility spectrometry with laser-produced ions
[AD-A197117] N89-12851
PHOTOLITHOGRAPHY
Ultrathin polymer films for microlithography
[AD-A197298] N89-12732
PHOTOLUMINESCENCE
Research on mercury cadmium telluride
[AD-A197238] N89-13282
PHOTOLYSIS
Aspects of CFC relative ozone destruction efficiencies determined in the LLNL 2-D model
[DE88-015431] N89-13106
PHOTOMASKS
Ultrathin polymer films for microlithography
[AD-A197298] N89-12732
PHOTOMETERS
The Instrument Test Dewar (ITD): Testing satellite instruments at 1.5 K N89-12604
Second Workshop on Improvements to Photometry
[NASA-CP-10015] N89-13310
The Hubble Space Telescope high speed photometer N89-13311
A multichannel fiber optic photometer present performance and future developments N89-13313
Tests of a multichannel photometer based on silicon diode detectors N89-13314
A fibre optic, four channel comparative photometer N89-13315
Absolute photometric calibration of detectors to 0.3 mmag using amplitude-stabilized lasers and a helium-cooled absolute radiometer N89-13318
A consideration of the use of optical fibers to remotely couple photometers to telescopes N89-13326
PHOTOMETRY
The Hubble Space Telescope high speed photometer N89-13311
Analog-to-digital conversion techniques for precision photometry N89-13319
Monitoring solar-type stars for luminosity variations N89-13321
Improvements to photometry. Part 1: Better estimation of derivatives in extinction and transformation equations N89-13322
PHOTOMULTIPLIER TUBES
An introduction to blocked impurity band detectors N89-13320
PHOTONS
The transfer of cyclotron photons through neutron star atamospheres N89-13378
PHYSICAL FACTORS
Physical modeling of bubble phenomena, electrolyte flow and mass transfer in simulated advanced Hall cells
[DE88-015585] N89-12828
PHYSICAL OPTICS
Focal region fields of distorted reflectors
[NASA-CR-183001] N89-12810
Shadows and wedges in scattering from the sea N89-12946
PHYSIOLOGICAL EFFECTS
The effects of hyperbaric oxygen and antioxidant deficiencies on rat retinal ultrastructure N89-12772
PICOSECOND PULSES
Surfaces and thin films studied by picosecond ultrasonics
[DE88-015268] N89-13233
PIEZOELECTRICITY
The standardized Bauer piezoelectric polymer shock gauge
[DE88-014963] N89-12840

PILOT PERFORMANCE
Pilot factors guidelines for the operational inspection of navigation systems
[NASA-CR-181644] N89-12557
Voice recognition and artificial intelligence in an air traffic control environment
[AD-A197219] N89-12559
The effect of attentional focus level on task performance utilizing information from different stimulus structure levels N89-12765
PIPES (TUBES)
Combined mechanical loading of composite tubes
[NASA-CR-183012] N89-12681
PITCHING MOMENTS
Unsteady structure of flow past a pitching delta wing N89-12541
PLANE WAVES
Focal region fields of distorted reflectors
[NASA-CR-183001] N89-12810
Laser speckle from thin and cascaded diffusers
[AD-A197066] N89-12850
PLANETARY ENVIRONMENTS
Moisture interaction and stability of ZOT (Zinc Orthotitanate) thermal control spacecraft coating N89-12618
PLANETARY EVOLUTION
Growth and sedimentation of dust grains in the primitive solar nebula N89-13374
PLANNING
Planner system for the application of indications and warning N89-13188
POPLAR: A testbed for cognitive modeling N89-13190
MANPRINT (Manpower and Personnel Integration Program) primer
[AD-A197681] N89-13296
PLASMA CHEMISTRY
Nonequilibrium effects in thermal plasmas: Radiation transport and chemical reactivity
[DE88-016841] N89-13262
Nonequilibrium effects in thermal plasma chemistry
[DE88-016842] N89-13263
PLASMA CONTROL
Modified magnetic confinement configurations based on understanding helicity dissipation and pressure driven modes in the spheromak
[DE88-009149] N89-13260
Tokamak equilibrium determination through function parameterization N89-13272
PLASMA DIODES
Fundamental studies and device development in beta silicon carbide
[AD-A197843] N89-12739
PLASMA EQUILIBRIUM
Toroidal studies of sawtooth oscillations in tokamaks
[DE88-017115] N89-13264
PLASMA HEATING
FOM Contributions to the 15th European Conference on Controlled Fusion and Plasma Heating
[REPT-88-178] N89-13266
The m=1 internal kink mode in a toroidal plasma with a flat q-profile near q=1 N89-13267
Kinetic effects on electron cyclotron emission during electron cyclotron heating in tokamaks N89-13268
Fundamental harmonic electron cyclotron emission for hot, loss-cone type distributions N89-13269
Transport code studies of m=2 mode control by local electron cyclotron heating in TFR N89-13270
Recent results of the toroidal screw pinch SPICA 2 N89-13271
PLASMA INTERACTIONS
RF stabilization of external kink modes --- tokamak plasmas N89-13275
PLASMA OSCILLATIONS
Investigation of acceleration and densification of electrons utilizing travelling magnetic waves
[AD-A197700] N89-13242
Internal kink modes in the ion-kinetic regime N89-13274
PLASMA PHYSICS
Nuclear technology for the year 2000
[DE88-005041] N89-13223
Tesla's coherent plasma discharge and a plan for megavolts at megahertz N89-13231
PLASMA SHEATHS
Injection of ionospheric ions into the plasma sheet in the Earth's magnetotail
[IFSI-88-13] N89-13113
PLASMA SPRAYING
Investigations into the plasma spray process
[DE88-014524] N89-12787
PLASMA-PARTICLE INTERACTIONS
The applicability of Rutherford scattering for Ti measurements at medium and large-sized experiments N89-13273
PLASMAS (PHYSICS)
Atomic oxygen studies on polymers N89-12591
A computer simulation of a plasma armature railgun N89-12780
Interaction of a hollow-cathode source with an ionospheric plasma
[IFSI-88-10] N89-13112
Sample introduction using the Hildebrand grid nebulizer for plasma spectrometry
[AD-A197145] N89-13257
Interaction of impurity ions with a weakly non-Maxwellian simple hydrogenic plasma
[DE88-017137] N89-13265
PLASTIC COATINGS
A methodology for characterizing reactive coatings: Time-Temperature-Transformation (TTT) analysis of the competition between cure, evaporation and thermal degradation for an epoxy-phenolic system
[AD-A197254] N89-12730
Soiling, cleaning, and weathering effects on aircraft polyurethane topcoats
[AD-A197302] N89-12733
PLASTIC DEFORMATION
Constitutive modeling for single crystal superalloys N89-12911
PLASTIC FLOW
Effect of grain size on the high temperature properties of B2 aluminides
[NASA-TM-101382] N89-12720
PLATES (STRUCTURAL MEMBERS)
Thermal transport between a continuously moving heated plate and a quiescent ambient medium N89-12824
PLATING
Determination of sulfuric acid, oxalic acid, and their matrix effects in aluminum anodizing solutions by ion chromatography
[AD-A197734] N89-12694
Corrosion of nickel and Monel welds of steel in chlorine trifluoride
[DE88-014122] N89-12706
PLAYAS
Monitoring playas using Thematic Mapper data N89-13028
PLUGS
Porous plug for reducing orifice induced pressure error in airfoils
[NASA-CASE-LAR-13569-1] N89-12841
POLAR ORBITS
Cloud track winds from polar orbiting satellites N89-13069
POLAR REGIONS
Cloud track winds from polar orbiting satellites N89-13069
POLARIMETERS
The development of a near-infrared polarimeter and its application to the continuum polarization of magnetic white dwarfs N89-12924
POLARIMETRY
Statistical analysis and some polarimetric signatures of a polarimetric synthetic aperture radar image N89-12952
On the concept of the polarimetric matched filter in high resolution radar imaging: An alternative for speckle radiation N89-12954
Cross-polar radar measurements in ice and rain N89-12993
Processing and interpretation of alternately polarised weather radar echoes N89-12996
Phase calibration of polarimetric SAR N89-13015
A fine resolution multifrequency polarimetric FM radar N89-13016
Examining the polarisation phase retrieval of a dual channel multipolarisation radar N89-13019
The NASA/JPL multifrequency, multipolarisation airborne SAR system N89-13020
Formulation of the proper equations for developing standards in coherent dual polarisation SAR imaging N89-13021
A 35 GHz helicopter-borne polarimeter radar N89-13038
POLARIZATION (WAVES)
The optimal polarizations for achieving maximum contrast in radar images
[NASA-CR-183349] N89-12794
Design considerations for advanced multi-polarisation SAR N89-13014
POLARIZATION CHARACTERISTICS
Modelling of SAR polarisation phase difference from trees N89-12951
Backscatter laser depolarization studies of simulated stratospheric aerosols: Crystallized sulfuric acid droplets
[NASA-CR-183387] N89-13111
POLICIES
United States space policy: Review and assessment
[DE88-015538] N89-13306
AGARD handbook N89-13392
POLLUTION TRANSPORT
The incorporation of sulfur dioxide into snow and depositing ice N89-13116
POLYATOMIC MOLECULES
Determination of stepsize parameters for intermolecular vibrational energy transfer
[DE88-010904] N89-13239
POLYIMIDES
Thermoplastic adhesives based on 4,4'-isophthaloyldiphthalic anhydride (IDPA)
[NASA-TM-101508] N89-12747
POLYMER CHEMISTRY
Charge transfer in multiple site chemical systems
[AD-A197143] N89-12666
High temperature adhesive systems
[AD-A197077] N89-12726
POLYMERIC FILMS
Polyenamines from aromatic diacetylenic diketones and diamines
[NASA-CASE-LAR-13444-2-CU] N89-12667
Studies of ultrathin polymer films for lithographic applications
[AD-A197297] N89-12731
Ultrathin polymer films for microlithography
[AD-A197298] N89-12732
Poly(ethyl acrylate) and poly(gamma-benzyl-L-glutamate): An interpenetrating polymer system
[AD-A197783] N89-12737
Re-evaluation of an improved efficiency polymeric web point-focus Fresnel lens
[DE88-016892] N89-13255
POLYMERIZATION
Atomic oxygen studies on polymers N89-12591
Polyenamines from aromatic diacetylenic diketones and diamines
[NASA-CASE-LAR-13444-2-CU] N89-12667
Electronic and ionic transport in polymers
[AD-A197142] N89-12728
Poly(ethyl acrylate) and poly(gamma-benzyl-L-glutamate): An interpenetrating polymer system
[AD-A197783] N89-12737
POLYMETHYL METHACRYLATE
Ultrathin polymer films for microlithography
[AD-A197298] N89-12732
POLYNOMIALS
Euclidean decoders for BCH codes
[AD-A197242] N89-13157
On the constrained Chebyshev approximation problem on ellipses
[NASA-CR-183209] N89-13200
POLYSACCHARIDES
Synthetic polymers as analogs of polysaccharides
[AD-A197842] N89-12738
POLYSTATION DOPPLER TRACKING SYSTEM
Phase coherence and Signal-To-Noise ratio considerations for sampled aperture radar systems
[AD-A197180] N89-12797
POLYURETHANE RESINS
Differential scanning calorimetry as a method for indicating hydrolysis of urethane elastomers
[AD-A197673] N89-12736
Development of polyisocyanurate pour foam formulation for space shuttle external tank thermal protection system
[NASA-CR-183511] N89-12745
POPULATION INVERSION
Population inversion non-equilibrium flow simulation calculations of the capabilities of convection flow lasers
[AD-A197741] N89-12854
POROSITY
Porous plug for reducing orifice induced pressure error in airfoils
[NASA-CASE-LAR-13569-1] N89-12841
POSITION (LOCATION)
Locating and search procedures with helicopters for sea and/or air emergencies
[FPN-0079] N89-12556
A comparison of propagation model predictions with EPLRS (Enhanced Position Location and Reporting System) UHF network measurements
[AD-A197473] N89-12804
Data collection system operating on Japan's first marine observation satellite: Inflight evaluation of the system performance N89-13007
POSITIONING DEVICES (MACHINERY)
Gripping device
[NASA-CASE-MSC-21365-1] N89-12865
POTATOES
Analysis of potato crop distribution using remotely sensed and environmental data in a pilot geographical information system N89-12967

POTENTIAL FLOW
Development and validation of an advanced low-order panel method
[NASA-TM-101024] N89-12554
POWDER (PARTICLES)
Highly magnetic powder
[DE88-010838] N89-12701
Amorphous powders of Al-Hf prepared by mechanical alloying
[DE88-014459] N89-12704
POWDER METALLURGY
Powder metallurgy bearings for advanced rocket engines N89-12641
Effect of grain size on the high temperature properties of B2 aluminides
[NASA-TM-101382] N89-12720
POWER CONDITIONING
Superionic conductors as fast, repetitive opening switches
[AD-A197365] N89-12817
POWER EFFICIENCY
The design of antenna matching networks using a microcomputer
[AD-A197364] N89-12802
PREAMPLIFIERS
Tests of a multichannel photometer based on silicon diode detectors N89-13314
PREBURNERS
Combustion modeling: Progress and projections N89-12652
PRECIPITATION (METEOROLOGY)
An algorithm to derive precipitation profiles from a downward viewing radar and a multifrequency passive radiometer N89-12992
Production of probability of precipitation maps over oceanic areas from automated cloud classification N89-12999
Precipitation detection with satellite microwave data
[PB88-240239] N89-13094
PRECIPITATION PARTICLE MEASUREMENT
Cross-polar radar measurements in ice and rain N89-12993
PRECISION
Precision limits of the twin-beam multiband URSULA N89-13312
Analog-to-digital conversion techniques for precision photometry N89-13319
PREDICTION ANALYSIS TECHNIQUES
Aerothermal modeling program, phase 2 N89-12890
Efficient numerical techniques for complex fluid flows N89-12894
Improved numerical methods for turbulent viscous recirculating flows N89-12895
Development of low Reynolds number two equation turbulence models for predicting external heat transfer on turbine blades N89-12901
Turbine airfoil film cooling N89-12903
Creep fatigue life prediction for engine hot section materials (isotropic): Fourth year progress review N89-12914
Life prediction and constitutive models for engine hot section N89-12916
Thermal barrier coating life prediction model development N89-12920
Thermal barrier coating life prediction model N89-12921
Thermal barrier coating life prediction model development N89-12922
Approximate mobilities of built up structures
[ISVR-TR-162] N89-12934
Spectral analysis of ocean wave imagery using 2-D linear prediction N89-12968
Improvement in NOAA-AVHRR snowcover determination for runoff prediction N89-13040
An analysis of the error characteristics of Atlantic tropical cyclone track prediction models N89-13117
An analysis of the error characteristics of Atlantic tropical cyclone track prediction models
[AD-A197146] N89-13119
Forecasting aids for setting tropical cyclone conditions: Sasebo and Iwakuni, Japan
[AD-A197802] N89-13122
PREDICTIONS
Aircraft technology opportunities for the 21st Century
[NASA-TM-101060] N89-12539
Prediction of fiber orientation during processing of short fiber composites N89-12671
Antenna pattern study
[ARI/R-88-510Z] N89-12790
A numerical method for computing unsteady 2-D boundary layer flows
[NASA-CR-4198] N89-12835
Prediction of stresses in aircraft panels subjected to acoustic forces
[NASA-CR-182513] N89-12923
Wavelength or sensor selection by minimization of prediction error
[AD-A197231] N89-13216
The next logical step in laser-fusion development
[DE88-007825] N89-13258
PRESSING
Slurry-pressing consolidation of silicon nitride
[NASA-TM-101365] N89-12746
PRESSURE
Theoretical study of turbulent channel flow: Bulk properties, pressure fluctuations, and propagation of electromagnetic waves
[NASA-TM-101248] N89-12830
PRESSURE EFFECTS
Survey of laser-produced pressure and impulse data
[AD-A197313] N89-12852
Combustor diffuser interaction program N89-12893
PRESSURE MEASUREMENT
The standardized Bauer piezoelectric polymer shock gauge
[DE88-014963] N89-12840
Porous plug for reducing orifice induced pressure error in airfoils
[NASA-CASE-LAR-13569-1] N89-12841
PRESSURE SENSORS
Porous plug for reducing orifice induced pressure error in airfoils
[NASA-CASE-LAR-13569-1] N89-12841
PRESSURE VESSELS
Fire spread in a three-dimensional pressure vessel with radiation exchange and wall heat losses
[AD-A197271] N89-12692
PRISMS
Fiber optic wavelength division multiplexing: Principles and applications in telecommunications and spectroscopy N89-13324
PROBABILITY DISTRIBUTION FUNCTIONS
A comparison of propagation model predictions with EPLRS (Enhanced Position Location and Reporting System) UHF network measurements
[AD-A197473] N89-12804
Production of probability of precipitation maps over oceanic areas from automated cloud classification N89-12999
PROBABILITY THEORY
A probabilistic approach to composite micromechanics
[NASA-TM-101366] N89-12684
On adaptive cell-averaging CFAR radar signal detection N89-12792
Bayesian reasoning tool
[AD-A197351] N89-13196
People versus probability
[DE88-017380] N89-13221
PROBLEM SOLVING
A fault diagnosis system based on an integrated knowledge base N89-13181
Distributed problem solving N89-13186
A shared knowledge base for independent problem solving agents N89-13187
Planner system for the application of indications and warning N89-13188
Bayesian reasoning tool
[AD-A197351] N89-13196
Engineering applications of heuristic multilevel optimization methods
[NASA-TM-101504] N89-13203
Sensitivity analysis for shortest Hamiltonian path and traveling salesman problems
[AD-A197167] N89-13204
PROCESS CONTROL (INDUSTRY)
Prediction of fiber orientation during processing of short fiber composites N89-12671
PROGRAM VERIFICATION (COMPUTERS)
Parallel debugging using graphical views
[AD-A197197] N89-13156
PROGRAMMING LANGUAGES
European Seminar on Neural Computing
[ONRL-8-010-C] N89-13173
Achieving speedups for a shared memory model language on an SIMD parallel computer
[AD-A197102] N89-13176
Artificial intelligence theory and reconfigurable control systems
[AD-A197255] N89-13195
PROJECTILES
Aerodynamics analysis of solid fuel Ramjet projectiles
[AD-A196755] N89-12548
Six degree of freedom simulation computer program for aeroelastic free-flight projectiles N89-12771
PROP-FAN TECHNOLOGY
Advanced turboprop project
[NASA-SP-495] N89-12565
PROPELLANT COMBUSTION
Aerojet TechSystems Company contribution to LOX/HC combustion and cooling technology N89-12646
Survey of LOX/hydrocarbon combustion and cooling N89-12647
LOX/hydrocarbon combustion and cooling survey N89-12648
RP-1 and methane combustion and cooling experiments N89-12650
Results of coaxial injector element testing N89-12651
Combustion modeling: Progress and projections N89-12652
Turbine Engine Hot Section Technology 1986
[NASA-CP-2444] N89-12876
PROPELLANT SENSITIVITY
Combined pressure-shear ignition sensitivity test
[AD-A197076] N89-12749
PROPELLANTS
Semiconductor bridge (SCB) igniter studies. 2: Comparison of SCB and hot-wire direct propulsion thrusters
[DE88-008803] N89-12625
PROPULSION
Fiber optic control system integration
[NASA-CR-179568] N89-13256
PROPULSION SYSTEM CONFIGURATIONS
Advanced Earth-to-Orbit Propulsion Technology 1986, volume 2
[NASA-CP-2437-VOL-2] N89-12626
Aerojet TechSystems Company contribution to LOX/HC combustion and cooling technology N89-12646
LOX/hydrocarbon combustion and cooling survey N89-12648
Liquid oxygen cooling of high pressure LOX/hydrocarbon rocket thrust chambers N89-12649
21st century propulsion concept
[AD-A197537] N89-12663
PROTECTION
Wave propagation in layered structures N89-12777
PROTECTIVE CLOTHING
Validity of heat index as indicator of level of heat storage for personnel wearing protective clothing in hot environments N89-12762
PROTECTIVE COATINGS
Atomic oxygen effects on candidate coatings for long-term spacecraft in low earth orbit N89-12592
Surface modification for wear resistance in a liquid oxygen turbopump environment N89-12644
Evaluation of boron carbide coatings N89-13228
PROTOCOL (COMPUTERS)
Boeing Military Airplane Company technical order transfer tests
[DE88-012233] N89-13151
PROVING
Two alternate proofs of Wang's lune formula for sparse distributed memory and an integral approximation
[NASA-CR-184555] N89-13214
PSYCHOACOUSTICS
Auditory models for speech analysis
[AD-A197322] N89-12801
PSYCHOLOGICAL FACTORS
Bayesian reasoning tool
[AD-A197351] N89-13196
PSYCHOLOGICAL TESTS
Differential-psychological analysis of a computer-based audio-visual test of vigilance
[DFVLR-FB-88-23] N89-13140
PSYCHOPHYSICS
Discrimination and identification of modulation-frequency using noise, tone and tonal-complex carriers
[AD-A197780] N89-13134
PUBLIC HEALTH
Bioelectromagnetic effects of EMP: Preliminary findings
[DE88-012118] N89-12791
Human exposure to dioxin from combustion sources
[DE88-013825] N89-13135
PULSE RADAR
Ionosphere 1970, Volume 58
[ISSN-0211-5166] N89-13114
PULTRUSION
Pultrusion die assembly
[NASA-CASE-LAR-13719-1] N89-12867
PYRAMIDS
PIPS: A Procedure for Interactive Pyramid Segmentation N89-12984
PYROTECHNICS
Pyro shock simulation: Experience with the MIPS simulator N89-12593
Laser illuminated high speed photography of energetic materials
[DE88-012870] N89-12848

Q

QUADRATIC PROGRAMMING
Temporal clustering in the multi-target tracking environment
[AD-A197153] N89-12796
QUADRUPOLES
A radio-frequency quadrupole accelerator longitudinal field stabilizer
[DE88-014399] N89-13246
Properties of stellar activity in F stars N89-13369
QUALIFICATIONS
Ariane 5 verification and associated test facilities N89-12611
The separation test in vacuum of the Ariane 4 payload fairing N89-12612
Requirements and test results for the qualification of thermal control coatings N89-12616
QUALITY
Survey of image restoration techniques
[AD-A197470] N89-13251
QUALITY CONTROL
Fingerprint test data report: FM 5834 test lots No. 1, 3, 4, and 5 --- resin matrix composites
[NASA-CR-179419] N89-12722
Fingerprint test data report: FM 5064J (Kaiser) lots No. 1 (K) - No. 4 (K) --- resin matrix composites
[NASA-CR-179409] N89-12723
Making statistical inferences about software reliability
[NASA-CR-4197] N89-13153
QUANTUM EFFICIENCY
Development of high efficiency opaque photocathodes for the Region 900 angstrom to 1200 angstrom
[NASA-CR-180597] N89-13249
QUANTUM MECHANICS
Quantum Monte Carlo calculation of the properties of atomic carbon and diamond
[DE88-014659] N89-12686
Stochastic stage of an inflationary universe model
[DE88-753149] N89-13373
QUANTUM THEORY
New gravitational forces from quantum theory
[DE88-016231] N89-13294
QUASARS
The large-scale structure of the universe: Some theoretical considerations N89-13381
QUATERNARY ALLOYS
Influence of alloying elements on the oxidation behavior of NbAl3
[NASA-TM-101398] N89-12717
QUEUEING THEORY
Performance studies of dynamic load balancing in distributed systems
[AD-A197130] N89-12926

R

RADAR
Phase coherence and Signal-To-Noise ratio considerations for sampled aperture radar systems
[AD-A197180] N89-12797
RADAR ANTENNAS
Examining the polarisation phase retrieval of a dual channel multipolarisation radar N89-13019
RADAR ATTENUATION
Polarization-dependent attenuation of dielectric cylinder arrays N89-12955
Attenuation and scattering measurements from dense media --- radar N89-13012
RADAR CROSS SECTIONS
Modeling and performance of HF/OTH (High-Frequency/Over-The-Horizon) radar target identification systems
[AD-A197850] N89-12808
EURACS: A European radar cross section database N89-12944
Constraints on two-scale descriptions of radar backscattering from the sea surface using scatterometer model functions N89-12945
Interpretation of coherent polarimetric signatures by dielectric cylinder models N89-12957
RADAR DATA
The effects of undersampling on multipolarization SAR images N89-12956
An intercomparison of SAR and buoy directional wave spectra from the Labrador Sea Extreme Waves Experiment (LEWEX) N89-12972
Some advantages of using polarisation diversity illustrated through the analysis of radar data from a storm in central Alberta (Canada) N89-12994
Processing and interpretation of alternately polarised weather radar echoes N89-12996
RADAR DETECTION
Modeling and performance of HF/OTH (High-Frequency/Over-The-Horizon) radar target identification systems
[AD-A197850] N89-12808
RADAR ECHOES
Processing and interpretation of alternately polarised weather radar echoes N89-12996
RADAR IMAGERY
The optimal polarizations for achieving maximum contrast in radar images
[NASA-CR-183349] N89-12794
Real-time adaptive radiometric correction for imaging radar systems N89-12943
Statistical analysis and some polarimetric signatures of a polarimetric synthetic aperture radar image N89-12952
On the concept of the polarimetric matched filter in high resolution radar imaging: An alternative for speckle radiation N89-12954
The effects of undersampling on multipolarization SAR images N89-12956
On the use of speckle statistics for the extraction of ocean wave spectra from SAR imagery N89-12969
Ocean wave number spectra and spatial autocorrelation functions from SAR images N89-12970
SAR-seen multimode waves in ice: Evidence of imaging nonlinearities N89-12971
Synthetic aperture radar over terrestrial ice N89-12977
Crop classification with multi-temporal X-band SAR data N89-12990
Image simulation of complex geometric targets for spaceborne synthetic aperture radar N89-13010
Bistatic frequency diverse imaging of complex scattering targets N89-13013
A synthetic apertures radar with multichannel and multipolarisation N89-13017
The relativity utility of LANDSAT MSS and SIR-A imagery in reconnaissance geological mapping in Northern Sudan N89-13022
Sea ice type classification of SAR imagery N89-13039
Statistics and high resolution imaging of snowpack at 35 GHz using a microcomputer N89-13047
Snow cover to alter terrain signatures on radar images N89-13048
The derivation of sub-canopy surface terrain models of coastal forests using synthetic aperture radar N89-13083
A luminance edge extraction method using gradient of gray level for synthetic aperture radar imageries N89-13086
RADAR MAPS
SAR image statistics related to atmospheric drag over sea ice N89-13034
RADAR MEASUREMENT
Cross-polar radar measurements in ice and rain N89-12993
Dual linear polarisation time series as an aid to hydrometeor identification N89-12995
Attenuation and scattering measurements from dense media --- radar N89-13012
Phase versus orbital velocity in SAR wave imaging: Paradox lost N89-13033
Microwave dielectric properties of low-salinity sea ice N89-13036
RADAR RECEPTION
Optimal reception in depolarising clutter N89-13008
RADAR RESOLUTION
A fine resolution multifrequency polarimetric FM radar N89-13016
RADAR SCATTERING
Constraints on two-scale descriptions of radar backscattering from the sea surface using scatterometer model functions N89-12945
Scattering from a skewed random surface --- radar scattering N89-12948
Polarimetric microwave scattering from known randomly rough surfaces N89-12949
Inference of geologic surface parameters from polarimetric radar observations and model inversion N89-12950
Modelling of SAR polarisation phase difference from trees N89-12951
Statistical properties of phase difference between two orthogonally-polarised SAR signals N89-12953
Attenuation and scattering measurements from dense media --- radar N89-13012
Bistatic frequency diverse imaging of complex scattering targets N89-13013
Modulation of the radar backscatter from the ocean surface by a long gravity wave N89-13031
A 35 GHz helicopter-borne polarimeter radar N89-13038
RADAR SIGNATURES
Snow cover to alter terrain signatures on radar images N89-13048
RADAR TARGETS
LORAN C Offshore Flight Following (LOFF) in the Gulf of Mexico
[AD-A197179] N89-12558
Image simulation of complex geometric targets for spaceborne synthetic aperture radar N89-13010
Bistatic frequency diverse imaging of complex scattering targets N89-13013
RADAR TRANSMISSION
On adaptive cell-averaging CFAR radar signal detection N89-12792
RADIAL VELOCITY
Use of optical fibers in spectrophotometry N89-13325
RADIANCE
A numerical model for the computation of radiance distributions in natural waters with wind-roughened surfaces
[AD-A197207] N89-13128
RADIANT HEATING
Fire spread in a three-dimensional pressure vessel with radiation exchange and wall heat losses
[AD-A197271] N89-12692
RADIATION COUNTERS
Holographic particle detection
[NASA-CR-183315] N89-13240
RADIATION DAMAGE
Fifteenth Space Simulation Conference: Support the Highway to Space Through Testing
[NASA-CP-3015] N89-12582
Atomic oxygen studies on polymers N89-12591
Atomic oxygen effects on candidate coatings for long-term spacecraft in low earth orbit N89-12592
RADIATION DISTRIBUTION
Laser speckle from thin and cascaded diffusers
[AD-A197086] N89-12850
RADIATION DOSAGE
Liquid scintillation counting with the Packard 1500 analyzer N89-12782
RADIATION EFFECTS
The NASA atomic oxygen effects test program N89-12589
Irradiation-assisted stress corrosion cracking and grain boundary segregation in heat treated Type 304SS
[DE88-008382] N89-12713
Radiation resistance and comparative performance of ITO/InP and n/p InP homojunction solar cells
[NASA-TM-101387] N89-12819
Radiation effects in semiconductor laser diode arrays
[DE88-016318] N89-12859
RADIATION HAZARDS
Space reactor assessment and validation study N89-13227
RADIATION MEASURING INSTRUMENTS
Application of PN and avalanche silicon photodiodes to low-level optical N89-13317
RADIATION PRESSURE
Nearfield acoustic radiation from a point-excited cylindrical shell
[AD-A197282] N89-13234
RADIATION PROTECTION
Lunar storm shelter conceptual design
[NASA-CR-172078] N89-13141
RADIATION SOURCES
Investigation of acceleration and densification of electrons utilizing travelling magnetic waves
[AD-A197700] N89-13242
RADIATION TRANSPORT
Nonequilibrium effects in thermal plasmas: Radiation transport and chemical reactivity
[DE88-016841] N89-13262
RADIATIVE TRANSFER
On the interactions of longwave radiation, microphysics and turbulence in boundary layer clouds N89-13109
Theoretical studies of mass loss and shock phenomena in cool star envelopes
[NASA-CR-182708] N89-13375
RADIO ALTIMETERS
Analysis of GEOSAT radar altimeter errors based on pre-launch test data
[NASA-TM-101230] N89-12806
RADIO COMMUNICATION
Application of autoregressive methods to adaptive excision of interfering tones from direct sequence spread spectrum communications systems
[AD-A197801] N89-12805
RADIO EQUIPMENT
A comparison of propagation model predictions with EPLRS (Enhanced Position Location and Reporting System) UHF network measurements
[AD-A197473] N89-12804

RADIO FREQUENCIES
Microwave RF coupling response through adjacent cavities
[DE88-012430] N89-12793
A radio-frequency quadrupole accelerator longitudinal field stabilizer
[DE88-014399] N89-13246
RF stabilization of external kink modes — tokamak plasmas N89-13275
RADIO SCATTERING
Inference of radio scattering parameters of Antarctic ice sheet using 179 MHz airborne radio echo sounding data N89-12975
RADIO TRANSMISSION
Review of electromagnetic surface waves, 1960 through 1987
[AD-A197278] N89-12798
RADIOACTIVE CONTAMINANTS
Liquid scintillation counting with the Packard 1500 analyzer N89-12782
RADIOACTIVE WASTES
Challenging applications for hydrated and chemically reacted ceramics
[DE88-015397] N89-12742
RADIOLOGY
Liquid scintillation counting with the Packard 1500 analyzer N89-12782
RADIOMETERS
Cost effective alternative to low irradiance measurements N89-12619
The Airborne Version Conical Scan Radiometer (AVCSR): An airborne radiometer as a tool for satellite data validation N89-12937
Verification results of MOS-1 multispectral self scanning radiometer (MESSR) data N89-13004
Optical and electrical measurements on UV sensitive photodiodes N89-13316
Absolute photometric calibration of detectors to 0.3 mmag using amplitude-stabilized lasers and a helium-cooled absolute radiometer N89-13318
RADIOMETRIC CORRECTION
Real-time adaptive radiometric correction for imaging radar systems N89-12943
RAILGUN ACCELERATORS
A decade of railgun development for high pressure research
[DE88-017024] N89-12578
A computer simulation of a plasma armature railgun N89-12780
RAIN
Cross-polar radar measurements in ice and rain N89-12993
Design of a spaceborne radar for tropical rain mapping at the climatological scale N89-12997
Rainfall index over oceans derived from SSM/I data — Special Sensor Microwave/Imager (SSM/I) N89-12998
Effects of rainfall on scatterometer derived wind speeds N89-13074
RAMAN SPECTRA
Optical modeling of clear ocean light fields: Raman scattering effects
[AD-A197249] N89-13129
RAMJET ENGINES
Aerodynamics analysis of solid fuel Ramjet projectiles
[AD-A196755] N89-12548
RANDOM NOISE
Neural network performance on the stochastic exclusive-or problem
[AD-A197789] N89-13179
RANDOM VARIABLES
Optimal rates of convergence for deconvolving a density
[AD-A197748] N89-13207
RANDOM VIBRATION
Multiple input/output random vibration control system N89-12594
RANGE (EXTREMES)
Precision limits of the twin-beam multiband URSULA N89-13312
RANGEFINDING
Micro-computer network architecture for range instrumentation applications
[AD-A196971] N89-13175
RAPID QUENCHING (METALLURGY)
Properties of rapidly solidified aluminum alloys. German-Norwegian Project (1983-1987)
[DFVLR-FB-88-24] N89-12719
RARE GASES
Surface structures and transitions and the evolution from firn to bulk behavior
[AD-A197788] N89-12695
RATES (PER TIME)
Micro-computer network architecture for range instrumentation applications
[AD-A196971] N89-13175
RATS
The effects of hyperbaric oxygen and antioxidant deficiencies on rat retinal ultrastructure N89-12772
NASA newsletters for the Weber Student Shuttle Involvement Project
[NASA-TM-101001] N89-13144
RAYLEIGH SCATTERING
Rayleigh lidar observations of gravity wave activity in the upper stratosphere at Urbana, Ill.
[NASA-CR-182738] N89-13107
REACTION KINETICS
Report on JANNAF Workshop Influence of Gas-Phase Chemical Kinetics on Low-Pressure Ignition and Flamespreading in Solid Propellant
[AD-A197854] N89-12751
Population inversion non-equilibrium flow simulation calculations of the capabilities of convection flow lasers
[AD-A197741] N89-12854
Nonequilibrium effects in thermal plasmas: Radiation transport and chemical reactivity
[DE88-016841] N89-13262
REACTIVITY
Materials selection for long life in LEO: A critical evaluation of atomic oxygen testing with thermal atom systems N89-12590
REACTOR CORES
Preliminary thermal analysis of a bimodal nuclear rocket core N89-12758
REACTOR DESIGN
The 5 kWe scale-down of the SPAR/SP-100 heat pipe reactor N89-13226
Laser driven inertial confinement fusion N89-13229
FIREBIRD: A conceptual design of a field reversed configuration Compact Torus Fusion Reactor (CTFR) N89-13230
REACTOR SAFETY
Fire aerosol experiment and comparisons with computer code predictions
[DE88-016328] N89-12788
Nuclear technology for the year 2000
[DE88-005041] N89-13223
Evaluation of boron carbide coatings N89-13228
REACTOR TECHNOLOGY
Radioisotope space power generators: Design concepts N89-13224
The 5 kWe scale-down of the SPAR/SP-100 heat pipe reactor N89-13226
REAL TIME OPERATION
Temporal clustering in the multi-target tracking environment
[AD-A197153] N89-12796
The behavior of disk electrodes: Optical imaging of the concentration distribution over a disk electrode under galvanostatic conditions
[AD-A197355] N89-12816
Real-time adaptive radiometric correction for imaging radar systems N89-12943
Artificial intelligence theory and reconfigurable control systems
[AD-A197255] N89-13195
Nonlinear effects in photorefractive crystals
[AD-A197152] N89-13281
RECEIVERS
Functional description of signal processing in the Rogue GPS receiver
[NASA-CR-183314] N89-12813
RECIRCULATIVE FLUID FLOW
Efficient numerical techniques for complex fluid flows N89-12894
Improved numerical methods for turbulent viscous recirculating flows N89-12895
RECOGNITION
Is word recognition automatic: A cognitive-anatomical approach
[AD-A197089] N89-13137
RECURSIVE FUNCTIONS
Application of autoregressive methods to adaptive excision of interfering tones from direct sequence spread spectrum communications systems
[AD-A197801] N89-12805
A GLR (Generalized Likelihood Ratio) algorithm for polyline approximation of waveforms
[AD-A197846] N89-13166
REDUCED GRAVITY
Control of the induced microgravity environment of the Man Tended Free Flyer (MTFF) N89-12606
Microgravity science and applications program tasks, 1987 revision
[NASA-TM-4068] N89-12752
Tank gauging apparatus and method
[NASA-CASE-MSC-21059-1] N89-12843
REFINING
Environmental management practices in oil refineries and terminals: An overview
[ISBN-92-807-1108-3] N89-13104
REFLECTANCE
A refined model for characterizing X-ray multilayers
[DE88-013592] N89-12872
Dual linear polarisation time series as an aid to hydrometeor identification N89-12995
Relationships between the nitrogen content of grass and reflectance N89-13002
Snow cover to alter terrain signatures on radar images N89-13048
A numerical model for the computation of radiance distributions in natural waters with wind-roughened surfaces
[AD-A197207] N89-13128
Light scattering of large rough particles application to cometary grains N89-13357
REFLECTION NEBULAE
Properties of interstellar dust in reflection nebulae N89-13365
REFRACTIVITY
Optical constants of minerals and other materials from the millimeter to the ultraviolet
[AD-A197803] N89-12696
Nonlinear effects in photorefractive crystals
[AD-A197152] N89-13281
Optical properties of cometary grains N89-13363
REFRACTORY MATERIALS
Round-robin measurements of the apparent thermal conductivity of two refractory insulation materials, using high-temperature guarded-hot-plate apparatus
[PB88-215421] N89-12670
Elevated temperature strain gages N89-12886
REFRIGERATORS
Self-actuating heat switches for redundant refrigeration systems
[NASA-CASE-NPO-17085-1-CU] N89-12785
REGENERATIVE COOLING
Survey of LOX/hydrocarbon combustion and cooling N89-12647
REGIONAL PLANNING
Large area TM land cover classification of Mittlerer Oberrhein County, southwest Germany, and its use for regional planning and crop surveys N89-12986
The detection of unimproved grassland in Berkshire using a binary decision tree approach N89-12988
Evaluation of LANDSAT TM and SPOT imagery for agricultural land use planning in less developed countries N89-13051
REGRESSION ANALYSIS
An analysis of the error characteristics of Atlantic tropical cyclone track prediction models
[AD-A197146] N89-13119
Identifying nonlinear covariate effects in semimartingale regression models
[AD-A197323] N89-13205
Multivariate regression with emphasis on multivariate spline methods
[AD-A197793] N89-13209
REINFORCING FIBERS
Short fiber reinforced thermoplastics N89-12673
Toughening by aligned, frictionally constrained fibers
[AD-A197194] N89-12676
RELATIVITY
How to test the special theory of relativity on rotating earth
[DE88-703048] N89-13293
RELEASING
Automatic release mechanism for the EL 32 bag — parachutes
[E-768] N89-12863
RELIABILITY
Robust recognition of loud and Lombard speech in the fighter cockpit environment
[AD-A197093] N89-12795
Making statistical inferences about software reliability
[NASA-CR-4197] N89-13153
REMOTE CONTROL
Remote guidance of payloads under maneuverable parachutes
[E-639] N89-12571
The flight robotics laboratory N89-12595
Improved docking alignment system
[NASA-CASE-MSC-21372-1] N89-12842
Magnetic attachment mechanism
[NASA-CASE-MSC-21095-1] N89-12866
REMOTE SENSING
Proceedings of the 1988 International Geoscience and Remote Sensing Symposium (IGARSS 1988) on Remote Sensing: Moving Towards the 21st Century, volume 1
[ESA-SP-284-VOL-1] N89-12936
Polarization-dependent attenuation of dielectric cylinder arrays N89-12955
The use of remote sensing in conjunction with geographic information systems for local planning N89-12959
An integrated remote sensing approach for regional agrostatistics and land monitoring N89-12960

Communication: The key to integrating remote sensing and geographic information systems N89-12963
Integrating remote sensing data into a geographical information system: A foundation for rural land use strategies: Nature Conservancy Council project N89-12964
Data bases and remote sensing N89-12965
An international approach to GIS based on remote sensing and terrain classification --- geographic information system (GIS) N89-12966
Analysis of potato crop distribution using remotely sensed and environmental data in a pilot geographical information system N89-12967
European remote sensing satellite platforms for the 1990's N89-12978
Spatial resolution for remote sensing of forest plantations N89-12991
Relationships between the nitrogen content of grass and reflectance N89-13002
The LIMEX 1987 pilot project, LIMEX 1989 and long-term objective for data collection on the Canadian East coast N89-13037
Microwave emission behavior of snow N89-13041
Average areal water equivalent of snow in a mountain basin using microwave and visible satellite data N89-13045
Microwave remote sensing at the Institute for Space Research (INPE) Brazil: Concepts and future prospects of soil moisture studies N89-13080
Important aspects of technology transfer: Training of inservice engineers and scientists; satellite remote sensing N89-13082
Applications of remote sensing for geological mapping in eastern Egypt N89-13087
Biogeochemical processes in sagebrush steppe: Interactions of terrain, vegetation and chemical cycles [NASA-CR-181486] N89-13088

REMOTE SENSORS
Analysis of GEOSAT radar altimeter errors based on pre-launch test data [NASA-TM-101230] N89-12806
Proposed design of the temperature control system for the variable temperature calibration target for the Advanced Microwave Sounding Unit B N89-12942
Effects of changing satellite sensor attributes N89-13059

REMOTELY PILOTED VEHICLES
DOD joint Unmanned Aerial Vehicle (UAV) program master plan, 1988 [AD-A197751] N89-12563

REPORTS
Biogeochemical processes in sagebrush steppe: Interactions of terrain, vegetation and chemical cycles [NASA-CR-181486] N89-13088
NASA newsletters for the Weber Student Shuttle Involvement Project [NASA-TM-101001] N89-13144

REQUIREMENTS
Requirements and test results for the qualification of thermal control coatings N89-12616
Moisture interaction and stability of ZOT (Zinc Orthotitanate) thermal control spacecraft coating N89-12618
A multimegawatt space power source radiator design [DE88-015185] N89-12662
Temporal clustering in the multi-target tracking environment [AD-A197153] N89-12796
EMP (electromagnetic pulse) mitigation program approach [AD-A197849] N89-12807
Lunar surface transportation systems conceptual design lunar base systems study Task 5.2 [NASA-CR-172077] N89-12862
Laser driven inertial confinement fusion N89-13229
Development of high efficiency opaque photocathodes for the Region 900 angstrom to 1200 angstrom [NASA-CR-180597] N89-13249

RESEARCH AND DEVELOPMENT
The RACE Program of the European Communities [ONRL-8-014-R] N89-12811
HOST instrumentation R and D program overview N89-12878
Establishment of center for rotorcraft education and research [AD-A197141] N89-13295
Survey of supply/demand relationships for Japanese Technical Information in the United States: The field of advanced ceramics research and development [PB88-210943] N89-13300
Federal Laboratory Consortium for Technology Transfer: Putting technology to work. Examples of industry-laboratory cooperation contributing to our nation's economic strength [PB88-243357] N89-13307
Soviet exoatmospheric neutral particle beam research [FASAC-TAR-3110] N89-13390
AGARD handbook N89-13392
Research and technology [NASA-TM-100051] N89-13393

RESEARCH FACILITIES
Establishment of center for rotorcraft education and research [AD-A197141] N89-13295
Application of PN and avalanche silicon photodiodes to low-level optical N89-13317
Research and technology [NASA-TM-100051] N89-13393

RESEARCH MANAGEMENT
United States Air Force Graduate Student Summer Support Program, volume 1 [AD-A191121] N89-12754
High temperature superconductivity research in selected laboratories in West Germany [ONRL-8-011-R] N89-13291
Danish Space Research Institute N89-13391
Research and technology [NASA-TM-100051] N89-13393

RESEARCH VEHICLES
Simulating vehicle dynamics: The importance of a valid forcing function [DE88-010527] N89-13167

RESIDUES
Precision cleaning methods for spacecraft applications N89-12588

RESIN MATRIX COMPOSITES
Fingerprint test data report: FM 5834 test lots No. 1, 3, 4, and 5 --- resin matrix composites [NASA-CR-179419] N89-12722
Fingerprint test data report: FM 5064J (Kaiser) lots No. 1 (K) - No. 4 (K) --- resin matrix composites [NASA-CR-179409] N89-12723

RESOLUTION
Time-resolved solid-state array imaging systems: Developments and applications [DE88-016274] N89-13254

RESONANCE
Directed motion Doppler shift effects on nitric oxide (0.0) gamma band resonance absorption N89-12760
The Frascati (Italy) gravitational antenna, 1987 [IFSI-88-4] N89-12846

RESONATORS
Construction of a phase conjugate laser resonator using Brillouin enhanced four wave mixing N89-12759
Resonator design with an intracavity time-varying index gradient [DE88-015259] N89-12857

RESPONSE TIME (COMPUTERS)
The solution of linear systems of equations with a structural analysis code on the NAS CRAY-2 [NASA-CR-4159] N89-13202

RESTORATION
Survey of image restoration techniques [AD-A197470] N89-13251

RETINA
The effects of hyperbaric oxygen and antioxidant deficiencies on rat retinal ultrastructure N89-12772

REUSABLE SPACECRAFT
A conceptual design study of the reusable reentry satellite [NASA-TM-101043] N89-12623

REUSE
Cryogenic insulation system [NASA-CASE-LAR-13506-1] N89-12741

REVERSE FIELD PINCH
FIREBIRD: A conceptual design of a field reversed configuration Compact Torus Fusion Reactor (CTFR) N89-13230
Confinement dynamics in the reversed field pinch [DE88-009148] N89-13259

REVISIONS
An artificial compression method for ENO schemes: The slope modification method [NASA-CR-184613] N89-13215

REYNOLDS NUMBER
The stability of time-dependent fluid flows N89-12825

RIO GRANDE (NORTH AMERICA)
Average areal water equivalent of snow in a mountain basin using microwave and visible satellite data N89-13045

RISK
Stochastic calculus and survival analysis [AD-A197324] N89-13217

ROBOTICS
The flight robotics laboratory N89-12595
Gripping device [NASA-CASE-MSC-21365-1] N89-12865
Optically controlled welding system [NASA-CASE-MFS-29291-1] N89-12868
Advancing automation and robotics technology for the space station and for the US economy [NASA-TM-100989] N89-13198

ROBOTS
Optically controlled welding system [NASA-CASE-MFS-29291-1] N89-12868

ROCKET ENGINE CASES
Lightweight structural design of a bolted case joint for the space shuttle solid rocket motor [NASA-TP-2851] N89-12580

ROCKET ENGINE DESIGN
Advanced Earth-to-Orbit Propulsion Technology 1986, volume 2 [NASA-CP-2437-VOL-2] N89-12626
Aerojet TechSystems Company contribution to LOX/HC combustion and cooling technology N89-12646
Survey of LOX/hydrocarbon combustion and cooling N89-12647
LOX/hydrocarbon combustion and cooling survey N89-12648
Results of coaxial injector element testing N89-12651
Hydrogen-environment embrittlement and its control in high pressure hydrogen/oxygen rocket engines N89-12654

ROCKET ENGINES
Considerations in development and implementation of elasto-viscoplastic constitutive model for high temperature applications [NASA-CR-183403] N89-12932

ROCKET EXHAUST
A steam inerting system for hydrogen disposal for the Vandenberg Shuttle N89-12608

ROCKET TEST FACILITIES
Ariane 5 verification and associated test facilities N89-12611

ROCKET VEHICLES
Antenna pattern study [ARI/R-88-510Z] N89-12790

ROCKY MOUNTAINS (NORTH AMERICA)
Average areal water equivalent of snow in a mountain basin using microwave and visible satellite data N89-13045

RODS
Composite rods in carbon-epoxy Fibredux 914 C/TS-6T-6K-34 [SARMA-TR-87-2431A] N89-12677
Carbon-epoxy composite rods Fibredux 914 C/TS-6T-6K-34 [SARMA-TR-872429-A] N89-12678

ROLLING CONTACT LOADS
Rolling contact fatigue life of zirconium and molybdenum nitride sputter plated AMS 5749 bearing steel N89-12642

ROTARY WING AIRCRAFT
Establishment of center for rotorcraft education and research [AD-A197141] N89-13295

ROTARY WINGS
Foundations of the blade-vortex interaction problem: Structure and behavior of travelling compressible vortices [AD-A197370] N89-12550

ROTATING SHAFTS
Measurement of rotordynamic coefficients for a hydrostatic radial bearing N89-12643

ROTATION
Improved docking alignment system [NASA-CASE-MSC-21372-1] N89-12842

ROTOR AERODYNAMICS
Low-speed flexible rotor balancing for smooth, high-speed operation N89-12628
Efficient transient analysis methods for the Space Shuttle Main Engine (SSME) turbopumps N89-12630
Vibrations induced by nonlinearities in rotordynamics N89-12631

ROTOR BLADES (TURBOMACHINERY)
Measurement of airfoil heat transfer coefficients on a turbine stage N89-12897
Heat transfer in the tip region of a rotor blade simulator N89-12898

ROTORS
Development of a thermal and structural analysis procedure for cooled radial turbines [NASA-TM-101416] N89-12568
Low-speed flexible rotor balancing for smooth, high-speed operation N89-12628
The effects of internal rotor friction on dynamic characteristics of turbopumps N89-12629
Efficient transient analysis methods for the Space Shuttle Main Engine (SSME) turbopumps N89-12630
Vibrations induced by nonlinearities in rotordynamics N89-12631

RP-1 ROCKET PROPELLANTS
LOX/hydrocarbon combustion and cooling survey N89-12648

Liquid oxygen cooling of high pressure LOX/hydrocarbon rocket thrust chambers N89-12649
RP-1 and methane combustion and cooling experiments N89-12650

RULES
Classification decision rule modification on the basis of information extracted from training data --- satellite imagery N89-13062

RURAL LAND USE
Integrating remote sensing data into a geographical information system: A foundation for rural land use strategies: Nature Conservancy Council project N89-12964
The detection of unimproved grassland in Berkshire using a binary decision tree approach N89-12988
Evaluation of LANDSAT TM and SPOT imagery for agricultural land use planning in less developed countries N89-13051

S

S MATRIX THEORY
De-embedding S-parameter measurements using TSD technique N89-12783
The effects of undersampling on multipolarization SAR images N89-12956

S WAVES
S-waves in the spectrum of cataclysmic binaries N89-13380

SAFETY
Fuel alcohol formulations [DE88-016753] N89-12748

SAHARA DESERT (AFRICA)
Applications of remote sensing for geological mapping in eastern Egypt N89-13087

SAMPLING
Phase coherence and Signal-To-Noise ratio considerations for sampled aperture radar systems [AD-A197180] N89-12797

SARGASSO SEA
Optical modeling of clear ocean light fields: Raman scattering effects [AD-A197249] N89-13129

SATELLITE ALTIMETRY
Geodynamics laser ranging system: Performance simulations and development of the EOS facility --- Earth Observing System (EOS) N89-12982

SATELLITE ATTITUDE CONTROL
Requirements for the Advanced Earth Observing Satellite (ADEOS) orbit, orbit and a attitude control, and rate jitter N89-12981

SATELLITE CONTROL
Advanced workstations for Meteosat command and control, volume 1 [BSO/AETR87030101-VOL-1] N89-12573
Advanced workstations for Meteosat command and control. Volume 2: Appendices [BSO/AETR87030101-VOL-2] N89-12574

SATELLITE DESIGN
Results of Advanced Earth Observing Satellite (ADEOS) conceptual study N89-12980

SATELLITE IMAGERY
An integrated remote sensing approach for regional agrostatistics and land monitoring N89-12960
Spectral analysis of ocean wave imagery using 2-D linear prediction N89-12968
Topographic effects on light scattering from snow N89-12976
Multitemporal resource complex analysis of Catinia province, Italy from LANDSAT-TM data N89-12985
Large area TM land cover classification of Mittlerer Oberrhein County, southwest Germany, and its use for regional planning and crop surveys N89-12986
Towards an urban land-use classification using textural and morphological criteria N89-12987
The detection of unimproved grassland in Berkshire using a binary decision tree approach N89-12988
Detection of seasonal and long-term changes in land cover from multitemporal LANDSAT MSS data N89-12989
Verification results of MOS-1 multispectral self scanning radiometer (MESSR) data N89-13004
Performance modeling and results for X-SAR N89-13009
A regional tectonic study of NE and E Africa and its implication for mineral exploration: A synoptic view from satellite imagery N89-13023
The interpretation of Icelandic tundra features from LANDSAT-MSS data N89-13027
Complex SAR imagery and speckle filtering for ERS-1 wave mode N89-13029
Analysis of Seasat SAR sea-ice data from the Beaufort Sea N89-13035
Improvement in NOAA-AVHRR snowcover determination for runoff prediction N89-13040
Snowmelt runoff estimation using snow cover extent data and its application to optimum control of dam water level N89-13042
Monitoring of seasonal snow cover on glaciers N89-13044
Microcomputers (PCs) for snow cover analyses using multisensor satellite data N89-13049
Evaluation of LANDSAT TM and SPOT imagery for agricultural land use planning in less developed countries N89-13051
Combining spectral and structural analyses to select useful cartographic information from SPOT imagery N89-13052
Extraction of dense digital elevation models from SPOT stereo imagery N89-13053
The differential rectification of SPOT HRV panchromatic and multispectral imagery using a digital elevation model N89-13054
LANDSAT Thematic Mapping (TM) and SPOT HRV for survey mapping of bedrock outcrops N89-13055
The production of anaglyphs from SPOT-HRV panchromatic data for geomorphological mapping N89-13056
An evaluation of satellite imagery, LANDSAT Thematic Mapper and SPOT-1 HRV, for grassland inventory in the UK N89-13057
Monitoring urban change from LANDSAT TM and SPOT satellite imagery by image differencing N89-13058
Effects of changing satellite sensor attributes N89-13059
Efficient classification of multispectral images by a best linear discriminant function N89-13060
A new spatial classification algorithm for high ground resolution images N89-13061
Classification decision rule modification on the basis of information extracted from training data --- satellite imagery N89-13062
Accuracy of land cover classification of Thematic Mapper (TM) and SPOT data N89-13066
The extrapolation of spectral signatures illustrates LANDSATS' potential to detect wetlands N89-13067
Change direction analysis using LANDSAT imagery: A review of methodology N89-13068
Building a monitoring system based on satellite data to detect vegetation and land use changes in a subtropical region of Mexico N89-13079
Important aspects of technology transfer: Training of inservice engineers and scientists; satellite remote sensing N89-13082

SATELLITE NETWORKS
Study of the integration of advanced communications satellite systems and terrestrial networks, executive summary [ESA-CR(P)-2655] N89-12809

SATELLITE ORBITS
Results of true-anomaly regularization in orbital mechanics N89-12577
Requirements for the Advanced Earth Observing Satellite (ADEOS) orbit, orbit and a attitude control, and rate jitter N89-12981

SATELLITE PERTURBATION
Results of true-anomaly regularization in orbital mechanics N89-12577

SATELLITE SOUNDING
Rainfall index over oceans derived from SSM/I data --- Special Sensor Microwave/Imager (SSM/I) N89-12998
Cloud track winds from polar orbiting satellites N89-13069
Precipitation detection with satellite microwave data [PB88-240239] N89-13094
Space-time spectral studies of global stratospheric temperature fields N89-13106

SATELLITE TRACKING
Functional description of signal processing in the Rogue GPS receiver [NASA-CR-183314] N89-12813

SATELLITE-BORNE INSTRUMENTS
The Airborne Version Conical Scan Radiometer (AVCSR): An airborne radiometer as a tool for satellite data validation N89-12937
The airborne radiometry experiment (ABREX) instrument, an experimental test bed for the specification of satellite-borne microwave radiometer at 90 GHz N89-12939
Verification results of MOS-1 multispectral self scanning radiometer (MESSR) data N89-13004
Performance of a scanning pencil-beam spaceborne scatterometer for ocean wind measurements N89-13073
The MEOSS experiment: A test case for future cartographic missions N89-13081

SATELLITE-BORNE RADAR
Design of a spaceborne radar for tropical rain mapping at the climatological scale N89-12997
Image simulation of complex geometric targets for spaceborne synthetic aperture radar N89-13010

SAUDI ARABIA
Mapping the distribution and abundance of lithological units and surface mineralogies at Jabal Sa'id, Saudi Arabia: An application of spectral mixture modelling N89-13024

SAWTOOTH WAVEFORMS
Toroidal studies of sawtooth oscillations in tokamaks [DE88-017115] N89-13264

SCALE (CORROSION)
In-situ high temperature oxidation studies [DE88-017092] N89-12716

SCANNING
Studies of ultrathin polymer films for lithographic applications [AD-A197297] N89-12731

SCATTERING
Theoretical study of turbulent channel flow: Bulk properties, pressure fluctuations, and propagation of electromagnetic waves [NASA-TM-101248] N89-12830
The applicability of Rutherford scattering for Ti measurements at medium and large-sized experiments N89-13273

SCATTERING CROSS SECTIONS
Constraints on two-scale descriptions of radar backscattering from the sea surface using scatterometer model functions N89-12945
Millimeter-wave backscatter measurements of various snow forms N89-13046

SCATTERING FUNCTIONS
Laser speckle from thin and cascaded diffusers [AD-A197066] N89-12850

SCATTEROMETERS
Constraints on two-scale descriptions of radar backscattering from the sea surface using scatterometer model functions N89-12945
Towards direct variational assimilation of scatterometer backscatter measurements into numerical weather prediction models N89-13000
Model-based estimation of wind fields over the ocean from wind scatterometer measurements N89-13070
An analysis of directional ambiguities in wind scatterometer measurements N89-13071
Multistatic scatterometry N89-13072
Performance of a scanning pencil-beam spaceborne scatterometer for ocean wind measurements N89-13073
Effects of rainfall on scatterometer derived wind speeds N89-13074
Radar control, detection and processing electronics design as used for the ERS-1 wind scatterometer space segment N89-13075
The Canada Centre for Remote Sensing (CCRS) ground-based microwave facility --- scatterometer N89-13076

SCENE ANALYSIS
The effect of attentional focus level on task performance utilizing information from different stimulus structure levels N89-12765
The structure of red-infrared scattergrams of semivegetated landscapes [NASA-CR-183385] N89-13091

SCINTILLATION COUNTERS
Liquid scintillation counting with the Packard 1500 analyzer N89-12782

SCREW PINCH
Recent results of the toroidal screw pinch SPICA 2 N89-13271

SEA ICE
SAR-seen multimode waves in ice: Evidence of imaging nonlinearities N89-12971
SAR image statistics related to atmospheric drag over sea ice N89-13034
Analysis of Seasat SAR sea-ice data from the Beaufort Sea N89-13035
Microwave dielectric properties of low-salinity sea ice N89-13036
The LIMEX 1987 pilot project, LIMEX 1989 and long-term objective for data collection on the Canadian East coast N89-13037
Sea ice type classification of SAR imagery N89-13039
Arctic oceanography and meteorology review [AD-A196533] N89-13126
Bering Sea wave and ice measurements in support of Arctic west winter 1986 [AD-A197196] N89-13127

SEA SURFACE TEMPERATURE
Estimation of sea surface temperature via NOAA-AVHRR sensor: Comparison with sea truth data by fixed buoys N89-13005

SEA TRUTH
Estimation of sea surface temperature via NOAA-AVHRR sensor: Comparison with sea truth data by fixed buoys N89-13005

SEALS (STOPPERS)
Damping seal tester progress and initial test results N89-12627
Dynamics of face and annular seals with two-phase flow
[NASA-CR-183352] N89-12870
SEARCH PROFILES
Locating and search procedures with helicopters for sea and/or air emergencies
[FPN-0079] N89-12556
SEASAT SATELLITES
Analysis of Seasat SAR sea-ice data from the Beaufort Sea N89-13035
SECONDARY FLOW
Influence of bulk turbulence and entrance boundary layer thickness on the curved duct flow field N89-12896
SECURITY
EMP (electromagnetic pulse) mitigation program approach
[AD-A197849] N89-12807
SEDIMENT TRANSPORT
Monitoring playas using Thematic Mapper data N89-13028
SEGMENTS
Alterations of segmental volume during orthostatic stress in nonhuman primates N89-12769
PIPS: A Procedure for Interactive Pyramid Segmentation N89-12984
SELF ADAPTIVE CONTROL SYSTEMS
Self-actuating heat switches for redundant refrigeration systems
[NASA-CASE-NPO-17085-1-CU] N89-12785
SEMANTICS
Natural language generation
[AD-A197321] N89-12800
Preattentive and attentive visual information processing
[AD-A197670] N89-13139
SNePS considered as a fully intensional propositional semantic network N89-13184
Belief revision in SNePS N89-13185
SEMICONDUCTOR DEVICES
Semiconductor bridge (SCB) igniter studies. 2: Comparison of SCB and hot-wire direct propulsion thrusters
[DE88-008803] N89-12625
Electrogenerated chemiluminescence
[AD-A197163] N89-12691
SEMICONDUCTOR DIODES
Tm,Ho:YLF laser end-pumped by a semiconductor diode laser array
[NASA-CASE-NPO-17282-1-CU] N89-12856
Radiation effects in semiconductor laser diode arrays
[DE88-016318] N89-12859
SEMICONDUCTOR LASERS
Radiation effects in semiconductor laser diode arrays
[DE88-016318] N89-12859
SEMICONDUCTOR PLASMAS
Fundamental studies and device development in beta silicon carbide
[AD-A197843] N89-12739
SEMICONDUCTORS (MATERIALS)
The 6th All-Union Conference on Nonlinear Optics (table of contents)
[AD-A197347] N89-13250
SENSORS
An optical sensor system for monitoring structural dynamics with applications to system identification N89-12775
Wavelength or sensor selection by minimization of prediction error
[AD-A197231] N89-13216
SENTENCES
The effects of high noise levels on the acoustic-phonetic structure of speech: A preliminary investigation N89-12764
SEPARATED FLOW
Unsteady structure of flow past a pitching delta wing N89-12541
Control of laminar separation over airfoils by acoustic excitation
[NASA-TM-101379] N89-12552
Evaluation of three turbulence models for the prediction of steady and unsteady airloads
[NASA-TM-101413] N89-12555
A comparative study of differing vortex structures arising in unsteady separated flows N89-12773
SEQUENCING
Achieving speedups for a shared memory model language on an SIMD parallel computer
[AD-A197102] N89-13176
SERIES EXPANSION
New methods for locating phase boundaries
[DE88-017084] N89-12700
SERVICE LIFE
Surface characteristics of liquid oxygen cooled ball bearings N89-12640
Research on mechanical properties for engine life prediction
[AD-A197816] N89-12864
Life prediction and constitutive models for engine hot section N89-12916
Thermal barrier coating life prediction model development N89-12920
Thermal barrier coating life prediction model N89-12921
Thermal barrier coating life prediction model development N89-12922
SEYFERT GALAXIES
Synthesis of accretion disk and nonthermal source models for AGN
[DE88-013098] N89-13384
SHADOWS
Shadows and wedges in scattering from the sea N89-12946
SHEAR FLOW
A spectral collocation solution to the compressible stability eigenvalue problem
[NASA-TP-2858] N89-12543
SHEAR PROPERTIES
Combined pressure-shear ignition sensitivity test
[AD-A197076] N89-12749
SHEAR STRENGTH
Thermoplastic adhesives based on 4,4'-isophthaloyldiphthalic anhydride (IDPA)
[NASA-TM-101508] N89-12747
SHELL THEORY
Two different methods for shell buckling calculation in the elastic-plastic region
[DFVLR-FB-88-26] N89-12933
SHELLS (STRUCTURAL FORMS)
Dynamic synthesis of joined/hermetic shell structures using state space method N89-12874
Non-isothermal buckling behavior of viscoplastic shell structures
[NASA-CR-183013] N89-12931
SHELTERS
Wave propagation in layered structures N89-12777
SHOCK HEATING
Recent results of the toroidal screw pinch SPICA 2 N89-13271
SHOCK SPECTRA
Pyro shock simulation: Experience with the MIPS simulator N89-12583
SHOCK TESTS
Pyro shock simulation: Experience with the MIPS simulator N89-12593
SHOCK WAVES
The standardized Bauer piezoelectric polymer shock gauge
[DE88-014963] N89-12840
Theoretical studies of mass loss and shock phenomena in cool star envelopes
[NASA-CR-182708] N89-13375
SHUTTLE DERIVED VEHICLES
Definition of a space transportation systems cargo element (Shuttle-C). Orientation
[NASA-CR-179404] N89-12579
SHUTTLE IMAGING RADAR
Directional ocean wave spectra: Prospects for acquiring a global data base from SIR-C N89-12973
The relativity utility of LANDSAT MSS and SIR-A imagery in reconnaissance geological mapping in Northern Sudan N89-13022
The derivation of sub-canopy surface terrain models of coastal forests using synthetic aperture radar N89-13083
SIGNAL ANALYSIS
Statistical properties of phase difference between two orthogonally-polarised SAR signals N89-12953
SIGNAL DETECTION
On adaptive cell-averaging CFAR radar signal detection N89-12792
SIGNAL DETECTORS
Wavelength or sensor selection by minimization of prediction error
[AD-A197231] N89-13216
SIGNAL PROCESSING
Functional description of signal processing in the Rogue GPS receiver
[NASA-CR-183314] N89-12813
Automatic control of a multi-channel millimeter wave radiometer N89-12938
An approach to automate digital signal processor code generation
[ETN-88-93530] N89-13172
Multivariate regression with emphasis on multivariate spline methods
[AD-A197793] N89-13209
On the simulation of harmonically related signals
[AD-A197821] N89-13235
SIGNAL TO NOISE RATIOS
Phase coherence and Signal-To-Noise ratio considerations for sampled aperture radar systems
[AD-A197180] N89-12797
SIGNATURE ANALYSIS
The extrapolation of spectral signatures illustrates LANDSATS' potential to detect wetlands N89-13067
Spectral characterization of forest damage in beech, oak and pine stands N89-13085
SILANES
Preparation and properties of high-deposition-rate a-Si:H films and solar cells using disilane
[DE88-001191] N89-13098
SILICATES
Optical properties of cometary grains N89-13363
SILICON
Ion beam mixing of metals and ceramics: Material considerations
[DE88-016797] N89-12744
Large silicon clusters: Confirmation of Phillips' conjecture
[AD-A197487] N89-13241
Tests of a multichannel photometer based on silicon diode detectors N89-13314
SILICON CARBIDES
Synthesis and characterization of VLS-derived silicon carbide whiskers
[DE88-016226] N89-12679
SiC whisker-reinforced MoSi2
[DE88-016674] N89-12680
Fundamental studies and device development in beta silicon carbide
[AD-A197843] N89-12739
SILICON DIOXIDE
Laboratory simulations of comet surfaces N89-13366
SILICON FILMS
As-deposited low-strain LPCVD (Low-Pressure, Chemical-Vapor-Deposition) polysilicon
[DE88-016980] N89-12789
Applications of polysilicon films in microsensors and microactuators
[DE88-016979] N89-12844
SILICON NITRIDES
Slurry-pressing consolidation of silicon nitride
[NASA-TM-101365] N89-12746
SILICON POLYMERS
As-deposited low-strain LPCVD (Low-Pressure, Chemical-Vapor-Deposition) polysilicon
[DE88-016980] N89-12789
Applications of polysilicon films in microsensors and microactuators
[DE88-016979] N89-12844
SIMD (COMPUTERS)
Practical algorithms for image component labeling on SIMD mesh connected computers
[AD-A197341] N89-13158
Achieving speedups for a shared memory model language on an SIMD parallel computer
[AD-A197102] N89-13176
SIMULATION
A two-dimensional numerical simulation of a supersonic, chemically reacting mixing layer
[NASA-TM-4055] N89-12542
LORAN C Offshore Flight Following (LOFF) in the Gulf of Mexico
[AD-A197179] N89-12558
An evaluation of ground collision avoidance system algorithm
[AD-A197831] N89-12560
The flight robotics laboratory N89-12595
IRIS thermal balance test within ESTEC LSS N89-12603
Simulation of the effects of the orbital debris environment on spacecraft N89-12607
The solar simulation test of the ITALSAT thermal structural model N89-12613
Corrosion of nickel and Monel welds of steel in chlorine trifluoride
[DE88-014122] N89-12706
Bioelectromagnetic effects of EMP: Preliminary findings
[DE88-012118] N89-12791
Backscatter laser depolarization studies of simulated stratospheric aerosols: Crystallized sulfuric acid droplets
[NASA-CR-183387] N89-13111
On the simulation of harmonically related signals
[AD-A197821] N89-13235
Improvements to photometry. Part 1: Better estimation of derivatives in extinction and transformation equations N89-13322
SIMULATORS
Pyro shock simulation: Experience with the MIPS simulator N89-12593

Image simulation of complex geometric targets for spaceborne synthetic aperture radar N89-13010

SINGLE CRYSTALS

Effects of high mean stress on the high-cycle fatigue of PWA 1480 and DS MAR M 246 + Hf at 1000 F N89-12633

Constitutive behavior of single crystal PWA 1480 and directionally solidified MAR-M 246 under monotonic and cyclic loads at high and low temperature N89-12634

Hydrogen effects on the fatigue and tensile behavior of CMSX-2 nickel base superalloy single crystals N89-12658

Surface structures and transitions and the evolution from firm to bulk behavior
[AD-A197788] N89-12695

Optical constants of minerals and other materials from the millimeter to the ultraviolet
[AD-A197803] N89-12696

Constitutive modeling for single crystal superalloys N89-12911

Constitutive modelling of single crystal and directionally solidified superalloys N89-12912

Preparation and structure of Li-stabilized Na(+) beta' alumina single crystals
[AD-A197245] N89-13283

Chemical precursors to zinc sulfide: ZnS whisker synthesis
[AD-A197262] N89-13284

SINTERING

Coble creep, cavity sintering and cavity growth
[DE88-013846] N89-12703

SITES

Charge transfer in multiple site chemical systems
[AD-A197143] N89-12666

SIZE DISTRIBUTION

Light extinction in a dispersion of small nematic droplets
[AD-A197201] N89-12729

SKEWNESS

Scattering from a skewed random surface --- radar scattering N89-12948

SKIN (STRUCTURAL MEMBER)

Analysis of the Space Shuttle Orbiter skin panels under simulated hydrodynamic loads
[NASA-TM-4082] N89-12935

SLABS

Temperature profile in semi-infinite planar slab with exponential source and convective boundary condition: Application to laser heating
[DE88-016746] N89-12831

SLOPES

An artificial compression method for ENO schemes: The slope modification method
[NASA-CR-184613] N89-13215

SLURRIES

Slurry-pressing consolidation of silicon nitride
[NASA-TM-101365] N89-12746

SNOW

Precision cleaning methods for spacecraft applications N89-12588

Topographic effects on light scattering from snow N89-12976

Microwave emission behavior of snow N89-13041

Polarisation of passive microwave signals as indicator of snow water equivalent N89-13043

Millimeter-wave backscatter measurements of various snow forms N89-13046

The incorporation of sulfur dioxide into snow and depositing ice N89-13116

SNOW COVER

Improvement in NOAA-AVHRR snowcover determination for runoff prediction N89-13040

Snowmelt runoff estimation using snow cover extent data and its application to optimum control of dam water level N89-13042

Monitoring of seasonal snow cover on glaciers N89-13044

Average areal water equivalent of snow in a mountain basin using microwave and visible satellite data N89-13045

Statistics and high resolution imaging of snowpack at 35 GHz using a microcomputer N89-13047

Snow cover to alter terrain signatures on radar images N89-13048

Microcomputers (PCs) for snow cover analyses using multisensor satellite data N89-13049

SOFTWARE ENGINEERING

Automation software for a materials testing laboratory N89-12917

Implementation issues for level O image processor software within an application package
[AD-A197768] N89-13162

SOFTWARE TOOLS

Making statistical inferences about software reliability
[NASA-CR-4197] N89-13153

SOIL MOISTURE

Laboratory evaluation of a field portable dielectric/soil moisture probe N89-13006

Microwave remote sensing at the Institute for Space Research (INPE) Brazil: Concepts and future prospects of soil moisture studies N89-13080

The structure of red-infrared scattergrams of semivegetated landscapes
[NASA-CR-183385] N89-13091

SOL-GEL PROCESSES

Sol-gel routes to superconducting ceramics
[DE88-015128] N89-12724

SOLAR ACTIVITY

Tenth European Regional Astronomy Meeting of the IAU: Abstracts
[DE88-703273] N89-13370

SOLAR CELLS

Radiation resistance and comparative performance of ITO/InP and n/p InP homojunction solar cells
[NASA-TM-101387] N89-12819

Metallization and characterization of a silicon p-n junction diode fabricated from a solar-cell-type silicon substrate
[DE88-703007] N89-13096

Solar photovoltaic technology: The thin film option
[DE88-001195] N89-13102

SOLAR COLLECTORS

Phase 2 testing of a molten salt central receiver
[DE88-012701] N89-13095

SOLAR CORONA

Aerodynamic properties of fractal grains: Implications for the primordial solar nebula N89-13361

Growth and sedimentation of dust grains in the primitive solar nebula N89-13374

SOLAR CYCLES

Evidence for temporal variation in the acoustic and f-mode eigenfrequency spectrum of the Sun
[DE88-015650] N89-13389

SOLAR FLARES

C IV fluxes from the Sun as a star, and the correlation with magnetic flux
[NASA-CR-182719] N89-13387

SOLAR NEUTRINOS

Solar monopoles and terrestrial neutrinos
[DE88-010677] N89-13388

SOLAR RADIATION

The NASA atomic oxygen effects test program N89-12589

The solar simulation test of the ITALSAT thermal structural model N89-12613

Evidence for temporal variation in the acoustic and f-mode eigenfrequency spectrum of the Sun
[DE88-015650] N89-13389

SOLAR SIMULATORS

Fifteenth Space Simulation Conference: Support the Highway to Space Through Testing
[NASA-CP-3015] N89-12582

Indian LSSC (Large Space Simulation Chamber) facility N89-12601

Solar simulation with a rectangular beam N89-12605

Test data acquisition system for the ESTEC large solar simulator at ESA/ESTEC N89-12620

SOLAR SYSTEM

Activities report of the Institute of Extraterrestrial Activities
[MPE-208] N89-13308

SOLID LUBRICANTS

Lubrication evaluation of SSME turbopump bearings N89-12639

Boric oxide as a solid lubricant additive in molybdenum disulfide
[AD-A197109] N89-12727

SOLID PROPELLANT COMBUSTION

Report on JANNAF Workshop Influence of Gas-Phase Chemical Kinetics on Low-Pressure Ignition and Flamespreading in Solid Propellant
[AD-A197854] N89-12751

SOLID PROPELLANT IGNITION

Report on JANNAF Workshop Influence of Gas-Phase Chemical Kinetics on Low-Pressure Ignition and Flamespreading in Solid Propellant
[AD-A197854] N89-12751

SOLID PROPELLANT ROCKET ENGINES

Test stand design and analysis for Titan 34D static firing N89-12609

Test stand for Titan 34D SRM static firing N89-12610

SOLID STATE

Time-resolved solid-state array imaging systems: Developments and applications
[DE88-016274] N89-13254

SOLIDIFICATION

Challenging applications for hydrated and chemically reacted ceramics
[DE88-015397] N89-12742

SOLIDS

Advanced instrumentation for local measurement of gas-solid suspension flows
[DE88-017087] N89-12833

SOLVENT RETENTION

Supercritical fluid chromatography: The effect of the partial molar volume in the stationary phase on retention
[DE88-016959] N89-12699

SONAR

Arctic oceanography and meteorology review
[AD-A196533] N89-13126

SONIC ANEMOMETERS

Wind tunnel investigation of the response of a sonic anemometer
[PB88-249826] N89-12847

SOUND FIELDS

Nearfield acoustic radiation from a point-excited cylindrical shell
[AD-A197282] N89-13234

SOUND TRANSMISSION

Parabolic equation model
[AD-A197480] N89-13161

SPACE COMMERCIALIZATION

SP-100 nuclear space power systems with application to space commercialization
[NASA-TM-101403] N89-12665

ERS data policy N89-13078

SPACE DEBRIS

Simulation of the effects of the orbital debris environment on spacecraft N89-12607

SPACE ENVIRONMENT SIMULATION

Fifteenth Space Simulation Conference: Support the Highway to Space Through Testing
[NASA-CP-3015] N89-12582

SPACE ERECTABLE STRUCTURES

Space station erectable manipulator placement system
[NASA-CASE-MSC-21096-1] N89-12621

SPACE EXPLORATION

SP-100 nuclear space power systems with application to space commercialization
[NASA-TM-101403] N89-12665

Preliminary applications of decentralized estimation to large flexible space structures N89-12761

SPACE FLIGHT

United States space policy: Review and assessment
[DE88-015538] N89-13306

SPACE LAW

United States space policy: Review and assessment
[DE88-015538] N89-13306

SPACE OBSERVATIONS (FROM EARTH)

The NASA Infrared Telescope Facility Comet Halley monitoring program 2: Post-perihelion results N89-13368

SPACE PLASMAS

Activities report of the Institute of Extraterrestrial Activities
[MPE-208] N89-13308

SPACE PLATFORMS

Control of the induced microgravity environment of the Man Tended Free Flyer (MTFF) N89-12606

SPACE POWER REACTORS

A multimegawatt space power source radiator design
[DE88-015185] N89-12662

SP-100 nuclear space power systems with application to space commercialization
[NASA-TM-101403] N89-12665

SPACE POWER UNIT REACTORS

Fission fragment rockets: A potential breakthrough
[DE88-016953] N89-12664

SPACE PROGRAMS

Australian preparations for the Polar Platform N89-12979

SPACE SHUTTLE MAIN ENGINE

Lightweight structural design of a bolted case joint for the space shuttle solid rocket motor
[NASA-TP-2851] N89-12580

A steam inerting system for hydrogen disposal for the Vandenberg Shuttle N89-12608

Advanced Earth-to-Orbit Propulsion Technology 1986, volume 2
[NASA-CP-2437-VOL-2] N89-12626

Damping seal tester progress and initial test results N89-12627

Low-speed flexible rotor balancing for smooth, high-speed operation N89-12628

Efficient transient analysis methods for the Space Shuttle Main Engine (SSME) turbopumps N89-12630

Vibrations induced by nonlinearities in rotordynamics N89-12631

Simplified cyclic structural analysis of SSME turbine blades N89-12632

Constitutive behavior of single crystal PWA 1480 and directionally solidified MAR-M 246 under monotonic and cyclic loads at high and low temperature N89-12634

Thermo-mechanical performance evaluation of cryogenic turbopump ball bearings N89-12637
Thermal analysis of SSME turbopump bearings N89-12638
Lubrication evaluation of SSME turbopump bearings N89-12639
Surface characteristics of liquid oxygen cooled ball bearings N89-12640
Powder metallurgy bearings for advanced rocket engines N89-12641
Measurement of rotordynamic coefficients for a hydrostatic radial bearing N89-12643
Surface modification for wear resistance in a liquid oxygen turbopump environment N89-12644
SSME bearing health monitoring using a fiberoptic deflectometer N89-12645
Combustion modeling: Progress and projections N89-12652
Effects of oxygen/hydrogen combustion chamber environment on copper alloys N89-12653
Hydrogen-environment embrittlement and its control in high pressure hydrogen/oxygen rocket engines N89-12654
Mass flow meter using the triboelectric effect for measurement in cryogenics [NASA-CR-179572] N89-12836

SPACE SHUTTLE MISSION 41-B
NASA newsletters for the Weber Student Shuttle Involvement Project [NASA-TM-101001] N89-13144

SPACE SHUTTLES
Definition of a space transportation systems cargo element (Shuttle-C). Orientation [NASA-CR-179404] N89-12579
IRIS thermal balance test within ESTEC LSS N89-12603
Development of polyisocyanurate pour foam formulation for space shuttle external tank thermal protection system [NASA-CR-183511] N89-12745
Analysis of the Space Shuttle Orbiter skin panels under simulated hydrodynamic loads [NASA-TM-4082] N89-12935

SPACE SIMULATORS
Fifteenth Space Simulation Conference: Support the Highway to Space Through Testing [NASA-CP-3015] N89-12582
Space simulators for laser optics N89-12597
Development of a two axis motion simulation system for thermal/vacuum satellite testing N89-12598
The two axis motion simulator for the large space simulator at ESTEC (European Space Research and Technology Center) N89-12600
IRIS thermal balance test within ESTEC LSS N89-12603
Solar simulation with a rectangular beam N89-12605
Cost effective alternative to low irradiance measurements N89-12619

SPACE STATION POLAR PLATFORMS
Australian preparations for the Polar Platform N89-12979
On-orbit servicing and cost effectiveness of Columbus Polar Platform concepts N89-12983

SPACE STATIONS
A teacher's companion to the space station: A multi-disciplinary resource N89-12575
Space station integrated propulsion and fluid systems study [NASA-CR-179393] N89-12581
Fifteenth Space Simulation Conference: Support the Highway to Space Through Testing [NASA-CP-3015] N89-12582
Atomic oxygen studies on polymers N89-12591
Space station docking mechanism dynamic testing N89-12596
Comparison of sulfuric and oxalic acid anodizing for preparation of thermal control coatings for spacecraft N89-12617
Space station erectable manipulator placement system [NASA-CASE-MSC-21096-1] N89-12621
Advancing automation and robotics technology for the space station and for the US economy [NASA-TM-100989] N89-13198

SPACE WEAPONS
United States space policy: Review and assessment [DE88-015538] N89-13306

SPACE-TIME FUNCTIONS
Space-time spectral studies of global stratospheric temperature fields N89-13108
How to test the special theory of relativity on rotating earth [DE88-703048] N89-13293
Gravitation, black holes and space-time physics [DE88-703054] N89-13377

SPACEBORNE EXPERIMENTS
Modes of operation of the RETE experiment [IFSI-88-5] N89-12576
Microgravity science and applications program tasks, 1987 revision [NASA-TM-4068] N89-12752

SPACECRAFT ANTENNAS
Antenna pattern study [ARI/R-88-510Z] N89-12790

SPACECRAFT COMPONENTS
Precision cleaning methods for spacecraft applications N89-12588
The NASA atomic oxygen effects test program N89-12589
Materials selection for long life in LEO: A critical evaluation of atomic oxygen testing with thermal atom systems N89-12590
Atomic oxygen studies on polymers N89-12591
Atomic oxygen effects on candidate coatings for long-term spacecraft in low earth orbit N89-12592
Indian LSSC (Large Space Simulation Chamber) facility N89-12601
Moisture interaction and stability of ZOT (Zinc Orthotitanate) thermal control spacecraft coating N89-12618
Superionic conductors as fast, repetitive opening switches [AD-A197365] N89-12817

SPACECRAFT CONSTRUCTION MATERIALS
The NASA atomic oxygen effects test program N89-12589
Materials selection for long life in LEO: A critical evaluation of atomic oxygen testing with thermal atom systems N89-12590
Atomic oxygen studies on polymers N89-12591
Atomic oxygen effects on candidate coatings for long-term spacecraft in low earth orbit N89-12592

SPACECRAFT CONTAMINATION
Fifteenth Space Simulation Conference: Support the Highway to Space Through Testing [NASA-CP-3015] N89-12582

SPACECRAFT CONTROL
Control of the induced microgravity environment of the Man Tended Free Flyer (MTFF) N89-12606

SPACECRAFT DESIGN
Class 100 large spacecraft facility N89-12586
Thermal/structural design verification strategies for large space structures N89-12602
A conceptual design study of the reusable reentry satellite [NASA-TM-101043] N89-12623

SPACECRAFT DOCKING
Space station docking mechanism dynamic testing N89-12596

SPACECRAFT ELECTRONIC EQUIPMENT
Radar control, detection and processing electronics design as used for the ERS-1 wind scatterometer space segment N89-13075

SPACECRAFT ENVIRONMENTS
The NASA atomic oxygen effects test program N89-12589
Materials selection for long life in LEO: A critical evaluation of atomic oxygen testing with thermal atom systems N89-12590
Atomic oxygen studies on polymers N89-12591
Atomic oxygen effects on candidate coatings for long-term spacecraft in low earth orbit N89-12592
Control of the induced microgravity environment of the Man Tended Free Flyer (MTFF) N89-12606
Simulation of the effects of the orbital debris environment on spacecraft N89-12607

SPACECRAFT EQUIPMENT
The flight robotics laboratory N89-12595

SPACECRAFT INSTRUMENTS
Correlation studies on surface particle detection methods N89-12587
Pyro shock simulation: Experience with the MIPS simulator N89-12593
The Instrument Test Dewar (ITD): Testing satellite instruments at 1.5 K N89-12604

SPACECRAFT LAUNCHING
Space reactor assessment and validation study N89-13227

SPACECRAFT POWER SUPPLIES
Nuclear technology for the year 2000 [DE88-005041] N89-13223
Radioisotope space power generators: Design concepts N89-13224
Down scale of the SP-100 concept for 5 kWe N89-13225
Space reactor assessment and validation study N89-13227

SPACECRAFT PROPULSION
Advanced Earth-to-Orbit Propulsion Technology 1986, volume 2 [NASA-CP-2437-VOL-2] N89-12626
Aerojet TechSystems Company contribution to LOX/HC combustion and cooling technology N89-12646
21st century propulsion concept [AD-A197537] N89-12663
Fission fragment rockets: A potential breakthrough [DE88-016953] N89-12664

SPACECRAFT STRUCTURES
IRIS thermal balance test within ESTEC LSS N89-12603

SPARK GAPS
Spark ignition of monodisperse fuel sprays N89-12685
Tesla's coherent plasma discharge and a plan for megavolts at megahertz N89-13231

SPARK IGNITION
Spark ignition of monodisperse fuel sprays N89-12685

SPATIAL DISTRIBUTION
A new spatial classification algorithm for high ground resolution images N89-13061
On the microstructure theory of a condensate layer in a white dwarf atmosphere [DE88-703324] N89-13385

SPATIAL RESOLUTION
Spatial resolution for remote sensing of forest plantations N89-12991
The interrelationship between resampling method and information extraction technique N89-13065
C IV fluxes from the Sun as a star, and the correlation with magnetic flux [NASA-CR-182719] N89-13387

SPECIFICATIONS
Fuel alcohol formulations [DE88-016753] N89-12748

SPECKLE INTERFEROMETRY
Summary of laser speckle photogrammetry for HOST N89-12889

SPECKLE PATTERNS
Summary of laser speckle photogrammetry for HOST N89-12889
On the concept of the polarimetric matched filter in high resolution radar imaging: An alternative for speckle radiation N89-12954
On the use of speckle statistics for the extraction of ocean wave spectra from SAR imagery N89-12969
Complex SAR imagery and speckle filtering for ERS-1 wave mode N89-13029

SPECTRAL BANDS
An introduction to blocked impurity band detectors N89-13320

SPECTRAL ENERGY DISTRIBUTION
Kinetic effects on electron cyclotron emission during electron cyclotron heating in tokamaks N89-13268

SPECTRAL REFLECTANCE
The structure of red-infrared scattergrams of semivegetated landscapes [NASA-CR-183385] N89-13091

SPECTRAL SIGNATURES
The extrapolation of spectral signatures illustrates LANDSATS' potential to detect wetlands N89-13067
Spectral characterization of forest damage in beech, oak and pine stands N89-13085

SPECTROMETERS
Performance of the forward scattering spectrometer probe in NASA's icing research tunnel [NASA-TM-101381] N89-12845
A far-infrared heterodyne spectrometer for airborne astronomy N89-13329

SPECTROPHOTOMETERS
Use of optical fibers in spectrophotometry N89-13325

SPECTROPHOTOMETRY
Use of optical fibers in spectrophotometry N89-13325
Airborne 20-65 micron spectrophotometry of Comet Halley N89-13354
Some 5-13 micrometer airborne observations of Comet Wilson 1986l: Preliminary results N89-13360

SPECTROSCOPY
Recent advances at NASA in calculating the electronic spectra of diatomic molecules [NASA-TM-101034] N89-12622
Laser applications in flow diagnostics [AGARD-AG-296] N89-12849
Fiber optic wavelength division multiplexing: Principles and applications in telecommunications and spectroscopy N89-13324

SPECTRUM ANALYSIS
Multiple input/output random vibration control system N89-12594
Spectral analysis of ocean wave imagery using 2-D linear prediction N89-12968
An intercomparison of SAR and buoy directional wave spectra from the Labrador Sea Extreme Waves Experiment (LEWEX) N89-12972

Estimating aircraft SAR response characteristics and approximating ocean wave spectra in the Labrador Sea N89-13032
Combining spectral and structural analyses to select useful cartographic information from SPOT imagery N89-13052
The 3.4 micrometer emission feature in Comet Halley N89-13338
The problem of clustering in laboratory studies of cometary dust N89-13356

SPECULAR REFLECTION
Laser speckle from thin and cascaded diffusers [AD-A197066] N89-12850

SPEECH
The effects of high noise levels on the acoustic-phonetic structure of speech: A preliminary investigation N89-12764
Auditory models for speech analysis [AD-A197322] N89-12801
Exploring the back-propagation network for speech applications [AD-A197385] N89-12803

SPEECH RECOGNITION
Voice recognition and artificial intelligence in an air traffic control environment [AD-A197219] N89-12559
Robust recognition of loud and Lombard speech in the fighter cockpit environment [AD-A197093] N89-12795
Auditory models for speech analysis [AD-A197322] N89-12801
Exploring the back-propagation network for speech applications [AD-A197385] N89-12803

SPENT FUELS
Evaluation of boron carbide coatings N89-13228

SPHEROMAKS
Modified magnetic confinement configurations based on understanding helicity dissipation and pressure driven modes in the spheromak [DE88-009149] N89-13260

SPLINES
The effects of internal rotor friction on dynamic characteristics of turbopumps N89-12629
Multivariate regression with emphasis on multivariate spline methods [AD-A197793] N89-13209

SPLIT FLAPS
Aerodynamic pressures and heating rates on surfaces between split elevons at Mach 6.6 [NASA-TP-2855] N89-12822

SPOT (FRENCH SATELLITE)
Agroelecological information content of SPOT data N89-13050
Evaluation of LANDSAT TM and SPOT imagery for agricultural land use planning in less developed countries N89-13051
Combining spectral and structural analyses to select useful cartographic information from SPOT imagery N89-13052
Extraction of dense digital elevation models from SPOT stereo imagery N89-13053
The differential rectification of SPOT HRV panchromatic and multispectral imagery using a digital elevation model N89-13054
LANDSAT Thematic Mapping (TM) and SPOT HRV for survey mapping of bedrock outcrops N89-13055
The production of anaglyphs from SPOT-HRV panchromatic data for geomorphological mapping N89-13056
An evaluation of satellite imagery, LANDSAT Thematic Mapper and SPOT-1 HRV, for grassland inventory in the UK N89-13057
Monitoring urban change from LANDSAT TM and SPOT satellite imagery by image differencing N89-13058
Accuracy of land cover classification of Thematic Mapper (TM) and SPOT data N89-13066

SPRAYED COATINGS
Development of polyisocyanurate pour foam formulation for space shuttle external tank thermal protection system [NASA-CR-183511] N89-12745

SPRAYERS
Sample introduction using the Hildebrand grid nebulizer for plasma spectrometry [AD-A197145] N89-13257

SPREAD SPECTRUM TRANSMISSION
Application of autoregressive methods to adaptive excision of interfering tones from direct sequence spread spectrum communications systems [AD-A197801] N89-12805

SPUTTERING
A refined model for characterizing X-ray multilayers [DE88-013592] N89-12872

STABILITY
Moisture interaction and stability of ZOT (Zinc Orthotitanate) thermal control spacecraft coating N89-12618

STABILITY AUGMENTATION
AH-1F Instrument Meteorological Conditions (IMC) flight evaluations [AD-A197128] N89-12562
Radiative augmented combustion [AD-A197300] N89-12693

STABILIZATION
LEC (Liquid Encapsulated Czochralski) growth of inP with magnetic field assisted melt stabilization and heat transfer control [AD-A196748] N89-12688
Preliminary applications of decentralized estimation to large flexible space structures N89-12761
Stabilization and oscillation of an acoustically levitated object [NASA-CASE-NPO-16896-1-CU] N89-13236
A radio-frequency quadrupole accelerator longitudinal field stabilizer [DE88-014399] N89-13246

STAINLESS STEELS
Determination of surfaces of constant inelastic strain rate at elevated temperature N89-12910

STANDARDIZATION
Derivation of anthropometry based body fat equations for the Army's weight control program [AD-A197371] N89-13132
Boeing Military Airplane Company technical order transfer tests [DE88-012233] N89-13151

STANDARDS
Formulation of the proper equations for developing standards in coherent dual polarisation SAR imaging N89-13021
A reference standard for bidirectional reflection distribution function and bidirectional transmission distribution function measurement [NASA-CASE-MFS-28183-1] N89-13253

STARS
A fibre optic, four channel comparative photometer N89-13315
Improvements to photometry. Part 1: Better estimation of derivatives in extinction and transformation equations N89-13322

STATIC FIRING
Test stand for Titan 34D SRM static firing N89-12610

STATIC PRESSURE
Porous plug for reducing orifice induced pressure error in airfoils [NASA-CASE-LAR-13569-1] N89-12841

STATIC TESTS
Test stand design and analysis for Titan 34D static firing N89-12609

STATISTICAL ANALYSIS
Making statistical inferences about software reliability [NASA-CR-4197] N89-13153
Optimal fix estimators and a variation on the Cramer Rao lower bound [NASA-CR-183011] N89-13211

STATISTICAL DISTRIBUTIONS
Performance analysis of the Alliant FX/8 multiprocessor using statistical clustering [NASA-CR-183221] N89-13145
Two-sample inference for median survival times based on one-sample procedures for censored survival data [AD-A197776] N89-13218

STATISTICAL TESTS
Stochastic calculus and survival analysis [AD-A197324] N89-13217
Use of distance versus statistical distance in acceptance tests [NASA-CR-183353] N89-13220

STATORS
HOST turbine heat transfer subproject overview N89-12880
Turbine stator flow field simulations N89-12902

STEAM
A steam inerting system for hydrogen disposal for the Vandenberg Shuttle N89-12608

STEELS
Rolling contact fatigue life of zirconium and molybdenum nitride sputter plated AMS 5749 bearing steel N89-12642
The determination of mobile hydrogen in aerospace engine alloys N89-12659
High strain rate properties of structural aluminium N89-12705
Fatigue crack growth of 5456-H116 aluminum and HSLA-80 weldments [AD-A197830] N89-12712

STELLAR ACTIVITY
Properties of stellar activity in F stars N89-13369

STELLAR ATMOSPHERES
The transfer of cyclotron photons through neutron star atamospheres N89-13378
On the microstructure theory of a condensate layer in a white dwarf atmosphere [DE88-703324] N89-13385

STELLAR COLOR
The near-infrared polarization and color of Comet Halley: What can we learn about the grains N89-13348

STELLAR ENVELOPES
Theoretical studies of mass loss and shock phenomena in cool star envelopes [NASA-CR-182708] N89-13375
Mixing and structural changes during mass transfer in binary systems N89-13382

STELLAR EVOLUTION
Activities report of the Institute of Extraterrestrial Activities [MPE-208] N89-13308
The evolutionary status of young stellar mass loss driving sources as derived from IRAS observations [IFSI-88-12] N89-13386

STELLAR LUMINOSITY
The evolutionary status of young stellar mass loss driving sources as derived from IRAS observations [IFSI-88-12] N89-13386

STELLAR MAGNITUDE
Carlsberg meridian catalog La Palma no. 3: Observations of positions of stars and planets made in the year 1986 [ISBN-0-98-87006-3] N89-13372

STELLAR MASS ACCRETION
Mixing and structural changes during mass transfer in binary systems N89-13382

STELLAR MASS EJECTION
The evolutionary status of young stellar mass loss driving sources as derived from IRAS observations [IFSI-88-12] N89-13386

STELLAR MOTIONS
Carlsberg meridian catalog La Palma no. 3: Observations of positions of stars and planets made in the year 1986 [ISBN-0-98-87006-3] N89-13372

STELLAR SPECTRA
Observations of a complete sample of emission-line galaxies N89-13328
On the carbon abundance in Comet Halley derived from the 3 micron feature: Comparison with interstellar dust N89-13341
S-waves in the spectrum of cataclysmic binaries N89-13380

STEPPING MOTORS
Circuit for actuation of a stepping motor [INPE-4633-NTE/281] N89-12814

STEREOPHOTOGRAPHY
Extraction of dense digital elevation models from SPOT stereo imagery N89-13053

STIFFNESS
The effects of internal rotor friction on dynamic characteristics of turbopumps N89-12629

STOCHASTIC PROCESSES
Neural network performance on the stochastic exclusive-or problem [AD-A197789] N89-13179
Stochastic calculus and survival analysis [AD-A197324] N89-13217
Stochastic stage of an inflationary universe model [DE88-753149] N89-13373

STOICHIOMETRY
Thin films from solvated metal atoms and metal-metal bonded compounds [AD-A197132] N89-12707

STOKES LAW OF RADIATION
The effects of undersampling on multipolarization SAR images N89-12956

STORAGE TANKS
Support of the eight-foot high-temperature tunnel modifications project [NASA-CR-183356] N89-12572

STRAIN GAGES
Applications of polysilicon films in microsensors and microactuators [DE88-016979] N89-12844
Elevated temperature strain gages N89-12886
Development of a high temperature static strain sensor N89-12887
The NASA Lewis Strain Gauge Laboratory: An update N89-12888

STRAIN MEASUREMENT
Elevated temperature strain gages N89-12886
Development of a high temperature static strain sensor N89-12887
The NASA Lewis Strain Gauge Laboratory: An update N89-12888
High temperature stress-strain analysis N89-12913

STRAIN RATE
High strain rate properties of structural aluminium N89-12705

Determination of surfaces of constant inelastic strain rate at elevated temperature N89-12910

STRATEGY

Some strategies for enhancing the performance of the block Lanczos method
[DE88-014401] N89-13212

STRATOCUMULUS CLOUDS

Radiometric observations of cloud liquid water during FIRE --- First ISCCP Regional Experiment (FIRE) N89-13001

Multispectral satellite analysis of marine stratocumulus cloud microphysics
[AD-A197316] N89-13092

STRATOSPHERE

Rayleigh lidar observations of gravity wave activity in the upper stratosphere at Urbana, Ill.
[NASA-CR-182738] N89-13107

Space-time spectral studies of global stratospheric temperature fields N89-13108

Backscatter laser depolarization studies of simulated stratospheric aerosols: Crystallized sulfuric acid droplets
[NASA-CR-183387] N89-13111

STRESS (PHYSIOLOGY)

Validity of heat index as indicator of level of heat storage for personnel wearing protective clothing in hot environments N89-12762

Alterations of segmental volume during orthostatic stress in nonhuman primates N89-12769

STRESS ANALYSIS

Effects of high mean stress on the high-cycle fatigue of PWA 1480 and DS MAR M 246 + Hf at 1000 F N89-12633

Powder metallurgy bearings for advanced rocket engines N89-12641

On 3D inelastic analysis methods for hot section components N89-12906

Component specific modeling N89-12907

A multiaxial theory of viscoplasticity for isotropic materials N89-12908

Constitutive modeling for single crystal superalloys N89-12911

High temperature stress-strain analysis N89-12913

Prediction of stresses in aircraft panels subjected to acoustic forces
[NASA-CR-182513] N89-12923

Structural response calculations for a metal booster tank model
[DE88-017095] N89-12929

STRESS CORROSION CRACKING

Powder metallurgy bearings for advanced rocket engines N89-12641

Irradiation-assisted stress corrosion cracking and grain boundary segregation in heat treated Type 304SS
[DE88-008382] N89-12713

STRESS CYCLES

HOST surface protection R and T overview N89-12883

STRESS INTENSITY FACTORS

Modified pull test for the testing of very adherent films
[DE88-016363] N89-12743

STRESS MEASUREMENT

High temperature stress-strain analysis N89-12913

STRESS-STRAIN DIAGRAMS

Simplified cyclic structural analysis of SSME turbine blades N89-12632

STRESS-STRAIN RELATIONSHIPS

High strain rate properties of structural aluminium N89-12705

Determination of surfaces of constant inelastic strain rate at elevated temperature N89-12910

Constitutive modelling of single crystal and directionally solidified superalloys N89-12912

High temperature stress-strain analysis N89-12913

STRONTIUM 90

Worldwide deposition of Sr-90 through 1985
[DE88-015577] N89-13105

STRUCTURAL ANALYSIS

Development of a thermal and structural analysis procedure for cooled radial turbines
[NASA-TM-101416] N89-12568

Lightweight structural design of a bolted case joint for the space shuttle solid rocket motor
[NASA-TP-2851] N89-12580

Simplified cyclic structural analysis of SSME turbine blades N89-12632

A multimegawatt space power source radiator design
[DE88-015185] N89-12662

Finite element analysis of composite laminates N89-12672

Turbine Engine Hot Section Technology 1986
[NASA-CP-2444] N89-12876

On 3-D inelastic analysis methods for hot section components N89-12905

On 3D inelastic analysis methods for hot section components N89-12906

Component specific modeling N89-12907

Two different methods for shell buckling calculation in the elastic-plastic region
[DFVLR-FB-88-26] N89-12933

Combining spectral and structural analyses to select useful cartographic information from SPOT imagery N89-13052

The solution of linear systems of equations with a structural analysis code on the NAS CRAY-2
[NASA-CR-4159] N89-13202

Nearfield acoustic radiation from a point-excited cylindrical shell
[AD-A197282] N89-13234

STRUCTURAL DESIGN

High-temperature LCF of Ni-201 and 304L stainless steel N89-12635

Liquid oxygen cooling of high pressure LOX/hydrocarbon rocket thrust chambers N89-12649

Assessment of Japanese variable speed heat pump technology
[DE88-013246] N89-12826

Lunar surface transportation systems conceptual design lunar base systems study Task 5.2
[NASA-CR-172077] N89-12862

Lunar storm shelter conceptual design
[NASA-CR-172078] N89-13141

Radioisotope space power generators: Design concepts N89-13224

FIREBIRD: A conceptual design of a field reversed configuration Compact Torus Fusion Reactor (CTFR) N89-13230

Establishment of center for rotorcraft education and research
[AD-A197141] N89-13295

STRUCTURAL ENGINEERING

Approximate mobilities of built up structures
[ISVR-TR-162] N89-12934

STRUCTURAL VIBRATION

Approximate mobilities of built up structures
[ISVR-TR-162] N89-12934

STUDENTS

United States Air Force Graduate Student Summer Support Program, volume 1
[AD-A191121] N89-12754

NASA newsletters for the Weber Student Shuttle Involvement Project
[NASA-TM-101001] N89-13144

SUBSTITUTES

Cost effective alternative to low irradiance measurements N89-12619

SUBSTRATES

Fundamental studies and device development in beta silicon carbide
[AD-A197843] N89-12739

SUBSTRUCTURES

Discovering substructure in examples
[AD-A197778] N89-13163

SULFUR DIOXIDES

The incorporation of sulfur dioxide into snow and depositing ice N89-13116

SULFUR FLUORIDES

Fundamental studies and device development in beta silicon carbide
[AD-A197843] N89-12739

SULFURIC ACID

Comparison of sulfuric and oxalic acid anodizing for preparation of thermal control coatings for spacecraft N89-12617

Determination of sulfuric acid, oxalic acid, and their matrix effects in aluminum anodizing solutions by ion chromatography
[AD-A197734] N89-12694

Backscatter laser depolarization studies of simulated stratospheric aerosols: Crystallized sulfuric acid droplets
[NASA-CR-183387] N89-13111

SUMMARIES

BES welding science contractors
[DE88-016589] N89-12869

SUMMER

United States Air Force Graduate Student Summer Support Program, volume 1
[AD-A191121] N89-12754

SUN

Evidence for temporal variation in the acoustic and f-mode eigenfrequency spectrum of the Sun
[DE88-015650] N89-13389

SUPERCOMPUTERS

Micro-computer network architecture for range instrumentation applications
[AD-A196971] N89-13175

SUPERCONDUCTIVITY

Sol-gel routes to superconducting ceramics
[DE88-015128] N89-12724

High T(sub c) superconductors: Will they replace helium temperature superconductors for magnets
[DE88-016632] N89-13279

Transition-metal oxide superconductivity
[AD-A197069] N89-13280

Overview of high-temperature superconductivity: Theory, surfaces, interfaces and bulk systems
[AD-A197383] N89-13285

Electronic properties and current carrying capacity of high-temperature ceramic superconductors
[AD-A197819] N89-13287

A novel excitonic mechanism for high temperature superconductivity
[DE88-016227] N89-13288

Superconductivity: Phenomenology
[DE88-016659] N89-13289

High temperature superconductivity research in selected laboratories in West Germany
[ONRL-8-011-R] N89-13291

SUPERCONDUCTORS

Sol-gel routes to superconducting ceramics
[DE88-015128] N89-12724

High T(sub c) superconductors: Will they replace helium temperature superconductors for magnets
[DE88-016632] N89-13279

Transition-metal oxide superconductivity
[AD-A197069] N89-13280

Overview of high-temperature superconductivity: Theory, surfaces, interfaces and bulk systems
[AD-A197383] N89-13285

Electronic properties and current carrying capacity of high-temperature ceramic superconductors
[AD-A197819] N89-13287

Low contact-resistivity junction to ceramic superconductors
[DE88-016155] N89-13292

SUPERCRITICAL FLOW

The effects of internal rotor friction on dynamic characteristics of turbopumps N89-12629

SUPERCRITICAL FLUIDS

Supercritical fluid chromatography: The effect of the partial molar volume in the stationary phase on retention
[DE88-016959] N89-12699

SUPERFLUIDITY

Neutron studies of liquid and solid helium
[DE88-009096] N89-13277

SUPERHIGH FREQUENCIES

Performance modeling and results for X-SAR N89-13009

Polarisation of passive microwave signals as indicator of snow water equivalent N89-13043

SUPERLATTICES

MBE growth, characterization and electronic device processing of HgCdTe, HgZnTe related heterojunctions and HgCdTe-CdTe superlattices
[AD-A197752] N89-13286

SUPERPLASTICITY

Mechanical behavior of superplastically-formed Al-Cu-Li-Zr alloy 2090
[DE88-016241] N89-12714

SUPERSATURATION

Research and development of anti-g life support systems. Part 2: Decompression sickness research
[AD-A197675] N89-13133

SUPERSONIC COMBUSTION

Radiative augmented combustion
[AD-A197300] N89-12693

SUPERSONIC FLOW

A two-dimensional numerical simulation of a supersonic, chemically reacting mixing layer
[NASA-TM-4055] N89-12542

SURFACE FINISHING

Soiling, cleaning, and weathering effects on aircraft polyurethane topcoats
[AD-A197302] N89-12733

SURFACE LAYERS

Surfaces and thin films studied by picosecond ultrasonics
[DE88-015268] N89-13233

SURFACE PROPERTIES

Focal region fields of distorted reflectors
[NASA-CR-183001] N89-12810

Laser speckle from thin and cascaded diffusers
[AD-A197066] N89-12850

Summary of laser speckle photogrammetry for HOST N89-12889

Generation of the J(sub c), H(sub c), T(sub c) surface for commercial superconductor using reduced-state parameters
[DE88-014038] N89-13278

SURFACE REACTIONS

Effects of oxygen/hydrogen combustion chamber environment on copper alloys N89-12653

Surface structures and transitions and the evolution from firm to bulk behavior
[AD-A197788] N89-12695

Heat transfer from roughened surfaces using interferometry N89-12827

SURFACE ROUGHNESS
Heat transfer to rough turbine blading N89-12823
Heat transfer from roughened surfaces using interferometry N89-12827
A numerical model for the computation of radiance distributions in natural waters with wind-roughened surfaces
[AD-A197207] N89-13128
SURFACE ROUGHNESS EFFECTS
Polarimetric microwave scattering from known randomly rough surfaces N89-12949
Inference of geologic surface parameters from polarimetric radar observations and model inversion N89-12950
Topographic effects on light scattering from snow N89-12976
SURFACE TEMPERATURE
Carbon, nitrogen and oxygen abundances in the chemically peculiar stars of the upper main sequence N89-13379
SURFACE TO AIR MISSILES
AUTOCREW implementation: Inbound surface-to-air missile simulation
[AD-A197674] N89-13143
SURFACE WAVES
Atomic oxygen studies on polymers N89-12591
SURVEYS
Automated Airframe Assembly Program (AAAP) survey of CIM status in the aircraft industry
[AD-A197368] N89-12535
SURVIVAL
Stochastic calculus and survival analysis
[AD-A197324] N89-13217
SWIRLING
Experimental study of isothermal flows in a dump combustor N89-12779
SWITCHES
Self-actuating heat switches for redundant refrigeration systems
[NASA-CASE-NPO-17085-1-CU] N89-12785
SWITCHING CIRCUITS
Superionic conductors as fast, repetitive opening switches
[AD-A197365] N89-12617
SYMBOLIC PROGRAMMING
Optical symbolic processor for expert system execution
[AD-A197668] N89-13252
SYMMETRY
21st century propulsion concept
[AD-A197537] N89-12663
An axisymmetric linear/high-order finite element for filament wound composite structures N89-12674
SYNCHRONISM
Auditory models for speech analysis
[AD-A197322] N89-12801
How to test the special theory of relativity on rotating earth
[DE88-703048] N89-13293
SYNCHRONOUS PLATFORMS
European remote sensing satellite platforms for the 1990's N89-12978
SYNTHESIS
A system to investigate synthesized voice feedback in man-machine interfaces N89-12776
SYNTHESIS (CHEMISTRY)
Polyenamines from aromatic diacetylenic diketones and diamines
[NASA-CASE-LAR-13444-2-CU] N89-12667
High temperature adhesive systems
[AD-A197077] N89-12726
Synthetic polymers as analogs of polysaccharides
[AD-A197842] N89-12738
Thermoplastic adhesives based on 4,4'-isophthaloyldiphthalic anhydride (IDPA)
[NASA-TM-101508] N89-12747
Chemical precursors to zinc sulfide: ZnS whisker synthesis
[AD-A197262] N89-13284
SYNTHETIC APERTURE RADAR
Modelling of SAR polarisation phase difference from trees N89-12951
Statistical analysis and some polarimetric signatures of a polarimetric synthetic aperture radar image N89-12952
Statistical properties of phase difference between two orthogonally-polarised SAR signals N89-12953
On the concept of the polarimetric matched filter in high resolution radar imaging: An alternative for speckle radiation N89-12954
The effects of undersampling on multipolarization SAR images N89-12956
On the use of speckle statistics for the extraction of ocean wave spectra from SAR imagery N89-12969
Ocean wave number spectra and spatial autocorrelation functions from SAR images N89-12970
SAR-seen multimode waves in ice: Evidence of imaging nonlinearities N89-12971
An intercomparison of SAR and buoy directional wave spectra from the Labrador Sea Extreme Waves Experiment (LEWEX) N89-12972
Synthetic aperture radar over terrestrial ice N89-12977
Crop classification with multi-temporal X-band SAR data N89-12990
Performance modeling and results for X-SAR N89-13009
Image simulation of complex geometric targets for spaceborne synthetic aperture radar N89-13010
Design considerations for advanced multi-polarisation SAR N89-13014
Phase calibration of polarimetric SAR N89-13015
A fine resolution multifrequency polarimetric FM radar N89-13016
A synthetic apertures radar with multichannel and multipolarisation N89-13017
Calibration of multipolarisation imaging radar N89-13018
The NASA/JPL multifrequency, multipolarisation airborne SAR system N89-13020
Formulation of the proper equations for developing standards in coherent dual polarisation SAR imaging N89-13021
Complex SAR imagery and speckle filtering for ERS-1 wave mode N89-13029
Estimating aircraft SAR response characteristics and approximating ocean wave spectra in the Labrador Sea N89-13032
Phase versus orbital velocity in SAR wave imaging: Paradox lost N89-13033
SAR image statistics related to atmospheric drag over sea ice N89-13034
Analysis of Seasat SAR sea-ice data from the Beaufort Sea N89-13035
Sea ice type classification of SAR imagery N89-13039
The derivation of sub-canopy surface terrain models of coastal forests using synthetic aperture radar N89-13083
A luminance edge extraction method using gradient of gray level for synthetic aperture radar imageries N89-13086
SYSTEM FAILURES
Fault diagnosis based on continuous simulation models
[NASA-CR-182737] N89-13152
SYSTEM IDENTIFICATION
Multiple input/output random vibration control system N89-12594
SYSTEMS ANALYSIS
Pilot factors guidelines for the operational inspection of navigation systems
[NASA-CR-181644] N89-12557
An optical sensor system for monitoring structural dynamics with applications to system identification N89-12775
Performance studies of dynamic load balancing in distributed systems
[AD-A197130] N89-12926
Is word recognition automatic: A cognitive-anatomical approach
[AD-A197089] N89-13137
AUTOCREW implementation: Inbound surface-to-air missile simulation
[AD-A197674] N89-13143
Software process modeling
[AD-A197137] N89-13154
Empirical analysis and refinement of expert system knowledge bases
[AD-A197241] N89-13303
SYSTEMS ENGINEERING
The design of antenna matching networks using a microcomputer
[AD-A197364] N89-12802
Design considerations for advanced multi-polarisation SAR N89-13014
A fine resolution multifrequency polarimetric FM radar N89-13016
A 35 GHz helicopter-borne polarimeter radar N89-13038
Radar control, detection and processing electronics design as used for the ERS-1 wind scatterometer space segment N89-13075
Speed and data structures in computer algebra systems
[AD-A197131] N89-13146
SYSTEMS INTEGRATION
Test data acquisition system for the ESTEC large solar simulator at ESA/ESTEC N89-12820
Study of the integration of advanced communications satellite systems and terrestrial networks, executive summary
[ESA-CR(P)-2655] N89-12809
Fiber optic control system integration
[NASA-CR-179568] N89-13256
SYSTEMS SIMULATION
Geodynamics laser ranging system: Performance simulations and development of the EOS facility --- Earth Observing System (EOS) N89-12982

T

T TAURI STARS
Theoretical studies of mass loss and shock phenomena in cool star envelopes
[NASA-CR-182708] N89-13375
TANKS (CONTAINERS)
Tank gauging apparatus and method
[NASA-CASE-MSC-21059-1] N89-12843
Structural response calculations for a metal booster tank model
[DE88-017095] N89-12929
TARGET RECOGNITION
Temporal clustering in the multi-target tracking environment
[AD-A197153] N89-12796
TARGETS
Phase coherence and Signal-To-Noise ratio considerations for sampled aperture radar systems
[AD-A197180] N89-12797
TASKS
Lunar surface transportation systems conceptual design lunar base systems study Task 5.2
[NASA-CR-172077] N89-12862
TECHNOLOGY ASSESSMENT
Aircraft technology opportunities for the 21st Century
[NASA-TM-101060] N89-12539
Assessment of Japanese variable speed heat pump technology
[DE88-013246] N89-12826
Large area TM land cover classification of Mittlerer Oberrhein County, southwest Germany, and its use for regional planning and crop surveys N89-12986
Verification results of MOS-1 multispectral self scanning radiometer (MESSR) data N89-13004
The relativity utility of LANDSAT MSS and SIR-A imagery in reconnaissance geological mapping in Northern Sudan N89-13022
Assessment and comparison of 100-MW coal gasification phosphoric acid fuel cell power plants
[NASA-CR-182189] N89-13103
User-computer interface technology: An assessment of the current state of the art
[AD-A196839] N89-13193
Radioisotope space power generators: Design concepts N89-13224
The next logical step in laser-fusion development
[DE88-007825] N89-13258
Soviet exoatmospheric neutral particle beam research
[FASAC-TAR-3110] N89-13390
TECHNOLOGY TRANSFER
Survey of supply/demand relationships for Japanese Technical Information in the United States: The field of advanced ceramics research and development
[PB88-210943] N89-13300
Federal Laboratory Consortium for Technology Transfer: Putting technology to work. Examples of industry-laboratory cooperation contributing to our nation's economic strength
[PB88-243357] N89-13307
TELECOMMUNICATION
The design of antenna matching networks using a microcomputer
[AD-A197364] N89-12802
Application of autoregressive methods to adaptive excision of interfering tones from direct sequence spread spectrum communications systems
[AD-A197801] N89-12805
EMP (electromagnetic pulse) mitigation program approach
[AD-A197849] N89-12807
Three-dimensional visual display for a prototype command and control workstation
[AD-A197319] N89-13142
Fiber optic wavelength division multiplexing: Principles and applications in telecommunications and spectroscopy N89-13324
TELEMETRY
Multispectral satellite analysis of marine stratocumulus cloud microphysics
[AD-A197316] N89-13092
TELEOPERATORS
The flight robotics laboratory N89-12595

TELEPHONES
Use of proximity effect in hearing aid microphones to increase telephone intelligibility in noise
[AD-A197311] N89-12799
TELESCOPES
A consideration of the use of optical fibers to remotely couple photometers to telescopes N89-13326
TEMPEL 2 COMET
IR-dust observations of Comet Tempel 2 with CRAF VIMS N89-13349
TEMPERATE REGIONS
Building a monitoring system based on satellite data to detect vegetation and land use changes in a subtropical region of Mexico N89-13079
TEMPERATURE
Fire spread in a three-dimensional pressure vessel with radiation exchange and wall heat losses
[AD-A197271] N89-12692
TEMPERATURE CONTROL
The solar simulation test of the ITALSAT thermal structural model N89-12613
LEC (Liquid Encapsulated Czochralski) growth of InP with magnetic field assisted melt stabilization and heat transfer control
[AD-A196748] N89-12688
Proposed design of the temperature control system for the variable temperature calibration target for the Advanced Microwave Sounding Unit B N89-12942
TEMPERATURE DISTRIBUTION
Prediction of heat transfer between the combustion space and the load
[DE88-016313] N89-12698
Heat transfer from roughened surfaces using interferometry N89-12827
Space-time spectral studies of global stratospheric temperature fields N89-13108
TEMPERATURE EFFECTS
Surface characteristics of liquid oxygen cooled ball bearings N89-12640
In-situ high temperature oxidation studies
[DE88-017092] N89-12716
Effect of grain size on the high temperature properties of B2 aluminides
[NASA-TM-101382] N89-12720
Coolant passage heat transfer with rotation N89-12899
Component specific modeling N89-12907
Generation of the J(sub c), H(sub c), T(sub c) surface for commercial superconductor using reduced-state parameters
[DE88-014038] N89-13278
TEMPERATURE GRADIENTS
Convective flows in enclosures with vertical temperature or concentration gradients
[NASA-TM-101373] N89-12753
TEMPERATURE MEASUREMENT
Cost effective alternative to low irradiance measurements N89-12619
Round-robin measurements of the apparent thermal conductivity of two refractory insulation materials, using high-temperature guarded-hot-plate apparatus
[PB88-215421] N89-12670
Further development of the dynamic gas temperature measurement system N89-12884
Estimation of sea surface temperature via NOAA-AVHRR sensor: Comparison with sea truth data by fixed buoys N89-13005
The applicability of Rutherford scattering for Ti measurements at medium and large-sized experiments N89-13273
TEMPERATURE MEASURING INSTRUMENTS
HOST instrumentation R and D program overview N89-12878
TEMPERATURE PROBES
Further development of the dynamic gas temperature measurement system N89-12884
TEMPERATURE PROFILES
Temperature profile in semi-infinite planar slab with exponential source and convective boundary condition: Application to laser heating
[DE88-016746] N89-12831
TEMPORAL DISTRIBUTION
Evidence for temporal variation in the acoustic and f-mode eigenfrequency spectrum of the Sun
[DE88-015650] N89-13389
TENSILE PROPERTIES
Hydrogen effects on the fatigue and tensile behavior of CMSX-2 nickel base superalloy single crystals N89-12658
LCF and crack growth rate of turbine blade alloys in hydrogen and hydrogen/steam environments N89-12660
The development of a hydrogen resistant alloy N89-12661
Synthesis and characterization of VLS-derived silicon carbide whiskers
[DE88-016226] N89-12679
Fundamental understanding of the intrinsic ductility in nickel-base L12 type alloys
[AD-A197605] N89-12711
Properties of rapidly solidified aluminum alloys. German-Norwegian Project (1983-1987)
[DFVLR-FB-88-24] N89-12719
TERMINAL BALLISTICS
On the resistance of ceramics to high velocity penetration
[AD-A197320] N89-12734
TERRAIN
An international approach to GIS based on remote sensing and terrain classification — geographic information system (GIS) N89-12966
Snow cover to alter terrain signatures on radar images N89-13048
Extraction of dense digital elevation models from SPOT stereo imagery N89-13053
The derivation of sub-canopy surface terrain models of coastal forests using synthetic aperture radar N89-13083
TERRAIN ANALYSIS
An evaluation of ground collision avoidance system algorithm
[AD-A197831] N89-12560
A comparison of propagation model predictions with EPLRS (Enhanced Position Location and Reporting System) UHF network measurements
[AD-A197473] N89-12804
TEST FACILITIES
A high pressure, high temperature hydrogen environment for metals properties testing system N89-12656
Fire spread in a three-dimensional pressure vessel with radiation exchange and wall heat losses
[AD-A197271] N89-12692
TEST STANDS
Test stand design and analysis for Titan 34D static firing N89-12609
Test stand for Titan 34D SRM static firing N89-12610
Damping seal tester progress and initial test results N89-12627
TEXTURES
Towards an urban land-use classification using textural and morphological criteria N89-12987
Co-occurrence matrix modification for small region texture measurement and comparison N89-13064
THEMATIC MAPPERS (LANDSAT)
Multitemporal resource complex analysis of Catinia province, Italy from LANDSAT-TM data N89-12985
Mapping the distribution and abundance of lithological units and surface mineralogies at Jabal Sa'id, Saudi Arabia: An application of spectral mixture modelling N89-13024
The need for volcano monitoring and the ability to detect activity using emitted short wavelength infrared N89-13025
Monitoring playas using Thematic Mapper data N89-13028
Evaluation of LANDSAT TM and SPOT imagery for agricultural land use planning in less developed countries N89-13051
LANDSAT Thematic Mapping (TM) and SPOT HRV for survey mapping of bedrock outcrops N89-13055
An evaluation of satellite imagery, LANDSAT Thematic Mapper and SPOT-1 HRV, for grassland inventory in the UK N89-13057
Monitoring urban change from LANDSAT TM and SPOT satellite imagery by image differencing N89-13058
The classification of semi-natural vegetation from LANDSAT Thematic Mapper imagery: A user's perspective N89-13084
Biogeochemical processes in sagebrush steppe: Interactions of terrain, vegetation and chemical cycles
[NASA-CR-181486] N89-13088
THEMATIC MAPPING
Development of a geographic information system with the aid of digital image processing techniques N89-12961
Large area TM land cover classification of Mittlerer Oberrhein County, southwest Germany, and its use for regional planning and crop surveys N89-12986
Mapping the distribution and abundance of lithological units and surface mineralogies at Jabal Sa'id, Saudi Arabia: An application of spectral mixture modelling N89-13024
Agroelecological information content of SPOT data N89-13050
LANDSAT Thematic Mapping (TM) and SPOT HRV for survey mapping of bedrock outcrops N89-13055
The production of anaglyphs from SPOT-HRV panchromatic data for geomorphological mapping N89-13056
Effects of changing satellite sensor attributes N89-13059
Cotton area mapping using multitemporal satellite data integrated within a geographical information system applied to a cotton boll weevil control programme in Paraguay N89-13077
Applications of remote sensing for geological mapping in eastern Egypt N89-13087
An albedo map of P/Halley on 13 March 1986 N89-13355
THEOREMS
Bearing error and the central limit theorem
[NASA-CR-183009] N89-13219
THERMAL ANALYSIS
Development of a thermal and structural analysis procedure for cooled radial turbines
[NASA-TM-101416] N89-12568
Thermo-mechanical performance evaluation of cryogenic turbopump ball bearings N89-12637
Thermal analysis of SSME turbopump bearings N89-12638
Sol-gel routes to superconducting ceramics
[DE88-015128] N89-12724
Differential scanning calorimetry as a method for indicating hydrolysis of urethane elastomers
[AD-A197673] N89-12736
Preliminary thermal analysis of a bimodal nuclear rocket core N89-12758
THERMAL BUCKLING
Non-isothermal buckling behavior of viscoplastic shell structures
[NASA-CR-183013] N89-12931
THERMAL COMFORT
Validity of heat index as indicator of level of heat storage for personnel wearing protective clothing in hot environments N89-12762
THERMAL CONDUCTIVITY
Round-robin measurements of the apparent thermal conductivity of two refractory insulation materials, using high-temperature guarded-hot-plate apparatus
[PB88-215421] N89-12670
THERMAL CONTROL COATINGS
Fifteenth Space Simulation Conference: Support the Highway to Space Through Testing
[NASA-CP-3015] N89-12582
Requirements and test results for the qualification of thermal control coatings N89-12616
Comparison of sulfuric and oxalic acid anodizing for preparation of thermal control coatings for spacecraft N89-12617
Moisture interaction and stability of ZOT (Zinc Orthotitanate) thermal control spacecraft coating N89-12618
Turbine Engine Hot Section Technology 1986
[NASA-CP-2444] N89-12876
HOST surface protection R and T overview N89-12883
A study on thermal barrier coatings including thermal expansion mismatch and bond coat oxidation N89-12919
Thermal barrier coating life prediction model development N89-12920
Thermal barrier coating life prediction model N89-12921
Thermal barrier coating life prediction model development N89-12922
THERMAL CYCLING TESTS
Indian LSSC (Large Space Simulation Chamber) facility N89-12601
Thermal/structural design verification strategies for large space structures N89-12602
THERMAL DEGRADATION
A methodology for characterizing reactive coatings: Time-Temperature-Transformation (TTT) analysis of the competition between cure, evaporation and thermal degradation for an epoxy-phenolic system
[AD-A197254] N89-12730
THERMAL EMISSION
A two component model for thermal emission from organic grains in Comet Halley N89-13340
The spectral appearance of comets from 5 to 20 micrometers: A survey of the data N89-13347
Properties of interstellar dust in reflection nebulae N89-13365
THERMAL ENERGY
Materials selection for long life in LEO: A critical evaluation of atomic oxygen testing with thermal atom systems N89-12590
THERMAL ENVIRONMENTS
Thermal/structural design verification strategies for large space structures N89-12602
THERMAL EXPANSION
The effects of expansion devices on the transient response characteristics of the air-source heat pump during the reverse cycle defrost
[AD-A197150] N89-12829

Heat transfer in the lip region of a rotor blade simulator N89-12898
A study on thermal barrier coatings including thermal expansion mismatch and bond coat oxidation N89-12919

THERMAL FATIGUE
High-temperature LCF of Ni-201 and 304L stainless steel N89-12635
Thermo-mechanical performance evaluation of cryogenic turbopump ball bearings N89-12637

THERMAL NEUTRONS
Neutron flux measurements in the Gran Sasso Underground Laboratory (Italy) (part 2) [IFSI-88-7] N89-13243

THERMAL PLASMAS
Nonequilibrium effects in thermal plasmas: Radiation transport and chemical reactivity [DE88-016841] N89-13262
Nonequilibrium effects in thermal plasma chemistry [DE88-016842] N89-13263

THERMAL PROTECTION
Heat pipe cooling system with sensible heat sink N89-12615

THERMAL RADIATION
A global analysis and correlation of Nimbus 7 cloud and longwave radiation data [AD-A197223] N89-13121

THERMAL STRESSES
HOST structural analysis program overview N89-12881
Coolant passage heat transfer with rotation N89-12899

THERMAL VACUUM TESTS
Development of a two axis motion simulation system for thermal/vacuum satellite testing N89-12596
Indian LSSC (Large Space Simulation Chamber) facility N89-12601

THERMODYNAMIC PROPERTIES
Thermal/structural design verification strategies for large space structures N89-12602
IRIS thermal balance test within ESTEC LSS N89-12603
Differential scanning calorimetry as a method for indicating hydrolysis of urethane elastomers [AD-A197673] N89-12736
Micro heat pipes [DE88-016113] N89-13100

THERMODYNAMICS
Supercritical fluid chromatography: The effect of the partial molar volume in the stationary phase on retention [DE88-016959] N89-12699
Fuel cells: A bibliography [DE88-001081] N89-13097

THERMOELASTICITY
Thermal/structural design verification strategies for large space structures N89-12602

THERMOELECTRIC GENERATORS
Radioisotope space power generators: Design concepts N89-13224

THERMOELECTRIC POWER GENERATION
Electronic properties and current carrying capacity of high-temperature ceramic superconductors [AD-A197819] N89-13287

THERMOGRAVIMETRY
Data acquisition of the thermogravimetric analysis testing summary [DE88-016062] N89-13147

THERMOMECHANICAL TREATMENT
Thermomechanical characterization of Hastelloy-X under uniaxial cyclic loading N89-12909

THERMOPLASTIC RESINS
Short fiber reinforced thermoplastics N89-12673
Pultrusion die assembly [NASA-CASE-LAR-13719-1] N89-12867

THERMOSTATS
The solar simulation test of the ITALSAT thermal structural model N89-12613

THESAURI
NASA thesaurus. Volume 2: Access vocabulary [NASA-SP-7064-VOL-2] N89-13298
NASA thesaurus. Volume 3: Definitions [NASA-SP-7064-VOL-3] N89-13301
NASA thesaurus. Volume 1: Hierarchical Listing [NASA-SP-7064-VOL-1] N89-13302

THIN FILMS
Thin films from solvated metal atoms and metal-metal bonded compounds [AD-A197132] N89-12707
Analysis of adhesion test methods and the evaluation of their use for ion-beam-mixed metal/ceramic systems [DE88-015358] N89-12725
Light extinction in a dispersion of small nematic droplets [AD-A197201] N89-12729
Studies of ultrathin polymer films for lithographic applications [AD-A197297] N89-12731
Ultrathin polymer films for microlithography [AD-A197298] N89-12732
Modified pull test for the testing of very adherent films [DE88-016363] N89-12743
A refined model for characterizing X-ray multilayers [DE88-013592] N89-12872
Preparation and properties of high-deposition-rate a-Si:H films and solar cells using disilane [DE88-001191] N89-13098
Solar photovoltaic technology: The thin film option [DE88-001195] N89-13102
Surfaces and thin films studied by picosecond ultrasonics [DE88-015268] N89-13233
Moisture adsorption in optical coatings N89-13327

THIN PLATES
The E-parallel polarization response of a two-dimensional heterogeneous layer modelled by two thin sheets --- electromagnetic geophysical sounding N89-12947

THREE DIMENSIONAL BOUNDARY LAYER
Influence of bulk turbulence and entrance boundary layer thickness on the curved duct flow field [NASA-CR-4186] N89-12838

THREE DIMENSIONAL FLOW
A zonal equation method for three-dimensional locally elliptic laminar and turbulent flows N89-12547
Direct simulation of three-dimensional flow about the AFE vehicle at high altitudes [NASA-TM-101492] N89-12834
Turbine stator flow field simulations N89-12902

THREE DIMENSIONAL MODELS
Development and validation of an advanced low-order panel method [NASA-TM-101024] N89-12554

THREE DIMENSIONAL MOTION
Improved docking alignment system [NASA-CASE-MSC-21372-1] N89-12842

THRUST AUGMENTATION
A control-volume method for analysis of unsteady thrust augmenting ejector flows [NASA-CR-182203] N89-12566

THRUST CHAMBERS
Liquid oxygen cooling of high pressure LOX/hydrocarbon rocket thrust chambers N89-12649

THRUST-WEIGHT RATIO
Combustor diffuser interaction program N89-12893

THULIUM
Tm,Ho:YLF laser end-pumped by a semiconductor diode laser array [NASA-CASE-NPO-17282-1-CU] N89-12856

TIME
Resonator design with an intracavity time-varying index gradient [DE88-015259] N89-12857

TIME DEPENDENCE
The stability of time-dependent fluid flows N89-12825
On the sampling in imaging microwave radiometers N89-12940
Worldwide deposition of Sr-90 through 1985 [DE88-015577] N89-13105
Time-resolved solid-state array imaging systems: Developments and applications [DE88-016274] N89-13254

TIME LAG
Phase versus orbital velocity in SAR wave imaging: Paradox lost N89-13033

TIME TEMPERATURE PARAMETER
A methodology for characterizing reactive coatings: Time-Temperature-Transformation (TTT) analysis of the competition between cure, evaporation and thermal degradation for an epoxy-phenolic system [AD-A197254] N89-12730

TISSUES (BIOLOGY)
Gordon Conference on Microbial Adhesion [AD-A197352] N89-12735
Electroporation: Theory of basic mechanisms [AD-A197391] N89-13130
Horizontally rotated cell culture system [NASA-CASE-MSC-21294-1] N89-13131
Research and development of anti-g life support systems. Part 2: Decompression sickness research [AD-A197675] N89-13133

TITAN LAUNCH VEHICLES
Test stand for Titan 34D SRM static firing N89-12610

TITANIUM
Moisture interaction and stability of ZOT (Zinc Orthotitanate) thermal control spacecraft coating N89-12618
High T(sub c) superconductors: Will they replace helium temperature superconductors for magnets [DE88-016632] N89-13279

TITANIUM ALLOYS
Fatigue crack retardation following overloads in Inconel 718, Ti-5Al-2.5Sn, and Haynes 188 N89-12636

TOKAMAK DEVICES
Toroidal studies of sawtooth oscillations in tokamaks [DE88-017115] N89-13264
FOM Contributions to the 15th European Conference on Controlled Fusion and Plasma Heating [REPT-88-178] N89-13266
Tokamak equilibrium determination through function parameterization N89-13272
RF stabilization of external kink modes --- tokamak plasmas N89-13275
Optimizing current drive by electron cyclotron waves in the presence of trapped particles N89-13276

TOMOGRAPHY
Bistatic frequency diverse imaging of complex scattering targets N89-13013

TOPOGRAPHY
Topographic effects on light scattering from snow N89-12976

TOROIDAL PLASMAS
The m=1 internal kink mode in a toroidal plasma with a flat q-profile near q=1 N89-13267
Recent results of the toroidal screw pinch SPICA 2 N89-13271

TOUGHNESS
Properties of rapidly solidified aluminum alloys. German-Norwegian Project (1983-1987) [DFVLR-FB-88-24] N89-12719

TRAJECTORY OPTIMIZATION
Design and numerical evaluation of full-authority flight control systems for conventional and thruster-augmented helicopters employed in NOE operations [NASA-CR-183311] N89-12570

TRANSDUCERS
Mass flow measurement of liquid cryogens using the triboelectric effect [NASA-CR-179519] N89-12837
The Frascati (Italy) gravitational antenna, 1987 [IFSI-88-4] N89-12846

TRANSFER FUNCTIONS
The transfer of cyclotron photons through neutron star atamospheres N89-13378

TRANSFORMATIONS (MATHEMATICS)
Implementation issues for level O image processor software within an application package [AD-A197768] N89-13162

TRANSIENT LOADS
Efficient transient analysis methods for the Space Shuttle Main Engine (SSME) turbopumps N89-12630

TRANSIENT RESPONSE
The effects of expansion devices on the transient response characteristics of the air-source heat pump during the reverse cycle defrost [AD-A197150] N89-12829

TRANSITION LAYERS
Electronic properties and current carrying capacity of high-temperature ceramic superconductors [AD-A197819] N89-13287

TRANSITION METALS
Transition-metal oxide superconductivity [AD-A197069] N89-13280

TRANSITION TEMPERATURE
Differential scanning calorimetry as a method for indicating hydrolysis of urethane elastomers [AD-A197673] N89-12736
A novel excitonic mechanism for high temperature superconductivity [DE88-016227] N89-13288
Superconductivity: Phenomenology [DE88-016659] N89-13289

TRANSLATIONAL MOTION
Improved docking alignment system [NASA-CASE-MSC-21372-1] N89-12842

TRANSMITTANCE
Laser speckle from thin and cascaded diffusers [AD-A197066] N89-12850
A numerical model for the computation of radiance distributions in natural waters with wind-roughened surfaces [AD-A197207] N89-13128

TRANSONIC FLOW
Theoretical and experimental studies of the transonic flow field and associated boundary conditions near a longitudinally-slotted wind-tunnel wall N89-12545

TRANSONIC WIND TUNNELS
Sidewall boundary-layer measurements with upstream suction in the Langley 0.3-meter transonic cryogenic tunnel [NASA-CR-4192] N89-12544

TRANSPORT PROPERTIES
Electronic properties and current carrying capacity of high-temperature ceramic superconductors
[AD-A197819] N89-13287
TRANSPORT THEORY
Electronic transport properties of the metallic glass Cu sub 100-x Ti sub x
[ETN-88-93231] N89-12718
TRANSPORTATION
Lunar surface transportation systems conceptual design lunar base systems study Task 5.2
[NASA-CR-172077] N89-12862
TRAPPED PARTICLES
Optimizing current drive by electron cyclotron waves in the presence of trapped particles N89-13276
TRAVELING SALESMAN PROBLEM
Sensitivity analysis for shortest Hamiltonian path and traveling salesman problems
[AD-A197167] N89-13204
TRAVELING WAVES
Investigation of acceleration and densification of electrons utilizing travelling magnetic waves
[AD-A197700] N89-13242
TREES (MATHEMATICS)
The detection of unimproved grassland in Berkshire using a binary decision tree approach N89-12988
TREES (PLANTS)
Modelling of SAR polarisation phase difference from trees N89-12951
Interpretation of coherent polarimetric signatures by dielectric cylinder models N89-12957
Spectral characterization of forest damage in beech, oak and pine stands N89-13085
TRIBOLOGY
Boric oxide as a solid lubricant additive in molybdenum disulfide
[AD-A197109] N89-12727
Mass flow meter using the triboelectric effect for measurement in cryogenics
[NASA-CR-179572] N89-12836
TROPICAL METEOROLOGY
Design of a spaceborne radar for tropical rain mapping at the climatological scale N89-12997
TROPICAL REGIONS
Building a monitoring system based on satellite data to detect vegetation and land use changes in a subtropical region of Mexico N89-13079
TROPICAL STORMS
An analysis of the error characteristics of Atlantic tropical cyclone track prediction models
[AD-A197146] N89-13119
The effect of vertical wind shear on tropical cyclone movement
[AD-A197218] N89-13120
TUNDRA
The interpretation of Icelandic tundra features from LANDSAT-MSS data N89-13027
TURBINE BLADES
Simplified cyclic structural analysis of SSME turbine blades N89-12632
Effects of high mean stress on the high-cycle fatigue of PWA 1480 and DS MAR M 246 + Hf at 1000 F N89-12633
Constitutive behavior of single crystal PWA 1480 and directionally solidified MAR-M 246 under monotonic and cyclic loads at high and low temperature N89-12634
LCF and crack growth rate of turbine blade alloys in hydrogen and hydrogen/steam environments N89-12660
Heat transfer to rough turbine blading N89-12823
Development of a high temperature static strain sensor N89-12887
Development of low Reynolds number two equation turbulence models for predicting external heat transfer on turbine blades N89-12901
On 3-D inelastic analysis methods for hot section components N89-12905
On 3D inelastic analysis methods for hot section components N89-12906
Component specific modeling N89-12907
Constitutive modelling of single crystal and directionally solidified superalloys N89-12912
Elevated temperature crack growth N89-12915
Preliminary results from the dynamic response testing of the Northern Power Systems 100-kW wind turbine
[DE88-001166] N89-13101
TURBINE ENGINES
Research on mechanical properties for engine life prediction
[AD-A197816] N89-12864
TURBINE PUMPS
Damping seal tester progress and initial test results N89-12627
Low-speed flexible rotor balancing for smooth, high-speed operation N89-12628
The effects of internal rotor friction on dynamic characteristics of turbopumps N89-12629
Efficient transient analysis methods for the Space Shuttle Main Engine (SSME) turbopumps N89-12630
Vibrations induced by nonlinearities in rotordynamics N89-12631
Thermo-mechanical performance evaluation of cryogenic turbopump ball bearings N89-12637
Thermal analysis of SSME turbopump bearings N89-12638
Lubrication evaluation of SSME turbopump bearings N89-12639
Surface characteristics of liquid oxygen cooled ball bearings N89-12640
Powder metallurgy bearings for advanced rocket engines N89-12641
Rolling contact fatigue life of zirconium and molybdenum nitride sputter plated AMS 5749 bearing steel N89-12642
Measurement of rotordynamic coefficients for a hydrostatic radial bearing N89-12643
Surface modification for wear resistance in a liquid oxygen turbopump environment N89-12644
SSME bearing health monitoring using a fiberoptic deflectometer N89-12645
TURBINES
Improving the efficiency of binary cycles
[DE88-015108] N89-13099
TURBOMACHINE BLADES
A review of turbomachinery blade-row interaction research
[NASA-CR-182211] N89-12567
Turbine airfoil film cooling N89-12903
TURBOPROP AIRCRAFT
Advanced turboprop project
[NASA-SP-495] N89-12565
TURBULENCE
Experimental study of isothermal flows in a dump combustor N89-12779
Parallel algorithms in the finite element approximation of flow problems
[AD-A197454] N89-13178
TURBULENCE MODELS
Influence of bulk turbulence and entrance boundary layer thickness on the curved duct flow field
[NASA-CR-4188] N89-12838
TURBULENT BOUNDARY LAYER
Method for laminar boundary layer transition visualization in flight
[NASA-CASE-LAR-13554-1] N89-12551
Structure measurements in a synthetic turbulent boundary layer N89-12821
On the interactions of longwave radiation, microphysics and turbulence in boundary layer clouds N89-13109
TURBULENT FLOW
A zonal equation method for three-dimensional locally elliptic laminar and turbulent flows N89-12547
Evaluation of three turbulence models for the prediction of steady and unsteady airloads
[NASA-TM-101413] N89-12555
Theoretical study of turbulent channel flow: Bulk properties, pressure fluctuations, and propagation of electromagnetic waves
[NASA-TM-101248] N89-12830
Advanced instrumentation for local measurement of gas-solid suspension flows
[DE88-017087] N89-12833
Influence of bulk turbulence and entrance boundary layer thickness on the curved duct flow field
[NASA-CR-4188] N89-12838
Gas flow and global code programme
[DE88-012635] N89-12861
Improved numerical methods for turbulent viscous recirculating flows N89-12895
Heat transfer with very high free-stream turbulence and streamwise vortices N89-12900
TURBULENT JETS
A control-volume method for analysis of unsteady thrust augmenting ejector flows
[NASA-CR-182203] N89-12566
TURBULENT MIXING
Mass and heat balances in the upper ocean N89-13089
TWO DIMENSIONAL BOUNDARY LAYER
A numerical method for computing unsteady 2-D boundary layer flows
[NASA-CR-4198] N89-12835
TWO PHASE FLOW
Dynamics of face and annular seals with two-phase flow
[NASA-CR-183352] N89-12870

U

ULTRAHIGH FREQUENCIES
A comparison of propagation model predictions with EPLRS (Enhanced Position Location and Reporting System) UHF network measurements
[AD-A197473] N89-12804
ULTRALIGHT AIRCRAFT
Small format air photo from ultrahigh aircraft as an aid for data collection of agricultural statistics in Sahelian countries N89-13003
ULTRASONIC FLAW DETECTION
Shock detection in composite structures. Test report 48-915/F — Impact damage
[REPT-48-915/F] N89-12683
ULTRASONIC SPECTROSCOPY
Laser dynamic photoelasticity and digital image analysis for nondestructive evaluation of surface and near surface flaws through ultrasonic spectroscopy N89-12871
ULTRASONIC WAVE TRANSDUCERS
Colloid vibration potentials
[VTT-RR-535] N89-13244
ULTRASONICS
Support of the eight-foot high-temperature tunnel modifications project
[NASA-CR-183356] N89-12572
Characterization of adhesively bonded joints using acousto-ultrasonics N89-12925
Surfaces and thin films studied by picosecond ultrasonics
[DE88-015268] N89-13233
ULTRAVIOLET RADIATION
Joint services electronics program
[AD-A197140] N89-12815
Optical and electrical measurements on UV sensitive photodiodes N89-13316
ULTRAVIOLET SPECTRA
WF/PC internal molecular contamination during system thermal-vacuum test N89-12583
The NASA atomic oxygen effects test program N89-12589
UNDERWATER ACOUSTICS
Arctic oceanography and meteorology review
[AD-A196533] N89-13126
Parabolic equation model
[AD-A197480] N89-13161
UNITED NATIONS
Environmental management practices in oil refineries and terminals: An overview
[ISBN-92-807-1108-3] N89-13104
UNITED STATES
Annual review of aircraft accident data, US general aviation, calendar year 1985
[PB88-115787] N89-12537
Survey of supply/demand relationships for Japanese Technical Information in the United States: The field of advanced ceramics research and development
[PB88-210943] N89-13300
UNIVERSE
Stochastic stage of an inflationary universe model
[DE88-753149] N89-13373
The large-scale structure of the universe: Some theoretical considerations N89-13381
UNIVERSITIES
United States Air Force Graduate Student Summer Support Program, volume 1
[AD-A191121] N89-12754
UNSTEADY AERODYNAMICS
A review of turbomachinery blade-row interaction research
[NASA-CR-182211] N89-12567
UNSTEADY FLOW
Unsteady structure of flow past a pitching delta wing N89-12541
A control-volume method for analysis of unsteady thrust augmenting ejector flows
[NASA-CR-182203] N89-12566
A comparative study of differing vortex structures arising in unsteady separated flows N89-12773
A numerical method for computing unsteady 2-D boundary layer flows
[NASA-CR-4198] N89-12835
URBAN PLANNING
The use of remote sensing in conjunction with geographic information systems for local planning N89-12959
Towards an urban land-use classification using textural and morphological criteria N89-12987
URBAN RESEARCH
Monitoring urban change from LANDSAT TM and SPOT satellite imagery by image differencing N89-13058
USER MANUALS (COMPUTER PROGRAMS)
Pilot factors guidelines for the operational inspection of navigation systems
[NASA-CR-181644] N89-12557

Providing on-line guidance to computer users N89-12766
C Cloud S (Climatology of Cloud Statistics) database (users manual)
[AD-A196497] N89-13118
HLP30: A set of linear programming procedures system manual
[DE88-016571] N89-13169
USER REQUIREMENTS
Installation of the ADINA FEM computer programs N89-12778
Requirements for ongoing development of the Pilot Land Data System (PLDS) N89-12958
Pan 1: An introduction for users, revision
[AD-A197344] N89-13160
Parabolic equation model
[AD-A197480] N89-13161

V

VACUUM
Wide Field/Planetary Camera (WF/PC) contamination control assessment N89-12584
Characterization of a graphite epoxy optical bench during thermal vacuum cycling N89-12585
Space simulators for laser optics N89-12597
VACUUM CHAMBERS
Design of vacuum chambers downstream of NSLS X-ray ring insertion devices
[DE88-015715] N89-13247
VACUUM SYSTEMS
LIGO vacuum system study N89-12599
VANES
Development of a high temperature static strain sensor N89-12887
On 3-D inelastic analysis methods for hot section components N89-12905
On 3D inelastic analysis methods for hot section components N89-12906
Component specific modeling N89-12907
Elevated temperature crack growth N89-12915
VAPOR DEPOSITION
As-deposited low-strain LPCVD (Low-Pressure, Chemical-Vapor-Deposition) polysilicon
[DE88-016980] N89-12789
Chemical precursors to zinc sulfide: ZnS whisker synthesis
[AD-A197262] N89-13264
VAPORS
Synthesis and characterization of VLS-derived silicon carbide whiskers
[DE88-016226] N89-12679
VARIABLE STARS
Spectral variability of Wolf-Rayet stars
[DE88-703325] N89-13371
VARIATIONS
Resonator design with an intracavity time-varying index gradient
[DE88-015259] N89-12857
Neural network performance on the stochastic exclusive-or problem
[AD-A197789] N89-13179
Monitoring solar-type stars for luminosity variations N89-13321
VARISTORS
Microstructure and nonlinearity of ZnO varistors, Volume 5, Number 8
[B8735659] N89-13290
VECTOR ANALYSIS
Euclidean decoders for BCH codes
[AD-A197242] N89-13157
VEGETATION
Modelling land resources within a pilot geographical information system N89-12962
Building a monitoring system based on satellite data to detect vegetation and land use changes in a subtropical region of Mexico N89-13079
The classification of semi-natural vegetation from LANDSAT Thematic Mapper imagery: A user's perspective N89-13084
VEGETATIVE INDEX
The structure of red-infrared scattergrams of semivegetated landscapes
[NASA-CR-183385] N89-13091
VELOCITY
Speed and data structures in computer algebra systems
[AD-A197131] N89-13146
VELOCITY DISTRIBUTION
Foundations of the blade-vortex interaction problem: Structure and behavior of travelling compressible vortices
[AD-A197370] N89-12550
VELOCITY MEASUREMENT
Wind tunnel investigation of the response of a sonic anemometer
[PB88-249826] N89-12847
Phase versus orbital velocity in SAR wave imaging: Paradox lost N89-13033
VERY LARGE SCALE INTEGRATION
Optical computing based on neuronal models
[AD-A197749] N89-13199
VIBRATION
Control of the induced microgravity environment of the Man Tended Free Flyer (MTFF) N89-12606
Vibrations induced by nonlinearities in rotordynamics N89-12631
VIBRATION DAMPING
Vibration suppression in a large space structure
[NASA-CR-182831] N89-12624
The effects of internal rotor friction on dynamic characteristics of turbopumps N89-12629
VIBRATION EFFECTS
Colloid vibration potentials
[VTT-RR-535] N89-13244
VISCOPLASTICITY
A multiaxial theory of viscoplasticity for isotropic materials N89-12908
Non-isothermal buckling behavior of viscoplastic shell structures
[NASA-CR-183013] N89-12931
Considerations in development and implementation of elasto-viscoplastic constitutive model for high temperature applications
[NASA-CR-183403] N89-12932
VISCOUS FLOW
Simulation of 2-dimensional viscous flow through cascades using a semi-elliptic analysis and hybrid C-H grids
[NASA-CR-4180] N89-12553
Improved numerical methods for turbulent viscous recirculating flows N89-12895
Parallel algorithms in the finite element approximation of flow problems
[AD-A197454] N89-13178
VISUAL PERCEPTION
A numerical model for the computation of radiance distributions in natural waters with wind-roughened surfaces
[AD-A197207] N89-13128
Preattentive and attentive visual information processing
[AD-A197670] N89-13139
VISUAL STIMULI
Differential-psychological analysis of a computer-based audio-visual test of vigilance
[DFVLR-FB-88-23] N89-13140
VOICE COMMUNICATION
A system to investigate synthesized voice feedback in man-machine interfaces N89-12776
Robust recognition of loud and Lombard speech in the fighter cockpit environment
[AD-A197093] N89-12795
VOICE CONTROL
Voice recognition and artificial intelligence in an air traffic control environment
[AD-A197219] N89-12559
VOLCANOLOGY
The need for volcano monitoring and the ability to detect activity using emitted short wavelength infrared N89-13025
VORTEX FILAMENTS
A vortex panel method for potential flows with applications to dynamics and control
[AD-A197091] N89-12549
VORTICES
The laminar boundary layer on an airfoil started impulsively from rest N89-12540
Foundations of the blade-vortex interaction problem: Structure and behavior of travelling compressible vortices
[AD-A197370] N89-12550
Structure measurements in a synthetic turbulent boundary layer N89-12821
Heat transfer with very high free-stream turbulence and streamwise vortices N89-12900
VORTICITY
A comparative study of differing vortex structures arising in unsteady separated flows N89-12773
VORTICITY EQUATIONS
Foundations of the blade-vortex interaction problem: Structure and behavior of travelling compressible vortices
[AD-A197370] N89-12550

W

WALLS
Fire spread in a three-dimensional pressure vessel with radiation exchange and wall heat losses
[AD-A197271] N89-12692
WARFARE
AUTOCREW implementation: Inbound surface-to-air missile simulation
[AD-A197674] N89-13143
WARNING SYSTEMS
Planner system for the application of indications and warning N89-13188
WASTE DISPOSAL
A steam inerting system for hydrogen disposal for the Vandenberg Shuttle N89-12608
Challenging applications for hydrated and chemically reacted ceramics
[DE88-015397] N89-12742
WASTE TREATMENT
Challenging applications for hydrated and chemically reacted ceramics
[DE88-015397] N89-12742
WATER
Homogeneous catalytic production of hydrogen and other molecules from water-DMF (N-dimethylformamide) solutions
[AD-A197072] N89-12690
Atomic and molecular abundances in comets N89-13376
WATER MANAGEMENT
Snowmelt runoff estimation using snow cover extent data and its application to optimum control of dam water level N89-13042
WATER RUNOFF
Improvement in NOAA-AVHRR snowcover determination for runoff prediction N89-13040
Snowmelt runoff estimation using snow cover extent data and its application to optimum control of dam water level N89-13042
WATER VAPOR
Verification of the accuracy of a network of water-vapor radiometers N89-12941
WATER WAVES
Spectral analysis of ocean wave imagery using 2-D linear prediction N89-12968
On the use of speckle statistics for the extraction of ocean wave spectra from SAR imagery N89-12969
Ocean wave number spectra and spatial autocorrelation functions from SAR images N89-12970
SAR-seen multimode waves in ice: Evidence of imaging nonlinearities N89-12971
An intercomparison of SAR and buoy directional wave spectra from the Labrador Sea Extreme Waves Experiment (LEWEX) N89-12972
Directional ocean wave spectra: Prospects for acquiring a global data base from SIR-C N89-12973
The Labrador Sea Extreme Waves Experiment: Objectives, status and plans N89-12974
Complex SAR imagery and speckle filtering for ERS-1 wave mode N89-13029
Some characteristics of short ocean waves as microwave scatterers N89-13030
Modulation of the radar backscatter from the ocean surface by a long gravity wave N89-13031
Estimating aircraft SAR response characteristics and approximating ocean wave spectra in the Labrador Sea N89-13032
Phase versus orbital velocity in SAR wave imaging: Paradox lost N89-13033
WAVE EQUATIONS
Formulation of the proper equations for developing standards in coherent dual polarisation SAR imaging N89-13021
WAVE PROPAGATION
Wave propagation in layered structures N89-12777
Theoretical study of turbulent channel flow: Bulk properties, pressure fluctuations, and propagation of electromagnetic waves
[NASA-TM-101248] N89-12830
Rayleigh lidar observations of gravity wave activity in the upper stratosphere at Urbana, Ill.
[NASA-CR-182738] N89-13107
WAVEFORMS
A GLR (Generalized Likelihood Ratio) algorithm for polyline approximation of waveforms
[AD-A197846] N89-13166
WAVEGUIDES
Mode extraction from an electromagnetic slow wave system N89-12767
WAVELENGTH DIVISION MULTIPLEXING
Fiber optic wavelength division multiplexing: Principles and applications in telecommunications and spectroscopy N89-13324

WAVELENGTHS
Wavelength or sensor selection by minimization of prediction error
[AD-A197231] N89-13216
Development of high efficiency opaque photocathodes for the Region 900 angstrom to 1200 angstrom
[NASA-CR-180597] N89-13249
WEAR
Surface characteristics of liquid oxygen cooled ball bearings N89-12640
Powder metallurgy bearings for advanced rocket engines N89-12641
Rolling contact fatigue life of zirconium and molybdenum nitride sputter plated AMS 5749 bearing steel N89-12642
WEAR RESISTANCE
Surface modification for wear resistance in a liquid oxygen turbopump environment N89-12644
Determination of sulfuric acid, oxalic acid, and their matrix effects in aluminum anodizing solutions by ion chromatography
[AD-A197734] N89-12694
WEATHER FORECASTING
An analysis of the error characteristics of Atlantic tropical cyclone track prediction models N89-13117
An analysis of the error characteristics of Atlantic tropical cyclone track prediction models
[AD-A197146] N89-13119
A global analysis and correlation of Nimbus 7 cloud and longwave radiation data
[AD-A197223] N89-13121
Forecasting aids for setting tropical cyclone conditions: Sasebo and Iwakuni, Japan
[AD-A197802] N89-13122
TURB: Turbulence forecasting for small/medium and large aircraft
[PB88-246368] N89-13125
WEATHER STATIONS
Hanford Meteorological Station computer codes. Volume 8: The REVIEW computer code
[DE88-015958] N89-13123
WEATHERING
Soiling, cleaning, and weathering effects on aircraft polyurethane topcoats
[AD-A197302] N89-12733
WEDGES
Shadows and wedges in scattering from the sea N89-12946
WEIBULL DENSITY FUNCTIONS
Calculation of Weibull strength parameters and Batdorf flow-density constants for volume- and surface-flaw-induced fracture in ceramics
[NASA-TM-100890] N89-12930
WEIGHT MEASUREMENT
Derivation of anthropometry based body fat equations for the Army's weight control program
[AD-A197371] N89-13132
WEIGHTLESSNESS SIMULATION
Glucose tolerance and insulin secretion during 0-g simulation
[DFVLR-FB-88-25] N89-13136
WELDABILITY
Influence of process parameters on laser weld characteristics in aluminum alloys
[AD-A197398] N89-12710
WELDED JOINTS
Influence of process parameters on laser weld characteristics in aluminum alloys
[AD-A197398] N89-12710
Fatigue crack growth of 5456-H116 aluminum and HSLA-80 weldments
[AD-A197830] N89-12712
BES welding science contractors
[DE88-016589] N89-12869
WELDING
Optically controlled welding system
[NASA-CASE-MFS-29291-1] N89-12868
WELLS
Development of Alaskan gas hydrate resources
[DE88-010270] N89-13093
WEST GERMANY
High temperature superconductivity research in selected laboratories in West Germany
[ONRL-8-011-R] N89-13291
WETLANDS
The extrapolation of spectral signatures illustrates LANDSATS' potential to detect wetlands N89-13067
WHEELS
Investigation into the applicability of fracture mechanics techniques to aircraft wheel life studies N89-12763
WHISKERS (CRYSTALS)
Synthesis and characterization of VLS-derived silicon carbide whiskers
[DE88-016226] N89-12679
SiC whisker-reinforced MoSi2
[DE88-016674] N89-12680
Chemical precursors to zinc sulfide: ZnS whisker synthesis
[AD-A197262] N89-13284
WHITE DWARF STARS
The development of a near-infrared polarimeter and its application to the continuum polarization of magnetic white dwarfs N89-12924
On the microstructure theory of a condensate layer in a white dwarf atmosphere
[DE88-703324] N89-13385
WICKS
Development of optimized, graded-permeability axial groove heat pipes N89-12614
WIND DIRECTION
An analysis of directional ambiguities in wind scatterometer measurements N89-13071
WIND EFFECTS
The Labrador Sea Extreme Waves Experiment: Objectives, status and plans N89-12974
WIND MEASUREMENT
Cloud track winds from polar orbiting satellites N89-13069
Model-based estimation of wind fields over the ocean from wind scatterometer measurements N89-13070
An analysis of directional ambiguities in wind scatterometer measurements N89-13071
Performance of a scanning pencil-beam spaceborne scatterometer for ocean wind measurements N89-13073
Effects of rainfall on scatterometer derived wind speeds N89-13074
WIND SHEAR
The effect of vertical wind shear on tropical cyclone movement
[AD-A197218] N89-13120
WIND TUNNEL STABILITY TESTS
Aerodynamics analysis of solid fuel Ramjet projectiles
[AD-A196755] N89-12548
WIND TUNNEL TESTS
Sidewall boundary-layer measurements with upstream suction in the Langley 0.3-meter transonic cryogenic tunnel
[NASA-CR-4192] N89-12544
Structure measurements in a synthetic turbulent boundary layer N89-12821
Wind tunnel investigation of the response of a sonic anemometer
[PB88-249826] N89-12847
WIND TUNNEL WALLS
Theoretical and experimental studies of the transonic flow field and associated boundary conditions near a longitudinally-slotted wind-tunnel wall N89-12545
WIND TUNNELS
Performance of the forward scattering spectrometer probe in NASA's icing research tunnel
[NASA-TM-101381] N89-12845
WIND TURBINES
Preliminary results from the dynamic response testing of the Northern Power Systems 100-kW wind turbine
[DE88-001166] N89-13101
WIND VELOCITY
Effects of rainfall on scatterometer derived wind speeds N89-13074
WINDPOWER UTILIZATION
21st century propulsion concept
[AD-A197537] N89-12663
WINTER
Bering Sea wave and ice measurements in support of Arctic west winter 1986
[AD-A197196] N89-13127
WOLF-RAYET STARS
Spectral variability of Wolf-Rayet stars
[DE88-703325] N89-13371
WOOD
Improving the fatigue resistance of adhesive joints in laminated wood structures
[NASA-CR-182165] N89-12675
WORDS (LANGUAGE)
Preattentive and attentive visual information processing
[AD-A197670] N89-13139
A lexical conceptual approach to generation for machine translation
[AD-A197356] N89-13304
WORKING FLUIDS
Improving the efficiency of binary cycles
[DE88-015108] N89-13099
WORKLOADS (PSYCHOPHYSIOLOGY)
Consequences of individual differences in brain organization for human performance
[AD-A197667] N89-13138
WORKSTATIONS
Advanced workstations for Meteosat command and control, volume 1
[BSO/AETR87030101-VOL-1] N89-12573
Advanced workstations for Meteosat command and control. Volume 2: Appendices
[BSO/AETR87030101-VOL-2] N89-12574
Three-dimensional visual display for a prototype command and control workstation
[AD-A197319] N89-13142
Providing intelligent assistance in distributed office environments N89-13189

X

X RAY DIFFRACTION
Characterization of graphite fibers by X-ray diffraction N89-12755
A refined model for characterizing X-ray multilayers
[DE88-013592] N89-12872
X RAY SOURCES
A refined model for characterizing X-ray multilayers
[DE88-013592] N89-12872
X RAYS
Design of vacuum chambers downstream of NSLS X-ray ring insertion devices
[DE88-015715] N89-13247

Y

YIELD STRENGTH
Simplified cyclic structural analysis of SSME turbine blades N89-12632
On the resistance of ceramics to high velocity penetration
[AD-A197320] N89-12734
YTTRIUM
Tm,Ho:YLF laser end-pumped by a semiconductor diode laser array
[NASA-CASE-NPO-17282-1-CU] N89-12856
YTTRIUM OXIDES
High T(sub c) superconductors: Will they replace helium temperature superconductors for magnets
[DE88-016632] N89-13279

Z

ZINC COATINGS
Moisture interaction and stability of ZOT (Zinc Orthotitanate) thermal control spacecraft coating N89-12618
ZINC OXIDES
Microstructure and nonlinearity of ZnO varistors, Volume 5, Number 8
[B8735659] N89-13290
ZINC SULFIDES
Chemical precursors to zinc sulfide: ZnS whisker synthesis
[AD-A197262] N89-13284
ZIRCONIUM ALLOYS
Mechanical behavior of superplastically-formed Al-Cu-Li-Zr alloy 2090
[DE88-016241] N89-12714

Typical Personal Author Index Listing

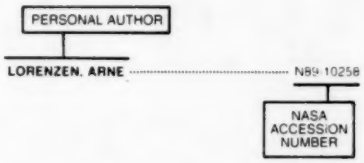

Listings in this index are arranged alphabetically by personal author. The NASA accession number denotes the number by which the citation is identified.

A

ABEYTA, J. R. N89-13299
ABICH, GERALD N89-12556
ABNER, MILTON D. N89-13142
ABOLGHASEM, H. N89-13293
ABRAMS, R. H. N89-13390
ADJEPONG, S. K. N89-13096
ADRIAN, JOHN M. N89-13226
ADVANI, SURESH GOPALDAS N89-12671
AFUWAPE, ANTHONY UYL N89-13201
Ai, CHIAYU N89-13248
AIKIN, R. M. N89-13292
AL-KHAYYAL, FAIZ A. N89-13206
AL-SARI, A. N89-13024
ALBERS, JAMES A. N89-12539
ALBRECHT, G. F. N89-12830
ALDEN, D. N89-12911
ALDRICH, T. E. N89-12791
ALEE, D. R. N89-12732
ALEXANDER, R. W., JR. N89-12696
ALHADDID, TALAL NAYEF MINWER N89-12705
ALLAMANDOLA, LOUIS J. N89-13337
N89-13346
N89-13367
ALLEN, D. H. N89-12906
ALLEN, G. P. N89-12909
ALLEN, J. F. N89-13180
ALLEN, L. E. N89-13314
ALVES, ADIL RAINIER N89-13109
AMAYENC, P. N89-12997
AMAZIGO, JOHN C. N89-12676
ANDERSON, M. N89-12584
ANDERSON, R. E. N89-12653
ANDERSON, WALLACE E. N89-13261
ANDERSON, WENDELL L. N89-13235
ANDREWS, G. L. N89-13123
ANDRIESSE, C. D. N89-13290
ANTOLOVICH, STEPHEN D. N89-12634
ARAI, K. N89-12981
ARAKERI, JAYWANT H. N89-12821
ARNEY, DAVID C. N89-13208
ARPIAINEN, VESA N89-13244
ARSENOVIC, PETER N89-12755
ARTILES, A. N89-12629
ASHBAUGH, NOEL E. N89-12864
ASHBY, DALE L. N89-12554
ATKINSON, P. N89-13065
ATKINSON, P. M. N89-12991
ATTA, RASHEED A. N89-12541
ATWATER, C. S. N89-12992
AYABE, K. N89-13007
AYDEMIR, A. Y. N89-13264

B

BAILEY, C. R. N89-12650
BAILEY, MARY L. N89-13156
N89-13177
BAILEY, RICHARD S. N89-12887
BAKER, C. BRUCE N89-12847
BALAKRISHNAN, N. N89-12996
BALCH, C. C. N89-13299
BALL, S. J. N89-12910
BALLESIO, MARINO N89-12603
BALSIGER, H. N89-13113
BAND, DAVID L. N89-13384
BANFIELD, L. J. N89-12942
BANKS, BRUCE A. N89-12589
BARBER, S. A. N89-12639
BARBIAN, E. P. N89-13273
BARD, ALLEN J. N89-12691
BARENGOLTZ, J. N89-12583
BARKAT, MOURAD N89-12792
BARKHOUDARIAN, SARKIS N89-12645
BARMATZ, MARTIN B. N89-13236
BARNES, C. W. N89-13260
BARRETT, C. A. N89-12717
BARRETT, W. P. N89-13299
BARTHELEMY, JEAN-FRANCOIS M. N89-13203
BARTHOLOME, E. N89-13003
BARTOLOTTA, P. A. N89-12909
BARWIG, H. N89-13313
BASS, ROBERT G. N89-12667
BASSAN, M. N89-12846
BASU, PRITHWISH N89-12870
BATTAGLIA, A. N89-12830
BATTAGLIA, ALESSANDRO N89-13374
BATTISTE, R. L. N89-12910
BAUDOT, Y. N89-12987
BAUER, F. N89-12840
BAUMGARTNER, M. F. N89-13049
BEAL, R. C. N89-12973
N89-12974
BEATTY, PAUL A. N89-12870
BEAUMONT, T. E. N89-13077
BECKEL, KURT A. N89-12600
BEEBE, KENNETH R. N89-13216
BEELER, RICHARD M. N89-12870
BEHRE, S. M. N89-13023
BELKIN, BRENDA L. N89-13143
BELKNAP, STUART B. N89-12608
BELL, J. F. N89-13349
BELL, R. J. N89-12696
BELLINI, P. X. N89-12684
BELWARD, A. S. N89-13084
BELZER, M. R. N89-13175
BENJAMIN, S. F. N89-12861
BENKE, STEVEN M. N89-13226
BENNETT, J. N89-13387
BENTON, DAVID N89-12602
BERAN, D. N89-13081
BERGERON, DOREEN W. N89-13222
BERGMAN, D. N89-12581
BERKER, A. N. N89-12695
BERNABEI, R. N89-13243
BERNATOWICZ, HENRY N89-12836
BERNSTEIN, I. MEL N89-12658
BERRA, P. B. N89-13180
BERRILLI, F. N89-13386
BERSHADER, DANIEL N89-12550
BEYER, A. N89-13011
BHAT, B. N. N89-12641
BHAT, P. K. N89-13098
BICKES, R. W., JR. N89-12625
BICKNELL, B. N89-12581
BIGIO, IRVING J. N89-12858
BIGNAL, E. N89-13084
BILES, J. A. N89-13180
BINIENDA, WIESLAW KAZIMIERZ N89-12669
BIRD, GRAEME A. N89-12834
BIRGENEAU, ROBERT J. N89-12695
BISHOP, A. R. N89-13288
BISOGNANO, JOSEPH J. N89-13245
BJORKMAN, MICHAEL D. N89-12607
BLACK, S. M. N89-13026
BLACKBURN, J. F. N89-12811
BLACKWELL, B. F. N89-12831
BLACKWOOD, WILLIAM O. N89-13296
BLAIR, MICHAEL F. N89-12897
BLAKE, OLIVER H. N89-12749
BLANCHARD, A. J. N89-12949
N89-13012
N89-13013
N89-13019
BLESS, R. C. N89-13311
BLIEM, C. J. N89-13099
BLIVEN, L. F. N89-13074
BOEHM, ROBERT F. N89-13095
BOERNER, W.-M. N89-12952
N89-12953
N89-12954
N89-13008
N89-13021
BONACUSE, PETER J. N89-12917
BONAS, A. G. N89-12625
BONIFAZI, P. N89-12846
BORDONI, F. N89-12846
BORNATICI, M. N89-13269
BORUCKI, WILLIAM J. N89-13310
N89-13314
BOS, A. M. N89-12573
N89-12574
BOSS, R. D. N89-13287
BOTTCHER, C. N89-13238
BOUCEK, G. P. N89-12557
BOUCHER, J.-M. N89-12968
BOWEN, K. A. N89-13180
BOWEN, THEODORE N89-13240
BOWERS, J. M. N89-13170
BOWLES, DAVID E. N89-12681
BOYLE, VINCENT M. N89-12749
BRADY, JOYCE A. N89-12589
BRAITHWAITE, T. N89-12591
BRANDT, G. L. N89-13170
BRAR, A. S. N89-12601
BREDOW, J. N89-13016
BREGMAN, JESSE D. N89-13347
N89-13360
N89-13367
BRENNAN, WILLIAM M. N89-12804
BRILEY, W. R. N89-12902
BRILL, MICHAEL H. N89-13222
BRINSON, H. F. N89-12928
BRISCO, B. N89-13076
BRISTOW, JULIAN N89-13252
BRITTAIN, J. O. N89-12886
BROCKHAUS, J. N89-12985
BROOKE, TIMOTHY Y. N89-13338
N89-13339
N89-13348
BROTHERTON, TIMOTHY J. N89-13257
BROWN, A. N89-13387
BROWN, JAMES A. N89-12635
BROWN, R. H. N89-13349
BROWN, R. J. N89-13076
BROWN, W. E. N89-13020
BROWNLEE, D. E. N89-13335
BRZUSKIEWICZ, J. E. N89-12616
BUDIANSKY, BERNARD N89-12676
BUGGELN, R. C. N89-12902
BUHL, HORST N89-12719
BULLOCK, JOHN N89-12757
BURIS, N. E. N89-12810
BURK, K. W. N89-13123
BURNS, B. A. N89-13034
BURONI, G. N89-12620
BUSH, HAROLD G. N89-12580
BUTCHER, J. R. N89-12612
BUTLER, JOHN M. N89-12745
BUTNER, MYLES N89-12640
BUTTNER, G. N89-13050

C

CALISE, A. J. N89-12538
CAMPBELL, JOHN H. N89-12860
CAMPINS, HUMBERTO C. N89-13331
N89-13354
N89-13360
CAMPION, D. G. N89-13077
CANDIDI, M. N89-13113
CANUTO, V. M. N89-12830
CAPPEL, K. L. N89-12627
CARDEN, HUEY D. N89-12935
CARDUS, J. O. N89-13114
N89-13309

CARIOU, C. N89-12968
CARLSON, G. E. N89-13064
CARLSON, JAMES E. N89-13155
CARLSSON, M. N89-13174
CAROL, M. N89-12571
CARPENTER, DAVID C. N89-12758
CARROLL, R. G. N89-12647
CARROLL, RAYMOND J. N89-13207
CARSON, RICHARD F. N89-12859
CARTER, BRUCE N89-12623
CARTER, DAVID H. N89-12680
CARTLEDGE, ALAN N89-12623
CARTWRIGHT, D. C. N89-13258
CASTELLANO, M. G. N89-12846
CASTRO, R. G. N89-13292
CATHCART, J. V. N89-12702
CATSIFF, E. H. N89-12726
CAYLOR, I. J. N89-12995
CECCARELLI, C. N89-13386
CELENLIGIL, M. CEVDET N89-12834
CHAI, A. T. N89-12753
CHAMBERLIN, RALPH V. N89-12708
CHAMIS, C. C. N89-12684
CHAN, CHUNG K. N89-12785
CHAN, H. C. N89-12797
CHAN, KWAI S. N89-12904
CHANDLER, W. T. N89-12654
CHANDRAMOULI, M. N89-12601
CHANG, A. T. C. N89-12998
N89-13045
CHANG, GEORGE C. N89-12919
CHAPLINE, GEORGE F. N89-12664
CHARTOFF, RICHARD P. N89-12745
CHASNOV, J. N89-12830
CHATHAM, H. N89-13098
CHAVEZ, JAMES M. N89-13095
CHEN, K. W. N89-13242
CHEN, M. F. N89-12949
CHEN, P. C. N89-12906
CHEN, PEHONG N89-13305
CHEN, ZONGZHI N89-13086
CHENGGANG, Y. N89-13094
CHERRY, S. M. N89-12993
CHIONCHIO, G. N89-12846
CHO, Y. M. N89-13175
CHOFFY, J. P. N89-12683
CHOI, KYUNAM N89-12759
CHOI, Y.-S. N89-12630
CHOY, L. N89-12806
CHRISTIANSEN, ALFRED W. N89-12675
CHRISTIANSON, D. E. N89-12679
CHUI, CHARLES K. N89-13209
CHURCHILL, P. N. N89-12944
CHYBA, CHRISTOPHER N89-13340
CHYU, M. K. N89-12858
CLARK, ALAN N89-13291
CLARK, B. C. N89-13334
CLARK, R. N. N89-13349
CLASPY, PAUL C. N89-12820
CLAUSING, R. E. N89-12713
CODY, JOE C. N89-12638
COHEN, M. C N89-13360
COHEN, S. C. N89-12982
COLLINS, CARL B. N89-12853
COLLINS, J. J. N89-12645
COLLINS, W. G. N89-13057
COMBES, M. N89-13352
COMBI, MICHAEL R. N89-13349
CONNELL, JOHN W. N89-12667
CONNELL, P. N89-13106
CONRY, S. E. N89-13180
N89-13187
CONRY, SUSAN E. N89-13186
CONWAY, J. A. N89-12945
COOK, R. T. N89-12648
COOK, T. S. N89-12921
CORBAN, J. E. N89-12538
CORDEY, R. A. N89-12945
N89-13029
N89-13072
CORKRAN, J. R. N89-12788
CORRIDAN, ROBERT E. N89-12623
COSMOVICI, C. B. N89-13112
COUTTS, T. J. N89-12819
COWLES, B. A. N89-12660
COWLEY, F. C. N89-13299
CRAWFORD, DAWN M. N89-12736
CRAWFORD, R. A. N89-12838
CRAWFORD, ROGER A. N89-12896
CRITCHLEY, B. R. N89-13077
CROFT, W. B. N89-13180
CROFT, W. BRUCE N89-13191
CROSS, J. B. N89-12592
CROVISIER, J. N89-13352
CRUICKSHANK, C. M. N89-13299
CRUIKSHANK, D. P. N89-13349
CSILLAG, F. N89-13050
CUNNINGHAM, JOCK N89-12836
CURRAN, P. J. N89-12990
CURTIS, D. N89-13084
CURTISS, H. C., JR. N89-12570
CUSHNIE, J. L. N89-12959
CYPHER, R. E. N89-13158
CZEKAJ, C. L. N89-13284

D

DAME, L. T. N89-12906
DANBERG, JAMES E. N89-12548
DANES, P. L. R. N89-13043
DANES, Z. F. N89-13043
DANFORD, MERLIN D. N89-12659
DANGELO, S. N89-13243
DANHOF, K. N89-13174
DANIS, ALLEN MICHAEL N89-12685
DANKS, ANTHONY C. N89-13342
DANSON, F. M. N89-12991
DARRAH, RODNEY C. N89-12754
DASCHBACH, J. N89-12816
DAVID, S. A. N89-12869
DAVIS, RANDALL C. N89-12741
N89-12786
DAVIS, ROBERT F. N89-12739
DAY, WILLIAM B. N89-12631
DEANNA, RUSSELL G. N89-12568
DEBIASE, G. A. N89-13312
DEBLANK, H. J. N89-13267
DEBROY, T. N89-12869
DEBSIKDAR, JAGADISH C. N89-12724
DEBUGARO, D. N89-12846
DECHENE, RONALD L. N89-12837
DELUCA, D. P. N89-12660
DEMASI, J. T. N89-12922
DEMORE, LOUIS N89-12598
DENORE, B. J. N89-13077
DEPASCALE, M. P. N89-13243
DERKS, WILLIAM N89-13229
DERRYBERRY, B. N89-13019
DERSTINE, MARK S. N89-12681
DESAI, S. S. N89-13149
DEVOS, W. N89-12960
DHAWAN, MEENA N89-13137
DHENDECOURT, LOUIS N89-13341
DICE, JACK W. N89-13296
DICKSON, PAUL W. N89-12664
DILLARD, D. A. N89-12928
DIMPSEY, ROBERT TOD N89-13145
DIONNE, GERALD F. N89-13280
DIPADUA, MARK A. N89-12560
DIPPOLITO, D. A. N89-13275
DIVINE, NEIL N89-13350
DOANE, J. W. N89-12729
DOBROWOLNY, M. N89-12576
DOLAN, FRED J. N89-12642
DOLAN, J. F. N89-13311
DOLATY, M. N89-13013
DOLLAR, M. N89-12658
DOMNANOVICH, A. N89-12658
DONN, BERTRAM N89-13361
DONNAY, J.-P. N89-12987
DORR, BONNIE J. N89-13304
DORSEY, JOHN T. N89-12580
DOSSER, LARRY R. N89-12848
DOUGHERTY, T. K. N89-12726
DOWDESWELL, J. A. N89-12976
DOWIE, P. N89-12964
DOYLE, R. J. N89-12735
DRAKE, N. N89-13024
N89-13026
DRAKES, JAMES A. N89-12760
DRESCHER, A. N89-13081
DRINAN, DAN N89-12657
DRING, ROBERT P. N89-12897
DRUMMOND, COLIN K. N89-12566
DRUMMOND, J. PHILIP N89-12542
DUBOIS, P. C. N89-12950
N89-12956
DUDERSTADT, E. C. N89-12921
DUDLEY, MICHAEL N89-12554
DUDZIAK, D. J. N89-13258
DUFOURD, J. F. N89-12965
DUFRANE, K. F. N89-12639
DUMBACHER, SUSAN M. N89-12761
DUNN, B. N89-13283
DWYER, THOMAS J. N89-12593
DYCKHOFF, WERNER N89-12718
DYKHUIZEN, R. C. N89-12787

E

EAGLESON, PETER S. N89-13091
EASTERLY, C. E. N89-12791
EASTMAN, WILLARD L. N89-13157
EATON, JOHN K. N89-12900
EATON, N. N89-13351
EBEL, W. J. N89-13064
EBONG, A. U. N89-13096
EDSINGER, LARRY E. N89-12623
EERENS, H. N89-12960
EGETH, HOWARD E. N89-13139
EHLERS, K. W. N89-13390
EINSTEIN, THEODORE L. N89-12715
EISBRECHER, HANS-DIETER N89-12556
ELIAS, W. E. N89-12726
ELKS, MICHAEL S. N89-13147
ELLIOT, J. L. N89-13311
ELLIS, J. R. N89-12908
N89-12909
ELM, JOE N89-12598
ELMORE, D. L. N89-12884
ELSEN, LIZ N89-12575
ELTOFT, T. N89-12970
ENCRENAZ, THERESE N89-13341
N89-13352
ENGLUND, D. R. N89-12878
ENLOW, K. SUZANNE N89-12762
ENNEKING, THOMAS J. N89-12763
ENSIGN, C. ROBERT N89-12877
EOM, H. J. N89-12952
N89-12953
EPPELDAUER, G. N89-13317
EPPLEY, K. N89-12812
ERBSCHLOE, DONALD R. N89-13281
ERDMANN, R. K. N89-13324
ESHAGHIAN, BIJAN N89-13133
ESKRIDGE, ROBERT E. N89-12847
ESPY, SUSAN K. N89-12754
ESSLINGER, MARIA N89-12933
ETTER, PAUL C. N89-13126
EVANS, BRAD N89-13225
EVANS, J. W. N89-12828
EVERHART, JOEL LEE N89-12545
EVES, JOHN W. N89-12841

F

FAHY, S. N89-12686
FALICOV, L. M. N89-13289
FAN, L. S. N89-12789
FAN, U. J. N89-12630
FARHAT, NABIL H. N89-13199
FARR, T. G. N89-12950
FARRELL, J. A. N89-13390
FASANELLA, EDWIN L. N89-12935
FATEMAN, RICHARD J. N89-13146
FAURIE, JEAN-PIERRE N89-13286
FEDEL, B. N89-13312
FEIL, O. G. N89-12605
FENSTERMACHER, C. A. N89-13258
FERGUSON, G. L. N89-13167
FERNANDEZ, J. C. N89-13260
FESCOS, GEORGE N89-12700
FEYOCK, STEFAN N89-13152
FILLERY, N. P. N89-13075
FINELL, GEORG N89-13140
FISCHER, BERND N89-13200
FISHER, STEVEN C. N89-12651
FITZGERALD, P. I. N89-13132
FLAHERTY, JOSEPH E. N89-13208
FLANAGAN, DAVID N89-12736
FLANDRO, G. A. N89-12538
FLEISCHMANN, M. N89-12816
FLOWERS, KENNETH D. N89-13235
FLYNN, GEORGE W. N89-12815
FOLDS, DENNIS F. N89-13138
FOODY, G. M. N89-12990
N89-13062
FORSMAN, TINA N89-13224
FOSTER, J. L. N89-13045
FOUT, S. L. N89-12706
FOWLER, J. N89-13314
FOX, D. S. N89-12717
FOX, T. N89-12630
FRANK, C. N89-13040
FRANK, C. W. N89-12731
N89-12732
FREEDMAN, MARC R. N89-12746
FREEMAN, A. N89-12956
N89-13014
N89-13018
N89-13020
FRENCH, J. B. N89-12591

FREUND, ROLAND N89-13200
FREY, H. U. N89-12605
FRIEDMAN, G. I. N89-12641
FRIEDMAN, JEROME H. N89-13213
FRIEMAN, J. N89-13388
FRYE, MARK W. N89-12867
FU, C. C. N89-12731
N89-12732
FUK, K. N89-13073
FUKUE, K. N89-13061
N89-13066
FUNG, A. K. N89-12948
N89-13012

G

GABLE, BEVERLEY A. N89-12764
GAGNON, DEBORAH A. N89-12765
GAILEY, P. C. N89-12791
GAISER, P. W. N89-13046
GALDON, E. N89-13114
GALL, PETER D. N89-12551
GAMBHIR, R. D. N89-12601
GAN, S. N89-12730
GARAND, L. N89-12999
GARBER, FRED D. N89-12808
GARDNER, C. S. N89-13107
GARDNER, FRANK H. N89-12597
GARRETT, STEVEN L. N89-13236
GARRITY, PATRICK J. N89-13306
GAUGLER, RAYMOND E. N89-12879
GAUSE, EMILY M. N89-13133
GEDEON, STEPHEN N89-13227
GEHRZ, R. D. N89-13333
GEHRZ, ROBERT D. N89-13353
GEILE, W. N89-13048
GEISELHART, RICHARD N89-12560
GEIST, JON N89-13320
GELLENBECK, EDWARD M. N89-12766
GELLER, JAMES N89-13181
GELLIN, S. N89-12906
GEOFFROY, G. L. N89-13284
GEORGE, THOMAS F. N89-13241
N89-13285
GERACHI, A. N89-12985
GERALD, JAMES A. N89-12767
GERBERICH, W. W. N89-12927
GERLACH, ALBERT A. N89-13235
GERLING, T. W. N89-12974
GESCH, D. B. N89-13083
GESLIN, D. N89-12886
GESSOW, ALFRED N89-13295
GHANDHI, S. K. N89-13282
GHIA, K. N. N89-12553
GHIA, U. N89-12553
GIBSON, PETER R. N89-12737
GIBSON, ROBERT B. N89-12858
GILLESPIE, G. H. N89-13390
GILLHAM, J. K. N89-12730
GINOUX, J. J. N89-12849
GIOMMI, M. N89-12613
GIORDANO, JOHN N89-12628
GIRARD, JEFFREY J. N89-12768
GIRTEN, BEVERLY ELAINE N89-12769
GIRUZZI, G. N89-13268
N89-13276
GIUSTI, LAURA N89-12770
GJERTSEN, A. K. N89-13059
GLACCUM, WILLIAM N89-13354
GLADDEN, HERBERT J. N89-12880
GLAESE, JOHN R. N89-12595
N89-12596
GLASHEEN, W. M. N89-13256
GLAZER, J. N89-12714
GLOSS, BLAIR B. N89-12841
GLOVER, ROLFE E., III N89-12715
GLOZMAN, VLADIMIR N89-12610
GLYDE, H. R. N89-13277
GODBOLE, S. P. N89-13093
GODDARD, J. F. W. N89-12993
GODFREY, BRENDAN B. N89-13164
GOEDBLOED, J. P. N89-13275
GOEDHEER, W. J. N89-13270
GOELTZ, RICHARD N89-13221
GOESSL, H. N89-12939
GOGINENI, S. N89-13016
GOGINENI, S. P. N89-13031
GOLDMAN, T. N89-13294
GOLEMME, A. N89-12729
GOLISCH, W. F. N89-13368
GOMBEER, P. N89-12960
GONG, XIN-GAO N89-12721
GONZALEZ, A. L. N89-12611
GONZALEZ, CHARLES C. N89-12618
GORDON, STEPHEN S. N89-12868
GORMAN, T. S. N89-13170
GRAHAM, R. A. N89-12840
GRAHAM, S. L. N89-13160
GRANT, HOWARD P. N89-12887
GRANT, K. N89-13106
GRASDALEN, GARY L. N89-13355
GRAY, E. R. N89-13246
GREEN, D. R. N89-12963
GREEN, JOANNE N89-13138
GREEN, MICHAEL A. N89-13278
N89-13279
GREEN, S. F. N89-13355
N89-13364
GREENLAW, RAY N89-13176
GREGOIRE, J.-M. N89-13003
GREGORY, W. S. N89-12788
GRIEP, D. M. N89-13368
GRIESEL, MARTHA A. N89-13165
GRIFFIN, D. C. N89-13238
GRIFFITHS, G. H. N89-13058
GRIFFITHS, P. S. N89-13022
GRIGORIEV, A. N89-13352
GRIMALDI, MARGARET E. N89-12621
GROOM, G. B. N89-12990
GROSSMAN, ERICH NATHAN N89-13329
GROSSMAN, JAMES W. N89-13095
GUHA, ALOKE N89-13252
GUIDONI, U. N89-12576
N89-13112
GUITON, T. A. N89-13284
GUNBURGER, MAX D. N89-13178
GUSTAFSON, BO A. S. N89-13366
GUTTMANN, S. N89-13085
GUYENNE, T. D. N89-12936
GYEKENYESI, JOHN P. N89-12930

H

HAAKE, F. K. N89-12660
HAEFNER, H. N89-13044
HAGAN, LYNN P. N89-12575
HAGER, ROY D. N89-12565
HAISLER, W. E. N89-12906
HAJA, S. R. N89-13053
HAJEK, T. J. N89-12899
HALFORD, GARY R. N89-12635
N89-12882
HALL, C. D. N89-13072
HALL, PETER N89-13207
HALL, ROBERT F. N89-12559
HALLIKAINEN, M. T. N89-13036
N89-13038
N89-13041
HAMILTON, C. B. N89-12791
HAMPSON, MICHAEL E. N89-12645
HANCOCK, D. N89-12806
HANNA, THOMAS E. N89-13134
HANNER, M. S. N89-13333
HANNER, MARTHA N89-13332
HANNER, MARTHA S. N89-13330
N89-13344
N89-13368
HANNIGAN, J. W. N89-12704
HANSEN, GREGORY A. N89-13154
HANSEN, PATRICIA A. N89-12585
HANTZIOS, PANAYIOTIS N89-13380
HARA, N. N89-12980
HARDIS, J. N89-13323
HARKINS, THOMAS N89-12771
HARMAN, E. A. N89-13132
HARPER, WARREN N89-12790
HARRIS, D. B. N89-13258
HARRIS, J. M. N89-12816
HARRISON, MICHAEL A. N89-13305
HARROLD, RONALD T. N89-12873
HARRUFF, PAUL W. N89-12873
HART, R. E., JR. N89-12819
HARTKE, G. J. N89-12830
HARTLE, M. N89-12906
HARTMAN, GEORGE A. N89-12864
HARTMANN, LEE N89-13375
HARTUP, DAVID C. N89-13138
HARVEY, JAMES A. N89-12745
HARVEY, WILLIAM T. N89-13133
HARWELL, WILLIAM D. N89-12866
HATHAWAY, R. G. W. N89-12983
HATTEMER-FREY, HOLLY A. N89-13135
HAUCK, M. N89-13081
HAWKE, R. S. N89-12578
HAYNE, G. N89-12806
HAYWARD, THOMAS L. N89-13355
HEACOX, WILLIAM D. N89-13326
HEADLEY, P. S. N89-12625
HEALEY, R N89-12964
HEATHERLY, L. N89-12713
HEBSUR, M. G. N89-12717
HEGEDUS, CHARLES R. N89-12733
HELD, D. N. N89-13020
HEMMATI, HAMID N89-12856
HENDERSON, DAVID N89-12598
HENINS, I. N89-13260
HENKE, BURKE L. N89-12872
HERGENROTHER, PAUL M. N89-12667
HERRMANN, HARTMUT N89-13124
HESS, DENNIS W. N89-13261
HETTMANSPERGER, THOMAS P. N89-13218
HILL, HENRY A. N89-13389
HILL, SCOTT M. N89-12820
HILLER, K. N89-13081
HILLERY, R. V. N89-12921
HIRST, DONALD J. N89-12733
HOBART, H. F. N89-12888
HOCK, S. M. N89-13101
HODGDON, J. A. N89-13132
HODGES, DONALD Y. N89-12572
HODO, J. N89-12657
HOGG, J. N89-12962
N89-12967
HOLBROOK, J. N89-12964
HOLDER, LAWRENCE B., JR. N89-13163
HOLLIS, ADRIENNE L. N89-12772
HOLLOWAY, K. N89-12993
HOLMES, BRUCE J. N89-12551
HOLMES, H. ROLLAND N89-12614
HOLT, A. R. N89-12994
HOLT, R. V. N89-12906
HOLTZMAN, J. C. N89-13031
HOMMA, M. N89-12980
HORST, REINER N89-13206
HOVENAC, EDWARD A. N89-12845
HOWE, ROGER T. N89-12844
HOWMAN, A. N89-13067
HOWSMAN, THOMAS G. N89-12596
HRESKO, G. C., III N89-12636
HSIAO, BRYAN C. N89-13297
HUANG, H. N89-12906
HUBER, G. N89-13313
HUBERT, J. N89-12591
HUFF, DENNIS L. N89-12555
HUFFMAN, DONALD R. N89-13356
HUGHES, J. STEVEN N89-13165
HUGHES, R. J. N89-13294
HUGHES, WILLIAM F. N89-12870
HULSE, CHARLES O. N89-12887
HUMPHRIES, R. G. N89-12994
HUMPHRIES, T. S. N89-12641
HUNT, J. J. N89-12936
HUNT, JOHN T. N89-12860
HUNT, L. ROANE N89-12822
HURON, ERIC S. N89-12634
HUSSAINI, M. YOUSUFF N89-12543
HUST, J. G. N89-12670
HUTCHISON, JOOP N89-12600
HUYER, STEPHEN A. N89-12773
HYLTON, LARRY D. N89-12903
HYVARINEN, OLLI N89-13172
HYYPPA, J. M. N89-13036

I

IAFOLLA, V. N89-12846
IANNILLI, M. N89-12846
IDE, ROBERT F. N89-12845
IESS, L. N89-13112
IGARASHI, T. N89-12980
IGUCHI, STEVEN K. N89-12554
IIKURA, Y. N89-13060
ILLINGWORTH, A. J. N89-12995
IMHOFF, M. L. N89-13083
ITIKAWA, YUKIKAZU N89-13237
ITTEN, K. I. N89-13040
IUCCI, N. N89-13243

J

JAASKELAINEN, V. I. N89-13041
JACKSON, J. T. N89-13144
JACKSON, L. ROBERT N89-12741
JACKSON, ROBERT N89-12786
JACKSON, ROBERT W. N89-12623
JACKSON, T. J. N89-13006
JACOBS, A. J. N89-12713
JACOBS, E. W. N89-13287
JACOBSEN, S. N89-12970
JAECKEL, LOUIS A. N89-13214
JAMES, B. D. N89-12954
JAMES, DAVID L. N89-12774
JAMES, GEORGE HENRY, III N89-12775
JAMESON, R. A. N89-13390

JARBOE, T. R. N89-13260
JARRELL, JERRY D. N89-13122
JARVIS, C. N89-13051
JASINSKI, MICHAEL F. N89-13091
JAYARAMAN, N. N89-12911
JEDRUCH, JACEK N89-12662
JELSKI, DANIEL A. N89-13241
JENKINS, T. N89-12583
JENKINS, TERESA K. N89-12585
JENTZ, R. R. N89-13039
JEWETT, R. P. N89-12636
JOHANSSON, ALLAN N89-13244
JOHNSEN, H. N89-12970
JOHNSON, B. V. N89-12899
JOHNSON, D. N89-13030
JOHNSON, GARY S. N89-12867
JOHNSON, L. R. N89-12635
JOHNSON, MICHELE E. N89-12776
JOHNSON, T. V. N89-13349
JONES, JAMES D. N89-13232
JONES, LISA E. N89-12935
JONES, T. E. N89-13287
JONGERT, J. N89-12573
N89-12574
JORDAN, E. H. N89-12912
JOSLYN, H. DAVID N89-12897
JUHASZ, I. N89-13050
JUVET, R. S., JR. N89-12738
JUZDAN, Z. RUSSELL N89-13105

K

KAEHNY, D. N89-12955
N89-12957
KAMATH, V. A. N89-13093
KAMINSKI, C. D. N89-13368
KANNEL, J. W. N89-12639
KAPOLNEK, MICHAEL R. N89-12614
KARKI, K. C. N89-12890
KAROUCHE, N. N89-12997
KARWE, MUKUND VISHNU N89-12824
KASISCHKE, E. S. N89-13015
KATZ, J. D. N89-12679
N89-13292
KATZER, EDGAR N89-12839
KAUFFMAN, D. S. N89-13053
KAUFFMAN, J. F. N89-12810
KAUFMAN, ALBERT N89-12632
KAUPP, V. N89-13019
KAWATA, Y. N89-13042
KAY, GREGORY J. N89-12929
KAY, S. N89-13054
KEEFE, D. N89-13390
KELHAE, VAEINOE N89-13244
KELLEHER, M. D. N89-12692
KELLER, GEORGE K. N89-12751
KELLER, M. N89-12961
KELLER, ROBERT N89-12623
KELLNER, MARC I. N89-13154
KELSO, THOMAS S. N89-12796
KENIK, E. A. N89-12702
KENNETT, R. G. N89-13073
KEYDEL, W. N89-12939
KHADJEHPOOR, M. R. N89-13293
KHOBAIB, M. N89-12864
KHORRAM, S. N89-12985
KIM, DONGMOON N89-12698
KIM, K. S. N89-12915
N89-12921
KIM, S. H. N89-13242
KINCAID, JOHN M. N89-12700
KING, A. M. N89-13148
KING, R. B. N89-13051
KINGWELL, J. N89-12979
KIRBY, F. M. N89-12648
KIRCHHOF, W. N89-13085
KIRKPATRICK, J. W. N89-13132
KISER, JAMES D. N89-12746
KLABUNDE, KENNETH J. N89-12707
KLEIN, J. D. N89-12956
N89-13014
N89-13020
KLENKE, CHRIS J. N89-12727
KNACKE, R. F. N89-13338
N89-13348
KNAUSS, W. G. N89-12726
KNOTT, W. M., III N89-13144
KODAMA, GOJI N89-12689
KOEHLER, H. A. N89-13254
KOENIG, KLAUS N89-12556
KOJIMA, M. N89-12740
KONG, J. A. N89-12794
KONNO, ICHISHIRO N89-13376
KOONTZ, S. L. N89-12590
KOSTINSKI, A. B. N89-12952
N89-12954
N89-13021
KOWALSKI, BRUCE R. N89-13216
KOZMINCHUK, BRIAN W. N89-12805
KRAINER, ANDREAS N89-12835
KRESS, J. D. N89-13212
KROGSTAD, H. E. N89-12972
KROLL, JAMES T. N89-13117
N89-13119
KROMP, W. N89-12658
KRUGER, CHARLES H. N89-13262
N89-13263
KRUGER, R. M. N89-12713
KRUTZ, ROBERT W. N89-13133
KUAN, S. W. N89-12731
N89-12732
KULIKOWSKI, CASIMIR A. N89-13303
KUMAR, GANESH N. N89-12568
KUMINECZ, J. N89-12590
KUMMEROW, C. D. N89-12992
KUNZ, EDWARD L. N89-13235
KUSAKA, T. N89-13042
KUX, H. J. H. N89-13080

L

LAAGER, P. N89-13044
LACONTI, ANTHONY B. N89-12818
LADWIG, A. M. N89-13144
LAFLEN, J. H. N89-12915
LAGOMASINO, ADOLFO N89-13197
LAIT, LESLIE ROBERT N89-13108
LAMBERT, D. L. N89-13342
LAMBERTY, M. N89-13085
LAMPTON, M. N89-13249
LAMY, PHILIPPE L. N89-13357
LAN, E. H. N89-12592
LANDEE-THOMPSON, SAM N89-13193
LANDIS, DAVID W. N89-12777
LANDIS, SHARON K. N89-12778
LANGENFELD, CRAIG A. N89-12779
LANGLOIS, P. M. N89-13046
LANGNER, A. N89-13285
LANGTON, C. A. N89-12742
LANZL, F. N89-13081
LAROUCHE, P. N89-12968
LASSING, H. S. N89-13271
LAU, STEPHEN N89-12870
LAUDER, K. N89-12616
LAUFENBERG, THEODORE L. N89-12675
LAUFER, P. M. N89-12852
LAURSEN, TOD A. N89-12929
LAVID, MOSHE N89-12693
LAW, C. C. N89-12711
LAWLESS, K. R. N89-12702
LAWRENCE, JOHN S. N89-12562
LAYCOCK, J. N89-13071
LE, HUONG G. N89-12617
LEBOFSKY, L. A. N89-13349
LECURU, D. N89-12683
LEE, C. N89-12629
LEE, L. M. N89-12840
LEFEBVRE, DIDIER R. N89-12928
LEGER, CHRISTOPHER B. N89-12780
LEGER, L. N89-12590
LEI, J. F. N89-12886
LEISS, J. E. N89-13390
LENNOX, JAMES E. N89-13162
LEPPARD, W. R. N89-12697
LESCHLY, K. N89-12583
LESLIE, I. H. N89-12788
LESSER, V. R. N89-13180
LESSER, VICTOR N89-13189
N89-13191
LESSNER, PHILIP N89-12818
LETTIS, DAVID STUART LAWRENCE N89-12825
LEUNG, T. N89-13016
LEVINE, R. Y. N89-13179
LEVINSKAS, DAVID N89-13228
LEVIS, ALEXANDER H. N89-13192
LEVY, RAM L. N89-12873
LI, S. T. N89-12802
LIANG, P. Y. N89-12652
LIBURA, MAREK N89-13204
LIBY, BRUCE W. N89-12781
LICKLIDER, J. C. N89-13159
LIEBENBERG, DONALD H. N89-13291
LIECHTI, K. M. N89-12726
LIEN, DAVID J. N89-13358
LIN, J. N89-12711
LINDEWALL, H. N89-12588
LINDHOLM, ULRIC S. N89-12904
LING, S. C. N89-12833
LINK, L. R. N89-12712
LINSKY, J. L. N89-13387
LISEAU, R. N89-13386
LITVA, J. N89-12797
LIU, A. N89-12920
LIU, C. H. N89-13107
LIU, H. W. N89-12918
LIVAS, JEFFREY C. N89-12599
LIVERANI, S. N89-12613
LOCKETT, JOHN FRANCIS N89-12827
LOCKWOOD, G. W. N89-13321
LOEWENSTEIN, R. F. N89-13354
LOK, J. N89-13271
LONG, D. G. N89-13070
LONG, L. L. N89-12696
LOPESCARDOZO, N. J. N89-13272
LORENZETTI, D. N89-13386
LORGE, FRANK N89-12558
LOU, Y. N89-13020
LOUIE, S. G. N89-12686
LOWDERMILK, W. HOWARD N89-12860
LU, CHENG-YI N89-13103
LUBMAN, DAVID M. N89-12851
LUND, J. N89-12629
LUNDEN, B. N89-13055
LUSE, STEPHEN N89-12803
LYALL, H. N89-13316
LYNCH, DAVID K. N89-13359
N89-13360

M

MAAG, C. N89-12584
MAAG, CARL R. N89-12585
MACARAEG, MICHELE G. N89-12543
MACARTHUR, J. L. N89-12973
MACCAGNO, P. N89-12732
MACHADOESILVA, ANTONIO JOSE F. N89-13090
MACIEJEWSKI, PAUL N89-12900
MACKIN, S. N89-13024
MACKLIN, J. T. N89-12945
N89-13029
MACLEOD, H. ANGUS N89-13327
MADAN, A. N89-13098
MAE, S. N89-12975
MAEDA, K. N89-13004
MAFFEO, R. J. N89-12907
MAGILL, J. H. N89-12740
MAIANI, M. N89-12846
MAJUMDAR, SAURIN N89-12633
MALEY, M. P. N89-13292
MALIK, S. N. N89-12915
MALKAN, MATTHEW A. N89-13384
MANDERSCHEID, J. M. N89-12632
MANDOCK, RANDAL L. N89-12782
MANSOURI, R. N89-13293
MARCHENKO, S. V. N89-13371
MARCI, GUENTER N89-12719
MARELLI, L. N89-13078
MARENGO, L. R. M. N89-13077
MARIS, H. J. N89-13233
MARKLIN, G. J. N89-13260
MARTEL, CHARLES R. N89-12750
MARTIN, DOUG N89-12803
MARTIN, JOHN R. N89-12562
MARTIN, R. L. N89-13288
MARTINEC, J. N89-13045
MARTINEZ, L. N89-12703
MARTINS, JOAO P. N89-13182
N89-13183
N89-13185
MARTY, DAVID N89-12638
MARTZ, JOSEPH C. N89-13261
MARYNICK, DENNIS S. N89-12728
MARZOUG, M. N89-12997
MASCHKE, PETER N89-13140
MASCY, ALFRED C. N89-12623
MASON, L. W. N89-13334
MASTERS, A. I. N89-12647
MATEJCZYK, DAN E. N89-12636
MATHEWS, J. N89-13084
MATLOCK, D. K. N89-12869
MATSON, D. L. N89-13349
MATSUMOTO, Y. N89-12989
MATTERN, JAMES W. N89-12783
MAXWELL, DAVID C. N89-12864
MAYBURY, MARK T. N89-12800
N89-12801
MAYES, LARRY L. N89-12709
MCAULIFFE, PATRICK S. N89-12741
MCBETH, MATTHEW B. N89-12784
MCCORD, T. B. N89-13349
MCDONALD, A. J. W. N89-13087
MCDONALD, H. N89-12902
MCDONALD, T. E. N89-13258
MCDONNELL, J. A. M. N89-13364
MCDONNELL, V. G. N89-12892
MCEVILY, A. J. N89-12869

MCGAW, MICHAEL A. N89-12917
MCGILL, COLIN ANDREW N89-13381
MCGINNIS, W. C. N89-13287
MCGUINNESS, B. N89-12994
MCGUINNESS, BRIAN B. N89-13345
MCGUIRE, J. N89-13057
MCHARGUE, C. J. N89-12743
MCHARGUE, CARL J. N89-12744
MCINTOSH, R. E. N89-13046
MCINTYRE, M. E. N89-13110
MCKAY, J. A. N89-12852
MCKEAGUE, IAN W. N89-13205
N89-13217
MCKILLIP, R. M., JR. N89-12570
MCKINZIE, D. J. N89-12552
MCKNIGHT, R. L. N89-12906
N89-12907
N89-12921
MCNUTT, L. N89-13037
MCPHERSON, W. BRYAN N89-12661
MEAKIN, P. N89-13361
MEECH, KAREN N89-13362
MEI, CHUH N89-12923
MENDEL, J. M. N89-13070
MERCER, STEPHEN D. N89-12646
MESSIDORO, PIERO N89-12603
METZGER, D. E. N89-12898
MEYER, H. M., III N89-13285
MEYER, R. A. N89-13180
N89-13187
MEYER, ROBERT A. N89-13186
MEYER, T. G. N89-12916
MEYER, THOMAS J. N89-12666
MIGDALL, A. L. N89-13323
MILAM, LAURA J. N89-12604
MILLARD, J. N89-12584
MILLER, ALLEN R. N89-13210
MILLER, D. N89-13009
MILLER, DOUGLAS R. N89-13153
MILLER, G. M. N89-12616
MILLER, L. N89-12806
MILLER, M. S. N89-13107
MILLER, PETER J. N89-13318
MILLER, ROBERT A. N89-12883
N89-12919
MILLER, T. N89-13020
MILLIGAN, WALTER W. N89-12634
MILLINGTON, A. C. N89-13028
MILNE, A. K. N89-13068
MINEART, GARY M. N89-13092
MINES, G. L. N89-13099
MITCHELL, A. J. B. N89-13051
MITCHELL, C. W. N89-12966
MIZOGUCHI, T. N89-13060
MO, TSAN N89-12951
MOBLEY, CURTIS D. N89-13128
MODENA, I. N89-12846
MODESTINO, J. W. N89-13180
MOFFAT, ROBERT J. N89-12900
MOISAN, M. N89-12591
MON, GORDON R. N89-12618
MONALDO, F. M. N89-12969
N89-12973
MONFORD, LEO G. N89-12842
MONGIA, H. C. N89-12890
N89-12891
N89-12892
MOON, H. K. N89-12898
MOON, T. J. N89-12832
MOORE, BETH R. N89-13165
MOORE, BOUDE C. N89-12599
MOORE, DENNIS N89-12657
MOORE, R. K. N89-13016
N89-13031
N89-13073
MOORHEAD, PAUL E. N89-12913
MORE, JORGE J. N89-13168
MOREIRA, J. A. N89-12943
MOREY-HOLTON, E. R. N89-13144
MOREY, DENNIS N89-13227
MORGAN, P. E. D. N89-13283
MORISON, W. D. N89-12591
MOROZ, V. I. N89-13352
MORRICE, J. G. N89-12967
MORRIS, BRIAN G. N89-12843
MORRIS, J. W., JR. N89-12714
MORRISON, GRAHAM N89-12700
MORTON, A. J. N89-12988
MOSELEY, S. H. N89-13354
MOSIER, RICHARD L. N89-12563
MOSS, JAMES N. N89-12834
MOSTAFA, A. A. N89-12892
MOUL, DAVID S. N89-12593
MOWLE, A. N89-12964
MOXSON, V. N89-12641
MRACEK, CURTIS P. N89-12549
MUKAI, TADASHI N89-13363
MULLER, R. S. N89-12789
MULLIGAN, JEFFREY B. N89-13171
MUNDAY, T. J. N89-13024
MUNRO, D. C. N89-12990
MURBACH, MARCUS S. N89-12623
MURMANIS, LIDIJA L. N89-12675
MURPHY, B. T. N89-12643
MURPHY, MIKE N89-12653
MURPHY, P. K. N89-13251
MURRAY, JOHN R. N89-12860
MURTHY, A. V. N89-12544
MURTHY, P. L. N. N89-12684
MURTHY, S. N. B. N89-12891
MUTALIK, PRALHAD N89-13093

N

NADASDI, I. N89-12987
NADEM, MEHRDAD N89-13093
NAERHEIM, YNGVE N89-12644
NAGLIC, STEVEN J. N89-13125
NAGY, G. N89-13180
NAIDU, DESINENI S. N89-12569
NAMBU, YASUSADA N89-13373
NANCE, C. E. N89-12949
NARAYANAN, R. M. N89-13046
NARENDRA, KUMPATI S. N89-12624
NASR, J. M. N89-13010
NATARAJAN, SUBRA N89-13252
NAVRATIL, G. A. N89-13271
NEAL, D. R. N89-12857
NELSON, RICHARD S. N89-12914
NEUMANN, J. F. N89-12920
NEWCOMER, J. A. N89-12958
NEWQUIST, L. A. N89-12696
NEY, E. P. N89-13353
NG, LILLIAN N89-12644
NGUYEN, Q. N89-13020
NICHOLS, B. D. N89-12788
NICHSON, JAMES D. N89-13231
NIEH, T. G. N89-12714
NIETO, MICHAEL MARTIN N89-13294
NIKJOOY, M. N89-12891
NIRENBURG, IRENE N89-13190
NIRENBURG, SERGEI N89-13188
N89-13189
N89-13190
NISHIO, F. N89-12975
NISSLEY, D. M. N89-12916
NOAH, SHERIF T. N89-12630
NORCROSS, G. N89-13074
NORDINE, P. N89-12590
NOTKIN, DAVID N89-13156
N89-13177
NOVAK, L. M. N89-12794
NUNAMAKER, ROBERT N89-13198
NUNN, STEPHEN N89-12803

O

OBERLE, LAWRENCE G. N89-12885
OCONNOR, E. A. N89-13087
ODEN, S. F. N89-12973
ODONNELL, TIMOTHY N89-12618
ODORICO, J. N89-12683
OEPTS, D. N89-13271
OGLESBY, PAUL H. N89-13389
OHMAE, H. N89-12975
OHTA, K. N89-12980
OLEARY, SCOTT T. N89-12619
OLNESS, DOLORES U. N89-13100
OLSEN, R. B. N89-12972
OLSON, D. L. N89-12869
OLSON, ROBERT M. N89-13133
OMARI, PIERPAOLO N89-13201
OMLIE, AUSTIN R. N89-12562
OOMENS, A. A. M. N89-13271
OPAL, CHET B. N89-13319
ORCHARD-HAYS, WILLIAM N89-13169
ORDAL, M. A. N89-12696
OREN, ABRAHAM L. N89-12872
ORR, HORACE A. N89-12560
ORSINI, S. N89-13113
OSGOOD, R. M. N89-13101
OSGOOD, RICHARD M., JR. N89-12815
OSHIDA, YOSHIKI N89-12918
OSULLIVAN, K. N. N89-12979
OTTO, G. P. N89-13063
OVERBEEK, R. N89-13174
OVERFELT, P. L. N89-12798
OVERMAN, ANDREA L. N89-13202

P

PACK, R. T. N89-13212
PAI, SHANTARAM S. N89-12930
PALLINI, ROBERT A. N89-12637
PANTANO, C. G. N89-13284
PAO, H. P. N89-12833
PAOLUZI, L. N89-13243
PARANJPE, SURESH G. N89-13093
PARDALOS, PANOS M. N89-13206
PARK, ROBERT L. N89-12715
PARKER, G. A. N89-13212
PARKER, R. K. N89-13390
PARKINSON, W. J. N89-12679
PARMA, GEORGE F. N89-12865
PARRY, ROBERT W. N89-12689
PARTINGTON, K. C. N89-13035
PATANKAR, SUHAS V. N89-12890
N89-12894
N89-12901
PATERNO, L. N89-13312
PATERSON, JOHN A. N89-12622
PATIL, S. L. N89-13093
PAUL, R. E. N89-12696
PAULEY, WAYNE N89-12900
PAVATE, T. V. N89-13082
PAWEL, J. E. N89-12725
N89-12743
PAZARGADI, SHAYAN N89-12609
PEASE, R. F. N89-12731
PEETERS, H. N89-12960
PEETERS, M. N89-12937
PEGORARO, F. N89-13274
PENDER, J. N89-13077
PENTTINEN, AUVO N89-13244
PERDU, DIDIER M. N89-13192
PERRI, TODD A. N89-12570
PERRIN, J. M. N89-13357
PERRY, C. H. N89-13364
PETERS, CARROLL E. N89-12896
PETERSON, KURT T. N89-12829
PETERSON, RONALD V. N89-12587
PETROVIC, J. J. N89-12679
PHELPS, A. V. N89-12855
PHILLIPS, D. S. N89-12679
PHUCHAROEN, WORAPHAT N89-12919
PILARSKI, DEBORAH L. N89-12749
PILSNER, B. H. N89-12921
PINDERA, MAREK-JERZY N89-12681
PINDZOLA, M. S. N89-13238
PINNINGTON, R. J. N89-12934
PITZ, W. J. N89-12697
PLENTOVICH, ELIZABETH B. N89-12841
PLUMMER, S. E. N89-13002
POBLOTZKI, GERT N89-12933
POETZSCH, W. N89-12943
POLLACK, FRANK G. N89-12889
POMERANTZ, MARTIN N89-12728
PONDER, CARL G. N89-13146
PONS, S. N89-12816
POOLE, EUGENE L. N89-13202
POOLE, I. N89-13063
POPOVICH, BERT N89-12598
POPPEL, G. L. N89-13256
PORCELLI, F. N89-13274
POSNER, MICHAEL I. N89-13137
POURRAT, J. C. N89-12678
N89-12682
POWELL, HOWARD T. N89-12860
PRASADARAO, V. S. N89-12601
PRATT, J. RICHARD N89-12747
PREISENDORFER, RUDOLPH W. N89-13128
PRICE, DOUGLAS B. N89-12589
PRICE, HAROLD G. N89-12649
PRIME, R. B. N89-12730
PROFFITT, CHARLES RAYMOND N89-13382
PROGAR, DONALD J. N89-12747
PRUVOST, B. N89-12678
N89-12682
PUGET, J. L. N89-13341
PULLIAINEN, J. T. N89-13038

Q

QUARMBY, N. A. N89-12959
N89-13028

R

RABAEY, GREGORY F. N89-13389
RAITHBY, G. D. N89-12895
RAJ, BABAK N89-12871
RAJESHWAR, KRISHNAN N89-12728

RAMAMURTI, R. N89-12553
RAMAN, ROGER N89-13230
RAMIREZ, DEANNA R. N89-13121
RAMSEY, LAWRENCE W. N89-13325
RANDALL, M. R. N89-12645
RANEY, R. K. N89-12971
N89-13033
N89-13037
RANGARAJAN, R. N89-13149
RANGO, A. N89-13045
N89-13049
RANK, D. M. N89-13360
RAPAPORT, WILLIAM J. N89-13184
RAPP, ROBERT A. N89-12716
RATIER, A. N89-13000
RAU, M. S. N89-13284
RAYCRAFT, J. N89-12692
RE, F. N89-13243
READING, A. J. N89-13028
REAGAN, J. A. N89-12938
REED, JOHN W. N89-12848
REED, R. P. N89-12840
REES, C. D. N89-13287
REES, W. G. N89-12976
N89-12977
REINERS, WILLIAM A. N89-13088
REININGER, TERRANCE L. N89-12562
REYNOLDS, JAMES H. N89-13190
REYNOLDS, JOHN R. N89-12728
RICHARDS, J. A. N89-12979
RICHMOND, R. J. N89-12626
RIEGGER, S. N89-12955
N89-12957
RIFF, RICHARD N89-12931
N89-12932
RILEY, EUGENE S. N89-13095
RITCHIE, R. O. N89-12927
RIVER, BRYAN H. N89-12675
ROBERTSON, R. C. N89-12047
ROBINS, GABRIEL N89-13194
ROBINSON, D. N. N89-12908
N89-12909
ROBINSON, E. L. N89-13311
ROBINSON, W. W. N89-12884
ROBY, SCOTT WILSON N89-13379
ROCKAERTS, M. N89-12960
ROGERS, CRAIG A. N89-12674
ROJASOVIEDO, RUBEN N89-12540
ROQUET, H. N89-13000
ROSE, L. N89-12581
ROSS, D. W. N89-13264
ROSS, RONALD G., JR. N89-12618
ROTH, B. N89-13011
ROTHER, MICHAEL J. N89-12656
ROTHERY, D. A. N89-13025
ROUSAR, DON C. N89-12646
N89-12653
ROUX, C. N89-12968
RUCEV, STEVEN W. N89-12756
RUDNICK, DANIEL LARS N89-13089
RUFFINA, U. N89-13269
RUNCHAL, A. K. N89-12890
RUSSELL, J. C. N89-13256
RUSSELL, RAY W. N89-13343
N89-13359
N89-13360
RUSSO, LUIS CARLOS N89-12814
RUTLEDGE, SHARON K. N89-12589
RYAN, L. E. N89-12586
N89-12588
RYYNAENEN, MATTI N89-13244

S

SAAR, S. H. N89-13387
SABISKY, E. S. N89-13102
SACHIDANANDA, M. N89-12996
SADLER, J. F. N89-12557
SAGAN, CARL N89-13340
SAGE, ANDREW P. N89-13197
SAHU, D. N89-13285
SAKATA, T. N89-13061
N89-13066
SAKIMOTO, KAZUHIRO N89-13237
SALZER, JOHN JOSEPH N89-13328
SAMUELSEN, G. S. N89-12892
SANDERS, WILLIAM A. N89-12746
SANDFORD, SCOTT A. N89-13336
N89-13337
N89-13346
N89-13367
SANDSON, JENNIFER N89-13137
SANJANA, ZAL N. N89-12873
SANKAR, L. N. N89-12555
SANTAGATI, G. N89-13312
SANTIN, G. P. N89-12613
SANTONICO, R. N89-13243
SANZ, J. L. N89-13158
SARACENO, P. N89-13386
SASAKI, MISAO N89-13373
SASS, PAUL F. N89-12804
SASSEN, KENNETH N89-13111
SATO, H. N89-13004
SATO, T. N89-13020
SAUBA, ROOKTABIR MANDAN N89-12687
SCANDURRA, L. N89-13112
SCARROTT, S. M. N89-13351
SCHAEFER, A. R. N89-13314
N89-13317
SCHEP, T. J. N89-13267
N89-13274
SCHINDLER, J. W. N89-13287
SCHLOBOHM, S. L. N89-12625
SCHLUND, JUERGEN N89-12606
SCHMIDT, D. W. N89-12636
SCHMIDT, RODNEY C. N89-12901
SCHMULLIUS, C. N89-12986
SCHNEIBEL, J. H. N89-12703
SCHNITZLER, BRICE G. N89-12664
SCHNURR, J. N89-13079
SCHOEMBS, R. N89-13313
SCHOENBERG, K. F. N89-13259
SCHOENDORF, JOHN F. N89-12914
SCHRAMM, M. N89-13085
SCHREINER, SERGE N89-12690
SCHRIJVER, C. J. N89-13387
SCHUCHMAN, J. C. N89-13247
SCHUELER, WILLIAM N89-13225
SCHUMACHER, PAUL WAYNE, JR. N89-12577
SCHWAB, SCOTT N89-12873
SCHWARZ, B. B. N89-13283
SCHWARZ, R. B. N89-12704
SCHWARZ, RAY N89-13131
SCOTT, JAMES N89-12817
SEARLEMAN, J. E. N89-13187
SEARLEMAN, JANICE E. N89-13186
SEASHOLTZ, RICHARD G. N89-12885
SEBESTA, P. D. N89-13144
SEIBOLD, R. W. N89-12726
SEIDEL, K. N89-12961
SEIFERT, RUDIGER N89-12564
SEIGNEURIE, T. E. F. N89-12863
SELLGREN, KRISTIN N89-13365
SETTLE, J. N89-13024
SHAFFER, TIMOTHY D. N89-12728
SHAH, D. W. N89-12711
SHALEK, P. D. N89-12679
SHAMROTH, S. J. N89-12902
SHAPIRO, A. N89-13246
SHAPIRO, STUART C. N89-13181
N89-13182
N89-13183
N89-13184
N89-13185
SHARMA, G. D. N89-13093
SHARMA, S. N89-13247
SHEBALIN, JOHN V. N89-12572
SHEEN, D. R. N89-13015
SHEFFLER, K. D. N89-12922
SHEH, M. N89-12911
SHEINBERG, H. N89-12704
SHEN, C. Q. N89-12546
SHEN, YUHSHEN N89-13018
SHIEH, FALIN N89-12561
SHIMABUKURO, S. N89-12726
SHIMADA, M. N89-13004
N89-13007
SHIMODA, H. N89-13061
N89-13066
SHIN, R. T. N89-12794
SHIPWAY, GEORGE N89-12610
SHIRLEY, LYLE GORDON N89-12850
SHOEMAKER, MARY N89-12640
SHUCHMAN, R. A. N89-13015
N89-13039
SHUHY, J. N89-12806
SHULMAN, GORDON L. N89-13137
SIEBER, A. J. N89-12944
N89-12957
SIEGMUND, O. N89-13249
SIGAL, ASHER N89-12548
SILBER, C. N89-12965
SILVERSTEIN, CALVIN C. N89-12615
SIMION, GEORGE N89-13224
SIMITSES, G. J. N89-12931
SIMPSON, S. F. N89-12816
SINSKY, MARK S. N89-12667
SKIFF, B. A. N89-13321
SKOU, N. N89-12940
SMIALEK, J. L. N89-12717
SMITH, CHARLES A. N89-12592
N89-12617
SMITH, D. R. N89-12670
SMITH, J. N89-12959
SMITH, JOHN M. N89-12665
SMITH, M. F. N89-12787
SMITH, P. N89-13030
SMITH, P. R. N89-12788
SMITH, R. D. N89-12699
SMITH, TODD E. N89-12567
SNIDER, J. B. N89-12941
N89-13001
SNYDER, J. J. N89-13323
SNYDER, LARRY N89-13158
N89-13176
SOARES, J. V. N89-13080
SOCHA, DAVID N89-13156
N89-13177
SOFKO, G. J. N89-13076
SOKOLOWSKI, DANIEL E. N89-12877
SONG, TAE-HO N89-12698
SONTI, NAGESH N89-12710
SOPOK, SAMUEL N89-12694
SPALEK, G. N89-13246
SPECK, D. RALPH N89-12860
SPINOGLIO, L. N89-13386
SRIHARI, SARGUR N. N89-13181
SRINIVASAN, RAM N89-12893
STACK, JOHN P. N89-12841
STAENZ, K. N89-13040
STANFIELD, CLARENCE E. N89-12867
STANIEK, GUENTER N89-12719
STANTON, BILL J., JR. N89-12795
STARK, MARGARET A. N89-12848
STAVN, ROBERT HANS N89-13129
STCLAIR, TERRY L. N89-12747
STECHER, JOSEPH N89-12582
STEFFEN, ANGELA ANN N89-12875
STEIN, PETER A. N89-12580
STEINBERG, RICHARD A. N89-13166
STENGEL, ROBERT F. N89-13195
STEPHENS, J. R. N89-12717
STEPHENS, JOHN R. N89-13366
STERNBERG, JOSEPH N89-12734
STILLWELL, CHARLES B. N89-13255
STOCK, T. A. N89-12684
STOKHOLM, M. N89-13113
STONE, LELAND S. N89-13171
STONER, WILLIAM W. N89-13222
STOUFFER, D. C. N89-12911
STRANGMAN, T. E. N89-12920
STRAUSBERGER, DONALD J. N89-12808
STREETT, CRAIG L. N89-12543
STREICHER, JUERGEN N89-13124
STUART, N. N89-12967
STUTTARD, M. J. N89-13084
STYLES, P. J. N89-13056
SULLIVAN, J. P. N89-12891
SULLIVAN, PATRICK J. N89-12562
SUN, D. J. N89-12753
SUREK, T. N89-13102
SWAMY, K. S. KRISHNA N89-13367
SWANSON, G. A. N89-12916
SWARTZ, A. A. N89-12794
SWARTZ, C. K. N89-12819
SWEATT, W. C. N89-12857
SWENSON, BYRON L. N89-12623
SYED, I. N89-13012
SZE, ROBERT C. N89-12858
SZEKELY, J. N89-12889

T

TABORGNA, N. N89-13243
TAIE, MING-RUEY N89-13181
TAKASHIRO, SHIGEAKI N89-12701
TALBERT, KIM M. N89-13120
TALLEY, ROBERT L. N89-12663
TAM, D. W. N89-12802
TANARY, SAMSIR N89-12925
TANBA, SUMIO N89-13005
TARADA, FATHI HASAN ALI N89-12823
TARDY, D. C. N89-13239
TASAKI, K. N89-13004
TAUC, J. N89-13233
TAVAKOLI, MASSOUD SEYED N89-12874
TAYLOR, ALLAN H. N89-12741
TAYLOR, ANTOINETTE J. N89-12858
TAYLOR, DANIEL M. N89-12583
N89-12585
TAYLOR, J. C. N89-13084
TAYLOR, L. E. N89-13170
TAYLOR, S. W. N89-13314
TEETS, ALAN R. N89-12736
TEKKANAT, BORA N89-12673
TENNYSON, R. C. N89-12591
TERRY, WILLIAM K. N89-13265

TESANOVIC, Z. N89-13288
THOM, ROBERT L. N89-12641
N89-12642
THOMAS, J. B. N89-12813
THOMAS, J. O. N89-13283
THOMAS, WILLIAM L., III N89-13127
THOMPSON, ROBERT L. N89-12881
N89-12913
THORP, DANIEL N89-12893
TIAINEN, T. N89-12704
TILLER, BRUCE K. N89-12638
TILLEY, D. G. N89-13032
TIMCHALK, A. N89-13094
TINTO, MASSINO N89-13383
TIPTON, M. T. N89-12907
TOBBE, PATRICK A. N89-12595
TODD, E. S. N89-12905
TOIKKA, M. V. O. N89-13036
TOKUNAGA, ALAN T. N89-13331
N89-13339
N89-13368
TONN, BRUCE N89-13221
TORALDO, GERARDO N89-13168
TORBET, E. B. N89-13314
TORCZYNSKI, J. R. N89-12857
TOTH, R. P. N89-12793
TOWNSHEND, J. R. G. N89-13028
TRACY, JOHN JOSEPH N89-12668
TRAN, JEAN-MARIE N89-13161
TRAVIS, CURTIS C. N89-13135
TRINH, TINH N89-13131
TRIOLO, J. N89-12583
TRODD, N. M. N89-12988
N89-13062
TROLINGER, J. D. N89-12849
TROSTEL, J. M. N89-13047
TRUMBACH, SABINE N89-13136
TRUSS, P. N89-12978
TSAU, LI-REN N89-12672
TSUIKI, A. N89-12980
TSUJI, M. N89-13007
TURAN, A. N89-12895
TURNER, J. N89-13069

U

UENO, S. N89-13042
ULIANA, A. N89-12806
ULLAL, H. S. N89-13102
ULLMANN, VOJTECH N89-13377
UNDERWOOD, J. H. N89-12927
UNRUH, JAMES F. N89-12594
URATSUKA, S. N89-12975
USHIMARU, KENJI N89-12826
UTIKAL, KLAUS J. N89-13205
N89-13217

V

VACHON, D. J. N89-12726
VACHON, P. W. N89-12971
N89-13033
VALDEZ, MARC PHILIP N89-13116
VALERO, F. P. J. N89-13346
VANBLOKLAND, A. A. E. N89-13273
VANCITTERS, G. W., JR. N89-13311
VANDENBERG, EDWIN J. N89-12738
VANDERMEER, A. F. G. N89-13271
VANDERSANDEN, J. J. N89-12963
VANDERSTAAK, H. P. A. M. N89-13290
VANDERVEN, H. W. N89-13273
VANDIVER, R. N89-12696
VANDOORMAAL, J. P. N89-12895
VANKATWIJK, V. N89-13045
VANKLEECK, J. A. N89-12653
VANLOON, A. J. N89-13290
VANMILLIGEN, B. PH. N89-13272
VANNARONI, G. N89-13112
VANSTONE, R. H. N89-12915
VANZYL, JAKOB J. N89-12950
VARSIK, JOHN ROGER N89-13369
VASKA, L. N89-12690
VAUGHAN, P. O. N89-13027
VAUGHAN, R. A. N89-13027
VEDRENNE, M. N89-12611
VENTURA, R. N89-13312
VERMA, S. K. N89-12655
VERRECK, M. N89-13271
VESSAZ, J. P. N89-12603
VIDAL-MADJAR, D. N89-13010
VILLORESI, G. N89-13243
VISEK, W. A. N89-12647
VITEK, J. M. N89-12869
VOAS, JEFFREY M. N89-13150
VOGEL, J. A. N89-13132
VOGELSONG, RICHARD D. N89-13234
VONEITZEN, ULRICH N89-12556
VONPRAGENAU, GEORGE L. N89-12627
N89-12628
VRABEL, DEBORAH N89-12565

W

WACKERMAN, C. C. N89-13039
WADSWORTH, J. N89-12714
WAGNER, J. N89-12899
WAGNER, M. N. N89-12643
WAKABAYASHI, H. N89-13004
WALKER, E. N. N89-13315
WALKER, J. S. N89-12832
WALKER, K. P. N89-12912
WALSTON, SCOTT N89-12658
WALTHER, M. N89-12952
WALTON, B. D. N89-13324
WALTON, J. N89-12629
WANG, J. R. N89-12951
WANG, JANE-LING N89-13218
WANG, JOHN CHI LIN N89-13378
WANG, L. W. N89-12753
WANG, X. W. N89-12686
WARFIELD, MATTHEW JAMES N89-12547
WARREN-SMITH, R. F. N89-13351
WARREN, D. N89-13069
WARREN, J. R. N89-12660
WASSENBERG, C. A. N89-12938
WATCHER, JOHN M. N89-12617
WATERS, JEFF N89-12803
WATKINS, W. B. N89-12884
WEAVER, J. H. N89-13285
WEAVER, JAMES C. N89-13130
WEBER, G. N89-12907
WEDDING, A. B. N89-12855
WEERASOORIYA, TUSIT N89-12864
WEGENER, A. N89-13034
WEIDEMANN, ALAN DEAN N89-13129
WEIKLE, DONALD H. N89-12885
WEINBERG, I. N89-12819
WEINMAN, J. A. N89-12992
WEISS, SHOLOM M. N89-13303
WEN, LIANG C. N89-12618
WERCINSKI, PAUL F. N89-12623
WERNER, C. N89-13018
WERNER, CHRISTIAN N89-13124
WERNET, MARK P. N89-12885
WEST, J. C. N89-13031
WEST, PHILIP D. N89-13138
WEST, STEVEN CHARLES N89-12924
WESTBROOK, C. K. N89-12697
WESTER, K. N89-13055
WESTERHOF, E. N89-13269
N89-13270
WETZEL, L. B. N89-12946
WHARTON, S. W. N89-12958
N89-12984
WHEELER, J. R. N89-13051
WHITE, B. W. N89-12788
WHITE, JAMES C. N89-12587
WHITE, R. J. N89-13051
WHITE, R. L. N89-13311
WHITING, ELLIS E. N89-12622
WHITTENBERGER, J. DANIEL N89-12720
WIESBECK, W. N89-12955
N89-12957
WILEY, J. C. N89-13264
WILHEIT, T. T. N89-12998
WILKINSON, G. G. N89-13063
WILLAND, JAMES H. N89-13118
WILLEMSEN, H. N89-13052
WILLIAMSON, MARLIN J. N89-12595
WILLIS, J. O. N89-13292
WILSON, A. D. N89-13316
WILSON, KATHRYN R. N89-12799
WILSON, MAYWOOD L. N89-12867
WILSON, S. N89-12581
WIRTH, GUENTER N89-12719
WIRTH, J. N89-12937
WITHEROW, WILLIAM K. N89-13253
WITT, AUGUST F. N89-12688
WITTEBORN, F. C. N89-13360
N89-13367
WOLF, DAVID A. N89-13131
WOLFF, STEVE N89-12836
WOOD, T. F. N89-13062
WOODRUFF, S. B. N89-13212
WOOLF, BEVERLY N89-13191
WOPENKA, B. N89-13337
WRIGHT, G. G. N89-12967
WU, CHANG-HSIAO N89-12757
WU, JIUNN-CHI N89-12555
WU, MITCHELL B. N89-12866
WU, S. T. N89-12626
WU, Z. C. N89-13241
WUEBBLES, D. N89-13106
WYSOCKI, F. J. N89-13260

X

XU, WEI N89-13086

Y

YAMAGUCHI, R. N89-13066
YAMAZAKI, T. N89-13007
YANG, H. Q. N89-12692
YANG, HUANAN N89-13215
YANG, K. Y. N89-12692
YASUOKA, Y. N89-13060
YOKOTA, T. N89-12989
YOKOYAMA, R. N89-13005
YONEHANA, YASUNORI N89-12701
YONKER, C. R. N89-12699
YOUNG, ANDREW T. N89-13322
YOUNG, J. A. T. N89-12963
YU, BING-KUN N89-13111
YU, JAMES Y. N89-12690
YUEH, H. A. N89-12794

Z

ZACHARIA, T. N89-12869
ZAMAN, K. B. M. Q. N89-12552
ZANOLIN, FABIO N89-13201
ZEBKER, H. A. N89-12950
N89-13020
ZENG, ZHI N89-12721
ZERLAUT, G. A. N89-12616
ZEYEN, R. N89-13003
ZHANG, CHENG BO N89-13017
ZHANG, ZI-JUE N89-13061
N89-13066
ZHAO, HONGJIE N89-13111
ZHENG, WING-QI N89-12721
ZHENG, YING CONG N89-13323
ZHONGXIANG, WU N89-12854
ZHOU, SONGNIAN N89-12926
ZIELINSKIE, D. A. N89-12938
ZOMZELY-NEURATH, CLAIRE N89-13173
ZORZI, E. N89-12628
ZRNIC, D. S. N89-12996
ZUBKO, V. G. N89-13385
ZUBRIN, ROBERT M. N89-13230
ZUCCONI, L. N89-12620
ZUK, JOHN N89-12539
ZUMER, S. N89-12729
ZWEIBEL, K. N89-13102
ZWENGER, I. N89-13085

Typical Corporate Source Index Listing

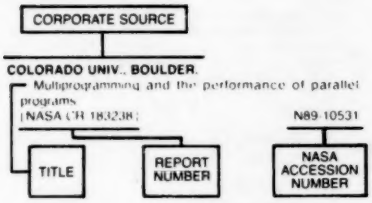

Listings in this index are arranged alphabetically by corporate source. The title of the document provides the user with a brief description of the subject matter. The report number helps to indicate the type of document cited (e.g., NASA report, translation, NASA contractor report). The NASA accession number denotes the number by which the citation is identified. The titles are arranged under each corporate source in ascending accession number order.

A

ABERDEEN UNIV. (SCOTLAND).
Communication: The key to integrating remote sensing and geographic information systems N89-12963

ACADEMIA SINICA, BEIJING (CHINA).
A synthetic apertures radar with multichannel and multipolarisation N89-13017
A luminance edge extraction method using gradient of gray level for synthetic aperture radar imageries N89-13086

ACADEMY OF SCIENCES OF THE UKRAINIAN SSR, KIEV.
Spectral variability of Wolf-Rayet stars [DE88-703325] N89-13371
On the microstructure theory of a condensate layer in a white dwarf atmosphere [DE88-703324] N89-13385

ADVANCED COMMUNICATIONS ENGINEERING CO., ALTAMONTE SPRINGS, FLA.
Fundamental understanding of the intrinsic ductility in nickel-base L12 type alloys [AD-A197605] N89-12711

ADVISORY GROUP FOR AEROSPACE RESEARCH AND DEVELOPMENT, NEUILLY-SUR-SEINE (FRANCE).
Guidance and Control/Flight Mechanics Panels Joint Symposium on The Man-Machine Interface in Tactical Aircraft Design and Combat Automation [AGARD-AR-249] N89-12564
Laser applications in flow diagnostics [AGARD-AG-296] N89-12649
AGARD handbook N89-13392

AERITALIA S.P.A., TURIN (ITALY).
IRIS thermal balance test within ESTEC LSS N89-12603

AEROJET TECHSYSTEMS CO., SACRAMENTO, CALIF.
Aerojet TechSystems Company contribution to LOX/HC combustion and cooling technology N89-12646
Effects of oxygen/hydrogen combustion chamber environment on copper alloys N89-12653

AERONAUTICAL SYSTEMS DIV., WRIGHT-PATTERSON AFB, OHIO.
An evaluation of ground collision avoidance system algorithm [AD-A197831] N89-12560

AEROSPACE CORP., EL SEGUNDO, CALIF.
A steam inerting system for hydrogen disposal for the Vandenberg Shuttle N89-12608

AEROSPACE CORP., LOS ANGELES, CALIF.
Laboratory investigations N89-13343
Comet Halley's colorful outbursts N89-13359

AEROSPATIALE, LES MUREAUX (FRANCE).
Image simulation of complex geometric targets for spaceborne synthetic aperture radar N89-13010

AEROSPATIALE, SURESNES (FRANCE).
Shock detection in composite structures. Test report 48-915/F [REPT-48-915/F] N89-12683

AIR FORCE INST. OF TECH., WRIGHT-PATTERSON AFB, OHIO.
A vortex panel method for potential flows with applications to dynamics and control [AD-A197091] N89-12549
Voice recognition and artificial intelligence in an air traffic control environment [AD-A197219] N89-12559
Robust recognition of loud and Lombard speech in the fighter cockpit environment [AD-A197093] N89-12795
Temporal clustering in the multi-target tracking environment [AD-A197153] N89-12796
Natural language generation [AD-A197321] N89-12800
Auditory models for speech analysis [AD-A197322] N89-12801
The effects of expansion devices on the transient response characteristics of the air-source heat pump during the reverse cycle defrost [AD-A197150] N89-12829
An analysis of the error characteristics of Atlantic tropical cyclone track prediction models [AD-A197146] N89-13119
The effect of vertical wind shear on tropical cyclone movement [AD-A197218] N89-13120
A global analysis and correlation of Nimbus 7 cloud and longwave radiation data [AD-A197223] N89-13121
Sample introduction using the Hildebrand grid nebulizer for plasma spectrometry [AD-A197145] N89-13257
Nonlinear effects in photorefractive crystals [AD-A197152] N89-13281

AIR FORCE SYSTEMS COMMAND, WRIGHT-PATTERSON AFB, OHIO.
Population inversion non-equilibrium flow simulation calculations of the capabilities of convection flow lasers [AD-A197741] N89-12854
The 6th All-Union Conference on Nonlinear Optics (table of contents) [AD-A197347] N89-13250

AIR FORCE WRIGHT AERONAUTICAL LABS., WRIGHT-PATTERSON AFB, OHIO.
Boric oxide as a solid lubricant additive in molybdenum disulfide [AD-A197109] N89-12727
Properties of JP-8 jet fuel [AD-A197270] N89-12750

AKRON UNIV., OHIO.
A multiaxial theory of viscoplasticity for isotropic materials N89-12908

ALABAMA UNIV., TUSCALOOSA.
Validity of heat index as indicator of level of heat storage for personnel wearing protective clothing in hot environments N89-12762

ALASKA UNIV., FAIRBANKS.
Development of Alaskan gas hydrate resources [DE88-010270] N89-13093

AMERICAN COLL. TESTING PROGRAM, IOWA CITY, IOWA.
Multidimensional item response theory estimation: A computer program [AD-A197160] N89-13155

ANALYTIC SCIENCES CORP., WASHINGTON, D. C.
Thermal/structural design verification strategies for large space structures N89-12602

ANALYTICAL SERVICES AND MATERIALS, INC., HAMPTON, VA.
The solution of linear systems of equations with a structural analysis code on the NAS CRAY-2 [NASA-CR-4159] N89-13202

APPLIED RESEARCH CORP., HUNTSVILLE, ALA.
Antenna pattern study [ARI/R-88-510Z] N89-12790

APPLIED RESEARCH CORP., LANDOVER, MD.
Possible identifications of the 3.4 micrometer feature N89-13342

APPLIED RESEARCH LAB., STATE COLLEGE, PA.
Influence of process parameters on laser weld characteristics in aluminum alloys [AD-A197398] N89-12710
Use of proximity effect in hearing aid microphones to increase telephone intelligibility in noise [AD-A197311] N89-12799

ARGONNE NATIONAL LAB., ILL.
Effects of high mean stress on the high-cycle fatigue of PWA 1480 and DS MAR M 246 + Hf at 1000 F N89-12633
Liquid metal flow in a large-radius elbow with a uniform magnetic fluid [DE88-016957] N89-12832
Algorithms for bound constrained quadratic programming problems [DE88-016470] N89-13168
Interaction of impurity ions with a weakly non-Maxwellian simple hydrogenic plasma [DE88-017137] N89-13265

ARIZONA STATE UNIV., TEMPE.
Fracton dynamics on fractal networks [AD-A197166] N89-12708
Synthetic polymers as analogs of polysaccharides [AD-A197842] N89-12738
Heat transfer in the tip region of a rotor blade simulator N89-12898
Laser driven inertial confinement fusion N89-13229
Atomic and molecular abundances in comets N89-13376

ARIZONA UNIV., TUCSON.
The development of a near-infrared polarimeter and its application to the continuum polarization of magnetic white dwarfs N89-12924
The incorporation of sulfur dioxide into snow and depositing ice N89-13116
Holographic particle detection [NASA-CR-183315] N89-13240
Phase measurement accuracy limitation in phase shifting interferometry N89-13248
Moisture adsorption in optical coatings N89-13327
The problem of clustering in laboratory studies of cometary dust N89-13356
Evidence for temporal variation in the acoustic and f-mode eigenfrequency spectrum of the Sun [DE88-015650] N89-13389

ARMY ARMAMENT RESEARCH, DEVELOPMENT AND ENGINEERING CENTER, WATERVLIET, N.Y.
Determination of sulfuric acid, oxalic acid, and their matrix effects in aluminum anodizing solutions by ion chromatography [AD-A197734] N89-12694

ARMY ARMAMENT RESEARCH AND DEVELOPMENT COMMAND, WATERVLIET, N. Y.
Fracture and fatigue [AD-A197310] N89-12927
An adaptive method with mesh moving and local mesh refinement for time-dependent partial differential equations [AD-A197772] N89-13208

ARMY AVIATION ENGINEERING FLIGHT ACTIVITY, EDWARDS AFB, CALIF.
AH-1F Instrument Meteorological Conditions (IMC) flight evaluations [AD-A197128] N89-12562

ARMY BELVOIR RESEARCH AND DEVELOPMENT CENTER, FORT BELVOIR, VA.
Differential scanning calorimetry as a method for indicating hydrolysis of urethane elastomers [AD-A197673] N89-12736

ARMY COMMUNICATIONS-ELECTRONICS COMMAND, FORT MONMOUTH, N.J.
A comparison of propagation model predictions with EPLRS (Enhanced Position Location and Reporting System) UHF network measurements [AD-A197473] N89-12804

ARMY INTELLIGENCE CENTER AND SCHOOL, FORT HUACHUCA, ARIZ.
Applications of parallelism to current algorithms for intelligence analysis
[NASA-CR-183351] N89-13165
Optimal fix estimators and a variation on the Cramer Rao lower bound
[NASA-CR-183011] N89-13211
Bearing error and the central limit theorem
[NASA-CR-183009] N89-13219
Use of distance versus statistical distance in acceptance tests
[NASA-CR-183353] N89-13220
ARMY MILITARY PERSONNEL CENTER, ALEXANDRIA, VA.
Poly(ethyl acrylate) and poly(gamma-benzyl-L-glutamate): An interpenetrating polymer system
[AD-A197783] N89-12737
ARMY RESEARCH INST. OF ENVIRONMENTAL MEDICINE, NATICK, MASS.
Derivation of anthropometry based body fat equations for the Army's weight control program
[AD-A197371] N89-13132
ASTON UNIV., BIRMINGHAM (ENGLAND).
An evaluation of satellite imagery, LANDSAT Thematic Mapper and SPOT-1 HRV, for grassland inventory in the UK N89-13057
ATMOSPHERIC AND ENVIRONMENTAL RESEARCH, INC., CAMBRIDGE, MASS.
IR-dust observations of Comet Tempel 2 with CRAF VIMS N89-13349
AUBURN INTERNATIONAL, INC., DANVERS, MASS.
Mass flow measurement of liquid cryogens using the triboelectric effect
[NASA-CR-179519] N89-12837
AUBURN UNIV., ALA.
The laminar boundary layer on an airfoil started impulsively from rest N89-12540
Vibrations induced by nonlinearities in rotordynamics N89-12631
Wave propagation in layered structures N89-12777
Installation of the ADINA FEM computer programs N89-12778
Electron-impact ionization of heavy atomic ions
[DE88-008371] N89-13238
AUTOMATION RESEARCH SYSTEMS LTD., ALEXANDRIA, VA.
MANPRINT (Manpower and Personnel Integration Program) primer
[AD-A197681] N89-13296
AVCO-EVERETT RESEARCH LAB., MASS.
Improved numerical methods for turbulent viscous recirculating flows N89-12895
AWESOME COMPUTING, INC.
The solution of linear systems of equations with a structural analysis code on the NAS CRAY-2
[NASA-CR-4159] N89-13202

B

BALLISTIC RESEARCH LABS., ABERDEEN PROVING GROUND, MD.
Aerodynamics analysis of solid fuel Ramjet projectiles
[AD-A196755] N89-12548
Combined pressure-shear ignition sensitivity test
[AD-A197076] N89-12749
Report on JANNAF Workshop Influence of Gas-Phase Chemical Kinetics on Low-Pressure Ignition and Flamespreading in Solid Propellant
[AD-A197854] N89-12751
BATTELLE COLUMBUS LABS., OHIO.
Lubrication evaluation of SSME turbopump bearings N89-12639
BOEING AEROSPACE CO., SEATTLE, WASH.
Simulation of the effects of the orbital debris environment on spacecraft N89-12607
BOEING COMMERCIAL AIRPLANE CO., SEATTLE, WASH.
Pilot factors guidelines for the operational inspection of navigation systems
[NASA-CR-181644] N89-12557
BOOZ-ALLEN AND HAMILTON, INC., BETHESDA, MD.
EMP (electromagnetic pulse) mitigation program approach
[AD-A197849] N89-12607
BRITISH AEROSPACE PUBLIC LTD. CO., BRISTOL (ENGLAND).
European remote sensing satellite platforms for the 1990's N89-12978
BRITISH ANTARCTIC SURVEY, CAMBRIDGE (ENGLAND).
Cloud track winds from polar orbiting satellites N89-13069
BROOKHAVEN NATIONAL LAB., UPTON, N. Y.
Design of vacuum chambers downstream of NSLS X-ray ring insertion devices
[DE88-015715] N89-13247
BROWN UNIV., PROVIDENCE, R. I.
Surfaces and thin films studied by picosecond ultrasonics
[DE88-015268] N89-13233
BSO/AEROSPACE B.V., UTRECHT (NETHERLANDS).
Advanced workstations for Meteosat command and control, volume 1
[BSO/AETR87030101-VOL-1] N89-12573
Advanced workstations for Meteosat command and control. Volume 2: Appendices
[BSO/AETR87030101-VOL-2] N89-12574

C

CALIFORNIA INST. OF TECH., PASADENA.
Structure measurements in a synthetic turbulent boundary layer N89-12821
A far-infrared heterodyne spectrometer for airborne astronomy N89-13329
CALIFORNIA POLYTECHNIC STATE UNIV., SAN LUIS OBISPO.
Test stand for Titan 34D SRM static firing N89-12610
CALIFORNIA UNIV., BERKELEY.
As-deposited low-strain LPCVD (Low-Pressure, Chemical-Vapor-Deposition) polysilicon
[DE88-016980] N89-12789
Physical modeling of bubble phenomena, electrolyte flow and mass transfer in simulated advanced Hall cells
[DE88-015585] N89-12828
Applications of polysilicon films in microsensors and microactuators
[DE88-016979] N89-12844
Performance studies of dynamic load balancing in distributed systems
[AD-A197130] N89-12926
Speed and data structures in computer algebra systems
[AD-A197131] N89-13146
Pan 1: An introduction for users, revision
[AD-A197344] N89-13160
Development of high efficiency opaque photocathodes for the Region 900 angstrom to 1200 angstrom
[NASA-CR-180597] N89-13249
Superconductivity: Phenomenology
[DE88-016659] N89-13289
Multiple representation document development
[AD-A197369] N89-13305
CALIFORNIA UNIV., BERKELEY. LAWRENCE BERKELEY LAB.
Quantum Monte Carlo calculation of the properties of atomic carbon and diamond
[DE88-014659] N89-12686
Mechanical behavior of superplastically-formed Al-Cu-Li-Zr alloy 2090
[DE88-016241] N89-12714
A refined model for characterizing X-ray multilayers
[DE88-013592] N89-12872
Generation of the J(sub c), H(sub c), T(sub c) surface for commercial superconductor using reduced-state parameters
[DE88-014038] N89-13278
High T(sub c) superconductors: Will they replace helium temperature superconductors for magnets
[DE88-016632] N89-13279
Superconductivity: Phenomenology
[DE88-016659] N89-13289
CALIFORNIA UNIV., IRVINE.
The effect of delamination on the response of advanced composite laminates N89-12668
CALIFORNIA UNIV., LOS ANGELES.
Numerical methods for the guidance and control of air-to-air missiles N89-12561
An artificial compression method for ENO schemes: The slope modification method
[NASA-CR-184613] N89-13215
Preparation and structure of Li-stabilized Na(+) beta' alumina single crystals
[AD-A197245] N89-13283
The processing of qualitative information in a natural language context N89-13297
CALIFORNIA UNIV., SAN DIEGO.
Mass and heat balances in the upper ocean N89-13089
CAMBRIDGE RESEARCH AND INSTRUMENTATION, INC., MASS.
Absolute photometric calibration of detectors to 0.3 mmag using amplitude-stabilized lasers and a helium-cooled absolute radiometer N89-13318
CAMBRIDGE UNIV. (ENGLAND).
Fundamentals of middle-atmospheric dynamics
[AD-A197358] N89-13110
CANADA CENTRE FOR REMOTE SENSING, OTTAWA (ONTARIO).
SAR-seen multimode waves in ice: Evidence of imaging nonlinearities N89-12971
Phase versus orbital velocity in SAR wave imaging: Paradox lost N89-13033
The LIMEX 1987 pilot project, LIMEX 1989 and long-term objective for data collection on the Canadian East coast N89-13037
The Canada Centre for Remote Sensing (CCRS) ground-based microwave facility N89-13076
CARNEGIE-MELLON UNIV., PITTSBURGH, PA.
Hydrogen effects on the fatigue and tensile behavior of CMSX-2 nickel base superalloy single crystals N89-12658
Dynamics of face and annular seals with two-phase flow
[NASA-CR-183352] N89-12870
Software process modeling
[AD-A197137] N89-13154
Parallel algorithms in the finite element approximation of flow problems
[AD-A197454] N89-13178
Sensitivity analysis for shortest Hamiltonian path and traveling salesman problems
[AD-A197167] N89-13204
CASE WESTERN RESERVE UNIV., CLEVELAND, OHIO.
Microwave characteristics of interdigitated photoconductors on a HEMT structure
[NASA-CR-182197] N89-12820
CATHOLIC UNIV. OF AMERICA, WASHINGTON, D.C.
Advanced instrumentation for local measurement of gas-solid suspension flows
[DE88-017087] N89-12833
CCS ASSOCIATES, BETHEL PARK, PA.
Heat pipe cooling system with sensible heat sink N89-12615
CENTRE AEROPORTE DE TOULOUSE (FRANCE).
Remote guidance of payloads under maneuverable parachutes
[E-639] N89-12571
Automatic release mechanism for the EL 32 bag
[E-768] N89-12863
CENTRE DE RECHERCHES EN PHYSIQUE DE L'ENVIRONNEMENT, ISSY-LES-MOULINEAUX (FRANCE).
Design of a spaceborne radar for tropical rain mapping at the climatological scale N89-12997
CESKOSLOVENSKA AKADEMIE VED, ONDREJOV.
Tenth European Regional Astronomy Meeting of the IAU: Abstracts
[DE88-703273] N89-13370
CESKOSLOVENSKA AKADEMIE VED, OSTRAVA.
Gravitation, black holes and space-time physics
[DE88-703054] N89-13377
CHINESE ACADEMY OF METEOROLOGICAL SCIENCES, BEIJING.
Precipitation detection with satellite microwave data
[PB88-240239] N89-13094
CINCINNATI UNIV., OHIO.
Simulation of 2-dimensional viscous flow through cascades using a semi-elliptic analysis and hybrid C-H grids
[NASA-CR-4180] N89-12553
Preliminary applications of decentralized estimation to large flexible space structures N89-12761
Constitutive modeling for single crystal superalloys N89-12911
CITY UNIV., LONDON (ENGLAND).
Heat transfer from roughened surfaces using interferometry N89-12827
CITY UNIV. OF NEW YORK, N.Y.
Growth and sedimentation of dust grains in the primitive solar nebula N89-13374
CLARKSON COLL. OF TECHNOLOGY, POTSDAM, N.Y.
Distributed problem solving N89-13186
A shared knowledge base for independent problem solving agents N89-13187
CLARKSON UNIV., POTSDAM, N.Y.
Homogeneous catalytic production of hydrogen and other molecules from water-DMF (N-dimethylformamide) solutions
[AD-A197072] N89-12690
CLEVELAND STATE UNIV., OHIO.
Assessment and comparison of 100-MW coal gasification phosphoric acid fuel cell power plants
[NASA-CR-182189] N89-13103
COLGATE UNIV., HAMILTON, N.Y.
Planner system for the application of indications and warning N89-13188
Providing intelligent assistance in distributed office environments N89-13189

POPLAR: A testbed for cognitive modeling N89-13190

COLLEGE OF WILLIAM AND MARY, WILLIAMSBURG, VA.
Design document for GCS version [NASA-CR-183278] N89-13150
Fault diagnosis based on continuous simulation models [NASA-CR-182737] N89-13152

COLOGNE UNIV. (WEST GERMANY).
The Airborne Version Conical Scan Radiometer (AVCSR): An airborne radiometer as a tool for satellite data validation N89-12937

COLORADO UNIV., BOULDER.
A comparative study of differing vortex structures arising in unsteady separated flows N89-12773
Superionic conductors as fast, repetitive opening switches [AD-A197365] N89-12817

COLUMBIA UNIV., NEW YORK, N.Y.
Joint services electronics program [AD-A197140] N89-12815

COMMERCE DEPT., WASHINGTON, D.C.
Survey of supply/demand relationships for Japanese Technical Information in the United States: The field of advanced ceramics research and development [PB88-210943] N89-13300

COMMUNICATIONS RESEARCH CENTRE, OTTAWA (ONTARIO).
Phase coherence and Signal-To-Noise ratio considerations for sampled aperture radar systems [AD-A197180] N89-12797

CONNECTICUT UNIV., STORRS.
Light extinction in a dispersion of small nematic droplets [AD-A197201] N89-12729
Constitutive modelling of single crystal and directionally solidified superalloys N89-12912

CONSIGLIO NAZIONALE DELLE RICERCHE, FRASCATI (ITALY).
Modes of operation of the RETE experiment [IFSI-88-5] N89-12576
The Frascati (Italy) gravitational antenna, 1987 [IFSI-88-4] N89-12846
Interaction of a hollow-cathode source with an ionospheric plasma [IFSI-88-10] N89-13112
Injection of ionospheric ions into the plasma sheet in the Earth's magnetotail [IFSI-88-13] N89-13113
Neutron flux measurements in the Gran Sasso Underground Laboratory (Italy) (part 2) [IFSI-88-7] N89-13243
The evolutionary status of young stellar mass loss driving sources as derived from IRAS observations [IFSI-88-12] N89-13386

CONTINUOUS ELECTRON BEAM ACCELERATOR FACILITY, NEWPORT NEW, VA.
Comments on the high frequency behavior of the coupling of an accelerator beam to its environment [CEBAF-PR-88-006] N89-13245

CONTRAVES CORP., ZURICH (SWITZERLAND).
The separation test in vacuum of the Ariane 4 payload fairing N89-12612

CONTRAVES GOERZ CORP., PITTSBURGH, PA.
Development of a two axis motion simulation system for thermal/vacuum satellite testing N89-12598

CONTROL DYNAMICS CO., HUNTSVILLE, ALA.
The flight robotics laboratory N89-12595
Space station docking mechanism dynamic testing N89-12596

COPENHAGEN UNIV. (DENMARK).
Carlsberg meridian catalog La Palma no. 3: Observations of positions of stars and planets made in the year 1986 [ISBN-0-98-87006-3] N89-13372

CORNELL UNIV., ITHACA, N.Y.
A system to investigate synthesized voice feedback in man-machine interfaces N89-12776
A two component model for thermal emission from organic grains in Comet Halley N89-13340
The transfer of cyclotron photons through neutron star atamospheres N89-13378

COUNCIL FOR NATIONAL ACADEMIC AWARDS (ENGLAND).
Stability limits and combustion measurements in low calorific value gas flames N89-12687
High strain rate properties of structural aluminium N89-12705

D

DANISH SPACE RESEARCH INST., LYNGBY.
Danish Space Research Institute N89-13391

DAYTON UNIV., OHIO.
Development of polyisocyanurate pour foam formulation for space shuttle external tank thermal protection system [NASA-CR-183511] N89-12745
Research on mechanical properties for engine life prediction [AD-A197816] N89-12864

DEFENCE RESEARCH ESTABLISHMENT, OTTAWA. (ONTARIO).
Application of autoregressive methods to adaptive excision of interfering tones from direct sequence spread spectrum communications systems [AD-A197801] N89-12805

DEFENSE SYSTEMS, INC., MCLEAN, VA.
User-computer interface technology: An assessment of the current state of the art [AD-A196839] N89-13193

DELAWARE UNIV., NEWARK.
Neutron studies of liquid and solid helium [DE88-009096] N89-13277

DEPARTMENT OF AGRICULTURE, BELTSVILLE, MD.
Laboratory evaluation of a field portable dielectric/soil moisture probe N89-13006
Microcomputers (PCs) for snow cover analyses using multisensor satellite data N89-13049

DEPARTMENT OF DEFENSE, WASHINGTON, D. C.
DOD joint Unmanned Aerial Vehicle (UAV) program master plan, 1988 [AD-A197751] N89-12563

DEPARTMENT OF ENERGY, MORGANTOWN, W. VA.
Fuel cells: A biblio hy [DE88-001081] N89-13097

DEPARTMENT OF ENERGY, NEW YORK.
Worldwide deposition of Sr-90 through 1985 [DE88-015577] N89-13105

DEPARTMENT OF ENERGY, OAK RIDGE, TENN.
Fuel cells: A bibliography [DE88-001081] N89-13097

DEPARTMENT OF ENERGY, WASHINGTON, D. C.
HLP30: A set of linear programming procedures system manual [DE88-016571] N89-13169

DEUTSCHE FORSCHUNGS- UND VERSUCHSANSTALT FUER LUFT- UND RAUMFAHRT, BRUNSWICK (WEST GERMANY).
Two different methods for shell buckling calculation in the elastic-plastic region [DFVLR-FB-88-26] N89-12933

DEUTSCHE FORSCHUNGS- UND VERSUCHSANSTALT FUER LUFT- UND RAUMFAHRT, COLOGNE (WEST GERMANY).
Properties of rapidly solidified aluminum alloys. German-Norwegian Project (1983-1987) [DFVLR-FB-88-24] N89-12719
Glucose tolerance and insulin secretion during 0-g simulation [DFVLR-FB-88-25] N89-13136

DEUTSCHE FORSCHUNGS- UND VERSUCHSANSTALT FUER LUFT- UND RAUMFAHRT, GOETTINGEN (WEST GERMANY).
Numerical integration of influence coefficients for panel methods about axisymmetric bodies by means of the ROMBERG algorithm [DFVLR-MITT-88-18] N89-12839

DEUTSCHE FORSCHUNGS- UND VERSUCHSANSTALT FUER LUFT- UND RAUMFAHRT, HAMBURG (WEST GERMANY).
Differential-psychological analysis of a computer-based audio-visual test of vigilance [DFVLR-FB-88-23] N89-13140

DEUTSCHE FORSCHUNGS- UND VERSUCHSANSTALT FUER LUFT- UND RAUMFAHRT, OBERPFAFFENHOFEN (WEST GERMANY).
The airborne radiometry experiment (ABREX) instrument, an experimental test bed for the specification of satellite-borne microwave radiometer at 90 GHz N89-12939
The MEOSS experiment: A test case for future cartographic missions N89-13081
Spectral characterization of forest damage in beech, oak and pine stands N89-13085
Cirrus-experiment ICE-1987: Microlidar measurements [DFVLR-MITT-88-17] N89-13124

DEUTSCHE FORSCHUNGS- UND VERSUCHSANSTALT FUER LUFT- UND RAUMFAHRT, WESSELING (WEST GERMANY).
Real-time adaptive radiometric correction for imaging radar systems N89-12943

DIRECTION DE LA METEOROLOGIE NATIONALE, PARIS (FRANCE).
Towards direct variational assimilation of scatterometer backscatter measurements into numerical weather prediction models N89-13000

DORNIER-WERKE G.M.B.H., FRIEDRICHSHAFEN (WEST GERMANY).
Performance modeling and results for X-SAR N89-13009

DREXEL UNIV., PHILADELPHIA, PA.
Mixed-mode fracture in fiber-reinforced composite materials N89-12689
Spark ignition of monodisperse fuel sprays N89-12685

DU PONT DE NEMOURS (E. I.) AND CO., AIKEN, S.C.
Challenging applications for hydrated and chemically reacted ceramics [DE88-015397] N89-12742
Data acquisition of the thermogravimetric analysis testing summary [DE88-016062] N89-13147

DUISBURG UNIV. (WEST GERMANY).
Scattering behavior of a three-axial ellipsoid N89-13011

DUNDEE UNIV. (SCOTLAND).
The interpretation of Icelandic tundra features from LANDSAT-MSS data N89-13027

DURHAM UNIV. (ENGLAND).
Polarization images of Comet Halley N89-13351

E

EAGLE ENGINEERING, INC., HOUSTON, TEX.
Lunar surface transportation systems conceptual design lunar base systems study Task 5.2 [NASA-CR-172077] N89-12862
Lunar storm shelter conceptual design [NASA-CR-172078] N89-13141

EBASCO SERVICES, INC., NEW YORK.
A multimegawatt space power source radiator design [DE88-015185] N89-12662

ECOLE NATIONALE SUPERIEURE DES TELECOMMUNICATIONS, BREST (FRANCE).
Spectral analysis of ocean wave imagery using 2-D linear prediction N89-12968

EDGERTON, GERMESHAUSEN AND GRIER, INC., IDAHO FALLS, IDAHO.
Fission fragment rockets: A potential breakthrough [DE88-016953] N89-12664
Sol-gel routes to superconducting ceramics [DE88-015128] N89-12724
Improving the efficiency of binary cycles [DE88-015108] N89-13099

EDINBURGH UNIV. (SCOTLAND).
Integrating remote sensing data into a geographical information system: A foundation for rural land use strategies: Nature Conservancy Council project N89-12964
Evaluation of LANDSAT TM and SPOT imagery for agricultural land use planning in less developed countries N89-13051

EIDGENOESSISCHE TECHNISCHE HOCHSCHULE, ZURICH (SWITZERLAND).
Development of a geographic information system with the aid of digital image processing techniques N89-12961

ENERGY INTERNATIONAL, INC., BELLEVUE, WASH.
Assessment of Japanese variable speed heat pump technology [DE88-013246] N89-12826

ENVIRONMENTAL PROTECTION AGENCY, RESEARCH TRIANGLE PARK, N.C.
Wind tunnel investigation of the response of a sonic anemometer [PB88-249826] N89-12847

ENVIRONMENTAL RESEARCH INST. OF MICHIGAN, ANN ARBOR.
Phase calibration of polarimetric SAR N89-13015
SAR image statistics related to atmospheric drag over sea ice N89-13034
Sea ice type classification of SAR imagery N89-13039

ESSEX UNIV., COLCHESTER (ENGLAND).
Some advantages of using polarisation diversity illustrated through the analysis of radar data from a storm in central Alberta (Canada) N89-12994

EUROPEAN SATELLITE CONSULTING ORGANIZATION, MONTROUGE (FRANCE).
Study of the integration of advanced communications satellite systems and terrestrial networks, executive summary [ESA-CR(P)-2655] N89-12809

EUROPEAN SPACE AGENCY, PARIS (FRANCE).
Ariane 5 verification and associated test facilities N89-12611
Proceedings of the 1988 International Geoscience and Remote Sensing Symposium (IGARSS 1988) on Remote Sensing: Moving Towards the 21st Century, volume 1 [ESA-SP-284-VOL-1] N89-12936

EUROPEAN SPACE AGENCY. ESRIN, FRASCATI (ITALY).
ERS data policy N89-13078
EUROPEAN SPACE AGENCY. EUROPEAN SPACE RESEARCH AND TECHNOLOGY CENTER, ESTEC, NOORDWIJK (NETHERLANDS).
The two axis motion simulator for the large space simulator at ESTEC (European Space Research and Technology Center) N89-12600
EXETER UNIV. (ENGLAND).
The stability of time-dependent fluid flows N89-12825

F

FEDERAL AVIATION ADMINISTRATION, ATLANTIC CITY, N.J.
LORAN C Offshore Flight Following (LOFF) in the Gulf of Mexico
[AD-A197179] N89-12558
FEDERAL LAB. CONSORTIUM, WASHINGTON, D. C.
Federal Laboratory Consortium for Technology Transfer: Putting technology to work. Examples of industry-laboratory cooperation contributing to our nation's economic strength
[PB88-243357] N89-13307
FLORIDA STATE UNIV., TALLAHASSEE.
Identifying nonlinear covariate effects in semimartingale regression models
[AD-A197323] N89-13205
Stochastic calculus and survival analysis
[AD-A197324] N89-13217
FOM-INST. VOOR PLASMAFYSICA, RIJNHUIZEN, JUTPHAAS (NETHERLANDS).
FOM Contributions to the 15th European Conference on Controlled Fusion and Plasma Heating
[REPT-88-178] N89-13266
The m=1 internal kink mode in a toroidal plasma with a flat q-profile near q=1 N89-13267
Kinetic effects on electron cyclotron emission during electron cyclotron heating in tokamaks N89-13268
Fundamental harmonic electron cyclotron emission for hot, loss-cone type distributions N89-13269
Transport code studies of m=2 mode control by local electron cyclotron heating in TFR N89-13270
Recent results of the toroidal screw pinch SPICA 2 N89-13271
Tokamak equilibrium determination through function parameterization N89-13272
The applicability of Rutherford scattering for Ti measurements at medium and large-sized experiments N89-13273
Internal kink modes in the ion-kinetic regime N89-13274
RF stabilization of external kink modes N89-13275
Optimizing current drive by electron cyclotron waves in the presence of trapped particles N89-13276
FOREST PRODUCTS LAB., MADISON, WIS.
Improving the fatigue resistance of adhesive joints in laminated wood structures
[NASA-CR-182165] N89-12675
FORUT, TROMSOE (NORWAY).
Ocean wave number spectra and spatial autocorrelation functions from SAR images N89-12970

G

GARRETT TURBINE ENGINE CO., PHOENIX, ARIZ.
Combustor diffuser interaction program N89-12893
Thermal barrier coating life prediction model development N89-12920
GAVAZZI (CARLO) CONTROLS S.P.A., MILAN (ITALY).
Test data acquisition system for the ESTEC large solar simulator at ESA/ESTEC N89-12620
GAYDON TECHNOLOGY LTD., WARWICK (ENGLAND).
Gas flow and global code programme
[DE88-012635] N89-12861
GEC-MARCONI ELECTRONICS LTD., CHELMSFORD (ENGLAND).
Constraints on two-scale descriptions of radar backscattering from the sea surface using scatterometer model functions N89-12945
Complex SAR imagery and speckle filtering for ERS-1 wave mode N89-13029
Analysis of Seasat SAR sea-ice data from the Beaufort Sea N89-13035
An analysis of directional ambiguities in wind scatterometer measurements N89-13071
GENERAL DYNAMICS CORP., ST. LOUIS, MO.
Trajectory optimization and guidance law development for national aerospace plane applications
[NASA-CR-182994] N89-12538
GENERAL ELECTRIC CO., CINCINNATI, OHIO.
Fiber optic control system integration
[NASA-CR-179568] N89-13256
GENERAL ELECTRIC CO., FAIRFIELD, CONN.
On 3D inelastic analysis methods for hot section components N89-12906
Component specific modeling N89-12907
Elevated temperature crack growth N89-12915
Thermal barrier coating life prediction model N89-12921
GENERAL ELECTRIC CO., PHILADELPHIA, PA.
Pyro shock simulation: Experience with the MIPS simulator N89-12593
GENERAL MOTORS CORP., DETROIT, MICH.
Aerothermal modeling program, phase 2 N89-12890
Aerothermal modeling program, phase 2. Element B: Flow interaction experiment N89-12891
Aerothermal modeling program, phase 2. Element C: Fuel injector-air swirl characterization N89-12892
Turbine airfoil film cooling N89-12903
GEOLOGICAL SURVEY OF BRITAIN, NOTTINGHAM.
Applications of remote sensing for geological mapping in eastern Egypt N89-13087
GEORGE MASON UNIV., FAIRFAX, VA.
Computer based intelligence support: An integrated expert system and decision support systems approach
[AD-A197386] N89-13197
GEORGE WASHINGTON UNIV., WASHINGTON, D.C.
Theoretical and experimental studies of the transonic flow field and associated boundary conditions near a longitudinally-slotted wind-tunnel wall N89-12545
Making statistical inferences about software reliability
[NASA-CR-4197] N89-13153
GEORGIA INST. OF TECH., ATLANTA.
Trajectory optimization and guidance law development for national aerospace plane applications
[NASA-CR-182994] N89-12538
Constitutive behavior of single crystal PWA 1480 and directionally solidified MAR-M 246 under monotonic and cyclic loads at high and low temperature N89-12634
Liquid scintillation counting with the Packard 1500 analyzer N89-12782
Non-isothermal buckling behavior of viscoplastic shell structures
[NASA-CR-183013] N89-12931
Considerations in development and implementation of elasto-viscoplastic constitutive model for high temperature applications
[NASA-CR-183403] N89-12932
Statistics and high resolution imaging of snowpack at 35 GHz using a microcomputer N89-13047
Consequences of individual differences in brain organization for human performance
[AD-A197667] N89-13138
Global optimization of concave functions subject to separable quadratic constraints and of all-quadratic separable problems
[AD-A197747] N89-13206
GINER, INC., WALTHAM, MASS.
Advanced double layer capacitor
[AD-A197739] N89-12818
GLASSTECH SOLAR, INC., WHEATRIDGE, COLO.
Preparation and properties of high-deposition-rate a-Si:H films and solar cells using disilane
[DE88-001191] N89-13098
GOETTINGEN UNIV. (WEST GERMANY).
Building a monitoring system based on satellite data to detect vegetation and land use changes in a subtropical region of Mexico N89-13079
GORDON RESEARCH CONFERENCES, INC., KINGSTON, R.I.
Gordon Conference on Microbial Adhesion
[AD-A197352] N89-12735
GRIFFITHS REMOTE SENSING, LONDON (ENGLAND).
The relativity utility of LANDSAT MSS and SIR-A imagery in reconnaissance geological mapping in Northern Sudan N89-13022

H

HARVARD UNIV., CAMBRIDGE, MASS.
Toughening by aligned, frictionally constrained fibers
[AD-A197194] N89-12676
HAWAII UNIV., HILO.
A consideration of the use of optical fibers to remotely couple photometers to telescopes N89-13326
HAWAII UNIV., HONOLULU.
Comparison of the 3.36 micrometer feature to the ISM N89-13339
Color gradients in the coma of P/Halley N89-13362
Properties of interstellar dust in reflection nebulae N89-13365
The NASA Infrared Telescope Facility Comet Halley monitoring program 2: Post-perihelion results N89-13368
Properties of stellar activity in F stars N89-13369
HELSINKI UNIV. OF TECHNOLOGY, ESPOO (FINLAND).
Microwave dielectric properties of low-salinity sea ice N89-13036
A 35 GHz helicopter-borne polarimeter radar N89-13036
Microwave emission behavior of snow N89-13041
An approach to automate digital signal processor code generation
[ETN-88-93530] N89-13172
HIGH VACUUM EQUIPMENT CORP., HINGHAM, MASS.
Indian LSSC (Large Space Simulation Chamber) facility N89-12601
HIROSHIMA UNIV., TAKEHARA (JAPAN).
Stochastic stage of an inflationary universe model
[DE88-753149] N89-13373
HITCO, SANTA ANA, CALIF.
Fingerprint test data report: FM 5834 test lots No. 1, 3, 4, and 5
[NASA-CR-179419] N89-12722
Fingerprint test data report: FM 5064J (Kaiser) lots No. 1 (K) - No. 4 (K)
[NASA-CR-179409] N89-12723
HONEYWELL, INC., BLOOMINGTON, MINN.
Optical symbolic processor for expert system execution
[AD-A197668] N89-13252
HENSCHEL FLUGZEUG-WERKE G.M.B.H., KASSEL (WEST GERMANY).
Locating and search procedures with helicopters for sea and/or air emergencies
[FPN-0079] N89-12556
HUGHES AIRCRAFT CO., EL SEGUNDO, CALIF.
High temperature adhesive systems
[AD-A197077] N89-12726
HUGHES AIRCRAFT CO., LONG BEACH, CALIF.
Correlation studies on surface particle detection methods N89-12587
HUGHES AIRCRAFT CO., TUCSON, ARIZ.
Automatic control of a multi-channel millimeter wave radiometer N89-12938
HYDROLOGICAL RESEARCH INST., PRETORIA (SOUTH AFRICA).
The extrapolation of spectral signatures illustrates LANDSATS' potential to detect wetlands N89-13067

I

IDAHO STATE UNIV., POCATELLO.
Evaluation of boron carbide coatings N89-13228
IIT RESEARCH INST., CHICAGO, ILL.
Multispecimen test facility for high-pressure hydrogen creep studies N89-12655
ILLINOIS UNIV., CHICAGO.
Statistical analysis and some polarimetric signatures of a polarimetric synthetic aperture radar image N89-12952
Statistical properties of phase difference between two orthogonally-polarised SAR signals N89-12953
On the concept of the polarimetric matched filter in high resolution radar imaging: An alternative for speckle radiation N89-12954
Optimal reception in depolarising clutter N89-13008
Formulation of the proper equations for developing standards in coherent dual polarisation SAR imaging N89-13021
MBE growth, characterization and electronic device processing of HgCdTe, HgZnTe related heterojunctions and HgCdTe-CdTe superlattices
[AD-A197752] N89-13286
ILLINOIS UNIV., URBANA.
Performance analysis of the Alliant FX/8 multiprocessor using statistical clustering
[NASA-CR-183221] N89-13145
Discovering substructure in examples
[AD-A197778] N89-13163
ILLINOIS UNIV., URBANA-CHAMPAIGN.
Prediction of fiber orientation during processing of short fiber composites N89-12671
Rayleigh lidar observations of gravity wave activity in the upper stratosphere at Urbana, Ill.
[NASA-CR-182738] N89-13107
INDIAN INST. OF TECH., BOMBAY.
Important aspects of technology transfer: Training of inservice engineers and scientists; satellite remote sensing N89-13082
INDUSTRIENLAGEN-BETRIEBSGESELLSCHAFT M.B.H., MUNICH (WEST GERMANY).
Solar simulation with a rectangular beam N89-12605
INSTITUTO DE PESQUISAS ESPACIAIS, CACHOEIRA PAULISTA (BRAZIL).
Photogrammetric model for correction of MSS-LANDSAT imagery
[INPE-4652-PRE/1359] N89-13090

INSTITUTO DE PESQUISAS ESPACIAIS, SAO JOSE DOS CAMPOS (BRAZIL).
Circuit for actuation of a stepping motor
[INPE-4633-NTE/281] N89-12814
Microwave remote sensing at the Institute for Space Research (INPE) Brazil: Concepts and future prospects of soil moisture studies N89-13080
INSTITUTO GEOGRAFICO NACIONAL, MADRID (SPAIN).
Activities report of the Canary Geophysical Center
[ISBN-8-45-055434-9] N89-13115
INSTITUTO SUPERIOR TECNICO, LISBON (PORTUGAL).
A logic for belief revision N89-13182
A model for belief revision N89-13183
Belief revision in SNePS N89-13185
INSTITUTO Y OBSERVATORIO ASTRONOMICO DE MARINA, SAN FERNANDO (SPAIN).
Carlsberg meridian catalog La Palma no. 3: Observations of positions of stars and planets made in the year 1986
[ISBN-0-98-87006-3] N89-13372
INTERNATIONAL CENTRE FOR THEORETICAL PHYSICS, TRIESTE (ITALY).
Electronic structure of light impurities in alpha-Fe and V
[DE88-702958] N89-12721
Metallization and characterization of a silicon p-n junction diode fabricated from a solar-cell-type silicon substrate
[DE88-703007] N89-13096
Nonlinear perturbations of differential operators with nontrivial kernel and applications to third order periodic boundary value problems
[DE88-702991] N89-13201
How to test the special theory of relativity on rotating earth
[DE88-703048] N89-13293
INTERNATIONAL INFORMATION SYSTEMS, INC., MCLEAN, VA.
User-computer interface technology: An assessment of the current state of the art
[AD-A196839] N89-13193
INTERNATIONAL RESEARCH AND DEVELOPMENT CO. LTD., NEWCASTLE (ENGLAND).
Optical and electrical measurements on UV sensitive photodiodes N89-13316
IOWA STATE UNIV. OF SCIENCE AND TECHNOLOGY, AMES.
Laser dynamic photoelasticity and digital image analysis for nondestructive evaluation of surface and near surface flaws through ultrasonic spectroscopy N89-12871
IOWA UNIV., IOWA CITY.
Space-time spectral studies of global stratospheric temperature fields N89-13108
Determination of stepsize parameters for intermolecular vibrational energy transfer
[DE88-010904] N89-13239
IWATE UNIV., MORIOKA (JAPAN).
Estimation of sea surface temperature via NOAA-AVHRR sensor: Comparison with sea truth data by fixed buoys N89-13005

J

JAYCOR, VIENNA, VA.
Bayesian reasoning tool
[AD-A197351] N89-13196
JET PROPULSION LAB., CALIFORNIA INST. OF TECH., PASADENA.
WF/PC internal molecular contamination during system thermal-vacuum test N89-12583
Wide Field/Planetary Camera (WF/PC) contamination control assessment N89-12584
Characterization of a graphite epoxy optical bench during thermal vacuum cycling N89-12585
Moisture interaction and stability of ZOT (Zinc Orthotitanate) thermal control spacecraft coating N89-12618
Functional description of signal processing in the Rogue GPS receiver
[NASA-CR-183314] N89-12813
Inference of geologic surface parameters from polarimetric radar observations and model inversion N89-12950
The effects of undersampling on multipolarization SAR images N89-12956
Design considerations for advanced multi-polarisation SAR N89-13014
Calibration of multipolarisation imaging radar N89-13018
The NASA/JPL multifrequency, multipolarisation airborne SAR system N89-13020
Performance of a scanning pencil-beam spaceborne scatterometer for ocean wind measurements N89-13073
Applications of parallelism to current algorithms for intelligence analysis
[NASA-CR-183351] N89-13165
Optimal fix estimators and a variation on the Cramer Rao lower bound
[NASA-CR-183011] N89-13211
Bearing error and the central limit theorem
[NASA-CR-183009] N89-13219
Use of distance versus statistical distance in acceptance tests
[NASA-CR-183353] N89-13220
Grain optical properties N89-13332
Focus on the future N89-13344
Cometary dust size distributions from flyby spacecraft N89-13350
JOHNS HOPKINS UNIV., BALTIMORE, MD.
Characterization of graphite fibers by X-ray diffraction N89-12755
Preattentive and attentive visual information processing
[AD-A197670] N89-13139
JOHNS HOPKINS UNIV., LAUREL, MD.
On the use of speckle statistics for the extraction of ocean wave spectra from SAR imagery N89-12969
Directional ocean wave spectra: Prospects for acquiring a global data base from SIR-C N89-12973
The Labrador Sea Extreme Waves Experiment: Objectives, status and plans N89-12974
Estimating aircraft SAR response characteristics and approximating ocean wave spectra in the Labrador Sea N89-13032
A GLR (Generalized Likelihood Ratio) algorithm for polyline approximation of waveforms
[AD-A197846] N89-13166
Survey of image restoration techniques
[AD-A197470] N89-13251
JOINT INST. FOR LAB. ASTROPHYSICS, BOULDER, COLO.
C IV fluxes from the Sun as a star, and the correlation with magnetic flux
[NASA-CR-182719] N89-13387
JOINT RESEARCH CENTRE OF THE EUROPEAN COMMUNITIES, ISPRA (ITALY).
EURACS: A European radar cross section database N89-12944
Small format air photo from ultrahigh aircraft as an aid for data collection of agricultural statistics in Sahelian countries N89-13003
The classification of semi-natural vegetation from LANDSAT Thematic Mapper imagery: A user's perspective N89-13084

K

KANAZAWA INST. OF TECH. (JAPAN).
Optical properties of cometary grains N89-13363
KANAZAWA UNIV. (JAPAN).
Snowmelt runoff estimation using snow cover extent data and its application to optimum control of dam water level N89-13042
KANSAS STATE UNIV., MANHATTAN.
Thin films from solvated metal atoms and metal-metal bonded compounds
[AD-A197132] N89-12707
Thermal properties of heterogeneous grains N89-13358
KANSAS UNIV., KANSAS CITY.
A fine resolution multifrequency polarimetric FM radar N89-13016
KANSAS UNIV., LAWRENCE.
Modulation of the radar backscatter from the ocean surface by a long gravity wave N89-13031
KARLSRUHE UNIV. (WEST GERMANY).
Polarization-dependent attenuation of dielectric cylinder arrays N89-12955
Interpretation of coherent polarimetric signatures by dielectric cylinder models N89-12957
Large area TM land cover classification of Mittlerer Oberrhein County, southwest Germany, and its use for regional planning and crop surveys N89-12986
KATHOLIEKE UNIVERSITEIT TE LEUVEN (BELGIUM).
An integrated remote sensing approach for regional agrostatistics and land monitoring N89-12960
KAWASAKI STEEL CORP., KOBE (JAPAN).
Highly magnetic powder
[DE88-010838] N89-12701
KENT STATE UNIV., OHIO.
Light extinction in a dispersion of small nematic droplets
[AD-A197201] N89-12729
Computer evaluation of ion-implanted dopant profile evolution during annealing N89-12756

KENT UNIV., CANTERBURY (ENGLAND).
A possible explanation for the inconsistency between the Giotto grain mass distribution and ground-based observations N89-13364
KEURING VAN ELECTROTECHNISCHE MATERIALEN N.V., ARNHEM (NETHERLANDS).
Microstructure and nonlinearity of ZnO varistors, Volume 5, Number 8
[B8735659] N89-13290
KINGSTON POLYTECHNIC, KINGSTON-UPON-THAMES (ENGLAND).
The detection of unimproved grassland in Berkshire using a binary decision tree approach N89-12988
Crop classification with multi-temporal X-band SAR data N89-12990
Classification decision rule modification on the basis of information extracted from training data N89-13062

L

LABORATOIRE D'ASTRONOMIE SPATIALE, MARSEILLE (FRANCE).
Light scattering of large rough particles application to cometary grains N89-13357
LAWRENCE LIVERMORE NATIONAL LAB., CALIF.
A decade of railgun development for high pressure research
[DE88-017024] N89-12578
Autoignition chemistry of n-butane in a motored engine: A comparison of experimental and modeling results
[DE88-014153] N89-12697
As-deposited low-strain LPCVD (Low-Pressure, Chemical-Vapor-Deposition) polysilicon
[DE88-016980] N89-12789
Applications of polysilicon films in microsensors and microactuators
[DE88-016979] N89-12844
High power Nd:glass lasers as drivers for inertial confinement fusion
[DE88-017016] N89-12860
Structural response calculations for a metal booster tank model
[DE88-017095] N89-12929
Micro heat pipes
[DE88-016113] N89-13100
Aspects of CFC relative ozone destruction efficiencies determined in the LLNL 2-D model
[DE88-015431] N89-13106
Boeing Military Airplane Company technical order transfer tests
[DE88-012233] N89-13151
The state of PC-based CADD (Computer-Aided Design and Drafting) systems
[DE88-017326] N89-13170
Time-resolved solid-state array imaging systems: Developments and applications
[DE88-016274] N89-13254
Synthesis of accretion disk and nonthermal source models for AGN
[DE88-013098] N89-13384
LEEDS UNIV. (ENGLAND).
Modelling land resources within a pilot geographical information system N89-12962
Analysis of potato crop distribution using remotely sensed and environmental data in a pilot geographical information system N89-12967
LEHIGH UNIV., BETHLEHEM, PA.
Unsteady structure of flow past a pitching delta wing N89-12541
LEICESTER UNIV. (ENGLAND).
Flow field characteristics around bluff parachute canopies N89-12546
LIEGE UNIV. (BELGIUM).
Towards an urban land-use classification using textural and morphological criteria N89-12987
LOCKHEED MISSILES AND SPACE CO., SUNNYVALE, CALIF.
Development of optimized, graded-permeability axial groove heat pipes N89-12614
LOS ALAMOS NATIONAL LAB., N. MEX.
Synthesis and characterization of VLS-derived silicon carbide whiskers
[DE88-016226] N89-12679
SiC whisker-reinforced MoSi2
[DE88-016674] N89-12680
Amorphous powders of Al-Hf prepared by mechanical alloying
[DE88-014459] N89-12704
Fire aerosol experiment and comparisons with computer code predictions
[DE88-016328] N89-12788
Overview of recent advances in excimer laser technology at Los Alamos
[DE88-016236] N89-12858

Some strategies for enhancing the performance of the block Lanczos method
[DE88-014401] N89-13212
The next logical step in laser-fusion development
[DE88-007825] N89-13258
Confinement dynamics in the reversed field pinch
[DE88-009148] N89-13259
Modified magnetic confinement configurations based on understanding helicity dissipation and pressure driven modes in the spheromak
[DE88-009149] N89-13260
A mass spectrometric analysis of CF4/O2 plasmas: Effect of oxygen concentration and plasma power
[DE88-016237] N89-13261
A novel excitonic mechanism for high temperature superconductivity
[DE88-016227] N89-13288
Low contact-resistivity junction to ceramic superconductors
[DE88-016155] N89-13292
New gravitational forces from quantum theory
[DE88-016231] N89-13294
United States space policy: Review and assessment
[DE88-015538] N89-13306
Laboratory simulations of comet surfaces N89-13366

LOUISIANA NATURE AND SCIENCE CENTER, NEW ORLEANS.
A teacher's companion to the space station: A multi-disciplinary resource N89-12575

LOUISIANA STATE UNIV., BATON ROUGE.
Six degree of freedom simulation computer program for aeroelastic free-flight projectiles N89-12771
A computer simulation of a plasma armature railgun N89-12780

LOWELL OBSERVATORY, FLAGSTAFF, ARIZ.
Monitoring solar-type stars for luminosity variations N89-13321

M

M L ENERGIA, INC., PRINCETON, N.J.
Radiative augmented combustion
[AD-A197300] N89-12693

MACDONALD, DETTWILER AND ASSOCIATES LTD., RICHMOND (BRITISH COLUMBIA).
Extraction of dense digital elevation models from SPOT stereo imagery N89-13053

MANCHESTER COLL. OF SCIENCE AND TECHNOLOGY (ENGLAND).
Dual linear polarisation time series as an aid to hydrometeor identification N89-12995

MARCONI SPACE AND DEFENCE SYSTEMS LTD., PORTSMOUTH (ENGLAND).
On-orbit servicing and cost effectiveness of Columbus Polar Platform concepts N89-12983
Radar control, detection and processing electronics design as used for the ERS-1 wind scatterometer space segment N89-13075

MARCONI SPACE SYSTEMS LTD., PORTSMOUTH (ENGLAND).
Proposed design of the temperature control system for the variable temperature calibration target for the Advanced Microwave Sounding Unit B N89-12942
Multistatic scatterometry N89-13072

MARTIN MARIETTA AEROSPACE, DENVER, COLO.
Space station integrated propulsion and fluid systems study
[NASA-CR-179393] N89-12581
Cost effective alternative to low irradiance measurements N89-12619
PIA update: Correlation analyses of mass spectra N89-13334

MARTIN MARIETTA AEROSPACE, NEW ORLEANS, LA.
Definition of a space transportation systems cargo element (Shuttle-C). Orientation
[NASA-CR-179404] N89-12579

MARTIN MARIETTA CORP., NEW ORLEANS, LA.
A teacher's companion to the space station: A multi-disciplinary resource N89-12575

MARYLAND UNIV., COLLEGE PARK.
Adsorption on metal surfaces
[DE88-016557] N89-12715
Establishment of center for rotorcraft education and research
[AD-A197141] N89-13295

MASSACHUSETTS INST. OF TECH., CAMBRIDGE.
LIGO vacuum system study N89-12599
LEC (Liquid Encapsulated Czochralski) growth of InP with magnetic field assisted melt stabilization and heat transfer control
[AD-A196748] N89-12688
Surface structures and transitions and the evolution from firm to bulk behavior
[AD-A197788] N89-12695
The optimal polarizations for achieving maximum contrast in radar images
[NASA-CR-183349] N89-12794
The structure of red-infrared scattergrams of semivegetated landscapes
[NASA-CR-183385] N89-13091
Electroporation: Theory of basic mechanisms
[AD-A197391] N89-13130
Graphical programming and monitoring
[AD-A197342] N89-13159
Evaluation of expert systems in decisionmaking organizations
[AD-A196448] N89-13192
A lexical conceptual approach to generation for machine translation
[AD-A197356] N89-13304

MASSACHUSETTS INST. OF TECH., LEXINGTON.
Neural network performance on the stochastic exclusive-or problem
[AD-A197789] N89-13179
Transition-metal oxide superconductivity
[AD-A197069] N89-13280

MASSACHUSETTS UNIV., AMHERST.
Millimeter-wave backscatter measurements of various snow forms N89-13046
Plan recognition, knowledge acquisition and explanation in an intelligent interface N89-13191

MATHEMATICAL ANALYSIS RESEARCH CORP., CLAREMONT, CALIF.
Bearing error and the central limit theorem
[NASA-CR-183009] N89-13219
Use of distance versus statistical distance in acceptance tests
[NASA-CR-183353] N89-13220

MAX-PLANCK-INST. FUER PHYSIK UND ASTROPHYSIK, GARCHING (WEST GERMANY).
Activities report of the Institute of Extraterrestrial Activities
[MPE-208] N89-13308

MCDONALD OBSERVATORY, AUSTIN, TEX.
Analog-to-digital conversion techniques for precision photometry N89-13319

MCDONNELL AIRCRAFT CO., ST. LOUIS, MO.
Composite curing process nondestructive evaluation
[AD-A197834] N89-12873

MCDONNELL-DOUGLAS ASTRONAUTICS CO., HUNTINGTON BEACH, CALIF.
Atomic oxygen effects on candidate coatings for long-term spacecraft in low earth orbit N89-12592

MCDONNELL-DOUGLAS CORP., HUNTINGTON BEACH, CALIF.
Comparison of sulfuric and oxalic acid anodizing for preparation of thermal control coatings for spacecraft N89-12617

MECHANICAL TECHNOLOGY, INC., LATHAM, N. Y.
The effects of internal rotor friction on dynamic characteristics of turbopumps N89-12629

MEHARRY MEDICAL COLL., NASHVILLE, TENN.
The effects of hyperbaric oxygen and antioxidant deficiencies on rat retinal ultrastructure N89-12772

MENTOR TECHNOLOGIES, INC., BAYSIDE, N.Y.
Micro-computer network architecture for range instrumentation applications
[AD-A196971] N89-13175

MESSERSCHMITT-BOELKOW-BLOHM G.M.B.H., BREMEN (WEST GERMANY).
Control of the induced microgravity environment of the Man Tended Free Flyer (MTFF) N89-12606

MICHIGAN UNIV., ANN ARBOR.
Short fiber reinforced thermoplastics N89-12673
Ion mobility spectrometry with laser-produced ions
[AD-A197117] N89-12851
Observations of a complete sample of emission-line galaxies N89-13328

MIDWEST RESEARCH INST., GOLDEN, COLO.
Preparation and properties of high-deposition-rate a-Si:H films and solar cells using disilane
[DE88-001191] N89-13098
Preliminary results from the dynamic response testing of the Northern Power Systems 100-kW wind turbine
[DE88-001166] N89-13101
Solar photovoltaic technology: The thin film option
[DE88-001195] N89-13102

MINISTRY OF POSTS AND TELECOMMUNICATIONS, TOKYO (JAPAN).
Inference of radio scattering parameters of Antarctic ice sheet using 179 MHz airborne radio echo sounding data N89-12975

MINNESOTA UNIV., MINNEAPOLIS.
Finite element analysis of composite laminates N89-12672
Efficient numerical techniques for complex fluid flows N89-12894
Development of low Reynolds number two equation turbulence models for predicting external heat transfer on turbine blades N89-12901
Cometary dust composition N89-13333
Infrared observations of P/Halley and P/Encke N89-13353

MISSION RESEARCH CORP., ALBUQUERQUE, N. MEX.
Microwave and electron beam computer programs
[AD-A197798] N89-13164

MISSOURI UNIV., ROLLA.
Optical constants of minerals and other materials from the millimeter to the ultraviolet
[AD-A197803] N89-12696
Isolation of osteogenic cells from the trauma-activated periosteum N89-12757
Co-occurrence matrix modification for small region texture measurement and comparison N89-13084

MITRE CORP., BEDFORD, MASS.
Euclidean decoders for BCH codes
[AD-A197242] N89-13157

MOUND LAB., MIAMISBURG, OHIO.
Laser illuminated high speed photography of energetic materials
[DE88-012870] N89-12848

MTS SYSTEMS CORP., MINNEAPOLIS, MINN.
A high pressure, high temperature hydrogen environment for metals properties testing system N89-12656

N

NATIONAL AERONAUTICAL LAB., BANGALORE (INDIA).
Mathematical modelling and computer simulation using Cartesian grid
[TM-AE-8804] N89-13149

NATIONAL AERONAUTICS AND SPACE ADMINISTRATION, WASHINGTON, D.C.
Aeronautical engineering: A continuing bibliography with indexes (supplement 232)
[NASA-SP-7037(232)] N89-12536
Microgravity science and applications program tasks, 1987 revision
[NASA-TM-4068] N89-12752
NASA thesaurus. Volume 2: Access vocabulary
[NASA-SP-7064-VOL-2] N89-13298
NASA thesaurus. Volume 3: Definitions
[NASA-SP-7064-VOL-3] N89-13301
NASA thesaurus. Volume 1: Hierarchical Listing
[NASA-SP-7064-VOL-1] N89-13302
Infrared Observations of Comets Halley and Wilson and Properties of the Grains
[NASA-CP-3004] N89-13330

NATIONAL AERONAUTICS AND SPACE ADMINISTRATION. AMES RESEARCH CENTER, MOFFETT FIELD, CALIF.
Aircraft technology opportunities for the 21st Century
[NASA-TM-101060] N89-12539
Development and validation of an advanced low-order panel method
[NASA-TM-101024] N89-12554
Recent advances at NASA in calculating the electronic spectra of diatomic molecules
[NASA-TM-101034] N89-12622
A conceptual design study of the reusable reentry satellite
[NASA-TM-101043] N89-12623
NASA newsletters for the Weber Student Shuttle Involvement Project
[NASA-TM-101001] N89-13144
Efficient use of bit planes in the generation of motion stimuli
[NASA-TM-101022] N89-13171
On the constrained Chebyshev approximation problem on ellipses
[NASA-CR-183209] N89-13200
Two alternate proofs of Wang's lune formula for sparse distributed memory and an integral approximation
[NASA-CR-184555] N89-13214
Second Workshop on Improvements to Photometry
[NASA-CP-10015] N89-13310
Tests of a multichannel photometer based on silicon diode detectors N89-13314
The spectral properties of interplanetary dust particles N89-13336
Aromatic components in cometary materials N89-13337
Interstellar grain chemistry and the composition of comets N89-13346
The spectral appearance of comets from 5 to 20 micrometers: A survey of the data N89-13347
Some 5-13 micrometer airborne observations of Comet Wilson 1986l: Preliminary results N89-13360
A multicomponent model of the infrared emission from Comet Halley N89-13367
Research and technology
[NASA-TM-100051] N89-13393

NATIONAL AERONAUTICS AND SPACE ADMINISTRATION. GODDARD SPACE FLIGHT CENTER, GREENBELT, MD.
Fifteenth Space Simulation Conference: Support the Highway to Space Through Testing
[NASA-CP-3015] N89-12582
The Instrument Test Dewar (ITD): Testing satellite instruments at 1.5 K N89-12604
Requirements and test results for the qualification of thermal control coatings N89-12616
Analysis of GEOSAT radar altimeter errors based on pre-launch test data
[NASA-TM-101230] N89-12806
Theoretical study of turbulent channel flow: Bulk properties, pressure fluctuations, and propagation of electromagnetic waves
[NASA-TM-101248] N89-12830
Modelling of SAR polarisation phase difference from trees N89-12951
Requirements for ongoing development of the Pilot Land Data System (PLDS) N89-12958
Geodynamics laser ranging system: Performance simulations and development of the EOS facility N89-12982
PIPS: A Procedure for Interactive Pyramid Segmentation N89-12984
An algorithm to derive precipitation profiles from a downward viewing radar and a multifrequency passive radiometer N89-12992
Rainfall index over oceans derived from SSM/I data N89-12998
Average areal water equivalent of snow in a mountain basin using microwave and visible satellite data N89-13045
The derivation of sub-canopy surface terrain models of coastal forests using synthetic aperture radar N89-13083
Airborne 20-65 micron spectrophotometry of Comet Halley N89-13354
Aerodynamic properties of fractal grains: Implications for the primordial solar nebula N89-13361

NATIONAL AERONAUTICS AND SPACE ADMINISTRATION. LYNDON B. JOHNSON SPACE CENTER, HOUSTON, TEX.
Materials selection for long life in LEO: A critical evaluation of atomic oxygen testing with thermal atom systems N89-12590
Space station erectable manipulator placement system
[NASA-CASE-MSC-21096-❶] N89-12621
Improved docking alignment system
[NASA-CASE-MSC-21372-1] N89-12842
Tank gauging apparatus and method
[NASA-CASE-MSC-21059-1] N89-12843
Gripping device
[NASA-CASE-MSC-21365-1] N89-12865
Magnetic attachment mechanism
[NASA-CASE-MSC-21095-1] N89-12866
Horizontally rotated cell culture system
[NASA-CASE-MSC-21294-1] N89-13131
Advancing automation and robotics technology for the space station and for the US economy
[NASA-TM-100989] N89-13198

NATIONAL AERONAUTICS AND SPACE ADMINISTRATION. LANGLEY RESEARCH CENTER, HAMPTON, VA.
A two-dimensional numerical simulation of a supersonic, chemically reacting mixing layer
[NASA-TM-4055] N89-12542
A spectral collocation solution to the compressible stability eigenvalue problem
[NASA-TP-2858] N89-12543
Method for laminar boundary layer transition visualization in flight
[NASA-CASE-LAR-13554-1] N89-12551
Singular perturbations and time scales in the design of digital flight control systems
[NASA-TP-2844] N89-12569
Lightweight structural design of a bolted case joint for the space shuttle solid rocket motor
[NASA-TP-2851] N89-12580
Polyenamines from aromatic diacetylenic diketones and diamines
[NASA-CASE-LAR-13444-2-CU] N89-12667
Cryogenic insulation system
[NASA-CASE-LAR-13506-1] N89-12741
Thermoplastic adhesives based on 4,4'-isophthaloyldiphthalic anhydride (IDPA)
[NASA-TM-101508] N89-12747
Truss-core corrugation for compressive loads
[NASA-CASE-LAR-13438-1] N89-12786
Aerodynamic pressures and heating rates on surfaces between split elevons at Mach 6.6
[NASA-TP-2855] N89-12822
Direct simulation of three-dimensional flow about the AFE vehicle at high altitudes
[NASA-TM-101492] N89-12834
Porous plug for reducing orifice induced pressure error in airfoils
[NASA-CASE-LAR-13569-1] N89-12841
Pultrusion die assembly
[NASA-CASE-LAR-13719-1] N89-12867
Analysis of the Space Shuttle Orbiter skin panels under simulated hydrodynamic loads
[NASA-TM-4082] N89-12935
Advancing automation and robotics technology for the space station and for the US economy
[NASA-TM-100989] N89-13198
Engineering applications of heuristic multilevel optimization methods
[NASA-TM-101504] N89-13203

NATIONAL AERONAUTICS AND SPACE ADMINISTRATION. LEWIS RESEARCH CENTER, CLEVELAND, OHIO.
Control of laminar separation over airfoils by acoustic excitation
[NASA-TM-101379] N89-12552
Evaluation of three turbulence models for the prediction of steady and unsteady airloads
[NASA-TM-101413] N89-12555
Advanced turboprop project
[NASA-SP-495] N89-12565
Development of a thermal and structural analysis procedure for cooled radial turbines
[NASA-TM-101416] N89-12568
The NASA atomic oxygen effects test program N89-12589
Simplified cyclic structural analysis of SSME turbine blades N89-12632
High-temperature LCF of Ni-201 and 304L stainless steel N89-12635
Liquid oxygen cooling of high pressure LOX/hydrocarbon rocket thrust chambers N89-12649
SP-100 nuclear space power systems with application to space commercialization
[NASA-TM-101403] N89-12665
A probabilistic approach to composite micromechanics
[NASA-TM-101366] N89-12684
Influence of alloying elements on the oxidation behavior of NbAl3
[NASA-TM-101398] N89-12717
Effect of grain size on the high temperature properties of B2 aluminides
[NASA-TM-101382] N89-12720
Slurry-pressing consolidation of silicon nitride
[NASA-TM-101365] N89-12746
Convective flows in enclosures with vertical temperature or concentration gradients
[NASA-TM-101373] N89-12753
Radiation resistance and comparative performance of ITO/InP and n/p InP homojunction solar cells
[NASA-TM-101387] N89-12819
Performance of the forward scattering spectrometer probe in NASA's icing research tunnel
[NASA-TM-101381] N89-12845
Turbine Engine Hot Section Technology 1986
[NASA-CP-2444] N89-12876
Turbine Engine Hot Section Technology (HOST) Project N89-12877
HOST instrumentation R and D program overview N89-12878
HOST combustion R and T overview N89-12879
HOST turbine heat transfer subproject overview N89-12880
HOST structural analysis program overview N89-12881
Fatigue and fracture overview N89-12882
HOST surface protection R and T overview N89-12883
Laser anemometry: A status report N89-12885
Development of a high temperature static strain sensor N89-12887
The NASA Lewis Strain Gauge Laboratory: An update N89-12888
Summary of laser speckle photogrammetry for HOST N89-12889
Turbine stator flow field simulations N89-12902
Thermomechanical characterization of Hastelloy-X under uniaxial cyclic loading N89-12909
High temperature stress-strain analysis N89-12913
Automation software for a materials testing laboratory N89-12917
A study on thermal barrier coatings including thermal expansion mismatch and bond coat oxidation N89-12919
Calculation of Weibull strength parameters and Batdorf flow-density constants for volume- and surface-flaw-induced fracture in ceramics
[NASA-TM-100890] N89-12930

NATIONAL AERONAUTICS AND SPACE ADMINISTRATION. MARSHALL SPACE FLIGHT CENTER, HUNTSVILLE, ALA.
Advanced Earth-to-Orbit Propulsion Technology 1986, volume 2
[NASA-CP-2437-VOL-2] N89-12626
Damping seal tester progress and initial test results N89-12627
Low-speed flexible rotor balancing for smooth, high-speed operation N89-12628
Efficient transient analysis methods for the Space Shuttle Main Engine (SSME) turbopumps N89-12630
Powder metallurgy bearings for advanced rocket engines N89-12641
Rolling contact fatigue life of zirconium and molybdenum nitride sputter plated AMS 5749 bearing steel N89-12642
RP-1 and methane combustion and cooling experiments N89-12650
Development of a computer-controlled technique to determine crack growth rate properties in controlled environments using crack opening displacement N89-12657
The determination of mobile hydrogen in aerospace engine alloys N89-12659
The development of a hydrogen resistant alloy N89-12661
Optically controlled welding system
[NASA-CASE-MFS-29291-1] • N89-12868
A reference standard for bidirectional reflection distribution function and bidirectional transmission distribution function measurement
[NASA-CASE-MFS-28183-1] N89-13253

NATIONAL AERONAUTICS AND SPACE ADMINISTRATION. PASADENA OFFICE, CALIF.
Self-actuating heat switches for redundant refrigeration systems
[NASA-CASE-NPO-17085-1-CU] N89-12785
Tm,Ho:YLF laser end-pumped by a semiconductor diode laser array
[NASA-CASE-NPO-17282-1-CU] N89-12856
Stabilization and oscillation of an acoustically levitated object
[NASA-CASE-NPO-16896-1-CU] N89-13236

NATIONAL AERONAUTICS AND SPACE ADMINISTRATION. WALLOPS FLIGHT FACILITY, WALLOPS ISLAND, VA.
Effects of rainfall on scatterometer derived wind speeds N89-13074

NATIONAL BUREAU OF STANDARDS, BOULDER, COLO.
Round-robin measurements of the apparent thermal conductivity of two refractory insulation materials, using high-temperature guarded-hot-plate apparatus
[PB88-215421] N89-12670
Detection of excited states by laser-induced fluorescence and analysis of energy transfer
[AD-A197770] N89-12855
C IV fluxes from the Sun as a star, and the correlation with magnetic flux
[NASA-CR-182719] N89-13387

NATIONAL BUREAU OF STANDARDS, GAITHERSBURG, MD.
Application of PN and avalanche silicon photodiodes to low-level optical N89-13317
An introduction to blocked impurity band detectors N89-13320
An optical heterodyne densitometer N89-13323

NATIONAL INST. FOR ENVIRONMENT, IBARAKI (JAPAN).
Efficient classification of multispectral images by a best linear discriminant function N89-13060

NATIONAL INST. FOR ENVIRONMENTAL STUDIES, TSUKUBA (JAPAN).
Detection of seasonal and long-term changes in land cover from multitemporal LANDSAT MSS data N89-12989

NATIONAL OCEANIC AND ATMOSPHERIC ADMINISTRATION, BOULDER, COLO.
Verification of the accuracy of a network of water-vapor radiometers N89-12941
Radiometric observations of cloud liquid water during FIRE N89-13001
Space environment laboratory data acquisition and display system 2
[PB88-205471] N89-13299

NATIONAL OCEANIC AND ATMOSPHERIC ADMINISTRATION, WASHINGTON, D. C.
Precipitation detection with satellite microwave data
[PB88-240239] N89-13094

NATIONAL REMOTE SENSING CENTRE, FARNBOROUGH (ENGLAND).
Monitoring urban change from LANDSAT TM and SPOT satellite imagery by image differencing N89-13058

NATIONAL SCIENCE FOUNDATION, WASHINGTON, D.C.
The Hubble Space Telescope high speed photometer N89-13311
NATIONAL SEVERE STORMS LAB., NORMAN, OKLA.
Processing and interpretation of alternately polarised weather radar echoes N89-12996
NATIONAL SPACE DEVELOPMENT AGENCY, OHASHI (JAPAN).
Requirements for the Advanced Earth Observing Satellite (ADEOS) orbit, orbit and a attitude control, and rate jitter N89-12981
Verification results of MOS-1 multispectral self scanning radiometer (MESSR) data N89-13004
Data collection system operating on Japan's first marine observation satellite: Inflight evaluation of the system performance N89-13007
NATIONAL SPACE DEVELOPMENT AGENCY, TOKYO (JAPAN).
Results of Advanced Earth Observing Satellite (ADEOS) conceptual study N89-12980
NATIONAL TRANSPORTATION SAFETY BOARD, WASHINGTON, D. C.
Annual review of aircraft accident data, US general aviation, calendar year 1985
[PB88-115787] N89-12537
NATIONAL WEATHER SERVICE, GARDEN CITY, N.Y.
TURB: Turbulence forecasting for small/medium and large aircraft
[PB88-246368] N89-13125
NAVAL AIR DEVELOPMENT CENTER, WARMINSTER, PA.
Soiling, cleaning, and weathering effects on aircraft polyurethane topcoats
[AD-A197302] N89-12733
NAVAL OCEAN RESEARCH AND DEVELOPMENT ACTIVITY, BAY ST. LOUIS, MISS.
Some characteristics of short ocean waves as microwave scatterers N89-13030
Implementation issues for level O image processor software within an application package
[AD-A197768] N89-13162
NAVAL OCEAN SYSTEMS CENTER, SAN DIEGO, CALIF.
The design of antenna matching networks using a microcomputer
[AD-A197364] N89-12802
Exploring the back-propagation network for speech applications
[AD-A197385] N89-12803
Electronic properties and current carrying capacity of high-temperature ceramic superconductors
[AD-A197819] N89-13287
NAVAL POSTGRADUATE SCHOOL, MONTEREY, CALIF.
Fire spread in a three-dimensional pressure vessel with radiation exchange and wall heat losses
[AD-A197271] N89-12692
An electron microscopy study of tweed microstructures and premartensitic effects in high damping 53Cu45Mn2Al alloy
[AD-A197317] N89-12709
On the resistance of ceramics to high velocity penetration
[AD-A197320] N89-12734
A numerical method for computing unsteady 2-D boundary layer flows
[NASA-CR-4198] N89-12835
Multispectral satellite analysis of marine stratocumulus cloud microphysics
[AD-A197316] N89-13092
Three-dimensional visual display for a prototype command and control workstation
[AD-A197319] N89-13142
NAVAL RESEARCH LAB., WASHINGTON, D.C.
Shadows and wedges in scattering from the sea N89-12946
A note on incomplete integrals of cylindrical functions
[AD-A197822] N89-13210
On the simulation of harmonically related signals
[AD-A197821] N89-13235
NAVAL SHIP RESEARCH AND DEVELOPMENT CENTER, BETHESDA, MD.
Fatigue crack growth of 5456-H116 aluminum and HSLA-80 weldments
[AD-A197830] N89-12712
Bering Sea wave and ice measurements in support of Arctic west winter 1986
[AD-A197196] N89-13127
NAVAL SUBMARINE MEDICAL CENTER, GROTON, CONN.
Discrimination and identification of modulation-frequency using noise, tone and tonal-complex carriers
[AD-A197780] N89-13134
NAVAL TRAINING SYSTEMS CENTER, ORLANDO, FLA.
Arctic oceanography and meteorology review
[AD-A196533] N89-13126
NAVAL UNDERWATER SYSTEMS CENTER, NEW LONDON, CONN.
Nearfield acoustic radiation from a point-excited cylindrical shell
[AD-A197282] N89-13234
NAVAL WEAPONS CENTER, CHINA LAKE, CALIF.
Review of electromagnetic surface waves, 1960 through 1987
[AD-A197278] N89-12798
NEW MEXICO STATE UNIV., UNIVERSITY PARK.
Mode extraction from an electromagnetic slow wave system N89-12767
NEW MEXICO UNIV., ALBUQUERQUE.
Construction of a phase conjugate laser resonator using Brillouin enhanced four wave mixing N89-12759
Investigation of laser diode coupling using nonlinear optics N89-12781
Nuclear technology for the year 2000
[DE88-005041] N89-13223
Radioisotope space power generators: Design concepts N89-13224
Down scale of the SP-100 concept for 5 kWe N89-13225
The 5 kWe scale-down of the SPAR/SP-100 heat pipe reactor N89-13226
Tesla's coherent plasma discharge and a plan for megavolts at megahertz N89-13231
NEW SOUTH WALES UNIV., KENSINGTON (AUSTRALIA).
Australian preparations for the Polar Platform N89-12979
Change direction analysis using LANDSAT imagery: A review of methodology N89-13068
NORTH CAROLINA STATE UNIV., RALEIGH.
Fundamental studies and device development in beta silicon carbide
[AD-A197843] N89-12739
Focal region fields of distorted reflectors
[NASA-CR-183001] N89-12810
An analysis of the error characteristics of Atlantic tropical cyclone track prediction models N89-13117
NORTH CAROLINA UNIV., CHAPEL HILL.
Charge transfer in multiple site chemical systems
[AD-A197143] N89-12666
NORTH CAROLINA UNIV., GREENSBORO.
Optical modeling of clear ocean light fields: Raman scattering effects
[AD-A197249] N89-13129
NORTH CAROLINA UNIV., RALEIGH.
Multitemporal resource complex analysis of Catinia province, Italy from LANDSAT-TM data N89-12985
NORTHROP CORP., HAWTHORNE, CALIF.
Automated Airframe Assembly Program (AAAP) survey of CIM status in the aircraft industry
[AD-A197368] N89-12535
NORTHWESTERN UNIV., EVANSTON, ILL.
Elevated temperature strain gages N89-12886
NOTRE DAME UNIV., IND.
Fire spread in a three-dimensional pressure vessel with radiation exchange and wall heat losses
[AD-A197271] N89-12692
Investigation into the applicability of fracture mechanics techniques to aircraft wheel life studies N89-12763

O

OAK RIDGE NATIONAL LAB., TENN.
Coble creep, cavity sintering and cavity growth
[DE88-013846] N89-12703
Irradiation-assisted stress corrosion cracking and grain boundary segregation in heat treated Type 304SS
[DE88-008382] N89-12713
Analysis of adhesion test methods and the evaluation of their use for ion-beam-mixed metal/ceramic systems
[DE88-015358] N89-12725
Ion beam mixing of metals and ceramics: Material considerations
[DE88-016797] N89-12744
Bioelectromagnetic effects of EMP: Preliminary findings
[DE88-012118] N89-12791
BES welding science contractors
[DE88-016589] N89-12869
Determination of surfaces of constant inelastic strain rate at elevated temperature N89-12910
Human exposure to dioxin from combustion sources
[DE88-013825] N89-13135
People versus probability
[DE88-017380] N89-13221
OBSERVATOIRE DE PARIS-MEUDON (FRANCE).
On the carbon abundance in Comet Halley derived from the 3 micron feature: Comparison with interstellar dust N89-13341
Detection of parent molecules in the IR spectrum of P/Halley with the IKS-Vega spectrometer N89-13352
OBSERVATORIO DEL EBRO, ROQUETAS (SPAIN).
Ionosphere 1970, Volume 58
[ISSN-0211-5166] N89-13114
OBSERVATORIO DEL EBRO, TORTOSA (SPAIN).
Geomagnetism, a dynamic science
[REPT-37] N89-13309
OCEANOR, TRONDHEIM (NORWAY).
An intercomparison of SAR and buoy directional wave spectra from the Labrador Sea Extreme Waves Experiment (LEWEX) N89-12972
OFFICE OF NAVAL RESEARCH, LONDON (ENGLAND).
The RACE Program of the European Communities
[ONRL-8-014-R] N89-12811
European Seminar on Neural Computing
[ONRL-8-010-C] N89-13173
High temperature superconductivity research in selected laboratories in West Germany
[ONRL-8-011-R] N89-13291
OHIO STATE UNIV., COLUMBUS.
In-situ high temperature oxidation studies
[DE88-017092] N89-12716
Alterations of segmental volume during orthostatic stress in nonhuman primates N89-12769
Experimental study of isothermal flows in a dump combustor N89-12779
Modeling and performance of HF/OTH (High-Frequency/Over-The-Horizon) radar target identification systems
[AD-A197850] N89-12808
Dynamic synthesis of joined/hermetic shell structures using state space method N89-12874
S-waves in the spectrum of cataclysmic binaries N89-13380
OHIO UNIV., LANCASTER.
The effects of high noise levels on the acoustic-phonetic structure of speech: A preliminary investigation N89-12764
OLD DOMINION UNIV., NORFOLK, VA.
Support of the eight-foot high-temperature tunnel modifications project
[NASA-CR-183356] N89-12572
Prediction of stresses in aircraft panels subjected to acoustic forces
[NASA-CR-182513] N89-12923
OPEN UNIV., MILTON (ENGLAND).
A regional tectonic study of NE and E Africa and its implication for mineral exploration: A synoptic view from satellite imagery N89-13023
The need for volcano monitoring and the ability to detect activity using emitted short wavelength infrared N89-13025
OREGON GRADUATE CENTER FOR STUDY AND RESEARCH, BEAVERTON.
De-embedding S-parameter measurements using TSD technique N89-12783
OREGON STATE UNIV., CORVALLIS.
Providing on-line guidance to computer users N89-12766
Space reactor assessment and validation study N89-13227
OSLO UNIV. (NORWAY).
Effects of changing satellite sensor attributes N89-13059
OTTAWA UNIV. (ONTARIO).
Characterization of adhesively bonded joints using acousto-ultrasonics N89-12925
OXFORD UNIV. (ENGLAND).
The large-scale structure of the universe: Some theoretical considerations N89-13381

P

PACIFIC NORTHWEST LABS., RICHLAND, WASH.
Prediction of heat transfer between the combustion space and the load
[DE88-016313] N89-12698
Supercritical fluid chromatography: The effect of the partial molar volume in the stationary phase on retention
[DE88-016959] N89-12699
Hanford Meteorological Station computer codes. Volume 8: The REVIEW computer code
[DE88-015958] N89-13123
PENNSYLVANIA STATE UNIV., UNIVERSITY PARK.
A zonal equation method for three-dimensional locally elliptic laminar and turbulent flows N89-12547
Two-sample inference for median survival times based on one-sample procedures for censored survival data
[AD-A197776] N89-13218

Chemical precursors to zinc sulfide: ZnS whisker synthesis
[AD-A197262] N89-13284
Use of optical fibers in spectrophotometry N89-13325

PENNSYLVANIA UNIV., PHILADELPHIA.
Optical computing based on neuronal models
[AD-A197749] N89-13199

PHYSICAL SCIENCES, INC., ALEXANDRIA, VA.
Survey of laser-produced pressure and impulse data
[AD-A197313] N89-12852

PITTSBURGH UNIV., PA.
Influence of side-groups on thermotropic behavior of polyorganophosphazenes
[AD-A197852] N89-12740

PLANETARY SCIENCE INST., TUCSON, ARIZ.
Infrared observations of the dust coma N89-13331

PLESSEY RESEARCH ROKE MANOR LTD., ROMSEY (ENGLAND).
Architectures for optoelectronic computing
[REPT-72/88/R260/U] N89-13148

PORTSMOUTH GASEOUS DIFFUSION PLANT, OHIO.
Corrosion of nickel and Monel welds of steel in chlorine trifluoride
[DE88-014122] N89-12706

PRATT AND WHITNEY AIRCRAFT, EAST HARTFORD, CONN.
Further development of the dynamic gas temperature measurement system N89-12884
Coolant passage heat transfer with rotation N89-12899
On 3-D inelastic analysis methods for hot section components N89-12905
Creep fatigue life prediction for engine hot section materials (isotropic): Fourth year progress review N89-12914
Life prediction and constitutive models for engine hot section N89-12916
Thermal barrier coating life prediction model development N89-12922

PRATT AND WHITNEY AIRCRAFT, WEST PALM BEACH, FLA.
Survey of LOX/hydrocarbon combustion and cooling N89-12647
LCF and crack growth rate of turbine blade alloys in hydrogen and hydrogen/steam environments N89-12660

PRINCETON UNIV., N. J.
Design and numerical evaluation of full-authority flight control systems for conventional and thruster-augmented helicopters employed in NOE operations
[NASA-CR-183311] N89-12570
A methodology for characterizing reactive coatings: Time-Temperature-Transformation (TTT) analysis of the competition between cure, evaporation and thermal degradation for an epoxy-phenolic system
[AD-A197254] N89-12730
AUTOCREW implementation: Inbound surface-to-air missile simulation
[AD-A197674] N89-13143
Artificial intelligence theory and reconfigurable control systems
[AD-A197255] N89-13195

PTR OPTICS CORP., WALTHAM, MASS.
Fiber optic wavelength division multiplexing: Principles and applications in telecommunications and spectroscopy N89-13324

PUGET SOUND UNIV., TACOMA, WASH.
Polarisation of passive microwave signals as indicator of snow water equivalent N89-13043

PURDUE UNIV., WEST LAFAYETTE, IND.
On the interactions of longwave radiation, microphysics and turbulence in boundary layer clouds N89-13109

R

READING UNIV. (ENGLAND).
The use of remote sensing in conjunction with geographic information systems for local planning N89-12959
An international approach to GIS based on remote sensing and terrain classification N89-12966
Mapping the distribution and abundance of lithological units and surface mineralogies at Jabal Sa'id, Saudi Arabia: An application of spectral mixture modelling N89-13024
Monitoring playas using Thematic Mapper data N89-13028
The production of anaglyphs from SPOT-HRV panchromatic data for geomorphological mapping N89-13056
The interrelationship between resampling method and information extraction technique N89-13065

REAL INST. Y OBSERVATORIO DE LA ARMADA, SAN FERNANDO (SPAIN).
Carlsberg meridian catalog La Palma no. 3: Observations of positions of stars and planets made in the year 1986
[ISBN-0-98-87006-3] N89-13372

RECHERCHE EN PREVISION NUMERIQUE, DORVAL (QUEBEC).
Production of probability of precipitation maps over oceanic areas from automated cloud classification N89-12999

REEDEREIGEMEINSCHAFT FORSCHUNGSSCHIFFAHRT G.M.B.H., BREMEN (WEST GERMANY).
Locating and search procedures with helicopters for sea and/or air emergencies
[FPN-0079] N89-12556

RENSSELAER POLYTECHNIC INST., TROY, N.Y.
Research on mercury cadmium telluride
[AD-A197238] N89-13282

RESEARCH INST. FOR SOIL SCIENCE AND AGRICULTURAL CHEMISTRY, BUDAPEST (TURKEY).
Agroelecological information content of SPOT data N89-13050

ROCHESTER UNIV., N. Y.
Laser speckle from thin and cascaded diffusers
[AD-A197066] N89-12850

ROCKWELL INTERNATIONAL CORP., CANOGA PARK, CALIF.
Fatigue crack retardation following overloads in Inconel 718, Ti-5Al-2.5Sn, and Haynes 188 N89-12636
Surface characteristics of liquid oxygen cooled ball bearings N89-12640
Measurement of rotordynamic coefficients for a hydrostatic radial bearing N89-12643
Surface modification for wear resistance in a liquid oxygen turbopump environment N89-12644
SSME bearing health monitoring using a fiberoptic deflectometer N89-12645
LOX/hydrocarbon combustion and cooling survey N89-12648
Results of coaxial injector element testing N89-12651
Combustion modeling: Progress and projections N89-12652
Hydrogen-environment embrittlement and its control in high pressure hydrogen/oxygen rocket engines N89-12654

ROME UNIV. (ITALY).
Precision limits of the twin-beam multiband URSULA N89-13312

ROTHAMSTED EXPERIMENTAL STATION, HARPENDEN (ENGLAND).
Spatial resolution for remote sensing of forest plantations N89-12991

ROYAL GREENWICH OBSERVATORY, HAILSHAM (ENGLAND).
Carlsberg meridian catalog La Palma no. 3: Observations of positions of stars and planets made in the year 1986
[ISBN-0-98-87006-3] N89-13372

ROYAL GREENWICH OBSERVATORY, HERSTMONCEUX (ENGLAND).
A fibre optic, four channel comparative photometer N89-13315

RUTGERS - THE STATE UNIV., NEW BRUNSWICK, N. J.
Thermal transport between a continuously moving heated plate and a quiescent ambient medium N89-12824
Empirical analysis and refinement of expert system knowledge bases
[AD-A197241] N89-13303

RUTHERFORD HIGH ENERGY LAB., CHILTON (ENGLAND).
Cross-polar radar measurements in ice and rain N89-12993

S

SAN DIEGO STATE UNIV., CALIF.
Designing simulator tasks to study the high speed, low altitude environment N89-12770
Improvements to photometry. Part 1: Better estimation of derivatives in extinction and transformation equations N89-13322

SANDIA NATIONAL LABS., ALBUQUERQUE, N. MEX.
Semiconductor bridge (SCB) igniter studies. 2: Comparison of SCB and hot-wire direct propulsion thrusters
[DE88-008803] N89-12625
Investigations into the plasma spray process
[DE88-014524] N89-12787
Microwave RF coupling response through adjacent cavities
[DE88-012430] N89-12793
Temperature profile in semi-infinite planar slab with exponential source and convective boundary condition: Application to laser heating
[DE88-016746] N89-12831
The standardized Bauer piezoelectric polymer shock gauge
[DE88-014963] N89-12840
Resonator design with an intracavity time-varying index gradient
[DE88-015259] N89-12857
Radiation effects in semiconductor laser diode arrays
[DE88-016318] N89-12859
Phase 2 testing of a molten salt central receiver
[DE88-012701] N89-13095
Simulating vehicle dynamics: The importance of a valid forcing function
[DE88-010527] N89-13167
A radio-frequency quadrupole accelerator longitudinal field stabilizer
[DE88-014399] N89-13246
Re-evaluation of an improved efficiency polymeric web point-focus Fresnel lens
[DE88-016892] N89-13255

SARMA EQUIPEMENT AVIATION, SAINT-VALLIER (FRANCE).
Composite rods in carbon-epoxy Fibredux 914 C/TS-6T-6K-34
[SARMA-TR-87-2431A] N89-12677
Carbon-epoxy composite rods Fibredux 914 C/TS-6T-6K-34
[SARMA-TR-872429-A] N89-12678
Damage of carbon fiber tubes and rods
[SARMA-TR-882401] N89-12682

SCIENCE APPLICATIONS INTERNATIONAL CORP., BILLERICA, MASS.
Adaptive machine vision
[AD-A197039] N89-13222

SCIENCE APPLICATIONS INTERNATIONAL CORP., MCLEAN, VA.
Soviet exoatmospheric neutral particle beam research
[FASAC-TAR-3110] N89-13390

SCIENCE APPLICATIONS INTERNATIONAL CORP., MONTEREY, CALIF.
Forecasting aids for setting tropical cyclone conditions: Sasebo and Iwakuni, Japan
[AD-A197802] N89-13122

SCIENCE APPLICATIONS INTERNATIONAL CORP., SAN DIEGO, CALIF.
Soviet exoatmospheric neutral particle beam research
[FASAC-TAR-3110] N89-13390

SCIENCE APPLICATIONS INTERNATIONAL CORP., SUNNYVALE, CALIF.
Mass flow meter using the triboelectric effect for measurement in cryogenics
[NASA-CR-179572] N89-12836

SCOTT, WILSON, KIRKPATRICK AND PARTNERS, BASINGSTOKE (ENGLAND).
Cotton area mapping using multitemporal satellite data integrated within a geographical information system applied to a cotton boll weevil control programme in Paraguay N89-13077

SCOTT POLAR RESEARCH INST., CAMBRIDGE (ENGLAND).
Topographic effects on light scattering from snow N89-12976
Synthetic aperture radar over terrestrial ice N89-12977

SCRIPPS INSTITUTION OF OCEANOGRAPHY, LA JOLLA, CALIF.
Parabolic equation model
[AD-A197480] N89-13161

SELENIA SPAZIO S.P.A., ROME (ITALY).
The solar simulation test of the ITALSAT thermal structural model N89-12613

SHEFFIELD UNIV. (ENGLAND).
Relationships between the nitrogen content of grass and reflectance N89-13002
Improving the accessibility of spatially referenced geological information N89-13026

SKF INDUSTRIES, INC., KING OF PRUSSIA, PA.
Thermo-mechanical performance evaluation of cryogenic turbopump ball bearings N89-12637

SMITHSONIAN ASTROPHYSICAL OBSERVATORY, CAMBRIDGE, MASS.
Theoretical studies of mass loss and shock phenomena in cool star envelopes
[NASA-CR-182708] N89-13375

SOUTHAMPTON UNIV. (ENGLAND).
Approximate mobilities of built up structures
[ISVR-TR-162] N89-12934

SOUTHERN METHODIST UNIV., DALLAS, TEX.
On the effect of R-ratio and Kfmax on fracture toughness measurement, fatigue crack propagation, and fatigue crack closure N89-12875

SOUTHWEST RESEARCH INST., SAN ANTONIO, TEX.
Multiple input/output random vibration control system N89-12594
Constitutive modeling for isotropic materials N89-12904
SPECTRA RESEARCH SYSTEMS, INC., HUNTSVILLE, ALA.
Thermal analysis of SSME turbopump bearings N89-12638
ST SYSTEMS CORP., LEXINGTON, MASS.
C Cloud S (Climatology of Cloud Statistics) database (users manual) [AD-A196497] N89-13118
STANFORD LINEAR ACCELERATOR CENTER, CALIF.
Algorithms for the self-consistent simulation of high power klystrons [DE88-010684] N89-12812
Fitting functions to noisy data in high dimensions [DE88-015922] N89-13213
Solar monopoles and terrestrial neutrinos [DE88-010677] N89-13388
STANFORD UNIV., CALIF.
Foundations of the blade-vortex interaction problem: Structure and behavior of travelling compressible vortices [AD-A197370] N89-12550
Studies of ultrathin polymer films for lithographic applications [AD-A197297] N89-12731
Ultrathin polymer films for microlithography [AD-A197298] N89-12732
Heat transfer with very high free-stream turbulence and streamwise vortices N89-12900
Nonequilibrium effects in thermal plasmas: Radiation transport and chemical reactivity [DE88-016841] N89-13262
Nonequilibrium effects in thermal plasma chemistry [DE88-016842] N89-13263
STATE UNIV. OF NEW YORK, BUFFALO.
The effect of attentional focus level on task performance utilizing information from different stimulus structure levels N89-12765
A fault diagnosis system based on an integrated knowledge base N89-13181
SNePS considered as a fully intensional propositional semantic network N89-13184
Large silicon clusters: Confirmation of Phillips' conjecture [AD-A197487] N89-13241
Overview of high-temperature superconductivity: Theory, surfaces, interfaces and bulk systems [AD-A197383] N89-13285
STATE UNIV. OF NEW YORK, STONY BROOK.
New methods for locating phase boundaries [DE88-017084] N89-12700
The 3.4 micrometer emission feature in Comet Halley N89-13338
Current status of the international Halley Watch infrared net archive N89-13345
The near-infrared polarization and color of Comet Halley: What can we learn about the grains N89-13348
STOCKHOLM UNIV. (SWEDEN).
LANDSAT Thematic Mapping (TM) and SPOT HRV for survey mapping of bedrock outcrops N89-13055
STRASBOURG UNIV. (FRANCE).
Data bases and remote sensing N89-12965
SUSSEX UNIV., BRIGHTON (ENGLAND).
Heat transfer to rough turbine blading N89-12623
SVENSK DRIVMEDEKSTEKNIK A.B., STOCKHOLM.
Fuel alcohol formulations [DE88-016753] N89-12748
SVERDRUP TECHNOLOGY, INC., CLEVELAND, OHIO.
A control-volume method for analysis of unsteady thrust augmenting ejector flows [NASA-CR-182203] N89-12566
A review of turbomachinery blade-row interaction research [NASA-CR-182211] N89-12567
SWEDISH INST. OF COMPUTER SCIENCE, UPPSALA.
Practical issues relating to the internal database predicates in an OR-parallel prolog: Extensions and useful hacks [DE88-010019] N89-13174
SYNTEK ENGINEERING AND COMPUTER SYSTEMS, INC., ROCKVILLE, MD.
Arctic oceanography and meteorology review [AD-A196533] N89-13126
SYRACUSE UNIV., N. Y.
On adaptive cell-averaging CFAR radar signal detection N89-12792
Grain boundary oxidation and its effects on high temperature fatigue life N89-12918
Northeast Artificial Intelligence Consortium (NAIC). Review of technical tasks, volume 2, part 1 [AD-A189773] N89-13180
SYSCON CORP., SAN DIEGO, CALIF.
Boeing Military Airplane Company technical order transfer tests [DE88-012233] N89-13151

T

TECHNICAL RESEARCH CENTRE OF FINLAND, ESPOO.
Colloid vibration potentials [VTT-RR-535] N89-13244
TECHNICAL UNIV. OF DENMARK, LYNGBY.
On the sampling in imaging microwave radiometers N89-12940
TECHNISCHE UNIV., MUNICH (WEST GERMANY).
Electronic transport properties of the metallic glass Cu sub 100-x Ti sub x [ETN-88-93231] N89-12718
A multichannel fiber optic photometer present performance and future developments N89-13313
TECHNOLOGY, INC., SAN ANTONIO, TEX.
Research and development of anti-g life support systems. Part 2: Decompression sickness research [AD-A197675] N89-13133
TECHNOLOGY INTERNATIONAL CORP., POTOMAC, MD.
Survey of supply/demand relationships for Japanese Technical Information in the United States: The field of advanced ceramics research and development [PB88-210943] N89-13300
TENNESSEE UNIV. SPACE INST., TULLAHOMA.
Directed motion Doppler shift effects on nitric oxide (0,0) gamma band resonance absorption N89-12760
Influence of bulk turbulence and entrance boundary layer thickness on the curved duct flow field [NASA-CR-4188] N89-12838
Influence of bulk turbulence and entrance boundary layer thickness on the curved duct flow field N89-12896
TENNEY ENGINEERING, INC.
Space simulators for laser optics N89-12597
TEXAS A&M UNIV., COLLEGE STATION.
Preliminary thermal analysis of a bimodal nuclear rocket core N89-12758
An optical sensor system for monitoring structural dynamics with applications to system identification N89-12775
Optimal rates of convergence for deconvolving a density [AD-A197748] N89-13207
Multivariate regression with emphasis on multivariate spline methods [AD-A197793] N89-13209
TEXAS INSTRUMENTS, INC., MCKINNEY.
Examining the polarisation phase retrieval of a dual channel multipolarisation radar N89-13019
TEXAS UNIV., ARLINGTON.
Electronic and ionic transport in polymers [AD-A197142] N89-12728
Scattering from a skewed random surface N89-12948
Polarimetric microwave scattering from known randomly rough surfaces N89-12949
Attenuation and scattering measurements from dense media N89-13012
Bistatic frequency diverse imaging of complex scattering targets N89-13013
Investigation of acceleration and densification of electrons utilizing travelling magnetic waves [AD-A197700] N89-13242
TEXAS UNIV., AUSTIN.
Electrogenerated chemiluminescence [AD-A197163] N89-12691
Toroidal studies of sawtooth oscillations in tokamaks [DE88-017115] N89-13264
Carbon, nitrogen and oxygen abundances in the chemically peculiar stars of the upper main sequence N89-13379
TEXAS UNIV., DALLAS.
Proof of the feasibility of coherent and incoherent schemes for pumping a gamma-ray laser [AD-A197333] N89-12853
TOKAI UNIV., KANAGAWA (JAPAN).
A new spatial classification algorithm for high ground resolution images N89-13061
Accuracy of land cover classification of Thematic Mapper (TM) and SPOT data N89-13066
TOKYO UNIV. (JAPAN).
Differential cross sections for electron-impact excitation of atomic ions [ISAS-RN-365] N89-13237
TORONTO UNIV., DOWNSVIEW (ONTARIO).
Atomic oxygen studies on polymers N89-12591
TRIER UNIV., TRIER-TARFORST (WEST GERMANY).
Snow cover to alter terrain signatures on radar images N89-13048
TRW DEFENSE AND SPACE SYSTEMS GROUP, REDONDO BEACH, CALIF.
Class 100 large spacecraft facility N89-12586
Precision cleaning methods for spacecraft applications N89-12588

U

UNITED NATIONS ENVIRONMENT PROGRAMME, PARIS (FRANCE).
Environmental management practices in oil refineries and terminals: An overview [ISBN-92-807-1108-3] N89-13104
UNITED TECHNOLOGIES RESEARCH CENTER, EAST HARTFORD, CONN.
Measurement of airfoil heat transfer coefficients on a turbine stage N89-12897
UNIVERSAL ENERGY SYSTEMS, INC., DAYTON, OHIO.
United States Air Force Graduate Student Summer Support Program, volume 1 [AD-A191121] N89-12754
UNIVERSITE CATHOLIQUE DE LOUVAIN (BELGIUM).
Combining spectral and structural analyses to select useful cartographic information from SPOT imagery N89-13052
UNIVERSITY COLL., LONDON (ENGLAND).
The differential rectification of SPOT HRV panchromatic and multispectral imagery using a digital elevation model N89-13054
Lapwing: A trainable spatial feature recognition system N89-13063
UNIVERSITY OF EASTERN ILLINOIS, CHARLESTON.
Perturbed functional iteration applied to the Navier-Stokes equations N89-12774
UNIVERSITY OF SOUTHERN CALIFORNIA, LOS ANGELES.
Model-based estimation of wind fields over the ocean from wind scatterometer measurements N89-13070
UNIVERSITY OF SOUTHERN CALIFORNIA, MARINA DEL REY.
Applications of the ISI (Information Sciences Institute) grapher [AD-A197230] N89-13194
UNIVERSITY OF WALES, SWANSEA.
Theoretical aspects of gravitational wave detection N89-13383
UTAH UNIV., SALT LAKE CITY.
The conversion of smaller borane fragments to larger structures. Systematics of boron hydride reactions [AD-A197068] N89-12689
The behavior of disk electrodes: Optical imaging of the concentration distribution over a disk electrode under galvanostatic conditions [AD-A197355] N89-12816
Backscatter laser depolarization studies of simulated stratospheric aerosols: Crystallized sulfuric acid droplets [NASA-CR-183387] N89-13111
UWOHALI, INC., HUNTSVILLE, ALA.
Antenna pattern study [ARI/R-88-510Z] N89-12790

V

VANDERBILT UNIV., NASHVILLE, TENN.
Modified pull test for the testing of very adherent films [DE88-016363] N89-12743
An expert system for diagnosis and repair of analog circuits N89-12784
VERITAY TECHNOLOGY, INC., AMHERST, N.Y.
21st century propulsion concept [AD-A197537] N89-12663
VIGYAN RESEARCH ASSOCIATES, INC., HAMPTON, VA.
Sidewall boundary-layer measurements with upstream suction in the Langley 0.3-meter transonic cryogenic tunnel [NASA-CR-4192] N89-12544
VIRGINIA POLYTECHNIC INST. AND STATE UNIV., BLACKSBURG.
Results of true-anomaly regularization in orbital mechanics N89-12577
An axisymmetric linear/high-order finite element for filament wound composite structures N89-12674
Combined mechanical loading of composite tubes [NASA-CR-183012] N89-12681
The durability of adhesive joints: An engineering study [AD-A197754] N89-12928
The E-parallel polarization response of a two-dimensional heterogeneous layer modelled by two thin sheets N89-12947
A study of active control techniques for noise reduction in an aircraft fuselage model N89-13232

VIRGINIA UNIV., CHARLOTTESVILLE.
In-situ oxidation of Ni3Al alloys
[DE88-007177] N89-12702

W

WASHINGTON STATE UNIV., PULLMAN.
Ground run-up afterburner detection and noise suppression N89-12768
WASHINGTON UNIV., SEATTLE.
A numerical model for the computation of radiance distributions in natural waters with wind-roughened surfaces
[AD-A197207] N89-13128
Parallel debugging using graphical views
[AD-A197197] N89-13156
Practical algorithms for image component labeling on SIMD mesh connected computers
[AD-A197341] N89-13158
Achieving speedups for a shared memory model language on an SIMD parallel computer
[AD-A197102] N89-13176
Voyeur: Graphical views of parallel programs
[AD-A197103] N89-13177
Wavelength or sensor selection by minimization of prediction error
[AD-A197231] N89-13216
FIREBIRD: A conceptual design of a field reversed configuration Compact Torus Fusion Reactor (CTFR)
N89-13230
A comparison of Halley dust with meteorites, interplanetary dust and interstellar grains N89-13335
Mixing and structural changes during mass transfer in binary systems N89-13382
WASHINGTON UNIV., ST. LOUIS, MO.
Is word recognition automatic: A cognitive-anatomical approach
[AD-A197089] N89-13137
WYLE LABS., INC., HUNTSVILLE, ALA.
Test stand design and analysis for Titan 34D static firing N89-12609
WYOMING UNIV., LARAMIE.
Biogeochemical processes in sagebrush steppe: Interactions of terrain, vegetation and chemical cycles
[NASA-CR-181486] N89-13088
An albedo map of P/Halley on 13 March 1986
N89-13355

Y

YALE UNIV., NEW HAVEN, CONN.
Vibration suppression in a large space structure
[NASA-CR-182831] N89-12624

Z

ZURICH UNIV. (SWITZERLAND).
Improvement in NOAA-AVHRR snowcover determination for runoff prediction N89-13040
Monitoring of seasonal snow cover on glaciers
N89-13044

Typical Contract Number Index Listing

Listings in this index are arranged alphanumerically by contract number. Under each contract number the NASA accession numbers denoting documents that have been produced as a result of research done under that contract are arranged in ascending order. The NASA accession number denotes the number by which the citation is identified.

AF PROJ. 2301 ..... N89-12855
N89-13178
N89-13242
AF PROJ. 2304 ..... N89-13180
AF PROJ. 2310 ..... N89-13118
AF PROJ. 2313 ..... N89-13139
AF PROJ. 3396 ..... N89-12754
AF-AFOSR-0023-88 ..... N89-13156
AF-AFOSR-0040-88 ..... N89-13205
AF-AFOSR-0101-83 ..... N89-13178
AF-AFOSR-0121-88 ..... N89-12995
AF-AFOSR-0180-87 ..... N89-13139
AF-AFOSR-0268-85 ..... N89-13218
AF-AFOSR-0368-83 ..... N89-13242
ARPA ORDER 4469 ..... N89-13159
ARPA ORDER 4871 ..... N89-12926
N89-13146
N89-13160
N89-13305
ARPA ORDER 5794 ..... N89-13252
ARPA ORDER 9526 ..... N89-12818
AUSPI-86-207 ..... N89-12591
BA-867/2-1 ..... N89-13313
DA PROJ. 2Q1-61102-B-74-F N89-13138
N89-13197
DA PROJ. 2Q1-62717-A-790 ..... N89-13193
DAAA15-85-K-0004 ..... N89-12696
DAAD07-87-C-0103 ..... N89-13175
DAAG28-85-K-0058 ..... N89-12695
DAAG29-83-K-0002 ..... N89-13295
DAAG29-83-K-0146 ..... N89-12550
DAAG29-84-K-0048 ..... N89-13143
N89-13195
DAAG29-84-K-0154 ..... N89-13209
DAAG29-85-K-0034 ..... N89-12689
DAAG29-85-K-0049 ..... N89-12815
DAAG29-85-K-0104 ..... N89-12691
DAAG29-85-K-0105 ..... N89-12851
DAAG29-85-K-0121 ..... N89-12666
DAAL03-86-K-0094 ..... N89-13205
N89-13217
DCA100-82-C-0034 ..... N89-12807
DE-AC02-76CH-00016 ..... N89-13247
DE-AC02-83CH-10093 ..... N89-13098
N89-13101
N89-13102
DE-AC03-76SF-00098 ..... N89-12686
N89-12714
N89-12872
N89-13278
N89-13279
N89-13289
DE-AC03-76SF-00515 ..... N89-12812
N89-13213
N89-13388
DE-AC04-76DP-00053 ..... N89-12848
DE-AC04-76DP-00789 ..... N89-12625
N89-12787
N89-12793
N89-12831
N89-12840
N89-12857
N89-12859
N89-13095
N89-13167
N89-13255
N89-13384
DE-AC05-76OR-00001 ..... N89-12706
DE-AC05-84ER-40150 ..... N89-13245
DE-AC05-84OR-21400 ..... N89-12701
N89-12702
N89-12703
N89-12713
N89-12725
N89-12743
N89-12744
N89-12791
N89-12826
N89-12869
N89-12910
N89-13135
N89-13221
N89-13238
DE-AC06-76RL-01830 ..... N89-12698
N89-12699
N89-13123
DE-AC07-76ID-01570 ..... N89-12662
N89-12664
N89-12724
N89-13099
DE-AC09-76SR-00001 ..... N89-12742
N89-13147
DE-AI01-76ET-20320 ..... N89-12675
DE-AI21-80ET-17088 ..... N89-13103
DE-AM03-76SF-00115 ..... N89-12828
DE-FG02-84ER-45082 ..... N89-13277
DE-FG02-84ER-45136 ..... N89-12716
DE-FG02-85ER-75172 ..... N89-13223
DE-FG02-86ER-45267 ..... N89-13233
DE-FG02-87ER-13648 ..... N89-12700
DE-FG02-87ER-13670 ..... N89-13389
DE-FG02-87ER-13700 ..... N89-13239
DE-FG03-85ER-13393 ..... N89-13262
N89-13263
DE-FG05-80ET-53088 ..... N89-13264
DE-FG05-84ER-45071 ..... N89-12715
DE-FG21-86FE-61114 ..... N89-13093
DE-FG22-86PC-90956 ..... N89-12833
DE-GI01-87CE-50181 ..... N89-12748
EEI-TO-87-57 ..... N89-12862
EN3E.0005.UK(H) N89-12861
ESA-6684/86-D-MD(SC) N89-12573
N89-12574
ESTEC-6781/86-NL-DG N89-12809
F06411-87-C-0058 ..... N89-12663
F19628-84-K-0011 ..... N89-12688
F19628-85-C-0002 ..... N89-13179
N89-13280
F19628-85-C-0003 ..... N89-13154
F19628-86-C-0001 ..... N89-13157
F19628-87-C-0046 ..... N89-13118
F20602-85-C-0279 ..... N89-12587
F29601-86-C-0216 ..... N89-13164
F30602-82-K-0170 ..... N89-13159
F30602-85-C-0008 ..... N89-13180
N89-13184
N89-13185
N89-13187
N89-13189
F33615-81-C-0600 ..... N89-13133
F33615-84-C-2427 ..... N89-12893
F33615-84-C-5051 ..... N89-12864
F33615-85-C-5024 ..... N89-12873
F33615-87-C-5217 ..... N89-12535
F49620-85-C-0013 ..... N89-12754
F49620-85-C-0144 ..... N89-13207
F49620-85-C-0145 ..... N89-12693
F49620-86-C-0033 ..... N89-12711
F49620-86-C-0082 ..... N89-13252
F49620-86-C-0115 ..... N89-13215
F49620-87-C-0021 ..... N89-13286
GS-14-08-0001-A-0353 ..... N89-13043
MDA903-81-C-0335 ..... N89-13194
MDA903-82-C-0124 ..... N89-13197
MDA903-86-C-0092 ..... N89-13296
MDA903-86-C-0204 ..... N89-13193
MDA903-86-K-0320 ..... N89-13138
MIPR-117-87 ..... N89-12738
NAGW-511 ..... N89-13375
NAG1-270 ..... N89-13215
NAG1-343 ..... N89-12681
NAG1-613 ..... N89-13145
NAG1-618 ..... N89-13152
NAG1-686 ..... N89-13111
NAG1-738 ..... N89-12810
NAG1-771 ..... N89-13153
NAG1-784 ..... N89-12538
NAG1-824 ..... N89-13150
NAG2-244 ..... N89-12570
NAG2-355 ..... N89-13088
NAG3-166 ..... N89-12870
NAG3-194 ..... N89-12553
NAG3-348 ..... N89-12918
NAG3-379 ..... N89-12908
NAG3-501 ..... N89-12886
NAG3-503 ..... N89-12634
NAG3-511 ..... N89-12911
NAG3-512 ..... N89-12912
NAG3-522 ..... N89-12900
NAG3-534 ..... N89-12931
N89-12932
NAG3-579 ..... N89-12901
NAG3-596 ..... N89-12894
NAG3-617 ..... N89-12838
N89-12896
NAG3-623 ..... N89-12898
NAG3-752 ..... N89-13227
NAG5-270 ..... N89-12794
NAG5-486 ..... N89-12949
N89-13013
NAG5-510 ..... N89-13091
NAG5-831 ..... N89-13240
NAG5-932 ..... N89-13387
NAG5-1007 ..... N89-13249
NASA ORDER C-80015-F N89-12675
NASA ORDER C-80017-F N89-12835
NAS1-17919 ..... N89-12544
NAS1-17993 ..... N89-12572
N89-12923
NAS1-18027 ..... N89-12557
NAS1-18599 ..... N89-13202
NAS2-12370 ..... N89-13359
N89-13360
NAS3-2317 ..... N89-12897
NAS3-23288 ..... N89-12914
NAS3-23687 ..... N89-12907
NAS3-23691 ..... N89-12899
NAS3-23698 ..... N89-12906
NAS3-23722 ..... N89-12887
NAS3-23925 ..... N89-12904
NAS3-23939 ..... N89-12916
NAS3-23940 ..... N89-12915
NAS3-23943 ..... N89-12921
NAS3-23944 ..... N89-12922
NAS3-23945 ..... N89-12920
NAS3-24228 ..... N89-12884
NAS3-24350 ..... N89-12890
N89-12891
N89-12892
NAS3-24351 ..... N89-12895
NAS3-24358 ..... N89-12902
NAS3-24619 ..... N89-12903
NAS3-24624 ..... N89-13256
NAS3-24648 ..... N89-12836
NAS3-24873 ..... N89-12837
NAS3-25266 ..... N89-12566
N89-12567
NAS7-918 ..... N89-12618
N89-12813
N89-12856
N89-13165
N89-13211
N89-13219
N89-13220
NAS8-27980 ..... N89-12640
N89-12654
NAS8-35341 ..... N89-12637

NAS8-35507 ..... N89-12636
NAS8-35601 ..... N89-12629
NAS8-35992 ..... N89-12631
NAS8-36182 ..... N89-12630
NAS8-36280 ..... N89-12745
NAS8-36298 ..... N89-12722
N89-12723
NAS8-36438 ..... N89-12581
NAS8-36475 ..... N89-12631
NAS8-36570 ..... N89-12595
NAS8-37143 ..... N89-12579
NAS9-17395 ..... N89-12624
NAS9-17878 ..... N89-12862
N89-13141
NCC2-367 ..... N89-13200
NCC2-408 ..... N89-13214
NCC3-17 ..... N89-13103
NCC3-27 ..... N89-12918
NCC3-99 ..... N89-12820
NERC-CASE-GT4/86/GS/90 ..... N89-13056
NERC-F60/G6/12 ..... N89-12959
N89-13028
NERC-GR3/5896 ..... N89-12995
NERC-GT4/83/TLS/43 ..... N89-13065
NERC-GT4/85/GS/85 ..... N89-13028
NSF CCR-84-16878 ..... N89-13177
NSF DCR-84-16878 ..... N89-13176
NSF DMS-85-03294 ..... N89-13215
NSF MCS-80-06314 ..... N89-13185
NSF PHY-88-03557 ..... N89-12599
NSG-5049 ..... N89-13107
N00014-75-C-0536 ..... N89-13216
N00014-80-C-0741 ..... N89-13218
N00014-81-C-0195 ..... N89-13039
N00014-81-C-0295 ..... N89-13034
N00014-82-K-0182 ..... N89-12739
N00014-82-K-0185 ..... N89-12928
N00014-82-K-0186 ..... N89-13163
N00014-83-K-0498 ..... N89-13283
N00014-84-K-0021 ..... N89-12730
N00014-84-K-0510 ..... N89-12676
N00014-84-K-0658 ..... N89-12690
N00014-85-C-0241 ..... N89-13155
N00014-85-C-0681 ..... N89-12726
N00014-85-K-0124 ..... N89-13304
N00014-85-K-0145 ..... N89-12928
N00014-85-K-0151 ..... N89-13282
N00014-85-K-0358 ..... N89-12740
N00014-85-K-0712 ..... N89-12816
N00014-85-K-0782 ..... N89-13192
N00014-85-K-0821 ..... N89-12707
N00014-85-K-2036 ..... N89-13199
N00014-86-C-0601 ..... N89-13222
N00014-86-C-2241 ..... N89-12852
N00014-86-C-2352 ..... N89-13196
N00014-86-C-2488 ..... N89-12853
N00014-86-K-0043 ..... N89-13241
N89-13285
N00014-86-K-0164 ..... N89-13158
N00014-86-K-0173 ..... N89-13206
N00014-86-K-0191 ..... N89-13284
N00014-86-K-0202 ..... N89-12808
N00014-86-K-0264 ..... N89-13156
N89-13176
N89-13177
N00014-86-K-0289 ..... N89-13137
N00014-86-K-0516 ..... N89-12817
N00014-86-K-0606 ..... N89-13129
N00014-86-K-0691 ..... N89-13215
N00014-86-K-0753 ..... N89-12676
N00014-86-K-0769 ..... N89-12728
N00014-86-K-0772 ..... N89-12729
N00014-87-C-0127 ..... N89-13161
N00014-87-C-0418 ..... N89-13039
N00014-87-G-0170 ..... N89-13110
N00014-87-G-0268 ..... N89-12735
N00014-87-K-0398 ..... N89-13303
N00014-87-K-0426 ..... N89-12731
N89-12732
N00014-87-K-0479 ..... N89-13130
N00014-87-K-0525 ..... N89-13128
N00014-87-K-0874 ..... N89-13163
N00014-88-C-0391 ..... N89-12818
N00014-88-K-0094 ..... N89-12708
N00024-85-C-6041 ..... N89-12710
N00039-84-C-0089 ..... N89-12926
N89-13146
N89-13160
N89-13305
N00039-87-C-5301 ..... N89-13166
N89-13251
N00228-86-C-3040 ..... N89-13122
N60530-85-C-0365 ..... N89-12948
N60921-86-C-A226 ..... N89-12591
ONR-146-70-03 ..... N89-13074
PROJ. RR0-2102 ..... N89-12739
PROJ. RR0-4106 ..... N89-12735
PROJ. RR0-4108 ..... N89-13130
PROJ. RR0-4206 ..... N89-13137
SERC-GR/E/27164 ..... N89-12994
SNL-33-0878 ..... N89-12615
STPA-84-96-013-00-471-75-86 ..... N89-12678
STPA-85-96-011-00-471-75-86 ..... N89-12677
STPA-86-96-009 ..... N89-12683
STPA-86-96-028-00-471-75-86 ..... N89-12682
SUNY-BRDF-150-9216 ..... N89-13184
TP2-325 ..... N89-12591
UTC-CSD-268024 ..... N89-12609
W-31-109-ENG-38 ..... N89-12633
N89-12832
N89-13168
N89-13174
N89-13265
W-7405-ENG-36 ..... N89-12679
N89-12680
N89-12704
N89-12788
N89-12858
N89-13212
N89-13258
N89-13259
N89-13260
N89-13261
N89-13288
N89-13292
N89-13294
N89-13306
W-7405-ENG-48 ..... N89-12578
N89-12664
N89-12697
N89-12789
N89-12830
N89-12844
N89-12860
N89-12929
N89-13100
N89-13106
N89-13151
N89-13170
N89-13246
N89-13254
157-05-50-04 ..... N89-13310
161-80-23 ..... N89-13074
314-40-50-55-09 ..... N89-12813
505-60-01-02 ..... N89-12542
N89-12543
505-61-01-02 ..... N89-12544
505-61-71 ..... N89-12554
505-62-21 ..... N89-12552
N89-12553
505-62-71 ..... N89-12566
505-63-1B N89-12567
N89-12930
505-63-01 ..... N89-12720
N89-12746
505-63-01-07 ..... N89-13203
505-63-01-10 ..... N89-13202
505-63-01-11 ..... N89-12935
505-63-11 ..... N89-12684
505-66-21-03 ..... N89-13153
505-68-1A N89-12845
505-69-51 ..... N89-12539
505-90-01 ..... N89-12555
506-40-21-01 ..... N89-12822
506-40-91-03 ..... N89-12834
506-41-11 ..... N89-12819
506-43-11-01 ..... N89-12747
506-43-41-02 ..... N89-12580
506-44-21 ..... N89-12820
506-46-21-01 ..... N89-12569
510-01-01 ..... N89-12717
533-04-11 ..... N89-12876
533-04-12 ..... N89-12838
535-03-01 ..... N89-12565
535-05-01 ..... N89-12568
582-01-11 ..... N89-12835
583-01-11 ..... N89-12622
674-25-05 ..... N89-12753
778-17-01 ..... N89-13103
805-18-10 ..... N89-13144
805-45-01 ..... N89-12623

Typical Report Number Index Listing

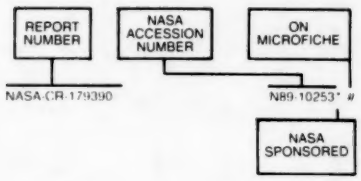

Listings in this index are arranged alphanumerically by report number. The NASA accession number denotes the number by which the citation is identified. An asterisk (*) indicates that the item is a NASA report. A pound sign (#) indicates that the item is available on microfiche.

A-88044 ..... N89-13393* #
A-88125 ..... N89-13310* #
A-88182 ..... N89-13144* #
A-88269 ..... N89-13171* #
A-88275 ..... N89-12554* #
A-88297 ..... N89-12622* #
A-88310 ..... N89-12623* #
A-89009 ..... N89-12539* #

ACT-RR-87-19 ..... N89-13155 #

AD-A189773 ..... N89-13180 #
AD-A191121 ..... N89-12754 #
AD-A196448 ..... N89-13192 #
AD-A196497 ..... N89-13118 #
AD-A196533 ..... N89-13126 #
AD-A196748 ..... N89-12688 #
AD-A196755 ..... N89-12548 #
AD-A196839 ..... N89-13193 #
AD-A196971 ..... N89-13175 #
AD-A197039 ..... N89-13222 #
AD-A197066 ..... N89-12850 #
AD-A197068 ..... N89-12689 #
AD-A197069 ..... N89-13280 #
AD-A197072 ..... N89-12690 #
AD-A197076 ..... N89-12749 #
AD-A197077 ..... N89-12726 #
AD-A197089 ..... N89-13137 #
AD-A197091 ..... N89-12549 #
AD-A197093 ..... N89-12795 #
AD-A197102 ..... N89-13176 #
AD-A197103 ..... N89-13177 #
AD-A197109 ..... N89-12727 #
AD-A197117 ..... N89-12851 #
AD-A197128 ..... N89-12562 #
AD-A197130 ..... N89-12926 #
AD-A197131 ..... N89-13146 #
AD-A197132 ..... N89-12707 #
AD-A197137 ..... N89-13154 #
AD-A197140 ..... N89-12815 #
AD-A197141 ..... N89-13295 #
AD-A197142 ..... N89-12728 #
AD-A197143 ..... N89-12666 #
AD-A197145 ..... N89-13257 #
AD-A197146 ..... N89-13119 #
AD-A197150 ..... N89-12829 #
AD-A197152 ..... N89-13281 #
AD-A197153 ..... N89-12796 #
AD-A197160 ..... N89-13155 #
AD-A197163 ..... N89-12691 #
AD-A197166 ..... N89-12708 #
AD-A197167 ..... N89-13204 #
AD-A197179 ..... N89-12558 #
AD-A197180 ..... N89-12797 #
AD-A197194 ..... N89-12676 #
AD-A197196 ..... N89-13127 #
AD-A197197 ..... N89-13156 #
AD-A197201 ..... N89-12729 #
AD-A197207 ..... N89-13128 #
AD-A197218 ..... N89-13120 #
AD-A197219 ..... N89-12559 #
AD-A197223 ..... N89-13121 #
AD-A197230 ..... N89-13194 #
AD-A197231 ..... N89-13216 #
AD-A197238 ..... N89-13282 #
AD-A197241 ..... N89-13303 #
AD-A197242 ..... N89-13157 #
AD-A197245 ..... N89-13283 #
AD-A197249 ..... N89-13129 #
AD-A197254 ..... N89-12730 #
AD-A197255 ..... N89-13195 #
AD-A197262 ..... N89-13284 #
AD-A197270 ..... N89-12750 #
AD-A197271 ..... N89-12692 #
AD-A197278 ..... N89-12798 #
AD-A197282 ..... N89-13234 #
AD-A197297 ..... N89-12731 #
AD-A197298 ..... N89-12732 #
AD-A197300 ..... N89-12693 #
AD-A197302 ..... N89-12733 #
AD-A197310 ..... N89-12927 #
AD-A197311 ..... N89-12799 #
AD-A197313 ..... N89-12852 #
AD-A197316 ..... N89-13092 #
AD-A197317 ..... N89-12709 #
AD-A197319 ..... N89-13142 #
AD-A197320 ..... N89-12734 #
AD-A197321 ..... N89-12800 #
AD-A197322 ..... N89-12801 #
AD-A197323 ..... N89-13205 #
AD-A197324 ..... N89-13217 #
AD-A197333 ..... N89-12853 #
AD-A197341 ..... N89-13158 #
AD-A197342 ..... N89-13159 #
AD-A197344 ..... N89-13160 #
AD-A197347 ..... N89-13250 #
AD-A197351 ..... N89-13196 #
AD-A197352 ..... N89-12735 #
AD-A197355 ..... N89-12816 #
AD-A197356 ..... N89-13304 #
AD-A197358 ..... N89-13110 #
AD-A197364 ..... N89-12802 #
AD-A197365 ..... N89-12817 #
AD-A197368 ..... N89-12535 #
AD-A197369 ..... N89-13305 #
AD-A197370 ..... N89-12550 #
AD-A197371 ..... N89-13132 #
AD-A197383 ..... N89-13285 #
AD-A197385 ..... N89-12803 #
AD-A197386 ..... N89-13197 #
AD-A197391 ..... N89-13130 #
AD-A197398 ..... N89-12710 #
AD-A197454 ..... N89-13178 #
AD-A197470 ..... N89-13251 #
AD-A197473 ..... N89-12804 #
AD-A197480 ..... N89-13161 #
AD-A197487 ..... N89-13241 #
AD-A197537 ..... N89-12663 #
AD-A197605 ..... N89-12711 #
AD-A197667 ..... N89-13138 #
AD-A197668 ..... N89-13252 #
AD-A197670 ..... N89-13139 #
AD-A197673 ..... N89-12736 #
AD-A197674 ..... N89-13143 #
AD-A197675 ..... N89-13133 #
AD-A197681 ..... N89-13296 #
AD-A197700 ..... N89-13242 #
AD-A197734 ..... N89-12694 #
AD-A197739 ..... N89-12818 #
AD-A197741 ..... N89-12854 #
AD-A197747 ..... N89-13206 #
AD-A197748 ..... N89-13207 #
AD-A197749 ..... N89-13199 #
AD-A197751 ..... N89-12563 #
AD-A197752 ..... N89-13286 #
AD-A197754 ..... N89-12928 #
AD-A197768 ..... N89-13162 #
AD-A197770 ..... N89-12855 #
AD-A197772 ..... N89-13208 #
AD-A197776 ..... N89-13218 #
AD-A197778 ..... N89-13163 #
AD-A197780 ..... N89-13134 #
AD-A197783 ..... N89-12737 #
AD-A197788 ..... N89-12695 #
AD-A197789 ..... N89-13179 #
AD-A197793 ..... N89-13209 #
AD-A197798 ..... N89-13164 #
AD-A197801 ..... N89-12805 #
AD-A197802 ..... N89-13122 #
AD-A197803 ..... N89-12696 #
AD-A197816 ..... N89-12864 #
AD-A197818 ..... N89-12806* #
AD-A197819 ..... N89-13287 #
AD-A197821 ..... N89-13235 #
AD-A197822 ..... N89-13210 #
AD-A197830 ..... N89-12712 #
AD-A197831 ..... N89-12560 #
AD-A197834 ..... N89-12873 #
AD-A197836 ..... N89-13211* #
AD-A197837 ..... N89-13219* #
AD-A197838 ..... N89-13165* #
AD-A197839 ..... N89-13220* #
AD-A197842 ..... N89-12738 #
AD-A197843 ..... N89-12739 #
AD-A197846 ..... N89-13166 #
AD-A197849 ..... N89-12807 #
AD-A197850 ..... N89-12808 #
AD-A197852 ..... N89-12740 #
AD-A197854 ..... N89-12751 #

AD-E900801 ..... N89-12798 #
AD-E900802 ..... N89-12692 #
AD-E900802 ..... N89-12750 #
AD-E900802 ..... N89-13284 #

AFAL-TR-88-031 ..... N89-12663 #

AFGL-TR-88-0060 ..... N89-13118 #

AFIT/CI/NR-88-112 ..... N89-13257 #
AFIT/CI/NR-88-132 ..... N89-13119 #
AFIT/CI/NR-88-133 ..... N89-13120 #
AFIT/CI/NR-88-142 ..... N89-12800 #
AFIT/CI/NR-88-143 ..... N89-12801 #
AFIT/CI/NR-88-170 ..... N89-12829 #
AFIT/CI/NR-88-171 ..... N89-12559 #
AFIT/CI/NR-88-174 ..... N89-13281 #
AFIT/CI/NR-88-178 ..... N89-12795 #
AFIT/CI/NR-88-179 ..... N89-12796 #
AFIT/CI/NR-88-181 ..... N89-13121 #
AFIT/CI/NR-88-182 ..... N89-12549 #

AFOSR-88-129TR ..... N89-13205 #
AFOSR-88-0209TR-VOL-1 ..... N89-12754 #
AFOSR-88-0494TR ..... N89-12693 #
AFOSR-88-0706TR ..... N89-13242 #
AFOSR-88-0723TR ..... N89-13286 #
AFOSR-88-0726TR ..... N89-13139 #
AFOSR-88-0735TR ..... N89-13252 #
AFOSR-88-0764TR ..... N89-13178 #
AFOSR-88-0771TR ..... N89-12711 #
AFOSR-88-0775TR ..... N89-13207 #

AFWAL-TR-88-2024 ..... N89-12727 #
AFWAL-TR-88-2033 ..... N89-12855 #
AFWAL-TR-88-2040 ..... N89-12750 #
AFWAL-TR-88-4051 ..... N89-12535 #
AFWAL-TR-88-4062 ..... N89-12864 #
AFWAL-TR-88-4085 ..... N89-12873 #

AFWL-TR-87-69 ..... N89-13164 #

AGARD-AG-296 ..... N89-12849 #

AGARD-AR-249 ..... N89-12564 #

AI-M-1015 ..... N89-13304 #

AIAA-89-0069 ..... N89-12753* #
AIAA-89-0565 ..... N89-12552* #
AIAA-89-0609 ..... N89-12555* #
AIAA-89-0769 ..... N89-12845* #

AITI-87-005 ..... N89-13151 #

ALGO-PUBL-0121 ..... N89-13219* #
ALGO-PUBL-0124 ..... N89-13211* #

ALGO-PUBL-0125 N89-13165* #
ALGO-PUBL-0144 N89-13220* #

AMRC-R-886 N89-13164 #

ANL/FPP/TM-215-REV-1 N89-13265 #
ANL/FPP/TM-227 N89-12832 #

ANL/MCS-TM-117 N89-13168 #

ARCCB-TR-88016 N89-12927 #
ARCCB-TR-88017 N89-13208 #
ARCCB-TR-88026 N89-12694 #

ARI-RN-88-41 N89-13197 #
ARI-RN-88-47 N89-13138 #
ARI-RN-88-50 N89-13193 #

ARI/R-88-510Z N89-12790 #

ARL/PSU/TR-88-007 N89-12799 #

ARO-19392.19-EG-RW N89-13295 #
ARO-20155.15-MA N89-13195 #
ARO-20155.16-MA N89-13143 #
ARO-20670.2-EG N89-12550 #
ARO-21091.17-MA N89-13209 #
ARO-21732.7-PH N89-12695 #
ARO-22284.3-CH N89-12738 #
ARO-22371.13-EL N89-12815 #
ARO-22381.15-CH N89-12689 #
ARO-22444.16-CH N89-12851 #
ARO-22448.9-CH N89-12691 #
ARO-22611.20-PH N89-12666 #
ARO-23699.18-MA N89-13217 #
ARO-23699.19-MA N89-13205 #
ARO-24626-PH-UIR N89-12850 #
ARO-24749-PH N89-12850 #

ASD-TR-87-5040 N89-12560 #

AVSCOM-TR-88-C-036 N89-12845* #
AVSCOM-TR-88-C-037 N89-12568* #

BNL-41555 N89-13247 #

BRDEC-2463 N89-12736 #

BRL-IMR-0896 N89-12548 #

BRL-MR-3687 N89-12548 #

BRL-TR-2918 N89-12751 #
BRL-TR-2927 N89-12749 #

BSO/AETR87030101-VOL-1 N89-12573 #
BSO/AETR87030101-VOL-2 N89-12574 #

B8735659 N89-13290 #

CASS/ESM-88-7 N89-12928 #

CCMS-88-11 N89-12681* #

CEBAF-PR-88-006 N89-13245 #

CECOM-TR-88-2 N89-12804 #

CMU/SEI-88-TR-9 N89-13154 #

CNSS-3 N89-13306 #

CONF-870715-9 N89-13238 #
CONF-870810-1 N89-13263 #
CONF-871124-104 N89-12844 #
CONF-880122-17 N89-12662 #
CONF-880178-5 N89-12812 #
CONF-880431-4 N89-12724 #
CONF-880477-11 N89-13099 #
CONF-880529-5 N89-12714 #
CONF-880552-6 N89-13247 #
CONF-880613-3 N89-12713 #
CONF-880621-1 N89-12699 #
CONF-880655-7 N89-13095 #
CONF-880667-2 N89-12704 #
CONF-880669-16 N89-13288 #
CONF-880724-24 N89-12698 #
CONF-880736-3 N89-13279 #
CONF-880750-2 N89-12625 #
CONF-880780-4 N89-13389 #
CONF-880812-2 N89-13292 #
CONF-880815-7 N89-12788 #
CONF-880841-3 N89-12702 #
CONF-880850-13 N89-13102 #
CONF-880859-1 N89-13174 #
CONF-880884-2 N89-12686 #

CONF-880885-1 N89-13101 #
CONF-880887-6 N89-12857 #
CONF-880911-18 N89-12664 #
CONF-880928-3 N89-12860 #
CONF-881015-1 N89-13260 #
CONF-881015-2 N89-13259 #
CONF-881026-1 N89-12787 #
CONF-881031-1 N89-13258 #
CONF-881049-1 N89-13246 #
CONF-881076-1 N89-13167 #
CONF-8703231-SUMMS N89-13223 #
CONF-8708269 N89-13370 #
CONF-8709275-2 N89-13388 #
CONF-8710344-1 N89-13384 #
CONF-8804100-2 N89-12826 #
CONF-8804159-2 N89-12848 #
CONF-8804183-1 N89-13213 #
CONF-8805106-2 N89-13262 #
CONF-8805132-8 N89-12793 #
CONF-8805164-1 N89-12703 #
CONF-8806103-2 N89-12679 #
CONF-8806227-1 N89-13135 #
CONF-8806233-1 N89-13269 #
CONF-8807102-1 N89-12742 #
CONF-8808102-4 N89-13106 #
CONF-8808103-2 N89-13254 #
CONF-8808108-1 N89-12743 #
CONF-8808108-4 N89-12744 #
CONF-8808112-1 N89-13294 #
CONF-8809109-3 N89-12840 #
CONF-8809109-5 N89-12578 #
CONF-8809111-2 N89-12859 #
CONF-8809124-1 N89-12858 #
CONF-8809125-1 N89-13261 #
CONF-8810119-2 N89-13212 #
CONF-8810120-1 N89-12697 #

CONTRIB-40 N89-13128 #

CRC-1412 N89-12797 #

CRDEC-CR-88074 N89-12696 #

CSG-91 N89-13145* #

C87A-25 N89-12818 #

DE88-001081 N89-13097 #
DE88-001166 N89-13101 #
DE88-001191 N89-13098 #
DE88-001195 N89-13102 #
DE88-005041 N89-13223 #
DE88-007177 N89-12702 #
DE88-007825 N89-13258 #
DE88-008371 N89-13238 #
DE88-008382 N89-12713 #
DE88-008803 N89-12625 #
DE88-009096 N89-13277 #
DE88-009148 N89-13259 #
DE88-009149 N89-13260 #
DE88-010019 N89-13174 #
DE88-010270 N89-13093 #
DE88-010527 N89-13167 #
DE88-010677 N89-13388 #
DE88-010684 N89-12812 #
DE88-010838 N89-12701 #
DE88-010904 N89-13239 #
DE88-012118 N89-12791 #
DE88-012233 N89-13151 #
DE88-012430 N89-12793 #
DE88-012635 N89-12861 #
DE88-012701 N89-13095 #
DE88-012870 N89-12848 #
DE88-013098 N89-13384 #
DE88-013246 N89-12826 #
DE88-013592 N89-12872 #
DE88-013825 N89-13135 #
DE88-013846 N89-12703 #
DE88-014038 N89-13278 #
DE88-014122 N89-12706 #
DE88-014153 N89-12697 #
DE88-014399 N89-13246 #
DE88-014401 N89-13212 #
DE88-014459 N89-12704 #
DE88-014524 N89-12787 #
DE88-014659 N89-12686 #
DE88-014963 N89-12840 #
DE88-015108 N89-13099 #
DE88-015128 N89-12724 #
DE88-015185 N89-12662 #
DE88-015259 N89-12857 #
DE88-015266 N89-13233 #
DE88-015358 N89-12725 #
DE88-015397 N89-12742 #
DE88-015431 N89-13106 #
DE88-015538 N89-13306 #

DE88-015577 N89-13105 #
DE88-015585 N89-12828 #
DE88-015650 N89-13389 #
DE88-015715 N89-13247 #
DE88-015922 N89-13213 #
DE88-015958 N89-13123 #
DE88-016062 N89-13147 #
DE88-016113 N89-13100 #
DE88-016155 N89-13292 #
DE88-016174 N89-12830* #
DE88-016226 N89-12679 #
DE88-016227 N89-13288 #
DE88-016231 N89-13294 #
DE88-016236 N89-12858 #
DE88-016237 N89-13261 #
DE88-016241 N89-12714 #
DE88-016274 N89-13254 #
DE88-016313 N89-12698 #
DE88-016318 N89-12859 #
DE88-016328 N89-12788 #
DE88-016363 N89-12743 #
DE88-016470 N89-13168 #
DE88-016557 N89-12715 #
DE88-016571 N89-13169 #
DE88-016589 N89-12869 #
DE88-016632 N89-13279 #
DE88-016659 N89-13289 #
DE88-016674 N89-12680 #
DE88-016746 N89-12831 #
DE88-016753 N89-12748 #
DE88-016797 N89-12744 #
DE88-016841 N89-13262 #
DE88-016842 N89-13263 #
DE88-016892 N89-13255 #
DE88-016953 N89-12664 #
DE88-016957 N89-12832 #
DE88-016959 N89-12699 #
DE88-016979 N89-12844 #
DE88-016980 N89-12789 #
DE88-017016 N89-12860 #
DE88-017024 N89-12578 #
DE88-017084 N89-12700 #
DE88-017087 N89-12833 #
DE88-017092 N89-12716 #
DE88-017095 N89-12929 #
DE88-017115 N89-13264 #
DE88-017137 N89-13265 #
DE88-017326 N89-13170 #
DE88-017380 N89-13221 #
DE88-702958 N89-12721 #
DE88-702991 N89-13201 #
DE88-703007 N89-13096 #
DE88-703048 N89-13293 #
DE88-703054 N89-13377 #
DE88-703273 N89-13370 #
DE88-703324 N89-13385 #
DE88-703325 N89-13371 #
DE88-753149 N89-13373 #

DFVLR-FB-88-23 N89-13140 #
DFVLR-FB-88-24 N89-12719 #
DFVLR-FB-88-25 N89-13136 #
DFVLR-FB-88-26 N89-12933 #

DFVLR-MITT-88-17 N89-13124 #
DFVLR-MITT-88-18 N89-12839 #

DOE/CE-50181/H1 N89-12748 #

DOE/EIA-M031 N89-13169 #

DOE/ER-13393/T3 N89-13262 #
DOE/ER-13393/T4 N89-13263 #
DOE/ER-13648/3 N89-12700 #
DOE/ER-13670/T1 N89-13389 #
DOE/ER-13700/1 N89-13239 #
DOE/ER-45071/T1 N89-12715 #
DOE/ER-45082/4 N89-13277 #
DOE/ER-45136/2 N89-12716 #
DOE/ER-45267/2 N89-13233 #
DOE/ER-75172/5 N89-13223 #

DOE/ET-53088/303 N89-13264 #

DOE/FE-61114/2608 N89-13093 #

DOE/METC-88-6091 N89-13097 #

DOE/NASA/0015-1 N89-12675* #
DOE/NASA/0017-7 N89-13103* #

DOE/OSTI-3359-SUPPL-3 N89-13097 #

DOE/PC-90956/T6 N89-12833 #

DOE/SF-00115/T13 N89-12828 #

DOT/FAA/CT-TN88/8 ..... N89-12558 #

DP-MS-88-163 ..... N89-12742 #

DPST-87-878 ..... N89-13147 #

DREO-TN-88-4 ..... N89-12805 #

DTRC/SHD-1212-03 ..... N89-13127 #

DTRC/SME-88-39 ..... N89-12712 #

E-639 ..... N89-12571 #
E-768 ..... N89-12863 #
E-3205 ..... N89-12876* #
E-3557 ..... N89-12720* #
E-4128 ..... N89-12930* #
E-4275 ..... N89-12717* #
E-4286 ..... N89-12553* #
E-4320 ..... N89-13103* #
E-4352 ..... N89-12746* #
E-4394 ..... N89-12835* #
E-4405 ..... N89-12684* #
E-4421 ..... N89-12753* #
E-4422 ..... N89-12567* #
E-4434 ..... N89-12552* #
E-4435 ..... N89-12845* #
E-4447 ..... N89-12819* #
E-4458 ..... N89-12838* #
E-4461 ..... N89-12566* #
E-4487 ..... N89-12665* #
E-4507 ..... N89-12555* #
E-4515 ..... N89-12568* #

EEI-88-188 ..... N89-12862* #
EEI-88-189 ..... N89-13141* #

EGG-M-38487 ..... N89-12662 #
EGG-M-88055 ..... N89-12724 #
EGG-M-88131 ..... N89-13099 #
EGG-M-88285 ..... N89-12664 #

EML-515 ..... N89-13105 #

EO/MO-14 ..... N89-13199 #

EPA-600/D-88-192 ..... N89-12847 #

ESA-CR(P)-2576-VOL-1 ..... N89-12573 #
ESA-CR(P)-2576-VOL-2 ..... N89-12574 #
ESA-CR(P)-2655 ..... N89-12809 #

ESA-SP-284-VOL-1 ..... N89-12936 #

ESD-TR-87-277 ..... N89-13280 #
ESD-TR-88-010 ..... N89-13154 #
ESD-TR-88-125 ..... N89-13179 #

ESL-718048-8 ..... N89-12808 #

ETN-88-93109 ..... N89-12571 #
ETN-88-93110 ..... N89-12863 #
ETN-88-93164 ..... N89-12573 #
ETN-88-93165 ..... N89-12574 #
ETN-88-93222 ..... N89-12556 #
ETN-88-93231 ..... N89-12718 #
ETN-88-93242 ..... N89-12936 #
ETN-88-93252 ..... N89-12809 #
ETN-88-93313 ..... N89-12682 #
ETN-88-93314 ..... N89-12677 #
ETN-88-93315 ..... N89-12678 #
ETN-88-93318 ..... N89-12683 #
ETN-88-93376 ..... N89-13266 #
ETN-88-93440 ..... N89-13290 #
ETN-88-93471 ..... N89-12846 #
ETN-88-93472 ..... N89-12576 #
ETN-88-93474 ..... N89-13243 #
ETN-88-93477 ..... N89-13112 #
ETN-88-93479 ..... N89-13386 #
ETN-88-93480 ..... N89-13113 #
ETN-88-93519 ..... N89-13308 #
ETN-88-93520 ..... N89-13124 #
ETN-88-93521 ..... N89-12839 #
ETN-88-93523 ..... N89-13140 #
ETN-88-93524 ..... N89-12719 #
ETN-88-93525 ..... N89-13136 #
ETN-88-93526 ..... N89-12933 #
ETN-88-93527 ..... N89-13114 #
ETN-88-93528 ..... N89-13115 #
ETN-88-93529 ..... N89-13372 #
ETN-88-93530 ..... N89-13172 #
ETN-88-93532 ..... N89-13244 #
ETN-88-93545 ..... N89-13309 #
ETN-88-93550 ..... N89-12934 #
ETN-88-93565 ..... N89-13148

EUR-11186 ..... N89-12861 #

FASAC-TAR-3110 ..... N89-13390 #

FPN-0079 ..... N89-12556 #

FSU-TR-M783 ..... N89-13205 #
FSU-TR-M790 ..... N89-13217 #

FTD-ID(RS)T-0263-88 ..... N89-12854 #
FTD-ID(RS)T-0463-88 ..... N89-13250 #

GRL/8704 ..... N89-12853 #

HAC-REF-F7896 ..... N89-12726 #

IC-87/198 ..... N89-12721 #
IC-87/371 ..... N89-13201 #
IC-87/405 ..... N89-13096 #
IC-88/44 ..... N89-13293 #

IEEE-88CH2497-6-VOL-1 ..... N89-12936 #

IFSI-88-4 ..... N89-12846 #
IFSI-88-5 ..... N89-12576 #
IFSI-88-7 ..... N89-13243 #
IFSI-88-10 ..... N89-13112 #
IFSI-88-12 ..... N89-13386 #
IFSI-88-13 ..... N89-13113 #

IFSR-303 ..... N89-13264 #

INIS-MF-11229 ..... N89-13377 #
INIS-MF-11267 ..... N89-13370 #

INPE-4633-NTE/281 ..... N89-12814 #
INPE-4652-PRE/1359 ..... N89-13090 #

ISAS-RN-365 ..... N89-13237 #

ISBN-0-98-87006-3 ..... N89-13372 #
ISBN-8-45-055434-9 ..... N89-13115 #
ISBN-9-03-530055-6 ..... N89-13290 #
ISBN-9-51-383158-2 ..... N89-13244 #
ISBN-92-807-1108-3 ..... N89-13104
ISBN-92-835-0480-1 ..... N89-12849 #

ISI/RS-88-210 ..... N89-13194 #

ISSN-0167-8590 ..... N89-13290 #
ISSN-0171-1342 ..... N89-12719 #
ISSN-0171-1342 ..... N89-12933 #
ISSN-0171-1342 ..... N89-13136 #
ISSN-0171-1342 ..... N89-13140 #
ISSN-0176-7739 ..... N89-12839 #
ISSN-0176-7739 ..... N89-13124 #
ISSN-0178-7101 ..... N89-13308 #
ISSN-0211-5166 ..... N89-13114 #
ISSN-0358-5077 ..... N89-13244 #
ISSN-0379-6566 ..... N89-12936 #

ISVR-TR-162 ..... N89-12934 #

ITF-87-52 ..... N89-13385 #
ITF-87-55 ..... N89-13371 #

JHU/APL/TG-1368 ..... N89-13251 #
JHU/APL/TG-1370 ..... N89-13166 #

JPL-D-4711 ..... N89-13219* #
JPL-D-4718 ..... N89-13211* #
JPL-D-4719 ..... N89-13165* #
JPL-D-4817 ..... N89-13220* #

JPL-PUBL-88-15 ..... N89-12813* #

L-16415 ..... N89-12542* #
L-16440 ..... N89-12569* #
L-16460 ..... N89-12822* #
L-16470 ..... N89-12543* #
L-16496 ..... N89-12580* #
L-16511 ..... N89-12935* #

LA-UR-88-981 ..... N89-13258 #
LA-UR-88-1103 ..... N89-13259 #
LA-UR-88-1104 ..... N89-13260 #
LA-UR-88-1820 ..... N89-12704 #
LA-UR-88-2465 ..... N89-13246 #
LA-UR-88-2482 ..... N89-13212 #
LA-UR-88-2535 ..... N89-13288 #
LA-UR-88-2536 ..... N89-12679 #
LA-UR-88-2563 ..... N89-13294 #
LA-UR-88-2666 ..... N89-12788 #
LA-UR-88-2745 ..... N89-12858 #
LA-UR-88-2751 ..... N89-13261 #
LA-UR-88-2815 ..... N89-13292 #

LA-11181 ..... N89-13306 #
LA-11411-T ..... N89-12680 #

LBL-24875 ..... N89-13278 #
LBL-25020 ..... N89-12714 #
LBL-25401 ..... N89-12872 #
LBL-25544 ..... N89-12686 #
LBL-25678 ..... N89-13289 #
LBL-25733 ..... N89-13279 #

LC-87-83254 ..... N89-12936 #

LCS-1986/AF 1 ..... N89-13159 #

LC88-1690 ..... N89-12565* #

LIDS-P-1788 ..... N89-13192 #

M-541-VOL-2 ..... N89-12626* #

MAE-1826 ..... N89-13195 #

MCR-87-580 ..... N89-12581* #

MECH-119 ..... N89-12676 #

MIPR-FY1455-86-N0652 ..... N89-12855 #

MLM-3498(OP) ..... N89-12848 #

MPE-208 ..... N89-13308 #

MPL-TM-401 ..... N89-13161 #

MPL-U-9/88 ..... N89-13161 #

MSRR-540 ..... N89-13204 #

MTR-101197 ..... N89-13157 #

NADC-88031-60 ..... N89-12733 #

NAS 1.15:4055 ..... N89-12542* #
NAS 1.15:4068 ..... N89-12752* #
NAS 1.15:4082 ..... N89-12935* #
NAS 1.15:100051 ..... N89-13393* #
NAS 1.15:100890 ..... N89-12930* #
NAS 1.15:100989 ..... N89-13198* #
NAS 1.15:101001 ..... N89-13144* #
NAS 1.15:101022 ..... N89-13171* #
NAS 1.15:101024 ..... N89-12554* #
NAS 1.15:101034 ..... N89-12622* #
NAS 1.15:101043 ..... N89-12623* #
NAS 1.15:101060 ..... N89-12539* #
NAS 1.15:101230 ..... N89-12806* #
NAS 1.15:101248 ..... N89-12830* #
NAS 1.15:101365 ..... N89-12746* #
NAS 1.15:101366 ..... N89-12684* #
NAS 1.15:101373 ..... N89-12753* #
NAS 1.15:101379 ..... N89-12552* #
NAS 1.15:101381 ..... N89-12845* #
NAS 1.15:101382 ..... N89-12720* #
NAS 1.15:101387 ..... N89-12819* #
NAS 1.15:101398 ..... N89-12717* #
NAS 1.15:101403 ..... N89-12665* #
NAS 1.15:101413 ..... N89-12555* #
NAS 1.15:101416 ..... N89-12568* #
NAS 1.15:101492 ..... N89-12834* #
NAS 1.15:101504 ..... N89-13203* #
NAS 1.15:101508 ..... N89-12747* #
NAS 1.21:495 ..... N89-12565* #
NAS 1.21:7037(232) N89-12536*
NAS 1.21:7064-VOL-1 ..... N89-13302* #
NAS 1.21:7064-VOL-2 ..... N89-13298* #
NAS 1.21:7064-VOL-3 ..... N89-13301* #
NAS 1.26:4159 ..... N89-13202* #
NAS 1.26:4180 ..... N89-12553* #
NAS 1.26:4188 ..... N89-12838* #
NAS 1.26:4192 ..... N89-12544* #
NAS 1.26:4197 ..... N89-13153* #
NAS 1.26:4198 ..... N89-12835* #
NAS 1.26:172077 ..... N89-12862* #
NAS 1.26:172078 ..... N89-13141* #
NAS 1.26:179393 ..... N89-12581* #
NAS 1.26:179404 ..... N89-12579* #
NAS 1.26:179409 ..... N89-12723* #
NAS 1.26:179419 ..... N89-12722* #
NAS 1.26:179519 ..... N89-12837* #
NAS 1.26:179568 ..... N89-13256* #
NAS 1.26:179572 ..... N89-12836* #
NAS 1.26:180597 ..... N89-13249* #
NAS 1.26:181486 ..... N89-13088* #
NAS 1.26:181644 ..... N89-12557* #
NAS 1.26:182165 ..... N89-12675* #
NAS 1.26:182189 ..... N89-13103* #
NAS 1.26:182197 ..... N89-12820* #

NAS 1.26:182203 ..... N89-12566* #
NAS 1.26:182211 ..... N89-12567* #
NAS 1.26:182513 ..... N89-12923* #
NAS 1.26:182706 ..... N89-13375* #
NAS 1.26:182719 ..... N89-13387* #
NAS 1.26:182737 ..... N89-13152* #
NAS 1.26:182738 ..... N89-13107* #
NAS 1.26:182831 ..... N89-12624* #
NAS 1.26:182994 ..... N89-12538* #
NAS 1.26:183001 ..... N89-12810* #
NAS 1.26:183009 ..... N89-13219* #
NAS 1.26:183011 ..... N89-13211* #
NAS 1.26:183012 ..... N89-12681* #
NAS 1.26:183013 ..... N89-12931* #
NAS 1.26:183209 ..... N89-13200* #
NAS 1.26:183221 ..... N89-13145* #
NAS 1.26:183278 ..... N89-13150* #
NAS 1.26:183311 ..... N89-12570* #
NAS 1.26:183314 ..... N89-12813* #
NAS 1.26:183315 ..... N89-13240* #
NAS 1.26:183349 ..... N89-12794* #
NAS 1.26:183351 ..... N89-13165* #
NAS 1.26:183352 ..... N89-12870* #
NAS 1.26:183353 ..... N89-13220* #
NAS 1.26:183356 ..... N89-12572* #
NAS 1.26:183385 ..... N89-13091* #
NAS 1.26:183387 ..... N89-13111* #
NAS 1.26:183403 ..... N89-12932* #
NAS 1.26:183511 ..... N89-12745* #
NAS 1.26:184555 ..... N89-13214* #
NAS 1.26:184613 ..... N89-13215* #
NAS 1.55:2437-VOL-2 ..... N89-12626* #
NAS 1.55:2444 ..... N89-12876* #
NAS 1.55:3004 ..... N89-13330* #
NAS 1.55:3015 ..... N89-12582* #
NAS 1.55:10015 ..... N89-13310* #
NAS 1.60:2844 ..... N89-12569* #
NAS 1.60:2851 ..... N89-12580* #
NAS 1.60:2855 ..... N89-12822* #
NAS 1.60:2858 ..... N89-12543* #
NAS 1.71:LAR-13719-1 ..... N89-12867* #
NAS 1.71:MFS-28183-1 ..... N89-13253* #
NAS 1.71:MFS-29291-1 ..... N89-12868* #
NAS 1.71:MSC-21059-1 ..... N89-12843* #
NAS 1.71:MSC-21095-1 ..... N89-12866* #
NAS 1.71:MSC-21294-1 ..... N89-13131* #
NAS 1.71:MSC-21365-1 ..... N89-12865* #
NAS 1.71:MSC-21372-1 ..... N89-12842* #
NAS 1.71:NPO-17282-1-CU ..... N89-12856* #

NASA-CASE-LAR-13438-1 ..... N89-12786*
NASA-CASE-LAR-13444-2-CU N89-12667*
NASA-CASE-LAR-13506-1 ..... N89-12741*
NASA-CASE-LAR-13554-1 ..... N89-12551*
NASA-CASE-LAR-13569-1 ..... N89-12841*
NASA-CASE-LAR-13719-1 ..... N89-12867* #

NASA-CASE-MFS-28183-1 ..... N89-13253* #
NASA-CASE-MFS-29291-1 ..... N89-12868* #

NASA-CASE-MSC-21059-1 ..... N89-12843* #
NASA-CASE-MSC-21095-1 ..... N89-12866* #
NASA-CASE-MSC-21096-1 ..... N89-12621*
NASA-CASE-MSC-21294-1 ..... N89-13131* #
NASA-CASE-MSC-21365-1 ..... N89-12865* #
NASA-CASE-MSC-21372-1 ..... N89-12842* #

NASA-CASE-NPO-16896-1-CU N89-13236*
NASA-CASE-NPO-17085-1-CU N89-12785*
NASA-CASE-NPO-17282-1-CU ..... N89-12856* #

NASA-CP-2437-VOL-2 ..... N89-12626* #
NASA-CP-2444 ..... N89-12876* #
NASA-CP-3004 ..... N89-13330* #
NASA-CP-3015 ..... N89-12582* #
NASA-CP-10015 ..... N89-13310* #

NASA-CR-4159 ..... N89-13202* #
NASA-CR-4180 ..... N89-12553* #
NASA-CR-4186 ..... N89-12838* #
NASA-CR-4192 ..... N89-12544* #
NASA-CR-4197 ..... N89-13153* #
NASA-CR-4198 ..... N89-12835* #
NASA-CR-172077 ..... N89-12862* #
NASA-CR-172078 ..... N89-13141* #
NASA-CR-179393 ..... N89-12581* #
NASA-CR-179404 ..... N89-12579* #
NASA-CR-179409 ..... N89-12723* #
NASA-CR-179419 ..... N89-12722* #
NASA-CR-179519 ..... N89-12837* #
NASA-CR-179566 ..... N89-13256* #
NASA-CR-179572 ..... N89-12836* #
NASA-CR-180597 ..... N89-13249* #
NASA-CR-181486 ..... N89-13068* #
NASA-CR-181644 ..... N89-12557* #
NASA-CR-182165 ..... N89-12675* #
NASA-CR-182189 ..... N89-13103* #
NASA-CR-182197 ..... N89-12820* #
NASA-CR-182203 ..... N89-12566* #
NASA-CR-182211 ..... N89-12567* #
NASA-CR-182513 ..... N89-12923* #
NASA-CR-182706 ..... N89-13375* #
NASA-CR-182719 ..... N89-13387* #
NASA-CR-182737 ..... N89-13152* #
NASA-CR-182738 ..... N89-13107* #
NASA-CR-182831 ..... N89-12624* #
NASA-CR-182994 ..... N89-12538* #
NASA-CR-183001 ..... N89-12810* #
NASA-CR-183009 ..... N89-13219* #
NASA-CR-183011 ..... N89-13211* #
NASA-CR-183012 ..... N89-12681* #
NASA-CR-183013 ..... N89-12931* #
NASA-CR-183209 ..... N89-13200* #
NASA-CR-183221 ..... N89-13145* #
NASA-CR-183278 ..... N89-13150* #
NASA-CR-183311 ..... N89-12570* #
NASA-CR-183314 ..... N89-12813* #
NASA-CR-183315 ..... N89-13240* #
NASA-CR-183349 ..... N89-12794* #
NASA-CR-183351 ..... N89-13165* #
NASA-CR-183352 ..... N89-12870* #
NASA-CR-183353 ..... N89-13220* #
NASA-CR-183356 ..... N89-12572* #
NASA-CR-183385 ..... N89-13091* #
NASA-CR-183387 ..... N89-13111* #
NASA-CR-183403 ..... N89-12932* #
NASA-CR-183511 ..... N89-12745* #
NASA-CR-184555 ..... N89-13214* #
NASA-CR-184613 ..... N89-13215* #

NASA-SP-495 ..... N89-12565* #
NASA-SP-7037(232) N89-12536*
NASA-SP-7064-VOL-1 ..... N89-13302* #
NASA-SP-7064-VOL-2 ..... N89-13298* #
NASA-SP-7064-VOL-3 ..... N89-13301* #

NASA-TM-4055 ..... N89-12542* #
NASA-TM-4066 ..... N89-12752* #
NASA-TM-4082 ..... N89-12935* #
NASA-TM-100051 ..... N89-13393* #
NASA-TM-100890 ..... N89-12930* #
NASA-TM-100989 ..... N89-13198* #
NASA-TM-101001 ..... N89-13144* #
NASA-TM-101022 ..... N89-13171* #
NASA-TM-101024 ..... N89-12554* #
NASA-TM-101034 ..... N89-12622* #
NASA-TM-101043 ..... N89-12623* #
NASA-TM-101060 ..... N89-12539* #
NASA-TM-101230 ..... N89-12806* #
NASA-TM-101248 ..... N89-12830* #
NASA-TM-101365 ..... N89-12746* #
NASA-TM-101366 ..... N89-12684* #
NASA-TM-101373 ..... N89-12753* #
NASA-TM-101379 ..... N89-12552* #
NASA-TM-101381 ..... N89-12845* #
NASA-TM-101382 ..... N89-12720* #
NASA-TM-101387 ..... N89-12819* #
NASA-TM-101398 ..... N89-12717* #
NASA-TM-101403 ..... N89-12665* #
NASA-TM-101413 ..... N89-12555* #
NASA-TM-101416 ..... N89-12568* #
NASA-TM-101492 ..... N89-12834* #
NASA-TM-101504 ..... N89-13203* #
NASA-TM-101508 ..... N89-12747* #

NASA-TP-2844 ..... N89-12569* #
NASA-TP-2851 ..... N89-12580* #
NASA-TP-2855 ..... N89-12822* #
NASA-TP-2858 ..... N89-12543* #

NBSIR-88-3087 ..... N89-12670 #

NCS-TIB-87-17 ..... N89-12807 #

NEPRF-CR-88-02 ..... N89-13122 #

NOAA-NWS-ERCP-44 ..... N89-13125 #

NOAA-TM-ERL-SEL-76 ..... N89-13299 #

NOAA-TR-NESDIS-32 ..... N89-13094 #

NOAA/PMEL-CONTRIB-813 ..... N89-13128 #

NOAA/PMEL-TM-75 ..... N89-13126 #

NORDA-203 ..... N89-13162 #

NOSC/TD-1306 ..... N89-13287 #

NPS-69-88-008 ..... N89-12692 #

NPS73-88-001 ..... N89-12734 #

NRL-MR-6244 ..... N89-12806* #

NRL-9125 ..... N89-13235 #
NRL-9127 ..... N89-13210 #

NSMRL-1117 ..... N89-13134 #

NTSB-ARG-87-03 ..... N89-12537 #

NTSC-TR-87-032 ..... N89-13126 #

NUSC-TD-8043 ..... N89-13234 #

NWC-TP-6880 ..... N89-12798 #

ONR-87-2 ..... N89-13155 #

ONRL-8-010-C ..... N89-13173 #
ONRL-8-011-R ..... N89-13291 #
ONRL-8-014-R ..... N89-12811 #

ORNL/M-612 ..... N89-12869 #

ORNL/TM-10468 ..... N89-12725 #
ORNL/TM-10784 ..... N89-12791 #
ORNL/TM-10998 ..... N89-13221 #

ORNL/TR-88/14 ..... N89-12701 #

PB88-115787 ..... N89-12537 #
PB88-205471 ..... N89-13299 #
PB88-210943 ..... N89-13300 #
PB88-215421 ..... N89-12670 #
PB88-240239 ..... N89-13094 #
PB88-243357 ..... N89-13307 #
PB88-246368 ..... N89-13125 #
PB88-249626 ..... N89-12847 #

PDRC-88-04 ..... N89-13206 #

PIPER-WP-87-5 ..... N89-13160 #

PNL-SA-15359 ..... N89-12698 #
PNL-SA-15424 ..... N89-12699 #

PNL-6279-VOL-8 ..... N89-13123 #

POEF-T-3487 ..... N89-12706 #

PR-87-6 ..... N89-12926 #

PSI-1012/TR-757 ..... N89-12852 #

PWA-FR-20424 ..... N89-12711 #

RADC-TR-TR-88-7 ..... N89-13159 #

RADC-TR-86-218-VOL-2-PT-1 ..... N89-13180 #
RADC-TR-88-27 ..... N89-12688 #
RADC-TR-88-44 ..... N89-13157 #

REPT-37 ..... N89-13309 #
REPT-48-915/F ..... N89-12683 #
REPT-72/88/R260/U N89-13148
REPT-86-9-71 ..... N89-12553* #
REPT-88-178 ..... N89-13266 #
REPT-88/03 ..... N89-12571 #
REPT-88/05 ..... N89-12863 #
REPT-88B0253 ..... N89-12582* #
REPT-153-4705 ..... N89-12817 #
REPT-243-043-00012 ..... N89-12739 #

RIACS-TR-88.5 ..... N89-13214* #
RIACS-TR-88.20 ..... N89-13200* #

RRK-87-31 ..... N89-13373 #

R87AEB111 ..... N89-13256* #

SAIC-PN-1-425-07-809 ..... N89-13122 #

SAIC-87/1612 ..... N89-12836* #

SAND-87-1940 ..... N89-12831 #
SAND-87-2872C ..... N89-12793 #
SAND-87-2921C ..... N89-13095 #
SAND-87-3095-C2 ..... N89-12625 #
SAND-88-0494C ..... N89-12857 #
SAND-88-0903 ..... N89-13255 #
SAND-88-1049C ..... N89-12859 #
SAND-88-1132C ..... N89-12787 #
SAND-88-1350C ..... N89-13167 #
SAND-88-2152C ..... N89-12840 #

SARMA-TR-87-2431A ..... N89-12677 #
SARMA-TR-872429-A ..... N89-12678 #
SARMA-TR-882401 ..... N89-12682 #

SERI/STR-211-3364 ..... N89-13098 #

SERI/TP-211-3390 ..... N89-13102 #
SERI/TP-217-3342 ..... N89-13101 #

SU-SLAC-PUB-4606 ..... N89-13388 #
SU-SLAC-PUB-4622 ..... N89-12812 #
SU-SLAC-PUB-4676 ..... N89-13213 #

TM-AE-8804 ..... N89-13149 #

TR-D102-ARO ..... N89-13217 #
TR-D103-ARO ..... N89-13205 #

TR-87-09-03 ..... N89-13176 #
TR-87-12-05 ..... N89-13158 #
TR-88-4-ONR ..... N89-13137 #
TR-88-03-05 ..... N89-13156 #
TR-88-04-03 ..... N89-13177 #
TR-68-011 ..... N89-12710 #
TR-802 ..... N89-13280 #
TR-1789T ..... N89-12570* #

UBUFFALO/DC/88/TR-75 ..... N89-13285 #
UBUFFALO/DC/88/TR-78 ..... N89-13241 #

UCB/CSD-87/367 ..... N89-13305 #
UCB/CSD-87/376 ..... N89-12926 #

UCID-21471 ..... N89-13100 #
UCID-21475 ..... N89-12929 #

UCRL-21058 ..... N89-13151 #
UCRL-21085 ..... N89-12830* #
UCRL-21091 ..... N89-12844 #
UCRL-21092 ..... N89-12789 #
UCRL-53877 ..... N89-13170 #
UCRL-97451 ..... N89-13384 #
UCRL-97987 ..... N89-13106 #
UCRL-98606 ..... N89-13254 #
UCRL-98970 ..... N89-12697 #
UCRL-99246 ..... N89-12578 #
UCRL-99517 ..... N89-12860 #

UDR-TR-88-08 ..... N89-12864 #
UDR-TR-88-96 ..... N89-12745* #

UILI-ENG-88-2223 ..... N89-13163 #

UILU-ENG-88-2255 ..... N89-13145* #

US-PATENT-APPL-SN-000692 ..... N89-12667*
US-PATENT-APPL-SN-010943 ..... N89-12841*
US-PATENT-APPL-SN-022298 ..... N89-12786*
US-PATENT-APPL-SN-060182 ..... N89-12741*
US-PATENT-APPL-SN-087282 ..... N89-12785*
US-PATENT-APPL-SN-087283 ..... N89-13236*
US-PATENT-APPL-SN-213558 ..... N89-13131* #
US-PATENT-APPL-SN-217725 ..... N89-12843* #
US-PATENT-APPL-SN-221388 ..... N89-12865* #
US-PATENT-APPL-SN-235150 ..... N89-12856* #
US-PATENT-APPL-SN-239260 ..... N89-12867* #
US-PATENT-APPL-SN-244367 ..... N89-13253* #
US-PATENT-APPL-SN-246595 ..... N89-12842* #
US-PATENT-APPL-SN-248010 ..... N89-12866* #
US-PATENT-APPL-SN-250196 ..... N89-12868* #
US-PATENT-APPL-SN-929862 ..... N89-12551*
US-PATENT-APPL-SN-929865 ..... N89-12621*

US-PATENT-CLASS-52-814 ..... N89-12786*
US-PATENT-CLASS-52-821 ..... N89-12786*
US-PATENT-CLASS-62-467 ..... N89-12785*
US-PATENT-CLASS-62-514-R N89-12785*
US-PATENT-CLASS-73-147 ..... N89-12551*
US-PATENT-CLASS-73-147 ..... N89-12841*
US-PATENT-CLASS-73-180 ..... N89-12841*
US-PATENT-CLASS-73-505 ..... N89-13236*
US-PATENT-CLASS-116-DIG.43 ..... N89-12551*
US-PATENT-CLASS-116-265 ..... N89-12551*
US-PATENT-CLASS-156-297 ..... N89-12741*
US-PATENT-CLASS-156-299 ..... N89-12741*
US-PATENT-CLASS-165-61 ..... N89-12785*
US-PATENT-CLASS-165-96 ..... N89-12785*
US-PATENT-CLASS-182-103 ..... N89-12621*
US-PATENT-CLASS-212-225 ..... N89-12621*
US-PATENT-CLASS-212-257 ..... N89-12621*
US-PATENT-CLASS-414-689 ..... N89-12621*
US-PATENT-CLASS-414-718 ..... N89-12621*
US-PATENT-CLASS-414-735 ..... N89-12621*
US-PATENT-CLASS-428-44 ..... N89-12741*
US-PATENT-CLASS-428-47 ..... N89-12741*
US-PATENT-CLASS-428-58 ..... N89-12741*
US-PATENT-CLASS-428-71 ..... N89-12741*
US-PATENT-CLASS-428-76 ..... N89-12741*
US-PATENT-CLASS-428-182 ..... N89-12786*
US-PATENT-CLASS-564-315 ..... N89-12667*
US-PATENT-CLASS-564-323 ..... N89-12667*
US-PATENT-CLASS-564-330 ..... N89-12667*
US-PATENT-CLASS-564-342 ..... N89-12667*
US-PATENT-CLASS-564-344 ..... N89-12667*
US-PATENT-CLASS-564-396 ..... N89-12667*
US-PATENT-CLASS-564-430 ..... N89-12667*

US-PATENT-4,769,968 ..... N89-12786*
US-PATENT-4,770,032 ..... N89-12841*
US-PATENT-4,771,823 ..... N89-12785*
US-PATENT-4,772,175 ..... N89-12621*
US-PATENT-4,773,266 ..... N89-13236*
US-PATENT-4,774,118 ..... N89-12741*
US-PATENT-4,774,359 ..... N89-12667*
US-PATENT-4,774,835 ..... N89-12551*

USAFSAM-TR-86-36-PT-2 ..... N89-13133 #

USARIEM-17-88 ..... N89-13132 #

UTSI/88-07 ..... N89-12838* #

VERITAY-F04-88-1 ..... N89-12663 #

VPI-E-88-18 ..... N89-12681* #

VPI-88-19 ..... N89-12928 #

VTT-RR-535 ..... N89-13244 #

WP-87-88-39 ..... N89-13204 #

FEDERAL REGIONAL DEPOSITORY LIBRARIES

ALABAMA

AUBURN UNIV. AT MONTGOMERY LIBRARY
Documents Department
Montgomery, AL 36193
(205) 271-9650

UNIV. OF ALABAMA LIBRARY
Documents Dept.-Box S
University, AL 35486
(205) 348-6046

ARIZONA

DEPT. OF LIBRARY, ARCHIVES AND PUBLIC RECORDS
Third Floor—State Cap.
1700 West Washington
Phoenix, AZ 85007
(602) 255-4121

UNIVERSITY OF ARIZONA LIB.
Government Documents Dept.
Tucson, AZ 85721
(602) 621-6433

ARKANSAS

ARKANSAS STATE LIBRARY
One Capitol Mall
Little Rock, AR 72201
(501) 371-2326

CALIFORNIA

CALIFORNIA STATE LIBRARY
Govt. Publications Section
P.O. Box 2037
Sacramento, CA 95809
(916) 324-4863

COLORADO

UNIV OF COLORADO LIB.
Government Pub. Division
Campus Box 184
Boulder, CO 80309
(303) 492-8834

DENVER PUBLIC LIBRARY
Govt. Pub. Department
1357 Broadway
Denver, CO 80203
(303) 571-2131

CONNECTICUT

CONNECTICUT STATE LIBRARY
Government Documents Unit
231 Capitol Avenue
Hartford, CT 06106
(203) 566-7029

FLORIDA

UNIV. OF FLORIDA LIBRARIES
Library West
Documents Department
Gainesville, FL 32611
(904) 392-0367

GEORGIA

UNIV. OF GEORGIA LIBRARIES
Government Reference Dept.
Athens, GA 30602
(404) 542-8949

HAWAII

UNIV. OF HAWAII LIBRARY
Govt. Documents Collection
2550 The Mall
Honolulu, HI 96822
(808) 948-8230

IDAHO

UNIV. OF IDAHO LIBRARY
Documents Section
Moscow, ID 83843
(208) 885-6344

ILLINOIS

ILLINOIS STATE LIBRARY
Information Services Branch
Centennial Building
Springfield, IL 62756
(217) 782-5185

INDIANA

INDIANA STATE LIBRARY
Serials Documents Section
140 North Senate Avenue
Indianapolis, IN 46204
(317) 232-3686

IOWA

UNIV. OF IOWA LIBRARIES
Govt. Documents Department
Iowa City, IA 52242
(319) 353-3318

KANSAS

UNIVERSITY OF KANSAS
Doc. Collect—Spencer Lib.
Lawrence, KS 66045-2800
(913) 864-4662

KENTUCKY

UNIV. OF KENTUCKY LIBRARIES
Govt. Pub. Department
Lexington, KY 40506-0039
(606) 257-3139

LOUISIANA

LOUISIANA STATE UNIVERSITY
Middleton Library
Govt. Docs. Dept.
Baton Rouge, LA 70803
(504) 388-2570

LOUISIANA TECHNICAL UNIV. LIBRARY
Documents Department
Ruston, LA 71272-0046
(318) 257-4962

MAINE

UNIVERSITY OF MAINE
Raymond H. Fogler Library
Tri-State Regional Documents Depository
Orono, ME 04469
(207) 581-1680

MARYLAND

UNIVERSITY OF MARYLAND
McKeldin Lib.—Doc. Div.
College Park, MD 20742
(301) 454-3034

MASSACHUSETTS

BOSTON PUBLIC LIBRARY
Government Docs. Dept.
Boston, MA 02117
(617) 536-5400 ext.226

MICHIGAN

DETROIT PUBLIC LIBRARY
Sociology Department
5201 Woodward Avenue
Detroit, MI 48202-4093
(313) 833-1409

MICHIGAN STATE LIBRARY
P.O. Box 30007
Lansing, MI 48909
(517) 373-1593

MINNESOTA

UNIVERSITY OF MINNESOTA
Government Pubs. Division
409 Wilson Library
309 19th Avenue South
Minneapolis, MN 55455
(612) 373-7870

MISSISSIPPI

UNIV. OF MISSISSIPPI LIB.
Documents Department
University, MS 38677
(601) 232-5857

MONTANA

UNIV. OF MONTANA
Mansfield Library
Documents Division
Missoula, MT 59812
(406) 243-6700

NEBRASKA

UNIVERSITY OF NEBRASKA - LINCOLN
Love Library
Documents Department
Lincoln, NE 68588-0410
(402) 472-2562

NEVADA

UNIVERSITY OF NEVADA LIB.
Govt. Pub. Department
Reno, NV 89557-0044
(702) 784-6579

NEW JERSEY

NEWARK PUBLIC LIBRARY
5 Washington Street
Newark, NJ 07101-0630
(201) 733-7812

NEW MEXICO

UNIVERSITY OF NEW MEXICO
Zimmerman Library
Government Pub. Dept.
Albuquerque, NM 87131
(505) 277-5441

NEW MEXICO STATE LIBRARY
Reference Department
325 Don Gaspar Avenue
Santa Fe, NM 87503
(505) 827-3826

NEW YORK

NEW YORK STATE LIBRARY
Empire State Plaza
Albany, NY 12230
(518) 474-5563

NORTH CAROLINA

UNIVERSITY OF NORTH CAROLINA AT CHAPEL HILL
Davis Library
BA/SS Documents Division
Chapel Hill, NC 27515
(919) 962-1151

NORTH DAKOTA

UNIVERSITY OF NORTH DAKOTA
Chester Fritz Library
Documents Department
Grand Forks, ND 58202
(701) 777-4629
In cooperation with North Dakota State Univ. Library

OHIO

STATE LIBRARY OF OHIO
Documents Department
65 South Front Street
Columbus, OH 43266-0334
(614) 462-7051

OKLAHOMA

OKLAHOMA DEPT. OF LIB.
Government Documents
200 NE 18th Street
Oklahoma City, OK 73105
(405) 521-2502, ext. 252

OKLAHOMA STATE UNIV. LIB.
Documents Department
Stillwater, OK 74078
(405) 624-6546

OREGON

PORTLAND STATE UNIV. LIB.
Documents Department
P.O. Box 1151
Portland, OR 97207
(503) 229-3673

PENNSYLVANIA

STATE LIBRARY OF PENN.
Government Pub. Section
P.O. Box 1601
Harrisburg, PA 17105
(717) 787-3752

TEXAS

TEXAS STATE LIBRARY
Public Services Department
P.O. Box 12927—Cap. Sta.
Austin, TX 78711
(512) 475-2996

TEXAS TECH. UNIV. LIBRARY
Govt. Documents Department
Lubbock, TX 79409
(806) 742-2268

UTAH

UTAH STATE UNIVERSITY
Merrill Library, U.M.C. 30
Logan, UT 84322
(801) 750-2682

VIRGINIA

UNIVERSITY OF VIRGINIA
Alderman Lib.—Public Doc.
Charlottesville, VA 22903-2498
(804) 924-3133

WASHINGTON

WASHINGTON STATE LIBRARY
Documents Section
Olympia, WA 98504
(206) 753-4027

WEST VIRGINIA

WEST VIRGINIA UNIV. LIB.
Documents Department
Morgantown, WV 26506-6069
(304) 293-3640

WISCONSIN

MILWAUKEE PUBLIC LIBRARY
814 West Wisconsin Avenue
Milwaukee, WI 53233
(414) 278-3065

ST. HIST LIB. OF WISCONSIN
Government Pub. Section
816 State Street
Madison, WI 53706
(608) 262-4347

WYOMING

WYOMING STATE LIBRARY
Supreme Ct. & Library Bld.
Cheyenne, WY 82002
(307) 777-5919

National Aeronautics and
Space Administration
Code NTT-4
Washington, D.C.
20546

Official Business

Penalty for Private Use, $300

SPECIAL FOURTH-CLASS RATE
POSTAGE & FEES PAID
NASA
PERMIT No. G 27

NASA

POSTMASTER: If Undeliverable (Section 158
Postal Manual) Do Not Return